PURINERGIC SIGNALING IN HEALTH AND DISEASE

EDITED BY: Eric Boué-Grabot, David Blum and Stefania Ceruti
PUBLISHED IN: Frontiers in Cellular Neuroscience and
Frontiers in Molecular Neuroscience

frontiers Research Topics

frontiers

ISSN 1664-8714
ISBN 978-2-88963-556-6
DOI 10.3389/978-2-88963-556-6

About Frontiers

Frontiers is more than just an open-access publisher of scholarly articles: it is a pioneering approach to the world of academia, radically improving the way scholarly research is managed. The grand vision of Frontiers is a world where all people have an equal opportunity to seek, share and generate knowledge. Frontiers provides immediate and permanent online open access to all its publications, but this alone is not enough to realize our grand goals.

Frontiers Journal Series

The Frontiers Journal Series is a multi-tier and interdisciplinary set of open-access, online journals, promising a paradigm shift from the current review, selection and dissemination processes in academic publishing. All Frontiers journals are driven by researchers for researchers; therefore, they constitute a service to the scholarly community. At the same time, the Frontiers Journal Series operates on a revolutionary invention, the tiered publishing system, initially addressing specific communities of scholars, and gradually climbing up to broader public understanding, thus serving the interests of the lay society, too.

Dedication to Quality

Each Frontiers article is a landmark of the highest quality, thanks to genuinely collaborative interactions between authors and review editors, who include some of the world's best academicians. Research must be certified by peers before entering a stream of knowledge that may eventually reach the public - and shape society; therefore, Frontiers only applies the most rigorous and unbiased reviews.
Frontiers revolutionizes research publishing by freely delivering the most outstanding research, evaluated with no bias from both the academic and social point of view. By applying the most advanced information technologies, Frontiers is catapulting scholarly publishing into a new generation.

What are Frontiers Research Topics?

Frontiers Research Topics are very popular trademarks of the Frontiers Journals Series: they are collections of at least ten articles, all centered on a particular subject. With their unique mix of varied contributions from Original Research to Review Articles, Frontiers Research Topics unify the most influential researchers, the latest key findings and historical advances in a hot research area! Find out more on how to host your own Frontiers Research Topic or contribute to one as an author by contacting the Frontiers Editorial Office: researchtopics@frontiersin.org

PURINERGIC SIGNALING IN HEALTH AND DISEASE

Topic Editors:
Eric Boué-Grabot, Université de Bordeaux, Institut des Maladies Neurodégénératives, CNRS UMR 5293, Bordeaux, France
David Blum, INSERM U1172 Centre de Recherche Jean Pierre Aubert, France
Stefania Ceruti, Università degli Studi di Milano, Italy

Citation: Boué-Grabot, E., Blum, D., Ceruti, S., eds. (2020). Purinergic Signaling in Health and Disease. Lausanne: Frontiers Media SA. doi: 10.3389/978-2-88963-556-6

Table of Contents

frontiers in Cellular Neuroscience

EDITORIAL
published: 04 February 2020
doi: 10.3389/fncel.2020.00015

Editorial: Purinergic Signaling in Health and Disease

Eric Boué-Grabot[1,2]*, *David Blum*[3] *and Stefania Ceruti*[4]

[1] Univ. de Bordeaux, Institut des Maladies Neurodégénératives, UMR 5293, Bordeaux, France, [2] CNRS, Institut des Maladies Neurodégénératives, UMR 5293, Bordeaux, France, [3] Université de Lille, Inserm, CHU, UMR-S1172, Lille Neuroscience & Cognition, Lille, France, [4] Department of Pharmacological and Biomolecular Sciences, Università Degli Studi di Milano, Milan, Italy

Keywords: purine, P2X, P2Y, adenosine (A(1), A(2A), A(2B)) receptors, purinergic signaling, CNS, CNS—disorder

Editorial on the Research Topic

Purinergic Signaling in Health and Disease

Adenosine 5′-triphosphate (ATP) is one of the most abundant molecules in living cells serving as universal energy "currency." After slow acceptance of the concept of the release and extracellular action of ATP and its breakdown products, ADP and adenosine, purinergic signaling has been recognized as a widespread mechanism for cell-to-cell communication in living organisms. Additionally, the contribution of pyrimidine nucleotides (such as UTP and UDP) and sugar-nucleotides (i.e., UDP-glucose and UDP-galactose) have been more recently discovered. Purinergic signaling plays major physiological roles in mammalian central nervous system (CNS) such as neurotransmission, neuromodulation, communication in glial network, and between neurons and glia. The high number of signaling molecules provides the versatile basis for complex purinergic signaling through the activation of several families of receptors. G-protein coupled P1 receptors for adenosine, ionotropic P2X receptors for ATP and G-protein coupled P2Y receptors for ATP and other nucleotides are abundant and widely distributed in central neurons at pre-and post-synapse and in glial cells. Dysregulations of purinergic signals are associated with major CNS disorders including chronic pain, brain trauma ischemia, epilepsy, neurodegenerative diseases such as Alzheimer's disease (AD) or Amyotrophic lateral sclerosis (ALS) associated with neuro-inflammation as well as neuropsychiatric diseases, including depression, anxiety, and schizophrenia.

In this Research Topic we have brought together 22 articles written by 145 authors containing 7 reviews, 1 hypothesis and theory, 1 brief research report, and 13 original research articles. Review articles present several up-to-date aspects of the biology of purinergic signaling in the nervous system, such as in the vertebrate olfactory system (Rotermund et al.) or in the preBötzinger Complex (Reklow et al.). Other reviews focus on the structure-function of P2X receptors (Peverini et al.) and on the function of adenosine receptor agonists, guanine-based purines and vesicular nucleotide transporter in health and disease emphasizing their therapeutic potential in neurological disorders (Jacobson et al.; Tasca et al.; Miras-Portugal et al.). The function of P2X7 receptor and its regulation by its wide interactome is also reviewed (Kanellopoulos and Delarasse; Kopp et al.). In addition, the diversity of P2X7 function is underlined in an original research article showing the role of P2X7 in the regulation of the whole-body energy metabolism (Giacovazzo et al.). P2X7 receptor distribution was also examined in a ß-amyloid mouse model and revealed its microglial upregulation at advanced and late stages of the disease (Martínez-Frailes et al.). The other original research papers are covering important aspects of purinergic receptor function and regulation in the CNS. Several papers focus on the role of adenosine A_{2A} receptors expressed in distinct brain region such as the prefrontal cortex (PFC), the hippocampus and the striatum and their role of associated behavior. By a selective downregulation of A_{2A}R selectively in prelimbic medial PFC the

OPEN ACCESS

Edited and reviewed by:
Arianna Maffei,
Stony Brook University, United States

Correspondence:
Eric Boué-Grabot
eric.boue-grabot@u-bordeaux.fr

Specialty section:
This article was submitted to Cellular Neurophysiology, a section of the journal Frontiers in Cellular Neuroscience

Received: *16 January 2020*
Accepted: *20 January 2020*
Published: *04 February 2020*

Citation:
Boué-Grabot E, Blum D and Ceruti S (2020) Editorial: Purinergic Signaling in Health and Disease. Front. Cell. Neurosci. 14:15. doi: 10.3389/fncel.2020.00015

authors revealed the role of A_{2A} in physiological behaviors such as decision making (Leffa et al.). A distinct strategy was used to knockdown A_{2A}R in two striatal regions, the nucleus accumbens and the dorsal medium striatum and results show that downregulation of A_{2A} increased attention and motivation (Zhou et al.). Long lasting blockade of A_{2A} receptor activity by a selective antagonist in a ß-amyloid mouse model of AD improves memory deficit and reduces cortical amyloid load consistent with a beneficial role of A_{2A}R blockade for AD (Faivre et al.) and with the idea that consumption of caffeine reduces the risk of developing the pathology. However, an article reveals that caffeine consumption during pregnancy may have opposite effect representing a risk-factor for early appearance of AD symptoms in the off-springs of a transgenic mouse model of tauopathy (Zappettini et al.). Several articles focus on P2X4 receptors describing new structural features based on the identification of a selective allosteric inhibitory site (Ase et al.) or novel specific monoclonal antibodies and nanobodies recognizing specifically P2X4 receptors in its native conformation (Bergmann et al.), as well as a role of intracellular P2X4 in lysosomal exocytosis that may be implicated in HIV associated neuropathy (Datta et al.). In the striatum, pharmacological manipulations of P2X4 and dopamine receptors show the role of the interplay between purinergic and dopaminergic signaling in the regulation of sensorimotor information processing (Khoja et al.). Spatio-temporal expression profile of P2X subunits during embryogenesis in *Xenopus* reveal that several P2X receptors may have distinct role during development including neurogenesis (Blanchard et al.). Neuromodulation of cortical excitatory or inhibitory synapses by P2X receptors activated by ATP released from neurons as well as from astrocytes in the neocortex is altered during aging, suggesting that alteration of ATP signaling may contribute to age-dependent impairment of synaptic activities, but can be partially rescued by positive experience, such as environmental enrichment (Lalo et al.). Fasting/refeeding conditions in rats show that increased expression of P2X2 is associated to increase neuronal activity in the supraoptic nucleus of the hypothalamus and arginine vasopressin release (Ivetic et al.). Finally, purinergic profiling of blood T cells of patients with migraine suggests the involvement of purinergic signaling in this disorder with increase of ATP-dependent pro-inflammatory and reduction of adenosine-mediated anti-inflammatory mechanism (Nurkhametova et al.).

Overall, this Research Topic provides an up-to-date overview of the diversity of the purinergic signaling function in the CNS and provides new insights on the importance of their engagement in physiological and pathological conditions.

AUTHOR CONTRIBUTIONS

All authors listed have made a substantial, direct and intellectual contribution to the work, and approved it for publication.

ACKNOWLEDGMENTS

We thank all authors for their contribution to this Research Topic and we would like also to acknowledge the work of reviewers whose constructive comments contributed to improve the quality of the articles.

Conflict of Interest: The authors declare that the research was conducted in the absence of any commercial or financial relationships that could be construed as a potential conflict of interest.

frontiers in Molecular Neuroscience

ORIGINAL RESEARCH
published: 12 July 2018
doi: 10.3389/fnmol.2018.00235

Beneficial Effect of a Selective Adenosine A_{2A} Receptor Antagonist in the APPswe/PS1dE9 Mouse Model of Alzheimer's Disease

*Emilie Faivre[1], Joana E. Coelho[2], Katja Zornbach[3], Enas Malik[4], Younis Baqi[4,5], Marion Schneider[4], Lucrezia Cellai[1], Kevin Carvalho[1], Shéhérazade Sebda[6], Martin Figeac[6], Sabiha Eddarkaoui[1], Raphaëlle Caillierez[1], Yijuang Chern[7], Michael Heneka[8,9], Nicolas Sergeant[1], Christa E. Müller[4], Annett Halle[3,8], Luc Buée[1], Luisa V. Lopes[2] and David Blum[1]**

[1]Université de Lille, Inserm, CHU-Lille, LabEx DISTALZ, Jean-Pierre Aubert Research Centre UMR-S1172, Alzheimer & Tauopathies, Lille, France, [2]Instituto de Medicina Molecular, Faculdade de Medicina de Lisboa, Universidade de Lisboa, Lisbon, Portugal, [3]Center of Advanced European Studies and Research, Bonn, Germany, [4]PharmaCenter Bonn, Pharmaceutical Institute, Pharmaceutical Chemistry I, University of Bonn, Bonn, Germany, [5]Department of Chemistry, Faculty of Science, Sultan Qaboos University, Muscat, Oman, [6]Plateau de Génomique Fonctionnelle et Structurale, CHU Lille, University of Lille, Lille, France, [7]Institute of Biomedical Sciences, Academia Sinica, Taipei, Taiwan, [8]German Center for Neurodegenerative Diseases (DZNE), Bonn, Germany, [9]Department of Neurodegenerative Diseases and Geropsychiatry/Neurology, University of Bonn Medical Center, Bonn, Germany

OPEN ACCESS

Edited by:
Detlev Boison, Legacy Health, United States

Reviewed by:
Annakaisa Haapasalo, A.I. Virtanen Institute for Molecular Sciences, Univeristy of Eastern Finland, Finland
Rodrigo A. Cunha, Faculdade de Medicina, Universidade de Coimbra, Portugal

***Correspondence:**
David Blum
david.blum@inserm.fr

Received: *25 April 2018*
Accepted: *15 June 2018*
Published: *12 July 2018*

Citation:
Faivre E, Coelho JE, Zornbach K, Malik E, Baqi Y, Schneider M, Cellai L, Carvalho K, Sebda S, Figeac M, Eddarkaoui S, Caillierez R, Chern Y, Heneka M, Sergeant N, Müller CE, Halle A, Buée L, Lopes LV and Blum D (2018) Beneficial Effect of a Selective Adenosine A_{2A} Receptor Antagonist in the APPswe/PS1dE9 Mouse Model of Alzheimer's Disease. Front. Mol. Neurosci. 11:235. doi: 10.3389/fnmol.2018.00235

Consumption of caffeine, a non-selective adenosine A_{2A} receptor ($A_{2A}R$) antagonist, reduces the risk of developing Alzheimer's disease (AD) and mitigates both amyloid and Tau lesions in transgenic mouse models of the disease. While short-term treatment with $A_{2A}R$ antagonists have been shown to alleviate cognitive deficits in mouse models of amyloidogenesis, impact of a chronic and long-term treatment on the development of amyloid burden, associated neuroinflammation and memory deficits has never been assessed. In the present study, we have evaluated the effect of a 6-month treatment of APPsw/PS1dE9 mice with the potent and selective $A_{2A}R$ antagonist MSX-3 from 3 to 9-10 months of age. At completion of the treatment, we found that the MSX-3 treatment prevented the development of memory deficits in APP/PS1dE9 mice, without significantly altering hippocampal and cortical gene expressions. Interestingly, MSX-3 treatment led to a significant decrease of Aβ1-42 levels in the cortex of APP/PS1dE9 animals, while Aβ1-40 increased, thereby strongly affecting the Aβ1-42/Aβ1-40 ratio. Together, these data support the idea that $A_{2A}R$ blockade is of therapeutic value for AD.

Keywords: Alzheimer's disease, amyloid, adenosine receptor, A_{2A}, memory

INTRODUCTION

Alzheimer's disease (AD) is the most common neurodegenerative disorder in the elderly. AD is characterized by a progressive cognitive decline and neuropathologically defined by two hallmarks: extracellular deposits constisting of aggregated β-amyloid (Aβ) peptides and intraneuronal fibrillar aggregates of hyper- and abnormally phosphorylated Tau proteins (Masters et al., 1985; Duyckaerts et al., 2015). AD is dependent on various genetic and environmental factors (Reitz et al., 2011; Cuyvers and Sleegers, 2016). Among protective factors, several epidemiological studies have

reported an inverse relation between caffeine intake, age-related cognitive impairments and the risk to develop AD later in life (for reviews see Flaten et al., 2014; Cunha, 2016). In accordance, we and others have shown that caffeine is beneficial towards memory impairments and pathology in transgenic mouse models of AD (Arendash et al., 2006, 2009; Cao et al., 2009; Laurent et al., 2014).

Beneficial effects of caffeine have been ascribed to its ability to block adenosine A_{2A} receptors (A_{2A}Rs), a G protein-coupled receptor whose endogenous ligand is adenosine (Cunha, 2016). In line with a role of A_{2A}Rs in AD, an association between a polymorphism of the ADORA2A gene with hippocampal volume in mild cognitive impairment and AD has been recently reported (Horgusluoglu-Moloch et al., 2017). Like caffeine, pharmacological and genetic A_{2A}R blockade was found to reduce hippocampal pathology, neuroinflammation and memory deficits in a model of AD-like Tau pathology (Laurent et al., 2016). A_{2A}R blockade or deletion was also found to counteract synaptotoxicity and memory deficits acutely induced by Aβ peptides (Dall'lgna et al., 2003, 2007; Canas et al., 2009). In line, recent data emphasize in transgenic models of amyloidogenesis (APP/PS1dE9 and hAPP-J20), that short-term treatments (from 1 to 3 weeks) with selective A_{2A}R antagonists (SCH58260 i.p. or KW6002 p.o.) revert memory alterations (Viana da Silva et al., 2016; Orr et al., 2018; Silva et al., 2018). However, the impact of a long-term and chronic A_{2A}R blockade on the development of amyloid pathology and associated memory impairment has not been investigated yet.

In the present study, we explored the outcomes of a chronic pharmacological blockade of A_{2A}R in the APPswe/PS1dE9 transgenic mouse model, using the selective water-soluble antagonist MSX-3. Our data demonstrate that chronic MSX-3 treatment delivered from 3 to 9-10 months of age in APPsw/PS1dE9 mice improves spatial memory deficits and moderately reduces cortical amyloid load. These data support the notion that targeting A_{2A}Rs is of therapeutic interest for AD.

MATERIALS AND METHODS

Animals

In this study, we used heterozygous male APPswe/PS1dE9 (herein referred to as APP/PS1, C57Bl6/J background; Jankowsky et al., 2001) and littermates controls. All animals were maintained in standard cages under conventional laboratory conditions (12 h/12 h light/dark cycle, 22°C), with *ad libitum* access to food and water. Animals were maintained 5–6 per cage with genotype segregated with enrichment as the form of small cylinder "cocoon," which offer the animal the possibility to fulfill their natural nesting instinct. The animals were used in compliance with European standards for the care and use of laboratory animals and experimental protocols approved by the local Animal Ethical Committee (agreement APAFIS#2264-2015101320441671 from CEEA75, Lille, France).

MSX-3 Treatment

MSX-3 is a water-soluble prodrug of the potent and highly selective A_{2A}R antagonist MSX-2 (Sauer et al., 2000), that crosses the blood-brain barrier (Collins et al., 2010). The drug was administered through drinking water at 0.3 g/L, a dose previously shown to provide benefit in Tau transgenic mice (Laurent et al., 2016). Chronic delivery at this dose achieved, in 10-month-old C57Bl6/J mice, plasma and brain concentrations of MSX-2 of about 13 nM and 50 nM, respectively (Supplementary Figure S1), compatible with A_{2A}R blockade (MSX-2 K_i = ca. 8 nM). Animals randomized according to their body weight, were assigned to the four following experimental groups: WT/H_2O, WT/MSX-3, APP/PS1/H_2O and APP/PS1/MSX-3. The MSX-3 solution was kept in bottles protected from light and changed weekly. Treatment started at 3 months of age, when amyloid pathology begins and before memory impairments in APP/PS1 mice, and continued until 9–10 months of age, when mice exhibit cortical and hippocampal amyloid pathology and memory deficits. MSX-3 consumption was assessed throughout treatment for each experimental cage. In average, mice consumed 6.6 ± 0.6 ml of the MSX-3 solution per day, corresponding to an average daily intake of 2 mg of the antagonist.

Anxiety Assessment Using Elevated Plus Maze

The elevated plus maze was used to investigate anxiety-related behavior. The apparatus consisted of a plus-shaped maze with two closed and two open arms (30 cm long × 6.5 cm wide). Mice were placed at the center of the maze with their face in the direction of a closed arm and were allowed to explore freely for 5 min. Distance moved, velocity and time spent in arms were recorded using the Ethovision XT tracking system (Noldus).

Spatial Memory Assessment Using the Morris Water Maze Task

Spatial memory abilities were evaluated in the standard hidden platform (PF) acquisition and retention version of the Morris Water Maze as previously described (Laurent et al., 2016). A 100-cm circular pool was filled with water, opacified with non-toxic white paint and kept at 21°C. A 10-cm round PF was hidden 1 cm beneath the surface of the water at a fixed position. Four positions around the edge of the tank were arbitrarily designated 1, 2, 3 and 4, thus dividing the tank into four quadrants (clockwise): target (hidden-PF contained), adjacent 1, opposite and adjacent 2. During the learning procedure, each mouse was given four swimming trials per day (15 min inter-trial interval) for five consecutive days. The start position (1, 2, 3, or 4) was pseudo-randomized across trials. A trial consisted of placing the mouse into the water facing the outer edge of the pool in one of the virtual quadrants and allowing it to escape to the hidden PF. A trial terminated when the animal reached the PF where it was allowed to remain for 15 s. If the animal failed to find the target before 120 s, it was manually guided to the PF where it was allowed to stay for 15 s. After completion of a trial, mice were removed from the pool and placed back to their home cages. Distance traveled to locate the hidden escape

PF (path length) and swimming speed (i.e., velocity, as a measure of possible motor defects that could interfere with their ability to perform in this task) were recorded using the Ethovision XT tracking system (Noldus). Seventy-two hours following the acquisition phase, a probe trial was conducted. During this probe trial (60 s), the PF was removed and search pattern of the mice was tracked again. Proportion of time spent in the target quadrant (T) vs. averaged non-target quadrants (O) was determined.

Sacrifice and Brain Tissue Preparation

Sacrifice of animals took place in the afternoon. Mice were deeply anesthetized with pentobarbital sodium (50 mg/kg, i.p.), then transcardially perfused with cold NaCl (0.9%). Brains were removed and one half of the hemisphere were post-fixed in 4% paraformaldehyde fixative in PBS (pH 7.4) for a week at 4°C and transferred to 30% sucrose solution overnight before being frozen. Coronal brains sections (35 μm) were obtained using a Leica cryostat. Free-floating sections were selected according the stereological rules, with the first section taken at random and every ninth sections afterwards and were stored in PBS-azide (0.2%) at 4°C. Cortex and hippocampus of the other hemisphere were dissected using a coronal acrylic slicer (Delta Microscopies) at 4°C and stored at −80°C until use.

Immunohistochemistry and Image Analysis

Antibodies used in this study are listed in **Table 1**. For Aβ immunohistochemistry (IHC), sections were pretreated with 80% formic acid for 3 min and were permeabilized with 0.2% Triton X-100/sodium phosphate buffer. Sections were then blocked with 10% "Mouse On Mouse" Kit serum (Vector Laboratories) for 1 h before incubation with mouse biotinylated anti-Aβ antibody (6E10) at 4°C overnight. After washing in PBS, the sections were incubated with the ABC kit (Vector Laboratories) for 2 h and developed using DAB (Sigma). Images were acquired using Leica ICC50 HD microscope. Quantification of the 6E10 staining intensity was performed using Mercator software (Explora Nova, Mountain View, CA, USA). The number of plaques, the average plaque size and the plaque burden, expressed as percentage of analyzed area, were calculated in the cortex and hippocampus of the APP/PS1 mice. For immunofluorescence studies, coronal brain sections were washed with sodium phosphate buffer and permeabilized with 0.2% Triton X-100/sodium phosphate buffer. Sections where blocked with normal goat serum (1/100; Vector Laboratories) before incubated with an anti-GFAP antibody (**Table 1**) at 4°C overnight. Primary antibody was detected with Alexa Fluor 488 or 633 goat anti-rabbit IgG (1/500, Thermo Fisher). After washes, sections were blocked with donkey serum (1/100; Sigma) and were incubated for 48 h at 4°C with an anti-A_{2A}R antibody followed by an incubation with Alexa Fluor 595 donkey anti-guinea pig IgG (1/500; Jackson) antibody for 2 h at RT. To visualize amyloid plaques, sections were pretreated with 80% formic acid for 3 min, blocked with 10% of Mouse On Mouse Kit serum (Vector Laboratories) for 1 h before incubated in mouse biotinylated anti-Aβ antibody at 4°C overnight. Sections were then incubated with streptavidin Alexa Fluo 488 conjugate (1/1000; Thermo Fisher Scientific). Sections were finally incubated with DAPI (1/5000; Sigma-Aldrich) for 10 min and treated for 10 min in 0.3% Suden Black (Sigma-Aldrich) with 70% ethanol to block autofluorescence. Images were acquired using a Zeiss LSM 710 confocal laser-scanning microscope to define co-localization of A_{2A}R with glial markers and amyloid plaques. 3D reconstruction of 2D confocal z stacks was performed using Imaris software (Bitplane, South Windsor, CT, USA).

Western Blots

For all biochemical experiments, tissue was homogenized in 200 μL Tris buffer (pH 7.4) containing 10% sucrose and protease inhibitors (Complete; Roche Diagnostics GmbH), sonicated, and kept at −80°C until use. Protein amounts were evaluated using

TABLE 1 | Antibodies used in this study.

Name	Epitope	Type	Origin	Provider	Dilution
Anti-A_{2A}R	CTER 33aa	Poly	Guinea Pig	Frontier Institute	1/200
Anti-GFAP	GFAP	Poly	Rabbit	Dako	1/1000
Anti-NeuN	NeuN	Mono	Mouse	Merck Mllipore	1/500 (IHC) 1/1000 (WB)
Anti-Aβ 1-16 (6E10)	Total Aβ (3-8 aa)	Mono	Mouse	Biolegend	1/1000
Anti-APP (C17)	Cter part of APP, CTFs	Poly	Rabbit	Home Made	1/5000
Anti-GluR1	Hulan GluR1 (840–850 aa)	Mono	Rabbit	Merck Mllipore	1/2000
Anti-phospho-GluRl (Ser831)	pSer831	Mono	Rabbit	Merck Mllipore	1/1000
Anti-phospho-GluR1 (Ser845)	pSer845	Mono	Rabbit	Merck Millipore	1/1000
Anti-GluR2	Mouse GluR2 (150–250 aa)	Poly	Rabbit	Abcam	1/5000
Anti-phospho-GluR2 (Ser88O)	pSer88O	Poly	Rabbit	Abcam	1/5000
Anti-NR2B	Mature NR2B (1437–1456 aa)	Poly	Rabbit	Cell Signaling	1/1000
Anti-phospho-NR2B (Tyr1472)	pTyr1472	Poly	Rabbit	Cell Signaling	1/1000
Anti-phospho-NR2B (Tyr1480)	pTyrl480	Poly	Rabbit	Thermo Fisher Scientific	1/1000
Anti-Munc-l8-1 (Muncl8)	Cter (577–594 aa)	Poly	Rabbit	Sigma	1/2000
Anti-PSD95	PSD95	Poly	Rabbit	Cell Signaling	1/1000
Anti-Spinophiline	Spinophiline	Poly	Rabbit	Merck Mllipore	1/1000
GAPDH	Hutnan GAPDH (FL 1–335)	Poly	Rabbit	Santa Cruz Biotechnology	1/1000

Abbreviations: Mono, monoclonal; Poly, polyclonal; IHC, dilution used in Immunohistochemistry; WB, dilution used in Western blotting; GFAP, glial fibrillary acidic protein; NeuN, neuronal nuclear; APP, amyloid precursor protein; GAPDH, glyceraldehyde-3-phosphate.

TABLE 2 | Primer sequences used in this study.

Name	Access number	Primer FW	Primer R	Amplicon size
GFAP	NM_001131020.1	cgcgaacaggaagagcgcca	gtggcgggccatctcctcct	104
Cd68	NM_009853.1	gacctacatcagagcccgagt	cgccatgaatgtccactg	95
TLR2	NM_011905.3	ggggcttcacttctctgctt	agcatcctctgcgatttgacg	110
CCL3	NM_011337.2	tgcccttgctgttcttctct	gtggaatcttccggctgtag	112
CCL5	NM_013653.3	ctcactgcagccgccctctg	ccgagccatatggtgaggcagg	51
Cyclophilin	NM_008907.1	agcatacaggtcctggcatc	ttcaccttcccaaagaccac	126

Abbreviations: FW, Forward; R, Reverse.

the BCA assay (Pierce). Protein amounts were evaluated using the BCA assay (Pierce), subsequently diluted with LDS 2X supplemented with reducing agents (Invitrogen) and then separated on 4%–12% NuPage Novex gels (Invitrogen). Proteins were transferred to nitrocellulose membranes, saturated (5% non-fat dry milk or 5% BSA) in TNT (Tris 15 mM pH 8, NaCl 140 mM, 0.05% Tween) and incubated with primary (see **Table 1**) overnight and then corresponding secondary antibodies (peroxidase labeled horse anti-rabbit 1/5000 or anti-mouse 1/50,000, Vector Laboratories). Immunoreactivity was visualized using chemiluminescence kits (ECL^{TM}, Amersham Bioscience) and a LAS3000 imaging system (Fujifilm). Results were normalized to GAPDH and quantifications were performed using ImageJ software (Scion Software).

mRNA Extraction and Quantitative Real-Time RT-PCR Analysis

Total RNA was extracted from hippocampi and cortex, and purified using the RNeasy Lipid Tissue Mini Kit (Qiagen, France). One microgram of total RNA was reverse-transcribed using the Applied Biosystems High-Capacity cDNA reverse transcription kit. Quantitative real-time RT-PCR analysis was performed on an Applied Biosystems Prism 7900 System using Power SYBR Green PCR Master Mix. The thermal cycler conditions were as follows: hold for 10 min at 95°C, followed by 45 cycles of a two-step PCR consisting of a 95°C step for 15 s followed by a 60°C step for 25 s. Sequences of primers used are given in **Table 2**. Cyclophilin A was used as internal control. Amplifications were carried out in triplicate and the relative expression of target genes was determined by the ΔΔCT method.

ELISA Measurements

Brain levels of human Aβ1-40 and Aβ1-42 were measured using ELISA kits (Invitrogen, Carlsbad, CA, USA; IBL-International, Hamburg, Germany) following manufactured' instructions. Briefly, for hippocampal and cortical samples, 20 μg of protein were diluted in Guanidine/Tris buffer (Guanidine HCl 5 M and Tris 50 mM pH 8), sonicated and incubated for 1 h at 4°C under agitation. Samples were then diluted in a BSAT-DPBS solution (KCl, KH_2PO_4, NaCl, Na_2HPO_4, BSA 5%, Tween-20 0.03% pH 7.4). The homogenates were centrifuged at 12,000 *g* for 15 min at 4°C. Supernatants were collected for the analysis of Aβ1-40 and Aβ1-42 by colorimetric immunoassays. Absorbance was measured by Multiskan Ascent counter (ThermoLab Systems). The normalized amounts of Aβ were expressed as pg/mL.

Evaluation of Microglial Phagocytosis

The effect of acute $A_{2A}R$ blockade on microglial phagocytosis was quantified in an *in situ* live cerebral slices assay similar to what has been described (Krabbe et al., 2013; Savage et al., 2015). APP/PS1 mice were crossbred with Csfr1r-EGFP mice (Sasmono et al., 2003) to readily visualize microglia. Coronal acute cerebral slices with a thickness of 130 μm were prepared from 12 month-old APP/PS1-Csf1r-EGFP mice and Csf1r-EGFP wildtype littermates using a vibratome (Leica VT1200 S). Acute slices were pre-incubated with the indicated concentration of MSX-3 (10–5000 nM) or vehicle for 60 min in artificial cerebrospinal fluid (aCSF) under constant carbogen saturation (three acute cerebral slices per condition). Live acute slices were then incubated with FCS-coated fluorescent microspheres (2 μm diameter, flash red, Bang Laboratories Inc.) at a concentration of 1.1×10^7 microspheres/mL for 60 min at 37°C in HBSS together with the indicated concentration of MSX-3 or vehicle. Slices were washed and fixed in 4% PFA. Aβ dense-core plaques were stained with 0.001% thiazine red (Sigma Aldrich) in PBS. Five corresponding regions of interest (ROIs) were recorded in the isocortex of each cerebral slice using a Nikon eclipse Ti-E confocal microscope (60× objective, 20 μm z stack, 1 μm z slice interval) and the phagocytic index, i.e., quotient between number of fluorescent microspheres internalized by GFP-positive plaque-associated microglia and the total number of plaque-associated microglia per ROI was quantified by an investigator blinded to the treatment condition.

Transcriptomic Analysis (Agilent Microarray)

Total RNA yield and quality were assessed on the Agilent 2100 bioanalyzer (Agilent Technologies, Massy, France). One color whole Mouse (074809_D_F_20150624 slides) 60-mer oligonucleotides 8× 60k microarrays (Agilent Technologies) were used to analyze gene expression. Six biological replicates for each condition were prepared for a total of 48 samples (Cortex or Hippocampus of WT-H_2O/WT-MSX-3/APP-H_2O/APP-MSX-3). cRNA labeling, hybridization and detection were carried out according to supplier's instructions (Agilent Technologies). For each microarray, Cyanine 3-labeled cRNA were synthesized with the low input QuickAmp labeling kit from 50 ng of total RNA. RNA Spike-In were added to all tubes and used as positive controls of labeling and amplification steps. The labeled cRNA were purified and 600 ng of each cRNA were then hybridized and washed following manufacturer's instructions. Microarrays were scanned on an Agilent G2505C scanner and data extracted using Agilent Feature Extraction Software© (FE

version 10.7.3.1). Microarray data are available through the GEO depository from NCBI (accession no. GSE113141).

The statistical analyses were performed with Genespring® software version GX13.0 (Agilent Technologies). Microarrays have been normalized to the 75th percentile. Probes below background under all conditions were removed from the analysis. Differentially expressed genes were identified by a moderated *t*-test with correction of multiple tests by the Benjamini Hochberg (BH) method. We selected significantly deregulated probes with a corrected *p*-value of less than 0.05 and with an expression differential of at least 1.5× (FC1.5). Differentially expressed probes were further analyzed in term of molecular function and biological process using the Ingenuity Pathways Analysis (Qiagen Inc.) software.

Statistics

Results are expressed as means ± SEM. Differences between mean values were determined using the Student's *t*-test, Two Way-analysis of variance (ANOVA) or One Way-ANOVA followed by a *post hoc* Fisher's LSD test using Graphpad Prism Software. *P* values < 0.05 were considered significant.

RESULTS

A_{2A}R Is Overexpressed by Astrocytes in APP/PS1 Transgenic Mice

We first examined A_{2A}R expression levels in APP/PS1 mice using IHC and confocal microscopy. Similar to what has been previously described in AD patients and in different APP models (Orr et al., 2015, 2018; Lee et al., 2018), we observed that APP/PS1 mice exhibit a progressive hippocampal upsurge of A_{2A}R immunoreactivity (**Figures 1G–I**), as compared to WT littermates (**Figures 1A–C**). Importantly, A_{2A}R immunopositive signal observed in the striatum and hippocampus of APP/PS1 mice was found abolished in APP/PS1 animals with genetically deleted A_{2A}R (Supplementary Figure S2) supporting the specificity of the A_{2A}R immunostaining provided in **Figure 1**. In APP/PS1 mice, increased A_{2A}R expression was observed in astrocytes in the hippocampus, starting at 3 months of age, and the cortex, starting at 9 months of age (**Figures 1D–F,J–N**). Astrocytic A_{2A}R overexpression was not found exclusively in the vicinity of 6E10-positive plaques but also in reactive astrocytes located at larger distance to plaques (**Figure 1O**). These data therefore indicate that the development of amyloid pathology elicits astrocytic A_{2A}R upsurge in APP/PS1 mice.

A_{2A}R Pharmacological Blockade Prevents Spatial Memory Impairments in APP/PS1 Transgenic Mice

In the present experimental paradigm, APP/PS1 mice and littermate controls were treated with MSX-3 in drinking water at 0.3 g/L, using a treatment paradigm we previously described to promote a significant benefit in a model of AD-like Tau pathology (Laurent et al., 2016). Mice were treated from 3 to 9-10 months of age, i.e along the development of amyloid pathology and cognitive deficits in this transgenic strain. At completion of the treatment, we evaluated the impact of the chronic A_{2A}R blockade on anxiety and spatial learning and memory using, respectively, the Elevated Plus Maze and the Morris Water Maze. We analyzed the impact of MSX-3 upon anxiety using the Elevated Plus Maze task. As shown in Supplementary Figure S3, we did not find any significant impact of MSX-3 upon velocity, distance moved and percentage of time spent in both closed and open arms ($p > 0.05$), suggesting that the treatment did not significantly impact anxiety behavior in both WT and APP/PS1 mice. Regarding Morris Water Maze, during the training phase, all groups showed a decrease in path length across trials ($p < 0.05$, two-way ANOVA). APP/PS1 animals demonstrated a slight learning deficit at day 2 ($p = 0.0002$, Two-Way ANOVA followed by Fisher LSD *post hoc* test) with no impact of the treatment ($p > 0.05$; **Figure 2A**). Neither APP/PS1 genotype nor the MSX-3 treatment influenced mouse velocity ($p > 0.05$; **Figure 2B**). Seventy-two hours following acquisition, a probe trial was performed to evaluate spatial memory. Regardless of treatment (H_2O or MSX-3), WT littermates exhibited a significant preference for the target quadrant (**Figure 2C**; WT H_2O: $p = 0.0003$; WT MSX3: $p = 0.039$ vs. O quadrants using One-way ANOVA followed by LSD Fisher *post hoc* test). As expected at this age, APP/PS1 H_2O mice showed spatial memory deficits, evidenced by the absence of preference for the target vs. the non-target (O) quadrants (**Figure 2C**; $p > 0.05$ vs. O quadrants using One-way ANOVA followed by LSD Fisher *post hoc* test). ANOVA analysis also indicated that the percentage of time spent in target quadrant for APP/PS1 H_2O mice was significantly reduced as compared to WT H_2O animals ($p = 0.037$). In sharp contrast, the blockade of A_{2A}R by MSX-3 significantly alleviated spatial memory impairment in APP/PS1 mice, as demonstrated by a significant preference of MSX-3-treated APP/PS1 mice for the target quadrant (**Figure 2C**, $p = 0.0002$ vs. O quadrants using One-way ANOVA followed by LSD Fisher *post hoc* test). ANOVA analysis also indicated that APP/PS1 mice treated with MSX-3 spent a higher percentage of time in the target quadrant as compared to water-treated APP/PS1 animals ($p = 0.027$; **Figure 2C**). Altogether, these data indicated that early onset chronic A_{2A}R blockade prevents the development of spatial memory alterations in APP/PS1 mice.

Effect of Chronic A_{2A}R Blockade on Hippocampal Synaptic Markers in APP/PS1 Transgenic Mice

To evaluate whether the beneficial effects of A_{2A}R blockade on spatial memory in the APP/PS1 mice could be ascribed to changes in the expression of hippocampal synaptic markers, we performed western blot evaluation of neuronal, pre/post-synaptic proteins as well as glutamatergic receptors. While MSX-3 did not modulate the expression of the studied neuronal and postsynaptic markers (NeuN, spinophiline and PSD95; $p > 0.05$, vs. APP/PS1 H_2O mice using Student's *t*-test; Supplementary Figure S4A) nor the expression and phosphorylation of AMPA and NMDA receptor subunits ($p > 0.05$, vs. APP/PS1 H_2O mice using Student's *t*-test;

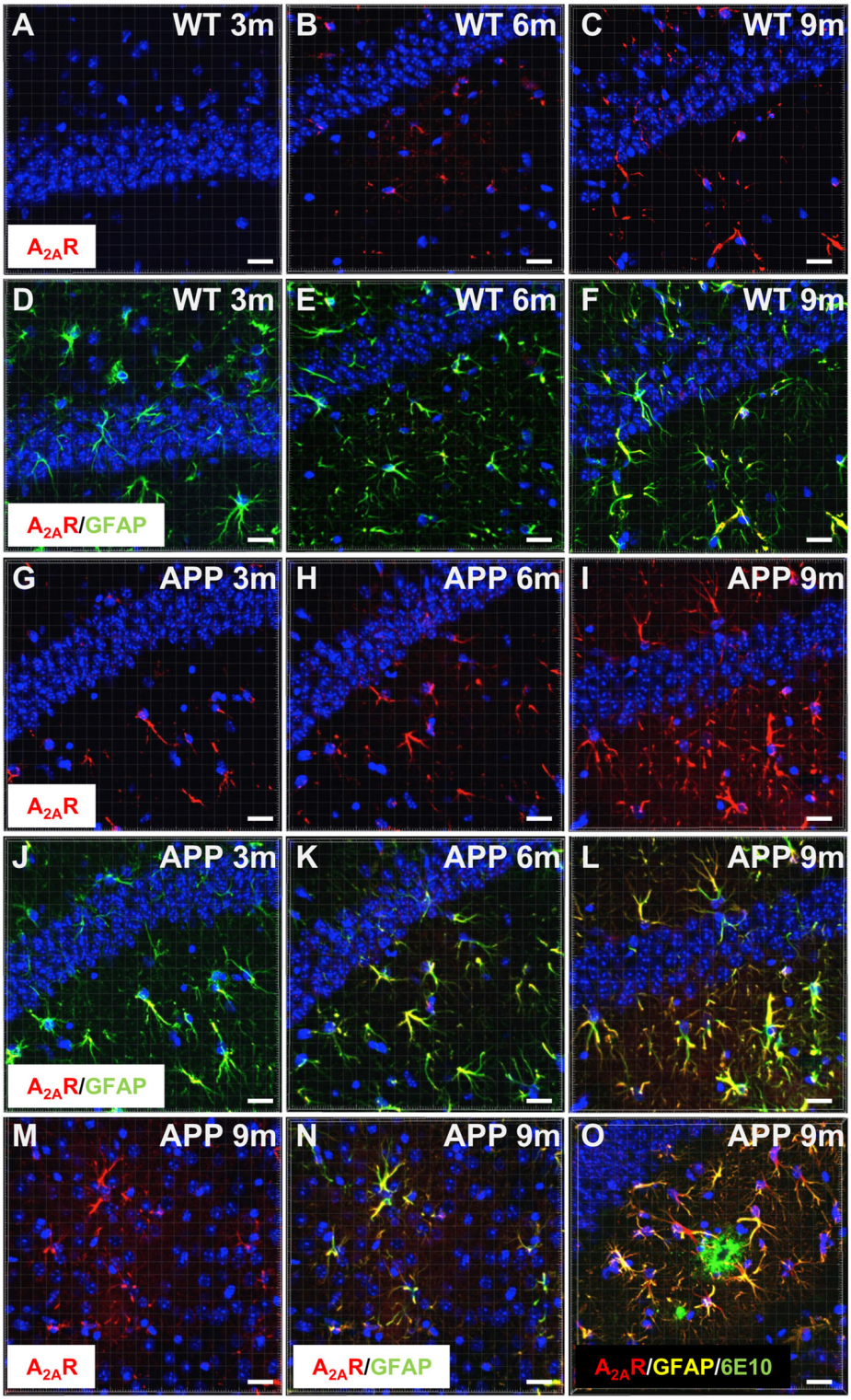

FIGURE 1 | Astrocytic upsurge of A_{2A}Rs in APP/PS1 mice. Representative photomicrographs of hippocampal immunostaining for the A_{2A} receptor (A_{2A}R; red) **(A–C,G–I)** and merged with the astrocyte marker GFAP (green) **(D–F,J–L)** from WT mice **(A–F)** and the APP/PS1 mice **(G–L)**, at different ages: 3 months **(A,D,G,J)**, 6 months **(B,E,H,K)**, and 9–10 months **(C,F,I,L)**. Representative photomicrographs of A_{2A}R expression (red) **(M)** and the merged with GFAP marker (green; **N**) in the cortex of 9-month-old APP/PS1 mice. Representative photomicrograph of A_{2A}R expression (red) GFAP (yellow) and 6E10-positive amyloid plaque marker (green) in the hippocampus of 9 month-old APP/PS1 mice **(O)**. Cell nuclei were labeled with DAPI (blue). Scale bar = 20 μm.

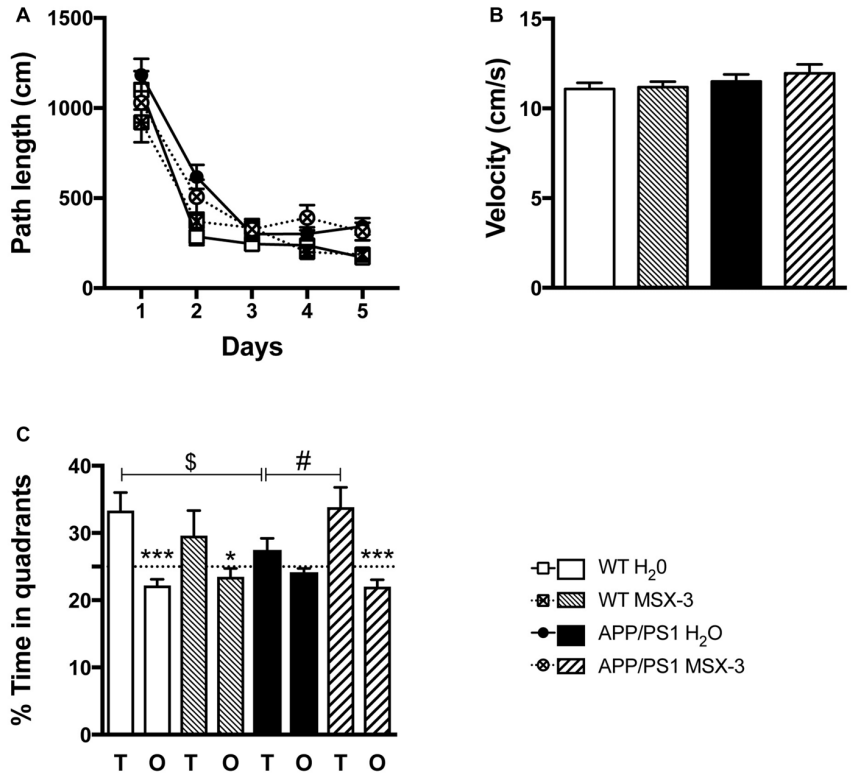

FIGURE 2 | A_{2A}R blockade prevents spatial memory impairments in APP/PS1 transgenic mice. Effect of MSX-3 treatment on spatial learning and memory using the Morris water-maze task. **(A)** Learning, as indicated by the equivalent path length needed to find the hidden platform (PF). At day 2, APP/PS1 mice exhibited a slight but significant higher path length as compared to WT animals (***$p < 0.001$ vs. WT H_2O using One-way analysis of variance (ANOVA) followed by LSD Fisher *post hoc* test). **(B)** All genotypes exhibited a comparable velocity in the maze, suggesting no motor deficits. **(C)** Spatial memory was assessed 72 h after the last day of learning. Results represent the percentage of time spent in the target (T) vs. non-target (O) quadrants. WT mice (both treated with water or MSX-3) spent significantly more time in the T quadrant, indicative of a preserved spatial memory. While APP/PS1 mice exhibited spatial memory deficits as underlined by their lack of preference for the T quadrant, APP/PS1-MSX-3 treated mice behaved as WT mice, suggesting a rescue of memory impairment. *$p < 0.05$ ***$p < 0.001$ T vs. O; $^{\$}p < 0.05$ WT vs. APP/PS1; $^{\#}p < 0.05$ APP/PS1-H_2O vs. APP/PS1 MSX-3 using One-way ANOVA followed by LSD Fisher *post hoc* test; N = 12–16 per group; Results are expressed as mean ± SEM.

Supplementary Figure S4B), we found that MSX-3 treatment significantly increased the hippocampal expression of the presynaptic marker Munc-18 in the APP/PS1 mice treated with MSX-3 ($p = 0.037$ vs. APP/PS1 H_2O using Student's t-test; Supplementary Figure S4A). Notably, none of the markers studied was found modified in the cortex of APP/PS1 MSX-3 animals (not shown).

Effect of Chronic A_{2A}R Blockade on Cortical and Hippocampal Transcriptome of APP/PS1 Transgenic Mice

In order to provide potential molecular insights on how chronic A_{2A}R blockade by MSX-3 improves memory of APP/PS1 mice, we evaluated gene expression changes in the cortex and hippocampus in the different groups of mice using Agilent technology. First, we determined gene expression changes between APP/PS1 H_2O vs. WT H_2O. In the cortex, 519 probes were significantly changed (BH adjusted p-values < 0.05) with a major effect (FC > 10) for Clec7a, Itgax, Cst, Ccl3, Ccl4 and Cxcl10 (Supplementary Table S1). In the hippocampus, 125 probes were significantly altered (BH adjusted p-values < 0.05; Supplementary Table S3) and we found the same highly modified genes, indicating highly concordant results between structures. The study of molecular functions by Ingenuity Pathway Analysis highlighted a significant number of deregulated genes in pathways related to immune functions (Supplementary Tables S2, S4), in accordance with the known link between amyloid load and the development of parenchymal neuroinflammation (Heneka et al., 2015 for review), which is known to favor cognitive deficits (Marciniak et al., 2015; Laurent et al., 2018 and references herein). Using quantitative PCR analysis, we validated several neuroinflammatory markers (GFAP, CD68, TLR2, CCL5 and CCL3) in both the cerebral cortex and the hippocampus of APP/PS1 H_2O mice as compared to WT H_2O animals ($p < 0.001$ vs. WT using One Way ANOVA followed by LSD Fisher *post hoc* text; Supplementary Figures S5A,B). We were then interested in comparing gene expression changes in the mouse groups treated with MSX-3. Notably, A_{2A}Rs were shown to modulate the function and

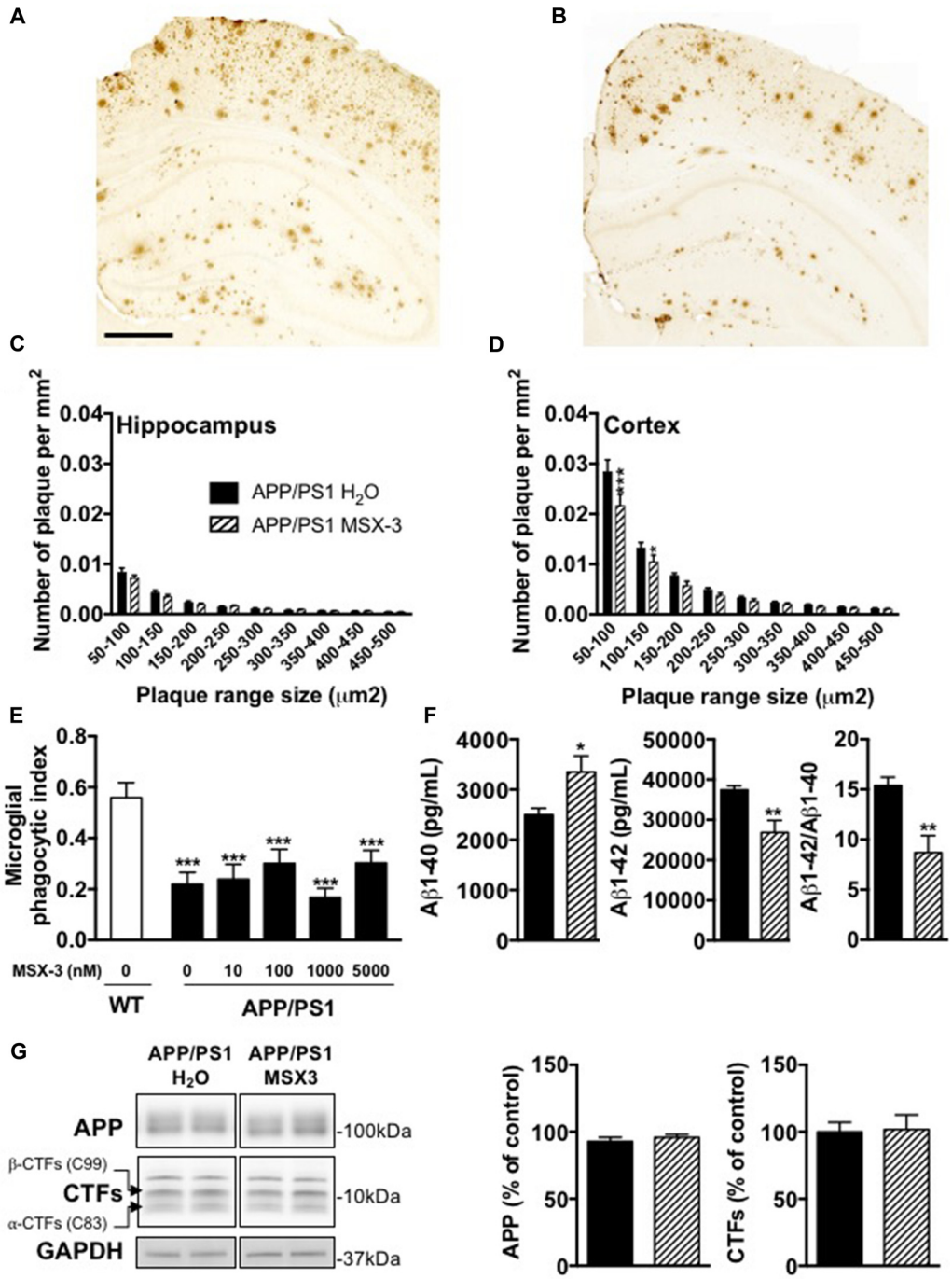

FIGURE 3 | Impact of MSX-3 treatment on amyloid load, Aβ levels and phagocytic capacity of microglia in APP/PS1 mice. Representative images of 6E10 staining in the brains of 10 months old APP/PS1 treated with water **(A)** or MSX-3 **(B)**. Scale bar = 500 μm. Distribution of amyloid plaques size were examined in the hippocampus **(C)** and cortex **(D)** of APP/PS1 mice. We found that the treatment with MSX-3 significantly reduced, in the cortex **(D)** but not in the hippocampus **(C)**, the density of plaques of lower size (between 50–150 μm^2) as compared with APP/PS1 H_2O animals (50–150 μm^2, $p < 0.001$; 100–150 μm^2, $p < 0.05$ vs. APP/PS1 H_2O using Two-Way ANOVA followed by LSD Fisher *post hoc* test; $N = 7–9$/group). **(E)** Effect of acute MSX-3 treatment on microglial phagocytic index determined in an *in situ* live cerebral slice assay of 12-month-old APP/PS1-Csf1r-EGFP mice and Csf1r-EGFP wildtype littermates after 60 min pre-incubation with the indicated concentration of MSX-3. Datasets were tested for significance with the One-way ANOVA and represent data from three independent experiments. $^{***}p < 0.001$ vs. WT **(F)** As measured by ELISA, MSX-3 treatment decreased Aβ1–42 levels in the cortex of APP/PS1 mice while Aβ1–40 levels was found increased. Overall, the Aβ1–42/Aβ1–40 ratio was found significantly reduced by the A_{2A} antagonist treatment ($^{*}p < 0.05$, $^{**}p < 0.01$ vs. APP/PS1 H_2O using Student's *t*-test; $N = 7–11$/group). **(G)** Western blot analysis performed in cortex of water and MSX-3 treated APP/PS1dE9 mice did not revealed any change in APP and Carboxyterminal fragments (CTFs) expression ($N = 6$/group). Results are expressed as mean ± SEM.

activation of brain innate immune cells (i.e., microglia and astrocytes; Cunha, 2016 for review) and blockade of these receptors may resolve brain neuroinflammation (Rebola et al., 2011; Laurent et al., 2016). Surprisingly, no significant effect of MSX-3, particularly for markers associated to immune functions (see also Supplementary Figures S5A,B), was observed in the cortex or hippocampus of WT or APP/PS1. Altogether, these data suggest that memory improvement in APP/PS1 treated with MSX-3 is associated with a weak transcriptional effect and a notable absence of impact on neuroinflammation.

Effect of Chronic A_{2A}R Blockade on Amyloid Burden in APP/PS1 Transgenic Mice

Age-dependent spatial memory impairment in APP/PS1 has been shown to correlate with increased brain amyloid burden (Savonenko et al., 2005; Garcia-Alloza et al., 2006; Zhang et al., 2011). Previous studies demonstrated that long-term caffeine treatment mitigates memory defects in APPsw mice, while reducing brain Aβ production (Arendash et al., 2006, 2009). While this is still controversial (Lu et al., 2016), other data indicated that A_{2A}R might impact on the production of Aβ *in vitro* (Nagpure and Bian, 2014). Altogether, these data supported a possible involvement of A_{2A}Rs in Aβ production and/or accumulation and, therefore upon memory. Using 6E10 IHC, we first performed the analysis of cortical and hippocampal Aβ plaque load in APP/PS1 mice treated with water or MSX-3 (**Figures 3A,B**). We found that the treatment with MSX-3 significantly reduced, in the cortex (**Figure 3D**) but not in the hippocampus (**Figure 3C**), the density of plaques of lower size (between 50–150 μm^2) as compared with APP/PS1 H_2O animals (50–150 μm^2, $p < 0.001$; 100–150 μm^2, $p < 0.05$ vs. APP/PS1 H_2O using Two-Way ANOVA followed by LSD Fisher *post hoc* test). Microglia surrounding amyloid plaques have an impaired phagocytic capacity (Krabbe et al., 2013; Savage et al., 2015). Since adenosine signaling and A_{2A}R activation has been shown to impair microglial phagocytosis in cell culture and *in situ* (Orr et al., 2009; Bulavina et al., 2013), we tested the possibility that MSX-3 could enhance the phagocytic capacity of microglia, thereby potentially explaining the moderate plaque reduction seen in the cortex of chronically MSX-3-treated APP/PS1 animals. To test whether A_{2A}R blockade has an immediate effect on microglial phagocytosis as has been shown for other microglial functions (Gyoneva et al., 2014, 2016), we used an *in situ* live acute slice assay and evaluated whether acute A_{2A}R blockade with MSX-3 in live cerebral slices could enhance the phagocytic capacity of microglia surrounding amyloid plaques. However, although our results confirmed that 12-month-old APP/PS1 mice exhibit a reduced phagocytic activity of microglia as compared with littermate controls, acute treatment of acute slices from APP/PS1 mice with MSX-3 of up to 5 μM failed to normalize phagocytosis of plaque-associated microglia (**Figure 3E**), suggesting that acute A_{2A}R blockade does not significantly affect microglial phagocytosis.

Next, we measured the concentration of Aβ1-42 and Aβ1-40 in the cortex and the hippocampus. The cortex of MSX-3-treated APP/PS1 mice exhibited a significant decrease of Aβ1-42 levels ($p = 0.0011$ vs. APP/PS1 H_2O using Student's *t*-test; **Figure 3F**) while Aβ1-40 levels were increased ($p = 0.012$ vs. APP/PS1 H_2O using Student's *t*-test; **Figure 3F**). Overall, in the cortex, the Aβ42/Aβ40 ratio was found to be significantly reduced in APP/PS1 MSX-3 mice as compared to APP/PS1 H_2O animals ($p = 0.0015$ vs. APP/PS1 H_2O using Student's *t*-test; **Figure 3F**). These cortical changes were not accompanied by a modification of APP expression or C-terminal fragments (CTF) of APP (**Figure 3G**). Also, none of the parameters studied was found changed in the hippocampus of APP/PS1 MSX-3 animals ($p > 0.05$, Student's *t*-test; not shown). Altogether, these data indicated that early and chronic A_{2A}R blockade reduces the development of cortical amyloid burden in APP/PS1 mice.

DISCUSSION

The present study demonstrates that an early, chronic and long-term treatment with a specific A_{2A}R antagonist, starting from an asymptomatic stage, prevents spatial memory impairments and reduces, at least in part, the development of amyloidogenesis in APPswe/PS1dE9 mice. These data extend previous findings showing that short-term treatment with different antagonists (KW6002 p.o. and SCH58261 i.p.; Viana da Silva et al., 2016; Orr et al., 2018; Silva et al., 2018) improves memory of three different models of amyloidogenesis (APP/PS1 and hAPP-J20). Here, we also provide the first experimental evidence that, *in vivo*, early blockade of A_{2A}Rs can reduce brain amyloid levels. Taken together with previous studies demonstrating the ability of A_{2A}R blockade to reduce Tau hyperphosphorylation and associated cognitive decline (Laurent et al., 2016; Zhao et al., 2017), these data support that A_{2A}R signaling is a target of interest in AD.

We found a progressive age-dependent astrocytic A_{2A}R upsurge in the hippocampus of APP/PS1dE9 mice, in accordance with recent studies demonstrating similar receptor dysregulation in several mouse models of cerebral amyloidosis (hAPP-J20, APP KI; Orr et al., 2015, 2018; Lee et al., 2018). A_{2A}R dysregulation likely contributes to memory deficits since conditional astrocytic-specific A_{2A}R deletion (Orr et al., 2015) or pharmacological blockade (Orr et al., 2018; the present data) of the receptors improve memory performance in APP mice. The idea that astrocytic upregulation of A_{2A}R might be detrimental for memory in AD models is in line with its physiological ability to control both glutamate and GABA uptake by these glial cells (Nishizaki et al., 2002; Matos et al., 2012; Cristóvão-Ferreira et al., 2013). In support of this, we recently demonstrated that A_{2A}R deletion improves memory while normalizing glutamate/GABA balance in the hippocampus of Tau transgenic mice (Laurent et al., 2016). Interestingly, recent data demonstrated that specific deletion of astrocytic A_{2A}Rs leads to neuronal adaptative changes in glutamatergic synapses, characterized by increased evoked release of glutamate from nerve terminals or enhanced density of NR2B (Matos et al., 2015). Further, it remains also possible that modulation of astrocytic A_{2A}Rs impacts the function of

synaptic A_{2A}Rs. Indeed, deletion of A_{2A}R in astrocytes has been shown to enhance the ability of A_{2A}R agonist CGS2160 to promote glutamate release by synaptosomes (Matos et al., 2015). Therefore, astrocytic A_{2A}R upsurge is likely prone to favor synaptic dysfunctions leading to memory deficits in APP/PS1 mice. Further, we cannot rule out that the benefit afforded by the pharmacological A_{2A}R blockade in APP/PS1 mice also result from the specific blockade of A_{2A}R on other receptor subpopulations, notably at the neuronal level. Indeed, neuronal upsurge of A_{2A}R have been observed in the brain of AD patients (Temido-Ferreira et al., 2018) and recent work demonstrated that APP/PS1 mice exhibit a significant increase of A_{2A}R binding on synaptic hippocampal membranes (Viana da Silva et al., 2016; Silva et al., 2018). It is thus highly conceivable that APP/PS1 mice exhibit both astrocytic and synaptic A_{2A}R upsurge, the latter being probably difficult to capture using classical immunohistofluorescence. In this regard, neuronal/synaptic modulation of A_{2A}Rs could also play an instrumental role in synaptic and memory deficits of APP mice. Indeed, mimicking neuronal A_{2A}R upsurge using conditional transgenic models or optogenetically enhancing intracellular signaling of the receptor was sufficient to promote plasticity and memory deficits (Giménez-Llort et al., 2007; Li et al., 2015; Batalha et al., 2016). Thus, it is likely that the pharmacological blockade of A_{2A}Rs also acts at the neuronal level to normalize memory deficits. It is also important to emphasize that the link between synaptic A_{2A}R upregulation and memory deficits goes far beyond the AD context, as demonstrated by the laboratories of Rodrigo Cunha and Luisa Lopes. For instance, synaptic A_{2A}R have been found dysregulated in models of aging, stress or depression with behavioral manifestations normalized by A_{2A}R receptor antagonists (Lopes et al., 1999; Rebola et al., 2003; Batalha et al., 2013; Kaster et al., 2015; Machado et al., 2017). Interestingly, in regard to presumable neuronal-based mechanisms, we observed, among the synaptic markers studied, an enhanced level of Munc-18 protein as seen by Western blot. Munc-18 is a neuronal (presynaptic) protein required for synaptic vesicles exocytosis (Carr and Rizo, 2010) and is considered as an important regulator of synaptic transmission and presynaptic strength (Toonen and Verhage, 2007; Genc et al., 2014), which is a crucial process in neuronal information processing and memory formation (Abbott and Regehr, 2004). Thus, enhancement of hippocampal Munc18 expression could also therefore contribute to memory improvement promoted by MSX-3. Besides memory impairments, it is important to mention that AD is also associated with neuropsychiatric symptoms. Recently, a study emphasized that long-term oral treatment with caffeine, a non-selective antagonist of A_{2A}Rs, exacerbate some behavioral symptoms in the triple Tg AD model (Baeta-Corral et al., 2018). While we only addressed the impact of MSX-3 on anxiety in our study behavior, which appears not affected by the antagonist, it will be important, in the future and from a therapeutic perspective, to evaluate more closely the impact of long-term A_{2A}R blockade on AD-related behavioral symptoms.

Our microarray data indicate that both cortex and hippocampus of 9–10-month-old APP/PS1 mice exhibit gene deregulation as compared to littermate controls. As expected, the number of deregulated genes was higher in the cortex, which harbors a more advanced pathology compared to the hippocampus in this mouse model (Kim et al., 2012). Several pathways were strongly dysregulated by the development of amyloid pathology (Suh and Checler, 2002), among them processes related to immune functions and neuroinflammation, which we confirmed by qPCR analysis. Interestingly and surprisingly, none of these pathways were impacted by MSX-3 treatment. Furthermore, chronic MSX-3 treatment of WT mice did not have a significant impact on the transcriptome either. These data indicate that, overall, chronic A_{2A}R inhibition is associated with very weak transcriptional effects. Actually, to the best of our knowledge, only one study reported an evaluation of transcriptomic changes following A_{2A}R blockade. This study reported that constitutive deletion of A_{2A}R in the striatum of knock-out mice leads to a significant deregulation of 152 genes compared to WT littermates (Yu et al., 2009). These data are difficult to compare to our experiments since the striatum is highly enriched in A_{2A}R as compared to cortex and hippocampus, with a major post-synaptic localization (Blum et al., 2003a,b; Cunha, 2016). The observation that MSX-3 improves memory of APP/PS1 mice is however in accordance with its acknowledged ability to fine tune synaptic plasticity in the hippocampus (Cunha, 2016). Recent data notably emphasized that A_{2A}R blockade can lead within minutes to an improvement of plasticity deficits in APP/PS1 mice (Viana da Silva et al., 2016).

However, improved memory in APP/SP1 MSX-3 mice in our data was found to be associated with reduced amyloid load. In APP/PS1dE9 mice, amyloid burden, and particularly hippocampal and cortical Aβ42 levels, strongly correlate with spatial memory deficits (Puoliväli et al., 2002; Garcia-Alloza et al., 2006; Sipos et al., 2007; Zhang et al., 2011). Our results demonstrate that MSX-3 treatment promotes a moderate but significant reduction of amyloid plaques in the cortex of APP/PS1 mice. Importantly, a significant reduction of the Aβ1-42/Aβ1-40 ratio was also observed in the cortex of APP/PS1 mice following A_{2A}R blockade. To our knowledge, this is the first report demonstrating an effect of an A_{2A}R ligand on amyloid pathology *in vivo*, in agreement with previous studies showing that chronic caffeine treatment reduces brain soluble Aβ in APPsw mice (Arendash et al., 2006, 2009). The decrease of amyloid burden following A_{2A}R blockade found in the cortex of APP/PS1 mice, a brain region involved in spatial navigation, could therefore explain, at least in part, the beneficial effect of MSX-3 on spatial memory. Reasons explaining a specific effect of MSX-3 on cortical amyloid pathology vs. hippocampus remain unclear. Similarly, the mechanisms underlying the changes of Aβ1-42/Aβ1-40 ratio and 6E10 immunoreactivity warrant further evaluations. However, the reduction of the Aβ1-42/Aβ1-40 is consistent with the reduction of amyloid burden, especially of small amyloid plaques. In fact, *in vitro* data indicated that Aβ42 facilitates amyloid nucleation while Aβ40 allows for Aβ elongation (Snyder et al., 1994). In the present

work, small plaques, reflecting amyloid nucleation, are decreased presumably due to the reduced amount of Aβ42 peptides. It cannot also be excluded that MSX-2 might bind to Aβ and act as a direct amyloid aggregation inhibitor, which warrants further exploration in the future. Interestingly, caffeine was shown, *in vivo* and *in vitro* to reduce both Aβ1-42 and Aβ1-40 levels (Arendash et al., 2006). This contrast with our data which indicate that MSX-3 modulates Aβ1-42/Aβ1-40 ratio, reducing Aβ1-42 and enhancing Aβ1-40 levels. Aβ length is under the control of the carboxypeptidase activity of the gamma-secretase which cleaves the Aβ peptide from its carboxy-terminal region. Thus, lack of PS1 exon 9 and exon 10 generates longer Aβ peptides (Le Guennec et al., 2017). Although speculative, MSX3 could promote the carboxypeptidase activity of the gamma-secretase and thus modify the ratio of Aβ towards the production of shorter species of Aβ peptides. In line with this hypothesis, A_{2A}R and gamma-secretase have been co-localized to endosomes and A_{2A}Rs have been suggested to modulate the gamma-secretase activity (Lu et al., 2016). Although controversial, our results also support a regulatory activity of A_{2A}R towards the gamma-secretase in APP/PS1 mouse. However, the underlying mechanism remains to be elucidated.

In conclusion, we have shown for the first time that a chronic and long-lasting treatment with an A_{2A}R antagonist reduces amyloid pathology and improves memory in a model of AD. Considering previous converging studies in different models of AD (Orr et al., 2015, 2018; Laurent et al., 2016; Viana da Silva et al., 2016; Silva et al., 2018), the present findings further highlight A_{2A}R as a promising therapeutic target in AD.

AUTHOR CONTRIBUTIONS

EF, JC, KZ, EM, YB, MS, LC, KC, SS, SE and RC performed experiments, analyzed data and corrected the manuscript. MF, YC, MH, NS, CM, AH, LB, LL and DB supervised the work, analyzed data and wrote the manuscript.

FUNDING

This work was supported by a cross-border grant from LECMA/Alzheimer Forschung Initiative/Vaincre Alzheimer (to DB and CM). We hereby thank Frédéric Leprêtre for submitting transcriptomics data to GEO. EF and KC are supported by Université de Lille, LC was supported by Italian Society of Pharmacology and LabEx DISTALZ.

ACKNOWLEDGMENTS

We thank the Bio Imaging Center Lille Nord de France (Campus Hospito-universitaire) as well as A. Bongiovanni and M. Tardivel for access microscopes and imagery analysis platform. We thank the animal core facility (animal facilities of Université de Lille) of Plateformes en Biologie Santé de Lille as well as M. Besegher-Dumoulin, C. Declerck, J. Devassine, Y. Lepage, C. Meunier, C. Degraeve and D. Taillieu for transgenic mouse production and care. Our laboratory is also supported by the France Alzheimer, FHU VasCog research network (Lille, France), and programs d'investissements d'avenir LabEx (excellence laboratory) Development of Innovative Strategies for a Transdisciplinary approach to ALZheimer's disease (DISTALZ), ANR (ADORATAU, SPREADTAU, GRAND), Fondation pour la Recherche Médicale, Fondation Plan Alzheimer, Inserm, CNRS, Université de Lille, Lille Métropole Communauté Urbaine, Région Hauts-de-France (COGNADORA), DN2M. AH is member of the DFG-funded Cluster of Excellence ImmunoSensation (EXC 1023).

SUPPLEMENTARY MATERIAL

The Supplementary Material for this article can be found online at: https://www.frontiersin.org/articles/10.3389/fnmol.2018.00235/full#supplementary-material

REFERENCES

Abbott, L. F., and Regehr, W. G. (2004). Synaptic computation. *Nature* 431, 796–803. doi: 10.1038/nature03010

Arendash, G. W., Mori, T., Cao, C., Mamcarz, M., Runfeldt, M., Dickson, A., et al. (2009). Caffeine reverses cognitive impairment and decreases brain amyloid-β levels in aged Alzheimer's disease mice. *J. Alzheimers Dis.* 17, 661–680. doi: 10.3233/JAD-2009-1087

Arendash, G. W., Schleif, W., Rezai-Zadeh, K., Jackson, E. K., Zacharia, L. C., Cracchiolo, J. R., et al. (2006). Caffeine protects Alzheimer's mice against cognitive impairment and reduces brain-amyloid production. *Neuroscience* 142, 941–952. doi: 10.1016/j.neuroscience.2006.07.021

Baeta-Corral, R., Johansson, B., and Giménez-Llort, L. (2018). Long-term treatment with low-dose caffeine worsens BPSD-like profile in 3xTg-AD mice model of Alzheimer's disease and affects mice with normal aging. *Front. Pharmacol.* 9:79. doi: 10.3389/fphar.2018.00079

Batalha, V. L., Ferreira, D. G., Coelho, J. E., Valadas, J. S., Gomes, R., Temido-Ferreira, M., et al. (2016). The caffeine-binding adenosine A_{2A} receptor induces age-like HPA-axis dysfunction by targeting glucocorticoid receptor function. *Sci. Rep.* 6:31493. doi: 10.1038/srep31493

Batalha, V. L., Pego, J. M., Fontinha, B. M., Costenla, A. R., Valadas, J. S., Baqi, Y., et al. (2013). Adenosine A_{2A} receptor blockade reverts hippocampal stress-induced deficits and restores corticosterone circadian oscillation. *Mol. Psychiatry* 18, 320–331. doi: 10.1038/mp.2012.8

Blum, D., Galas, M.-C., Pintor, A., Brouillet, E., Ledent, C., Muller, C. E., et al. (2003a). A dual role of adenosine A_{2A} receptors in 3-nitropropionic acid-induced striatal lesions: implications for the neuroprotective potential of A_{2A} antagonists. *J. Neurosci.* 23, 5361–5369. doi: 10.1523/JNEUROSCI.23-12-05361.2003

Blum, D., Hourez, R., Galas, M.-C., Popoli, P., and Schiffmann, S. N. (2003b). Adenosine receptors and Huntington's disease: implications for pathogenesis and therapeutics. *Lancet Neurol.* 2, 366–374. doi: 10.1016/s1474-4422(03)00411-3

Bulavina, L., Szulzewsky, F., Rocha, A., Krabbe, G., Robson, S. C., Matyash, V., et al. (2013). NTPDase1 activity attenuates microglial phagocytosis. *Purinergic Signal.* 9, 199–205. doi: 10.1007/s11302-012-9339-y

Canas, P. M., Porciuncula, L. O., Cunha, G. M. A., Silva, C. G., Machado, N. J., Oliveira, J. M. A., et al. (2009). Adenosine A_{2A} receptor blockade prevents synaptotoxicity and memory dysfunction caused by β-amyloid peptides via p38 mitogen-activated protein kinase pathway. *J. Neurosci.* 29, 14741–14751. doi: 10.1523/JNEUROSCI.3728-09.2009

Cao, C., Cirrito, J. R., Lin, X., Wang, L., Verges, D. K., Dickson, A., et al. (2009). Caffeine suppresses amyloid-β levels in plasma and brain of Alzheimer's disease transgenic mice. *J. Alzheimers Dis.* 17, 681–697. doi: 10.3233/JAD-2009-1071

Carr, C. M., and Rizo, J. (2010). At the junction of SNARE and SM protein function. *Curr. Opin. Cell Biol.* 22, 519–527. doi: 10.1016/j.ceb.2010.04.006

Collins, L. E., Galtieri, D. J., Brennum, L. T., Sager, T. N., Hockemeyer, J., Müller, C. E., et al. (2010). Oral tremor induced by the muscarinic agonist pilocarpine is suppressed by the adenosine A_{2A} antagonists MSX-3 and SCH58261, but not the adenosine A_1 antagonist DPCPX. *Pharmacol. Biochem. Behav.* 94, 561–569. doi: 10.1016/j.pbb.2009.11.011

Cristóvão-Ferreira, S., Navarro, G., Brugarolas, M., Pérez-Capote, K., Vaz, S. H., Fattorini, G., et al. (2013). A1R-A_{2A} R heteromers coupled to Gsand Gi/0proteins modulate GABA transport into astrocytes. *Purinergic Signal.* 9, 433–449. doi: 10.1007/s11302-013-9364-5

Cunha, R. A. (2016). How does adenosine control neuronal dysfunction and neurodegeneration? *J. Neurochem.* 139, 1019–1055. doi: 10.1111/jnc.13724

Cuyvers, E., and Sleegers, K. (2016). Genetic variations underlying Alzheimer's disease: evidence from genome-wide association studies and beyond. *Lancet Neurol.* 15, 857–868. doi: 10.1016/S1474-4422(16)00127-7

Dall'lgna, O. P., Fett, P., Gomes, M. W., Souza, D. O., Cunha, R. A., and Lara, D. R. (2007). Caffeine and adenosine A_{2A} receptor antagonists prevent β-amyloid (25–35)-induced cognitive deficits in mice. *Exp. Neurol.* 203, 241–245. doi: 10.1016/j.expneurol.2006.08.008

Dall'lgna, O. P., Porciúncula, L. O., Souza, D. O., Cunha, R. A., and Lara, D. R. (2003). Neuroprotection by caffeine and adenosine A_{2A} receptor blockade of β -amyloid neurotoxicity. *Br. J. Pharmacol.* 138, 1207–1209. doi: 10.1038/sj.bjp.0705185

Duyckaerts, C., Braak, H., Brion, J., Buée, L., Del Tredici, K., Goedert, M., et al. (2015). PART is part of Alzheimer disease. *Acta Neuropathol.* 129, 749–756. doi: 10.1007/s00401-015-1390-7

Flaten, V., Laurent, C., Coelho, J. E., Sandau, U., Batalha, V. L., Burnouf, S., et al. (2014). From epidemiology to pathophysiology: what about caffeine in Alzheimer's disease? *Biochem. Soc. Trans.* 42, 587–592. doi: 10.1042/BST20130229

Garcia-Alloza, M., Robbins, E. M., Zhang-Nunes, S. X., Purcell, S. M., Betensky, R. A., Raju, S., et al. (2006). Characterization of amyloid deposition in the APPswe/PS1dE9 mouse model of Alzheimer disease. *Neurobiol. Dis.* 24, 516–524. doi: 10.1016/j.nbd.2006.08.017

Genc, O., Kochubey, O., Toonen, R. F., Verhage, M., and Schneggenburger, R. (2014). Munc18–1 is a dynamically regulated PKC target during short-term enhancement of transmitter release. *Elife* 3:e01715. doi: 10.7554/eLife.01715

Giménez-Llort, L., Schiffmann, S. N., Shmidt, T., Canela, L., Camón, L., Wassholm, M., et al. (2007). Working memory deficits in transgenic rats overexpressing human adenosine A_{2A} receptors in the brain. *Neurobiol. Learn. Mem.* 87, 42–56. doi: 10.1016/j.nlm.2006.05.004

Gyoneva, S., Shapiro, L., Lazo, C., Garnier-Amblard, E., Smith, Y., Miller, G. W., et al. (2014). Adenosine A_{2A} receptor antagonism reverses inflammation-induced impairment of microglial process extension in a model of Parkinson's disease. *Neurobiol. Dis.* 67, 191–202. doi: 10.1016/j.nbd.2014.03.004

Gyoneva, S., Swanger, S. A., Zhang, J., Weinshenker, D., and Traynelis, S. F. (2016). Altered motility of plaque-associated microglia in a model of Alzheimer's disease. *Neuroscience* 330, 410–420. doi: 10.1016/j.neuroscience.2016.05.061

Heneka, M. T., Carson, M. J., El Khoury, J., Landreth, G. E., Brosseron, F., Feinstein, D. L., et al. (2015). Neuroinflammation in Alzheimer's disease. *Lancet Neurol.* 14, 388–405. doi: 10.1016/S1474-4422(15)70016-5

Horgusluoglu-Moloch, E., Nho, K., Risacher, S. L., Kim, S., Foroud, T., Shaw, L. M., et al. (2017). Targeted neurogenesis pathway-based gene analysis identifies ADORA2A associated with hippocampal volume in mild cognitive impairment and Alzheimer's disease. *Neurobiol. Aging* 60, 92–103. doi: 10.1016/j.neurobiolaging.2017.08.010

Jankowsky, J. L., Slunt, H. H., Ratovitski, T., Jenkins, N. A., Copeland, N. G., and Borchelt, D. R. (2001). Co-expression of multiple transgenes in mouse CNS: a comparison of strategies. *Biomol. Eng.* 17, 157–165. doi: 10.1016/s1389-0344(01)00067-3

Kaster, M. P., Machado, N. J., Silva, H. B., Nunes, A., Ardais, A. P., Santana, M., et al. (2015). Caffeine acts through neuronal adenosine A_{2A} receptors to prevent mood and memory dysfunction triggered by chronic stress. *Proc. Natl. Acad. Sci. U S A* 112, 7833–7838. doi: 10.1073/pnas.1423088112

Kim, T.-K., Lee, J.-E., Park, S.-K., Lee, K.-W., Seo, J.-S., Im, J.-Y., et al. (2012). Analysis of differential plaque depositions in the brains of Tg2576 and Tg-APPswe/PS1dE9 transgenic mouse models of Alzheimer disease. *Exp. Mol. Med.* 44, 492–502. doi: 10.3858/emm.2012.44.8.056

Krabbe, G., Halle, A., Matyash, V., Rinnenthal, J. L., Eom, G. D., Bernhardt, U., et al. (2013). Functional impairment of microglia coincides with beta-amyloid deposition in mice with Alzheimer-like pathology. *PLoS One* 8:e60921. doi: 10.1371/journal.pone.0060921

Laurent, C., Buée, L., and Blum, D. (2018). Tau and neuroinflammation: what impact for Alzheimer's disease and tauopathies? *Biomed. J.* 41, 21–33. doi: 10.1016/j.bj.2018.01.003

Laurent, C., Burnouf, S., Ferry, B., Batalha, V. L., Coelho, J. E., Baqi, Y., et al. (2016). A_{2A} adenosine receptor deletion is protective in a mouse model of Tauopathy. *Mol. Psychiatry* 21, 97–107. doi: 10.1038/mp.2014.151

Laurent, C., Eddarkaoui, S., Derisbourg, M., Leboucher, A., Demeyer, D., Carrier, S., et al. (2014). Beneficial effects of caffeine in a transgenic model of Alzheimer's disease-like tau pathology. *Neurobiol. Aging* 35, 2079–2090. doi: 10.1016/j.neurobiolaging.2014.03.027

Le Guennec, K., Veugelen, S., Quenez, O., Szaruga, M., Rousseau, S., Nicolas, G., et al. (2017). Deletion of exons 9 and 10 of the Presenilin 1 gene in a patient with Early-onset alzheimer disease generates longer amyloid seeds. *Neurobiol. Dis.* 104, 97–103. doi: 10.1016/j.nbd.2017.04.020

Lee, C.-C., Chang, C.-P., Lin, C.-J., Lai, H.-L., Kao, Y.-H., Cheng, S.-J., et al. (2018). Adenosine augmentation evoked by an ENT1 inhibitor improves memory impairment and neuronal plasticity in the APP/PS1 mouse model of Alzheimer's disease. *Mol. Neurobiol.* doi: 10.1007/s12035-018-1030-z [Epub ahead of print].

Li, P., Rial, D., Canas, P. M., Yoo, J.-H., Li, W., Zhou, X., et al. (2015). Optogenetic activation of intracellular adenosine A_{2A} receptor signaling in the hippocampus is sufficient to trigger CREB phosphorylation and impair memory. *Mol. Psychiatry* 20, 1339–1349. doi: 10.1038/mp.2014.182

Lopes, L. V., Cunha, R. A., and Ribeiro, J. A. (1999). Increase in the number, G protein coupling and efficiency of facilitatory adenosine A_{2A} receptors in the limbic cortex, but not striatum, of aged rats. *J. Neurochem.* 73, 1733–1738. doi: 10.1046/j.1471-4159.1999.731733.x

Lu, J., Cui, J., Li, X., Wang, X., Zhou, Y., Yang, W., et al. (2016). An Anti-Parkinson's disease drug via targeting adenosine A_{2A} receptor enhances amyloid-β generation and γ-secretase activity. *PLoS One* 11:e0166415. doi: 10.1371/journal.pone.0166415

Machado, N. J., Simões, A. P., Silva, H. B., Ardais, A. P., Kaster, M. P., Garção, P., et al. (2017). Caffeine reverts memory but not mood impairment in a depression-prone mouse strain with up-regulated adenosine A_{2A} receptor in hippocampal glutamate synapses. *Mol. Neurobiol.* 54, 1552–1563. doi: 10.1007/s12035-016-9774-9

Marciniak, E., Faivre, E., Dutar, P., Alves Pires, C., Demeyer, D., Caillierez, R., et al. (2015). The Chemokine MIP-1α/CCL3 impairs mouse hippocampal synaptic transmission, plasticity and memory. *Sci. Rep.* 5:15862. doi: 10.1038/srep15862

Masters, C. L., Simms, G., Weinman, N. A., Multhaup, G., McDonald, B. L., and Beyreuther, K. (1985). Amyloid plaque core protein in Alzheimer disease and Down syndrome. *Proc. Natl. Acad. Sci. U S A* 82, 4245–4249. doi: 10.1073/pnas.82.12.4245

Matos, M., Augusto, E., Santos-Rodrigues, A. D., Schwarzschild, M. A., Chen, J.-F., Cunha, R. A., et al. (2012). Adenosine A_{2A} receptors modulate glutamate uptake in cultured astrocytes and gliosomes. *Glia* 60, 702–716. doi: 10.1002/glia.22290

Matos, M., Shen, H. Y., Augusto, E., Wang, Y., Wei, C. J., Wang, Y. T., et al. (2015). Deletion of adenosine A_{2A} receptors from astrocytes disrupts glutamate homeostasis leading to psychomotor and cognitive impairment: relevance to schizophrenia. *Biol. Psychiatry* 78, 763–774. doi: 10.1016/j.biopsych.2015.02.026

Nagpure, B. V., and Bian, J. S. (2014). Hydrogen sulfide inhibits A_{2A} adenosine receptor agonist induced β-amyloid production in SH-SY5Y neuroblastoma

cells via a cAMP dependent pathway. *PLoS One* 9:e88508. doi: 10.1371/journal.pone.0088508

Nishizaki, T., Nagai, K., Nomura, T., Tada, H., Kanno, T., Tozaki, H., et al. (2002). A new neuromodulatory pathway with a glial contribution mediated via A_{2A} adenosine receptors. *Glia* 39, 133–147. doi: 10.1002/glia.10100

Orr, A. G., Orr, A. L., Li, X. J., Gross, R. E., and Traynelis, S. F. (2009). Adenosine A_{2A} receptor mediates microglial process retraction. *Nat. Neurosci.* 12, 872–878. doi: 10.1038/nn.2341

Orr, A. G., Hsiao, E. C., Wang, M. M., Ho, K., Kim, D. H., Wang, X., et al. (2015). Astrocytic adenosine receptor A_{2A} and G_s-coupled signaling regulate memory. *Nat. Neurosci.* 18, 423–434. doi: 10.1038/nn.3930

Orr, A. G., Lo, I., Schumacher, H., Ho, K., Gill, M., Guo, W., et al. (2018). Istradefylline reduces memory deficits in aging mice with amyloid pathology. *Neurobiol. Dis.* 110, 29–36. doi: 10.1016/j.nbd.2017.10.014

Puoliväli, J., Wang, J., Heikkinen, T., Heikkilä, M., Tapiola, T., van Groen, T., et al. (2002). Hippocampal Abeta42 levels correlate with spatial memory deficit in APP and PS1 double transgenic mice. *Neurobiol. Dis.* 9, 339–347. doi: 10.1006/nbdi.2002.0481

Rebola, N., Sebastião, A. M., de Mendonca, A., Oliveira, C. R., Ribeiro, J. A., and Cunha, R. A. (2003). Enhanced adenosine A_{2A} receptor facilitation of synaptic transmission in the hippocampus of aged rats. *J. Neurophysiol.* 90, 1295–1303. doi: 10.1152/jn.00896.2002

Rebola, N., Simões, A. P., Canas, P. M., Tomé, A. R., Andrade, G. M., Barry, C. E., et al. (2011). Adenosine A_{2A} receptors control neuroinflammation and consequent hippocampal neuronal dysfunction. *J. Neurochem.* 117, 100–111. doi: 10.1111/j.1471-4159.2011.07178.x

Reitz, C., Brayne, C., and Mayeux, R. (2011). Epidemiology of Alzheimer disease. *Nat. Rev. Neurol.* 7, 137–152. doi: 10.1038/nrneurol.2011.2

Sasmono, R. T., Oceandy, D., Pollard, J. W., Tong, W., Pavli, P., Wainwright, B. J., et al. (2003). A macrophage colony-stimulating factor receptor-green fluorescent protein transgene is expressed throughout the mononuclear phagocyte system of the mouse. *Blood* 101, 1155–1163. doi: 10.1182/blood-2002-02-0569

Sauer, R., Maurinsh, J., Reith, U., Fülle, F., Klotz, K. N., and Müller, C. E. (2000). Water-soluble phosphate prodrugs of 1-propargyl-8-styrylxanthine derivatives, A_{2A}-selective adenosine receptor antagonists. *J. Med. Chem.* 43, 440–448. doi: 10.1021/jm9911480

Savage, J. C., Jay, T., Goduni, E., Quigley, C., Mariani, M. M., Malm, T., et al. (2015). Nuclear receptors license phagocytosis by trem2$^+$ myeloid cells in mouse models of Alzheimer's disease. *J. Neurosci.* 35, 6532–6543. doi: 10.1523/JNEUROSCI.4586-14.2015

Savonenko, A., Xu, G. M., Melnikova, T., Morton, J. L., Gonzales, V., Wong, M. P. F., et al. (2005). Episodic-like memory deficits in the APPswe/PS1dE9 mouse model of Alzheimer's disease: relationships to β-amyloid deposition and neurotransmitter abnormalities. *Neurobiol. Dis.* 18, 602–617. doi: 10.1016/j.nbd.2004.10.022

Silva, A. C., Lemos, C., Gonçalves, F. Q., Pliássova, A. V., Machado, N. J., Silva, H. B., et al. (2018). Blockade of adenosine A_{2A} receptors recovers early deficits of memory and plasticity in the triple transgenic mouse model of Alzheimer's disease. *Neurobiol Dis.* 31, 72–81. doi: 10.1016/j.nbd.2018.05.024

Sipos, E., Kurunczi, A., Kasza, Á., Horváth, J., Felszeghy, K., Laroche, S., et al. (2007). β-Amyloid pathology in the entorhinal cortex of rats induces memory deficits: implications for Alzheimer's disease. *Neuroscience* 147, 28–36. doi: 10.1016/j.neuroscience.2007.04.011

Snyder, S. W., Ladror, U. S., Wade, W. S., Wang, G. T., Barrett, L. W., Matayoshi, E. D., et al. (1994). Amyloid-beta aggregation: selective inhibition of aggregation in mixtures of amyloid with different chain lengths. *Biophys. J.* 67, 1216–1228. doi: 10.1016/s0006-3495(94)80591-0

Suh, Y.-H., and Checler, F. (2002). Amyloid precursor protein, presenilins, and alpha synuclein: molecular pathogenesis and pharmacological applications in Alzheimer's disease. *Pharmacol. Rev.* 54, 469–525. doi: 10.1124/pr.54.3.469

Temido-Ferreira, M., Ferreira, D. G., Batalha, V. L., Marques-Morgado, I., Coelho, J. E., Pereira, P., et al. (2018). Age-related shift in LTD is dependent on neuronal adenosine A_{2A} receptors interplay with mGluR5 and NMDA receptors. *Mol. Psychiatry* doi: 10.1038/s41380-018-0110-9 [Epub ahead of print].

Toonen, R. F. G., and Verhage, M. (2007). Munc18–1 in secretion: lonely Munc joins SNARE team and takes control. *Trends Neurosci.* 30, 564–572. doi: 10.1016/j.tins.2007.08.008

Viana da Silva, S., Haberl, M. G., Zhang, P., Bethge, P., Lemos, C., Gonçalves, N., et al. (2016). Early synaptic deficits in the APP/PS1 mouse model of Alzheimer's disease involve neuronal adenosine A_{2A} receptors. *Nat. Commun.* 7:11915. doi: 10.1038/ncomms11915

Yu, L., Coelho, J. E., Zhang, X., Fu, Y., Tillman, A., Karaoz, U., et al. (2009). Uncovering multiple molecular targets for caffeine using a drug target validation strategy combining A_{2A} receptor knockout mice with microarray profiling. *Physiol. Genomics* 37, 199–210. doi: 10.1152/physiolgenomics.90353.2008

Zhang, W., Hao, J., Liu, R., Zhang, Z., Lei, G., Su, C., et al. (2011). Soluble Aβ levels correlate with cognitive deficits in the 12-month-old APPswe/PS1dE9 mouse model of Alzheimer's disease. *Behav. Brain Res.* 222, 342–350. doi: 10.1016/j.bbr.2011.03.072

Zhao, Z. A., Zhao, Y., Ning, Y. L., Yang, N., Peng, Y., Li, P., et al. (2017). Adenosine A_{2A} receptor inactivation alleviates early-onset cognitive dysfunction after traumatic brain injury involving an inhibition of tau hyperphosphorylation. *Transl. Psychiatry* 7:e1123. doi: 10.1038/tp.2017.98

Conflict of Interest Statement: The authors declare that the research was conducted in the absence of any commercial or financial relationships that could be construed as a potential conflict of interest.

frontiers in Molecular Neuroscience

REVIEW
published: 31 July 2018
doi: 10.3389/fnmol.2018.00265

New Insights Into Permeation of Large Cations Through ATP-Gated P2X Receptors

*Laurie Peverini, Juline Beudez, Kate Dunning, Thierry Chataigneau and Thomas Grutter**

CNRS, CAMB UMR 7199, Équipe de Chimie et Neurobiologie Moléculaire, Université de Strasbourg, Strasbourg, France

The permeability of large cations through the P2X pore has remained arguably the most controversial and complicated topic in P2X-related research, with the emergence of conflicting studies on the existence, mechanism and physiological relevance of a so-called "dilated" state. Due to the important role of several "dilating" P2X subtypes in numerous diseases, a clear and detailed understanding of this phenomenon represents a research priority. Recent advances, however, have challenged the existence of a progressive, ATP-induced pore dilation, by demonstrating that this phenomenon is an artifact of the method employed. Here, we discuss briefly the history of this controversial and enigmatic dilated state, from its initial discovery to its recent reconsideration. We will discuss the literature in which mechanistic pathways to a large cation-permeable state are proposed, as well as important advances in the methodology employed to study this elusive state. Considering recent literature, we will also open the discussion as to whether an intrinsically dilating P2X pore exists, as well as the physiological relevance of such a large cation-permeable pore and its potential use as therapeutic pathway.

Keywords: LGICs, P2X receptors, dilation, spermidine, ion permeation

OPEN ACCESS

Edited by:
Joe Lynch,
The University of Queensland,
Australia

Reviewed by:
Toshi Kawate,
Cornell University, United States
Elsa Fabbretti,
University of Trieste, Italy

***Correspondence:**
Thomas Grutter
grutter@unistra.fr

Received: *29 May 2018*
Accepted: *13 July 2018*
Published: *31 July 2018*

Citation:
Peverini L, Beudez J, Dunning K, Chataigneau T and Grutter T (2018) New Insights Into Permeation of Large Cations Through ATP-Gated P2X Receptors. Front. Mol. Neurosci. 11:265. doi: 10.3389/fnmol.2018.00265

INTRODUCTION

For most ion channels, ion selectivity remains stable over time once the pore has opened, allowing small metal ions, such as Na^+, K^+ and Ca^{2+} to flow across the cell membrane. However, a few channels, namely TRPV1 (Chung et al., 2008), TRPV2 (Nabissi et al., 2013; Zubcevic et al., 2018), TRPA1 (Banke et al., 2010), acid-sensing ion channels (ASICs; Lingueglia et al., 1997; de Weille et al., 1998) and ATP-gated P2X receptors (Khakh and Lester, 1999; Virginio et al., 1999a) exhibit a striking increase in their permeability to larger cations, such as fluorescent dyes or synthetic organic molecules. This phenomenon was initially thought to occur through a time-dependent change of their ion selectivity upon repeated stimulation, a process known as "pore dilation." However, recent advances have challenged the idea of a slow dynamic change in ion selectivity (Puopolo et al., 2013; Li et al., 2015). In the case of P2X receptors, for which this phenomenon was first described several decades ago, pore dilation has failed to be unanimously accepted due to the increasing emergence of conflicting studies, and alternative mechanisms have been tentatively suggested (Jiang et al., 2005; Rokic and Stojilkovic, 2013; Wei et al., 2016). Given the importance of these ligand-gated ion channels in various physiological and pathological processes, including inflammation and neuropathic pain (Khakh and Alan North, 2006; Abbracchio et al., 2009; Khakh and North, 2012; Lemoine et al., 2012; Bernier et al., 2017),

a clear and detailed understanding of this unusual process at the molecular level is of utmost importance.

First cloned in 1994 (Brake et al., 1994; Valera et al., 1994), the family of P2X receptors is comprised of seven different subunit subtypes (P2X1-P2X7). A functional receptor is composed of three subunits, which are assembled as homo- or heterotrimers (Saul et al., 2013). Each subtype monomer shares a common architecture: two transmembrane domains (named TM1 and TM2) linked by a large, multi-glycosylated and disulfide bridge-containing extracellular domain, and intracellular C- and N-termini (Kawate et al., 2009; **Figure 1**). There are three ATP-binding sites which are found within the extracellular domain, positioned in cavities at the interface of adjacent subunits (Chataigneau et al., 2013; Habermacher et al., 2016a). In response to ATP binding, P2X receptors cycle between a number of different allosteric conformational states for which X-ray structures are now available (Kawate et al., 2009; Hattori and Gouaux, 2012; Mansoor et al., 2016; **Figure 1**). Initial ATP binding to the resting, closed channel state triggers a conformational change, resulting in the displacement of all six transmembrane helices and subsequent opening of the transmembrane pore (Li et al., 2008; Kracun et al., 2010). This transition (termed "gating") usually takes place on the millisecond time scale and allows the small metal cations Na^+, K^+ and Ca^{2+} to pass through the open pore (sometimes called I_1 state) according to their electrochemical gradient (North, 2002). Sustained application of ATP then leads to the inactivation of the pore (with the exception of P2X7), a process called desensitization, in which ion flux is terminated despite the fact that ATP remains bound to the receptor. ATP dissociation from these states reverts the pore to the initial closed state, from which the receptor is able to undergo further gating cycles upon re-activation (**Figure 1**).

To account for the gradual increase of permeability to larger cations, several mechanistic pathways linked to the P2X gating cycle have been proposed (Jiang et al., 2005; Rokic and Stojilkovic, 2013; Wei et al., 2016). For one of these routes, a putative dilated state (called I_2 state) corresponding to a progressive pore expansion of the open I_1 state following sustained ATP application has been suggested (Khakh and Lester, 1999; Virginio et al., 1999a; **Figure 1**). However, recent studies have seriously challenged this pore dilation hypothesis, by demonstrating that this phenomenon is rather an artifact of the method used to measure ion permeability change. In this review, we will discuss briefly the historical emergence of the controversial dilated state in the P2X family, as well as the recent important advances in the methodology employed that have led to the reconsideration of pore dilation. Finally, we will open the discussion to new physiological and therapeutic perspectives.

BRIEF HISTORY OF THE INCREASE OF PERMEABILITY

The ability of ATP to permeabilize membranes from different cells, such as mast cells, macrophages and transformed fibroblasts, was first discovered in the late 70s by demonstrating that the membrane permeability of cells gradually increases with increasing concentrations of ATP (Cockcroft and Gomperts, 1979). Besides small inorganic cations, larger organic molecules, such as carboxyfluorescein (376 Da), ethidium bromide (394 Da), lucifer yellow (444 Da) and fura-2 (636 Da) were also shown to be able to cross membranes following ATP application. However, solutes of higher molecular weight, such as Trypan Blue (872 Da), Evans Blue (961 Da) and inulin (more than 5000 Da) did not permeate the membrane (Steinberg et al., 1987; Steinberg and Silverstein, 1989), suggesting that molecules exceeding a certain radius cannot pass. At this point in time, the protein responsible for this behavior was unknown, and additionally, the observed "pore formation" features largely varied according to the cellular subtypes studied (Heppel et al., 1985).

Following these observations, and the discovery of ATP-activated purinergic receptors (P2X and P2Y; Burnstock, 1990), the passage of such large molecules across cell membranes was attributed to the fact that those cell types, in particular immune cells, express an unusual P2 receptor with an apparently non-selective pore. This was initially classified as the P2Z receptor: the "pore-forming" protein was thus named (Gordon, 1986; Abbracchio and Burnstock, 1994). P2Z receptors were then extensively studied for their ability to allow the permeation of large organic molecules into macrophages through a "macropore" (Nuttle and Dubyak, 1994), leading to cytolysis (Di Virgilio, 1995). The link with a putative P2X-related mechanism arose from the identification of the close proximity between P2Z receptor and P2X family receptor sequences. This similarity led to the re-classification of P2Z as the P2X7 receptor subtype (Surprenant et al., 1996). A few years later, two seminal articles reported that other P2X subtypes, the P2X2 and P2X4, also exhibit a striking increase in the permeability of large cations following several seconds of ATP application (Khakh et al., 1999; Virginio et al., 1999b). The concept of P2X "pore dilation" was born and multiple research groups have since confirmed and extended the concept to homomeric and heteromeric receptors (e.g., P2X2/3 and P2X2/5) expressed either in recombinant systems or in native tissues (Khakh et al., 1999; Virginio et al., 1999b; Yan et al., 2008; Compan et al., 2012; Browne et al., 2013). However, certain P2X subtypes, namely P2X1 and P2X3 which are fast desensitizing receptors, were classified as "non-dilating" channels as there was no evidence for an apparent increase in the permeability to large cations. Moreover, distinctive behaviors have been observed for P2X7 receptor splice variants, of which there are nine in humans, classified from P2X7B to P2X7J, and four in rodents (P2X7B, P2X7C, P2X7D and P2X7K); P2X7A is the full-length common P2X7 subunit (Rassendren et al., 1997; Cheewatrakoolpong et al., 2005; Sluyter, 2017). Some of these variants show an altered permeability for large cations. For instance, P2X7B, a variant bearing a largely truncated C terminus, is considered "non-dilating" (Cheewatrakoolpong et al., 2005; Adinolfi et al., 2010). On the contrary, P2X7K, which features a modified TM1 sequence as well as a more lipophilic N terminus, has been shown to be

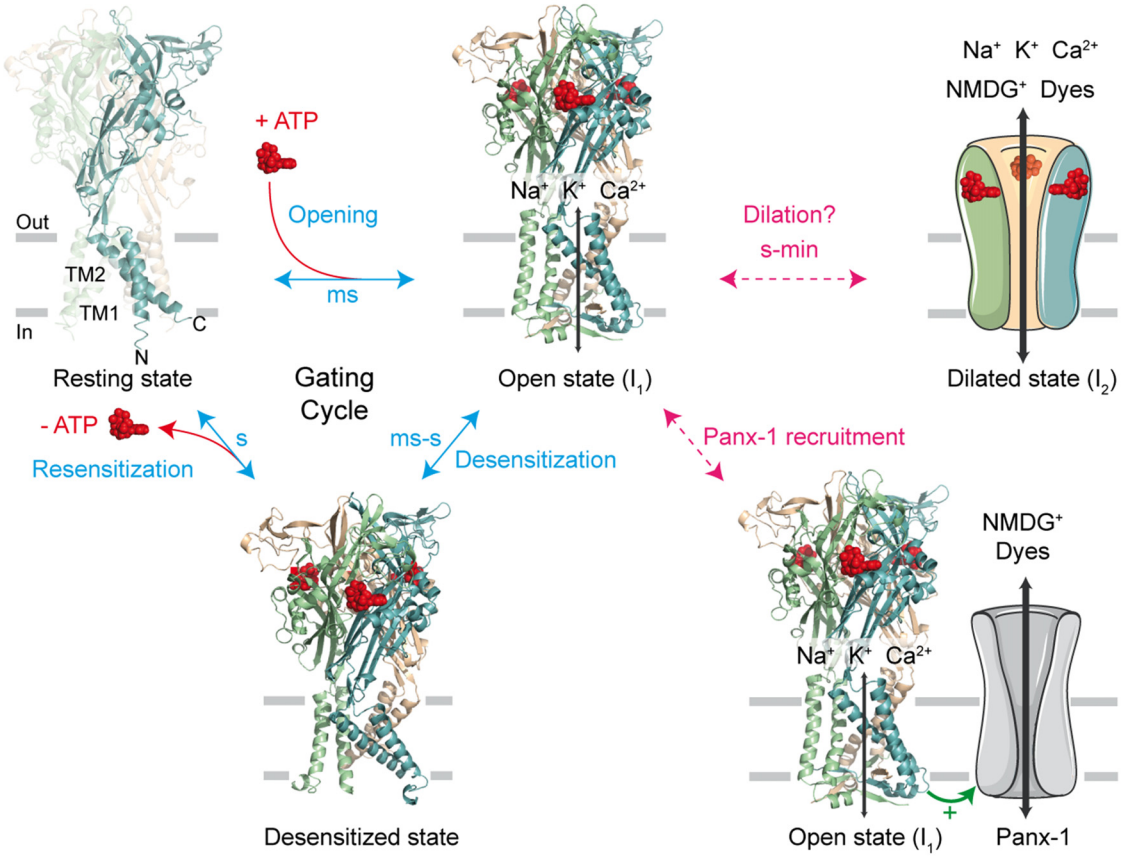

FIGURE 1 | The gating cycle and hypothetical pathways associated to permeation of large cations. In response to ATP binding, the receptor cycles between at least three functional states: the resting state, the open state (sometimes called I_1 state) and the desensitized state. X-ray structures are from the human P2X3 receptor solved in the apo, resting state (PDB ID 5SVJ), ATP-bound, open channel state (5SVK) and ATP-bound, desensitized state (5SVL; Mansoor et al., 2016). Ribbon structures are viewed laterally from the membrane and each subunit is color coded (one subunit is highlighted in the resting state, in which the N and C termini are indicated). ATP is shown as a space-filling model and the lipid bilayer is symbolized by gray bars. It has been initially suggested that sustained ATP application allows the passage of large cations, such as *N*-methyl-D-glucamine ($NMDG^+$) and fluorescent dyes, through two main putative, controversial routes. The first one involves a gradual pore dilation of the open I_1 state to reach a dilated state (I_2); the second pathway involves the recruitment of the hemichannel pannexin-1 (Panx-1) by P2X receptor. The two models were suggested not to be mutually exclusive.

constitutively and immediately dilated (Nicke et al., 2009; Xu et al., 2012).

METHODS AND INTERPRETATIONS LEADING TO THE CONTROVERTED DILATED STATE

Two main experimental approaches have been used to monitor the apparent gradual increase in large cation permeability. In the first approach, the cellular uptake of fluorescent dyes, such as YO-PRO-1 or ethidium bromide, is observed as a function of time. Dye uptake usually develops several seconds after ATP application. As these cationic dyes become fluorescent when bound to DNA, this method is a simple and direct read-out of the passage of large molecules following P2X activation. Studies involving cysteine reactive compounds, such as methanethiosulfonate (MTS) reagents, have also shown the ability of larger sized molecules to pass into the cell (Browne et al., 2013). This method has been employed for P2X2, P2X4 and P2X7 receptors (Khakh et al., 1999; Virginio et al., 1999a,b; Yan et al., 2008).

In the second approach, the permeability of large cations is measured by patch-clamp electrophysiology (Khakh et al., 1999; Virginio et al., 1999b). In this indirect method, reversal potentials (E_{rev}) are measured in bi-ionic solutions, where *N*-methyl-D-glucamine ($NMDG^+$), a synthetic large organic cation, is the sole permeating ion present outside the cell ($NMDG^+_{out}$) and Na^+ is the sole permeating cation present inside the cell (Na^+_{in}). According to the Goldman-Hodgkin-Katz voltage equation, a shift in E_{rev} signals a change in membrane permeability to one or both cations provided the concentrations of ions on either side of the membrane remain unchanged. The gradual and positive shifts in E_{rev} measured during long applications of ATP have been interpreted as a time-dependent change in the relative permeability of $NMDG^+$ relative to Na^+ (P_{NMDG^+}/P_{Na^+}). At the

beginning of extracellular ATP application, the agonist opens a pore that is initially more permeable to Na^+ than $NMDG^+$, but during sustained activation of the channel, E_{rev} shifts towards less negative values that signify a dramatic increase in the permeability to $NMDG^+$ (Khakh et al., 1999; Virginio et al., 1999b). This method has been extensively employed to probe shifts in E_{rev} for many P2X receptors, such as P2X2, P2X2/3, P2X2/5, P2X4 and P2X7 (Khakh et al., 1999; Virginio et al., 1999a,b; Compan et al., 2012).

The fact that shifts of E_{rev} and dye uptake occur on the same time scale has led to the belief that a common mechanism would be at work. Two main hypotheses have then emerged (**Figure 1**). One hypothesis involves the recruitment of an auxiliary protein by P2X receptors. This protein is pannexin-1 (Panx-1), a hemichannel that is responsible for the passage of larger molecules. This hypothesis is supported by the observation that P2X permeability to large cations is inhibited when inhibitors of Panx-1 are applied (Pelegrin and Surprenant, 2006). In addition, colchicine, a drug that disrupts the cytoskeleton, has been shown to affect YO-PRO-1 uptake into cells transfected with P2X2 or P2X7 subtypes, but not the permeability for small cations. This would indicate that these two types of permeability result from different pathways (Marques-da-Silva et al., 2011).

On the other hand, a second hypothesis postulates the existence of an intrinsic "pore dilation" mechanism, whereby the P2X pore itself undergoes a slow conformational change. This would lead to a physical expansion in the diameter of the P2X ion pore from the I_1 state to the putative I_2 dilated state, allowing the passage of larger molecules. This "pore dilation" mechanism has been extensively studied by site-directed mutagenesis, patch-clamp electrophysiology, fluorescent dye uptake and use of chemical reagents (Khakh et al., 1999; Virginio et al., 1999a,b; Eickhorst et al., 2002; Khakh and Egan, 2005; Browne et al., 2013). Moreover, it has been shown that cells which do not express Panx-1 nonetheless exhibit "dilating" properties and, in agreement with this hypothesis, overexpression or inhibition of Panx-1 by carbenoxolone does not affect dilation of P2X2 receptors expressed in HEK-293 cells (Chaumont and Khakh, 2008; Yan et al., 2008).

As evidence has been found both in support of and against each hypothetical pathway, the question has been raised as to whether these two distinct mechanisms may in fact co-exist (Jiang et al., 2005; Cankurtaran-Sayar et al., 2009). One mechanism would be dedicated to $NMDG^+$ permeability and the other to larger molecules such as YO-PRO-1 and even occasionally the permeation of organic anions (Browne et al., 2013). Moreover, interactions with other proteins may play a role. For instance, cytoskeletal proteins have been described as important for pore dilation in P2X7 receptor subtype (Kim et al., 2001; Gu et al., 2009). In addition, characterization of the apparent "pore dilation" has been shown to be dependent on cell types used for experiments as well as expression levels of receptors (Fujiwara and Kubo, 2004). Of greatest importance is the fact that dynamic changes of unitary conductance following prolonged ATP application have never been observed at the single channel level (Ding and Sachs, 1999; Riedel et al., 2007b), thus bringing into question the reality of an intrinsic "pore dilation".

CHANGING THE PARADIGM

In 2015, the team of K. Swartz offered an alternative explanation of the change in E_{rev} measured in bi-ionic $NMDG^+_{out}/Na^+_{in}$ solutions (Li et al., 2015). The authors elegantly demonstrate in the P2X2 receptor that shifts in E_{rev}, although very real, are not caused by a time-dependent change in channel permeability, but rather by a dramatic and unappreciated change of the intracellular ion concentrations, which may vary by more than 100 mM throughout the course of the experiment. Combining electrophysiology and mathematical modeling, the authors were able to convincingly demonstrate that prolonged ATP activation leads to a depletion of intracellular Na^+, from 140 mM to around 20 mM, and accumulation of $NMDG^+$, from 0 mM to over 200 mM. They further showed that physical parameters such as channel densities, pore conductance, cell volume, and access resistance (R_{access}) between the cell and the pipette electrode, may directly change ion concentrations inside the cell following sustained exposure to ATP. Because of these changes, the Goldman-Hodgkin-Katz voltage equation cannot be used to reliably determine the relative permeability of ions. This study therefore proved that the time-dependent shift in the E_{rev} measured in bi-ionic solutions is an artifact of the method employed, and that extreme caution must be taken when measuring permeability changes during whole-cell patch-clamp recordings.

This outstanding article seriously challenges the pore dilation paradigm which held true for almost two decades. However, it is important to emphasize that the study did not question the ability of $NMDG^+$ to permeate through the activated P2X pore, as initially suggested by the seminal articles (Khakh et al., 1999; Virginio et al., 1999b), but that this $NMDG^+$ permeation occurs soon after ATP activation. As a direct proof of this assumption, Li et al. (2015) showed that whole-cell currents carried by $NMDG^+$ using symmetrical solutions (whereby both intracellular and extracellular solutions contain $NMDG^+$) developed immediately following ATP application. These observations indicate that a gradual pore dilation mechanism is not necessary to account for $NMDG^+$ permeation.

A NEW MECHANISTIC POINT OF VIEW

The publication of Li et al. (2015) opens an appealing hypothesis: the dimensions of the pore itself may be directly adequate for the direct passage of $NMDG^+$ following several milliseconds of ATP application. From a mechanistic point of view, the I_1 state would represent the most parsimonious hypothesis, provided the diameter of the narrowest part of its open pore is sufficiently wide to allow the passage of such large molecules. We have investigated this possibility by combining single-channel recordings, molecular modeling and

the use of photo-switchable tweezers (Harkat et al., 2017), a recently developed technology that allows identification of the molecular motions involved in channel activation (Habermacher et al., 2016b). By covalently tethering synthetic azobenzene cross-linkers to a pair of selected engineered cysteine residues, these "molecular tweezers" are capable of pulling or pushing on gating elements once azobenzene isomerization is triggered by light irradiation. To provide a read-out of the large cation permeation, we used symmetric $NMDG^+$ solutions, where $NMDG^+$ was the sole permeating ion. A rapid solution exchange of the extracellular solutions from an $NMDG^+$-containing to a Na^+-containing solution allowed direct comparison of molecular motions involved in pore opening and permeation of $NMDG^+$ and Na^+. We screened several positions near a flexible region of TM2 in the P2X2 receptor, as well as a region of the pore surrounding a kink that was previously identified in channel gating (Habermacher et al., 2016b; Mansoor et al., 2016). Firstly, we identified two types of molecular motions involved in the permeation of large cations: a horizontal expansion of the upper end of TM2 helices and a vertical flexing of the extremities of two adjacent TM2 helices. Surprisingly, we observed no $NMDG^+$ permeation for mutants bearing no permeability to Na^+, suggesting that none of the molecular motions that we monitored can produce a pathway dedicated exclusively to $NMDG^+$ permeation. Secondly, for the motions that allowed the passage of both $NMDG^+$ and Na^+, the ratio of the current I_{NMDG^+}/I_{Na^+} was around 10%, suggesting that $NMDG^+$ follows the same pathway as Na^+ across the P2X pore but is not able to permeate as easily.

To further support this observation, we recorded ATP-induced single-channel currents from outside-out patches using symmetrical $NMDG^+$ solutions (**Figure 2A**). We not only showed that P2X2 receptors are $NMDG^+$-permeable channels, activated on the millisecond timescale, with kinetics similar to those observed when Na^+ is the primary permeating ion, but we also established the first measurements of the unitary conductance of $NMDG^+$ currents (around four pS for several ATP concentrations). This is approximately 10 times lower than that of Na^+ currents. We further confirmed these experimental data by molecular dynamic simulations carried out on a model of ATP-bound P2X receptors. These computations represent a step forwards in the understanding of the molecular mechanism of $NMDG^+$ permeation, which is the result of a conformational and orientational selection process (Harkat et al., 2017). We further validated our methodology by measuring YO-PRO-1 uptake in cells expressing engineered receptors, to discount the presence of possible artifacts caused by the use of non-physiological media for electrophysiological recordings. For the mutants exhibiting light-induced motions leading to a "desensitizing-like" phenotype, we were not able to show fluorescence uptake, but for those associated with a stable opening induced by light, YO-PRO-1 was successfully incorporated into cells, suggesting that desensitization may hinder dye accumulation into cells. However, no YO-PRO-1 uptake was observed during molecular dynamic simulations, which brings back the possibility of two distinct mechanisms for YO-PRO-1 and $NMDG^+$ uptake. Alternatively, this could be the result of a limitation of the method used, as it is possible that the sampling time for computations may not have been sufficient to observe the passage of low-conductance YO-PRO-1. Altogether, our data support that the open I_1 state likely represents the main route for both small and large cations (**Figure 2B**).

In agreement with data obtained from P2X2 receptors, two recent reports carried out on P2X7 receptors further support an instantaneous permeation of large cations upon ATP activation (Karasawa et al., 2017; Pippel et al., 2017). In the first study, a rigorous and thorough analysis of single-channel currents demonstrate that the unitary conductance of the human P2X7 channel remains stable over time following prolonged ATP application (up to 30 min; Riedel et al., 2007a,b; Pippel et al., 2017). Interestingly, the authors even showed that chemical modification of engineered cysteine side chains with charged MTS reagents increased dramatically the open probability of the channel, with no sign of apparent pore dilation (Pippel et al., 2017). In the second study, the biophysical properties of the "macropore" feature of P2X7 channel have been scrutinized in a synthetic system, in which the functionality of the P2X7 protein has been monitored in the absence of other protein cellular components (Karasawa et al., 2017). To do so, a purified, yet truncated, version of the giant panda P2X7 receptor (pdP2X7-ΔNC) was reconstituted into manufactured liposomes. To distinguish channel activity (I_1 state) from "macropore" formation (I_2 state), proteoliposomes encapsulated either Fluo-4, a Ca^{2+}-sensing fluorescent probe, or DNA, to which binding of YO-PRO-1 enhances dye fluorescence emission. The authors elegantly and convincingly showed that pdP2X7-ΔNC was not only permeable to YO-PRO-1, but also to Ca^{2+} with the same apparent kinetics, suggesting a common pathway for both small and large cations (Karasawa et al., 2017). Therefore, in a reconstituted system, the purified P2X7 receptor is able to form an intrinsic and immediate dye-permeable pore with no apparent time-lag, a finding that is apparently not compatible with the slow and progressive process of pore dilation.

IS THE CONCEPT OF PORE DILATION DEAD?

As stated above, recent data now support the hypothesis that the open I_1 state would be sufficiently wide to allow the passage of relatively large molecules, without the need for an ATP-induced pore dilation. However, comparison of the structure of the largest permeating molecules with recent X-ray structures of the ATP-bound, open state casts doubt on the fact that the open I_1 state truly represents the sole ion pathway (**Figure 3**). This is particularly true for P2X7 receptors, for which MTS-rhodamine, a nanometer-sized dye, was shown to penetrate the open channel and block at a cysteine-substituted residue located deeply in the pore (Browne et al., 2013), whereas the structure of the open pore derived from the human P2X3 receptor (the structure of P2X7 open pore is not yet determined) appears to be too narrow to accommodate such a molecule. Interestingly, molecules of similar size, such as Texas Red-MTSEA, cannot

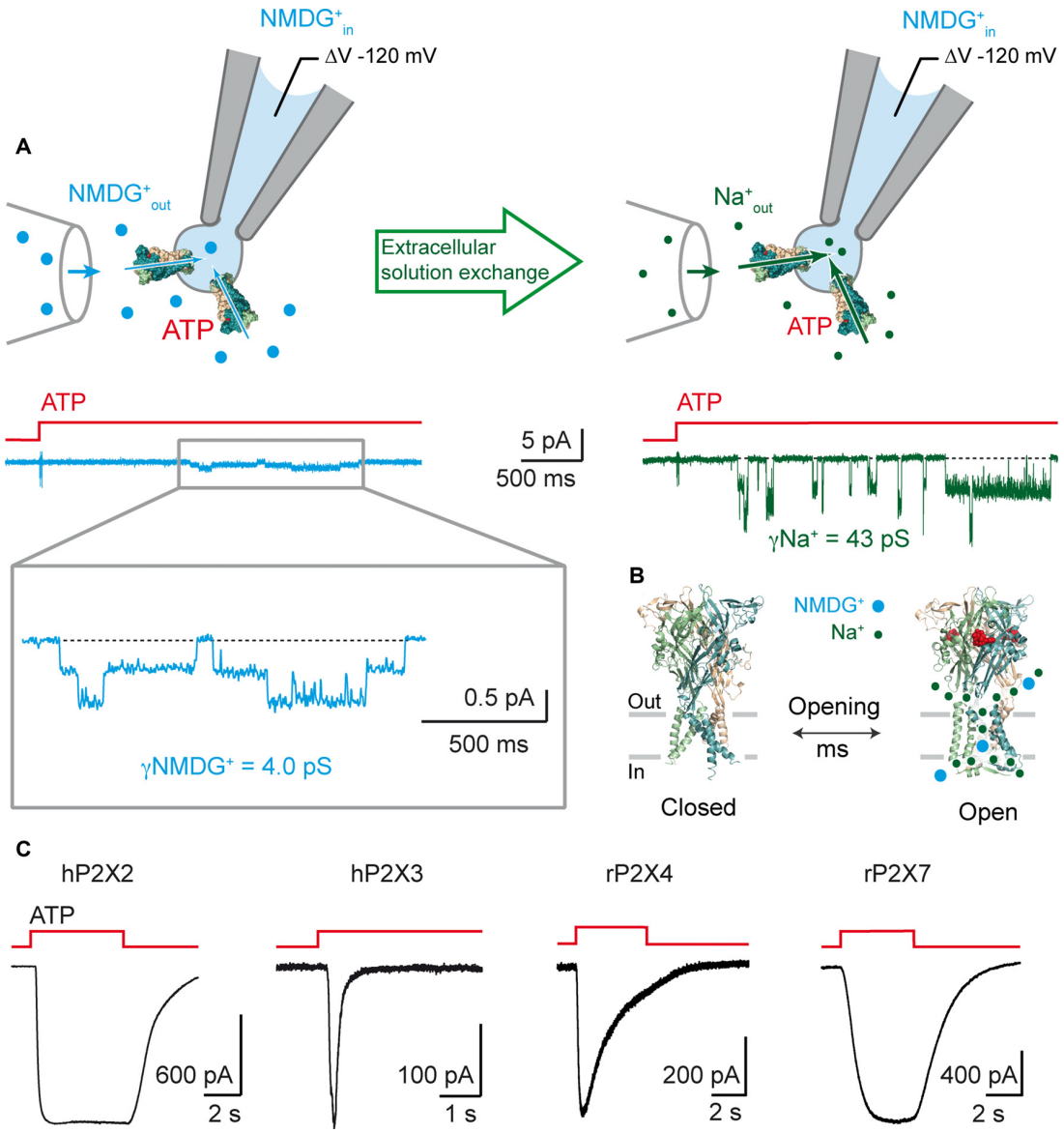

FIGURE 2 | P2X receptors are rapidly permeable to large cations. **(A)** Rapid onset of single-channel $NMDG^+$ currents following ATP application. Top: schematic drawing of the outside-out configuration and perfusion glass tube. Note that patch pipette contains $NMDG^+$. Bottom: Single-channel currents elicited by 1 μM ATP from an outside-out patch expressing the rat P2X2 receptor. Currents were first recorded in extracellular $NMDG^+_{out}$ solution (symmetric $NMDG^+_{out}/NMDG^+_{in}$, left, blue), and then in extracellular Na^+_{out} solution ($Na^+_{out}/NMDG^+_{in}$, right, green), following rapid solution exchange. Currents were recorded at −120 mV and filtered at 1 kHz. Inset shows magnification of $NMDG^+$ currents filtered at 100 Hz. ATP applications are indicated by red stepped bars. Adapted from Harkat et al. (2017). **(B)** Proposed model in which $NMDG^+$ and Na^+ ions transit through the same open pore at different flow rates following rapid ATP activation (~2.5 × 10^6 $NMDG^+$ ions/s at −120 mV with 132.6 mM $NMDG^+$, 32 × 10^6 Na^+ ions/s at -120 mV with 132.6 mM Na^+; data taken from Harkat et al. (2017)). **(C)** Whole-cell ATP-gated currents recorded in symmetric spermidine solution at -60 mV from HEK-293 cells expressing the indicated P2X receptors. Traces for hP2X2 and hP2X3 are adapted from Harkat et al. (2017). ATP concentration was 30 μM for hP2X2 and hP2X3, 100 μM for rP2X4, and 1000 μM for rP2X7.

enter the P2X2 pore (Li et al., 2015) suggesting that the P2X7 receptor, when activated by ATP, can reach a diameter that is larger than that of the P2X2 receptor (**Figure 3**). Other routes specifically dedicated to the permeation of such very large molecules may also exist. As stated above, Panx-1 is a candidate, as close proximity between Panx-1 and P2X7 channels has been established in human and mouse macrophages cells (Pelegrin and Surprenant, 2006). Alternatively, there is still a possibility that P2X7 receptors do indeed dilate under certain conditions that remain to be determined.

A finding which may reconcile P2X7 (and perhaps other P2X subtypes) with the concept of "pore dilation" comes from recent studies that emphasize the importance of the lipid composition of the membrane for the passage of large cations through the P2X pore. Although lipids, such as phosphoinositides (Bernier et al., 2008a,b) and cholesterol (Murrell-Lagnado, 2017),

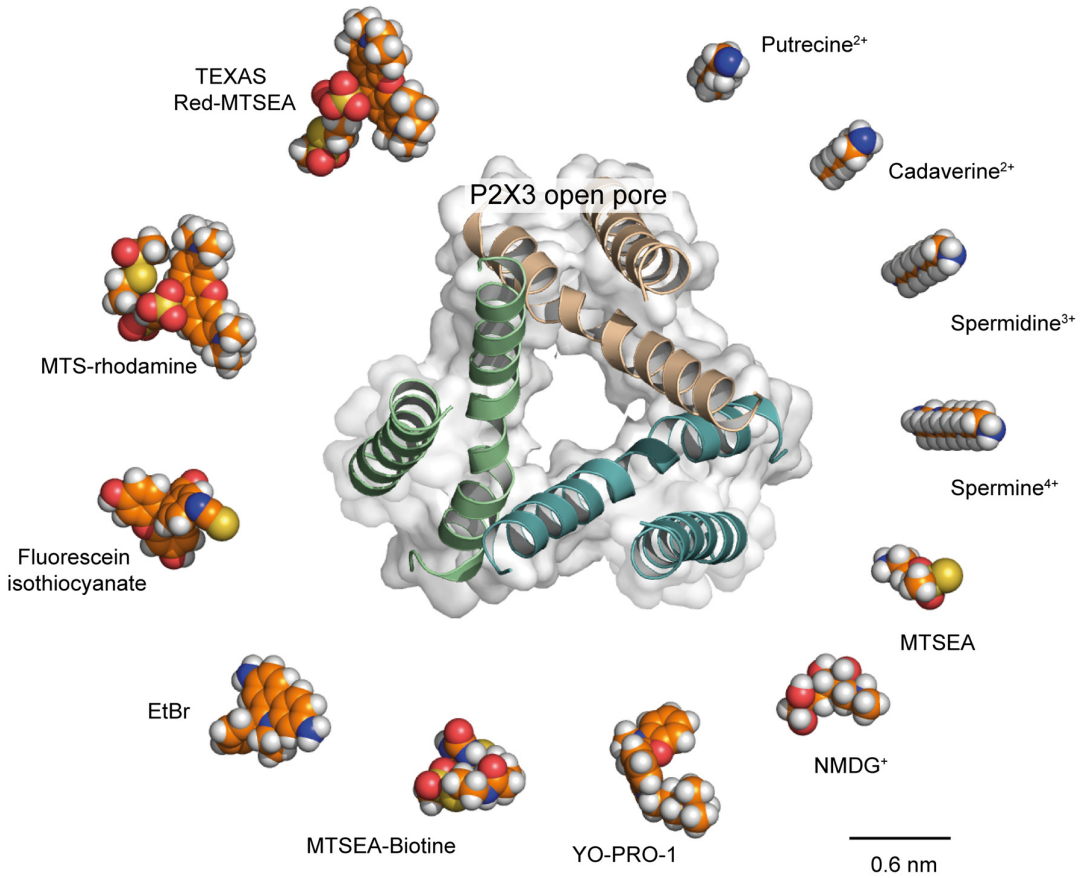

FIGURE 3 | Is the P2X open pore sufficiently wide to allow the passage of large molecules? Comparison of structures of selected organic molecules, shown as space-filling models, scaled to the X-ray structure of the P2X3 open pore (PDB ID: 5SVK), viewed along the three-fold axis of symmetry. Receptor ribbon structure is superimposed to the protein surface. Shown is a clockwise ranking of molecules, from the smallest (putrescine, top right) to the largest dimensions (Texas Red-MTSEA, top left). Valency of cations is also indicated. Recent evidence supporting permeation of $NMDG^+$ and spermidine through the P2X2 open I_1 state (Harkat et al., 2017) suggests that molecules of similar size to these cations should also permeate the P2X open pore. For slightly larger molecules, such as YO-PRO-1, for which their dimensions reach those of the open pore, we propose that such molecules follow the same pathway as Na^+ across the P2X pore but are not able to permeate as easily. For the largest molecules, such as Texas Red-MTSEA, there is evidence that they cannot enter the P2X2 pore (Li et al., 2010). However, methanethiosulfonate (MTS)-rhodamine, which has a size that is similar to that of Texas Red-MTSEA, has been shown to directly permeate the P2X7 pore (Browne et al., 2013), suggesting the P2X7 open pore is larger than that of P2X2. From a structural point of view, the open state of the P2X3 receptor seems too narrow to allow the passage of MTS-rhodamine. Therefore, either the structure of P2X7 open state is different from that of the P2X3 receptor or other routes specifically dedicated to the permeation of such very large molecules in P2X7 receptors exist. Carbon atoms are indicated in orange; nitrogen atoms in blue, oxygen atoms in red; phosphorus atoms in yellow, and hydrogen atoms in white.

seem to be important for the regulation of allosteric states of P2X receptors, this factor has been underestimated in "dilation" studies thus far. However, Kawate and co-workers (Karasawa et al., 2017) have very recently demonstrated in reconstituted liposomes that sphingomyelin and phosphatidylglycerol-containing membranes facilitate pdP2X7-ΔNC-dependent dye uptake, whereas the presence of cholesterol rather inhibits this process. It is thus conceivable that the lipid composition may have a direct impact on the physical diameter of the P2X7 open channel state that would allow the passage of very large molecules (up to 900 Da). Alternatively, a conformational plasticity in the selectivity filter of the P2X pore may allow the passage of large molecules, as very recently shown on TRPV2 ion channel (Zubcevic et al., 2018). Although appealing, these hypotheses need convincing evidence; in particular the structure of the P2X7 open channel state (and also other P2X subtypes) solved in a lipid bilayer will certainly advance this issue.

PHYSIOPATHOLOGICAL ROLE OF LARGE CATION PERMEATION

Now that there is no doubt that P2X receptors are permeable to large cations, is there any link between this feature and pathological states? Evidence exists indicating a possible link at least involving the P2X7 receptor, which is arguably of most therapeutic interest due to its implication in a large variety of diseases. Expressed in a range of immune and microglial

TABLE 1 | Polyamine modulation of ion channels and ligand-gated ion channels.

Ion channel/ligand-gated ion channel	Nature of the interaction with polyamines	Observations suggesting a possible implication of P2X receptors
AMPA receptors	Voltage-dependent block by intracellular polyamines (Bowie et al., 1998)	Co-localization Synaptic scaling Synaptic depression Functional interactions (Pougnet et al., 2014)
Kainate receptors	Voltage-dependent block by intracellular polyamines (Perrais et al., 2010)	Co-expression of kainate receptors and P2X receptors in some populations of neurons (Lucifora et al., 2006)
NMDA receptors	Potentiation by extracellular polyamines, existence of a polyamine binding site (Han et al., 2008; Mony et al., 2011)	Modulation of NMDA-dependent plasticity (Boué-Grabot and Pankratov, 2017)
Nicotinic receptors	Binding site for polyamine-derived toxins (Bixel et al., 2001)	Interaction between nicotinic receptors and P2X receptors: cross inhibition (Khakh et al., 2005)
Inward rectifier K^+ (Kir) channels	Voltage-dependent blockage by intracellular polyamines Existence of a polyamine binding site (Kurata et al., 2006)	*To be determined*
ASICs	Potentiation by spermine (Babini et al., 2002)	Functional interaction between P2X receptors and ASICs (Birdsong et al., 2010; Stephan et al., 2018)
TRPV1 receptors	Polyamines can act as ligands and are able to pass through TRPV1 (Ahern et al., 2006)	Cross-talk between TRPV1 and P2X receptors (Stanchev et al., 2009)

cells, P2X7 receptors are widely involved in the immune and inflammatory response, notably in the nervous system. Several recent reviews extensively cover the involvement of P2X7 receptors in pathological immune-related conditions, such as neuropathic pain, Alzheimer's disease, Huntington's disease and multiple sclerosis to name but a few (De Marchi et al., 2016; Di Virgilio et al., 2017; Savio et al., 2018). A first possible link may involve the ability of Panx-1 channels to allow entry of large cations into the cell, as it has been demonstrated that an increase in extracellular ATP induces the clustering of Panx-1 with P2X7 receptors, leading to their internalization (Boyce et al., 2015). An impairment of this internalization mechanism could contribute to the over-activity of P2X-mediated signaling that may lead to pathophysiological states, such as neuropathic pain (Swayne and Boyce, 2017). Another possible link may involve the P2X7 protein itself. An association between nerve-induced pain behavior (mechanical allodynia) and the P451L mutation found in the mouse *P2rx7* gene has been identified. This mutation impaired "pore formation" by affecting the entry of YO-PRO-1 and ethidium bromide in HEK-293 cells and calcein dye into macrophages, but interestingly the mutation did not affect Ca^{2+} entry (Adriouch et al., 2002; Young et al., 2006; Sorge et al., 2012). Mice in which P2X7 receptors have impaired pore formation as a result of this mutation showed less allodynia than mice with the pore-forming receptors. Moreover, in two independent human chronic pain cohorts, it has been shown that human mutations affecting the amino acid sequence of P2X7 receptor modify the chronic pain sensitivity (Sorge et al., 2012). For instance, in the cohort experiencing post-mastectomy chronic pain, the H155Y single nucleotide polymorphism, which leads to hyperfunctional P2X7 receptors, was associated with an increased pain sensitivity. In contrast, mastectomized women with the hypofunctional mutation R270H of P2X7 receptor, experienced reduced chronic pain (Sorge et al., 2012). These correlations thus clearly suggest that the level of pore activity is related to pathological states and indicate that P2X7 receptors are vital targets for the treatment of diseases such as neuropathic pain. Differences in Na^+, K^+ and Ca^{2+} ion flux may trigger such pathological responses, but permeation of large, pathologically relevant cations may also be involved. These large molecules remain to be identified.

NEW DIRECTIONS CONCERNING THE P2X PERMEATION OF LARGE CATIONS: THE CASE OF POLYAMINES

What is the physiological implication of P2X permeability to large cations? To answer to this question, it is first important to consider whether this unusual large cation permeation feature is shared by all members of the P2X family. Before 2017, a striking observation was that fast-desensitizing receptors, namely P2X1 and P2X3 receptors, were apparently unable to allow the entry of larger cations through the pore. By using symmetric solutions, we have provided evidence that P2X3 receptors are actually permeable to $NMDG^+$, suggesting that these receptors should be reconsidered as channels permeable to large cations (Harkat et al., 2017). However, $NMDG^+$ is a synthetic molecule, and we sought rather to establish the permeability of large, naturally occurring cations through the P2X pore. We have very recently found that spermidine permeates through the human P2X2 and P2X3 receptor ion channels (Harkat et al., 2017). Now we have extended this permeation to the rat P2X4 and P2X7 receptors, suggesting permeation of spermidine may be a common feature

shared by many, if not all members of the P2X family (**Figure 2C**).

Spermidine is a natural, ubiquitously distributed polyamine that is vital for the cell (Guerra et al., 2016; Madeo et al., 2018). It is formed intracellularly and is involved in several important cellular functions, such as growth, division and proliferation. Spermidine is also recognized as an allosteric modulator of many ion channels, including ionotropic glutamate receptors, nicotinic acetylcholine receptor, potassium channels, ASICs and TRPV1 channels (**Table 1**). For some of these channels, spermidine must exit the cell through dedicated pathways to reach the targeted extracellular sites. One of these such pathways may be the vesicular polyamine transporter (VPAT) that stores polyamines in secretory vesicles in astrocytes and mast cells (Hiasa et al., 2014; Takeuchi et al., 2017). As we provide evidence that spermidine permeates through the open pore of P2X receptors (**Figure 2C**), we propose that P2X receptors may represent an alternative polyamine pathway that is under the control of ATP. Given the importance of spermidine for the function of several other ion channels, as well as the known interactions of P2X receptors with such channels (Khakh et al., 2005; Stanchev et al., 2009; Pougnet et al., 2014; Boué-Grabot and Pankratov, 2017; Stephan et al., 2018), the question is now raised as to what extent can P2X receptors be the physiological mediator of spermidine transit.

By discovering spermidine permeation through P2X receptors, our results uncover a possible overlooked P2X signaling pathway that may be extended to other natural large molecules. Earlier work provided strong evidence that P2X7 receptors are sites of release of important molecules, such as ATP and excitatory amino acids (Duan et al., 2003; Pellegatti et al., 2005; Suadicani et al., 2006; Di Virgilio et al., 2018). It now remains to determine whether these signaling molecules are physically able to cross directly through the P2X7 open pore. Identification of the mechanisms involved will undoubtedly advance the biology of P2X receptors and their role in pathological states.

COULD P2X RECEPTORS ACT AS A PATHWAY FOR THERAPEUTIC APPLICATIONS?

P2X receptors can act as a pathway for the entry of large molecules into cells—to what extent can this property be exploited for therapeutic applications? Two examples of P2X receptors being used as pathways for the passage of azobenzene-based molecules have been published by the team of R. Kramer. The first example is related to the control of nociception, by manipulation of neurons involved in pain signaling via voltage-gated ion channels (Mourot et al., 2012). This was carried out by the incorporation of QAQ, an azobenzene-based photoswitch bearing two quaternary ammonium moieties, into cells through the P2X pore. Control of nociception is based on the activation/deactivation process of local voltage-gated ion channels (calcium, potassium, sodium), which is provided by the geometrical switching between *trans* and *cis* isomers of QAQ. The route responsible for the entry of QAQ, which is otherwise a membrane-impermeable molecule, can be TRPV1 or alternatively P2X7 receptors (Mourot et al., 2012). In 2016, they further developed this concept of P2X-mediated membrane passage in order to resurrect light-sensitivity of retinal ganglion cells of degenerated retina in blind mice. They employed the same methodology: a charged photoswitchable molecule based on an azobenzene moiety is applied to cells and permeates the membrane via P2X receptors. This molecule is then able to act on voltage-gated ion channels, restoring the responsiveness of retinal-ganglion cells to light (Tochitsky et al., 2016).

As stated above, the presence and implication of P2X7 in many diseases could inspire new approaches, whereby the permeability of the receptor to large cations may be utilized to therapeutic effect, in the delivery of biological effectors to P2X7-expressing cells. Equally, P2X7 has been found in over-expressed levels in several types of cancers, such as chronic B lymphocytic leukemia (De Marchi et al., 2016) and thyroid papillary cancer (Solini et al., 2008). One could envisage the exploitation of these high expression levels in conjunction with the permeability of P2X7 to large molecules, to deliver anti-cancer drugs through the P2X7 pathway.

CONCLUSION

For some time now, there has been much controversy surrounding the passage of large cations through the P2X pore, and a clear explanation on the mechanism of this particular permeation pathway has remained highly elusive. However, recent advances in experimental technique allow a more just study of large cation permeation. Equally, new information showing the highly sensitive nature of P2X7 function to lipid membrane composition, which can vary between cellular types, may be considered in future studies probing the permeability of P2X7 to large cations.

New important features of P2X receptor permeability are now being brought to light. First, it is important to reconsider the structure of the open state, which exhibits an immediate extended permeability, and to consider more closely the critical role of the membrane lipid environment in order to fully understand the functionality of these proteins. Secondly, their physiological importance must also be reconsidered, with the new information that they are able to allow the passage of important physiological modulators. A final interesting point is to look further into the potential application of P2X receptors as pathway for drug delivery.

AUTHOR CONTRIBUTIONS

LP, KD, TC and TG wrote the manuscript. JB made the figures.

FUNDING

This work was supported by the Agence Nationale de la Recherche (grant no. ANR-14-CE11-0004-01) and the Ministère de la Recherche.

REFERENCES

Abbracchio, M. P., and Burnstock, G. (1994). Purinoceptors: are there families of P2X and P2Y purinoceptors? *Pharmacol. Ther.* 64, 445–475. doi: 10.1016/0163-7258(94)00048-4

Abbracchio, M. P., Burnstock, G., Verkhratsky, A., and Zimmermann, H. (2009). Purinergic signalling in the nervous system: an overview. *Trends Neurosci.* 32, 19–29. doi: 10.1016/j.tins.2008.10.001

Adinolfi, E., Cirillo, M., Woltersdorf, R., Falzoni, S., Chiozzi, P., Pellegatti, P., et al. (2010). Trophic activity of a naturally occurring truncated isoform of the P2X7 receptor. *FASEB J.* 24, 3393–3404. doi: 10.1096/fj.09-153601

Adriouch, S., Dox, C., Welge, V., Seman, M., Koch-Nolte, F., and Haag, F. (2002). Cutting edge: a natural P451L mutation in the cytoplasmic domain impairs the function of the mouse P2X7 receptor. *J. Immunol.* 169, 4108–4112. doi: 10.4049/jimmunol.169.8.4108

Ahern, G. P., Wang, X., and Miyares, R. L. (2006). Polyamines are potent ligands for the capsaicin receptor TRPV1. *J. Biol. Chem.* 281, 8991–8995. doi: 10.1074/jbc.M513429200

Babini, E., Paukert, M., Geisler, H.-S., and Grunder, S. (2002). Alternative splicing and interaction with di- and polyvalent cations control the dynamic range of acid-sensing ion channel 1 (ASIC1). *J. Biol. Chem.* 277, 41597–41603. doi: 10.1074/jbc.m205877200

Banke, T. G., Chaplan, S. R., and Wickenden, A. D. (2010). Dynamic changes in the TRPA1 selectivity filter lead to progressive but reversible pore dilation. *Am. J. Physiol. Cell Physiol.* 298, C1457–C1468. doi: 10.1152/ajpcell.00489.2009

Bernier, L.-P., Ase, A. R., Chevallier, S., Blais, D., Zhao, Q., Boué-Grabot, E., et al. (2008a). Phosphoinositides regulate $P2X_4$ ATP-gated channels through direct interactions. *J. Neurosci.* 28, 12938–12945. doi: 10.1523/JNEUROSCI.3038-08.2008

Bernier, L.-P., Ase, A. R., Tong, X., Hamel, E., Blais, D., Zhao, Q., et al. (2008b). Direct modulation of $P2X_1$ receptor-channels by the lipid phosphatidylinositol 4,5-bisphosphate. *Mol. Pharmacol.* 74, 785–792. doi: 10.1124/mol.108.047019

Bernier, L.-P., Ase, A. R., and Séguéla, P. (2017). P2X receptor channels in chronic pain pathways. *Br. J. Pharmacol.* 175, 2219–2230. doi: 10.1111/bph.13957

Birdsong, W. T., Fierro, L., Williams, F. G., Spelta, V., Naves, L. A., Knowles, M., et al. (2010). Sensing muscle ischemia: coincident detection of acid and ATP via interplay of two ion channels. *Neuron* 68, 739–749. doi: 10.1016/j.neuron.2010.09.029

Bixel, M. G., Weise, C., Bolognesi, M. L., Rosini, M., Brierly, M. J., Mellor, I. R., et al. (2001). Location of the polyamine binding site in the vestibule of the nicotinic acetylcholine receptor ion channel. *J. Biol. Chem.* 276, 6151–6160. doi: 10.1074/jbc.M008467200

Boué-Grabot, E., and Pankratov, Y. (2017). Modulation of central synapses by astrocyte-released ATP and postsynaptic P2X receptors. *Neural Plast.* 2017:9454275. doi: 10.1155/2017/9454275

Bowie, D., Lange, G. D., and Mayer, M. L. (1998). Activity-dependent modulation of glutamate receptors by polyamines. *J. Neurosci.* 18, 8175–8185. doi: 10.1523/JNEUROSCI.18-20-08175.1998

Boyce, A. K. J., Kim, M. S., Wicki-Stordeur, L. E., and Swayne, L. A. (2015). ATP stimulates pannexin 1 internalization to endosomal compartments. *Biochem. J.* 470, 319–330. doi: 10.1042/bj20141551

Brake, A. J., Wagenbach, M. J., and Julius, D. (1994). New structural motif for ligand-gated ion channels defined by an ionotropic ATP receptor. *Nature* 371, 519–523. doi: 10.1038/371519a0

Browne, L. E., Compan, V., Bragg, L., and North, R. A. (2013). P2X7 receptor channels allow direct permeation of nanometer-sized dyes. *J. Neurosci.* 33, 3557–3566. doi: 10.1523/JNEUROSCI.2235-12.2013

Burnstock, G. (1990). Overview. Purinergic mechanisms. *Ann. N Y Acad. Sci.* 603, 1–17; discussion 18. doi: 10.1111/j.1749-6632.1990.tb37657.x

Cankurtaran-Sayar, S., Sayar, K., and Ugur, M. (2009). P2X7 receptor activates multiple selective dye-permeation pathways in RAW 264.7 and human embryonic kidney 293 cells. *Mol. Pharmacol.* 76, 1323–1332. doi: 10.1124/mol.109.059923

Chataigneau, T., Lemoine, D., and Grutter, T. (2013). Exploring the ATP-binding site of P2X receptors. *Front. Cell. Neurosci.* 7:273. doi: 10.3389/fncel.2013.00273

Chaumont, S., and Khakh, B. S. (2008). Patch-clamp coordinated spectroscopy shows P2X2 receptor permeability dynamics require cytosolic domain rearrangements but not Panx-1 channels. *Proc. Natl. Acad. Sci. U S A* 105, 12063–12068. doi: 10.1073/pnas.0803008105

Cheewatrakoolpong, B., Gilchrest, H., Anthes, J. C., and Greenfeder, S. (2005). Identification and characterization of splice variants of the human $P2X_7$ ATP channel. *Biochem. Biophys. Res. Commun.* 332, 17–27. doi: 10.1016/j.bbrc.2005.04.087

Chung, M.-K., Güler, A. D., and Caterina, M. J. (2008). TRPV1 shows dynamic ionic selectivity during agonist stimulation. *Nat. Neurosci.* 11, 555–564. doi: 10.1038/nn.2102

Cockcroft, S., and Gomperts, B. D. (1979). ATP induces nucleotide permeability in rat mast cells. *Nature* 279, 541–542. doi: 10.1038/279541a0

Compan, V., Ulmann, L., Stelmashenko, O., Chemin, J., Chaumont, S., and Rassendren, F. (2012). P2X2 and P2X5 subunits define a new heteromeric receptor with P2X7-like properties. *J. Neurosci.* 32, 4284–4296. doi: 10.1523/JNEUROSCI.6332-11.2012

De Marchi, E., Orioli, E., Dal Ben, D., and Adinolfi, E. (2016). P2X7 receptor as a therapeutic target. *Adv. Protein Chem. Struct. Biol.* 104, 39–79. doi: 10.1016/bs.apcsb.2015.11.004

de Weille, J. R., Bassilana, F., Lazdunski, M., and Waldmann, R. (1998). Identification, functional expression and chromosomal localisation of a sustained human proton-gated cation channel. *FEBS Lett.* 433, 257–260. doi: 10.1016/s0014-5793(98)00916-8

Di Virgilio, F. (1995). The P2Z purinoceptor: an intriguing role in immunity, inflammation and cell death. *Immunol. Today* 16, 524–528. doi: 10.1016/0167-5699(95)80045-x

Di Virgilio, F., Dal Ben, D., Sarti, A. C., Giuliani, A. L., and Falzoni, S. (2017). The P2X7 receptor in infection and inflammation. *Immunity* 47, 15–31. doi: 10.1016/j.immuni.2017.06.020

Di Virgilio, F., Sarti, A. C., and Grassi, F. (2018). Modulation of innate and adaptive immunity by P2X ion channels. *Curr. Opin. Immunol.* 52, 51–59. doi: 10.1016/j.coi.2018.03.026

Ding, S., and Sachs, F. (1999). Single channel properties of $P2X_2$ purinoceptors. *J. Gen. Physiol.* 113, 695–720. doi: 10.1085/jgp.113.5.695

Duan, K., Yu, X., Zhang, C., and Zhou, Z. (2003). Control of secretion by temporal patterns of action potentials in adrenal chromaffin cells. *J. Neurosci.* 23, 11235–11243. doi: 10.1523/JNEUROSCI.23-35-11235.2003

Eickhorst, A. N., Berson, A., Cockayne, D., Lester, H. A., and Khakh, B. S. (2002). Control of $P2X_2$ channel permeability by the cytosolic domain. *J. Gen. Physiol.* 120, 119–131. doi: 10.1085/jgp.20028535

Fujiwara, Y., and Kubo, Y. (2004). Density-dependent changes of the pore properties of the $P2X_2$ receptor channel. *J. Physiol.* 558, 31–43. doi: 10.1113/jphysiol.2004.064568

Gordon, J. L. (1986). Extracellular ATP: effects, sources and fate. *Biochem. J.* 233, 309–319. doi: 10.1042/bj2330309

Gu, B. J., Rathsam, C., Stokes, L., McGeachie, A. B., and Wiley, J. S. (2009). Extracellular ATP dissociates nonmuscle myosin from $P2X_7$ complex: this dissociation regulates $P2X_7$ pore formation. *Am. J. Physiol. Cell Physiol.* 297, C430–C439. doi: 10.1152/ajpcell.00079.2009

Guerra, G. P., Rubin, M. A., and Mello, C. F. (2016). Modulation of learning and memory by natural polyamines. *Pharmacol. Res.* 112, 99–118. doi: 10.1016/j.phrs.2016.03.023

Habermacher, C., Dunning, K., Chataigneau, T., and Grutter, T. (2016a). Molecular structure and function of P2X receptors. *Neuropharmacology* 104, 18–30. doi: 10.1016/j.neuropharm.2015.07.032

Habermacher, C., Martz, A., Calimet, N., Lemoine, D., Peverini, L., Specht, A., et al. (2016b). Photo-switchable tweezers illuminate pore-opening motions of an ATP-gated P2X ion channel. *ELife* 5:e11050. doi: 10.7554/eLife.11050

Han, X., Tomitori, H., Mizuno, S., Higashi, K., Füll, C., Fukiwake, T., et al. (2008). Binding of spermine and ifenprodil to a purified, soluble regulatory domain of the N-methyl-d-aspartate receptor. *J. Neurochem.* 107, 1566–1577. doi: 10.1111/j.1471-4159.2008.05729.x

Harkat, M., Peverini, L., Cerdan, A. H., Dunning, K., Beudez, J., Martz, A., et al. (2017). On the permeation of large organic cations through the pore of ATP-gated P2X receptors. *Proc. Natl. Acad. Sci. U S A* 114, E3786–E3795. doi: 10.1016/j.bpj.2016.11.22514

Hattori, M., and Gouaux, E. (2012). Molecular mechanism of ATP binding and ion channel activation in P2X receptors. *Nature* 485, 207–212. doi: 10.1038/nature11010

Heppel, L. A., Weisman, G. A., and Friedberg, I. (1985). Permeabilization of transformed cells in culture by external ATP. *J. Membr. Biol.* 86, 189–196. doi: 10.1007/bf01870597

Hiasa, M., Miyaji, T., Haruna, Y., Takeuchi, T., Harada, Y., Moriyama, S., et al. (2014). Identification of a mammalian vesicular polyamine transporter. *Sci. Rep.* 4:6836. doi: 10.1038/srep06836

Jiang, L.-H., Rassendren, F., Mackenzie, A., Zhang, Y. H., Surprenant, A., and North, R. A. (2005). N-methyl-D-glucamine and propidium dyes utilize different permeation pathways at rat $P2X_7$ receptors. *Am. J. Physiol. Cell Physiol.* 289, C1295–C1302. doi: 10.1152/ajpcell.00253.2005

Karasawa, A., Michalski, K., Mikhelzon, P., and Kawate, T. (2017). The P2X7 receptor forms a dye-permeable pore independent of its intracellular domain but dependent on membrane lipid composition. *Elife* 6:e31186. doi: 10.7554/eLife.31186

Kawate, T., Michel, J. C., Birdsong, W. T., and Gouaux, E. (2009). Crystal structure of the ATP-gated $P2X_4$ ion channel in the closed state. *Nature* 460, 592–598. doi: 10.1038/nature08198

Khakh, B. S., and Alan North, R. (2006). P2X receptors as cell-surface ATP sensors in health and disease. *Nature* 442, 527–532. doi: 10.1038/nature04886

Khakh, B. S., and Egan, T. M. (2005). Contribution of transmembrane regions to ATP-gated $P2X_2$ channel permeability dynamics. *J. Biol. Chem.* 280, 6118–6129. doi: 10.1074/jbc.M411324200

Khakh, B. S., Bao, X. R., Labarca, C., and Lester, H. A. (1999). Neuronal P2X transmitter-gated cation channels change their ion selectivity in seconds. *Nat. Neurosci.* 2, 322–330. doi: 10.1038/7233

Khakh, B. S., Fisher, J. A., Nashmi, R., Bowser, D. N., and Lester, H. A. (2005). An angstrom scale interaction between plasma membrane ATP-gated $P2X_2$ and $\alpha_4\beta_2$ nicotinic channels measured with fluorescence resonance energy transfer and total internal reflection fluorescence microscopy. *J. Neurosci.* 25, 6911–6920. doi: 10.1523/JNEUROSCI.0561-05.2005

Khakh, B. S., and Lester, H. A. (1999). Dynamic selectivity filters in ion channels. *Neuron* 23, 653–658. doi: 10.1016/s0896-6273(01)80025-8

Khakh, B. S., and North, R. A. (2012). Neuromodulation by extracellular ATP and P2X receptors in the CNS. *Neuron* 76, 51–69. doi: 10.1016/j.neuron.2012.09.024

Kim, M., Jiang, L. H., Wilson, H. L., North, R. A., and Surprenant, A. (2001). Proteomic and functional evidence for a $P2X_7$ receptor signalling complex. *EMBO J.* 20, 6347–6358. doi: 10.1093/emboj/20.22.6347

Kracun, S., Chaptal, V., Abramson, J., and Khakh, B. S. (2010). Gated access to the pore of a P2X receptor: structural implications for closed-open transitions. *J. Biol. Chem.* 285, 10110–10121. doi: 10.1074/jbc.M109.089185

Kurata, H. T., Marton, L. J., and Nichols, C. G. (2006). The polyamine binding site in inward rectifier K^+ channels. *J. Gen. Physiol.* 127, 467–480. doi: 10.1085/jgp.200509467

Lemoine, D., Jiang, R., Taly, A., Chataigneau, T., Specht, A., and Grutter, T. (2012). Ligand-gated ion channels: new insights into neurological disorders and ligand recognition. *Chem. Rev.* 112, 6285–6318. doi: 10.1021/cr3000829

Li, M., Chang, T.-H., Silberberg, S. D., and Swartz, K. J. (2008). Gating the pore of P2X receptor channels. *Nat. Neurosci.* 11, 883–887. doi: 10.1038/nn.2151

Li, M., Kawate, T., Silberberg, S. D., and Swartz, K. J. (2010). Pore-opening mechanism in trimeric P2X receptor channels. *Nat. Commun.* 1:44. doi: 10.1038/ncomms1048

Li, M., Toombes, G. E. S., Silberberg, S. D., and Swartz, K. J. (2015). Physical basis of apparent pore dilation of ATP-activated P2X receptor channels. *Nat. Neurosci.* 18, 1577–1583. doi: 10.1038/nn.4120

Lingueglia, E., de Weille, J. R., Bassilana, F., Heurteaux, C., Sakai, H., Waldmann, R., et al. (1997). A modulatory subunit of acid sensing ion channels in brain and dorsal root ganglion cells. *J. Biol. Chem.* 272, 29778–29783. doi: 10.1074/jbc.272.47.29778

Lucifora, S., Willcockson, H. H., Lu, C.-R., Darstein, M., Phend, K. D., Valtschanoff, J. G., et al. (2006). Presynaptic low- and high-affinity kainate receptors in nociceptive spinal afferents. *Pain* 120, 97–105. doi: 10.1016/j.pain.2005.10.018

Madeo, F., Eisenberg, T., Pietrocola, F., and Kroemer, G. (2018). Spermidine in health and disease. *Science* 359:eaan2788. doi: 10.1126/science.aan2788

Mansoor, S. E., Lü, W., Oosterheert, W., Shekhar, M., Tajkhorshid, E., and Gouaux, E. (2016). X-ray structures define human $P2X_3$ receptor gating cycle and antagonist action. *Nature* 538, 66–71. doi: 10.1038/nature19367

Marques-da-Silva, C., Chaves, M., Castro, N., Coutinho-Silva, R., and Guimaraes, M. (2011). Colchicine inhibits cationic dye uptake induced by ATP in P2X2 and P2X7 receptor-expressing cells: implications for its therapeutic action. *Br. J. Pharmacol.* 163, 912–926. doi: 10.1111/j.1476-5381.2011.01254.x

Mony, L., Zhu, S., Carvalho, S., and Paoletti, P. (2011). Molecular basis of positive allosteric modulation of GluN2B NMDA receptors by polyamines. *EMBO J.* 30, 3134–3146. doi: 10.1038/emboj.2011.203

Mourot, A., Fehrentz, T., Le Feuvre, Y., Smith, C. M., Herold, C., Dalkara, D., et al. (2012). Rapid optical control of nociception with an ion-channel photoswitch. *Nat. Methods* 9, 396–402. doi: 10.1038/nmeth.1897

Murrell-Lagnado, R. D. (2017). Regulation of P2X purinergic receptor signaling by cholesterol. *Curr. Top. Membr.* 80, 211–232. doi: 10.1016/bs.ctm.2017.05.004

Nabissi, M., Morelli, M. B., Santoni, M., and Santoni, G. (2013). Triggering of the TRPV2 channel by cannabidiol sensitizes glioblastoma cells to cytotoxic chemotherapeutic agents. *Carcinogenesis* 34, 48–57. doi: 10.1093/carcin/bgs328

Nicke, A., Kuan, Y.-H., Masin, M., Rettinger, J., Marquez-Klaka, B., Bender, O., et al. (2009). A functional P2X7 splice variant with an alternative transmembrane domain 1 escapes gene inactivation in P2X7 knock-out mice. *J. Biol. Chem.* 284, 25813–25822. doi: 10.1074/jbc.M109.033134

North, R. A. (2002). Molecular physiology of P2X receptors. *Physiol. Rev.* 82, 1013–1067. doi: 10.1152/physrev.00015.2002

Nuttle, L. C., and Dubyak, G. R. (1994). Differential activation of cation channels and non-selective pores by macrophage $P2_Z$ purinergic receptors expressed in *Xenopus* oocytes. *J. Biol. Chem.* 269, 13988–13996.

Pelegrin, P., and Surprenant, A. (2006). Pannexin-1 mediates large pore formation and interleukin-1β release by the ATP-gated $P2X_7$ receptor. *EMBO J.* 25, 5071–5082. doi: 10.1038/sj.emboj.7601378

Pellegatti, P., Falzoni, S., Pinton, P., Rizzuto, R., and Di Virgilio, F. (2005). A novel recombinant plasma membrane-targeted luciferase reveals a new pathway for ATP secretion. *Mol. Biol. Cell* 16, 3659–3665. doi: 10.1091/mbc.e05-03-0222

Perrais, D., Veran, J., and Mulle, C. (2010). Gating and permeation of kainate receptors: differences unveiled. *Trends Pharmacol. Sci.* 31, 516–522. doi: 10.1016/j.tips.2010.08.004

Pippel, A., Stolz, M., Woltersdorf, R., Kless, A., Schmalzing, G., and Markwardt, F. (2017). Localization of the gate and selectivity filter of the full-length P2X7 receptor. *Proc. Natl. Acad. Sci. U S A* 114, E2156–E2165. doi: 10.1073/pnas.1610414114

Pougnet, J.-T., Toulme, E., Martinez, A., Choquet, D., Hosy, E., and Boué-Grabot, E. (2014). ATP P2X receptors downregulate AMPA receptor trafficking and postsynaptic efficacy in hippocampal neurons. *Neuron* 83, 417–430. doi: 10.1016/j.neuron.2014.06.005

Puopolo, M., Binshtok, A. M., Yao, G.-L., Oh, S. B., Woolf, C. J., and Bean, B. P. (2013). Permeation and block of TRPV1 channels by the cationic lidocaine derivative QX-314. *J. Neurophysiol.* 109, 1704–1712. doi: 10.1152/jn.00012.2013

Rassendren, F., Buell, G. N., Virginio, C., Collo, G., North, R. A., and Surprenant, A. (1997). The permeabilizing ATP receptor, $P2X_7$. Cloning and expression of a human cDNA. *J. Biol. Chem.* 272, 5482–5486. doi: 10.1074/jbc.272.9.5482

Riedel, T., Lozinsky, I., Schmalzing, G., and Markwardt, F. (2007a). Kinetics of $P2X_7$ receptor-operated single channels currents. *Biophys. J.* 92, 2377–2391. doi: 10.1529/biophysj.106.091413

Riedel, T., Schmalzing, G., and Markwardt, F. (2007b). Influence of extracellular monovalent cations on pore and gating properties of $P2X_7$ receptor-operated single-channel currents. *Biophys. J.* 93, 846–858. doi: 10.1529/biophysj.106.103614

Rokic, M. B., and Stojilkovic, S. S. (2013). Two open states of P2X receptor channels. *Front. Cell. Neurosci.* 7:215. doi: 10.3389/fncel.2013.00215

Saul, A., Hausmann, R., Kless, A., and Nicke, A. (2013). Heteromeric assembly of P2X subunits. *Front. Cell. Neurosci.* 7:250. doi: 10.3389/fncel.2013.00250

Savio, L. E. B., de Andrade Mello, P., da Silva, C. G., and Coutinho-Silva, R. (2018). The P2X7 receptor in inflammatory diseases: angel or demon? *Front. Pharmacol.* 9:52. doi: 10.3389/fphar.2018.00052

Sluyter, R. (2017). The P2X7 receptor. *Adv. Exp. Med. Biol.* 1051, 17–53. doi: 10.1007/5584_2017_59

Solini, A., Cuccato, S., Ferrari, D., Santini, E., Gulinelli, S., Callegari, M. G., et al. (2008). Increased $P2X_7$ receptor expression and function in thyroid papillary cancer: a new potential marker of the disease? *Endocrinology* 149, 389–396. doi: 10.1210/en.2007-1223

Sorge, R. E., Trang, T., Dorfman, R., Smith, S. B., Beggs, S., Ritchie, J., et al. (2012). Genetically determined P2X7 receptor pore formation regulates variability in chronic pain sensitivity. *Nat. Med.* 18, 595–599. doi: 10.1038/nm.2710

Stanchev, D., Blosa, M., Milius, D., Gerevich, Z., Rubini, P., Schmalzing, G., et al. (2009). Cross-inhibition between native and recombinant TRPV1 and $P2X_3$ receptors. *Pain* 143, 26–36. doi: 10.1016/j.pain.2009.01.006

Steinberg, T. H., Newman, A. S., Swanson, J. A., and Silverstein, S. C. (1987). ATP4-permeabilizes the plasma membrane of mouse macrophages to fluorescent dyes. *J. Biol. Chem.* 262, 8884–8888.

Steinberg, T. H., and Silverstein, S. C. (1989). "Chapter 3 ATP permeabilization of the plasma membrane," in *Methods in Cell Biology*, ed. A. M. Tartakoff (New York, NY: Academic Press), 45–61.

Stephan, G., Huang, L., Tang, Y., Vilotti, S., Fabbretti, E., Yu, Y., et al. (2018). The ASIC3/P2X3 cognate receptor is a pain-relevant and ligand-gated cationic channel. *Nat. Commun.* 9:1354. doi: 10.1038/s41467-018-03728-5

Suadicani, S. O., Brosnan, C. F., and Scemes, E. (2006). $P2X_7$ receptors mediate ATP release and amplification of astrocytic intercellular Ca^{2+} signaling. *J. Neurosci.* 26, 1378–1385. doi: 10.1523/JNEUROSCI.3902-05.2006

Surprenant, A., Rassendren, F., Kawashima, E., North, R. A., and Buell, G. (1996). The cytolytic P_{2Z} receptor for extracellular ATP identified as a P_{2X} receptor ($P2X_7$). *Science* 272, 735–738.

Swayne, L. A., and Boyce, A. K. J. (2017). Regulation of pannexin 1 surface expression by extracellular ATP: potential implications for nervous system function in health and disease. *Front. Cell. Neurosci.* 11:230. doi: 10.3389/fncel.2017.00230

Takeuchi, T., Harada, Y., Moriyama, S., Furuta, K., Tanaka, S., Miyaji, T., et al. (2017). Vesicular polyamine transporter mediates vesicular storage and release of polyamine from mast cells. *J. Biol. Chem.* 292, 3909–3918. doi: 10.1074/jbc.M116.756197

Tochitsky, I., Helft, Z., Meseguer, V., Fletcher, R. B., Vessey, K. A., Telias, M., et al. (2016). How azobenzene photoswitches restore visual responses to the blind retina. *Neuron* 92, 100–113. doi: 10.1016/j.neuron.2016.08.038

Valera, S., Hussy, N., Evans, R. J., Adami, N., North, R. A., Surprenant, A., et al. (1994). A new class of ligand-gated ion channel defined by P2X receptor for extracellular ATP. *Nature* 371, 516–519. doi: 10.1038/371516a0

Virginio, C., MacKenzie, A., North, R. A., and Surprenant, A. (1999a). Kinetics of cell lysis, dye uptake and permeability changes in cells expressing the rat $P2X_7$ receptor. *J. Physiol.* 519, 335–346. doi: 10.1111/j.1469-7793.1999.0335m.x

Virginio, C., MacKenzie, A., Rassendren, F. A., North, R. A., and Surprenant, A. (1999b). Pore dilation of neuronal P2X receptor channels. *Nat. Neurosci.* 2, 315–321. doi: 10.1038/7225

Wei, L., Caseley, E., Li, D., and Jiang, L.-H. (2016). ATP-induced P2X receptor-dependent large pore formation: how much do we know? *Front. Pharmacol.* 7:5. doi: 10.3389/fphar.2016.00005

Xu, X. J., Boumechache, M., Robinson, L. E., Marschall, V., Gorecki, D. C., Masin, M., et al. (2012). Splice variants of the P2X7 receptor reveal differential agonist dependence and functional coupling with pannexin-1. *J. Cell Sci.* 125, 3776–3789. doi: 10.1242/jcs.099374

Yan, Z., Li, S., Liang, Z., Tomić, M., and Stojilkovic, S. S. (2008). The $P2X_7$ receptor channel pore dilates under physiological ion conditions. *J. Gen. Physiol.* 132, 563–573. doi: 10.1085/jgp.200810059

Young, M. T., Pelegrin, P., and Surprenant, A. (2006). Identification of Thr_{283} as a key determinant of $P2X_7$ receptor function. *Br. J. Pharmacol.* 149, 261–268. doi: 10.1038/sj.bjp.0706880

Zubcevic, L., Le, S., Yang, H., and Lee, S.-Y. (2018). Conformational plasticity in the selectivity filter of the TRPV2 ion channel. *Nat. Struct. Mol. Biol.* 25, 405–415. doi: 10.1038/s41594-018-0059-z

Conflict of Interest Statement: The authors declare that the research was conducted in the absence of any commercial or financial relationships that could be construed as a potential conflict of interest.

frontiers in Cellular Neuroscience

ORIGINAL RESEARCH
published: 25 September 2018
doi: 10.3389/fncel.2018.00326

Purinergic Profiling of Regulatory T-cells in Patients With Episodic Migraine

Dilyara Nurkhametova[1,2†], Igor Kudryavtsev[3,4†], Olga Khayrutdinova[5†], Maria Serebryakova[3], Rashid Altunbaev[5‡], Tarja Malm[1] and Rashid Giniatullin[1,2]*

[1] A.I. Virtanen Institute for Molecular Sciences, University of Eastern Finland, Kuopio, Finland, [2] Laboratory of Neurobiology, Kazan Federal University, Kazan, Russia, [3] Department of Immunology, Institute of Experimental Medicine, St. Petersburg, Russia, [4] Department of Fundamental Medicine, Far Eastern Federal University, Vladivostok, Russia, [5] Department of Neurology and Rehabilitation, Kazan State Medical University, Kazan, Russia

Objectives: Immune responses in migraine are poorly characterized, yet implicated in the disease pathogenesis. This study was carried out to characterize purinergic profiles of T-cells in patients with episodic migraine without aura (MWoA) to provide mechanistic evidence for ATP and adenosine involvement in modulation of immune regulation in migraine.

Methods: Peripheral blood samples were obtained from patients with migraine (n = 16) and age-matched control subjects (n = 21). Subsets of T-cells were identified by flow cytometry based on specific membrane markers.

Results: Migraine patients showed reduced total T-cell counts in the peripheral blood. Whereas the total number of CD3+CD4+, CD3+CD8+, or regulatory T lymphocytes (Treg) was not changed, the proportion of Treg CD45R0+CD62L– and CD45R0–CD62L– cells was increased. Interestingly, in migraine, less Treg cells expressed CD39 and CD73 suggesting disrupted ATP breakdown to adenosine. The negative correlations were observed between the duration of migraine and the relative number of CD73+CD39– Tregs and total number of CD73-positive CD45R0+CD62L+ Tregs.

Conclusion: Obtained data indicate that T-cell populations are altered in episodic migraine and suggest the involvement of Tregs in the pathophysiology of this disorder. Reduced expression of CD39 and CD73 suggests promotion of ATP-dependent pro-inflammatory and reduction of adenosine-mediated anti-inflammatory mechanisms in migraine.

Keywords: purinergic signaling, ATP, adenosine, regulatory T cells, migraine

OPEN ACCESS

Edited by:
Eric Boué-Grabot, Université de Bordeaux, France

Reviewed by:
Cecile Delarasse, Institut National de la Santé et de la Recherche Médicale (INSERM), France
Beata Sperlagh, Institute of Experimental Medicine (MTA), Hungary

***Correspondence:**
Rashid Giniatullin
Rashid.Giniatullin@uef.fi

[†] These authors have contributed equally to this work

[‡] Deceased 29 December 2016

Received: *14 June 2018*
Accepted: *07 September 2018*
Published: *25 September 2018*

Citation:
Nurkhametova D, Kudryavtsev I, Khayrutdinova O, Serebryakova M, Altunbaev R, Malm T and Giniatullin R (2018) Purinergic Profiling of Regulatory T-cells in Patients With Episodic Migraine. Front. Cell. Neurosci. 12:326. doi: 10.3389/fncel.2018.00326

INTRODUCTION

Migraine is a very common neurological disorder in the modern population. There are two main types of migraine: migraine with aura (MWA) and migraine without aura (MWoA). Migraine aura is presented with 'recurrent attacks, lasting minutes, of unilateral fully reversible visual, sensory, or other central nervous system symptoms that usually develop gradually and are usually

followed by headache and associated migraine symptoms' (Headache Classification Committee of the International Headache Society (IHS), 2018) ICHD-3. Currently, it is generally accepted that migraine aura is associated with the phenomenon called cortical spreading depression which is a slowly propagating wave of depolarization of brain cells (Somjen, 2001).

Recent evidence suggests the involvement of immune system in the pathogenesis of migraine. Nociceptive trigeminal nerves in dura mater, a likely source of migraine pain (Moskowitz and Cutrer, 1993; Bolay et al., 2002; Olesen et al., 2009; Zakharov et al., 2015), are surrounded by mast cells (Levy, 2009; Kilinc et al., 2017) and T-cells, apparently associated with recently discovered meningeal lymphatic vessels (Aspelund et al., 2015; Louveau et al., 2015). These findings are consistent with local inflammatory reactions leading to neuroinflammation in meninges. The idea of local neurogenic inflammation (sterile inflammation) due to release of neuropeptides from meningeal nerves in migraine was first suggested by M. Moskowitz with colleagues (Moskowitz et al., 1979; Moskowitz and Cutrer, 1993). This view was further developed by many other researchers suggesting involvement of various immune cells and pro-inflammatory substances in development of local meningeal inflammation (Strassman et al., 1996; Reuter et al., 2001, Peroutka, 2005; Levy, 2009; Ramachandran, 2018). In addition, several recent studies have revealed signs of systemic inflammation in migraine. Specifically, the levels of C-reactive protein (CRP) are elevated in serum of migraine patients (Welch et al., 2006; Vanmolkot and de Hoon, 2007). During migraine attacks procalcitonin, another marker of inflammation, is also elevated (Turan et al., 2011). Moreover, a soluble urokinase-type plasminogen activator receptor (suPAR) has been suggested as a prognostic marker for migraine, especially during attack periods. The levels of SuPAR have been reported to be elevated during migraine attack compared to healthy individuals and patients with migraine in the interictal period (Yılmaz et al., 2017).

These data are in line with reported increased levels of several pro-inflammatory cytokines, such as interleukin-1β (IL-1β), IL-6, and tumor necrosis factor-alpha (TNFα) in serum of migraineurs (Sarchielli et al., 2006; Wang et al., 2015; Yücel et al., 2016). Importantly, plasma levels of pro-inflammatory IL-1α and TNFα are elevated not only in adults but also in children with migraine (Bońkowski et al., 2009). At the same time the plasma levels of anti-inflammatory cytokine IL-10, produced by T-cells, are increased during attacks in patients with migraine without aura (Munno et al., 2001). These data indicate that the local (in dura mater) as well as systemic (triggered by cytokines with pleiotropic effects) inflammation are implicated in the pathogenesis of migraine.

The systemic inflammatory reactions are largely mediated by T-cells. T-cells are categorized in subpopulations based on their functional properties and these can be identified based on their expression of specific cell surface markers. From the various T-cell populations, such as helper (CD3+CD4+), cytotoxic (CD3+CD8+) and regulatory (CD3+CD4+CD25high) T cells, the regulatory T cells (Tregs) are specialized in immune suppression and have been recognized as key players in regulation of inflammation (Vignali et al., 2008). Recently the anti-inflammatory capacity of Tregs was suggested to be mediated by purinergic mechanisms and their ability to convert ATP to adenosine via the function of cell-surface ecto-nucleoside triphosphate diphosphohydrolase 1, E-NTPDase1 (CD39), and ecto-5′-nucleotidase (CD73) (Grant et al., 2015; de Oliveira Bravo et al., 2016; Rueda et al., 2016). ATP is known as a powerful pro-inflammatory compound and its concentration is dramatically elevated during inflammation and tissue damage (la Sala et al., 2003). ATP is dephosphorylated by CD39 expressed on Tregs to form ADP/AMP, which is further converted to anti-inflammatory adenosine by CD73. This reaction likely underlies the immunosuppressive effects of Tregs (Takenaka et al., 2016).

Albeit for evidence pointing toward the involvement of T-cells in the pathogenesis of migraine, no studies have analyzed the levels of specific T-cell subtypes in migraine. Here we show for the first time that the level of immunosuppressive Tregs are reduced in migraine patients. Furthermore, we demonstrate that the Treg expression of CD39 and CD73 is reduced suggesting promotion of purinergic mechanisms of inflammation. Our study supports the involvement of systemic inflammatory responses in the disease course of migraine.

MATERIALS AND METHODS

General Description of Patients

Total of 38 patients were assessed for correspondence to inclusion criteria. The criteria were age 18 to 55 years and previously diagnosed migraine without aura, as defined in The International Classification of Headache Disorders-3-beta. Exclusion criteria were oncology, pregnancy, breast-feeding, chronic diseases in stage of decompensation, and migraine with aura. Of initial set of patients, 23 fulfilled inclusion criteria. Twelve patients had oncology, pregnancy or breast feeding, three had migraine with aura, seven declined to participate in the study.

16 patients (all females) were included in the final analysis. **Table 1** provides patients' detailed demographic characteristics.

The data were compared to the results obtained from 21 age-matched healthy female volunteers. Current study was approved by the Medical Ethics Committee of Kazan State Medical University (Kazan, Russia) (protocol No 10 from 20.12.2016). All participants provided written informed consent in accordance with the 2013 Declaration of Helsinki.

Sample Collection

All experiments were performed on the day of blood collection. Peripheral blood samples were collected into vacuum test tubes containing the K3-EDTA anti-coagulant (cat. 2130122, Weihai Hongyu Medical Devices Co., Ltd, China) and then processed to analyze the frequency of T-cell subsets by using flow cytometry.

TABLE 1 | Clinical and demographic characteristics of patients with migraine without aura.

Number of patients	Age	Disease duration (years)	Attacks frequency/per month	Max intensity VAS	Attack duration	Number of days after last attack
1	26	11	8	10	~24 h	4
2	26	2	2	6	~24 h	35
3	37	10	2	7	~48 h	17
4	48	20	3	9	~72 h	10
5	28	3	1	7	~24 h	7
6	37	10	2	8	~24 h	4
7	55	20	4	10	~24 h	2
8	36	15	3	8	~48 h	6
9	47	15	2	8	~24 h	6
10	38	6	0.5	10	~24 h	28
11	21	6	2	6	~48 h	5
12	53	20	8	9	~72 h	2
13	40	10	5	8	~72 h	1
14	41	11	3	7	~48 h	7
15	45	20	1	8	~24 h	14
16	35	6	1	7	~24 h	12

Multicolor Flow Cytometry Assay

The subsets of T cells were analyzed using CytoFLEX and Navios flow cytometers (Beckman Coulter, United States). In brief, 100 μl of peripheral blood was stained with the following cocktail of anti-human antibodies: CD39-FITC (clone A1, cat. 328206, BioLegend, Inc., United States), CD25-PE (clone B1.49.9, cat. A07774, Beckman Coulter, United States), CD62L-ECD (clone DREG56, cat. IM2713U, Beckman Coulter, United States), CD45R0-PC5.5 (clone UCHL1, cat. IM2712U, Beckman Coulter, United States), CD4-PC7 (clone SFCI12T4D11 (T4), cat 737660, Beckman Coulter, United States), CD8-APC (clone B9.11, cat. IM2469, Beckman Coulter, United States), CD3-APC-Alexa Fluor 750 (clone UCHT1, cat. A94680, Beckman Coulter, United States), CD73-Pacific Blue (clone AD2, cat. 344012, BioLegend, Inc., United States) and CD45-Krome Orange (clone J33, cat. A96416, Beckman Coulter, United States). Optimal combinations of antibodies directly conjugated with various fluorochromes were used according to that of previously published (Mahnke and Roederer, 2007). Stainings were carried out in dark at room temperature for 15 min after which red blood cells were lysed by adding 975 μl VersaLyse Lysing Solution (cat. A09777, Beckman Coulter, United States) supplied with 25 μl of IOTest 3 Fixative Solution (cat. A07800, Beckman Coulter, United States) in dark at room temperature for 15 min. The samples were washed once with PBS for 7 min at 330g, resuspended in 250 μl of PBS supplied with 2% of neutral formalin (cat. HT5011-1CS, Sigma-Aldrich Co., United States) and subjected to flow cytometry analysis.

Gating Strategy of Main T-cell Subsets

Gating scheme used for identification of T cell subsets is shown in **Figure 1**. Helper T (Th) and cytotoxic T cells (Tcyt) were immunophenotyped by using the CD3, CD4, and CD8 antibodies. Th were identified as CD3+CD4+, while Tcyt were CD3+CD8+. Tregs were characterized by the expression of CD3, CD4 and high levels of the IL-2R alpha chain (CD25high). T cell differentiation subsets were defined based on expression pattern of CD45R0 and CD62L as 'naïve' (N, CD45R0–CD62L+), central memory (CM, CD45R0+CD62L+), effector memory (EM, CD45R0+CD62L–), and terminally differentiated CD45RA-positive effector T-cells (TEMRA, CD45R0–CD62L–) (Gronert et al., 2015; Ambada et al., 2017). The expression of CD39 and CD73 was evaluated in all above mentioned T-cell subsets. The raw data supporting the conclusions of this manuscript will be made available by the authors, without undue reservation, to any qualified researcher.

Statistical Analysis

The data were analyzed by using CytExpert Software v.1.1 and Kaluza^{TM} software v.1.5a (Beckman Coulter, United States), Statistica 8 Software (Quest Software Inc., United States) and GraphPad Prism 4 (GraphPad Software, United States). The Shapiro-Wilk's W test was used to test data for normality. Mann-Whitney U test was employed for comparisons between two different groups of samples. Correlations were evaluated by the Spearman rank correlation test. All data were expressed as mean ± SEM. The level of significance was set as $p < 0.05$.

RESULTS

Clinical Description of Patients

The clinical characteristics of patients are shown in **Table 1**. The age of the patients ranged from 21 to 55 years (40.3 ± 2.6). The intensity of pain in most cases was at the level 7–10 (8.0 ± 0.3, visual analog scale (VAS)) with frequency of attacks varying from 0.5 up to 8 per month (2.7 ± 0.6) and disease duration from 2 to 20 years (years from diagnosis made). The patients did not

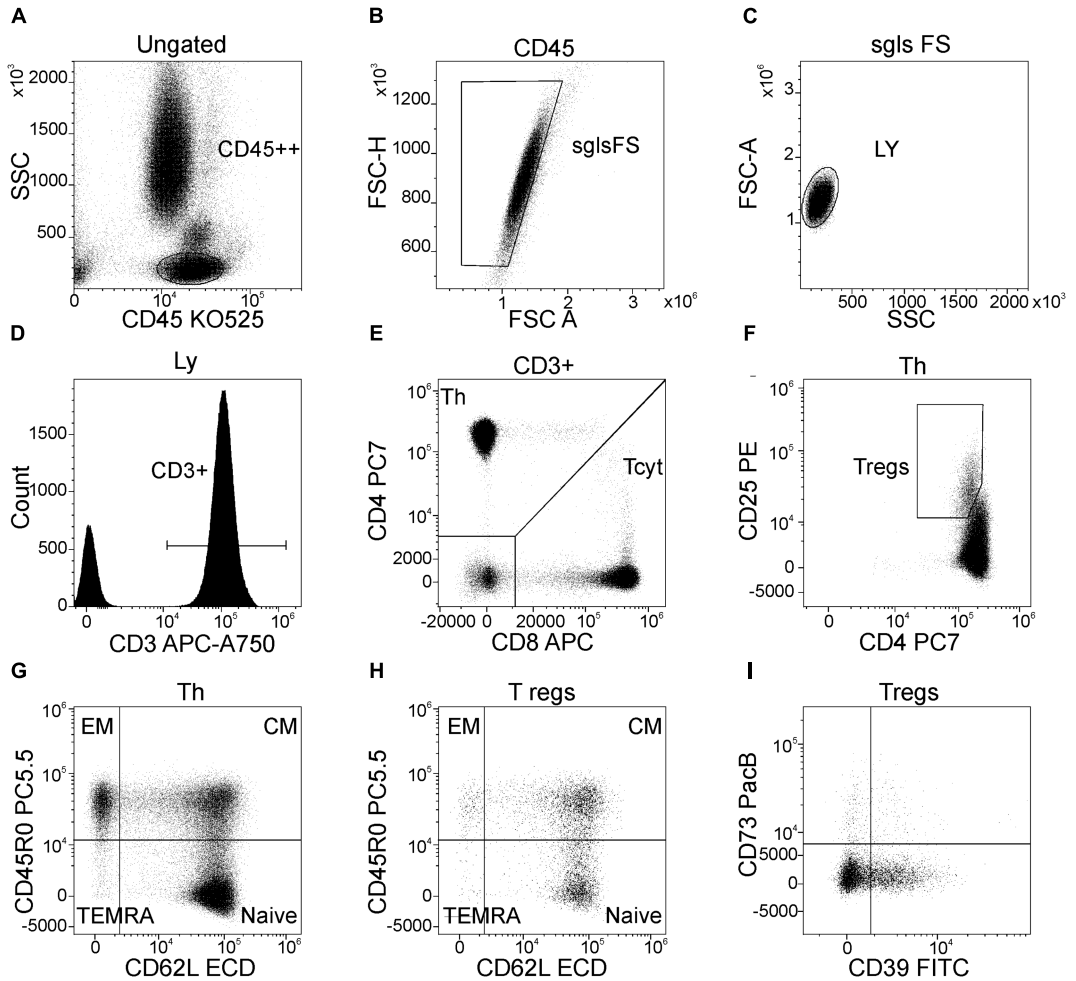

FIGURE 1 | Flow cytometric gating strategy used to identify main peripheral blood T-cell subsets, their differentiation stages, and the expression of CD39 and CD73 by Treg subsets. **(A)** Lymphocytes were selected on the side scatter (SSC) versus CD45 expression plot with a gate "CD45++"; **(B)** Discrimination of lymphocyte doublets, single T-cell gating based on FSC H versus FSC A (the region "sgls FS" is set on single cells); **(C)** All lymphocytes were gated on the side scatter/forward scatter plot with a gate "LY"; **(D)** T-cells were identified from the gate of lymphocytes as "CD3+" within total lymphocyte subset; **(E)** Th (CD3+CD4+) and cytotoxic T-cells (CD3+CD8+) were identified within CD3-positive cells based on CD4 and CD8 expression, respectively; **(F)** Regulatory T-cells (Tregs) were purified as CD4+CD25hi subset within total CD3+CD4+ cells; **(G)** Dot plot representing the expression of CD45R0 and CD62L by Th cells, naïve Th cells are CD45R0–CD62L+, central memory cells are CD45R0+CD62L+, effector memory cells are CD45R0+CD62L– and effector or "terminally-differentiated" Th cells are CD45R0–CD62L– (the same dot plot was used to identify the same differentiation stages of cytotoxic T-cells); **(H)** main differentiation stages of Tregs (the quadrant gate is set at the same position as for total Th cells as well as for cytotoxic T-cells, for that purpose linked quadrant gates were used); **(I)** expression of CD39 and CD73 by total Treg subsets (the same dot plots with the same position of quadrant gates were used when the expression of CD39 and CD73 by naïve, CM, and EM Treg subsets were studied).

take migraine medications at least two days prior the analysis, except for one patient who used migraine medication one day prior the blood sampling (this patient was excluded from the final analysis).

Migraine Patients Show Increased Levels of EM and TEMRA Treg Cells

Figure 1 demonstrates the gating strategy for our flow cytometric analysis. Our data revealed that the total CD3+ T cell population was slightly decreased in migraine patients compared to healthy controls (p = 0.021, **Table 2**). We further evaluated the percentages of various subsets of T cells that express different patterns of CD45R0 and CD62L (**Figure 2**). Quantitative analysis revealed that the total proportions of Tcyt, Th, and Tregs were not significantly altered in patients with migraine (**Table 2**). However, the percentage of effector memory (EM) and terminally differentiated CD45RA-positive effector (TEMRA) Treg subsets were significantly increased in the peripheral blood from migraine patients (**Table 2** and **Figure 2**).

Changed Expression of CD73 and CD39 by Treg Subsets in Patients With Migraine

We next characterized the expression of CD73 and CD39 on the peripheral blood Treg subsets at different stages of Treg

TABLE 2 | The relative number of main T-cell subsets in peripheral blood from healthy volunteers and patients with migraine (percentage of T-cell subsets in total lymphocyte subset, data are mean ± SEM.

Main subsets	Control, %	Migraine, %	p
	Mean ± SEM	Mean ± SEM	
Total T-cells	77.04 ± 0.98	72.07 ± 1.66	0.021
Total Tcyt (CD3+CD8+)	26.1 ± 1.44	23.6 ± 1.43	0.198
'naïve' Tcyt (CD45R0–CD62L+)	9.37 ± 1.02	8.75 ± 0.98	0.806
CM Tcyt (CD45R0+CD62L+)	1.46 ± 0.19	1.25 ± 0.18	0.520
EM Tcyt (CD45R0+CD62L–)	6.10 ± 0.69	4.72 ± 0.96	0.061
TEMRA Tcyt (CD45R0–CD62L–)	9.19 ± 0.92	8.92 ± 0.83	0.736
Total Th (CD3+CD4+)	47.56 ± 1.25	44.95 ± 1.18	0.177
'naive' Th (CD45R0–CD62L+)	22.8 ± 1.65	20.67 ± 1.16	0.481
CM Th (CD45R0+CD62L+)	13.7 ± 0.59	12.85 ± 0.74	0.244
EM Th (CD45R0+CD62L–)	9.61 ± 0.65	9.77 ± 0.41	0.939
TEMRA Th (CD45R0–CD62L–)	1.47 ± 0.33	1.65 ± 0.31	0.141
Total Treg (CD3+CD4+CD25high)	2.98 ± 0.17	3.54 ± 0.24	0.177
'naive' Treg (CD45R0–CD62L+)	1.09 ± 0.12	1.27 ± 0.11	0.297
CM Treg (CD45R0+CD62L+)	1.56 ± 0.08	1.69 ± 0.16	0.902
EM Treg (CD45R0+CD62L–)	0.32 ± 0.03	0.49 ± 0.05	0.004
TEMRA Treg (CD45R0–CD62L–)	0.019 ± 0.004	0.086 ± 0.011	< 0.001

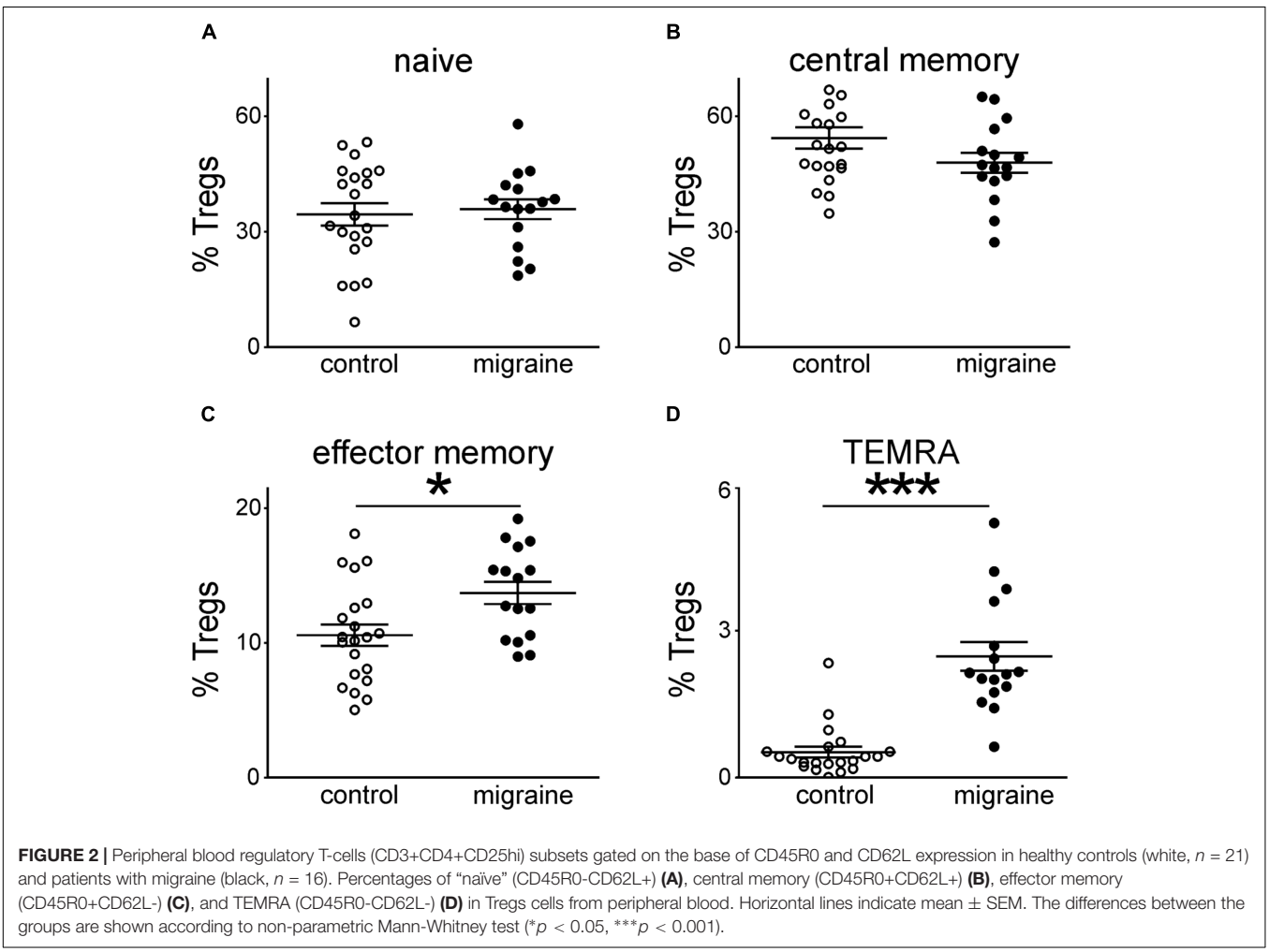

FIGURE 2 | Peripheral blood regulatory T-cells (CD3+CD4+CD25hi) subsets gated on the base of CD45R0 and CD62L expression in healthy controls (white, $n = 21$) and patients with migraine (black, $n = 16$). Percentages of "naïve" (CD45R0-CD62L+) **(A)**, central memory (CD45R0+CD62L+) **(B)**, effector memory (CD45R0+CD62L-) **(C)**, and TEMRA (CD45R0-CD62L-) **(D)** in Tregs cells from peripheral blood. Horizontal lines indicate mean ± SEM. The differences between the groups are shown according to non-parametric Mann-Whitney test (*$p < 0.05$, ***$p < 0.001$).

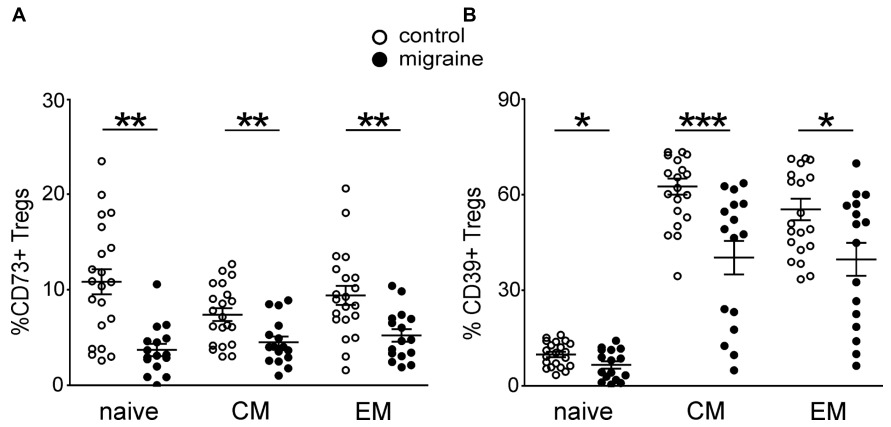

FIGURE 3 | CD73 and CD 39 expression by Treg subsets gated based on CD45R0 and CD62L expression in healthy controls (white, $n = 21$) and migraine patients (black, $n = 16$). **(A)** Percentages of CD73-positive cells within "naïve" (CD45R0-CD62L+), central memory (CD45R0+CD62L+), and effector memory (CD45R0+CD62L-) Tregs. **(B)** Percentages of CD39-positive cells within "naïve" (CD45R0-CD62L+), central memory (CD45R0+CD62L+), effector memory (CD45R0+CD62L-) Tregs. Horizontal lines indicate mean ± SEM. The differences between the groups are shown according to non-parametric Mann-Whitney test (*$p < 0.05$, **$p < 0.01$, ***$p < 0.001$).

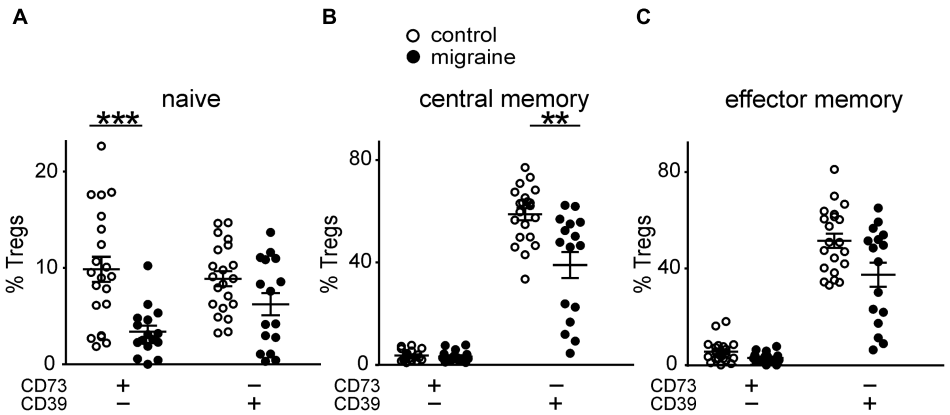

FIGURE 4 | Co-expression of CD39 and CD73 by Treg subsets gated based on the CD45R0 and CD62L expression in healthy controls (white, $n = 21$) and patients with migraine (black, $n = 16$). Percentages of CD73+CD39- and CD73-CD39+ cells within "naïve" (CD45R0-CD62L+) **(A)**, central memory (CD45R0+CD62L+) **(B)**, effector memory (CD45R0+CD62L-) **(C)** Tregs. Horizontal lines indicate mean ± SEM. The differences between the groups are shown according to non-parametric Mann-Whitney test (**$p < 0.01$, ***$p < 0.001$).

maturation in migraine patients (**Figure 3**). From the total Treg subset 8.96 ± 0.83% and 42.4 ± 3.13% of the cells were positive for CD73+ and CD39+, respectively, in the control group whereas in patients with migraine the proportion of these cell was significantly lower. Thus, only 4.53 ± 0.56% and 27.6 ± 3.63% of Tregs were CD73 or CD39-positive ($p < 0.001$ and $p = 0.006$, respectively). Our data also show that migraine is associated with reduction of CD73 and CD39 expression in all subsets of Tregs. In healthy controls 10.8 ± 1.32% of the 'naïve' CD62L+CD45RO- Tregs were CD73+ and 9.8 ± 0.84% were CD39+, while in patients with migraine these values were significantly lower (3.7 ± 0.64% and 6.5 ± 1.17%, respectively) (**Figure 3**). Similar decrease in the expression of CD39 and CD73 was also observed in CM and EM Tregs (**Figure 3**).

We further measured the number of cells, which express either one of the molecules CD39/CD73 or co-express both of them.

Patients with migraine had significantly less CD73+CD39– 'naïve' Tregs when comparing to control group (3.37 ± 0.64% and 9.86 ± 1.3%, respectively, $p < 0.001$ (**Figure 4A**). The number of CD73–CD39+ cells in 'naïve' Tregs tended to be lower in migraine patients (6.23 ± 1.15% versus 8.87 ± 0.78% in control), although this difference did not reach a significance (**Figure 4A**).

No significant differences were found in CD73+CD39– CM Tregs between migraine patients and healthy volunteers (**Figure 4B**). However, the relative number of CD73–CD39+ CM Tregs was significantly higher ($p = 0.002$) in control group (**Figure 4B**).

Co-expression of CD73 and CD39 on effector memory Tregs did not significantly differ between the groups (**Figure 4C**).

Patients with migraine had higher levels of Tregs negative for both CD73 and CD39 (**Figure 5A**) and correspondingly lower levels of CD73+CD39+ Tregs (**Figure 5B**).

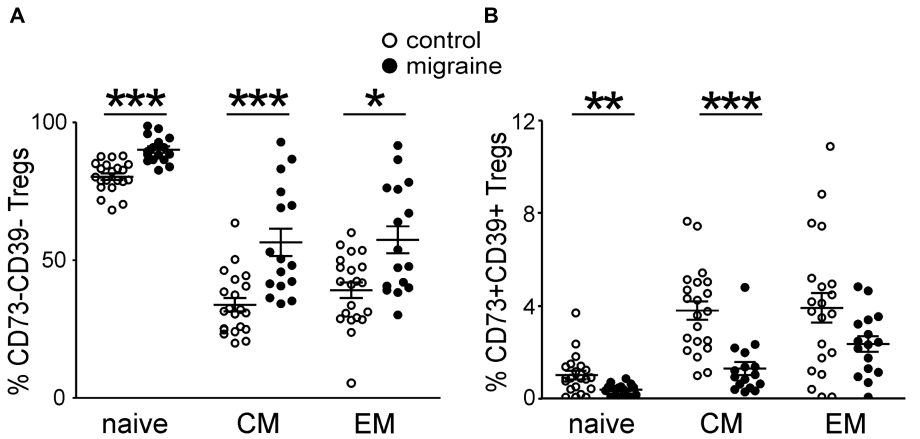

FIGURE 5 | Co-expression of CD39 and CD73 by Treg subsets gated based on the CD45R0 and CD62L expression in healthy controls (white, $n = 21$) and patients with migraine (black, $n = 16$). Percentage of CD73-CD39- **(A)** and CD73+CD39+ **(B)** in "naïve", central memory, and effector memory Tregs. Horizontal lines indicate mean ± SEM. The differences between the groups are shown according to non-parametric Mann-Whitney test (*$p < 0.05$, **$p < 0.01$, ***$p < 0.001$).

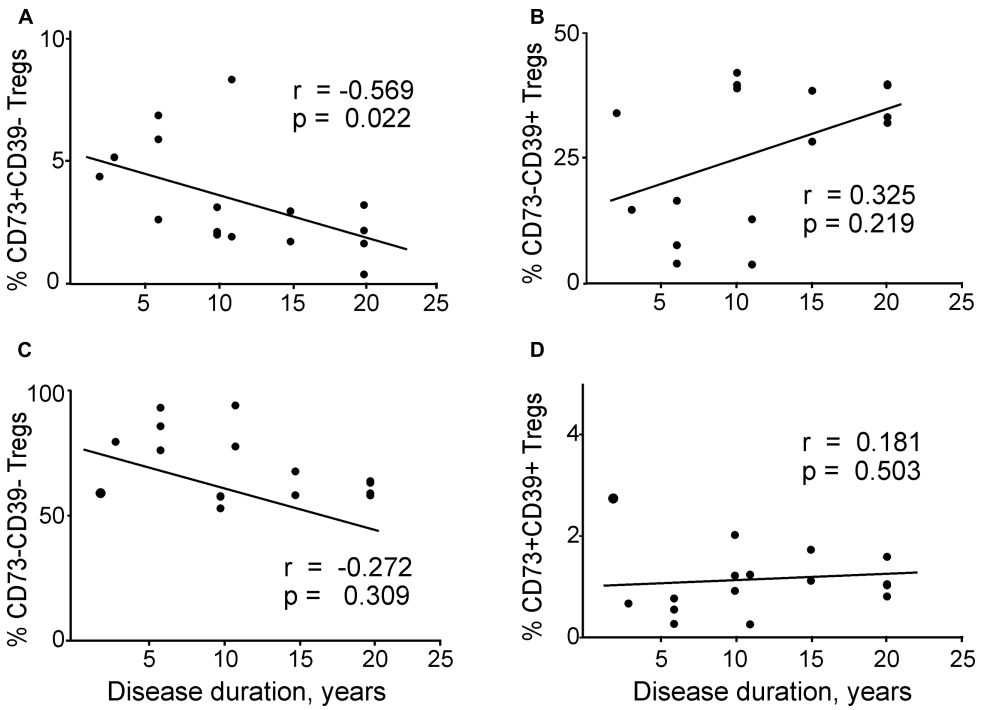

FIGURE 6 | Correlations between disease duration and regulatory T cells expressing different patterns of CD73 and CD39 in patients with migraine according to Spearman rank correlation test: **(A)** CD73+CD39–, **(B)** CD73–CD39+, **(C)** CD73–CD39–, **(D)** CD73+CD39+ in patients with migraine.

Then we analyzed the association between the disease duration and co-expression of CD73 and CD39 in Tregs (**Figure 6**). We found a significant negative correlation between disease duration and CD73+CD39– Tregs (**Figure 6A**). CD73–CD39– subset of general Tregs population also had a tendency to negative correlate with disease duration (**Figure 6C**), however the values did not reach significance. In contrast, CD73–CD39+ and CD73+CD39+ subsets did not correlate with the disease duration (**Figures 6B,D**).

Additionally, duration of migraine negatively correlated with the central memory Tregs subset expressing CD73+, including CD73+CD39- CM Tregs (**Supplementary Figures 1A,B**) but not with expression of CD39+ (**Supplementary Figures 1C,D**). We also explored the correlation between the expression of CD39 and CD73 in Tregs and the number of days after attack (**Supplementary Figure 2**). However, in contrast to the duration of migraine, this analysis failed to reveal significant correlations ($p > 0.05$ for all combinations of CD39 and CD73 expression in Tregs).

DISCUSSION

Here we describe for the first time changes in Treg subsets and their CD39/73 expression in patients suffering from migraine. The most important finding of our study was that Tregs showed remarkable migraine-associated changes in their expression of CD39 and CD73. These enzymes control the levels of ATP and adenosine - two key purinergic compounds recently emerged as potential modulators of migraine pathology.

Despite accumulating evidence of local and systemic inflammation in migraine, there is only one study of Tregs in this disorder (Arumugam and Parthasarathy, 2016). This study reported that migraine patients, compared to healthy volunteers, exhibited significantly higher percentage of Th cells in their peripheral blood and their Tcyt cell population was significantly reduced (Arumugam and Parthasarathy, 2016). We also observed a trend toward reduced number of Tcyt, however these changes failed to reach statistical significance. Arumugam and Parthasarathy (2016) also suggested the presence of autoimmune response in migraine based on their findings of lower levels of Tregs in patients with migraine. However, purinergic mechanisms including expression of CD39 and CD73 which are important for the function of Tregs (Kobie et al., 2006; Borsellino et al., 2007) were not studied.

Tregs have attracted much attention recently as immune cells capable of controlling excessive inflammation and likely play a crucial role in the maintenance of immune balance (Sakaguchi et al., 2010). There are several mechanisms how Tregs suppress the adaptive immune responses (Vignali et al., 2008). The most well-known is the production of anti-inflammatory cytokines such as IL-10, IL-35 and TGF-β (Grant et al., 2015; Rueda et al., 2016). Tregs can also induce apoptosis of effector T cells through formation of adenosine via CD39/CD73-controlled pathways (Kobie et al., 2006; Borsellino et al., 2007; Grant et al., 2015; Rueda et al., 2016). Notably, the lack of CD39 (Li et al., 2015; Yoshida et al., 2015) or CD73 (Ehrentraut et al., 2013; Wang et al., 2013) may diminish the function of Tregs.

Previous studies showed that calcitonin gene-related peptide (CGRP) – the main mediator of migraine – is involved in the differentiation and polarization of T cells (reviewed by Granstein et al., 2015; Hu et al., 2016). It has been found that CGRP transfected dendritic cells are able to increase the differentiation of CD4+CD25+Foxp3+ Tregs (Matsuda et al., 2012). Whereas this peptide triggers the secretion of pro-inflammatory cytokines from cultured trigeminal glial cells (Thalakoti et al., 2007), in T cells, CGRP promotes expression of the main lineage-specification factor of Tregs, Foxp3 (Rochlitzer et al., 2016; Szklany et al., 2016). Notably, CGRP levels have been reported to be significantly increased in serum of patients with chronic migraine (Ashina et al., 2000; Cernuda-Morollón et al., 2014). In addition, CGRP stimulates the release of ATP in the trigeminovascular system (Yegutkin et al., 2016) and can sensitize ATP receptors in trigeminal neurons (Giniatullin et al., 2008).

Tregs are highly heterogeneous population of peripheral blood lymphocytes and include several subsets. Different classifications of Tregs are used in clinical studies based on their expression of various functional antigens (Sakaguchi et al., 2010; Gronert et al., 2015; Ambada et al., 2017). In our work we identified subsets of Tregs based on their expression of CD45R0 and CD62L, as outlined by previous studies (Sakaguchi et al., 2010; Gronert et al., 2015; Ambada et al., 2017). Out of the four main Treg subsets – 'naïve', CM, EM, and TEMRA – we found that the last two were significantly higher in the peripheral blood of migraine patients. Together with CCR7, CD62L is the main antigen responsible for 'homing' of T cells to lymphoid tissues. Notably, the latter two Treg subsets lack the expression of CD62L and they have the ability to migrate to peripheral tissues and participate to the suppression of inflammatory reactions. This may be specifically important to migraine-associated neuroinflammation in the meningeal tissues (Pietrobon and Moskowitz, 2013). The changes we observed here in the subsets of Tregs in migraine patients suggest that these reactive cells can contribute to the suppression of migraine-related neuroinflammatory processes in the peripheral tissues.

Another important aspect of this study was the profile of CD39 and CD73, molecules implicated in purinergic signaling. ATP is currently recognized as a key player in triggering neuroinflammatory processes (Burnstock, 2016; Chen et al., 2017) and implicated in migraine pathology (Burnstock, 1981; Magni and Ceruti, 2013; Yegutkin et al., 2016; Zakharov et al., 2016). One key enzyme responsible for the fast deactivation of the pro-nociceptive and pro-inflammatory extracellular ATP is CD39, whereas CD73 is responsible for the transformation of ADP and AMP into anti-nociceptive adenosine (Yegutkin, 2008).

CD39 is expressed in various T cells, including Tregs, and in other effector T helper subsets, such as Th1 and Th17 cells. CD39+ Tregs are more effective than CD39- Tregs in the production of the anti-inflammatory TGF-β in response to activation (Fletcher et al., 2009). Furthermore, CD4+CD25highCD39+ Tregs are effective in suppressing the pro-inflammatory IL-17 implicated in pathological pain (Hung et al., 2017). In contrast, CD4+CD25highCD39- Tregs do not suppress IL-17 secretion (Fletcher et al., 2009). CD39 expression is upregulated in T cells following their infiltration into ATP-rich tissues, such as into tumor microenvironments (Bono et al., 2015). We found that the number of Tregs expressing CD39 was significantly lower in migraine patients, suggesting the accumulation of pro-inflammatory ATP in the extracellular space. This effect was highly significant in the 'naïve', CM, and EM Treg subsets. As on potential mechanism for this, we could thus hypothesize that the levels of CD39+CD73+ Tregs were reduced in the systemic circulation because they were recruited to meningeal tissues.

In contrast to high CD39 expression on Tregs, CD73 expression was relatively low. Thus, about 80% in the CD4+CD25high subset were CD39 positive, but only 1–7% of Tregs expressed CD73 on their cell membrane (Mandapathil et al., 2010). Similar to CD39, we found down-regulation in the expression of CD73 in patients' Tregs. Furthermore, this reduction was present in the 'naïve', CM, and EM CD73-positive Tregs. This suggests a reduced level of extracellular adenosine in the peripheral blood of migraine patients and potential 'disinhibition' of the inhibitory tone on pain signaling

in migraine. The number of Tregs co-expressing both ecto-nucleotidases CD39 and CD73 simultaneously was also significantly lower in patients suffering from migraine. These data indicate that the effective degradation of pro-inflammatory ATP into anti-inflammatory adenosine is disturbed at two sequential stages: ATP → ADP and AMP → adenosine. Impaired effector functions of Tregs in ATP degradation may cause imbalance in the anti- and pro-inflammatory Th subsets, primarily in Th17 cells. Extracellular ATP promotes the synthesis and secretion of pro-inflammatory IL-17, and CD39 on Treg cell surfaces and CD39 ectonucleotidase activity can play a central part in IL-17 down-regulation via ATP removal. For example, during the remission phase of multiple sclerosis, patients could counterbalance Th17 cells that play the main part in neuroinflammation maintenance by triggering an expansion of CD39+ Treg (Peelen et al., 2011). Considering the low expression of CD39 and CD73 in the CD62L-positive subsets of Tregs ('naïve' and CM), and the high level of IL-6 in migraine patients (Khaiboullina et al., 2017), it is possible that Th17 cells may mediate Th cell polarization in lymph nodes and mucosa-associated lymphoid tissues. Disrupted ATP homeostasis can also change the functional role of ATP-driven P2X7 receptors implicated in migraine (Gölöncsér and Sperlágh, 2014; Yegutkin et al., 2016) and in triggering the release of the key pro-inflammatory cytokine, IL-1β (Ferrari et al., 2006; Karmakar et al., 2016). The variable CD39/CD73 expression in subsets of Tregs suggests that these cells might differentially participate in different stages of the migraine attack, possibly supporting a pro-inflammatory role of ATP in the initial phase of migraine and later contributing to the termination of the attack via the anti-nociceptive action of adenosine.

In general, our findings show an imbalance in Treg subsets in migraine patients and suggest the inability of Tregs to effectively suppress inflammation in migraine. Further studies should test the contribution of other pro- and anti-inflammatory immune cells (for instance, cytokine-induced killer (CIK) T cells (Horenstein et al., 2018), in migraine pathophysiology, especially in its severe and chronic forms when the inflammatory components are better presented. Several studies have investigated the neuroprotective role of Tregs in various pathological conditions such as stroke, HIV-induced encephalitis and neurodegeneration (Liu et al., 2009; Gong et al., 2011; Li et al., 2013; Huang et al., 2017; Neal et al., 2018). The neuroprotective role is important in the light of recent findings showing that the brains of migrainers may exhibit microinfarctions and microlesions (Colombo et al., 2011; Bashir et al., 2013; Hougaard et al., 2014). Notably, the main migraine mediator CGRP, apart from its' ability to promote Treg differentiation, is directly neuroprotective in cortical neurons (Abushik et al., 2017) demonstrating a range of previously not appreciated intrinsic defensive mechanisms in migraine.

In summary, we suggest that mobilization of Tregs with functional CD39 and CD73 toward inflammation-affected meninges may be anti-inflammatory and neuroprotective in migraine.

AUTHOR CONTRIBUTIONS

DN and IK contributed to data collection, analysis, interpretation, and manuscript writing. OK contributed to patient enrollment, data interpretation, and manuscript writing. MS contributed to data collection and analysis. RA contributed to study design, and patients' enrollment. TM supervised, wrote, and edited final manuscript. RG contributed to study design and supervision, manuscript writing.

FUNDING

RG was supported by the Finnish Academy (Grant 277442) and by the program of competitive growth of Kazan Federal University and the subsidy (6.2313.2017/4.6) allocated to Kazan Federal University for the state assignment in the sphere of scientific activities.

SUPPLEMENTARY MATERIAL

The Supplementary Material for this article can be found online at: https://www.frontiersin.org/articles/10.3389/fncel.2018.00326/full#supplementary-material

REFERENCES

Abushik, P. A., Bart, G., Korhonen, P., Leinonen, H., Giniatullina, R., Sibarov, D. A., et al. (2017). Pro-nociceptive migraine mediator CGRP provides neuroprotection of sensory, cortical and cerebellar neurons via multi-kinase signaling. *Cephalalgia* 37, 1373–1383. doi: 10.1177/0333102416681588

Ambada, G. N., Ntsama, C. E., Nji, N. N., Ngu, L. N., Sake, C. N., Lissom, A., et al. (2017). Phenotypic characterization of regulatory T cells from antiretroviral-naïve HIV-1-infected people. *Immunology* 1514, 405–416. doi: 10.1111/imm.12738

Arumugam, M., and Parthasarathy, V. (2016). Reduction of CD4 + CD25 + regulatory t-cells in migraine: is migraine an autoimmune disorder? *J. Neuroimmunol.* 290, 54–59. doi: 10.1016/j.jneuroim.2015.11.015

Ashina, M., Bendtsen, L., Jensen, R., Schifter, S., and Olesen, J. (2000). Evidence for increased plasma levels of calcitonin gene-related peptide in migraine outside of attacks. *Pain* 86, 133–138. doi: 10.1016/S0304-3959(00)00232-3

Aspelund, A., Antila, S., Proulx, S. T., Karlsen, T. V., Karaman, S., Detmar, M., et al. (2015). A dural lymphatic vascular system that drains brain interstitial fluid and macromolecules. *J. Exp. Med.* 212, 991–999. doi: 10.1084/jem.20142290

Bashir, A., Lipton, R. B., and Ashina, S. (2013). Migraine and structural changes in the brain: a systematic review and meta-analysis. *Neurology* 81, 1260–1268. doi: 10.1212/WNL.0b013e3182a6cb32

Boćkowski, L., Sobaniec, W., and Żelazowska-Rutkowska, B. (2009). Proinflammatory plasma cytokines in children with migraine. *Pediatr. Neurol.* 41, 17–21. doi: 10.1016/j.pediatrneurol.2009.02.001

Bolay, H., Reuter, U., Dunn, A., Huang, Z., Boas, D. A., and Moskowitz, M. A. (2002). Intrinsic brain activity triggers trigeminal meningeal afferents in a migraine model. *Nat. Med.* 8, 136–142. doi: 10.1038/nm0202-136

Bono, M. R., Fernández, D., Flores-Santibáñez, F., Rosemblatt, M., and Sauma, D. (2015). CD73 and CD39 ectonucleotidases in T cell differentiation: beyond immunosuppression. *FEBS Lett.* 589, 3454–3460. doi: 10.1016/j.febslet.2015.07.027

Borsellino, G., Kleinewietfeld, M., Di Mitri, D., Sternjak, A., Diamantini, A., Giometto, R., et al. (2007). Expression of ectonucleotidase CD39 by Foxp3 + Treg cells: hydrolysis of extracellular ATP and immune suppression. *Blood* 110, 1225–1232. doi: 10.1182/blood-2006-12-064527

Burnstock, G. (1981). Pathophysiology of migraine: a new hypothesis. *Lancet* 317, 1397–1399. doi: 10.1016/S0140-6736(81)92572-1

Burnstock, G. (2016). P2X ion channel receptors and inflammation. *Purinergic Signal.* 12, 59–67. doi: 10.1007/s11302-015-9493-0

Cernuda-Morollón, E., Martínez-Camblor, P., Ramón, C., Larrosa, D., Serrano-Pertierra, E., and Pascual, J. (2014). CGRP and VIP levels as predictors of efficacy of Onabotulinumtoxin type A in chronic migraine. *Headache* 54, 987–995. doi: 10.1111/head.12372

Chen, S. P., Qin, T., Seidel, J. L., Zheng, Y., Eikermann, M., Ferrari, M. D., et al. (2017). Inhibition of the P2X7-PANX1 complex suppresses spreading depolarization and neuroinflammation. *Brain* 140, 1643–1656. doi: 10.1093/brain/awx085

Colombo, B., Dalla Libera, D., and Comi, G. (2011). Brain white matter lesions in migraine: What's the meaning? *Neurol. Sci.* 32, S37–S40. doi: 10.1007/s10072-011-0530-7

de Oliveira Bravo, M., Carvalho, J., and Saldanha-Araujo, F. (2016). Adenosine production: a common path for mesenchymal stem-cell and regulatory T-cell-mediated immunosuppression. *Purinergic Signal.* 12, 595–609. doi: 10.1007/s11302-016-9529-0

Ehrentraut, H., Clambey, E. T., McNamee, E. N., Brodsky, K. S., Ehrentraut, S. F., Poth, J. M., et al. (2013). CD73 + regulatory T cells contribute to adenosine-mediated resolution of acute lung injury. *FASEB J.* 27, 2207–2219. doi: 10.1096/fj.12-225201

Ferrari, D., Pizzirani, C., Adinolfi, E., Lemoli, R. M., Curti, A., Idzko, M., et al. (2006). The P2X7 receptor: a key player in IL-1 processing and release. *J. Immunol.* 176, 3877–3883. doi: 10.4049/jimmunol.176.7.3877

Fletcher, J. M., Lonergan, R., Costelloe, L., Kinsella, K., Moran, B., O'Farrelly, C., et al. (2009). CD39 + Foxp3 + regulatory T cells suppress pathogenic Th17 cells and are impaired in multiple sclerosis. *J. Immunol.* 183, 7602–7610. doi: 10.4049/jimmunol.0901881

Giniatullin, R., Nistri, A., and Fabbretti, E. (2008). Molecular mechanisms of sensitization of pain-transducing P2X3 receptors by the migraine mediators CGRP and NGF. *Mol. Neurobiol.* 37, 83–90. doi: 10.1007/s12035-008-8020-5

Gölöncsér, F., and Sperlágh, B. (2014). Effect of genetic deletion and pharmacological antagonism of P2X7 receptors in a mouse animal model of migraine. *J. Headache Pain* 15:24. doi: 10.1186/1129-2377-15-24

Gong, N., Liu, J., Reynolds, A. D., Gorantla, S., Mosley, R. L., and Gendelman, H. E. (2011). Brain ingress of regulatory T cells in a murine model of HIV-1 encephalitis. *J. Neuroimmunol.* 230, 33–41. doi: 10.1016/j.jneuroim.2010.08.014

Granstein, R. D., Wagner, J. A., Stohl, L. L., and Ding, W. (2015). Calcitonin gene-related peptide: key regulator of cutaneous immunity. *Acta Physiol.* 213, 586–594. doi: 10.1111/apha.12442

Grant, C. R., Liberal, R., Mieli-Vergani, G., Vergani, D., and Longhi, M. S. (2015). Regulatory T-cells in autoimmune diseases: challenges, controversies and—yet—unanswered questions. *Autoimmun. Rev.* 14, 105–116. doi: 10.1016/j.autrev.2014.10.012

Gronert, A. A., Fytili, P., Suneetha, P. V., Kraft, A. R., Brauner, C., Schlue, J., et al. (2015). Comprehensive phenotyping of regulatory T cells after liver transplantation. *Liver Transpl.* 21, 381–395. doi: 10.1002/lt.24050

Headache Classification Committee of the International Headache Society (IHS) (2018). The international classification of headache disorders, 3rd edition. *Cephalalgia* 33, 629–808. doi: 10.1177/0333102417738202

Horenstein, A. L., Chillemi, A., Zini, R., Quarona, V., Bianchi, N., Manfredini, R., et al. (2018). Cytokine-induced killer cells express CD39, CD38, CD203a, CD73 ectoenzymes and P1 adenosinergic receptors. *Front. Pharmacol.* 9:196. doi: 10.3389/fphar.2018.00196

Hougaard, A., Amin, F. M., and Ashina, M. (2014). Migraine and structural abnormalities in the brain. *Curr. Opin. Neurol.* 27, 309–314. doi: 10.1097/WCO.0000000000000086

Hu, R., Li, Y. J., and Li, X. H. (2016). An overview of non-neural sources of calcitonin gene-related peptide. *Curr. Med. Chem.* 23, 763–773. doi: 10.2174/0929867323666160210125416

Huang, Y., Liu, Z., Cao, B. B., Qiu, Y. H., and Peng, Y. P. (2017). Treg cells protect dopaminergic neurons against MPP + neurotoxicity via CD47-SIRPA interaction. *Cell. Physiol. Biochem.* 41, 1240–1254. doi: 10.1159/000464388

Hung, A. L., Lim, M., and Doshi, T. L. (2017). Targeting cytokines for treatment of neuropathic pain. *Scand. J. Pain* 17, 287–293. doi: 10.1016/j.sjpain.2017.08.002

Karmakar, M., Katsnelson, M. A., Dubyak, G. R., and Pearlman, E. (2016). Neutrophil P2X7 receptors mediate NLRP3 inflammasome-dependent IL-1β secretion in response to ATP. *Nat. Commun.* 7:10555. doi: 10.1038/ncomms10555

Khaiboullina, S., Mendelevich, E., Shigapova, L., Shagimardanova, E., Gazizova, G., Nikitin, A., et al. (2017). Cerebellar atrophy and changes in cytokines associated with the CACNA1A R583Q mutation in a russian familial hemiplegic migraine type 1 family. *Front. Cell. Neurosci.* 11:263. doi: 10.3389/fncel.2017.00263

Kilinc, E., Guerrero-Toro, C., Zakharov, A., Vitale, C., Gubert-Olive, M., Koroleva, K., et al. (2017). Serotonergic mechanisms of trigeminal meningeal nociception: implications for migraine pain. *Neuropharmacology* 166, 160–173. doi: 10.1016/j.neuropharm.2016

Kobie, J. J., Shah, P. R., Yang, L., Rebhahn, J. A., Fowell, D. J., and Mosmann, T. R. (2006). T regulatory and primed uncommitted CD4 T cells express CD73, which suppresses effector CD4 T cells by converting 5'-adenosine monophosphate to adenosine. *J. Immunol.* 177, 6780–6786. doi: 10.4049/jimmunol.177.10.6780

la Sala, A., Ferrari, D., Di Virgilio, F., Idzko, M., Norgauer, J., and Girolomoni, G. (2003). Alerting and tuning the immune response by extracellular nucleotides. *J. Leukoc. Biol.* 73, 339–343. doi: 10.1189/jlb.0802418

Levy, D. (2009). Migraine pain, meningeal inflammation, and mast cells. *Curr. Pain Headache Rep.* 13, 237–240. doi: 10.1016/j.neuropharm.2016.12.024

Li, P., Gan, Y., Sun, B. L., Zhang, F., Lu, B., Gao, Y., et al. (2013). Adoptive regulatory T-cell therapy protects against cerebral ischemia. *Ann. Neurol.* 74, 458–471. doi: 10.1002/ana.23815

Li, P., Gao, Y., Cao, J., Wang, W., Chen, Y., Zhang, G., et al. (2015). CD39 + regulatory T cells attenuate allergic airway inflammation. *Clin. Exp. Allergy* 45, 1126–1137. doi: 10.1111/cea.12521

Liu, J., Gong, N., Huang, X., Reynolds, A. D., Mosley, R. L., and Gendelman, H. E. (2009). Neuromodulatory activities of CD4 + CD25 + regulatory T cells in a murine model of HIV-1-associated neurodegeneration. *J. Immunol.* 182, 3855–3865. doi: 10.4049/jimmunol.0803330

Louveau, A., Smirnov, I., Keyes, T. J., Eccles, J. D., Rouhani, S. J., Peske, J. D., et al. (2015). Structural and functional features of central nervous system lymphatic vessels. *Nature* 523, 337–341. doi: 10.1038/nature14432

Magni, G., and Ceruti, S. (2013). P2Y purinergic receptors: new targets for analgesic and antimigraine drugs. *Biochem. Pharmacol.* 85, 466–477. doi: 10.1016/j.bcp.2012.10.027

Mahnke, Y. D., and Roederer, M. (2007). Optimizing a multicolor immunophenotyping assay. *Clin. Lab. Med.* 27, 469–485. doi: 10.1016/j.cll.2007.05.002

Mandapathil, M., Hilldorfer, B., Szczepanski, M. J., Czystowska, M., Szajnik, M., Ren, J., et al. (2010). Generation and accumulation of immunosuppressive adenosine by human CD4 + CD25highFOXP3 + regulatory T cells. *J. Biol. Chem.* 285, 7176–7186. doi: 10.1074/jbc.M109.047423

Matsuda, R., Kezuka, T., Nishiyama, C., Usui, Y., Matsunaga, Y., Okunuki, Y., et al. (2012). Suppression of murine experimental autoimmune optic neuritis by mature dendritic cells transfected with calcitonin gene-related peptide gene. *Invest. Ophthalmol. Vis. Sci.* 53, 5475–5485. doi: 10.1167/iovs.12-9935

Moskowitz, M. A., and Cutrer, F. M. (1993). Sumatriptan: a receptor-targeted treatment for migraine. *Annu. Rev. Med.* 44, 145–154. doi: 10.1146/annurev.me.44.020193.001045

Moskowitz, M. A., Reinhard, J. F. Jr., Romero, J., Melamed, E., and Pettibone, D. J. (1979). Neurotransmitters and the fifth cranial nerve: is there a relation to the headache phase of migraine? *Lancet* 2, 883–885.

Munno, I., Marinaro, M., Bassi, A., Cassiano, M. A., Causarano, V., and Centonze, V. (2001). Immunological aspects in migraine: increase of IL-10 plasma levels during attack. *Headache* 41, 764–767. doi: 10.1046/j.1526-4610.2001.01140.x

Neal, E. G., Acosta, S. A., Kaneko, Y., Ji, X., and Borlongan, C. V. (2018). Regulatory T-cells within bone marrow-derived stem cells actively confer immunomodulatory and neuroprotective effects against stroke. *J. Cereb. Blood Flow Metab.* doi: 10.1177/0271678X18766172 [Epub ahead of print].

Olesen, J., Burstein, R., Ashina, M., and Tfelt-Hansen, P. (2009). Origin of pain in migraine: evidence for peripheral sensitisation. *Lancet Neurol.* 8, 679–690. doi: 10.1016/S1474-4422(09)70090-0

Peelen, E., Damoiseaux, J., Smolders, J., Knippenberg, S., Menheere, P., Tervaert, J., et al. (2011). Th17 expansion in MS patients is counterbalanced by an expanded CD39 + regulatory T Cell population during remission but not during relapse. *J. Neuroimmunol.* 24, 97–103. doi: 10.1016/j.jneuroim.2011.09.013

Peroutka, S. J. (2005). Neurogenic inflammation and migraine: implications for the therapeutics. *Mol. Interv.* 5, 304–311. doi: 10.1124/mi.5.5.10

Pietrobon, D., and Moskowitz, M. A. (2013). Pathophysiology of migraine. *Annu. Rev. Physiol.* 75, 365–391. doi: 10.1146/annurev-physiol-030212-183717

Ramachandran, R. (2018). Neurogenic inflammation and its role in migraine. *Semin. Immunopathol.* 40, 301–314. doi: 10.1007/s00281-018-0676-y

Reuter, U., Bolay, H., Jansen-Olesen, I., Chiarugi, A., Sanchez del Rio, M., Letourneau, R., et al. (2001). Delayed inflammation in rat meninges: implications for migraine pathophysiology. *Brain* 124, 2490–2502. doi: 10.1093/brain/124.12.2490

Rochlitzer, S., Veres, T. Z., Kühne, K., Prenzler, F., Pilzner, C., Knothe, S., et al. (2016). The neuropeptide calcitonin gene-related peptide affects allergic airway inflammation by modulating dendritic cell function. *Clin. Exp. Allergy* 41, 1609–1621. doi: 10.1111/j.1365-2222.2011.03822.x

Rueda, C. M., Jackson, C. M., and Chougnet, C. A. (2016). Regulatory T-cell-mediated suppression of conventional T-cells and dendritic cells by different cAMP intracellular pathways. *Front. Immunol.* 7:216. doi: 10.3389/fimmu.2016.00216

Sakaguchi, S., Miyara, M., Costantino, C. M., and Hafler, D. A. (2010). FOXP3 + regulatory T cells in the human immune system. *Nat. Rev. Immunol.* 10, 490–500. doi: 10.1038/nri2785

Sarchielli, P., Alberti, A., Baldi, A., Coppola, F., Rossi, C., Pierguidi, L., et al. (2006). Proinflammatory cytokines, adhesion molecules, and lymphocyte integrin expression in the internal jugular blood of migraine patients without aura assessed ictally. *Headache* 46, 200–207. doi: 10.1111/j.1526-4610.2006.00337.x

Somjen, G. G. (2001). Mechanisms of spreading depression and hypoxic spreading depression-like depolarization. *Physiol. Rev.* 81, 1065–1096. doi: 10.1152/physrev.2001.81.3.1065

Strassman, A. M., Raymond, S. A., and Burstein, R. (1996). Sensitization of meningeal sensory neurons and the origin of headaches. *Nature* 384, 560–564.

Szklany, K., Ruiter, E., Mian, F., Kunze, W., Bienenstock, J., Forsythe, P., et al. (2016). Superior cervical ganglia neurons induce Foxp3 + regulatory T cells via calcitonin gene-related peptide. *PLoS One* 11:e0152443. doi: 10.1371/journal.pone.0152443

Takenaka, M. C., Robson, S., and Quintana, F. J. (2016). Regulation of the T cell response by CD39. *Trends Immunol.* 37, 427–439. doi: 10.1016/j.it.2016.04.009

Thalakoti, S., Patil, V. V., Damodaram, S., Vause, C. V., Langford, L. E., Freeman, S. E., et al. (2007). Neuron-glia signaling in trigeminal ganglion: implications for migraine pathology. *Headache* 47, 1008–1023. doi: 10.1111/j.1526-4610.2007.00854.x

Turan, H., Horasanli, B., Ugur, M., and Arslan, H. (2011). Procalcitonin levels in migraine patients. *Can. J. Neurol. Sci.* 38, 124–128. doi: 10.1017/S0317167100011161

Vanmolkot, F. H., and de Hoon, J. N. (2007). Increased C-reactive protein in young adult patients with migraine. *Cephalalgia* 27, 843–846. doi: 10.1111/j.1468-2982.2007.01324.x

Vignali, D. A., Collison, L. W., and Workman, C. J. (2008). How regulatory T cells work. *Nat. Rev. Immunol.* 8, 523–532. doi: 10.1038/nri2343

Wang, F., He, Q., Ren, Z., Li, F., Chen, W., Lin, X., et al. (2015). Association of serum levels of intercellular adhesion molecule-1 and interleukin-6 with migraine. *Neurol. Sci.* 36, 535–540. doi: 10.1007/s10072-014-2010-3

Wang, L., Fan, J., Chen, S., Zhang, Y., Curiel, T. J., and Zhang, B. (2013). Graft-versus-host disease is enhanced by selective CD73 blockade in mice. *PLoS One* 8:e58397. doi: 10.1371/journal.pone.0058397

Welch, K. M., Brandes, A. W., Salerno, L., and Brandes, J. L. (2006). C-reactive protein may be increased in migraine patients who present with complex clinical features. *Headache* 46, 197–199. doi: 10.1111/j.1526-4610.2006.00330.x

Yegutkin, G. G. (2008). Nucleotide- and nucleoside-converting ectoenzymes: important modulators of purinergic signalling cascade. *Biochim. Biophys. Acta* 1783, 673–694. doi: 10.1016/j.bbamcr.2008.01.024

Yegutkin, G. G., Guerrero-Toro, C., Kilinc, E., Koroleva, K., Ishchenko, Y., Abushik, P., et al. (2016). Nucleotide homeostasis and purinergic nociceptive signaling in rat meninges in migraine-like conditions. *Purinergic Signal.* 12, 561–574. doi: 10.1007/s11302-016-9521-8

Yılmaz, N., Yılmaz, M., Sirin, B., Yılmaztekin, S., and Kutlu, G. (2017). The relationship between levels of plasma-soluble urokinase plasminogen activator receptor (suPAR) and presence of migraine attack and aura. *J. Recept. Signal. Transduct. Res.* 37, 447–452. doi: 10.1080/10799893.2017.1328440

Yoshida, O., Dou, L., Kimura, S., Yokota, S., Isse, K., Robson, S. C., et al. (2015). CD39 deficiency in murine liver allografts promotes inflammatory injury and immune-mediated rejection. *Transpl. Immunol.* 32, 76–83. doi: 10.1016/j.trim.2015.01.003

Yücel, M., Kotan, D., Gurol Çiftçi, G., Çiftçi, I. H., and Cikriklar, H. I. (2016). Serum Levels of endocan, claudin-5 and cytokines in migraine. *Eur. Rev. Med. Pharmacol. Sci.* 20, 930–936.

Zakharov, A., Koroleva, K., and Giniatullin, R. (2016). Clustering analysis for aorting ATP-induced nociceptive firing in rat meninges. *BioNanoScience* 6, 508–512. doi: 10.1007/s12668-016-0276-z

Zakharov, A., Vitale, C., Kilinc, E., Koroleva, K., Fayuk, D., Shelukhina, I., et al. (2015). Hunting for origins of migraine pain: cluster analysis of spontaneous and capsaicin-induced firing in meningeal trigeminal nerve fibers. *Front. Cell Neurosci.* 9:287. doi: 10.3389/fncel.2015.00287

Conflict of Interest Statement: The authors declare that the research was conducted in the absence of any commercial or financial relationships that could be construed as a potential conflict of interest.

frontiers in Cellular Neuroscience

REVIEW
published: 23 October 2018
doi: 10.3389/fncel.2018.00376

Neuromodulatory Effects of Guanine-Based Purines in Health and Disease

Carla I. Tasca[1,2], Débora Lanznaster[2,3]*, Karen A. Oliveira[1,2], Victor Fernández-Dueñas[4,5] and Francisco Ciruela[4,5]**

[1]*Departamento de Bioquímica, Centro de Ciências Biológicas, Universidade Federal de Santa Catarina, Florianópolis, Brazil,* [2]*Programa de Pós-Graduação em Bioquímica, Centro de Ciências Biológicas, Universidade Federal de Santa Catarina, Florianópolis, Brazil,* [3]*UMR 1253, Team 2, INSERM/University of Tours, Tours, France,* [4]*Unitat de Farmacologia, Departament de Patologia i Terapèutica Experimental, Facultat de Medicina, IDIBELL, Universitat de Barcelona, L'Hospitalet de Llobregat, Barcelona, Spain,* [5]*Institut de Neurociències, Universitat de Barcelona, Barcelona, Spain*

The function of guanine-based purines (GBPs) is mostly attributed to the intracellular modulation of heteromeric and monomeric G proteins. However, extracellular effects of guanine derivatives have also been recognized. Thus, in the central nervous system (CNS), a guanine-based purinergic system that exerts neuromodulator effects, has been postulated. The thesis that GBPs are neuromodulators emerged from *in vivo* and *in vitro* studies, in which neurotrophic and neuroprotective effects of these kinds of molecules (i.e., guanosine) were demonstrated. GBPs induce several important biological effects in rodent models and have been shown to reduce seizures and pain, stabilize mood disorder behavior and protect against gliomas and diseases related with aging, such as ischemia or Parkinson and Alzheimer diseases. *In vitro* studies to evaluate the protective and trophic effects of guanosine, and of the nitrogenous base guanine, have been fundamental for understanding the mechanisms of action of GBPs, as well as the signaling pathways involved in their biological roles. Conversely, although selective binding sites for guanosine have been identified in the rat brain, GBP receptors have not been still described. In addition, GBP neuromodulation may depend on the capacity of GBPs to interact with well-known membrane proteins in glutamatergic and adenosinergic systems. Overall, in this review article, we present up-to-date GBP biology, focusing mainly on the mechanisms of action that may lead to the neuromodulator role of GBPs observed in neurological disorders.

Keywords: guanosine, neuromodulation, purinergic system, Parkinson's disease, Alzheimer's disease, glutamatergic system

OPEN ACCESS

Edited by:
David Blum, INSERM U1172 Centre de Recherche Jean Pierre Aubert, France

Reviewed by:
Elisabetta Coppi, Università degli Studi di Firenze, Italy
Lisiane Oliveira Porciúncula, Universidade Federal do Rio Grande do Sul (UFRGS), Brazil

****Correspondence:***
Carla I. Tasca
carla.tasca@ufsc.br
Débora Lanznaster
de_lanz@hotmail.com
Francisco Ciruela
fciruela@ub.edu

Received: *28 July 2018*
Accepted: *02 October 2018*
Published: *23 October 2018*

Citation:
Tasca CI, Lanznaster D, Oliveira KA, Fernández-Dueñas V and Ciruela F (2018) Neuromodulatory Effects of Guanine-Based Purines in Health and Disease. Front. Cell. Neurosci. 12:376. doi: 10.3389/fncel.2018.00376

PURINES AS INTERCELLULAR MODULATORS

Purines are endogenous organic molecules that are essential for all cells. For instance, they are structural constituents of nucleic acids, are part of coenzyme structures and act as second messengers in intracellular signaling pathways. Purines consist of the two-ring nitrogenous bases adenine and guanine, together with the derivatives of these: nucleosides (nitrogenous bases plus a pentose sugar, usually ribose) and nucleotides (nitrogenous bases plus ribose and phosphate) that are mono-, di- or tri-phosphorylated. Adenine derivatives include the nucleoside adenosine, and the nucleotides adenosine-5′-monophosphate (AMP),

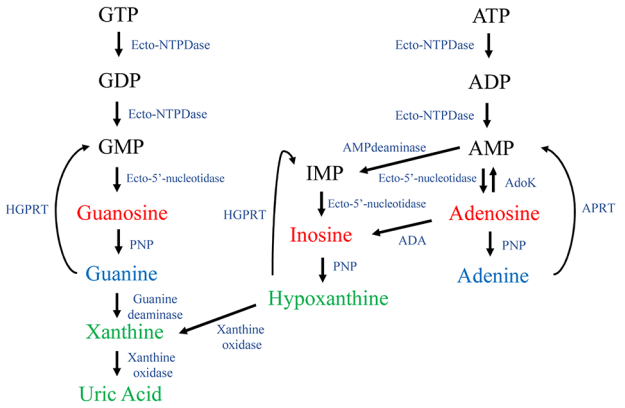

FIGURE 1 | Purine metabolism. The guanine nucleotides guanosine-5′-triphosphate (GTP), guanosine-5′-diphosphate (GDP) and guanosine-5′-monophosphate (GMP) are sequentially dephosphorylated by ecto-nucleotidases (i.e., Ecto-NTPDase and Ecto-5'-nucleotidase), thus generating guanosine. Guanosine is hydrolyzed by PNP generating the purine base guanine. By action of a guanine deaminase (GDA), guanine is converted into xanthine and subsequently to uric acid by the action of a xanthine oxidase. Adenine nucleotides are also hydrolyzed forming the nucleosides adenosine and inosine. The following nitrogenous bases, hypoxanthine, xanthine and uric acid, are formed intracellularly. Ecto-NTPDase, ecto-nucleotide diphosphohydrolase or apyrase; ADA, adenosine deaminase; AdoK, adenosine kinase; APRT, adenine phosphoribosyl transferase; HGPRT, hypoxanthine-guanine phosphoribosyl transferase; PNP, purine nucleoside phosphorylase. APRT and HGPRT are mainly involved in the intracellular salvage purines pathway.

adenosine-5′-diphosphate (ADP) and adenosine-5′-triphosphate (ATP). Guanine derivatives include the nucleoside guanosine, and the nucleotides guanosine-5′-monophosphate (GMP), guanosine-5′-diphosphate (GDP) and guanosine-5′-triphosphate (GTP). Purines also include some related metabolites, such as the nucleoside inosine and the nitrogenous base hypoxanthine, from the catabolism pathway of adenosine; and the bases xanthine and uric acid, from the catabolism of guanine and hypoxanthine (**Figure 1**). When released into the extracellular space, nucleotides are hydrolyzed by ecto-nucleotidases located at the cellular membrane surface (Zimmermann and Braun, 1996). The main ecto-nucleotide triphosphatase (ecto-NTPase) are: ecto-ATPase, which hydrolyzes ATP to ADP and GTP to GDP; ecto-ATP-diphosphohydrolase or apyrase (ecto-NTPDase), which leads to AMP from either ATP or ADP, and forms GMP from GTP or GDP (Schadeck et al., 1989). Next, the nucleosides adenosine and guanosine are the result of AMP or GMP hydrolization by ecto-5′-nucleotidase (Zimmermann, 1996). Furthermore, ecto-purine nucleoside phosphorylase (ecto-PNP) produces guanine from guanosine (Giuliani et al., 2016), while guanine deaminase (GDA) or cypin mediates guanine deamination to xanthine (Miyamoto et al., 1982; **Figure 1**).

The concept of purines as intercellular modulators emerged from the identification of extracellular effects of adenine-based purines (ABPs) in different cell types. Drury and Szent-Györgyi (1929) demonstrated that, after heart ischemia, adenosine is released into the extracellular space, where it promotes a negative chronotropic effect and also produces coronary vessels vasodilatation. Later, ATP was recognized to have both extracellular and intracellular effects, i.e., in the maintenance of energetic cellular metabolism (Lipmann, 1941). In the 1970s, Geoffrey Burnstock introduced the concept of purinergic nerves and purinergic neurotransmission (Burnstock et al., 1970; Burnstock, 1972). Since then, adenosine and ATP have been considered to be important neuromodulators in the central nervous system (CNS; Cunha, 2005; Jacobson and Gao, 2006; Burnstock et al., 2011; Tozaki-Saitoh et al., 2011; Ciruela et al., 2012). Meanwhile, opposed to the multiple actions reported for ABP, the importance of guanine-based purines (GBPs) has mostly been ascribed to their role as regulators of G protein function. G proteins (formerly named guanine-nucleotide regulatory proteins or GTP-binding proteins) are key to signal transduction of the so-called G protein-coupled receptors (GPCRs) to intracellular effectors (Rodbell et al., 1971). Thus, G protein activity is, up to now, modulated by the interactions with GDP or GTP in the basal and activated states, respectively (Taylor, 1990). Similarly, low molecular monomeric G protein activity is also modulated by interaction with GTP and GDP (Hepler and Gilman, 1992); while other GBPs, such as GMP, guanosine or guanine, have not been reported to interact with G proteins.

In recent years, it has been shown that, apart from the intracellular regulation of G proteins, GBPs have important extracellular effects in different tissues, especially in the CNS. Indeed, similarly to the vesicular storage reported for ATP (Gualix et al., 1999), it was found that GTP was also stored in synaptic vesicles, suggesting this guanine nucleotide would be a neurotransmitter in the brain (Santos et al., 2006). Thus, together with the existence of an adenosine-based purinergic system, a guanine-based purinergic system has been proposed (Schmidt et al., 2007). In the present review article, we report and discuss how the guanine-based purinergic system is organized in the nervous system and highlight the fundamental neuromodulator and regulatory role of these molecules.

EXTRACELLULAR ROLES OF GUANINE-BASED PURINES

GBPs function in the extracellular milieu was first observed when assessing GBP levels after ischemic injury. Interestingly, it was observed that GBP were rapidly released and that their levels remain elevated until 7 days (Uemura et al., 1991). Similarly, astrocytes subjected to hypoxic or hypoglycaemic situations released different kinds of purine nucleotides, and extracellular levels of GBPs were shown to reach levels three-fold higher than those of ABPs (Ciccarelli et al., 1999). Also, it was possible to detect extracellular GBPs in human cerebrospinal fluid (CSF), both in physiological and pathological conditions (Regner et al., 1997). These findings prompted the proposal that GBPs might represent an endogenous restorative system that is activated after injury. In this context, upon brain injury, hydrolysis of the released nucleotides would occur, leading to the formation of the respective nucleosides, which may possess a protective effect.

In the CNS, the first modulatory effects of extracellular GBPs were demonstrated in the glutamatergic system (Schmidt et al., 2007), the main excitatory neurotransmission system in the brain (Meldrum, 2000; Segovia et al., 2001). Besides its essential trophic effects in the CNS, glutamate is capable of promoting a cascade of events leading to cellular death, widely known as excitotoxicity. Therefore, molecules that modulate glutamate excitotoxicity without interfering with the physiological functions of glutamate may play a fundamental role in neuroprotection. In line with this, initial studies evaluating extracellular GBP functions, indicated that guanine nucleotides would displace glutamate from its receptors (Schmidt et al., 2007; Lanznaster et al., 2016). GBPs would also modulate glutamate-induced cell responses in physiological (Tasca et al., 1995, 1998, 1999b; Regner et al., 1998; Tasca and Souza, 2000) and pathological (Regner et al., 1998; Burgos et al., 2000b) situations. Additionally, GBPs were shown to cause a delay in glutamate uptake into synaptic vesicles (Tasca et al., 2004), suggesting they modulate synaptic glutamate turnover. Moreover, other studies showed that guanosine would also modulate glutamate transporter activity (Dal-Cim et al., 2011, 2013; Lanznaster et al., 2016). In short, the identification of the extracellular actions of GBPs as intercellular messengers was possible due to five pieces of evidences: (1) GBPs can be found in the extracellular space, where they are released upon certain harmful conditions; (2) hydrolization of extracellular guanine nucleotides leads to the formation of guanosine and guanine; (3) GTP is stored in synaptic vesicles; (4) glutamate binding is displaced by guanine nucleotides; and (5) GBPs modulate glutamate transporter activity. Based on these findings, it can be concluded that GBPs act as endogenous modulators of glutamatergic transmission, and it might result in the potentially critical role that these molecules play in neuroprotection.

NEUROTROPHIC AND NEUROPROTECTIVE EFFECTS OF GBPs

GBPs as Neurotrophic Agents

The trophic effects of GBPs, especially GTP and guanosine, in the CNS (i.e., proliferation in astrocytes and neuritogenesis in neurons) have been widely studied and are supported by many data (Neary et al., 1996; Rathbone et al., 1999; Ciccarelli et al., 2001). For example, it was first shown that GTP or guanosine treatment of cultured astrocytes promoted cell proliferation due to guanosine-induced adenosine release (Ciccarelli et al., 2001). Similarly, GTP or guanosine was also capable of stimulating the release of neurotrophic factors (i.e., fibroblast growth factor-2, FGF-2; nerve growth factor, NGF) from cultured astrocytes (Middlemiss et al., 1995; Gysbers and Rathbone, 1996a). In pheochromocytoma (PC12) cells, GTP or guanosine enhanced NGF-induced neurite arborization outgrowth (Gysbers and Rathbone, 1992, 1996b). Similarly, guanosine induced this kind of neurite arborization in PC12 cells, and also in cerebellar neurons, upon hypoxic conditions (Thauerer et al., 2010). Finally, guanosine and NGF co-treatment of PC12 cells enhanced the activity of antioxidant enzyme heme-oxygenase-1 (HO-1) and also produced an increase of cyclic GMP (cGMP) intracellular levels (Bau et al., 2005).

There are also robust findings that support the idea that GBPs play a role in neuron–astrocyte interactions. Thus, the trophic effects of GBPs were evaluated in neurons co-cultured with astrocytes, where GMP or guanosine increased the amount of cerebellar neurons and modulated the organization of the extracellular matrix proteins laminin and fibronectin in astrocytes (Decker et al., 2007). Additionally, in another work, it was demonstrated that GMP or guanosine increased the number of cultured cerebellar neurons (Tasca et al., 2010). Therefore, besides having a direct positive effect on neuronal viability, GMP or guanosine may also induce the release of soluble factors from astrocytes that favor the survival of cultured neurons. Altogether, it would be stated that GBP effects are importantly involved in neuronal migration and cell proliferation.

It should be noted that, in adulthood, neurogenesis occurs in two brain areas: the subventricular zone (SVZ) of the lateral ventricles and the subgranular zone (SGZ) in the dentate gyrus of the hippocampus (Gage et al., 1998; Gage, 2000). Indeed, in cultures of neural stem cell from the SVZ, it was recently shown that guanosine treatment increased cell proliferation and expression of brain-derived neurotrophic factor (BDNF; Su et al., 2013). Interestingly, another role for guanosine was reported. Thus, in a Parkinson's disease (PD) mouse model, the systemic administration of guanosine stimulated neuroprogenitor cell proliferation in the SVZ (Su et al., 2009). Moreover, guanosine was also capable of increasing the number of FGF-2-positive cells, which have been shown to be critical regulators of neuroprogenitor/stem cell proliferation, survival and differentiation (Zhao et al., 2008).

Neuroprotective Effects of GBPs

GBPs-mediated neuroprotective effects have been demonstrated using *in vivo* animal models of CNS disorders and *in vitro and ex vivo* models of excitotoxicity or oxidative damage. Here, we mainly focus on reviewing the effects of GBPs in animal models of seizures, ischemia, PD and Alzheimer's disease (AD). Also, we review some of the related *in vitro* and *ex vivo* models of degeneration designed to identify the mechanisms of GBP-induced neuroprotection. The effects of GBPs on other CNS diseases are also briefly discussed.

Seizures

In vivo evaluation of seizures in rats or mice can be performed by using quinolinic acid, an agonist of the ionotropic glutamate receptor *N*-methyl-D-aspartate (NMDA) subtype, which causes overstimulation of glutamatergic activity (Heyes et al., 1990; Nakano et al., 1993; Meldrum, 1994). Interestingly, acute administration of GMP or guanosine reduced quinolinic acid-induced seizures by about 60% (Schmidt et al., 2000; Soares et al., 2004; Tavares et al., 2005, 2008; Torres et al., 2010). In one of those studies, the anticonvulsant effect of GMP was blocked with the 5'-nucleotidase inhibitor alpha-beta-methylene-adenosine-5'-diphosphate (AOPCP), which impedes the

conversion of GMP to guanosine (Soares et al., 2004). This result suggested that guanosine is the biologically active anticonvulsant molecule. In line with this, guanosine was demonstrated to be protective both when administered intracerebroventricularly (Schmidt et al., 2005) and orally (Lara et al., 2001; de Oliveira et al., 2004); showing that its anticonvulsant effect occurs regardless the route of administration. Similarly, chronic (2 weeks) oral guanosine administration was shown to decrease quinolinic acid- and α-dendrotoxin-induced seizures (Vinadé et al., 2003, 2005). It was also shown that guanosine can modulate the changes induced in electroencephalographic (EEG) signals by quinolinic acid intracerebroventricular infusion and prevent behavioral seizures (Torres et al., 2010). Finally, in WAG/Rij rats, which is a genetic model of absence epilepsy, it was observed that guanosine decreased spike-wave discharges related. This effect was not dependent on adenosine receptor activation, since guanosine-mediated effects were not altered by using the non-selective adenosine receptor antagonist theophylline (Kovács et al., 2015).

Taken together, the data from all these studies indicate that GBPs (mainly guanosine) may modulate exacerbation of glutamatergic transmission by decreasing epileptic activity and seizures.

Ischemia

The most common cause of disability worldwide is brain ischemia. In the brain, blood flow reduction leads to reduced oxygen and glucose supplying, which leads to the failure of cellular bioenergetics and ultimately to excitotoxicity and oxidative stress (Durukan and Tatlisumak, 2007). GBPs-mediated neuroprotective effects can be evaluated in different brain ischemia models. One of them consists of the unilateral occlusion of the carotid artery, which is then exposed to a hypoxic atmosphere. This model is known as a perinatal hypoxia-ischemia (HI). Interestingly, guanosine was able to restore HI-induced reduction in glutamate uptake (Moretto et al., 2005, 2009). Similarly, in a model of neurological damage, such as the unilateral middle cerebral artery occlusion (MCAO), it was observed that guanosine displayed a neuroprotective effect, since it reduced the infarcted area and it also improved gait disturbances or spontaneous activity (Chang et al., 2008; Rathbone et al., 2011; Connell et al., 2013). Additionally, the neuroprotective effects of guanosine were evaluated in a rodent model of cerebral hypoperfusion (reduced blood flow) due to permanent bilateral occlusion of common carotid arteries. Interestingly, it was observed that guanosine administration (orally, for 2 weeks) reversed pyramidal neurons loss and glial fibrillary acidic protein (GFAP) expression in the hippocampus. However, guanosine did not prevent the cognitive deficit induced in this model of cerebral hypoperfusion (Ganzella et al., 2012). Another ischemic model in which the neuroprotective effects of guanosine have been shown is that induced by thermocoagulation (Hansel et al., 2014, 2015). Of note, when inducing permanent cortical focal ischemia in rats, guanosine treatment reduced the percentage of the infarcted area (around 40%). In addition, guanosine reduced neuronal degeneration, prevented reactive oxygen species (ROS) production and lipid peroxidation, which led to an improvement in forelimb dysfunction. Guanosine also reduced activation of microglia and restored the levels of inflammatory mediators (i.e., tumor necrosis factor (TNF-α), interleukins IL-1 or IL-6) in the infarcted area (Hansel et al., 2015). Importantly, these neuroprotective effects occurred when guanosine treatment was initiated just after the focal ischemia.

Apart from the data obtained from animal models, *in vitro* and *ex vivo* protocols can be useful tools to demonstrate the neuroprotective effects of GBPs in ischemic situations. For instance, brain slices subjected to oxygen and glucose deprivation (OGD) is an *ex vivo* ischemia model that allows the study of neuroprotective agents (Tasca et al., 2015). In this way, guanosine-mediated neuroprotection was observed in OGD-deprived hippocampal slices (Oleskovicz et al., 2008). Interestingly, these effects were identified to depend on the modulation of glutamate transporter activity (Dal-Cim et al., 2016), since glutamate uptake was restored to basal levels (Dal-Cim et al., 2011). Of note, guanosine would also produce antioxidant effects, since it reduced oxidative parameters (e.g., ROS production) and prevented the depolarization of the mitochondrial membrane. Interestingly, in the OGD model, guanosine has been shown to display a number of important anti-inflammatory effects. Thus, guanosine inhibited p65 (the active subunit of nuclear factor kappa B (NF-κB) transcription factor) translocation to the nucleus, or it also reduced inducible nitric oxide synthase (iNOS) expression (Dal-Cim et al., 2013). Similarly, guanosine diminished NO levels, similar to that obtained with neuronal NOS (nNOS) or iNOS isoforms inhibition (Thomaz et al., 2016).

Interestingly, glutamate challenge can also be used as an ischemic-like protocol, since ischemic events increase glutamate release and excitotoxicity. In hippocampal slices, upon glutamate-mediated damage, guanosine decreased glutamate release and prevented iNOS induction (Molz et al., 2011). Guanosine was also capable of attenuating glutamate-induced ROS production (Dalla Corte et al., 2012).

Altogether, these studies support a role for GBPs against ischemia, which may act as neuroprotective agents. Thus, GBPs would have the capacity of increasing the clearance of extracellular glutamate, prevent inflammatory events, activate antioxidant defenses and maintain mitochondria bioenergetics.

Parkinson's Disease

PD is a neurodegenerative disorder, which is characterized by the selective death of dopaminergic neurons at the substantia nigra pars compacta (SNc). This loss causes important motor symptoms (i.e., bradykinesia, rigidity or postural complications; Olanow and Tatton, 1999). Several studies have evaluated the effects of GBPs in *in vivo* models of PD and the mechanisms of action of GBPs in *ex vivo* and *in vitro* models of PD.

Interestingly, guanosine was shown to decrease neuronal cell death and even produce an increase in SNc dopaminergic terminals, which ultimately led to reduce bradykinesia in a model of PD (i.e., proteasome inhibitor administration;

Su et al., 2009). Another example of such neuroprotective role for guanosine was found in the PD-related alpha-synuclein A53T transgenic mouse model. Thus, this mutation led to higher guanosine brain levels when mice grew (the guanosine content would increase with aging), thus eliciting a putative protective effect (Chen et al., 2015).

Recently, the effectiveness of guanosine against dyskinesia in three rodent models of movement impairment was reported for the first time. Thus, guanosine ameliorated tremolous jaw movements (TJM) and catalepsy of reserpinized mice. In addition, guanosine potentiated contralateral rotations induced by L-DOPA in unilaterally 6-hydroxydopamine (6-OHDA)-injured rats and displayed antidyskinetic efficacy in the L-DOPA-induced dyskinesia (LID) animal model. These results support the potential usefulness of guanosine in PD management, including its capacity to reduce dyskinesia when used in combination with L-DOPA (Massari et al., 2017).

Moving to *in vitro* PD models, one of the most used is the 1-methyl-4-phenyl pyridinium (MPP^+) model. This active metabolite of the neurotoxin 1-methyl-4-phenyl-1,2,3,6-tetrahydropyridine (MPTP) inhibits complex I activity in mitochondria (Vila and Przedborski, 2003). Notably, guanosine was able to prevent MPP^+-induced apoptosis in SH-SY5Y neuroblastoma cells (Pettifer et al., 2007). Conversely this effect was not observed in C6 astroglial cells exposed to 6-OHDA, which is another PD model (Giuliani et al., 2016).

Alzheimer's Disease (AD)

AD is a neurodegenerative condition that affects approximately 36 million people worldwide (Mazurek, 2000; Karran et al., 2011; Masters and Selkoe, 2012). Along with neuronal death, amyloid-β (Aβ) plaques and neurofibrillary tangles are the main neuropathological hallmarks of the brain of AD patients.

Different models have been used to study the neuroprotective effects of GBPs in AD. For instance, in an *in vivo* model of the pathology (intracerebroventricular infusion of $A\beta_{1-40}$), chronic guanosine treatment prevented the cognitive deficit and anhedonic-like behavior induced in mice. Interestingly, it was shown that $A\beta_{1-40}$ altered glutamate transport, mainly by increasing Na^+-independent glutamate uptake, and that guanosine treatment led to recovery from this glutamatergic transmission imbalance (Lanznaster et al., 2017).

A few studies have evaluated the neuroprotective effects of GBPs in *in vitro* models of AD (i.e., using Aβ peptides). Thus, in Aβ-treated SH-SY5Y neuroblastoma cells, guanosine was able to prevent apoptosis and ROS production (Pettifer et al., 2004; Tarozzi et al., 2010). In addition, guanosine also prevented β-secretase over activity and reduced $A\beta_{1-42}$ levels upon oxidative stress (Tarozzi et al., 2010). Similarly, in hippocampal astrocytes, guanosine prevented lipopolysaccharide (LPS)-induced inflammatory and oxidative damage as well as decreasing TNF- α and NF-κB levels by induction of HO-1 (Bellaver et al., 2015). Taken together, these data suggest that guanosine attenuates the neuroinflammation and oxidative stress induced by Aβ peptides.

Hepatic Encephalopathy (HE)

HE is a neurological disease that leads to cognitive impairment, which is initiated by liver dysfunction and continues with ammonia accumulation that causes alterations in extracellular glutamate levels (Butterworth et al., 1987; Albrecht and Jones, 1999). To our knowledge, only a single study has evaluated the effects of GBPs in HE. Thus, in rats subjected to bile duct ligation (BDL), guanosine was able to reverse cognitive impairment, although no changes were observed in ammonia levels. Of note, in this model oxidative stress and increased CSF glutamate levels were observed in the striatum and hippocampus, indicating that guanosine could act at this level (Paniz et al., 2014).

Sepsis

Sepsis, which is a potentially fatal syndrome of physiological, pathological and biochemical abnormalities associated with infection, is another condition in which GBPs may be effective. One of the existent models consists of caecal ligation and perforation. This intervention leads to oxidative stress in a number of brain regions (i.e., hippocampus, striatum, cerebellum and cerebral cortex). Interestingly, guanosine (acute administration) was shown to reduce lipid peroxidation, suggesting it would be one of the mechanisms explaining guanosine-mediated neuroprotective effects. In addition, chronic (10 days) could reduce cognitive impairment and depressive-like behavior (Petronilho et al., 2012).

Spinal Cord Injury

The neuroprotective effects of GBPs against spinal cord injury have also been demonstrated. In a model in which the spinal cord from rats was moderately damaged, thus leading to chronic traumatic spinal cord injury, guanosine was able to induce locomotor activity recovery (Jiang et al., 2003). Notably, guanosine treatment also led to spinal cord higher levels of bromo-deoxy-uridine (BrdU), which is a marker of cell proliferation. Thus, new mature oligodendrocytes were observed at the damaged area, which would allow remyelination and the recovery of motor activity (Jiang et al., 2003, 2008). Indeed, it is well-accepted that remyelination of the damaged area in the spinal cord is critical for functional recovery (Gilson and Blakemore, 1993; Horner et al., 2000).

Gliomas

Gliomas are considered the most aggressive type of brain tumors. Therapies involve surgical resection, radiotherapy or chemotherapy. One of the chemotherapeutic compounds most commonly used is temozolomide (TMZ), which is an alkylating drug that inhibits DNA replication and that has been shown to have some efficacy in early diagnosed gliomas. A few studies have analyzed the effects of GBPs on tumoral cells. Thus, guanosine was evaluated as a therapeutic strategy in several types of tumors, including lung cancer cells (Su et al., 2010), melanoma cells (Naliwaiko et al., 2008), hepatoma cells (Yang et al., 2005), leukemia and mastocytoma models (Iigo et al., 1987) and an *in vivo* Ehrlich carcinoma model (Kim et al., 1997).

In CNS tumors, the effect of guanosine was evaluated in the A172 glioma cell line. Interestingly, guanosine was cytotoxic to

glioma in concentrations that were not toxic to native brain tissue (Molz et al., 2009), and to astrocytes in culture (Oliveira et al., 2017). By evaluating the combination of guanosine with the alkylating agent TMZ, it was shown that their cytotoxicity arises from the potentiation of the apoptotic process and the reduction of glioma cells migration. Guanosine also decreased mitochondrial membrane potential, intracellular ATP levels, and prevented the increase in glutamate release evoked by TMZ in glioma cells (Oliveira et al., 2017). Despite all the evidences of GBPs-mediated modulation of glutamatergic transmission, no effects of guanosine on glutamate uptake release or on the activity of glutamine synthetase have been observed (Yin et al., 2013). Additionally, the cytotoxic effect of guanosine in gliomas was not affected by glutamate receptors or transporters pharmacological blockage; while, on the other hand, adenosine receptors would be involved in guanosine-mediated cytotoxic effects (Oliveira et al., 2017). To the best of our knowledge, the anti-tumorigenic effects of guanosine in glioma cells still need further investigation. Thus, it was clearly shown that guanosine activates survival signaling pathways, which are able to induce neuroprotection or trophic effects in non-tumoral cells (Lanznaster et al., 2016). Accordingly, the cytotoxic effects of guanosine would also be related to the regulation of cell growing and survival in tumoral cells. These interesting results, together with the mechanisms that confer a dual-effect to guanosine (i.e., displaying a protective action to healthy neural cells subjected to pathological conditions and cytotoxic effect to SNC tumoral cells), need additional evaluation to be unraveled.

Overall, the studies discussed here support important neurotrophic and neuroprotective effects of GBPs, mainly GTP, GMP and guanosine. We should note that most of the neuroprotective effects observed in different pathological models were obtained using guanosine, which may be probably due to nucleotide hydrolysis occurring in the extracellular space.

GBP EFFECTS ON MODELS OF PAIN AND MOOD DISORDERS

Anxiety, depression and pain are among the major causes of disability worldwide. Glutamate transmission has been described to be involved in the etiology and treatment of such pathologies. For instance, ketamine, which is an antagonist for NMDA glutamate receptors, was able to produce a fast-acting antidepressant effect (Chaki and Fukumoto, 2015). Furthermore, metabotropic glutamate receptor ligands have been shown to possess analgesic properties (Kolber, 2015). Considering that GBPs modulate glutamatergic transmission, it is reasonable to infer that these molecules may also present anxiolytic, antidepressant and analgesic effects.

The anxiolytic and antidepressant effects of GBPs have been studied in some well-accepted models. For instance, rats treated once with GMP or guanosine showed a decrease in anxiogenic-like behavior, which were similar to that observed with diazepam, a classic anxiolytic drug (Almeida et al., 2010). Anxiolytic-like behavior induced by guanosine was also observed after chronic treatment. Thus, guanosine (2 weeks administration) increased anxiolytic-like behavior (Da Silva and Elisabetsky, 2001; Vinadé et al., 2003). Also, a rapid antidepressant effect, similar to that of ketamine, was observed after a single oral administration of guanosine in mice (Bettio et al., 2012). Guanosine also induced antidepressant-like effects in mice subjected to acute restraint stress, a more translational model associated with mood disorders that are secondary effects of stressful lifetime events (for a review, see Yang et al., 2015). Interestingly, the antidepressant-like effects of guanosine could be due to its antioxidant activity, which would reduce hippocampal oxidative damage induced by acute restraint stress (Bettio et al., 2014). Finally, it was recently shown that chronic guanosine treatment promoted an antidepressant-like effect that might be associated with hippocampal neuroblasts differentiation (Bettio et al., 2016b), suggesting a connection between the antidepressant and neurogenic effects of guanosine (Bettio et al., 2016a).

The possible analgesic effects of GBPs have also been explored in different rodent models of pain. Guanosine reduced nociception in several acute pain models, such as acetic acid, formalin, glutamate or capsaicin injections. Guanosine treatment inhibited nociception induced by intrathecal administration of nociceptive substances, such as non-NMDA receptor agonists (Schmidt et al., 2010). Similarly, guanine inhibited nociception induced by glutamate and AMPA (de Oliveira et al., 2016). Moreover, central administration of GMP, guanosine or guanine in mice induced anti-nociception against thermal or chemical (i.e., glutamate, capsaicin) stimuli (Schmidt et al., 2008; de Oliveira et al., 2016), reinforcing the hypothesis of a CNS action of GBPs.

MECHANISMS OF ACTION OF THE PROTECTIVE AND TROPHIC EFFECTS OF GBPs

As commented on above, the neuromodulatory effects of GBPs have been studied in different models of ischemia and neurodegenerative diseases, based on its action in neuroinflammation, glutamatergic toxicity and mitochondrial stress. These effects are mainly attributed to the capacity of GBPs to modulate glutamatergic transport and inhibit both oxidative stress and inflammatory damage. Meanwhile, the nucleoside guanosine, which can activate several intracellular pathways of second messengers that ultimately lead to a decrease in apoptosis, would be the main element responsible for the protective and trophic effects observed. Accordingly, most of the work aiming to elucidate the mechanisms of action of GBPs has focused on guanosine.

Several studies have demonstrated that GBP modulation of glutamate transport has a major impact on the induction of protection against excitotoxicity. Guanosine prevented glutamate release in hippocampal slices subjected to glutamatergic toxicity (Molz et al., 2011). Also, guanosine stimulated glutamate uptake both in C6 astroglial cells deprived from glucose (Quincozes-Santos et al., 2013) and in hippocampal slices subjected to OGD (Dal-Cim et al., 2013). Interestingly,

these effects were all mediated by phosphatidylinositol-3 protein kinase (PI3K) and protein kinase B (Akt) pathways induction, followed by activation of mitogen-activated protein kinase/extracellular-regulated kinase (MAPK/ERK). In C6 cells, guanosine also activated protein kinase C (PKC) and $p38^{MAPK}$ pathways to induce its protective effect. Hence, based on these studies, we can conclude that the effects of GBPs on glutamate transporters are dependent on activation of these intracellular signaling pathways. Supporting this view, a study showed that chronic administration of GMP decreased the expression of NMDA and AMPA receptor subunits and the glutamate transporters EAAC1 and GLT-1 in the rat cerebral cortex (Ganzella et al., 2012).

Regarding the ischemia and neurodegenerative models, some intracellular pathways have been identified. Thus, guanosine induced an increase in cell viability in hippocampal slices subjected to OGD, which involved the activation of several signaling pathways, including PKC, protein kinase A (PKA), MAPK/ERK and PI3K (Oleskovicz et al., 2008). PI3K activation is also involved in the anti-apoptotic effect of guanosine in cultured human neuroblastoma cells challenged with β-amyloid, which may include an increase in phospho-Akt (Pettifer et al., 2004). Similarly, Akt expression and activation was increased by guanosine, which protected astrocytes challenged with the apoptotic drug staurosporine (Di Iorio et al., 2004). Also, guanosine activated the PI3K/Akt/GSK3β pathway, which inhibits the oxidative damage produced by blocking mitochondrial complexes I and V (Dal-Cim et al., 2012). Furthermore, in 6-OHDA-treated SH-SY5Y cells, a model for PD, guanosine reduced $p38^{MAPK}$ and Jun Kinase (JNK) activation, and increased phospho-Akt and the expression of the anti-apoptotic protein, Bcl-2 (Giuliani et al., 2012b). Finally, guanosine also activated the PI3K pathway, which promotes anti-inflammatory effects. It also inhibited iNOS induction via PI3K and MAPK/ERK activation in hippocampal slices subjected to OGD (Dal-Cim et al., 2013).

Notably, the involvement of the PI3K/Akt pathway in GBP mechanisms of action has also been reported for the antidepressant effects of guanosine. In addition, guanosine-mediated antidepressant effects would also depend on the activation of the mammalian target of rapamycin (mTOR; Bettio et al., 2012).

Finally, regarding GBP-induced trophic effects, similar signaling pathways have been reported. Guanosine promoted neurite outgrowth in primary cerebellar neurons culture by activation of PCK-related kinase-1 (PRK1; Thauerer et al., 2010), which is a kinase involved in neuronal differentiation (Manser et al., 2008). Similarly, by increasing cAMP accumulation, phosphorylation of cAMP response element-binding protein (CREB), and BDNF mRNA levels, guanosine induced neural stem cell proliferation (Su et al., 2013). ERK, CaMKII, PKC, PI3K and PKA were also involved in the trophic effect of guanosine in cultured cerebellar neurons (Tasca et al., 2010). Indeed, the effects of guanosine in the MAPK/ERK, CaMKII, PKC, PI3K and PKA signaling pathways were observed to correlate with the reorganization (from a diffuse to a fibrillary matrix) of extracellular matrix proteins (Decker et al., 2007).

Overall, GBPs have been shown to activate several intracellular pathways that promote biological effects (**Figure 2**). It could then be concluded that the PI3K pathway is one of the main intracellular routes involved in guanosine-induced neuroprotection. Importantly, the identification of GBP receptor(s), which is discussed below, will help to determine the exact sequence of cell signaling pathways activated by GBPs.

GBP RECEPTORS: ARE GBPs ORPHAN MOLECULES?

Selective binding sites for GBPs have already been confirmed in rat brain membranes (Traversa et al., 2002, 2003); but GBP receptors have not yet been identified. The existence of exclusive protein receptors for GBPs are mainly supported by the use of [^{3}H]guanosine in rat brains. Accordingly, it was possible to identify a single high-affinity guanosine binding site (dissociation constant (*Kd*): 95.4 ± 11.9 nM; and apparent number of maximal binding sites (Bmax): 0.57 ± 0.03 pmol/mg protein). Other GBP and guanine metabolites were not potent displacers of guanosine binding, strengthening the hypothesis that guanosine is the ultimate GBP with biological effects. Nevertheless, recent studies also highlighted biological effects for guanine, mainly through modulating memory and learning impairment (Giuliani et al., 2012a; Zuccarini et al., 2018).

One of the hypotheses to identify GBP (or guanosine) receptors consists of their interaction with adenosine receptors. However, given that adenosine, together with caffeine or theophylline (non-selective adenosine receptor antagonists) were not capable of displacing guanosine binding, it would seem likely that other receptors may be involved. Indeed, in 2011, it was identified a new putative GPCR that could be selectively activated by guanosine (Volpini et al., 2011). On the other hand, it would also seem likely that guanosine-mediated effects depend on $G\alpha_i$-protein activation. In this way, by means of the pertussis toxin (PTX), an inhibitor of $G\alpha_i$ family proteins, it was possible to reduce guanosine binding by 45% (Traversa et al., 2003). Interestingly, other studies have focused on assessing whether GBPs could also interact with transporters in the purinergic system. Thus, it was found that a nucleoside transporter inhibitor (nitrobenzylthioinosine) and an inhibitor of adenosine reuptake (propentofylline) had no effect on guanosine binding (Traversa et al., 2003).

Although the identification of putative GBP receptors is a major goal, research has also focused on elucidating the role of some well-characterized membrane proteins, such as glutamate receptors and transporters, adenosine receptors and potassium channels, which have been shown to be involved in the effects of GBPs. The diverse findings suggest that GBPs, especially the nucleoside guanosine, may act as multi-target neuromodulators (Lanznaster et al., 2016).

Glutamate Transporters or Receptors

As discussed above, GBPs can modulate the activity of the glutamatergic system; therefore, a possible direct interaction

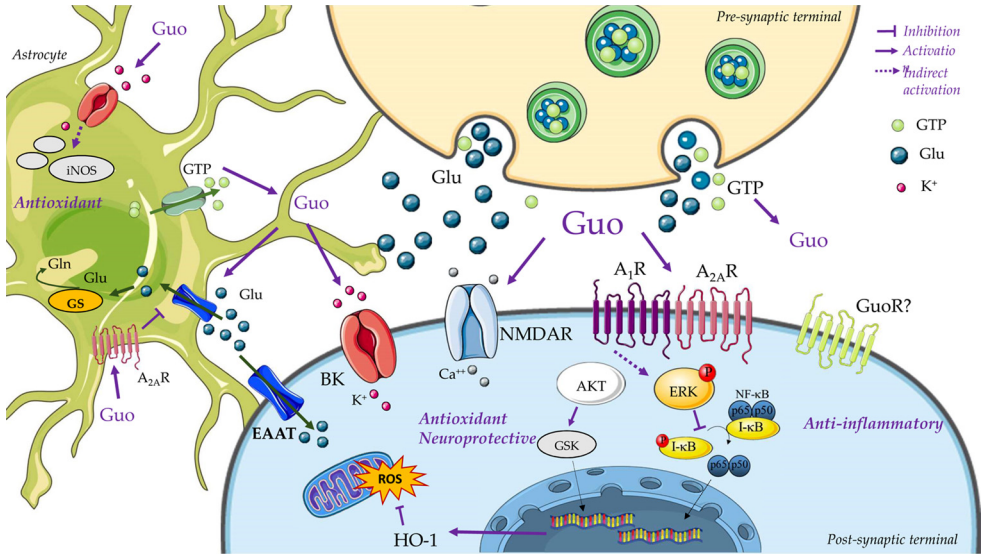

FIGURE 2 | Guanine-based purinergic signaling. This cartoon presents an overview of the main mechanisms involved in the neuroprotective effects of guanosine. The release of guanine nucleotides (i.e., GTP) from synaptic vesicles or astrocytes produces extracellular guanosine (Guo) following hydrolysis by ecto-nucleotidases. Guanine may also be formed by PNP activity on guanosine (not represented). A specific binding site for Guo has not been disclosed yet (i.e., guanosine receptor, GuoR), but guanosine effects through calcium-dependent (big) conductance potassium (BK) channels, A_1R and $A_{2A}R$ adenosine receptors, and glutamatergic N-methyl-D-aspartate receptors (NMDARs) has been described. Guanosine promotes neuroprotection through an anti-inflammatory effect of inhibiting nuclear factor kappa B (NF-κB) activation via MAPK/ERK. Additionally, guanosine presents antioxidant effects, as reducing the reactive oxygen species (ROS) generation, preventing inducible nitric oxide synthase (iNOS) expression, and by increasing antioxidant defenses, as Heme-oxygenase-1 (HO-1) levels. Activation of PI3K/Akt, protein kinase C (PKC) and MAPK/ERK by guanosine leads to stimulation of excitatory amino acid transporters (EAATs) activity. Guo also increases glutamine (Gln) synthetase (GS) activity, thus reducing extracellular levels of glutamate (Glu) and protecting from glutamate excitotoxicity. Figure designed using image templates from Servier Medical Art https://smart.servier.com/image-set-download/.

with glutamate receptors has been explored. Initial binding studies showed that GBPs can displace the binding of glutamate and its analogs to receptors in cell membrane preparations (Sharif and Roberts, 1981; Butcher et al., 1986; Monahan et al., 1988; Baron et al., 1989; Hood et al., 1990; Paas et al., 1996). It was also shown that GBP-induced glutamate displacement would not depend on the interaction with G proteins or on the reduction of agonist binding to other GPCRs (Souza and Ramírez, 1991; Paz et al., 1994; Ramos et al., 1997; Porciúncula et al., 2002; Rotta et al., 2004). Reinforcing this hypothesis, several studies showed that GMP is capable of decreasing glutamate binding to receptors that do not interact with G proteins (Burgos et al., 1998, 2000a,b; Aleu et al., 1999; Tasca et al., 1999a; Tasca and Souza, 2000). Meanwhile, a number of studies failed to observe a direct interaction of other GBPs with glutamate receptors; guanosine and guanine had no effect on the binding of glutamate and its analogs in total rat brain membranes (Traversa et al., 2002; Vinadé et al., 2003). Binding experiments with the post-synaptic density-enriched fraction showed that GppNp (a poor hydrolyzable GTP analog) and GMP displaced 40% and 36%, respectively, of glutamate binding, while guanosine only displaced 23%. Similarly, AMPA binding was not affected by guanosine, but was inhibited 21% and 25% by GppNp and GMP, respectively (Porciúncula et al., 2002).

Considering the capacity of GBPs to modulate glutamate transport, they could also interact with glutamate transporters. Interestingly, the enhancement of glutamate uptake by guanosine was first identified (Dal-Cim et al., 2011, 2013) together with the fact that guanosine reduced glutamate release (Molz et al., 2011). More recently, it was shown that synthetic glutamate transporter inhibitors also inhibited the decrease in glutamate release promoted by guanosine in an *in vitro* ischemia model (Dal-Cim et al., 2016); suggesting a direct interaction of guanosine with glutamate transporters. Nevertheless, despite these data, a direct guanosine-glutamate transporter interaction has still not been demonstrated.

Adenosine Receptors

To date, the involvement of the adenosinergic system in guanosine-mediated effects is still a matter of debate. As discussed above, binding studies seemed to rule out a direct interaction of guanosine with adenosine receptors. However, several biological effects induced by guanosine seem to be dependent on adenosine receptors, namely on A_1R and $A_{2A}R$. For example, although caffeine (a non-selective adenosine receptor antagonist) did not alter guanosine binding in rat brain (Traversa et al., 2003), it reversed the guanosine-mediated anxiolytic-like behavior. In contrast, caffeine was not able to block the effects of guanosine in capsaicin-induced nociception (Schmidt et al., 2008), and the anticonvulsant effect of guanosine on QA-induced seizures in mice (Lara et al., 2001). Similarly, DPCPX, a selective A_1R antagonist blocked guanosine anti-nociceptive effects, but not SCH58361, an $A_{2A}R$

antagonist (Schmidt et al., 2008). Contradictorily, in cultured cerebellar neurons, the trophic effects of guanosine depended on $A_{2A}R$, since the selective antagonist ZM241385 blocked increased neuronal adhesion mediated by guanosine (Tasca et al., 2010).

The involvement of A_1R and $A_{2A}R$ in the guanosine cytoprotective effects has been well characterized in *in vitro* and *ex vivo* studies. In a human neuroblastoma cell line (SH-SY5Y) subjected to mitochondrial oxidative stress, the protective effects of guanosine were blocked by DPCPX and ZM241385 (Dal-Cim et al., 2012). Guanosine induced a decrease in ROS formation and mitochondrial membrane potential in hippocampal slices subjected to OGD, which was dependent on A_1R, since DPCPX treatment inhibited the protective effect of guanosine; however, A_1R inhibition did not affect the effect of guanosine on glutamate uptake. Also, PTX blocked the effects of guanosine mediating recovery from OGD-induced glutamate uptake impairment, suggesting an interaction with a $G\alpha_i$ protein-coupled receptor. In contrast, activation of $A_{2A}R$ by agonist CGS21680 inhibited guanosine-induced neuroprotection, but $A_{2A}R$ blockade with the antagonist ZM241385 did not; both assessed by cellular viability and glutamate uptake (Dal-Cim et al., 2013). These controversial results support the hypothesis that guanosine needs the presence of both A_1R and $A_{2A}R$, which could be related to the fact that these receptors directly interact forming the so-called receptor oligomers. Indeed, it was demonstrated that these receptors associate in the membrane of cells and interact with each other in an antagonistic manner (Ciruela et al., 2006a,b; Ciruela, 2013). Further studies should be performed to demonstrate this hypothesis.

Potassium Channels

Apart from its effects on GPCRs commented on above, guanosine has also been shown to modulate the activity and expression of K^+ channels. In this way, the function of inward rectifier K^+ channels was increased upon guanosine challenge in cultured rat cortical astrocytes (Benfenati et al., 2006). Also, the neuroprotective effects of guanosine would also depend on K^+ channel activity. In line with this, charybdotoxin, which blocks large-conductance Ca^{2+}-activated K^+ channels (BK), was able to impede guanosine-mediated cellular viability increase in OGD-treated hippocampal slices and also blocked the protective effects of guanosine on SH-SY5Y cells subjected to mitochondrial damage (Dal-Cim et al., 2011, 2012). BK blockage also inhibited guanosine-mediated recovery of the decreased glutamate uptake in hippocampal slices subjected to OGD (Dal-Cim et al., 2011). It should be noted that other potassium channels do not seem to modulate guanosine-mediated neuroprotective effects. Thus, guanosine-induced neuroprotection was not affected by the inhibition of ATP-sensitive K^+ channels (with glibenclamide) or small-conductance Ca^{2+}-activated K^+ (SK) channels (with apamin; Dal-Cim et al., 2011). Indeed, guanosine increased K^+ conductance in cells transiently transfected with the functional α-subunit of BK channels but not with SK channels (Tasca et al., 2013).

From the reports discussed here, it seems clear that additional studies are necessary to unravel the putative molecular targets of guanosine (and even of guanine), in order to understand the actual complexity of the GBP system.

PERSPECTIVES ON THE GUANINE-BASED PURINERGIC SYSTEM

GBPs exert a plethora of beneficial (i.e., neuroprotective, neurotrophic, antidepressant, anxiolytic and analgesic) effects throughout the CNS. Accordingly, in recent years, much effort has been devoted to fully characterize these kinds of effects and elucidating the still unresolved mechanisms of action of these molecules. Importantly, the lack of identification of putative GBP receptors, which may mediate some of the observed effects (other receptors, such as glutamate or adenosine receptors, and ion channels, may also be involved) has slowed this process. For this reason, in the next few years, an exponential rise in GBP studies is expected, in which the elucidation of both the mechanism of action of these molecules and the exact role they play in some pathologies (e.g., AD and PD) may be the main goals. Meanwhile, some empirical data can already be successfully used in a number of clinical situations. For instance, drugs facilitating the salvage pathway of purine recycling, such as allopurinol, a xanthine oxidase activity inhibitor, could be included as an option for refractory epilepsy (Togha et al., 2007). Similarly, alteration of purine metabolism may be considered a possible biomarker for PD diagnosis. Thus, a reduction in uric acid plasma levels can be observed in PD patients (Schwarzschild et al., 2008), while increased urate levels have been found in post-mortem PD brains. Altogether, these data reinforce the notion that purine levels and metabolism may modulate response of the organism to injury, acting as a retaliatory system responsible for modulating unbalanced neurotransmission in damaging situations. Overall, together with evidences showing that GBPs may have both trophic effects on neural cells and beneficial behavioral effects, present knowledge of GBP biology in the CNS supports the rationale for further studies of this system and the development of novel drugs that may be useful in the near future.

AUTHOR CONTRIBUTIONS

CT wrote the article and made illustrations. DL, KO, VF-D and FC wrote the article.

FUNDING

This work was supported by MINECO/ISCIII (SAF2017-87349-R and PIE14/00034), the Catalan government (2017 SGR 1604), Fundació la Marató de TV3 (Grant 20152031), FWO (SBO-140028) to FC; and by CAPES (PVE 052/2012), CNPq (INCT for Excitotoxicity and Neuroprotection) and FAPESC (NENASC/PRONEX) to CT. CT is recipient of CNPq productivity fellowship. Also, this work was funded by CAPES/PVE 052/2012 and CNPq process 207161/2014-3, who provided doctoral fellowships for DL.

REFERENCES

Albrecht, J., and Jones, E. A. (1999). Hepatic encephalopathy: molecular mechanisms underlying the clinical syndrome. *J. Neurol. Sci.* 170, 138–146. doi: 10.1016/s0022-510x(99)00169-0

Aleu, J., Barat, A., Burgos, J. S., Solsona, C., Marsal, J., and Ramírez, G. (1999). Guanine nucleotides, including GMP, antagonize kainate responses in *Xenopus* oocytes injected with chick cerebellar membranes. *J. Neurochem.* 72, 2170–2176. doi: 10.1046/j.1471-4159.1999.0722170.x

Almeida, R. F., Cereser, V. H., Faraco, R. B., Böhmer, A. E., Souza, D. O., and Ganzella, M. (2010). Systemic administration of GMP induces anxiolytic-like behavior in rats. *Pharmacol. Biochem. Behav.* 96, 306–311. doi: 10.1016/j.pbb.2010.05.022

Baron, B. M., Dudley, M. W., McCarty, D. R., Miller, F. P., Reynolds, I. J., and Schmidt, C. J. (1989). Guanine nucleotides are competitive inhibitors of N-methyl-D-aspartate at its receptor site both *in vitro* and *in vivo*. *J. Pharmacol. Exp. Ther.* 250, 162–169.

Bau, C., Middlemiss, P. J., Hindley, S., Jiang, S., Ciccarelli, R., Caciagli, F., et al. (2005). Guanosine stimulates neurite outgrowth in PC12 cells via activation of heme oxygenase and cyclic GMP. *Purinergic Signal.* 1, 161–172. doi: 10.1007/s11302-005-6214-0

Bellaver, B., Souza, D. G., Bobermin, L. D., Gonçalves, C.-A., Souza, D. O., and Quincozes-Santos, A. (2015). Guanosine inhibits LPS-induced pro-inflammatory response and oxidative stress in hippocampal astrocytes through the heme oxygenase-1 pathway. *Purinergic Signal.* 11, 571–580. doi: 10.1007/s11302-015-9475-2

Benfenati, V., Caprini, M., Nobile, M., Rapisarda, C., and Ferroni, S. (2006). Guanosine promotes the up-regulation of inward rectifier potassium current mediated by Kir4.1 in cultured rat cortical astrocytes. *J. Neurochem.* 98, 430–445. doi: 10.1111/j.1471-4159.2006.03877.x

Bettio, L. E. B., Cunha, M. P., Budni, J., Pazini, F. L., Oliveira, Á., Colla, A. R., et al. (2012). Guanosine produces an antidepressant-like effect through the modulation of NMDA receptors, nitric oxide-cGMP and PI3K/mTOR pathways. *Behav. Brain Res.* 234, 137–148. doi: 10.1016/j.bbr.2012.06.021

Bettio, L. E. B., Freitas, A. E., Neis, V. B., Santos, D. B., Ribeiro, C. M., Rosa, P. B., et al. (2014). Guanosine prevents behavioral alterations in the forced swimming test and hippocampal oxidative damage induced by acute restraint stress. *Pharmacol. Biochem. Behav.* 127, 7–14. doi: 10.1016/j.pbb.2014.10.002

Bettio, L. E. B., Gil-Mohapel, J., and Rodrigues, A. L. (2016a). Current perspectives on the antidepressant-like effects of guanosine. *Neural Regen. Res.* 11, 1411–1413. doi: 10.4103/1673-5374.191209

Bettio, L. E. B., Neis, V. B., Pazini, F. L., Brocardo, P. S., Patten, A. R., Gil-Mohapel, J., et al. (2016b). The antidepressant-like effect of chronic guanosine treatment is associated with increased hippocampal neuronal differentiation. *Eur. J. Neurosci.* 43, 1006–1015. doi: 10.1111/ejn.13172

Burgos, J. S., Barat, A., and Ramirez, G. (2000a). Ca^{2+}-dependent kainate excitotoxicity in the chick embryonic neural retina *ex vivo*. *Neuroreport* 11, 3855–3858. doi: 10.1097/00001756-200011270-00050

Burgos, J. S., Barat, A., and Ramírez, G. (2000b). Guanine nucleotides block agonist-driven 45Ca2+ influx in chick embryo retinal explants. *Neuroreport* 11, 2303–2305. doi: 10.1097/00001756-200007140-00047

Burgos, J. S., Barat, A., Souza, D. O., and Ramírez, G. (1998). Guanine nucleotides protect against kainate toxicity in an *ex vivo* chick retinal preparation. *FEBS Lett.* 430, 176–180. doi: 10.1016/s0014-5793(98)00651-6

Burnstock, G. (1972). Purinergic nerves. *Pharmacol. Rev.* 24, 509–581.

Burnstock, G., Campbell, G., Satchell, D., and Smythe, A. (1970). Evidence that adenosine triphosphate or a related nucleotide is the transmitter substance released by non-adrenergic inhibitory nerves in the gut. *Br. J. Pharmacol.* 40, 668–688. doi: 10.1111/j.1476-5381.1970.tb10646.x

Burnstock, G., Fredholm, B. B., and Verkhratsky, A. (2011). Adenosine and ATP receptors in the brain. *Curr. Top. Med. Chem.* 11, 973–1011. doi: 10.2174/156802611795347627

Butcher, S. P., Roberts, P. J., and Collins, J. F. (1986). Purine nucleotides inhibit the binding of DL-[^{3}H] 2-amino-4-phosphonobutyrate (DL-[^{3}H] APB) to L-glutamate-sensitive sites on rat brain membranes. *Biochem. Pharmacol.* 35, 991–994. doi: 10.1016/0006-2952(86)90088-2

Butterworth, R. F., Giguère, J.-F., Michaud, J., Lavoie, J., and Layrargues, G. P. (1987). Ammonia: key factor in the pathogenesis of hepatic encephalopathy. *Neurochem. Pathol.* 6, 1–12. doi: 10.1007/bf02833598

Chaki, S., and Fukumoto, K. (2015). Potential of glutamate-based drug discovery for next generation antidepressants. *Pharmaceuticals* 8, 590–606. doi: 10.3390/ph8030590

Chang, R., Algird, A., Bau, C., Rathbone, M. P., and Jiang, S. (2008). Neuroprotective effects of guanosine on stroke models *in vitro* and *in vivo*. *Neurosci. Lett.* 431, 101–105. doi: 10.1016/j.neulet.2007.11.072

Chen, X., Xie, C., Sun, L., Ding, J., and Cai, H. (2015). Longitudinal metabolomics profiling of Parkinson's disease-related α-synuclein A53T transgenic mice. *PLoS One* 10:e0136612. doi: 10.1371/journal.pone.0136612

Ciccarelli, R., Ballerini, P., Sabatino, G., Rathbone, M. P., D'Onofrio, M., Caciagli, F., et al. (2001). Involvement of astrocytes in purine-mediated reparative processes in the brain. *Int. J. Dev. Neurosci.* 19, 395–414. doi: 10.1016/s0736-5748(00)00084-8

Ciccarelli, R., Di Iorio, P., Giuliani, P., D'Alimonte, I., Ballerini, P., Caciagli, F., et al. (1999). Rat cultured astrocytes release guanine-based purines in basal conditions and after hypoxia/hypoglycemia. *Glia* 25, 93–98. doi: 10.1002/(sici)1098-1136(19990101)25:1<93::aid-glia9>3.0.co;2-n

Ciruela, F. (2013). Guanosine behind the scene. *J. Neurochem.* 126, 425–427. doi: 10.1111/jnc.12328

Ciruela, F., Casado, V., Rodrigues, R. J., Lujan, R., Burgueño, J., Canals, M., et al. (2006a). Presynaptic control of striatal glutamatergic neurotransmission by adenosine A_1–A_{2A} receptor heteromers. *J. Neurosci.* 26, 2080–2087. doi: 10.1523/JNEUROSCI.3574-05.2006

Ciruela, F., Ferré, S., Casadó, V., Cortés, A., Cunha, R. A., Lluis, C., et al. (2006b). Heterodimeric adenosine receptors: a device to regulate neurotransmitter release. *Cell. Mol. Life Sci.* 63, 2427–2431. doi: 10.1007/s00018-006-6216-2

Ciruela, F., Fernández-Dueñas, V., Llorente, J., Borroto-Escuela, D., Cuffí, M. L., Carbonell, L., et al. (2012). G protein-coupled receptor oligomerization and brain integration: focus on adenosinergic transmission. *Brain Res.* 1476, 86–95. doi: 10.1016/j.brainres.2012.04.056

Connell, B. J., Di Iorio, P., Sayeed, I., Ballerini, P., Saleh, M. C., Giuliani, P., et al. (2013). Guanosine protects against reperfusion injury in rat brains after ischemic stroke. *J. Neurosci. Res.* 91, 262–272. doi: 10.1002/jnr.23156

Cunha, R. A. (2005). Neuroprotection by adenosine in the brain: from A_1 receptor activation to A_{2A} receptor blockade. *Purinergic Signal.* 1, 111–134. doi: 10.1007/s11302-005-0649-1

Da Silva, A. L., and Elisabetsky, E. (2001). Interference of propylene glycol with the hole-board test. *Braz. J. Med. Biol. Res.* 34, 545–547. doi: 10.1590/s0100-879x2001000400016

Dal-Cim, T., Ludka, F. K., Martins, W. C., Reginato, C., Parada, E., Egea, J., et al. (2013). Guanosine controls inflammatory pathways to afford neuroprotection of hippocampal slices under oxygen and glucose deprivation conditions. *J. Neurochem.* 126, 437–450. doi: 10.1111/jnc.12324

Dal-Cim, T., Martins, W. C., Santos, A. R. S., and Tasca, C. I. (2011). Guanosine is neuroprotective against oxygen/glucose deprivation in hippocampal slices via large conductance Ca^{2+}-activated K^+ channels, phosphatidilinositol-3 kinase/protein kinase B pathway activation and glutamate uptake. *Neuroscience* 183, 212–220. doi: 10.1016/j.neuroscience.2011.03.022

Dal-Cim, T., Martins, W. C., Thomaz, D. T., Coelho, V., Poluceno, G. G., Lanznaster, D., et al. (2016). Neuroprotection promoted by guanosine depends on glutamine synthetase and glutamate transporters activity in hippocampal slices subjected to oxygen/glucose deprivation. *Neurotox. Res.* 29, 460–468. doi: 10.1007/s12640-015-9595-z

Dal-Cim, T., Molz, S., Egea, J., Parada, E., Romero, A., Budni, J., et al. (2012). Guanosine protects human neuroblastoma SH-SY5Y cells against mitochondrial oxidative stress by inducing heme oxigenase-1 via PI3K/Akt/GSK-3β pathway. *Neurochem. Int.* 61, 397–404. doi: 10.1016/j.neuint.2012.05.021

Dalla Corte, C. L., Bastos, L. L., Dobrachinski, F., Rocha, J. B. T., and Soares, F. A. A. (2012). The combination of organoselenium compounds and guanosine prevents glutamate-induced oxidative stress in different regions of rat brains. *Brain Res.* 1430, 101–111. doi: 10.1016/j.brainres.2011.10.049

de Oliveira, D. L., Horn, J. F., Rodrigues, J. M., Frizzo, M. E. S., Moriguchi, E., Souza, D. O., et al. (2004). Quinolinic acid promotes seizures and decreases glutamate uptake in young rats: reversal by orally administered guanosine. *Brain Res.* 1018, 48–54. doi: 10.1016/j.brainres.2004.05.033

de Oliveira, E. D., Schallenberger, C., Böhmer, A. E., Hansel, G., Fagundes, A. C., Milman, M., et al. (2016). Mechanisms involved in the antinociception induced by spinal administration of inosine or guanine in mice. *Eur. J. Pharmacol.* 772, 71–82. doi: 10.1016/j.ejphar.2015.12.034

Decker, H., Francisco, S. S., Mendes-de-Aguiar, C. B. N., Romão, L. F., Boeck, C. R., Trentin, A. G., et al. (2007). Guanine derivatives modulate extracellular matrix proteins organization and improve neuron-astrocyte co-culture. *J. Neurosci. Res.* 85, 1943–1951. doi: 10.1002/jnr.21332

Di Iorio, P., Ballerini, P., Traversa, U., Nicoletti, F., D'Alimonte, I., Kleywegt, S., et al. (2004). The antiapoptotic effect of guanosine is mediated by the activation of the PI 3-kinase/AKT/PKB pathway in cultured rat astrocytes. *Glia* 46, 356–368. doi: 10.1002/glia.20002

Drury, A. N., and Szent-Györgyi, A. (1929). The physiological activity of adenine compounds with especial reference to their action upon the mammalian heart. *J. Physiol.* 68, 213–237. doi: 10.1113/jphysiol.1929.sp002608

Durukan, A., and Tatlisumak, T. (2007). Acute ischemic stroke: overview of major experimental rodent models, pathophysiology, and therapy of focal cerebral ischemia. *Pharmacol. Biochem. Behav.* 87, 179–197. doi: 10.1016/j.pbb.2007.04.015

Gage, F. H. (2000). Mammalian neural stem cells. *Science* 287, 1433–1438. doi: 10.1126/science.287.5457.1433

Gage, F. H., Kempermann, G., Palmer, T. D., Peterson, D. A., and Ray, J. (1998). Multipotent progenitor cells in the adult dentate gyrus. *J. Neurobiol.* 36, 249–266. doi: 10.1002/(sici)1097-4695(199808)36:2<249::aid-neu11>3.0.co;2-9

Ganzella, M., de Oliveira, E. D. A., Comassetto, D. D., Cechetti, F., Cereser, V. H., Moreira, J. D., et al. (2012). Effects of chronic guanosine treatment on hippocampal damage and cognitive impairment of rats submitted to chronic cerebral hypoperfusion. *Neurol. Sci.* 33, 985–997. doi: 10.1007/s10072-011-0872-1

Gilson, J., and Blakemore, W. F. (1993). Failure of remyelination in areas of demyelination produced in the spinal cord of old rats. *Neuropathol. Appl. Neurobiol.* 19, 173–181. doi: 10.1111/j.1365-2990.1993.tb00424.x

Giuliani, P., Buccella, S., Ballerini, P., Ciccarelli, R., D'Alimonte, I., Cicchitti, S., et al. (2012a). Guanine-based purines modulate the effect of L-NAME on learning and memory in rats. *Panminerva Med.* 54, 53–58.

Giuliani, P., Romano, S., Ballerini, P., Ciccarelli, R., Petragnani, N., Cicchitti, S., et al. (2012b). Protective activity of guanosine in an *in vitro* model of Parkinson's disease. *Panminerva Med.* 54, 43–51.

Giuliani, P., Zuccarini, M., Buccella, S., Rossini, M., D'Alimonte, I., Ciccarelli, R., et al. (2016). Development of a new HPLC method using fluorescence detection without derivatization for determining purine nucleoside phosphorylase activity in human plasma. *J. Chromatogr. B Analyt. Technol. Biomed. Life Sci.* 1009–1010, 114–121. doi: 10.1016/j.jchromb.2015.12.012

Gualix, J., Pintor, J., and Miras-Portugal, M. T. (1999). Characterization of nucleotide transport into rat brain synaptic vesicles. *J. Neurochem.* 73, 1098–1104. doi: 10.1046/j.1471-4159.1999.0731098.x

Gysbers, J. W., and Rathbone, M. P. (1992). Guanosine enhances NGF-stimulated neurite outgrowth in PC12 cells. *Neuroreport* 3, 997–1000. doi: 10.1097/00001756-199211000-00013

Gysbers, J. W., and Rathbone, M. P. (1996a). GTP and guanosine synergistically enhance NGF-induced neurite outgrowth from PC12 cells. *Int. J. Dev. Neurosci.* 14, 19–34. doi: 10.1016/0736-5748(95)00083-6

Gysbers, J. W., and Rathbone, M. P. (1996b). Neurite outgrowth in PC12 cells is enhanced by guanosine through both cAMP-dependent and -independent mechanisms. *Neurosci. Lett.* 220, 175–178. doi: 10.1016/s0304-3940(96)13253-5

Hansel, G., Ramos, D. B., Delgado, C. A., Souza, D. G., Almeida, R. F., Portela, L. V., et al. (2014). The potential therapeutic effect of guanosine after cortical focal ischemia in rats. *PLoS One* 9:e90693. doi: 10.1371/journal.pone.0090693

Hansel, G., Tonon, A. C., Guella, F. L., Pettenuzzo, L. F., Duarte, T., Duarte, M. M. M. F., et al. (2015). Guanosine protects against cortical focal ischemia. Involvement of inflammatory response. *Mol. Neurobiol.* 52, 1791–1803. doi: 10.1007/s12035-014-8978-0

Hepler, J. R., and Gilman, A. G. (1992). G proteins. *Trends Biochem. Sci.* 17, 383–387. doi: 10.1016/0968-0004(92)90005-T

Heyes, M. P., Wyler, A. R., Devinsky, O., Yergey, J. A., Markey, S. P., and Nadi, N. S. (1990). Quinolinic acid concentrations in brain and cerebrospinal fluid of patients with intractable complex partial seizures. *Epilepsia* 31, 172–177. doi: 10.1111/j.1528-1167.1990.tb06302.x

Hood, W. F., Thomas, J. W., Compton, R. P., and Monahan, J. B. (1990). Guanine nucleotide modulation of [^{3}H]TCP binding to the NMDA receptor complex. *Eur. J. Pharmacol.* 188, 43–49. doi: 10.1016/0922-4106(90)90246-t

Horner, P. J., Power, A. E., Kempermann, G., Kuhn, H. G., Palmer, T. D., Winkler, J., et al. (2000). Proliferation and differentiation of progenitor cells throughout the intact adult rat spinal cord. *J. Neurosci.* 20, 2218–2228. doi: 10.1523/JNEUROSCI.20-06-02218.2000

Iigo, M., Miwa, M., Ishitsuka, H., and Nitta, K. (1987). Potentiation of the chemotherapeutic action of 5'-deoxy-5-fluorouridine in combination with guanosine and related compounds. *Cancer Chemother. Pharmacol.* 19, 61–64. doi: 10.1007/bf00296258

Jacobson, K. A., and Gao, Z. G. (2006). Adenosine receptors as therapeutic targets. *Nat. Rev. Drug Discov.* 5, 247–264. doi: 10.1038/nrd1983

Jiang, S., Ballerini, P., Buccella, S., Giuliani, P., Jiang, C., Huang, X., et al. (2008). Remyelination after chronic spinal cord injury is associated with proliferation of endogenous adult progenitor cells after systemic administration of guanosine. *Purinergic Signal.* 4, 61–71. doi: 10.1007/s11302-007-9093-8

Jiang, S., Khan, M. I., Lu, Y., Wang, J., Buttigieg, J., Werstiuk, E. S., et al. (2003). Guanosine promotes myelination and functional recovery in chronic spinal injury. *Neuroreport* 14, 2463–2467. doi: 10.1097/00001756-200312190-00034

Karran, E., Mercken, M., and De Strooper, B. (2011). The amyloid cascade hypothesis for Alzheimer's disease: an appraisal for the development of therapeutics. *Nat. Rev. Drug Discov.* 10, 698–712. doi: 10.1038/nrd3505

Kim, S. G., Kim, C. W., Ahn, E.-T., Lee, K.-Y., Hong, E.-K., Yoo, B.-I., et al. (1997). Enhanced anti-tumor effects of acriflavine in combination with guanosine in mice. *J. Pharm. Pharmacol.* 49, 216–222. doi: 10.1111/j.2042-7158.1997.tb06783.x

Kolber, B. J. (2015). mGluRs head to toe in pain. *Prog. Mol. Biol. Transl. Sci.* 131, 281–324. doi: 10.1016/bs.pmbts.2014.12.003

Kovács, Z., Kékesi, K. A., Dobolyi, Á., Lakatos, R., and Juhász, G. (2015). Absence epileptic activity changing effects of non-adenosine nucleoside inosine, guanosine and uridine in Wistar Albino Glaxo Rijswijk rats. *Neuroscience* 300, 593–608. doi: 10.1016/j.neuroscience.2015.05.054

Lanznaster, D., Dal-Cim, T., Piermartiri, T. C. B., and Tasca, C. I. (2016). Guanosine: a neuromodulator with therapeutic potential in brain disorders. *Aging Dis.* 7, 657–679. doi: 10.14336/ad.2016.0208

Lanznaster, D., Mack, J. M., Coelho, V., Ganzella, M., Almeida, R. F., Dal-Cim, T., et al. (2017). Guanosine prevents anhedonic-like behavior and impairment in hippocampal glutamate transport following amyloid-β1–40 administration in mice. *Mol. Neurobiol.* 54, 5482–5496. doi: 10.1007/s12035-016-0082-1

Lara, D. R., Schmidt, A. P., Frizzo, M. E., Burgos, J. S., Ramírez, G., and Souza, D. O. (2001). Effect of orally administered guanosine on seizures and death induced by glutamatergic agents. *Brain Res.* 912, 176–180. doi: 10.1016/s0006-8993(01)02734-2

Lipmann, F. (1941). "Metabolic generation and utilization of phosphate bond energy," in *Advances in Enzymology and Related Subjects*, eds F. F. Nord and C. H. Werkman (New York, NY: Interscience Publishers), 99–162.

Manser, C., Stevenson, A., Banner, S., Davies, J., Tudor, E. L., Ono, Y., et al. (2008). Deregulation of PKN1 activity disrupts neurofilament organisation and axonal transport. *FEBS Lett.* 582, 2303–2308. doi: 10.1016/j.febslet.2008.05.034

Massari, C. M., López-Cano, M., Núñez, F., Fernández-Dueñas, V., Tasca, C. I., and Ciruela, F. (2017). Antiparkinsonian efficacy of guanosine in rodent models of movement disorder. *Front. Pharmacol.* 8:700. doi: 10.3389/fphar.2017.00700

Masters, C. L., and Selkoe, D. J. (2012). Biochemistry of amyloid β-protein and amyloid deposits in Alzheimer disease. *Cold Spring Harb. Perspect. Med.* 2:a006262. doi: 10.1101/cshperspect.a006262

Mazurek, A. A. (2000). Treatment of Alzheimer's disease. *N. Engl. J. Med.* 342:821; author reply 821–822. doi: 10.1056/NEJM200003163421114

Meldrum, B. S. (1994). The role of glutamate in epilepsy and other CNS disorders. *Neurology* 44, S14–S23.

Meldrum, B. S. (2000). Glutamate as a neurotransmitter in the brain: review of physiology and pathology. *J. Nutr.* 130, 1007S–1015S. doi: 10.1093/jn/130.4.1007s

Middlemiss, P. J., Gysbers, J. W., and Rathbone, M. P. (1995). Extracellular guanosine and guanosine-5'-triphosphate increase: NGF synthesis and release from cultured mouse neopallial astrocytes. *Brain Res.* 677, 152–156. doi: 10.1016/0006-8993(95)00156-k

Miyamoto, S., Ogawa, H., Shiraki, H., and Nakagawa, H. (1982). Guanine deaminase from rat brain. Purification, characteristics, and contribution to ammoniagenesis in the brain. *J. Biochem.* 91, 167–176. doi: 10.1093/oxfordjournals.jbchem.a133673

Molz, S., Dal-Cim, T., Budni, J., Martín-de-Saavedra, M. D., Egea, J., Romero, A., et al. (2011). Neuroprotective effect of guanosine against glutamate-induced cell death in rat hippocampal slices is mediated by the phosphatidylinositol-3 kinase/Akt/glycogen synthase kinase 3β pathway activation and inducible nitric oxide synthase inhibition. *J. Neurosci. Res.* 89, 1400–1408. doi: 10.1002/jnr.22681

Molz, S., Dal-Cim, T., and Tasca, C. I. (2009). Guanosine-5'-monophosphate induces cell death in rat hippocampal slices via ionotropic glutamate receptors activation and glutamate uptake inhibition. *Neurochem. Int.* 55, 703–709. doi: 10.1016/j.neuint.2009.06.015

Monahan, J. B., Hood, W. F., Michel, J., and Compton, R. P. (1988). Effects of guanine nucleotides on N-methyl-D-aspartate receptor-ligand interactions. *Mol. Pharmacol.* 34, 111–116.

Moretto, M. B., Arteni, N. S., Lavinsky, D., Netto, C. A., Rocha, J. B. T., Souza, D. O., et al. (2005). Hypoxic-ischemic insult decreases glutamate uptake by hippocampal slices from neonatal rats: prevention by guanosine. *Exp. Neurol.* 195, 400–406. doi: 10.1016/j.expneurol.2005.06.005

Moretto, M. B., Boff, B., Lavinsky, D., Netto, C. A., Rocha, J. B. T., Souza, D. O., et al. (2009). Importance of schedule of administration in the therapeutic efficacy of guanosine: early intervention after injury enhances glutamate uptake in model of hypoxia-ischemia. *J. Mol. Neurosci.* 38, 216–219. doi: 10.1007/s12031-008-9154-7

Nakano, K., Takahashi, S., Mizobuchi, M., Kuroda, T., Masuda, K., and Kitoh, J. (1993). High levels of quinolinic acid in brain of epilepsy-prone E1 mice. *Brain Res.* 619, 195–198. doi: 10.1016/0006-8993(93)91612-v

Naliwaiko, K., Luvizon, A. C., Donatti, L., Chammas, R., Mercadante, A. F., Zanata, S. M., et al. (2008). Guanosine promotes B16F10 melanoma cell differentiation through PKC-ERK 1/2 pathway. *Chem. Biol. Interact.* 173, 122–128. doi: 10.1016/j.cbi.2008.03.010

Neary, J. T., Rathbone, M. P., Cattabeni, F., Abbracchio, M. P., and Burnstock, G. (1996). Trophic actions of extracellular nucleotides and nucleosides on glial and neuronal cells. *Trends Neurosci.* 19, 13–18. doi: 10.1016/0166-2236(96)81861-3

Olanow, C. W., and Tatton, W. G. (1999). Etiology and pathogenesis of Parkinson's disease. *Annu. Rev. Neurosci.* 22, 123–144. doi: 10.1146/annurev.neuro.22.1.123

Oleskovicz, S. P., Martins, W. C., Leal, R. B., and Tasca, C. I. (2008). Mechanism of guanosine-induced neuroprotection in rat hippocampal slices submitted to oxygen-glucose deprivation. *Neurochem. Int.* 52, 411–418. doi: 10.1016/j.neuint.2007.07.017

Oliveira, K. A., Dal-Cim, T. A., Lopes, F. G., Nedel, C. B., and Tasca, C. I. (2017). Guanosine promotes cytotoxicity via adenosine receptors and induces apoptosis in temozolomide-treated A172 glioma cells. *Purinergic Signal.* 13, 305–318. doi: 10.1007/s11302-017-9562-7

Paas, Y., Devillers-Thiéry, A., Changeux, J. P., Medevielle, F., and Teichberg, V. I. (1996). Identification of an extracellular motif involved in the binding of guanine nucleotides by a glutamate receptor. *EMBO J.* 15, 1548–1556. doi: 10.1002/j.1460-2075.1996.tb00499.x

Paniz, L. G., Calcagnotto, M. E., Pandolfo, P., Machado, D. G., Santos, G. F., Hansel, G., et al. (2014). Neuroprotective effects of guanosine administration on behavioral, brain activity, neurochemical and redox parameters in a rat model of chronic hepatic encephalopathy. *Metab. Brain Dis.* 29, 645–654. doi: 10.1007/s11011-014-9548-x

Paz, M. M., Ramos, M., Ramírez, G., and Souza, D. (1994). Differential effects of guanine nucleotides on kainic acid binding and on adenylate cyclase activity in chick optic tectum. *FEBS Lett.* 355, 205–208. doi: 10.1016/0014-5793(94)01208-3

Petronilho, F., Périco, S. R., Vuolo, F., Mina, F., Constantino, L., Comim, C. M., et al. (2012). Protective effects of guanosine against sepsis-induced damage in rat brain and cognitive impairment. *Brain Behav. Immun.* 26, 904–910. doi: 10.1016/j.bbi.2012.03.007

Pettifer, K. M., Jiang, S., Bau, C., Ballerini, P., D'Alimonte, I., Werstiuk, E. S., et al. (2007). MPP^+-induced cytotoxicity in neuroblastoma cells: antagonism and reversal by guanosine. *Purinergic Signal.* 3, 399–409. doi: 10.1007/s11302-007-9073-z

Pettifer, K. M., Kleywegt, S., Bau, C. J., Ramsbottom, J. D., Vertes, E., Ciccarelli, R., et al. (2004). Guanosine protects SH-SY5Y cells against β-amyloid-induced apoptosis. *Neuroreport* 15, 833–836. doi: 10.1097/00001756-200404090-00019

Porciúncula, L. O., Vinadé, L., Wofchuk, S., and Souza, D. O. (2002). Guanine based purines inhibit [^{3}H]glutamate and [^{3}H]AMPA binding at postsynaptic densities from cerebral cortex of rats. *Brain Res.* 928, 106–112. doi: 10.1016/s0006-8993(01)03368-6

Quincozes-Santos, A., Bobermin, L. D., de Souza, D. G., Bellaver, B., Gonçalves, C.-A., and Souza, D. O. (2013). Gliopreventive effects of guanosine against glucose deprivation *in vitro*. *Purinergic Signal.* 9, 643–654. doi: 10.1007/s11302-013-9377-0

Ramos, M., Souza, D. O., and Ramírez, G. (1997). Specific binding of [^{3}H]GppNHp to extracellular membrane receptors in chick cerebellum: possible involvement of kainic acid receptors. *FEBS Lett.* 406, 114–118. doi: 10.1016/s0014-5793(97)00260-3

Rathbone, M. P., Middlemiss, P. J., Gysbers, J. W., Andrew, C., Herman, M. A., Reed, J. K., et al. (1999). Trophic effects of purines in neurons and glial cells. *Prog. Neurobiol.* 59, 663–690. doi: 10.1016/s0301-0082(99)00017-9

Rathbone, M. P., Saleh, T. M., Connell, B. J., Chang, R., Su, C., Worley, B., et al. (2011). Systemic administration of guanosine promotes functional and histological improvement following an ischemic stroke in rats. *Brain Res.* 1407, 79–89. doi: 10.1016/j.brainres.2011.06.027

Regner, A., Crestana, R. E., Silveira F, J. P., Friedman, G., Chemale, I., and Souza, D. (1997). Guanine nucleotides are present in human CSF. *Neuroreport* 8, 3771–3774. doi: 10.1097/00001756-199712010-00023

Regner, A., Ramirez, G., Belló-Klein, A., and Souza, D. (1998). Effects of guanine nucleotides on glutamate-induced chemiluminescence in rat hippocampal slices submitted to hypoxia. *Neurochem. Res.* 23, 519–524. doi: 10.1023/A:1022430501454

Rodbell, M., Birnbaumer, L., Pohl, S. L., and Krans, H. M. (1971). The glucagon-sensitive adenyl cyclase system in plasma membranes of rat liver. V. An obligatory role of guanylnucleotides in glucagon action. *J. Biol. Chem.* 246, 1877–1882.

Rotta, L. N., Soares, F. A. A., Nogueira, C. W., Martini, L. H., Perry, M. L. S., and Souza, D. O. (2004). Characterization of imido [8–^{3}H] guanosine 5'-triphosphate binding sites to rat brain membranes. *Neurochem. Res.* 29, 805–809. doi: 10.1023/b:nere.0000018854.67768.47

Santos, T. G., Souza, D. O., and Tasca, C. I. (2006). GTP uptake into rat brain synaptic vesicles. *Brain Res.* 1070, 71–76. doi: 10.1016/j.brainres.2005.10.099

Schadeck, R. J., Sarkis, J. J., Dias, R. D., Araujo, H. M., and Souza, D. O. (1989). Synaptosomal apyrase in the hypothalamus of adult rats. *Braz. J. Med. Biol. Res.* 22, 303–314.

Schmidt, A. P., Avila, T. T., and Souza, D. O. (2005). Intracerebroventricular guanine-based purines protect against seizures induced by quinolinic acid in mice. *Neurochem. Res.* 30, 69–73. doi: 10.1007/s11064-004-9687-2

Schmidt, A., Böhmer, A., Schallenberger, C., Antunes, C., Tavares, R., Wofchuk, S., et al. (2010). Mechanisms involved in the antinociception induced by systemic administration of guanosine in mice. *Br. J. Pharmacol.* 159, 1247–1263. doi: 10.1111/j.1476-5381.2009.00597.x

Schmidt, A. P., Böhmer, A. E., Leke, R., Schallenberger, C., Antunes, C., Pereira, M. S. L., et al. (2008). Antinociceptive effects of intracerebroventricular administration of guanine-based purines in mice: evidences for the mechanism of action. *Brain Res.* 1234, 50–58. doi: 10.1016/j.brainres.2008.07.091

Schmidt, A. P., Lara, D. R., de Faria Maraschin, J., da Silveira Perla, A., and Onofre Souza, D. (2000). Guanosine and GMP prevent seizures induced by

quinolinic acid in mice. *Brain Res.* 864, 40–43. doi: 10.1016/s0006-8993(00)02106-5

Schmidt, A. P., Lara, D. R., and Souza, D. O. (2007). Proposal of a guanine-based purinergic system in the mammalian central nervous system. *Pharmacol. Ther.* 116, 401–416. doi: 10.1016/j.pharmthera.2007.07.004

Schwarzschild, M. A., Schwid, S. R., Marek, K., Watts, A., Lang, A. E., Oakes, D., et al. (2008). Serum urate as a predictor of clinical and radiographic progression in Parkinson disease. *Arch. Neurol.* 65, 716–723. doi: 10.1001/archneur.2008.65.6.nct70003

Segovia, G., Porras, A., Del Arco, A., and Mora, F. (2001). Glutamatergic neurotransmission in aging: a critical perspective. *Mech. Ageing Dev.* 122, 1–29. doi: 10.1016/s0047-6374(00)00225-6

Sharif, N. A., and Roberts, P. J. (1981). Regulation of cerebellar L-[^{3}H]glutamate binding: influence of guanine nucleotides and Na^+ ions. *Biochem. Pharmacol.* 30, 3019–3022. doi: 10.1016/0006-2952(81)90273-2

Soares, F. A., Schmidt, A. P., Farina, M., Frizzo, M. E. S., Tavares, R. G., Portela, L. V. C., et al. (2004). Anticonvulsant effect of GMP depends on its conversion to guanosine. *Brain Res.* 1005, 182–186. doi: 10.1016/j.brainres.2004.01.053

Souza, D. O., and Ramírez, G. (1991). Effects of guanine nucleotides on kainic acid binding and on adenylate cyclase in chick optic tectum and cerebellum. *J. Mol. Neurosci.* 3, 39–45. doi: 10.1007/bf02896847

Su, C., Elfeki, N., Ballerini, P., D'Alimonte, I., Bau, C., Ciccarelli, R., et al. (2009). Guanosine improves motor behavior, reduces apoptosis and stimulates neurogenesis in rats with parkinsonism. *J. Neurosci. Res.* 87, 617–625. doi: 10.1002/jnr.21883

Su, C., Picard, P., Rathbone, M. P., and Jiang, S. (2010). Guanosine-induced decrease in side population of lung cancer cells: lack of correlation with ABCG2 expression. *J. Biol. Regul. Homeost. Agents* 24, 19–25.

Su, C., Wang, P., Jiang, C., Ballerini, P., Caciagli, F., Rathbone, M. P., et al. (2013). Guanosine promotes proliferation of neural stem cells through cAMP-CREB pathway. *J. Biol. Regul. Homeost. Agents* 27, 673–680.

Tarozzi, A., Merlicco, A., Morroni, F., Bolondi, C., Di Iorio, P., Ciccarelli, R., et al. (2010). Guanosine protects human neuroblastoma cells from oxidative stress and toxicity induced by Amyloid-β peptide oligomers. *J. Biol. Regul. Homeost. Agents* 24, 297–306.

Tasca, C. I., Burgos, J. S., Barat, A., Souza, D. O., and Ramírez, G. (1999a). Chick kainate binding protein lacks GTPase activity. *Neuroreport* 10, 1981–1983. doi: 10.1097/00001756-199906230-00034

Tasca, C. I., Cardoso, L. F., and Souza, D. O. (1999b). Effects of guanine nucleotides on adenosine and glutamate modulation of cAMP levels in optic tectum slices from chicks. *Neurochem. Int.* 34, 213–220. doi: 10.1016/s0197-0186(99)00006-6

Tasca, C. I., Cardoso, L. F., Martini, L. H., Ramírez, G., and Souza, D. O. (1998). Guanine nucleotides inhibit cAMP accumulation induced by metabotropic glutamate receptor activation. *Neurochem. Res.* 23, 183–188. doi: 10.1023/A:1022480825290

Tasca, C. I., Dal-Cim, T., and Cimarosti, H. (2015). *In vitro* oxygen-glucose deprivation to study ischemic cell death. *Methods Mol. Biol.* 1254, 197–210. doi: 10.1007/978-1-4939-2152-2_15

Tasca, C., Decker, H., de Aguiar, C., Romao, L., Boeck, H., and Moura-Neto, V. (2010). A2A adenosine receptors and ionotropic glutamate receptors are involved on gmp-or guanosine-induced trophic effects in cultured cerebellar granule neuronse. *Purinergic Signal.* 6, 42–42. doi: 10.1007/s11302-010-9187-6

Tasca, C., Llorente, J., Dal-Cim, T., Fernandez-Duenas, V., Gomez-Soler, M., Gandia, J., et al. (2013). The neuroprotective agent Guanosine activates big conductance Ca^{2+}-activated Potassium channels (BK) transfected to HEK-293 cells. *J. Neurochem.* 125, 273–273. doi: 10.1111/jnc.12186

Tasca, C. I., Santos, T. G., Tavares, R. G., Battastini, A. M. O., Rocha, J. B. T., and Souza, D. O. (2004). Guanine derivatives modulate L-glutamate uptake into rat brain synaptic vesicles. *Neurochem. Int.* 44, 423–431. doi: 10.1016/j.neuint.2003.08.001

Tasca, C. I., and Souza, D. O. (2000). Interaction of adenosine and guanine derivatives in the rat hippocampus: effects on cyclic AMP levels and on the binding of adenosine analogues and GMP. *Neurochem. Res.* 25, 181–188. doi: 10.1023/A:1007557600687

Tasca, C. I., Wofchuk, S. T., Souza, D. O., Ramirez, G., and Rodnight, R. (1995). Guanine nucleotides inhibit the stimulation of GFAP phosphorylation by glutamate. *Neuroreport* 6, 249–252. doi: 10.1097/00001756-199501000-00006

Tavares, R. G., Schmidt, A. P., Abud, J., Tasca, C. I., and Souza, D. O. (2005). *In vivo* quinolinic acid increases synaptosomal glutamate release in rats: reversal by guanosine. *Neurochem. Res.* 30, 439–444. doi: 10.1007/s11064-005-2678-0

Tavares, R. G., Schmidt, A. P., Tasca, C. I., and Souza, D. O. (2008). Quinolinic acid-induced seizures stimulate glutamate uptake into synaptic vesicles from rat brain: effects prevented by guanine-based purines. *Neurochem. Res.* 33, 97–102. doi: 10.1007/s11064-007-9421-y

Taylor, C. W. (1990). The role of G proteins in transmembrane signalling. *Biochem. J.* 272, 1–13. doi: 10.1042/bj2720001

Thauerer, B., zur Nedden, S., and Baier-Bitterlich, G. (2010). Vital role of protein kinase C-related kinase in the formation and stability of neurites during hypoxia. *J. Neurochem.* 113, 432–446. doi: 10.1111/j.1471-4159.2010.06624.x

Thomaz, D. T., Dal-Cim, T. A., Martins, W. C., Cunha, M. P., Lanznaster, D., de Bem, A. F., et al. (2016). Guanosine prevents nitroxidative stress and recovers mitochondrial membrane potential disruption in hippocampal slices subjected to oxygen/glucose deprivation. *Purinergic Signal.* 12, 707–718. doi: 10.1007/s11302-016-9534-3

Togha, M., Akhondzadeh, S., Motamedi, M., Ahmadi, B., and Razeghi, S. (2007). Allopurinol as adjunctive therapy in intractable epilepsy: a double-blind and placebo-controlled trial. *Arch. Med. Res.* 38, 313–316. doi: 10.1016/j.arcmed.2006.10.010

Torres, F. V., da Silva Filho, M., Antunes, C., Kalinine, E., Antoniolli, E., Portela, L. V. C., et al. (2010). Electrophysiological effects of guanosine and MK-801 in a quinolinic acid-induced seizure model. *Exp. Neurol.* 221, 296–306. doi: 10.1016/j.expneurol.2009.11.013

Tozaki-Saitoh, H., Tsuda, M., and Inoue, K. (2011). "Role of purinergic receptors in CNS function and neuroprotection," in *Advances in Pharmacology*, eds K. A. Jacobson and J. Linden (San Diego, CA: Elsevier), 495–528.

Traversa, U., Bombi, G., Camaioni, E., Macchiarulo, A., Costantino, G., Palmieri, C., et al. (2003). Rat brain guanosine binding site. Biological studies and pseudo-receptor construction. *Bioorg. Med. Chem.* 11, 5417–5425. doi: 10.1016/j.bmc.2003.09.043

Traversa, U., Bombi, G., Di Iorio, P., Ciccarelli, R., Werstiuk, E. S., and Rathbone, M. P. (2002). Specific [^{3}H]-guanosine binding sites in rat brain membranes. *Br. J. Pharmacol.* 135, 969–976. doi: 10.1038/sj.bjp.0704542

Uemura, Y., Miller, J. M., Matson, W. R., and Beal, M. F. (1991). Neurochemical analysis of focal ischemia in rats. *Stroke* 22, 1548–1553. doi: 10.1161/01.str.22.12.1548

Vila, M., and Przedborski, S. (2003). Targeting programmed cell death in neurodegenerative diseases. *Nat. Rev. Neurosci.* 4, 365–375. doi: 10.1038/nrn1100

Vinadé, E. R., Schmidt, A. P., Frizzo, M. E. S., Izquierdo, I., Elisabetsky, E., and Souza, D. O. (2003). Chronically administered guanosine is anticonvulsant, amnesic and anxiolytic in mice. *Brain Res.* 977, 97–102. doi: 10.1016/s0006-8993(03)02769-0

Vinadé, E. R., Schmidt, A. P., Frizzo, M. E. S., Portela, L. V., Soares, F. A., Schwalm, F. D., et al. (2005). Effects of chronic administered guanosine on behavioral parameters and brain glutamate uptake in rats. *J. Neurosci. Res.* 79, 248–253. doi: 10.1002/jnr.20327

Volpini, R., Marucci, G., Buccioni, M., Dal Ben, D., Lambertucci, C., Lammi, C., et al. (2011). Evidence for the existence of a specific g protein-coupled receptor activated by guanosine. *ChemMedChem* 6, 1074–1080. doi: 10.1002/cmdc.201100100

Yang, S.-C., Chiu, C.-L., Huang, C.-C., and Chen, J.-R. (2005). Apoptosis induced by nucleosides in the human hepatoma HepG2. *World J. Gastroenterol.* 11, 6381–6384. doi: 10.3748/wjg.v11.i40.6381

Yang, L., Zhao, Y., Wang, Y., Liu, L., Zhang, X., Li, B., et al. (2015). The effects of psychological stress on depression. *Curr. Neuropharmacol.* 13, 494–504. doi: 10.2174/1570159x1304150831150507

Yin, Y., Sun, W., Xiang, J., Deng, L., Zhang, B., Xie, P., et al. (2013). Glutamine synthetase functions as a negative growth regulator in glioma. *J. Neurooncol.* 114, 59–69. doi: 10.1007/s11060-013-1168-5

Zhao, C., Deng, W., and Gage, F. H. (2008). Mechanisms and functional implications of adult neurogenesis. *Cell* 132, 645–660. doi: 10.1016/j.cell.2008.01.033

Zimmermann, H. (1996). Biochemistry, localization and functional roles of ecto-nucleotidases in the nervous system. *Prog. Neurobiol.* 49, 589–618. doi: 10.1016/0301-0082(96)00026-3

Zimmermann, H., and Braun, N. (1996). Extracellular metabolism of nucleotides in the nervous system. *J. Auton. Pharmacol.* 16, 397–400. doi: 10.1111/j.1474-8673.1996.tb00062.x

Zuccarini, M., Giuliani, P., Frinchi, M., Mudò, G., Serio, R. M., Belluardo, N., et al. (2018). Uncovering the signaling pathway behind extracellular guanine-induced activation of NO system: new perspectives in memory-related disorders. *Front. Pharmacol.* 9:110. doi: 10.3389/fphar.2018.00110

Conflict of Interest Statement: The authors declare that the research was conducted in the absence of any commercial or financial relationships that could be construed as a potential conflict of interest.

frontiers in Molecular Neuroscience

ORIGINAL RESEARCH
published: 20 December 2018
doi: 10.3389/fnmol.2018.00475

Adenosine A_{2A} Receptors in the Rat Prelimbic Medial Prefrontal Cortex Control Delay-Based Cost-Benefit Decision Making

*Douglas T. Leffa[1,2†], Pablo Pandolfo[2,3†], Nélio Gonçalves[1], Nuno J. Machado[1], Carolina M. de Souza[1,4], Joana I. Real[1], António C. Silva[1], Henrique B. Silva[1], Attila Köfalvi[1], Rodrigo A. Cunha[1,5] and Samira G. Ferreira[1]**

[1]CNC-Center for Neuroscience and Cell Biology, University of Coimbra, Coimbra, Portugal, [2]Department of Biochemistry, Federal University of Rio Grande do Sul, Porto Alegre, Brazil, [3]Department of Neurobiology, Fluminense Federal University, Niterói, Brazil, [4]Post-Graduate Program in Medical Sciences, Faculty of Medicine, Federal University of Ceará, Fortaleza, Brazil, [5]Faculty of Medicine, University of Coimbra, Coimbra, Portugal

Adenosine A_{2A} receptors (A_{2A}Rs) were recently described to control synaptic plasticity and network activity in the prefrontal cortex (PFC). We now probed the role of these PFC A_{2A}R by evaluating the behavioral performance (locomotor activity, anxiety-related behavior, cost-benefit decision making and working memory) of rats upon downregulation of A_{2A}R selectively in the prelimbic medial PFC (PLmPFC) via viral small hairpin RNA targeting the A_{2A}R (shA_{2A}R). The most evident alteration observed in shA_{2A}R-treated rats, when compared to sh-control (shCTRL)-treated rats, was a decrease in the choice of the large reward upon an imposed delay of 15 s assessed in a T-maze-based cost-benefit decision-making paradigm, suggestive of impulsive decision making. Spontaneous locomotion in the open field was not altered, suggesting no changes in exploratory behavior. Furthermore, rats treated with shA_{2A}R in the PLmPFC also displayed a tendency for higher anxiety levels in the elevated plus maze (less entries in the open arms), but not in the open field test (time spent in the center was not affected). Finally, working memory performance was not significantly altered, as revealed by the spontaneous alternation in the Y-maze test and the latency to reach the platform in the repeated trial Morris water maze. These findings constitute the first direct demonstration of a role of PFC A_{2A}R in the control of behavior in physiological conditions, showing their major contribution for the control of delay-based cost-benefit decisions.

Keywords: adenosine A_{2A} receptors, impulsive choice, prefrontal cortex (PFC), anxiety, working memory, cost-benefit decision making

OPEN ACCESS

Edited by:
David Blum, INSERM U1172 Centre de Recherche Jean Pierre Aubert, France

Reviewed by:
Joana Esteves Coelho, Instituto de Medicina Molecular (IMM), Portugal
Ryan K. Bachtell, University of Colorado Boulder, United States

****Correspondence:***
Samira G. Ferreira
carsamira@gmail.com

†These authors have contributed equally to this work

Received: *22 May 2018*
Accepted: *05 December 2018*
Published: *20 December 2018*

Citation:
Leffa DT, Pandolfo P, Gonçalves N, Machado NJ, de Souza CM, Real JI, Silva AC, Silva HB, Köfalvi A, Cunha RA and Ferreira SG (2018) Adenosine A_{2A} Receptors in the Rat Prelimbic Medial Prefrontal Cortex Control Delay-Based Cost-Benefit Decision Making. Front. Mol. Neurosci. 11:475. doi: 10.3389/fnmol.2018.00475

INTRODUCTION

Adenosine A_{2A} receptors (A_{2A}Rs) are mostly known to control long-term synaptic plasticity throughout the brain (reviewed in Cunha, 2016), namely in the prefrontal cortex (PFC) where they facilitate long-term potentiation (LTP) in excitatory synapses onto fast spiking interneurons and control network activity (Kerkhofs et al., 2018). The PFC mediates cognitive and executive functions including working memory, attention and inhibitory control

(Goldman-Rakic, 1999; Fuster, 2001), which are disrupted in major neuropsychiatric disorders such as attention deficit and hyperactivity disorder (ADHD), addiction and schizophrenia (Arnsten et al., 2015). Notably, the antagonism of $A_{2A}R$ has been tied to the improvement of mood and memory deficits in several neuropsychiatric disorders (Chen, 2014; Kaster et al., 2015; Viana da Silva et al., 2016). The contribution of $A_{2A}R$ in the PFC is suggested by the observation that the antagonism of adenosine receptors with their general antagonist caffeine improves attention and short-term memory in animal models of ADHD (Caballero et al., 2011; Pandolfo et al., 2013). Furthermore, $A_{2A}R$ antagonism increases impulsivity (Oliveros et al., 2017), attenuate the effects of dopamine D_2 receptor antagonism on effort-based decision making (Pardo et al., 2012) and attenuate working memory deficits in rats with PFC dopamine depletion (Horita et al., 2013).

While optogenetic activation of $A_{2A}R$ signaling pathways in the medial PFC improves maintenance of spatial working memory (Li et al., 2018), there are still no direct evidence supporting a role for the endogenous activation of $A_{2A}R$ in the PFC to modulate behavior. This is of particular relevance since $A_{2A}R$ are present in different areas of the forebrain (i.e., cerebral cortex, hippocampus and striatum) with different impacts on different behavioral outputs, as heralded by the striking opposite phenotypes resulting from the selective deletion of $A_{2A}R$ from only the striatum or forebrain neurons (Shen et al., 2008, 2013; Wei et al., 2014). Thus, to better understand the role of the endogenous activation of $A_{2A}R$ in the PFC, we now selectively downregulated $A_{2A}R$ in the rat prelimbic medial PFC (PLmPFC) and evaluated the consequences on PFC-related behaviors such as working memory, anxiety-related behavior and delay-based cost-benefit decision-making. Our findings reveal that the downregulation of $A_{2A}R$ in the PLmPFC decreased the choice of the large reward in a T-maze-based cost-benefit paradigm in which the cost was delay, suggesting an increase in impulsive decision making, a finding relevant for disorders with impaired decision making, such as Parkinson's disease, schizophrenia, ADHD and addiction (Lee, 2013).

MATERIALS AND METHODS

Animals

Male Wistar rats (7-week-old) were purchased from Charles River (Barcelona, Spain) and housed in a temperature and humidity-controlled environment with 12 h light on/off cycles and *ad libitum* access to food and water. All studies were conducted in accordance with the principles and procedures outlined as "3Rs" in the EU guidelines (210/63), FELASA, and the National Centre for the 3Rs (the ARRIVE; Kilkenny et al., 2010), and were approved by the Animal Care Committee of the Center for Neuroscience and Cell Biology (ORBEA 78/2013).

Generation and Bilateral Administration of Lentiviral Vectors Into the PLmPFC

A small hairpin RNA targeting $A_{2A}R$ ($shA_{2A}R$, nt 419–437) was inserted into a lentivector together with an enhanced green fluorescent protein (EGFP) reporter gene, as previously detailed (Simões et al., 2016; Viana da Silva et al., 2016). This $shA_{2A}R$ has been shown to cause a 68% decrease of $A_{2A}R$ mRNA expression and a 55% decrease of $A_{2A}R$ protein density in the striatum, where the high density of $A_{2A}R$ allows a faithful quantification (Viana da Silva et al., 2016). A hairpin targeting the coding region of red fluorescent protein (nt 22–41) was used as an internal control (shCTRL). These lentivectors (1 μL per hemisphere at 750,000 ng of p24 antigen/mL) were stereotaxically delivered into the PLmPFC of the two hemispheres at an infusion rate of 0.2 μL/min in the following coordinates: antero-posterior: +3.20 mm; lateral: ±0.60 mm; dorso-ventral: −3.80 mm (Paxinos and Watson, 2009).

Radioligand Binding Assay in Total Membranes From the PLmPFC

The amount of tissue allowed a single point radioligand binding which was carried out with slight modification to our previous studies (Cunha et al., 1999; Ferreira et al., 2015). Three male Wistar rats of 6–8 weeks of age were bilaterally injected $shA_{2A}R$ in their PLmPFC, while four Wistar rats were bilaterally injected with the shCTRL. At 5 weeks post-injection, rats were decapitated under halothane anesthesia, and their brains transferred to ice-cold artificial cerebrospinal fluid (composition in mM: NaCl 125, KCl 3, $MgSO_4$ 1, $CaCl_2$ 2, Na_2HPO_4 1.25, $NaHCO_3$ 25–26 and glucose 11, pH 7.4 (osmolality of 300 mOsmol/kg), oxygenated with carbogen (95% O_2 + 5% CO_2). We obtained coronal brain slices from which we dissected the PLmPFC, which was homogenized in 1.8 mL of ice-cold membrane preparation solution of the following composition: sucrose (320 mM), EDTA (2 mM), $MgCl_2$ (3 mM), HEPES (15 mM), pH 7.4, supplied with a protease inhibitor cocktail (Sigma-Aldrich, 1 μL/mL). The homogenates were then centrifuged at 1,000 *g* for 30 min, at 4°C to decant intracellular debris. The membrane-rich supernatant was then re-centrifuged at 20,000 *g* for 30 min, and the pellets were vigorously resuspended in 450 μL binding assay buffer of the following composition: NaCl (100 mM), Tris-HCl (50 mM), EDTA (1 mM), $MgCl_2$ (3 mM), protease inhibitor (1 μL/mL), pH 7.4. Next, 100 μL of the protein suspension was mixed with 200 μL of assay buffer containing adenosine deaminase (Sigma-Aldrich; final concentration, 3 U/mL), guanosine 5′-diphosphate (Abcam; 100 μM), and either the $A_{2A}R$-selective antagonist, SCH58261 (Tocris; 1 μM) to measure non-specific binding or its vehicle, DMSO (0.1% v/v) to yield the total binding. This mixture also contained the $A_{2A}R$-selective radioligand ^{3}H-ZM241385 (American Radiolabeled Chemicals, St. Louis, MO, USA; specific activity, 30 mCi/mmol) at a final concentration of 2.63 nM. The binding assay was carried out in duplicate. The remaining 50 μL of protein aliquots were used to determine protein concentration with the BCA method. The mixtures (containing 20.6 ± 1.4 μg of protein) were left to incubate for 2 h at room temperature in Eppendorf-tubes, then were rapidly transferred into 15 mL of ice-cold washing solution (Tris-HCl, 50 mM, BSA 0.1% v/w), and instantly vacuum-filtered with the help of a Millipore filtration unit, containing Whatman GF/B glass microfiber filters, which had been soaked overnight in Tris-HCl

(10 mM), pH 9.1, containing 0.25% v/v of the cationic polymer polyethylenimine (Sigma; Bruns et al., 1983). The glass tubes were rinsed with an additional 15 mL of washing solution onto the filters. The filters then were harvested into 3 mL of Aquasafe scintillation liquid and after 24 h, were counted for tritium with the help of a Tricarb β-counter (PerkinElmer). Binding values are expressed as fmol binding sites per mg protein.

Behavioral Experiments

Behavioral analyses started 21 days post-surgery and were conducted between 8:00 AM and 6:00 PM under a low intensity red light (12 lx), after habituation of the animals to the room for at least 1 h and with care to clean all apparatus with ethanol after testing each animal to eliminate olfactory cues. We carried out two groups of experiments, all video-taped and analyzed using the ANY-maze video tracking system (Stoelting, Wood Dale, IL, USA).

Experimental Set I

The first group of rats were sequentially exposed to the following behavioral tests with a 24 h interval in between them: the elevated plus maze, in order to assess anxiety-like behavior; the open field test to assess locomotor activity as well as anxiety-like behavior; and the splash test in order to evaluate mood alterations.

The elevated plus maze was carried out in an elevated plus-shaped maze with two open arms arranged perpendicularly to two closed arms, as previously described (Kaster et al., 2015). Rats were allowed to explore the maze for 10 min. The general principle of this test is that more "anxious" animals will likely explore less the risky open arms as opposed to the closed arms, which are perceived as safer. Thus, anxiety-like behavior was measured as a lower percentage of open arm entries (Pellow et al., 1985). Entries were counted whenever all the four paws of the animal crossed into one of the arms. The open field test was carried out in a square-shaped arena (1 × 1 m) with defined peripheral and central (36% of total area) zones. Rats were allowed to explore the arena for 10 min and only the first 5 min were analyzed (Gonçalves et al., 2015). Locomotor activity was measured as the total distance traveled and anxiety-like behavior was measured by the time spent in the center zone of the arena, which is perceived as a more threatening area (Choleris et al., 2001; Prut and Belzung, 2003).

The splash test was used as a measure of anxiety- and depressive-like behavior as previously described (Kaster et al., 2015). We measured grooming bouts (head washing and nose/face and body grooming) over 5 min after a 10% sucrose solution was splashed on the dorsal coat of the animal (Yalcin et al., 2005).

Experimental Set II

This second set of experiments sequentially tested rats in a delay-based cost-benefit decision making paradigm in a T-maze, followed by spatial working memory tests using a Y-maze and a repeated trial Morris water maze (MWM).

Delay-Based Cost-Benefit Decision-Making Paradigm in a T-maze

This test is based on delay aversion, which is used as a measure of impulsive decision making or impulsive choice (Pattij and Vanderschuren, 2008). Animals had to choose between a large-but-delayed and small-but-immediate reward (adapted from Bizot et al., 2007). The testing apparatus was a gray-colored T-maze, built out of PVC, with 50-cm-high walls, consisting of a starting runway, ending in two perpendicular 50-cm-long, 15-cm-wide arms. Four removable guillotine wood doors were vertically inserted at the entry and 10-cm from the end of each arm. The space between doors in each arm was enough to accommodate a rat. One week before starting the behavioral tests, rats were food-restricted to achieve 90% of their original weight. During that time, palatable dog chow pellets (Royal Canin Junior®) were given to the rats to habituate them to the new food. The task was divided into three different phases: habituation, training and testing phase.

Habituation

Rats were individually placed on the starting runway and allowed to freely explore the apparatus. Each arm had three pellets, including the starting runway. After 5 min, the number of pellets ingested was verified. If an animal had not eaten all the pellets, it was subjected to a new habituation trial. Up to five trials were conducted each day. After eating all the pellets, the rats progressed to the training phase. The number of habituation trials to reach training criterion was recorded.

Training Phase

Rats were run in the maze where one arm of the apparatus had a small reward (0.5 pellet) and the other had a large (two pellets) reward. The arm where the large reward was placed was randomly selected for each rat, but it was always on the same side throughout the experiment for a given rat. Rats were individually placed on the starting runway and had equal access to both arms. Both doors in the chosen arm were opened when the animal turned to its direction. As soon as the first door was crossed, it was closed to prevent the rat from escaping. The second door in that arm remained open to allow the animal to eat the reward. Then, another trial was carried out until a session of five trials was complete. Up to two sessions of five trials were conducted in the same day. The criterion to progress to the testing phase was choosing the large reward at least four times in five trials in two consecutive sessions. Otherwise, further trials were carried out in the next day. The number of training sessions to reach testing criterion was recorded.

Testing Phase

The test was conducted in five consecutive days, each day consisting of five trials. A delay of 15 s was imposed before the rat had access to the large reward, i.e., after choosing the arm with the large reward, both doors were closed right after the animal crossed the first one, keeping the animal between doors during this period. No delay was imposed after entering the small reward

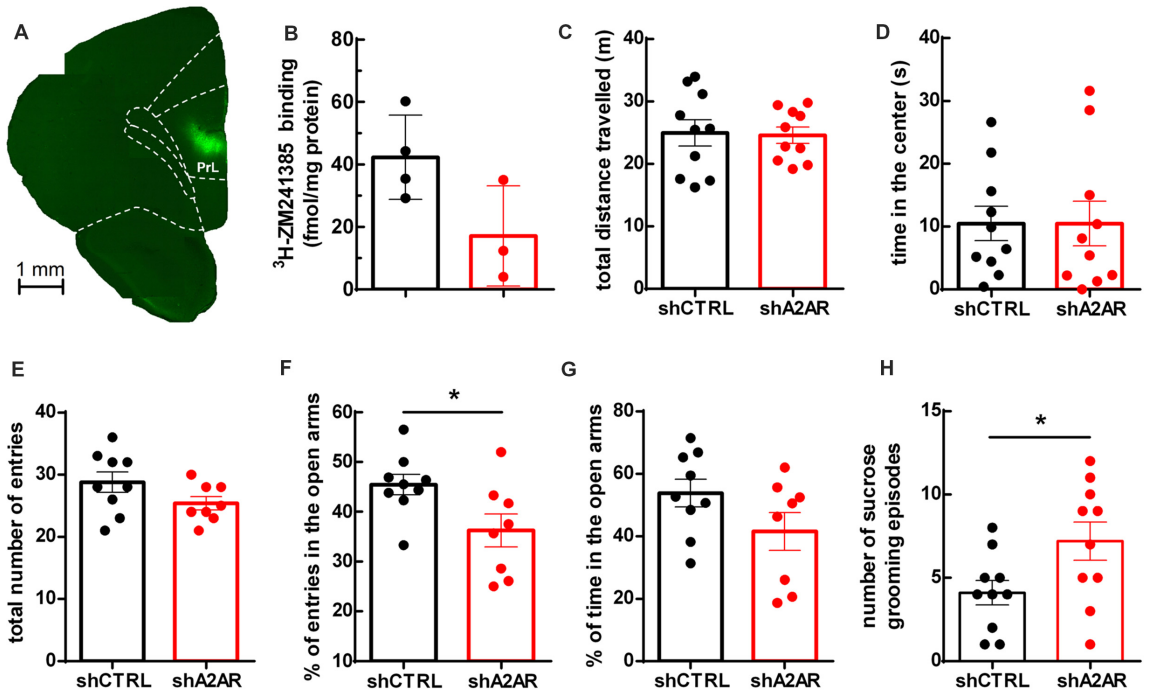

FIGURE 1 | Effect of downregulating adenosine A_{2A} receptors (A_{2A}R) in the prelimbic medial prefrontal cortex (PLmPFC) on locomotion and anxiety- and depressive-like behavior. **(A)** Lentivector constructs containing small hairpin RNA targeting A_{2A}R (shA_{2A}R) together with enhanced green fluorescent protein (EGFP) reporter gene was effectively transduced in the PLmPFC, as shown by EGFP labeling in the region. **(B)** Specific binding of the selective A_{2A}R antagonist ^{3}H-ZM241385 shows a decrease in A_{2A}R protein density in shA_{2A}R- as compared to shCTRL-treated rats (n = 3–4, p = 0.07). **(C)** The analysis of the performance in the open field test suggests no alteration of exploratory activity, since the total distance traveled was similar between shA_{2A}R- and shCTRL-treated rats. **(D)** There was also no change in the time spent in the center of the open field between shA_{2A}R- and shCTRL-treated rats. **(E)** In the elevated plus maze there was no change in the total number of arm entries. **(F)** The performance in the elevated plus maze test suggests a mild anxiogenic effect resulting from the downregulation of PLmPFC A_{2A}R, since shA_{2A}R-treated rats entered less in the open arms when compared with shCTRL-treated rats. **(G)** Time spent in the open arms was not significantly affected (p = 0.1173). **(H)** Likewise, the performance in the splash test (with 10% sucrose solution) revealed an increased number of sucrose grooming episodes in shA_{2A}R- compared with shCTRL-treated rats. Behavioral data are mean ± SEM of 9–10 rats per group; *$p < 0.05$, unpaired Student's t-test.

arm. The number of choices of the large reward was recorded for each day.

Working Memory Tests

The Y-maze spontaneous alternation test was carried out as previously described (Augusto et al., 2013). The rats explored the maze for 8 min. The spontaneous alternation test takes advantage of the natural tendency of animals to choose a different arm than the one previously chosen (Dudchenko, 2004). In a correct sequence, a rat chooses a different arm in each of the successive three entries. The percentage of alternation in correct sequences was used to evaluate spatial working memory.

The repeated trial MWM was carried out in a circular pool (100 cm in diameter, 55 cm high), filled with water at 26°C. A platform (10 cm in diameter) was placed just under the surface of the water. The extra-maze cues in the testing room were kept constant. The test was adapted from a four-trial repeated acquisition protocol described in previous studies (Whishaw, 1985; Zhou et al., 2009) with four consecutive daily trials repeated during four consecutive days. The interval between trials was less than 1 min. The platform was moved to a new quadrant every day, but kept in the same position for all trials on the same day. The rats were allowed to swim until they reach the platform. Working memory was evaluated through the latency of escape from the starting point to the platform.

Statistical Analysis

Statistical analyses were performed using Prism 6 GraphPad Software. Data are expressed as mean ± standard error of the mean (SEM). Data were analyzed using unpaired Student's t-test and two-way ANOVA for repeated measures, followed by Bonferroni *post hoc* test as appropriate. $p < 0.05$ was taken as statistically significant.

RESULTS

We generated lentivectors, with neuronal tropism (Lundberg et al., 2008), encoding shRNAs to selectively neutralize A_{2A}R (shA_{2A}R) together with EGFP. These lentivectors were injected into the PLmPFC (**Figure 1A**) of rats. Upon dissection of the PLmPFC 5 weeks post-injection, we performed radioligand biding assay with ^{3}H-ZM241385, an A_{2A}R ligand, to assess A_{2A}R density. The density of A_{2A}R in PLmPFC total membranes was 42.28 ± 13.46 fmol/mg protein for shCTRL-treated rats (n = 4)

and 17.13 ± 16.03 fmol/mg protein in PLmPFC total membranes from shA_{2A}R-treated rats **Figure 1B**), representing a 59 ± 18% decrease in A_{2A}R protein density as compared to shCTRL-treated rats (n = 3–4), a down-regulation similar to that achieved in the striatum (Viana da Silva et al., 2016).

Downregulation of A_{2A}R in the PLmPFC Induces Slight Mood Alterations With No Changes of Locomotor Activity

We then evaluated if the downregulation of A_{2A}R in the PLmPFC impacted on locomotor activity. As shown in **Figure 1C**, there was no difference in the total distance traveled between shA_{2A}R- and shCTRL-treated rats (24.59 ± 1.28 m for shA_{2A}R-treated rats vs. 24.96 ± 2.10 m for shCTRL-treated rats, n = 10, p = 0.8830), suggesting that the exploratory behavior was not affected. Regarding anxiety-like behavior, the results were less clear: there was no difference in the time spent in the center of the open field between shA_{2A}R- and shCTRL-treated rats (10.48 ± 3.58 s for shA_{2A}R-treated rats vs. 10.49 ± 2.72 s for shCTRL-treated rats, n = 10, p = 0.9983; **Figure 1D**). However, in the elevated plus maze test, while total number of arm entries remained unchanged (25.38 ± 1.07 n = 8, for shA_{2A}R-treated rats vs. 28.78 ± 1.64, n = 9, for shCTRL-treated, p = 0.1116; **Figure 1E**), shA_{2A}R-treated rats entered less in the open arms as compared with shCTRL-treated rats (36.24 ± 3.32%, n = 8, for shA_{2A}R-treated rats vs. 53.86 ± 4.46%, n = 9, for shCTRL-treated, p = 0.0289; **Figure 1F**). In contrast, the time spent in the open arms was not significantly altered (41.56 ± 6.04% n = 8, for shA_{2A}R-treated rats vs. 53.86 ± 4.46%, n = 9, for shCTRL-treated, p = 0.1173; **Figure 1G**). In the splash test, there was an increase in sucrose grooming frequency (7.20 ± 1.14 events for shA_{2A}R-treated rats vs. 4.10 ± 0.737 events for shCTRL-treated rats, n = 10, p = 0.0351; **Figure 1H**). Altogether, these data suggest that downregulating PLmPFC A_{2A}R might result in a discrete anxiogenic profile.

Downregulation of A_{2A}R in the PLmPFC Renders Rats More Averse to Delay

We used a delay-based cost-benefit decision making paradigm in a T-maze (**Figures 2A,B**) to evaluate preference for a small immediate reward over a larger, but delayed reward. In the habituation phase, shA_{2A}R- and shCTRL-treated rats needed a similar number of habituation trials to reach training criterion, i.e., they learned similarly that there was a reward at the end of two arms (shA_{2A}R-treated rats learned over 7.25 ± 0.88 trials, whereas shCTRL-treated rats learned over 8.38 ± 1.64 trials, n = 8, p = 0.5575; **Figure 2C**). In the training phase, shA_{2A}R-treated rats needed a lower number of training sessions to reach testing criterion, i.e., they learned faster to choose the larger reward as compared to shCTRL-treated rats (shA_{2A}R-treated rats learned over 3.25 ± 0.16 sessions,

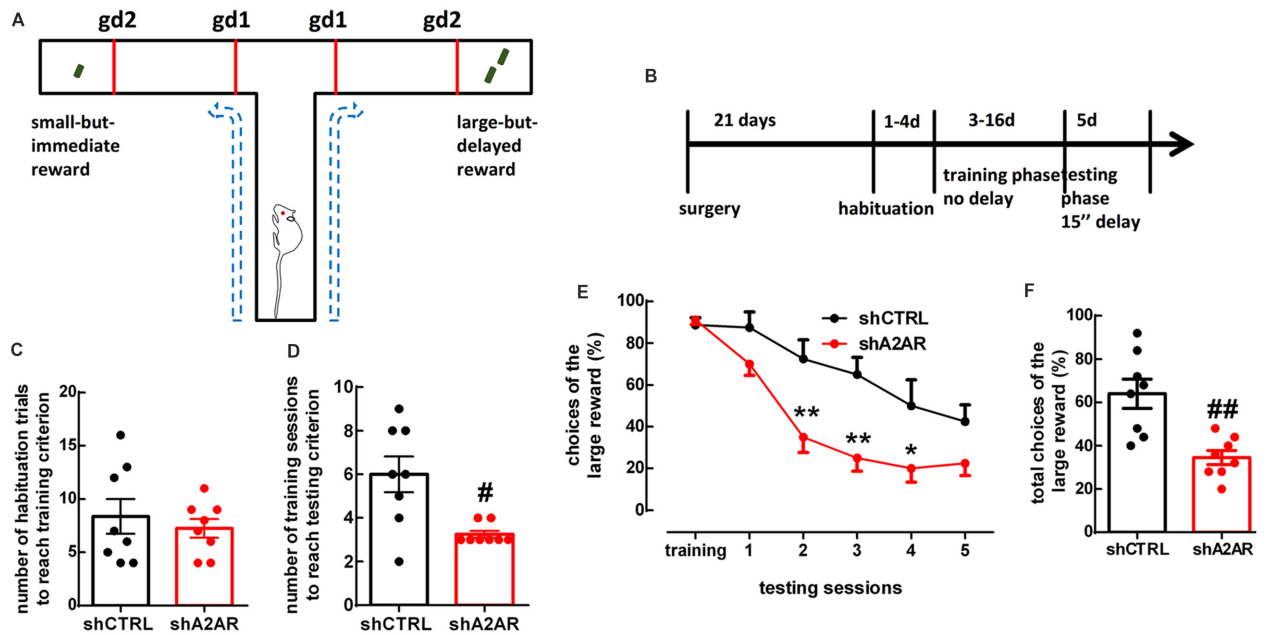

FIGURE 2 | Downregulation of A_{2A}R in the PLmPFC increases impulsive choice. **(A)** Scheme of the testing apparatus (gd, guillotine door). **(B)** Scheme of the experimental design. **(C)** shA_{2A}R- and shCTRL-treated rats required a similar number of habituation trials to reach training criterion. **(D)** shA_{2A}R-treated rats required less training sessions than shCTRL-treated rats to reach testing criterion (when they learn to choose the large reward); **(E,F)** with a 15-s-imposed delay, shA_{2A}R-treated rats were more intolerant to delay as compared to shCTRL-treated rats, as shown by their decreased choice of the large reward. Data are mean ± SEM. $^{\#}p < 0.05$ and $^{\#\#}p < 0.01$, unpaired Student's t-test; $^{*}p < 0.05$ and $^{**}p < 0.01$, two-way analysis of variance (ANOVA) for repeated measures, followed by Bonferroni *post hoc* test.

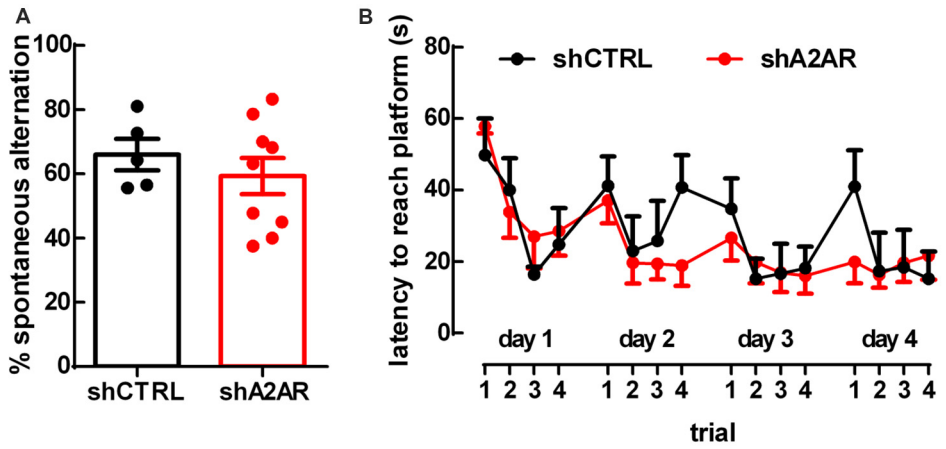

FIGURE 3 | Downregulation of $A_{2A}R$ in the PLmPFC does not affect spatial working memory. **(A)** The performance in the Y-maze test revealed no change of the percentage of spontaneous alternation in $shA_{2A}R$-compared to shCTRL-treated rats. **(B)** The repeated trial Morris water maze (MWM) paradigm revealed that $shA_{2A}R$-treated rats had no changes in the latency to reach the platform as compared to shCTRL-treated rats. Data are mean ± SEM of $n = 5$ for shCTRL- and $n = 9$ for $shA_{2A}R$-treated rats.

whereas shCTRL-treated rats learned over 6.00 ± 0.82 sessions, $n = 8$, $p = 0.0122$; **Figure 2D**). However, in the testing phase, $shA_{2A}R$-treated rats were more intolerant to a 15-s-imposed delay as compared to shCTRL-treated rats, suggesting an increase in impulsive choice upon down-regulation of $A_{2A}R$ in the PLmPFC. A repeated measures ANOVA analysis indicated a decrease in the choices of the large reward with increased number of sessions ($F_{(5,70)} = 28.08$, $p < 0.0001$), with $shA_{2A}R$ treatment ($F_{(1,14)} = 13.64$, $p = 0.0024$), and a session × $shA_{2A}R$ treatment interaction ($F_{(5,70)} = 3.10$, $p = 0.0138$; **Figure 2E**). The total number of choices of the large reward was 8.63 ± 0.82 in $shA_{2A}R$-treated rats and 16.00 ± 1.67 in shCTRL-treated rats ($n = 8$, $p = 0.0026$; **Figure 2F**).

Downregulation of $A_{2A}R$ in the PLmPFC Does Not Affect Spatial Working Memory

There were no differences in spontaneous alternation in the Y-maze test between $shA_{2A}R$- and shCTRL-treated rats (65.87 ± 5.61%, $n = 9$, for $shA_{2A}R$-treated rats vs. 66.44 ± 3.99%, $n = 5$, for shCTRL-treated rats, $p = 0.9350$; **Figure 3A**). In the MWM test, repeated measures ANOVA revealed an effect for trial ($F_{(15,180)} = 4.63$, $p < 0.0001$), but not for $shA_{2A}R$ treatment ($F_{(1,12)} = 0.31$, $p = 0.5853$; **Figure 3B**). Overall, these data suggest that $A_{2A}R$ in the PLmPFC have no impact on spatial working memory.

DISCUSSION

We have recently reported that $A_{2A}R$ in the PLmPFC control long-term plasticity of excitatory synaptic transmission onto fast spiking interneurons (Kerkhofs et al., 2018) and that they are necessary for dopamine-induced decrease in population activity (Real et al., 2018). Thus, we anticipated a role for PFC $A_{2A}R$ in the control of PFC-dependent behaviors, which include anxiety-like behavior (Calhoon and Tye, 2015; Tovote et al., 2015), cost-benefit decision-making (Bailey et al., 2016) and working memory (Goldman-Rakic, 1999; Fuster, 2001). The most evident effect resulting from the down-regulation of $A_{2A}R$ selectively in the PLmPFC was increased aversion to delay, suggestive of increased impulsive decision making, while only a discrete increase in anxiety-like behavior was observed, and spatial working memory was not significantly affected.

$A_{2A}R$, in particular those in the nucleus accumbens, have been consistently implicated in cost-benefit decision-making in which the cost is physical effort (e.g., Font et al., 2008; Mingote et al., 2008; Pardo et al., 2012; Nunes et al., 2013). Specifically, activation of $A_{2A}R$ decreased lever pressing for the preferred food as opposed to eating the readily available less preferred chow (Font et al., 2008) and disrupted performance in an instrumental task with high work demands (Mingote et al., 2008), while $A_{2A}R$ blockade or genetic deletion attenuated haloperidol (dopamine D_2 receptor antagonist)-induced decrease in the choice of the high reward arm of a T-maze that was accessible after climbing a barrier (Pardo et al., 2012). Now, we show that PLmPFC $A_{2A}R$ have the opposite effect on a cost-benefit decision-making task in which the cost was delay. Decisions about different, yet interrelated, types of costs have dissociable neural circuits and neurochemical mechanisms (Rudebeck et al., 2006; Floresco et al., 2008; Bailey et al., 2016), which may have contributed to this difference. Furthermore, it is known that $A_{2A}R$ are able to modulate the same behavior in opposite direction, depending on the brain region that is being manipulated. That is, for instance, the case for fear memory (Wei et al., 2014; Simões et al., 2016) and psychomotor activity (Shen et al., 2008). Thus, a more comprehensive study involving region-selective manipulations of $A_{2A}R$ will be necessary to dissect their role across different types of decision costs.

The impact of PFC $A_{2A}R$ on delay-based decision making could either be due to a control of: (i) aversion to the holding chamber before the reward; (ii) an altered goal-directed to habit-based strategy; (iii) an altered subjective value of the reward; (iv) an altered spatial memory encoding; and (v) impulsivity. This is compatible with the main involvement of the accumbens-PFC-amygdala circuitry (Floresco and Ghods-Sharifi, 2007; Hauber and Sommer, 2009) as well as of the dorsal hippocampus (Liu et al., 2016) in T-maze based analysis of effort-based decision making, and with the ability of the PFC to control aversive memories (Courtin et al., 2013), goal-directed behavior (Gourley and Taylor, 2016), the subjective value of rewards (Kable and Glimcher, 2007), processing of spatial memory (Jin and Maren, 2015) and impulsivity (Kim and Lee, 2011). However, the previous analysis of the role of $A_{2A}R$ in these different behaviors leads us to propose that PFC-$A_{2A}R$ mostly control delay-based decision making by controlling impulsivity. This contention stems from observations that: (i) $A_{2A}R$ control aversive memories, but this is fully accounted by the impact of amygdalar $A_{2A}R$ (Simões et al., 2016); (ii) $A_{2A}R$ control the shift from goal-directed to habit-based strategies, but this is fully accounted by the activity of $A_{2A}R$ in medial spiny neurons of different striatal regions (Yu et al., 2009; Li et al., 2016); (iii) $A_{2A}R$ control reward, but this is dependent on $A_{2A}R$ in the nucleus accumbens rather than PFC $A_{2A}R$ (Harper et al., 2006; Wydra et al., 2018); and (iv) $A_{2A}R$ control spatial memory, but this is fully accounted by $A_{2A}R$ in the dorsal hippocampus (Li P. et al., 2015; Pagnussat et al., 2015). Furthermore, we now report that PFC $A_{2A}R$ have a discrete impact on anxiety-like behaviors. Therefore, it is likely that the control by PFC $A_{2A}R$ of delay-based decision making might be a consequence of an ability of PFC $A_{2A}R$ to control impulsivity, which is often inferred from the analysis of delay-based decision tasks (Dalley et al., 2011; Kim and Lee, 2011). This contention that PFC $A_{2A}R$ might control delay-based decision making by controlling impulsivity is in agreement with the key role of the PFC in gating impulsivity (Sripada et al., 2011; Mason et al., 2014). However, it should be made clear that this is an indirect inference rather than a direct demonstration and future work should address if PFC $A_{2A}R$ also control others forms of impulsivity apart from impulsive intertemporal choice, such as impulsivity based on speed instead of accuracy (see Kim and Lee, 2011).

Our finding of increased delay aversion upon decreased function of PLmPFC $A_{2A}R$ seems to fully account for the exacerbation of waiting impulsivity observed upon systemic antagonism of $A_{2A}R$ (Oliveros et al., 2017). Likewise, there also seems to be a positive correlation between the intake of caffeine (Grant and Chamberlain, 2018) or caffeinated alcoholic beverages (Amlung et al., 2013; Heinz et al., 2013) and higher impulsivity. Although caffeine is a mixed antagonist of $A_1/A_{2A}R$ antagonist (Fredholm et al., 2005), and its intake is already biased by the predisposition to impulsivity (Waldeck and Miller, 1997; Jones and Lejuez, 2005), animal studies indicate that caffeine can actually reduce impulsive choice behavior only in the sub-population of rodents with medium-to-high basal level of impulsivity (Barbelivien et al., 2008). Thus, blockade of adenosine receptors seems to work as a normalizer of function, bolstering impulsivity in low-impulsivity individuals and dampening impulsivity when it is already elevated. This putative shift of $A_{2A}R$ function may be associated with stressful conditions in the brain (reviewed in Cunha, 2016) or with a disbalance among the PFC, dorsal hippocampus and nucleus accumbens in the control of impulsivity (Kim and Lee, 2011; Monterosso et al., 2001), since synaptic plasticity is differently regulated by $A_{2A}R$ in each of these brain areas (D'Alcantara et al., 2001; Costenla et al., 2011; Kerkhofs et al., 2018). This possibility allows reconciling the presently observed increased impulsivity upon selective downregulation of $A_{2A}R$ in the PLmPFC with the beneficial effect of caffeine and $A_{2A}R$ antagonists in processes such as memory deterioration (Cunha and Agostinho, 2010; Chen, 2014), ADHD (Pandolfo et al., 2013), schizophrenia (Rial et al., 2014), effort-based decision-making (e.g., Pardo et al., 2012; Nunes et al., 2013), ethanol consumption (Nam et al., 2013) or psychomotor responses triggered by drugs of abuse (e.g., Shen et al., 2008; Matos et al., 2015), all of which are worsened with increased impulsivity.

The role of $A_{2A}R$ in the control of anxiety is not straightforward (reviewed in Cunha et al., 2008; Yamada et al., 2014). Accordingly, there was a discrete effect upon downregulating $A_{2A}R$ selectively in the PLmPFC on anxiety-like behavior in the elevated plus maze test and in the splash test, whereas no effect was observed in the open field test. Although previous human genetic association studies implicate polymorphisms of the $A_{2A}R$ gene in caffeine-induced anxiety (Alsene et al., 2003; Tsai et al., 2006), there is some discrepancy on the impact on anxiety-like behaviors of $A_{2A}R$ genetic deletions and $A_{2A}R$ pharmacological antagonism (e.g., Ledent et al., 1997; El Yacoubi et al., 2000; Kaster et al., 2015) as well as $A_{2A}R$ overexpression (Giménez-Llort et al., 2007; Coelho et al., 2014). The inconsistency in these global manipulations of $A_{2A}R$ might result from a differential contribution of $A_{2A}R$ in different brain regions. This is exemplified by the observations that the deletion of $A_{2A}R$ in striatal neurons does not affect anxiety-like behavior, while deletion of $A_{2A}R$ in the entire forebrain or focal deletion of hippocampal $A_{2A}R$ both produce an anxiolytic phenotype (Wei et al., 2014). Our results add further complexity to the $A_{2A}R$-mediated modulation of anxious behavior and warrants future region-selective studies to unravel the impact of $A_{2A}R$ in different circuits in the control this behavior.

Given that the downregulation of $A_{2A}R$ in the PLmPFC resulted in a discrete anxious phenotype, caution must be taken when inferring impulsive choice behavior from a T-maze delay-based cost-benefit decision making analysis. The enclosure of animals with an anxious phenotype in a small compartment between two arms of the T-maze during the delay period could have induced a context aversion, leading the rats to choose the small reward solely as a result of a cost-benefit re-evaluation rather than impulsivity. Furthermore, the subjective value of the large food reward was greater in sh$A_{2A}R$- as compared to shCTRL-treated rats as they needed lower number of training sessions to reach testing criterion. Because of this, the extinction of this subjective value could also be faster, adding a confound to our observations. It is known that PLmPFC and $A_{2A}R$ regulate

fear responses. However, the involvement of A_{2A}R in fear responses is complex, as the nature of regulation depends on the manipulated brain region (Wei et al., 2014; Simões et al., 2016). If A_{2A}R in the PLmPFC also regulates fear responses is not known. Interestingly, impulsive choice behavior has been shown to predict greater anxiety-like behavior in rats (Stein et al., 2015), and in humans, anxious individuals were shown to be impulsive decision-makers in the delay discounting task (Xia et al., 2017), both in agreement with our findings. Thus, future studies to clarify the role of A_{2A}R in anxiety and fear responses and their relationship to impulsive behavior will be useful to dissociate between the impact of PLmPFC A_{2A}R on impulsive decision making vs. on reward value- and context-dependent re-evaluation of cost-benefit during decision making.

The final PFC-related behavioral output that was investigated was working memory, which is bolstered upon pharmacological and genetic ablation of A_{2A}R, both in physiological and pathological situations (reviewed in Chen, 2014), whereas transgenic overexpression of A_{2A}R in the cortex of rats impairs working memory (Giménez-Llort et al., 2007). Working memory is a short-lasting on-line memory buffer system that holds behaviorally relevant information to ongoing tasks and relies on a network of brain regions connected to and orchestrated by the PFC (Goldman-Rakic, 1999; Fuster, 2001). However, we now show that the genetic downregulation of A_{2A}R selectively in the PLmPFC of rats does not affect spatial working memory when assessed as the spontaneous alternation in the Y-maze and it has an inconsistent effect on working memory assessed in the repeated trial MWM test. Our findings are in line with a recent report that optogenetic activation of A_{2A}R signaling pathways in the mPFC did not affect spatial working in the Y-maze test (Li et al., 2018); in contrast, the selective manipulation of A_{2A}R in the striatum is sufficient to control working memory (Zhou et al., 2009; Wei et al., 2011) in a manner equivalent to the improvement of spatial working memory upon systemic antagonism of A_{2A}R (Augusto et al., 2013; Li et al., 2018). Thus, it seems that striatal A_{2A}R override mPFC A_{2A}R in controlling working memory performance in physiological conditions. However, it remains to be determined to which extent PFC A_{2A}R might contribute to the recovery of the deterioration of working memory performance afforded by A_{2A}R blockade in different pathological conditions (Horita et al., 2013; Li W. et al., 2015).

Altogether, our findings that PLmPFC A_{2A}R mediate impulsive choice constitutes the first direct demonstration of a role of A_{2A}R in the control of behavior in physiological conditions. We have recently shown that PFC A_{2A}R LTP in excitatory synapses onto fast spiking interneurons and control PLmPFC network activity (Kerkhofs et al., 2018). Thus, future research targeting selectively A_{2A}R in PLmPFC fast spiking interneurons will be needed to clarify whether specifically A_{2A}R located on glutamatergic synapses impinging on fast spiking interneurons control decision making and impulsive choice, or these behaviors are rather dependent on cooperation among A_{2A}R located in different cell types. Furthermore, the differences observed between the selective manipulation of A_{2A}R in the PLmPFC and more global alterations of A_{2A}R function clearly warrant the need of future studies to dissect the hierarchy of the different roles of A_{2A}R in different brain regions in the control of mood and cognition. Additionally, since decision making and impulsive choice is also modulated by dopamine receptors, it will also be interesting to probe whether the effect of A_{2A}R on impulsive choice involves interaction with dopamine D_2R, especially because antagonism and genetic deletion of A_{2A}R dampen dopamine-mediated decrease in PFC network activity (Real et al., 2018). Finally, the up-regulation of A_{2A}R in synapses upon brain disease condition (reviewed in Cunha, 2016), namely in the PFC (Pandolfo et al., 2013), heralds the potential of A_{2A}R as relevant players controlling the pathophysiology of several neuropsychiatric disorders (Cunha et al., 2008), which still remains to be explored.

AUTHOR CONTRIBUTIONS

DL, PP, NG, RC and SF designed the research. DL, PP, NG, NM, CS, JR, HS, AK and SF performed the experiments and analyzed the data. SF wrote the first draft of the manuscript. All authors commented on the manuscript text.

FUNDING

This work was supported by Maratona da Saúde, Fundacion LaCaixa, Pepita-FMUC and Banco Santander-Totta, NARSAD, Centro 2020 (project CENTRO-01-0145-FEDER-000008:BrainHealth 2020 and CENTRO-01-0246-FEDER-000010), and FCT (projects POCI-01-0145-FEDER-007440 and PTDC/NEU-NMC/4154/2016) to RC.

REFERENCES

Alsene, K., Deckert, J., Sand, P., and de Wit, H. (2003). Association between A_{2A} receptor gene polymorphisms and caffeine-induced anxiety. *Neuropsychopharmacology* 28, 1694–1702. doi: 10.1038/sj.npp.1300232

Amlung, M., Few, L. R., Howland, J., Rohsenow, D. J., Metrik, J., and MacKillop, J. (2013). Impulsivity and alcohol demand in relation to combined alcohol and caffeine use. *Exp. Clin. Psychopharmacol.* 21, 467–474. doi: 10.1037/a0034214

Arnsten, A. F. T., Wang, M., and Paspalas, C. D. (2015). Dopamine's actions in primate prefrontal cortex: challenges for treating cognitive disorders. *Pharmacol. Rev.* 67, 681–696. doi: 10.1124/pr.115.010512

Augusto, E., Matos, M., Sévigny, J., El-Tayeb, A., Bynoe, M. S., Müller, C. E., et al. (2013). Ecto-5′-nucleotidase (CD73)-mediated formation of adenosine is critical for the striatal adenosine A_{2A} receptor functions. *J. Neurosci.* 33, 11390–11399. doi: 10.1523/jneurosci.5817-12.2013

Bailey, M. R., Simpson, E. H., and Balsam, P. D. (2016). Neural substrates underlying effort, time and risk-based decision making in motivated behavior. *Neurobiol. Learn. Mem.* 133, 233–256. doi: 10.1016/j.nlm.2016.07.015

Barbelivien, A., Billy, E., Lazarus, C., Kelche, C., and Majchrzak, M. (2008). Rats with different profiles of impulsive choice behavior exhibit differences in responses to caffeine and d-amphetamine and in medial prefrontal cortex 5-HT utilization. *Behav. Brain Res.* 187, 273–283. doi: 10.1016/j.bbr.2007.09.020

Bizot, J. C., Chenault, N., Houzé, B., Herpin, A., David, S., Pothion, S., et al. (2007). Methylphenidate reduces impulsive behaviour in juvenile Wistar rats, but not in adult Wistar, SHR and WKY rats. *Psychopharmacology* 193, 215–223. doi: 10.1007/s00213-007-0781-4

Bruns, R. F., Lawson-Wendling, K., and Pugsley, T. A. (1983). A rapid filtration assay for soluble receptors using polyethylenimine-treated filters. *Anal. Biochem.* 132, 74–81. doi: 10.1016/0003-2697(83)90427-x

Caballero, M., Núñez, F., Ahern, S., Cuffí, M. L., Carbonell, L., Sánchez, S., et al. (2011). Caffeine improves attention deficit in neonatal 6-OHDA lesioned rats, an animal model of attention deficit hyperactivity disorder (ADHD). *Neurosci. Lett.* 494, 44–48. doi: 10.1016/j.neulet.2011.02.050

Calhoon, G. G., and Tye, K. M. (2015). Resolving the neural circuits of anxiety. *Nat. Neurosci.* 18, 1394–1404. doi: 10.1038/nn.4101

Chen, J. F. (2014). Adenosine receptor control of cognition in normal and disease. *Int. Rev. Neurobiol.* 119, 257–307. doi: 10.1016/b978-0-12-801022-8.00012-x

Choleris, E., Thomas, A. W., Kavaliers, M., and Prato, F. S. (2001). A detailed ethological analysis of the mouse open field test: effects of diazepam, chlordiazepoxide and an extremely low frequency pulsed magnetic field. *Neurosci. Biobehav. Rev.* 25, 235–260. doi: 10.1016/s0149-7634(01)00011-2

Coelho, J. E., Alves, P., Canas, P. M., Valadas, J. S., Shmidt, T., Batalha, V. L., et al. (2014). Overexpression of adenosine A_{2A} receptors in rats: effects on depression, locomotion and anxiety. *Front. Psychiatry* 5:67. doi: 10.3389/fpsyt.2014.00067

Costenla, A. R., Diógenes, M. J., Canas, P. M., Rodrigues, R. J., Nogueira, C., Maroco, J., et al. (2011). Enhanced role of adenosine A_{2A} receptors in the modulation of LTP in the rat hippocampus upon ageing. *Eur. J. Neurosci.* 34, 12–21. doi: 10.1111/j.1460-9568.2011.07719.x

Courtin, J., Bienvenu, T. C., Einarsson, E. Ö., and Herry, C. (2013). Medial prefrontal cortex neuronal circuits in fear behavior. *Neuroscience* 240, 219–242. doi: 10.1016/j.neuroscience.2013.03.001

Cunha, R. A. (2016). How does adenosine control neuronal dysfunction and neurodegeneration? *J. Neurochem.* 139, 1019–1055. doi: 10.1111/jnc.13724

Cunha, R. A., and Agostinho, P. M. (2010). Chronic caffeine consumption prevents memory disturbance in different animal models of memory decline. *J. Alzheimers Dis.* 20, S95–S116. doi: 10.3233/jad-2010-1408

Cunha, R. A., Constantino, M. D., and Ribeiro, J. A. (1999). G protein coupling of CGS 21680 binding sites in the rat hippocampus and cortex is different from that of adenosine A_1 and striatal A_{2A} receptors. *Naunyn Schmiedebergs Arch. Pharmacol.* 359, 295–302. doi: 10.1007/pl00005355

Cunha, R. A., Ferré, S., Vaugeois, J. M., and Chen, J. F. (2008). Potential therapeutic interest of adenosine A_{2A} receptors in psychiatric disorders. *Curr. Pharm. Des.* 14, 1512–1524. doi: 10.2174/138161208784480090

D'Alcantara, P., Ledent, C., Swillens, S., and Schiffmann, S. N. (2001). Inactivation of adenosine A_{2A} receptor impairs long term potentiation in the accumbens nucleus without altering basal synaptic transmission. *Neuroscience* 107, 455–464. doi: 10.1016/S0306-4522(01)00372-4

Dalley, J. W., Everitt, B. J., and Robbins, T. W. (2011). Impulsivity, compulsivity and top-down cognitive control. *Neuron* 69, 680–694. doi: 10.1016/j.neuron.2011.01.020

Dudchenko, P. A. (2004). An overview of the tasks used to test working memory in rodents. *Neurosci. Biobehav. Rev.* 28, 699–709. doi: 10.1016/j.neubiorev.2004.09.002

El Yacoubi, M., Ledent, C., Parmentier, M., Costentin, J., and Vaugeois, J. M. (2000). The anxiogenic-like effect of caffeine in two experimental procedures measuring anxiety in the mouse is not shared by selective A_{2A} adenosine receptor antagonists. *Psychopharmacology* 148, 153–163. doi: 10.1007/s002130050037

Ferreira, S. G., Gonçalves, F. Q., Marques, J. M., Tomé, Â. R., Rodrigues, R. J., Nunes-Correia, I., et al. (2015). Presynaptic adenosine A_{2A} receptors dampen cannabinoid CB_1 receptor-mediated inhibition of corticostriatal glutamatergic transmission. *Br. J. Pharmacol.* 172, 1074–1086. doi: 10.1111/bph.12970

Floresco, S. B., and Ghods-Sharifi, S. (2007). Amygdala-prefrontal cortical circuitry regulates effort-based decision making. *Cereb. Cortex* 17, 251–260. doi: 10.1093/cercor/bhj143

Floresco, S. B., Tse, M. T. L., and Ghods-Sharifi, S. (2008). Dopaminergic and glutamatergic regulation of effort- and delay-based decision making. *Neuropsychopharmacology* 33, 1966–1979. doi: 10.1038/sj.npp.1301565

Font, L., Mingote, S., Farrar, A. M., Pereira, M., Worden, L., Stopper, C., et al. (2008). Intra-accumbens injections of the adenosine A_{2A} agonist CGS21680 affect effort-related choice behavior in rats. *Psychopharmacology* 199, 515–526. doi: 10.1007/s00213-008-1174-z

Fredholm, B. B., Chen, J. F., Cunha, R. A., Svenningsson, P., and Vaugeois, J. M. (2005). Adenosine and brain function. *Int. Rev. Neurobiol.* 63, 191–270. doi: 10.1016/S0074-7742(05)63007-3

Fuster, J. M. (2001). The prefrontal cortex—an update: time is of the essence. *Neuron* 30, 319–333. doi: 10.1016/s0896-6273(01)00285-9

Giménez-Llort, L., Schiffmann, S. N., Shmidt, T., Canela, L., Camón, L., Wassholm, M., et al. (2007). Working memory deficits in transgenic rats overexpressing human adenosine A_{2A} receptors in the brain. *Neurobiol. Learn. Mem.* 87, 42–56. doi: 10.1016/j.nlm.2006.05.004

Goldman-Rakic, P. S. (1999). The physiological approach: functional architecture of working memory and disordered cognition in schizophrenia. *Biol. Psychiatry* 46, 650–661. doi: 10.1016/s0006-3223(99)00130-4

Gonçalves, F. Q., Pires, J., Pliassova, A., Beleza, R., Lemos, C., Marques, J. M., et al. (2015). Adenosine A_{2B} receptors control A_1 receptor-mediated inhibition of synaptic transmission in the mouse hippocampus. *Eur. J. Neurosci.* 41, 878–888. doi: 10.1111/ejn.12851

Gourley, S. L., and Taylor, J. R. (2016). Going and stopping: dichotomies in behavioral control by the prefrontal cortex. *Nat. Neurosci.* 19, 656–664. doi: 10.1038/nn.4275

Grant, J. E., and Chamberlain, S. R. (2018). Caffeine's influence on gambling behavior and other types of impulsivity. *Addict. Behav.* 76, 156–160. doi: 10.1016/j.addbeh.2017.08.007

Harper, L. K., Beckett, S. R., Marsden, C. A., McCreary, A. C., and Alexander, S. P. (2006). Effects of the A_{2A} adenosine receptor antagonist KW6002 in the nucleus accumbens *in vitro* and *in vivo*. *Pharmacol. Biochem. Behav.* 83, 114–121. doi: 10.1016/j.pbb.2005.12.014

Hauber, W., and Sommer, S. (2009). Prefrontostriatal circuitry regulates effort-related decision making. *Cereb. Cortex* 19, 2240–2247. doi: 10.1093/cercor/bhn241

Heinz, A. J., de Wit, H., Lilje, T. C., and Kassel, J. D. (2013). The combined effects of alcohol, caffeine and expectancies on subjective experience, impulsivity and risk-taking. *Exp. Clin. Psychopharmacol.* 21, 222–234. doi: 10.1037/a0032337

Horita, T. K., Kobayashi, M., Mori, A., Jenner, P., and Kanda, T. (2013). Effects of the adenosine A_{2A} antagonist istradefylline on cognitive performance in rats with a 6-OHDA lesion in prefrontal cortex. *Psychopharmacology* 23, 345–352. doi: 10.1007/s00213-013-3158-x

Jin, J., and Maren, S. (2015). Prefrontal-hippocampal interactions in memory and emotion. *Front. Syst. Neurosci.* 9:170. doi: 10.3389/fnsys.2015.00170

Jones, H. A., and Lejuez, C. W. (2005). Personality correlates of caffeine dependence: the role of sensation seeking, impulsivity and risk taking. *Exp. Clin. Psychopharmacol.* 13, 259–266. doi: 10.1037/1064-1297.13.3.259

Kable, J. W., and Glimcher, P. W. (2007). The neural correlates of subjective value during intertemporal choice. *Nat. Neurosci.* 10, 1625–1633. doi: 10.1038/nn2007

Kaster, M. P., Machado, N. J., Silva, H. B., Nunes, A., Ardais, A. P., Santana, M., et al. (2015). Caffeine acts through neuronal adenosine A_{2A} receptors to prevent mood and memory dysfunction triggered by chronic stress. *Proc. Natl. Acad. Sci. U S A* 112, 7833–7838. doi: 10.1073/pnas.1423088112

Kerkhofs, A., Canas, P. M., Timmerman, A. J., Real, J. I., Xavier, C., Cunha, R. A., et al. (2018). Adenosine A_{2A} receptors control glutamatergic synaptic plasticity in fast spiking interneurons of the prefrontal cortex. *Front. Pharmacol.* 9:133. doi: 10.3389/fphar.2018.00133

Kilkenny, C., Browne, W., Cuthill, I. C., Emerson, M., Altman, D. G., and NC3Rs Reporting Guidelines Working Group. (2010). Animal research: reporting *in vivo* experiments: the ARRIVE guidelines. *Br. J. Pharmacol.* 160, 1577–1579. doi: 10.1111/j.1476-5381.2010.00872.x

Kim, S., and Lee, D. (2011). Prefrontal cortex and impulsive decision making. *Biol. Psychiatry* 69, 1140–1146. doi: 10.1016/j.biopsych.2010.07.005

Ledent, C., Vaugeois, J. M., Schiffmann, S. N., Pedrazzini, T., El Yacoubi, M., Vanderhaeghen, J. J., et al. (1997). Aggressiveness, hypoalgesia and high blood pressure in mice lacking the adenosine A_{2A} receptor. *Nature* 388, 674–678. doi: 10.1038/41771

Lee, D. (2013). Decision making: from neuroscience to psychiatry. *Neuron* 78, 233–248. doi: 10.1016/j.neuron.2013.04.008

Li, Z., Chen, X., Wang, T., Gao, Y., Li, F., Chen, L., et al. (2018). The corticostriatal adenosine A_{2A} receptor controls maintenance and retrieval of spatial working memory. *Biol. Psychiatry* 83, 530–541. doi: 10.1016/j.biopsych.2017.07.017

Li, Y., He, Y., Chen, M., Pu, Z., Chen, L., Li, P., et al. (2016). Optogenetic activation of adenosine A_{2A} receptor signaling in the dorsomedial striatopallidal neurons suppresses goal-directed behavior. *Neuropsychopharmacology* 41, 1003–1013. doi: 10.1038/npp.2015.227

Li, P., Rial, D., Canas, P. M., Yoo, J. H., Li, W., Zhou, X., et al. (2015). Optogenetic activation of intracellular adenosine A_{2A} receptor signaling in the hippocampus is sufficient to trigger CREB phosphorylation and impair memory. *Mol. Psychiatry* 20, 1339–1349. doi: 10.1038/mp.2015.43

Li, W., Silva, H. B., Real, J., Wang, Y.-M., Rial, D., Li, P., et al. (2015). Inactivation of adenosine A_{2A} receptors reverses working memory deficits at early stages of Huntington's disease models. *Neurobiol. Dis.* 79, 70–80. doi: 10.1016/j.nbd.2015.03.030

Liu, K. C., Li, J. Y., Xie, W., Li, L. B., Zhang, J., Du, C. X., et al. (2016). Activation and blockade of serotonin6 receptors in the dorsal hippocampus enhance T maze and hole-board performance in a unilateral 6-hydroxydopamine rat model of Parkinson's disease. *Brain Res.* 1650, 184–195. doi: 10.1016/j.brainres.2016.09.009

Lundberg, C., Björklund, T., Carlsson, T., Jakobsson, J., Hantraye, P., Déglon, N., et al. (2008). Applications of lentiviral vectors for biology and gene therapy of neurological disorders. *Curr. Gene Ther.* 8, 461–473. doi: 10.2174/156652308786847996

Mason, L., O'Sullivan, N., Montaldi, D., Bentall, R. P., and El-Deredy, W. (2014). Decision-making and trait impulsivity in bipolar disorder are associated with reduced prefrontal regulation of striatal reward valuation. *Brain* 137, 2346–2355. doi: 10.1093/brain/awu152

Matos, M., Shen, H. Y., Augusto, E., Wang, Y., Wei, C. J., Wang, Y. T., et al. (2015). Deletion of adenosine A_{2A} receptors from astrocytes disrupts glutamate homeostasis leading to psychomotor and cognitive impairment: relevance to schizophrenia. *Biol. Psychiatry* 78, 763–774. doi: 10.1016/j.biopsych.2015.02.026

Mingote, S., Font, L., Farrar, A. M., Vontell, R., Worden, L. T., Stopper, C. M., et al. (2008). Nucleus accumbens adenosine A_{2A} receptors regulate exertion of effort by acting on the ventral striatopallidal pathway. *J. Neurosci.* 28, 9037–9046. doi: 10.1523/JNEUROSCI.1525-08.2008

Monterosso, J., Ehrman, R., Napier, K. L., O'Brien, C. P., and Childress, A. R. (2001). Three decision-making tasks in cocaine-dependent patients: do they measure the same construct? *Addiction* 96, 1825–1837. doi: 10.1080/09652140120089571

Nam, H. W., Hinton, D. J., Kang, N. Y., Kim, T., Lee, M. R., Oliveros, A., et al. (2013). Adenosine transporter ENT1 regulates the acquisition of goal-directed behavior and ethanol drinking through A_{2A} receptor in the dorsomedial striatum. *J. Neurosci.* 33, 4329–4338. doi: 10.1523/JNEUROSCI.3094-12.2013

Nunes, E. J., Randall, P. A., Podurgiel, S., Correa, M., and Salamone, J. D. (2013). Nucleus accumbens neurotransmission and effort-related choice behavior in food motivation: effects of drugs acting on dopamine, adenosine and muscarinic acetylcholine receptors. *Neurosci. Biobehav. Rev.* 37, 2015–2025. doi: 10.1016/j.neubiorev.2013.04.002

Oliveros, A., Cho, C. H., Cui, A., Choi, S., Lindberg, D., Hinton, D., et al. (2017). Adenosine A_{2A} receptor and ERK-driven impulsivity potentiates hippocampal neuroblastproliferation. *Transl. Psychiatry* 7:e1095. doi: 10.1038/tp.2017.64

Pagnussat, N., Almeida, A. S., Marques, D. M., Nunes, F., Chenet, G. C., Botton, P. H., et al. (2015). Adenosine A_{2A} receptors are necessary and sufficient to trigger memory impairment in adult mice. *Br. J. Pharmacol.* 172, 3831–3845. doi: 10.1111/bph.13180

Pandolfo, P., Machado, N. J., Köfalvi, A., Takahashi, R. N., and Cunha, R. A. (2013). Caffeine regulates frontocorticostriatal dopamine transporter density and improves attention and cognitive deficits in an animal model of attention deficit hyperactivity disorder. *Eur. Neuropsychopharmacol.* 23, 317–328. doi: 10.1016/j.euroneuro.2012.04.011

Pardo, M., Lopez-Cruz, L., Valverde, O., Ledent, C., Baqi, Y., Müller, C. E., et al. (2012). Adenosine A_{2A} receptor antagonism and genetic deletion attenuate the effects of dopamine D_2 antagonism on effort-based decision making in mice. *Neuropharmacology* 62, 2068–2077. doi: 10.1016/j.neuropharm.2011.12.033

Pattij, T., and Vanderschuren, L. J. (2008). The neuropharmacology of impulsive behaviour. *Trends Pharmacol. Sci.* 29, 192–199. doi: 10.1016/j.tips.2008.01.002

Paxinos, G., and Watson, C. (2009). *The Rat Brain In Stereotaxic Coordinates*. 6th Edn. London: Elsevier Academic Press.

Pellow, S., Chopin, P., File, S. E., and Briley, M. (1985). Validation of open: closed arm entries in an elevated plus-maze as a measure of anxiety in the rat. *J. Neurosci. Methods* 14, 149–167. doi: 10.1016/0165-0270(85)90031-7

Prut, L., and Belzung, C. (2003). The open field as a paradigm to measure the effects of drugs on anxiety-like behaviors: a review. *Eur. J. Pharmacol.* 463, 3–33. doi: 10.1016/s0014-2999(03)01272-x

Real, J. I., Simões, A. P., Cunha, R. A., Ferreira, S. G., and Rial, D. (2018). Adenosine A_{2A} receptors modulate the dopamine D2 receptor-mediated inhibition of synaptic transmission in the mouse prefrontal cortex. *Eur. J. Neurosci.* 47, 1127–1134. doi: 10.1111/ejn.13912

Rial, D., Lara, D. R., and Cunha, R. A. (2014). The adenosine neuromodulation system in schizophrenia. *Int. Rev. Neurobiol.* 119, 395–449. doi: 10.1016/b978-0-12-801022-8.00016-7

Rudebeck, P. H., Walton, M. E., Smyth, A. N., Bannerman, D. M., and Rushworth, M. F. S. (2006). Separate neural pathways process different decision costs. *Nat. Neurosci.* 9, 1161–1168. doi: 10.1038/nn1756

Shen, H. Y., Canas, P. M., Garcia-Sanz, P., Lan, J. Q., Boison, D., Moratalla, R., et al. (2013). Adenosine A_{2A} receptors in striatal glutamatergic terminals and GABAergic neurons oppositely modulate psychostimulant action and DARPP-32 phosphorylation. *PLoS One* 8:e80902. doi: 10.1371/journal.pone.0080902

Shen, H. Y., Coelho, J. E., Ohtsuka, N., Canas, P. M., Day, Y. J., Huang, Q. Y., et al. (2008). A critical role of the adenosine A_{2A} receptor in extrastriatal neurons in modulating psychomotor activity as revealed by opposite phenotypes of striatum and forebrain A_{2A} receptor knockouts. *J. Neurosci.* 28, 2970–2975. doi: 10.1523/JNEUROSCI.5255-07.2008

Simões, A. P., Machado, N. J., Gonçalves, N., Kaster, M. P., Simões, A. T., Nunes, A., et al. (2016). Adenosine A_{2A} receptors in the amygdala control synaptic plasticity and contextual fear memory. *Neuropsychopharmacology* 41, 2862–2871. doi: 10.1038/npp.2016.98

Sripada, C. S., Gonzalez, R., Phan, K. L., and Liberzon, I. (2011). The neural correlates of intertemporal decision-making: contributions of subjective value, stimulus type and trait impulsivity. *Hum. Brain Mapp.* 32, 1637–1648. doi: 10.1002/hbm.21136

Stein, J. S., Renda, C. R., Barker, S. M., Liston, K. J., Shahan, T. A., and Madden, G. J. (2015). Impulsive choice predicts anxiety-like behavior, but not alcohol or sucrose consumption, in male long-evans rats. *Alcohol. Clin. Exp. Res.* 39, 932–940. doi: 10.1111/acer.12713

Tovote, P., Fadok, J. P., and Lüthi, A. (2015). Neuronal circuits for fear and anxiety. *Nat. Rev. Neurosci.* 16, 317–331. doi: 10.1038/nrn3945

Tsai, S. J., Hong, C. J., Hou, S. J., and Yen, F. C. (2006). Association study of adenosine A_{2A} receptor (1976C>T) genetic polymorphism and mood disorders and age of onset. *Psychiatr. Genet.* 16:185. doi: 10.1097/01.ypg.0000218627.26622.eb

Viana da Silva, S., Haberl, M. G., Zhang, P., Bethge, P., Lemos, C., Gonçalves, N., et al. (2016). Early synaptic deficits in the APP/PS1 mouse model of Alzheimer's disease involve neuronal adenosine A_{2A} receptors. *Nat. Commun.* 7:11915. doi: 10.1038/ncomms11915

Waldeck, T. L., and Miller, L. S. (1997). Gender and impulsivity differences in licit substance use. *J. Subst. Abuse* 9, 269–275. doi: 10.1016/s0899-3289(97)90021-3

Wei, C. J., Augusto, E., Gomes, C. A., Singer, P., Wang, Y., Boison, D., et al. (2014). Regulation of fear responses by striatal and extrastriatal adenosine A_{2A} receptors in forebrain. *Biol. Psychiatry* 75, 855–863. doi: 10.1016/j.biopsych.2013.05.003

Wei, C. J., Singer, P., Coelho, J., Boison, D., Feldon, J., Yee, B. K., et al. (2011). Selective inactivation of adenosine A_{2A} receptors in striatal neurons enhances working memory and reversal learning. *Learn. Mem.* 18, 459–474. doi: 10.1101/lm.2136011

Whishaw, I. Q. (1985). Formation of a place learning-set by the rat: a new paradigm for neurobehavioral studies. *Physiol. Behav.* 35, 139–143. doi: 10.1016/0031-9384(85)90186-6

Wydra, K., Suder, A., Frankowska, M., Borroto Escuela, D. O., Fuxe, K., and Filip, M. (2018). Effects of intra-accumbal or intra-prefrontal cortex microinjections of adenosine 2A receptor ligands on responses to cocaine reward and seeking in rats. *Psychopharmacology* 235, 3509–3523. doi: 10.1007/s00213-018-5072-8

Xia, L., Gu, R., Zhang, D., and Luo, Y. (2017). Anxious individuals are impulsive decision-makers in the delay discounting task: an ERP study. *Front. Behav. Neurosci.* 11:5. doi: 10.3389/fnbeh.2017.00005

Yalcin, I., Aksu, F., and Belzung, C. (2005). Effects of desipramine and tramadol in a chronic mild stress model in mice are altered by yohimbine but not by pindolol. *Eur. J. Pharmacol.* 514, 165–174. doi: 10.1016/j.ejphar.2005.03.029

Yamada, K., Kobayashi, M., and Kanda, T. (2014). Involvement of adenosine A_{2A} receptors in depression and anxiety. *Int. Rev. Neurobiol.* 119, 373–393. doi: 10.1016/b978-0-12-801022-8.00015-5

Yu, C., Gupta, J., Chen, J. F., and Yin, H. H. (2009). Genetic deletion of A_{2A} adenosine receptors in the striatum selectively impairs habit formation. *J. Neurosci.* 29, 15100–15103. doi: 10.1523/JNEUROSCI.4215-09.2009

Zhou, S. J., Zhu, M. E., Shu, D., Du, X. P., Song, X. H., Wang, X. T., et al. (2009). Preferential enhancement of working memory in mice lacking adenosine A_{2A} receptors. *Brain Res.* 1303, 74–83. doi: 10.1016/j.brainres.2009.09.082

Conflict of Interest Statement: RC is a scientific consultant for the Institute for Scientific Information on Coffee.

The remaining authors declare that the research was conducted in the absence of any commercial or financial relationships that could be construed as a potential conflict of interest.

frontiers in Cellular Neuroscience

REVIEW
published: 28 March 2019
doi: 10.3389/fncel.2019.00124

Historical and Current Adenosine Receptor Agonists in Preclinical and Clinical Development

Kenneth A. Jacobson, Dilip K. Tosh, Shanu Jain and Zhan-Guo Gao*

Molecular Recognition Section, Laboratory of Bioorganic Chemistry, National Institute of Diabetes and Digestive and Kidney Diseases, National Institutes of Health, Bethesda, MD, United States

Adenosine receptors (ARs) function in the body's response to conditions of pathology and stress associated with a functional imbalance, such as in the supply and demand of energy/oxygen/nutrients. Extracellular adenosine concentrations vary widely to raise or lower the basal activation of four subtypes of ARs. Endogenous adenosine can correct an energy imbalance during hypoxia and other stress, for example, by slowing the heart rate by A_1AR activation or increasing the blood supply to heart muscle by the A_{2A}AR. Moreover, exogenous AR agonists, antagonists, or allosteric modulators can be applied for therapeutic benefit, and medicinal chemists working toward that goal have reported thousands of such agents. Thus, numerous clinical trials have ensued, using promising agents to modulate adenosinergic signaling, most of which have not succeeded. Currently, short-acting, parenteral agonists, adenosine and Regadenoson, are the only AR agonists approved for human use. However, new concepts and compounds are currently being developed and applied toward preclinical and clinical evaluation, and initial results are encouraging. This review focuses on key compounds as AR agonists and positive allosteric modulators (PAMs) for disease treatment or diagnosis. AR agonists for treating inflammation, pain, cancer, non-alcoholic steatohepatitis, angina, sickle cell disease, ischemic conditions and diabetes have been under development. Multiple clinical trials with two A_3AR agonists are ongoing.

Keywords: purinergic signaling, adenosine receptors, inflammation, pain, CNS

OPEN ACCESS

Edited by:
David Blum,
INSERM U1172 Centre de Recherche Jean-Pierre Aubert, France

Reviewed by:
Sergi Ferre,
Intramural Research Program (NIDA), United States
Francisco Ciruela,
University of Barcelona, Spain
Patrizia Popoli,
Istituto Superiore di Sanità (ISS), Italy

****Correspondence:***
Kenneth A. Jacobson
kennethJ@niddk.nih.gov;
kajacobs@helix.nih.gov

Received: *08 January 2019*
Accepted: *13 March 2019*
Published: *28 March 2019*

Citation:
Jacobson KA, Tosh DK, Jain S and Gao Z-G (2019) Historical and Current Adenosine Receptor Agonists in Preclinical and Clinical Development. Front. Cell. Neurosci. 13:124. doi: 10.3389/fncel.2019.00124

INTRODUCTION

Adenosine receptors (ARs) are G protein-coupled receptors (GPCRs) that sense an imbalance of demand and supply of energy/oxygen/nutrients. Extracellular adenosine concentrations rise in response to hypoxia and other stress, to act upon four subtypes of ARs (A_1AR, A_{2A}AR, A_{2B}AR, and A_3AR) (Fredholm et al., 2001; Chen et al., 2013). As shown with mice lacking all four AR subtypes, extracellular adenosine is mainly a sensor of tissue damage or danger, rather than a homeostatic regulator under baseline conditions (Xiao et al., 2019). Elevated adenosine can correct an energy imbalance during distress of an organ, for example by slowing the heart rate by A_1AR activation or increasing the blood supply to heart muscle by the A_{2A}AR (Borea et al., 2016). However, there are conditions in which chronic adenosine overproduction can be harmful, leading to increased inflammation, fibrosis, cytokine release, brain dopamine depletion, and kidney damage (Borea et al., 2017). Moreover, exogenous AR agonists, antagonists, or allosteric modulators can be applied for therapeutic benefit, and thousands of such agents have been reported by medicinal chemists working toward that goal (Jacobson and Gao, 2006; Kiesman et al., 2009). Clinically important

effects of adenosine also include suppression of the immune response, glomerular filtration, seizures and pain (Fredholm et al., 2001; Cekic and Linden, 2016; Antonioli et al., 2018). Adenosine 5′-triphosphate (ATP) released from cells under stress conditions or damage is the source of much of the extracellular adenosine. There is typically a basal level of AR stimulation, especially for A_1AR, A_{2A}AR and A_3AR at low nM concentrations, while A_{2B}AR activation generally occurs at higher (μM) adenosine concentrations (Fredholm et al., 2001). Therefore, AR antagonists have distinct biological effects *in vivo*. Purinergic signaling is also to be considered in the larger context of ligand (ATP)-gated P2X receptors or G protein-coupled P2Y receptors that respond to extracellular purine and pyrimidine mono- and di-nucleotides (Burnstock and Boeynaems, 2014).

There are many approaches to small molecule therapeutics based on experimental modulators of ARs (Chen et al., 2013; Borea et al., 2018). Numerous subtype-selective agonists and antagonists have been introduced, both as pharmacological probes and as clinical candidate molecules, and representative compounds are described here. AR knockout (KO) mice are increasingly used to validate *in vivo* results with agonists and antagonists, which can actually have variable selectivity (Carlin et al., 2018). This review covers both directly acting AR modulators, i.e., agonists, and several positive allosteric modulators (PAMs). It describes compounds that have been in human trials, for both therapeutics and diagnostics, and some compounds for which clinical trials have only been contemplated. Other reviews cover the use of enzymatic or transport inhibitors to increase – such as inhibitors of adenosine kinase or adenosine deaminase that deplete adenosine levels, or uptake inhibitors – or to decrease, such as inhibitors of ectonucleotidases, the levels of endogenous nucleosides (Boison, 2013; Allard et al., 2017; Vuerich et al., 2019). These enzymes are often upregulated in inflammatory states (Boison, 2013; Haskó et al., 2018).

AR AGONISTS FOR CLINICAL DEVELOPMENT

Agonists of the A_1AR, A_{2A}AR and A_3AR have been the subject of preclinical and clinical evaluation (**Figures 1, 2** and **Tables 1**, **2**). A_{2B}AR agonist development is the most limited among the ARs, and agonists for this AR subtype have not yet entered clinical trials. There is also much controversy about whether A_{2B}AR agonists or antagonists would be more useful clinically (Eisenstein et al., 2015; Sun and Huang, 2016; Gao and Jacobson, 2017).

Each AR can signal through multiple pathways, and different agonists may show a signaling preference, i.e., bias. For example, the A_{2B}AR acts through G_s, G_q, or G_i, depending on the tissue, receptor density and final measure of activity (Gao et al., 2018). The possibility of biased signaling of AR agonists or PAMs could provide a means to increase selectivity for a particular tissue or condition (Gao et al., 2011; Baltos et al., 2017; Gao et al., 2018; Vecchio et al., 2018).

One limitation of AR agonists for human therapeutics is that their target GPCRs might be subject to agonist-induced desensitization as shown for all four ARs in cell lines (Mundell and Kelly, 2011). However, in other cases, depending on multiple pharmacological factors, a prolonged agonist exposure did not lead to *in vivo* desensitization of the desired effect (Little et al., 2015), even with a full A_3AR agonist. Two possible approaches to circumvent GPCR desensitization are the use of partial agonists in cases where the desired effect is maintained, such as in A_1AR antiarrhythmic activity (Elzein and Zablocki, 2008; Voors et al., 2017), and the use of PAMs (Vincenzi et al., 2014). Partial agonists are also known to display tissue or organ selectivity, because of the differential receptor expression level (Van der Graaf et al., 1999). Thus, when spare receptors are present, i.e., overexpression or high level of endogenous expression, a partial agonist could be fully efficacious in tissues where there is a receptor reserve and activation of only a fraction of the receptors suffices.

Positron emission tomography (PET) for *in vivo* imaging of ARs has been extensively explored (van Waarde et al., 2018). PET imaging could potentially be essential in drug discovery and clinical development of AR modulators, to determine the target engagement and to assess the role of endogenous adenosine. Although most high affinity ligands designed for *in vivo* AR imaging by PET have been antagonists, some agonists have also been labeled with positron-emitting ^{18}F, ^{76}Br or ^{11}C isotopes (Kiesewetter et al., 2009; Guo et al., 2018).

A_1AR and A_{2A}AR are examples of the growing list of GPCRs for which physically determined three-dimensional structures with a bound agonist are known (Lebon et al., 2011; Xu et al., 2011). This understanding facilitates the structure-based design of novel AR agonists (Tosh et al., 2019). Several structures determined by X-ray crystallography and cryo-electron microscopy contain a G-protein or G-protein fragment, which is more representative of the active state AR structures (Draper-Joyce et al., 2018; García-Nafría et al., 2018). NMR studies of assigned A_{2A}AR Trp and Gly residues are informative about microswitches involved in the signal propagation from bound agonist toward the intracellular region for G protein binding (Eddy et al., 2018). There can be multiple active conformations of a given GPCR, and agonist-induced changes are nuanced with respect to both structure and signaling. Thus, direct biophysical methods for receptor characterization can impact agonist design.

The following examples of AR drugs and molecular probes are arranged according to their target receptor: A_1 (**1** – **20**, **39**, **40**), A_{2A} (**21** – **29**), A_{2B} (**30**), A_3 (**31** – **38**, **41**). It has also been suggested that coactivation of two AR subtypes might be beneficial, such as both A_1AR and A_3AR in cardioprotection (Jacobson et al., 2005).

Early AR Agonists

Adenosine 1

Arrhythmias

Many pathophysiological conditions including hypoxia and ischemia may cause arrhythmias. Adenosine is considered as an endogenous antiarrhythmic agent partly due to its endogenous anti-ischemic property (Kiesman et al., 2009; Szentmiklosi

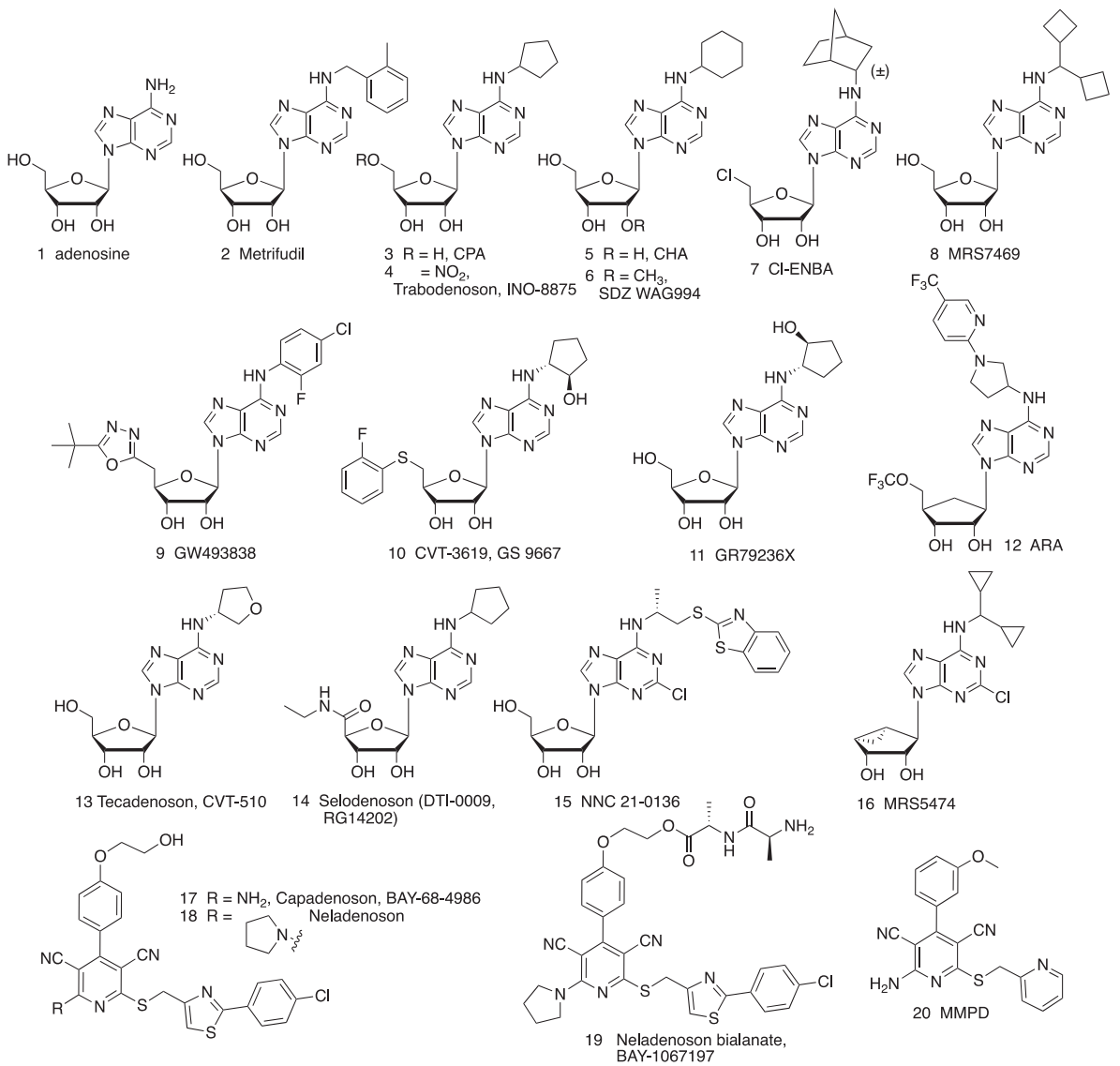

FIGURE 1 | Adenosine **(1)**, a non-selective AR agonist, and its derivatives as A_1AR-selective agonists, including nucleosides **(2–16)** and non-nucleosides **(17–20)**.

et al., 2015). As described earlier, infused adenosine (under the name of Adenocard, approved in 1989, Olsson, 2003) and its precursor ATP have long been used for the treatment of paroxysmal supraventricular tachycardia (PSVT) (Pelleg et al., 2012; Szentmiklosi et al., 2015). The antiarrhythmic action of adenosine has been suggested to occur via the A_1AR in the sinoatrial and atrioventricular nodes, which leads to modification of AV nodal conduction (Kiesman et al., 2009). A_1AR activation is known to induce opening of ATP-sensitive potassium channels (Fredholm et al., 2001; Jacobson and Gao, 2006). Adenosine infusion (under the name of Adenoscan, approved in 1995) is used for myocardial perfusion imaging (MPI), through its short-lived A_{2A}AR activation, to dilate the coronary artery (Olsson, 2003). Many recent clinical trials in various cardiovascular and ischemic conditions have utilized adenosine as an approved drug being tested for new uses (**Table 1**). For example, a clinical trial of adenosine to reverse left ventricular impairment in Takotsubo syndrome (Galiuto et al., 2010) was initiated, but terminated in 2018.

Dermatological conditions

Adenosine applied topically has been used to promote hair growth and skin health (Abella, 2006; Faghihi et al., 2013). For the treatment of androgenetic alopecia, adenosine (0.75% solution) displayed efficacy similar to minoxidil but was preferred by patients because of the response speed and its quality. Applied in cosmetic preparations (0.1% cream or 1% dissolvable film) for 2 months, adenosine significantly improved skin smoothness and reduced facial wrinkles.

Epilepsy

Adenosine is considered an endogenous antiseizure agent and also attenuates epileptogenesis by an epigenetic

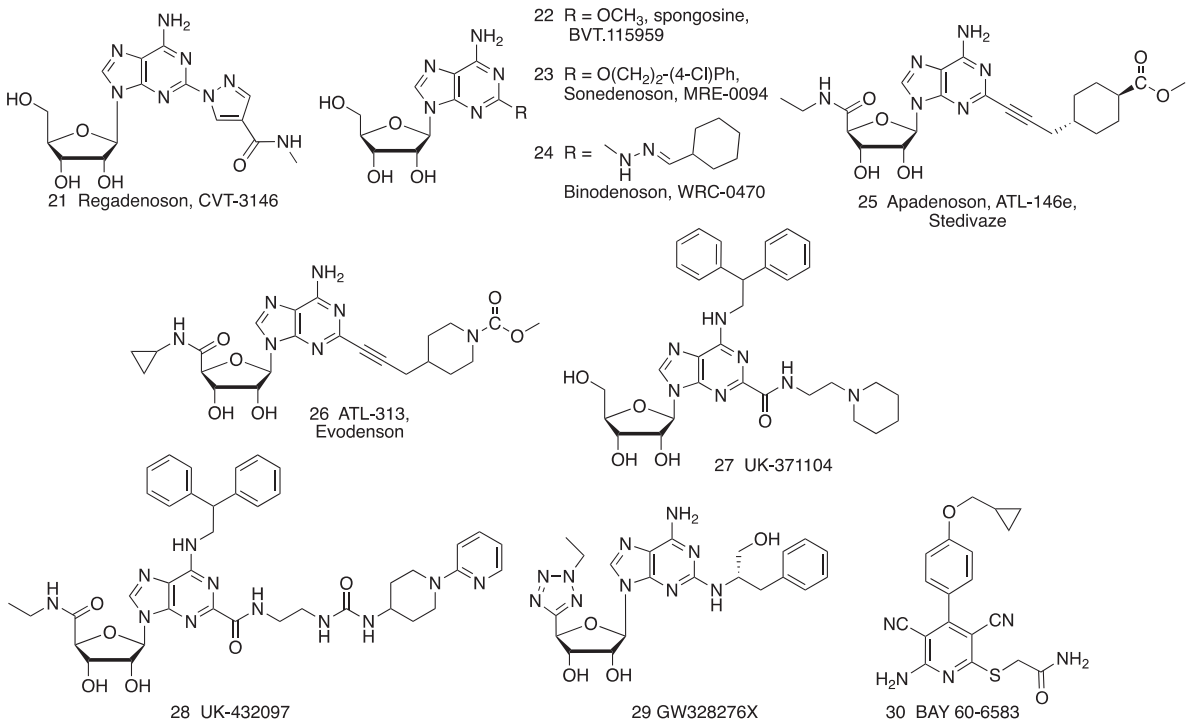

FIGURE 2 | A_{2A}AR- **(21–29)** and A_{2B}AR- **(30)** selective agonists.

mechanism, i.e., nuclear adenosine reduces DNA methylation (Boison, 2013). Elevated adenosine indirectly inhibits DNA methyltransferases through two stages of enzymatic product inhibition, beginning with *S*-adenosylhomocysteine hydrolase (SAH). In the epileptic brain there is an overexpression of adenosine kinase in astrocytes, which depletes adenosine both inside and outside the cell. Because peripheral adenosine itself is rapidly removed from circulation in seconds, drug delivery systems are needed to raise its brain concentration. Experimental use of an adenosine-releasing silk brain implant was found to be an efficacious form of adenosine augmentation therapy (AAT) for treating refractory epilepsy in a rat model of kindling epileptogenesis (Szybala et al., 2009). Adenosine was encapsulated in microspheres, which were embedded into nanofilm-coated silk fibroin scaffolds. The polymer was introduced surgically into the infrahippocampal cleft, and when monitored for 10 days, demonstrated a lack of convulsive seizures. This protective effect was antagonized by an A_1AR-selective antagonist 8-cyclopentyl-1,3-dipropylxanthine (DPCPX).

AMP (Adenosine 5′-Monophosphate) and ATP (Adenosine 5′-Triphosphate)

Asthmatic drug testing

Ectonucleotidases readily cleave the naturally occurring 5′-phosphoesters of adenosine 5′-phosphates to produce adenosine *in situ*. Adenosine 5′-monophosphate (AMP) is used diagnostically in inhalation challenge testing (Basoglu et al., 2005; Isogai et al., 2017). AMP readily forms adenosine *in situ* and thus most of its actions occur through ARs, but not all of its *in vivo* effects arise from AR activation (Carlin et al., 2018; Xiao et al., 2019).

Cancer

Adenosine 5′-triphosphate plays a physiological role in obstructive airway disease to increase inflammation and to induce bronchoconstriction and cough (Pelleg et al., 2016). ATP has been administered in humans intravenously in clinical trials for the treatment of both cachexia in cancer and the cancer itself (Rapaport et al., 2015). The working hypothesis was that by increasing the intracellular ATP pools in erythrocytes, the energy balance could be restored. Alternatively, an action on P2 receptors was considered, but the extracellular ATP pools were elevated only briefly in patients with advanced solid tumors. Nevertheless, with the ubiquitous presence of ectonucleotidases, one main action of ATP would be through increased adenosine acting at ARs.

Metrifudil 2

Glomerulonephritis

Many adenosine derivatives found in early studies (1960s and 1970s) to be biologically active at what were later termed the A_1AR and A_{2A}AR, contain bulky, hydrophobic substitution at the adenine N^6 position (Olsson, 2003; Jacobson and Gao, 2006; Mantell et al., 2010). This describes two potent agonists, Metrifudil **2** and *R*-PIA (*R*-N^6-phenylisopropyladenosine (structure not shown), which

TABLE 1 | Representative recent clinical trials of AR agonists and an A_1AR PAM (data from ClinicalTrials.gov, accessed 12-28-2018).

Receptor	Condition	Compound	Years	Phase, NCT#	Reference
A_1	Neuropathic pain	**1**	2014–2018	**2**, 00349921	Zylka, 2011
	SVT[a]	**1**	2011–2017	**–**, 01495481	Chrysostomou et al., 2013
	Perioperative pain	**1**	2006	**2**, 00298636	Jin and Mi, 2017
	Pediatric heart transpl.	**1**	2015–2018	**1**, 02462941	Flyer et al., 2017
	Takotsubo syndrome	**1**	2016–2018	**2**, 02867878	Galiuto et al., 2010
	Paroxysmal AF	**1**	2017	**2**, 03032965	Letsas et al., 2017
	Glaucoma	**4**	2015–2016	**3**, 02565173	Myers et al., 2016
	Neuropathic pain	**9**	2002–2003	**2**, 00376454	Elzein and Zablocki, 2008
	T2D	**10**	∼2009	**1**, **–**	Staehr et al., 2013
	AF	**13**	2008–2014	**2**, 00713401	Corino et al., 2015
	AF	**14**	2015–2018	**2**, 00040001	Elzein and Zablocki, 2008
	Stable angina	**17**	2007–2011	**2**, 00518921	Tendera et al., 2012
	AF	**17**	2008	**2**, 00568945	Kiesman et al., 2009
	Heart failure[b]	**19**	2014–2016	**2**, 02040233	Lam et al., 2018
	Heart failure[c]	**19**	2016–2018	**2**, 02580851	Voors et al., 2017
	Posthepetic neuralgia	**39**	2008–2012	**2**, 00809679	Miao et al., 2018
A_{2A}	CAD (MPI)	**21**	2005–2009	**3**, 00208312	Zoghbi and Iskandrian, 2012
	Sickle cell anemia	**21**	2013–2018	**2**, 01788631	Field et al., 2014, 2017
	Lung transplant	**21**	2017–	**1**, 03072589	Sharma et al., 2016
	IHD (MRI)	**21**	2011–2012	**1**, 00881218	Lasley, 2018
	Pulmonary hypertens.	**21**	2014–2018	**–**, 02220634	Palani and Ananthasubramaniam, 2013
	Heart transplant (MRI)	**21**	2017–	**4**, 03102125	Palani and Ananthasubramaniam, 2013
	BBB defect	**21**	2015–2018	**1**, 02389738	Jackson et al., 2018
	Diabetic nerve pain	**22**	2007–2014	**2**, 00452777	Knezevic et al., 2015
	Diabetic foot ulcers	**23**	2006–2012	**2**, 00318214	Montesinos et al., 2015
	CAD	**24**	2009–2012	**3**, 00944294	Zoghbi and Iskandrian, 2012
	CAD (SPECT-MPI)	**25**	2009–2012	**3**, 00990327	Zoghbi and Iskandrian, 2012
	CAD (MPI)	**25**	2011–2012	**3**, 01313572	Zoghbi and Iskandrian, 2012
	COPD	**28**	2007–2013	**2**, 00430300	Mantell et al., 2010
	Healthy subjects (PK)	**29**	2012–2017	**1**, 01640990	Allen et al., 2013
A_{2B}- A_3		–	–		Sun and Huang, 2016
	Rheumatoid arthritis	**31**	2016–	**3**, 02467762	Fishman et al., 2012
	Plaque psoriasis	**31**	2017–	**3**, 03168256	David et al., 2016;
	Glaucoma	**31**	2009–2015	**2**, 01033422	Jacobson and Civan, 2016
	Dry eye disease	**31**	2010–2015	**3**, 01235234	Avni et al., 2010
	NASH	**32**	2016–	**2**, 02927314	Fishman et al., 2018
	HCC	**32**	2008–2015	**1/2**, 00790218	Stemmer et al., 2013
	HCC	**32**	2014–	**2**, 02128958	Stemmer et al., 2013
	Chronic HCV	**32**	2008–2015	**1/2**, 00790673	Bar-Yehuda et al., 2008

[a]*Comparison to dexmedetomidine.* [b]*With preserved ejection fraction.* [c]*With reduced ejection fraction. SVT, supraventricular tachycardia; AF, atrial fibrillation; CAD, coronary artery disease; MPI, myocardial perfusion imaging; MRI, magnetic resonance imaging; SPECT, single-photon emission computed tomography; BBB, blood brain barrier; IHD, ischemic heart disease; PK, pharmacokinetics; NASH, nonalcoholic steatohepatitis; HCC, hepatocellular carcinoma; HCV, hepatitis C virus.*

are moderately A_1AR-selective. Metrifudil (60 mg oral dose) was one of the earliest synthetic adenosine agonists to be studied in humans (Schaumann and Kutscha, 1972; Wilbrandt et al., 1972), along with *R*-PIA (Schaumann et al., 1972). Following the discovery that vasodilator dipyridamole (equilibrative adenosine transporter ENT1 inhibitor) was active against glomerulonephritis by an adenosinergic mechanism, Metrifudil was applied to its treatment, which resulted in limited improvement in three patients. However, no subsequent trials of Metrifudil or *R*-PIA were reported, probably because of their cardiovascular side effects.

A_1AR-Selective Agonists

Trabodenoson (INO-8875, PJ-875) 4

Glaucoma

A_1AR partial agonist Trabodenoson (INO-8875) **4**, which is a 5′-nitrate ester derived from CPA **3**, was in advanced clinical trials as an ophthalmic formulation for primary

TABLE 2 | AR Binding affinity of selected AR agonists described here (human, if not specified; p, pig; r, rat; m, mouse).[a,b]

Compound		pK_i A_1AR	pK_i $A_{2A}AR$	pK_i A_3AR
1	Adenosine	7.0	6.5	6.5
2	Metrifudil	7.22 (r)	7.62 (r)	7.33, 7.46 (r)
3	CPA	8.64, 9.66 (m)	6.10, 6.09 (m)	7.37, 6.27 (m)
4	Trabodenoson	9.0	ND	ND
5	CHA	8.62	5.86	7.14
6	SDZ WAG994	7.64 (p), 7.12 (r)	4.64 (p), 5.24 (r)	ND
7	Cl-ENBA	9.29, 9.70 (m)	5.87	5.89, 5.62 (m)
8	MRS7469	8.67, 9.43 (m)	5.45	4.97, 6.05 (m)
10	GS 9667	7.92	<5	<6
11	GR79236X	8.51 (r)	5.89 (r)	ND
13	Tecadenoson	8.52	ND	ND
14	Selodenoson	8.22	ND	ND
15	NNC 21-0136	8.33 (r)	5.89 (r)	ND
16	MRS5474	7.30	5.40	6.33
17	Capadenoson	8.85	<5	<5
18[c]	Neladenoson	10.0	6.17	<5.52
20	MMPD	9.31, 9.68 (r)	7.15, 7.28 (r)	<5
21	Regadenoson	<5, 8.11 (m)	6.34, 7.11 (m)	<5, <5 (m)
22	BVT.115959	6.81	6.01	6.81
23	Sonedenson	<5	6.31	ND
24	Binodenoson	4.32	6.57	<4
25	Apadenson	7.11	9.30	7.35
26	Evodenoson	7.24	9.15	6.60
27[c]	UK-371104	6.99	7.70	<6
28	UK-432097	ND	8.40	ND
29	GW328276X	6.05	8.63	8.38
30	Bay 60-6583	6.41, 6.45 (m)	<5, <5 (m)	6.94, 6.87 (m)
31	Piclodenoson	7.29, 7.79 (m)	5.50, 5.54 (m)	8.74, 9.66 (m)
32	Namodenoson	6.66	5.27	8.85
33	LJ-529	6.71	6.65	9.42
34	CP-532,903	6.05 (m)	<5 (m)	8.05 (m)
35	CP-608,039	5.14	<4.3	8.24
36	MRS5698	<5	<5	8.52
37	MRS5980	<5	<5	9.15

[a] *References: Knutsen et al., 1999; Gao et al., 2003; Kiesman et al., 2009; Alnouri et al., 2015; Meibom et al., 2017; Baraldi et al., 2018; Jacobson et al., 2018; Tosh et al., 2019.* [b] *$A_{2B}AR$ affinity (pKi; h, unless noted): **1**, 4.8; **18**, 7.10 (pEC_{50}); **21**, <5; **23**, <5; **25**, <6; **26**, <6; **27**, 5.36 (pEC_{50}); **29**, 8.30; **30**, 6.94, 7.00 (r), 6.87 (m); **31**, 4.96; **34**, <5 (m).* [c] *pEC_{50} in cAMP assays. ND, not determined.*

open-angle glaucoma and ocular hypertension. However, the development was terminated in 2017 following a Phase 3 trial due to failure to achieve its primary endpoint (Jacobson and Civan, 2016). Trabodenoson and its congeners were also considered for treatment of arrhythmias (Elzein and Zablocki, 2008; see below). Another analog containing a 5′-nitrate ester, but with a N^6-3-aminotetrahydrofuryl group was found to lose its nitro group *in vivo* to form the parent full agonist, which was associated with side effects.

CHA 5

Hypothermia

The use of A_1AR agonist CHA **5** for inducing therapeutic hypothermia has been proposed (Jinka et al., 2015). However, it is likely that the hypothermic effect of CHA in rodents may be through both a peripheral A_3AR, and a central A_1AR (Carlin et al., 2017).

SDZ WAG994 6

Diabetes and obesity

A_1AR is highly expressed in adipose tissue and involved in triglyceride (TG) storage. Breakdown of TG and the subsequent increase in plasma free fatty acids (FFA) results in development of insulin resistance in peripheral organs. Insulin resistance is associated with obesity and development of type 2 diabetes (Antonioli et al., 2015). Adenosine-mediated A_1AR activation or A_1AR overexpression in adipocytes results in suppression of lipolysis and reduction of plasma FFA. Various adenosine analogs have been developed for their potential intervention in diabetes. N^6-Cyclopentyladenosine (CPA, **3**) reduced FFA and cholesterol levels and increased glycogen synthesis in skeletal muscle in

streptozotocin (STZ) diabetic rats (Cheng et al., 2000). Thus, A_1AR agonists may have beneficial effects on glucose utilization by peripheral tissues to lower plasma glucose.

Typically, both 2′- and 3′-hydroxyl groups are important for nucleoside recognition in the AR binding sites. SDZ WAG994 **6** is a structurally unusual 2′-*O*-methyl A_1AR agonist that did not display hemodynamic side effects in humans. However, SDZ WAG994 increased PR interval, consistent with A_1AR activation in the AV node and its suggested use in tachycardia (Jacobson and Knutsen, 2001).

SDZ WAG994 **6** was also under development as an antilipolytic agent for treating diabetes (Ishikawa et al., 1998). Oral administration of SDZ WAG994 and another A_1AR agonist Selodenoson (RG14202, **14**) in STX-treated rats decreased FFA, TG levels and heart rate in a dose-dependent manner (Cox et al., 1997). A human study revealed that RPR749 (structure not shown), was capable of decreasing circulating FFA levels and thus may be beneficial in treating hyperlipidemia (Shah et al., 2004). These compounds have therapeutic potential for the treatment of cardiovascular and metabolic disorders.

Cl-ENBA 7 and MRS7469 8

Hypothermia and pain

Several A_1AR agonists, Cl-ENBA **7** and MRS7469 **8**, were recently reported to activate in the mouse A_1AR in the brain when administered peripherally, without comparable peripheral A_3AR activation (Carlin et al., 2017; Tosh et al., 2019). Cl-ENBA **7** is a highly A_1AR-selective adenosine agonist that is used as a pharmacological probe (Tosh et al., 2019), and its efficacy in pain models demonstrated (Luongo et al., 2012). It consists of a mixture of two diastereoisomers, and thus its *in vivo* A_1AR target engagement is complicated. However, when administered intraperitoneally in mice, it activated the central A_1AR preferentially over the peripheral A_3AR in mast cells, due partly its being a full agonist for the A_1AR but a partial agonist of low efficacy or an antagonist at the A_3AR (Carlin et al., 2017). This is consistent with a report that *S*-N^6-endo-norbornyl-adenosine (*S*-ENBA) is a full agonist at the A_1AR but low-efficacy partial agonist at the A_3AR (Gao et al., 2003).

Like Cl-ENBA, MRS7469 **8** is a highly selective agonist that activated the central A_1AR preferentially when administered peripherally, leading to A_1AR-dependent hypothermia and locomotor depression (Tosh et al., 2019). When administered icv. (52 μg/kg) it caused intense hypothermia. Thus, it crosses the blood brain barrier (BBB) sufficiently, given its high affinity (K_i 0.37 nM at mouse A_1AR), to activate the A_1AR. Moreover, MRS7469 with a non-chiral N^6 group is a pure diastereoisomer, which is advantageous for *in vivo* studies.

GW493838 9

Pain

The A_1AR is involved in depressant and protective functions in the brain and spinal cord, including suppressing pain (Sawynok, 1998; Zylka, 2011; Giorgi and Nieri, 2013). Intrathecal opioids induce local adenosine release (Eisenach et al., 2004), and exogenously applied adenosine and other A_1AR agonists and PAMs reduce pain (Eisenach et al., 2013; Vincenzi et al., 2014). A_1AR agonist GW493838 **9**, which is an adenosine analog highly modified at N^6 and 5′ positions, showed efficacy in animal models of pain (Imlach et al., 2015). However, GW493838 (50 mg oral dose) failed to show significant efficacy in a clinical trial for treatment of chronic pain (diabetic pain). Also, a meta-analysis of patient postoperative pain in clinical data showed no analgesic effect of adenosine (Jin and Mi, 2017).

CVT-3619 (GS-9667) 10, GR79236 11 and ARA 12

Diabetes

Increasing evidence indicates a crucial role of A_1AR in the regulation of insulin sensitivity and glucose homeostasis especially in metabolically active organs such as adipose tissue, liver and skeletal muscle, which are related to diabetes mellitus (Peleli and Carlstrom, 2017). It has been convincingly demonstrated that A_1AR is critical for regulation of lipid metabolism, and thus A_1AR agonists have been proposed for the treatment of type II diabetes (T2D) and obesity (Antonioli et al., 2018). The white adipocyte A_1AR inhibits lipolysis. Curiously, a functional A_{2A}AR activates thermogenic brown adipose tissue (BAT) as indicated using human PET imaging (Lahesmaa et al., 2018), and A_{2A}AR agonists might prove beneficial in metabolic conditions (Tozzi and Novak, 2017). Cold exposure in human subjects reduced PET ligand binding in BAT, indicative of elevated local adenosine release.

Several A_1AR agonists, GR79236 **11**, ARA **12**, and CVT-3619 **10**, have been in clinical trials for T2D due to their ability to increase insulin sensitivity (Bigot et al., 2004; Kiesman et al., 2009; Staehr et al., 2013). However, development of full agonists, such as GR79236 and ARA, was not successful due to cardiovascular side effects (Elzein and Zablocki, 2008). Although both full and partial agonists may lower non-esterified fatty acid levels, it is suggested that partial agonists may improve insulin sensitivity without producing severe cardiovascular side effects (Elzein and Zablocki, 2008). A single dose of ARA given to healthy individuals during a phase I clinical trial reduced plasma FFA levels, but individuals developed tolerance to the drug (Zannikos et al., 2001). The A_1AR partial agonist CVT-3619 (GS-9667) has been reported to lower FFA in both healthy and obese subjects without showing evidence of A_1AR desensitization (Staehr et al., 2013), but oral doses of $\geq$ 300 mg were required to see the FFA effect. The individual benefits of GS-9667 and sitagliptin [Januvia, an inhibitor of DPP4 (dipeptidyl peptidase 4)] on glucose and lipid homeostasis were enhanced in combination (Ning et al., 2011).

Tecadenoson 13 and Selodenoson 14

Arrhythmias

Despite its demonstrated A_1AR-dependent beneficial effect in PSVT, adenosine is known to cause atrial fibrillation (AF) in about 15% of patients by decreasing the refractory period of the atrium and causes other adverse effects related to the activation of other AR subtypes (Glatter et al., 1999). Thus, extensive efforts have been made in developing selective A_1AR agonists as anti-arrhythmic agents (Mason and DiMarco, 2009). A_1AR full agonists Tecadenoson **13** (Corino et al., 2015), Selodenoson **14** and Trabodenoson **4** (Kiesman et al.,

2009; Mason and DiMarco, 2009) have been under development. However, full agonists are known to cause tachyphylaxis, presumably due to A_1AR desensitization. Tecadenoson has been in a Phase 3 trial for the termination of supraventricular tachycardia (SVT) (Elzein and Zablocki, 2008; Mason and DiMarco, 2009), but its development was discontinued in 2009. A clinical safety study of Tecadenoson for the treatment of AF was performed, but its clinical development was also curtailed.

NNC-21-0136 15

Stroke

NNC-21-0136 **15** is an A_1AR selective agonist that was designed for neuroprotection. Its hemodynamic effects were minimal, revealing a brain-protective effect in stroke models (Knutsen et al., 1999; Jacobson and Knutsen, 2001), but it did not enter human testing.

MRS5474 16

Seizures and depression

A_1AR agonists are of interest in the CNS for their anxiolytic, antinociceptive, antidepressant and antiseizure properties, and behavioral results with A_1AR KO mice support the use of A_1AR in this context. Unfortunately, many adenosine derivatives display minimal ability to cross the BBB (Schaddelee et al., 2005; Tosh et al., 2019). 4′-Truncated nucleosides, thionucleosides and methanocarba-nucleosides (containing a [3.1.0]bicyclohexyl ring system) were originally characterized as A_3AR low-efficacy, selective partial agonists. However, an N^6-dicyclopropylmethyl group present in MRS5474 **16** substantially shifts the selectivity toward A_1AR, especially in mouse (204-fold compared to mouse A_3AR), compared to other a-branched N^6 groups (Tosh et al., 2012, 2019; Carlin et al., 2017). The small molecular weight (376), polar surface area (93 Å^2) and number of H-bond donor groups (3) positioned MRS5474 for potential brain application. MRS5474 showed antidepressant activity in a mouse model that was mediated by homer1 protein in the medial prefrontal cortex, and upregulation of homer1 by an AR agonist was lost in A_1AR KO mice (Serchov et al., 2015). Nevertheless, it also activated a peripheral mA_3AR (Carlin et al., 2017).

Capadenoson 17 and Neladenoson 18

Angina

Anti-ischemic effect of A_1AR agonists has been demonstrated in animal studies, but clinical successes are lacking, and more relevant clinical models are needed (Borea et al., 2016; Lasley, 2018).

Most known AR agonists are adenosine derivatives, but two classes of pyridine-derived agonists are known (Guo et al., 2018). The non-nucleoside A_1AR agonist Capadenoson **17** (BAY68-4986), having an atypical 3,5-dicyanopyridine structure, was evaluated in patients with stable angina using an oral dose of 4 mg, once daily (Kiesman et al., 2009; Tendera et al., 2012). However, Capadenoson was withdrawn from clinical trials for angina and for AF.

Heart failure

Rather than full agonists, an A_1AR partial agonist Neladenoson **18** (in the form of a dipeptide ester prodrug **19**) is now being tested in patients with chronic heart failure (Greene et al., 2016; Dinh et al., 2017; Meibom et al., 2017; Voors et al., 2017). Compared with Capadenoson (Baltos et al., 2017), Neladenoson is a more selective partial agonist for A_1AR. Neladenoson has been shown to improve cardiac function without producing bradycardia, atrioventricular blocks, or undesirable effect on blood pressure (Meibom et al., 2017; Voors et al., 2017). The rationale for using partial A_1AR agonists is based on the observation that the activation of myocardial A_1ARs by partial agonists protects cardiac function related to ischemia and reperfusion injury without producing severe side effects (Albrecht-Küpper et al., 2012; Voors et al., 2017). A multiple dose study of Neladenoson (BAY 1067197) (ParSiFAL, 5 – 40 mg oral dose, once daily) in heart failure is ongoing.

MMPD 20

Imaging

Numerous A_1AR ligands have been in development for potential use in diagnosis of various conditions, such as depression, Parkinson's disease, Alzheimer's disease, epilepsy, ischemia, and sleep disorders. The A_1AR is highly expressed in many brain regions, such as the hippocampus, neocortex, thalamus and basal ganglia (Fredholm et al., 2001). *In vivo* imaging of A_1AR in the human brain is therefore an attractive approach for diagnosis, and various AR agonists and antagonists have been developed for PET brain imaging (van Waarde et al., 2018). Although varied AR subtype selectivities and agonist efficacies are seen with the class of atypical 3,5-dicyanopyridine ligands, partial agonist MMPD **20** was recently shown to be highly A_1AR selective, with 16% maximal human A_1AR activation, and suitable for the PET imaging in the rat brain (Guo et al., 2018). It has a relatively low molecular weight (373) and polar surface area (108 Å^2), which allows it to cross the BBB. Typical ribose-containing A_1AR agonists have limited utility to be administered therapeutically for CNS treatment due to their low degree of brain uptake from the periphery (Schaddelee et al., 2005).

A_{2A}AR-Selective Agonists

Regadenoson 21

Imaging

Regadenoson **21** (CVT-3146, Lexiscan) is a moderately selective, short acting A_{2A}AR agonist that is administered i.v. for MPI (Palani and Ananthasubramaniam, 2013). It was first approved as a pharmacologic stress agent in 2008. At present, it is the only synthetic AR agonist that is approved for human use, although it is not highly potent or selective for the A_{2A}AR. Nevertheless, Regadenoson's A_{2A}AR selectivity is higher in human than in mouse, in which it is actually 10-fold A_1AR selective compared to A_{2A}AR (Carlin et al., 2018). The availability of an FDA-approved new chemical entity (NCE) allows it to be tested in diverse clinical trials for cardiovascular treatment and diagnosis (>60 currently listed in ClinicalTrials.gov, accessed 12-31-2018).

Sickle cell disease

In addition to their diagnostic application in MPI, A_{2A}AR agonists have been considered for treatment of inflammation (Cekic and Linden, 2016) and sickle cell disease (SCD, Field et al.,

2014). A_{2A}AR activation in natural killer T (iNKT) cells is anti-inflammatory as demonstrated in a transgenic mouse model of SCD. However, A_{2B}AR activation in erythrocytes is predicted to have a harmful effect in SCD. The effects of Regadenoson **21** as an A_{2A}AR agonist in SCD patients were evaluated in a clinical trial, but there was no statistically significant benefit (Field et al., 2017).

Lung transplantation

Murine lung ischemia reperfusion injury occurring via NADPH oxidase 2 (NOX2) and IL-17 is also attenuated by A_{2A}AR agonist **26** (Sharma et al., 2016), which has led to an ongoing clinical trial of Regadenoson **21** in lung transplantation. The safety of using Regadenoson for MPI in patients with mild to moderate COPD and asthma was established (Golzar and Doukky, 2014).

Glioblastoma

A_{2A}AR agonists transiently increase BBB permeability (Kim and Bynoe, 2016), and this is being evaluated as a novel pharmacological approach to drug delivery to the brain. Regadenoson was tested clinically in an attempt to raise the concentration of the anticancer drug temozolomide in the brain interstitium, determined using microdialysis in glioblastoma patients (Jackson et al., 2018).

Spongosine (BVT.115959, CBT-1008) 22 and Other Naturally Occurring AR Agonists

Pain

Numerous other A_{2A}AR agonists were studied in preclinical testing or clinical trials prior to the approval of Regadenoson. Among the first such agonists was the simple 2-methoxy derivative of adenosine, spongosine (BVT.115959) **22**, a marine natural product (García et al., 2018). Actually, spongosine is slightly selective for and equipotent at the human A_1AR and A_3AR. It was shown to be effective in a clinical trial for diabetic neuropathic pain (7 mg oral dose, 3X daily), which was terminated because the company discontinued small molecule research (Knezevic et al., 2015).

Inflammation

Activation of the A_{2A}AR by endogenous adenosine provides benefit in animal models of inflammation and rheumatic disease, for example in rat models of osteoarthritis (Cronstein and Sitkovsky, 2017; Haskó et al., 2018). Other naturally occurring adenosine or deoxyadenosine derivatives have been applied as AR agonists. Polydeoxyribonucleotide (PDRN, structure not shown), of molecular weight 80–200 KD and extracted from trout or salmon sperm, is degraded by plasma DNA nucleases or cell membrane-bound nucleases giving rise to nucleosides and nucleotides. It is asserted that the degraded products pharmacologically activate the A_{2A}AR, based on antagonism by the relatively weak and non-selective A_{2A}AR antagonist 3,7-dimethyl-1-propargylxanthine (DMPX). PRDN's therapeutic effects include tissue repairing, anti-ischemic, and anti-inflammatory, making it suitable in regenerative medicine and for treating diabetic foot ulcers. Topically applied PDRN was in a clinical trial for reducing inflammation to promote wound healing in cases of diabetic foot ulcers (Squadrito et al., 2017). Also, topically applied PDRN significantly reduced pain and increased joint function in an animal model of osteoarthritis and increased neurogenesis in a spinal cord injury model (Irrera et al., 2018).

Sonedenoson (MRE-0094) 23 and Binodenoson (WRC-0470, MRE-0470) 24

Imaging

Many adenosine derivatives that proved to be A_{2A}AR-selective agonists have bulky, hydrophobic substitution at the C2 position of adenine (Jacobson and Gao, 2006). A_{2A}AR agonist Binodenoson **24** ($\leq$ 1.5 μg/kg, i.v.) administered for MPI of patients with coronary artery disease did not cause the side effect of bronchoconstriction (Murray et al., 2009).

Wound healing

Sonedenoson (MRE-0094) **23** was effective in the treatment of poorly healing wounds in animal models (Victor-Vega et al., 2002), an A_{2A}AR-agonist effect later found to be dependent on tissue plasminogen activator (Montesinos et al., 2015). A Phase 2 clinical trial of Sonedenoson administered as a topical gel for diabetic foot ulcers had poor enrollment and was terminated in 2008.

Apadenoson (ATL-146e, BMS 068645) 25 and Evodenoson (ATL-313, DE-112) 26

Imaging

Apadenoson **25** (Rieger et al., 2001; Zoghbi and Iskandrian, 2012) was in several clinical trials for MPI and SCD, which has a component of hypoxia. Apadenoson contains a labile ester moiety, which is cleaved *in vivo* to limit its duration of action. Its more stable, urethane-containing congener Evodenoson (ATL-313) **26**, was developed as a candidate drug for treating multiple myeloma (Rickles et al., 2010; van Waarde et al., 2018).

UK-371104 27 and UK-432097 28

Pulmonary inflammation

Intratracheal administration of A_{2A}AR agonist UK-371104 **27**, with sterically bulky N^6 and C2 substituents, in anesthetized guinea pig, inhibited the capsaicin-induced bronchoconstriction without affecting blood pressure (Trevethick et al., 2008). Thus, additional lung-focused A_{2A}AR agonists were explored for treating lung inflammation.

UK-432097 **28** is a selective A_{2A}AR agonist that was in a failed clinical trial for COPD (Mantell et al., 2010), although its pharmacology is comparable to its preceding congener, UK-371104 **27**. UK-432097 as an inhaled dry powder was not efficacious in human trials (discontinued in 2008), possibly due to its agonist activity at the A_1 and A_3ARs, and/or its high MW (778), and multiple H-bond donor (7) and acceptor (13) groups reduced its bioavailability, even when administered directly in the lungs by inhalation. However, it displays a favorably slow off-rate from the receptor, which has been suggested to contribute to its sustained agonist effects (Hothersall et al., 2017). The extended N^6 and C2 substituents of UK-432097 and its congeners interact with A_{2A}AR extracellular regions to impede their dissociation. The bulky N^6 and C2 substitutions of UK-432097 enabled the structural determination of its A_{2A}AR complex (Xu et al., 2011).

GW328267X 29

Asthma and allergy

A dual A_{2A}AR agonist and A_3AR antagonist GW328267X **29** failed to show efficacy in a clinical trial for asthma (inhaled) and allergic rhinitis (intranasal) (Trevethick et al., 2008), despite its anti-inflammatory efficacy in animal models. Its structure is unusual in that it contains an ethyl-tetrazole group at the ribose 4′ position, thus contributing to its dual action at the two AR subtypes (Trevethick et al., 2008). Its side effects (hypotension, tachycardia) even when administered by inhalation were dose-limiting in the clinical trials. However, intravenous infusion of GW328267X in humans (52 μg/kg, over 5.5 h) resulted in a mechanism-related tachycardia that was ascribed to A_{2A}AR activation in the carotid bodies, which was not alleviated upon prolonged agonist exposure. The lack of tachyphylaxis leading to prolonged tachycardia was not acceptable (Allen et al., 2013), and its clinical testing was discontinued. The translational failure of A_{2A}AR agonists is likely due to their limited selectivity, especially their agonist activity at the A_1AR. It has been suggested that A_1AR antagonists and A_{2A}AR agonists may have beneficial effects for asthma (Gao and Jacobson, 2017).

A_{2B}AR-Selective Agonist

BAY 60-6583 30

Ischemia, inflammation, diabetes, asthma, and cancer

Although there are no A_{2B}AR agonists currently in clinical evaluation, animal models suggest its activation might result in beneficial effects in acute lung injury, ischemia and vascular leakage (Eltzschig et al., 2003; Eltzschig, 2009). The non-nucleoside (3,5-dicyanopyridine) agonist BAY 60-6583 **30** has been used as an *in vitro* and *in vivo* pharmacological probe, although its degree of efficacy and its species dependence of affinity/selectivity can vary (Gao et al., 2014). In some models, including insulin release in MIN6 mouse insulinoma cells, the compound was reported to act as an A_{2B}AR antagonist. Therefore, highly selective and reliably efficacious A_{2B}AR agonists are still lacking. Moreover, the signaling pathways activated or inhibited by the nominally G_s-coupled A_{2B}AR are complex and involve multiple G proteins (Gao et al., 2018).

Mast cell A_{2B}AR activation might be useful in the treatment of asthma (Gao and Jacobson, 2017). In the intestines, kidney and other organs, this receptor has an anti-ischemic effect (Grenz et al., 2008; Hart et al., 2011). A_{2B}AR activation is predicted to have beneficial cardiovascular effects and maintain the endothelial cell barrier (Eltzschig et al., 2003). BAY 60-6583 was shown to have protective effects in a model of myocardial reperfusion injury (Tian et al., 2015). A_{2B}AR activation leading to the PI3K/Akt pathway is anti-inflammatory by shifting macrophages to an M2 phenotype. Pre-ischemic administration of BAY 60-6583 stimulated leukocyte PI3K/Akt in the mouse spleen to reduce myocardial reperfusion injury in an IL-10-dependent manner (Ni et al., 2018).

A_{2B}AR activation might also be useful in treating T2D and atherosclerosis, and preventing vascular lesions due to smooth muscle cell proliferation after angioplasty (Koupenova et al., 2012; Sun and Huang, 2016). A_{2B}AR KO mice displayed increased fatty liver pathology, tissue inflammation and insulin resistance due to the lack of this receptor in macrophages (Johnston-Cox et al., 2014). A_{2B}AR activation reduced inflammation and macrophage activation resulting from FFA (Csóka et al., 2014). The receptor was highly upregulated in mice subjected to a high-fat diet (HFD), and A_{2B}AR KO mice on this diet developed obesity and insulin resistance. BAY 60-6583 administered for 4 weeks HFD restored endocrine function and reduced inflammation. However, A_{2B}AR gene expression was found to be elevated in cases of human gestational diabetes, but this observation did not establish whether an A_{2B}AR agonist or antagonist would be more beneficial (Wojcik et al., 2014).

Although blocking the A_{2B}AR is considered a target in conjunction with cancer immunotherapy, its activation also has been reported to reduce proliferation of cancer cells (Koussémou et al., 2018). A_{2B}AR activation led to ERK1/2 dephosphorylation and reduced cell proliferation through inhibition of the MAPK signaling pathway in the MDA-MB-231 breast cancer cell line.

A_3AR-Selective Agonists

IB-MECA 31

Autoimmune inflammatory diseases

A_3AR agonists display anti-inflammatory and anticancer effects in various *in vivo* disease models (Cronstein and Sitkovsky, 2017; Jacobson et al., 2018). A_3AR agonists stimulate chemotaxis in neutrophils through the leading edge, which could be pro-inflammatory. However, systemic A_3AR agonist administration could actually have an anti-inflammatory effect by inhibiting neutrophil chemotaxis because of the non-directional agonist exposure (Chen et al., 2006).

IB-MECA (CF101, Piclodenoson) **31**, the first moderately selective A_3 agonist (Gallo-Rodriguez et al., 1994), is being developed for the treatment of autoimmune anti-inflammatory diseases, including rheumatoid arthritis (RA) and psoriasis (both in Phase 3) (Fishman et al., 2012). In Phase 2 trials, its action in RA and psoriasis compared favorably to existing treatments for those conditions, but it did not display serious adverse effects, as do the current treatments. In a comparison of 1, 2, and 4 mg oral IB-MECA doses in a 12-week Phase 2 psoriasis trial, the greatest patient improvement was observed with the 2 mg dose (Fishman et al., 2012). Similarly in a Phase 2 RA trial, the middle (1 mg, compared to 0.1 and 4 mg) oral dose achieved the highest responses. Peripheral blood mononuclear cells (PBMCs) from psoriasis patients showed elevated A_3AR expression. IB-MECA inhibited proliferation and formation of IL-17 and IL-23 in a human keratinocyte cell line (Cohen et al., 2018). IB-MECA was previously in Phase 2 clinical trials for dry eye disease and glaucoma, 1 mg and 2 mg, respectively (oral, twice daily), which failed to demonstrate efficacy (Avni et al., 2010; Jacobson and Civan, 2016).

Cl-IB-MECA 32

Liver diseases

Cl-IB-MECA **32**, was initially shown to display a higher A_3AR agonist selectivity than IB-MECA at the rat ARs. However, at the mA_3AR, IB-MECA is more potent and selective than Cl-IB-MECA (Carlin et al., 2017). Cl-IB-MECA (CF102,

Namodenoson) is being developed for the treatment of liver conditions, including hepatocellular carcinoma (HCC) and non-alcoholic steatohepatitis (NASH) (Fishman et al., 2018). A_3AR agonists have apoptotic and anticancer effects *in vivo* induced by Wnt signaling deregulation (Bar-Yehuda et al., 2008). The US Food and Drug Administration and the European Medicines Agency granted fast track designation to **32** for the treatment of liver cancer. Cl-IB-MECA (up to a 25 mg oral dose) increased the median overall survival in patients with advanced HCC by 7.8 months in patients (Stemmer et al., 2013), which was improved over the current treatment. There were no serious adverse effects or dose-limiting toxicity. Secondarily, the trial examined using the A_3AR as a predictive marker of the CF102 clinical response. The use of A_3AR to prevent cytokine release syndrome in cancer immunotherapy has been proposed (Cohen and Fishman, 2019).

An anti-steatotic effect of Cl-IB-MECA in an HFD mouse model of NASH, induced by STZ administered 2 days after birth, was mediated via a molecular mechanism leading to decreased α-smooth muscle actin (αSMA, a marker of pathological fibroblasts) and cytokeratin 18 (CK-18, a predictor of NASH severity). A Phase 2 trial of CF-102 (12.5 and 25 mg oral doses, twice daily) for NASH treatment is underway.

Skeletal muscle protection

A_3AR agonists, including Cl-IB-MECA, protect skeletal muscle in ischemic models in a phospholipase C-b2/b3-dependent manner (Zheng et al., 2007).

CP-608,039 34 and CP-608,039 35

Cardioprotection

DeNinno et al. (2003) reported that CP-608,039 **35** is a highly A_3AR selective and water-soluble agonist that was being evaluated for the prevention of perioperative myocardial ischemic injury. This follows numerous other reports showing that A_3AR activation protects ischemic cardiomyocytes by preconditioning (Lasley, 2018).

Recently, selective A_3AR deletion in mouse cardiomyocytes was used to demonstrate that activation by selective agonist CP-532,903 (**34**) of a myocardial A_3AR provides ischemic tolerance that is dependent on K_{ATP} channels (Wan et al., 2019). This study resolves a long-standing controversy by showing that a protective A_3AR is present in adult ventricular cardiomyocytes, although expressed at very low levels (copy number of 85 per 100 ng total RNA versus 12,830 for the A_1AR).

MRS5698 36

Pain

As noted above, A_1AR agonists and PAMs are already under consideration for pain treatment. The efficacy of A_3AR agonists for chronic pain was first explored depth in 2011 (Chen et al., 2012). The approach of using A_3AR agonists for pain treatment was initially controversial, as A_3AR activation had been described in earlier review papers as an uninteresting target or even an anti-target for pain relief (Nascimento et al., 2012; Janes et al., 2016). Reasons for this premature characterization were: truly selective A_3AR agonists were not initially available and the A_3AR causes release of inflammatory mediators, e.g., histamine and serotonin, from peripheral mast cells in rodents, but not human and other species (Auchampach et al., 1997; Leung et al., 2014; Gao and Jacobson, 2017). These mediators can contribute to inflammation in mouse and rat, and Sawynok (1998) concluded that A_3AR activation induces pain and paw oedema. However, consistent with the now well-documented action of A_3AR activation in various chronic pain models, A_3AR KO mice had a lower pain threshold in the hind-paw hot-plate test (40% greater latency, Fedorova et al., 2003). Curiously, there was no difference between A_3AR KO and WT mice in the acute pain response in the tail-flick test.

The two selective A_3AR agonists in already clinical trials, IB-MECA and Cl-IB-MECA, at high doses *in vivo* might interact with other ARs, as has been observed in experimental models (Fozard, 2010). A new series of C2-extended (N)-methanocarba analogs displayed even greater A_3AR selectivity, estimated to be in the range of at least 10,000-fold in comparison to other ARs (Jacobson et al., 2018). Among these agonists is MRS5698 **33**, which has been shown to reduce chronic neuropathic pain, including oxaliplatin-induced neuropathic pain (Little et al., 2015; Wahlman et al., 2018). MRS5698 has many drug-like properties – it is non-toxic and relatively stable *in vivo*, except that its oral bioavailability in the rat is only 5%F (Tosh et al., 2015). Nevertheless, by various modes of administration it is efficacious in pain models *in vivo*, including chronic constriction injury-induced, chemotherapy-induced and cancer-induced. Its ability to reduce chronic hyperalgesia is not affected by the A_3AR-induced histamine release observed in rodent but not human mast cells (Carlin et al., 2016).

MRS5980 37

Pain

MRS5980 **37** is a highly selective C2-arylethynyl (N)-methanocarba A_3AR agonist, which has been demonstrated to be highly efficacious in *in vivo* pain models following administered by oral gavage, with a protective effect lasting up to 3 h (Tosh et al., 2014; Janes et al., 2016), and its metabolomics has been studied (Fang et al., 2015). The 2-chlorothienyl group is stable *in vivo*, and the aryl alkyne group was shown to be not highly reactive. MRS5980 and other A_3AR agonist were shown to indirectly block a pro-nociceptive N-type Ca^{2+} calcium channels, a proven target in controlling pain, and cell excitability in the spinal cord dorsal horn (Coppi et al., 2019). Thus, therapeutic application of A_3AR agonists appears to be a promising approach for treating pain of different etiologies.

LJ-529 33 and MRS4322 38

Stroke

von Lubitz et al. (1999) found that both A_1AR and A_3AR agonists have cerebroprotective properties in a model of gerbil forebrain ischemia. An (N)-methanocarba nucleoside MRS4322 **38** was proposed in a patent application (Korinek et al., 2018) as a treatment for stroke and traumatic brain injury. The nucleoside appears to act through the A_3AR, to which it binds in the μM range, because a selective A_3AR antagonist propyl 6-ethyl-5-((ethylthio)carbonyl)-2-phenyl-4-propylnicotinate (MRS1523)

diminished the benefit of reduced stroke lesions. LJ-529 **33** (4′-thio-Cl-IB-MECA) is a selective A_3 adenosine agonist that was shown to be protective in a rat stroke model and inhibited brain migration of inflammatory cells (Choi et al., 2011). However, platelet A_{2A}AR activation by LJ-529 increased the bleeding risk.

AR Allosteric Enhancers (PAMs)

PAMs of the A_1AR and A_3AR have been the subject of preclinical and clinical evaluation (**Figure 3** and **Table 2**). PAMs, in principle, may remain silent until a large rise in the extracellular adenosine occurs, at which time the PAM would amplify adenosine's action at a particular AR subtype. Thus, PAMs are described as temporally and spatially specific modulators (Gao et al., 2011). Also, PAMs tend to be more subtype selective than orthosteric agonists, because their non-canonical binding regions on the GPCRs are those that have the most diverse sequences within the receptor family (Vecchio et al., 2018).

T-62 39

Benzoylthiophenes are the earliest and most extensively studied class of A_1AR PAMs, and they have allosteric agonist properties as well as enhancing the effect of other A_1AR agonists (Vincenzi et al., 2014; Jacobson and Gao, 2017). The benzoylthiophenes Just as A_1AR agonists have been considered for pain treatment, a representative benzoylthiophene T-62 **39** entered a clinical trial for postherpetic neuropathic pain in 2008 that was discontinued because of its lack of efficacy (Giorgi and Nieri, 2013). Also, some patients displayed transient, elevated liver transaminases. Nevertheless, T-62 reduced hypersensitivity in animal models of neuropathic pain. The structural basis for recognition of benzoylthiophene PAMs involving A_1AR extracellular loops (ELs) has been predicted using Gaussian accelerated molecular dynamics (Miao et al., 2018).

TRR469 40

Pain

A later generation benzoylthiophene TRR469 **40** was shown to be an A_1AR PAM that increases the affinity of A_1AR agonists (Vincenzi et al., 2014, 2016). It reduced pain, comparably to morphine, in writhing and formalin tests and in chronic STZ-induced diabetic neuropathy, and it displayed fewer behavioral side effects than an A_1AR orthosteric agonist. Furthermore, the same A_1AR PAM was anxiolytic in four behavioral models in the mouse, in a manner comparable to the anxiolytic drug diazepam (Vincenzi et al., 2016). This activity of **40**, which was blocked by a selective A_1AR antagonist (DPCPX), is consistent with the previously noted anxiolytic activity of A_1AR agonists.

LUF6000 41

Inflammation and erectile dysfunction

LUF6000 **41** is a imidazoquinolinamine A_3AR allosteric enhancer (PAM). It enhanced the maximal efficacy of A_3AR agonists but had no agonism on its own (Gao et al., 2011). Its interaction with the A_3AR was species-dependent (Du et al., 2018). Although it was more efficacious in human, canine and rabbit than in rodent species, it was shown to produce an anti-inflammatory effect in rat models of adjuvant-induced arthritis and iodoacetate-induced osteoarthritis and in a mouse model of concanavalin A-induced liver inflammation (Cohen et al., 2014). The molecule is termed CF602 and is on a translational path for treatment of erectile dysfunction (Cohen et al., 2016).

CONCLUSION

The structural and pharmacological features of key AR agonists and positive allosteric modulators (PAMs) have been summarized, with an emphasis on molecules that have been

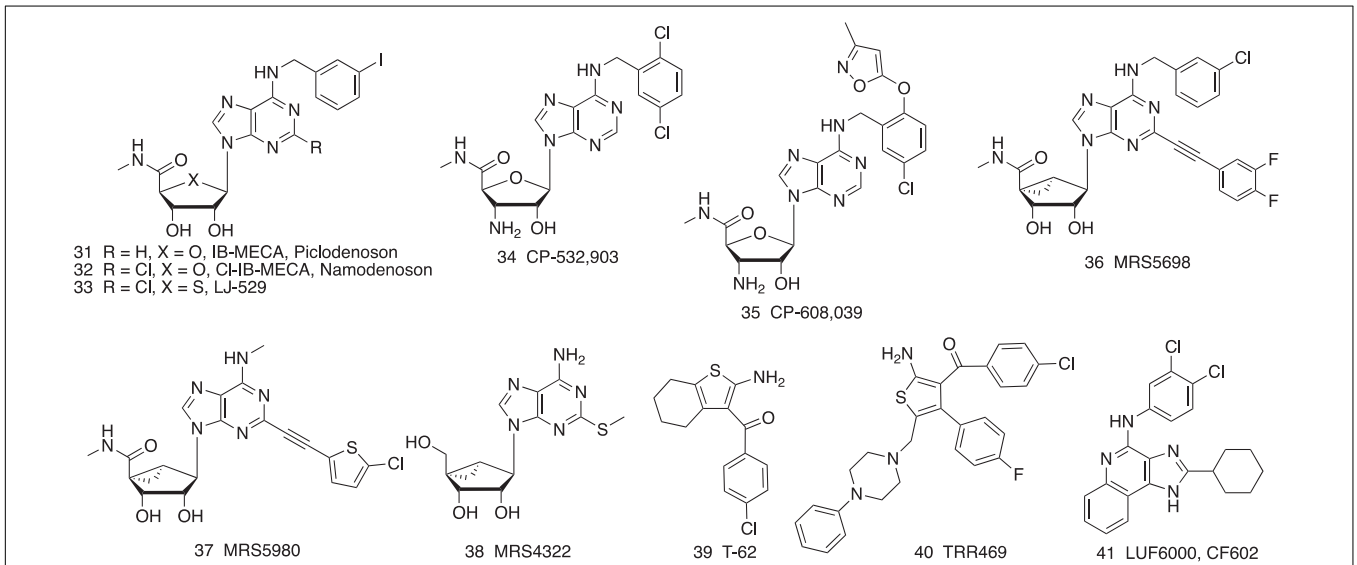

FIGURE 3 | A_3AR- (**31**-**38**) selective agonists and allosteric enhancers (PAMs) of the A_1AR (**39**, **40**) and A_3AR (**41**).

in humans or that were considered for human testing. From the thousands of selective AR agonists or allosteric enhancers reported, there are few translational successes. Many AR agonists have been in clinical trials for disease treatment or diagnosis, but only two are approved for human use, i.e., short-acting agonists adenosine and Regadenoson. However, new concepts and compounds are currently being developed and applied toward preclinical and clinical evaluation, and initial results are encouraging. AR agonists for treating inflammation, pain, cancer, NASH, angina, sickle cell disease, ischemic conditions and diabetes are under development. Multiple clinical trials with two A_3AR agonists are ongoing.

AUTHOR CONTRIBUTIONS

KJ organized the outline and wrote most of the text. DT contributed to the writing and researching the topic. SJ contributed to the writing and researching the topic. Z-GG contributed to the writing and researching the topic.

ACKNOWLEDGMENTS

We thank the NIDDK Intramural Research Program for funding (ZIA DK-31117).

REFERENCES

Abella, M. L. (2006). Evaluation of anti-wrinkle efficacy of adenosine-containing products using the FOITS technique. *Int. J. Cosmetic Sci.* 28, 447–451. doi: 10.1111/j.1467-2494.2006.00349.x

Albrecht-Küpper, B. E., Leineweber, K., and Nell, P. G. (2012). Partial adenosine A1 receptor agonists for cardiovascular therapies. *Purinergic Signal.* 8(Suppl. 1), 91–99. doi: 10.1007/s11302-011-9274-3

Allard, B., Longhi, M. S., Robson, S. C., and Stagg, J. (2017). The ectonucleotidases CD39 and CD73: novel checkpoint inhibitor targets. *Immunol. Rev.* 276, 121–144. doi: 10.1111/imr.12528

Allen, A., Koch, A., Garman, N., Cahn, A., Dewitt, O. E., and Rambaran, C. N. (2013). A PK/PD study of a selective A2a agonist, (GW328267X) a potential IV therapeutic for acute lung injury: no tachyphylaxis to the heart rate effect. Abstract PC028. *Br. Pharmacol. Soc.* Available at: https://bps.conference-services.net/resources/344/3654/pdf/PHARM13_0008.pdf

Alnouri, M. W., Jepards, S., Casari, A., Schiedel, A. C., Hinz, S., and Müller, C. E. (2015). Selectivity is species-dependent: characterization of standard agonists and antagonists at human, rat, and mouse adenosine receptors. *Purinergic Signal.* 11, 389–407. doi: 10.1007/s11302-015-9460-9

Antonioli, L., Blandizzi, C., Csóka, B., Pacher, P., and Haskó, G. (2015). Adenosine signalling in diabetes mellitus–pathophysiology and therapeutic considerations. *Nat. Rev. Endocrinol.* 11, 228–241. doi: 10.1038/nrendo.2015.10

Antonioli, L., Fornai, M., Blandizzi, C., and Haskó, G. (2018). "Adenosine Regulation of the Immune System," in *BT - The Adenosine Receptors*, eds P. A. Borea, K. Varani, S. Gessi, S. Merighi, and F. Vincenzi (Cham: Springer International Publishing), 499–514. doi: 10.1007/978-3-319-90808-3_20

Auchampach, J. A., Jin, X., Wan, T. C., Caughey, G. H., and Linden, J. (1997). Canine mast cell adenosine receptors: cloning and expression of the A3 receptor and evidence that degranulation is mediated by the A2B receptor. *Mol. Pharmacol.* 52, 846–860. doi: 10.1124/mol.52.5.846

Avni, I., Garzozi, H. J., Barequet, I. S., Segev, F., Varssano, D., Sartani, G., et al. (2010). Treatment of dry eye syndrome with orally-administered CF101: data from a Phase 2 clinical trial. *Ophthalmology* 117, 1287–1293. doi: 10.1016/j.ophtha.2009.11.029

Baltos, J. A., Vecchio, E. A., Harris, M. A., Qin, C. X., Ritchie, R. H., Christopoulos, A., et al. (2017). Capadenoson, a clinically trialed partial adenosine A1 receptor agonist, can stimulate adenosine A2B receptor biased agonism. *Biochem. Pharmacol.* 135, 79–89. doi: 10.1016/j.bcp.2017.03.014

Baraldi, S., Baraldi, P. G., Oliva, P., Toti, K. S., Ciancetta, A., and Jacobson, K. A. (2018). "Chapter 5. A2A adenosine receptor: structures, modeling and medicinal chemistry," in *The Adenosine Receptors, The Receptors*, Vol. 34, ed. K. Varani (Berlin: Springer), 91–136.

Bar-Yehuda, S., Stemmer, S. M., Madi, L., Castel, D., Ochaion, A., Cohen, S., et al. (2008). The A3 adenosine receptor agonist CF102 induces apoptosis of hepatocellular carcinoma via de-regulation of the Wnt and NF-kappaB signal transduction pathways. *Int. J. Oncol.* 33, 287–295.

Basoglu, O. K., Pelleg, A., Essilfie-Quaye, S., Brindicci, C., Barnes, P. J., and Kharitonov, S. A. (2005). Effects of aerosolized adenosine 5′-triphosphate vs adenosine 5′-monophosphate on dyspnea and airway caliber in healthy nonsmokers and patients with asthma. *Chest* 128, 1905–1909. doi: 10.1378/chest.128.4.1905

Bigot, A., Stengelin, S., Jähne, G., Herling, A., Müller, G., Hock, F. J., et al. (2004). Aventis Pharma Deutschland. Novel Adenosine Analoguexs and their use as Pharmaceutical Agents. US Patent WO04003002.

Boison, D. (2013). Adenosine kinase: exploitation for therapeutic gain. *Pharmacol. Rev.* 65, 906–943. doi: 10.1124/pr.112.006361

Borea, P. A., Gessi, S., Merighi, S., and Varani, K. (2016). Adenosine as a multi-signalling guardian angel in human diseases: When, where and how does it exert its protective effects? *Trends Pharmacol. Sci.* 37, 419–434. doi: 10.1016/j.tips.2016.02.006

Borea, P. A., Gessi, S., Merighi, S., Vincenzi, F., and Varani, K. (2017). Pathological overproduction: the bad side of adenosine. *Br. J. Pharmacol.* 174, 1945–1960. doi: 10.1111/bph.13763

Borea, P. A., Gessi, S., Merighi, S., Vincenzi, F., and Varani, K. (2018). Pharmacology of adenosine receptors: the state of the art. *Physiol. Rev.* 98, 1591–1625. doi: 10.1152/physrev.00049.2017

Burnstock, G., and Boeynaems, J. M. (2014). Purinergic signalling and immune cells. *Purinergic Signal.* 10, 529–564. doi: 10.1007/s11302-014-9427-2

Carlin, J. L., Jain, S., Duroux, R., Suresh, R. R., Xiao, C., Auchampach, J. A., et al. (2018). Activation of adenosine A2A or A2B receptors causes hypothermia in mice. *Neuropharmacology* 139, 268–278. doi: 10.1016/j.neuropharm.2018.02.035

Carlin, J. L., Jain, S., Gizewski, E., Wan, T. C., Tosh, D. K., Xiao, C., et al. (2017). Hypothermia in mouse is caused by adenosine A1 and A3 receptor agonists and AMP via three distinct mechanisms. *Neuropharmacology* 114, 101–113. doi: 10.1016/j.neuropharm.2016.11.026

Carlin, J. L., Tosh, D. K., Xiao, C., Piñol, R. A., Chen, Z., Salvemini, D., et al. (2016). Peripheral adenosine A3 receptor activation causes regulated hypothermia in mice that is dependent on central histamine H1 receptors. *J. Pharmacol. Exp. Ther.* 356, 474–482. doi: 10.1124/jpet.115.229872

Cekic, C., and Linden, J. (2016). Purinergic regulation of the immune system. *Nat. Rev. Immunol.* 16, 177–192. doi: 10.1038/nri.2016.4

Chen, J. F., Eltzschig, H. K., and Fredholm, B. B. (2013). Adenosine receptors as drug targets - What are the challenges? *Nat. Rev. Drug Discov.* 12, 265–286. doi: 10.1038/nrd3955

Chen, Y., Corriden, R., Inoue, Y., Yip, L., Hashiguchi, N., Zinkernagel, A., et al. (2006). ATP release guides neutrophil chemotaxis via P2Y2 and A3 receptors. *Science* 314, 1792–1795. doi: 10.1126/science.1132559

Chen, Z., Janes, K., Chen, C., Doyle, T., Tosh, D. K., Jacobson, K. A., et al. (2012). Controlling murine and rat chronic pain through A3 adenosine receptor activation. *FASEB J.* 26, 1855–1865. doi: 10.1096/fj.11-201541

Cheng, J. T., Chi, T. C., and Liu, I. M. (2000). Activation of adenosine A1 receptors by drugs to lower plasma glucose in streptozotocin-induced diabetic rats. *Auton. Neurosci.* 83, 127–133. doi: 10.1016/S0165-1838(00)00106-5

Choi, I.-Y., Lee, J.-C., Ju, C., Hwang, S., Cho, G.-S., Lee, H. W., et al. (2011). A3 adenosine receptor agonist reduces brain ischemic injury and inhibits inflammatory cell migration in rats. *Am. J. Pathol.* 179, 2042–2052. doi: 10.1016/j.ajpath.2011.07.006

Chrysostomou, C., Morell, V. O., Wearden, P., Sanchez-de-Toledo, J., Jooste, E. H., and Beerman, L. (2013). Dexmedetomidine: therapeutic use for the termination

of reentrant supraventricular tachycardia. *Congenit. Heart Dis.* 8, 48–56. doi: 10.1111/j.1747-0803.2012.00669.x

Cohen, S., Barer, F., Bar-Yehuda, S., IJzerman, A. P., Jacobson, K. A., and Fishman, P. (2014). A3 adenosine receptor allosteric modulator induces an anti-inflammatory effect: In vivo studies and molecular mechanism of action. *Mediators Inflamm.* 2014:708746. doi: 10.1155/2014/708746

Cohen, S., Barer, F., Itzhak, I., Silverman, M. H., and Fishman, P. (2018). Inhibition of IL-17 and IL-23 in human keratinocytes by the A3 adenosine receptor agonist piclidenoson. *J. Immunol. Res.* 2018:2310970. doi: 10.1155/2018/2310970

Cohen, S., and Fishman, P. (2019). Targeting the A3 adenosine receptor to treat cytokine release syndrome in cancer immunotherapy. *Drug Des. Dev. Ther.* 13, 491–497. doi: 10.2147/DDDT.S195294

Cohen, S., Fishman, P., and Tikva, P. (2016). CF602 improves erectile dysfunction in diabetic rats. *J. Urol.* 195:e1138. doi: 10.1016/j.juro.2016.02.2465

Coppi, E., Cherchi, F., Fusco, I., Failli, P., Vona, A., Dettori, I., et al. (2019). Adenosine A3 receptor activation inhibits pro-nociceptive N-type Ca2+ currents in dorsal root ganglion neurons. *Pain* doi: 10.1097/j.pain.0000000000001488

Corino, V. D. A., Sandberg, F., Mainardi, L. T., Platonov, P. G., and Sörnmo, L. (2015). Noninvasive characterization of atrioventricular conduction in patients with atrial fibrillation. *J. Electrocardiol.* 48, 938–942. doi: 10.1016/j.jelectrocard.2015.08.010

Cox, B. F., Clark, K. L., Perrone, M. H., Welzel, G. E., Greenland, B. D., Colussi, D. J., et al. (1997). Cardiovascular and metabolic effects of adenosine A1-receptor agonists in streptozotocin-treated rats. *J. Cardiovasc. Pharmacol.* 29, 417–426. doi: 10.1097/00005344-199703000-00017

Cronstein, B. N., and Sitkovsky, M. (2017). Adenosine and adenosine receptors in the pathogenesis and treatment of rheumatic diseases. *Nat. Rev. Rheumatol.* 13, 41–51. doi: 10.1038/nrrheum.2016.178

Csóka, B., Koscsó, B., Törö, G., Kókai, E., Virág, L., Németh, Z. H., et al. (2014). A2B adenosine receptors prevent insulin resistance by inhibiting adipose tissue inflammation via maintaining alternative macrophage activation. *Diabetes* 63, 850–866. doi: 10.2337/db13-0573

David, M., Gospodinov, D. K., Gheorghe, N., Mateev, G. S., Rusinova, M. V., Hristakieva, E., et al. (2016). Treatment of plaque-type psoriasis with oral CF101: data from a phase II/III multicenter, randomized, controlled trial. *J. Drugs Dermatol.* 15, 931–938.

DeNinno, M. P., Masamune, H., Chenard, L. K., DiRico, K. J., Eller, C., Etienne, J. B., et al. (2003). 3′-Aminoadenosine-5′-uronamides: discovery of the first highly selective agonist at the human adenosine A3 receptor. *J. Med. Chem.* 46, 353–355. doi: 10.1021/jm0255724

Dinh, W., Albrecht-Küpper, B., Gheorghiade, M., Voors, A. A., van der Laan, M., and Sabbah, H. N. (2017). Partial adenosine A1 agonist in heart failure. *Handb. Exp. Pharmacol.* 243, 177–203. doi: 10.1007/164_2016_83

Draper-Joyce, C. J., Khoshouei, M., Thal, D. M., Liang, Y.-L., Nguyen, A. T. N., Furness, S. G. B., et al. (2018). Structure of the adenosine-bound human adenosine A1 receptor–Gi complex. *Nature* 558, 559–563. doi: 10.1038/s41586-018-0236-6

Du, L., Gao, Z. G., Paoletta, S., Wan, T. C., Barbour, S., van Veldhoven, J. P., et al. (2018). Species differences and mechanism of action of A3 adenosine receptor allosteric modulators. *Purinergic Signal.* 14, 59–71. doi: 10.1007/s11302-017-9592-1

Eddy, M. T., Lee, M. Y., Gao, Z. G., White, K. L., Didenko, T., Horst, R., et al. (2018). Allosteric coupling of drug binding and intracellular signaling in the A2A adenosine receptor. *Cell* 172, 68–80. doi: 10.1016/j.cell.2017.12.004

Eisenach, J. C., Hood, D. D., Curry, R., Sawynok, J., Yaksh, T. L., and Li, X. (2004). Intrathecal but not intravenous opioids release adenosine from the spinal cord. *J. Pain* 5, 64–68. doi: 10.1016/j.jpain.2003.10.001

Eisenach, J. C., Rauck, R. L., and Curry, R. (2013). Intrathecal, but not intravenous adenosine reduces allodynia in patients with neuropathic pain. *Pain* 105, 65–70. doi: 10.1016/S0304-3959(03)00158-1

Eisenstein, A., Patterson, S., and Ravid, K. (2015). The many faces of the A2b adenosine receptor in cardiovascular and metabolic diseases. *J. Cell. Physiol.* 230, 2891–2897. doi: 10.1002/jcp.25043

Eltzschig, H. K. (2009). Adenosine: an old drug newly discovered. *Anesthesiology* 111, 904–915. doi: 10.1097/ALN.0b013e3181b060f2

Eltzschig, H. K., Ibla, J. C., Furuta, G. T., Leonard, M. O., Jacobson, K. A., Enjyoji, K., et al. (2003). Coordinated adenine nucleotide phosphohydrolysis and nucleoside signaling in post-hypoxic endothelium: role of ectonucleotidases and adenosine A2B-receptors. *J. Exp. Med.* 198, 783–796. doi: 10.1084/jem.20030891

Elzein, E., and Zablocki, J. (2008). A1 adenosine receptor agonists and their potential therapeutic applications. *Expert Opin. Invest. Drugs* 17, 1901–1910. doi: 10.1517/13543780802497284

Faghihi, G., Iraji, F., Rajaee Harandi, M., Nilforoushzadeh, M. A., and Askari, G. (2013). Comparison of the efficacy of topical minoxidil 5% and adenosine 0.75% solutions on male androgenetic alopecia and measuring patient satisfaction rate. *Acta Dermatovenerol. Croat.* 21, 155–159.

Fang, Z. Z., Tosh, D. K., Tanaka, N., Wang, H., Krausz, K. W., O'Connor, R., et al. (2015). Metabolic mapping of A3 adenosine receptor agonist MRS5980. *Biochem. Pharmacol.* 97, 215–223. doi: 10.1016/j.bcp.2015.07.007

Fedorova, I. M., Jacobson, M. A., Basile, A., and Jacobson, K. A. (2003). Behavioral characterization of mice lacking the A3 adenosine receptor: sensitivity to hypoxic neurodegeneration. *Cell Mol. Neurobiol.* 23, 431–447. doi: 10.1023/A:1023601007518

Field, J. J., Majerus, E., Gordeuk, V. R., Gowhari, M., Hoppe, C., Heeney, M. M., et al. (2017). Randomized phase 2 trial of regadenoson for treatment of acute vaso-occlusive crises in sickle cell disease. *Blood Adv.* 1, 1645–1649. doi: 10.1182/bloodadvances.2017009613

Field, J. J., Nathan, D. G., and Linden, J. (2014). The role of adenosine signaling in sickle cell therapeutics. *Hematol. Oncol. Clin. North Am.* 28, 287–299. doi: 10.1016/j.hoc.2013.11.003

Fishman, P., Bar-Yehuda, S., Liang, B. T., and Jacobson, K. A. (2012). Pharmacological and therapeutic effects of A3 adenosine receptor (A3AR) agonists. *Drug Discov. Today* 17, 359–366. doi: 10.1016/j.drudis.2011.10.007

Fishman, P., Salhab, A., Cohen, S., Amer, J., Itzhak, I., Barer, F., et al. (2018). The anti-inflammatory and anto-fibrogenic effects of namodenoson in NAFLD/NASH animal models. Abstract Thu-487. *J. Hepatol.* 68:S349. doi: 10.1016/S0168-8278(18)30921-8

Flyer, J. N., Zuckerman, W. A., Richmond, M. E., Anderson, B. R., Mendelsberg, T. G., McAllister, J. M., et al. (2017). Prospective study of adenosine on atrioventricular nodal conduction in pediatric and young adult patients after heart transplantation. *Circulation* 135, 2485–2493. doi: 10.1161/CIRCULATIONAHA.117.028087

Fozard, J. R. (2010). "From hypertension (+) to asthma: interactions with the adenosine A3 receptor from a personal perspective," in *A3 Adenosine Receptors from Cell Biology to Pharmacology and Therapeutics*, ed. P. A. Borea (Dordrecht: Springer Science+Business Media B.V), 3–26. doi: 10.1007/978-90-481-3144-0_1

Fredholm, B. B., IJzerman, A. P., Jacobson, K. A., Klotz, K. N., and Linden, J. (2001). International Union of Pharmacology. XXV. Nomenclature and classification of adenosine receptors. *Pharmacol. Rev.* 53, 527–552.

Galiuto, L., De Caterina, A. R., Porfidia, A., Paraggio, L., Barchetta, S., Locorotondo, G., et al. (2010). Reversible coronary microvascular dysfunction: a common pathogenetic mechanism in apical ballooning or tako-tsubo syndrome. *Eur. Heart J.* 31, 1319–1327. doi: 10.1093/eurheartj/ehq039

Gallo-Rodriguez, C., Ji, X.-D., Melman, N., Siegman, B. D., Sanders, L. H., Orlina, J., et al. (1994). Structure-activity relationships of N6-benzyladenosine-5(-uronamides as A3-selective adenosine agonists. *J. Med. Chem.* 37, 636–646. doi: 10.1021/jm00031a014

Gao, Z. G., Balasubramanian, R., Kiselev, E., Wei, Q., and Jacobson, K. A. (2014). Probing biased/partial agonism at the G protein-coupled A2B adenosine receptor. *Biochem. Pharmacol.* 90, 297–306. doi: 10.1016/j.bcp.2014.05.008

Gao, Z. G., Blaustein, J., Gross, A. S., Melman, N., and Jacobson, K. A. (2003). N6-Substituted adenosine derivatives: selectivity, efficacy, and species differences at A3 adenosine receptors. *Biochem. Pharmacol.* 65, 1675–1684. doi: 10.1016/S0006-2952(03)00153-9

Gao, Z. G., Inoue, A., and Jacobson, K. A. (2018). On the G protein-coupling selectivity of the native A2B adenosine receptor. *Biochem. Pharmacol.* 151, 201–213. doi: 10.1016/j.bcp.2017.12.003

Gao, Z. G., and Jacobson, K. A. (2017). Purinergic signaling in mast cell degranulation and asthma. *Front. Pharmacol.* 8:947. doi: 10.3389/fphar.2017.00947

Gao, Z. G., Verzijl, D., Zweemer, A., Ye, K., Göblyös, A., IJzerman, A. P., et al. (2011). Functionally biased modulation of A3 adenosine receptor agonist efficacy and potency by imidazoquinolinamine allosteric enhancers. *Biochem. Pharmacol.* 82, 658–668. doi: 10.1016/j.bcp.2011.06.017

García, P. A., Valles, E., Díez, D., and Castro, M. -Á (2018). Marine alkylpurines: a promising group of bioactive marine natural products. *Mar. Drugs* 16:E6. doi: 10.3390/md16010006

García-Nafría, J., Lee, Y., Bai, X., Carpenter, B., and Tate, C. G. (2018). Cryo-EM structure of the adenosine A2A receptor coupled to an engineered heterotrimeric G protein. *Elife* 7:e35946. doi: 10.7554/eLife.35946

Giorgi, I., and Nieri, P. (2013). Adenosine A1 modulators: a patent update (2008 to present). *Expert Opin. Ther. Pat.* 23, 1109–1121. doi: 10.1517/13543776.2013.799142

Glatter, K. A., Cheng, J., and Dorostkar, P. (1999). Electrophysiologic effects of adenosine in patients with supraventricular tachycardia. *Circulation* 99, 1034–1040. doi: 10.1161/01.CIR.99.8.1034

Golzar, Y., and Doukky, R. (2014). Regadenoson use in patients with chronic obstructive pulmonary disease: the state of current knowledge. *Int. J. Chron. Obstruct. Pulmon. Dis.* 9, 129–137. doi: 10.2147/COPD.S56879

Greene, S. J., Sabbah, H. N., Butler, J., Voors, A. A., Albrecht-Küpper, B., Düngen, H. D., et al. (2016). Partial adenosine A1 receptor agonism: a potential new therapeutic strategy for heart failure. *Heart Fail. Rev.* 21, 95–102. doi: 10.1007/s10741-015-9522-7

Grenz, A., Osswald, H., Eckle, T., Yang, D., Zhang, H., Tran, Z. V., et al. (2008). The reno-vascular A2B adenosine receptor protects the kidney from ischemia. *PLoS Med.* 5:e137. doi: 10.1371/journal.pmed.0050137

Guo, M., Gao, Z.-G., Tyler, R., Stodden, T., Wang, G.-J., Wiers, C., et al. (2018). Preclinical evaluation of the first adenosine A1 receptor partial agonist radioligand for positron emission tomography (PET) imaging. *J. Med. Chem.* 61, 9966–9975. doi: 10.1021/acs.jmedchem.8b01009

Hart, M. L., Grenz, A., Gorzolla, I. C., Schittenhelm, J., Dalton, J. H., and Eltzschig, H. K. (2011). Hypoxia-inducible factor-1α-dependent protection from intestinal ischemia/reperfusion injury involves ecto-5′-nucleotidase (CD73) and the A2B adenosine receptor. *J. Immunol.* 186, 4367–4374. doi: 10.4049/jimmunol.0903617

Haskó, G., Antonioli, L., and Cronstein, B. N. (2018). Adenosine metabolism, immunity and joint health. *Biochem. Pharmacol.* 151, 307–313. doi: 10.1016/j.bcp.2018.02.002

Hothersall, J. D., Guo, D., Sarda, S., Sheppard, R. J., Chen, H., Keur, W., et al. (2017). Structure-activity relationships of the sustained effects of adenosine A2A receptor agonists driven by slow dissociation kinetics. *Mol. Pharmacol.* 91, 25–38. doi: 10.1124/mol.116.105551

Imlach, W. L., Bhola, R. F., May, L. T., Christopoulos, A., and Christie, M. J. (2015). A positive allosteric modulator of the adenosine A1 receptor selectively inhibits primary afferent synaptic transmission in a neuropathic pain model. *Mol. Pharmacol.* 88, 460–468. doi: 10.1124/mol.115.099499

Irrera, N., Arcoraci, V., Mannino, F., Vermiglio, G., Pallio, G., Minutoli, L., et al. (2018). Activation of A2A receptor by PDRN reduces neuronal damage and stimulates WNT/β-catenin driven neurogenesis in spinal cord injury. *Front. Pharmacol.* 9:506. doi: 10.3389/fphar.2018.00506

Ishikawa, J., Mitani, H., Bandoh, T., Kimura, M., Totsuka, T., and Hayashi, S. (1998). Hypoglycemic and hypotensive effects of 6-cyclohexyl-2′-O-methyl-adenosine, an adenosine A1 receptor agonist, in spontaneous hypertensive rat complicated with hyperglycemia. *Diabetes Res. Clin. Pract.* 39, 3–9. doi: 10.1016/S0168-8227(97)00116-2

Isogai, S., Niwa, Y., Yatsuya, H., Hayashi, M., Yamamoto, N., Okamura, T., et al. (2017). Increased airway hyperresponsiveness to adenosine in patients with aspirin intolerant asthma. *Allergol. Int.* 66, 360–362. doi: 10.1016/j.alit.2016.10.001

Jackson, S., Weingart, J., Nduom, E. K., Harfi, T. T., George, R. T., McAreavey, D., et al. (2018). The effect of an adenosine A2A agonist on intra-tumoral concentrations of temozolomide in patients with recurrent glioblastoma. *Fluids Barriers CNS* 15:2. doi: 10.1186/s12987-017-0088-8

Jacobson, K. A., and Civan, M. M. (2016). Ocular purine receptors as drug targets in the eye. *J. Ocular Pharmacol. Ther.* 32, 534–547. doi: 10.1089/jop.2016.0090

Jacobson, K. A., and Gao, Z. G. (2006). Adenosine receptors as therapeutic targets. *Nat. Rev. Drug Discov.* 5, 247–264. doi: 10.1038/nrd1983

Jacobson, K. A., and Gao, Z. G. (2017). "Allosteric modulators of adenosine, P2Y and P2X receptors," in *Chapter* 11 in Allosterism in Drug Discovery (RSC Drug Discovery Series No. 56), ed. D. Doller (London: Royal Society of Chemistry), 247–270. doi: 10.1039/9781782629276

Jacobson, K. A., Gao, Z. G., Tchilibon, S., Duong, H. T., Joshi, B. V., Sonin, D., et al. (2005). Semirational design of (N)-methanocarba nucleosides as dual acting A1 and A3 adenosine receptor agonists: novel prototypes for cardioprotection. *J. Med. Chem.* 48, 8103–8107. doi: 10.1021/jm050726b

Jacobson, K. A., and Knutsen, L. J. S. (2001). P1 and P2 purine and pyrimidine receptors. *Handb. Exp. Pharmacol.* 151, 129–175.

Jacobson, K. A., Merighi, S., Varani, K., Borea, P. A., Baraldi, S., Tabrizi, M. A., et al. (2018). A3 adenosine receptors as modulators of inflammation: from medicinal chemistry to therapy. *Med. Res. Rev.* 38, 1031–1072. doi: 10.1002/med.21456

Janes, K., Symons-Liguori, A. M., Jacobson, K. A., and Salvemini, D. (2016). Identification of A3 adenosine receptor agonists as novel non-narcotic analgesics. *Br. J. Pharmacol.* 173, 1253–1267. doi: 10.1111/bph.13446

Jin, X., and Mi, W. (2017). Adenosine for postoperative analgesia: a systematic review and meta-analysis. *PLoS One* 12:e0173518. doi: 10.1371/journal.pone.0173518

Jinka, T. R., Combs, V. M., and Drew, K. L. (2015). Translating drug-induced hibernation to therapeutic hypothermia. *ACS Chem. Neurosci.* 6, 899–904. doi: 10.1021/acschemneuro.5b00056

Johnston-Cox, H., Eisenstein, A. S., Koupenova, M., Carroll, S., and Ravid, K. (2014). The macrophage A2B adenosine receptor regulates tissue insulin sensitivity. *PLoS One* 9:e98775. doi: 10.1371/journal.pone.0098775

Kiesewetter, D. O., Lang, L., Ma, Y., Bhattacharjee, A. K., Gao, Z. G., Joshi, B. V., et al. (2009). Synthesis and characterization of [76Br]-labeled high affinity A3 adenosine receptor ligands for positron emission tomography. *Nucl. Med. Biol.* 36, 3–10. doi: 10.1016/j.nucmedbio.2008.10.003

Kiesman, W. F., Elzein, E., and Zablocki, J. (2009). A1 Adenosine receptor antagonists, agonists, and allosteric enhancers. *Handb. Exp. Pharmacol.* 193, 25–58. doi: 10.1007/978-3-540-89615-9_2

Kim, D.-G., and Bynoe, M. S. (2016). A2A adenosine receptor modulates drug efflux transporter P-glycoprotein at the blood-brain barrier. *J. Clin. Invest.* 126, 1717–1733. doi: 10.1172/JCI76207

Knezevic, N. N., Cicmil, N., Knezevic, I., and Candido, K. D. (2015). Discontinued neuropathic pain therapy between 2009–2015. *Exp. Opin. Invest. Drugs* 24, 1631–1646. doi: 10.1517/13543784.2015.1099627

Knutsen, L. J. S., Lau, J., Petersen, H., Thomsen, C., Weis, J. U., Shalmi, M., et al. (1999). N-Substituted adenosines as novel neuroprotective A1 agonists with diminished hypotensive effects. *J. Med. Chem.* 42, 3463–3477. doi: 10.1021/jm960682u

Korinek, W. S., Lechleiter, J. D., and Liston, T. E. (2018). *Compounds and Methods for Treating Neurological and Cardiovascular Conditions*. Washington, DC: U.S. Patent and Trademark Office.

Koupenova, M., Johnston-Cox, H., Vezeridis, A., Gavras, H., Yang, D., Zannis, V., et al. (2012). A2b adenosine receptor regulates hyperlipidemia and atherosclerosis. *Circulation* 125, 354–363. doi: 10.1161/CIRCULATIONAHA.111.057596

Koussémou, M., Lorenz, K., and Klotz, K.-N. (2018). The A2B adenosine receptor in MDA-MB-231 breast cancer cells diminishes ERK1/2 phosphorylation by activation of MAPK-phosphatase-1. *PLoS One* 13:e0202914. doi: 10.1371/journal.pone.0202914

Lahesmaa, M., Oikonen, V., Helin, S., Luoto, P., U Din, M., Pfeifer, A., et al. (2018). Regulation of human brown adipose tissue by adenosine and A2A receptors – studies with [15O]H2O and [11C]TMSX PET/CT. *Eur. J. Nucl. Med. Mol. Imaging* 46, 743–750. doi: 10.1007/s00259-018-4120-2

Lam, C. S. P., Voors, A. A., de Boer, R. A., Solomon, S. D., and van Veldhuisen, D. J. (2018). Heart failure with preserved ejection fraction: from mechanisms to therapies. *Eur. Heart J.* 39, 2780–2792. doi: 10.1093/eurheartj/ehy301

Lasley, R. D. (2018). Adenosine receptor-mediated cardioprotection - current limitations and future directions. *Front. Pharmacol.* 9:310. doi: 10.3389/fphar.2018.00310

Lebon, G., Warne, T., Edwards, P. C., Bennett, K., Langmead, C. J., Leslie, A. G. W., et al. (2011). Agonist-bound adenosine A2A receptor structures reveal common features of GPCR activation. *Nature* 474, 521–525. doi: 10.1038/nature10136

Letsas, K. P., Georgopoulos, S., Efremidis, M., Liu, T., Bazoukis, G., Vlachos, K., et al. (2017). Adenosine-guided radiofrequency catheter ablation of atrial fibrillation: a meta-analysis of randomized control trials. *J. Arrhythm.* 33, 247–255. doi: 10.1016/j.joa.2017.02.002

Leung, C. T., Li, A., Banerjee, J., Gao, Z. G., Kambayashi, T., Jacobson, K. A., et al. (2014). The role of activated adenosine receptors in degranulation of human LAD2 mast cells. *Purinergic Signal.* 10, 465–475. doi: 10.1007/s11302-014-9409-4

Little, J. W., Ford, A., Symons-Liguori, A. M., Chen, Z., Janes, K., Doyle, T., et al. (2015). Endogenous adenosine A3 receptor activation selectively alleviates persistent pain states. *Brain* 138, 28–35. doi: 10.1093/brain/awu330

Luongo, L., Petrelli, R., Gatta, L., Giordano, C., Guida, F., Vita, P., et al. (2012). 5′-Chloro-5′-deoxy-(±)-ENBA, a potent and selective adenosine A1 receptor agonist, alleviates neuropathic pain in mice through functional glial and microglial changes without affecting motor or cardiovascular functions. *Molecules* 17, 13712–13726. doi: 10.3390/molecules171213712

Mantell, S., Jones, R., and Trevethick, M. (2010). Design and application of locally delivered agonists of the adenosine A2A receptor. *Expert Rev. Clin. Pharmacol.* 3, 55–72. doi: 10.1586/ecp.09.57

Mason, P. K., and DiMarco, J. P. (2009). New pharmacological agents for arrhythmias. *Circ. Arrhythm. Electrophysiol.* 2, 588–597. doi: 10.1161/CIRCEP.109.884429

Meibom, D., Albrecht-Küpper, B., Diedrichs, N., Hübsch, W., Kast, R., Krämer, T., et al. (2017). Neladenoson Bialanate hydrochloride: a prodrug of a partial adenosine A1 receptor agonist for the chronic treatment of heart diseases. *Chem. Med. Chem.* 12, 728–737. doi: 10.1002/cmdc.201700151

Miao, Y., Bhattarai, A., Nguyen, A. T. N., Christopoulos, A., and May, L. T. (2018). Structural basis for binding of allosteric drug leads in the adenosine A1 receptor. *Sci. Rep.* 8:16836. doi: 10.1038/s41598-018-35266-x

Montesinos, M. C., Desai-Merchant, A., and Cronstein, B. N. (2015). Promotion of wound healing by an agonist of adenosine A2A Receptor is dependent on tissue plasminogen activator. *Inflammation* 38, 2036–2041. doi: 10.1007/s10753-015-0184-3

Mundell, S., and Kelly, E. (2011). Adenosine receptor desensitization and trafficking. *Biochim. Biophys. Acta* 1808, 1319–1328. doi: 10.1016/j.bbamem.2010.06.007

Murray, J. J., Weiler, J. M., Schwartz, L. B., Busse, W. W., Katial, R. K., Lockey, R. F., et al. (2009). Safety of binodenoson, a selective adenosine A2A receptor agonist vasodilator pharmacological stress agent, in healthy subjects with mild intermittent asthma. *Circ. Cardiovasc. Imaging* 2, 492–498. doi: 10.1161/CIRCIMAGING.108.817932

Myers, J. S., Sall, K. N., DuBiner, H., Slomowitz, N., McVicar, W., Rich, C. C., et al. (2016). A dose-escalation study to evaluate the safety, tolerability, pharmacokinetics, and efficacy of 2 and 4 weeks of twice-daily ocular trabodenoson in adults with ocular hypertension or primary open-angle glaucoma. *J. Ocul. Pharmacol. Ther.* 32, 555–562. doi: 10.1089/jop.2015.0148

Nascimento, F. P., Macedo, S.T., and Santos, A. R. (2012). "The involvement of purinergic system in pain: adenosine receptors and inosine as pharmacological tools in future treatments," in *Chap. 28 in Pharmacology*, eds S. J. Macedo Jr. and L. Gallelli (London: InTech).

Ni, Y., Liang, D., Tian, Y., Kron, I. L., French, B. A., and Yang, Z. (2018). Infarct-sparing effect of adenosine A2B receptor agonist is primarily due to its action on splenic leukocytes via a PI3K/Akt/IL-10 pathway. *J. Surg. Res.* 232, 442–449. doi: 10.1016/j.jss.2018.06.042

Ning, Y., Jiang, J., Belardinelli, L., and Dhalla, A. K. (2011). *Short-Term Treatment of GS-9667 in Combination with Sitagliptin Improves Glucose and Lipid Homeostasis in ZDF rats.* Arlington, VI: American Diabetes Association.

Olsson, R. A. (2003). Robert Berne: his place in the history of purine research. *Drug Dev. Res.* 58, 296–301. doi: 10.1002/ddr.10197

Palani, G., and Ananthasubramaniam, K. (2013). Regadenoson: review of its established role in myocardial perfusion imaging and emerging applications. *Cardiol. Rev.* 21, 42–48. doi: 10.1097/CRD.0b013e3182613db6

Peleli, M., and Carlstrom, M. (2017). Adenosine signaling in diabetes mellitus and associated cardiovascular and renal complications. *Mol. Aspects Med.* 55, 62–74. doi: 10.1016/j.mam.2016.12.001

Pelleg, A., Kutalek, S. P., Flammang, D., and Benditt, D. (2012). ATPaceTM: injectable adenosine 5′-triphosphate: diagnostic and therapeutic indications. *Purinergic Signal.* 8(Suppl. 1), 57–60. doi: 10.1007/s11302-011-9268-1

Pelleg, A., Schulman, E. S., and Barnes, P. J. (2016). Extracellular adenosine 5′-triphosphate in obstructive airway diseases. *Chest* 150, 908–915. doi: 10.1016/j.chest.2016.06.045

Rapaport, E., Salikhova, A., and Abraham, E. H. (2015). Continuous intravenous infusion of ATP in humans yields large expansions of erythrocyte ATP pools but extracellular ATP pools are elevated only at the start followed by rapid declines. *Purinergic Signal.* 11, 251–262. doi: 10.1007/s11302-015-9450-y

Rickles, R. J., Padval, M., Giordano, T., Rieger, J. M., and Lee, M. S. (2010). ATL313, a potent, and selective A2A agonist as a novel drug candidate for the treatment of multiple myeloma. *Blood* 116:2990.

Rieger, J. M., Brown, M. L., Sullivan, G. W., Linden, J., and Macdonald, T. L. (2001). Design, synthesis, and evaluation of novel A_{2A} adenosine receptor agonists. *J. Med. Chem.* 44, 531–539. doi: 10.1021/jm0003642

Sawynok, J. (1998). Adenosine receptor activation and nociception. *Eur. J. Pharmacol.* 347, 1–11. doi: 10.1016/S0014-2999(97)01605-1

Schaddelee, M. P., Read, K. D., Cleypool, C. G., IJzerman, A. P., Danhof, M., and de Boer, A. G. (2005). Brain penetration of synthetic adenosine A1 receptor agonists in situ: role of the rENT1 nucleoside transporter and binding to blood constituents. *Eur. J. Pharm. Sci.* 24, 59–66. doi: 10.1016/j.ejps.2004.09.010

Schaumann, E., and Kutscha, W. (1972). Clinical-pharmacological studies with a new orally active adenosine derivative. *Drug Res.* 22, 783–790.

Schaumann, E., Schlierf, G., Ptleiderer, T., and Weber, E. (1972). Effect of repeated doses of phenylisopropyladenosine on lipid and carbohydrate metabolism in healthy fasting subjects. *Arzneim. Forsch.* 22, 593–596.

Serchov, T., Clement, H.-W., Schwarz, M. K., Iasevoli, F., Tosh, D. K., Idzko, M., et al. (2015). Increased signaling via adenosine A1 receptors, sleep deprivation, imipramine, and ketamine inhibit depressive-like behavior via induction of homer1a. *Neuron* 87, 549–562. doi: 10.1016/j.neuron.2015.07.010

Shah, B., Rohatagi, S., Natarajan, C., Kirkesseli, S., Baybutt, R., and Jensen, B. K. (2004). Pharmacokinetics, pharmacodynamics, and safety of a lipid-lowering adenosine A1 agonist, RPR749, in healthy subjects. *Am. J. Ther.* 11, 175–189. doi: 10.1097/00045391-200405000-00005

Sharma, A. K., LaPar, D. J., Stone, M. L., Zhao, Y., Mehta, C. K., Kron, I. L., et al. (2016). NOX2 activation of natural killer T cells is blocked by the adenosine A2A receptor to inhibit lung ischemia-reperfusion injury. *Am. J. Respir. Crit. Care Med.* 193, 988–999. doi: 10.1164/rccm.201506-1253OC

Squadrito, F., Bitto, A., Irrera, N., Pizzino, G., Pallio, G., Minutoli, L., et al. (2017). Pharmacological activity and clinical use of PDRN. *Front. Pharmacol.* 8:224. doi: 10.3389/fphar.2017.00224

Staehr, P. M., Dhalla, A. K., Zack, J., Wang, X., Ho, Y. L., Bingham, J., et al. (2013). Reduction of free fatty acids, safety, and pharmacokinetics of oral GS-9667, an A1 adenosine receptor partial agonist. *J. Clin. Pharmacol.* 53, 385–392. doi: 10.1002/jcph.9

Stemmer, S. M., Benjaminov, O., Medalia, G., Ciuraru, N. B., Silverman, M. H., Bar-Yehuda, S., et al. (2013). CF102 for the treatment of hepatocellular carcinoma: a phaseI/II, open- label, dose-escalation study. *Oncologist* 18, 25–26. doi: 10.1634/theoncologist.2012-0211

Sun, Y., and Huang, P. (2016). Adenosine A2B receptor: from cell biology to human diseases. *Front. Chem.* 4:37. doi: 10.3389/fchem.2016.00037

Szentmiklosi, A. J., Galajda, Z., Cseppento, A., Gesztelyi, R., Susan, Z., Hegyi, B., et al. (2015). The Janus face of adenosine: antiarrhythmic and proarrhythmic actions. *Curr. Pharm. Des.* 21, 965–976. doi: 10.2174/1381612820666141029100346

Szybala, C., Pritchard, E. M., Lusardi, T. A., Li, T., Wilz, A., Kaplan, D. L., et al. (2009). Antiepileptic effects of silk-polymer based adenosine release in kindled rats. *Exp. Neurol.* 219, 126–135. doi: 10.1016/j.expneurol.2009.05.018

Tendera, M., Gaszewska-Żurek, E., Parma, Z., Ponikowski, P., Jankowska, E., Kawecka-Jaszcz, K., et al. (2012). The new oral adenosine A1 receptor agonist capadenoson in male patients with stable angina. *Clin. Res. Cardiol.* 101, 585–591. doi: 10.1007/s00392-012-0430-8

Tian, Y., Piras, B. A., Kron, I. L., French, B. A., and Yang, Z. (2015). Adenosine 2B receptor activation reduces myocardial reperfusion injury by promoting anti-inflammatory macrophages differentiation via PI3K/Akt pathway. *Oxid. Med. Cell. Longev.* 2015:585297. doi: 10.1155/2015/585297

Tosh, D. K., Finley, A., Paoletta, S., Moss, S. M., Gao, Z. G., Gizewski, E., et al. (2014). In vivo phenotypic screening for treating chronic neuropathic pain: modification of C2-arylethynyl group of conformationally constrained A3 adenosine receptor agonists. *J. Med. Chem.* 57, 9901–9914. doi: 10.1021/jm501021n

Tosh, D. K., Padia, J., Salvemini, D., and Jacobson, K. A. (2015). Efficient, large-scale synthesis and preclinical studies of MRS5698, a highly selective A3 adenosine receptor agonist that protects against chronic neuropathic pain. *Purinergic Signal.* 11, 371–387. doi: 10.1007/s11302-015-9459-2

Tosh, D. K., Paoletta, S., Deflorian, F., Phan, K., Moss, S. M., Gao, Z. G., et al. (2012). Structural sweet spot for A1 adenosine receptor activation by truncated (N)-methanocarba nucleosides: receptor docking and potent anticonvulsant activity. *J. Med. Chem.* 55, 8075–8090. doi: 10.1021/jm300965a

Tosh, D. K., Rao, H., Bitant, A., Salmaso, V., Mannes, P., Lieberman, D. I., et al. (2019). Design and in vivo characterization of A1 adenosine receptor agonists in the native ribose and conformationally-constrained (N)-methanocarba series. *J. Med. Chem.* 62, 1502–1522. doi: 10.1021/acs.jmedchem.8b01662

Tozzi, M., and Novak, I. (2017). Purinergic receptors in adipose tissue as potential targets in metabolic disorders. *Front. Pharmacol.* 8:878. doi: 10.3389/fphar.2017.00878

Trevethick, M. A., Mantell, S. J., Stuart, E. F., Barnard, A., Wright, K. N., and Yeadon, M. (2008). Treating lung inflammation with agonists of the adenosine A2A receptor: promises, problems and potential solutions. *Br. J. Pharmacol.* 155, 463–474. doi: 10.1038/bjp.2008.329

Van der Graaf, P. H., Van Schaick, E. A., Visser, S. A. G., De Greef, H. J. M. M., IJzerman, A. P., and Danhof, M. (1999). Mechanism-based pharmacokinetic-pharmacodynamic modeling of antilipolytic effects of adenosine A1 receptor agonists in rats: prediction of tissue-dependent efficacy in vivo. *J. Pharmacol. Exp. Ther.* 290, 702–709.

van Waarde, A., Dierckx, R. A. J. O., Zhou, X., Khanapur, S., Tsukada, H., Ishiwata, K., et al. (2018). Potential therapeutic applications of adenosine A2A receptor ligands and opportunities for A2A receptor imaging. *Med. Res. Rev.* 38, 5–56. doi: 10.1002/med.21432

Vecchio, E. A., Baltos, J. A., Nguyen, A. T. N., Christopoulos, A., White, P. J., and May, L. T. (2018). New paradigms in adenosine receptor pharmacology: allostery, oligomerization and biased agonism. *Br. J. Pharmacol.* 175, 4036–4046. doi: 10.1111/bph.14337

Victor-Vega, C., Victor-Vega, C., Desai, A., Montesinos, M. C., and Cronstein, B. N. (2002). Adenosine A2A receptor agonists pro- mote more rapid wound healing than recombinant human platelet- derived growth factor (Becaplermin gel). *Inflammation* 26, 19–24. doi: 10.1023/A:1014417728325

Vincenzi, F., Ravani, A., Pasquini, S., Merighi, S., Gessi, S., Romagnoli, R., et al. (2016). Positive allosteric modulation of A1 adenosine receptors as a novel and promising therapeutic strategy for anxiety. *Neuropharmacology* 111, 283–292. doi: 10.1016/j.neuropharm.2016.09.015

Vincenzi, F., Targa, M., Romagnoli, R., Merighi, S., Gessi, S., Baraldi, P. G., et al. (2014). TRR469, a potent A1 adenosine receptor allosteric modulator, exhibits antinociceptive properties in acute and neuropathic pain models in mice. *Neuropharmacology* 82, 6–14. doi: 10.1016/j.neuropharm.2014.01.028

von Lubitz, D. K. J. E., Lin, R.-C., Boyd, M., Bischofberger, N., and Jacobson, K. A. (1999). Chronic administration of adenosine A3 receptor agonist and cerebral ischemia: neuronal and glial effects. *Eur. J. Pharmacol.* 367, 157–163. doi: 10.1016/S0014-2999(98)00977-7

Voors, A. A., Düngen, H. D., Senni, M., Nodari, S., Agostoni, P., Ponikowski, P., et al. (2017). Safety and tolerability of Neladenoson Bialanate, a novel oral partial adenosine A1 receptor agonist, in patients with chronic heart failure. *J. Clin. Pharmacol.* 57, 440–451. doi: 10.1002/jcph.828

Vuerich, M., Harshe, R. P., Robson, S. C., and Longhi, M. S. (2019). Dysregulation of adenosinergic signaling in systemic and organ-specific autoimmunity. *Int. J. Mol. Sci.* 20:528. doi: 10.3390/ijms20030528

Wahlman, C., Doyle, T., Little, J. W., Luongo, L., Janes, K., Chen, Z., et al. (2018). Chemotherapy-induced pain is promoted by enhanced spinal adenosine kinase levels via astrocyte-dependent mechanisms. *Pain* 159, 1025–1034. doi: 10.1097/j.pain.0000000000001177

Wan, T. C., Tampob, A., Kwokb, W. M., and Auchampach, J. A. (2019). Ability of CP-532,903 to protect mouse hearts from ischemia/reperfusion injury is dependent on expression of A3 adenosine receptors in cardiomyoyctes. *Biochem. Pharmacol.* 163, 21–31. doi: 10.1016/j.bcp.2019.01.022

Wilbrandt, R., Frotscher, U., Freyland, M., Messerschmidt, W., Richter, R., Schulte-Lippern, M., et al. (1972). Zur Behandlung der Glomerulonephritis mit Metrifudil. *Medizinische Klinik* 67, 1138–1140.

Wojcik, M., Zieleniak, A., Mac-Marcjanek, K., Wozniak, L. A., and Cypryk, K. (2014). The elevated gene expression level of the A2B adenosine receptor is associated with hyperglycemia in women with gestational diabetes mellitus. *Diabetes Metab. Res. Rev.* 30, 42–53. doi: 10.1002/dmrr.2446

Xiao, C., Liu, N., Jacobson, K. A., Gavrilova, O., and Reitman, M. L. (2019). Physiology and effects of nucleosides in mice lacking all four adenosine receptors. *PLoS Biol.* 17:e3000161. doi: 10.1371/journal.pbio.3000161

Xu, F., Wu, H., Katritch, V., Han, G. W., Jacobson, K. A., Gao, Z. G., et al. (2011). Structure of an agonist-bound human A2A adenosine receptor. *Science* 332, 322–327. doi: 10.1126/science.1202793

Zannikos, P. N., Rohatagi, S., and Jensen, B. K. (2001). Pharmacokinetic-pharmacodynamic modeling of the antilipolytic effects of an adenosine receptor agonist in healthy volunteers. *J. Clin. Pharmacol.* 41, 61–69. doi: 10.1177/00912700122009845

Zheng, J., Wang, R., Zambraski, E., Wu, D., Jacobson, K. A., and Liang, B. T. (2007). Protective roles of adenosine A1, A2A, and A3 receptors in skeletal muscle ischemia and reperfusion injury. *Am. J. Physiol. Heart Circ. Physiol.* 293, 3685–3691. doi: 10.1152/ajpheart.00819.2007

Zoghbi, G. J., and Iskandrian, A. E. (2012). Selective adenosine agonists and myocardial perfusion imaging. *J. Nucl. Cardiol.* 19, 126–141. doi: 10.1007/s12350-011-9474-9

Zylka, M. J. (2011). Pain-relieving prospects for adenosine receptors and ectonucleotidases. *Trends Mol. Med.* 17, 188–196. doi: 10.1016/j.molmed.2010.12.006

Conflict of Interest Statement: The authors declare that the research was conducted in the absence of any commercial or financial relationships that could be construed as a potential conflict of interest.

frontiers in Cellular Neuroscience

ORIGINAL RESEARCH
published: 09 April 2019
doi: 10.3389/fncel.2019.00121

An Allosteric Inhibitory Site Conserved in the Ectodomain of P2X Receptor Channels

Ariel R. Ase[1], *Éric Therrien*[2†] *and Philippe Séguéla*[1*]

[1]Alan Edwards Centre for Research on Pain, Department of Neurology and Neurosurgery, Montreal Neurological Institute, McGill University, Montreal, QC, Canada, [2]Molecular Forecaster Inc., Montreal, QC, Canada

P2X receptors constitute a gene family of cation channels gated by extracellular ATP. They mediate fast ionotropic purinergic signaling in neurons and non-excitable cell types in vertebrates. The highly calcium-permeable P2X4 subtype has been shown to play a significant role in cardiovascular physiology, inflammatory responses and neuro-immune communication. We previously reported the discovery of a P2X4-selective antagonist, the small organic compound BX430, with submicromolar potency for human P2X4 receptors and marked species-dependence (Ase et al., 2015). The present study investigates the molecular basis of P2X4 inhibition by the non-competitive blocker BX430 using a structural and functional approach relying on mutagenesis and electrophysiology. We provide evidence for the critical contribution of a single hydrophobic residue located in the ectodomain of P2X4 channel subunits, Ile312 in human P2X4, which determines blockade by BX430. We also show that the nature of this extracellular residue in various vertebrate P2X4 orthologs underlies their specific sensitivity or resistance to the inhibitory effects of BX430. Taking advantage of high-resolution crystallographic data available on zebrafish P2X4, we used molecular dynamics simulation to model the docking of BX430 on an allosteric binding site around Ile315 (zebrafish numbering) in the ectodomain of P2X4. We also observed that the only substitution I312D (human numbering) that renders P2X4 silent by itself has also a profound silencing effect on all other P2X subtypes tested when introduced at homologous positions. The generic impact of this aspartate mutation on P2X function indicates that the pre-TM2 subregion involved is conserved functionally and defines a novel allosteric inhibitory site present in all P2X receptor channels. This conserved structure-channel activity relationship might be exploited for the rational design of potent P2X subtype-selective antagonists of therapeutic value.

Keywords: purinoceptor, ATP, nucleotides, ionotropic, calcium, inflammation, pain

OPEN ACCESS

Edited by:
Eric Boué-Grabot,
Université de Bordeaux, France

Reviewed by:
Thomas Grutter,
Université de Strasbourg, France
Claudio Coddou,
Universidad Católica del Norte Coquimbo, Chile

***Correspondence:**
Philippe Séguéla
philippe.seguela@mcgill.ca

†Present address:
Éric Therrien,
Schrödinger LLC, New York, NY, United States

Received: *16 January 2019*
Accepted: *12 March 2019*
Published: *09 April 2019*

Citation:
Ase AR, Therrien É and Séguéla P (2019) An Allosteric Inhibitory Site Conserved in the Ectodomain of P2X Receptor Channels. Front. Cell. Neurosci. 13:121. doi: 10.3389/fncel.2019.00121

INTRODUCTION

P2X receptors are ATP-gated nonselective cation channels, formed by the trimeric assembly of homologous subunits encoded by seven genes in mammals (P2rx1–7), resulting in homomeric or heteromeric channels (North, 2002; Saul et al., 2013). P2X channel subunits share a common topology, with intracellular amino- and carboxy-termini, two transmembrane domains and a large ectodomain constrained in a complex folded conformation by five disulfide bridges

(Stojilkovic et al., 2005; Hattori and Gouaux, 2012). The P2X ectodomain contains the binding sites for the endogenous agonist ATP and for antagonists, protons and modulatory metallic ions, whereas the transmembrane helical domains form a non-selective cationic pore permeable to calcium ions (Coddou et al., 2011; Habermacher et al., 2016).

Among the mammalian P2X subtypes, the P2X4 receptor is an ATP-gated channel highly permeable to calcium ions that plays a significant pathophysiological role in cardiovascular, inflammatory and neuropathic disorders (Burnstock and Kennedy, 2011). Knockout mice lacking P2X4 receptors display deficits in shear stress-induced vasodilation, indicating a significant contribution of these channels to the regulation of vascular tone by endothelial cells (Yamamoto et al., 2006). P2X4 is also expressed in monocytes, macrophages and microglia where it is involved in the release of inflammatory mediators and cytokines (Bowler et al., 2003; Tsuda et al., 2003; Raouf et al., 2007; Ulmann et al., 2008). In the central nervous system, P2X4 is upregulated at the surface of spinal microglia following peripheral nerve injury and P2X4-dependent BDNF release was shown to trigger the development of neuronal hyperexcitability underlying tactile allodynia in conditions of chronic neuropathic pain (Trang et al., 2012).

Recently, using a stable cell line expressing human P2X4 and high throughput screening with calcium uptake readout, we have reported the identification of the phenylurea BX430 endowed with the properties of a potent non-competitive antagonist with remarkable selectivity for the P2X4 subtype (Ase et al., 2015). Here, we have extended this previous study to identify the domain(s) responsible for the non-competitive inhibitory effect of BX430 on human P2X4 receptor channels. Based on our observation of the differential blockade of human and rodent P2X4 orthologs by BX430 (Ase et al., 2015) and taking advantage of the high conservation of P2X4 primary sequences among vertebrates, we successfully identified a single key extracellular amino acid critical for the non-competitive binding of BX430 on specific P2X4 orthologs. Based on high-resolution structures of invertebrate and vertebrate P2X receptors in apo as well as liganded states (Pasqualetto et al., 2018), we modeled the 3D structure of zebrafish and human P2X4 channels liganded with BX430. Interestingly, the basic structure and function of this BX430-binding domain present in P2X4 is conserved in the P2X gene family and we show that all the P2X subtypes tested share this allosteric inhibitory site.

MATERIALS AND METHODS

Cell Culture and Plasmids

Human embryonic kidney (HEK293) cells were cultured in Dulbecco's modified Eagle's medium and 10% heat-inactivated fetal bovine serum (Invitrogen, Carlsbad, CA, USA) containing penicillin and streptomycin. HEK293 cells stably expressing human His-tagged P2X4 channels (hP2X4-HEK293 cells) were a kind gift from R. Alan North (University of Manchester, UK). They were kept in DMEM:F12 (1:1) containing 10% FBS, penicillin and streptomycin, supplemented with G418 (250 μg/ml) for selection. For experiments involving comparisons between wild-type and mutant P2X4 receptors, HEK293 cells were transiently co-transfected with the fluorescent reporter mCherry and the following cDNAs subcloned in pCDNA3 expression vector (DNA ratio 1:5) : wild-type human P2X4 (hP2X4), mutants hP2X4 I312T, I312G, I312D, I312E, I315K, I312A, I312V, I312L, I312F, I312Y, I312W, wild-type rat P2X4, mutant rat P2X4 T312I, bovine P2X4, xenopus P2X4, wild-type zebrafish P2X4 (zfP2X4), mutants zfP2X4 I315T, I315D, ΔzfP2X4(A)-GFP, human P2X1, human P2X1 F308D, human P2X2, human P2X2 I307D, human P2X3, human P2X3 L298D, human P2X5, human P2X5 M313D, human P2X7 or human P2X7 I310D. Site-directed mutations were introduced using the QuikChange method (Agilent). Transfected cells were used for electrophysiological recordings 48 h post-transfection.

Electrophysiology

Whole-cell patch-clamp recording of hP2X4-HEK293 cells and transiently transfected HEK293 cells (V_{hold}= −60 mV) were performed using pipettes filled with internal solution, pH 7.2, containing (in mM): 120 K-gluconate, 1 $MgCl_2$, 5 EGTA and 10 HEPES. The recording solution, pH 7.4, comprised (in mM): 140 NaCl, 5 KCl, 2 $CaCl_2$, 2 $MgCl_2$, 10 HEPES and 10 glucose. Membrane currents were recorded using an Axopatch 200B amplifier and digitized at 500 Hz with a Digidata 1330 interface (Axon Instruments, Molecular Devices, Sunnyvale, CA, USA). Only recordings with series resistance below 10 MΩ and stable for the duration of the recording were considered for analysis. The liquid junction potential was calculated to be 3.7 mV and was not compensated. Drugs were dissolved in recording solution and applied using a SF-77B fast perfusion system (Warner Instruments, Hamden, CT, USA) at a rate of 1 ml/min. All experiments were performed at 22°C. For each individual experiment, current amplitudes before and after drug treatment were compared and expressed as a percentage.

Homology Modeling and Ligand Docking

Putative binding sites were identified using the *Roll* algorithm[1]. Molecular dynamics was performed on the closed state of the P2X4 receptor (pdb 4DW0) using the GROMACS package[1]. The protein was prepared for docking using PREPARE (hydrogen atoms were added, rotamers and tautomers were evaluated). The ligand BX430 was converted from 2D in 3D and hydrogens were added using the CONVERT program. BX430 was prepared for docking using the SMART program. The ligand was docked using the FITTED docking program with the default settings. PREPARE, CONVERT, PROCESS, SMART, and FITTED are part of the FORECASTER platform (Molecular Forecaster, Montreal, QC, Canada). PyMOL is a graphical program distributed as open-source from Schrödinger (Cambridge, MA, USA). Discovery Studio Visualizer is a graphical program from Accelrys (San Diego, CA, USA).

[1]http://www.gromacs.org/

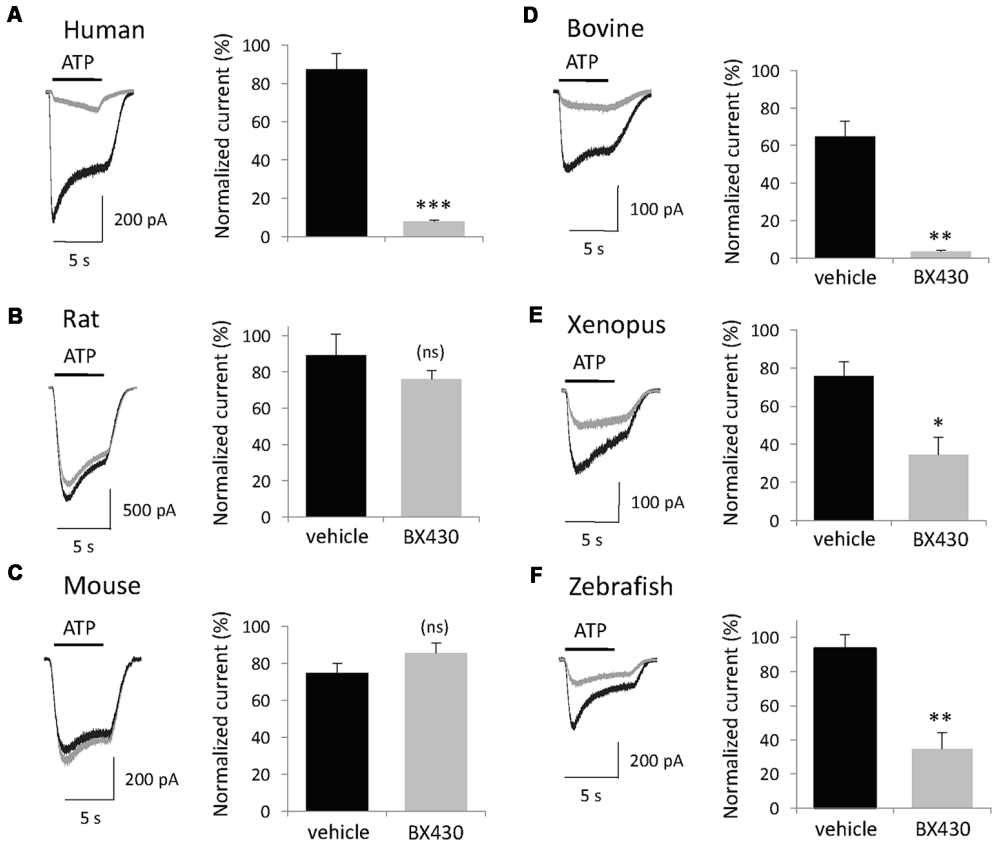

FIGURE 1 | The inhibitory effect of the P2X4 antagonist BX430 compound is species-dependent. **(A,D,E,F)** Representative responses and quantitative results showing ATP (50 μM)-evoked currents recorded in patch clamp from HEK293 cells transfected with human, bovine, xenopus and zebrafish P2X4 receptor channels displaying sensitivity to BX430. **(B,C)** Representative responses and quantitative data showing that rat and mouse P2X4 receptor channels are not affected by treatment with BX430 (10 μM). In all panels: current traces from vehicle-treated cells in black, from BX430-treated cells in gray. $^{*}P < 0.05$; $^{**}P < 0.01$; $^{***}P < 0.001$ ($n = 5$–7).

Statistics

Current amplitudes recorded during ATP applications were measured and mean values were calculated for comparative analysis. Data are presented as mean ± standard error of the mean (SEM) unless indicated otherwise, analyzed using Student's *t* test, non-paired two-tailed distribution, paired or one-way analysis of variance (ANOVA) followed by a Sidak's multiple comparisons test.

RESULTS

Species-Selectivity of the Antagonist BX430

The primary sequence of P2X4 subunits is significantly conserved between vertebrates from fish to primates, therefore, we investigated the sensitivity of diverse P2X4 orthologs to the inhibitory effect of BX430, a small organic compound (MW = 413) that blocks selectively human P2X4 channels with submicromolar potency (Ase et al., 2015). Plasmids encoding P2X4 subunits from human, rat, mouse, bovine, xenopus and zebrafish were transiently transfected in HEK293 cells and patch-clamp recording was performed 48 h later. To monitor both desensitization and recovery kinetics, the protocol consisted of several short (5 s) applications of ATP 2 min apart under voltage clamp conditions (Vh = −60 mV). Following the second control application of ATP, transfected cells were exposed to vehicle (DMSO 0.1%) or BX430 for 2 min and then tested for ATP + BX430 (co-application then ATP alone was applied again to measure the recovery response. As shown in **Figure 1**, BX430 blockade of ATP-evoked current was species-dependent. In spite of high similarity with human P2X4 sequence, rat and mouse P2X4 channels (both 87% amino acid identity) mediated ATP-evoked current responses that were not significantly affected by the application of 10 μM BX430. This lack of sensitivity was also confirmed using higher concentrations of BX430 (up to 100 μM; data not shown). In contrast, bovine P2X4 receptors displayed high sensitivity to BX430 (95% blockade), similar to human P2X4 (91%) while zebrafish and xenopus P2X4 orthologs displayed lower but nevertheless significant sensitivity to blockade by BX430 (63% and 55% inhibition, respectively).

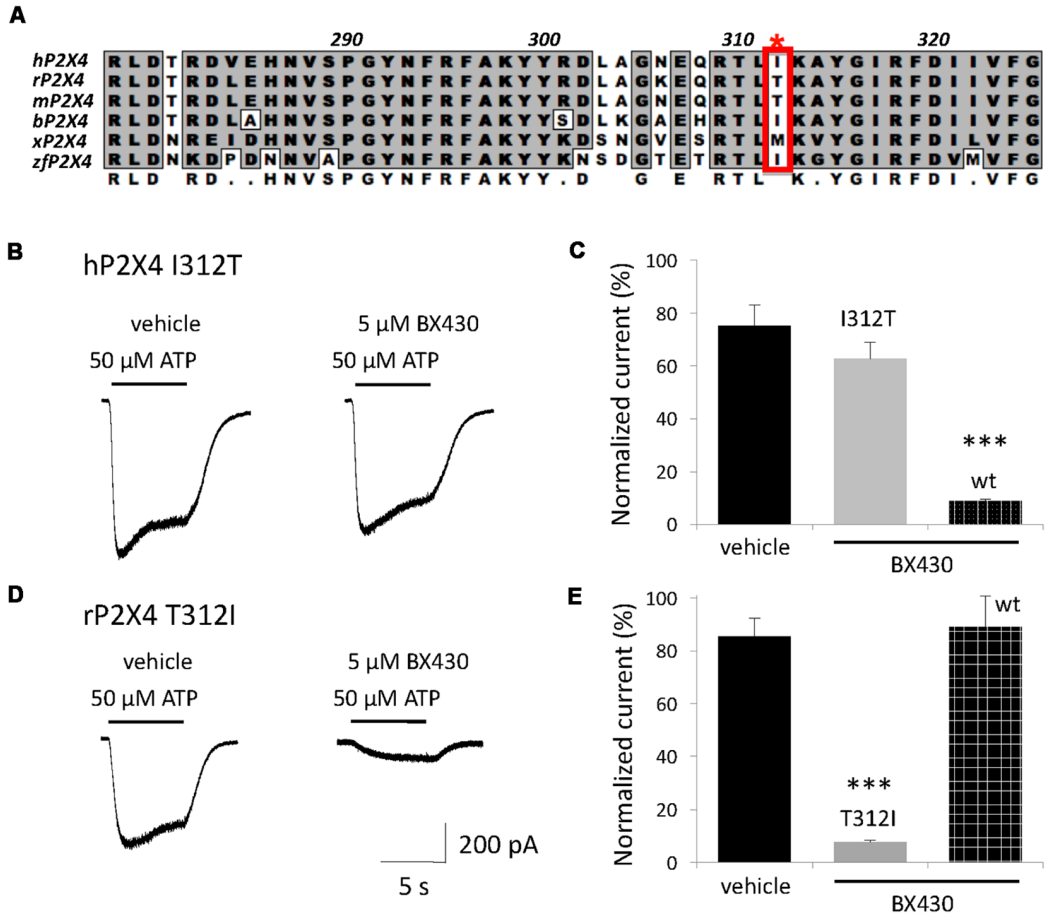

FIGURE 2 | A single residue in the ectodomain, Ile312 in human P2X4, determines BX430 antagonist effect and sensitivity of P2X4 orthologs. **(A)** Alignment of a subregion of the ectodomain of human P2X4 with several vertebrate P2X4 orthologs showing Ile312 in its proximal environment. r, rat; m, mouse; b, bovine; x, xenopus; zf, zebrafish. **(B,C)** Representative traces and quantitative results showing a complete loss of sensitivity to BX430 caused by the single mutation I312T on human P2X4 receptor channels expressed in HEK293 cells. **(D,E)** Representative traces and quantitative results showing the gain of sensitivity to BX430 caused by the single mutation T312I on rat P2X4 receptor channels. ***$P < 0.001$ ($n = 5–8$).

We previously reported electrophysiological evidence for an extracellular site of action of the ligand BX430 on P2X4 receptors (Ase et al., 2015). The alignment of the ectodomains of P2X4 orthologs (**Figure 2A**) combined with their differential sensitivity to blockade by BX430 was used as a strategy for the identification of amino acids or subdomains responsible for the inhibitory effect of BX430. We specifically looked for residues identical or similar in the ectodomain of BX430-sensitive human, bovine, xenopus and zebrafish P2X4 orthologs while physicochemically different in BX430-resistant rodent orthologs. Among six candidates, the aliphatic isoleucine Ile312 (human P2X4 numbering) was particularly interesting because it is replaced by polar threonines in BX430-resistant rat and mouse P2X4 subunits. We generated the mutant hP2X4 I312T and observed that this single mutation resulted in an almost complete loss of sensitivity to BX430 (**Figures 2B,C**). Reciprocally, substituting threonine 312 for isoleucine in the rat sequence (mutant rP2X4 T312I) conferred *de novo* sensitivity to BX430 to the rat P2X4 receptor (**Figures 2D,E**), demonstrating that the extracellular residue Ile312 in human P2X4 is a necessary component of the binding domain for the antagonist BX430.

Structural Basis for the Pharmacological Properties of BX430

To look closer into the nature of interactions between BX430 and human P2X4, we carried out a series of systematic substitutions of I312 for amino acids with different side chains, such as polar uncharged, negatively- or positively-charged, aliphatic or aromatic (**Figure 3**, see also summary of results in **Table 1**). Except for the only silent mutant hP2X4 I312D, all the mutants of human P2X4 generated responses evoked by 50 µM ATP, with current phenotypes similar to wild-type hP2X4 (data not shown). We observed a similar impact of replacing isoleucine with polar (threonine) or small apolar (glycine) uncharged amino acid, both inducing a loss of sensitivity to BX430 in the mutants I312T and I312G. Substitutions for aspartate and glutamate with negatively charged side chains produced contrasting results:

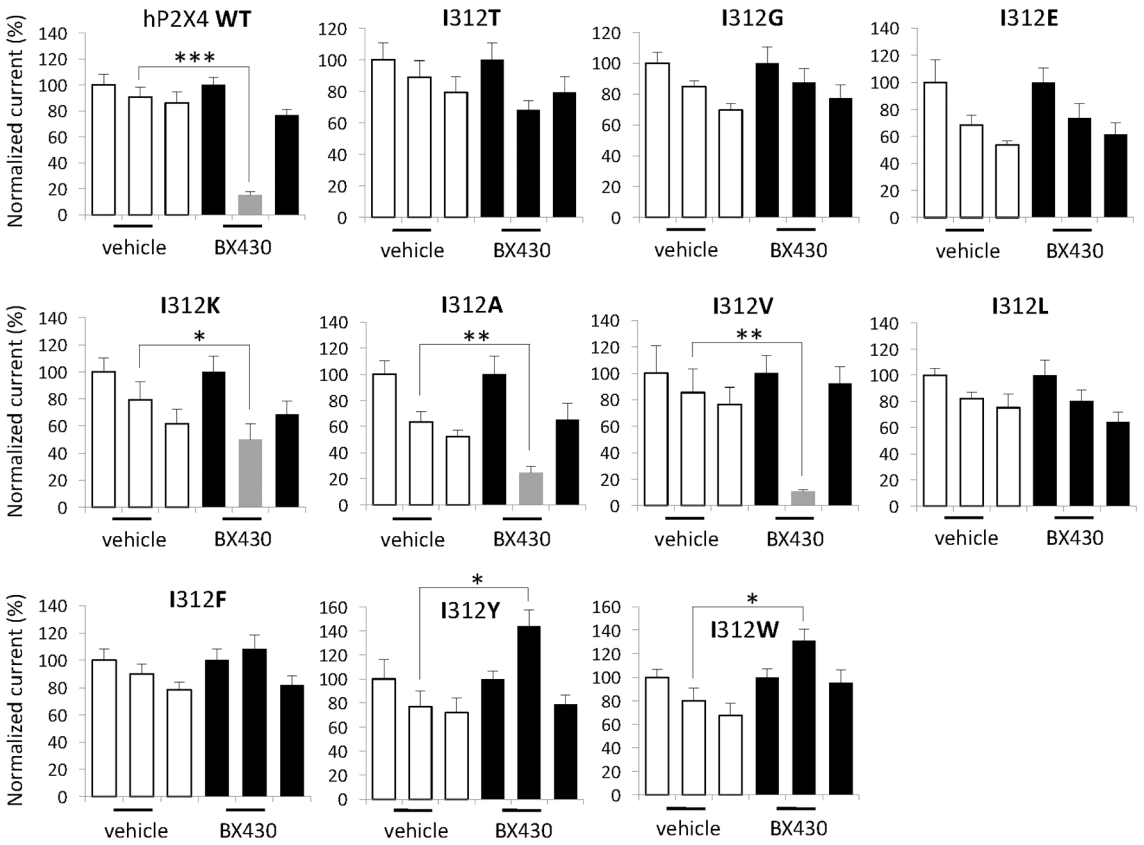

FIGURE 3 | Differential impact of amino acid substitutions at position 312 on the sensitivity of human P2X4 to BX430. Quantitative analysis of the electrophysiological recordings shows that the mutations on human P2X4 I312K, I312A and I312V do not interfere with BX430 binding and blockade, whereas the mutations I312T, I312G, I312E, I312L and I312F induce a loss of sensitivity to BX430. Human P2X4 mutants with I312Y or I312W display significant BX430-evoked potentiation of ATP responses. $^{*}P < 0.05$; $^{**}P < 0.01$; $^{***}P < 0.001$ (n = 6–12).

the mutant I312D was silent, even when stimulated by up to 500 μM ATP (data not shown), while the mutant I312E was fully functional but did not display any sensitivity to BX430. The mutation with a positively charged amino acid I312K preserved both functionality and blockade by BX430, but with lower sensitivity. The aliphatic side chain of valine is similar in size to isoleucine and the mutant I312V mirrored the wild-type phenotype regarding sensitivity to BX430. Mutant hP2X4 I312A was also found significantly sensitive to BX430 but with lower potency than the wild-type version. Unexpectedly, when isoleucine was replaced by its regioisomer leucine in the mutant I312L, human P2X4 lost its sensitivity to BX430. BX430 also lost its antagonist properties on the mutants with aromatic side chains I312F, I312Y and I312W. On the contrary, we recorded a significant potentiation of the current response in the presence of BX430 in the cases of I312Y and I312W (**Figure 3**).

Reports of the crystal structure of zebrafish P2X4 and other invertebrate and vertebrate P2X subtypes solved at high resolution in closed as well as ATP-bound open states provided a breakthrough in the understanding of structure-activity relationships that underlie gating mechanisms by specific nucleotides, desensitization, antagonist binding or ion selectivity of P2X channels (review in Pasqualetto et al., 2018). We first checked that wild-type zebrafish P2X4 is effectively blocked by BX430 in a dose-dependent manner (**Figure 4A**) and confirmed that the residue Ile315 homologous to Ile312 in human P2X4 plays also a key role in the inhibitory effect of BX430. Moreover, substituting Ile315 for threonine effectively suppressed blockade of zebrafish P2X4 by BX430 (**Figure 4B**): as for hP2X4 I312T, zfP2X4 I315T became insensitive to 10 μM BX430 (vehicle: 98 ± 5.5% vs. BX430 95 ± 4.5%; n = 5). Compared to wild-type, the mutant zfP2X4 I312T was also found less sensitive to 500 μM ATP (peak current amplitude = 44 ± 10 pA for mutant vs. 147 ± 13 pA for wild-type, n = 5). In order to use them as structural references for the 3D modeling of human P2X4, we wondered then if the truncated forms of zebrafish P2X4 that were crystallized were also subject to blockade by BX430. As shown in **Figure 4C**, the truncated mutant ΔzfP2X4(A)-GFP (Kawate et al., 2009) expressed in HEK293 cells was significantly inhibited by BX430, with 56% blockade at 10 μM and 86% blockade at 50 μM. Thus, both the wild-type and its truncated counterpart show similar sensitivity to the antagonist BX430. We were not able to reach sufficient

TABLE 1 | Summary of electrophysiological data obtained in single amino acid substitution experiments targeting Ile312 (human, h) or Ile315 (zebrafish, zf) in the ectodomain of P2X4 receptor channels.

Mutant	Function	Blockade by BX430
Polar uncharged side chain		
hP2X4 I312T	Yes	No
zfP2X4 I315T	Yes	No
Negatively-charged side chain		
hP2X4 I312D	No	n.a.
zfP2X4 I315D	No	n.a.
hP2X4 I312E	Yes	No
Positively-charged side chain		
hP2X4 I312K	Yes	Yes
Apolar aliphatic side chain		
hP2X4 I312G	Yes	No
hP2X4 I312A	Yes	Yes
hP2X4 I312V	Yes	Yes
hP2X4 I312L	Yes	No
Aromatic side chain		
hP2X4 I312F	Yes	No
hP2X4 I312Y	Yes	No (potentiation)
hP2X4 I312W	Yes	No (potentiation)

levels of surface expression in HEK293 cells for the other reported versions of crystallized truncated zfP2X4 constructs in HEK293 cells or the mutant ΔzfP2X4(A)-GFP I315T (data not shown). Nevertheless, we could conclude that human and zebrafish P2X4 receptors share homologous binding sites for the antagonist BX430 around the same Ile312/315 residue in their ectodomain.

Available crystal structures of P2X4 receptor channels were inspected (pdb 4DW0, 4DW1, 3H9V, and 3I5D) and the structure of zebrafish P2X4 in its closed, apo state (pdb code 4DW0) was selected to identify putative BX430 binding sites by detecting pockets and cavities on the receptor using complementary *Roll* and DogSiteScorer modeling approaches. The docking sites in zebrafish P2X4 were set to sample the region proximal to Ile315 in the upper body region of the channel subunit. The ligand BX430 was prepared using the FORECASTER platform. The docking poses were generated for the identified putative binding sites using the rigid and flexible protein docking modes available in the FITTED program. Visual inspection of the proposed poses led to the identification of the binding site that showed the best interactions with most of the relevant residues (**Figures 5A,B**).

Homology models for human P2X4 were built based on the zebrafish P2X4 crystal structure (pdb code 4DW0) using the SWISS-MODEL web server. Docking poses were generated by the same protocol using the FITTED program. Visual inspection of the proposed poses led to the selection of the best receptor conformations—binding sites combination. The selected docking modes of BX430 for human P2X4 were used as starting structures for molecular dynamics simulations. The simulations were performed in GROMACS (version 4.5.4) with the amber ff99sb and GAFF force fields using AM1-BCC partial charges for BX430. The receptor and BX430 were solvated in a triclinic TIP3P water box and neutralized by adding counter-ions. The systems were energy-minimized to ensure the systems have no steric clashes or inappropriate geometry. The energy-minimized systems were equilibrated with position restraints for 100 ps at constant volume and temperature (300 K). Production runs were for 2 ns with 2-fs time steps using the LINCS algorithm to constrain bonds between hydrogens and heavy atoms. Trajectories were analyzed using PyMOL. Representative conformations were extracted from clustering and up to three structures were selected for further evaluation. Then, the BX430 ligand was docked within these conformations using the flexible protein docking mode of FITTED. Using the human P2X4 model as a template, homology models for the mutated hP2X4 I312T structure was built. The BX430 ligand was docked to each model and the region around Ile/Thr312 in the upper body region was used to define the overall docking site of BX430 on wild-type and mutant human P2X4 receptor (**Figure 5C**). The identification of negative charges (Asp88) and hydrogen bond donor (Tyr300) around the Ile312 residue was the starting point for molecular docking studies. We propose that the amines in the urea moiety of BX430 interact with the C = O of Asp88 while the C = O of BX430 makes an H-bond with the hydroxyl of Tyr300. The dibromo-isopropylphenyl group of BX430 fills a hydrophobic pocket around Ile312 and Leu107 (Ile110 in zebrafish P2X4; **Figures 5A–C**) that is disrupted in the mutant Ile312T while the pyridine moiety of BX430 is solvent-exposed and interacts with surrounding water molecules. The significant physical distance observed between the docking site of BX430 and the ATP-binding site (**Figure 5D**) provides a structural basis for the non-competitive nature of the inhibition induced by the binding of BX430 on P2X4 receptor channels.

The Function of the BX430-Binding Domain in P2X4 is Conserved in the Whole P2X Family

Only one specific mutation in human P2X4 receptor, isoleucine to aspartate (I312D), had a profound functional impact by itself as P2X4 channels became completely insensitive to ATP. This suggested a critical role for this Ile312 residue and/or its immediate surrounding environment in the basic function of P2X4 receptor channels. Taking into account the high level of conservation of this pre-TM2 subdomain in the P2X family (see the alignment in **Figure 6A**), we considered the possibility that the strong antagonist effect of this single mutation might be extended to other P2X channel subtypes. We mutated all human P2X receptor subunits known to assemble into functional homotrimers (P2X1–4, P2X5–7) by substituting the residue homologous to Ile312 in human P2X4 (either isoleucine, leucine or methionine in the other P2X subtypes) for aspartate. These mutant receptors, i.e., P2X1 I308D, P2X2 I307D, P2X3 L298D, P2X4 I312D, P2X5 M313D and P2X7 I310D, were expressed in HEK293 cells and tested for agonist (ATP or BzATP)-evoked current responses (**Figures 6B–H**). We did not test mutant human P2X6 because the wild-type homomeric P2X6 channel is insensitive to ATP. As illustrated in **Figure 6**, all the homomeric P2X subtypes tested were rendered silent by this mutation, except P2X3 L298D. However, the response of the mutant P2X3 channels to ATP was severely impaired, as the amplitude

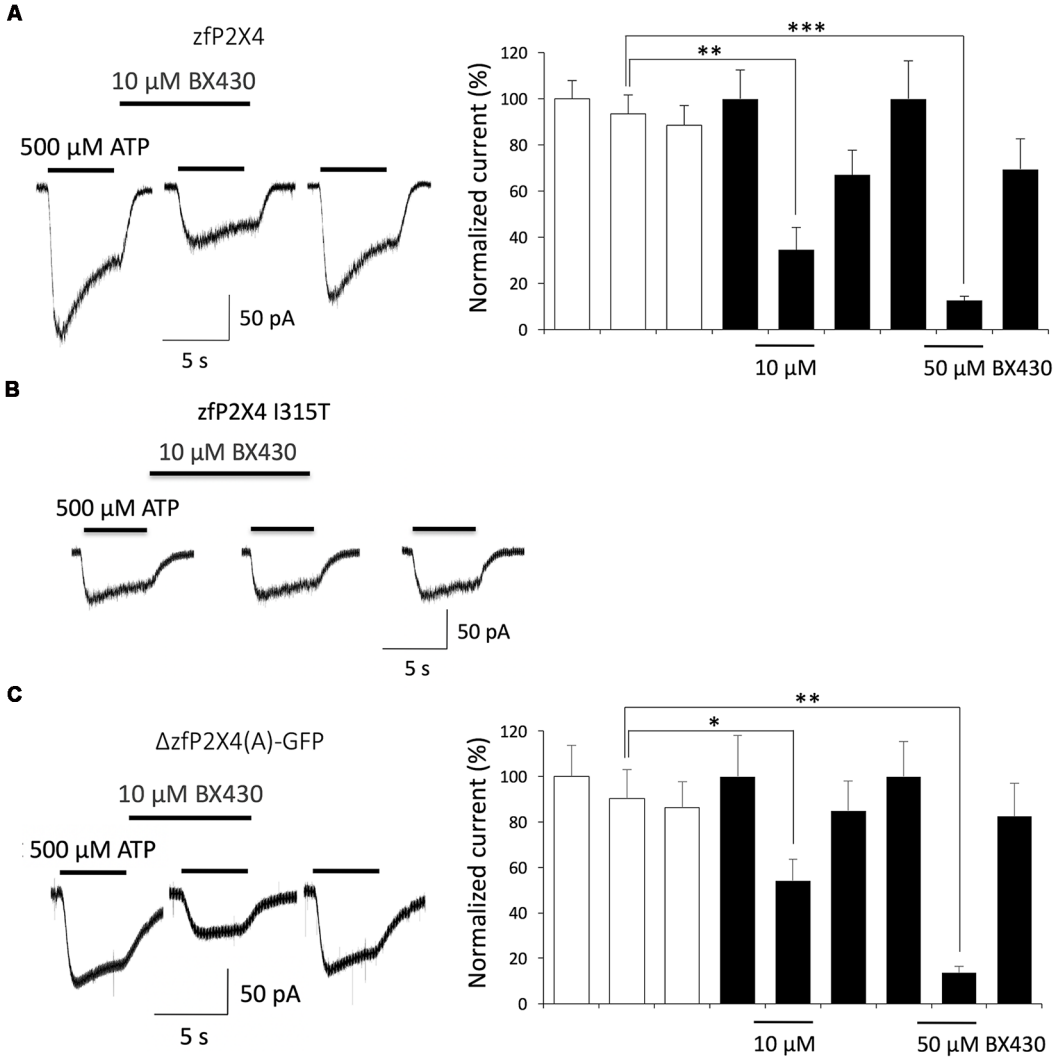

FIGURE 4 | Both wild-type zebrafish P2X4 and the crystallized truncated form ΔzfP2X4(A)-GFP are sensitive to the antagonist BX430. **(A)** Typical ATP-evoked current responses and quantitative results documenting dose-dependent inhibition of wild-type zebrafish P2X4 by BX430. **(B)** Representative traces showing that the mutation I315T in zebrafish P2X4 induces a complete loss of sensitivity to BX430. **(C)** Typical ATP-evoked current responses and quantitative results showing that BX430 is also an antagonist of the truncated form of zebrafish P2X4 ΔzfP2X4(A)-GFP used in X-ray crystallography (Kawate et al., 2009). $^{*}P < 0.05$; $^{**}P < 0.01$; $^{***}P < 0.001$ (n = 5–9).

of their peak currents was about 10 times lower compared to wild-type P2X3 (**Figure 6D**). The homologous mutation introduced in zebrafish P2X4, I315D, fully suppressed channel activity (**Figure 6F**). These results indicate that this aspartate mutation targeting a conserved subregion of the ectodomain, which happens to be a BX430-binding site in P2X4 selectively, disrupts a basic functional mechanism shared by all the P2X receptor subtypes tested.

DISCUSSION

Altogether, our results provide convincing evidence for the existence of a novel allosteric binding site for the selective antagonist BX430 in the ectodomain of P2X4 receptor channels. By comparing the primary sequences of several BX430-sensitive and -resistant P2X4 orthologs, we were able to identify one extracellular residue (at position 312 in human P2X4) in the ectodomain of P2X4 as the single critical determinant for the inhibitory effect of BX430. The structure of the subdomain involved is conserved in the whole P2X family and we showed that its disruption has a generic silencing effect on the function of all P2X receptor channels.

Molecular Basis for Species-Specific Sensitivity to the Antagonist BX430

We have reported that the P2X4-selective antagonist BX430 is an effective blocker of human P2X4 with submicromolar potency but it has no measurable effect on mouse P2X4 receptors

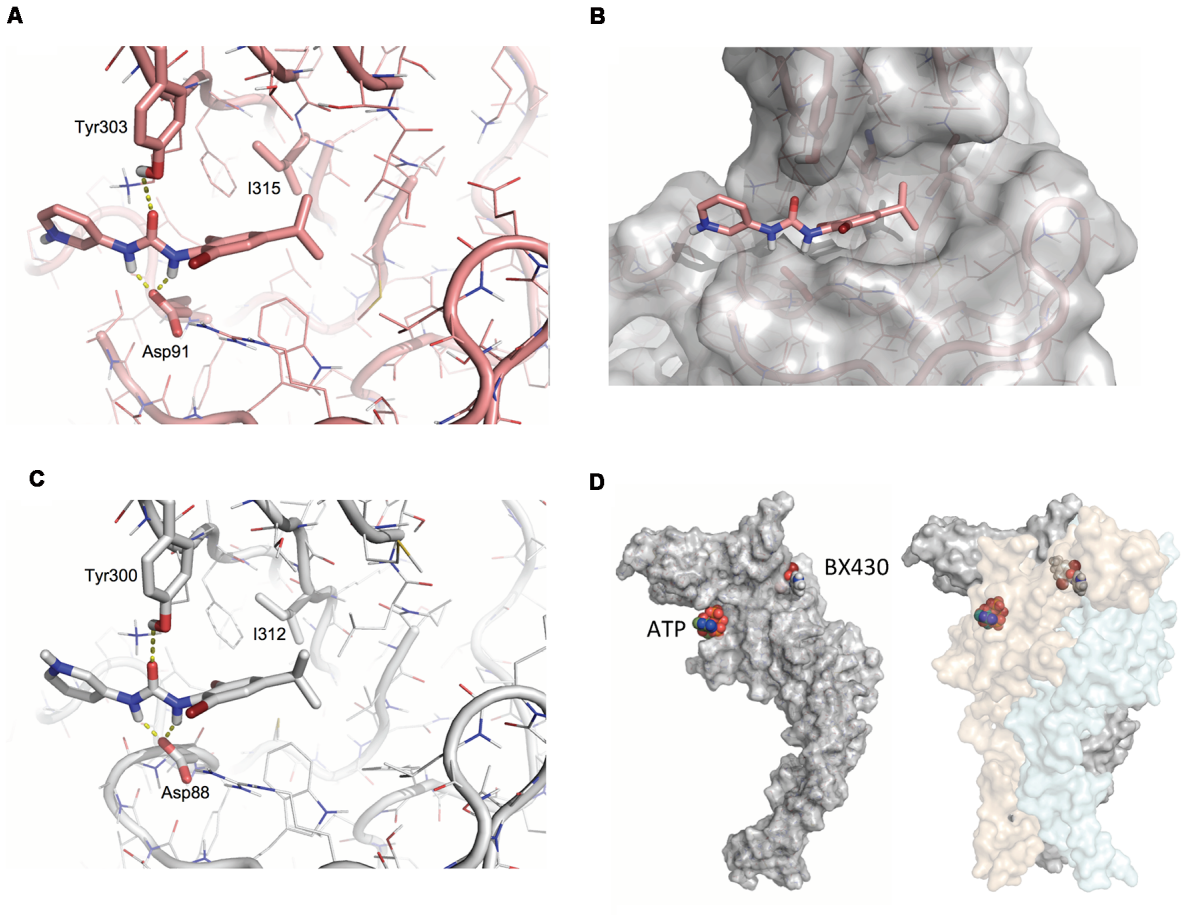

FIGURE 5 | Modeling of the BX430 binding domain in zebrafish and human P2X4 structures. **(A)** Docking of the antagonist BX430 using molecular dynamics simulation on the model of zebrafish P2X4 based on X-ray crystallographic data of the construct ΔzfP2X4(A)-GFP (pdb code 4DW0). Key isoleucine (Ile315), as well as tyrosine (Tyr303) and aspartate (Asp91) residues contributing to the binding of BX430, are indicated. **(B)** 3D surface representation of docked BX430 in ΔzfP2X4(A)-GFP. **(C)** Homologous docking of BX430 on the model of human P2X4 subunit and key amino acids involved in the binding domain. **(D)** Model of a single human P2X4 subunit in surface view (left) and global quaternary structure of the trimeric P2X4 complex (right), illustrating the relative positions of the agonist-binding site occupied by ATP and the allosteric antagonist-binding site occupied by BX430.

(Ase et al., 2015). Previous cases of species-specific pharmacology in the field of P2X receptors include, among others, the P2X3 antagonist RO51 (Serrano et al., 2012), the P2X4 antagonists suramin and PPADS (Garcia-Guzman et al., 1997; Jones et al., 2000), the P2X7 antagonist AZ11645373 (Michel et al., 2009) and the positive allosteric modulation of P2X7 by ivermectin (Nörenberg et al., 2012). We tested several other vertebrate P2X4 orthologs (rodents, bovine, xenopus, zebrafish) for their sensitivity to BX450 and noticed that the antagonist property of BX430 is not directly related to the degree of homology with human P2X4. Human and bovine P2X4 (94% sequence similarity) share a high sensitivity to BX430. However, xenopus and zebrafish P2X4 receptor channels (only 81% and 75% similarity with human P2X4, respectively) also display a significant sensitivity to BX430 while rodent P2X4 orthologs (93% sequence similarity with human P2X4 for rat and mouse subunits) are resistant to BX430 blockade. All vertebrate P2X4 receptors tested display similar current phenotypes, therefore, a differential effect of BX430 independent from the global homology strongly implies that a specific sequence or subdomain is shared between BX430-sensitive P2X4 orthologs. Focusing on the ectodomain, which was found to be site of action of BX430 (Ase et al., 2015), we identified a hydrophobic residue (isoleucine or methionine) at position 312 (human numbering), present in all BX430-sensitive P2X4 receptors but replaced by the polar residue threonine in rodents, as the determinant of BX430 antagonist effect. Indeed we demonstrated that Ile312 plays a critical role by introducing the loss-of-inhibition mutation I312T in human P2X4 and showing that it converts it into a rodent-like BX430-insensitive receptor. Reciprocally, we conferred a BX430-sensitive phenotype to the rat P2X4 receptor channel by introducing the gain-of-inhibition mutation T312I, convincingly proving that the nature of the amino acid at position 312 determines sensitivity or resistance to BX430.

Since isoleucine and methionine are two hydrophobic amino acids with an aliphatic side chain, these physicochemical

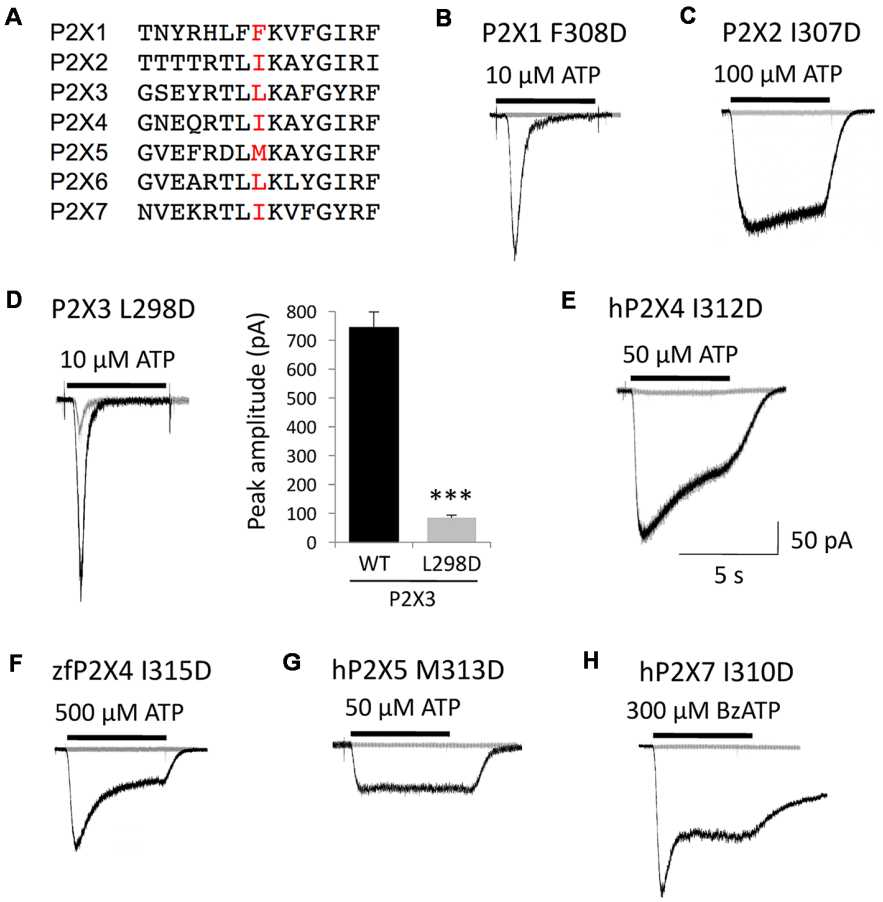

FIGURE 6 | The silencing mutation I312D in human P2X4 disrupts a key functional domain conserved in the P2X gene family. **(A)** Alignment of partial primary sequences of human P2X channel subunits with a focus on the homologous extracellular domain around Ile312 in P2X4. **(B–H)** Representative agonist-evoked current traces showing the profound inhibitory impact of mutation I312D on human P2X4 and of the equivalent substitutions indicated on all other human homomeric P2X subtypes, as well as on zebrafish P2X4. **(D)** Whereas all other subtypes are rendered silent, the P2X3 receptor remains functional although its ATP-gated channel activity is severely disrupted by the mutation L298D, as indicated by quantitative comparison of peak current amplitudes. ***$P < 0.001$ (n = 6–13).

properties might be required for BX430 binding and inhibitory effects. This was tested by swapping isoleucine for various amino acids. Systematic single mutations on the isoleucine315 of human P2X4 with amino acids with different types of side-chain structures (see **Table 1**) revealed that its substitution by amino acids with negatively-charged polar, polar uncharged, or aromatic side chains renders the P2X4 channel either silent or insensitive to blockade by BX430. Unexpectedly, replacing isoleucine with its regioisomer leucine or with glycine also disrupts BX430 sensitivity while inserting the bulky aromatic side chains of tyrosine and tryptophan at position 312 in human P2X4 converts BX430 into a positive allosteric modulator. The residues preserving BX430 sensitivity were found to be the hydrophobic alanine or valine and to a lesser extent the positively-charged lysine.

From this series of mutagenesis experiments, apart from the exclusion of polar uncharged, negatively-charged or aromatic side chains at position 312 (in human P2X4), the diversity of side chains compatible with binding and inhibitory effects of BX430 confirms the folding complexity of the ectodomain in P2X channel subunits. We took advantage of the fact that the homologous isoleucine in the ectodomain of wild-type zebrafish P2X4 (Ile315) is also critical for its blockade by BX430, and that the crystallized form ΔzfP2X4(A)-GFP remains sensitive to BX430, to look at the 3D structure of the BX430 binding pocket in models of zebrafish and human P2X4 receptors. Molecular dynamics simulation based on the crystal structure of ΔzfP2X4(A)-GFP allowed us to identify a groove at the surface of the ectodomain around Ile315 where BX430 could bind with relevant affinity. A homologous binding domain was confirmed in the virtual model of human P2X4, also based on ΔzfP2X4(A)-GFP. These simulations predict that Tyr300 and Asp88, with Ile312 (human numbering), participate in the coordination of the BX430 binding. Another interesting observation from these structural models is that the docking site for BX430 was found to not overlap with the ATP binding site, confirming our empiric results on the noncompetitive allosteric nature of the inhibitory effects of BX430 (Ase et al., 2015). From these modeling data, we conclude that the most likely mechanisms of action of BX430 on P2X4 receptor channels is a structural locking of this subregion

of the ectodomain (Jiang et al., 2013; Mansoor et al., 2016) induced by its binding to the allosteric site involving Asp88, Tyr300 and Ile312 in human P2X4. Locking or stabilization mechanisms involving different parts of the ectodomain have been proposed for the inhibition of P2X3 by the antagonists TNP-ATP (Mansoor et al., 2016) and AF-219 (Wang et al., 2018), and also for the inhibition of P2X7 by TNP-ATP (Kasuya et al., 2017) based on crystal structures.

A Key Functional Domain Conserved in the P2X Family

In our extended series of amino acid substitutions targeting Ile312 in human P2X4, the only mutation that induced a loss of ATP-gated channel activity in the absence of antagonist was I312D. It remains to be elucidated why the mutation to glutamate, also with a negatively charged side chain, does not affect hP2X4 as does aspartate. Nevertheless, such a strong functional impact of replacing a single isoleucine residue with aspartate highlighted an important role of Ile312 and its proximal environment in the normal function of the P2X4 channel. The selective binding of BX430 likely requires multiple P2X4-specific interactions beyond the key conserved residues identified in our docking model. However, as all P2X receptor channels share similar basic mechanisms of operation and a significant degree of homology in the corresponding pre-TM2 region, we predicted that mutation of this binding domain in other P2X subtypes would have similar loss-of-function effects. Indeed, virtually all human P2X subtypes, as well as zebrafish P2X4, were fully silenced by a single mutation replacing the residue at position 312 (human P2X4 numbering) with aspartate. The only exception was the mutation L298D introduced in P2X3, although the channel activity was severely reduced. Therefore, we can conclude that this aspartate mutation reveals the existence of a conserved inhibitory allosteric site present in most, if not all, P2X receptor subtypes. Interestingly, the residue I310 in P2X7 (homologous to I312 in P2X4) has been reported to be in close proximity to a non-competitive allosteric antagonist site and the mutation I310C was found to disrupt P2X7 channel activity after modification with the cysteine reagent MTS-TPAE (Karasawa and Kawate, 2016). Altogether, this provides further evidence that the structure around I312 (human P2X4 numbering), located in β-strand #14 in the pre-TM2 region of the "upper body" of P2X subunits (Hattori and Gouaux, 2012), plays a key role in P2X function.

A cluster of positively-charged amino acids is responsible for coordinating the phosphate groups of the bound ATP (Evans, 2010; Hattori and Gouaux, 2012) and one of these, Lys313 (human P2X4 numbering), is adjacent to the aspartate mutation in all the P2X receptors. This might lead to the neutralization of the positive charge of Lys313 and could explain the insensitivity to ATP. Alternatively, the aspartate mutation could compromise the channel by disrupting the proper folding of the ectodomain required for trimeric assembly, for translocation to the plasma membrane and/or for gating the opening of the cationic pore. We did not observe a dominant-negative effect of the mutant P2X4 I312D subunit on the current amplitude of co-expressed wild-type P2X4 channels (data not shown), therefore a disruption of subunit oligomerization and/or trafficking is unlikely. The structural changes induced by the aspartate mutation could mimic the inhibitory effects of BX430 bound on P2X4 receptor channels by hindering ATP-induced gating movements (Jiang et al., 2013; Karasawa and Kawate, 2016; Wang et al., 2018).

From a translational point of view, the localization of a generic allosteric inhibitory site conserved in all P2X receptors might facilitate the discovery and design of P2X subtype-selective non-competitive antagonists of therapeutic value, for example through the virtual screening of compound libraries on high-resolution crystal structures.

AUTHOR CONTRIBUTIONS

AA performed the experiments, analyzed the data and wrote the manuscript. ÉT performed modeling, molecular dynamics simulations and wrote the manuscript. PS designed the project, analyzed the data and wrote the manuscript.

FUNDING

This work was possible with the support of operating grants from Canadian Institutes of Health Research (CIHR; PJT-153098; PS) and Natural Sciences and Engineering Research Council of Canada (NSERC; RGPIN-2015-04876; PS).

ACKNOWLEDGMENTS

We thank Dominique Blais (Montreal Neurological Institute) and Helmi Zaghdane (Zamboni Chemical Solutions, Montreal, Canada) for their expert technical assistance.

REFERENCES

Ase, A. R., Honson, N. S., Zaghdane, H., Pfeifer, T. A., and Séguéla, P. (2015). Identification and characterization of a selective allosteric antagonist of human P2X4 receptor channels. *Mol. Pharmacol.* 87, 606–616. doi: 10.1124/mol.114.096222

Bowler, J. W., Bailey, R. J., North, R. A., and Surprenant, A. (2003). P2X4, P2Y1 and P2Y2 receptors on rat alveolar macrophages. *Br. J. Pharmacol.* 140, 567–575. doi: 10.1038/sj.bjp.0705459

Burnstock, G., and Kennedy, C. (2011). P2X receptors in health and disease. *Adv. Pharmacol.* 61, 333–372. doi: 10.1016/b978-0-12-385526-8.00011-4

Coddou, C., Yan, Z., Obsil, T., Huidobro-Toro, J. P., and Stojilkovic, S. S. (2011). Activation and regulation of purinergic P2X receptor channels. *Pharmacol. Rev.* 63, 641–683. doi: 10.1124/pr.110.003129

Evans, R. J. (2010). Structural interpretation of P2X receptor mutagenesis studies on drug action. *Br. J. Pharmacol.* 161, 961–971. doi: 10.1111/j.1476-5381.2010.00728.x

Garcia-Guzman, M., Soto, F., Gomez-Hernandez, J. M., Lund, P. E., and Stühmer, W. (1997). Characterization of recombinant human P2X4 receptor reveals pharmacological differences to the rat homologue. *Mol. Pharmacol.* 51, 109–118. doi: 10.1124/mol.51.1.109

Habermacher, C., Dunning, K., Chataigneau, T., and Grutter, T. (2016). Molecular structure and function of P2X receptors. *Neuropharmacology* 104, 18–30. doi: 10.1016/j.neuropharm.2015.07.032

Hattori, M., and Gouaux, E. (2012). Molecular mechanism of ATP binding and ion channel activation in P2X receptors. *Nature* 485, 207–212. doi: 10.1038/nature11010

Jiang, R., Taly, A., and Grutter, T. (2013). Moving through the gate in ATP-activated P2X receptors. *Trends Biochem. Sci.* 38, 20–29. doi: 10.1016/j.tibs.2012.10.006

Jones, C. A., Chessell, I. P., Simon, J., Barnard, E. A., Miller, K. J., Michel, A. D., et al. (2000). Functional characterization of the $P2X_4$ receptor orthologues. *Br. J. Pharmacol.* 129, 388–394. doi: 10.1038/sj.bjp.0703059

Karasawa, A., and Kawate, T. (2016). Structural basis for subtype-specific inhibition of the P2X7 receptor. *Elife* 5:e22153. doi: 10.7554/elife.22153

Kasuya, G., Yamaura, T., Ma, X. B., Nakamura, R., Takemoto, M., Nagumo, H., et al. (2017). Structural insights into the competitive inhibition of the ATP-gated P2X receptor channel. *Nat. Commun.* 8:876. doi: 10.1038/s41467-017-00887-9

Kawate, T., Michel, J. C., Birdsong, W. T., and Gouaux, E. (2009). Crystal structure of the ATP-gated $P2X_4$ ion channel in the closed state. *Nature* 460, 592–598. doi: 10.1038/nature08198

Mansoor, S. E., Lü, W., Oosterheert, W., Shekhar, M., Tajkhorshid, E., and Gouaux, E. (2016). X-ray structures define human $P2X_3$ receptor gating cycle and antagonist action. *Nature* 538, 66–71. doi: 10.1038/nature19367

Michel, A. D., Ng, S. W., Roman, S., Clay, W. C., Dean, D. K., and Walter, D. S. (2009). Mechanism of action of species-selective $P2X_7$ receptor antagonists. *Br. J. Pharmacol.* 156, 1312–1325. doi: 10.1111/j.1476-5381.2009.00135.x

Nörenberg, W., Sobottka, H., Hempel, C., Plötz, T., Fischer, W., Schmalzing, G., et al. (2012). Positive allosteric modulation by ivermectin of human but not murine P2X7 receptors. *Br. J. Pharmacol.* 167, 48–66. doi: 10.1111/j.1476-5381.2012.01987.x

North, R. A. (2002). Molecular physiology of P2X receptors. *Physiol. Rev.* 82, 1013–1067. doi: 10.1152/physrev.00015.2002

Pasqualetto, G., Brancale, A., and Young, M. T. (2018). The molecular determinants of small-molecule ligand binding at P2X receptors. *Front. Pharmacol.* 9:58. doi: 10.3389/fphar.2018.00058

Raouf, R., Chabot-Doré, A. J., Ase, A. R., Blais, D., and Séguéla, P. (2007). Differential regulation of microglial P2X4 and P2X7 ATP receptors following LPS-induced activation. *Neuropharmacology* 53, 496–504. doi: 10.1016/j.neuropharm.2007.06.010

Saul, A., Hausmann, R., Kless, A., and Nicke, A. (2013). Heteromeric assembly of P2X subunits. *Front. Cell. Neurosci.* 7:250. doi: 10.3389/fncel.2013.00250

Serrano, A., Mo, G., Grant, R., Paré, M., O'Donnell, D., Yu, X. H., et al. (2012). Differential expression and pharmacology of native P2X receptors in rat and primate sensory neurons. *J. Neurosci.* 32, 11890–11896. doi: 10.1523/JNEUROSCI.0698-12.2012

Stojilkovic, S. S., Tomic, M., He, M. L., Yan, Z., Koshimizu, T. A., and Zemkova, H. (2005). Molecular dissection of purinergic P2X receptor channels. *Ann. N Y Acad. Sci.* 1048, 116–130. doi: 10.1196/annals.1342.011

Trang, T., Beggs, S., and Salter, M. W. (2012). ATP receptors gate microglia signaling in neuropathic pain. *Exp. Neurol.* 234, 354–361. doi: 10.1016/j.expneurol.2011.11.012

Tsuda, M., Shigemoto-Mogami, Y., Koisumi, S., Mizokoshi, A., Kohsaka, S., Salter, M. W., et al. (2003). P2X4 receptors induced in spinal microglia gate tactile allodynia after nerve injury. *Nature* 424, 778–783. doi: 10.1038/nature01786

Ulmann, L., Hatcher, J. P., Hughes, J. P., Chaumont, S., Green, P. J., Conquet, F., et al. (2008). Up-regulation of P2X4 receptors in spinal microglia after peripheral nerve injury mediates BDNF release and neuropathic pain. *J. Neurosci.* 28, 11263–11268. doi: 10.1523/JNEUROSCI.2308-08.2008

Wang, J., Wang, Y., Cui, W. W., Huang, Y., Yang, Y., Liu, Y., et al. (2018). Druggable allosteric site of P2X3 receptors. *Proc. Natl. Acad. Sci. U S A* 115, 4939–4944. doi: 10.1073/pnas.1800907115

Yamamoto, K., Sokabe, T., Matsumoto, T., Yoshimura, K., Shibata, M., Ohura, N., et al. (2006). Impaired flow-dependent control of vascular tone and remodeling in P2X4-deficient mice. *Nat. Med.* 12, 133–137. doi: 10.1038/nm1338

Conflict of Interest Statement: ÉT was employed by the company Molecular Forecaster Inc.

The remaining authors declare that the research was conducted in the absence of any commercial or financial relationships that could be construed as a potential conflict of interest.

frontiers in Cellular Neuroscience

ORIGINAL RESEARCH
published: 11 April 2019
doi: 10.3389/fncel.2019.00130

Accumbal Adenosine A_{2A} Receptors Enhance Cognitive Flexibility by Facilitating Strategy Shifting

*Jianhong Zhou[1,2], Beibei Wu[1,2], Xiangxiang Lin[1,2], Yuwei Dai[1,2], Tingting Li[1,2], Wu Zheng[1,2], Wei Guo[1,2], Sergii Vakal[1], Xingjun Chen[1,2] and Jiang-Fan Chen[1,2]**

[1]Molecular Neuropharmacology Laboratory, School of Optometry and Ophthalmology and Eye Hospital, Wenzhou Medical University, Wenzhou, China, [2]State Key Laboratory of Optometry & Vision Science, Wenzhou, China

The deficits of cognitive flexibility (including attentional set-shifting and reversal learning) concomitant with dysfunction of the striatum are observed in several neuropsychiatric disorders. Rodent and human studies have identified the striatum [particularly the dorsomedial striatum (DMS) and nucleus accumbens (NAc)] as the critical locus for control of cognitive flexibility, but the effective neuromodulator and pharmacological control of cognitive flexibility remains to be determined. The adenosine A_{2A} receptors (A_{2A}Rs) are highly enriched in the striatopallidal neurons where they integrate dopamine and glutamate signals to modulate several cognitive behaviors, but their contribution to cognitive flexibility control is unclear. In this study, by coupling an automated operant cognitive flexibility task with striatal subregional knockdown (KD) of the A_{2A}R *via* the Cre-loxP strategy, we demonstrated that NAc A_{2A}R KD improved cognitive flexibility with enhanced attentional set-shifting and reversal learning by decreasing regressive and perseverative errors, respectively. This facilitation was not attributed to mnemonic process or motor activity as NAc A_{2A}R KD did not affect the visual discrimination, lever-pressing acquisition, and locomotor activity, but was associated with increased attention and motivation as evident by the progressive ratio test (PRT). In contrast to NAc A_{2A}Rs, DMS A_{2A}Rs KD neither affected visual discrimination nor improved set-shifting nor reversal learning, but promoted the effort-related motivation. Thus, NAc and DMS A_{2A}Rs exert dissociable controls of cognitive flexibility with NAc A_{2A}Rs KD selectively enhancing cognitive flexibility by facilitating strategy shifting with increased motivation/attention.

Keywords: adenosine A_{2A} receptors, nucleus accumbens, dorsomedial striatum, attentional set-shifting, reversal learning, motivation, attention

OPEN ACCESS

Edited by:
David Blum, INSERM U1172 Centre de Recherche Jean Pierre Aubert, France

Reviewed by:
Serge N. Schiffmann, Free University of Brussels, Belgium
Rodrigo A. Cunha, Universidade de Coimbra, Portugal

****Correspondence:***
Jiang-Fan Chen
chenjf555@gmail.com

Received: *16 February 2019*
Accepted: *14 March 2019*
Published: *11 April 2019*

Citation:
Zhou J, Wu B, Lin X, Dai Y, Li T, Zheng W, Guo W, Vakal S, Chen X and Chen J-F (2019) Accumbal Adenosine A_{2A} Receptors Enhance Cognitive Flexibility by Facilitating Strategy Shifting. Front. Cell. Neurosci. 13:130. doi: 10.3389/fncel.2019.00130

INTRODUCTION

Cognitive flexibility is an essential executive function that enables individuals and species to adapt to new surroundings in the constantly changing environment and can be divided into two distinct components including attentional set-shifting (extra-dimensional shifting) and reversal learning (intra-dimensional shifting). The impairment of cognitive flexibility is often observed in several mental disorders concomitant with dysfunction of the basal ganglia, including attentional deficit and hyperactivity disorder (ADHD; Reeve and Schandler, 2001), early Parkinson's disease (Cools et al., 2001), schizophrenia (Pantelis et al., 1999), drug addiction (Kalivas and Volkow, 2005) and

autism (Leung and Zakzanis, 2014). The effective pharmacological strategies to improve the deficit in cognitive flexibility in neuropsychiatric disorders are critically needed.

Rodent and primate studies have revealed the distinct cortical-subcortical circuits subserved cognitive flexibility (Birrell and Brown, 2000; McAlonan and Brown, 2003; Ragozzino, 2007). Furthermore, as the primary brain region receiving cortical glutamatergic inputs, striatum also plays an essential role in neuronal control of cognitive flexibility. The striatum is an anatomically and functionally heterogeneous structure that can be distinguished into the dorsomedial striatum (DMS, involving goal-directed behavior), dorsolateral striatum (involving habit formation) and the ventral striatum [nucleus accumbens (NAc), involving reward, motivation and emotion; Yin and Knowlton, 2006; Bagot et al., 2015; Li et al., 2016]. The dorsal striatum receives glutamatergic excitatory afferents from the sensorimotor, prefrontal cortical areas and the intralaminar thalamic nuclei (Hunnicutt et al., 2016; Kato et al., 2018), as well as dopaminergic innervations from the substantia nigra pars compacta (Horvitz, 2002). The ventral striatum mainly receives convergent glutamatergic inputs/projections from the ventral hippocampus (vHIP), medial prefrontal cortex (mPFC), basolateral amygdala (BLA) and paraventricular thalamus (French and Totterdell, 2002; Sesack and Grace, 2010; Britt et al., 2012), and dopaminergic inputs from the ventral tegmental area (VTA; Goto and Grace, 2008). Accordingly, NAc has been shown to be critical to control cognitive flexibility (Haluk and Floresco, 2009; Ding et al., 2014; Cui et al., 2018). This NAc control of cognitive flexibility may be associated with NAc ability to modulate attention (Christakou et al., 2004; Salgado and Kaplitt, 2015), working memory (Takahashi et al., 2011; Laplante et al., 2012) and goal-directed behavior (Mannella et al., 2013). Similarly, DMS has also an important role in the control of cognitive flexibility and other cognitive behavior (Li et al., 2016, 2018; Kato et al., 2018; Zhu et al., 2018).

Both glutamatergic and dopaminergic signaling in the striatum are critical for the control of cognitive flexibility by strategy shifting. For example, the glutamatergic signaling from the mPFC is engaged, specifically, in mediating attentional set-shifting extradimensionally, while the glutamate signaling from the orbitofrontal cortex (OFC) selectively controls reversal learning intradimensionally (Birrell and Brown, 2000; Ragozzino, 2007). Moreover, the dopaminergic signaling regulates some elements of behavior flexibility as well as various learning and memory-associated behaviors (Haluk and Floresco, 2009; Cui et al., 2018). In addition, other neuromodulators such as endocannabinoid (Varvel and Lichtman, 2002; Klugmann et al., 2011), acetylcholine (Aoki et al., 2015; Prado et al., 2017), GABA (Yawata et al., 2012) and BDNF (Parikh et al., 2016a,b) and adenosine (Wei et al., 2011) have been implicated in the control of cognitive flexibility. However, the control of cognitive flexibility by neuromodulators other than glutamate and dopamine systems in the different striatal regions is still largely unexplored.

The adenosine A_{2A} receptors (A_{2A}Rs) are highly enriched in the striatopallidal neurons (Svenningsson et al., 1999) where A_{2A}Rs interact with dopamine D_2 receptors (Schiffmann et al., 2010) and N-methyl-D-aspartate receptors (NMDARs; Higley and Sabatini, 2010), as well as metabotropic glutamate 5 receptors (mGlu5; Ferré et al., 2002). Striatopallidal A_{2A}Rs can integrate glutamatergic and dopaminergic signals to control striatal synaptic plasticity and various cognitive behaviors in both normal and abnormal conditions (Chen et al., 2013; Chen, 2014). Recent studies from our and other labs have demonstrated that activation of the striatopallidal A_{2A}Rs exerts inhibitory control of various cognitive behaviors such as working memory and goal-directed behavior (Wei et al., 2014; Li et al., 2016, 2018). Thus, we propose that the A_{2A}R inaction represents a novel target for reversing cognitive deficit in neuropsychiatric disorders (Chen, 2014). This proposal has high translational potential given that the A_{2A}R antagonist is in clinical phase III trial for the treatment of Parkinson's disease with a notable safety profile (Chen et al., 2013). However, the exact role of striatal A_{2A}Rs in the control of cognitive flexibility (i.e., attentional set-shifting and reversal learning) is mostly unclear. Limited studies showed that A_{2A}R inactivation is associated either with impaired (Amodeo et al., 2018) or enhanced (Wei et al., 2011) or no effect (O'Neill and Brown, 2007) on cognitive flexibility. Moreover, as the dorsomedial and dorsolateral striatum A_{2A}Rs exert distinct control of goal-directed and habitual behaviors, respectively (Li et al., 2016), the specific contributions of the striatopallidal A_{2A}Rs in NAc and DMS to the control of strategy shifting remain to be determined.

In this study, we adapted the automated operant cognitive flexibility task which minimizes the procedural disadvantages and vulnerability to manual error and subjective interpretation of the cross-maze task and the digging task to test behavioral flexibility in rodents (Haluk and Floresco, 2009; Brady and Floresco, 2015; Parikh et al., 2016a). This task (including visual discrimination, attentional set-shifting, and reversal learning) placed heavier emphasis on response conflicts and shared similar features to the Wisconsin Card Sorting Task established to assess the cognitive flexibility of human beings (Monchi et al., 2001). By coupling this cognitive flexibility task with the Cre-loxP-mediated focal knockdown (KD) of A_{2A}Rs in the DMS and NAc, we critically determined the effects of DMS and NAc A_{2A}R on cognitive flexibility. We further explored the possible role of a motivational factor in the modulation of A_{2A}R control of strategy shifting by progressive ratio test (PRT).

MATERIALS AND METHODS

Subjects

The animal protocols were approved by the Institutional Ethics Committee for Animal Use in Research and Education at Wenzhou Medical University, China. All mice were housed at a constant temperature (24 ± 0.5°C) with a relative humidity of 60 ± 2% and controlled by a 12-h light-dark cycle (light on at 8:00 A.M.). Except for the periods of food-restriction for the purpose of behavioral training and testing, all mice were given *ad libitum* access to food and water. The $A_{2A}R^{flox/flox}$ mice were generated and then backcrossed to C57BL/6 for 10 generations to generate congenic $A_{2A}R^{flox/flox}$ in the C57BL/6 genetic

background, and characterized as we described previously (Shen et al., 2008; Augusto et al., 2013).

The Cre-loxP-Mediated Conditional A_{2A}Rs Knockdown Strategy

Male $A_{2A}R^{flox/flox}$ mice, aged 8–12 weeks, were used in the experiments. Conditional KD of the A_{2A}R gene was achieved by injecting Cre recombinase-expressing AAV to the DMS (AP, +0.98 mm; ML, ±1.20 mm; DV, 2.50 mm) or NAc (AP, +1.3 mm; ML, ±1.00 mm; DV, 3.90 mm). Specifically, AAV8-CAG-Cre-ZsGreen (200 nl) was injected bilaterally into $A_{2A}Rs^{flox/flox}$ mice *via* a Hamilton injection syringe to achieve focal KD of A_{2A}Rs in targeted subregions. $A_{2A}R^{flox/flox}$ mice injected with AAV8-CAG-ZsGreen were used as the control. The mice were allowed to recover for 3 weeks, and the conditional KD of A_{2A}Rs was carried out before behavioral training.

Open-Field Test and Spontaneous Alternation Test in the Y-maze

For the open-field test, mice were placed in the center of a white, dimly lit open-field chamber (40 × 40 cm) and allowed to explore the environment for a total of 10 min freely. The center of the open-field was defined as >20 cm apart from all four walls. Total movement distance and the time spent in the center and periphery were recorded by an automated video tracking system (EthoVision system, Noldus). For spontaneous alternation test in the Y-maze, all the mice were placed into a Y-maze and allowed to navigate for 8 min freely. The sequence of animal entries to each arm and the number of entries were recorded. Correct spontaneous alternation was defined as the continuous entry into three arms (such as 1, 2, 3 or 1, 3, 2) as described previously (Zheng et al., 2018).

Mouse Operant Cognitive Flexibility Task

We adapted standard operant conditioning chambers (MED Associates., Albans, VT, USA) for an automated operant cognitive flexibility task as described previously with slight modifications (Haluk and Floresco, 2009; Brady and Floresco, 2015; Parikh et al., 2016a). All the operant procedures and data collection in this task can be automatically controlled by a customized program. Briefly, in the operant conditioning chambers, two retractable levers were mounted at either side of the receptacle with a central reward port attached to a fluid dipper between them, and a light stimulus was placed above each lever. Animals were manually handled, and their body weight was restricted to 80%–85% of their original weight before the beginning of the test.

Autoshaping and Side Preference Task

When shaping in the operant chambers, all the mice had 1 day magazine training in which as long as the mice poked the central reward port, they would receive 10 μl of 20% sucrose solution as a reward. After that, all the mice were autoshaped on an FR-1 schedule of reinforcement in which mice were required to press the lever to get the reward (each lever press leading to one reinforcement delivered). In this training, only one lever was present, but the reinforced lever (left or right lever) was counterbalanced across animals and training days to prevent the mice from forming a lever bias. After meeting the criterion of getting 50 rewards per session for two consecutive days, mice were advanced to the retractable lever training sessions to familiarize them with the extension and retraction of the levers. In these training sessions, each trial consisted of a lever presentation (either left or right) for 8 s, and the lever was extended in a pseudorandom order with no more than two consecutive trials extending the same lever. Each lever press response was rewarded and terminated the lever extension. If the animal did not respond within 8 s, the lever would automatically be retracted, and the trial was recorded as an omission. To control for any novelty effect that might be associated with the visual stimulus during the subsequent stage of the task, the activated lever was randomly associated with an unpredictably occurring illumination of the panel light. Trials were presented with an inter-trial interval (ITI) of 9 ± 3 s. The day after reaching the criteria (40 rewards and ≤20% omissions for two consecutive days), the side preference of animals was assessed. The side preference task consisted of 10 trials. In every trial, both levers were inserted into the chamber simultaneously, and the initial reward was available after responding on either lever, but the mice had to respond on the lever opposite to the one chosen initially to get a reward upon the following response. If the mice pressed the same lever as the initial choice, no reinforcement would be delivered. This task continued until the animals chose the lever opposite to that chosen initially and the number of responses on each lever would be recorded. After choosing both levers with an ITI of 12 s, a new trial commenced. The lever (right or left) that mice responded on the initial choice of a trial was recorded and counted as its bias lever. If the total number of responses on each lever was comparable, the lever that mice chose initially six or more times over 10 total trials was considered its side bias. However, if a disproportional number of responses was made on one lever (greater than a 2:1 ratio), the lever was considered its side bias.

After the side preference testing, all the mice were officially progressed to the mouse operant cognitive flexibility task, which consisted of three different phases: visual discrimination, strategy set-shifting, and reversal learning.

Visual Discrimination Phase

During the visual discrimination phase, the two levers were present at the same time, and either of the levers was randomly illuminated with the light stimulus, and mice were required to discern the lever with an activated cue light to get a reward within 8-s test period after the lever extension. All trials were started with a 2-s acoustic stimulus, the lever and cue light were automatically retracted and turned off if any lever pressing happened or no response happened within 8 s (the trial counted as an omission response). The ITI was 9 ± 3 s. A lever press response on the cued lever was scored as "correct response," whereas pressing the non-illuminated lever was defined as "incorrect response." Each session included 40 trials, and all the mice were trained for one session per day. When the animals were able to meet the criterion with 75% correct responses for three consecutive days in the phase of visual discrimination,

all the mice were advanced to the phase of the attentional set-shifting.

Set-Shifting Phase

During this phase, animals were required to shift to the lever-pressing response task, which reinforced animals for responding on the lever opposite their side preference, regardless of stimulus light (cue) illumination. The experimental parameters remained identical to the visual discrimination phase except that the contingencies were altered in such a way that the animals were requested to press the lever other than their bias lever to get reward irrespective of the cue presentation which remained pseudorandom. For example, if the mice bias lever is the left lever, in this phase the mice have to press the right lever to get a reward and ignore the cue presentation. Animals that had successfully attained the criterion (80% correct responses for three consecutive days) at this stage were moved to the reversal learning phase. The visual discrimination task was the "Set" task in this phase, and the response task was the "Shift" task in this phase. The Set-shifting phase also can be termed as extradimensional shifting which referred to the ability to actively suppress a previously learned response strategy while acquiring a new competing strategy, particularly across stimulus dimensions—for example, switching from performing visually-based discrimination to lever-pressing response discrimination in our behavioral paradigm.

Reversal Phase

During this phase of training, the reinforced lever was reversed again; animals were required to press the opposite lever, which was assigned to the correct lever during the preceding phase (set-shifting) regardless of the position of the illuminated cue until reaching the criterion (80% correct responses for three consecutive days). For example, the mice have to press the left lever to get a reward in this phase, if the mice were required to press the right lever to get a reward in the Set-shifting phase. Reversal learning also can be termed as intradimensional shifting which involved a change in response strategy but within the same stimulus dimension—for example, switching from a left lever-based reinforcement to a right lever-based reinforcement in our reversal phase.

The number of correct responses, errors, omissions and response latencies were automatically obtained for each behavioral session. Response accuracies were calculated for each session according to the formula: correct responses/(correct + incorrect responses) $\times$ 100%. The total number of performed trials to criterion, errors to criterion, and omissions were obtained for each training phase using the above-described criteria. The incorrect responses were divided into three different error types: perseverative, regressive and never-reinforced errors. In the strategy set-shifting phase, these errors were classified as perseverative if the animal responded to the incorrect lever when the visual cue was illuminated above it on more than 12 out of 20 trials ($\geq$60%) within a session. If the animals made $<$60% incorrect responses, these errors were identified as regressive in all subsequent sessions. Never-reinforced errors occurred when the animal responded on the incorrect lever while the visual cue was presented on the other side. In the reversal learning phase, if the animals made $\geq$60% incorrect presses ($\geq$24/40 of performed trials), these errors were scored as perseverative. If the animals made $<$60% incorrect responses, errors were scored as regressive in all subsequent sessions. There were no never-reinforced errors in the reversal learning test.

Progressive Ratio Test

The PR task was used to evaluate effort-related motivation by quantifying the number of lever presses that a subject was willing to expend to earn a reward in operant conditioning chambers. The experimental paradigm was adapted from the method described previously with minor modifications (Carvalho Poyraz et al., 2016; Tsutsui-Kimura et al., 2017). Briefly, mice were initially trained to press the lever on a fixed ratio (FR)-1 reinforcement schedule whereby a single lever press elicited the delivery of 10 μl of 20% sucrose solution as a reward in the magazine. Only one lever was present, and the allocation of right and left levers was counterbalanced between mice. Following four successive sessions of FR-1 reinforcement schedule, the schedule was upgraded to FR-5 in which five active lever presses triggered the delivery of the reward and lasted for 3 days. Each FR training session lasted 1 h or until the delivery of 60 rewards. After that, all the mice were moved to the PRT. The response ratio schedule during PR testing was calculated according to the formula: [5e (R$\times$0.2)]-5, where R was equal to the number of food rewards already earned plus 1. Thus, the number of responses required to earn a reward followed the order: 1, 2, 4, 6, 9, 12, 15, 20, 25, 32, 40, 50, 62, 77, 95, and so on. The final completed ratio represented the breakpoint. A PR session lasted up to 1 h maximum and failure to press the lever in any 3-min period resulted in the termination of the session.

Immunofluorescence

Mice were deeply transcardially perfused with 4% paraformaldehyde. Brain slices (30 μm) were sectioned, and immunofluorescence staining was performed on free-floating sections as described previously (Li et al., 2016). Brain slices were incubated with primary anti-A_{2A}R (Santa Cruz, 1:50) antibodies overnight. The sections were then rinsed and incubated with Alexa 488 conjugated secondary antibodies (Invitrogen, 1:1,000). The slices were washed and mounted, and images were acquired and quantified as mean integrated optical density using Image Pro Plus software.

Statistical Analyses

All data were presented as means $\pm$ standard error of the mean (SEM). Two-way analysis of variance (ANOVA) for repeated-measures with *post hoc* Bonferroni's test was used for the comparison of multiple factors (i.e., A_{2A}R KD $\times$ training sessions). Error subtype and latency to lever were analyzed separately using Two-way ANOVAs, with Treatment as the between-subjects factor and Error Type (perseverative, regressive and never-reinforced errors) or Choice (correct/incorrect) as a within-subjects factor. Significant main effects of Treatment were followed up with multiple comparisons using Bonferroni's test. Student's *t*-test was performed for comparison of the two groups (A_{2A}R KD vs. control). Statistical comparisons were

performed using SPSS statistics version 25. The significance of the differences was considered for $p < 0.05$.

RESULTS

Conditional A_{2A}R Knockdown in the NAc by the Cre-loxP Strategy

To focally knockdown the A_{2A}Rs in the NAc, we employed Cre-loxP strategy by injecting AAV8-CAG-Cre-ZsGreen (200 nl) or AAV8-CAG-ZsGreen (control virus) bilaterally into the NAc of $A_{2A}R^{flox/flox}$ mice. Three weeks later, the specific areas of virus expression were verified by immunofluorescence. As can be seen in **Figure 1C**, the black color represents the largest area of virus transfection, and the gray color depicts the smallest one. Furthermore, we observed that the A_{2A}Rs expression (the red fluorescence) was reduced selectively in the Cre-expressing regions of the NAc (indicated by green fluorescence, **Figure 1B**, right panels) but not in the control virus-expressing regions (**Figure 1A**, right panels). Optical intensity analysis of the A_{2A}R immunostaining confirmed that the expression level of A_{2A}R in the NAc was decreased by 71% after transfection with AAV8-CAG-Cre-ZsGreen, as compared with the NAc transfected with AAV8-CAG-ZsGreen (**Figure 1C**). Thus, the A_{2A}R expression was selectively and efficiently knocked down in NAc.

NAc A_{2A}R Knockdown Does Not Affect Visual Discrimination but Facilitates Attentional Set-Shifting and Reversal Learning

Three weeks after the surgery, we implemented the mouse operant cognitive flexibility task to determine the functional involvement of striatal subregion-specific A_{2A}Rs in the behavioral cognitive flexibility. This paradigm consists of three different phases: visual discrimination, attentional set-shifting, and reversal learning. In the phase of the visual discrimination, mice were trained to press the specific (left or right) lever above which the cue light was randomly illuminated to get the reward (**Figure 2I**). NAc A_{2A}R KD did not change the total number of trials needed to reach the criterion compared to control (**Figures 2A–C**, $p > 0.05$). The total number of errors and omissions needed to reach the criterion were also similar between the two groups (**Figure 2B**, errors, $p = 0.1164$; **Figure 2C**, omissions, $p = 0.637$). Thus, NAc A_{2A}R KD did not affect the performance of visual discrimination.

After reaching the criterion of an average correct response of >75% on three consecutive days in the visual discrimination test, the mice were moved to the attentional set-shifting phase which required shifting attention away from a visual cue-reinforced dimension to the spatial location-reinforced dimension to obtain the reward. In this phase, the animals were required to press the non-preferred lever to obtain the reward regardless of the position of the cue light (**Figure 2II**). Both control and NAc A_{2A}R KD groups increased their correct response ratio with increasing sessions (**Figure 2D**, the training session effect, $F_{(4,44)} = 124.187$, $p < 0.001$, two-way ANOVA for repeated measures). However, the correct response ratio in the A_{2A}R KD group increased much faster than in the control (**Figure 2D**, the group effect, $F_{(1,11)} = 10.123$, $p = 0.009$) and this effect was dependent on the training sessions (**Figure 2D**, the group × session interaction: $F_{(4,44)} = 3.819$, $p = 0.035$). There were group differences in the second and third training sessions (**Figure 3D**, both $p < 0.05$). The number of the trials and errors needed to reach the criterion also differed between the two groups (**Figure 2E**, trials, $p < 0.05$; **Figure 2F**, errors, $p < 0.05$). Furthermore, error type analysis revealed a significant effect of the NAc A_{2A}R KD (**Figure 2G**, $F_{(1,30)} = 8.189$, $p < 0.001$) and the NAc A_{2A}R KD × error type interaction (**Figure 2G**, $F_{(2,30)} = 4.565$, $p = 0.0186$). Multiple-comparison analysis indicated that NAc A_{2A}R KD significantly decreased the regressive errors ($p < 0.05$) but had no effect on perseverative errors and non-reinforced errors (**Figure 2G**, both $p > 0.05$). The omissions and correct response latencies showed a decreasing tendency but failed to reach statistical significance after NAc A_{2A}R KD (**Figure 2H**, omissions, $p = 0.1865$; **Figure 2I**, correct response latencies, $p = 0.0622$). Thus, NAc A_{2A}R KD did not affect the performance of visual discrimination but facilitated attentional set-shifting by decreasing regressive errors.

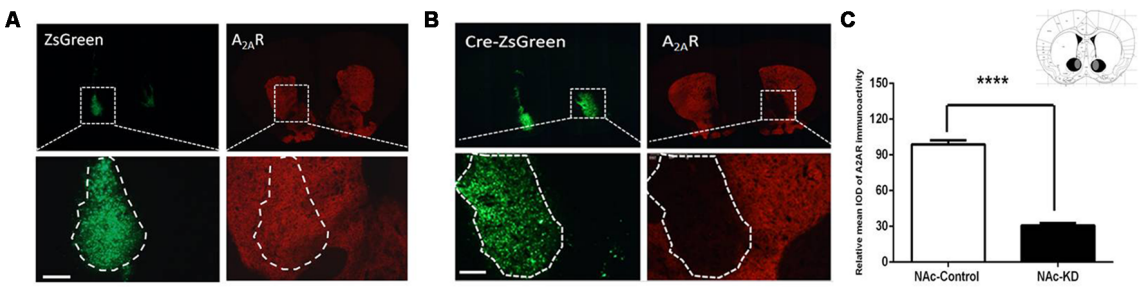

FIGURE 1 | Conditional A_{2A}R knockdown (KD) in the nucleus accumbens (NAc) by the Cre-loxP system. **(A,B)** Representative immunofluorescent photomicrographs showing focal KD expression of A_{2A} receptors (A_{2A}Rs) in the NAc after injection of AAV8-CAG-ZsGreen **(A)** and AAV8-CAG-Cre-ZsGreen into the $A_{2A}R^{(flox/flox)}$ mice **(B)**. The intensity of A_{2A}Rs signal (red) was decreased in the overlapping area with Cre-zsGreen expression (**B**; right panels) but not the control (**A**; right panels). **(C)** Schematic illustration of the maximal (black) and minimal (gray) A_{2A}R KD areas in the NAc. Quantitative analysis showed that A_{2A}Rs expression was markedly reduced in the AAV8-CAG-Cre-zsGreen-transfected regions compared with control virus ($n \geq 5$). Scale bar = 150 μm. ****$p < 0.0001$.

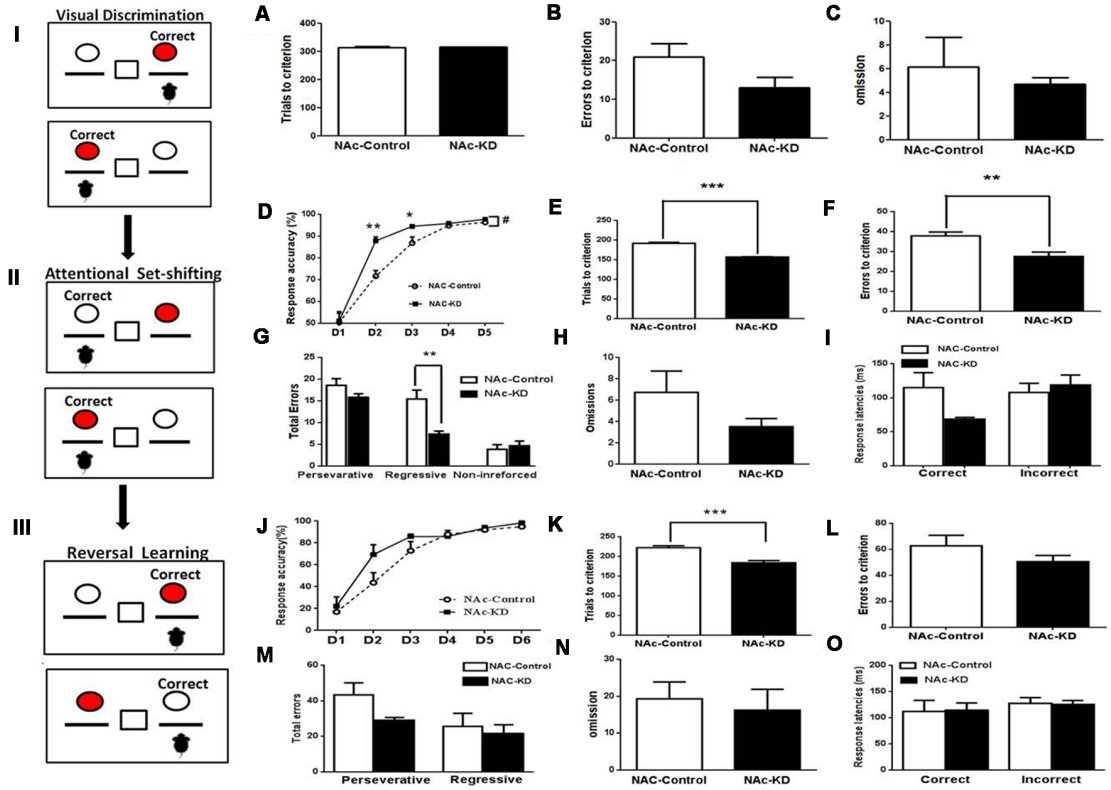

FIGURE 2 | NAc A_{2A}R KD did not affect visual discrimination but facilitated attentional set-shifting and reversal learning. (Left panels I, II, III) A schematic illustration of mouse operant cognitive flexibility task. **(A–C)** The NAc A_{2A}R blockade did not affect the performance of visual discrimination (total number of trials needed to reach the criterion: $p > 0.05$; total number of errors, $p = 0.1164$; total number of omission, $p = 0.637$, Student's *t*-test) compared with the control group. **(D–I)** A_{2A}R KD in the NAc facilitated attentional set-shifting by decreasing regressive errors. **(D)** A two-way repeated measures analysis of variance (ANOVA) showed that both groups increased their correct response ratio along with increasing sessions (main effect of training session, $F_{(4,44)} = 124.187$, $p < 0.001$), but the correct response ratio in the A_{2A}R-KD group increased faster than the control (group effect of group, $F_{(1,11)} = 10.123$, $p = 0.009$). This group effect interacted with the training sessions (group × session interaction, $F_{(4,44)} = 3.819$, $p = 0.035$). **(E,F)** The number of the trials and errors needed to reach the criterion also differed between the two groups (**Figure 2E**, trials, $p < 0.05$; **Figure 2F**, errors, $p < 0.05$). There was a significant effect of the NAc A_{2A}R KD (**Figure 2G**, $F_{(1,30)} = 8.189$, $p < 0.001$) and the NAc A_{2A}R KD × error type interaction (**Figure 2G**, $F_{(2,30)} = 4.565$, $p = 0.0186$). Multiple-comparison analysis indicated that NAc A_{2A}R KD decreased the regressive errors ($p < 0.05$) but had no effect on the perseverative errors and non-reinforced errors (**Figure 2G**, both $p > 0.05$). The omissions and correct response latencies showed a decreasing tendency but failed to reach statistical significance after NAc A_{2A}R KD (**Figure 2H**, omissions, $p = 0.1865$; **Figure 2I**, correct response latencies, $p = 0.0622$). **(J–O)** NAc A_{2A}R KD improved reversal learning. **(J)** Response accuracy analysis revealed the session-dependent learning rates across both groups ($F_{(4,44)} = 99.01$, $p < 0.01$), but there was no group difference ($F_{(1,11)} = 0.679$, $p > 0.05$, first 5 days) and group × session interaction effect ($F_{(4,44)} = 0.812$, $p > 0.05$). **(K)** The total number of trials needed for the NAc A_{2A}R-KD group was lower than in the control ($p < 0.001$). **(L–O)** NAc A_{2A}R KD did not affect the errors to criterion, omissions and response latencies compared to the control group (all $p > 0.05$), but there was a decreasing tendency in the perseverative errors (**Figure 2M**, $p = 0.0915$). Data are presented as the mean ± standard error of the mean (SEM), $^{\#}p < 0.05$, $^{*}p < 0.05$, $^{**}p < 0.01$, $^{***}p < 0.001$.

Following the set-shifting phase, reversal learning was implemented during which the reward contingencies were reversed (i.e., the reinforced lever was opposite to the lever in the set-shifting phase, **Figure 2III**) until the criterion was achieved. Response accuracy analysis revealed session-dependent learning rates across both groups (**Figure 2J**, $F_{(4,44)} = 99.01$, $p < 0.01$). However, two-way ANOVA revealed that there was no group difference ($F_{(1,11)} = 0.679$, $p > 0.05$) and group × session interaction effect ($F_{(4,44)} = 0.812$, $p > 0.05$). Nonetheless, NAc A_{2A}R KD was associated with an improved tendency in the correct response accuracy on Day 2 compared to the control. Moreover, NAc A_{2A}R KD facilitated the mice to reach the criterion earlier with the total number of trials needed to reach the criterion being lower than that in the control (**Figure 2K**, $p < 0.001$). However, in addition to having a decreasing tendency in the perseverative errors (**Figure 2M**, $p = 0.0915$), the errors to criterion, the omissions, and the response latencies were indistinguishable between the two groups (**Figures 2L–O**, $p > 0.05$).

NAc A_{2A}Rs Knockdown-Mediated Facilitation of Cognitive Flexibility Is Not Attributed to Motor Activity but Associated With Enhanced Motivation

The decreasing tendency of the omission number and the correct response latency induced by NAc A_{2A}R KD in the attentional set-shifting test prompted us to evaluate the effect of NAc

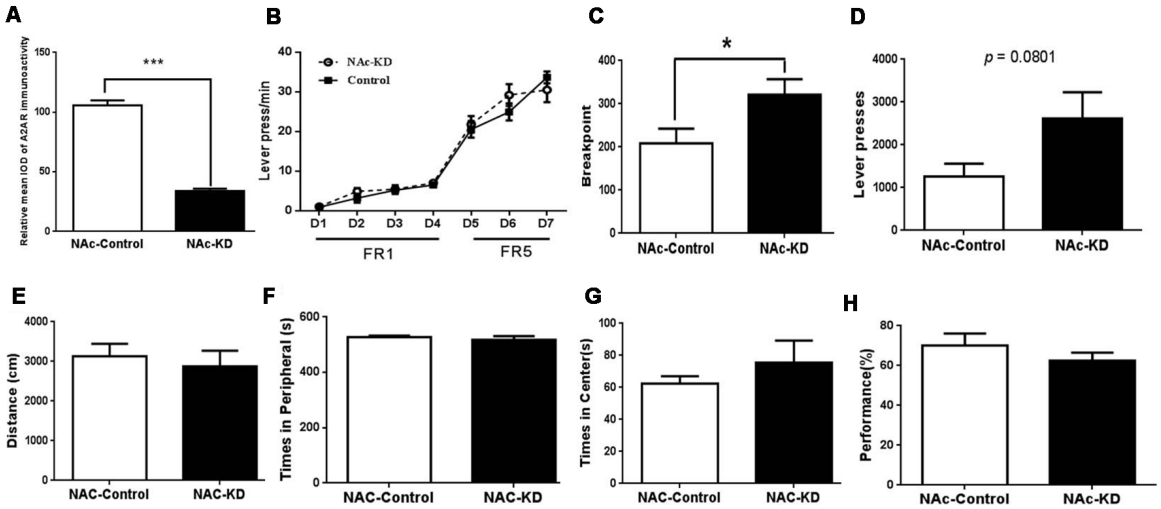

FIGURE 3 | NAc A_{2A}R KD-mediated facilitation of cognitive flexibility is not due to the motor activity but associated with enhanced motivation. **(A)** The expression level of NAc A_{2A}R in these new groups was validated to have a ∼71% decrease after AAV8-CAG-Cre-ZsGreen transfection. **(B)** Both groups of mice gradually increased their lever pressing rates to obtain the reward ($F_{(6,78)} = 114.564$, $p < 0.01$). Two-way ANOVA for repeated-measures revealed neither the main effect of A_{2A}R KD ($F_{(1,13)} = 1.366$, $p = 0.264$) nor the manipulation × training session interaction effect ($F_{(6,78)} = 1.56$, $p = 0.225$). **(C)** NAc A_{2A}R KD increased the breakpoint (63.2% increase, $p = 0.0477$) and **(D)** had a decreased tendency in the total number of presses (121.4% increase, $p = 0.0801$). **(E)** NAc A_{2A}R KD did not affect the total moving distance in the open-field test in comparison with the control ($p > 0.05$, Student's *t*-test). **(F,G)** NAc A_{2A}R KD did not alter the time spent in the peripheral (**F**, $p > 0.05$) vs. central areas (**G**, $p > 0.05$). **(H)** NAc A_{2A}R KD also did not affect the performance of spontaneous alternations in Y-maze (**H**, $p > 0.05$). Data are presented as the mean ± SEM, $^{*}p < 0.05$, $^{***}p < 0.001$.

A_{2A}R KD on the effort-related motivation by the PRT using a separate set of NAc A_{2A}R KD and control mice. The selective KD of NAc A_{2A}R (71%) by transfection with the AAV8-CAG-Cre-ZsGreen virus in these new groups was confirmed by fluorescence histochemistry (**Figure 3A**). In the training stage, both groups of mice gradually increased their lever pressing rates to obtain the reward (**Figure 3B**, $F_{(6,78)} = 114.564$, $p < 0.01$). We did not observe the main effect of NAc A_{2A}R KD (**Figure 3B**, $F_{(1,13)} = 1.366$, $p = 0.264$) nor NAc A_{2A}R × training course interaction ($F_{(6,78)} = 1.56$, $p = 0.225$, two-way ANOVA for repeated measures). However, NAc A_{2A}R KD increased the breakpoint (**Figure 3C**, 63% increase, $p = 0.0477$) and had an increasing tendency in the total number of presses (**Figure 3D**, 121% increase, $p = 0.0801$) in the test stage.

To exclude the possible confounding effect of NAc A_{2A}Rs KD on locomotion, anxiety-like behavior, and working memory, we evaluated the locomotor activity in the open-field test and spontaneous alternations in the Y-maze test. NAc A_{2A}R KD did not affect locomotion (**Figure 3E**, $p > 0.05$, Student's *t*-test) and the residence time in both central (**Figure 3G**, $p < 0.05$) and peripheral (**Figure 3F**, $p < 0.05$,) areas were indistinguishable between the control and NAc A_{2A}R KD groups. There was also no difference in possible working memory performance by the spontaneous alternation in the Y-maze test between these two groups (**Figure 3H**, $p < 0.05$).

Conditional A_{2A}R Knockdown in the DMS by the Cre-loxP Strategy

Due to the heterogeneity of the striatum, we further examined the contributions of the DMS A_{2A}Rs to cognitive flexibility. To selectively knockdown the A_{2A}Rs in the DMS, the same Cre-loxP strategy was used by injecting AAV8-CAG-Cre-ZsGreen or AAV8-CAG-ZsGreen (control virus) bilaterally into the DMS of $A_{2A}R^{flox/flox}$ mice. Three weeks later, the specific area of virus expression was verified by immunofluorescence, as can be seen in the **Figure 4C** in which the black color represents the largest area of virus transfection and the gray color depicts the smallest one. Furthermore, we observed that A_{2A}Rs expression (the red fluorescence) was reduced selectively in the Cre-expressing regions of the DMS (indicated by green fluorescence, **Figure 4B**, right panels; but not in the control DMS, **Figure 4A**, right panel). Optical intensity analysis of the A_{2A}R immunohistochemistry (**Figure 4C**) confirmed that the expression level of A_{2A}Rs in the DMS was decreased by 74%, compared with the control groups.

DMS A_{2A}R Knockdown Does Not Affect Visual Discrimination, Attentional Set-Shifting and Reversal Learning

Similarly, the DMS A_{2A}R KD and control mice were tested by mouse operant cognitive flexibility task to decipher the possible heterogeneous function of striatal subregion A_{2A}Rs. In the visual discrimination stage, DMS A_{2A}R KD also did not affect the performance of visual discrimination (**Figures 5A–C**, $p > 0.05$, Student's *t*-test). Two-way ANOVA analysis revealed that there was a main effect of the training session (**Figure 5D**, $F_{(4,48)} = 54.609$, $p < 0.01$), but in contrast to NAc A_{2A}R KD, neither the effect of the DMS A_{2A}R KD ($F_{(1,12)} = 0.17$, $p = 0.9$) nor the training × DMS A_{2A}R KD interaction ($F_{(4,48)} = 0.412$, $p = 0.799$) were observed in the attentional set-shifting phase. Also, the trial number ($p = 0.6328$), learning errors ($p = 0.991$),

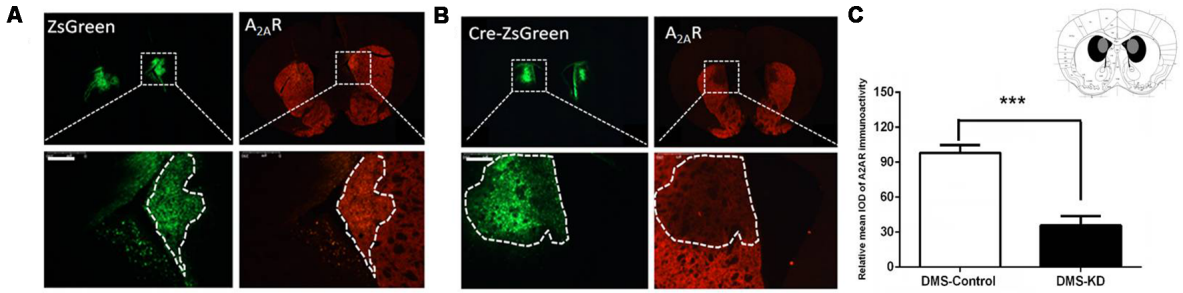

FIGURE 4 | Conditional A_{2A}R KD in the dorsomedial striatum (DMS) *via* the Cre-loxP system. **(A,B)** We employed the same Cre-loxP strategy to selectively knockdown the A_{2A}R in the DMS by injecting AAV8-CAG-ZsGreen (control virus) or AAV8-CAG-Cre-ZsGreen bilaterally into the DMS of $A_{2A}R^{flox/flox}$ mice. A_{2A}R expression (the red fluorescence) was reduced selectively in the Cre-expressing regions of the DMS (**B**; right panels) but not in the control DMS (**A**; right panels). **(C)** Schematic illustration of the maximal (black) and minimal (gray) A_{2A}R KD areas in the DMS and optical intensity analysis confirmed that the expression level of A_{2A}R in the DMS was decreased by 74% compared to the control group. ***$p < 0.001$.

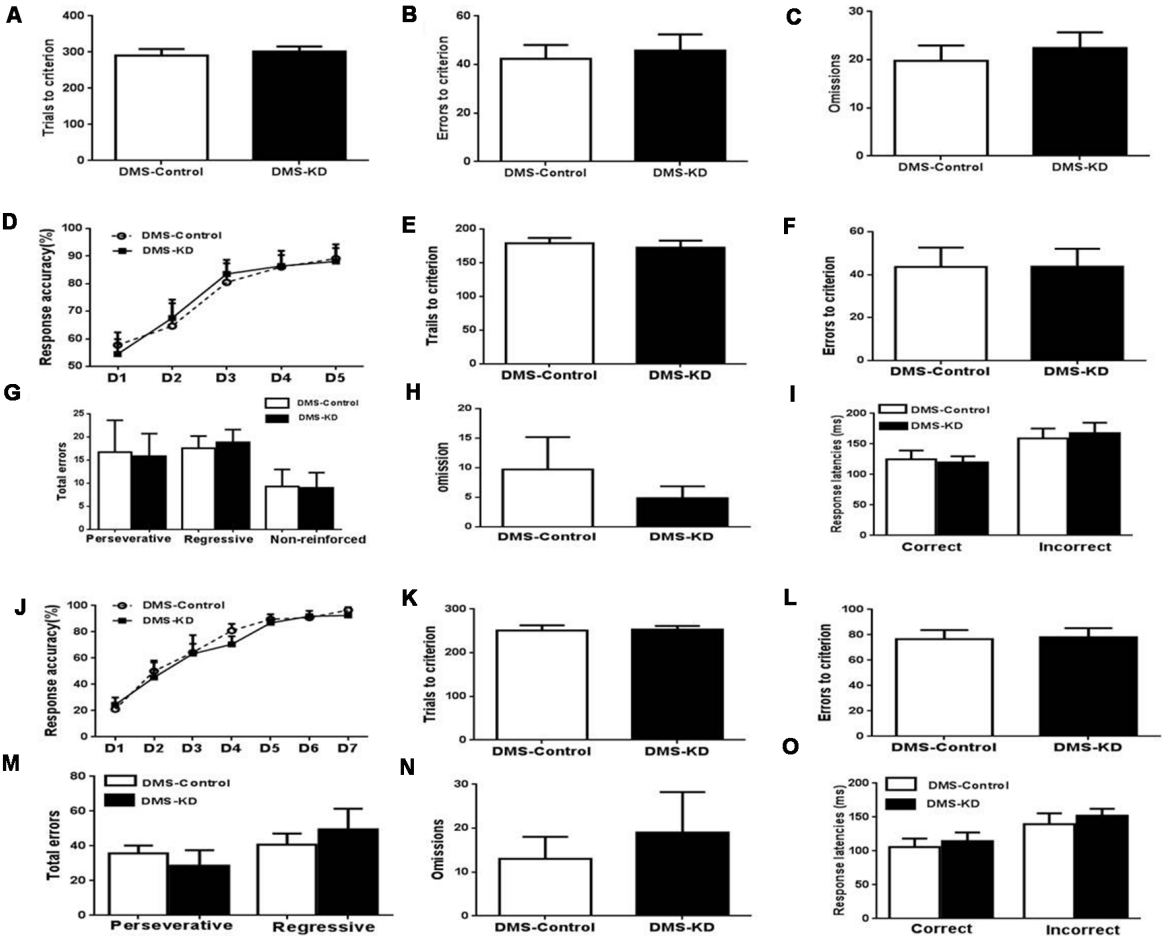

FIGURE 5 | DMS A_{2A}R KD did not affect visual discrimination, attentional set-shifting, and reversal learning. **(A–C)** A_{2A}R KD in the DMS did not affect the performance in task acquisition of visual discrimination (all $p > 0.05$). **(D–I)** A_{2A}R KD in the DMS did not affect the attentional set-shifting. **(D)** A two-way repeated measures ANOVA showed the main effect of the training session ($F_{(4,48)} = 54.609$, $p < 0.01$), but no effect of the manipulation ($F_{(1,12)} = 0.17$, $p = 0.9$) and training × manipulation interaction ($F_{(4,48)} = 0.412$, $p = 0.799$). **(E–I)** There was no significant difference in the trial number ($p = 0.6328$), learning errors ($p = 0.991$), omission ($p = 0.4199$) and response latencies ($p > 0.05$). **(J–O)** Knockdown of A_{2A}Rs in the DMS did not affect reversal learning. **(J)** Response accuracy analysis revealed the session-dependent learning rates across DMS A_{2A}R KD and control groups ($F_{(4,32)} = 37.371$, $p < 0.01$, two-way ANOVA with repeated measures), but no group difference ($F_{(1,8)} = 0.175$, $p > 0.05$, first 5 days) and group × session interaction effect ($F_{(4,32)} = 0.382$, $p > 0.05$). **(K–O)** DMS A_{2A}R KD did not affect total trials, errors to criterion, omissions, and response latencies, as compared to the control group (all $p > 0.05$).

omission ($p = 0.4199$) and response latencies ($p > 0.05$) were all indistinguishable between the DMS A_{2A}R KD and control groups (**Figures 5E–I**). Similarly, we found that DMS A_{2A}R KD did not affect the performance (i.e., the number of correct responses, errors, omissions and response latencies) in the reversal phase (**Figures 5J–O**). Collectively, these data suggested that DMS A_{2A}R KD did not affect the performance in visual discrimination, attentional set-shifting, and reversal learning.

DMS A_{2A}R Knockdown Does Not Affect Locomotion but Enhances Motivation

Using a new set of the mice with confirmed KD (by 70%) of DMS A_{2A}R after transfection with AAV8-CAG-Cre-ZsGreen (**Figure 6A**), we showed that DMS A_{2A}R KD also did not affect locomotion, the residence time in the central and peripheral area in the open-field test and possible working memory by a spontaneous alternation in Y-maze compared to the control (**Figures 6E–H**, all $p < 0.05$). However, PR task revealed that the breakpoint (**Figure 6C**, 30.6% increase, $p = 0.0233$) and total number of presses (**Figure 6D**, 62.6% increase, $p = 0.0179$) were also significantly increased by DMS A_{2A}R KD, although there were no significant differences in the training stage between these two groups (**Figure 6B**, effect of training session, $F_{(6,96)} = 51.558$, $p < 0.05$; DMS A_{2A}R KD × training course interaction effect, $F_{(6,96)} = 1.57$, $p > 0.05$; effect of DMS A_{2A}R KD, $F_{(1,16)} = 0.6$, $p > 0.05$). Thus, DMS A_{2A}R KD can enhance motivation.

DISCUSSION

The Striatopallidal A_{2A}Rs in the NAc Modulate Cognitive Flexibility by Facilitating Strategy Shifting

The important finding in this study is that NAc A_{2A}R KD enhances cognitive flexibility by increasing set-shifting as well as reversal learning. First, NAc A_{2A}Rs blockade improved attentional set-shifting as evident from the increased response accuracy and decreased the number of trials to reach the criterion. The enhanced cognitive flexibility by NAc A_{2A}R KD is associated with the decreased regressive errors, indicating that the A_{2A}R KD mice can efficiently identify the newly reinforced choice and strongly maintain this new response, or accelerate the learning about the irrelevant stimuli (the right or left lever was irrelevant in the visual discrimination but turned into the relevant stimuli in the stage of the attentional set-shifting). This finding is consistent with the other reports showing that inactivation of the NAc enhanced learning about the irrelevant stimuli in the set-shifting (Tai et al., 1995; Jongen-Rêlo et al., 2002; Floresco et al., 2006). Thus, NAc A_{2A}R KD selectively improved attentional set-shifting by increasing the ability of learning and maintaining the new extradimensional strategy.

Furthermore, NAc A_{2A}R KD also improves reversal learning as evident from the decreased number of trials to reach the criterion and the increased correct response accuracy on day 2 in the phase of reversal learning. This improvement is associated with apparently decreasing perseverative errors, indicating the increased inhibition of previously learned (old) strategy to facilitate the strategy shifting. This finding is consistent with our previous finding that A_{2A}R KO increases performance in the omission test, in which the mice learn to suppress lever pressing for 20 s in order to obtain the reward, indicating an increased behavioral inhibition (Yu et al., 2009).

The facilitation of search for a new strategy in the set-shifting phase by reduced regressing errors and inhibition of the previous strategy in the reversal phase by the tendency for a reduction in perseverative errors suggests that NAc A_{2A}R controls cognitive flexibility by two distinct processes that are distinctly controlled by glutamatergic inputs from mPFC

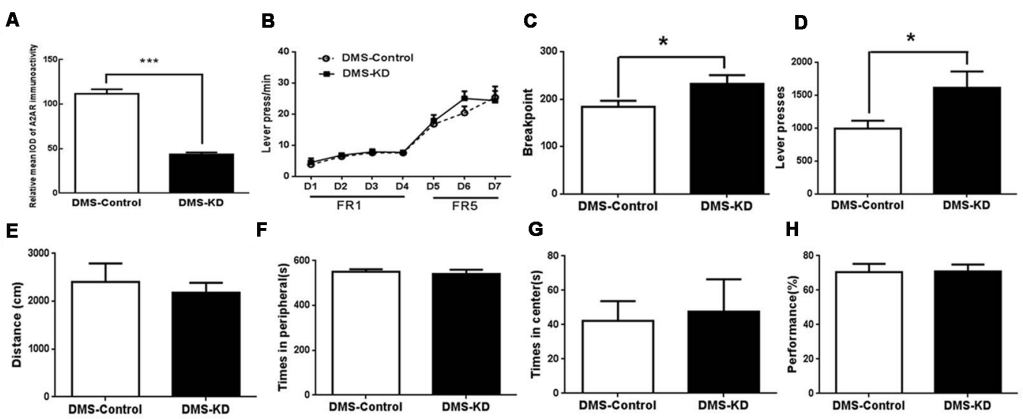

FIGURE 6 | DMS A_{2A}R KD did not affect locomotion but enhanced motivation. **(A)** The expression level of DMS A_{2A}R in these new groups was decreased by ∼70% after AAV8-CAG-Cre-ZsGreen transfection. **(B–D)** DMS A_{2A}R KD enhanced motivation. **(B)** There was no significant difference in the training stage between these two groups (effect of training session, $F_{(6,96)} = 51.558$, $p < 0.05$; DMS A_{2A}R KD × training course interaction effect, $F_{(6,96)} = 1.57$, $p > 0.05$; effect of DMS A_{2A}R KD, $F_{(1,16)} = 0.6$, $p > 0.05$, two-way ANOVA with repeated measures). **(C,D)** DMS A_{2A}R KD increased the breakpoint by 30.6% ($p = 0.0233$, Student's t-test) and a total number of presses by 62.6% ($p = 0.0179$, Student's t-test) in the PRT stage. **(E–H)** DMS A_{2A}R KD did not affect locomotion, the residence time in the central and peripheral area in the open-field test, and working memory by a spontaneous alternation in Y-maze, compared to the control (all $p > 0.05$). $^*p < 0.05$; $^{***}p < 0.001$.

and orbitofrontal cortex (OFC) into the NAc, respectively (Birrell and Brown, 2000; McAlonan and Brown, 2003; Cui et al., 2018). Importantly, modulation of both processes leads to the enhanced strategy shifting by the A_{2A}R KD in the NAc. This view is also consistent with that A_{2A}R KO enhances goal-directed behavior in instrumental conditioning (Yu et al., 2009) and strategy shifting in water maze paradigm (Wei et al., 2011), and is supported by the finding that caffeine (a non-specific antagonist of A_{2A}R) treatment significantly improves attention and cognitive deficits in an attentional deficit and hyperactivity disorder (ADHD) animal model (Pandolfo et al., 2013). Furthermore, the NAc A_{2A}R KD seems only to modulate the early phases of set-shifting instead of consolidating the new searching strategy, since the response of reversal learning on the Day 1 was similar between these two groups and the NAc A_{2A}R KD even improves reversal learning by decreasing the number of trials to reach the criterion. These indicate that NAc A_{2A}R may only control short-term memory or goal-directed behavior, which is also supported by our unpublished data which reveal that NAc A_{2A}R KD can improve short-term working memory in a delayed non-match-to-place (DNMTP) task and goal-directed behavior in the instrumental behavior.

Collectively, these findings suggest that NAc A_{2A}R enhances cognitive flexibility by facilitating strategy shifting *via* increasing the ability of learning and maintenance of new extradimensional strategy and possible inhibition of intradimensional old strategy. Except for the D1R agonists (Haluk and Floresco, 2009), most studies with pharmacological and genetic manipulation of neuromodulators and focal lesioning produced almost exclusive impairment of cognitive flexibility (Ding et al., 2014; Parikh et al., 2016b; Grospe et al., 2018). Our finding may shed new light on the striatopallidal pathway control of cognitive flexibility as the A_{2A}R is selectively expressed in the striatopallidal neurons and the A_{2A}R KD is expected to reduce the striatopallidal neuron activity. The previous studies have produced different results on cognitive flexibility. For example, optogenetic (ChR2) activation in DMS (Wang et al., 2019) or by toxin-induced depletion of the striatopallidal pathway in NAc (Yawata et al., 2012) can facilitate or impair cognitive flexibility, while optogenetic (NpHR) silencing of striatopallidal pathway in DMS produces no effect (Wang et al., 2019). In this regard, NAc A_{2A}R KD selectively improving cognitive flexibility, combined with the noted safety profile of A_{2A}R antagonists and caffeine in clinical phase III trials for motor benefits in Parkinson's disease (Chase et al., 2003) suggests that pharmacological targeting striatal A_{2A}R may represent a novel treatment strategy for the deficits of cognitive flexibility in various neuropsychiatric disorders.

The NAc A_{2A}R KD May Enhance Cognitive Flexibility by Modulating Motivation/Attention

The mechanism underlying the NAc A_{2A}R KD-mediated facilitation of cognitive flexibility is not clear. Notably, this facilitation by NAc A_{2A}R KD is not attributed to the mnemonic process or possible working memory, as NAc A_{2A}R KD did not affect the performance in the visual discrimination phase (**Figures 2A–C**) and the acquisition of lever pressing in the PRT (**Figure 3A**) and spontaneous alternations in Y-maze. This is consistent with previous finding that this task is specifically sensitive to the manipulation to disruption of cognitive flexibility (i.e., set-shifting and reversal learning) but relatively insensitive to mnemonic process since manipulation of glutamate and dopamine signaling mainly alter cognitive flexibility without affecting visual discrimination (Parikh et al., 2016b; Cui et al., 2018; Kato et al., 2018). Moreover, this NAc A_{2A}Rs-mediated modification of cognitive flexibility is neither confounded by motor activity nor possibly anxiety-like behavior (**Figures 3E–G**). As the motivational factor is critical to the control of cognitive flexibility (Liu and Wang, 2014) and NAc is the critical locus for motivational control, we propose that NAc A_{2A}Rs may improve cognitive flexibility with facilitated strategy shifting by enhancing the motivation. This proposal is supported by the finding of a decreased tendency of the number of omissions and correct response latency induced by NAc A_{2A}R KD in attentional set-shifting test (**Figures 2H–I**). This contention is further validated by the finding that NAc A_{2A}R KD increases the breakpoint and enhances the motivation in PRT. The enhanced response induced by A_{2A}R KD in PRT can be explained by an enhanced sensitivity to reinforcement, rapid initiation of lever pressing or enhanced persistence of the action. These results are in line with the findings that A_{2A}R antagonism and genetic deletion can improve effort-based decision making (Pardo et al., 2012; López-Cruz et al., 2018). We noted that A_{2A}R KD in both NAc and DMS increased motivation (i.e., breakpoint in PRT), consistent with the previous study that showed the inhibition of the indirect pathway in either the NAc or DMS leads to enhanced motivation (Carvalho Poyraz et al., 2016). However, the NAc A_{2A}R KD produces a higher breakpoint than DMS A_{2A}R KD. It is possible that different intensities of motivation may lead to the different control of cognitive flexibility by NAc vs. DMS A_{2A}R KD and additional studies are needed to clarify this issue.

Additionally, the reduced response latency in the set-shifting after NAc A_{2A}R KD may indicate an increased attention. The enhanced response induced by A_{2A}R KD in the set-shifting can also be attributed to an enhanced sensitivity to environmental sensory stimulation (or enhanced attention to the detection of novel features). The NAc receives dense direct glutamatergic projections from vHIP with sensory inputs to generate new attention (Voorn et al., 2004; Mannella et al., 2013; Floresco, 2015), from the paraventricular thalamus to track context-dependent salience (Zhu et al., 2018), from the BLA to modulate cue-triggered motivated behavior (Stuber et al., 2011) and dopaminergic projections from VTA to control attention, approach initiation and flexible reward-seeking (Syed et al., 2016; Boekhoudt et al., 2018; Cui et al., 2018). These pathways confer the NAc the unique feature to modulate cognitive flexibility by modifying sensitivity to environmental sensory stimulation and attention to the detection of novel features, resulting in action selection with motivation.

Dopamine signaling in the striatum is also critical to cognitive flexibility control (Parikh et al., 2016b; Cui et al., 2018). Individual differences in the dopamine D2-type receptor (D2R) levels in the caudate nucleus of human subjects and monkeys correlate with performance in a discrimination reversal task (Horst et al., 2019). As striatal A_{2A}Rs exert an inhibitory effect on D2R signaling, possibly through the A_{2A}R-D2R heterodimers in the striatopallidal neurons where they almost exclusively colocalized, it can be speculated that NAc A_{2A}R KD may facilitate cognitive flexibility with enhanced motivation by modulating D2R signaling in the striatum. Consistent with this view, global D2R knockout has been shown to disrupt reversal learning in mice (Horst et al., 2019). However, focal injection of the D2R agonist quinpirole into NAc produces opposite effects to NAc A_{2A}R KD, i.e., disruption of both set-shifting and reversal learning (Haluk and Floresco, 2009; Horst et al., 2019). Whether NAc A_{2A}Rs control cognitive flexibility by interacting with the D2R remains to be clarified. In addition, A_{2A}R activity can also modulate glutamate signaling through the antagonistic interactions with NMDARs and metabotropic glutamate receptor 5 (mGlu5) in the striatum (Parsons et al., 2007; Zhu et al., 2016, 2018). In agreement with this proposal, NMDAR antagonists have been shown to impair both set-shifting and reversal learning (Darrah et al., 2008; Ding et al., 2014).

Striatopallidal A_{2A}Rs Exert NAc- and DMS-Specific Control of Cognitive Flexibility

Another noted observation is that striatopallidal A_{2A}Rs exert NAc- and DMS-specific control of cognitive flexibility. Consistent with the critical role of the NAc in modulating the cognitive flexibility (Haluk and Floresco, 2009; Ding et al., 2014; Cui et al., 2018), NAc A_{2A}R KD enhances cognitive flexibility (i.e., both set-shifting and reversal learning) by facilitating strategy shifting. By contrast, DMS A_{2A}R KD is devoid of effects on cognitive flexibility, as evident by the lack of effects of DMS A_{2A}R KD on set-shifting and reversal learning. As DMS has been shown to control cognitive flexibility (Aoki et al., 2015; Grospe et al., 2018), the lack of effects of DMS A_{2A}R on cognitive flexibility indicates that neuromodulators other than the A_{2A}R (such as acetylcholine and glutamate signaling) may mediate DMS control of cognitive flexibility. Furthermore, DMS A_{2A}R KD can enhance goal-directed behavior (Li et al., 2016) and working memory (Li et al., 2018), two behavioral elements involved in cognitive flexibility control. Thus, other behavioral elements such as attention and impulsivity control (associated mainly with the NAc function) may play critical roles in this control. The dissociable function of striatal subregion A_{2A}Rs in modulating cognitive flexibility collaborate with several previous studies including ours showing that the cortico-striatal A_{2A}Rs can exert different or opposite effects on behaviors. For example, we have recently shown that prefrontal and striatal A_{2A}Rs have the opposite effect on working memory (Li et al., 2018), fear memory (Wei et al., 2014) and psychomotor activity (Shen et al., 2008). Similarly, selective down-regulation of A_{2A}Rs in the prefrontal cortex has been shown to cause an impulsive-like behavior in the delay-based cost-benefit decision-making paradigm (Leffa et al., 2018), while pharmacological blockade or genetic inactivation of A_{2A}Rs can reverse the impairment induced by D2R antagonist in an effort-related cost-benefit decision-making paradigm (Pardo et al., 2012). Also, the distinct functions of the cortico-striatal A_{2A}Rs at the presynaptic vs. postsynaptic sites may underlie opposite control of cognitive behaviors by A_{2A}Rs in the prefrontal cortex and striatum, as different behaviors may be preferentially controlled by postsynaptic striatal A_{2A}Rs (such as working memory; Li et al., 2018) or presynaptic cortical A_{2A}Rs (such as THC self-administration; Tebano et al., 2004; Justinová et al., 2014). This opposite control of behaviors by A_{2A}Rs in different brain regions (at the presynaptic vs. postsynaptic levels) may confer A_{2A}Rs with the ability to keep each behavior in balance and to fine-tune behaviors.

As the A_{2A}R signaling and functional interaction with other neurotransmitters are similar in different subregions of the striatum (Svenningsson et al., 1999), the functional divergence of striatal subregion-specific A_{2A}Rs in controlling strategy shifting may be primarily attributed to the distinct input-output mapping. NAc mainly receives inputs from mPFC, orbital prefrontal cortex, vHIP, BLA and VTA and projects to ventral pallidum whereas DMS mainly receives inputs from mPFC, intralaminar thalamic nuclei and SNc and projects to globus pallidus external (Britt et al., 2012; Papp et al., 2012; Hunnicutt et al., 2016; Kato et al., 2018). Functionally, the hippocampus is essential in processing the relationships between different stimuli and recognition of novelty (Mannella et al., 2013) and vHIP-NAc stimulation may increase VTA dopamine neuron population activity (Floresco et al., 2001). The BLA also plays a crucial role in forming associations between neutral stimuli and guiding action selection in situations involving reward uncertainty (McLaughlin and Floresco, 2007; Bercovici et al., 2018). Also, the VTA dopamine preferentially projecting to NAc is critical to the control of motivation, rewarding behavior, and affection, whereas the SNc dopamine mostly projecting to DMS mainly contributes to the motor and possibly motivation functions (Le Moal and Simon, 1991; Nieoullon and Coquerel, 2003; Björklund and Dunnett, 2007). Moreover, activation of VTA dopaminergic neurons impaired sustained attention (Boekhoudt et al., 2017) and increased responsiveness to sucrose and enhanced motivation for the reward in the PRT (Boekhoudt et al., 2018) while activation of SNc dopaminergic neurons impaired attention and delayed responsiveness and had no effects on sucrose seeking and motivation (Boekhoudt et al., 2017, 2018); meanwhile, a recent study has demonstrated that NAc and dorsal striatum have differences in the sensitivity and timing of D2-receptor signaling with higher sensitivity for dopamine in the NAc by preferential coupling to $G_{\alpha o}$ (Engeln et al., 2018; Marcott et al., 2018). The subregional heterogeneities of D2R signaling and function in the striatum may also underlie distinct control of cognitive flexibility by NAc vs. DMS A_{2A}Rs.

It should be noted that NAc A_{2A}Rs may control cognitive flexibility by striatal collateral control and striatal local microcircuits involving interneurons and glial cells, as recent studies have demonstrated that there are collateral synapses between striatopallidal neurons and striatonigral neurons (Lalchandani et al., 2013; Wei et al., 2017) and the striatonigral neurons (so-called direct pathway) played important roles in controlling cognitive flexibility (Haluk and Floresco, 2009; Wang et al., 2019). Meanwhile, the striatal cholinergic interneurons and astrocyte calcium signaling also can modulate set-shifting and repetitive behavior possibly by controlling local microcircuits (Aoki et al., 2015; Yu et al., 2018). However, to confirm these possible mechanisms, additional studies are needed to dissect out the circuit and neurochemical basis of the differential control of cognitive flexibility by NAc vs. DMS A_{2A}Rs.

DATA AVAILABILITY

The raw data supporting the conclusions of this manuscript will be made available by the authors, without undue reservation, to any qualified researcher.

ETHICS STATEMENT

The animal protocols were approved by the Institutional Ethics Committee for Animal Use in Research and Education at Wenzhou Medical University, China.

AUTHOR CONTRIBUTIONS

J-FC and JZ conceived and designed the experiments and wrote the article. JZ, BW, XL, YD, TL, and XC performed the experiments. JZ, WZ, GW, and SV analyzed the data. JZ, WZ, WG, and XC contributed reagents, materials and analysis tools. SV also contributed to the manuscript text edition.

FUNDING

This work was supported by National Natural Science Foundation of China (Grant Nos. 81630040, 31600854, 81600991, 31600859, 81801092 and 31800903), Natural Science Foundation of Zhejiang Province (Grant Nos. LQ17H090005 and LQ16H090006), Wenzhou Science and Technology Program (Grant Nos. Y20170189, Y20160088 and Y20160012).

REFERENCES

Amodeo, D. A., Cuevas, L., Dunn, J. T., Sweeney, J. A., and Ragozzino, M. E. (2018). The adenosine A_{2A} receptor agonist, CGS 21680, attenuates a probabilistic reversal learning deficit and elevated grooming behavior in BTBR mice. *Autism Res.* 11, 223–233. doi: 10.1002/aur.1901

Aoki, S., Liu, A. W., Zucca, A., Zucca, S., and Wickens, J. R. (2015). Role of striatal cholinergic interneurons in set-shifting in the rat. *J. Neurosci.* 35, 9424–9431. doi: 10.1523/JNEUROSCI.0490-15.2015

Augusto, E., Matos, M., Sévigny, J., El-Tayeb, A., Bynoe, M. S., Müller, C. E., et al. (2013). Ecto-5'-nucleotidase (CD73)-mediated formation of adenosine is critical for the striatal adenosine A_{2A} receptor functions. *J. Neurosci.* 33, 11390–11399. doi: 10.1523/jneurosci.5817-12.2013

Bagot, R. C., Parise, E. M., Peña, C. J., Zhang, H. X., Maze, I., Chaudhury, D., et al. (2015). Ventral hippocampal afferents to the nucleus accumbens regulate susceptibility to depression. *Nat. Commun.* 6:7626. doi: 10.1038/ncomms8626

Bercovici, D. A., Princz-Lebel, O., Tse, M. T., Moorman, D. E., and Floresco, S. B. (2018). Optogenetic dissection of temporal dynamics of amygdala-striatal interplay during risk/reward decision making. *eNeuro* 5:ENEURO.0422-18.2018. doi: 10.1523/ENEURO.0422-18.2018

Birrell, J. M., and Brown, V. J. (2000). Medial frontal cortex mediates perceptual attentional set shifting in the rat. *J. Neurosci.* 20, 4320–4324. doi: 10.1523/jneurosci.20-11-04320.2000

Björklund, A., and Dunnett, S. B. (2007). Dopamine neuron systems in the brain: an update. *Trends Neurosci.* 30, 194–202. doi: 10.1016/j.tins.2007.03.006

Boekhoudt, L., Voets, E. S., Flores-Dourojeanni, J. P., Luijendijk, M. C., Vanderschuren, L. J., and Adan, R. A. (2017). Chemogenetic activation of midbrain dopamine neurons affects attention, but not impulsivity, in the five-choice serial reaction time task in rats. *Neuropsychopharmacology* 42, 1315–1325. doi: 10.1038/npp.2016.235

Boekhoudt, L., Wijbrans, E. C., Man, J. H. K., Luijendijk, M. C. M., de Jong, J. W., van der Plasse, G., et al. (2018). Enhancing excitability of dopamine neurons promotes motivational behaviour through increased action initiation. *Eur. Neuropsychopharmacol.* 28, 171–184. doi: 10.1016/j.euroneuro.2017.11.005

Brady, A. M., and Floresco, S. B. (2015). Operant procedures for assessing behavioral flexibility in rats. *J. Vis. Exp.* 96:e52387. doi: 10.3791/52387

Britt, J. P., Benaliouad, F., McDevitt, R. A., Stuber, G. D., Wise, R. A., and Bonci, A. (2012). Synaptic and behavioral profile of multiple glutamatergic inputs to the nucleus accumbens. *Neuron* 76, 790–803. doi: 10.1016/j.neuron.2012.09.040

Carvalho Poyraz, F., Holzner, E., Bailey, M. R., Meszaros, J., Kenney, L., Kheirbek, M. A., et al. (2016). Decreasing striatopallidal pathway function enhances motivation by energizing the initiation of goal-directed action. *J. Neurosci.* 36, 5988–6001. doi: 10.1523/jneurosci.0444-16.2016

Chase, T. N., Bibbiani, F., Bara-Jimenez, W., Dimitrova, T., and Oh-Lee, J. D. (2003). Translating A_{2A} antagonist KW6002 from animal models to parkinsonian patients. *Neurology* 61, S107–111. doi: 10.1212/01.wnl.0000095223.08711.48

Chen, J. F. (2014). Adenosine receptor control of cognition in normal and disease. *Int. Rev. Neurobiol.* 119, 257–307. doi: 10.1016/b978-0-12-801022-8.00012-x

Chen, J. F., Eltzschig, H. K., and Fredholm, B. B. (2013). Adenosine receptors as drug targets–what are the challenges?. *Nat. Rev. Drug Discov.* 12, 265–286. doi: 10.1038/nrd3955

Christakou, A., Robbins, T. W., and Everitt, B. J. (2004). Prefrontal cortical-ventral striatal interactions involved in affective modulation of attentional performance: implications for corticostriatal circuit function. *J. Neurosci.* 24, 773–780. doi: 10.1523/JNEUROSCI.0949-03.2004

Cools, R., Barker, R. A., Sahakian, B. J., and Robbins, T. W. (2001). Mechanisms of cognitive set flexibility in Parkinson's disease. *Brain* 124, 2503–2512. doi: 10.1093/brain/124.12.2503

Cui, Q., Li, Q., Geng, H., Chen, L., Ip, N. Y., Ke, Y., et al. (2018). Dopamine receptors mediate strategy abandoning via modulation of a specific prelimbic cortex-nucleus accumbens pathway in mice. *Proc. Natl. Acad. Sci. U S A* 115, E4890–E4899. doi: 10.1073/pnas.1717106115

Darrah, J. M., Stefani, M. R., and Moghaddam, B. (2008). Interaction of N-methyl-D-aspartate and group 5 metabotropic glutamate receptors on behavioral flexibility using a novel operant set-shift paradigm. *Behav. Pharmacol.* 19, 225–234. doi: 10.1097/fbp.0b013e3282feb0ac

Ding, X. K., Qiao, Y. H., Piao, C. J., Zheng, X. G., Liu, Z. K., and Liang, J. (2014). N-methyl-D-aspartate receptor-mediated glutamate transmission in nucleus accumbens plays a more important role than that in dorsal striatum in cognitive flexibility. *Front. Behav. Neurosci.* 8:304. doi: 10.3389/fnbeh.2014.00304

Engeln, M., Fox, M. E., and Lobo, M. K. (2018). Dopamine is differentially encoded by D2 receptors in striatal subregions. *Neuron* 98, 459–461. doi: 10.1016/j.neuron.2018.04.016

Ferré, S., Karcz-Kubicha, M., Hope, B. T., Popoli, P., Burgueño, J., Gutiérrez, M. A., et al. (2002). Synergistic interaction between adenosine A_{2A} and glutamate mGlu5 receptors: implications for striatal neuronal function. *Proc. Natl. Acad. Sci. U S A* 99, 11940–11945. doi: 10.1073/pnas.172393799

Floresco, S. B. (2015). The nucleus accumbens: an interface between cognition, emotion and action. *Annu. Rev. Psychol.* 66, 25–52. doi: 10.1146/annurev-psych-010213-115159

Floresco, S. B., Ghods-Sharifi, S., Vexelman, C., and Magyar, O. (2006). Dissociable roles for the nucleus accumbens core and shell in regulating set shifting. *J. Neurosci.* 26, 2449–2457. doi: 10.1523/jneurosci.4431-05.2006

Floresco, S. B., Todd, C. L., and Grace, A. A. (2001). Glutamatergic afferents from the hippocampus to the nucleus accumbens regulate activity of ventral tegmental area dopamine neurons. *J. Neurosci.* 21, 4915–4922. doi: 10.1523/jneurosci.21-13-04915.2001

French, S. J., and Totterdell, S. (2002). Hippocampal and prefrontal cortical inputs monosynaptically converge with individual projection neurons of the nucleus accumbens. *J. Comp. Neurol.* 446, 151–165. doi: 10.1002/cne.10191

Goto, Y., and Grace, A. A. (2008). Limbic and cortical information processing in the nucleus accumbens. *Trends Neurosci.* 31, 552–558. doi: 10.1016/j.tins.2008.08.002

Grospe, G. M., Baker, P. M., and Ragozzino, M. E. (2018). Cognitive flexibility deficits following 6-OHDA lesions of the rat dorsomedial striatum. *Neuroscience* 374, 80–90. doi: 10.1016/j.neuroscience.2018.01.032

Haluk, D. M., and Floresco, S. B. (2009). Ventral striatal dopamine modulation of different forms of behavioral flexibility. *Neuropsychopharmacology* 34, 2041–2052. doi: 10.1038/npp.2009.21

Higley, M. J., and Sabatini, B. L. (2010). Competitive regulation of synaptic Ca^{2+} influx by D2 dopamine and A_{2A} adenosine receptors. *Nat. Neurosci.* 13, 958–966. doi: 10.1038/nn.2592

Horst, N. K., Jupp, B., Roberts, A. C., and Robbins, T. W. (2019). D2 receptors and cognitive flexibility in marmosets: tri-phasic dose-response effects of intra-striatal quinpirole on serial reversal performance. *Neuropsychopharmacology* 44, 564–571. doi: 10.1038/s41386-018-0272-9

Horvitz, J. C. (2002). Dopamine gating of glutamatergic sensorimotor and incentive motivational input signals to the striatum. *Behav. Brain Res.* 137, 65–74. doi: 10.1016/s0166-4328(02)00285-1

Hunnicutt, B. J., Jongbloets, B. C., Birdsong, W. T., Gertz, K. J., Zhong, H., and Mao, T. (2016). A comprehensive excitatory input map of the striatum reveals novel functional organization. *Elife* 5:e19103. doi: 10.7554/elife.19103

Jongen-Rêlo, A. L., Kaufmann, S., and Feldon, J. (2002). A differential involvement of the shell and core subterritories of the nucleus accumbens of rats in attentional processes. *Neuroscience* 111, 95–109. doi: 10.1016/s0306-4522(01)00521-8

Justinová, Z., Redhi, G. H., Goldberg, S. R., and Ferré, S. (2014). Differential effects of presynaptic versus postsynaptic adenosine A_{2A} receptor blockade on Δ9-tetrahydrocannabinol (THC) self-administration in squirrel monkeys. *J. Neurosci.* 34, 6480–6484. doi: 10.1523/jneurosci.5073-13.2014

Kalivas, P. W., and Volkow, N. D. (2005). The neural basis of addiction: a pathology of motivation and choice. *Am. J. Psychiatry* 162, 1403–1413. doi: 10.1176/appi.ajp.162.8.1403

Kato, S., Fukabori, R., Nishizawa, K., Okada, K., Yoshioka, N., Sugawara, M., et al. (2018). Action selection and flexible switching controlled by the intralaminar thalamic neurons. *Cell Rep.* 22, 2370–2382. doi: 10.1016/j.celrep.2018.02.016

Klugmann, M., Goepfrich, A., Friemel, C. M., and Schneider, M. (2011). AAV-mediated overexpression of the CB1 receptor in the mPFC of adult rats alters cognitive flexibility, social behavior and emotional reactivity. *Front. Behav. Neurosci.* 5:37. doi: 10.3389/fnbeh.2011.00037

Lalchandani, R. R., van der Goes, M. S., Partridge, J. G., and Vicini, S. (2013). Dopamine D2 receptors regulate collateral inhibition between striatal medium spiny neurons. *J. Neurosci.* 33, 14075–14086. doi: 10.1523/JNEUROSCI.0692-13.2013

Laplante, F., Zhang, Z. W., Huppé-Gourgues, F., Dufresne, M. M., Vaucher, E., and Sullivan, R. M. (2012). Cholinergic depletion in nucleus accumbens impairs mesocortical dopamine activation and cognitive function in rats. *Neuropharmacology* 63, 1075–1084. doi: 10.1016/j.neuropharm.2012.07.033

Le Moal, M., and Simon, H. (1991). Mesocorticolimbic dopaminergic network: functional and regulatory roles. *Physiol. Rev.* 71, 155–234. doi: 10.1152/physrev.1991.71.1.155

Leffa, D. T., Pandolfo, P., Goncalves, N., Machado, N. J., de Souza, C. M., Real, J. I., et al. (2018). Adenosine A_{2A} receptors in the rat prelimbic medial prefrontal cortex control delay-based cost-benefit decision making. *Front. Mol. Neurosci.* 11:475. doi: 10.3389/fnmol.2018.00475

Leung, R. C., and Zakzanis, K. K. (2014). Brief report: cognitive flexibility in autism spectrum disorders: a quantitative review. *J. Autism Dev. Disord.* 44, 2628–2645. doi: 10.1007/s10803-014-2136-4

Li, Y., He, Y., Chen, M., Pu, Z., Chen, L., Li, P., et al. (2016). Optogenetic activation of adenosine A_{2A} receptor signaling in the dorsomedial striatopallidal neurons suppresses goal-directed behavior. *Neuropsychopharmacology* 41, 1003–1013. doi: 10.1038/npp.2015.227

Li, Z., Chen, X., Wang, T., Gao, Y., Li, F., Chen, L., et al. (2018). The corticostriatal adenosine A_{2A} receptor controls maintenance and retrieval of spatial working memory. *Biol. Psychiatry* 83, 530–541. doi: 10.1016/j.biopsych.2017.07.017

Liu, Y., and Wang, Z. (2014). Positive affect and cognitive control: approach-motivation intensity influences the balance between cognitive flexibility and stability. *Psychol. Sci.* 25, 1116–1123. doi: 10.1177/0956797614525213

López-Cruz, L., Salamone, J. D., and Correa, M. (2018). Caffeine and selective adenosine receptor antagonists as new therapeutic tools for the motivational symptoms of depression. *Front. Pharmacol.* 9:526. doi: 10.3389/fphar.2018.00526

Mannella, F., Gurney, K., and Baldassarre, G. (2013). The nucleus accumbens as a nexus between values and goals in goal-directed behaviour: a review and a new hypothesis. *Front. Behav. Neurosci.* 7:135. doi: 10.3389/fnbeh.2013.00135

Marcott, P. F., Gong, S., Donthamsetti, P., Grinnell, S. G., Nelson, M. N., Newman, A. H., et al. (2018). Regional heterogeneity of D2-receptor signaling in the dorsal striatum and nucleus accumbens. *Neuron* 98, 575–587. doi: 10.1016/j.neuron.2018.03.038

McAlonan, K., and Brown, V. J. (2003). Orbital prefrontal cortex mediates reversal learning and not attentional set shifting in the rat. *Behav. Brain Res.* 146, 97–103. doi: 10.1016/j.bbr.2003.09.019

McLaughlin, R. J., and Floresco, S. B. (2007). The role of different subregions of the basolateral amygdala in cue-induced reinstatement and extinction of food-seeking behavior. *Neuroscience* 146, 1484–1494. doi: 10.1016/j.neuroscience.2007.03.025

Monchi, O., Petrides, M., Petre, V., Worsley, K., and Dagher, A. (2001). Wisconsin card sorting revisited: distinct neural circuits participating in different stages of the task identified by event-related functional magnetic resonance imaging. *J. Neurosci.* 21, 7733–7741. doi: 10.1523/jneurosci.21-19-07733.2001

Nieoullon, A., and Coquerel, A. (2003). Dopamine: a key regulator to adapt action, emotion, motivation and cognition. *Curr. Opin. Neurol.* 16, S3–9. doi: 10.1097/00019052-200312002-00002

O'Neill, M., and Brown, V. J. (2007). The effect of striatal dopamine depletion and the adenosine A_{2A} antagonist KW-6002 on reversal learning in rats. *Neurobiol Learn Mem* 88, 75–81. doi: 10.1016/j.nlm.2007.03.003

Pandolfo, P., Machado, N. J., Köfalvi, A., Takahashi, R. N., and Cunha, R. A. (2013). Caffeine regulates frontocorticostriatal dopamine transporter density and improves attention and cognitive deficits in an animal model of attention deficit hyperactivity disorder. *Eur. Neuropsychopharmacol.* 23, 317–328. doi: 10.1016/j.euroneuro.2012.04.011

Pantelis, C., Barber, F. Z., Barnes, T. R. E., Nelson, H. E., Owen, A. M., and Robbins, T. W. (1999). Comparison of set-shifting ability in patients with chronic schizophrenia and frontal lobe damage. *Schizophr. Res.* 37, 251–270. doi: 10.1016/s0920-9964(98)00156-x

Papp, E., Borhegyi, Z., Tomioka, R., Rockland, K. S., Mody, I., and Freund, T. F. (2012). Glutamatergic input from specific sources influences the nucleus accumbens-ventral pallidum information flow. *Brain Struct. Funct.* 217, 37–48. doi: 10.1007/s00429-011-0331-z

Pardo, M., Lopez-Cruz, L., Valverde, O., Ledent, C., Baqi, Y., Müller, C. E., et al. (2012). Adenosine A_{2A} receptor antagonism and genetic deletion attenuate the effects of dopamine D2 antagonism on effort-based decision making in mice. *Neuropharmacology* 62, 2068–2077. doi: 10.1016/j.neuropharm.2011.12.033

Parikh, V., Cole, R. D., Patel, P. J., Poole, R. L., and Gould, T. J. (2016a). Cognitive control deficits during mecamylamine-precipitated withdrawal in mice: possible links to frontostriatal BDNF imbalance. *Neurobiol. Learn. Mem.* 128, 110–116. doi: 10.1016/j.nlm.2016.01.003

Parikh, V., Naughton, S. X., Yegla, B., and Guzman, D. M. (2016b). Impact of partial dopamine depletion on cognitive flexibility in BDNF heterozygous mice. *Psychopharmacology* 233, 1361–1375. doi: 10.1007/s00213-016-4229-6

Parsons, M. P., Li, S., and Kirouac, G. J. (2007). Functional and anatomical connection between the paraventricular nucleus of the thalamus and dopamine fibers of the nucleus accumbens. *J. Comp. Neurol.* 500, 1050–1063. doi: 10.1002/cne.21224

Prado, V. F., Janickova, H., Al-Onaizi, M. A., and Prado, M. A. (2017). Cholinergic circuits in cognitive flexibility. *Neuroscience* 345, 130–141. doi: 10.1016/j.neuroscience.2016.09.013

Ragozzino, M. E. (2007). The contribution of the medial prefrontal cortex, orbitofrontal cortex and dorsomedial striatum to behavioral flexibility. *Ann. N. Y. Acad. Sci.* 1121, 355–375. doi: 10.1196/annals.1401.013

Reeve, W. V., and Schandler, S. L. (2001). Frontal lobe functioning in adolescents with attention deficit hyperactivity disorder. *Adolescence* 36, 749–765.

Salgado, S., and Kaplitt, M. G. (2015). The nucleus accumbens: a comprehensive review. *Stereotact. Funct. Neurosurg.* 93, 75–93. doi: 10.1159/000368279

Schiffmann, S., Gall, D., Ferré, S., and Azdad, K. (2010). Dopamine D2 and adenosine A_{2A} receptors regulate activity of striatopallidal neurons through A_{2A} -D2 receptor heteromerization. *Purinergic Signalling* 6, 98–99. doi: 10.1038/npp.2008.144

Sesack, S. R., and Grace, A. A. (2010). Cortico-basal ganglia reward network: microcircuitry. *Neuropsychopharmacology* 35, 27–47. doi: 10.1038/npp.2009.93

Shen, H. Y., Coelho, J. E., Ohtsuka, N., Canas, P. M., Day, Y. J., Huang, Q. Y., et al. (2008). A critical role of the adenosine A_{2A} receptor in extrastriatal neurons in modulating psychomotor activity as revealed by opposite phenotypes of striatum and forebrain A_{2A} receptor knock-outs. *J. Neurosci.* 28, 2970–2975. doi: 10.1523/jneurosci.5255-07.2008

Stuber, G. D., Sparta, D. R., Stamatakis, A. M., van Leeuwen, W. A., Hardjoprajitno, J. E., Cho, S., et al. (2011). Excitatory transmission from the amygdala to nucleus accumbens facilitates reward seeking. *Nature* 475, 377–380. doi: 10.1038/nature10194

Svenningsson, P., Le Moine, C., Fisone, G., and Fredholm, B. B. (1999). Distribution, biochemistry and function of striatal adenosine A_{2A} receptors. *Prog. Neurobiol.* 59, 355–396. doi: 10.1016/s0301-0082(99)00011-8

Syed, E. C., Grima, L. L., Magill, P. J., Bogacz, R., Brown, P., and Walton, M. E. (2016). Action initiation shapes mesolimbic dopamine encoding of future rewards. *Nat. Neurosci.* 19, 34–36. doi: 10.1038/nn.4187

Tai, C. T., Cassaday, H. J., Feldon, J., and Rawlins, J. N. (1995). Both electrolytic and excitotoxic lesions of nucleus accumbens disrupt latent inhibition of learning in rats. *Neurobiol. Learn. Mem.* 64, 36–48. doi: 10.1006/nlme.1995.1042

Takahashi, E., Niimi, K., and Itakura, C. (2011). Role of Ca(V)2.1-mediated NMDA receptor signaling in the nucleus accumbens in spatial short-term memory. *Behav. Brain Res.* 218, 353–356. doi: 10.1016/j.bbr.2010.12.019

Tebano, M. T., Pintor, A., Frank, C., Domenici, M. R., Martire, A., Pepponi, R., et al. (2004). Adenosine A_{2A} receptor blockade differentially influences excitotoxic mechanisms at pre- and postsynaptic sites in the rat striatum. *J. Neurosci. Res.* 77, 100–107. doi: 10.1002/jnr.20138

Tsutsui-Kimura, I., Takiue, H., Yoshida, K., Xu, M., Yano, R., Ohta, H., et al. (2017). Dysfunction of ventrolateral striatal dopamine receptor type 2-expressing medium spiny neurons impairs instrumental motivation. *Nat. Commun.* 8:14304. doi: 10.1038/ncomms14304

Varvel, S. A., and Lichtman, A. H. (2002). Evaluation of CB1 receptor knockout mice in the morris water maze. *J. Pharmacol. Exp. Ther.* 301, 915–924. doi: 10.1124/jpet.301.3.915

Voorn, P., Vanderschuren, L. J., Groenewegen, H. J., Robbins, T. W., and Pennartz, C. M. (2004). Putting a spin on the dorsal-ventral divide of the striatum. *Trends Neurosci.* 27, 468–474. doi: 10.1016/j.tins.2004.06.006

Wang, X. Y., Qiao, Y. H., Dai, Z. H., Sui, N., Shen, F., Zhang, J. J., et al. (2019). Medium spiny neurons of the anterior dorsomedial striatum mediate reversal learning in a cell-type-dependent manner. *Brain Struct. Funct.* 224, 419–434. doi: 10.1007/s00429-018-1780-4

Wei, C. J., Augusto, E., Gomes, C. A., Singer, P., Wang, Y., Boison, D., et al. (2014). Regulation of fear responses by striatal and extrastriatal adenosine A_{2A} receptors in forebrain. *Biol. Psychiatry* 75, 855–863. doi: 10.1016/j.biopsych.2013.05.003

Wei, W., Ding, S., and Zhou, F. M. (2017). Dopaminergic treatment weakens medium spiny neuron collateral inhibition in the parkinsonian striatum. *J. Neurophysiol.* 117, 987–999. doi: 10.1152/jn.00683.2016

Wei, C. J., Singer, P., Coelho, J., Boison, D., Feldon, J., Yee, B. K., et al. (2011). Selective inactivation of adenosine A_{2A} receptors in striatal neurons enhances working memory and reversal learning. *Learn. Mem.* 18, 459–474. doi: 10.1101/lm.2136011

Yawata, S., Yamaguchi, T., Danjo, T., Hikida, T., and Nakanishi, S. (2012). Pathway-specific control of reward learning and its flexibility via selective dopamine receptors in the nucleus accumbens. *Proc. Natl. Acad. Sci. U S A* 109, 12764–12769. doi: 10.1073/pnas.1210797109

Yin, H. H., and Knowlton, B. J. (2006). The role of the basal ganglia in habit formation. *Nat. Rev. Neurosci.* 7, 464–476. doi: 10.1038/nrn1919

Yu, C., Gupta, J., Chen, J. F., and Yin, H. H. (2009). Genetic deletion of A_{2A} adenosine receptors in the striatum selectively impairs habit formation. *J. Neurosci.* 29, 15100–15103. doi: 10.1523/jneurosci.4215-09.2009

Yu, X. Z., Taylor, A. M. W., Nagai, J., Golshani, P., Evans, C. J., Coppola, G., et al. (2018). Reducing astrocyte calcium signaling in vivo alters striatal microcircuits and causes repetitive behavior. *Neuron* 99, 1170–1187. doi: 10.1016/j.neuron.2018.08.015

Zheng, W., Zhou, J., Luan, Y., Yang, J., Ge, Y., Wang, M., et al. (2018). Spatiotemporal control of GPR37 signaling and its behavioral effects by optogenetics. *Front. Mol. Neurosci.* 11:95. doi: 10.3389/fnmol.2018.00095

Zhu, Y., Nachtrab, G., Keyes, P. C., Allen, W. E., Luo, L., and Chen, X. (2018). Dynamic salience processing in paraventricular thalamus gates associative learning. *Science* 362, 423–429. doi: 10.1126/science.aat0481

Zhu, Y., Wienecke, C. F., Nachtrab, G., and Chen, X. (2016). A thalamic input to the nucleus accumbens mediates opiate dependence. *Nature* 530, 219–222. doi: 10.1038/nature16954

Conflict of Interest Statement: The authors declare that the research was conducted in the absence of any commercial or financial relationships that could be construed as a potential conflict of interest.

frontiers in Cellular Neuroscience

ORIGINAL RESEARCH
published: 12 April 2019
doi: 10.3389/fncel.2019.00143

Amyloid Peptide Induced Neuroinflammation Increases the P2X7 Receptor Expression in Microglial Cells, Impacting on Its Functionality

Carlos Martínez-Frailes[1,2†], Caterina Di Lauro[1,2†], Carolina Bianchi[1,2], Laura de Diego-García[1,3‡], Álvaro Sebastián-Serrano[1,2,3‡], Lisardo Boscá[3‡] and Miguel Díaz-Hernández[1,2]*

[1] Department of Biochemistry and Molecular Biology, Veterinary School, Complutense University of Madrid, Madrid, Spain, [2] Instituto de Investigación Sanitaria del Hospital Clínico San Carlos, Madrid, Spain, [3] Instituto de Investigaciones Biomedicas "Alberto Sols", Consejo Superior de Investigaciones Científicas-Universidad Autónoma de Madrid, Madrid, Spain

Alzheimer disease is a neurodegenerative disease characterized by the presence of senile plaques composed of amyloid-β (Aβ) peptide, neurofibrillary tangles, neuronal loss and neuroinflammation. Previous works have revealed that extracellular ATP, through its selective receptor P2X7 (P2X7R), is essential to neuroinflammation and neurotoxicity induced by Aβ. P2X7R is upregulated on microglial cells around the senile plaques. This upregulation progressively rises with age and is parallel with an accumulation of senile plaques and also correlates with the synaptic toxicity detected both in animal models reproducing AD and human patients of AD. Furthermore, the late onset of the first AD-associated symptoms suggests that aging associated-changes may be relevant to the disease progression. Thus, microglia motility and its capacity to respond to exogenous ATP stimulus decrease with aging. To evaluate whether the P2X7R age related-changes on microglia cells may be relevant to the AD progression, we generated a new transgenic mouse model crossing an Aβ peptide mouse model, J20 mice and the P2X7R reporter mice ^{P2X7R}EGFP. Our results indicate that neuroinflammation induced by Aβ peptide causes changes in the P2X7R distribution pattern, increasing it s expression in microglial cells at advanced and late stages, when microgliosis occurs, but not in the early stages, in the absence of microgliosis. In addition, we found that P2X7R activation promotes microglial cells migration to senile plaques but decreases their phagocytic capacity. Moreover, we found a significant reduction of P2X7R transcription on neuronal cells at the early and advanced stages, but not at the late stages. Since previous studies have reported that either pharmacological inhibition or selective downregulation of P2X7R significantly improve behavioral alterations and reduce the incidence and size of senile plaques in the early and advanced stages of AD, the results presented here provide new evidence, indicating that this therapeutic approach could be also efficient in the late stages of the disease.

Keywords: senile plaques, neuroinflammation, LPS, BzATP, ATP, Alzheimer disease, phagocytosis, migration

OPEN ACCESS

Edited by:
Eric Boué-Grabot, Université de Bordeaux, France

Reviewed by:
Francesco Di Virgilio, University of Ferrara, Italy
Robson Coutinho-Silva, Federal University of Rio de Janeiro, Brazil
Luiz Eduardo Baggio Savio, Federal University of Rio de Janeiro, Brazil

***Correspondence:**
Miguel Díaz-Hernández
migueldiaz@ucm.es

[†] These authors have contributed equally to this work

*[‡] **Present address:***
Laura de Diego-García, Department of Physiology and Medical Physics, Royal College of Surgeons in Ireland, Dublin, Ireland
Álvaro Sebastián-Serrano, Centro de Investigación Biomédica en Red sobre Enfermedades Neurodegenerativas, Instituto de Salud Carlos III, Madrid, Spain
Lisardo Boscá, Centro de Investigación Biomédica en Red sobre Enfermedades Cardiovasculares, Instituto de Salud Carlos III, Madrid, Spain

***Received:** 24 January 2019*
***Accepted:** 22 March 2019*
***Published:** 12 April 2019*

Citation:
Martínez-Frailes C, Di Lauro C, Bianchi C, de Diego-García L, Sebastián-Serrano Á, Boscá L and Díaz-Hernández M (2019) Amyloid Peptide Induced Neuroinflammation Increases the P2X7 Receptor Expression in Microglial Cells, Impacting on Its Functionality. Front. Cell. Neurosci. 13:143. doi: 10.3389/fncel.2019.00143

INTRODUCTION

Alzheimer disease (AD) is a neurodegenerative disease for which, currently, there is no effective treatment available. At a neuropathological level, the disease is characterized by the presence of a profound cortical atrophy associated with a generalized neuroinflammation state (Gahtan and Overmier, 1999), synaptic contacts loss, neuronal depletion and two histopathological hallmarks, the extracellular amyloid plaques and the intracellular neurofibrillary tangles (Selkoe, 2001; Avila, 2006). Neurofibrillary tangles are assembled by hyperphosphorylated tau protein whereas the amyloid plaques are primarily composed of Aβ-amyloid (Aβ) peptide, which is derived from sequential proteolysis of the APP by β- and γ-secretases (Selkoe, 2001). In 2–5% of AD cases have been found mutations both in APP protein and enzymes related in its processing (PS1 and PS2). These cases are denominated as Familiar Alzheimer disease or FAD (Price and Sisodia, 1998; Ling et al., 2003). The development of different transgenic animal models that mimic the FAD symptoms have allowed the confirmation that Aβ peptide is one of the toxic species involved in AD (Hsiao et al., 1996; Mucke et al., 2000; Radde et al., 2006).

Over recent years, several pieces of evidence, provided by different groups, indicate that extracellular ATP plays a crucial role in APP-induced toxicity, primarily through the activation of its selective ionotropic receptor P2X7 (P2X7R). It was found that ATP regulates APP processing via P2X7R (Delarasse et al., 2011; Leon-Otegui et al., 2011; Diaz-Hernandez et al., 2012). A negative association between the P2X7R 489C > T polymorphism and AD has also been established (Sanz et al., 2014). Upregulation of P2X7R was found in AD patients (McLarnon et al., 2006; Sanz et al., 2009; Martin et al., 2018), especially in microglial cells around the senile plaques (Parvathenani et al., 2003). Interestingly, P2X7R upregulation was seen to progressively rise with age and parallels the accumulation of senile plaques (Lee et al., 2011), and correlates with the synaptic toxicity associated to AD (Lee et al., 2011). In agreement with these findings, i.c. of Aβ peptides induced gliosis, hippocampal neurons loss and an increase of hippocampal P2X7R expression (Ryu and Mclarnon, 2008), and the pharmacological P2X7R-blockage reverted the memory impairment associated (Chen et al., 2014). The fact that i.c. of Aβ to P2X7R deficient mice did not cause the above alterations mentioned, suggests that P2X7R is essential for the microglial activation induced by Aβ peptide (Sanz et al., 2009). Furthermore, it also reported that its selective downregulation promotes microglial phagocytosis of Aβ peptide (Ni et al., 2013). Nevertheless, the late onset of the first AD-associated symptoms suggests that aging associated-changes may be relevant to the disease progression (Mosher and Wyss-Coray, 2014). In accordance with this hypothesis, age induced-changes on microglial morphology are exacerbated in AD patients (Serrano-Pozo et al., 2013). Microglia motility and its capacity to respond to exogenous ATP stimulus decrease with aging (Koenigsknecht-Talboo et al., 2008; Damani et al., 2011). It has consequently been seen that microglial cells are removing Aβ in early stages more efficiently than in later stages of AD (Solito and Sastre, 2012). All these data suggest that P2X7R age related-changes on microglia cells are relevant to the AD progression.

In previous studies, we found that *in vivo* pharmacological P2X7R blockage reduced the number and size of senile plaques downregulating the amyloidogenic processing and promoting the non- amyloidogenic processing of APP in young J20 mice, a FAD mouse model (Diaz-Hernandez et al., 2012). However, J20 mice treated with P2X7R antagonist did not show, either a decreased microglial recruitment toward senile plaques or a significant increase in microglial population, at least, at the tested-age (Diaz-Hernandez et al., 2012). Taking into account the repercussion that the microglia aging appears to have on AD progression, in the current study, we decided to analyze whether P2X7R-regulated microglial functions, such as microglial activation, phagocytosis or migration are altered over the AD progression. To address this question, we generated a new transgenic mouse by crossing the AD mouse model, J20 mice, and the P2X7R reporter mice ^{P2X7R}EGFP.

MATERIALS AND METHODS

Animals

All animal procedures were carried out at the Universidad Complutense of Madrid, in compliance with National and European regulations (RD1201/2005; 86/609/CEE) following the guidelines of the International Council for the Laboratory Animal Science. The protocol was approved by the Committee of Animal Experiments of the Complutense University of Madrid and the Environmental Counseling of the Comunidad de Madrid, Spain. All animals were housed with food and water available *ad libitum* and maintained in a temperature-controlled environment on a 12/12 h light/dark cycle with light onset at 08:00 A.M. All surgery was performed under isoflurane anesthesia, and all efforts were made to minimize suffering.

^{P2X7R}EGFP reporter mice (Tg [P2rx7-EGFP] FY174Gsat/Mmcd, stock 011959-UCD) expressing EGFP immediately downstream of P2X7R promoter (Sebastian-Serrano et al., 2016). J20 hAPP transgenic mouse line express a mutant form of the human amyloid protein precursor bearing both the Swedish (K670N/M671L) and the Indiana (V717F) mutations (APPSwInd), labeled as strain B6.Cg-Tg (PDGFB-APPSwInd) 20Lms/2J. This mouse strain develops the

Abbreviations: Aβ peptide, amyloid-β; AD, Alzheimer disease; APP, amyloid precursor protein; ATP, Adenosine 5′-triphosphate; BSA, bovine serum albumin; BzATP, 2′,3′-O-(4-benzoyl)-benzoyl ATP; CNS, central nervous system; CytoD, Cytochalasin D; DAPI, 4′,6-Diamidine-2′-phenylindole dihydrochloride; DMEM, Dulbecco's Modified Eagle Medium; DMSO, dimethyl sulfoxide; EGFP, enhance green fluorescent protein; FAD, Familiar Alzheimer disease; FBS, fetal bovine serum; GLDG, granular layer of the dentate gyrus; HEPES, 4-(2-hydroxyethyl)-1-piperazineethanesulfonic acid; HRP, horseradish peroxidase; i.c., intracranial administration; i.p., intraperitoneally; J20 mice, mouse model of Familiar Alzheimer disease; p, postnatal day; P2X7R, P2X7 receptor; ^{P2X7R}EGFP mice, P2X7R reporter mice ^{P2X7R}EGFP; ^{P2X7R}EGFP/J20, mice generated crossing ^{P2X7R}EGFP and J20 mice; PBS, Phosphate-Buffered saline; PBS-T, PBS-buffer containing 0.1 % (v/v) Tween-20; PFA, paraformaldehyde; PS1 and PS2, presenilin-1 and -2; s.e.m., mean ± standard error of the mean; SDS-PAGE, Sodium dodecyl sulfate-polyacrylamide gel electrophoresis; WT, wild-type mice.

characteristic amyloid peptide deposits by 6–8 months of age (Mucke et al., 2000). ^{P2X7}EGFP/J20 mice were generated crossing heterozygous ^{P2X7}EGFP mice by heterozygous J20 mice.

PCR Genotyping

Genomic DNA was obtained from tail biopsies using Wizard® SV Genomic DNA Purification System (Promega, Madison, WI, United States) according to the manufacturer's protocol.

Simple PCR reactions were carried out using DNA Amplitools Master Mix (Biotools, Madrid, Spain), specific primers (400 nM each) and 5 μL of genomic DNA in a final volume of 25 μL. Animals were genotyped using specific primers for ^{P2X7R}EGFP Fw 5′-CCTACGGCGTGCAGTGCTTCAGC-3′ and Rv 5′-CGGCGAGCTGCACGCTGCGTCCTC-3′; primers for J20 Fw 5′-GGTGAGTTTGTAAGTGATGCC-3′ and Rv 5′-TCTTCTTCTTCCACCTCAGC-3′. PCR was carried out over 40 cycles of 94°C for 30 s, 60°C for 45 s, and 72°C for 45 s for EGFP primers or over 40 cycles of 94°C for 30 s, 60°C for 45 s, and 72°C for 45 s for J20 primers.

PCR amplification products were electrophoresed on a 1.5% (w/v) agarose gel and stained with SYBR® Safe DNA Gel Stain (Life Technologies, Carlsbad, CA, United States). PCR bands were visualized by gel imaging system Gel Logic 200 Imaging System (Kodak, Rochester, NY, United States).

Human Samples

The Netherlands Brain Bank provided the human brain tissues, which supplies postmortem specimens from clinically well documented and neuropathologically confirmed AD patients and non-diseased donors (NBB, Netherlands Institute for Neuroscience, Amsterdam). The NBB works following all national laws and regulations. Frozen samples used were obtained from three different regions of the temporal lobe (inferior, medial, and superior) from four patients with the clinical diagnosis of AD (three women aged 73, 83, and 85 years old and one man aged 85 years) and four non-demented controls (three women aged 70, 72, and 85 years old and one man aged 73 years) following the protocols of nervous tissue donation approved by the local Ethical Committees of the Netherlands Brain Bank. The postmortem delay in tissue processing was between 4 and 5 h in both groups.

Microglial Cell Culture

Primary microglial cultures were prepared from the hippocampus of WT at postnatal (p) 4–5 days as previously described (de Diego Garcia et al., 2018). Mixed glial culture containing both astrocytes and microglial was maintained in a 37°C incubator with a humidified atmosphere of 5% CO_2 for 14 days in 75 cm^2 flasks containing DMEM medium supplemented with 10% fetal calf serum (Gibco) 2 mM glutamine, 100 μ/ml penicillin, 100 μg/ml streptomycin, 50 μg/ml kanamycin, and 0.25 μg/ml Amphotericin B (all from Sigma-Aldrich). The medium was replaced every 3 days. Microglial cells were de-attached by shaking the culture flasks at 250 rpm for 2 h at 37°C in an orbital shaker. Microglia cells were plated at 5×10^5 cells/well in six-well plates and cultured in supplemented DMEM media (Thermo Fisher).

Chemical and Antibodies

LPS, ATP, BzATP (catalog number B6396), and the antibody anti-α-tubulin (catalog number T6199) were purchased from Sigma-Aldrich (Madrid, Spain). Anti-NeuN antibody (catalog number MAB377) were obtained from Merck Millipore (Tullagreen, Ireland). A438079 (catalog number 2972/10) was obtained from Tocris BioScience (Bristol, United Kingdom). Monoclonal anti Aβ 4–10 residues clone WO2 (catalog number MABN10) was purchased from Merck Chemicals (Madrid, Spain). The commercial antibody for P2X7R (catalog number APR-004) was purchased from Alomone Labs (Jerusalem, Israel). Antibodies against enhanced green fluorescent protein (EGFP) were obtained from Thermo Fisher (catalog number A11122) and AVESLab (catalog number GFP-1020) (Tigard, OR, United States). Red Fluorescent 2 μm diameter microspheres (catalog number F8826) (Life technologies). Antibody against Iba-1 (catalog number 019-19741) was provided from Wako (Richmond, VA, United States). CytoD (catalog number sc-201442) was provided by Santa Cruz (Dallas, TX, United States). Selective P2X7R antagonist GSK 1482160A was provided by GlaxoSmithKline (Madrid, Spain)

Phagocytosis Assays

In vitro; Phagocytosis assays were performed 24 h after microglial cell seeding on coverslips of 35-mm of diameter. Pharmacological treatments were applied 20 min before adding the fluorescencent microspheres. Red Fluorescent 2 μm diameter microspheres (Life Technologies) at 0,002% in DMEM medium were added to microglial cells, and afterward, cells were put back in the incubator and left to rest for 2 h. Then, the medium was removed, and cells were washed thoroughly with PBS three times and fixed in PFA 4%.

Microglial cells were stained with a rabbit polyclonal anti-Iba1 (1/200) obtained from Wako and revealed with goat anti-rabbit IgG labeled with Alexa 488 (1/400) obtained from Molecular Probes. For each coverslip, 4 random pictures were taken, using the TCS SPE confocal microscope (Leica Microsystems, Wetzlar, Germany). Images were analyzed using ImageJ software (US National Institutes of Health, Bethesda, MD, United States). The number of fluorescent beads inside each cell was counted, and the average number of phagocyted microspheres per microglial cell was calculated for each experiment and treatment. Experiments were repeated at least 3 times for each condition.

In vivo; 6-month-old ^{P2X7R}EGFP mice (n = 6) were anesthetized with isoflurane (1-chloro-2, 2, 2-trifuoroethyl-difluormethylether) (Isovet®, BRAUN, Rubi, Barcelona, Spain) diluted in 50% O_2. The scalp was incised along the midline, and one hole was made at the appropriate stereotaxic coordinates from Bregma (mediolateral, 1 mm; anteroposterior, 2 mm; dorsoventral, 1.8 mm). 1 μL of 0.02% red Fluorescent 2 μm microspheres in PBS was intracranial administrated (i.c.) at a rate of ≈1 μL/min.

In some cases, the selective P2X7R antagonist GSK 1482160A (from GlaxoSmithKline, Madrid, Spain) was i.p. administrated at 100mg/Kg dosage every 24 h for 1 week. GSK 1482160A was

diluted in vehicle solution composed of 20% hydroxypropyl-β-cyclodextrin plus 0.2% DMSO in sterile PBS. Control littermates were treated with vehicle solution using the same relationship (volume per body weight).

Migration Assay

The migration assays were performed placing 1.5×10^5 hippocampal microglia cells contained in 200 μL of serum free in the upper chamber of the 24-well format, 8.0 μm pore size *trans*-well inserts (Costar, New York, NY, United States), and 600 μL of the same medium containing 10% of FBS in the lower chamber. In some cases, cells were pre-treated with 1 μM GSK 1482160A before stimulating them with 1 mM ATP or 300 μM BzATP for 24 h at 37°C in 5% of CO_2. The inserts were subsequently removed rinsing twice with PBS and fixed in 4% PFA for 10 min, followed by staining with DAPI for 10 min. The cells on the upper side of the filter were removed with cotton-tipped swabs. The microglial migration was quantified by counting the number of cells that migrated through the membrane to the other side. The images were selected from 20 random fields for each treatment with microscopy at 50x magnification, and the number of migrating cells was quantified. Each experiment was repeated at least three times.

LPS Treatment

^{P2X7R}EGFP mice weighing at the indicated ages were i.p. treated with either sterile PBS or LPS (5 mg/Kg, *Escherichia coli*, serotype 055: B5) ($n = 5$ per age and treatment). Mice were sacrificed 24 h (acute) or 7 days (chronic) after injection.

Immunofluorescence Studies

For confocal microscopy, animals were transcardially perfused with 4% PFA in Sorensen's buffer for 10 min, post-fixed, and brains were cryoprotected in sucrose before sectioning. Brain slices were washed in PBS and treated with blocking solution containing 5 % FBS, 1% BSA, and 0.2% Triton-X 100 in PBS buffer. After that, samples were incubated with primary antibodies diluted in blocking solution. After washed them, sections were incubated with fluorescent-tagged secondary antibodies to be counterstained with DAPI (Thermo Fisher) and mounted in FluorSave (Merck Millipore) later. The following primary antibodies were used at the indicated dilutions: mouse anti-APP clone (WO2) 1:200, rabbit anti-GFP 1:400, chicken anti-EGFP 1:400, rabbit anti-P2X7R 1:200, rabbit anti-Iba-1 1:200. Donkey anti-rabbit, anti-mouse or anti-chicken secondary antibodies, conjugated with Alexa 488, 594 or 647 (Life Technologies, Madrid, Spain) were used at 1:400. Confocal images were acquired with a TCS SPE. Confocal images stacks were acquired with a TCS SPE microscope from Leica Microsystems equipped with a Plan Fluor 10X dry objective lens NA = 0.30, 40X Apochromat NA = 1.15 oil objective lens and 63X Apochromat NA = 1.3 oil objective lens (Leica Microsystems GmbH) at room temperature. The images stacks are composite by a sequence of at least 20 pictures acquired every 0.5 μm on the *Z*-axis. For the detection of DAPI, 405 nm laser line was used. For Alexa Fluor 594, the 561 nm laser line was used. For Alexa Fluor 488, the 488 nm laser line was used. For Alexa 647, the 645 nm laser line was used. Images were acquired using the Leica software LAS AF v2.2.1 software (Leica Microsystems GmbH) and the Z projection of images stacks was made using ImageJ 1.47d (NIH). In some cases, it also shows orthogonal views corresponding to specific locations (indicated by dashed lines) of images stack. Green cells in the hippocampus were considered those cells positively marked with antibodies against GFP with an identifiable cellular morphology and whose nucleus was positively stained with DAPI.

Quantification of GFP Positive Microglial and Neuron Cells and Distances Measurement

For each case (at least 4 mice per phenotype, age and treatment) 4 series (16 sections, 90 μm apart, approximately spanning from Bregma −0.95 mm to −3.78 mm according to Paxinos and Franklin (2001) of sections (30 μm thick) were selected to be immunostained with antibodies anti-GFP, anti-Iba-1, anti-P2X7R or anti-APP (clone WO2) respectively. In some cases, hippocampal slices were stained with more than one antibody.

The number of cells corresponding to each cell type was counted, identified by specific antibodies (neurons using NeuN antibody and microglial cells with Iba-1 antibody). The counting was performed using blind-coded on grayscale 8-byte images from whole-hippocampal area acquired at low magnification. The background signal was determined by visual analysis, obtaining a cut-off value of 150 on a 0–255 scale with 0 = white and 255 = black using the free software ImageJ 1.45h (US National Institutes of Health, Bethesda, MD, United States).

Distances of GFP positive or P2X7R positive cells to the senile plate were measured from the core of the cellular body, to the border of the nearest senile plate bigger than 30 nm in its longer axis.

Western Blotting

Hippocampal samples from WT, J20, ^{P2X7R}EGFP or ^{P2X7R}EGFP/J20 mice and Human samples were treated with lysis buffer containing 20 mM HEPES, 100 mM NaCl, 50 mM NaF, 5 mM EDTA, 5 mM Na_3VO_4 (all salts from Sigma-Aldrich), 1% Triton X-100, okadaic acid and CompleteTM Protease Inhibitor Cocktail Tablets, pH 7.4 (Roche Diagnostics GmbH). Protein concentration was determined, and then, samples were boiled in a gel-loading buffer and separated by SDS-PAGE. Proteins were transferred to nitrocellulose membranes and probed with the following primary antibodies: rabbit anti- P2X7R (1:1000) antibody or mouse anti-α-tubulin (1:10000) antibody. Blots were then washed in PBS-T and incubated with goat anti-rabbit or goat anti-mouse IgGs coupled with HRP (Amersham GE Healthcare), used at 1:1000 and 1:5000, respectively. Protein bands were visualized by chemiluminescence (Pierce Biotechnology, Rockford, IL, United States) using ImageQuant LAS500 (GE Healthcare Life Sciences) and analyzed using ImageJ software (v1, 47d, NIH, Bethesda, MD, United States).

Statistical Analysis

Results were analyzed by unpaired *t*-test or ANOVA test followed by Bonferroni's or Sidak's multiple comparisons tests using GRAPH PAD PRISM 6 (Graph Pad Software Inc., San Diego, CA, United States) and expressed as the s.e.m. Differences were considered to be significant at $p < 0.05$.

RESULTS

In a Familiar Alzheimer Disease Mouse Model (FAD), Microglial Cells Begin to Express P2X7R at Adult Stages, Once Microgliosis Takes Place

To elucidate if Aβ peptide conditions the P2X7R expression on microglial cells along the AD progression, we generated a new transgenic mouse model by crossbreeding the amyloid mice model of the AD, J20 mice with the ^{P2X7R}EGFP mice that express EGFP under the control of the P2X7R promoter. ^{P2X7R}EGFP/J20 and their corresponding control littermates ^{P2X7R}EGFP mice were sacrificed to analyze their hippocampus by immunofluorescence techniques at the following ages; 4–6 months-old (early stage), 10–12 months-old (advanced stage), and 16–20 months-old (late stage). Results showed that EGFP positive cells were mainly found on the GLDG on both genotypes and at all ages tested. In addition, disseminated EGFP-positive cells throughout the whole hippocampus were also found (**Figure 1A**). Double immunofluorescence studies using specific neuronal marker NeuN or glial markers GFAP and Iba-1 for astroglial cells and microglial cells respectively revealed that EGFP positive cells on GLDG were neurons while disseminated extra granular EGFP-positive green cells were microglial cells (**Supplementary Figure 1**). Curiously, in the early and advanced stages, the number of EGFP-positive neurons in GLDG was lower in ^{P2X7R}EGFP/J20 than observed in ^{P2X7R}EGFP mice ($7.9 \pm 0.4\ 10^4$ vs. $5.4 \pm 0.5\ 10^4$ in the early stages and $8.3 \pm 0.4\ 10^4$ vs. $6.3 \pm 0.6\ 10^4$ in the advanced stages, **Figures 1A,D**). However, no change on EGFP-positive neurons in GLDG was found between ^{P2X7R}EGFP/J20 and ^{P2X7R}EGFP mice at late stages ($8.7 \pm 0.3\ 10^4$ vs. $8.2 \pm 0.5\ 10^4$ in the late stages, **Figures 1A,D**). Otherwise, ^{P2X7R}EGFP/J20 mice presented a higher number of disseminated EGFP-positive microglial cells than those observed in their corresponding control littermates ^{P2X7R}EGFP mice both in the advanced and late stages (1.5 ± 0.3 vs. 6.4 ± 1.0 in the advanced stages and 4.3 ± 0.6 vs. 7.7 ± 0.6 in late stages, **Figures 1A,C**). Non-differences in the number of EGFP-positive microglial cells were found between ^{P2X7R}EGFP/J20 and ^{P2X7R}EGFP mice in the early stages (0.6 ± 0.2 vs. 1.6 ± 0.5, **Figures 1A,C**). It is worth highlighting that while ^{P2X7R}EGFP/J20 and ^{P2X7R}EGFP mice showed, in the early stages, a similar number of hippocampal microglial cells, in the advanced and late stages, ^{P2X7R}EGFP/J20 mice presented a significant increase of microglial cells compared with those detected in their corresponding littermates ^{P2X7R}EGFP mice (**Figures 1A,B**). These data indicate that in the FAD early stages, when a microgliosis had not yet taken place but the senile plaques start to be detected (**Figure 1A**), negative modulation of P2X7R transcription occurs in neurons, but did not affect microglial cells. Conversely, in FAD advanced stages, once a significant microgliosis begins to be detected and the number of senile plates increase (**Figures 1A,B**), a rise of P2X7R transcription occurs in microglial cells, but the reduction of P2X7R transcription is maintained in neurons. Finally, in the late stages of the FAD, when microgliosis remains over time, the increased of P2X7R transcription remains in microglial cells, but the neuronal reduction of P2X7R transcription disappears.

In the following step, we decided to check if the changes observed in P2X7R transcription affected the protein expression of this receptor. To this end, we measured P2X7R protein expression levels in hippocampal samples from WT and J20 mice at the same ages as those we had previously analyzed ^{P2X7R}EGFP/J20 and ^{P2X7R}EGFP mice. Results revealed that J20 mice, at the early stages, presented similar P2X7R levels to those observed in their control littermates. However, in their advanced and late stages, J20 mice showed higher P2X7R expression levels than those detected in their corresponding control littermates ($209 \pm 34\%$ in the advanced stages and $140 \pm 9\%$ in the late stages, **Figures 2A,B**). Double immunofluorescence studies using P2X7R and Iba-1 antibodies showed that, similarly to that observed in ^{P2X7R}EGFP/J20 mice, J20 mice presented a higher number of P2X7R positive microglial cells than those detected in their corresponding control littermate WT mice both in the advanced and late stages ($4 \pm 1\%$ vs. $13 \pm 1\%$ in the advanced stages and $5 \pm 1\%$ vs. $18 \pm 1\%$ in the late stages (**Figures 2C,D**). Interestingly, something similar was observed in ^{P2X7R}EGFP mice, the percentage of positive P2X7R microglial cells was low in WT mice at all ages tested (**Figures 1C**, **2C**). When we analyzed the distribution pattern of P2X7R positive microglial cells, we found them mainly localized inside senile plaques at all ages tested (**Figure 2F**). However, P2X7R positive microglial cells were not abundant at this location (**Figure 2E**). It is also worth noting that the J20 mice did not show any significant differences, either in the total number (12.0 ± 1.2 and 15.3 ± 1.2 respectively), or in the percentage of EGFP-positive microglial cells ($9 \pm 2\%$ and $90 \pm 2\%$ respectively) inside the senile plates between their advanced and late stages (**Figures 2E,F**).

Similar to what was observed in J20 mice at advanced and late stages, we detected a significantly increased of P2X7R expression in samples from human AD patients (**Figures 3E,F**). Immunofluorescence studies using human brain samples confirmed that P2X7R is expressed in microglial cells (**Figure 3A**), although the number of microglial cells expressing P2X7R was lower than those non-expressing this receptor (**Figure 3B**). Regarding their distribution pattern, we observed, once again, that positive P2X7R microglial cells were preferentially inside extracellular β-amyloid deposits (**Figures 3C,D**). These results confirm that J20 mice mimics the microglial P2X7R location observed in human AD patients.

Neuroinflammation Changes the P2X7R Distribution Pattern

Once we had observed that, both in FAD mouse models and human AD patients, the increased P2X7R expression occurred in

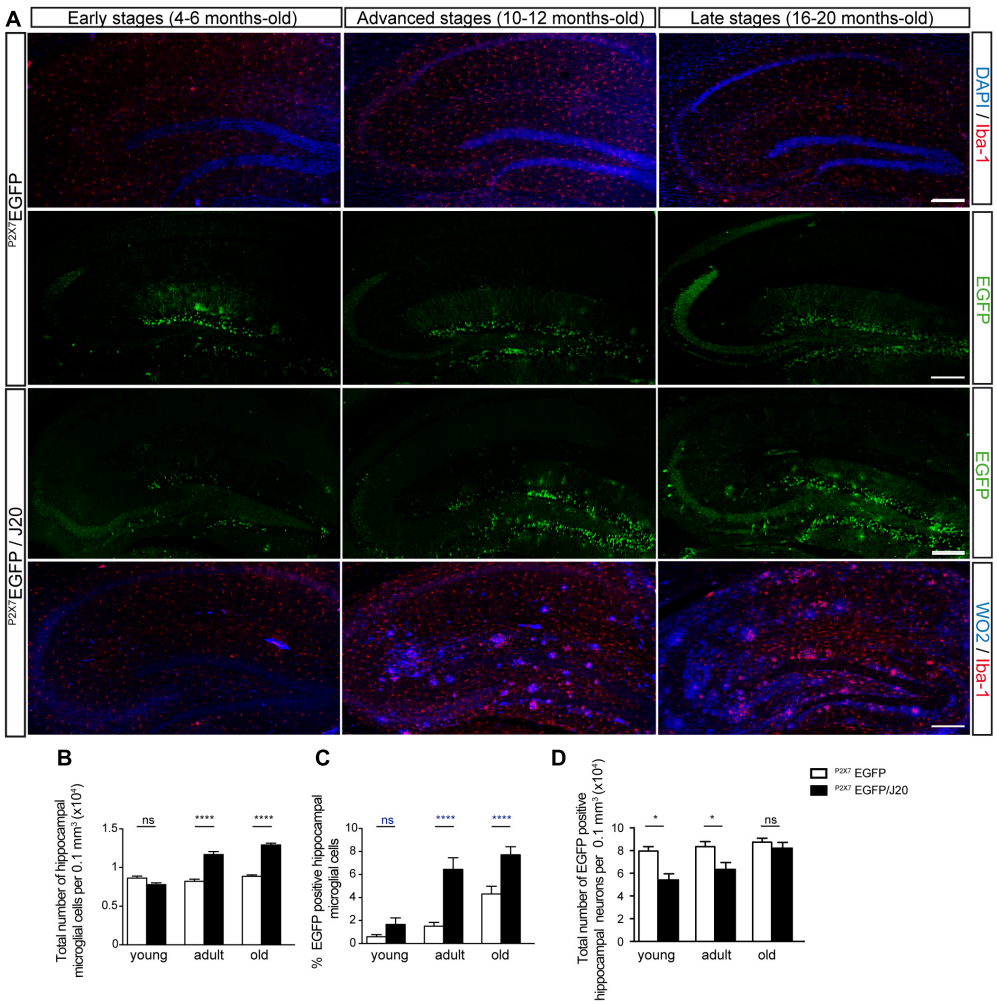

FIGURE 1 | Microgliosis in ^{P2X7R}EGFP/J20 mice promotes increased expression of the P2X7R reporter protein in microglial cells and reduces it in neurons. **(A)** Representative images of hippocampal coronal sections from ^{P2X7R}EGFP and ^{P2X7R}EGFP/J20 mice at 4–6 months-old (early stage), 10–12 months-old (advanced stage) and 16–20 months-old (late stage). Sections from ^{P2X7R}EGFP mice stained with nuclear marker DAPI plus microglial marker Iba-1 or antibodies against EGFP. Sections from ^{P2X7R}EGFP/J20 mice were stained with antibodies against EGFP or antibodies against APP protein (WO2) plus antibodies against Iba-1. Scale bar: 200 μm. **(B)** The total number of microglia cells per 0.1 mm^3 of the hippocampal section on ^{P2X7R}EGFP mice (white bars) and ^{P2X7R}EGFP/J20 mice (black bars) at each analyzed age. **(C)** Percentage of hippocampal EGFP positive microglial cells on ^{P2X7R}EGFP mice (white bars) and ^{P2X7R}EGFP/J20 mice (black bars) at each indicated age ($n \geq 5$ mice per genotype and age; sections ≥ 9 per mouse). **(D)** Quantification of EGFP positive neurons per 0.1 mm^3 of the hippocampal section on ^{P2X7R}EGFP mice (white bars) and P2X7REGFP/J20 mice (black bars) at each analyzed age ($n \geq 5$ mice per genotype and age; sections ≥ 9 per mouse). *$p < 0.05$ and ****$p < 0.0001$ using an unpaired t-test, ns not statistically significant. Data in bar graphs represent mean ± s.e.m.

microglial cells, we decided to identify the factors causing it, as well as its consequences on microglial functionality.

As, in studies using J20 mice, we observed that the P2X7R distribution pattern changed when a significant increase in microglial cells took place, initially, we decided to evaluate if the associated neuroinflammation process might be one of the factors involved in it. To assess this hypothesis, we decided to resort to the LPS-induced neuroinflammation model. Additional groups of young, adult and old ^{P2X7R}EGFP mice were treated i.p. with LPS or vehicle solution for 24 h or 7 days. Results showed that, although the LPS administration did not modify the P2X7R hippocampal expression levels (**Figure 4A**), it did, however, induce a similar P2X7R distribution pattern change to the one observed in ^{P2X7R}EGFP/J20 mice (**Figure 4B**). LPS-treated ^{P2X7R}EGFP mice presented a significant increase in EGFP-positive microglial cells throughout the hippocampus at all ages tested. This change was independent of the treatment duration (**Figures 4B,D**). This fact was linked to a significant increase in the total number of hippocampal microglial cells (**Figure 4C**). Curiously, only 7 days-LPS-treated ^{P2X7R}EGFP old mice did not show a significant increase of EGFP-positive microglial cells when compared to their respective 7 days-vehicle-treated ^{P2X7R}EGFP old mice (4.6 ± 0.9 vs. 7.8 ± 0.7, **Figures 4B,D**). Moreover, we found, once more, in young and adult LPS-treated ^{P2X7R}EGFP mice, a significant decrease in the EGFP-positive neurons in GLDG

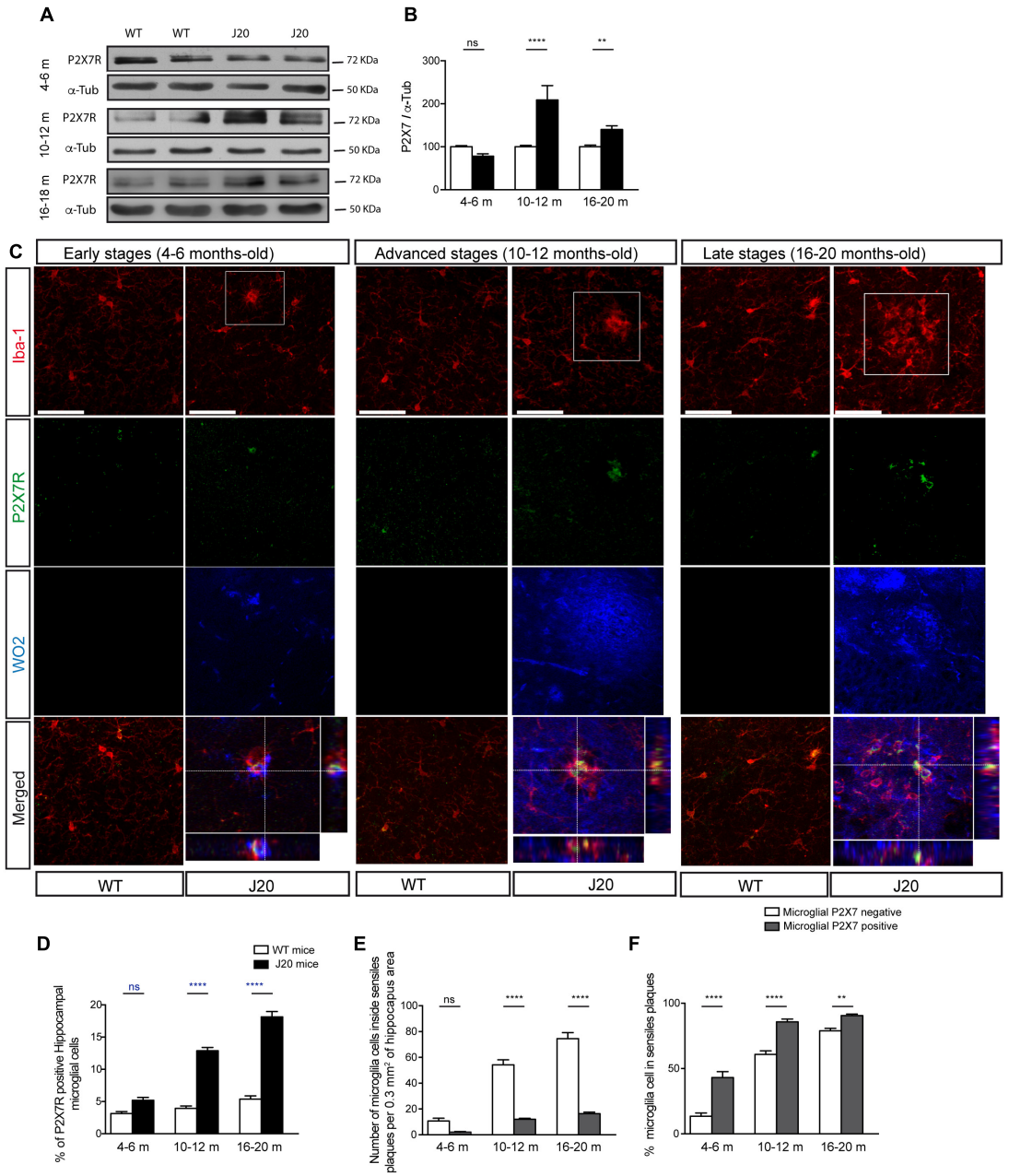

FIGURE 2 | J20 mice increase the P2X7R expression levels in microglial cells at advanced and late stages when they develop a significant microgliosis. **(A)** Representative images of Western blot using hippocampal samples from J20 at 4–6 months-old (early stage), 10–12 months-old (advanced stage), and 16–20 months-old (late stage) and their corresponding control-littermates (WT) mice stained with antibodies against constitutive P2X7R or α-tubulin. **(B)** Graphs show quantification of the protein expression of P2X7 receptor ($n \geq 6$ mice per genotype and age). Data were normalized using α-tubulin levels. The 100% value indicates the corresponding P2X7R protein expression detected in WT mice. $^{**}p < 0.01$ and $^{****}p < 0.0001$ using unpaired *t*-test. **(C)** Representative micrographs of hippocampal sections from J20 and WT mice at early, advanced or late stages stained with antibodies against P2X7 receptor (green), microglial marker Iba-1 (red), and APP protein (WO2) (blue). Merged images both the full field and a magnification 1.5x of the area indicated in upper images are shown at the bottom with their corresponding orthogonal views. Dashed lines represent the locations where orthogonal views were obtained. Scale bar: 50 μm. **(D)** The graph shows the percentage of positive P2X7R microglial cells in WT (white) or J20 (black) mice per 0.1 mm^3 of hippocampal section ($n \geq 5$ mice per genotype and age; sections ≥ 10 per mouse). **(E)** Quantification of the total number of microglial cells expressing (gray) or not P2X7R (white) inside of senile plaques per 0.3 mm^3 of the hippocampal section. **(F)** Percentage of hippocampal microglial cells expressing (gray) or not P2X7R (white) inside of senile plaques ($n \geq 5$ mice per genotype and age; sections ≥ 8 per mouse). The 100% value corresponded to the total number of microglial cells expressing or not P2X7R. $^{**}p < 0.01$ and $^{****}p < 0.0001$ using an unpaired *t*-test, ns not statistically significant. Data in bar graphs represent mean ± s.e.m.

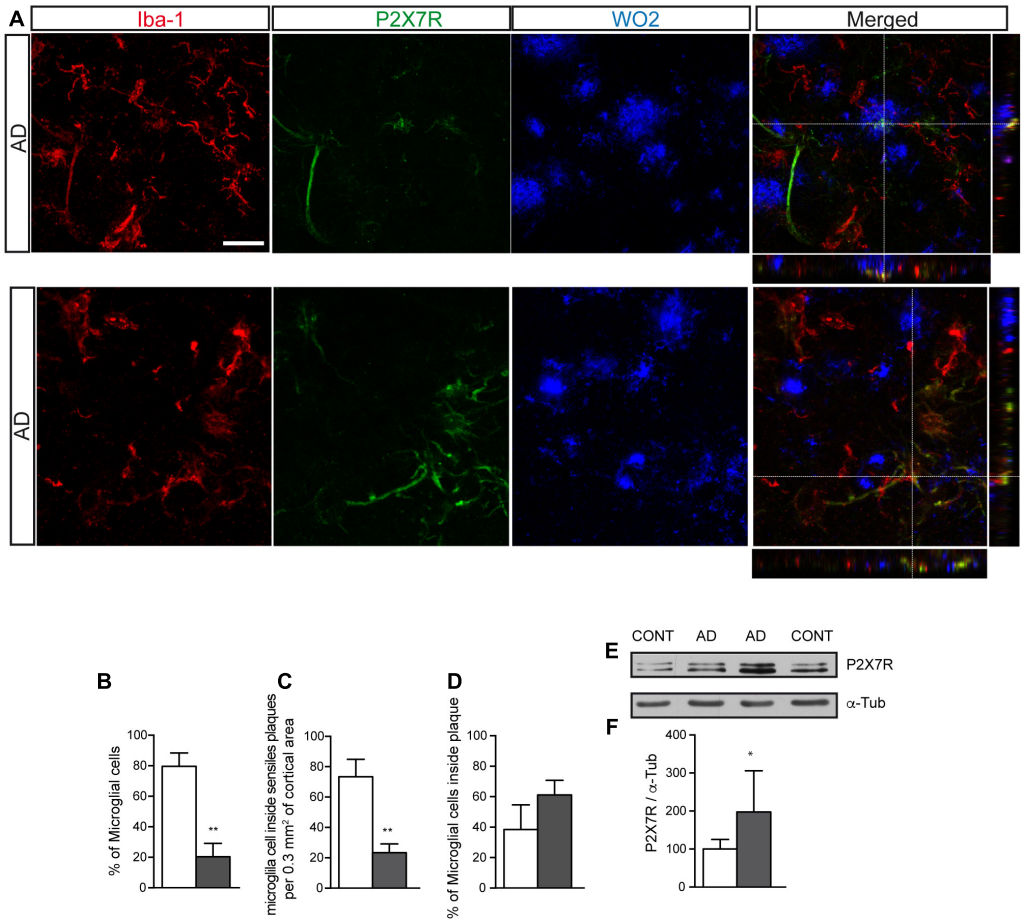

FIGURE 3 | Human AD patients showed a significantly increased P2X7R expression in microglial cells, preferably localized inside of senile plaques. **(A)** Representative images of post-mortem cortical sections from AD patients stained with antibodies against P2X7 receptor (green), microglial marker Iba-1 (red) and APP protein (WO2) (blue). Merged images and orthogonal views are also shown. Dashed lines represent the locations where orthogonal views were obtained. Scale bar: 20 μm. **(B)** The graph shows the percentage of microglial cells expressing (gray) or not (white) P2X7R in post-mortem cortical sections from human AD patients (n = 4; sections ≥ 10 per case). **(C)** Quantification of the total number of microglial cells expressing (gray) or not P2X7R (white) inside of senile plaques per 0.3 mm^3 of the cortical area. **(D)** Percentage of hippocampal microglial cells expressing (gray) or not P2X7R (white) inside of senile plaques. (n = 4; sections ≥ 10 per case). The 100% value corresponded to the total number of microglial cells. $^{**}p < 0.01$ using unpaired t-test. **(E)** Representative images of Western blot using post-mortem cortical samples from human AD patients or non-demented controls stained with antibodies against P2X7R or α-tubulin. **(F)** Graphs show a quantification of the protein expression of P2X7 receptor (n = 4 AD and n = 4 controls). Data were normalized to the expression levels of α-tubulin. The 100% value indicates the corresponding P2X7R protein levels detected in non-demented controls. $^{*}p < 0.05$ using unpaired t-test. Data in bar graphs represent mean ± s.e.m.

(63.1 ± 7.2% and 48.1 ± 10.5% for 24 h or 7 days of LPS-treatment respectively on young mice and 66.4 ± 9.0% and 40.5 ± 12.9% for 24 h or 7 days of LPS-treatment respectively on adult mice, **Figures 4B,E**). However, this reduction was not observed in old LPS-treated ^{P2X7R}EGFP mice independently of the treatment duration (**Figures 4B,E**). To validate the results obtained with ^{P2X7R}EGFP reporter protein, we performed a new analysis using anti-P2X7R antibodies. Results revealed that LPS-treatment induced a significant increase in P2X7R-positive microglial cells at all ages tested (**Figures 4F,G**). It is important to consider that, by using this approach, we found a significant increase in the number of P2X7R-positive microglial cells even in LPS-treated old mice (**Figures 4F,G**). These data are suggesting that P2X7R distribution pattern change detected in J20 mice may be caused by the associated neuroinflammation developed by mice during the progression of the disease.

P2X7R Regulates the Microglial Cell Recruitment to Senile Plate

Taking into account that our preliminary data revealed that P2X7R positive microglial cells were mainly inside senile plates, we wondered if P2X7R favors the migration of microglial cells toward them. To address this point, initially, we decided to evaluate the role of P2X7R on microglial cell migration, using primary microglial cells cultures isolated from the hippocampus. Results showed that high ATP concentration (1 mM) promotes microglial cells migration (6.9 ± 3.0 migrated microglial cells stimulated by PBS vs. 228.2 ± 14.2 migrated microglial cells

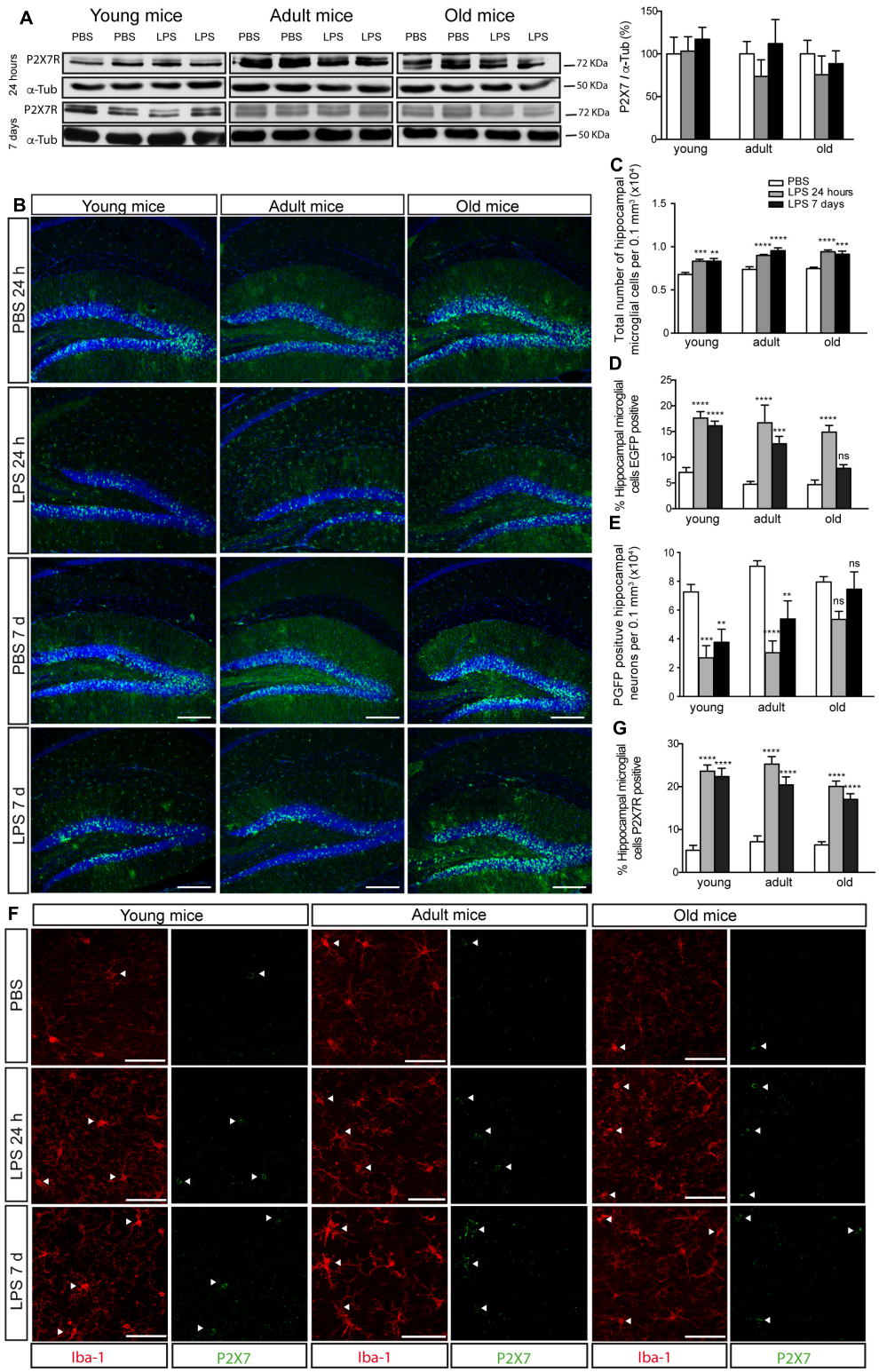

FIGURE 4 | LPS-induced neuroinflammation increases P2X7R in microglial cells and reduces its levels in neurons. **(A)** Representative images of Western blot using hippocampal samples from young (4–6 months–old), adult (10–12 months old), or old ^{P2X7R}EGFP mice (16–20 months-old) intraperitoneally PBS- or LPS-treated for 24 h or 7 days and stained with antibodies against P2X7R or α-tubulin. The graph shows the quantification of P2X7R protein levels ($n \geq 5$ mice per age and treatment). Data were normalized using α-tubulin levels. The 100% value corresponds to P2X7R protein levels detected in PBS-treated mice. Data in bar graphs

(Continued)

FIGURE 4 | Continued
depict mean ± s.e.m. **(B)** Representative images of hippocampal coronal sections from young, adult or old ^{P2X7R}EGFP mice intraperitoneally PBS- or LPS-treated for 24 h or 7 days and stained with an antibody against EGFP plus nuclear marker DAPI (lower panels). Scale bar: 200 μm. **(C)** Quantification of the total number of microglial cells per 0.3 mm^3 of the hippocampal section on young, adult or old ^{P2X7R}EGFP mice intraperitoneally PBS- or LPS-treated for 24 h or 7 days. **(D)** Percentage of hippocampal EGFP positive microglial cells on young, adult or old ^{P2X7R}EGFP mice intraperitoneally PBS- or LPS-treated for 24 h or 7 days. 100% value corresponded to the total number of microglial cells expressing EGFP in PBS-treated mice. **(E)** Graphs show the total number of hippocampal neurons expressing EGFP on young, adult or old ^{P2X7R}EGFP mice intraperitoneally PBS- or LPS-treated for 24 h or 7 days ($n \geq 5$ mice per age and treatment; sections ≥ 8 per mouse). $^{**}p < 0.01$, $^{***}p < 0.001$, and $^{****}p < 0.0001$ using ANOVA test followed by Bonferroni's tests, ns not statistically significant. Data in bar graphs depict mean ± s.e.m. **(F)** Representative micrographs of hippocampal sections from young, adult or old ^{P2X7R}EGFP mice intraperitoneally PBS- or LPS-treated for 24 h or 7 days and stained with antibodies against P2X7 receptor (green) and microglial marker Iba-1 (red). Arrowheads show the microglial cells expressing P2X7R. Scale bar: 50 μm. **(G)** The graph shows the percentage of hippocampal microglial cells expressing P2X7R on young, adult or old ^{P2X7R}EGFP mice intraperitoneally PBS- or LPS-treated for 24 h or 7 days ($n \geq 5$ mice per age and treatment; sections ≥ 10 per mouse). $^{****}p < 0.0001$ using ANOVA test followed by Bonferroni's tests. Data in bar graphs represent mean ± s.e.m.

ATP-stimulated, **Figure 5A**). Since acute stimulation of P2X7R by high ATP concentrations can induce cellular death (Miras-Portugal et al., 2017), we decided to stimulate the microglial cells with lower concentrations of ATP (0.3 mM) or with the selective P2X7R agonist BzATP (0.3 mM, **Supplementary Figure 2**). Both stimulations caused similar results on microglial mobility than that induced high ATP concentration (**Supplementary Figure 2**). The involvement of P2X7R was confirmed when the selective P2X7R antagonist GSK 1482160A prevented the microglial migration induced by 1mM ATP (13.5 ± 2.6 migrated microglial cells after being stimulated by ATP in presence GSK 1482160A, **Figure 5A**) or 300 μM BzATP (**Supplementary Figure 2**). These results point to the fact that P2X7R is regulating the microglial mobility, and, consequently, ATP may be considered as a chemotaxis signal for microglial cells.

In the following step, to determine whether P2X7R regulates microglial cells recruitment to senile plates, we decided to analyze ^{P2X7R}EGFP/J20 mice. In this study, we measured the number of both EGFP-positive and EGFP-negative microglial cells inside senile plates, as well as the distance between the center of microglial cell to the border of the most closed senile plate. As shown in **Figure 5B**, in all ages tested we observed higher percentages of EGFP-positive than EGFP-negative microglial inside the senile plates, although only in the advanced and late stages this increase was significant (37.1 ± 11.8% vs. 15.2 ± 3.5% respectively in young mice, 66.1 ± 7.6% vs. 31.1 ± 0.8% respectively in adult mice and 71.2 ± 1.1% vs. 38.7 ± 4.5% respectively in old mice, **Figure 5B**). Furthermore, in the early stages, we detected a higher percentage of EGFP-positive microglial cells at the most closed environment of senile plates than EGFP-negative ones (55.0 ± 2.8% vs. 43.8 ± 2.2% respectively, **Figure 5B**). On the other hand, we found a lower percentage of EGFP-positive microglial cells than EGFP-negative ones at distances further away from the senile plates (45.0 ± 2.8% vs. 56.1 ± 2.2% respectively, **Figure 5B**). A similar tendency, but not statistically significative, was found in the advanced stages (63.3 ± 1.3% vs. 58.3 ± 1.0% and 36.6 ± 1.3% vs. 41.6 ± 1.1% respectively, **Figure 5B**). In the late stages, we did not find any difference in the distribution pattern of microglial cells outside senile plates (91.4 ± 2.0% vs. 95.3 ± 1.7% and 2.9 ± 1.0% vs. 1.5 ± 0.9% respectively). Although our findings suggest that P2X7R-activation promotes the microglial recruitment toward senile plates, in comparison, inside the senile plates, the majority of microglial cells did not express this receptor.

P2X7R Modules the Phagocytic Capacity of Microglia Cells

To elucidate what role P2X7R plays on recruited microglial cells inside senile plates, we decided to evaluate the possible role of this receptor in another of the most relevant microglial functions, the phagocytosis. Initially, we decided to use, once again, primary microglial cells cultures. To evaluate phagocytic capacity of cultured microglial cells, we measured the number of fluorescence microspheres phagocyted after them were stimulated with BzATP in the presence or absence of the selective P2X7R antagonists (**Figure 6A**).

Our results showed that BzATP stimulation reduced the phagocytic ability of microglial cells (8.9 ± 0.8 microspheres per microglial cell treated with PBS vs. 3.8 ± 0.4 microspheres per microglial cell treated with BzATP, **Figures 6A,B**). Interestingly, selective P2X7R antagonists reverted the reduced phagocytic capacity induced by BzATP (6.5 ± 1.5 microspheres per microglial cell treated with A438072 plus BzATP and 7.1 ± 0.7 microspheres per microglial cell treated with GSK 1482160A plus BzATP, **Figures 6A,B**). As negative phagocytosis control, microglial cells were treated with CytoD, an inhibitor of actin polymerization that blocks more than 90% of the phagocytosis capacity (1.3 ± 0.1 microspheres per microglial cell treated with Cyto D, **Figures 6A,B**). Interestingly, the negative effect induced by P2X7R activation on microglial phagocytic capacity was not modified when cells were LPS-pre-treated (8.4 ± 0.6 microspheres per microglial cell treated with LPS vs. 2.9 ± 0.8 microspheres per microglial cell treated with LPS plus BzATP, **Supplementary Figure 3**). To consolidate these results, in the following step, we decided to administrate fluorescence microspheres i.c. to the hippocampus of ^{P2X7R}EGFP mice. After i.c. injection, ^{P2X7R}EGFP mice were daily i.p. treated for 7 days with the P2X7R antagonist GSK 1482160A or vehicle solution before being sacrificed. Hippocampus from ^{P2X7R}EGFP mice was analyzed by immunofluorescence techniques using anti-EGFP, and anti-Iba-1 antibodies (**Figure 6C**). Results revealed that *in vivo* pharmacology P2X7R blockage promoted the phagocytic capacity of the microglial cells (**Figure 6D**). Interesting, most of the phagocytic microglial cells on vehicle-treated mice expressed the P2X7R reporter protein EGFP

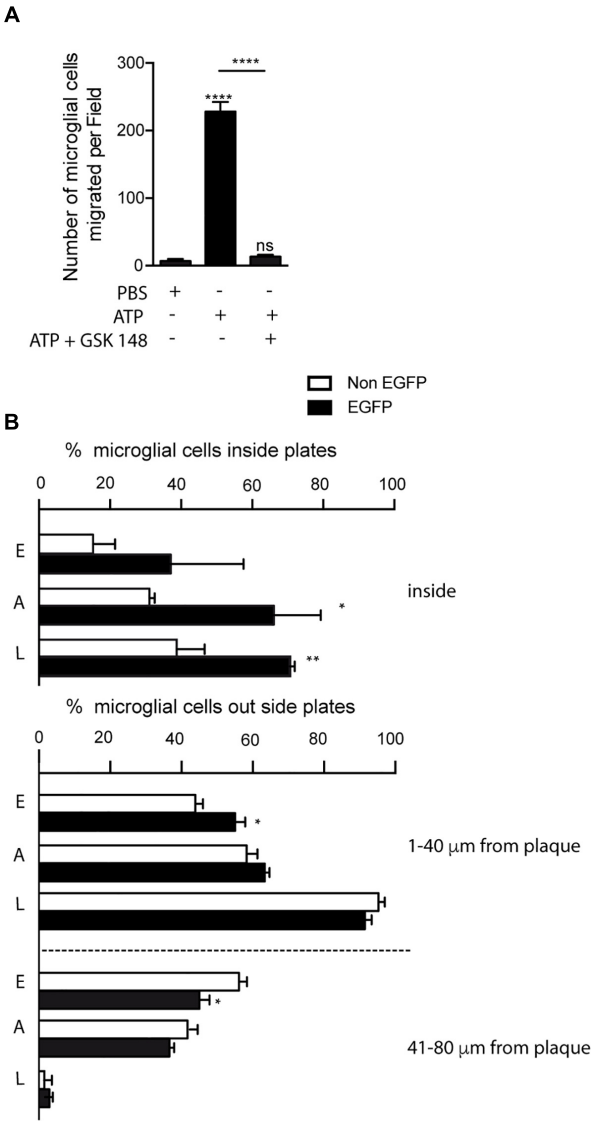

FIGURE 5 | Selective P2X7R activation promotes microglial migration to senile plates. **(A)** The graph shows the number of cultured microglial cells from the hippocampus of WT mice migrating through trans-well inserts after being stimulated with 1 mM ATP in the presence or absence of 1 μM GSK 1482160A. Values represent, at least, the mean ± s.e.m of 3 independent cultures run in duplicate. ****$p < 0.0001$ using ANOVA test followed by Bonferroni's tests, ns not statistically significant. **(B)** Graphs show the number of hippocampal microglial cells expressing (black bars) or not (white bars) the P2X7 receptor reporter protein (EGFP) inside (upper graph) or in the nearness (lower graph) of senile plaques identified ^{P2X7R}EGFP/J20 mice at early, advanced or late stages ($n \geq 5$ mice per age; sections ≥ 8 per mouse; plaques ≥ 15 per sections). *$p < 0.05$, **$p < 0.01$, using unpaired *t*-test. Data in bar graphs represent mean ± s.e.m. E meaning early stages, A meaning advances stages and L meaning late stages.

(81.9 ± 2.4% was EGFP-negative vs. 18.1 ± 2.4% was EGFP-positive). However, in GSK 1482160A-treated mice, no significant differences were detected between both microglial populations (51.5 ± 5.0% was EGFP-negative vs. 45.5 ± 5.0% was EGFP-positive) (**Figure 6E**). It is worth highlighting that P2X7R inhibition also caused the EGFP-positive microglial cells to increase their phagocytic capacity, so these cells passed to phagocyte a mean of 0.7 ± 0.1 to 1.7 ± 0.2 microspheres per cell (**Figure 6F**). However, the pharmacological blockage of P2X7R did not modify the phagocytic capacity of EGFP-negative cells (1.6 ± 0.2 vehicle vs. 1.5 ± 0.1 GSK 1482160A) (**Figure 6F**). All these data suggest that P2X7R negatively modulates the microglial phagocyte capacity.

DISCUSSION

In the present study, we have evaluated the impact of microglial cells expressing P2X7R on FAD progression analyzing the new transgenic mouse model ^{P2X7R}EGFP/J20 mice. In the early stages, when Aβ peptide begins assembling on detectable extracellular β-amyloid deposits, but still non-evident microglial proliferation takes place, we did not observe significant changes in the percentage of microglial cells expressing P2X7R. However, at this stage, we found that outside plaques, microglial cells expressing P2X7R were closer to nascent plaques than those non-expressing this receptor. On the other hand, both in advanced and late stages, when J20 mice experience microgliosis and an evident cognitive and motor impairments (Mucke et al., 2000), significant increases in P2X7R expression levels and in the percentage of P2X7R expressing microglial cells were detected. Furthermore, at both stages, although P2X7R-expressing microglial cells were mostly found inside the senile plaques, this microglial population was not the most abundant, either inside the senile plaques or in the whole hippocampus. We also found a significant reduction in the number of neuronal cells transcribing P2X7R in the early and advanced, but not in the late stages.

As observed in J20 mice, we detected in brain samples from AD patients, both a significant increase of P2X7R expression levels and a preferred location of microglial cells expressing P2X7R inside senile plaques, but this was not, once again, the most abundant microglial population at this location. Our data confirm that P2X7R mediated signaling is increased in microglial cells on AD, as previously reported by other groups (Parvathenani et al., 2003; McLarnon et al., 2006; Lee et al., 2011). However, on these works did not identify the factors causing the increased P2X7R expression in microglial cells or what consequences had on microglial functionality.

It is well known that ATP-signaling via P2X7R regulates different microglial functions. It is also reported that ATP-induced morphological changes related with their migratory ability, allowing them rapidly to migrate toward the injury (Davalos et al., 2005), in an ATP-induced ATP-release dependent mechanism (Dou et al., 2012). Our *in vitro* studies confirmed that ATP promotes the microglial mobility by P2X7R activation. Furthermore, using ^{P2X7R}EGFP/J20 mice, we have demonstrated that microglial cells expressing P2X7R migrate more quickly toward the extracellular β-amyloid deposits than those non-expressing this receptor. These results suggest that the enrichment of P2X7R-expressing microglial cells around β-amyloid deposits observed in the last stages of AD by other

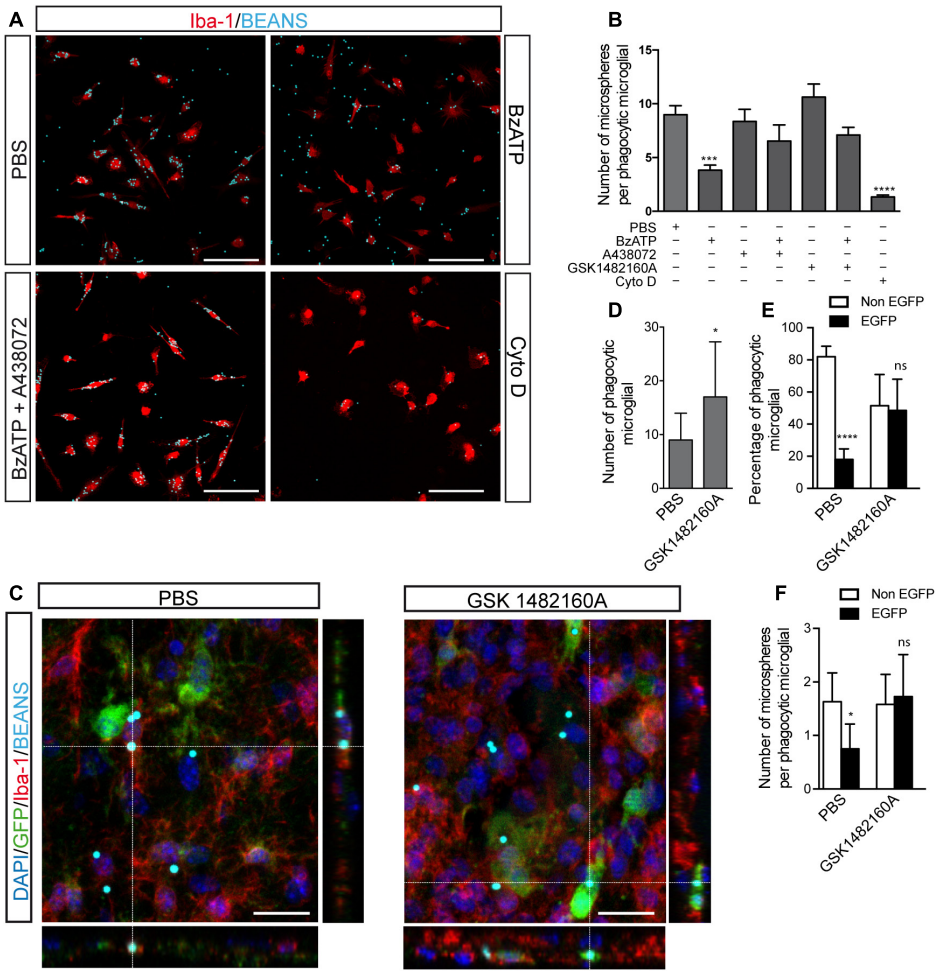

FIGURE 6 | Selective P2X7R inhibition promotes microglial phagocytosis. **(A)** Representative fluorescence micrographs of cultured microglial cells from the hippocampus of WT mice identified using antibodies against the microglial marker Iba-1 (red) uptaking fluorescence microparticles (cyan) after stimulated with 300 μM BzATP in presence or absence of the selective P2X7R antagonists 10 μM A438072 or 1 μM GSK 1482160A. In some cases, the cultured microglial cells were treated with 10 μM cytochalasin D (CytoD) as a negative control. **(B)** The graph shows the number of phagocyted microfluorescent particles per microglial cell under different experimental conditions. Values represent, at least, the mean ± s.e.m of 4 independent cultures run in duplicate. ***$p < 0.001$ and ****$p < 0.0001$ using ANOVA test followed by Bonferroni's tests. **(C)** Representative confocal images and its corresponding orthogonal views of hippocampal sections from 6 months-old ^{P2X7R}EGFP mice intraperitoneally GSK 1482160A-treated for 7 days after intracranial administration of fluorescent microspheres to the hippocampus. Dashed lines represent the locations where orthogonal views were obtained. Sections were stained with antibodies against EGFP (green), microglial marker Iba-1 (red), nuclear marker DAPI (blue), being microspheres visualized in cyan. Scale bar: 50 μm. **(D)** The graph shows the number of microglial cells uptaking fluorescent microspheres on PBS- or GSK 1482160A-treated ^{P2X7R}EGFP mice ($n \geq 4$ mice per treatment; sections ≥ 8 per mouse). **(E)** The graph shows the percentage of phagocytic microglial cells expressing (black) or not (white) the P2X7 receptor reporter protein EGFP on PBS- or GSK 1482160A-treated ^{P2X7R}EGFP mice ($n \geq 4$ mice per treatment; sections ≥ 8 per mouse). **(F)** The graph shows the number of incorporated fluorescent microspheres by microglial cells expressing (black) or not (white) the P2X7 receptor reporter protein EGFP on PBS- or GSK 1482160A-treated ^{P2X7R}EGFP mice ($n \geq 4$ mice per treatment; sections ≥ 8 per mouse). *$p < 0.05$, ****$p < 0.0001$, using unpaired *t*-test, ns not statistically significant. Data in bar graphs represent mean ± s.e.m.

authors (Parvathenani et al., 2003; McLarnon et al., 2006; Lee et al., 2011) may result from the increased migratory capacity of these cells by the increase of P2X7R expression levels. This hypothesis is in accordance with the fact that the upregulation of P2X7R on microglial cells increases parallel to the incidence of senile plaques in the brain (Lee et al., 2011). Moreover, since microglial P2X7R activation also triggers the cytokines release (Di Virgilio et al., 2017), P2X7R activation on migratory microglial would favor, in turn, the recruitment of microglial cells toward the plaques. In this way, we found that outside of extracellular β-amyloid deposits, the non-positive P2X7R microglial cells present delayed recruitment toward them compared to microglial cells expressing P2X7R.

It has also been reported that cytoskeleton changes in microglial cells caused by ATP-induced P2X7R activation, reduce their phagocytic capacity (Fang et al., 2009). Accordingly, downregulation of P2X7R using small RNA interference favors the Aβ peptide phagocytosis (Ni et al., 2013). Here, using both *in vitro* and *in vivo* approaches, we found that selective pharmacological P2X7R inhibition promotes

microglial phagocytosis. In agreement with an inverse relationship between P2X7R expression and microglial phagocytic capacity, we discovered that most microglial cells in the senile plaques did not express P2X7R. It is worth highlighting that, although there was a higher number of microglial cells inside senile plaques in the late, rather than in the advanced stages, the percentage of P2X7R positive microglial cells inside extracellular Aβ deposits is similar in both phases. Considering that microglial recruitment toward senile plaques remains over AD progression, one possible explanation is that, after promotes migration of microglial cells to senile plaques, once they reach the plaque, P2X7R expression is decreased favoring the Aβ peptide phagocytosis. Supporting this hypothesis, we found that the low phagocytosis capacity detected in P2X7R-expressing microglial cells increases once the receptor is pharmacologically blocked. However, additional experiments should be made to confirm this hypothesis.

Over recent years, there has been an active debate in the field about the preferential expression of P2X7R on neural cells (Illes et al., 2017; Miras-Portugal et al., 2017). These opposing points of view are mainly due to that fact that some groups found P2X7R in neurons (Miras-Portugal et al., 2017), whereas other groups detected it mainly in glial cells, especially in microglial cells, but not in neurons (Illes et al., 2017). In the present work, using a well-characterized P2X7R reporter mice ^{P2X7R}EGFP (Engel et al., 2012; Sebastian-Serrano et al., 2016), we found that, at hippocampal level, under physiological conditions, P2X7R is mainly transcribed in neurons, expressing on the nerve endings from those granular neurons on dentate gyrus that project their axons toward the CA3 region, as previously reported (Sebastian-Serrano et al., 2016). However, under pathological conditions where neuroinflammation causes microglial proliferation and activation, as occurs in J20 mice at advanced and late stages or in LPS treated mice, the P2X7R distribution pattern changes, decreasing its transcription on neurons and increasing in microglial cells. These results suggest that neuroinflammation regulates the expression of P2X7R both in neurons and in glial cells. In agreement with this idea it has been reported that P2X7R pharmacological blockage or its downregulation by small RNA interference attenuated LPS-induced neuroinflammation by avoiding the microglial activation and the subsequence inflammation (Lu et al., 2013), and decreased microglial proliferation (Bianco et al., 2006). Since proinflammatory cytokines released by P2X7R may cause the receptor upregulation, this positive feedback loop might promote and maintain, over time, an exacerbating microglial response contributing in this way to the adverse effects associated with neuroinflammation (Mosher and Wyss-Coray, 2014). Supporting this hypothesis, a close relationship has been detected between P2X7R upregulation in microglial cells and synaptic toxicity on AD (Lee et al., 2011). In this sense, it is worth noting that the compression of brain tissue by the extracellular Aβ deposits may cause a mechanical ATP release (Burnstock et al., 2011), which, in addition to favoring the migration of P2X7R-expressing microglial cells toward these deposits, may also promote a sustained activation of neuronal P2X7R. Since the persistent activation of P2X7R on neurons by high extracellular ATP levels may also lead to compromise the cellular viability, the reduction of P2X7R transcription observed in neurons both the early and advanced stages, may be an adaptive physiological response to avoid or at least reduce the neuronal loss associated to AD. In this way, the loss of this regulatory mechanism might be contributing to the neuronal loss detected in the late stages of AD.

CONCLUSION

We found that neuroinflammation associated with AD induces a change in the P2X7R distribution pattern, increasing its expression on microglial cells at advanced and late stages of AD, when there is evident microgliosis. P2X7R activation improves the migratory faculty of microglial cells to senile plaques but decreases their phagocytic capacity. Additionally, we found a significant reduction of P2X7R transcription in neuronal cells at the early and advanced, but not at the late stages of AD. Because different studies have demonstrated that both pharmacological inhibition or the selective downregulation of P2X7R significantly improve behavioral alterations and reduce the incidence and size of senile plaques in the early and advanced stages of AD (Diaz-Hernandez et al., 2012; Chen et al., 2014; Martin et al., 2018), the results presented here provide new pieces of evidences indicating that this therapeutic approach may also be useful in the late stages of the disease.

ETHICS STATEMENT

This study was carried out in accordance with the recommendations of 'Ethical Committees of the Netherlands Brain Bank with written informed consent from all subjects. All subjects gave written informed consent in accordance with the Declaration of Helsinki. The protocol was approved by the Ethical Committees of the Netherlands Brain Bank.' This study was carried out in accordance with the recommendations of 'International Council for the Laboratory Animal Science'. The protocol was approved by the Committee of Animal Experiments of the Complutense University of Madrid and the Environmental Counseling of the Comunidad de Madrid, Spain.

AUTHOR CONTRIBUTIONS

CM-F treated and processed the mice generating and analyzing the samples, participated in experimental design, and contributed to the interpretation of the data. CDL contributed the processing and analyzing of samples and contributed to the interpretation of the data. AS-S, LdD-G, CB, and LB revised the manuscript

and helped in the interpretation of data. MD-H participated in the experimental design, in the interpretation of the results, wrote the manuscript, and also provided the financial support for the work.

FUNDING

This work was supported by funding from the Spanish Ministry of Science and Education BFU2012-31195 (to MD-H), SAF2017-82436R (to LB), European Union project H2020-MSCA-ITN-2017 number 766124 (to MD-H), and from Universidad Complutense of Madrid (UCM)-Santander Central Hispano Bank PR41/17-21014 (to MD-H). CM-F had an FPI pre-doctoral fellowship associated to BFU2012-31195. CDL and CB were hired by H2020-MSCA-ITN-2017 number 766124. AS-S was hired by BFU2012-31195 grant and LdD-G had an UCM pre-doctoral fellowship supervised by MD-H. This work was supported in part by FEDER.

ACKNOWLEDGMENTS

We would like to thank Dra Maria Teresa de Frailes-Alvaro for her help in providing us with the selective P2X7R antagonist GSK 1482160A (from GlaxoSmithKline, Madrid, Spain).

SUPPLEMENTARY MATERIAL

The Supplementary Material for this article can be found online at: https://www.frontiersin.org/articles/10.3389/fncel.2019.00143/full#supplementary-material

REFERENCES

Avila, J. (2006). Tau protein, the main component of paired helical filaments. *J. Alzheimers Dis.* 9, 171–175. doi: 10.3233/JAD-2006-9S320

Bianco, F., Ceruti, S., Colombo, A., Fumagalli, M., Ferrari, D., Pizzirani, C., et al. (2006). A role for P2X7 in microglial proliferation. *J. Neurochem.* 99, 745–758. doi: 10.1111/j.1471-4159.2006.04101.x

Burnstock, G., Fredholm, B. B., and Verkhratsky, A. (2011). Adenosine and ATP receptors in the brain. *Curr. Top. Med. Chem.* 11, 973–1011. doi: 10.2174/156802611795347627

Chen, X., Hu, J., Jiang, L., Xu, S., Zheng, B., Wang, C., et al. (2014). Brilliant Blue G improves cognition in an animal model of Alzheimer's disease and inhibits amyloid-beta-induced loss of filopodia and dendrite spines in hippocampal neurons. *Neuroscience* 279, 94–101. doi: 10.1016/j.neuroscience.2014.08.036

Damani, M. R., Zhao, L., Fontainhas, A. M., Amaral, J., Fariss, R. N., and Wong, W. T. (2011). Age-related alterations in the dynamic behavior of microglia. *Aging Cell* 10, 263–276. doi: 10.1111/j.1474-9726.2010.00660.x

Davalos, D., Grutzendler, J., Yang, G., Kim, J. V., Zuo, Y., Jung, S., et al. (2005). ATP mediates rapid microglial response to local brain injury in vivo. *Nat. Neurosci.* 8, 752–758. doi: 10.1038/nn1472

de Diego Garcia, L., Sebastian-Serrano, A., Hernandez, I. H., Pintor, J., Lucas, J. J., and Diaz-Hernandez, M. (2018). The regulation of proteostasis in glial cells by nucleotide receptors is key in acute neuroinflammation. *FASEB J.* 32, 3020–3032. doi: 10.1096/fj.201701064RR

Delarasse, C., Auger, R., Gonnord, P., Fontaine, B., and Kanellopoulos, J. M. (2011). The purinergic receptor P2X7 triggers alpha-secretase-dependent processing of the amyloid precursor protein. *J. Biol. Chem.* 286, 2596–2606. doi: 10.1074/jbc.M110.200618

Di Virgilio, F., Dal Ben, D., Sarti, A. C., Giuliani, A. L., and Falzoni, S. (2017). The P2X7 receptor in infection and inflammation. *Immunity* 47, 15–31. doi: 10.1016/j.immuni.2017.06.020

Diaz-Hernandez, J. I., Gomez-Villafuertes, R., Leon-Otegui, M., Hontecillas-Prieto, L., Del Puerto, A., Trejo, J. L., et al. (2012). In vivo P2X7 inhibition reduces amyloid plaques in Alzheimer's disease through GSK3beta and secretases. *Neurobiol. Aging* 33, 1816–1828. doi: 10.1016/j.neurobiolaging.2011.09.040

Dou, Y., Wu, H. J., Li, H. Q., Qin, S., Wang, Y. E., Li, J., et al. (2012). Microglial migration mediated by ATP-induced ATP release from lysosomes. *Cell Res.* 22, 1022–1033. doi: 10.1038/cr.2012.10

Engel, T., Gomez-Villafuertes, R., Tanaka, K., Mesuret, G., Sanz-Rodriguez, A., Garcia-Huerta, P., et al. (2012). Seizure suppression and neuroprotection by targeting the purinergic P2X7 receptor during status epilepticus in mice. *FASEB J.* 26, 1616–1628. doi: 10.1096/fj.11-196089

Fang, K. M., Yang, C. S., Sun, S. H., and Tzeng, S. F. (2009). Microglial phagocytosis attenuated by short-term exposure to exogenous ATP through P2X receptor action. *J. Neurochem.* 111, 1225–1237. doi: 10.1111/j.1471-4159.2009.06409.x

Gahtan, E., and Overmier, J. B. (1999). Inflammatory pathogenesis in Alzheimer's disease: biological mechanisms and cognitive sequeli. *Neurosci. Biobehav. Rev.* 23, 615–633. doi: 10.1016/S0149-7634(98)00058-X

Hsiao, K., Chapman, P., Nilsen, S., Eckman, C., Harigaya, Y., Younkin, S., et al. (1996). Correlative memory deficits, Abeta elevation, and amyloid plaques in transgenic mice. *Science* 274, 99–102. doi: 10.1126/science.274.5284.99

Illes, P., Khan, T. M., and Rubini, P. (2017). Neuronal P2X7 receptors revisited: do they really exist? *J. Neurosci.* 37, 7049–7062. doi: 10.1523/JNEUROSCI.3103-16.2017

Koenigsknecht-Talboo, J., Meyer-Luehmann, M., Parsadanian, M., Garcia-Alloza, M., Finn, M. B., Hyman, B. T., et al. (2008). Rapid microglial response around amyloid pathology after systemic anti-Abeta antibody administration in PDAPP mice. *J. Neurosci.* 28, 14156–14164. doi: 10.1523/JNEUROSCI.4147-08.2008

Lee, H. G., Won, S. M., Gwag, B. J., and Lee, Y. B. (2011). Microglial P2X(7) receptor expression is accompanied by neuronal damage in the cerebral cortex of the APPswe/PS1dE9 mouse model of Alzheimer's disease. *Exp. Mol. Med.* 43, 7–14. doi: 10.3858/emm.2011.43.1.001

Leon-Otegui, M., Gomez-Villafuertes, R., Diaz-Hernandez, J. I., Diaz-Hernandez, M., Miras-Portugal, M. T., and Gualix, J. (2011). Opposite effects of P2X7 and P2Y2 nucleotide receptors on alpha-secretase-dependent APP processing in Neuro-2a cells. *FEBS Lett.* 585, 2255–2262. doi: 10.1016/j.febslet.2011.05.048

Ling, Y., Morgan, K., and Kalsheker, N. (2003). Amyloid precursor protein (APP) and the biology of proteolytic processing: relevance to Alzheimer's disease. *Int. J. Biochem. Cell Biol.* 35, 1505–1535. doi: 10.1016/S1357-2725(03)00133-X

Lu, K., Wang, J., Hu, B., Shi, X., Zhou, J., Tang, Y., et al. (2013). Brilliant blue G attenuates lipopolysaccharide-mediated microglial activation and inflammation. *Neural Regen. Res.* 8, 599–608. doi: 10.3969/j.issn.1673-5374.2013.07.003

Martin, E., Amar, M., Dalle, C., Youssef, I., Boucher, C., Le Duigou, C., et al. (2018). New role of P2X7 receptor in an Alzheimer's disease mouse model. *Mol. Psychiatry* 24, 108–125. doi: 10.1038/s41380-018-0108-3

McLarnon, J. G., Ryu, J. K., Walker, D. G., and Choi, H. B. (2006). Upregulated expression of purinergic P2X(7) receptor in Alzheimer disease and amyloid-beta peptide-treated microglia and in peptide-injected rat hippocampus. *J. Neuropathol. Exp. Neurol.* 65, 1090–1097. doi: 10.1097/01.jnen.0000240470.97295.d3

Miras-Portugal, M. T., Sebastian-Serrano, A., De Diego Garcia, L., and Diaz-Hernandez, M. (2017). Neuronal P2X7 receptor: involvement in neuronal physiology and pathology. *J. Neurosci.* 37, 7063–7072. doi: 10.1523/JNEUROSCI.3104-16.2017

Mosher, K. I., and Wyss-Coray, T. (2014). Microglial dysfunction in brain aging and Alzheimer's disease. *Biochem. Pharmacol.* 88, 594–604. doi: 10.1016/j.bcp.2014.01.008

Mucke, L., Masliah, E., Yu, G. Q., Mallory, M., Rockenstein, E. M., Tatsuno, G., et al. (2000). High-level neuronal expression of abeta 1-42 in wild-type human amyloid protein precursor transgenic mice: synaptotoxicity without plaque formation. *J. Neurosci.* 20, 4050–4058. doi: 10.1523/JNEUROSCI.20-11-04050.2000

Ni, J., Wang, P., Zhang, J., Chen, W., and Gu, L. (2013). Silencing of the P2X(7) receptor enhances amyloid-beta phagocytosis by microglia. *Biochem. Biophys. Res. Commun.* 434, 363–369. doi: 10.1016/j.bbrc.2013.03.079

Parvathenani, L. K., Tertyshnikova, S., Greco, C. R., Roberts, S. B., Robertson, B., and Posmantur, R. (2003). P2X7 mediates superoxide production in primary microglia and is up-regulated in a transgenic mouse model of Alzheimer's disease. *J. Biol. Chem.* 278, 13309–13317. doi: 10.1074/jbc.M209478200

Paxinos, G., and Franklin, K. B. J. (2001). *The Mouse Brain in Stereotaxic Coordinates*, 2nd Edn. San Diego, CA: Academic Press.

Price, D. L., and Sisodia, S. S. (1998). Mutant genes in familial Alzheimer's disease and transgenic models. *Annu. Rev. Neurosci.* 21, 479–505. doi: 10.1146/annurev.neuro.21.1.479

Radde, R., Bolmont, T., Kaeser, S. A., Coomaraswamy, J., Lindau, D., Stoltze, L., et al. (2006). Abeta42-driven cerebral amyloidosis in transgenic mice reveals early and robust pathology. *EMBO Rep.* 7, 940–946. doi: 10.1038/sj.embor.7400784

Ryu, J. K., and Mclarnon, J. G. (2008). Block of purinergic P2X(7) receptor is neuroprotective in an animal model of Alzheimer's disease. *Neuroreport* 19, 1715–1719. doi: 10.1097/WNR.0b013e3283179333

Sanz, J. M., Chiozzi, P., Ferrari, D., Colaianna, M., Idzko, M., Falzoni, S., et al. (2009). Activation of microglia by amyloid {beta} requires P2X7 receptor expression. *J. Immunol.* 182, 4378–4385. doi: 10.4049/jimmunol.0803612

Sanz, J. M., Falzoni, S., Rizzo, R., Cipollone, F., Zuliani, G., and Di Virgilio, F. (2014). Possible protective role of the 489C > T P2X7R polymorphism in Alzheimer's disease. *Exp. Gerontol.* 60, 117–119. doi: 10.1016/j.exger.2014.10.009

Sebastian-Serrano, A., Engel, T., De Diego-Garcia, L., Olivos-Ore, L. A., Arribas-Blazquez, M., Martinez-Frailes, C., et al. (2016). Neurodevelopmental alterations and seizures developed by mouse model of infantile hypophosphatasia are associated with purinergic signalling deregulation. *Hum. Mol. Genet.* 25, 4143–4156. doi: 10.1093/hmg/ddw248

Selkoe, D. J. (2001). Alzheimer's disease: genes, proteins, and therapy. *Physiol. Rev.* 81, 741–766. doi: 10.1152/physrev.2001.81.2.741

Serrano-Pozo, A., Gomez-Isla, T., Growdon, J. H., Frosch, M. P., and Hyman, B. T. (2013). A phenotypic change but not proliferation underlies glial responses in Alzheimer disease. *Am. J. Pathol.* 182, 2332–2344. doi: 10.1016/j.ajpath.2013.02.031

Solito, E., and Sastre, M. (2012). Microglia function in Alzheimer's disease. *Front. Pharmacol.* 3:14. doi: 10.3389/fphar.2012.00014

Conflict of Interest Statement: The authors declare that the research was conducted in the absence of any commercial or financial relationships that could be construed as a potential conflict of interest.

frontiers in Cellular Neuroscience

REVIEW
published: 16 April 2019
doi: 10.3389/fncel.2019.00112

Purinergic Signaling in the Vertebrate Olfactory System

*Natalie Rotermund, Kristina Schulz, Daniela Hirnet and Christian Lohr**

Division of Neurophysiology, University of Hamburg, Hamburg, Germany

Adenosine 5′-triphosphate (ATP) is an ubiquitous co-transmitter in the vertebrate brain. ATP itself, as well as its breakdown products ADP and adenosine are involved in synaptic transmission and plasticity, neuron-glia communication and neural development. Although purinoceptors have been demonstrated in the vertebrate olfactory system by means of histological techniques for many years, detailed insights into physiological properties and functional significance of purinergic signaling in olfaction have been published only recently. We review the current literature on purinergic neuromodulation, neuron-glia interactions and neurogenesis in the vertebrate olfactory system.

Keywords: purinergic signaling, olfactory system, olfaction, ATP, adenosine receptor, P2X receptor, P2Y receptor

INTRODUCTION

Since the discovery of adenosine 5′-triphosphate (ATP) release from sensory nerve terminals (Holton, 1959) and peripheral purinergic neurotransmission (Burnstock et al., 1970), ATP has been described as a (co-)transmitter in most if not all parts of the vertebrate nervous system. ATP is stored in and released from synaptic vesicles but alternative release pathways such as diffusion through connexin and pannexin hemichannels, volume-regulated anion channels and $P2X_7$ receptor channels have been published (Bodin and Burnstock, 2001; Taruno, 2018). Once released into the extracellular space, ATP activates a specific subclass of purinoceptors, the P2 receptors. P2 receptors can further be subdivided into ionotropic P2X receptors and metabotropic P2Y receptors (Burnstock et al., 2011). P2X receptors comprise seven subtypes, named $P2X_1$ to $P2X_7$, that form non-selective cation channels with high calcium permeability (North, 2016; Schmid and Evans, 2019). In the extracellular space, ATP immediately undergoes enzymatic degradation. Remarkably, a variety of purinoceptors is additionally, if not exclusively, sensitive for the degradation products. The first step of enzymatic ATP degradation yields adenosine 5′-diphosphate (ADP), which is able to activate P2Y receptors in addition to ATP. Some P2Y receptors are also activated by the pyrimidines uridine 5′-triphosphate (UTP) and uridine 5′-diphosphate (UDP; Abbracchio et al., 2006). At least nine different P2Y receptors are expressed in vertebrates, however, $P2Y_3$ appears to be an avian-specific receptor (Webb et al., 1996). $P2Y_{1,2,4,6,11,12,13,14}$ are found in mammals and many of them are expressed by brain cells. The primary intracellular targets of P2Y receptors are heterotrimeric G proteins, in particular, those containing $G\alpha_{q/11}$ ($P2Y_{1,2,4,6,11}$) and $G\alpha_i$ ($P2Y_{12,13,14}$; Abbracchio et al., 2006; Köles et al., 2011). Hence, activation of P2Y receptors results in PLC-mediated calcium signaling and PKC activation as well as inhibition of adenylate cyclase. Besides P2 receptors, the family of purinoceptors comprises P1 receptors (Burnstock et al., 2011). P1 receptors are activated by adenosine, which is usually derived from extracellular degradation of ATP, ADP and AMP by ecto-nucleotidases (CD39/NTPDases, E-NPP, CD73) and alkaline phosphatase (Abbracchio et al., 2009; Zimmermann et al., 2012). P1 are subdivided into A_1, A_{2A}, A_{2B} and A_3 receptors. Mostly, A_1 and A_3 are linked to G_i proteins, while A_{2A} and A_{2B} are linked to G_s

OPEN ACCESS

Edited by:
Eric Boué-Grabot,
Université de Bordeaux, France

Reviewed by:
Antje Grosche,
Ludwig Maximilian University of Munich, Germany
Ivan Milenkovic,
Leipzig University, Germany

****Correspondence:***
Christian Lohr
christian.lohr@uni-hamburg.de

Received: *14 January 2019*
Accepted: *07 March 2019*
Published: *16 April 2019*

Citation:
Rotermund N, Schulz K, Hirnet D and Lohr C (2019) Purinergic Signaling in the Vertebrate Olfactory System. Front. Cell. Neurosci. 13:112. doi: 10.3389/fncel.2019.00112

proteins exerting an impact on the cellular cAMP levels. To finally terminate the purinergic signaling cascade, adenosine is removed by adenosine transporters or converted by adenosine deaminase and adenosine kinase to inosine and AMP, respectively (Boison, 2013; Bagatini et al., 2018; Pastor-Anglada and Pérez-Torras, 2018). Thus, in contrast to other neurotransmitter systems, the degradation of the neurotransmitter ATP does not immediately terminate transmission but generates the neuromodulators ADP and adenosine, which possess their own subsets of receptors and evoke additional cellular responses. Hence, purinergic signaling is by far more complex than other neurotransmitter systems and is determined by the combination of purinoceptors, ATP/adenosine-degrading enzymes and nucleotide/nucleoside transporters. Since this combination changes during development and circadian rhythm and differs significantly between different brain regions and even between microenvironments, purinergic signaling has multiple facets and fulfills a plethora of functions. Postsynaptic P2X receptors, e.g., mediate fast synaptic transmission (Edwards et al., 1992; Evans et al., 1992; Pankratov et al., 2007), whereas P2Y and P1 receptors rather act as neuromodulators. Adenosine, for instance, is a well-known modulator of presynaptic neurotransmitter release at central synapses (Snyder, 1985; Sebastião and Ribeiro, 2009, 2015). In addition, P2Y receptors inhibit presynaptic calcium channels, thereby reducing neurotransmitter release (Sperlágh et al., 2007; Guzman and Gerevich, 2016). Both P1 and P2 receptors are not only expressed by neurons, but also by glial cells (Deitmer et al., 1998; Verkhratsky et al., 2009; Boison et al., 2010). Activation of purinoceptors induces calcium signaling in astrocytes, which triggers the release of gliotransmitters and mediates neurovascular coupling (Pelligrino et al., 2011; Lohr et al., 2014; Köles et al., 2016). Purinergic signaling is also involved in sensory systems, both in sensory organs such as the eye and the cochlea as well as in brain regions contributing to sensory information processing (Housley et al., 2009; Lohr et al., 2011, 2014). In this review article, we summarize recent data on the role of purinergic signaling in cell physiology, adult neurogenesis and odor information processing in the vertebrate olfactory system. Purinergic signaling has also been shown to play important roles in the development of the nervous system (Zimmermann, 2011). However, studies in the olfactory system, even when performed in the developing animal, rarely address the functional role of purines in development, for which reason we will not elaborate on this topic.

STRUCTURE OF THE VERTEBRATE OLFACTORY SYSTEM

Olfactory Epithelium

The vertebrate main olfactory system can be divided into distinct hierarchical levels, mainly the olfactory epithelium, the olfactory bulb and the olfactory cortex (**Figure 1**). In addition, the vomeronasal organ is also part of the vertebrate olfactory system (forming the sensory organ of the additional olfactory system) conveying the detection of pheromones, but we will focus here on the main olfactory system. Odor sensation is initiated by odor molecules flooding the nasal cavity and their detection by olfactory sensory neurons embedded in the olfactory epithelium, a specialized epithelial tissue located in the nasal cavity. Four main cell types provide its functionality; sensory neurons, basal cells, sustentacular cells and microvillar (brush) cells. Olfactory sensory neurons are bipolar neurons with apical poles equipped with cilia that reach into the mucosa covering the epithelium. On the cilia, odorant receptors are located which are activated by odor molecules resulting in excitation of olfactory sensory neurons. Specialized odorant-binding proteins facilitate the solubility of odor molecules in the mucus and therefore are actively involved in the availability of odor molecules for the odorant receptors (Heydel et al., 2013; Pelosi et al., 2014). Since the sensory neurons of the olfactory epithelium are in constant contact with respiratory air containing pathogens and hazardous substances, they have a very limited span of life and have to be replaced by newborn neurons generated from basal cells every few weeks (Brann and Firestein, 2014). Basal cells are stem cells located nearby the basal lamina of the olfactory epithelium. Microvillar cells are microvilli-bearing columnar cells that contact the afferent nerve endings of the trigeminal nerve with their basal surface and mediate the transduction of general sensation (Lucero, 2013). In addition to these cells, the undermost layer of the olfactory epithelium, the lamina propria, harbors olfactory glands (Bowman's glands). They deliver the protein-rich secret onto the air-facing side of the epithelium. Supporting cells, as the name suggests, are non-neuronal cells providing metabolic and physical support for the cell types described above. The axons of olfactory sensory neurons project into the central nervous system forming the first cranial nerve. Many small nerve fascicles pass the perforated cribriform plate to enter the cranial cavity and eventually spread over the surface of their destination area, the olfactory bulb.

Olfactory Bulb

The vertebrate olfactory bulb, the first relay station of the olfactory sensory pathway, is a highly structured area of the forebrain with a complex cellular architecture. Morphologically and functionally distinct layers harbor diverse specialized populations of neurons and glial cells (**Figure 1**). The most superficial layer of the olfactory bulb is the olfactory nerve layer. It is composed of sensory axons, which are assembled into fascicles and surrounded by a unique type of glial cells, the olfactory ensheathing cells. Eventually, the axons of the olfactory sensory neurons exit the nerve layer towards deeper layers to terminate in the glomerular layer. Here, they synapse onto apical dendrites of mitral and tufted cells in so-called glomeruli, separated globular neuropil compartments that form distinct processing units for the incoming odor signals. Mitral and tufted cells, the projection neurons of the olfactory bulb, are often regarded as functionally homogenous and therefore collectively named mitral/tufted cells. In addition to sensory axons and mitral/tufted cell dendrites, glomeruli comprise the processes of local interneurons and astrocytes, whose somata are surrounding the glomerular neuropil in which they project

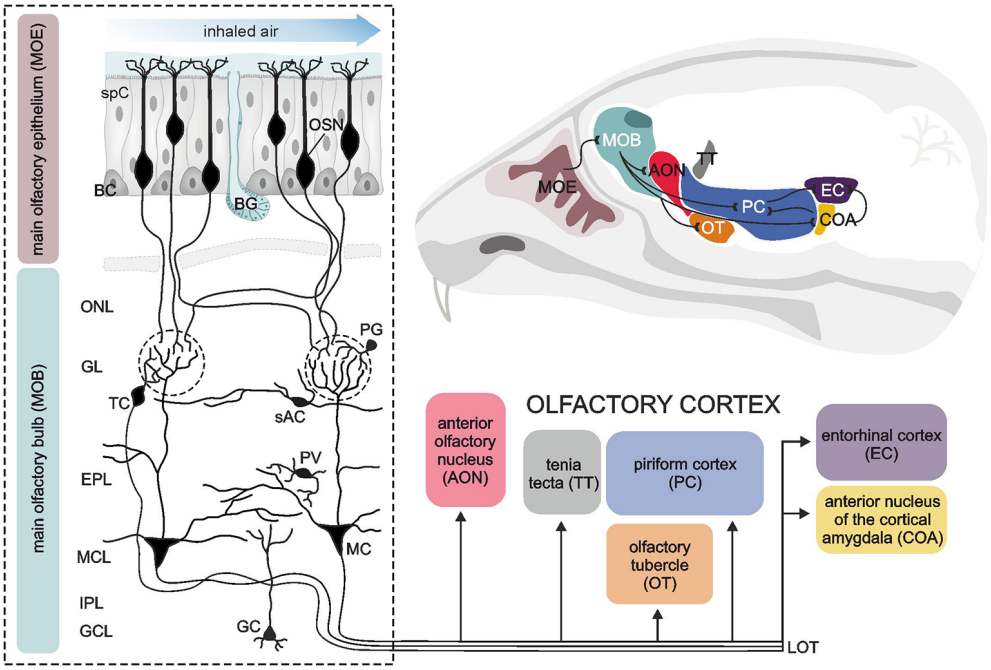

FIGURE 1 | Sensory pathways in the vertebrate olfactory system. A sagittal section of the murine brain (upper right corner) illustrates the components of the vertebrate olfactory system and the connections amongst them (black lines). The dashed box on the left shows a detailed view of the neuronal architecture of the main olfactory epithelium (MOE) and the main olfactory bulb (MOB). The MOE mainly consists of olfactory sensory neurons (OSN), supporting cells (spC) and basal cells (BC) as well as Bowman's glands (BG) providing a mucosa covering the MOE. Volatile odorant molecules are drawn to the nasal cavity by sniffing, pass the mucosa and are detected by OSN. OSN project their axons to the MOB. After passing the olfactory nerve layer (ONL), all OSN expressing the same olfactory receptor converge to the same glomerulus (dashed circles), where the information is synaptically transmitted to second-order neurons, mitral (MC) and tufted cells (TC). The MOB also harbors different types of interneurons, such as periglomerular neurons (PG), short axon cells (sAC), parvalbumin-positive neurons (PV) and granule cells (GC). These interneurons form complex synaptic networks with MC and TC, particularly in the glomerular layer (GL) and the adjacent external plexiform layer (EPL). The somata of MC are located in the mitral cell layer (MCL). The internal plexiform layer (IPL) mainly consists of axons from MC and TC, forming the lateral olfactory tract (LOT). MC and TC generate output *via* LOT and project their axons to different brain areas referred to as the olfactory cortex, consisting of the anterior olfactory nucleus, tenia tecta, olfactory tubercle, piriform cortex, anterior nucleus of the cortical amygdala and the entorhinal cortex. Illustration by SciGraphics.

(Valverde and Lopez-Mascaraque, 1991; Berkowicz et al., 1994; Ennis et al., 1996; De Saint Jan and Westbrook, 2005; De Saint Jan et al., 2009; Lohr et al., 2014). In the glomeruli, the first level of neuronal processing of odor information is established by feed-forward excitation and feedback inhibition within the axo-dendritic and dendro-dendritic glomerular network. The somata of tufted cells lie in the lower part of the glomerular layer and the adjacent so-called external plexiform layer. Below the external plexiform layer, the cell bodies of mitral cells are located in a single-rowed layer, the mitral cell layer. Mitral cells possess a characteristic morphology with a relatively large, pyramidal cell body and an apical dendrite ending in a single glomerulus. They have few lateral dendrites, branching in the external plexiform layer, where they build reciprocal dendro-dendritic synapses with granule cells and other local interneurons. Thus, the external plexiform layer demarcates a second area of odor signal processing besides the glomerular layer, meaning that mitral/tufted cells integrate two spatially and functionally independent levels of information processing. Just below the mitral cell layer, the axons of mitral/tufted cells assemble and proceed caudally, forming the internal plexiform layer. The deepest layer of the olfactory bulb is mainly filled with granule cells, small axon-less interneurons that project their dendrites to the external plexiform layer.

Primary Olfactory Cortex

On their way towards the cortical areas, the axons of mitral/tufted cells converge to the lateral olfactory tract, leaving the olfactory bulbs to project to areas of higher ordered sensory processing. The olfactory pathway shows some unique features compared to neuronal pathways of other senses such as vision, hearing and somatosensation. The main part of the information from the olfactory bulb is conveyed straight to cortical areas without passing a thalamic relay first (Gottfried, 2006). These cortical areas, receiving direct input from the olfactory bulb, are designated primary olfactory cortex and extend to the dorsomedial surface of the temporal lobe. As main elements, the primary olfactory cortex comprises (from rostral to caudal) the anterior olfactory nucleus (a.k.a. anterior olfactory cortex), olfactory tubercle, tenia tecta, piriform cortex, anterior cortical nucleus of the amygdala and entorhinal cortex (**Figure 1**). Apart from the entorhinal cortex, the areas of the primary olfactory cortex

consist of a three-layered allo-(palaeo-)cortex, pointing to its ancient evolutionary origins (Gottfried, 2006). Notably, all these regions are not exclusively destined to process olfactory information, but, being elements of the limbic system, rather fulfil multiple functions such as processing emotions and memory formation, which can anecdotally be experienced as highly vivid and emotional autobiographical memories triggered by olfactory sensation (Gottfried, 2006; Wilson et al., 2014). The connection between primary olfactory cortex structures and the olfactory bulb is reciprocal, apart from the olfactory tubercle, a structure which is rudimentary in humans and does not feed back to the olfactory bulb (Gottfried, 2006). Most subregions of the primary olfactory cortex are intensely interconnected *via* cortical fibers with each other and with higher-ordered secondary cortical areas such as the orbitofrontal cortex, mediodorsal thalamus and amygdala (Wilson et al., 2014). A key area of this network producing olfactory perception is the piriform cortex. Despite the relatively simple three-layered cytoarchitecture, the piriform cortex executes diverse operations, which are attributed to higher-ordered associative cortices rather than to primary sensory cortices. For instance, the piriform cortex contributes to decorrelation of odor responses in order to discriminate different odors, pattern completion allowing perceptual stability and encoding the value associated with the odor creating an odor context memory (Haberly, 2001; Courtiol and Wilson, 2017).

SOURCES AND BREAKDOWN OF ATP AND ADENOSINE

ATP, as intracellular energy supply, is present in all cells and therefore ubiquitously available as an intercellular signaling molecule. Thus, the presence of high amounts of ATP in the extracellular space as a result of injury or cell death seems to be a common signal of cell damage (Burnstock and Verkhratsky, 2009). Apart from that, a controlled release of ATP by exocytosis, active transport or membrane pores is also known for most brain areas (North and Verkhratsky, 2006; Lohr et al., 2011; Burnstock, 2013). Depending on the release pathway, achieved local concentration, the rate of degradation or uptake and the presence of different types of purinoceptors, ATP and other nucleotides transduce or modulate physiological responses in a highly specific manner.

In the olfactory system, the active release of ATP, ADP or adenosine has been described in the olfactory epithelium, the olfactory bulb and the olfactory cortex. ATP is released by exocytosis in the olfactory epithelium and activates both P2Y and P2X receptors (Hegg et al., 2009; Hayoz et al., 2012). In the olfactory bulb, electrical stimulation of axons of olfactory sensory neurons results in co-release of ATP and glutamate at the axon terminals in the glomerular layer as well as alongside the axons in the nerve layer, which was termed "ectopic" release (Thyssen et al., 2010). The concentration of extracellular ATP released from these neurons was estimated to reach the upper micromolar range (Thyssen et al., 2010). The release of ATP from olfactory sensory neurons depends on a rise in intracellular calcium and is suppressed by impairing exocytosis with botulinum toxin, indicating vesicular release (Thyssen et al., 2010). In addition, astrocytes provide a source for extracellular ATP in the olfactory bulb. Roux et al. (2015) demonstrated the significance of astrocytic connexin 43 hemichannels for purinergic neuron-glia communication and baseline ATP levels in the mouse olfactory bulb. ATP-mediated effects on mitral cells are blocked in mice deficient in connexin 43, a connexin mainly expressed by astrocytes, and by the connexin 43-specific inhibitory peptide Gap26. On the other hand, ATP release from astrocytes *via* the opening of connexin 43 hemichannels is reduced by tetrodotoxin (TTX) and hence depends on neuronal activity (Roux et al., 2015). The prominent role of astrocytic hemichannels in controlling extracellular ATP is further confirmed by the finding that Gap26 results in a reduction of ambient ATP levels by about 50% (Roux et al., 2015).

Purinergic signaling is more complex than most other neurotransmitter systems, since extracellular degradation of ATP is not the endpoint of its action, but activates other parts of the purinergic signaling system. A variety of extracellular enzymes, e.g., tissue non-specific alkaline phosphatases and ecto-nucleotidases, catalyze the successive degradation of ATP (Zimmermann, 2006). The activity of these enzymes and of adenosine deaminase is notably high in the olfactory bulb, compared to other brain regions, suggesting a rapid extracellular breakdown from ATP to adenosine and great significance of ATP dephosphorylation products as signaling molecules in the olfactory bulb (Geiger and Nagy, 1987; Schoen and Kreutzberg, 1995, 1997; Clemow and Brunjes, 1996; Langer et al., 2008). Interestingly, the activity of different nucleotide-degrading enzymes differs significantly between different layers of the olfactory bulb. Ecto 5′-nucleotidase (CD73), e.g., has a very high activity in the external and internal plexiform layers as well as in the granule cell layer, while tissue non-specific alkaline phosphatase is active in the glomerular, external and internal plexiform layers (Langer et al., 2008). Physiological experiments in acute olfactory bulb slices provide additional evidence for the importance of tissue non-specific alkaline phosphatase, since its inhibition suppresses the A_{2A} receptor-dependent calcium response in periglomerular astrocytes upon application of ATP, while inhibition of ecto-nucleotidases with ARL 67156 had no effect (Doengi et al., 2008). A study by Pani et al. (2014) provides data about baseline levels of ATP, ADP, AMP and adenosine in five brain regions, including the olfactory bulb, of five different strains of mice. Using high-performance liquid chromatography with electrochemical detection, they found significant variations of baseline purine levels between brain regions and mouse strains. In the olfactory bulb, total adenosine concentrations varied significantly from about 3,000 pg/mg wet weight in C57BL/6J mice to about 600,000 pg/mg wet weight in BALB/c mice. In C57BL/6J mice, both adenosine and ATP showed the lowest concentrations in the olfactory bulb compared to the other brain regions such as the cerebral cortex and hippocampus (Pani et al., 2014). Yet, whether these variations in total purine concentration also reflect diversity in extracellular purine levels and purinergic

neuromodulation in different brain areas or mouse strains remains an open question.

PURINERGIC SIGNALING IN THE OLFACTORY EPITHELIUM

The olfactory epithelium mainly consists of sensory neurons, sustentacular cells, microvillar cells and basal cells (**Figure 2**). All four cell types have been found to express purinoceptors (Hegg et al., 2003). Immunohistochemical, electrophysiological and calcium imaging studies demonstrated the presence of P2X and P2Y receptors in olfactory sensory neurons (Hegg et al., 2003). Application of ATP excites olfactory sensory neurons and leads to an increase in the cytosolic calcium concentration in explants of the olfactory epithelium of mice and *Xenopus* tadpoles (Hegg et al., 2003; Czesnik et al., 2006). Despite the excitatory effect of ATP on non-stimulated olfactory sensory neurons, calcium responses upon stimulation by odors are inhibited by co-application of ATP (Hegg et al., 2003). In line with this, odor-evoked responses in olfactory sensory neurons are increased in amplitude when purinoceptors are blocked by the non-specific P2 antagonists PPADS and suramin, indicating purinergic modulation of odor responses by endogenously released ATP (Hegg et al., 2003).

Besides the impact on sensory signal transduction, purinergic agonists such as ATP, ADP and UTP also evoke calcium signaling in sustentacular cells and microvillar cells, linking neuronal activity and trophic functions (Hegg et al., 2003, 2009; Czesnik et al., 2006; Hassenklöver et al., 2008; Jia and Hegg, 2015). In sustentacular cells, ATP and UTP stimulate calcium signaling *via* P2Y receptor-mediated calcium release from internal stores (Hassenklöver et al., 2008; Hegg et al., 2009). These calcium signals occur as calcium oscillations in individual cells but can also travel as calcium waves through the gap junction-coupled syncytium of sustentacular cells in the olfactory epithelium (Vogalis et al., 2005a; Hassenklöver et al., 2008; Hegg et al., 2009). Calcium transients in sustentacular cells are accompanied by activation of calcium-dependent BK potassium channels, which results in hyperpolarization of the cell membrane (Vogalis et al., 2005a,b). Degeneration of sensory neurons in the olfactory epithelium evokes the release of ATP (Jia and Hegg, 2010; Hayoz et al., 2012). In neonatal mice, this ATP release is potentiated by ATP-induced ATP release, which involves $P2X_7$ and P2Y receptors and results in extracellular ATP concentrations in the low micromolar range (Hayoz et al., 2012). Besides sustentacular cells, the second type of supporting cells, microvillar cells, resides in the olfactory epithelium and expresses purinoceptors (Hegg et al., 2010; Fu et al., 2018). Extracellular ATP evokes calcium signaling in both, sustentacular and microvillar cells, by activation of $P2Y_2$ and $P2X_7$ receptors (**Figure 2**). A subpopulation of microvillar cells that expresses type 3 inositol trisphosphate receptor (IP3R3) and transient receptor potential channel M5 (TRPM5) also expresses the neurotrophic factor neuropeptide Y (NPY); in these cells, P2 receptor-dependent calcium signaling leads to release of NPY (Montani et al., 2006; Kanekar et al., 2009; Jia and Hegg, 2015). Activation of Y1 NPY receptors in basal cells stimulates p44/42 extracellular signal-regulated kinase (ERK), thereby promoting proliferation of basal cells that differentiate into mature olfactory sensory neurons (Jia et al., 2009, 2013; Jia and Hegg, 2012). Upon maturation, these sensory neurons grow

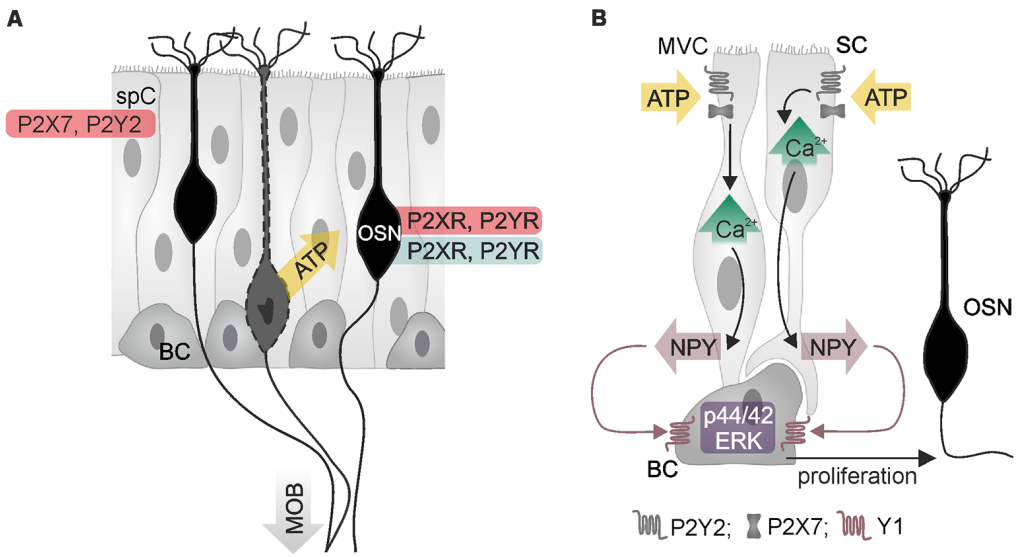

FIGURE 2 | Purinergic signaling in the main olfactory epithelium. **(A)** Olfactory sensory neurons (OSN) and supporting cells (spC) express P2X and P2Y receptors, as demonstrated by physiological (red) and histological data (blue). Adenosine 5′-triphosphate (ATP) is released from injured or degenerating OSN (yellow arrow). BC, basal cell; MOB, main olfactory bulb. **(B)** ATP stimulates calcium signaling in two types of supporting cells, microvillar cells (MVC) and sustentacular cells (SC), resulting in the release of neuropeptide Y (NPY). Activation of Y1 NPY receptors of basal cells stimulates proliferation *via* p44/42 mitogen-activated protein kinase (extracellular signal-regulated kinase; ERK), which generates new OSN. Illustration by SciGraphics.

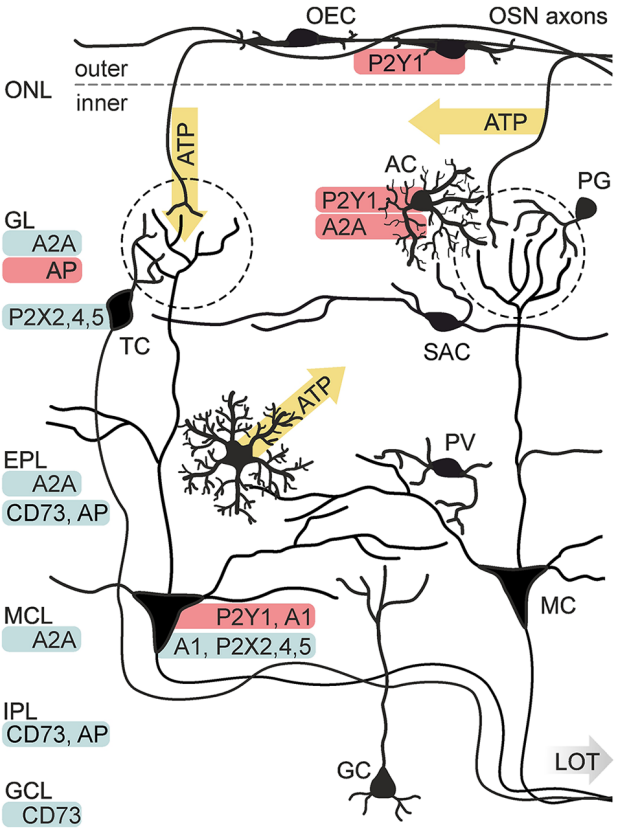

FIGURE 3 | Purinergic signaling in the olfactory bulb. Known release sides of purines (yellow) and distribution (red: physiological data, blue: histological data) of purinoceptors and degrading enzymes in the cellular network of the olfactory bulb. Electrical stimulation of axons of olfactory sensory neurons (OSN) results in the release of ATP from axon terminals in the GL and alongside the axons in the ONL. ATP is released from astrocytes (AC) *via* the opening of connexin 43 hemichannels. $P2X_{2/4/5}$ receptors have been identified histologically in mitral cells (MC) and tufted cells (TC). Physiological evidence exists for the expression of $P2Y_1$ receptors in AC and MC, as well as for A_1 receptor expression in MC and A_{2A} receptor expression in AC. Expression of the A_{2A} receptor has been shown histologically for the GL, EPL and mitral cell layer (MCL). Activity of nucleotide-degrading enzymes alkaline phosphatase (AP) and ecto 5′-nucleotidase (CD73) has been demonstrated in several layers. Abbr.: GC, granule cell; GCL, granule cell layer; IPL, internal plexiform layer; LOT, lateral olfactory tract; OEC, olfactory ensheathing cell; PG, periglomerular neuron; PV, parvalbumin-positive neuron; SAC, short axon cell. Illustration by SciGraphics.

their axons into the olfactory bulb and form synapses with mitral and tufted cells.

PURINERGIC SIGNALING IN THE OLFACTORY BULB

Purinoceptor Expression

With a growing number of studies showing the influence of purinergic signaling in olfaction, a widespread involvement of purinoceptors in this sensory system becomes obvious. By now, the presence of purinoceptors has been shown for all layers of the olfactory bulb by means of physiological studies, antibody staining, *in situ* hybridization and binding studies with radio-labeled receptor ligands (**Figure 3**). $P2X_2$, $P2X_4$, $P2X_5$ and $P2X_6$ receptor expression has been demonstrated in the principal neurons of the olfactory bulb, mitral and tufted cells, by *in situ* hybridization and immunolabeling, while P2X receptors have so far not been found in glial cells of the olfactory bulb (Collo et al., 1996; Vulchanova et al., 1996; Lê et al., 1998; Guo et al., 2008; Kaneda et al., 2010). For the family of P2Y receptors, only little information about expression in the olfactory bulb is published. Staining with a radio-labeled $P2Y_1$ ligand showed positive results for all layers of the olfactory bulb, with a pronounced staining in the glomerular layer (Simon et al., 1997). In olfactory bulb tissue, mRNA expression of all four types of adenosine receptors has been demonstrated by Northern blot (Mahan et al., 1991; Dixon et al., 1996). A_1 receptors, as well as A_{2A} receptors have been found by *in situ* hybridization and antibody staining (Johansson et al., 1997; Rosin et al., 1998; Kaelin-Lang et al., 1999). Noteworthy, the expression levels of A_1 and A_{2A} were among the highest in the entire mouse brain. In the olfactory bulb mRNA of A_1 receptors is predominantly expressed in a pattern resembling the localization, size and abundance of mitral and tufted cells (Rotermund et al., 2018). *In situ* hybridization depicts a more widespread expression of the A_{2A} receptor, with intense staining in mitral and tufted cells, but also in periglomerular interneurons and granule cells (Rotermund et al., 2018).

Glial Cell Physiology and Function

Purinergic signaling in the olfactory bulb has first been described in glial cells, corroborating the important role of purines for neuron-glia interaction. Olfactory ensheathing cells, exclusively found in the olfactory nerve including the olfactory bulb nerve layer, respond to application of ATP with a $P2Y_1$-mediated calcium increase in neonates (Rieger et al., 2007; Thyssen et al., 2010) as well as in adults (Thyssen et al., 2013; Stavermann et al., 2015). In contrast, application of adenosine has no impact on calcium levels in these cells (Thyssen et al., 2013). A recent study demonstrates that the observed effect of $P2Y_1$-mediated calcium signaling is restricted to P75 neurotrophin receptor-positive olfactory ensheathing cells of the outer nerve layer, whereas P75-negative olfactory ensheathing cells of the inner nerve layer do not generate calcium signals in response to ATP or other purinergic ligands (Thyssen et al., 2013; Stavermann et al., 2015). Like most other neurotransmitter-mediated calcium responses in glial cells, the $P2Y_1$-mediated intracellular calcium increase in olfactory ensheathing cells is based on calcium release driven by IP3 receptors, being amplified by calcium-induced calcium release and prolonged by store-operated calcium entry (Stavermann et al., 2012; Thyssen et al., 2013).

In addition to olfactory ensheathing cells, olfactory bulb astrocytes express purinoceptors. Periglomerular astrocytes have been shown to possess $P2Y_1$ and A_{2A} receptors that are linked to intracellular calcium signaling (Doengi et al., 2008; Lohr and Deitmer, 2010). ATP, which is co-released with glutamate at axon terminals of olfactory sensory neurons, is degraded extracellularly to ADP and adenosine. It was shown that both ADP and adenosine elicit a rise in intracellular calcium levels in olfactory bulb astrocytes, mediated by $P2Y_1$ and A_{2A} receptors,

while the co-released glutamate activates metabotropic glutamate receptor 5 ($mGluR_5$) and calcium-permeable AMPA receptors in these cells (Petzold et al., 2008; Verkhratsky et al., 2009; Droste et al., 2017). Calcium signaling evoked by $mGluR_5$ activation is only found in astrocytes of developing animals, while the $P2Y_1$-, A_{2A}- and AMPA receptor-evoked calcium responses persist in adults (Doengi et al., 2008; Otsu et al., 2015; Droste et al., 2017; Beiersdorfer et al., 2019). In accordance with calcium signaling in olfactory ensheathing cells, ATP- and ADP-evoked rises in intracellular calcium in olfactory bulb astrocytes are driven by calcium release *via* IP3 signaling and subsequent calcium entry by the activation of store-operated calcium channels (Singaravelu et al., 2006; Doengi et al., 2009). Interestingly, the calculated EC50 (4.5 μM) for ADP-induced calcium signaling in glomerular astrocytes is higher by more than one order of magnitude compared to the EC50 value (0.23 μM) for A_{2A} receptor-dependent calcium signals (Doengi et al., 2008). This concentration-dependent activation may result in a differentiated activation of purinergic receptors: only high amounts of ATP above 1 μM are sufficient to activate $P2Y_1$ receptors in glomerular astrocytes, whereas lower amounts of ATP bypass P2 receptor activation and directly target adenosinergic P1 receptors providing the possibility of graduated responses to different neuronal activity.

In other brain areas, astrocytes have been shown to respond to neurotransmitters released from presynaptic terminals with increases in the cytosolic calcium concentration, which can result in release of so-called gliotransmitters (e.g., glutamate, D-serin and ATP) and other substances such as arachidonic acid and prostaglandins which affect adjacent synapses and blood vessels (Haydon and Carmignoto, 2006; Attwell et al., 2010; Verkhratsky et al., 2012; Shigetomi et al., 2016; Dallérac et al., 2018). Calcium-dependent modulation of blood vessels by astrocytes upon neuronal activity is called neurovascular coupling and has also been studied in the olfactory bulb (Petzold et al., 2008; Doengi et al., 2009; Lohr et al., 2011; Otsu et al., 2015). Neurovascular coupling is an important mechanism to cope with the increasing energy demand upon neuronal activity, since action potential firing and synaptic transmission are the main energy sinks in the brain (Attwell and Laughlin, 2001; Attwell and Gibb, 2005; Barros and Deitmer, 2010). In addition, neurovascular coupling regulates and stabilizes the blood pressure in brain arterioles (Iadecola and Nedergaard, 2007). In olfactory bulbs of living, anesthetized mice, odor stimulation evokes $mGluR_5$- and $P2Y_1/A_{2A}$-dependent calcium signaling in astrocytes that trigger dilation of adjacent capillaries and hyperemia (Petzold et al., 2008; Otsu et al., 2015). However, since $mGluR_5$ is down-regulated in astrocytes of the cortex and the olfactory bulb in adult mice, glial $mGluR_5$ is unlikely to mediate neurovascular coupling in adult animals (Sun et al., 2013; Otsu et al., 2015; Beiersdorfer et al., 2019). In contrast, calcium signaling evoked by ATP and possibly ADP and adenosine persists from neonates to adults (Doengi et al., 2008; Beiersdorfer et al., 2019), resulting in astrocytic calcium responses upon odor stimulation even in the absence of $mGluR_5$ (Otsu et al., 2015). Calcium transients in astrocytic microdomains of perivascular endfeet are followed by a drop in calcium in perivascular pericytes and, finally, vasodilation as well as hyperemia in the glomerular layer (Otsu et al., 2015; Rungta et al., 2018). The olfactory nerve layer comprises axons of olfactory sensory neurons and olfactory ensheathing cells but lacks astrocytes with the exception of astrocytic processes that enwrap arterioles that penetrate the nerve layer. Calcium signaling in astrocytes around penetrating arterioles is able to mediate neurovascular coupling (Petzold et al., 2008), however, capillaries in the nerve layer require a different mechanism to adapt to neuronal activity. Capillaries in the nerve layer are enwrapped by the fine processes of olfactory ensheathing cells (Thyssen et al., 2010). Olfactory ensheathing cells express $mGluR_1$ as well as $P2Y_1$ receptors and respond to glutamate and ATP released from axons of sensory neurons with calcium transients (Rieger et al., 2007; Thyssen et al., 2010, 2013). Similar to astrocytes, mGluRs are down-regulated during the first postnatal weeks, whereas purinoceptor expression persists until adulthood (Thyssen et al., 2013; Stavermann et al., 2015; Beiersdorfer et al., 2019). Neuronal activity, local stimulation of $P2Y_1$ receptors and induction of calcium signaling in single olfactory ensheathing cells trigger vasoresponses in the olfactory bulb capillaries, indicating that in addition to astrocytes, olfactory ensheathing cells are able to mediate neurovascular coupling *via* purinergic signaling (Thyssen et al., 2010; Lohr et al., 2011, 2014; Beiersdorfer et al., 2019).

Neuromodulation

ATP and its breakdown products ADP and adenosine have been described as neuromodulators in many instances (Chen et al., 2014; Sebastião and Ribeiro, 2015; Guzman and Gerevich, 2016; Köles et al., 2016; Boué-Grabot and Pankratov, 2017). In developing as well as mature olfactory bulbs, ATP increases neuronal network activity leading to excitation of output neurons, the mitral and tufted cells (Fischer et al., 2012; Schulz, 2018). In these studies, wide-field photoapplication of ATP (by photolysis of caged ATP) evokes an increase of synaptic inputs and excitation of mitral cells, measured as whole-cell current and voltage responses. In addition, local release of ATP by photoapplication in a single glomerulus produces an increase of synaptic inputs in the mitral cell which is accompanied by an increase in intracellular calcium in the mitral cell tuft (Fischer et al., 2012). The ATP response depends on the activation of $P2Y_1$ receptors, as inhibition of $P2Y_1$ receptors by the specific antagonist MRS2179 impeded the effect. The rise in network activity is not the consequence of direct $P2Y_1$-mediated excitation of the mitral cell itself, but of other neurons, since suppression of neuronal firing with TTX and inhibition of NMDA and AMPA receptors, respectively, not only abolished the network response but also eliminated $P2Y_1$-mediated current responses in mitral cells almost entirely (Fischer et al., 2012). So far, the identity of these $P2Y_1$-expressing neurons has not been resolved. Despite the high expression of P2X receptors in mitral and tufted cells, as shown by *in situ* hybridization and immunolabeling (Lê et al., 1998; Kanjhan et al., 1999; Guo et al., 2008), P2X-mediated currents could not be measured yet (**Figure 3**). In summary, the studies show that purinoceptors are abundant

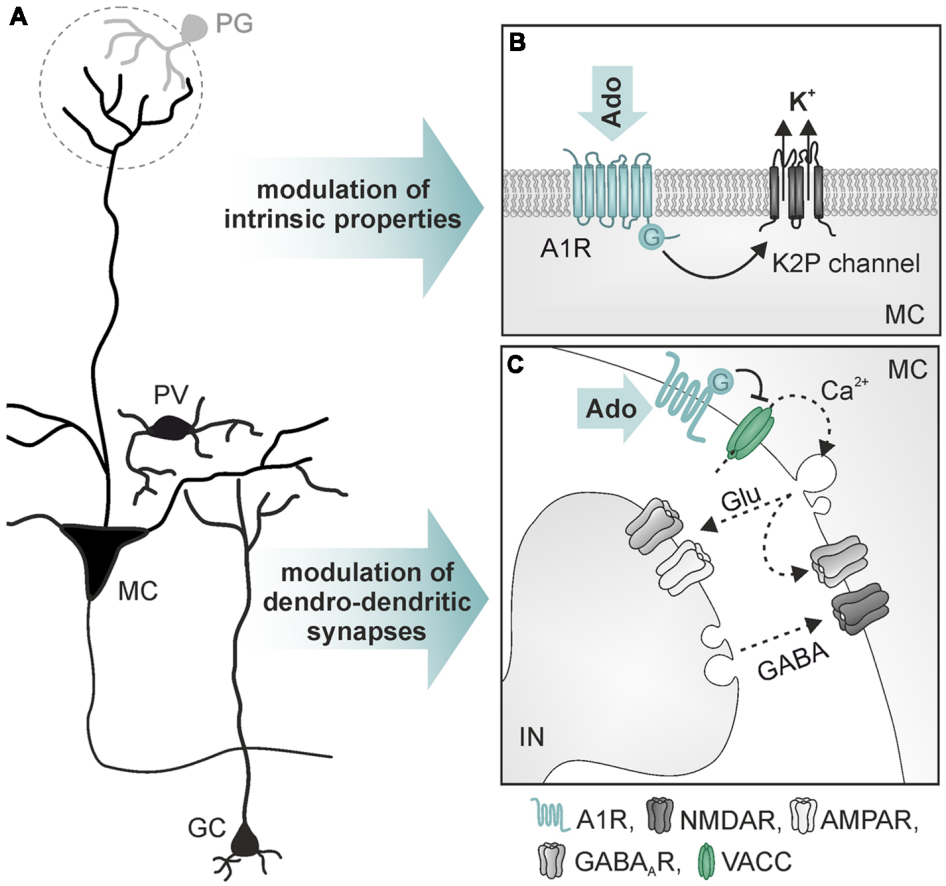

FIGURE 4 | Mechanisms of action of adenosine in mitral cells. **(A)** Simplified neuronal network in the olfactory bulb. **(B)** Opening of two-pore domain potassium channels (K2P) by activation of A_1 receptors leads to hyperpolarization of mitral cells (MC). **(C)** A_1 receptor-mediated reduction of Ca^{2+} influx into presynaptic sites of MC reduces dendro-dendritic inhibition at reciprocal synapses between MC and interneurons (IN; GC and parvalbumin-positive interneurons). Abbr.: Ado, adenosine; Glu, glutamate; GC, granule cells; PG, periglomerular interneuron; PV, parvalbumin-positive interneuron; VACC, voltage-activated calcium channel. Illustration by SciGraphics.

in the olfactory bulb and ATP has a strong excitatory effect on neuronal network activity, however, the exact mechanisms by which ATP modulates neuronal performance still need to be elucidated.

A well-established role of adenosine is the regulation of glutamatergic synaptic transmission by activation of presynaptic P1 receptors (Sebastião and Ribeiro, 2009; Chen et al., 2014). In the olfactory bulb, A_1 and A_{2A} receptors are highly expressed (Kaelin-Lang et al., 1999; Rotermund et al., 2018). In addition, the activity of ATP-degrading ectoenzymes required for the production of adenosine from ATP is among the highest activities found in the rodent brain (Langer et al., 2008). It has been shown that adenosine acts as a neuromodulator in the olfactory bulb (Roux et al., 2015; Rotermund et al., 2018; Schulz et al., 2018; **Figure 4**). Whole cell patch clamp recordings show that activation of A_1 receptors hyperpolarizes mitral cells and reduces the network activity in olfactory bulb brain slice preparations of wild type mice, but not of A_1 receptor knockout mice (Rotermund et al., 2018). The hyperpolarization is mediated by increasing the potassium conductance of the mitral cell membrane. While in other brain areas, A_1 receptor activation leads to stimulation of G protein-coupled inwardly rectifying potassium (GIRK) channels (Sickmann and Alzheimer, 2003; Kim and Johnston, 2015), the effect of adenosine on mitral cells is based on an A_1 receptor-dependent opening of two-pore domain potassium channels (**Figure 4B**), probably reflecting very ancient cellular mechanisms in this archicortex (Rotermund et al., 2018). Roux et al. (2015) found constitutive release of ATP from astrocytes that is degraded to adenosine, resulting in DPCPX-sensitive alteration of slow membrane oscillations of mitral cells. In another study, DPCPX had no effect on steady-state excitability of mitral cells but inhibited adenosine-evoked hyperpolarization (Rotermund et al., 2018). The adenosine-evoked hyperpolarization is associated with a decrease in spontaneous action potential firing. In contrast, bursting activity of mitral cells upon synaptic input from sensory fibers is unaffected by adenosine, indicating lack of adenosine-mediated plasticity at synapses between sensory neurons and mitral cells (Rotermund et al., 2018). This results in a significant increase in the ratio of synaptically evoked firing over spontaneous firing

and hence, in the signal-to-noise ratio of the output signaling of mitral cells (Rotermund et al., 2018).

Mitral and tufted cells establish numerous reciprocal dendro-dendritic synapses between their lateral dendrites and inhibitory interneurons (**Figure 4C**), mainly granule cells and parvalbumin-positive cells (Crespo et al., 2013). Mitral cells express A_1 receptors that are located in the presynaptic membrane of the mitral-to-interneuron synaptic connection of these reciprocal synapses. Activation of A_1 receptors inhibits presynaptic voltage-dependent calcium channels of the N- and P/Q-type, thus reducing glutamate release from mitral cell lateral dendrites (Schulz et al., 2018). Consequently, interneurons receive less excitation and thus respond with diminished GABA release, resulting in attenuated recurrent inhibition in mitral cells. The attenuation of NMDA, as well as AMPA receptor-mediated dendro-dendritic inhibition, indicates that reciprocal synapses of mitral cells with both, granule cells (NMDA receptor-driven) and with parvalbumin-positive cells (AMPA receptor-driven), are modulated by adenosine (Schulz et al., 2018). Recurrent inhibition between mitral cells and GABAergic interneurons is fundamental for odor discrimination. Increasing recurrent inhibition by, for instance, optogenetic excitation of granule cells or enhanced GABA release from granule cells due to ablation of GluA2 subunits (thereby amplifying glutamate-evoked calcium influx) improves odor discrimination, whereas inhibition of granule cells impairs odor discrimination (Abraham et al., 2010; Gschwend et al., 2015). Consequently, A_1 receptor-deficient mice that lack adenosine-mediated depression of recurrent inhibition outperform wild type mice in a behavioral olfaction test, emphasizing the role of adenosine in olfactory information processing (Schulz et al., 2018).

PURINERGIC SIGNALING IN THE OLFACTORY CORTEX

Expression of Purinoceptors and Nucleotidases

As already known for many years, adenosine modulates synaptic transmission in the olfactory cortex (Kuroda, 1978;

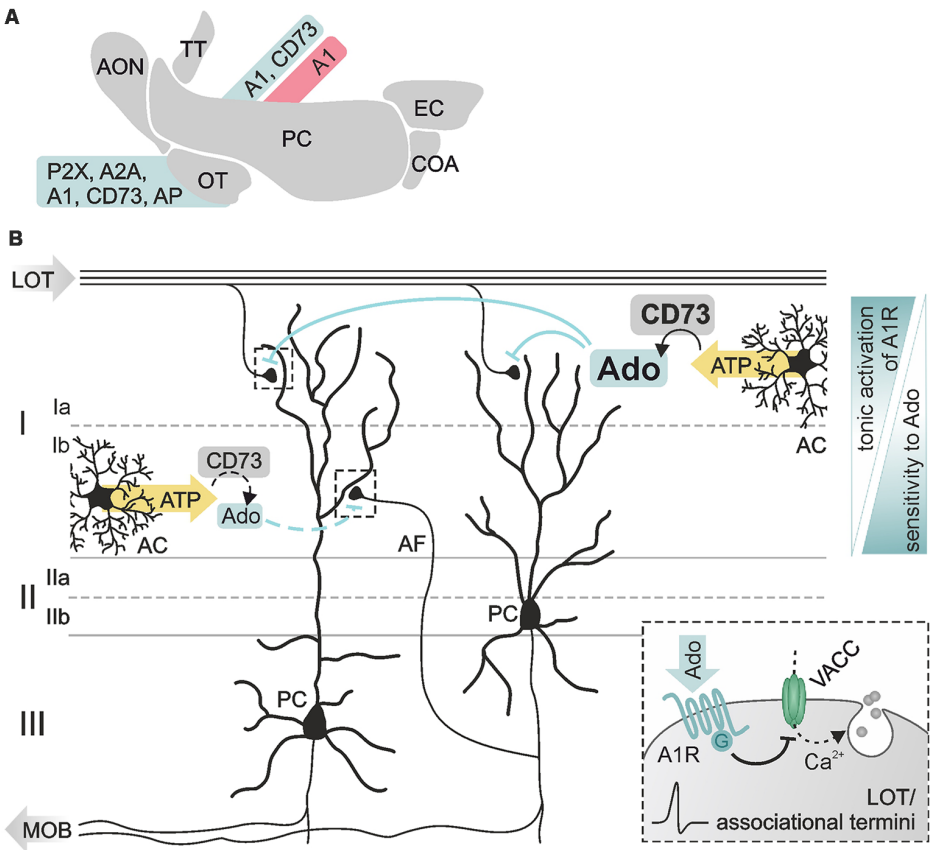

FIGURE 5 | Purinergic modulation in the piriform cortex. **(A)** Expression of members of the purinergic signaling pathway in the olfactory cortex documented by physiological (red) and histological (blue) data. **(B)** Pyramidal cells (PC) reside in layer II/III of the piriform cortex with dendritic arbors spreading in superficial layer I. Synaptic inputs at PC dendrites are segregated in distinct sublayers, sublayer Ia exclusively receiving excitatory input from fibers of the LOT, sublayer Ib receiving input from intracortical associational fibers (AF). Adenosine affects both types of inputs by A1 receptor-dependent inhibition of presynaptic voltage-activated calcium channels (VACC) and thereby inhibition of glutamate release (see inset). Ecto 5′-nucleotidase (CD73) is differentially expressed in the sublayers resulting in higher basal levels of extracellular adenosine in layer Ia compared to layer Ib. Synaptic transmission in both layers shows different sensitivity to adenosine, associative synapses in layer Ib being more sensitive to adenosine than LOT synapses in layer Ia. Abbr.: AC, astrocyte; MOB, main olfactory bulb. Illustration by SciGraphics.

Scholfield, 1978; Okada and Kuroda, 1980; Collins and Anson, 1985) There is a number of studies demonstrating the expression of enzymes and receptors of the purinergic signaling cascade in the primary olfactory cortex (**Figure 5A**). Kidd et al. (1995) detected P2X receptor mRNA in the olfactory tubercle, implying a contribution of ATP to fast neurotransmission in this brain area. The majority of available data, though, concerns adenosinergic signaling. In the olfactory tubercle, the expression of adenosine A_{2A} receptors is the highest apart from expression in the striatum and the olfactory bulb as shown by *in situ* hybridization, antibody staining and autoradiographic labeling studies (Johansson and Fredholm, 1995; Luthin et al., 1995; Rosin et al., 1998, 2003; DeMet and Chicz-DeMet, 2002; Rotermund et al., 2018). A_1 receptors are also expressed in the olfactory tubercle, albeit to a lesser degree (Fastbom et al., 1987; Rotermund et al., 2018). Antibody staining of the ecto-nucleotidase CD73 clearly labels the olfactory tubercle (Kulesskaya et al., 2013). Furthermore, enzymatic activity of ecto 5′-nucleotidases and alkaline phosphatase is very high in the olfactory tubercle, emphasizing the role of purinergic neurotransmission and -modulation in this brain area (Langer et al., 2008).

Modulation of Synaptic Plasticity

Expression of A_1 receptors and ecto 5′-nucleotidases has been found in the piriform cortex, pointing to a role of adenosine in neuromodulation (Goodman and Synder, 1982; Trieu et al., 2015). The main targets of adenosinergic modulation in the piriform cortex are excitatory synaptic inputs in pyramidal cell dendrites (Rezvani et al., 2007; Yang et al., 2007; Trieu et al., 2015; Perrier et al., 2019). The somata of pyramidal cells reside in layer II/III of the piriform cortex, while their apical dendritic arbors extend into the superficial layer I (**Figure 5B**). There they receive spatially segregated excitatory input from different sources: axons of mitral cells carry odor information *via* the lateral olfactory tract and synapse on pyramidal cell dendrites in layer Ia (**Figure 5B**, LOT), while intrinsic afferent fibers from piriform cortex pyramidal cells and other cortical areas (forming the piriform cortex association network) establish synapses with pyramidal cell dendrites in layer Ib (**Figure 5B**, AF; Luskin and Price, 1983a,b; Nevill and Haberly, 2004). Stimulation of lateral olfactory tract fibers evokes field excitatory postsynaptic potentials (fEPSP) in the piriform cortex with a characteristic bipolar waveform reflecting the two different kinds of input in pyramidal cells (Haberly, 1973). The initial peak represents the monosynaptic sensory transmission (lateral olfactory tract-to-pyramidal cell), followed by a compound signal representing the activity of associational network fibers within the piriform cortex (pyramidal cell-to-pyramidal cell). Both types of synapses are modulated by adenosine; in *in vivo* experiments, activation of A_1 receptors has been shown to reduce both the initial peak as well as the subsequent compound signal of the fEPSP (Rezvani et al., 2007). This depression of synaptic transmission is mediated by A_1 receptor-dependent inhibition of presynaptic voltage-gated calcium entry *via* N- and P/Q-type calcium channels (Yang et al., 2007). In addition, adenosine increases paired-pulse facilitation in layer Ia while decreasing paired-pulse depression in layer Ib (Yang et al., 2007). Hence, A_1 receptor-mediated inhibition of calcium channels decreases the release probability at these synapses. Interestingly, synapses between associational network fibers and pyramidal cells in layer Ib are more sensitive for modulation by experimentally added adenosine compared to synapses between lateral olfactory tract fibers and pyramidal cells in layer Ia, indicating a lower concentration of endogenous adenosine in layer Ib (Yang et al., 2007). The low ambient adenosine concentration at layer Ib synapses results from slow ATP-to-adenosine conversion due to low abundance of ecto 5′-nucleotidase and lack of synaptic ensheathment by glial cell processes, which provide one major source of ATP in the cortex (Haberly and Behan, 1983; Nevill and Haberly, 2004; Pankratov and Lalo, 2015; Trieu et al., 2015; Yi et al., 2017). Synapses between lateral olfactory tract fibers and pyramidal cell dendrites in layer Ia are not only depressed by adenosine, but can also be facilitated dependent on the frequency of synaptic activation (Perrier et al., 2019). While adenosine has no effect on the amplitude of fEPSP evoked by a train of stimuli at frequencies between 3 and 25 Hz, it strongly facilitates fEPSP at frequencies between 50 and 100 Hz (Perrier et al., 2019). Since the entire range of stimulation frequencies used in that study reflects frequencies naturally occurring during odor perception depending on, e.g., odor concentrations, adenosine might fine-tune odor perception in an intensity-dependent manner. However, while the studies above clearly demonstrate neuromodulatory functions of adenosine in synaptic transmission and plasticity in the olfactory cortex, its role in olfactory learning and memory formation remains to be shown.

CONCLUSION

Purinergic signaling is a universal and versatile system of neurotransmission and -modulation. The extraordinary high expression of purinoceptors and nucleotide-degrading enzymes in regions of the olfactory pathway such as the olfactory bulb and olfactory tubercle emphasize the significance of purinergic signaling for this sensory system. P2X, P2Y and adenosine receptors are involved in adult neurogenesis in the olfactory epithelium, link neuronal activity to vascular responses in the olfactory bulb and modulate synaptic transmission in the olfactory bulb as well as the olfactory cortex. However, research on the functional role of purinergic signaling in olfaction has only started recently. Based on the recent physiological studies that reveal a broad range of specific purinoceptor-dependent effects, further research faces the challenge to link these findings to olfactory perception and behavior. In addition, given the fact that olfactory impairment is an early symptom in many neurodegenerative and neuroinflammatory diseases, the involvement of purinergic signaling in neuronal degeneration in the olfactory system is expected to move into focus in the future. The use of cell-specific knockout

animals in combination with disease models and behavioral tests might be a promising strategy to gain insights into the mechanisms of purinergic neuromodulation in health and disease.

AUTHOR CONTRIBUTIONS

NR, DH and CL wrote the text. KS designed the figures. All authors edited the manuscript.

FUNDING

The research that served as basis for this review article was financed by the Deutsche Forschungsgemeinschaft (HI 1288/3; LO 779/6; LO 779/10; SFB 1328-TP07 and -TP16).

ACKNOWLEDGMENTS

We thank SciGraphics (contact@scigraphics.de) for contributing the illustrations.

REFERENCES

Abbracchio, M. P., Burnstock, G., Boeynaems, J. M., Barnard, E. A., Boyer, J. L., Kennedy, C., et al. (2006). International Union of Pharmacology LVIII: update on the P2Y G protein-coupled nucleotide receptors: from molecular mechanisms and pathophysiology to therapy. *Pharmacol. Rev.* 58, 281–341. doi: 10.1124/pr.58.3.3

Abbracchio, M. P., Burnstock, G., Verkhratsky, A., and Zimmermann, H. (2009). Purinergic signalling in the nervous system: an overview. *Trends Neurosci.* 32, 19–29. doi: 10.1016/j.tins.2008.10.001

Abraham, N. M., Egger, V., Shimshek, D. R., Renden, R., Fukunaga, I., Sprengel, R., et al. (2010). Synaptic inhibition in the olfactory bulb accelerates odor discrimination in mice. *Neuron* 65, 399–411. doi: 10.1016/j.neuron.2010.01.009

Attwell, D., Buchan, A. M., Charpak, S., Lauritzen, M., MacVicar, B. A., and Newman, E. A. (2010). Glial and neuronal control of brain blood flow. *Nature* 468, 232–243. doi: 10.1038/nature09613

Attwell, D., and Gibb, A. (2005). Neuroenergetics and the kinetic design of excitatory synapses. *Nat. Rev. Neurosci.* 6, 841–849. doi: 10.1038/nrn1784

Attwell, D., and Laughlin, S. B. (2001). An energy budget for signaling in the grey matter of the brain. *J. Cereb. Blood Flow Metab.* 21, 1133–1145. doi: 10.1097/00004647-200110000-00001

Bagatini, M. D., Dos Santos, A. A., Cardoso, A. M., Manica, A., Reschke, C. R., and Carvalho, F. B. (2018). The impact of purinergic system enzymes on noncommunicable, neurological and degenerative diseases. *J. Immunol. Res.* 2018:4892473. doi: 10.1155/2018/4892473

Barros, L. F., and Deitmer, J. W. (2010). Glucose and lactate supply to the synapse. *Brain Res. Rev.* 63, 149–159. doi: 10.1016/j.brainresrev.2009.10.002

Beiersdorfer, A., Scheller, A., Kirchhoff, F., and Lohr, C. (2019). Panglial gap junctions between astrocytes and olfactory ensheathing cells mediate transmission of Ca^{2+} transients and neurovascular coupling. *Glia* doi: 10.1002/glia.23613 [Epub ahead of print].

Berkowicz, D. A., Trombley, P. Q., and Shepherd, G. M. (1994). Evidence for glutamate as the olfactory receptor cell neurotransmitter. *J. Neurophysiol.* 71, 2557–2561. doi: 10.1152/jn.1994.71.6.2557

Bodin, P., and Burnstock, G. (2001). Purinergic signalling: ATP release. *Neurochem. Res.* 26, 959–969. doi: 10.1023/A:1012388618693

Boison, D. (2013). Adenosine kinase: exploitation for therapeutic gain. *Pharmacol. Rev.* 65, 906–943. doi: 10.1124/pr.112.006361

Boison, D., Chen, J. F., and Fredholm, B. B. (2010). Adenosine signaling and function in glial cells. *Cell Death Differ.* 17, 1071–1082. doi: 10.1038/cdd.2009.131

Boué-Grabot, E., and Pankratov, Y. (2017). Modulation of central synapses by astrocyte-released ATP and postsynaptic P2X receptors. *Neural Plast.* 2017:9454275. doi: 10.1155/2017/9454275

Brann, J. H., and Firestein, S. J. (2014). A lifetime of neurogenesis in the olfactory system. *Front. Neurosci.* 8:182. doi: 10.3389/fnins.2014.00182

Burnstock, G. (2013). Introduction to purinergic signalling in the brain. *Adv. Exp. Med. Biol.* 986, 1–12. doi: 10.1007/978-94-007-4719-7_1

Burnstock, G., Campbell, G., Satchell, D., and Smythe, A. (1970). Evidence that adenosine triphosphate or a related nucleotide is the transmitter substance released by non-adrenergic inhibitory nerves in the gut. *Br. J. Pharmacol.* 40, 668–688. doi: 10.1111/j.1476-5381.1970.tb10646.x

Burnstock, G., Fredholm, B. B., and Verkhratsky, A. (2011). Adenosine and ATP receptors in the brain. *Curr. Top. Med. Chem.* 11, 973–1011. doi: 10.2174/156802611795347627

Burnstock, G., and Verkhratsky, A. (2009). Evolutionary origins of the purinergic signalling system. *Acta Physiol.* 195, 415–447. doi: 10.1111/j.1748-1716.2009.01957.x

Chen, J. F., Lee, C. F., and Chern, Y. (2014). Adenosine receptor neurobiology: overview. *Int. Rev. Neurobiol.* 119, 1–49. doi: 10.1016/B978-0-12-801022-8.00001-5

Clemow, D. B., and Brunjes, P. C. (1996). Development of 5′-nucleotidase staining in the olfactory bulbs of normal and naris-occluded rats. *Int. J. Dev. Neurosci.* 14, 901–911. doi: 10.1016/s0736-5748(96)00040-8

Collins, G. G., and Anson, J. (1985). Adenosine A1 receptors mediate the inhibitory effects of exogenous adenosine in the rat olfactory cortex slice. *Neuropharmacology* 24, 1077–1084. doi: 10.1016/0028-3908(85)90195-9

Collo, G., North, R. A., Kawashima, E., MerloPich, E., Neidhart, S., Surprenant, A., et al. (1996). Cloning of $P2X_5$ and $P2X_6$ receptors and the distribution and properties of an extended family of ATP-gated ion channels. *J. Neurosci.* 16, 2495–2507. doi: 10.1523/JNEUROSCI.16-08-02495.1996

Courtiol, E., and Wilson, D. A. (2017). The olfactory mosaic: bringing an olfactory network together for odor perception. *Perception* 46, 320–332. doi: 10.1177/0301006616663216

Crespo, C., Liberia, T., Blasco-Ibanez, J. M., Nacher, J., and Varea, E. (2013). The circuits of the olfactory bulb. The exception as a rule. *Anat. Rec.* 296, 1401–1412. doi: 10.1002/ar.22732

Czesnik, D., Kuduz, J., Schild, D., and Manzini, I. (2006). ATP activates both receptor and sustentacular supporting cells in the olfactory epithelium of Xenopus laevis tadpoles. *Eur. J. Neurosci.* 23, 119–128. doi: 10.1111/j.1460-9568.2005.04533.x

Dallérac, G., Zapata, J., and Rouach, N. (2018). Versatile control of synaptic circuits by astrocytes: where, when and how? *Nat. Rev. Neurosci.* 19, 729–743. doi: 10.1038/s41583-018-0080-6

De Saint Jan, D., Hirnet, D., Westbrook, G. L., and Charpak, S. (2009). External tufted cells drive the output of olfactory bulb glomeruli. *J. Neurosci.* 29, 2043–2052. doi: 10.1523/jneurosci.5317-08.2009

De Saint Jan, D., and Westbrook, G. L. (2005). Detecting activity in olfactory bulb glomeruli with astrocyte recording. *J. Neurosci.* 25, 2917–2924. doi: 10.1523/JNEUROSCI.5042-04.2005

Deitmer, J. W., Verkhratsky, A. J., and Lohr, C. (1998). Calcium signalling in glial cells. *Cell Calcium* 24, 405–416. doi: 10.1016/s0143-4160(98)90063-x

DeMet, E. M., and Chicz-DeMet, A. (2002). Localization of adenosine A2A-receptors in rat brain with [^{3}H]ZM-241385. *Naunyn Schmiedebergs. Arch. Pharmacol.* 366, 478–481. doi: 10.1007/s00210-002-0613-3

Dixon, A. K., Gubitz, A. K., Sirinathsinghji, D. J. S., Richardson, P. J., and Freeman, T. C. (1996). Tissue distribution of adenosine receptor mRNAs in the rat. *Br. J. Pharmacol.* 118, 1461–1468. doi: 10.1111/j.1476-5381.1996.tb15561.x

Doengi, M., Deitmer, J. W., and Lohr, C. (2008). New evidence for purinergic signaling in the olfactory bulb: A_{2A} and $P2Y_1$ receptors mediate intracellular calcium release in astrocytes. *FASEB J.* 22, 2368–2378. doi: 10.1096/fj.07-101782

Doengi, M., Hirnet, D., Coulon, P., Pape, H.-C., Deitmer, J. W., and Lohr, C. (2009). GABA uptake-dependent Ca^{2+} signaling in developing olfactory bulb astrocytes. *Proc. Natl. Acad. Sci. U S A* 106, 17570–17575. doi: 10.1073/pnas.0809513106

Droste, D., Seifert, G., Seddar, L., Jadtke, O., Steinhauser, C., and Lohr, C. (2017). Ca^{2+}-permeable AMPA receptors in mouse olfactory bulb astrocytes. *Sci. Rep.* 7:44817. doi: 10.1038/srep44817

Edwards, F. A., Gibb, A. J., and Colquhoun, D. (1992). ATP receptor-mediated synaptic currents in the central nervous system. *Nature* 359, 144–147. doi: 10.1038/359144a0

Ennis, M., Zimmer, L. A., and Shipley, M. T. (1996). Olfactory nerve stimulation activates rat mitral cells via NMDA and non-NMDA receptors *in vitro*. *Neuroreport* 7, 989–992. doi: 10.1097/00001756-199604100-00007

Evans, R. J., Derkach, V., and Surprenant, A. (1992). ATP mediates fast synaptic transmission in mammalian neurons. *Nature* 357, 503–505. doi: 10.1038/357503a0

Fastbom, J., Pazos, A., Probst, A., and Palacios, J. M. (1987). Adenosine A1 receptors in the human brain: a quantitative autoradiographic study. *Neuroscience* 22, 827–839. doi: 10.1016/0306-4522(87)92962-9

Fischer, T., Rotermund, N., Lohr, C., and Hirnet, D. (2012). $P2Y_1$ receptor activation by photolysis of caged ATP enhances neuronal network activity in the developing olfactory bulb. *Purinergic Signal.* 8, 191–198. doi: 10.1007/s11302-011-9286-z

Fu, Z., Ogura, T., Luo, W., and Lin, W. (2018). ATP and odor mixture activate TRPM5-expressing microvillous cells and potentially induce acetylcholine release to enhance supporting cell endocytosis in mouse main olfactory epithelium. *Front. Cell. Neurosci.* 12:71. doi: 10.3389/fncel.2018.00071

Geiger, J. D., and Nagy, J. I. (1987). Ontogenesis of adenosine deaminase activity in rat brain. *J. Neurochem.* 48, 147–153. doi: 10.1111/j.1471-4159.1987.tb13139.x

Goodman, R. R., and Synder, S. H. (1982). Autoradiographic localization of adenosine receptors in rat brain using [^{3}H]cyclohexyladenosine. *J. Neurosci.* 2, 1230–1241. doi: 10.1523/jneurosci.02-09-01230.1982

Gottfried, J. A. (2006). Smell: central nervous processing. *Adv. Otorhinolaryngol.* 63, 44–69. doi: 10.1159/000093750

Gschwend, O., Abraham, N. M., Lagier, S., Begnaud, F., Rodriguez, I., and Carleton, A. (2015). Neuronal pattern separation in the olfactory bulb improves odor discrimination learning. *Nat. Neurosci.* 18, 1474–1482. doi: 10.1038/nn.4089

Guo, W., Xu, X., Gao, X., Burnstock, G., He, C., and Xiang, Z. (2008). Expression of P2X5 receptors in the mouse CNS. *Neuroscience* 156, 673–692. doi: 10.1016/j.neuroscience.2008.07.062

Guzman, S. J., and Gerevich, Z. (2016). P2Y receptors in synaptic transmission and plasticity: therapeutic potential in cognitive dysfunction. *Neural Plast.* 2016:1207393. doi: 10.1155/2016/1207393

Haberly, L. B. (1973). Summed potentials evoked in opossum prepyriform cortex. *J. Neurophysiol.* 36, 775–788. doi: 10.1152/jn.1973.36.4.775

Haberly, L. B. (2001). Parallel-distributed processing in olfactory cortex: new insights from morphological and physiological analysis of neuronal circuitry. *Chem. Senses* 26, 551–576. doi: 10.1093/chemse/26.5.551

Haberly, L., and Behan, M. (1983). Structure of the piriform cortex of the opossum. III. Ultrastructural characterization of synaptic terminals of association and olfactory bulb afferent fibers. *J. Comp. Neurol.* 219, 448–460. doi: 10.1002/cne.902190406

Hassenklöver, T., Kurtanska, S., Bartoszek, I., Junek, S., Schild, D., and Manzini, I. (2008). Nucleotide-induced Ca^{2+} signaling in sustentacular supporting cells of the olfactory epithelium. *Glia* 56, 1614–1624. doi: 10.1002/glia.20714

Haydon, P. G., and Carmignoto, G. (2006). Astrocyte control of synaptic transmission and neurovascular coupling. *Physiol. Rev.* 86, 1009–1031. doi: 10.1152/physrev.00049.2005

Hayoz, S., Jia, C., and Hegg, C. C. (2012). Mechanisms of constitutive and ATP-evoked ATP release in neonatal mouse olfactory epithelium. *BMC Neurosci.* 13:53. doi: 10.1186/1471-2202-13-53

Hegg, C. C., Greenwood, D., Huang, W., Han, P., and Lucero, M. T. (2003). Activation of purinergic receptor subtypes modulates odor sensitivity. *J. Neurosci.* 23, 8291–8301. doi: 10.1523/jneurosci.23-23-08291.2003

Hegg, C. C., Irwin, M., and Lucero, M. T. (2009). Calcium store-mediated signaling in sustentacular cells of the mouse olfactory epithelium. *Glia* 57, 634–644. doi: 10.1002/glia.20792

Hegg, C. C., Jia, C., Chick, W. S., Restrepo, D., and Hansen, A. (2010). Microvillous cells expressing IP3 receptor type 3 in the olfactory epithelium of mice. *Eur. J. Neurosci.* 32, 1632–1645. doi: 10.1111/j.1460-9568.2010.07449.x

Heydel, J. M., Coelho, A., Thiebaud, N., Legendre, A., Le Bon, A. M., Faure, P., et al. (2013). Odorant-binding proteins and xenobiotic metabolizing enzymes: implications in olfactory perireceptor events. *Anat. Rec.* 296, 1333–1345. doi: 10.1002/ar.22735

Holton, P. (1959). The liberation of adenosine triphosphate on antidromic stimulation of sensory nerves. *J. Physiol.* 145, 494–504. doi: 10.1113/jphysiol.1959.sp006157

Housley, G. D., Bringmann, A., and Reichenbach, A. (2009). Purinergic signaling in special senses. *Trends Neurosci.* 32, 128–141. doi: 10.1016/j.tins.2009.01.001

Iadecola, C., and Nedergaard, M. (2007). Glial regulation of the cerebral microvasculature. *Nat. Neurosci.* 10, 1369–1376. doi: 10.1038/nn2003

Jia, C., Doherty, J. P., Crudgington, S., and Hegg, C. C. (2009). Activation of purinergic receptors induces proliferation and neuronal differentiation in Swiss Webster mouse olfactory epithelium. *Neuroscience* 163, 120–128. doi: 10.1016/j.neuroscience.2009.06.040

Jia, C., Hayoz, S., Hutch, C. R., Iqbal, T. R., Pooley, A. E., and Hegg, C. C. (2013). An IP3R3- and NPY-expressing microvillous cell mediates tissue homeostasis and regeneration in the mouse olfactory epithelium. *PLoS One* 8:e58668. doi: 10.1371/journal.pone.0058668

Jia, C., and Hegg, C. C. (2010). NPY mediates ATP-induced neuroproliferation in adult mouse olfactory epithelium. *Neurobiol. Dis.* 38, 405–413. doi: 10.1016/j.nbd.2010.02.013

Jia, C., and Hegg, C. C. (2012). Neuropeptide Y and extracellular signal-regulated kinase mediate injury-induced neuroregeneration in mouse olfactory epithelium. *Mol. Cell. Neurosci.* 49, 158–170. doi: 10.1016/j.mcn.2011.11.004

Jia, C., and Hegg, C. C. (2015). Effect of IP3R3 and NPY on age-related declines in olfactory stem cell proliferation. *Neurobiol. Aging* 36, 1045–1056. doi: 10.1016/j.neurobiolaging.2014.11.007

Johansson, B., and Fredholm, B. B. (1995). Further characterization of the binding of the adenosine receptor agonist [^{3H}]CGS 21680 to rat brain using autoradiography. *Neuropharmacology* 34, 393–403. doi: 10.1016/0028-3908(95)00009-u

Johansson, B., Georgiev, V., and Fredholm, B. B. (1997). Distribution and postnatal ontogeny of adenosine A_{2A} receptors in rat brain: comparison with dopamine receptors. *Neuroscience* 80, 1187–1207. doi: 10.1016/s0306-4522(97)00143-7

Kaelin-Lang, A., Lauterburg, T., and Burgunder, J. M. (1999). Expression of adenosine A2a receptors gene in the olfactory bulb and spinal cord of rat and mouse. *Neurosci. Lett.* 261, 189–191. doi: 10.1016/s0304-3940(99)00022-1

Kaneda, M., Ito, K., Shigematsu, Y., and Shimoda, Y. (2010). The OFF-pathway dominance of P2X(2)-purinoceptors is formed without visual experience. *Neurosci. Res.* 66, 86–91. doi: 10.1016/j.neures.2009.09.1714

Kanekar, S., Jia, C., and Hegg, C. C. (2009). Purinergic receptor activation evokes neurotrophic factor neuropeptide Y release from neonatal mouse olfactory epithelial slices. *J. Neurosci. Res.* 87, 1424–1434. doi: 10.1002/jnr.21954

Kanjhan, R., Housley, G. D., Burton, L. D., Christie, D. L., Kippenberger, A., Thorne, P. R., et al. (1999). Distribution of the P2X(2) receptor subunit of the ATP-gated ion channels in the rat central nervous system. *J. Comp. Neurol.* 407, 11–32. doi: 10.1002/(sici)1096-9861(19990428)407:1<11::aid-cne2>3.0.co;2-r

Kidd, E. J., Grahames, C. B., Simon, J., Michel, A. D., Barnard, E. A., and Humphrey, P. P. (1995). Localization of P2X purinoceptor transcripts in the rat nervous system. *Mol. Pharmacol.* 48, 569–573.

Kim, C. S., and Johnston, D. (2015). A1 adenosine receptor-mediated GIRK channels contribute to the resting conductance of CA1 neurons in the dorsal hippocampus. *J. Neurophysiol.* 113, 2511–2523. doi: 10.1152/jn.00951.2014

Köles, L., Kató, E., Hanuska, A., Zádori, Z. S., Al-Khrasani, M., Zelles, T., et al. (2016). Modulation of excitatory neurotransmission by neuronal/glial signalling molecules: interplay between purinergic and glutamatergic systems. *Purinergic Signal.* 12, 1–24. doi: 10.1007/s11302-015-9480-5

Köles, L., Leichsenring, A., Rubini, P., and Illes, P. (2011). P2 receptor signaling in neurons and glial cells of the central nervous system. *Adv. Pharmacol.* 61, 441–493. doi: 10.1016/b978-0-12-385526-8.00014-x

Kulesskaya, N., Võikar, V., Peltola, M., Yegutkin, G. G., Salmi, M., Jalkanen, S., et al. (2013). CD73 is a major regulator of adenosinergic signalling in mouse brain. *PLoS One* 8:e66896. doi: 10.1371/journal.pone.0066896

Kuroda, Y. (1978). Physiological roles of adenosine derivatives which are released during neurotransmission in mammalian brain. *J. Physiol.* 74, 463–470.

Langer, D., Hammer, K., Koszalka, P., Schrader, J., Robson, S., and Zimmermann, H. (2008). Distribution of ectonucleotidases in the rodent brain revisited. *Cell Tissue Res.* 334, 199–217. doi: 10.1007/s00441-008-0681-x

Lê, K. T., Villeneuve, P., Ramjaun, A. R., McPherson, P. S., Beaudet, A., and Seguela, P. (1998). Sensory presynaptic and widespread somatodendritic immunolocalization of central ionotropic P2X ATP receptors. *Neuroscience* 83, 177–190. doi: 10.1016/s0306-4522(97)00365-5

Lohr, C., and Deitmer, J. W. (2010). Ca^{2+} imaging of glia. *Calcium Meas. Methods* 43, 221–249. doi: 10.1007/978-1-60761-476-0_12

Lohr, C., Grosche, A., Reichenbach, A., and Hirnet, D. (2014). Purinergic neuron-glia interactions in sensory systems. *Pflugers Arch.* 466, 1859–1872. doi: 10.1007/s00424-014-1510-6

Lohr, C., Thyssen, A., and Hirnet, D. (2011). Extrasynaptic neuron-glia communication: the how and why. *Commun. Integr. Biol.* 4, 109–111. doi: 10.4161/cib.4.1.14184

Lucero, M. T. (2013). Peripheral modulation of smell: fact or fiction? *Semin. Cell Dev. Biol.* 24, 58–70. doi: 10.1016/j.semcdb.2012.09.001

Luskin, M. B., and Price, J. L. (1983a). The laminar distribution of intracortical fibers originating in the olfactory cortex of the rat. *J. Comp. Neurol.* 216, 292–302. doi: 10.1002/cne.902160306

Luskin, M. B., and Price, J. L. (1983b). The topographic organization of associational fibers of the olfactory system in the rat, including centrifugal fibers to the olfactory bulb. *J. Comp. Neurol.* 216, 264–291. doi: 10.1002/cne.902160305

Luthin, D. R., Lee, K. S., Okonkwo, D., Zhang, P., and Linden, J. (1995). Photoaffinity labeling with 2−[2−(4-azido-3−[^{125}I]-iodophenyl) ethylamino]adenosine and autoradiography with 2−[2−(4-amino-3−[^{125}I] iodophenyl)ethylamino]adenosine of A_{2A} adenosine receptors in rat brain. *J. Neurochem.* 65, 2072–2079. doi: 10.1046/j.1471-4159.1995.65052072.x

Mahan, L. C., McVittie, L. D., Smykrandall, E. M., Nakata, H., Monsma, F. J., Gerfen, C. R., et al. (1991). Cloning and expression of an A1 adenosine receptor from rat-brain. *Mol. Pharmacol.* 40, 1–7.

Montani, G., Tonelli, S., Elsaesser, R., Paysan, J., and Tirindelli, R. (2006). Neuropeptide Y in the olfactory microvillar cells. *Eur. J. Neurosci.* 24, 20–24. doi: 10.1111/j.1460-9568.2006.04878.x

Nevill, K. R., and Haberly, L. B. (2004). "Olfactory cortex," in *The Synaptic Organization of the Brain*, 5th Edn. G. M. Shepherd (New York, NY: Oxford University Press), 415–454.

North, R. A. (2016). P2X receptors. *Philos. Trans. R. Soc. Lond. B Biol. Sci.* 371:20150427. doi: 10.1098/rstb.2015.0427

North, R. A., and Verkhratsky, A. (2006). Purinergic transmission in the central nervous system. *Pflugers Arch.* 452, 479–485. doi: 10.1007/s00424-006-0060-y

Okada, Y., and Kuroda, Y. (1980). Inhibitory action of adenosine and adenosine analogs on neurotransmission in the olfactory cortex slice of guinea pig - structure-activity relationships. *Eur. J. Pharmacol.* 61, 137–146. doi: 10.1016/0014-2999(80)90156-9

Otsu, Y., Couchman, K., Lyons, D. G., Collot, M., Agarwal, A., Mallet, J. M., et al. (2015). Calcium dynamics in astrocyte processes during neurovascular coupling. *Nat. Neurosci.* 18, 210–218. doi: 10.1038/nn.3906

Pani, A. K., Jiao, Y., Sample, K. J., and Smeyne, R. J. (2014). Neurochemical measurement of adenosine in discrete brain regions of five strains of inbred mice. *PLoS One* 9:e92422. doi: 10.1371/journal.pone.0092422

Pankratov, Y., and Lalo, U. (2015). Role for astroglial α1-adrenoreceptors in gliotransmission and control of synaptic plasticity in the neocortex. *Front. Cell. Neurosci.* 9:230. doi: 10.3389/fncel.2015.00230

Pankratov, Y., Lalo, U., Verkhratsky, A., and North, R. A. (2007). Quantal release of ATP in mouse cortex. *J. Gen. Physiol.* 129, 257–265. doi: 10.1085/jgp.200609693

Pastor-Anglada, M., and Pérez-Torras, S. (2018). Who is who in adenosine transport. *Front. Pharmacol.* 9:627. doi: 10.3389/fphar.2018.00627

Pelligrino, D. A., Vetri, F., and Xu, H. L. (2011). Purinergic mechanisms in gliovascular coupling. *Semin. Cell Dev. Biol.* 22, 229–236. doi: 10.1016/j.semcdb.2011.02.010

Pelosi, P., Mastrogiacomo, R., Iovinella, I., Tuccori, E., and Persaud, K. C. (2014). Structure and biotechnological applications of odorant-binding proteins. *Appl. Microbiol. Biotechnol.* 98, 61–70. doi: 10.1007/s00253-013-5383-y

Perrier, S. P., Gleizes, M., Fonta, C., and Nowak, L. G. (2019). Effect of adenosine on short-term synaptic plasticity in mouse piriform cortex *in vitro*: adenosine acts as a high-pass filter. *Physiol. Rep.* 7:e13992. doi: 10.14814/phy2.13992

Petzold, G. C., Albeanu, D. F., Sato, T. F., and Murthy, V. N. (2008). Coupling of neural activity to blood flow in olfactory glomeruli is mediated by astrocytic pathways. *Neuron* 58, 897–910. doi: 10.1016/j.neuron.2008.04.029

Rezvani, M. E., Mirnajafi-Zadeh, J., Fathollahi, Y., and Palizvan, M. R. (2007). Changes in neuromodulatory effect of adenosine A1 receptors on piriform cortex field potentials in amygdala kindled rats. *Eur. J. Pharmacol.* 565, 60–67. doi: 10.1016/j.ejphar.2007.02.010

Rieger, A., Deitmer, J. W., and Lohr, C. (2007). Axon-glia communication evokes calcium signaling in olfactory ensheathing cells of the developing olfactory bulb. *Glia* 55, 352–359. doi: 10.1002/glia.20460

Rosin, D. L., Hettinger, B. D., Lee, A., and Linden, J. (2003). Anatomy of adenosine A_{2A} receptors in brain: morphological substrates for integration of striatal function. *Neurology* 61, S12–S18. doi: 10.1212/01.wnl.0000095205.33940.99

Rosin, D. L., Robeva, A., Woodard, R. L., Guyenet, P. G., and Linden, J. (1998). Immunohistochemical localization of adenosine A_{2A} receptors in the rat central nervous system. *J. Comp. Neurol.* 401, 163–186. doi: 10.1016/b978-0-12-803724-9.00005-3

Rotermund, N., Winandy, S., Fischer, T., Schulz, K., Fregin, T., Alstedt, N., et al. (2018). Adenosine A1 receptor activates background potassium channels and modulates information processing in olfactory bulb mitral cells. *J. Physiol.* 596, 717–733. doi: 10.1113/jp275503

Roux, L., Madar, A., Lacroix, M. M., Yi, C., Benchenane, K., and Giaume, C. (2015). Astroglial connexin 43 hemichannels modulate olfactory bulb slow oscillations. *J. Neurosci.* 35, 15339–15352. doi: 10.1523/JNEUROSCI.0861-15.2015

Rungta, R. L., Chaigneau, E., Osmanski, B. F., and Charpak, S. (2018). Vascular compartmentalization of functional hyperemia from the synapse to the pia. *Neuron* 99, 362.e4–375.e4. doi: 10.1016/j.neuron.2018.06.012

Schmid, R., and Evans, R. J. (2019). ATP-gated P2X receptor channels: molecular insights into functional roles. *Annu. Rev. Physiol.* 81, 43–62. doi: 10.1146/annurev-physiol-020518-114259

Schoen, S. W., and Kreutzberg, G. W. (1995). Evidence that 5'-Nucleotidase is associated with malleable synapses—an enzyme cytochemical investigation of the olfactory bulb of adult rats. *Neuroscience* 65, 37–50. doi: 10.1016/0306-4522(94)00469-l

Schoen, S. W., and Kreutzberg, G. W. (1997). 5'-nucleotidase enzyme cytochemistry as a tool for revealing activated glial cells and malleable synapses in CNS development and regeneration. *Brain Res. Protoc.* 1, 33–43. doi: 10.1016/s1385-299x(96)00006-2

Scholfield, C. N. (1978). Depression of evoked potentials in brain slices by adenosine compounds. *Br. J. Pharmacol.* 63, 239–244. doi: 10.1111/j.1476-5381.1978.tb09752.x

Schulz, K. (2018). *ATP und Adenosin als Modulatoren Neuronaler Kommunikation im Bulbus Olfactorius der Maus.* Ph. D. thesis. Hamburg: University of Hamburg.

Schulz, K., Rotermund, N., Grzelka, K., Benz, J., Lohr, C., and Hirnet, D. (2018). Adenosine A1 receptor-mediated attenuation of reciprocal dendro-dendritic inhibition in the mouse olfactory bulb. *Front. Cell. Neurosci.* 11:435. doi: 10.3389/fncel.2017.00435

Sebastião, A. M., and Ribeiro, J. A. (2009). Tuning and fine-tuning of synapses with adenosine. *Curr. Neuropharmacol.* 7, 180–194. doi: 10.2174/157015909789152128

Sebastião, A. M., and Ribeiro, J. A. (2015). Neuromodulation and metamodulation by adenosine: impact and subtleties upon synaptic plasticity regulation. *Brain Res.* 1621, 102–113. doi: 10.1016/j.brainres.2014.11.008

Shigetomi, E., Patel, S., and Khakh, B. S. (2016). Probing the complexities of astrocyte calcium signaling. *Trends Cell Biol.* 26, 300–312. doi: 10.1016/j.tcb.2016.01.003

Sickmann, T., and Alzheimer, C. (2003). Short-term desensitization of G-protein-activated, inwardly rectifying K^+ (GIRK) currents in pyramidal neurons of rat neocortex. *J. Neurophysiol.* 90, 2494–2503. doi: 10.1152/jn.00112.2003

Simon, J., Webb, T. E., and Barnard, E. A. (1997). Distribution of S-35 dATP α S binding sites in the adult rat neuraxis. *Neuropharmacology* 36, 1243–1251. doi: 10.1016/s0028-3908(97)00124-x

Singaravelu, K., Lohr, C., and Deitmer, J. W. (2006). Regulation of store-operated calcium entry by calcium-independent phospholipase A_2 in rat cerebellar astrocytes. *J. Neurosci.* 26, 9579–9592. doi: 10.1523/JNEUROSCI.2604-06.2006

Snyder, S. H. (1985). Adenosine as a neuromodulator. *Annu. Rev. Neurosci.* 8, 103–124. doi: 10.1146/annurev.ne.08.030185.000535

Sperlágh, B., Heinrich, A., and Csölle, C. (2007). P2 receptor-mediated modulation of neurotransmitter release-an update. *Purinergic Signal.* 3, 269–284. doi: 10.1007/s11302-007-9080-0

Stavermann, M., Buddrus, K., St John, J. A., Ekberg, J. A. K., Nilius, B., Deitmer, J. W., et al. (2012). Temperature-dependent calcium-induced calcium release via $InsP_3$ receptors in mouse olfactory ensheathing glial cells. *Cell Calcium* 52, 113–123. doi: 10.1016/j.ceca.2012.04.017

Stavermann, M., Meuth, P., Doengi, M., Thyssen, A., Deitmer, J. W., and Lohr, C. (2015). Calcium-induced calcium release and gap junctions mediate large-scale calcium waves in olfactory ensheathing cells *in situ*. *Cell Calcium* 58, 215–225. doi: 10.1016/j.ceca.2015.05.003

Sun, W., McConnell, E., Pare, J.-F., Xu, Q., Chen, M., Peng, W., et al. (2013). Glutamate-dependent neuroglial calcium signaling differs between young and adult brain. *Science* 339, 197–200. doi: 10.1126/science.1226740

Taruno, A. (2018). ATP release channels. *Int. J. Mol. Sci.* 19:E808. doi: 10.3390/ijms19030808

Thyssen, A., Hirnet, D., Wolburg, H., Schmalzing, G., Deitmer, J. W., and Lohr, C. (2010). Ectopic vesicular neurotransmitter release along sensory axons mediates neurovascular coupling via glial calcium signaling. *Proc. Natl. Acad. Sci. U S A* 107, 15258–15263. doi: 10.1073/pnas.1003501107

Thyssen, A., Stavermann, M., Buddrus, K., Doengi, M., Ekberg, J. A., St John, J. A., et al. (2013). Spatial and developmental heterogeneity of calcium signaling in olfactory ensheathing cells. *Glia* 61, 327–337. doi: 10.1002/glia.22434

Trieu, B. H., Kramár, E. A., Cox, C. D., Jia, Y., Wang, W., Gall, C. M., et al. (2015). Pronounced differences in signal processing and synaptic plasticity between piriform-hippocampal network stages: a prominent role for adenosine. *J. Physiol.* 593, 2889–2907. doi: 10.1113/jp270398

Valverde, F., and Lopez-Mascaraque, L. (1991). Neuronal arrangements in the olfactory glomeruli of the hedgehog. *J. Comp. Neurol.* 307, 658–674. doi: 10.1002/cne.903070411

Verkhratsky, A., Krishtal, O. A., and Burnstock, G. (2009). Purinoceptors on Neuroglia. *Mol. Neurobiol.* 39, 190–208. doi: 10.1007/s12035-009-8063-2

Verkhratsky, A., Rodríguez, J. J., and Parpura, V. (2012). Calcium signalling in astroglia. *Mol. Cell. Endocrinol.* 353, 45–56. doi: 10.1016/j.mce.2011.08.039

Vogalis, F., Hegg, C. C., and Lucero, M. T. (2005a). Electrical coupling in sustentacular cells of the mouse olfactory epithelium. *J. Neurophysiol.* 94, 1001–1012. doi: 10.1152/jn.01299.2004

Vogalis, F., Hegg, C. C., and Lucero, M. T. (2005b). Ionic conductances in sustentacular cells of the mouse olfactory epithelium. *J. Physiol.* 562, 785–799. doi: 10.1113/jphysiol.2004.079228

Vulchanova, L., Arvidsson, U., Riedl, M., Wang, J., Buell, G., Surprenant, A., et al. (1996). Differential distribution of two ATP-gated ion channels (P-2X receptors) determined by immunocytochemistry. *Proc. Natl. Acad. Sci. U S A* 93, 8063–8067. doi: 10.1073/pnas.93.15.8063

Webb, T. E., Henderson, D., King, B. F., Wang, S., Simon, J., Bateson, A. N., et al. (1996). A novel G protein-coupled P2 purinoceptor (P2Y3) activated preferentially by nucleoside diphosphates. *Mol. Pharmacol.* 50, 258–265.

Wilson, D. A., Xu, W., Sadrian, B., Courtiol, E., Cohen, Y., and Barnes, D. C. (2014). Cortical odor processing in health and disease. *Prog. Brain Res.* 208, 275–305. doi: 10.1016/b978-0-444-63350-7.00011-5

Yang, S. C., Chiu, T. H., Yang, H. W., and Min, M. Y. (2007). Presynaptic adenosine A1 receptors modulate excitatory synaptic transmission in the posterior piriform cortex in rats. *Brain Res.* 1156, 67–79. doi: 10.1016/j.brainres.2007.04.049

Yi, C., Ezan, P., Fernández, P., Schmitt, J., Sáez, J. C., Giaume, C., et al. (2017). Inhibition of glial hemichannels by boldine treatment reduces neuronal suffering in a murine model of Alzheimer's disease. *Glia* 65, 1607–1625. doi: 10.1002/glia.23182

Zimmermann, H. (2006). Nucleotide signaling in nervous system development. *Pflugers Arch.* 452, 573–588. doi: 10.1007/s00424-006-0067-4

Zimmermann, H. (2011). Purinergic signaling in neural development. *Semin. Cell Dev. Biol.* 22, 194–204. doi: 10.1016/j.semcdb.2011.02.007

Zimmermann, H., Zebisch, M., and Sträter, N. (2012). Cellular function and molecular structure of ecto-nucleotidases. *Purinergic Signal.* 8, 437–502. doi: 10.1007/s11302-012-9309-4

Conflict of Interest Statement: The authors declare that the research was conducted in the absence of any commercial or financial relationships that could be construed as a potential conflict of interest.

frontiers in Cellular Neuroscience

REVIEW
published: 17 May 2019
doi: 10.3389/fncel.2019.00224

Physiopathological Role of the Vesicular Nucleotide Transporter (VNUT) in the Central Nervous System: Relevance of the Vesicular Nucleotide Release as a Potential Therapeutic Target

*María T. Miras-Portugal[1,2,3], Aida Menéndez-Méndez[1,2,3], Rosa Gómez-Villafuertes[1,2,3], Felipe Ortega[1,2,3], Esmerilda G. Delicado[1,2,3], Raquel Pérez-Sen[1,2,3] and Javier Gualix[1,2,3]**

[1] Departamento de Bioquímica y Biología Molecular, Facultad de Veterinaria, Universidad Complutense de Madrid, Madrid, Spain, [2] Instituto Universitario de Investigación en Neuroquímica, Universidad Complutense de Madrid, Madrid, Spain, [3] Instituto de Investigación Sanitaria del Hospital Clínico San Carlos, Madrid, Spain

OPEN ACCESS

Edited by:
Eric Boué-Grabot,
Université de Bordeaux, France

Reviewed by:
Frank Kirchhoff,
Saarland University, Germany
Simona Candiani,
University of Genoa, Italy

***Correspondence:**
Javier Gualix
jgualix@ucm.es

Specialty section:
This article was submitted to Cellular Neurophysiology, a section of the journal Frontiers in Cellular Neuroscience

Received: 18 February 2019
Accepted: 02 May 2019
Published: 17 May 2019

Citation:
Miras-Portugal MT, Menéndez-Méndez A, Gómez-Villafuertes R, Ortega F, Delicado EG, Pérez-Sen R and Gualix J (2019) Physiopathological Role of the Vesicular Nucleotide Transporter (VNUT) in the Central Nervous System: Relevance of the Vesicular Nucleotide Release as a Potential Therapeutic Target. Front. Cell. Neurosci. 13:224. doi: 10.3389/fncel.2019.00224

Vesicular storage of neurotransmitters, which allows their subsequent exocytotic release, is essential for chemical transmission in the central nervous system. Neurotransmitter uptake into secretory vesicles is carried out by vesicular transporters, which use the electrochemical proton gradient generated by a vacuolar H^+-ATPase to drive neurotransmitter vesicular accumulation. ATP and other nucleotides are relevant extracellular signaling molecules that participate in a variety of biological processes. Although the active transport of nucleotides into secretory vesicles has been characterized from the pharmacological and biochemical point of view, the protein responsible for such vesicular accumulation remained unidentified for some time. In 2008, the human *SLC17A9* gene, the last identified member of the SLC17 transporters, was found to encode the vesicular nucleotide transporter (VNUT). VNUT is expressed in various ATP-secreting cells and is able to transport a wide variety of nucleotides in a vesicular membrane potential-dependent manner. VNUT knockout mice lack vesicular storage and release of ATP, resulting in blockage of the purinergic transmission. This review summarizes the current studies on VNUT and analyzes the physiological relevance of the vesicular nucleotide transport in the central nervous system. The possible role of VNUT in the development of some pathological processes, such as chronic neuropathic pain or glaucoma is also discussed. The putative involvement of VNUT in these pathologies raises the possibility of the use of VNUT inhibitors for therapeutic purposes.

Keywords: VNUT, vesicular ATP release, purinergic signaling, neuropathic pain, glaucoma, clodronate

INTRODUCTION

Chemical transmission at the synapse plays a central role in cellular communication in both the central and peripheral nervous system. This process requires the previous storage of neurotransmitters into synaptic vesicles and their subsequent release through Ca^{2+}-dependent exocytosis. The released neurotransmitters interact with specific receptors on the plasma membrane of target cells, thus triggering intracellular signals. Vesicular neurotransmitter transporters (VNTs) are the proteins responsible for the storage of these compounds into synaptic vesicles, thus determining the amount of neurotransmitter available to be released by exocytosis and, therefore, are essential components of chemical transmission in the nervous system (Blakely and Edwards, 2012; Omote and Moriyama, 2013; Omote et al., 2016). Different types of transporters are known to be involved in the uptake of neurotransmitters into synaptic vesicles. These include the vesicular glutamate transporters (VGLUTs), vesicular monoamine transporters (VMATs), vesicular acetylcholine transporter (VAChT), and vesicular inhibitory amino acid transporter (VIAAT) (Eiden et al., 2004; Gasnier, 2004; Reimer, 2013). These vesicular transporters are active transport systems that mediate the accumulation of their respective neurotransmitters by means of an electrochemical proton gradient ($\Delta\mu H^+$) across the vesicular membrane, which is generated by a vacuolar H^+-ATPase (V-ATPase) (Njus et al., 1986; Whittaker, 1987). $\Delta\mu H^+$ is composed of a proton gradient (ΔpH, lumen acidic) and the membrane potential ($\Delta\Psi$, lumen-positive). Vesicular neurotransmitter transporters use the chemical (ΔpH), electrical ($\Delta\Psi$) or both components of $\Delta\mu H^+$ as driving forces to mediate transport of neurotransmitters against their concentration gradient (Chaudhry et al., 2008).

ATP is a relevant chemical transmitter released from neurons and non-neuronal cells. In the extracellular space, this nucleotide undergoes successive hydrolysis by ectonucleotidases and both ATP and some of its enzymatic breakdown products (ADP and adenosine) can interact with specific cell-surface purinoceptors (Burnstock, 2007b). In the nervous system, purinergic signaling is involved in a great variety of either physiological or pathological processes such as mechanosensory transduction, central control of autonomic functions, glia-glia and neuronal-glial interaction, pain, trauma, ischemia or inflammation. In addition, extracellular nucleotides exert potent long-term effects in cell proliferation, growth and development (Burnstock, 2007a; Abbracchio et al., 2009; Burnstock et al., 2011). In spite of the relatively well-known features of the signaling cascade after ATP secretion and activation of the purinergic receptors, the mechanism by which ATP is released from cells remains less understood. There is compelling evidence for neuronal exocytotic release of ATP (Richardson and Brown, 1987; Sawynok et al., 1993; Jo and Schlichter, 1999; Pankratov et al., 2006, 2007; Tompkins and Parsons, 2006) and studies also support a vesicular release of ATP from glial cells (Pascual et al., 2005; Pankratov et al., 2006; Bowser and Khakh, 2007; Pangrsic et al., 2007; Zhang et al., 2007; Parpura and Zorec, 2010; Lalo et al., 2014), although additional mechanisms of nucleotide release through ATP-binding cassette transporters, pannexin or connexin hemichannels, voltage-dependent anion channels or P2X7 receptors cannot be ruled out (Lazarowski, 2012; Baroja-Mazo et al., 2013). Consistent with this, the determination of the mechanism and physiological relevance of vesicular ATP storage and its exocytotic release, that is, vesicular ATP release, appear to be critical for the full understanding of purinergic chemical transmission at the nervous system.

In the past decades, it has been recognized that ATP is a common constituent of secretory vesicles (Winkler, 1976; Holmsen and Weiss, 1979; Hutton et al., 1983; Njus et al., 1986; Johnson, 1988). The presence of an active transport mechanism that mediate nucleotide accumulation in a $\Delta\Psi$-dependent manner has been described in adrenal medulla chromaffin granules and the kinetic behavior, solute specificity and pharmacology of the nucleotide vesicular transporter have been extensively analyzed in this secretory vesicle model (Kostron et al., 1977; Aberer et al., 1978; Weber and Winkler, 1981; Bankston and Guidotti, 1996; Gualix et al., 1996, 1997, 1999a). When transport was assayed using a wide range of substrate concentrations, complex non-hyperbolic saturation curves were obtained. This complex dependence of transport capacity with substrate concentration was explained on the basis of a mnemonical kinetic model (Gualix et al., 1996, 1997). The mnemonic kinetic behavior of the nucleotide vesicular transporter was further corroborated by flow cytometry analysis of fluorescent nucleotide analogs incorporation into single chromaffin granules (Gualix et al., 1999a). Another remarkable feature of the nucleotide vesicular transporter in chromaffin granules is its low specificity (Aberer et al., 1978; Weber and Winkler, 1981; Bankston and Guidotti, 1996; Gualix et al., 1996, 1997), this transporter being able to internalize a wide diversity of nucleotides such as ATP, ADP, AMP, GTP, and UTP (**Figure 1A**), as well as the diadenosine polyphosphates (Ap_nA), a group of dinucleotides that are also constituents of secretory vesicles (Rodriguez del Castillo et al., 1988; Pintor et al., 1992a,b,c) and can be detected in the extracellular media both under basal conditions (Gualix et al., 2014) or after stimulation of the cells with depolarizing agents or secretagogues (Pintor et al., 1992a,c). Nucleotide uptake into chromaffin granules is significantly reduced in the presence of atractyloside (**Figure 1B**), a compound previously described as an inhibitor of the mitochondrial ADP/ATP exchanger, and the anion transport inhibitor 4,4′-diisothiocyanatostilbene-2,2′-disulfonic acid (DIDS) (Kostron et al., 1977; Aberer et al., 1978; Weber and Winkler, 1981; Bankston and Guidotti, 1996; Gualix et al., 1996, 1997). A nucleotide vesicular transporter with strong similarities to that described in chromaffin granules can be also observed in cholinergic synaptic vesicles isolated from *Torpedo marmorata* electric organ and brain synaptic vesicles. Again, several different nucleotides can be incorporated into the vesicles through this vesicular transporter (Luqmani, 1981; Gualix et al., 1999b), which also exhibits a complex kinetic behavior that can be explained by means of a mnemonical model (Gualix et al., 1999b). As occurs in chromaffin granules, nucleotide transport into synaptic vesicles is affected by atractyloside and DIDS, although the compound that showed more effectivity to reduce ATP uptake into the

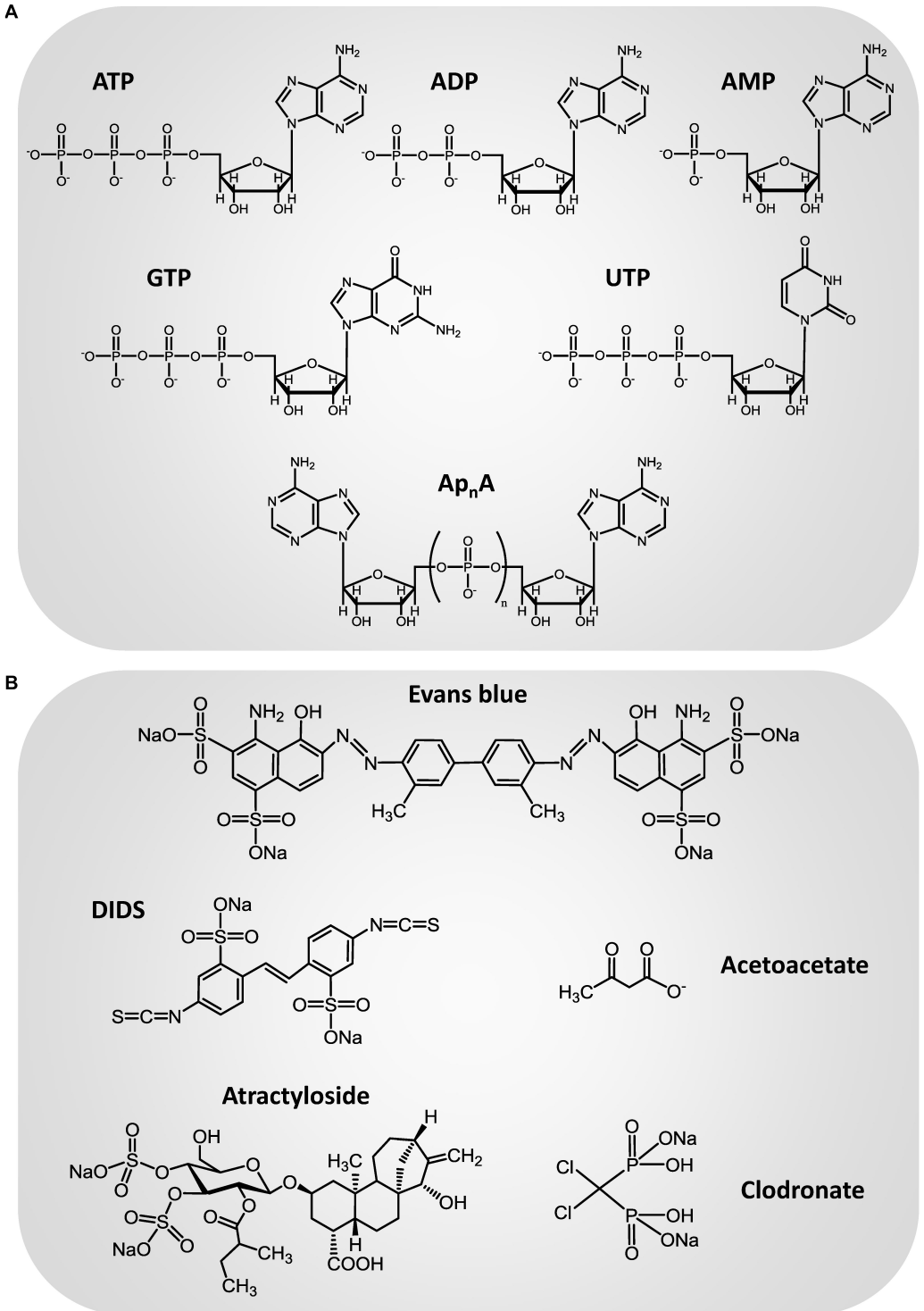

FIGURE 1 | Chemical structure of the main transport substrates **(A)** and inhibitors **(B)** of the vesicular nucleotide transporter.

vesicles was Evans blue (**Figure 1B**; Gualix et al., 1999b), a dye which was previously described as a potent inhibitor of the vesicular glutamate transporter (Roseth et al., 1995). However, in spite of the accumulating evidence of the presence of an active mechanism of nucleotide transport into secretory vesicles, such as synaptic vesicles and adrenal chromaffin granules, the protein responsible for the nucleotide vesicular accumulation remained unidentified for some time.

Solute carrier 17 (SLC17) type I inorganic phosphate transporters are a group of structurally related proteins that mediate the transmembrane transport of organic anions. Members of this transporter family include the three identified isoforms of the vesicular glutamate transporter VGLUT1 (*SLC17A7*), VGLUT2 (*SLC17A6*), and VGLUT3 (*SLC17A8*) (Reimer, 2013). In 2008, *SLC17A9*, the last identified member of this family was found to encode the vesicular nucleotide transporter (VNUT). Northern blot analysis revealed that *SLC17A9* gene is expressed in several organs, being especially abundant in the brain and the adrenal gland, regions where nucleotide vesicular transport might be relevant (Sawada et al., 2008). Moreover, in the adrenal gland, the SLC17A9 protein is specifically expressed in the medulla, where it is associated with chromaffin granules, as revealed by immunohistochemistry, immunoelectron microscopy and Western blot (Sawada et al., 2008). These data are compatible with the hypothesis that SLC17A9 could be responsible for the granular storage of the nucleotides. The human SLC17A9 protein was expressed, purified and incorporated into liposomes and an internal positive $\Delta\psi$ was generated by diffusion of K^+ into the liposomes by the addition of valinomycin, in order to supply a driving force for nucleotide uptake. As anticipated, the SLC17A9 protein actively transported ATP at the expense of $\Delta\psi$ but not of ΔpH. This protein carried several nucleotides with the following order of efficacy: ATP > UTP > GTP > ITP, ADP > > AMP. Adenosine cannot be transported by the SLC17A9 protein, whereas the diadenosine polyphosphate Ap_3A is a good transport substrate. The substrate selectivity of the SLC17A9 protein approximately matches the nucleotide content of the organelles that store ATP (Sawada et al., 2008). Additionally, SLC17A9 does not transport substrates of other members of the SLC17 family such as glutamate, aspartate, or hippuric acid, which indicates that the SLC17A9 protein is a carrier that specifically recognizes a variety of nucleotides as transport substrates. SLC17A9-mediated ATP transport is inhibited by DIDS and Evans blue (Sawada et al., 2008). Atractyloside is also a partial inhibitor but only when Mg^{2+} is present in the assay medium. These characteristics are similar, if not identical, to those observed for the transport of nucleotides to chromaffin granules and synaptic vesicles. Moreover, SLC17A9 protein is endogenously expressed by PC12 pheochromocytoma cells, where it is associated with secretory granules. Suppression of SLC17A9 gene expression by RNA interference (RNAi) strongly decreased vesicular storage and release of ATP from PC12 cells. Taken together, all these results demonstrate that *SLC17A9* encodes VNUT (Sawada et al., 2008; Moriyama et al., 2017). When mouse VNUT protein was purified and reconstituted in liposomes (Larsson et al., 2012) it exhibited similar functional properties to the previously characterized human orthologue (Sawada et al., 2008), thus indicating that *SLC17A9* also encodes the VNUT in rodents. An additional evidence of the essential role of this protein in the vesicular storage of nucleotides is that the vesicular release of ATP is lost from neurons and neuroendocrine cells of *VNUT* knockout ($VNUT^{-/-}$) mice (Sakamoto et al., 2014; Masuda et al., 2016; Nakagomi et al., 2016; Moriyama et al., 2017).

VNUT DISTRIBUTION IN NEURONAL AND GLIAL POPULATIONS OF THE CENTRAL NERVOUS SYSTEM

Expression and Distribution of VNUT in the Brain

The seminal work of Sawada et al. (2008) showed the expression of VNUT in human and mouse brain but its cellular and subcellular distribution was not known.

Allen Mouse Brain Atlas provides a comprehensive atlas of gene expression in the adult C57BL/6J mouse brain. Data were generated using automated high-throughput procedures for *in situ* hybridization and data acquisition (Lein et al., 2007), and are publicly accessible online[1]. As shown in **Figure 2**, VNUT transcript is widely expressed throughout the adult mouse brain, with a prominent expression found in areas such as the hippocampus or the cerebellum.

Immunoperoxidase labeling of rat brain tissue also showed that VNUT is widely distributed throughout the brain with particular strong VNUT immunoreactivity in the cerebellum, the hippocampus and the olfactory bulb (Larsson et al., 2012).

VNUT in the Hippocampus

Figure 3 shows immunofluorescence images demonstrating the presence of VNUT in cultured mouse hippocampal neurons at 7 days *in vitro*.

Vesicular nucleotide transporter immunofluorescence could be detected in the soma and neurites of cultured hippocampal neurons, which also showed VNUT-dependent ATP release, as K^+-evoked ATP release was attenuated by RNAi-mediated knockdown of VNUT (Larsson et al., 2012). The staining pattern of VNUT in the hippocampal neurons only partially overlapped with the presynaptic terminal markers synaptophysin and synaptotagmin 1, thus indicating that VNUT was located in different neuronal compartments. The analysis of the subcellular localization of VNUT in the hippocampal neuropil by immunogold labeling and electron microscopy showed that the nucleotide transporter is associated with synaptic vesicles in both excitatory and inhibitory terminals (Larsson et al., 2012). Moreover, VNUT immunoreactivity can be also detected in preterminal axons, where it was mainly located to the axoplasm as opposed to near the plasma membrane, indicating that VNUT-possessing vesicles are undergoing axonal transport (Larsson et al., 2012). VNUT also appears to be associated with vesicular structures in postsynaptic dendritic spines in the hippocampal formation. Although the role of the postsynaptically localized VNUT have to be clarified in further studies, authors hypothesize that postsynaptic spines can be an additional potential source of extracellular ATP, which may act as a retrograde signal, thus modulating presynaptic transmitter release (Larsson et al., 2012). Immunoisolation experiments showed that some, but not all, VGLUT1-possessing synaptic vesicles also contain VNUT, thus indicating that ATP is stored only in a subpopulation of glutamatergic vesicles. Analysis of immunogold labeling in

[1] http://portal.brain-map.org/

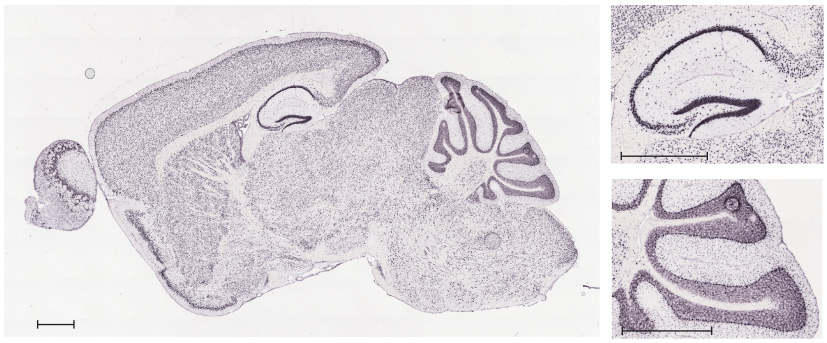

FIGURE 2 | *In situ* hybridization analysis of VNUT transcript expression in a sagittal section of adult mouse brain. Inserts show magnification of the hippocampal and cerebellar areas. Scale bar: 850 μm. Image credit: Allen Mouse Brain Atlas (http://mouse.brain-map.org/gene/show/86822). Image is reproduced with permission of the copyright holders.

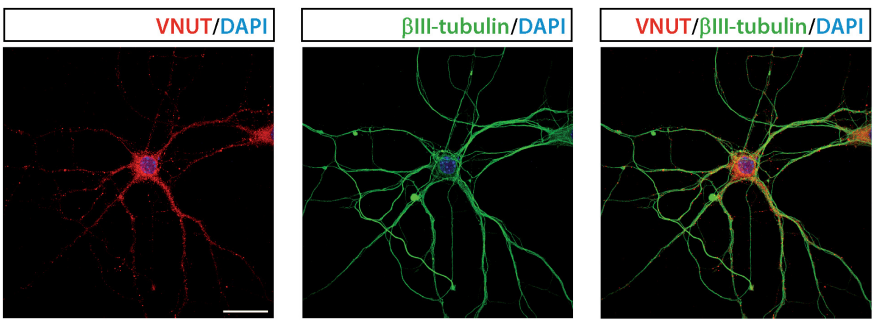

FIGURE 3 | Vesicular nucleotide transporter is expressed by cultured hippocampal neurons. Representative immunofluorescence images showing immunostaining for VNUT (red) and the cytoskeletal protein βIII-tubulin (green) in cultured hippocampal neurons at 7 days *in vitro*. The nuclei are counterstained with DAPI (blue). Scale bar: 20 μm. Adapted from Menéndez Méndez (2017). Images are reproduced with permission of the copyright holders.

hippocampal inhibitory terminals suggested that a similar partial segregation exists between VNUT- and VGAT-possessing vesicles (Larsson et al., 2012). Taken together, all these data indicate that VNUT may confer a purinergic phenotype to hippocampal neurons by establishing an exocytotically releasable vesicular pool of ATP. Hippocampal neurons from *VNUT*$^{-/-}$ mice completely loss their capacity to release ATP in response to K^+ stimulation (Sakamoto et al., 2014), which is an additional confirmation of the essential role of VNUT in the neuronal vesicular storage and vesicular release of ATP in the hippocampus.

VNUT in the Cerebellum

When localization of VNUT was analyzed by immunoperoxidase labeling in the rat brain, particularly strong immunoreactivity was observed in the cerebellar cortex. VNUT immunolabeling was detected in the somatodendritic extent of Purkinje cells, being also relevant throughout the molecular layer (Larsson et al., 2012).

Further studies have shown that cultured cerebellar granule neurons express a functional VNUT that participates in the exocytotic release of ATP from these cells (Menendez-Mendez et al., 2017). VNUT can be detected by western blotting and immunofluorescence in the cultured granule neurons, which release ATP in a Ca^{2+}-dependent manner, as stimulation of the cells with the calcium-selective ionophore ionomycin induces a significant increase of extracellular ATP (Menendez-Mendez et al., 2017). Exocytosis of ATP-containing vesicles can be visualized by fluorescence microscopy using quinacrine. This acidophilic antimalarial drug interacts with ATP stored in vesicles and has been extensively used as a fluorescent marker of intracellular ATP storage sites (Orriss et al., 2009; Liu et al., 2016). When granule cells were loaded with quinacrine, a punctate staining was observed, which appeared not only throughout the soma but was also evident in cell prolongations, thus indicating the presence of numerous ATP enriched vesicles in the granule neurons. Depolarization of the cells with K^+ reduced quinacrine-associated fluorescence in granule cells, showing that they release ATP via Ca^{2+}-dependent exocytosis (Menendez-Mendez et al., 2017). Ionomicin-induced ATP release was reduced when granule neurons were treated with the VNUT inhibitor Evans blue, thus indicating the involvement of VNUT in the vesicular storage and release of ATP. Moreover, immunofluorescence assays showed the co-localization of the vesicular protein synaptophysin and VNUT immunostaining in granule neurons, which further supports the exocytotic nature of ATP release (Menendez-Mendez et al., 2017). However, co-localization of VNUT and the synaptic vesicle marker was incomplete, suggesting that VNUT may be

also present in another type of storage vesicles or subcellular structures. The subcellular distribution of VNUT in cerebellar granule neurons was analyzed by the use of specific axonal and somatodendritic markers, such as the pan-axonal neurofilament marker SMI 312 and the microtubule-associated protein 2 (MAP2), respectively. VNUT showed co-localization with both subcellular markers, suggesting that this transporter exists both pre- and post-synaptically in the granule cells. The presence of VNUT in postsynaptic domains was confirmed by the clear co-localization of the transporter protein with the postsynaptic density protein 95 (PSD95). Interestingly, the co-localization of VNUT and the lysosomal marker LAMP-1 in certain cytosolic areas indicated that VNUT can be also found in lysosomes (Menendez-Mendez et al., 2017).

The glutamatergic phenotype of cerebellar granule neurons requires the vesicular storage of glutamate through VGLUTs, of which the most abundant isoform is VGLUT1. Immunofluoresecence assays showed a weak co-localization between VNUT and VGLUT1 in the granule neurons, suggesting that ATP- and glutamate-containing vesicle pools are segregated in these cells (Menendez-Mendez et al., 2017). Nevertheless, it should be taken into account that these studies were performed *in vitro*, in cultured granule cells. To assess whether such distribution also reflects the situation *in vivo*, slices of mouse cerebellum were immunolabeled with antibodies to VNUT and VLGUT1. These two vesicular transporters clearly showed a non-overlapping distribution with only a few examples of co-localization between VGLUT and VNUT in both the molecular or granular layers, which was consistent with the results obtained in cultured cells (Menendez-Mendez et al., 2017).

Cerebellar sections of P5 and P15 mice were used to analyze the distribution of VNUT during the postnatal development of the cerebellar cortex. At P5 stage, cortical layers of the cerebellum are not well defined and immature granule neurons are still migrating from the external to the internal granular layer, where they reach their final location. At this stage, VNUT was abundantly expressed and can be found in granule cell precursors and immature neurons that have not completely differentiated (Menendez-Mendez et al., 2017), suggesting a possible role of this transporter in the initial stages of granule cells maturation. Committed granule cells become mature neurons during the subsequent development of the cerebellum. Consistent with this, markers of neuronal progenitors and immature neurons are dramatically reduced at P15 stage. Nevertheless, VNUT expression persisted at this stage (Menendez-Mendez et al., 2017), indicating the relevance of VNUT during the commitment and differentiation of granule cells. These results correlate with the observations *in vitro*. VNUT expression could be detected from the first day of culture, when cerebellar granule neurons are still immature, persisting once the cells have matured and established synaptic contacts (Menendez-Mendez et al., 2017). Although further studies are required to fully understand the role of VNUT in the maturation of the granule cells and the development of the cerebellum, these findings, showing the localization and activity of VNUT in cerebellar granule neurons *in vitro* and their correlation with the situation *in vivo*, opens exciting new questions that need to be addressed in the future.

Double immunolabeling with antibodies against calbindin and VNUT revealed that the vesicular nucleotide transported is located adjacent to Purkinje neurons in P15 cerebellar sections, showing a filamentous morphology. Besides, co-localization between VNUT and the glial fibrillary acidic protein (GFAP) could be observed (**Figure 4A**). This staining pattern is consistent with the presence of VNUT in Bergmann glia, a population of radial glia present in the Purkinje cell layer. Moreover, the same pattern of VNUT immunolabeling persisted in the adult stage (**Figure 4B**), thus indicating that VNUT is present in this type of glial cells both in the advanced stages of cerebellar development and in the adult cerebellum. Bergmann glia has been postulated as one of the neurogenic populations in the cerebellum, as expression of neural stem cell markers, such as Sox2, a transcription factor that plays a key role in neurogenesis during the development of the nervous system, has been described in these cells (Sottile et al., 2006; Alcock et al., 2009). Presence of VNUT in these putative stem cells also supports a potential role of this vesicular transporter in the development of the cerebellum.

VNUT in Midbrain Dopaminergic Neurons

Immunohistochemical studies showed the presence of VNUT in tyrosine hydroxylase (TH)-positive dopaminergic neurons of the *substantia nigra* and ventral tegmental area of the midbrain (Ho et al., 2015). All TH-positive dopaminergic neurons in these areas were VNUT-positive. Nevertheless, expression of VNUT was not restricted to dopaminergic neurons, as VNUT-positive TH-negative cells can be detected in the *substantia nigra* and other regions of the brain (Ho et al., 2015). These findings, together with the fact that VNUT is expressed by retinal dopaminergic neurons, which incorporate ATP into vesicles and release ATP when stimulated (see below), indicate that the machinery necessary for vesicular ATP release is present in dopaminergic neurons from different regions of the central nervous system, and that these dopaminergic neurons can be a source of extracellular ATP and its bioactive breakdown products (Ho et al., 2015). These purinergic ligands would mediate their actions trough purinoceptors which are pre-synaptically expressed on dopaminergic neurons and co-expressed with dopamine receptors on neurons in regions that receive the dopaminergic input (Amadio et al., 2007; Morin and Di Paolo, 2014). As dopaminergic neurons in the midbrain are involved in the modulation of a wide range of behaviors, such as motor control, motivation and reward responses (Wise, 2008; Joshua et al., 2009; Cachope and Cheer, 2014), it is likely that purinergic transmission could play a role in these processes. Likewise, purinergic neurotransmission could have a role in neurological disorders involving dysregulation of midbrain dopaminergic pathways, such as Parkinson's disease (Chinta and Andersen, 2005; Hracsko et al., 2011).

VNUT in Glial Cells

VNUT in Astrocytes

Several studies have shown that astrocytes respond to neurotransmitters and release different gliotransmitters, including ATP, which can trigger propagation of Ca^{2+} waves

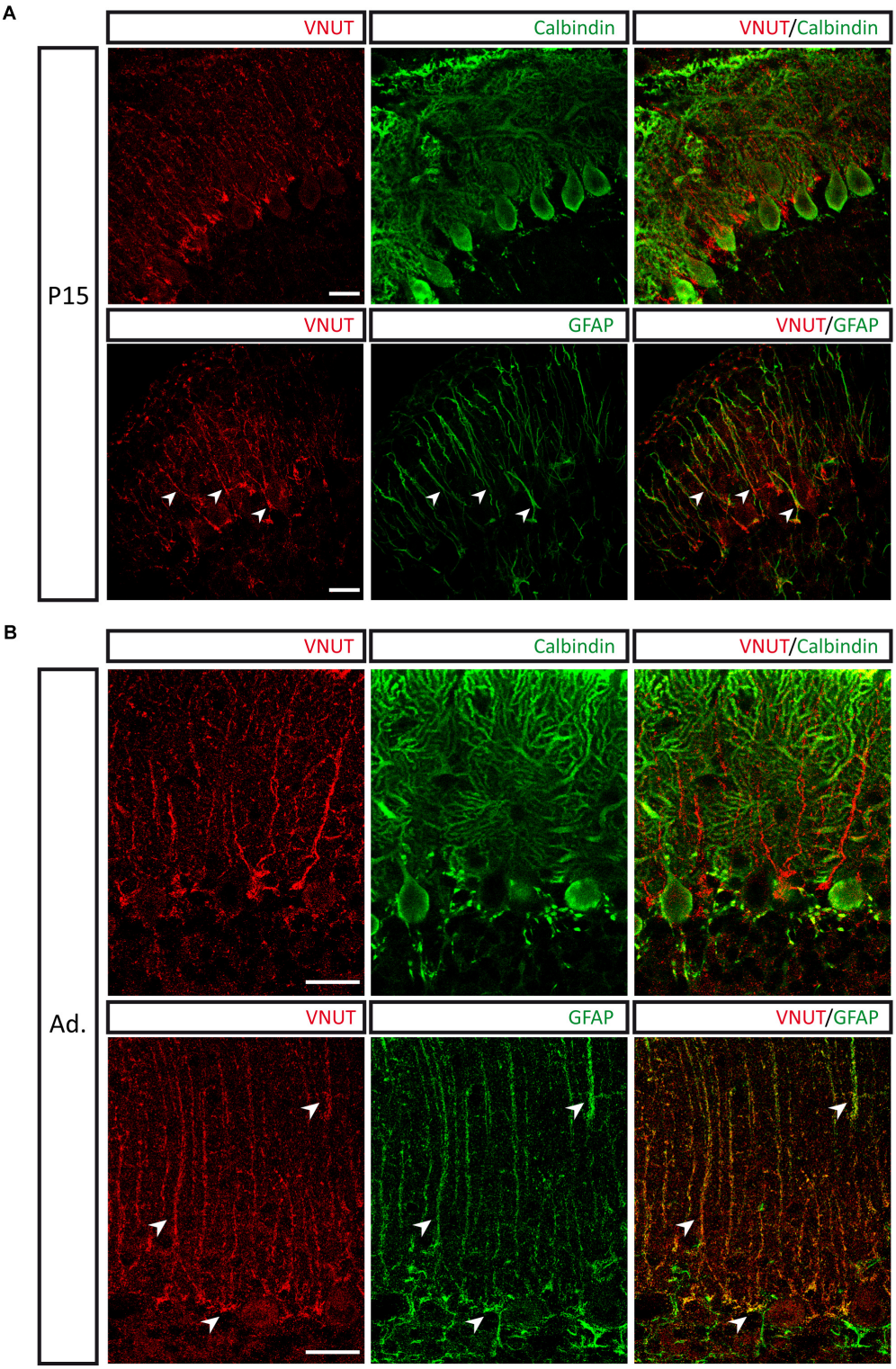

FIGURE 4 | Presence of VNUT in Bergmann glia. Representative immunofluorescence images showing double immunostaining for VNUT (red) and calbindin or GFAP (green) in cerebellar sections of P15 **(A)** and adult **(B)** mice. Arrowheads indicate co-localization of the immunoreactivity for VNUT and GFAP. Scale bar: 20 μm. Adapted from Menéndez Méndez (2017). Images are reproduced with permission of the copyright holders.

in these cells and modulate the activity of surrounding neurons (Stout et al., 2002; Coco et al., 2003; Newman, 2003; Zhang et al., 2003; Bowser and Khakh, 2007; Chen et al., 2013). However, the precise mechanism by which astrocytes release ATP are not well understood and both Ca^{2+}-dependent exocytosis (Coco et al., 2003; Pascual et al., 2005; Pangrsic et al., 2007; Parpura and Zorec, 2010; Lalo et al., 2014) and non-vesicular release pathways (Stout et al., 2002; Suadicani et al., 2006, 2012; Liu et al., 2008) have been described. Lysosomes can be a relevant source of vesicular ATP release from astrocytes, with the fusion of lysosomal and plasma membranes leading to ATP exocytosis (Zhang et al., 2007; Verderio et al., 2012).

Vesicular nucleotide transporter is expressed in C6 glioma cells and primary cultures of cortical astrocytes, where it is mainly associated to lysosomes, as demonstrated by the co-localization of VNUT-EGFP with lysosomal markers (Oya et al., 2013). Interestingly, VNUT-associated lysosomes release their content in response to elevations of the intracellular Ca^{2+} concentration, but they do not completely collapse into the plasma membrane after lysosomal exocytosis, as VNUT remains associated with the secretory lysosome and failed to spread into the plasma membrane, suggesting that lysosomes retain their spherical structure for a long time after fusion to plasma membrane. Such "kiss and stay" mechanism is quite different from the behavior of synaptic or dense-core vesicles, which easily spread into the plasma membrane during fusion events (Oya et al., 2013). ATP uptake into the secretory lysosomes decreased by pharmacological inhibition of VNUT by Evans blue. Moreover, silencing of VNUT expression by siRNA or inhibition of VNUT function by Evans blue reduced the amount of ATP released by the cells, whereas overexpression of VNUT increased it. Collectively, these data demonstrate the implication of VNUT in ATP storage in secretory lysosomes in astrocytes and its relevant role in astrocytic ATP release by lysosomal exocytosis (Oya et al., 2013). VNUT co-localize with the lysosomal marker LAMP3 in rat optic nerve head astrocytes that release lysosomal ATP after stimulation of the toll-like receptor 3 (TLR3), which is an additional evidence supporting the role of VNUT in the storage of ATP in secretory lysosomes in astrocytes (Beckel et al., 2018).

Astrocytes residing near the brainstem ventral surface (central respiratory chemosensitive area) respond to physiological reductions in pH with elevations in intracellular Ca^{2+} and ATP release. ATP stimulates the brainstem respiratory network, thus contributing to adaptive changes in lung ventilation. In terms of their sensitivity to pH, ventral brainstem astrocytes clearly differ from astrocytes that reside in other parts of the brain, such as cerebral cortex astrocytes, which indicates that these cells are functionally specialized (Kasymov et al., 2013). Compared to cortical astrocytes, ventral brainstem astrocytes showed increased levels of expression of genes encoding proteins associated with vesicular ATP transport and vesicular fusion, including VNUT (Kasymov et al., 2013), which suggests that astrocytes of the brainstem chemosensitive area are able to respond to acidification with enhanced vesicular release of ATP. Moreover, ATP released from astrocytes, possibly by the exocytosis of VNUT-possesing vesicular compartments, is involved in sensing of physiological changes in oxygen concentration in the brain (Angelova et al., 2015).

ATP derived from astrocytes modulates depressive behaviors in mice (Cao et al., 2013). In this sense, VNUT-dependent ATP release from astrocytes seems to play a pivotal role in the therapeutic effect of the anti-depressant fluoxetine (Kinoshita et al., 2018). Fluoxetine increases exocytotic ATP release in primary cultures of hippocampal astrocytes. Fluoxetine-induced ATP release was significantly reduced in astrocytes obtained from VNUT-knockdown mice, indicating that fluoxetine, at least in part, stimulates the release of ATP by VNUT-dependent exocytosis (Kinoshita et al., 2018). Fluoxetine-induced anti-depressive behavior was decreased in VNUT-knockdown mice and, relevantly, the anti-depressive effects of fluoxetine were dependent on astrocytic VNUT, as demonstrated in mice with selective knockout or overexpression of the VNUT gene in astrocytes. A decrease or increase of VNUT in astrocytes, resulted in a decrease or increase in the anti-depressive effects induced by fluoxetine, respectively. These findings demonstrate that fluoxetine acts on astrocytes and mediates its anti-depressive effect by increasing VNUT-dependent ATP exocytosis from these cells (Kinoshita et al., 2018). Released ATP and its metabolite adenosine act on $P2Y_{11}$ and adenosine A2b receptors expressed by astrocytes, inducing an increase in brain-derived neurotrophic factor (BDNF), which is considered to have a relevant role in the therapeutic action of anti-depressants (Kinoshita et al., 2018).

VNUT in the Microglia

Microglial cells constitute the resident immune cell population of the mammalian central nervous system. These cells monitor environmental changes and act as damage sensors within the brain. Any type of injury or pathological process induces the activation of the microglia, which change their morphology, migrate to the site of injury, proliferate, produce/release several substances that affect pathological processes, or even phagocytose damaged cells or debris to restore the brain homeostasis (Kettenmann et al., 2011). Extracellular nucleotides are relevant mediators that regulate the function of the microglia and, consequently, purinoceptor-mediated microglial responses have received much attention (Calovi et al., 2018). Microglia release ATP in response to different stimuli, such as ATP or glutamate (Liu et al., 2006; Dou et al., 2012). The mechanisms involved in ATP release from microglia remain unclear, although participation of connexin 43 (Cx43) hemichannels has been described (Ma et al., 2014).

Vesicular nucleotide transporter was found to be expressed in vesicular-like structures in primary cultured microglia and exhibited no co-localization with lysosomes (Imura et al., 2013). When cells where incubated with the fluorescent ATP analog 2′/3′-O-(*N*-Methyl-anthraniloyl)-adenosine-5′-triphosphate (MANT-ATP), the existence of many ATP-possessing vesicular structures could be observed. Microglia release ATP in an exocytotic manner: when cells were stimulated with ionomycin they released ATP and such release was dependent on Ca^{2+}, vesicular H^{+}-ATPase and soluble *N*-ethylmaleimide sensitive factor attachment protein receptors (SNAREs), but independent on connexin/pannexin hemichannels. Additionally, exocytotic

events of ATP-containing vesicles could be visualized by quinacrine-based TIRF microscopy in the microglial cell line MG5 (Imura et al., 2013). Ionomycin-induced ATP release from microglial cells was dependent upon VNUT, as release was significantly reduced when cells were treated with VNUT-siRNA. These findings demonstrated that microglia possess functional VNUT by which microglial cells store and release ATP in an exocytotic process (Imura et al., 2013). Moreover, stimulation of MG5 cells with the bacterial endotoxin lipopolysaccharide (LPS) significantly increased ionomycin-evoked ATP release, which was associated with an increase in VNUT expression. The increase in ATP release by LPS was abolished by the knockdown of VNUT (treatment of the cells with VNUT siRNA), indicating that the increase in VNUT by LPS should be responsible for the enhancement of the ATP release in microglial MG5 cells. This could be of relevance because, during infections or brain injuries, microglia could increase exocytotic ATP release by increasing VNUT (Imura et al., 2013).

Methylmercury (MeHg) is a well-known environmental pollutant that easily crosses the blood-brain barrier, inducing severe neuronal damage. It has been described that cultured microglia sense low concentrations of MeHg and release ATP in response to this neurotoxicant (Shinozaki et al., 2014). MeHg-evoked ATP release is significantly reduced by treatment with the botulinum toxin A, a toxin that cleaves synaptosomal-associated proteins (SNAPs), thereby preventing exocytosis. Moreover, microglia cultures prepared from VNUT knockout mice showed no ATP release when exposed to MeHg, in contrast to the significant ATP release from wild-type microglia. These results indicate that MeHg stimulates the exocytic release of ATP from microglial cells via a VNUT-dependent pathway (Shinozaki et al., 2014). The microglia-derived ATP in turn stimulates $P2Y_1$ receptors in astrocytes, which induces the release of interleukin-6 (IL-6), thus protecting neurons against MeHg. These neuroprotective effects were observed in organotypic slices from the hippocampus of wild-type mice, but not in slices obtained from VNUT knockdown mice, where MeHg failed to induce ATP release or IL-6production, which resulted in neuronal damage induced by MeHg (Shinozaki et al., 2014).

ROLE OF VNUT IN CENTRAL NERVOUS SYSTEM PHYSIOLOGY AND DISEASE

Role of VNUT in the Regulation of Neuronal Differentiation and Neuritogenesis

Differentiation of the axon is a pivotal process that gives rise to a complex morphology and physiology of neurons. Axon formation and growth is regulated by a variety of extracellular mediators, such as neurotransmitters, neurotrophic factors and other signaling molecules. Stimulating cultured hippocampal neurons with ATP evokes Ca^{2+} transients in the distal part of the axon which exerts a negative effect on axon growth, reducing both axonal length and branching (Diaz-Hernandez et al., 2008). This effect is mediated through P2X7 receptors that are expressed at the growth cone of the axon. Either the pharmacological inhibition of P2X7 receptor or its silencing by shRNA results in longer and more-branched axons, which is coupled to morphological changes of the growth cone (Diaz-Hernandez et al., 2008). This effect of ATP on axonal growth was corroborated by the finding that tissue-nonspecific alkaline phosphatase (TNAP) regulates axonal elongation and branching in hippocampal neurons by controlling the local availability of growth-inhibiting extracellular ATP (Diez-Zaera et al., 2011). Moreover, P2X7 receptors negatively regulate neurite formation in mouse Neuro-2a (N2a) neuroblastoma cell line (Gomez-Villafuertes et al., 2009). Pharmacological inhibition and interference of P2X7 receptor expression were associated with neuritogenesis in N2a cells, whereas P2X7 overexpression significantly reduced neurite formation. Neurotrophic effects of P2X7 were mediated through the modulation of the activity of the Ca^{2+}/calmodulin-dependent kinase II and some of its downstream effectors, which have been related to axonal growth and neuronal differentiation processes (Gomez-Villafuertes et al., 2009). Thus, N2a cells have been shown to be a suitable model to analyze the sequence of purinergic events that regulate neuronal differentiation.

Although N2a cells express very small amounts of endogenous VNUT, this transporter can be successfully heterologously expressed in this cell line, and co-localization of VNUT with the vesicular marker synaptophysin could be observed by confocal microscopy imaging (Menendez-Mendez et al., 2015). Retinoic acid-induced differentiation keeps VNUT expression in transfected N2a cells. Functionality of the vesicular transporter was assessed by luciferin-luciferase assays to measure ionomycin-induced ATP release from differentiated N2a cells (Menendez-Mendez et al., 2015). Expression of VNUT clearly decreases neuritogenesis in retinoic acid-treated N2a cells, as both the number and length of neurites are reduced when compared to control (VNUT non-expressing) cells. To corroborate the VNUT negative effect on neuritogenesis, shVNUT was used to knockdown VNUT expression in VNUT-transfected and differentiated cells. These cells, where VNUT expression was reduced, showed more prominent neuritogenesis, with an increase in both the number and length of neurites. These results highlight the role of VNUT as a key component in the sequence of events involved in extracellular ATP regulation of neuritogenesis and neuronal differentiation processes (Menendez-Mendez et al., 2015).

VNUT in the Spinal Cord: Role of VNUT-Dependent ATP Release in Neuropathic Pain

In the spinal cord, VNUT has been related to neuropathic pain, a hypersensitivity to pain that occurs after damage of a peripheral nerve as a consequence of traumatic injury or diseases such as diabetes mellitus, multiple sclerosis or cancer. Accumulating evidence indicated the crucial role of microglial cells in the spinal cord in the development of neuropathic pain. After damage of a peripheral nerve, spinal microglia turn into a reactive state through a sequence of molecular and

cellular changes, which include the increase in the expression of genes that encode purinergic receptors, such as P2X4 or $P2Y_{12}$. In response to the activation of these ATP receptors, microglial cells release different bioactive factors that cause abnormal neurotransmission in the nociceptive network in spinal dorsal horn (SDH). These pathological alterations result in pain hypersensitivity that converts initially innocuous stimuli into nociceptive signals (Tsuda et al., 2003; Tozaki-Saitoh et al., 2008).

Spinal dorsal horn neurons have been identified as a source of extracellular ATP that contributes to peripheral nerve injury (PNI) induced pain hypersensitivity (Masuda et al., 2016). PNI increases VNUT expression in the spinal cord and this upregulation of VNUT is required for the development of tactile allodynia (abnormal pain hypersensitivity evoked by innocuous stimuli), as the intrathecal administration of siRNA targeting *VNUT* in mice subjected to PNI, significantly reduced the expression of spinal VNUT and ameliorated PNI-evoked allodynia. Moreover, PNI also increased extracellular ATP content within the spinal cord and this increase was suppressed by vesicular exocytosis inhibitors (Masuda et al., 2016). VNUT-deficient ($VNUT^{-/-}$) mice did not shown PNI-evoked increase in extracellular ATP concentration and had attenuated pain hypersensitivity. Attenuation of PNI-induced allodynia and reduction in spinal extracellular ATP content was also observed in mice with specific deletion of VNUT in SDH neurons, but not in mice lacking VNUT in primary sensory neurons, astrocytes or microglia. Moreover, ectopic expression of VNUT in SDH neurons of VNUT-deficient mice restored PNI-evoked increase in extracellular ATP and pain. These results showed that VNUT-dependent exocytotic ATP release from dorsal horn neurons is an essential mechanism for neuropathic pain after PNI (Masuda et al., 2016).

Vesicular nucleotide transporter is expressed in subpopulations of rat dorsal root ganglion (DRG) neurons (Nishida et al., 2014). In a model of rats subjected to nerve injury (L5 spinal nerve ligation), an increase in VNUT expression was observed in injured DRG neurons. Moreover, VNUT co-localize with the lysosomal protein LAMP1 in these cells (Jung et al., 2016). Fluorescent labeling of lysosomal vesicles demonstrated that ATP containing VNUT-positive lysosomes are transported to the central nerve terminals of DRG neurons in the dorsal horn. Although there is no direct evidence of ATP release from primary afferent nerve terminals in dorsal horn through lysosomal exocytosis, a previous *in vitro* study revealed exocytotic ATP release from lysosomes in primary cultured DRG neurons (Jung et al., 2013). In the light of these findings, it has been suggested that lysosomal exocytosis from central terminals of DRG neurons could be an additional source of ATP that contribute to activation of the microglia in the dorsal horn after nerve injury (Jung et al., 2016).

Vesicular nucleotide transporter shows strong similarities with other members of the family of SCL17 anion transporters, such as the vesicular glutamate transporter (VGLUT). VGLUT undergoes unusual regulation by Cl^-. Glutamate uptake into vesicles shows biphasic dependence with the concentration of this ion: low Cl^- concentrations (2–8 mM) stimulate glutamate transport while high concentrations (>20 mM) inhibit it. It has been suggested that Cl^- acts as an allosteric modulator of VGLUT that triggers glutamate uptake upon binding to the transporter (Juge et al., 2010), whereas the inhibition of vesicular glutamate accumulation by high Cl^- concentrations could be related to the dissipation of $\Delta\psi$, the component of $\Delta\mu H^+$ that drives vesicular glutamate uptake. However, the precise molecular mechanism underlying the regulation of VGLUT by Cl^- is still to be clarified. Ketone bodies inhibit vesicular glutamate transport by competing with Cl^- at the site of allosteric regulation (Juge et al., 2010), which suggest a metabolic control of vesicular glutamate release. The strong dependence on transport activity with Cl^- concentration is a characteristic shared by other members of the SLC17 family such as VNUT. Presence of this ion is an absolute requirement for ATP transport activity in VNUT, as nucleotide transport cannot be detected in the absence of Cl^-. Br^- also activates transport, whereas I^-, F^-, nitrate, sulfate, and thiocyanate are ineffective (Sawada et al., 2008). This anion dependence is very similar to that of VGLUT2 (Juge et al., 2010). Moreover, VNUT is also inhibited by ketone bodies such as acetoacetate (**Figure 1B**), the inhibitory effect being reversible and prevented by high concentrations of Cl^- (Juge et al., 2010). Although detailed kinetic studies have not been carried out, these findings suggest the existence of similar anion binding sites and regulatory mechanisms in both members of the SLC17 family of transporters, VNUT and VGLUT.

Clodronate is a first-generation bisphosphonate used in antiresorptive therapy for osteoporosis. Nevertheless, studies have proved that clodronate also has analgesic properties, although the mechanism underlying this analgesic effect was unknown. Recently, clodronate was identified as a potent and selective inhibitor of ATP vesicular storage and release (**Figure 1B**; Kato et al., 2017). *In vitro* assays demonstrated that clodronate inhibits VNUT (IC_{50} = 15.6 nM) without affecting other vesicular neurotransmitter transporters, acting as an allosteric modulator that interacts with the Cl^- binding site. Clodronate shifted the Cl^- concentration necessary for VNUT activation toward a higher activation level, suggesting a competitive interaction. Consistent with this, clodronate modulates vesicular ATP release. Low concentrations of clodronate completely inhibited ATP release from microglia, neurons and immune cells (human monocyte cell line THP-1). *In vivo* analysis revealed that clodronate attenuates neuropathic and inflammatory pain, in addition to the accompanying inflammation, in wild type but no $VNUT^{-/-}$ mice, without altering basal nociception (Kato et al., 2017). These results demonstrated that clodronate exerts analgesic and anti-inflammatory actions by targeting VNUT. Noticeably, clodronate is approved for clinical use in the treatment of osteoporosis and its clinical safety in humans is well established (Muratore et al., 2011). Moreover, clodronate attenuates inflammatory and neuropathic pain with stronger, faster acting, and longer lasting effects than existing drugs (Kato et al., 2017; Moriyama and Nomura, 2018). Thereby, clodronate is likely to be clinically useful in the treatment of chronic neuropathic pain and could

open new perspectives regarding the use of VNUT inhibitors that block vesicular ATP release as therapeutic drugs.

VNUT in the Retina: Possible Role of VNUT in the Development of Glaucoma

Using laser microdissected retinal samples, VNUT mRNA expression was detected in photoreceptor and inner nuclear layer/ganglion cell layer (INL/GCL) samples (Vessey and Fletcher, 2012). Immunochemical studies have shown that VNUT appear to be widely distributed throughout the inner and outer retinal layers, with particular strong immunoreactivity detected in the outer segments of photoreceptors, outer plexiform layer, inner plexiform layer and ganglion cell layer. Presence of VNUT in these retinal areas was confirmed by the loss of VNUT immunoreactivity in the retina from VNUT knockout ($VNUT^{-/-}$) mice (Moriyama and Hiasa, 2016). Double-labeling immunochemistry showed that VNUT is co-localized with synaptophysin and VGLUT1 in photoreceptor cells, whereas it is co-localized with vesicular γ-aminobutyric acid (GABA) transporter (VGAT) in bipolar and amacrine cells. VNUT is also present in astrocytes and Müller cells. Retinal membrane fraction took up radiolabeled ATP in a DIDS and bafilomycin A1 (a vacuolar ATPase inhibitor) sensitive manner, this ATP-uptake activity being absent in retinal membrane vesicles prepared from $VNUT^{-/-}$ mice (Moriyama and Hiasa, 2016). Thus, these results indicate that VNUT is widely present in retina, where ATP can be stored and released to initiate purinergic chemical transmission.

Vesicular nucleotide transporter immunoreactivity can be detected in TH positive dopaminergic amacrine/interplexiform cells (Ho et al., 2015). Three-dimensional reconstruction of retinal flatmounts immunolabelled with VNUT showed that VNUT-positive amacrine/plexiform cells processes are closely associated with cone photoreceptors terminals and horizontal cells, which are known to express P2 purinergic receptors. In order to assess function, dissociated retinal neurons were loaded with fluorescent dopamine (FFN102) and ATP (MANT-ATP, quinacrine) markers and immunostained with a VNUT antibody. VNUT-immunoreactive neurons load fluorescent ATP and dopamine markers in vesicles. Moreover, ATP and dopamine markers co-localize in these cells, thus indicating co-loading of ATP and dopamine in vesicles within the VNUT-positive neurons. Fluorescence of the ATP marker quinacrine was reduced upon K^+ stimulation, this response being blocked in the presence of cadmium. Taken together, all these results indicate that dopaminergic neurons in the retina release ATP via calcium dependent exocytosis, which may modulate the visual response by stimulating purinergic receptors in closely associated cells (Ho et al., 2015).

Retinal extracellular ATP levels and changes in VNUT expression have been analyzed in the DBA/2J mouse model of glaucoma during the development of the disease (Perez de Lara et al., 2015). For this purpose, retinas were dissected from glaucomatous animals at 3, 9, 15, and 22 months of age. C57BL/6J mice were used as age-matched controls. Retinal net ATP release increased with the progression of the pathology, varying from 0.32 pmol/retina (3 months) to 1.10 pmol/retina (15 months, threefold increase). Concomitantly, a significant increase in VNUT expression in DBA/2J mice retina during glaucoma progression was detected. These data may suggest a possible correlation between retinal dysfunction and increased levels of extracellular ATP and nucleotide transporter (Perez de Lara et al., 2015).

TABLE 1 | Expression, localization, and function of VNUT in the central nervous system.

Organ	Location (vesicle)	Role	References
Brain	Hippocampal neurons (synaptic vesicles, postsynaptic vesicular structures)	VNUT-dependent ATP release	Larsson et al., 2012; Sakamoto et al., 2014
	Cerebellar granule neurons (synaptic vesicles, lysosomes)	Granule cell development	Menendez-Mendez et al., 2017
	Bergmann glia	ND	Menéndez Méndez, 2017
	Midbrain dopaminergic neurons	Vesicular ATP release	Ho et al., 2015
	Cortical astrocytes (lysosomes)	Lysosomal ATP release	Oya et al., 2013; Beckel et al., 2018
	Brainstem astrocytes	Response to changes in pH and brain oxygenation	Kasymov et al., 2013; Angelova et al., 2015
	Hippocampal astrocytes	Effect of antidepressants	Kinoshita et al., 2018
	Microglia (vesicular-like structures)	Exocytotic ATP release. Neuroprotective response to neurotoxicants	Imura et al., 2013; Shinozaki et al., 2014
Spinal cord	Dorsal horn neurons	Neuropathic pain	Masuda et al., 2016
	Dorsal root ganglion neurons (lysosomes)	Microglial activation in dorsal horn after nerve injury	Nishida et al., 2014; Jung et al., 2016
Retina	Photoreceptor cells, bipolar cells, astrocytes, Müller cells	ND	Moriyama and Hiasa, 2016
	Amacrine cells	Calcium-dependent ATP exocytosis	Ho et al., 2015; Moriyama and Hiasa, 2016

ND, not determined.

CONCLUDING REMARKS

It is widely accepted that VNUT is responsible for the storage of ATP and other nucleotides into secretory vesicles and therefore plays an essential role in the vesicular release of nucleotides and the initiation of purinergic chemical transmission. Both the reduction in the expression of VNUT and the inhibition of its activity reduce the vesicular release of ATP and lead to a decrease in purinergic chemical signaling. VNUT appear to be widely expressed in the central nervous system, being present in neurons, astrocytes and microglial cells. Accumulating evidence indicate the involvement of VNUT-dependent nucleotide release in a diversity of biological processes in the central nervous system, which include development of the cerebellar cortex, neuronal differentiation and neuritogenesis, sensing of physiological changes in pH and brain oxygenation, protection against neurotoxicants or modulation of depressive behaviors. The expression pattern, localization and functions of VNUT in the central nervous system are summarized in **Table 1**. Deficiencies in the vesicular release of ATP could have beneficial effects in certain pathological conditions. In particular, increased levels of extracellular ATP have correlated with retinal dysfunction during the development of glaucoma. Moreover, mice deficient in VNUT show attenuated neuropathic pain, and the selective inhibitor of VNUT, clodronate, exerts analgesic effects. Therefore, VNUT could constitute a new and relevant molecular target in the context of the pathophysiology of purinergic transmission. Impairment of purinergic signaling by inhibiting the activity of VNUT or silencing VNUT gene expression may represent a new and promising therapeutical strategy for the treatment of a variety of pathological conditions.

AUTHOR CONTRIBUTIONS

JG wrote the manuscript and made illustrations. MM-P, AM-M, RG-V, FO, ED, and RP-S wrote the manuscript.

FUNDING

This work was supported by the Spanish Ministerio de Economia y Competitividad (MINECO, BFU 2014-53654-P) and the "Red de Excelencia Consolider-Ingenio Spanish Ion Channel Initiative" (BFU2015-70067REDC), by the Comunidad de Madrid (BRADE-CM S2013/ICE-2958), and by a Fundación Ramón Areces Grant (PR2018/16-02). FO is the recipient of a Ramón y Cajal contract (RYC-2013-13290).

REFERENCES

Abbracchio, M. P., Burnstock, G., Verkhratsky, A., and Zimmermann, H. (2009). Purinergic signalling in the nervous system: an overview. *Trends Neurosci.* 32, 19–29. doi: 10.1016/j.tins.2008.10.001

Aberer, W., Kostron, H., Huber, E., and Winkler, H. (1978). A characterization of the nucleotide uptake of chromaffin granules of bovine adrenal medulla. *Biochem. J.* 172, 353–360. doi: 10.1042/bj1720353b

Alcock, J., Lowe, J., England, T., Bath, P., and Sottile, V. (2009). Expression of Sox1, Sox2 and Sox9 is maintained in adult human cerebellar cortex. *Neurosci. Lett.* 450, 114–116. doi: 10.1016/j.neulet.2008.11.047

Amadio, S., Montilli, C., Picconi, B., Calabresi, P., and Volonte, C. (2007). Mapping P2X and P2Y receptor proteins in striatum and substantia nigra: an immunohistological study. *Purinergic Signal.* 3, 389–398. doi: 10.1007/s11302-007-9069-8

Angelova, P. R., Kasymov, V., Christie, I., Sheikhbahaei, S., Turovsky, E., Marina, N., et al. (2015). Functional oxygen sensitivity of astrocytes. *J. Neurosci.* 35, 10460–10473. doi: 10.1523/JNEUROSCI.0045-15.2015

Bankston, L. A., and Guidotti, G. (1996). Characterization of ATP transport into chromaffin granule ghosts. synergy of ATP and serotonin accumulation in chromaffin granule ghosts. *J. Biol. Chem.* 271, 17132–17138. doi: 10.1074/jbc.271.29.17132

Baroja-Mazo, A., Barbera-Cremades, M., and Pelegrin, P. (2013). The participation of plasma membrane hemichannels to purinergic signaling. *Biochim. Biophys. Acta* 1828, 79–93. doi: 10.1016/j.bbamem.2012.01.002

Beckel, J. M., Gomez, N. M., Lu, W., Campagno, K. E., Nabet, B., Albalawi, F., et al. (2018). Stimulation of TLR3 triggers release of lysosomal ATP in astrocytes and epithelial cells that requires TRPML1 channels. *Sci. Rep.* 8:5726. doi: 10.1038/s41598-018-23877-3

Blakely, R. D., and Edwards, R. H. (2012). Vesicular and plasma membrane transporters for neurotransmitters. *Cold Spring Harb. Perspect. Biol.* 4:a005595. doi: 10.1101/cshperspect.a005595

Bowser, D. N., and Khakh, B. S. (2007). Vesicular ATP is the predominant cause of intercellular calcium waves in astrocytes. *J. Gen. Physiol.* 129, 485–491. doi: 10.1085/jgp.200709780

Burnstock, G. (2007a). Physiology and pathophysiology of purinergic neurotransmission. *Physiol. Rev.* 87, 659–797. doi: 10.1152/physrev.00043.2006

Burnstock, G. (2007b). Purine and pyrimidine receptors. *Cell. Mol. Life Sci.* 64, 1471–1483.

Burnstock, G., Krugel, U., Abbracchio, M. P., and Illes, P. (2011). Purinergic signalling: from normal behaviour to pathological brain function. *Prog. Neurobiol.* 95, 229–274. doi: 10.1016/j.pneurobio.2011.08.006

Cachope, R., and Cheer, J. F. (2014). Local control of striatal dopamine release. *Front. Behav. Neurosci.* 8:188. doi: 10.3389/fnbeh.2014.00188

Calovi, S., Mut-Arbona, P., and Sperlagh, B. (2018). Microglia and the purinergic signaling system. *Neuroscience* 405, 137–147. doi: 10.1016/j.neuroscience.2018.12.021

Cao, X., Li, L. P., Wang, Q., Wu, Q., Hu, H. H., Zhang, M., et al. (2013). Astrocyte-derived ATP modulates depressive-like behaviors. *Nat. Med.* 19, 773–777. doi: 10.1038/nm.3162

Chaudhry, F. A., Edwards, R. H., and Fonnum, F. (2008). Vesicular neurotransmitter transporters as targets for endogenous and exogenous toxic substances. *Annu. Rev. Pharmacol. Toxicol.* 48, 277–301. doi: 10.1146/annurev.pharmtox.46.120604.141146

Chen, J., Tan, Z., Zeng, L., Zhang, X., He, Y., Gao, W., et al. (2013). Heterosynaptic long-term depression mediated by ATP released from astrocytes. *Glia* 61, 178–191. doi: 10.1002/glia.22425

Chinta, S. J., and Andersen, J. K. (2005). Dopaminergic neurons. *Int. J. Biochem. Cell Biol.* 37, 942–946. doi: 10.1016/j.biocel.2004.09.009

Coco, S., Calegari, F., Pravettoni, E., Pozzi, D., Taverna, E., Rosa, P., et al. (2003). Storage and release of ATP from astrocytes in culture. *J. Biol. Chem.* 278, 1354–1362. doi: 10.1074/jbc.M209454200

Diaz-Hernandez, M., del Puerto, A., Diaz-Hernandez, J. I., Diez-Zaera, M., Lucas, J. J., Garrido, J. J., et al. (2008). Inhibition of the ATP-gated P2X7 receptor promotes axonal growth and branching in cultured hippocampal neurons. *J. Cell. Sci.* 121(Pt 22), 3717–3728. doi: 10.1242/jcs.034082

Diez-Zaera, M., Diaz-Hernandez, J. I., Hernandez-Alvarez, E., Zimmermann, H., Diaz-Hernandez, M., and Miras-Portugal, M. T. (2011). Tissue-nonspecific alkaline phosphatase promotes axonal growth of hippocampal neurons. *Mol. Biol. Cell.* 22, 1014–1024. doi: 10.1091/mbc.E10-09-0740

Dou, Y., Wu, H. J., Li, H. Q., Qin, S., Wang, Y. E., Li, J., et al. (2012). Microglial migration mediated by ATP-induced ATP release from lysosomes. *Cell Res.* 22, 1022–1033. doi: 10.1038/cr.2012.10

Eiden, L. E., Schafer, M. K., Weihe, E., and Schutz, B. (2004). The vesicular amine transporter family (SLC18): amine/proton antiporters required for vesicular accumulation and regulated exocytotic secretion of monoamines and acetylcholine. *Pflugers Arch.* 447, 636–640. doi: 10.1007/s00424-003-1100-5

Gasnier, B. (2004). The SLC32 transporter, a key protein for the synaptic release of inhibitory amino acids. *Pflugers Arch.* 447, 756–759. doi: 10.1007/s00424-003-1091-2

Gomez-Villafuertes, R., del Puerto, A., Diaz-Hernandez, M., Bustillo, D., Diaz-Hernandez, J. I., Huerta, P. G., et al. (2009). Ca2+/calmodulin-dependent kinase II signalling cascade mediates P2X7 receptor-dependent inhibition of neuritogenesis in neuroblastoma cells. *FEBS J.* 276, 5307–5325. doi: 10.1111/j.1742-4658.2009.07228.x

Gualix, J., Abal, M., Pintor, J., Garcia-Carmona, F., and Miras-Portugal, M. T. (1996). Nucleotide vesicular transporter of bovine chromaffin granules. Evidence for a mnemonic regulation. *J. Biol. Chem.* 271, 1957–1965. doi: 10.1074/jbc.271.4.1957

Gualix, J., Alvarez, A. M., Pintor, J., and Miras-Portugal, M. T. (1999a). Studies of chromaffin granule functioning by flow cytometry: transport of fluorescent epsilon-ATP and granular size increase induced by ATP. *Receptors Channels* 6, 449–461.

Gualix, J., Pintor, J., and Miras-Portugal, M. T. (1999b). Characterization of nucleotide transport into rat brain synaptic vesicles. *J. Neurochem.* 73, 1098–1104. doi: 10.1046/j.1471-4159.1999.0731098.x

Gualix, J., Fideu, M. D., Pintor, J., Rotllan, P., Garcia-Carmona, F., and Miras-Portugal, M. T. (1997). Characterization of diadenosine polyphosphate transport into chromaffin granules from adrenal medulla. *FASEB J.* 11, 981–990. doi: 10.1096/fasebj.11.12.9337151

Gualix, J., Gomez-Villafuertes, R., Pintor, J., Llansola, M., Felipo, V., and Miras-Portugal, M. T. (2014). Presence of diadenosine polyphosphates in microdialysis samples from rat cerebellum in vivo: effect of mild hyperammonemia on their receptors. *Purinergic Signal.* 10, 349–356. doi: 10.1007/s11302-013-9382-3

Ho, T., Jobling, A. I., Greferath, U., Chuang, T., Ramesh, A., Fletcher, E. L., et al. (2015). Vesicular expression and release of ATP from dopaminergic neurons of the mouse retina and midbrain. *Front. Cell. Neurosci.* 9:389. doi: 10.3389/fncel.2015.00389

Holmsen, H., and Weiss, H. J. (1979). Secretable storage pools in platelets. *Annu. Rev. Med.* 30, 119–134. doi: 10.1146/annurev.me.30.020179.001003

Hracsko, Z., Baranyi, M., Csolle, C., Goloncser, F., Madarasz, E., Kittel, A., et al. (2011). Lack of neuroprotection in the absence of P2X7 receptors in toxin-induced animal models of parkinson's disease. *Mol. Neurodegener.* 6:28. doi: 10.1186/1750-1326-6-28

Hutton, J. C., Penn, E. J., and Peshavaria, M. (1983). Low-molecular-weight constituents of isolated insulin-secretory granules. Bivalent cations, adenine nucleotides and inorganic phosphate. *Biochem. J.* 210, 297–305. doi: 10.1042/bj2100297

Imura, Y., Morizawa, Y., Komatsu, R., Shibata, K., Shinozaki, Y., Kasai, H., et al. (2013). Microglia release ATP by exocytosis. *Glia* 61, 1320–1330. doi: 10.1002/glia.22517

Jo, Y. H., and Schlichter, R. (1999). Synaptic corelease of ATP and GABA in cultured spinal neurons. *Nat. Neurosci.* 2, 241–245. doi: 10.1038/6344

Johnson, R. G. Jr. (1988). Accumulation of biological amines into chromaffin granules: a model for hormone and neurotransmitter transport. *Physiol. Rev.* 68, 232–307. doi: 10.1152/physrev.1988.68.1.232

Joshua, M., Adler, A., and Bergman, H. (2009). The dynamics of dopamine in control of motor behavior. *Curr. Opin. Neurobiol.* 19, 615–620. doi: 10.1016/j.conb.2009.10.001

Juge, N., Gray, J. A., Omote, H., Miyaji, T., Inoue, T., Hara, C., et al. (2010). Metabolic control of vesicular glutamate transport and release. *Neuron* 68, 99–112. doi: 10.1016/j.neuron.2010.09.002

Jung, J., Shin, Y. H., Konishi, H., Lee, S. J., and Kiyama, H. (2013). Possible ATP release through lysosomal exocytosis from primary sensory neurons. *Biochem. Biophys. Res. Commun.* 430, 488–493. doi: 10.1016/j.bbrc.2012.12.009

Jung, J., Uesugi, N., Jeong, N. Y., Park, B. S., Konishi, H., and Kiyama, H. (2016). Increase of transcription factor EB (TFEB) and lysosomes in rat DRG neurons and their transportation to the central nerve terminal in dorsal horn after nerve injury. *Neuroscience* 313, 10–22. doi: 10.1016/j.neuroscience.2015.11.028

Kasymov, V., Larina, O., Castaldo, C., Marina, N., Patrushev, M., Kasparov, S., et al. (2013). Differential sensitivity of brainstem versus cortical astrocytes to changes in pH reveals functional regional specialization of astroglia. *J. Neurosci.* 33, 435–441. doi: 10.1523/JNEUROSCI.2813-12.2013

Kato, Y., Hiasa, M., Ichikawa, R., Hasuzawa, N., Kadowaki, A., Iwatsuki, K., et al. (2017). Identification of a vesicular ATP release inhibitor for the treatment of neuropathic and inflammatory pain. *Proc. Natl. Acad. Sci. U.S.A.* doi: 10.1073/pnas.1704847114 [Epub ahead of print].

Kettenmann, H., Hanisch, U. K., Noda, M., and Verkhratsky, A. (2011). Physiology of microglia. *Physiol. Rev.* 91, 461–553. doi: 10.1152/physrev.00011.2010

Kinoshita, M., Hirayama, Y., Fujishita, K., Shibata, K., Shinozaki, Y., Shigetomi, E., et al. (2018). Anti-Depressant fluoxetine reveals its therapeutic effect via astrocytes. *EBioMedicine* 32, 72–83. doi: 10.1016/j.ebiom.2018.05.036

Kostron, H., Winkler, H., Peer, L. J., and Konig, P. (1977). Uptake of adenosine triphosphate by isolated adrenal chromaffin granules: a carrier-mediated transport. *Neuroscience* 2, 159–166. doi: 10.1016/0306-4522(77)90077-x

Lalo, U., Palygin, O., Rasooli-Nejad, S., Andrew, J., Haydon, P. G., and Pankratov, Y. (2014). Exocytosis of ATP from astrocytes modulates phasic and tonic inhibition in the neocortex. *PLoS Biol.* 12:e1001747. doi: 10.1371/journal.pbio.1001747

Larsson, M., Sawada, K., Morland, C., Hiasa, M., Ormel, L., Moriyama, Y., et al. (2012). Functional and anatomical identification of a vesicular transporter mediating neuronal ATP release. *Cereb. Cortex* 22, 1203–1214. doi: 10.1093/cercor/bhr203

Lazarowski, E. R. (2012). Vesicular and conductive mechanisms of nucleotide release. *Purinergic Signal.* 8, 359–373. doi: 10.1007/s11302-012-9304-9

Lein, E. S., Hawrylycz, M. J., Ao, N., Ayres, M., Bensinger, A., Bernard, A., et al. (2007). Genome-wide atlas of gene expression in the adult mouse brain. *Nature* 445, 168–176. doi: 10.1038/nature05453

Liu, G. J., Kalous, A., Werry, E. L., and Bennett, M. R. (2006). Purine release from spinal cord microglia after elevation of calcium by glutamate. *Mol. Pharmacol.* 70, 851–859. doi: 10.1124/mol.105.021436

Liu, H. T., Toychiev, A. H., Takahashi, N., Sabirov, R. Z., and Okada, Y. (2008). Maxi-anion channel as a candidate pathway for osmosensitive ATP release from mouse astrocytes in primary culture. *Cell Res.* 18, 558–565. doi: 10.1038/cr.2008.49

Liu, J., Liu, W., and Yang, J. (2016). ATP-containing vesicles in stria vascular marginal cell cytoplasms in neonatal rat cochlea are lysosomes. *Sci. Rep.* 6:20903. doi: 10.1038/srep20903

Luqmani, Y. A. (1981). Nucleotide uptake by isolated cholinergic synaptic vesicles: evidence for a carrier of adenosine 5′-triphosphate. *Neuroscience* 6, 1011–1021. doi: 10.1016/0306-4522(81)90067-1

Ma, Y., Cao, W., Wang, L., Jiang, J., Nie, H., Wang, B., et al. (2014). Basal CD38/cyclic ADP-ribose-dependent signaling mediates ATP release and survival of microglia by modulating connexin 43 hemichannels. *Glia* 62, 943–955. doi: 10.1002/glia.22651

Masuda, T., Ozono, Y., Mikuriya, S., Kohro, Y., Tozaki-Saitoh, H., Iwatsuki, K., et al. (2016). Dorsal horn neurons release extracellular ATP in a VNUT-dependent manner that underlies neuropathic pain. *Nat. Commun.* 7:12529. doi: 10.1038/ncomms12529

Menéndez Méndez, A. (2017). *Caracterización Del Transportador Vesicular De Nucleótidos En Tejidos Neurales*. Ph.D. thesis, Complutense University of Madrid, Madrid.

Menendez-Mendez, A., Diaz-Hernandez, J. I., and Miras-Portugal, M. T. (2015). The vesicular nucleotide transporter (VNUT) is involved in the extracellular ATP effect on neuronal differentiation. *Purinergic Signal.* 11, 239–249. doi: 10.1007/s11302-015-9449-4

Menendez-Mendez, A., Diaz-Hernandez, J. I., Ortega, F., Gualix, J., Gomez-Villafuertes, R., and Miras-Portugal, M. T. (2017). Specific temporal distribution and subcellular localization of a functional vesicular nucleotide transporter (VNUT) in cerebellar granule neurons. *Front. Pharmacol.* 8:951. doi: 10.3389/fphar.2017.00951

Morin, N., and Di Paolo, T. (2014). Interaction of adenosine receptors with other receptors from therapeutic perspective in Parkinson's disease.

Int. Rev. Neurobiol. 119, 151–167. doi: 10.1016/B978-0-12-801022-8.00007-6

Moriyama, S., and Hiasa, M. (2016). Expression of vesicular nucleotide transporter in the mouse retina. *Biol. Pharm. Bull.* 39, 564–569. doi: 10.1248/bpb.b15-00872

Moriyama, Y., Hiasa, M., Sakamoto, S., Omote, H., and Nomura, M. (2017). Vesicular nucleotide transporter (VNUT): appearance of an actress on the stage of purinergic signaling. *Purinergic Signal.* 13, 387–404. doi: 10.1007/s11302-017-9568-1

Moriyama, Y., and Nomura, M. (2018). Clodronate: a vesicular ATP release blocker. *Trends Pharmacol. Sci.* 39, 13–23. doi: 10.1016/j.tips.2017.10.007

Muratore, M., Quarta, E., Grimaldi, A., Calcagnile, F., and Quarta, L. (2011). Clinical utility of clodronate in the prevention and management of osteoporosis in patients intolerant of oral bisphosphonates. *Drug Des. Devel. Ther.* 5, 445–454. doi: 10.2147/DDDT.S12139

Nakagomi, H., Yoshiyama, M., Mochizuki, T., Miyamoto, T., Komatsu, R., Imura, Y., et al. (2016). Urothelial ATP exocytosis: regulation of bladder compliance in the urine storage phase. *Sci. Rep.* 6:29761. doi: 10.1038/srep29761

Newman, E. A. (2003). Glial cell inhibition of neurons by release of ATP. *J. Neurosci.* 23, 1659–1666. doi: 10.1523/jneurosci.23-05-01659.2003

Nishida, K., Nomura, Y., Kawamori, K., Moriyama, Y., and Nagasawa, K. (2014). Expression profile of vesicular nucleotide transporter (VNUT, SLC17A9) in subpopulations of rat dorsal root ganglion neurons. *Neurosci. Lett.* 579, 75–79. doi: 10.1016/j.neulet.2014.07.017

Njus, D., Kelley, P. M., and Harnadek, G. J. (1986). Bioenergetics of secretory vesicles. *Biochim. Biophys. Acta* 853, 237–265. doi: 10.1016/0304-4173(87)90003-6

Omote, H., Miyaji, T., Hiasa, M., Juge, N., and Moriyama, Y. (2016). Structure, function, and drug interactions of neurotransmitter transporters in the postgenomic era. *Annu. Rev. Pharmacol. Toxicol.* 56, 385–402. doi: 10.1146/annurev-pharmtox-010814-124816

Omote, H., and Moriyama, Y. (2013). Vesicular neurotransmitter transporters: an approach for studying transporters with purified proteins. *Physiology* 28, 39–50. doi: 10.1152/physiol.00033.2012

Orriss, I. R., Knight, G. E., Utting, J. C., Taylor, S. E., Burnstock, G., and Arnett, T. R. (2009). Hypoxia stimulates vesicular ATP release from rat osteoblasts. *J. Cell. Physiol.* 220, 155–162. doi: 10.1002/jcp.21745

Oya, M., Kitaguchi, T., Yanagihara, Y., Numano, R., Kakeyama, M., Ikematsu, K., et al. (2013). Vesicular nucleotide transporter is involved in ATP storage of secretory lysosomes in astrocytes. *Biochem. Biophys. Res. Commun.* 438, 145–151. doi: 10.1016/j.bbrc.2013.07.043

Pangrsic, T., Potokar, M., Stenovec, M., Kreft, M., Fabbretti, E., Nistri, A., et al. (2007). Exocytotic release of ATP from cultured astrocytes. *J. Biol. Chem.* 282, 28749–28758. doi: 10.1074/jbc.M700290200

Pankratov, Y., Lalo, U., Verkhratsky, A., and North, R. A. (2006). Vesicular release of ATP at central synapses. *Pflugers Arch.* 452, 589–597. doi: 10.1007/s00424-006-0061-x

Pankratov, Y., Lalo, U., Verkhratsky, A., and North, R. A. (2007). Quantal release of ATP in mouse cortex. *J. Gen. Physiol.* 129, 257–265.doi: 10.1085/jgp.200609693

Parpura, V., and Zorec, R. (2010). Gliotransmission: exocytotic release from astrocytes. *Brain Res. Rev.* 63, 83–92. doi: 10.1016/j.brainresrev.2009.11.008

Pascual, O., Casper, K. B., Kubera, C., Zhang, J., Revilla-Sanchez, R., Sul, J. Y., et al. (2005). Astrocytic purinergic signaling coordinates synaptic networks. *Science* 310, 113–116. doi: 10.1126/science.1116916

Perez de Lara, M. J., Guzman-Aranguez, A., de la Villa, P., Diaz-Hernandez, J. I., Miras-Portugal, M. T., and Pintor, J. (2015). Increased levels of extracellular ATP in glaucomatous retinas: possible role of the vesicular nucleotide transporter during the development of the pathology. *Mol. Vis.* 21,1060–1070.

Pintor, J., Diaz-Rey, M. A., Torres, M., and Miras-Portugal, M. T. (1992a). Presence of diadenosine polyphosphates–Ap4A and Ap5A–in rat brain synaptic terminals. Ca2+ dependent release evoked by 4-aminopyridine and veratridine. *Neurosci. Lett.* 136, 141–144. doi: 10.1016/0304-3940(92)90034-5

Pintor, J., Kowalewski, H. J., Torres, M., Mirasportugal, M. T., and Zimmermann, H. (1992b). Synaptic vesicle storage of diadenosine polyphosphates in the torpedo electric organ. *Neurosci. Res. Commun.* 10, 9–15.

Pintor, J., Rotllan, P., Torres, M., and Miras-Portugal, M. T. (1992c). Characterization and quantification of diadenosine hexaphosphate in chromaffin cells: granular storage and secretagogue-induced release. *Anal. Biochem.* 200, 296–300. doi: 10.1016/0003-2697(92)90469-n

Reimer, R. J. (2013). SLC17: a functionally diverse family of organic anion transporters. *Mol. Aspects Med.* 34, 350–359. doi: 10.1016/j.mam.2012.05.004

Richardson, P. J., and Brown, S. J. (1987). ATP release from affinity-purified rat cholinergic nerve terminals. *J. Neurochem.* 48, 622–630. doi: 10.1111/j.1471-4159.1987.tb04138.x

Rodriguez del Castillo, A., Torres, M., Delicado, E. G., and Miras-Portugal, M. T. (1988). Subcellular distribution studies of diadenosine polyphosphates–Ap4A and Ap5A–in bovine adrenal medulla: presence in chromaffin granules. *J. Neurochem.* 51, 1696–1703. doi: 10.1111/j.1471-4159.1988.tb01147.x

Roseth, S., Fykse, E. M., and Fonnum, F. (1995). Uptake of L-glutamate into rat brain synaptic vesicles: effect of inhibitors that bind specifically to the glutamate transporter. *J. Neurochem.* 65, 96–103. doi: 10.1046/j.1471-4159.1995.65010096.x

Sakamoto, S., Miyaji, T., Hiasa, M., Ichikawa, R., Uematsu, A., Iwatsuki, K., et al. (2014). Impairment of vesicular ATP release affects glucose metabolism and increases insulin sensitivity. *Sci. Rep.* 4:6689. doi: 10.1038/srep06689

Sawada, K., Echigo, N., Juge, N., Miyaji, T., Otsuka, M., Omote, H., et al. (2008). Identification of a vesicular nucleotide transporter. *Proc. Natl. Acad. Sci. U.S.A.* 105, 5683–5686. doi: 10.1073/pnas.0800141105

Sawynok, J., Downie, J. W., Reid, A. R., Cahill, C. M., and White, T. D. (1993). ATP release from dorsal spinal cord synaptosomes: characterization and neuronal origin. *Brain Res.* 610, 32–38. doi: 10.1016/0006-8993(93)91213-c

Shinozaki, Y., Nomura, M., Iwatsuki, K., Moriyama, Y., Gachet, C., and Koizumi, S. (2014). Microglia trigger astrocyte-mediated neuroprotection via purinergic gliotransmission. *Sci. Rep.* 4:4329. doi: 10.1038/srep04329

Sottile, V., Li, M., and Scotting, P. J. (2006). Stem cell marker expression in the bergmann glia population of the adult mouse brain. *Brain Res.* 1099, 8–17. doi: 10.1016/j.brainres.2006.04.127

Stout, C. E., Costantin, J. L., Naus, C. C., and Charles, A. C. (2002). Intercellular calcium signaling in astrocytes via ATP release through connexin hemichannels. *J. Biol. Chem.* 277, 10482–10488. doi: 10.1074/jbc.M109902200

Suadicani, S. O., Brosnan, C. F., and Scemes, E. (2006). P2X7 receptors mediate ATP release and amplification of astrocytic intercellular Ca2+ signaling. *J. Neurosci.* 26, 1378–1385. doi: 10.1523/JNEUROSCI.3902-05.2006

Suadicani, S. O., Iglesias, R., Wang, J., Dahl, G., Spray, D. C., and Scemes, E. (2012). ATP signaling is deficient in cultured Pannexin1-null mouse astrocytes. *Glia* 60, 1106–1116. doi: 10.1002/glia.22338

Tompkins, J. D., and Parsons, R. L. (2006). Exocytotic release of ATP and activation of P2X receptors in dissociated guinea pig stellate neurons. *Am. J. Physiol. Cell Physiol.* 291, C1062–C1071. doi: 10.1152/ajpcell.00472.2005

Tozaki-Saitoh, H., Tsuda, M., Miyata, H., Ueda, K., Kohsaka, S., and Inoue, K. (2008). P2Y12 receptors in spinal microglia are required for neuropathic pain after peripheral nerve injury. *J. Neurosci.* 28, 4949–4956. doi: 10.1523/JNEUROSCI.0323-08.2008

Tsuda, M., Shigemoto-Mogami, Y., Koizumi, S., Mizokoshi, A., Kohsaka, S., Salter, M. W., et al. (2003). P2X4 receptors induced in spinal microglia gate tactile allodynia after nerve injury. *Nature* 424, 778–783. doi: 10.1038/nature01786

Verderio, C., Cagnoli, C., Bergami, M., Francolini, M., Schenk, U., Colombo, A., et al. (2012). TI-VAMP/VAMP7 is the SNARE of secretory lysosomes contributing to ATP secretion from astrocytes. *Biol. Cell.* 104, 213–228. doi: 10.1111/boc.201100070

Vessey, K. A., and Fletcher, E. L. (2012). Rod and cone pathway signalling is altered in the P2X7 receptor knock out mouse. *PLoS One* 7:e29990. doi: 10.1371/journal.pone.0029990

Weber, A., and Winkler, H. (1981). Specificity and mechanism of nucleotide uptake by adrenal chromaffin granules. *Neuroscience* 6, 2269–2276. doi: 10.1016/0306-4522(81)90016-6

Whittaker, V. P. (1987). Cholinergic synaptic vesicles from the electromotor nerve terminals of torpedo. Composition and life cycle. *Ann. N. Y. Acad. Sci.* 493, 77–91. doi: 10.1111/j.1749-6632.1987.tb27185.x

Winkler, H. (1976). The composition of adrenal chromaffin granules: an assessment of controversial results. *Neuroscience* 1, 65–80. doi: 10.1016/0306-4522(76)90001-4

Wise, R. A. (2008). Dopamine and reward: the anhedonia hypothesis 30 years on. *Neurotox. Res.* 14, 169–183. doi: 10.1007/BF03033808

Zhang, J. M., Wang, H. K., Ye, C. Q., Ge, W., Chen, Y., Jiang, Z. L., et al. (2003). ATP released by astrocytes mediates glutamatergic activity-dependent heterosynaptic suppression. *Neuron* 40, 971–982. doi: 10.1016/s0896-6273(03)00717-7

Zhang, Z., Chen, G., Zhou, W., Song, A., Xu, T., Luo, Q., et al. (2007). Regulated ATP release from astrocytes through lysosome exocytosis. *Nat. Cell Biol.* 9, 945–953. doi: 10.1038/ncb1620

Conflict of Interest Statement: The authors declare that the research was conducted in the absence of any commercial or financial relationships that could be construed as a potential conflict of interest.

frontiers in Cellular Neuroscience

ORIGINAL RESEARCH
published: 29 May 2019
doi: 10.3389/fncel.2019.00242

Age- and Experience-Related Plasticity of ATP-Mediated Signaling in the Neocortex

*Ulyana Lalo[1], Alexander Bogdanov[2] and Yuriy Pankratov[1]**

[1] School of Life Sciences, Gibbet Hill Campus, University of Warwick, Coventry, United Kingdom, [2] Institute for Chemistry and Biology, Immanuel Kant Baltic Federal University, Kaliningrad, Russia

There is growing recognition of the important role of interaction between neurons and glial cells for brain longevity. The extracellular ATP have been shown to bring significant contribution into bi-directional glia-neuron communications, in particular into astrocyte-driven modulation of synaptic plasticity. To elucidate a putative impact of brain aging on neuron-glia networks, we explored the aging-related plasticity of the purinoreceptors-mediated signaling in cortical neurons and astrocytes. We investigated the age- and experience-related alterations in purinergic components of neuronal synaptic currents and astroglial calcium signaling in the layer2/3 of neocortex of mice exposed to the mild caloric restriction (CR) and environmental enrichment (EE) which included *ad libitum* physical exercise. We observed the considerable age-related decline in the neuronal P2X receptor-mediated miniature spontaneous currents which originated from the release of ATP from both synapses and astrocytes. We also found out that purinergic astrocytic Ca^{2+}-signaling underwent the substantial age-related decline but EE and CR rescued astroglial signaling, in particular mediated by P2X1, P2X1/5, and P2Y1 receptors. Our data showed that age-related attenuation in the astroglial calcium signaling caused a substantial decrease in the exocytosis of ATP leading to impairment of astroglia-derived purinergic modulation of excitatory synaptic currents and GABAergic tonic inhibitory currents. On a contrary, exposure to EE and CR, which enhanced purinergic astrocytic calcium signaling, up-regulated the excitatory and down-regulated the inhibitory currents in neurons of old mice, thus counterbalancing the impact of aging on synaptic signaling. Combined, our results strongly support the physiological importance of ATP-mediated signaling for glia-neuron interactions and brain function. Our data also show that P2 purinoreceptor-mediated communication between astrocytes and neurons in the neocortex undergoes remodeling during brain aging and decrease in the ATP release may contribute to the age-related impairment of synaptic transmission.

Keywords: ageing, synaptic strength, glia-neuron interaction, diet, exercise, GABA receptor A, AMPA receptor, calcium

OPEN ACCESS

Edited by:
Eric Boué-Grabot,
Université de Bordeaux, France

Reviewed by:
Rashid Giniatullin,
University of Eastern Finland, Finland
Arthur Morgan Butt,
University of Portsmouth,
United Kingdom

****Correspondence:***
Yuriy Pankratov
y.pankratov@warwick.ac.uk

Specialty section:
This article was submitted to Cellular Neurophysiology, a section of the journal Frontiers in Cellular Neuroscience

Received: *17 March 2019*
Accepted: *15 May 2019*
Published: *29 May 2019*

Citation:
Lalo U, Bogdanov A and Pankratov Y (2019) Age- and Experience-Related Plasticity of ATP-Mediated Signaling in the Neocortex. Front. Cell. Neurosci. 13:242. doi: 10.3389/fncel.2019.00242

INTRODUCTION

Adaptation of mammalian brain to environmental and biochemical challenges across a life-time is associated with remodeling of synaptic contacts and plastic changes in the neural networks (Hillman et al., 2008; Nithianantharajah and Hannan, 2009; van Praag, 2009; Mercken et al., 2012; Merzenich et al., 2014). The responsiveness of neural networks and synapses to enriched environment (EE), physical activity, and caloric restriction (CR) (Hillman et al., 2008; Nithianantharajah and Hannan, 2009; van Praag, 2009; Mercken et al., 2012; Merzenich et al., 2014) provides an opportunity to ameliorate the negative consequences of aging on cognitive function. Still, cellular and molecular mechanisms underlying effects of exercise and CR on synaptic plasticity are yet to be fully understood.

It is now widely acknowledged that maintenance and modification of synaptic networks depends on the interaction between neurons and neuroglia (Araque et al., 2014; Hulme et al., 2014; Gundersen et al., 2015; De Strooper and Karran, 2016). However, a great deal of information on this interaction has been derived from the experiments on young animals, whereas the age-dependent modification of glia-neuron communications remains unknown.

There is an accumulating evidence of importance of extracellular ATP for transmitting signals between brain neurons and glia. ATP can be released from nerve terminals, mainly by exocytosis, and astrocytes, both by vesicular release and diffusion through the plasmalemmal channels (Fields and Stevens, 2000; Pangrsic et al., 2007; Abbracchio et al., 2009; Butt, 2011; Khakh and North, 2012; Lalo et al., 2014a). The role for synaptically released ATP in neuronal signaling has been established for several brain areas, such as medial habenula, hippocampus and somatosensory cortex (Robertson et al., 1999; Pankratov et al., 2003, 2007, 2009). Release of ATP from astrocytes represents a powerful pathway of glia-neuron interaction implicated in the synaptic plasticity (Araque et al., 2014; Rasooli-Nejad et al., 2014; Pankratov and Lalo, 2015; Lalo et al., 2016), meta-plasticity (Hulme et al., 2014; Lalo et al., 2018), and neurological disorders (Butt, 2011; Rodrigues et al., 2015; Rivera et al., 2016; Verkhratsky et al., 2017). Apart from mediating a significant component of glia-to-neuron signaling, astrocyte-derived ATP can also act in autocrine manner activating purinoreceptor-mediated Ca^{2+}-signaling in astroglial networks (Fields and Stevens, 2000; Fields and Burnstock, 2006; Gourine et al., 2010; Butt, 2011; Lalo et al., 2011b; Wells et al., 2015).

Effects of ATP as neuro- and gliotransmitter are mediated by ionotropic P2X and metabotropic P2Y purinoreceptors which are abundantly expressed in the brain and can bring significant contribution to the intracellular Ca^{2+}-signaling in various types of cells and (Burnstock, 2007; Abbracchio et al., 2009; Khakh and North, 2012; Pankratov and Lalo, 2014). Acting via P2X and P2Y receptors, extracellular ATP can exert various neuro-modulatory effects on excitatory and inhibitory synaptic transmission both at pre- and post-synaptic loci (Khakh and North, 2012; Boue-Grabot and Pankratov, 2017).

Hence, ATP as extracellular transmitter can bring significant contribution into the bi-directional communications between neurons and astrocytes. Our recent data highlighted an important role of glia-neuron interactions in the experience-induced metaplasticity in aging brain (Lalo et al., 2018). We also reported previously that ATP-mediated signaling in astrocytes can undergo significant age-dependent remodeling. Our data, as well as reports of other groups, suggest that alterations in neuronal and glial ATP-mediated signaling can be involved in (patho)physiological changes in synaptic transmission in aging and neurodegenerative diseases (Delekate et al., 2014; Verkhratsky et al., 2017; Zorec et al., 2017; Lalo et al., 2018). Still, aging-related plasticity of purinergic component of glia-neuron communications remains largely unexplored. Here we report in depth analysis of the age-dependent changes in purinergic signaling in neocortical astrocytes and neurons which we performed aiming to understand how brain aging affects signaling in tripartite synapse. We also elucidated the putative impact of environmental enrichment (EE) and CR on purinergic signaling.

MATERIALS AND METHODS

All animal work has been carried out in accordance with United Kingdom legislation and "3R" strategy; research has not involved non-human primates. Experiments were performed in astrocytes and pyramidal neurons of somatosensory cortex of transgenic mice expressing enhanced green fluorescent protein (EGFP) under control of the human glial fibrillary acidic protein (GFAP) promoter (GFAP-EGFP mice; see Lalo et al., 2008). We used mice of four age groups: 3–6 (average 4.2 ± 1.1) weeks (young), 3–6 (4.4 ± 1.2) months (adult), 8–12 (10.3 ± 1.4) months (old), and 16–28 (21.4 ± 3.2) months (very old). We compared animals kept under standard housing conditions (SH) vs animals exposed to the enriched environment (EE) from birth (Correa et al., 2012), including *ad libitum* access to the running wheel, or kept on mild CR diet (food intake individually regulated to maintain the body weight loss of 10–15%) for 4–6 weeks.

Slice and Cell Preparation

Mice were anesthetized by halothane and then decapitated, in accordance with United Kingdom legislation. Brains were removed rapidly after decapitation and placed into ice-cold physiological saline containing (mM): NaCl 130, KCl 3, $CaCl_2$ 0.5, $MgCl_2$ 2.5, NaH_2PO_4 1, $NaHCO_3$ 25, glucose 15, and pH of 7.4 gassed with 95% O_2 – 5% CO_2. Transverse slices (260 μm) were cut at 4°C and then placed in physiological saline containing (mM): NaCl 130, KCl 3, $CaCl_2$ 2.5, $MgCl_2$ 1, NaH_2PO_4 1, $NaHCO_3$ 22, glucose 15, pH of 7.4 gassed with 95% O_2 - 5% CO_2, and kept for 1.5 – 5 h prior to cell isolation and recording.

Astrocytes were initially identified by their morphology under DIC observation and EGFP fluorescence. After the recordings, the identification of astrocyte was confirmed via functional properties (high potassium conductance, low input resistance, and strong activity of glutamate transporters) as described previously (Lalo et al., 2014a; Rasooli-Nejad et al., 2014; Pankratov and Lalo, 2015). To facilitate the high-quality

whole-cell recordings in the brain tissue slices of old mice, tissue slices were treated with vibrating glass ball remove the upper layer of dead cells and expose healthy neurons (Lalo and Pankratov, 2017).

Whole-cell voltage clamp recordings from cortical neurones and astrocytes cells were made with patch pipettes (4 – 5 MΩ) filled with intracellular solution (in mM): 60 CsCl, 50 CsGluconate, 10 NaCl, 10 HEPES, 5 MgATP, 1 D-Serine, 0.1 EGTA, and pH 7.35; Currents were monitored using an MultiClamp 700B patch-clamp amplifier (Axon Instruments, United States) filtered at 2 kHz and digitized at 4 kHz. Experiments were controlled by Digidata 1440A data acquisition board (Axon Instruments, United States) and WinWCP software (University of Strathclyde, United Kingdom); data were analyzed by self-designed software. Liquid junction potentials were compensated with the patch-clamp amplifier. The series and input resistances were, respectively 5–7 MΩ and 600–1100 MΩ; both series and input resistance varied by less than 20% in the cells accepted for analysis. In the younger mice (up to age of 6 months), the 90% of neurons tested showed acceptable parameters (as above) of whole-cell recordings, in the older mice, only 60% of neurons tests were suitable for long-time high-quality whole-cell recordings.

For activation of synaptic responses, axons originating from layer IV–VI neurons were stimulated with a bipolar coaxial electrode (WPI, United States) placed in layer V close to the layer IV border, approximately opposite the site of recording; stimulus duration was 300 μs, train of 5 stimuli was delivered at 100 Hz. The stimulus magnitude was set 3 – 4 times higher than the minimal stimulus necessary to elicit a response in layer II pyramidal neurons (Rasooli-Nejad et al., 2014; Pankratov and Lalo, 2015; Lalo et al., 2016).

Multi-Photon Fluorescent Ca^{2+}-Imaging in Astrocytes

To monitor the cytoplasmic free Ca^{2+}concentration ($[Ca^{2+}]_i$) *in situ*, astrocytes of neocortical slices were loaded via 30 min incubation with 1 μM of Rhod-2AM (dnSNARE mice) or Oregon Green Bapta-2AM and sulforhodamine 101 (wild-type and MSK1 KD mice) at 33°C. Two-photon images of neurons and astrocytes were acquired at 5 Hz frame-rate using a Zeiss LSM 7MP multi-photon microscope coupled to a Spectra-Physics MaiTai pulsing laser; experiments were controlled by ZEN LSM software (Carl Zeiss, Germany). Images were further analyzed off-line using ZEN LSM (Carl Zeiss) and ImageJ (NIH) software (Schneider et al., 2012). The $[Ca^{2+}]_i$ levels were expressed as ΔF/F ratio averaged over a region of interest (ROI). For analysis of spontaneous Ca^{2+}–transients in astrocytes, 5–10 ROIs located over the astrocytic branches and 1 ROI located over the soma were chosen. Overall Ca^{2+} -response to receptors agonists or synaptic stimulation was quantified using an ROI covering the whole cell image.

Data Analysis

All data are presented as mean ± SD and the statistical significance of differences between data groups was tested by two-tailed unpaired *t*-test, unless indicated otherwise. For all cases of statistical significance reported, the statistical power of the test was 0.8–0.9.

The spontaneous transmembrane currents recorded in neurons were analyzed off-line using methods described previously (Lalo et al., 2014a, 2016). The amplitude distributions of spontaneous and evoked currents were analyzed with the aid of probability density functions and likelihood maximization techniques; all histograms shown were calculated as probability density functions. The amplitude distributions were fitted with either multi-quantal binomial model or bi-modal function consisting of two Gaussians with variable peak location, width and amplitude. Parameters of models were fit using likelihood maximization routine.

RESULTS

Age- and Environment-Related Alterations in Astroglial Ca^{2+}-Signaling

We recorded spontaneous and evoked cytosolic Ca^{2+}-transients in the branches and somata of neocortical astrocytes of EFGP/GFAP mice of four age groups: young (average 4.2 weeks), adult (4.4 months), old (10.3 months), and very old (21.4 months). Mice were kept under SH or exposed either to enriched environment (EE) or CR; the details are given in *Methods*. The astrocytes in brain slices were loaded with fluorescent Ca^{2+}-probe Rhod-2AM and identified by their green fluorescence (**Figure 1A**) and, after the recordings, by their characteristic electrophysiological signature (Lalo et al., 2011a, 2014b).

In baseline, before synaptic stimulation or agonists application, astrocytes of mice of all age groups exhibited spontaneous Ca^{2+}-transients, which were more prominent in the astrocytic branches (**Figure 1A**). The average frequency of spontaneous Ca^{2+}-transients in astrocytes of young SH mice was 0.23 ± 0.11 min^{-1} in the soma but reached of 1.38 ± 0.41 min^{-1} in the astrocytic arborization (i.e., calculated for the whole cell image except soma). For the sake of simplicity, the further analysis of alterations in the spontaneous Ca^{2+}-signaling used data evaluated for the whole astrocyte image. This predominantly reflected a situation in the astrocytic branches but would not distort the overall picture since the changes in purinergic signaling in the somata followed the same trend as in branches. Also, it is widely recognized that Ca^{2+}-events relevant for astroglia functions and glia-neuron interaction occur mainly in the astrocytic processes (Khakh and McCarthy, 2015; Bazargani and Attwell, 2016; Agarwal et al., 2017).

We observed a moderate increase in the amplitude and frequency of spontaneous astrocytic Ca^{2+}-transients of SH mice during maturation (i.e., between age groups I and II) which was the followed by strong age-dependent decrease (**Figure 1B**). Exposure to the EE or CR significantly increased the spontaneous astroglial Ca^{2+}-signaling in the old mice (**Figure 1B**). To evaluate the overall contribution of ATP receptors to spontaneous astroglial signaling, we applied purinoreceptor antagonists PPADS which, in concentration used (10 μM), efficiently and selectively inhibits P2X and P2Y receptors. The application

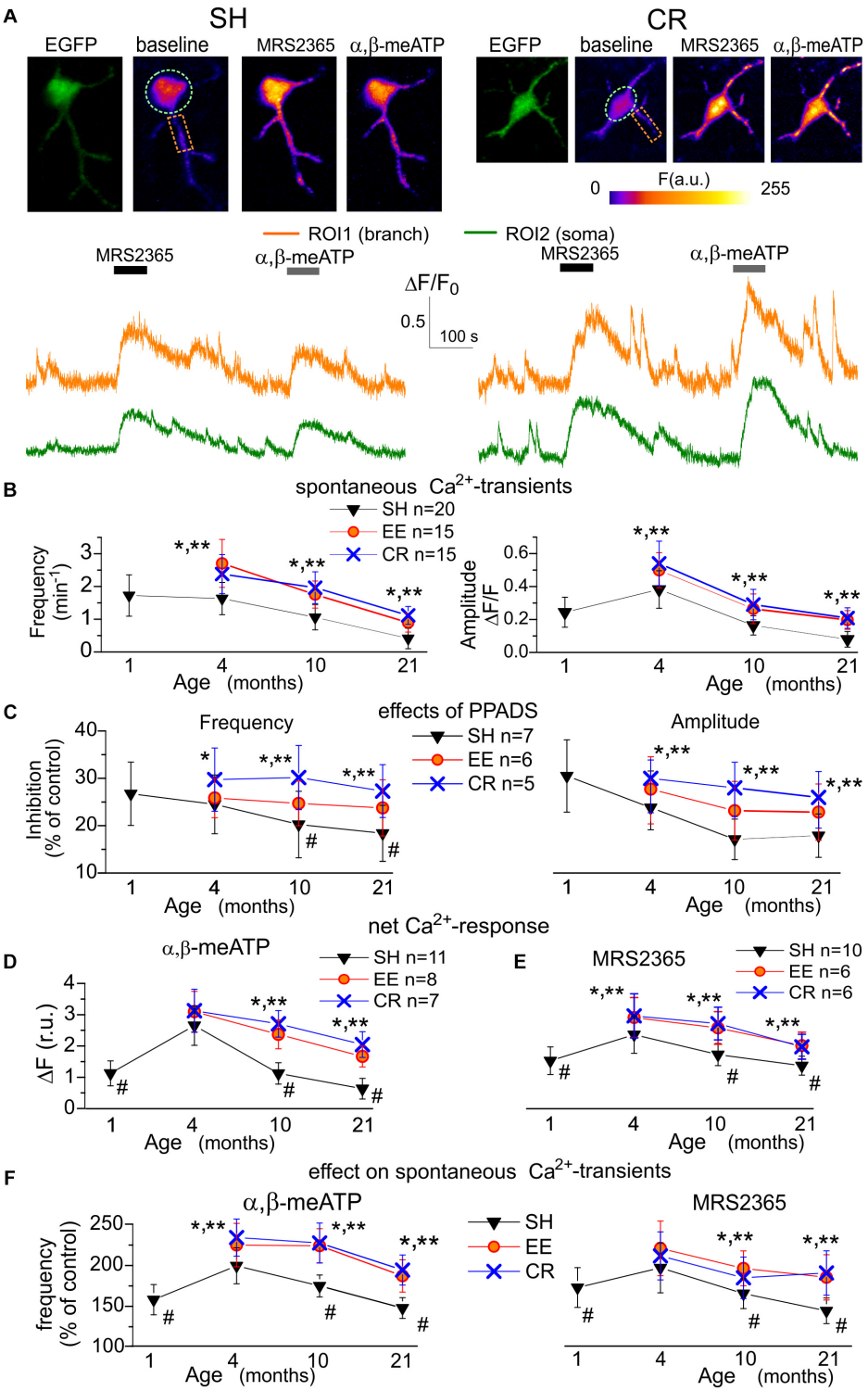

FIGURE 1 | Age- and experience-related changes in the purinergic astrocytic Ca^{2+} signaling. **(A)** Representative multi-photon images of EGFP fluorescence and pseudo-color images of Rhod-2 fluorescence recorded in the astrocytes of old GFAP-EGFP (GFEC) mice kept in the standard housing conditions (SH) and exposed to calorie restriction diet (CR). Images were acquired before (baseline) and after the application of specific agonists of P2X (α,β-me ATP) and P2Y1 (MRS2365) receptors. Graphs below show the time course of Rhod-2 fluorescence averaged over regions of interests (ROI) indicated in the fluorescence images. Note the marked increase in the spontaneous Ca^{2+}-elevations and Ca^{2+}-responses to α,β-me ATP and MRS2365. **(B)** The pooled data on the peak amplitude and frequency of baseline spontaneous Ca^{2+}-transients recorded in the astrocytes of mice of different age and treatment groups. **(C)** The pooled data on the effect of

(Continued)

FIGURE 1 | Continued
P2 purinoreceptor antagonist PPADS on the peak amplitude and frequency of spontaneous Ca^{2+}-transients. **(D,E)** The pooled data on the net responses to application of α,β-me ATP and MRS2365 in the different age groups. Net response was evaluated as an integral Ca^{2+}-signal measured within 3 min after stimulation and normalized to the baseline integral Ca^{2+} signal. **(F)** The pooled data on the changes in the frequency of spontaneous Ca^{2+}-transients (relative to the baseline) registered in the neocortical astrocytes within 5 min after application of α,β-me ATP and MRS2365; the cell numbers are the same as in **(D,E)**. Data in the panels **(B–F)** are shown as mean ± SD for the 6–12 astrocytes (as indicated) from 3 to 6 animals. The hush symbols (#) indicate statistical significance ($P < 0.02$) of the difference between the adult SH mice and SH mice of other age groups. Asterisks (*, **) correspondingly indicate statistical significance ($P < 0.05$) of the effect of EE- or CR-treatment (as compared to SH mice of the same age group). Note the significant increase in the spontaneous and agonist-evoked Ca^{2+}-signaling in astrocytes of mice exposed to EE and CR.

of PPADS partially inhibited spontaneous Ca^{2+} events in the astrocytes of mice of all ages and treatments. The relative effect of PPADS on the amplitude and frequency of Ca^{2+} -events was correspondingly 30.5 ± 7.8% and 26.7 ± 6.7% in the astrocytes of young SH mice with a tendency of moderate decrease in the old age (**Figure 1C**). Interestingly, exposure to CR led to the notable increase in the relative contribution of P2 purinoreceptors to astroglial Ca^{2+} -transients (**Figure 1C**). Hence, the age- and experience-related alterations in the spontaneous Ca^{2+} -transients might be attributed to the changes in the functional expression of P2X and/or P2Y receptors as important components of astrocytic signaling.

As previous works suggested $P2X_1$ and $P2Y_1$ subunits-containing receptors to bring main contribution to purinergic signaling in cortical astrocytes (Lalo et al., 2008; Butt, 2011; Di Castro et al., 2011; Mederos et al., 2019) we applied their agonists α,β-me ATP (10 μM) and MRS2365 (10 nM) to activate correspondingly ionotropic and metabotropic components of Ca^{2+}-signaling (**Figures 1A,D,E**). Application of both agonists induced notable Ca^{2+}-responses in the neocortical astrocytes of mice of all age groups (**Figures 1A,D,E**). Also, both α,β-me ATP and MRS2365 significantly increased the frequency of spontaneous Ca^{2+}-transients (**Figure 1F**). The P2X-mediated response and effect of α,β-meATP on spontaneous signaling showed significant age-related decline but were rescued in the astrocytes of EE and CR-exposed mice (**Figures 1D,F**). In contrast to the P2X-mediated component, the metabotropic MRS2365-evoked Ca^{2+}-response showed a moderate age-dependent decline (**Figure 1E**). Still, effects of EE and CR on $P2Y_1$-mediated astrocytic signaling in the old mice were statistically significant.

Since age-related alterations in the repertoire of P2 purinoreceptors expressed in astrocytes could not be ruled out *a priori*, we also tested the effects of drugs selective for $P2X_7$, $P2X_4$, and $P2Y_2$ receptors (**Figure 2**). Although we observed a notable elevation of cytosolic Ca^{2+} in astrocytes after application of P2X7 receptor agonist BzATP (100 μM), these Ca^{2+}-responses were weakly sensitive to the specific P2X7 antagonist A740003 (1 μM) but were effectively inhibited by PPADS in moderate (10 μM) concentrations (**Figures 2A,B**). In parallel, application of P2X7 antagonist A740003 did not had a significant inhibitory effect of the spontaneous Ca^{2+}-transients in astrocytes. These results argue against a significant contribution of $P2X_7$ receptors in the purinergic signaling in neocortical astrocytes, at least in our experimental paradigm.

We also observed only marginal inhibitory effects of selective $P2X_4$ antagonist 5-BDBD on the amplitude and frequency of spontaneous astrocytic Ca^{2+}-transients in the SH mice of all age groups (overall 3.8 ± 3.1%, $n = 14$; data not shown). In contrast, application of $P2Y_2$ subtype-specific agonist MRS2678 (10 μM) elicited a modest elevation of cytosolic Ca^{2+} in the branches and soma of astrocytes in all age groups (**Figures 2C,D**); these Ca^{2+}-responses were not sensitive to the specific $P2Y_1$ antagonist. The $P2Y_2$-mediated Ca^{2+}-transients reached about 10–15% of signals activated via $P2Y_1$ receptors and exhibited a weak age-dependent decline (**Figure 2C**).

These results strongly support the dominant role of $P2X_1$ and $P2Y_1$ subunit-containing receptors in the purinergic signaling in neocortical astrocytes and suggest that surface expression of functional purinoreceptors can undergo significant remodeling across a life-time and in response to the experience and diet. Age-related changes in the surface expression of P2 receptors can alter the responsiveness of astrocytes to the ATP released from the neighboring synapses as a co-transmitter (Pankratov et al., 2007; Lalo et al., 2016) and, thereby, affect their ability to monitor neuronal activity. To explore this, we investigated the changes in the Ca^{2+}-responses of astrocytes to the stimulation of surrounding synapses.

Synaptically Activated Ca^{2+}-Transients in Cortical Astrocytes

As in our previous study of electrical signaling in astrocytes (Lalo et al., 2011a), we recorded synaptically activated Ca^{2+}-responses evoked in the layer II/III astrocytes by the stimulation of neuronal afferents originating from layers IV-VI (**Figure 3A**). The synaptically evoked astroglial Ca^{2+}-signaling moderately increased in the mature adult animals and then exhibited the significant age-dependent decline both in the somata and branches (**Figures 3A,B**). An exposure to EE and CR caused statistically significant increase in the evoked astrocytic Ca^{2+}-response in mice of all age groups (**Figure 3B**).

As several different types of receptors, including NMDA, mGluR, and CB1, could participate in Ca^{2+}-responses of astrocytes to synaptic stimulation (Lalo et al., 2008; Palygin et al., 2010; Rasooli-Nejad et al., 2014), we dissected the contribution of P2X and P2Y receptors pharmacologically, by applying a range of specific antagonists. We used highly subtype-specific antagonists NF449 (10 nM) and MRS2279 (300 nM) targeting correspondingly $P2X_1/P2X_{1-5}$ and $P2Y_1$ receptors which were expected to bring major contribution into astroglial purinergic signaling in young mice (Lalo et al., 2008, 2011a; Butt, 2011).

The inhibitory effect of NF449 on the synaptically activated Ca^{2+}-transients reached 18.7 ± 4.9% ($n = 9$, $P < 0.05$) in the

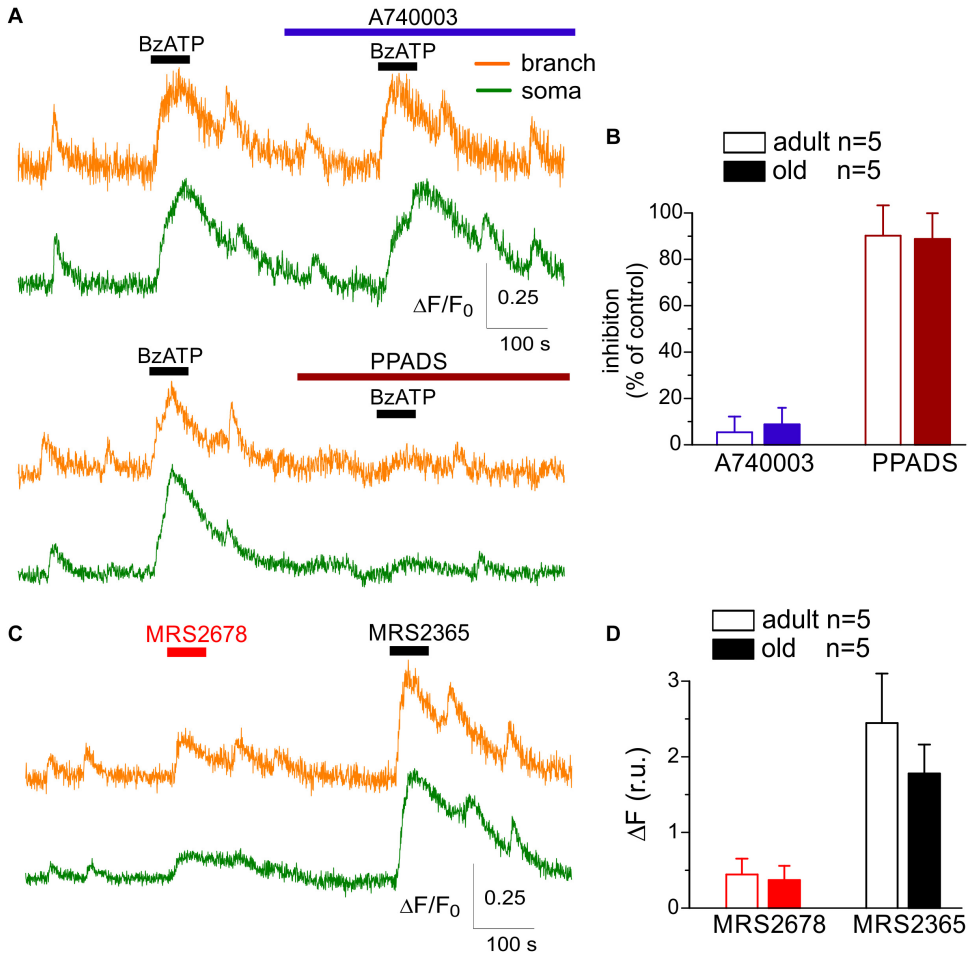

FIGURE 2 | Action of subtype-specific drugs on Ca^{2+}-signaling in cortical astrocytes. **(A,B)** Effect of P2X7 subtype-specific drugs. **(A)** Representative traces of Rhod-2 fluorescence recorded in the branches and somata of astrocytes of old SH mice. Fluorescence was measured before and after the application of P2X7 receptor agonist BzATP in control and in the presence of highly selective P2X7 antagonist A740003 and general P2 purinoreceptor antagonist PPADS. **(B)** The pooled data on the relative inhibitory effects of A740003 and PPADS on the net Ca^{2+}-response to BzATP recorded in astrocytes of adult (4 month-old) and old (10 month-old) SH mice. The net response was evaluated as an integral Ca^{2+}-signal measured within 3 min after stimulation, averaged over the whole cell image and normalized to the baseline integral Ca^{2+} signal. Note the lack of effect of P2X7-selective inhibitor A740003. **(C,D)** Effect of P2Y2 subtype-specific agonist MRS2678. **(D)** Representative traces of Rhod-2 fluorescence recorded in the branches and somata of astrocytes of old SH mice before and after application of selective agonists P2Y2 (MRS2678) and P2Y1 receptors (MRS2365). **(D)** The pooled data on the net Ca^{2+}-response to MRS2365 and MRS2678 recorded in astrocytes of adult (4 month-old) and old (10 month-old) SH mice.

young SH mice (**Figure 3C**) and showed moderate increase in the adult mice but declined sharply in the old and very old age. The age-related decline in the ionotropic purinergic (NF449-sensitive) Ca^{2+}-signaling was partially ameliorated in the astrocytes of EE and CR-exposed mice (**Figure 3C**). In contrast to the P2X-mediated component, the metabotropic MRS2279-sensitive component of synaptically evoked Ca^{2+}-transients showed a sharp decrease in old and very old age and rather modest EE- and CR-induced enhancement (**Figure 3D**).

Interestingly, both P2X- and P2Y-mediated components of synaptically activated response (**Figure 3**) showed steeper age-related decline and were less susceptible to EE and CR as their agonist-induced counterparts (**Figure 1**). The most likely explanation could be that, in parallel to alterations in the density of purinoreceptors, the release of ATP from synaptic terminals also underwent considerable changes. The decline in the synaptic release of ATP should have led to alterations in the purinergic synaptic currents in neurons which we explored in the next series of experiments.

Age- and Environment-Related Alterations in Neuronal Purinergic Signaling

We have shown in the series of previous work that cortical pyramidal neurons of young mice express ionotropic P2X purinoreceptors which can be activated by release of ATP from both synaptic terminals and astrocytes (Lalo et al., 2014a, 2016). So, it might be plausible to detect P2X-mediated spontaneous currents in neurons of older animals. We recorded

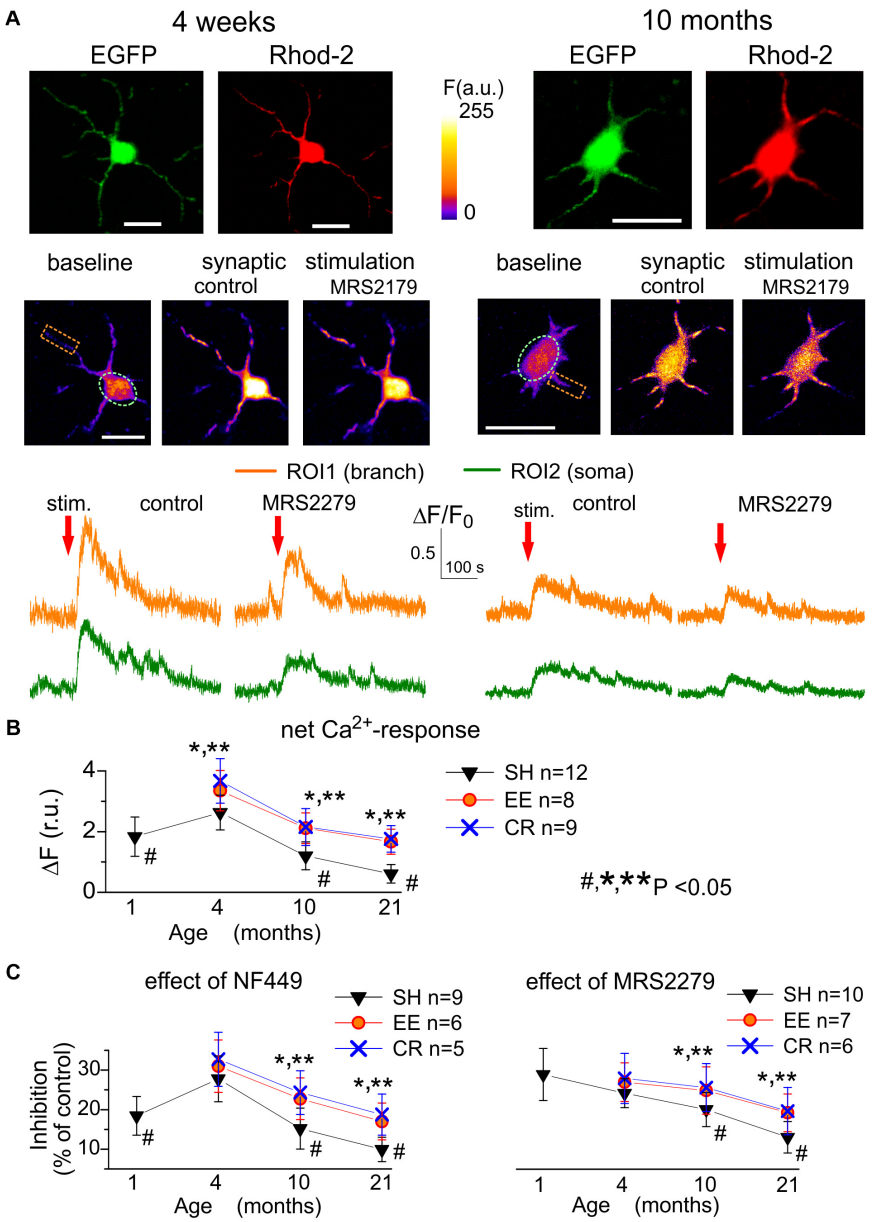

FIGURE 3 | Age- and experience-related plasticity of astroglial Ca^{2+}-response to synaptic stimulation. Ca^{2+} -signaling was monitored in cortical astrocytes loaded with Rhod-2AM using multi-photon fluorescent microscopy similar to the **Figure 1**. **(A)** Representative multi-photon images of EGFP fluorescence and pseudo-color images of Rhod-2 fluorescence recorded in the astrocytes of young (4 weeks) and very old (11 months) SH mice before (baseline) and after the stimulation (stim.) of cortical afferents under control conditions and in the presence of selective P2Y1 antagonist MRS2279 (10 nM). **(B,C)** The pooled data on the net responses of astrocytes (quantified similar to **Figure 1**) to the synaptic stimulation **(B)** and inhibitory effects of selective antagonists of P2X1 and P2Y1 receptors **(C)**. Data in the panels **(B,C)** are shown as mean ± SD for the 5–12 astrocytes (as indicated) from 3 to 5 animals. The hush symbols (#) indicate statistical significance ($P < 0.02$) of the difference between the adult SH mice and SH mice of other age groups. Asterisks (*, **) correspondingly indicate statistical significance ($P < 0.05$) of the effect of EE- or CR-treatment (as compared to SH mice of the same age group). Note the significant increase in the synaptically evoked Ca^{2+}-signaling in astrocytes of mice exposed to EE and CR.

the whole-cell currents in neocortical pyramidal neurons at a membrane potential of −80 mV in the presence of picrotoxin (100 μM), D-APV (30 μM), and NBQX (30 μM), to eliminate the signals mediated correspondingly by the GABAA, NMDA, and AMPA receptors (**Figure 4**). We observed the residual non-glutamatergic miniature excitatory spontaneous synaptic currents (mEPSCs) in neurons of adult (91% of cells tested), old (85% of neurons), and very old mice (77% of neurons). These residual non-glutamatergic mEPSCs were abolished by application of specific P2XRs antagonists PPADS (10 μM) and 5-BDBD (5 μM) in neurons of adult, old and very old mice (correspondingly 15,11 and 11 cells). Based on this results as

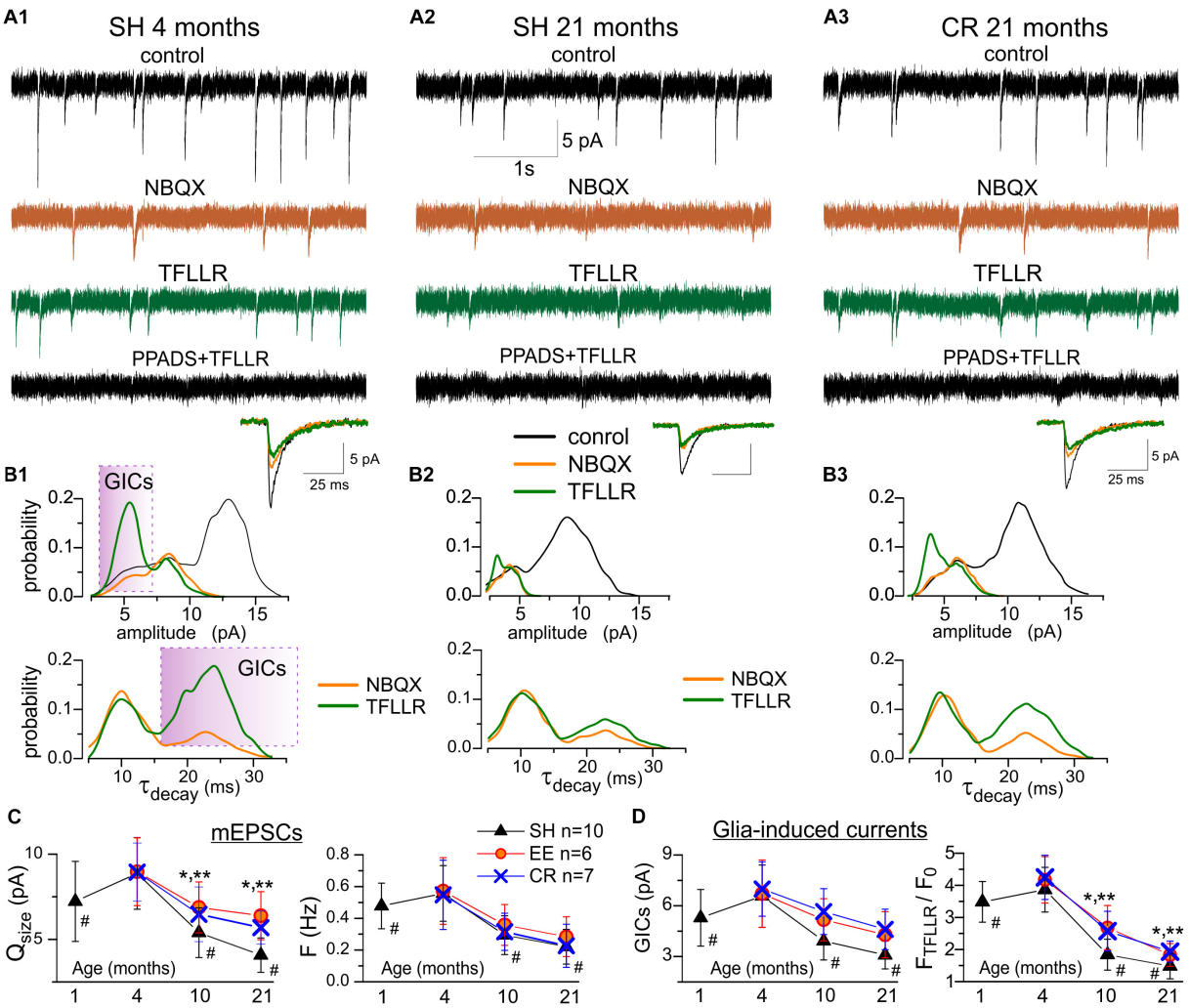

FIGURE 4 | Age- and experience-related alterations in purinergic currents in neocortical neurons. The spontaneous transmembrane currents were recorded in the layer 2/3 pyramidal neurons of neocortical slices of the adult **(A1,B1)** and very old mice **(A2,3,B2,3)** at holding potential of –80 mV in presence of picrotoxin (100 μM). **(A1–3)**, *upper row* shows the representative transmembrane currents recorded before the application of NBQX (control), the AMPA receptors-mediated mEPSCs comprise the main fraction of spontaneous events; two *middle rows* show the non-glutamatergic inward spontaneous currents, recoded under NBQX before and 1 min after activation of Ca^{2+} -signaling in the astrocytes by selective agonist of astroglial PAR-1 receptors (TFLLR 10 μM); *bottom row* show transmembrane currents recorded after inhibition of P2X receptors with selective antagonists PPADS and 5-BDBD. The inserts at the bottom show an average mEPSCs waveforms under different conditions. Note the large increase in the number of non-glutamatergic currents in the adult mice under TFLLR and their disappearance under PPADS and 5-BDBD. **(B1–3)** the corresponding distributions (probability density functions) of the amplitude (*upper row*), and decay time (*lower row*) of spontaneous currents recorded before and after application of NBQX and TFLLR. Distributions reveal the presence of distinct population of spontaneous currents of smaller amplitude and slower kinetics in mice of both age groups. Stimulation of astrocytes with TFLLR significantly increases the peaks corresponding to smaller and slower sEPSCs, thus verifying their origin from astroglial release of ATP, as previously reported in Lalo et al. (2014a). Shaded areas indicate the range of decay times and amplitudes used to discriminate the glia-induced currents (GICs) from the currents of synaptic origin (mEPSCs) for the subsequent analysis of age-related plasticity **(C,D)**. **(C)** Pooled data on the quantal size (determined for each neuron as position of corresponding peak at the amplitude histogram) and frequency of purinergic mEPSCs in the mice of different age and experience groups. **(D)** pooled data on the quantal size of relative TFLLR-induced increase in the frequency of purinergic GICs. The data in the panels **(C,D)** are shown as mean ± SD for the 6–10 neurons (as indicated in **C**) from 3 to 4 animals. The hush symbols (#) indicate statistical significance ($P < 0.02$) of the difference between the adult SH mice and SH mice of other age groups. Asterisks (*, **) correspondingly indicate statistical significance ($P < 0.05$) of the effect of EE- or CR-treatment (as compared to SH mice of the same age group). Note the significant decrease in the quantal size and frequency of purinergic currents in the old and very old mice (10–21 months) and increase in the synaptic and glia-induced neuronal purinergic signaling in mice exposed to EE and CR.

well as our previous work (Pankratov et al., 2003, 2007; Lalo et al., 2014a, 2016), the spontaneous inward currents observed in the neocortical neurons in the presence of glutamatergic and GABAergic antagonists can be confidently attributed to the P2X receptors.

The spontaneous purinergic currents recorded in neurons of the adult SH mice under baseline conditions had an average amplitude of 8.1 ± 2.5 pA and an average decay time of 9.8 ± 2.9 ms ($n = 12$). We previously showed (Lalo et al., 2014a) that in neurons of young mice spontaneous purinergic currents

could be divided into two populations: events of larger amplitude and faster decay kinetics and events of smaller amplitude and slower decay kinetics; the former population comprised events of synaptic origin whereas the latter population was elicited by exocytosis of ATP from astrocytes. Existence of two population of events manifested in the appearance of two peaks at amplitude and decay time distribution histograms (Lalo et al., 2014a). Activation of Ca^{2+}-signaling in astrocytes, in particular via astroglia-specific PAR-1 receptors, dramatically increase the frequency of the smaller-and-slower currents, verifying their astroglial origin (Lalo et al., 2014a).

In consistence with our previous findings in young mice (Lalo et al., 2014a), the amplitude distribution of purinergic currents in pyramidal neurons of adult animals (**Figure 4A1**) exhibited a bimodal pattern with minor peak of smaller amplitude (5.5 ± 1.6 pA) and major peak of larger amplitude (8.7 ± 2.3 pA, $n = 12$). The distribution of mEPSCs decay time in these neurones exhibited peaks at 9.1 ± 1.4 ms and 21.8 ± 5.7 ms. The number of purinergic events of smaller amplitude and slow kinetics dramatically increased upon activation of astrocytes with PAR-1 agonist TFLLR (10 μM) which manifested in the enhancement of the corresponding peaks in the amplitude and decay time distributions (**Figure 4B1**). Hence, both in young and old mice (**Figures 4A2–B3**), quantal purinergic currents originating from the release of ATP from synaptic terminals and astrocytes can be distinguished by their biophysical properties. The baseline spontaneous purinergic currents of faster kinetics and larger amplitudes represent events elicited by release of ATP from synaptic terminals (referred further as purinergic mEPSCs) whereas the currents of slower kinetics, whose frequency increased upon stimulation of astrocytes with TFLLR, originate from glial release of ATP (referred further as glia-induced currents, GICs).

Thus, we used the amplitude and frequency of the baseline mEPSCs as post- and presynaptic readouts for ATP-mediated synaptic transmission (**Figure 4C**). Conversely, the TFFLR-induced elevation in the GICs frequency was used as a readout for astrocytic ATP release (**Figure 4D**). The mean amplitude and frequency of purinergic mEPSCs underwent significant decrease in the neurons of old and very old SH mice (**Figures 4A2,B2,C**); this result suggests that aging can affect both the surface density of synaptic P2X receptors and probability of ATP release from synaptic terminals. In parallel, the frequency of TFLLR-induced purinergic GICs exhibited strong age-dependent decrease (**Figures 4A2,B2,D**). This results implies that glia release of ATP can undergo substantial decline with aging which closely agrees with our previous data obtained using ATP microelectrode biosensors (Lalo et al., 2018).

Exposure to EE and CR caused an enhancement in the purinergic mEPSCs and GICs in all age groups, especially in the old and very old mice (**Figures 4A3,C,D**). In line with their effects on functional expression of P2X receptors in astrocytes (**Figure 1**), EE and CR substantially increased the amplitude of neuronal mEPSCs (**Figure 4C**). However, the effect of EE and, especially CR, on synaptic and astroglial release of ATP were not that prominent. Both treatments did not have significant effect on the frequency of mEPSCs (**Figure 4C**) and just moderately enhanced the frequency GICs in old and very old mice (**Figure 4D**). The weaker effects of EE and CR on the synaptic and astroglial exocytosis of ATP in the old age might be attributed to the general decline in metabolic functions of aging brain (Mercken et al., 2012; Lopez-Otin et al., 2016) which would very likely affect the production of ATP and its accumulation in synaptic/glial vesicles.

Combined together, our results demonstrate that the purinergic component of synaptic transmission and astrocyte-to-neuron communications can undergo substantial decline in the aging brain. It was shown previously in young mice that activation of post-synaptic purinoreceptors can up-regulate AMPA-receptor-mediated synaptic currents and down-regulate GABAergic inhibition (Boue-Grabot and Pankratov, 2017). Hence, one might expect astrocyte-driven purinergic modulation to change in the adult and very old mice.

Changes in the Purinergic Modulation of AMPA Receptor-Mediated Synaptic Currents

We recorded the AMPA receptor-mediated miniature spontaneous synaptic currents in the pyramidal neurons at membrane potential of −80 mV in presence of picrotoxin and TTX. Under this conditions, the main fraction of spontaneous events was represented by the AMPA- receptor-mediated mEPSCs, which could be easily discriminated from the purinergic events by much larger quantal size, as evidenced by **Figures 4A1,B1**. In the adult mice, the mean amplitude of AMPAR-mediated mEPSCs showed significant increase (up to 25–30%) upon activation of astrocytes with TFLLR (**Figures 5A,C**); the mean mEPSCs frequency did not undergo marked changes. Analysis of the mEPSCs amplitude distribution showed the considerable rightward shift after TFLLR application indicating the increase in the quantal size. The effect of TFLLR was abolished by inhibition of P2X receptors with PPADS and 5-BDBD (**Figure 5C**). These results verify the post-synaptic locus and purinergic mechanism of the astroglia-driven enhancement of excitatory synapses.

Importantly, the TFLLR-induced modulation of AMPAR-mediated mEPSCs was significantly decreased (**Figures 5A,C**) in the very old mice where neuronal purinergic signaling and exocytosis of ATP from astrocytes is impaired (**Figure 4**). One might expect that manipulations which ameliorate age-related decline in purinergic signaling would also rescue purinergic modulation in the old mice. Indeed, exposure to EE significantly increased the effect of TFLLR on the quantal size of glutamatergic mEPSCs. The CR had much less prominent but still statistically significant effect (**Figure 5C**).

Changes in the Purinergic Modulation of GABAergic Inhibition

As a readout for astroglia-driven modulation of GABAergic inhibition, we evaluated the TFLLR-induced modulation of tonic bicuculline-sensitive inhibitory currents, using experimental paradigm similar to our previous work in the young mice

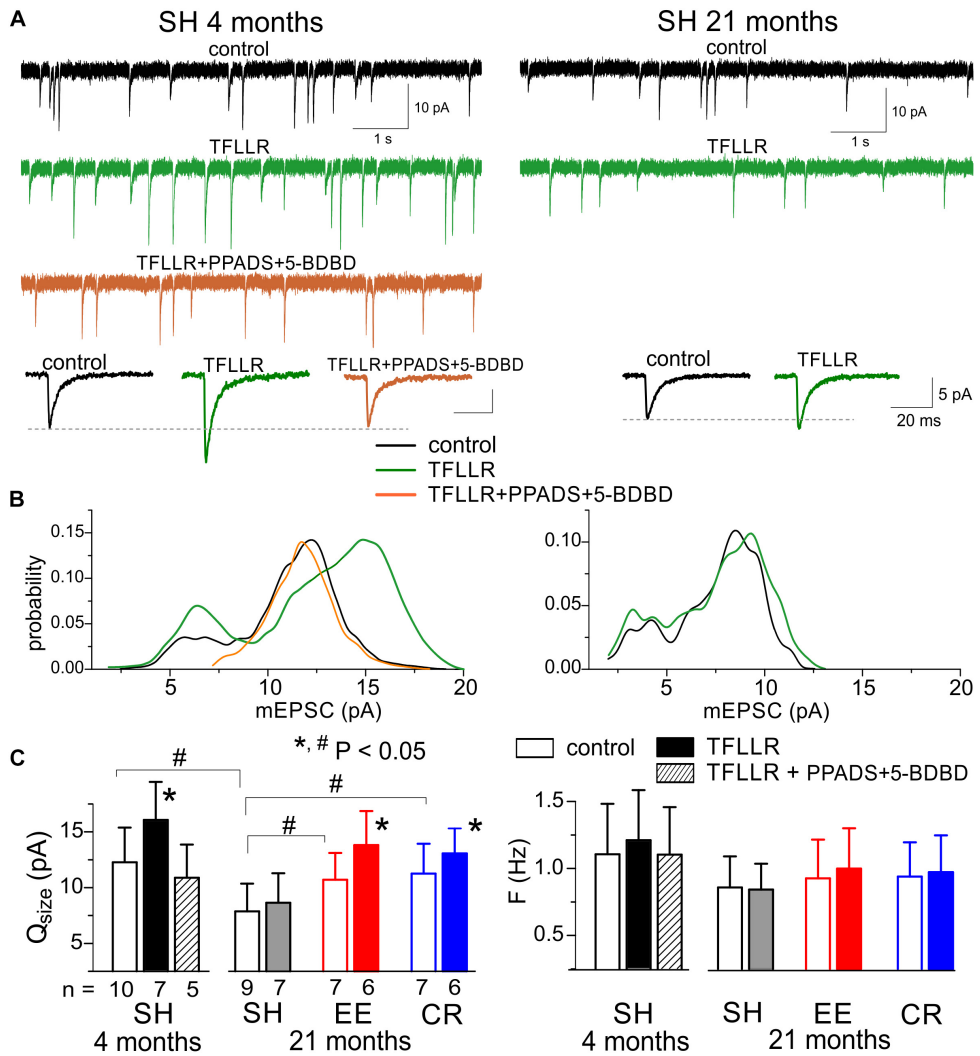

FIGURE 5 | Astrocyte-driven modulation of excitatory synaptic currents in neocortical neurons. The AMPA receptor-mediated spontaneous mEPSCs were recorded in the neocortical neurons of adult (4 months) and very old (21 months) mice at –80 mV in presence of 100 μM picrotoxin, 1 μM TTX, and 30 μM D-APV. Astroglial modulation of mEPSCs was triggered by 3 min-long bath application of TFLLR. **(A)** the representative whole-cell currents recorded in the pyramidal neurons before (baseline) and 1 min after application of TFLLR alone or in the presence of P2X receptor antagonists PPADS and 5-BDBD. The insets below show the average mEPSCs waveforms recorded under different conditions. **(B)** The corresponding amplitude distributions (probability density functions calculated for 100–300 events registered over 5 min period). Note the significant increase in the mEPSCs amplitude after application of TFLLR in the neurons of adult mice and the lack of changes when TFLLR was applied in the presence of P2X receptor blockers. The post-synaptic alteration in the quantal size of mEPSCs is evidenced by rightward shift of the peak of amplitude distribution. **(C)** Diagrams show the quantal size and frequency of AMPAR-mediated mEPSCs in adult and very old mice of different environment groups; the data are shown as mean ± SD for the number of neurons indicated below. The hush symbols (#) indicate statistical significance ($P < 0.05$) of the difference between the age and environment groups. Asterisks (*) correspondingly indicate statistical significance ($P < 0.05$) of the effect of TFLLR (as compared to the control).

(Lalo et al., 2014a). Activation of astroglial PAR-1 receptors by TFLLR, which has been shown to induce ATP release (Lalo et al., 2014a), caused a significant decrease in the tonic inhibitory currents in the neocortical pyramidal neurons of adult mice (**Figure 6A**). This effect was occluded after inhibition of P2 purinoreceptors with PPADS and 5-BDBD, confirming the crucial role astrocyte-derived ATP (**Figures 6A,C**).

We observed the substantial up-regulation in the baseline tonic inhibitory currents in the neurons of very old mice which was accompanied by the marked attenuation of the effect of TFLLR (**Figure 6B**). These alterations resembled the previously reported phenotype (Lalo et al., 2014a) of mice with the deficit of astrocytic exocytosis of ATP (dnSNARE line). In line with data on modulation of excitatory currents, the astroglia-driven modulation of tonic inhibition in the very old mice was rescued by EE and CR (**Figures 6C,D**). In contrast to experience-dependent changes in the excitatory currents (**Figure 5**), the effects of CR on the baseline tonic inhibition and its TFLLR-induced attenuation were much stronger than effects of EE (**Figure 6D**).

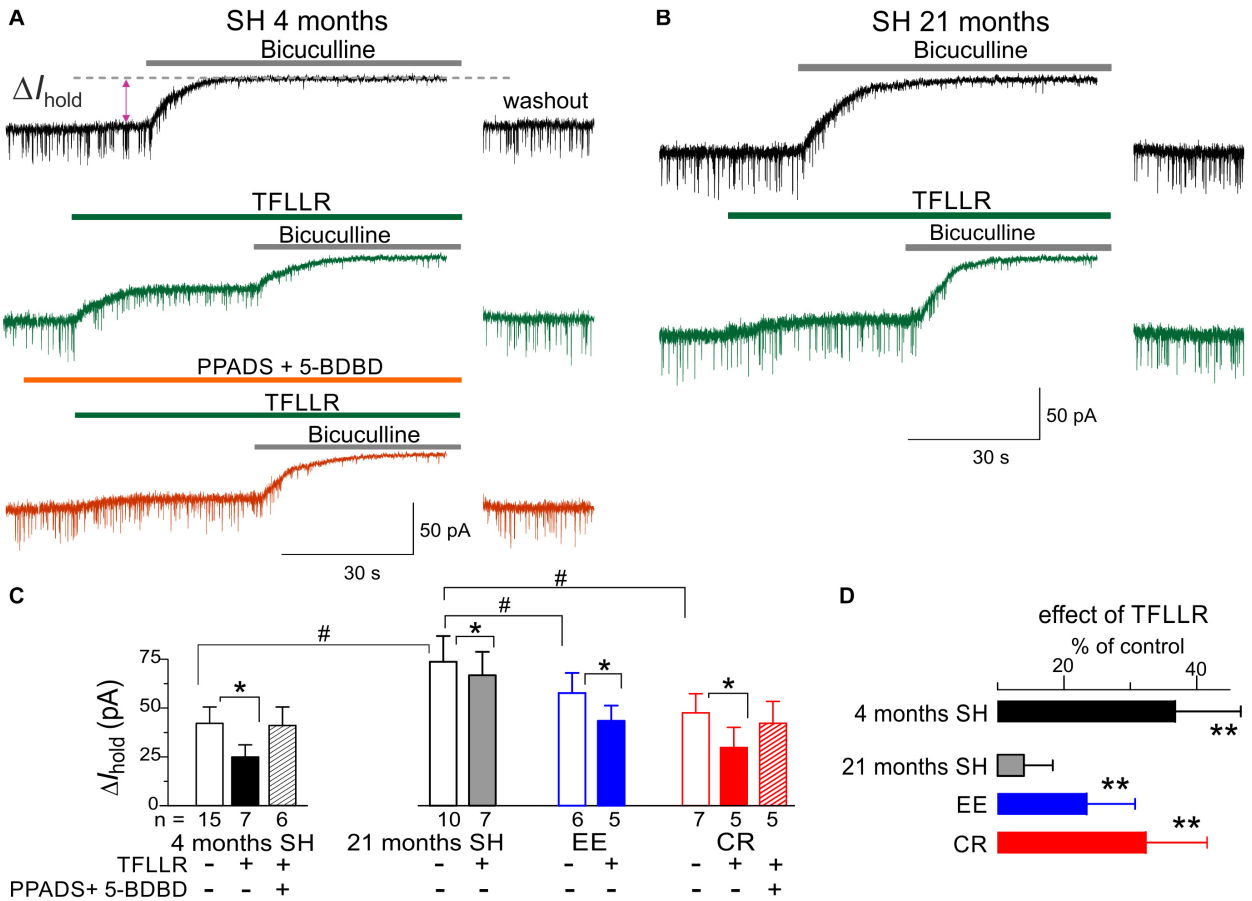

FIGURE 6 | Astrocyte-driven modulation of tonic GABAergic currents in neocortical neurons. **(A,B)** The tonic GABA-mediated currents were evaluated by upward shift in the whole-cell holding current (ΔI_{hold}) caused by application of bicuculline (50 μM) to the layer 2/3 pyramidal neurons in brain slices of adult (4 months) and very old (21 months) mice. Bicuculline was applied either in control (upper traces) or after activation of astrocytic signaling by 10 μM TFLLR (middle traces, *green*) or after application of TFLLR in presence of P2X receptors antagonist PPADS and 5-BDBD (bottom trace, *orange*). Currents were recorded in presence of NBQX (50 μM) and D-APV (30 μM) at holding potential of –80 mV. **(C)** The average amplitude of tonic GABA-mediated current measured in the mice of different age and environment groups; the data are shown as mean ± SD for the number of neurons indicated below. The hush symbols (#) indicate statistical significance ($P < 0.05$) of the difference between the age and environment groups. Asterisks (*) correspondingly indicate statistical significance ($P < 0.05$) of the effect of TFLLR (as compared to the control). **(D)** The pooled data (mean ± SD) on the relative effect of TFLLR on the tonic currents. Asterisks (**) indicate the statistical significance ($P < 0.01$) of difference from the very old mice of standard housing (21 months SH). Note that in the very old SH mice, the tonic inhibitory current was significantly up-regulated and activation of astroglial Ca^{2+} had much smaller effect on the tonic current than in the adult mice. The impact of aging on the TFLLR-induced modulation of the tonic current was ameliorated in the EE and CR mice.

DISCUSSION

Taken together, our results show that purinergic component of bi-directional communications between astrocytes and neurons can undergo marked remodeling across a lifetime and, in particular, in response to environment and experience. The data on age-dependent alterations in the P2X and P2Y receptors-mediated evoked and spontaneous signaling in astrocytes presented above (**Figures 1**, **2**) closely agree with our previous data on alterations in the ionotropic astrocytic signaling (Lalo et al., 2011a). We observed the general trend of significant decrease in the astrocytic purinergic signaling in the old and very old age which is in line with other reports on detrimental morphological and molecular changes in the astrocytes (Lalo et al., 2011a, 2014b; Rodriguez et al., 2014; Verkhratsky et al., 2014). These data suggest that ability of astrocytes to monitor and integrate activity of neighboring neuronal networks, which is crucial for many astroglia functions, can be compromised in the aged brain. So, the age-related decline in the astroglial purinergic signaling could play a specific role in onset and progression of neurodegenerative disorders.

Our results (**Figures 1**, **3**) also suggest that purinergic P2X and P2Y receptors can bring considerable contribution into Ca^{2+}-signaling in cortical astrocytes across a lifetime. We would like to note that, while the role for P2Y receptors in glial signaling is widely recognized (Abbracchio et al., 2009; Butt, 2011; Araque et al., 2014; Verkhratsky et al., 2017), a contribution of ionotropic P2X receptors remains often overlooked. This may result from some confusion about the specificity of the most frequently used and highly efficient P2Y1 antagonist MRS2179

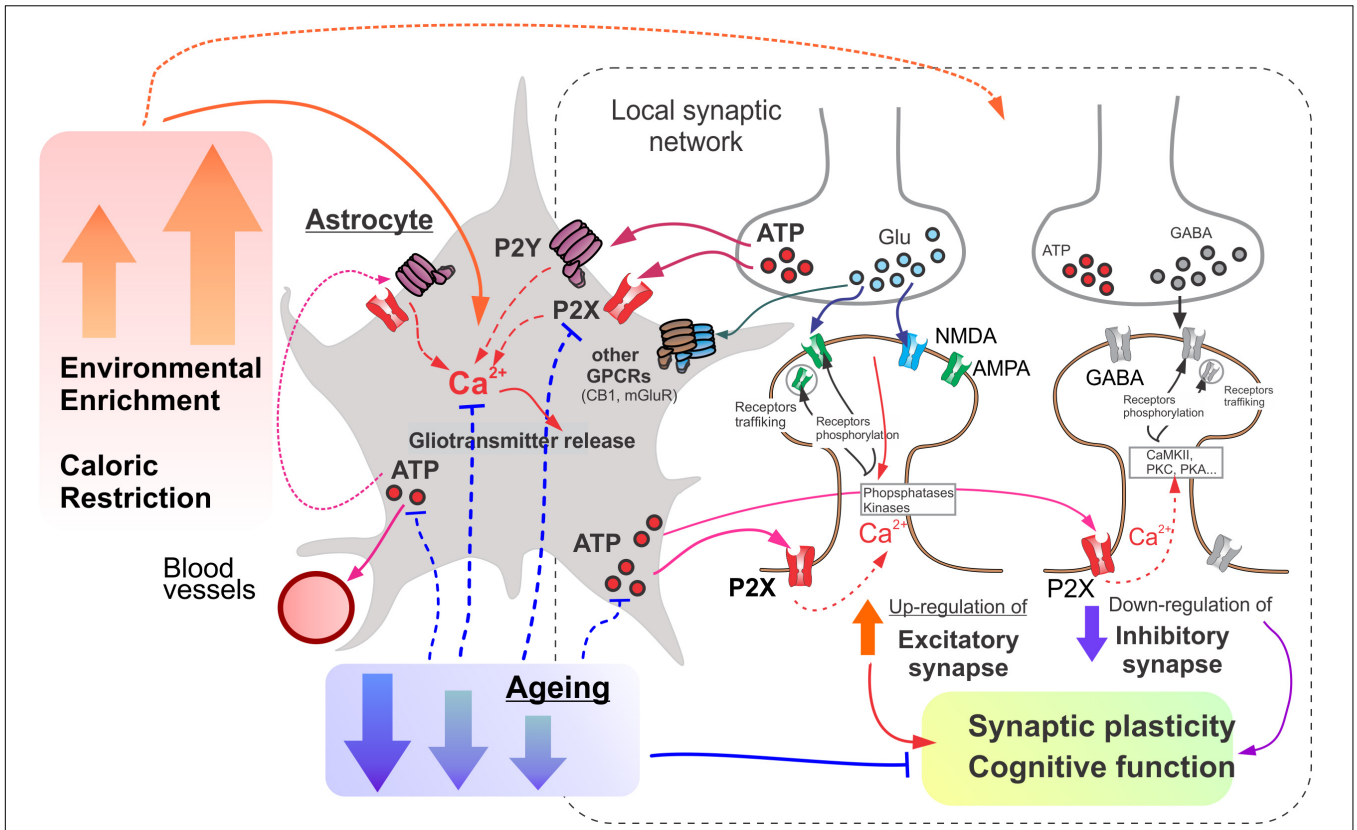

FIGURE 7 | The putative mechanisms underlying the involvement of astroglial purinergic signaling on the age- and experience-related brain plasticity. Astrocytes act a "Brain Hub" receiving signals from neurons and regulating synaptic transmission, neuronal metabolism, and neurovascular coupling. Astroglial purinergic Ca^{2+} signaling is activated by ATP released from synaptic terminals as a co-transmitter and ATP released from astrocytes. Astrocytes up-regulate excitatory and down-regulate inhibitory synapse by releasing ATP (as well as other gliotransmitters) thereby facilitating synaptic plasticity and cognitive functions. Age-related attenuation in astrocytic purinergic signaling compromises glial control of synaptic homeostasis. Environmental enrichment (EE) and caloric restriction (CR) enhance purinergic signaling in astrocytes and ameliorate the age-related decline in their function.

which was applied in many cases in the overkill concentrations (>1 μM). At such concentrations, MRS2179 can also inhibit the P2X1 subunit-containing receptors (Brown et al., 2000), which accordingly to our results, mediate the substantial part of ionotropic Ca^{2+}-signaling in astrocytes (Lalo et al., 2008; see also **Figures 1**, **3**). So, usage of MRS2179 at high concentrations can lead to overestimation the P2Y-mediated component for the expense of P2X-mediated component. To circumvent this problem, we used the more specific P2Y1 antagonist MRS2279 (Boyer et al., 2002). Our present results (**Figures 1**, **3**) confirm our previous conclusions on the importance of P2X receptor-mediated Ca^{2+}-influx in the function of neocortical astrocytes across a lifetime (Lalo et al., 2011a). Interestingly, the ionotropic component of purinergic Ca^{2+}-signaling showed sharp age-related changes (as compared to P2Y-mediated component) and turned out to be highly responsive to the beneficial effects of EE and CR. This may imply a novel physiological role for P2X receptors in astrocytes which are yet to be investigated.

Rather surprisingly, our data do not show any significant contribution of P2X7 receptors into spontaneous or evoked purinergic signaling in neocortical astrocytes (**Figure 2**) that may seem to disagree with numerous reports of P2X7 expression in glial cells (Butt, 2011; Rivera et al., 2016). Our results also support the previously expressed cautions against usage of BzATP as a definitive proof of P2X7-mediated activity (Anderson and Nedergaard, 2006). We would like to emphasize that present work has been focused primarily on changes in the purinergic signaling during physiological aging; particularly we optimized our tissue preparation procedure to minimize the risk of inflammation and ischemia in the brain slices of old mice. Accordingly to our estimations (Lalo et al., 2014a), the concentration of ATP in the extracellular space after vesicular release from neurons or astrocytes cannot exceed 10–100 μM which is not sufficient to activate the P2X7 receptors. The P2X7-mediated signaling, however, is usually associated with various pathological conditions such as neuro-inflammation, epilepsy and ischemia, where excessive ATP release can occur (Abbracchio et al., 2009; Rivera et al., 2016). The plausible function of astroglial P2X7 receptors upon these conditions surely deserves a further study, especially in the context of brain aging.

Our observation of decrease in astroglia-driven P2X-mediated currents in pyramidal neurons goes in line with data on the decline in astroglial exocytosis of ATP and other gliotransmitters (Lalo et al., 2014b, 2018). In parallel, we observed a decrease

in the quantal size of neuronal purinergic currents, which was, most likely, due to decrease in the density of post-synaptic P2X receptors. Hence, all parts of purinergic signaling with "tripartite synapse" can undergo significant decline with aging. Importantly, the purinergic signaling within a "tripartite synapse" turned out to be very responsive to EE and CR both at the post-synaptic and astroglial side (**Figures 1**, **4**).

Although (patho)physiological consequences of alterations of purinergic glia-neuron communications are yet to be fully understood, our data can give few important insights into this topic. In particular, our data show that ATP, in particular glia-derived, does not cease to play a neuro-modulatory functions in the synapses of aging brain but extent of purinergic modulation can decrease due to decline in the release of ATP and density of post-synaptic ATP receptors (**Figure 5**). Our present (**Figure 4**) and previous data (Lalo et al., 2014b, 2018) demonstrate that release of ATP can undergo significant decline with aging. This in turn can cause an impairment of purinergic astroglia-driven modulation of synaptic signaling, manifested in particular in the decrease in the glutamatergic (**Figures 5**, **7**) and increase in the GABAergic signaling (**Figures 6**, **7**). Such shift of the balance toward inhibition can affect the induction of long-term synaptic plasticity. So, the deficit in the purinergic component of glia-neuron communications could contribute to the age-related impairment of synaptic plasticity (**Figure 7**). This notion is supported by our previous data on the impairment of LTP in the neocortex of old mice which was rescued by additional stimulation of astrocytes or supplementing the ATP by exogenous non-hydrolysable analogs (Lalo et al., 2014b, 2018). This notion is further supported by our observations that manipulations facilitating neuronal P2X-mediated signaling and astroglial release of ATP, e.g., EE and CR, reversed the changes in excitatory and inhibitory synaptic signaling back to "younger" state (**Figures 5**, **6**). Interestingly, that effect of CR on the GABAergic currents in the very old mice was unexcitingly high (being large than effect of EE) taking into account rather moderate effect of CR on neuronal P2X-mediated currents (**Figure 4**). This suggest than mechanisms of beneficial effects of CR on neuronal signaling might involve other molecular cascades, particular modulation of autophagic processes in astrocytes and neurons (Lopez-Otin et al., 2016; Nikoletopoulou and Tavernarakis, 2018).

CONCLUSION

To conclude, our results strongly support physiological importance of astroglial purinergic signaling and glia-derived ATP for communication between astrocytes and neurons across a lifetime. The age-related decline in the purinergic component of glia-neuron interactions can lead to a dysregulation of excitatory and inhibitory synaptic signaling and thereby can be an aggravating factor, if not the cause, of cognitive decline in aging and neurodegenerative diseases. On another hand, our data demonstrate that EE and CR can enhance purinergic glia-neuron communications and ameliorate negative effects of aging on synaptic transmission.

DATA AVAILABILITY

The datasets generated for this study are available on request to the corresponding author.

ETHICS STATEMENT

All animal work was carried out in accordance with United Kingdom legislation and "3R" strategy; research did not involve non-human primates. This project was approved by the University of Warwick Animal Welfare and Ethical Review Body (AWERB), approval number G13-19, and regulated under the auspices of the United Kingdom Home Office Animals (Scientific Procedures) Act licenses P1D8E11D6 and I3EBF4DB9.

AUTHOR CONTRIBUTIONS

YP and UL conceived the study and wrote the manuscript. UL, AB, and YP performed the experiments and data analysis.

FUNDING

This work was supported by the grant from BBSRC UK (BB/K009192/1) to YP.

REFERENCES

Abbracchio, M. P., Burnstock, G., Verkhratsky, A., and Zimmermann, H. (2009). Purinergic signalling in the nervous system: an overview. *Trends Neurosci.* 32, 19–29. doi: 10.1016/j.tins.2008.10.001

Agarwal, A., Wu, P. H., Hughes, E. G., Fukaya, M., Tischfield, M. A., Langseth, A. J., et al. (2017). Transient opening of the mitochondrial permeability transition pore induces microdomain calcium transients in astrocyte processes. *Neuron* 93 587–605. doi: 10.1016/j.neuron.2016.12.034

Anderson, C. M., and Nedergaard, M. (2006). Emerging challenges of assigning P2X7 receptor function and immunoreactivity in neurons. *Trends Neurosci.* 29, 257–262. doi: 10.1016/j.tins.2006.03.003

Araque, A., Carmignoto, G., Haydon, P. G., Oliet, S. H., Robitaille, R., and Volterra, A. (2014). Gliotransmitters travel in time and space. *Neuron* 81, 728–739. doi: 10.1016/j.neuron.2014.02.007

Bazargani, N., and Attwell, D. (2016). Astrocyte calcium signaling: the third wave. *Nat. Neurosci.* 19, 182–189. doi: 10.1038/nn.4201

Boue-Grabot, E., and Pankratov, Y. (2017). Modulation of central synapses by astrocyte-released ATP and postsynaptic P2X receptors. *Neural. Plast* 2017:9454275. doi: 10.1155/2017/9454275

Boyer, J. L., Adams, M., Ravi, R. G., Jacobson, K. A., and Harden, T. K. (2002). 2-Chloro N(6)-methyl-(N)-methanocarba-2′-deoxyadenosine-3′,5′-bisphosphate is a selective high affinity P2Y(1) receptor antagonist. *Br. J. Pharmacol.* 135, 2004–2010. doi: 10.1038/sj.bjp.0704673

Brown, S. G., King, B. F., Kim, Y. C., Jang, S. Y., Burnstock, G., and Jacobson, K. A. (2000). Activity of novel adenine nucleotide derivatives as agonists and antagonists at recombinant Rat P2X receptors. *Drug Dev. Res.* 49, 253–259.

Burnstock, G. (2007). Physiology and pathophysiology of purinergic neurotransmission. *Physiol. Rev.* 87, 659–797.

Butt, A. M. (2011). ATP: a ubiquitous gliotransmitter integrating neuron-glial networks. *Semin. Cell Dev. Biol.* 22, 205–213. doi: 10.1016/j.semcdb.2011.02.023

Correa, S. A., Hunter, C. J., Palygin, O., Wauters, S. C., Martin, K. J., McKenzie, C., et al. (2012). MSK1 regulates homeostatic and experience-dependent synaptic

plasticity. *J. Neurosci.* 32, 13039–13051. doi: 10.1523/JNEUROSCI.0930-12.2012

De Strooper, B., and Karran, E. (2016). The cellular phase of alzheimer's disease. *Cell* 164, 603–615. doi: 10.1016/j.cell.2015.12.056

Delekate, A., Fuchtemeier, M., Schumacher, T., Ulbrich, C., Foddis, M., and Petzold, G. C. (2014). Metabotropic P2Y1 receptor signalling mediates astrocytic hyperactivity in vivo in an Alzheimer's disease mouse model. *Nat. Commun.* 5:5422. doi: 10.1038/ncomms6422

Di Castro, M. A., Chuquet, J., Liaudet, N., Bhaukaurally, K., Santello, M., Bouvier, D., et al. (2011). Local Ca2+ detection and modulation of synaptic release by astrocytes. *Nat. Neurosci.* 14, 1276–1284. doi: 10.1038/nn.2929

Fields, R. D., and Burnstock, G. (2006). Purinergic signalling in neuron-glia interactions. *Nat. Rev. Neurosci.* 7, 423–436.

Fields, R. D., and Stevens, B. (2000). ATP: an extracellular signaling molecule between neurons and glia. *Trends Neurosci.* 23, 625–633.

Gourine, A. V., Kasymov, V., Marina, N., Tang, F., Figueiredo, M. F., Lane, S., et al. (2010). Astrocytes control breathing through pH-dependent release of ATP. *Science* 329, 571–575. doi: 10.1126/science.1190721

Gundersen, V., Storm-Mathisen, J., and Bergersen, L. H. (2015). Neuroglial Transmission. *Physiol. Rev.* 95, 695–726. doi: 10.1152/physrev.00024.2014

Hillman, C. H., Erickson, K. I., and Kramer, A. F. (2008). Be smart, exercise your heart: exercise effects on brain and cognition. *Nat. Rev. Neurosci.* 9, 58–65. doi: 10.1038/nrn2298

Hulme, S. R., Jones, O. D., Raymond, C. R., Sah, P., and Abraham, W. C. (2014). Mechanisms of heterosynaptic metaplasticity. *Philos. Trans. R. Soc. Lond. B Biol. Sci.* 369:20130148. doi: 10.1098/rstb.2013.0148

Khakh, B. S., and McCarthy, K. D. (2015). Astrocyte calcium signaling: from observations to functions and the challenges therein. *Cold Spring Harb. Perspect. Biol.* 7:a020404. doi: 10.1101/cshperspect.a020404

Khakh, B. S., and North, R. A. (2012). Neuromodulation by extracellular ATP and P2X receptors in the CNS. *Neuron* 76, 51–69. doi: 10.1016/j.neuron.2012.09.024

Lalo, U., Bogdanov, A., and Pankratov, Y. (2018). Diversity of astroglial effects on aging- and experience-related cortical metaplasticity. *Front. Mol. Neurosci.* 11:239. doi: 10.3389/fnmol.2018.00239

Lalo, U., Palygin, O., North, R. A., Verkhratsky, A., and Pankratov, Y. (2011a). Age-dependent remodelling of ionotropic signalling in cortical astroglia. *Aging Cell* 10, 392–402. doi: 10.1111/j.1474-9726.2011.00682.x

Lalo, U., Verkhratsky, A., and Pankratov, Y. (2011b). Ionotropic ATP receptors in neuronal-glial communication. *Semin. Cell Dev. Biol.* 22, 220–228. doi: 10.1016/j.semcdb.2011.02.012

Lalo, U., Palygin, O., Rasooli-Nejad, S., Andrew, J., Haydon, P. G., and Pankratov, Y. (2014a). Exocytosis of ATP from astrocytes modulates phasic and tonic inhibition in the neocortex. *PLoS Biol.* 12:e1001747. doi: 10.1371/journal.pbio.1001747

Lalo, U., Rasooli-Nejad, S., and Pankratov, Y. (2014b). Exocytosis of gliotransmitters from cortical astrocytes: implications for synaptic plasticity and aging. *Biochem. Soc. Trans.* 42, 1275–1281. doi: 10.1042/BST20140163

Lalo, U., Palygin, O., Verkhratsky, A., Grant, S. G., and Pankratov, Y. (2016). ATP from synaptic terminals and astrocytes regulates NMDA receptors and synaptic plasticity through PSD-95 multi-protein complex. *Sci. Rep.* 6:33609. doi: 10.1038/srep33609

Lalo, U., and Pankratov, Y. (2017). Exploring the Ca2+-dependent synaptic dynamics in vibro-dissociated cells. *Cell. Calcium* 64, 91–101. doi: 10.1016/j.ceca.2017.01.008

Lalo, U., Pankratov, Y., Wichert, S. P., Rossner, M. J., North, R. A., Kirchhoff, F., et al. (2008). P2X1 and P2X5 subunits form the functional P2X receptor in mouse cortical astrocytes. *J. Neurosci.* 28, 5473–5480. doi: 10.1523/JNEUROSCI.1149-08.2008

Lopez-Otin, C., Galluzzi, L., Freije, J. M., Madeo, F., and Kroemer, G. (2016). Metabolic control of longevity. *Cell* 166, 802–821. doi: 10.1016/j.cell.2016.07.031

Mederos, S., Hernandez-Vivanco, A., Ramirez-Franco, J., Martin-Fernandez, M., Navarrete, M., Yang, A., et al. (2019). Melanopsin for precise optogenetic activation of astrocyte-neuron networks. *Glia* 67, 915–934. doi: 10.1002/glia.23580

Mercken, E. M., Carboneau, B. A., Krzysik-Walker, S. M., and de Cabo, R. (2012). Of mice and men: the benefits of caloric restriction, exercise, and mimetics. *Ageing Res. Rev.* 11, 390–398. doi: 10.1016/j.arr.2011.11.005

Merzenich, M. M., Van Vleet, T. M., and Nahum, M. (2014). Brain plasticity-based therapeutics. *Front. Hum. Neurosci.* 8:385. doi: 10.3389/fnhum.2014.00385

Nikoletopoulou, V., and Tavernarakis, N. (2018). regulation and roles of autophagy at synapses. *Trends Cell. Biol.* 28, 646–661. doi: 10.1016/j.tcb.2018.03.006

Nithianantharajah, J., and Hannan, A. J. (2009). The neurobiology of brain and cognitive reserve: mental and physical activity as modulators of brain disorders. *Prog. Neurobiol.* 89, 369–382. doi: 10.1016/j.pneurobio.2009.10.001

Palygin, O., Lalo, U., Verkhratsky, A., and Pankratov, Y. (2010). Ionotropic NMDA and P2X1/5 receptors mediate synaptically induced Ca2+ signalling in cortical astrocytes. *Cell. Calcium* 48, 225–231. doi: 10.1016/j.ceca.2010.09.004

Pangrsic, T., Potokar, M., Stenovec, M., Kreft, M., Fabbretti, E., Nistri, A., et al. (2007). Exocytotic release of ATP from cultured astrocytes. *J. Biol. Chem.* 282, 28749–28758. doi: 10.1074/jbc.M700290200

Pankratov, Y., and Lalo, U. (2014). Calcium permeability of ligand-gated Ca2+ channels. *Eur. J. Pharmacol.* 739, 60–73. doi: 10.1016/j.ejphar.2013.11.017

Pankratov, Y., and Lalo, U. (2015). Role for astroglial alpha1-adrenoreceptors in gliotransmission and control of synaptic plasticity in the neocortex. *Front. Cell. Neurosci.* 9:230. doi: 10.3389/fncel.2015.00230

Pankratov, Y., Lalo, U., Krishtal, O., and Verkhratsky, A. (2003). P2X receptor-mediated excitatory synaptic currents in somatosensory cortex. *Mol. Cell. Neurosci.* 24, 842–849.

Pankratov, Y., Lalo, U., Krishtal, O. A., and Verkhratsky, A. (2009). P2X receptors and synaptic plasticity. *Neuroscience* 158, 137–148. doi: 10.1016/j.neuroscience.2008.03.076

Pankratov, Y., Lalo, U., Verkhratsky, A., and North, R. A. (2007). Quantal release of ATP in mouse cortex. *J. Gen. Physiol.* 129, 257–265. doi: 10.1085/jgp.200609693

Rasooli-Nejad, S., Palygin, O., Lalo, U., and Pankratov, Y. (2014). Cannabinoid receptors contribute to astroglial Ca(2)(+)-signalling and control of synaptic plasticity in the neocortex. *Philos. Trans. R. Soc. Lond. B Biol. Sci.* 369:20140077. doi: 10.1098/rstb.2014.0077

Rivera, A., Vanzulli, I., and Butt, A. M. (2016). A Central Role for ATP Signalling in Glial Interactions in the CNS. *Curr. Drug Targets* 17, 1829–1833.

Robertson, S. J., Burnashev, N., and Edwards, F. A. (1999). Ca2+ permeability and kinetics of glutamate receptors in rat medial habenula neurones: implications for purinergic transmission in this nucleus. *J. Physiol.* 518(Pt 2), 539–549.

Rodrigues, R. J., Tome, A. R., and Cunha, R. A. (2015). ATP as a multi-target danger signal in the brain. *Front. Neurosci.* 9:148. doi: 10.3389/fnins.2015.00148

Rodriguez, J. J., Yeh, C. Y., Terzieva, S., Olabarria, M., Kulijewicz-Nawrot, M., and Verkhratsky, A. (2014). Complex and region-specific changes in astroglial markers in the aging brain. *Neurobiol. Aging* 35, 15–23. doi: 10.1016/j.neurobiolaging.2013.07.002

Schneider, C. A., Rasband, W. S., and Eliceiri, K. W. (2012). NIH Image to ImageJ: 25 years of image analysis. *Nat. Methods* 9, 671–675.

van Praag, H. (2009). Exercise and the brain: something to chew on. *Trends Neurosci.* 32, 283–290. doi: 10.1016/j.tins.2008.12.007

Verkhratsky, A., Rodriguez, J. J., and Parpura, V. (2014). Neuroglia in ageing and disease. *Cell Tissue Res.* 357, 493–503. doi: 10.1007/s00441-014-1814-z

Verkhratsky, A., Rodriguez-Arellano, J. J., Parpura, V., and Zorec, R. (2017). Astroglial calcium signalling in Alzheimer's disease. *Biochem. Biophys. Res. Commun.* 483, 1005–1012. doi: 10.1016/j.bbrc.2016.08.088

Wells, J. A., Christie, I. N., Hosford, P. S., Huckstepp, R. T., Angelova, P. R., Vihko, P., et al. (2015). A critical role for purinergic signalling in the mechanisms underlying generation of BOLD fMRI responses. *J. Neurosci.* 35, 5284–5292. doi: 10.1523/JNEUROSCI.3787-14.2015

Zorec, R., Parpura, V., Vardjan, N., and Verkhratsky, A. (2017). Astrocytic face of Alzheimer's disease. *Behav. Brain Res.* 322(Pt B), 250–257. doi: 10.1016/j.bbr.2016.05.021

Conflict of Interest Statement: The authors declare that the research was conducted in the absence of any commercial or financial relationships that could be construed as a potential conflict of interest.

frontiers in Cellular Neuroscience

ORIGINAL RESEARCH
published: 26 June 2019
doi: 10.3389/fncel.2019.00284

P2X2 Receptor Expression and Function Is Upregulated in the Rat Supraoptic Nucleus Stimulated Through Refeeding After Fasting

*Milorad Ivetic, Anirban Bhattacharyya and Hana Zemkova**

Department of Cellular and Molecular Neuroendocrinology, Institute of Physiology, Academy of Sciences of the Czech Republic, Prague, Czechia

Magnocellular neurons in the supraoptic nucleus (SON), which synthesize and release arginine vasopressin (AVP) and oxytocin (OT), express several subtypes of ATP-stimulated purinergic P2X receptors (P2XR) that modulate neuronal activity as well as neurotransmitter and hormone release. However, the physiological impact of this modulation is not well understood. Here, we tested a hypothesis that P2XRs play a role in the sustained release of hormones from SON neurons stimulated through fasting/refeeding. We studied the effect of 2 h of refeeding after 48 h of fasting on P2XR and P2YR mRNA expression and ATP-induced presynaptic and postsynaptic responses in the SON of 30-day-old rats. Quantitative real-time PCR revealed that the expression of P2X2R and AVP mRNA was upregulated, whereas P2X4R, P2X7R, P2Y2R, and OT mRNA levels were not significantly changed and P2Y1R mRNA expression was decreased. Whole-cell patch clamp recordings performed on isolated rat brain slices showed that the amplitude of the ATP-stimulated somatic current and the ATP-induced increases in the frequency of spontaneous GABAergic inhibitory postsynaptic currents were significantly higher in SON neurons from fasted/refed rats than in SON neurons from normally fed rats. No evidence was found for changes in the presynaptic effect of ATP in SON neurons not expressing somatic P2XRs. These results suggest that the increased activity of SON neurons synthesizing AVP is associated with enhanced expression of P2X2Rs on neuronal cell bodies and their GABAergic presynaptic nerve terminals.

Keywords: supraoptic nucleus, P2X receptor, P2Y receptor, ATP, GABA, arginine vasopressin, oxytocin

OPEN ACCESS

Edited by:
David Blum,
INSERM U1172 Centre de Recherche Jean-Pierre Aubert, France

Reviewed by:
Peter Illes,
Leipzig University, Germany
Ivan Milenkovic,
Leipzig University, Germany

***Correspondence:**
Hana Zemkova
Hana.Zemkova@fgu.cas.cz

Specialty section:
This article was submitted to Cellular Neurophysiology, a section of the journal Frontiers in Cellular Neuroscience

Received: *25 February 2019*
Accepted: *12 June 2019*
Published: *26 June 2019*

Citation:
Ivetic M, Bhattacharyya A and Zemkova H (2019) P2X2 Receptor Expression and Function Is Upregulated in the Rat Supraoptic Nucleus Stimulated Through Refeeding After Fasting. Front. Cell. Neurosci. 13:284. doi: 10.3389/fncel.2019.00284

INTRODUCTION

Mammalian magnocellular neurons in the supraoptic nucleus (SON) and paraventricular nucleus (PVN) secrete either vasopressin (AVP) or oxytocin (OT) from their nerve terminals in the posterior pituitary in response to a variety of different physiological stimuli. AVP release increases as a function of plasma osmolality and water status of the body (Oliet and Bourque, 1993; Israel et al., 2010; Choe et al., 2015), whereas OT release is mainly caused by parturition and

suckling-induced reflex milk ejection (Moos, 1995; Voisin et al., 1995; Jourdain et al., 1998; Brussaard and Kits, 1999), These two peptides are also locally released in various brain regions (Richard et al., 1991), including within the PVN and SON, where AVP and OT have local regulatory actions (Ludwig, 1998; Kombian et al., 2002; Leng and Ludwig, 2008). The secretion of both hormones is dependent on electrical activity of magnocellular neurons (Leng et al., 1999; Sladek and Kapoor, 2001; Armstrong, 2007; Li et al., 2007; Choe et al., 2015), which is under the control of various excitatory and inhibitory synaptic inputs (Hu and Bourque, 1991; Wuarin and Dudek, 1993; Shibuya et al., 2000; Israel et al., 2010). These inputs, in particular those using glutamate (Decavel and Curras, 1997; Boudaba et al., 2003; Iremonger et al., 2010; Vilhena-Franco et al., 2018) and γ-aminobutyric acid (GABA) (Brussaard and Kits, 1999) as neurotransmitters, play an important role in the generation of the specific pattern of activity in AVP and OT neurons (Moos, 1995; Voisin et al., 1995; Jourdain et al., 1998; Brussaard and Kits, 1999; Israel et al., 2010; Choe et al., 2015).

Two experimental conditions that have been widely used to stimulate the synthesis and release of these peptides are lactation for OT (de Kock et al., 2004; Panatier and Oliet, 2006) and water deprivation or refeeding after fasting for AVP (Carreno et al., 2011; Gottlieb et al., 2011; Yao et al., 2012; Yoshimura et al., 2013; Lucio-Oliveira et al., 2015). Refeeding after fasting represents a complex stimulation to hormone secretion involving the volume/baroreceptors and peripheral/central osmoreceptors (Burlet et al., 1992) that may involve neurotransmitter signaling at different levels. For example, the NR1 subunit of NMDA receptors, expressed in both AVP and OT magnocellular neurons of the SON and PVN, is upregulated after dehydration in these areas (Decavel and Curras, 1997). A higher incidence of GABA(A) receptor-mediated spontaneous inhibitory postsynaptic currents (sIPSCs) has been found in the SON neurons of pregnant rats than in those of virgin rats, consistent with the observations of an increase in the density of GABA-containing synaptic boutons (Brussaard and Kits, 1999).

The secretion of hormones by magnocellular neurosecretory cells in the hypothalamic SON and PVN can be modulated by ATP (adenosine-5′-triphosphate), which is co-released with noradrenaline during stimulation of these cells (Day et al., 1993; Knott et al., 2008; Gordon et al., 2009). Extracellular ATP and its metabolic products, ADP and adenosine, act as agonists or extracellular messengers on ionotropic P2X receptors (P2XRs) and G-protein coupled adenosine receptors and P2Y receptors (P2YRs) (Burnstock, 2006). Locally applied ATP increases cytosolic free Ca^{2+} concentrations in identified somata of dissociated SON neurons (Troadec et al., 1998; Shibuya et al., 1999; Song et al., 2007) and evokes AVP release from isolated posterior pituitary nerve terminals but not OT release (Troadec et al., 1998; Song and Sladek, 2006; Knott et al., 2008; Gomes et al., 2009; Custer et al., 2012; Lemos et al., 2018). In addition, activation of presynaptic P2XRs by the application of ATP dramatically facilitates glutamate and GABA release in SON slices (Vavra et al., 2011).

Although presynaptic P2XR responses have been described in many parts of the brain (Khakh and North, 2012), a satisfactory understanding and the precise physiological function of this form of modulation of synaptic transmission is still lacking. In the present study, we tested a hypothesis that P2XRs might play a role in the release of AVP from SON neurons stimulated through fasting/refeeding. We examined the effect of 2 h of food intake after 48 h of starvation (Lucio-Oliveira et al., 2015) on AVP, OT, P2XR and P2YR mRNA expression and ATP-induced electrophysiological responses in the SON neurons in rat brain slices. Normally fed rats of the same age and sex were used as controls for this condition. We show that fasting/refeeding increases the level of P2X2R mRNA expression and potentiates both postsynaptic and presynaptic ATP-induced responses.

MATERIALS AND METHODS

Animals and Brain Slices

Animals were obtained from established breeding couples in the animal facility (Animal facility of the Institute of Physiology, Czech Academy of Sciences; approval number #56379/2015-MZE-17214). All animal procedures were approved by the Animal Care and Use Committee of the Czech Academy of Sciences (dissection protocol # 67985823). The animals were kept since their birth under conditions of stable temperature and humidity, 12 h light/dark cycles and food and water provided *ad libitum* (Animal Facility of the Institute of Physiology, Czech Academy of Sciences). We employed a previously reported protocol to challenge the peptide producing system of the SON, refeeding with standard chow for 2 h after 2 days of fasting (**Figure 1A**), which increases the activity of AVP neurons (Lucio-Oliveira et al., 2015). Experiments were performed in 30- to 32-day-old Wistar rats. A total of 64 Wistar rats (37 normally fed and 27 fasted/refed) of both sexes were investigated. Euthanasia was performed by decapitation after anesthesia with isofuranum (Forane, AbbVie s.r.o. Czechia) that does not smell and does not damage epithelium in the respiratory system. Brains were removed and placed into ice-cold (4°C) oxygenated (95% O_2 + 5% CO_2) artificial cerebrospinal fluid (ACSF). Hypothalamic slices (200- to 300-μm-thick) containing SONs were cut with a vibratome (DTK-1000, D.S.K., Dosaka, Japan). The slices were allowed to recover for at least 1 h in oxygenated ACSF at 32–33°C before being transferred into a recording chamber. During the experiments, slices were submerged in continuously flowing oxygenated ACSF at 1–2 ml min^{-1} at room temperature (20–25°C). Slices were viewed with an upright microscope (Olympus BX50WI, Melville, NY, United States) mounted on a Gibraltar X-Y table (Burleigh) using a water immersion lens (60× and 10×) and Dodt infrared gradient contrast (Luigs & Neumann, GmbH, Germany). The SON of rats was identified by the position relative to the chiasma opticum (Vavra et al., 2011).

Quantitative Real-Time RT-PCR

Coronal hypothalamic slices (1000 μm) containing SON(s) were dissected from rat brains using a Vibratome slicer, and

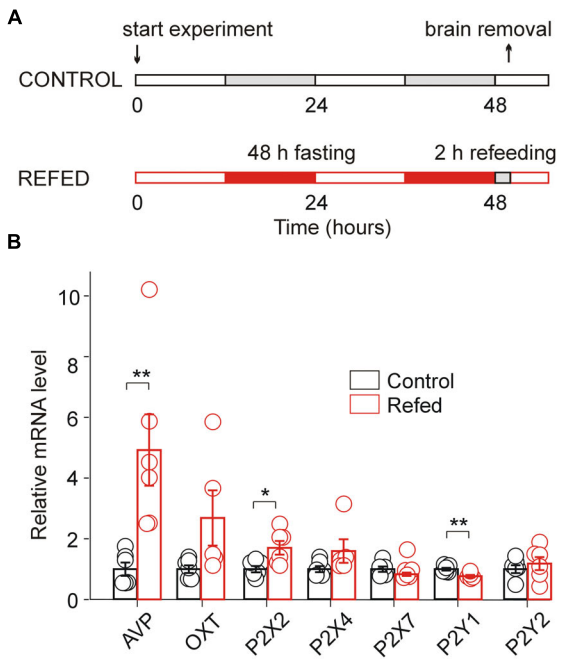

FIGURE 1 | Effect of fasting/refeeding on purinergic P2 receptor expression. **(A)** Schematic diagram of the fasting/refeeding experiment. One group of 30-day-old rats was fed food *ad libitum* for the entire experiment (Control), and the second group of 30-day-old rats was fasted for 48 h and subsequently refed with standard chow for 2 h (Refed). Both groups were allowed to drink water *ad libitum*. At the end of this procedure, hypothalamic slices were prepared from both groups. **(B)** Effect of fasting/refeeding on the relative mRNA expression (calculated as probe/18sRNA ratio) of the P2X2, P2X4, P2X7, P2Y1, and P2Y2 receptors as well as AVP and OT in the SON normalized to the control group. Data represent the mean ± S.E.M with a scatterplot of the individual data points (n = 6 tissue samples from three animals). Significant differences between control and fasted/refed animals were estimated using the unpaired t-test, $p < 0.01$ (**) and $p < 0.05$ (*).

SON(s) were punched out of the slices under visual control (magnification 20×) using a needle punch with an internal diameter of approximately 1 mm. Samples were either used immediately or frozen in RNA*later*™ (Sigma-Aldrich) at −80°C. Total RNA was extracted from the tissues using the mirVana™ miRNA Isolation Kit (Ambion™, Thermo Fisher Scientific, United States). Briefly, samples were homogenized in lysis buffer provided with the kit using ceramic balls (MagNA Lyser Green Beads) and a MagNA Lyser homogenizer (Roche Diagnostics GmbH, Germany). RNA was then extracted from the tissue homogenate using acid-phenol:chloroform extraction and subsequent column purification with glass-fiber filter containing columns according to the manufacturer's protocol. The concentration of total RNA in each sample was measured using a NanoDrop™ spectrophotometer (Thermo Fisher Scientific, Wilmington, DE, United States). Samples were volume adjusted with DNAase and RNAase free DEPC treated water provided with the RT kit and normalized for their RNA content. The first strand cDNA was synthesized from up to 1 μg of isolated RNA using SuperScript™ VILO™ cDNA Synthesis Kit (Invitrogen, Thermo Fisher Scientific, United States) in a 20-μL reaction volume using random primers provided with the kit according to the manufacturer's protocol. The expression levels of specific mRNA(s) for the AVP, OT, P2X receptors 2, 4, and 7 (P2X2, P2X4, and P2X7), P2Y1 and P2Y2 genes were measured using a ViiA™ 7 Real-Time PCR System (Applied Biosystems, Foster City, United States). The probes and primers (TaqMan® probes) used for these experiments were developed as TaqMan Gene Expression Assay by Applied Biosystems. Specifically, AVP (Rn00566449_m1), OT (Rn00564446_g1), P2X2 (Rn00586491_m1), P2X4 (Rn00580949_m1), P2X7 (Rn00570451_m1), P2Y1 (Rn00562996_m1), and P2Y2 (Rn00568476_m1) were used. Eukaryotic 18 s rRNA endogenous control (VIC®/MGB Probe, Primer Limited; Hs99999901_s1) was used as a housekeeping gene/endogenous control. Real-time PCR amplification was performed in 30 μl aliquots on a 96-well fast optical plate in a duplex reaction format. Each reaction contained TaqMan target gene probes labeled with FAM/TAMRA, 18 s RNA probes (VIC/MGB), TaqMan Universal Master Mix II, no UNG (Applied Biosystems) and cDNA. The efficiency of different probes was found to be very similar, and therefore, the $2^{-\Delta\Delta}C_T$ method was used to calculate the relative mRNA levels of all genes of interest normalized to the endogenous control (18 s RNA). Final results were expressed as fold changes in relative mRNA expression with the treatment of the animals (controls vs. 2 h fasted/refed groups).

Patch Clamp Recordings

ATP-induced currents and membrane potentials were recorded from SON slices using standard whole-cell patch clamp techniques with an Axopatch-200B amplifier (Axon Instruments, Union City, CA, United States). Patch pipettes were pulled on the horizontal Flaming Brown P-97 model puller (Sutter Instruments, Novato, CA, United States) from borosilicate glass (World Precision Instruments, Sarasota, FL) and polished by heat to a tip resistance of 4–6 MΩ. The access resistance (average 14.2 ± 1.2 MΩ, n = 18) was monitored throughout each experiment. The mean capacitance of the cells was 6–8 pF, 50–80% series resistance compensation was used, and liquid junction potential (∼4 mV), calculated using the program CLAMPEX 9, was corrected offline when determining the resting membrane potential of SON cells. Data were captured and stored using the pClamp 9 software package in conjunction with the Digidata 1322A A/D converter (Axon Instruments). Signals were filtered at 1 kHz and sampled at 10 kHz. The ATP-induced currents and spontaneous miniature postsynaptic currents (mPSCs) were recorded from cells voltage-clamped in the presence of 0.5 μM tetrodotoxin (TTX) that was used to block action potentials. The cell membrane potential was held at –60 mV.

Drug Application

ATP (100 μM) was applied in HEPES-buffered extracellular solution (see *Solutions*). The solutions were delivered to the recorded cells by a gravity-driven microperfusion system containing nine glass tubes with a common outlet approximately 300 μM in diameter (RSC-200 Rapid Solution Changer, Biologic, Claix, France). The application tip was routinely positioned approximately 500 μm away from the recorded cell and ∼50 μm

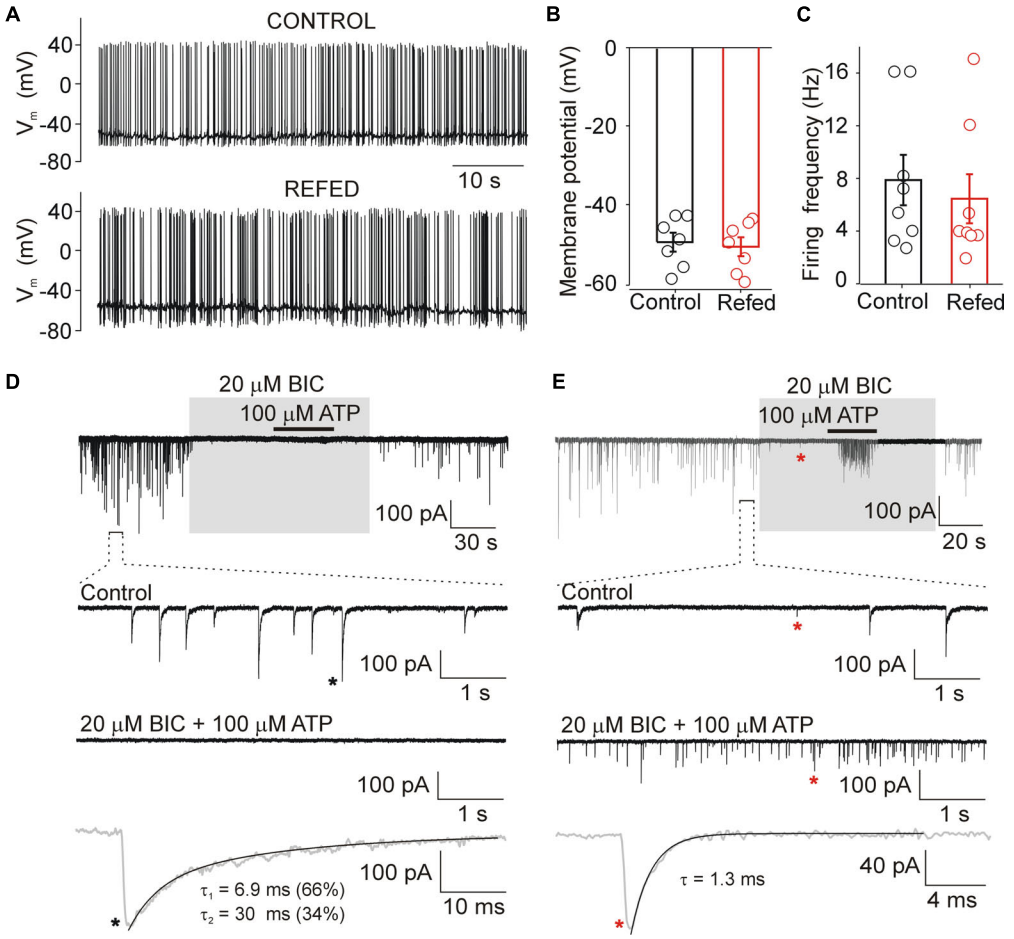

FIGURE 2 | Biophysical properties of SON neurons. **(A)** Action potentials recorded from SON neurons in slices from normally fed (Control) and fasted/refed (Refed) animals using current clamp patch clamp configuration. Resting membrane potential **(B)** and frequency of action potentials **(C)** in both animal groups. Data represent the mean ± S.E.M of 6–8 cells from three independent experiments. **(D,E)** Miniature postsynaptic currents recorded from SON neurons voltage-clamped at –60 mV in the presence of TTX (0.5 μM). (D) Example record from cell with mIPSCs. Application of bicuculline (BIC, 20 μM) inhibited all GABAergic synaptic currents both in the presence and absence of ATP (100 μM). Lower trace shows mIPSC (black asterisk) on expanded time scale. **(E)** Example record from cell exhibiting both mIPSCs and mEPSCs. Application of bicuculline (BIC, 20 μM) inhibited GABAergic synaptic currents and glutamatergic excitatory postsynaptic currents persisted. Lower trace shows mEPSC (red asterisk, in the presence of ATP and BIC) on expanded time scale. The time constants (τ, τ_1, and τ_2) were measured by fitting the curve to a monoexponential (mEPSCs.) or biexponential (mIPSCs) functions.

above the surface of the slice. The time of each ATP application (5–20 s) was controlled.

Solutions

Slices were preincubated at 32–33°C in oxygenated ACSF that contained (in mM): 130 NaCl, 3 KCl, 1 $MgCl_2$, 2 $CaCl_2$, 19 $NaHCO_3$, 1.25 NaH_2PO_4 and 10 glucose (pH 7.3–7.4; osmolality 300–315 mOsm). ATP was diluted and applied in a N-2-hydroxyethylpiperazine-N′-2-ethanesulfonic acid (HEPES)-buffered extracellular solution (ECS) containing (in mM): 142 NaCl, 3 KCl, 1 $MgCl_2$, 2 $CaCl_2$, 10 glucose and 10 HEPES, the osmolality was 300–315 mOsm and the pH was adjusted to 7.3 with 1 M NaOH. While testing the effect of ATP application, neurons were exposed to HEPES-buffered ECS for no more than 2 min. The patch electrodes used for whole-cell recording were filled with an intracellular solution containing (in mM): 140 KCl, 3 $MgCl_2$, 0.5 $CaCl_2$, 10 HEPES and 5 EGTA, and the pH was adjusted to 7.2 with KOH. The osmolality of the intracellular solutions was 285–295 mOsm.

Data Analysis

The frequencies and amplitudes of miniature GABAergic inhibitory postsynaptic currents (mIPSCs) were manually analyzed off-line using pClamp 10 software (Molecular Devices, United States). The currents were detected using a threshold-based event search and visually evaluated by the experimenters. Only events exceeding 10 pA and lasting 15–20 ms were used in subsequent analysis. Miniature glutamatergic excitatory postsynaptic currents (mEPSCs) identified as smaller and shorter (∼5 ms) events (Vavra et al., 2011), were ignored. The amplitudes of individual events were determined by the detection program, and the frequency was calculated by dividing number of events

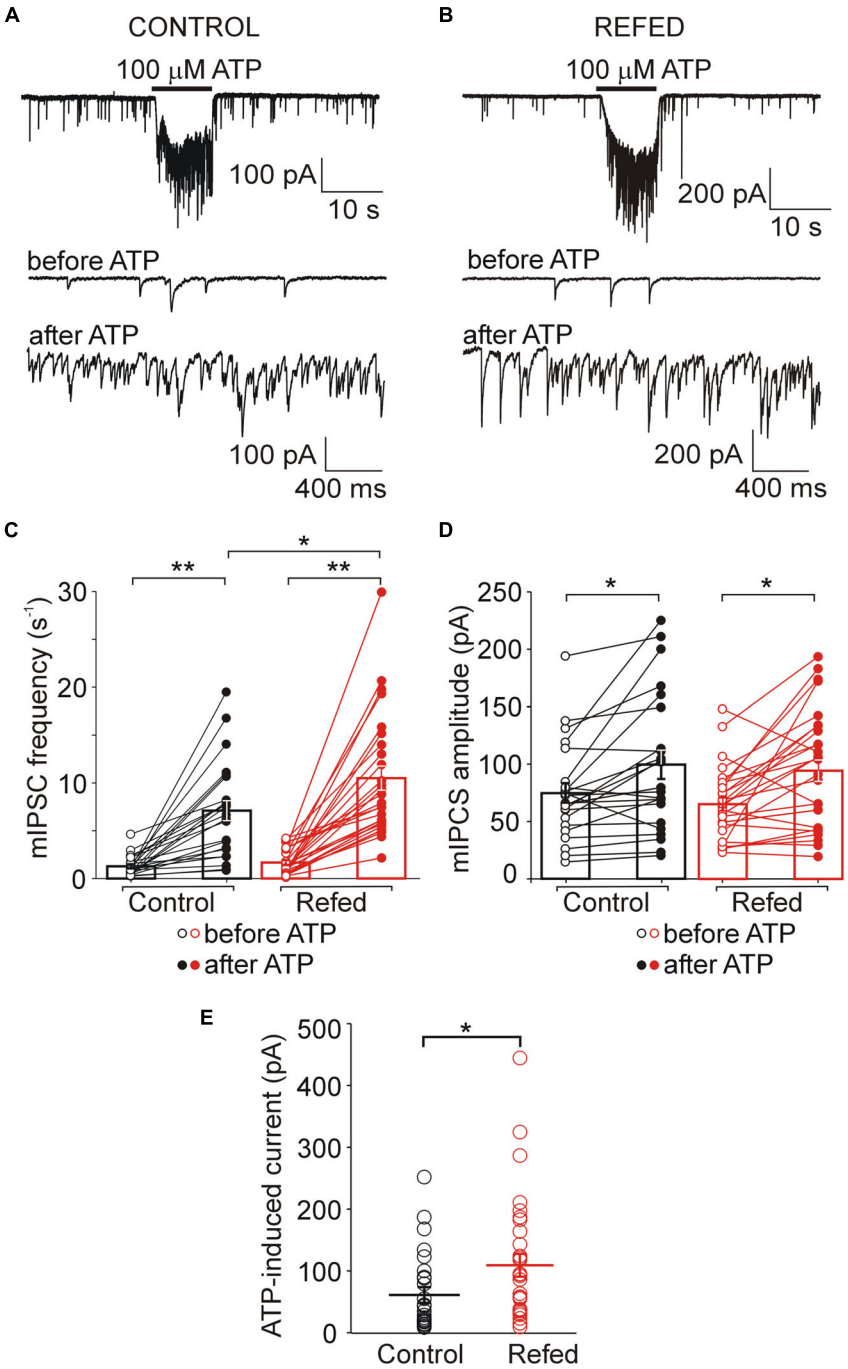

FIGURE 3 | The difference between control and fasted/refed rats in ATP-induced somatic and presynaptic effects. ATP evoked somatic current and increased the frequency of mIPSC in SON neurons from control **(A)** and fasted/refed **(B)** animals. Traces on an expanded time scale show spontaneous inhibitory synaptic currents before and after ATP application. **(C,D)** The frequency **(C)** and amplitude **(D)** of mIPSCs in control (black) and refed (red) animals in the presence (closed symbols) and absence (open symbols) of ATP. Data represent the mean ± S.E.M with a scatterplot of the individual data points (control, n = 17 cells; refed, n = 26 cells). **(E)** The amplitude of current induced by 5–10 s ATP application. Data represent the mean ± S.E.M with a scatterplot of the individual data points (control, n = 26 cells; refed, n = 34 cells). Analysis was performed by two-way ANOVA and Tukey's *post hoc* test. $^{**}p < 0.01$, $^{*}p < 0.05$. The ATP-induced current and ATP-induced frequency increase were significantly higher in fasted/refed rats than control rats.

by the recording time. The average time of recordings used for frequency calculation was 19.6 ± 0.4 s and 8.6 ± 1.0 s (n = 10) before and after ATP application, respectively. The kinetics of mEPSC and mIPSC current decay were fitted by a single exponential function [$y = A \exp(-t/\tau)$] and by the sum of two exponentials [$y = A1 \exp(-t/\tau_1) + A2 \exp(-t/\tau_2)$],

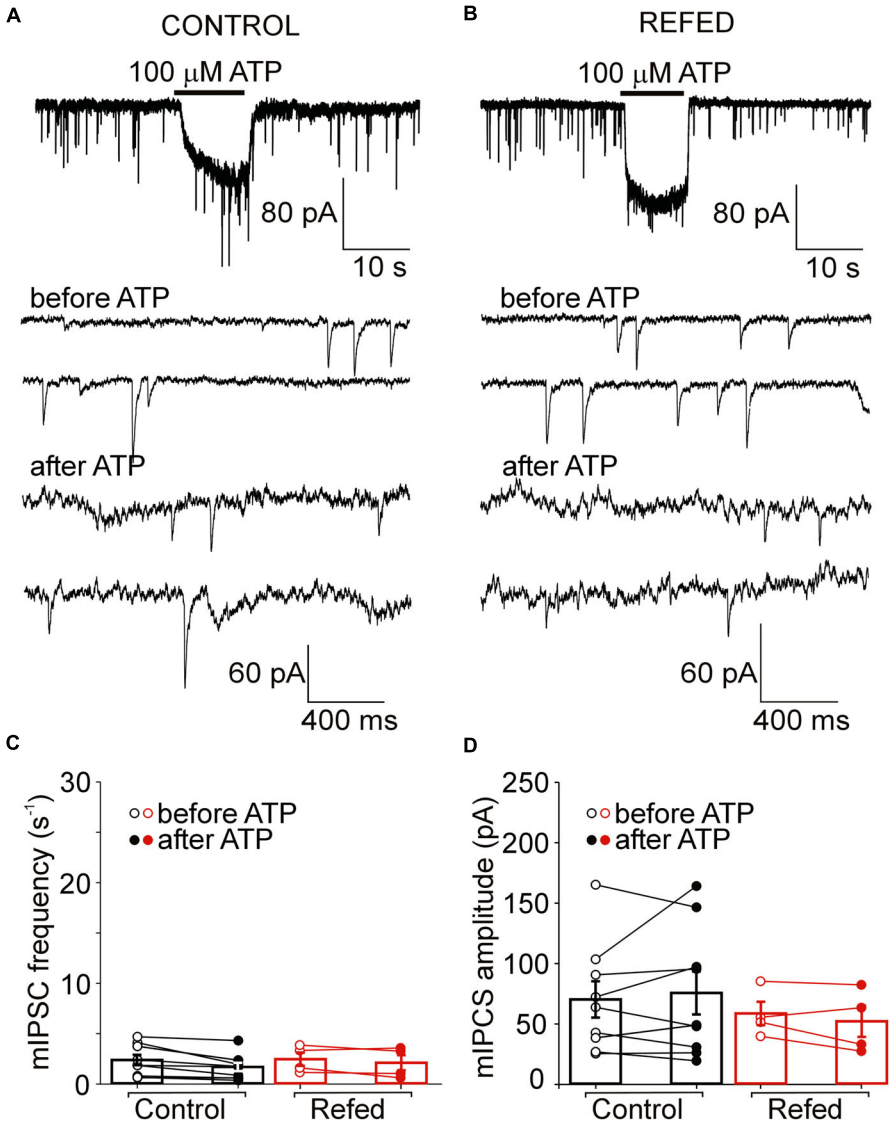

FIGURE 4 | The absence of a presynaptic effect of ATP in a subpopulation of P2XR-expressing SON neurons in both animal groups. **(A,B)** ATP-induced current without increases in the frequency of mIPSCs in control **(A)** and refed **(B)** animals. Traces on an expanded time scale show spontaneous inhibitory synaptic currents before and after ATP application **(C,D)** The frequency **(C)** and amplitude **(D)** of mIPSCs in control (black) and refed (red) animals in the presence (closed symbols) and absence (open symbols) of ATP. Data represent the mean ± S.E.M with a scatterplot of the individual data points (control, n = 9 cells; refed, n = 4 cells).

respectively, using the program CLAMPFIT 9, where A1 and A2 are relative amplitudes of the first and second exponential, and τ_1 and τ_2 are time constants. The derived time constant for current decay was labeled as τ. All values are reported as the mean ± SEM. Significant differences were determined by two-way analysis of variance (ANOVA) and Tukey's *post hoc* test using SigmaStat 2000 v9.01, or Student's *t*-test using SigmaPlot v10.01 with $p < 0.01$ (**) and $p < 0.05$ (*). Graphing was performed using SigmaPlot and CorelDraw software.

Chemicals

TTX was from Tocris Bioscience. ATP and all other chemicals were from Sigma (St. Louis, MO).

RESULTS

Upregulation of AVP and P2X2R mRNA in the Hypothalamic SON Stimulated Through Fasting/Refeeding

Our previous analysis of the mRNA expression of seven P2XRs (P2X1–P2X7) and three P2YRs (P2Y1, P2Y2, and P2Y12) in rat SON tissue revealed significant differential expression (P2X2R > P2X7R > P2X4R > P2Y1R = P2Y2R), while the mRNA expression for the other P2 receptors was minimal (Vavra et al., 2011). Therefore, to address whether the increased synthesizing and releasing activity of AVP neurons induced by the fasting/refeeding protocol (**Figure 1A**;

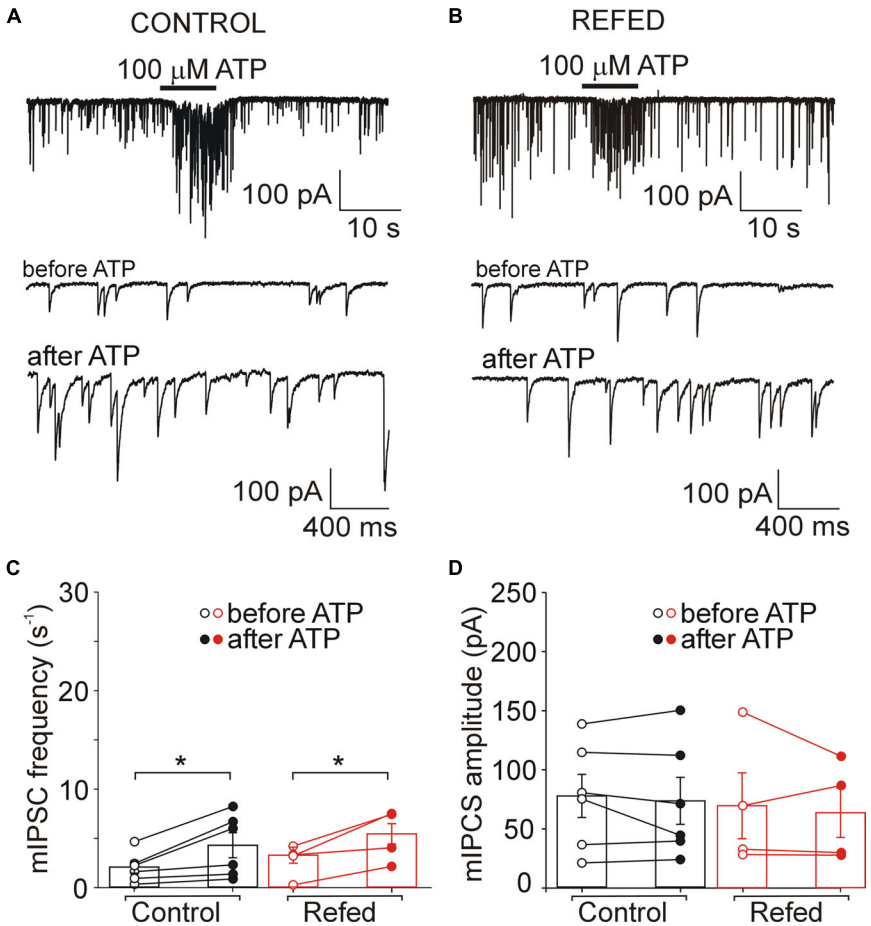

FIGURE 5 | Presynaptic effect of ATP in SON neurons not expressing P2XRs is similar in both animal groups. **(A,B)** ATP-induced increases in the frequency of mIPSCs in control **(A)** and refed **(B)** animals. Traces on an expanded time scale show spontaneous inhibitory synaptic currents before and after ATP application **(C,D)** The frequency **(C)** and amplitude **(D)** of mIPSCs in control (black) and refed (red) animals in the presence (closed symbols) and absence (open symbols) of ATP. Data represent the mean ± S.E.M with a scatterplot of the individual data points (control, $n = 6$ cells; refed, $n = 4$ cells). Analysis was performed by two-way ANOVA and Tukey's *post hoc* test. $^*p < 0.05$.

Lucio-Oliveira et al., 2015) regulates P2XR gene expression in the SON, we performed quantitative PCR analysis with reverse transcription (RT-qPCR) to compare the mRNA expression of P2X2R, P2X4R, P2X7R, P2Y1R, and P2Y2R in SON tissue from 30-day-old rats refed for 2 h after 48 h of starvation with that in SON tissue isolated from controls, i.e., normally fed rats (**Figure 1B**). Additionally, we examined the mRNA expression levels of AVP and OT in both animal groups (**Figure 1B**). These experiments showed a significant increase in the expression of AVP (ratio = 4.93 ± 1.17, $n = 3$, unpaired t-test, $p = 0.0074$) and P2X2R (ratio = 1.61 ± 0.17, $n = 3$, $p = 0.0199$) mRNA, a decrease in P2Y1 mRNA (ratio = 0.78 ± 0.04, $n = 3$, $p = 0.0060$) in fasted/refed animals compared to controls (**Figure 1B**). However, changes in the mRNA expression of OT, P2X4R, P2X7R, and P2Y2R were non-significant. These results showed that fasting/refeeding increases the expression of P2X2R and this effect correlates with the upregulation of AVP in the SON.

Biophysical Properties of SON Neurons in Slices From Fasted/Refed Rats and Controls

We used acutely isolated hypothalamic slices to determine the basic electrophysiological properties of SON neurons from fasted/refed and normally fed rats. Whole-cell current clamp recordings performed 1–6 h after isolation showed that the resting membrane potential of SON neurons was −49.1 ± 2.3 mV ($n = 8$ cells) in control rats and −50.7 ± 2.3 mV ($n = 8$ cells) in fasted/refed rats (**Figures 2A,B**). The average frequency of action potentials was 6.5 ± 1.8 mV ($n = 8$) and 7.9 ± 1.9 mV ($n = 8$, $p = 0{,}571$) in control and fasted/refed rats, respectively (**Figures 2A,C**). Thus, no significant change in the basal membrane properties and spontaneous neuronal activity was observed in SON neurons stimulated to secrete hormones through fasting/refeeding.

In the presence of 0.5 μM TTX, whole-cell voltage clamp recordings showed that under our experimental conditions

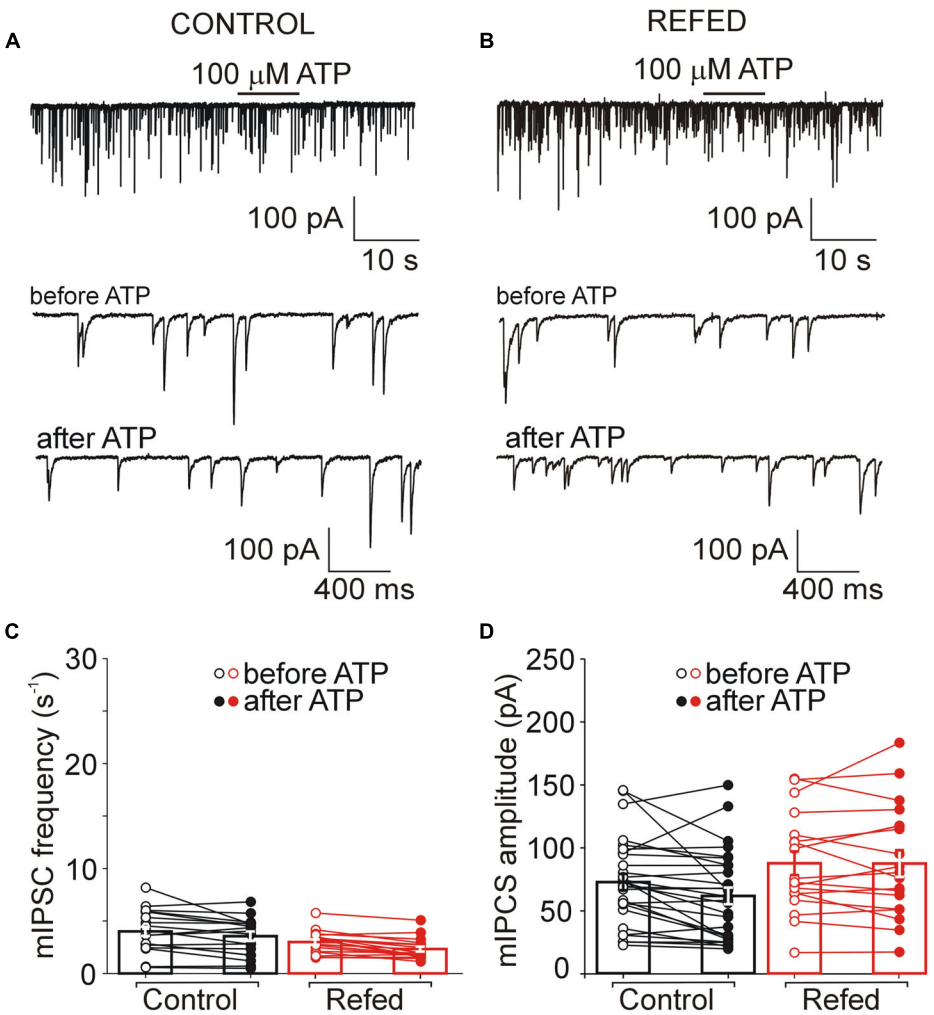

FIGURE 6 | The absence of both somatic and presynaptic effects of ATP in a subpopulation of SON neurons. **(A,B)** Lack of effect of ATP on the frequency of mIPSCs in control **(A)** and refed **(B)** animals. Traces on an expanded time scale show spontaneous inhibitory synaptic currents before and after ATP application **(C,D)** The frequency **(C)** and amplitude **(D)** of mIPSCs in control (black) and refed (red) animals in the presence (closed symbols) and absence (open symbols) of ATP. Data represent the mean ± S.E.M with a scatterplot of the individual data points (control, n = 28 cells; refed, n = 18 cells).

(intracellular [Cl^-], 144 mM; extracellular [Cl^-], 151 mM; holding potential, −60 mV; the theoretical equilibrium potential for Cl calculated by the Nernst equation is about 0 mV), both mEPSCs and mIPSCs could be recorded as small inward currents (**Figures 2D,E**). Using ATP to stimulate the frequency of mEPSCs and mIPSCs (Vavra et al., 2011) and bicuculline (BIC; 20 μM) to block GABAergic currents, we found that mEPSCs and mIPSCs differ in their amplitudes and decay time constants. The amplitude of BIC-sensitive currents (mIPSCs) was 72 ± 4 pA, and the decay phase was well fitted by a sum of two exponentials with weight time constant of 6.1 ± 0.6 ms (contribution 41 ± 16%) and 33 ± 6 ms (n = 8 cells; **Figure 2D**). The amplitude of BIC-insensitive currents was much smaller, 22 ± 4 pA, and the decay phase was well fitted with a single exponential with a time constant of 1.5 ± 0.3 ms (n = 5 cells; **Figure 2E**). Previously we have shown that these events are inhibited with 6,7-dinitroquinoxaline-2, 3-dione (DNQX; 20 μM) that blocks α-amino-3-hydroxy-5-methyl-4-isoxazolepropionic acid (AMPA) currents and 2-amino-5-phosphonopentanoic acid (AP5; 50 μM) that blocks *N*-Methyl-D-aspartate (NMDA) currents (Vavra et al., 2011), indicating that these are mEPSCs. These events were observed in only about 30% of SON neurons from both animal groups, and were not studied further. The differences in the amplitude and time course allowed us to examine the effects of ATP on mIPSCs in the absence of specific glutamatergic blockers (see Methods for mEPCs discrimination). The GABAergic mIPSCs could be recorded in all SON neurons, and the average basal frequency was not significantly different between the two animal groups (control, 2.9 ± 0.3 Hz, n = 60; fasted/refed, 2.2 ± 0.2 Hz; n = 52; p = 0.5745). The frequency of mEPSCs was 0.24 ± 0.10 Hz (n = 6) and

0.32 ± 0.08 Hz (n = 8; p = 0,4556) in controls and fasted/refed rats, respectively.

Increased Amplitude of ATP-Induced Somatic Current in the SON Neurons of Fasted/Refed Rats

Next, we applied 100 μM ATP to SON neurons voltage-clamped at −60 mV to characterize ATP-induced somatic current. This concentration of ATP is close to the effective concentration producing a half-maximal effect of ATP in SON slices from control rats [EC_{50} = 70 ± 10 μM; (Vavra et al., 2011)], and was used throughout the study. Voltage clamp whole cell recording revealed that the brief application (5−10 s) of ATP evoked inward currents in 26 out of 60 control neurons (57 slices from 37 rats; **Figures 3A**, **4A**) and in 30 out of 52 neurons from fasted/refed rats (43 slices from 27 rats; **Figures 3B**, **4B**). The mean amplitude of ATP-induced somatic current was significantly higher in fasted/refed rats than controls (control, 75 ± 18 pA; fasted/refed, 132 ± 25 pA; p = 0.043; **Figure 3E**). These results indicate that refeeding after fasting upregulates the P2XR protein level on the cell somata of SON neurons compared to SON neurons from normally fed rats.

Increased ATP-Induced Potentiation of GABA Release in the P2XR-Expressing SON Neurons of Fasted/Refed Rats

In addition to the amplitude of ATP-evoked somatic current, we studied the effect of presynaptic P2XR activation on the frequency and amplitude of miniature mIPSCs. We first examined the effect of ATP on mIPSC frequency in SON neurons exhibiting ATP-evoked somatic current (**Figures 3**, **4**); these neurons will be called "P2XR-expressing" neurons in this study. In 65% (17/26) of control P2XR-expressing SON neurons, the application of ATP increased the mIPSC frequency by 1198 ± 202% (before ATP, 1.29 ± 0.23 Hz; after ATP, 8.60 ± 1.26 Hz; p = 0.00005; **Figure 3C**, left) and increased the amplitude from 66.60 ± 7.38 pA to 99.71 ± 15.33 pA (p = 0.0055; **Figure 3D**, left). The remaining 35% (9/26) of cells showed ATP-evoked somatic current without ATP-induced increase in mIPSC frequency (before ATP, 2.35 ± 0.52 Hz; after ATP, 1.95 ± 0.42, **Figure 4C**, left) and amplitude (before ATP, 68.98 ± 15.01 pA; after ATP, 76.30 ± 17.78 pA; n = 9, **Figure 4D**, left).

In fasted/refed rats, ATP-induced increase in mIPSC frequency and amplitude was observed more often, increasing to 87% (26/30) of P2XR-expressing neurons (**Figure 3B**). The application of ATP increased the mIPSC frequency by 1102 ± 241% (before ATP, 1.45 ± 0.23; after ATP, 10.79 ± 1.35 Hz; p = 0.0000005; **Figure 3C**, right) and increased the amplitude from 64.01 ± 5.35 pA to 98.16 ± 9.81 pA (p = 0.0003, **Figure 3D**, right). The difference between control and fasted/refed rats in the ATP-induced increase in mIPSC frequency was significant (two-way ANOVA, p = 0.0469; **Figure 3C**), but the difference in the ATP-induced increase in mIPSC amplitude was not (**Figure 3D**). The remaining 13% (4/30) of cells from fasted/refed animals exhibited ATP-evoked somatic current without ATP-induced increase in mIPSC frequency (before ATP, 2.25 ± 0.85 Hz; after ATP, 2.07 ± 0.75 Hz; **Figure 4C**, right) and amplitude (before ATP, 58.94 ± 9.67 pA; after ATP, 53.46 ± 10.15 pA; n = 4, **Figure 4D**, right).

These data revealed that fasting/refeeding increases expression of the P2XRs in the nerve terminals releasing GABA on P2XR-expressing SON neurons.

No Effect of Refeeding After Fasting on ATP-Evoked Presynaptic Responses in a Subpopulation of SON Neurons Not Expressing Somatic P2XRs

Next, we investigated the effect of ATP on GABAergic synaptic transmission in SON neurons not exhibiting ATP-evoked somatic current (**Figures 5**, **6**). In 18% (6/34) of control SON neurons, ATP application increased mIPSC frequency by 207 ± 22% (before ATP, 2.06 ± 0.62 Hz; after ATP, 4.27 ± 1.26 Hz; p = 0.031; **Figures 5A,C**, left), without impacting the amplitude (before ATP, 67.30 ± 20.56 pA; after ATP, 63.01 ± 22.51 pA; p = 0.509; **Figure 5D**, left). The remaining 82% (28/34) of neurons exhibited no effect of ATP on mIPSC frequency (before ATP, 4.05 ± 0.44 Hz; after ATP, 3.59 ± 0.45 Hz; **Figures 6A,C**, left) and amplitude (before ATP, 72.61 ± 6.49 pA; after ATP, 60.78 ± 6.51 pA; n = 28; **Figure 6D**, left).

Similarly, in 18% (4/22) of SON neurons from fasted/refed animals, ATP application increased mIPSC frequency by 296 ± 140% (before ATP, 3.02 ± 1.00 Hz; after ATP, 4.95 ± 1.26 Hz; p = 0,048; **Figures 5B,C**, right), without impacting sIPSC amplitude (before, 69.61 ± 27.87 pA; after ATP, 63.68 ± 20.88 pA; p = 0,638; **Figure 5D**, right). The difference between control and fasted/refed rats in the ATP-induced increase in mIPSC frequency was not significant (two-way ANOVA, p = 0.6660). The remaining 82% (18/22) of cells displayed no ATP-induced increase in mIPSC frequency (before ATP, 3.02 ± 0.25 Hz; after ATP, 2.35 ± 0.24 Hz; **Figures 6B,C**, right) and amplitude (ECS, 85.36 ± 9.61 pA; ATP, 84.97 ± 10.91 pA; n = 18; **Figure 6D**, right).

These data reveal that fasting/refeeding has no effect on presynaptic ATP-induced responses in SON neurons not expressing somatic P2XRs. In addition, these data also show that the amplitude of postsynaptic current did not increase when ATP application induces moderate increase in mIPSC frequency.

DISCUSSION

We found significantly increased AVP and P2X2R expression and decreased P2Y1R expression, but no changes in OT, P2X4R, P2X7R, and P2Y2R mRNA expression in the rat SON after 48 h of starvation and 2 h after food intake. Using acutely isolated rat brain slices, we showed that the changes in P2X2R mRNA expression are accompanied by functional effects such that the amplitude of ATP-stimulated somatic current and the incidence of P2XRs mediated presynaptic facilitation of GABA release onto P2XR-expressing SON neurons increases. These data suggest that the recruitment of P2X2Rs to both

postsynaptic and presynaptic sites could be associated with the increased synthesis and release of AVP in the SON of fasted/refed rats.

Food deprivation for 48 h causes a decline in the AVP level in the SON, while little change in the OT concentration was detected (Burlet et al., 1992). Food intake after 48 h of fasting evokes increases in plasma AVP (Lucio-Oliveira et al., 2015) and OT (Lucio-Oliveira and Franci, 2012) levels. Previous studies also revealed that 2–4 h of refeeding after 48 h of fasting significantly increases the mRNA levels of both OT and AVP in the mouse hypothalamus compared to the OT and AVP mRNA expression in normally fed mice (Poplawski et al., 2010). Refeeding after fasting increases the expression of the immediate early gene c-FOS in identified AVP and, to a lesser extent, OT cells, indicating that AVP-positive neurons in the SON could show higher activity than OT-positive neurons under these experimental conditions (Timofeeva et al., 2005; Johnstone et al., 2006; Kohno et al., 2008; Lucio-Oliveira and Franci, 2012; Lucio-Oliveira et al., 2015). In agreement with this, we found that refeeding after fasting significantly increases AVP mRNA expression, while changes in OT mRNA expression were not significant.

Previous studies on the hypothalamic SON and/or PVN showed the presence of mRNA transcripts not only for P2X2 but also for the P2X3, P2X4, P2X6, and P2X7 receptors (Bo et al., 1995; Collo et al., 1996; Vulchanova et al., 1996; Xiang et al., 1998; Shibuya et al., 1999; Vavra et al., 2011). Experiments with specific P2XR knockout mice revealed that endogenously released ATP acts on P2X2R but not P2X3R or P2X7R in posterior pituitary nerve terminals (Custer et al., 2012). Functional and pharmacological studies on SON neurons also identified P2X2R as a dominant subtype of the P2X receptor (Troadec et al., 1998; Song and Sladek, 2006; Gomes et al., 2009; Vavra et al., 2011). P2X2R activation increases the release of AVP from hypothalamo-neurohypophyseal system explants (Troadec et al., 1998; Song and Sladek, 2006; Gomes et al., 2009) and evokes somatic current in the SON neurons of hypothalamic slices (Vavra et al., 2011; Bhattacharya et al., 2013). There are lines of evidence indicating that P2X2R-expressing neurons are magnocellular AVP neurons. First, locally applied ATP increases cytosolic free Ca^{2+} concentrations in identified somata of dissociated AVP neurons from the SON (Troadec et al., 1998; Shibuya et al., 1999; Song et al., 2007) and evokes AVP release from isolated posterior pituitary nerve terminals, but no significant OT release (Troadec et al., 1998; Song and Sladek, 2006; Gomes et al., 2009; Lemos et al., 2018). Second, ATP endogenously released from the posterior pituitary during electrical stimulation depolarizes the nerve terminals and potentiates AVP secretion (Knott et al., 2008). Finally, the data presented here show that the increased expression of P2X2R mRNA and functionality in terms of ATP-induced current in the SON of 2 h refed animals corresponds with the increased expression of AVP mRNA. Thus, these results altogether support the idea that the upregulation of P2X2Rs during fasting/refeeding could be selectively associated with increased synthesizing and releasing activity of AVP neurons.

P2X2R has also been shown to be expressed on presynaptic nerve terminals in hypothalamic slices and its activation facilitates glutamate and GABA release in a subpopulation of SON neurons (Vavra et al., 2011; Bhattacharya et al., 2013). The ATP-induced increase in mIPSC amplitude observed here in P2XR-expressing neurons might represent multiquantal release of GABA that was due to a dramatic influx of calcium through a high number of presynaptic P2X2R channels. This idea is supported by the fact that the amplitude of postsynaptic current did not increase when ATP-induced increase in frequency was moderate, such as in neurons not-expressing somatic P2XRs. Quantitative analysis of GABA-synthesizing enzyme glutamate decarboxylase or GABA immunostaining combined with OT and AVP immunolocalization previously showed that GABAergic innervation within the SON is very extensive and uniformly distributed within the nucleus and that GABAergic nerve terminals contact OT and AVP neurons to a similar extent (Theodosis et al., 1986; Meeker et al., 1993). Electron microscopy observations has also shown that not all axons in the rat SON display immunoreactivity to P2X2Rs (Loesch et al., 1999). Our electrophysiology results revealed that most of P2XR-expressing GABAergic inputs terminate on P2XR-expressing neurons (probably AVP neurons), while most GABAergic inputs without presynaptic P2XRs terminate on neurons not expressing P2XRs (probably OT neurons). These results also support idea that upregulation of P2X2Rs during fasting/refeeding is selectively associated with increased activity of AVP neurons, in this case at presynaptic level.

Both P2XRs and P2YRs participate in the ATP-induced increase in $[Ca^{2+}]_i$ in the SON cells (Song et al., 2007) and P2YRs have been reported in rat SON astrocytes (Espallergues et al., 2007). P2YRs couple with the phospholipase C (PLC) pathway, the activation of which results in $[Ca^{2+}]_i$ increase due to Ca^{2+} release from intracellular stores and the stimulation of a Ca^{2+}−dependent K^+ current (Schicker et al., 2010). This indicates that P2YR activation might hyperpolarize the membrane and inhibit neuronal firing. In this scenario, reduced expression of P2Y1R mRNA might contribute to increased excitatory effect of ATP on neuronal somata. Since ADP was not found to significantly inhibit the frequency of action potentials in SON neurons of slices (Vavra et al., 2011), functional consequences of reduced expression of P2Y1R mRNA observed in SON from fasted/refed animals need further investigation.

SON neurons receive GABAergic afferent inputs from osmosensitive neurons of the circumventricular subfornical organ that communicate chronic changes in plasma osmolality through direct projections to the AVP neurons, thus modulating the synthesis of AVP as well as its transport to and release from the posterior lobe of the pituitary (Weiss and Hatton, 1990). Some inputs to AVP cells could originate from GABA-containing cells in the locus coeruleus (Jones and Moore, 1977; Leng et al., 1999) or interneurons within the perinuclear zone (Tappaz et al., 1983), which presumably mediate the projections from other regions, and regulate the excitatory and inhibitory inputs into the SON neurons (Leng et al., 1999; Wang et al., 2015). Neurons in this zone could account for the large number of intact synapses remaining in the SON after its surgical isolation by

slicing (Leranth et al., 1975). The perinuclear GABAergic neurons are thought to mediate the rapid inhibition of AVP neurons following transient hypertension (Jhamandas et al., 1989; Nissen et al., 1993). We can speculate that the observed food-intake related changes in GABAergic synaptic input might be associated with changes in the patterning of the discharge of AVP neurons so that synthesis and release of AVP is increased.

Overall, our observations indicate that ATP and P2X2R signaling could be significantly linked with the complex stimulation of AVP neurons and corresponding hormone secretion induced in rats by refeeding after fasting.

DATA AVAILABILITY

The raw data supporting the conclusions of this manuscript will be made available by the authors, without undue reservation, to any qualified researcher.

ETHICS STATEMENT

Animals were obtained from established breeding couples in the animal facility (Animal facility of the Institute of Physiology, Czech Academy of Sciences; approval number #56379/2015-MZE-17214). All animal procedures were approved by the Animal Care and Use Committee of the Czech Academy of Sciences (dissection protocol # 67985823).

AUTHOR CONTRIBUTIONS

MI prepared rat brain slices, carried out electrophysiological experiments, and contributed to the conception of the work. AB did quantitative real-time RT-PCR. HZ designed the experiments and finalized the manuscript. All authors analyzed the data, contributed to drafting the work, approved the version to be published, and agreed to be accountable for all aspects of the work.

FUNDING

This research was financed by the Grant Agency of the Czech Republic (16-12695S and 18-05413S), the Ministry of Education, Youth and Sports of the Czech Republic within the LQ1604 National Sustainability Program II (Project BIOCEV-FAR), the project BIOCEV (CZ.1.05/1.1.00/02.0109), and by the Czech Academy of Sciences research project RVO 67985823.

REFERENCES

Armstrong, W. E. (2007). The neurophysiology of neurosecretory cells. *J. Physiol.* 585, 645–647. doi: 10.1113/jphysiol.2007.145755

Bhattacharya, A., Vavra, V., Svobodova, I., Bendova, Z., Vereb, G., and Zemkova, H. (2013). Potentiation of inhibitory synaptic transmission by extracellular ATP in rat suprachiasmatic nuclei. *J. Neurosci.* 33, 8035–8044. doi: 10.1523/JNEUROSCI.4682-12.2013

Bo, X., Zhang, Y., Nassar, M., Burnstock, G., and Schoepfer, R. (1995). A P2X purinoceptor cDNA conferring a novel pharmacological profile. *FEBS Lett.* 375, 129–133. doi: 10.1016/0014-5793(95)01203-q

Boudaba, C., Di, S., and Tasker, J. G. (2003). Presynaptic noradrenergic regulation of glutamate inputs to hypothalamic magnocellular neurones. *J. Neuroendocrinol.* 15, 803–810. doi: 10.1046/j.1365-2826.2003.01063.x

Brussaard, A. B., and Kits, K. S. (1999). Changes in GABAA receptor-mediated synaptic transmission in oxytocin neurons during female reproduction: plasticity in a neuroendocrine context. *Ann. N. Y. Acad. Sci.* 868, 677–680. doi: 10.1111/j.1749-6632.1999.tb11344.x

Burlet, A. J., Jhanwar-Uniyal, M., Chapleur-Chateau, M., Burlet, C. R., and Leibowitz, S. F. (1992). Effect of food deprivation and refeeding on the concentration of vasopressin and oxytocin in discrete hypothalamic sites. *Pharmacol. Biochem. Behav.* 43, 897–905. doi: 10.1016/0091-3057(92)90423-d

Burnstock, G. (2006). Purinergic signalling–an overview. *Novartis Found Symp.* 276, 26–48.

Carreno, F. R., Walch, J. D., Dutta, M., Nedungadi, T. P., and Cunningham, J. T. (2011). Brain-derived neurotrophic factor-tyrosine kinase B pathway mediates NMDA receptor NR2B subunit phosphorylation in the supraoptic nuclei following progressive dehydration. *J. Neuroendocrinol.* 23, 894–905. doi: 10.1111/j.1365-2826.2011.02209.x

Choe, K. Y., Han, S. Y., Gaub, P., Shell, B., Voisin, D. L., Knapp, B. A., et al. (2015). High salt intake increases blood pressure via BDNF-mediated downregulation of KCC2 and impaired baroreflex inhibition of vasopressin neurons. *Neuron* 85, 549–560. doi: 10.1016/j.neuron.2014.12.048

Collo, G., North, R. A., Kawashima, E., Merlo-Pich, E., Neidhart, S., Surprenant, A., et al. (1996). Cloning OF P2X5 and P2X6 receptors and the distribution and properties of an extended family of ATP-gated ion channels. *J. Neurosci.* 16, 2495–2507. doi: 10.1523/jneurosci.16-08-02495.1996

Custer, E. E., Knott, T. K., Cuadra, A. E., Ortiz-Miranda, S., and Lemos, J. R. (2012). P2X purinergic receptor knockout mice reveal endogenous ATP modulation of both vasopressin and oxytocin release from the intact neurohypophysis. *J. Neuroendocrinol.* 24, 674–680. doi: 10.1111/j.1365-2826.2012.02299.x

Day, T. A., Sibbald, J. R., and Khanna, S. (1993). ATP mediates an excitatory noradrenergic neuron input to supraoptic vasopressin cells. *Brain Res.* 607, 341–344. doi: 10.1016/0006-8993(93)91528-Z

de Kock, C. P., Burnashev, N., Lodder, J. C., Mansvelder, H. D., and Brussaard, A. B. (2004). NMDA receptors induce somatodendritic secretion in hypothalamic neurones of lactating female rats. *J. Physiol.* 561, 53–64. doi: 10.1113/jphysiol.2004.069005

Decavel, C., and Curras, M. C. (1997). Increased expression of the N-methyl-D-aspartate receptor subunit. NR1, in immunohistochemically identified magnocellular hypothalamic neurons during dehydration. *Neuroscience* 78, 191–202. doi: 10.1016/s0306-4522(96)00544-1

Espallergues, J., Solovieva, O., Técher, V., Bauer, K., Alonso, G., Vincent, A., et al. (2007). Synergistic activation of astrocytes by ATP and norepinephrine in the rat supraoptic nucleus. *Neuroscience* 148, 712–723. doi: 10.1016/j.neuroscience.2007.03.043

Gomes, D. A., Song, Z., Stevens, W., and Sladek, C. D. (2009). Sustained stimulation of vasopressin and oxytocin release by ATP and phenylephrine requires recruitment of desensitization-resistant P2X purinergic receptors. *Am. J. Physiol. Regul. Integr. Comp. Physiol.* 297, R940–R949. doi: 10.1152/ajpregu.00358.2009

Gordon, G. R., Iremonger, K. J., Kantevari, S., Ellis-Davies, G. C., MacVicar, B. A., and Bains, J. S. (2009). Astrocyte-mediated distributed plasticity at hypothalamic glutamate synapses. *Neuron* 64, 391–403. doi: 10.1016/j.neuron.2009.10.021

Gottlieb, H. B., Ji, L. L., and Cunningham, J. T. (2011). Role of superior laryngeal nerve and Fos staining following dehydration and rehydration in the rat. *Physiol. Behav.* 104, 1053–1058. doi: 10.1016/j.physbeh.2011.07.008

Hu, B., and Bourque, C. W. (1991). Functional N-Methyl-D-Aspartate and non-N-Methyl-D-aspartate receptors are expressed by rat supraoptic neurosecretory cells in vitro. *J. Neuroendocrinol.* 3, 509–514. doi: 10.1111/j.1365-2826.1991.tb00311.x

Iremonger, K. J., Benediktsson, A. M., and Bains, J. S. (2010). Glutamatergic synaptic transmission in neuroendocrine cells: basic principles and mechanisms of plasticity. *Front. Neuroendocrinol.* 31:296–306. doi: 10.1016/j.yfrne.2010.03.002

Israel, J. M., Poulain, D. A., and Oliet, S. H. (2010). Glutamatergic inputs contribute to phasic activity in vasopressin neurons. *J. Neurosci.* 30, 1221–1232. doi: 10.1523/JNEUROSCI.2948-09.2010

Jhamandas, J. H., Raby, W., Rogers, J., Buijs, R. M., and Renaud, L. P. (1989). Diagonal band projection towards the hypothalamic supraoptic nucleus: light and electron microscopic observations in the rat. *J. Comp. Neurol.* 282, 15–23. doi: 10.1002/cne.902820103

Johnstone, L. E., Fong, T. M., and Leng, G. (2006). Neuronal activation in the hypothalamus and brainstem during feeding in rats. *Cell Metab.* 4, 313–321. doi: 10.1016/j.cmet.2006.08.003

Jones, B. E., and Moore, R. Y. (1977). Ascending projections of the locus coeruleus in the rat. II. autoradiographic study. *Brain Res.* 127, 25–53.

Jourdain, P., Israel, J. M., Dupouy, B., Oliet, S. H., Allard, M., Vitiello, S., et al. (1998). Evidence for a hypothalamic oxytocin-sensitive pattern-generating network governing oxytocin neurons in vitro. *J. Neurosci.* 18, 6641–6649. doi: 10.1523/jneurosci.18-17-06641.1998

Khakh, B. S., and North, R. A. (2012). Neuromodulation by extracellular ATP and P2X receptors in the CNS. *Neuron* 76, 51–69. doi: 10.1016/j.neuron.2012.09.024

Knott, T. K., Marrero, H. G., Custer, E. E., and Lemos, J. R. (2008). Endogenous ATP potentiates only vasopressin secretion from neurohypophysial terminals. *J. Cell Physiol.* 217, 155–161. doi: 10.1002/jcp.21485

Kohno, D., Nakata, M., Maejima, Y., Shimizu, H., Sedbazar, U., Yoshida, N., et al. (2008). Nesfatin-1 neurons in paraventricular and supraoptic nuclei of the rat hypothalamus coexpress oxytocin and vasopressin and are activated by refeeding. *Endocrinology* 149, 1295–1301. doi: 10.1210/en.2007-1276

Kombian, S. B., Hirasawa, M., Mouginot, D., and Pittman, Q. J. (2002). Modulation of synaptic transmission by oxytocin and vasopressin in the supraoptic nucleus. *Prog Brain Res.* 139, 235–246. doi: 10.1016/s0079-6123(02)39020-4

Lemos, J. R., Custer, E. E., and Ortiz-Miranda, S. (2018). Purinergic receptor types in the hypothalamic-neurohypophysial system. *J. Neuroendocrinol.* [Epub ahead of print],

Leng, G., Brown, C. H., and Russell, J. A. (1999). Physiological pathways regulating the activity of magnocellular neurosecretory cells. *Progr. Neurobiol.* 57, 625–655. doi: 10.1016/s0301-0082(98)00072-0

Leng, G., and Ludwig, M. (2008). Neurotransmitters and peptides: whispered secrets and public announcements. *J. Physiol.* 586, 5625–5632. doi: 10.1113/jphysiol.2008.159103

Leranth, C., Zaborszky, L., Marton, J., and Palkovits, M. (1975). Quantitative studies on the supraoptic nucleus in the rat. I. synaptic organization. *Exp. Brain Res.* 22, 509–523.

Li, C., Tripathi, P. K., and Armstrong, W. E. (2007). Differences in spike train variability in rat vasopressin and oxytocin neurons and their relationship to synaptic activity. *J. Physiol.* 581, 221–240. doi: 10.1113/jphysiol.2006.123810

Loesch, A., Miah, S., and Burnstock, G. (1999). Ultrastructural localisation of ATP-gated P2X2 receptor immunoreactivity in the rat hypothalamo-neurohypophysial system. *J. Neurocytol.* 28, 495–504.

Lucio-Oliveira, F., and Franci, C. R. (2012). Effect of the interaction between food state and the action of estrogen on oxytocinergic system activity. *J. Endocrinol.* 212, 129–138. doi: 10.1530/JOE-11-0272

Lucio-Oliveira, F., Traslavina, G. A., Borges, B. D., and Franci, C. R. (2015). Modulation of the activity of vasopressinergic neurons by estrogen in rats refed with normal or sodium-free food after fasting. *Neuroscience* 284, 325–336. doi: 10.1016/j.neuroscience.2014.09.076

Ludwig, M. (1998). Dendritic release of vasopressin and oxytocin. *J. Neuroendocrinol.* 10, 881–895. doi: 10.1046/j.1365-2826.1998.00279.x

Meeker, R. B., Swanson, D. J., Greenwood, R. S., and Hayward, J. N. (1993). Quantitative mapping of glutamate presynaptic terminals in the supraoptic nucleus and surrounding hypothalamus. *Brain Res.* 600, 112–122. doi: 10.1016/0006-8993(93)90408-f

Moos, F. C. (1995). GABA-induced facilitation of the periodic bursting activity of oxytocin neurones in suckled rats. *J. Physiol.* 488(Pt 1), 103–114. doi: 10.1113/jphysiol.1995.sp020949

Nissen, R., Cunningham, J. T., and Renaud, L. P. (1993). Lateral hypothalamic lesions alter baroreceptor-evoked inhibition of rat supraoptic vasopressin neurones. *J. Physiol.* 470, 751–766. doi: 10.1113/jphysiol.1993.sp019886

Oliet, S. H., and Bourque, C. W. (1993). Mechanosensitive channels transduce osmosensitivity in supraoptic neurons. *Nature* 364, 341–343. doi: 10.1038/364341a0

Panatier, A., and Oliet, S. H. (2006). Neuron-glia interactions in the hypothalamus. *Neuron Glia Biol.* 2, 51–58. doi: 10.1017/S1740925X06000019

Poplawski, M. M., Mastaitis, J. W., Yang, X. J., and Mobbs, C. V. (2010). Hypothalamic responses to fasting indicate metabolic reprogramming away from glycolysis toward lipid oxidation. *Endocrinology* 151, 5206–5217. doi: 10.1210/en.2010-0702

Richard, P., Moos, F., and Freund-Mercier, M. J. (1991). Central effects of oxytocin. *Physiol. Rev.* 71, 331–370. doi: 10.1152/physrev.1991.71.2.331

Schicker, K. W., Chandaka, G. K., Geier, P., Kubista, H., and Boehm, S. (2010). P2Y1 receptors mediate an activation of neuronal calcium-dependent K+ channels. *J. Physiol.* 588, 3713–3725. doi: 10.1113/jphysiol.2010.193367

Shibuya, I., Kabashima, N., Ibrahim, N., Setiadji, S. V., Ueta, Y., and Yamashita, H. (2000). Pre- and postsynaptic modulation of the electrical activity of rat supraoptic neurones. *Exp. Physiol.* 85, 145S–151S. doi: 10.1111/j.1469-445x.2000.tb00018.x

Shibuya, I., Tanaka, K., Hattori, Y., Uezono, Y., Harayama, N., Noguchi, J., et al. (1999). Evidence that multiple P2X purinoceptors are functionally expressed in rat supraoptic neurones. *J. Physiol.* 514, 351–367. doi: 10.1111/j.1469-7793.1999.351ae.x

Sladek, C. D., and Kapoor, J. R. (2001). Neurotransmitter/neuropeptide interactions in the regulation of neurohypophyseal hormone release. *Exp. Neurol.* 171, 200–209. doi: 10.1006/exnr.2001.7779

Song, Z., and Sladek, C. D. (2006). Site of ATP and phenylephrine synergistic stimulation of vasopressin release from the hypothalamo-neurohypophyseal system. *J. Neuroendocrinol.* 18, 266–272. doi: 10.1111/j.1365-2826.2006.01411.x

Song, Z., Vijayaraghavan, S., and Sladek, C. D. (2007). ATP increases intracellular calcium in supraoptic neurons by activation of both P2X and P2Y purinergic receptors. *Am. J. Physiol. Regul. Integr. Comp. Physiol.* 292, R423–R431.

Tappaz, M. L., Wassef, M., Oertel, W. H., Paut, L., and Pujol, J. F. (1983). Light- and electron-microscopic immunocytochemistry of glutamic acid decarboxylase (GAD) in the basal hypothalamus: morphological evidence for neuroendocrine gamma-aminobutyrate (GABA). *Neuroscience* 9, 271–287. doi: 10.1016/0306-4522(83)90293-2

Theodosis, D. T., Paut, L., and Tappaz, M. L. (1986). Immunocytochemical analysis of the GABAergic innervation of oxytocin- and vasopressin-secreting neurons in the rat supraoptic nucleus. *Neuroscience* 19, 207–222. doi: 10.1016/0306-4522(86)90016-3

Timofeeva, E., Baraboi, E. D., and Richard, D. (2005). Contribution of the vagus nerve and lamina terminalis to brain activation induced by refeeding. *Eur. J. Neurosci.* 22, 1489–1501. doi: 10.1111/j.1460-9568.2005.04330.x

Troadec, J. D., Thirion, S., Nicaise, G., Lemos, J. R., and Dayanithi, G. (1998). ATP-evoked increases in [Ca2+]i and peptide release from rat isolated neurohypophysial terminals via a P2X2 purinoceptor. *J. Physiol.* 511, 89–103. doi: 10.1111/j.1469-7793.1998.089bi.x

Vavra, V., Bhattacharya, A., and Zemkova, H. (2011). Facilitation of glutamate and GABA release by P2X receptor activation in supraoptic neurons from freshly isolated rat brain slices. *Neuroscience* 188, 1–12. doi: 10.1016/j.neuroscience.2011.04.067

Vilhena-Franco, T., Valentim-Lima, E., Reis, L. C., Elias, L. L. K., Antunes-Rodrigues, J., and Mecawi, A. S. (2018). Role of AMPA and NMDA receptors on vasopressin and oxytocin secretion induced by hypertonic extracellular volume expansion. *J. Neuroendocrinol.* 12:e12633. doi: 10.1111/jne.12633

Voisin, D. L., Herbison, A. E., and Poulain, D. A. (1995). Central inhibitory effects of muscimol and bicuculline on the milk ejection reflex in the anaesthetized rat. *J. Physiol.* 483(Pt 1), 211–224. doi: 10.1113/jphysiol.1995.sp020579

Vulchanova, L., Arvidsson, U., Riedl, M., Wang, J., Buell, G., Surprenant, A., et al. (1996). Differential distribution of two ATP-gated channels (P2X receptors) determined by immunocytochemistry. *Proc. Natl. Acad. Sci. U.S.A.* 93, 8063–8067. doi: 10.1073/pnas.93.15.8063

Wang, L., Ennis, M., Szabo, G., and Armstrong, W. E. (2015). Characteristics of GABAergic and cholinergic neurons in perinuclear zone of mouse supraoptic nucleus. *J. Neurophysiol.* 113, 754–767. doi: 10.1152/jn.00561.2014

Weiss, M. L., and Hatton, G. I. (1990). Collateral input to the paraventricular and supraoptic nuclei in rat. I. Afferents from the subfornical organ and the anteroventral third ventricle region. *Brain Res. Bull.* 24, 231–238. doi: 10.1016/0361-9230(90)90210-q

Wuarin, J. P., and Dudek, F. E. (1993). Patch-clamp analysis of spontaneous synaptic currents in supraoptic neuroendocrine cells of the rat hypothalamus. *J. Neurosci.* 13, 2323–2331. doi: 10.1523/jneurosci.13-06-02323.1993

Xiang, Z., Bo, X., Oglesby, I., Ford, A., and Burnstock, G. (1998). Localization of ATP-gated P2X2 receptor immunoreactivity in the rat hypothalamus. *Brain Res.* 813, 390–397. doi: 10.1016/s0006-8993(98)01073-7

Yao, S. T., Gouraud, S. S., Qiu, J., Cunningham, J. T., Paton, J. F., and Murphy, D. (2012). Selective up-regulation of JunD transcript and protein expression in vasopressinergic supraoptic nucleus neurones in water-deprived rats. *J. Neuroendocrinol.* 24, 1542–1552. doi: 10.1111/j.1365-2826.2012.02362.x

Yoshimura, M., Ohkubo, J., Katoh, A., Ohno, M., Ishikura, T., Kakuma, T., et al. (2013). A c-fos-monomeric red fluorescent protein 1 fusion transgene is differentially expressed in rat forebrain and brainstem after chronic dehydration and rehydration. *J. Neuroendocrinol.* 25, 478–487. doi: 10.1111/jne.12022

Conflict of Interest Statement: The authors declare that the research was conducted in the absence of any commercial or financial relationships that could be construed as a potential conflict of interest.

frontiers in Cellular Neuroscience

ORIGINAL RESEARCH
published: 17 July 2019
doi: 10.3389/fncel.2019.00329

HIV-1 gp120 Promotes Lysosomal Exocytosis in Human Schwann Cells

*Gaurav Datta, Nicole M. Miller, Zahra Afghah, Jonathan D. Geiger and Xuesong Chen**

Department of Biomedical Sciences, University of North Dakota School of Medicine and Health Sciences, Grand Forks, ND, United States

Human immunodeficiency virus type 1 (HIV-1) associated neuropathy is the most common neurological complication of HIV-1, with debilitating pain affecting the quality of life. HIV-1 gp120 plays an important role in the pathogenesis of HIV neuropathy via direct neurotoxic effects or indirect pro-inflammatory responses. Studies have shown that gp120-induced release of mediators from Schwann cells induce CCR5-dependent DRG neurotoxicity, however, CCR5 antagonists failed to improve pain in HIV- infected individuals. Thus, there is an urgent need for a better understanding of neuropathic pain pathogenesis and developing effective therapeutic strategies. Because lysosomal exocytosis in Schwann cells is an indispensable process for regulating myelination and demyelination, we determined the extent to which gp120 affected lysosomal exocytosis in human Schwann cells. We demonstrated that gp120 promoted the movement of lysosomes toward plasma membranes, induced lysosomal exocytosis, and increased the release of ATP into the extracellular media. Mechanistically, we demonstrated lysosome de-acidification, and activation of P2X4 and VNUT to underlie gp120-induced lysosome exocytosis. Functionally, we demonstrated that gp120-induced lysosome exocytosis and release of ATP from Schwann cells leads to increases in intracellular calcium and generation of cytosolic reactive oxygen species in DRG neurons. Our results suggest that gp120-induced lysosome exocytosis and release of ATP from Schwann cells and DRG neurons contribute to the pathogenesis of HIV-1 associated neuropathy.

Keywords: gp120, lysosome exocytosis, P2X4, ATP, Schwann cell, DRG neuron

OPEN ACCESS

Edited by:
Stefania Ceruti,
University of Milan, Italy

Reviewed by:
Archan Ganguly,
University of California, San Diego, United States
Jorge Matias-Guiu,
Complutense University of Madrid, Spain

***Correspondence:**
Xuesong Chen
xuesong.chen@med.und.edu

Specialty section:
This article was submitted to Non-Neuronal Cells, a section of the journal Frontiers in Cellular Neuroscience

Received: *27 March 2019*
Accepted: *03 July 2019*
Published: *17 July 2019*

Citation:
Datta G, Miller NM, Afghah Z, Geiger JD and Chen X (2019) HIV-1 gp120 Promotes Lysosomal Exocytosis in Human Schwann Cells. Front. Cell. Neurosci. 13:329. doi: 10.3389/fncel.2019.00329

INTRODUCTION

Schwann cells are the most abundant glial cells in the peripheral nervous system, ensheathing all axons of peripheral nerves as either myelinating or non-myelinating cells. In addition to its role as insulators of axons, Schwann cells are crucial for the proper function and maintenance of peripheral nerves by providing metabolic and/or trophic support (Beirowski et al., 2014; Feldman et al., 2017; Sasaki et al., 2018) and modulating responses to nerve injury (Jessen and Mirsky, 2016; Kim et al., 2018). Disrupting Schwann cell function can compromise glial–axon communication, nerve homeostasis, and ultimately lead to fiber loss, neurodegeneration, and pain. Although cellular and molecular mechanisms underlying communication between Schwann cells and dorsal root ganglia (DRG) neurons remain to be investigated, Schwann cell dysfunction could play a key role in the pathogenesis of peripheral neuropathy, a highly complex and prevalent disease affecting 2.4% of the general population. The prevalence of peripheral neuropathy increases with age, with 8% in individuals 55 years of age or older in Europe and 14.8% in individuals 40 years of age or older in

United States (Martyn and Hughes, 1997; Gregg et al., 2004). The causes of peripheral neuropathy, which may be hereditary or iatrogenic from the toxicity of drugs given as part of antiretroviral or chemotherapy regiments, are often secondary to systemic illnesses including diabetes and infectious causes such as human immunodeficiency virus type 1 (HIV-1).

Human immunodeficiency virus type 1 infection affects 35 million people worldwide. Although combined anti-retroviral therapy (ART) successfully suppresses HIV-1 and dramatically increases the lifespan of HIV-infected individuals, neurological complication of HIV-1 infection persists. Between 30 and 60% of HIV-infected individuals develop HIV-associated distal symmetric polyneuropathy (DSP), a peripheral sensory neuropathy that is characterized clinically by numbness, tingling, pain, paresthesia, and allodynia that begin in distal lower extremities symmetrically and extend to more proximal areas and the upper extremities later in the disease (Centner et al., 2013). Pathologically, DSP is characterized by loss of intraepidermal nerve fibers, nerve fiber swelling, mononuclear inflammation, distal degeneration of long axons in a "dying back" pattern and concurrent damage to the DRG (Schütz and Robinson-Papp, 2013; Bilgrami and O'Keefe, 2014; Kaku and Simpson, 2014; Aziz-Donnelly and Harrison, 2017; Prior et al., 2018). The pathogenesis of DSP was originally attributed to neurotoxic effects of HIV-1 infection, but this is likely to be an indirect effect because evidence of viral infection of sensory neurons is lacking (Keswani et al., 2003; Melli et al., 2006). Since the introduction of ART, sensory neuropathy resulting from neurotoxic antiretrovirals, especially stavudine (d4T), didanosine (ddI), and zalcitabine (ddC), commonly referred to as d−drugs, has been recognized. However, in resource-rich countries where these neurotoxic drugs are no longer widely used, the rate of HIV-1 sensory neuropathies remains unsatisfactorily high (Ellis et al., 2008; Letendre et al., 2009). Furthermore, the prevalence of HIV-1 DSP was high before the introduction of highly active antiretroviral therapy (Hall et al., 1991; Fuller et al., 1993).

The pathogenesis of DSP remains elusive, but several underlying mechanisms have been proposed (Schütz and Robinson-Papp, 2013; Stavros and Simpson, 2014; Prior et al., 2018); peripheral nerve degeneration could result from HIV-induced dysfunction of macrophages that release inflammatory mediators, from age-related HIV-comorbidities such as diabetes, or from neurotoxicity of gp120, a glycoprotein on the HIV-1 envelope. Although gp120 is able to bind to DRG neurons and may have a direct neurotoxic effect (Apostolski et al., 1993; Melli et al., 2006; Wallace et al., 2007; Berth et al., 2016; Wenzel et al., 2017), Schwann cell-dependent DRG neurotoxicity of gp120 has also been implicated; gp120 can bind to chemokine receptors (CXCR4) of Schwann cells and the subsequent release of chemokines can induce apoptosis of DRG neurons via the activation of the C-C chemokine receptor type 5 (CCR5) (Keswani et al., 2003; Melli et al., 2006). However, vicriviroc, a CCR5 antagonist, did not improve pain compared to placebo in a trial of 118 patients with HIV DSP (Yeh et al., 2010). Thus, further mechanistic studies of HIV DSP are warranted.

Lysosomes are acidic organelles responsible for the degradation of macromolecules derived from endocytic and autophagic substrates. Besides their classical role in degradation, lysosomes have been implicated in intercellular communications via lysosome exocytosis; lysosomes can respond to extracellular stimuli by docking at the interior of the cell surface, fuse with the plasma membranes, and release their contents. In the nervous system, lysosomal exocytosis represents as a new pathway for gliotransmitters secreted from astrocytes (Zhang et al., 2007; Li et al., 2008; Liu et al., 2011). In Schwann cells, lysosome exocytosis has also been demonstrated (Chen et al., 2012; Shin et al., 2012; Jung et al., 2014; Su et al., 2019) and lysosome exocytosis can play an important role in regulating myelination and the release of ATP, an important mediator of peripheral pain via activation of purinergic receptors (Surprenant et al., 1996; Hattori and Gouaux, 2012; Yamashita et al., 2016; Jurga et al., 2017; Ying et al., 2017). Thus, disturbances in Schwann cell function could be an important underlying factor for axonal degeneration as occurs in HIV-1 neuropathy (Orita et al., 2013; Viader et al., 2013; Beirowski et al., 2014; Bacallao and Monje, 2015; Monk et al., 2015; Brosius Lutz et al., 2017).

Based on recent findings in non-neural cells that ATP is transported to lysosomes by the vesicular nucleotide transporter (VNUT), where it regulates lysosomal P2X4 function (Cao et al., 2014; Zhong et al., 2016; Moriyama and Nomura, 2017; Moriyama et al., 2017), we investigated the role of gp120 in regulating lysosome exocytosis in Schwann cells and subsequently affecting DRG neuron function. We demonstrated that gp120 induced the movement of lysosomes toward the cell periphery, increased lysosomal exocytosis, and enhanced release of ATP from Schwann cells, and that these processes were sensitive to P2X4 and VNUT inhibition. Using a simplified model of Schwann cell-DRG neuron interaction, we further showed that gp120-induced lysosomal exocytosis in Schwann cells increased cytosolic calcium and generation of reactive oxygen species (ROS) in DRG neurons. Our finding suggests that gp120-induced lysosome exocytotic release of ATP from Schwann cells contributes to the pathogenesis of HIV DSP.

MATERIALS AND METHODS

Cell Culture

Primary human schwann cells (hSCs) were obtained from ScienCell (Carlsbad, CA, United States). The hSCs were cultured in Schwann Cell Medium supplemented with Schwann Cell Growth Supplement, 10% Fetal Bovine Serum and 1% Pen/Strep, and maintained at 37°C in a 5% CO_2 atmosphere following manufacturer's instructions. For the present study, only cells from passage 2–5 were used.

Rat Schwannoma RT4-D6P2T cells were obtained from ATCC (Manassas, VA, United States) and maintained in DMEM supplemented with 10% FBS. For the present study, only cells from passage 2–5 were used.

Rat embryonic DRG neurons were obtained from Lonza (Walkersville, MD, United States), and cultured according to manufacturer's instructions. Rat DRG neurons were cultured in primary neuron basal medium (PNBM) supplemented

with 2 mmol/L L-Glutamine, 50 μg/ml Gentamicin/37 ng/ml Amphotericin, and 2% NSF-1. To get a pure DRG neuron culture without Schwann cells, mitotic inhibitors (17.5 μg/ml uridine and 7.5 μg/ml of 5-fluoro-2′-deoxyuridine) were added. DRG neurons were used for assay between DIV 7–10.

Plasmids and Transfection

The P2X4-pHluorin123 plasmid was a kind gift from Baljit Khakh (Addgene plasmid # 52926). The construct is based on the mouse P2X4 sequence, with the initiating methionine of pHluorin at position 123 of the reconstructed P2X4 receptor (Xu et al., 2014). The extracellular domain of P2X4 was chosen for pHluorin insertion because it avoided regions of known function. The total size of the insert was 1953 bp and was cloned into pcDNA3.1. For transient expression, RT4 Schwann cells were plated onto poly D-lysine coated 6-well plates at a density of 7000 cells/cm^2 and transfected with 1.0 μg plasmid and 3.0 μL Lipofectamine 2000 transfection reagent at ∼70% confluency. On reaching confluency, cells were then split on to 35 mm^2 poly D-lysine coated glass bottom dishes (MatTek) and imaged after 48–72 h.

Antibodies and Reagents

The following primary antibodies were used in immunofluorescent staining; rabbit anti-LAMP1-CD107a (1:100 for surface staining, AB2971, EMD Millipore), rabbit anti-LAMP1-D2D11 (1:250 for intracellular staining, Catalog #9091, Cell Signaling), mouse monoclonal anti-pan cadherin (1:500, Catalog # C1821, Sigma-Aldrich), rabbit anti-TFEB (1:250, Catalog # AV100809, Sigma-Aldrich), goat anti-VNUT (1:200, Catalog # ABN110, EMD Millipore), rabbit anti-P2X4 (1:500, Catalog # AB5226, EMD Millipore), rabbit anti-RILP (1:250, Catalog # ab128616, Abcam). Alexa Fluor 594 goat anti-rabbit, 488 goat anti-rabbit, 594 goat anti-mouse, 488 goat anti-mouse antibodies were from Thermo Fisher, and Donkey Anti-Goat IgG Alexa 488 was from Abcam. All secondary antibodies were used at 1:250 dilutions.

Recombinant HIV-1 MN gp120 (Baculovirus) was from ImmunoDX (Catalog # 1021), and heat -inactivated gp120 was used as a control. Acid Phosphatase Activity Fluorometric Kit was from Sigma-Aldrich (Catalog # MAK087).

PKH 26 Red Fluorescent Cell Linker Kit was from Sigma-Aldrich (Catalog # PKH26GL). Magic Red Cathepsin B kit was from Bio-Rad (Catalog # ICT937). Lysotracker DND-99 Red (Catalog # L7528), Thermo Fisher) was used at a final concentration of 50 nmol/L, Alexa Fluor 647 Dextran (Catalog # D22914, Thermo Fisher) was used at a final concentration of 10 μg/ml, BODIPY FL ATP (Catalog # A12410, Thermo Fisher) was used at 5 μmol/L, Fluo-8 AM (Catalog # ab142773, Abcam) was used at 2 μmol/L, and H2DCFDA (Catalog # D399, Thermo Fisher) was used at 5 μmol/L.

Bx430 was from Tocris Bioscience (Catalog #5545), ATP disodium salt was from Sigma-Aldrich (Catalog# FLAAS-5VL), and clodronate disodium salt and BzATP triethylammonium salt were from Calbiochem (Catalog # 233183 and 5057340001, respectively).

Acid Phosphatase Activity Assay

Human schwann cells were plated on to poly-D-lysine coated 24-well plates at a density of 10,000 per cm^2 and treated with either recombinant gp120 or heat-inactivated gp120 (as control) for 24 h or 40 min. The media supernatant (500 μL) was collected and 110 μL were used per sample (in triplicates) for acid phosphatase activity assay following manufacturer's instructions. Acid phosphatase activity was expressed as relative fluorescence, which was measured at Ex/Em-360/440 nm in a Spectra Max Plate Reader (Molecular Devices, San Jose, CA, United States).

LAMP1 Surface Staining

Human schwann cells were plated on to poly-D-lysine coated coverslips in 24-well plates at a density of 5000 per cm^2 and treated with either recombinant gp120 or heat-inactivated gp120 (as control) for 40 min. The plate was chilled on ice and washed twice with ice-cold PBS (containing 1 mM $CaCl_2$, 2 mM $MgCl_2$) and LAMP1 antibody CD107a was added in 0.1% BSA in PBS for 30 min on ice. Following three washes with ice-cold PBS, plasma membranes were co-stained with PKH26 (4 μL/mL) for 90 s on ice. The cells were then washed three times with PBS, fixed in 4% PFA for 3 min on ice, and stained with secondary antibody (0.1% BSA in PBS) for 30 min. Coverslips were then washed, and mounted on frosted glass slides (Fisher Scientific) with ProLong Gold antifade (Catalog # P36935, Thermo Fisher) before imaging on a Zeiss LSM800 Confocal Microscope.

Surface Biotinylation Assay

Human schwann cells grown on poly-D-lysine coated 100 mm^2 dishes were washed twice with PBS (Ca^{+2}, Mg^{+2} free) and treated with recombinant gp120 (8.3 nM) or heat-inactivated gp120 (control) for 40 min. Following the treatments, cells were washed twice with ice-cold PBS and incubated with sulfo-NHS-SS-Biotin (0.5 mg/ml, 4°C, 30 min) and washed with quenching buffer (20 mM Tris and 120 mM NaCl, pH = 7.4) three-times to remove unreacted biotin. After washing twice with ice-cold PBS, hSCs were lysed with 200 μL of radioimmunoprecipitation assay (RIPA) buffer containing protease inhibitor cocktail (Catalog # A32963, Pierce, Thermo Fisher) followed by sonication. After centrifugation (10,000 × *g* for 10 min), supernatants were collected, and protein concentrations were determined with a DC protein assay (Bio-Rad). Further steps were followed as per Pierce Cell Surface Protein Isolation Kit (Catalog # 89881, Thermo Fisher). Labeled proteins were isolated with NeutrAvidin Agarose columns and eluted with sample buffer before immunoblotting. LAMP1 levels were normalized to pan-Cadherin levels for analysis.

Immunoblotting

Cells were harvested and lysed in 1 × RIPA lysis buffer (Thermo Fisher) plus 10 mM NaF, 1 mM Na_3VO_4, and Protease Inhibitor Cocktail (Pierce). After centrifugation (13,000 × *g* for 10 min at 4°C), supernatants were collected, and protein concentrations were determined with a DC protein assay (Bio-Rad). Proteins (10 μg) were separated by SDS-PAGE (12% gel) and transferred to polyvinylidene difluoride membranes

(Millipore). The membranes were incubated overnight at 4°C with appropriate primary and secondary antibodies. The blots were developed with enhanced chemiluminescence, and bands were visualized and analyzed by LI-COR Odyssey Fc Imaging System. Pan-Cadherin or GAPDH was used as loading control to normalize LAMP1/P2X4 and TFEB levels, respectively. Quantification of results was performed by densitometry and the results were analyzed as total integrated densitometric volume values (arbitrary units).

ATP Measurement

ATP released from hSCs into extracellular media was measured with ATP Bioluminescent Assay Kit (Catalog # FLAA, Sigma-Aldrich) following manufacturer's instructions. ATP levels were expressed as relative luminescence, which was measured using a Spectra Max Gemini EM plate reader (Molecular Devices).

Immunofluorescence

Human schwann cells seeded onto poly-D-lysine coated coverslips were treated with gp120 or heat-inactivated gp120 (control) and washed twice with PBS, and fixed with 4% PFA (Electron Microscopy Sciences) for 30 min at RT. The cells were then permeabilized with 0.01% Tween-20, washed twice with PBS and blocked with 3% BSA + 1% normal goat serum for 90 min at 4°C. Incubations with primary antibodies were done overnight at 4°C followed by two washes with PBS and incubation with secondary antibody for 90 min at 4°C. Coverslips were then washed and mounted on frosted glass slides (Fisher Scientific) with ProLong Gold antifade with DAPI before imaging on a Zeiss LSM800 confocal microscope. Controls for immunostaining specificity included staining neurons with primary antibodies without fluorescence-conjugated secondary antibodies (background controls), and staining neurons with only secondary antibodies; these controls helped eliminate auto-fluorescence in each channel and bleed-through (crossover) between channels. For live cell imaging, hSCs on poly D-lysine coated 35 mm^2 glass bottom petridishes (MatTek, P35GC-0-10-C) were transduced with BacMam Lysosome GFP for 36 h prior to imaging. Time lapse imaging with z-stacks at 2 min intervals were captured using a Zeiss LSM800 confocal microscope. Images were processed using ZEISS ZEN and Imaris 9.2 software.

Cathepsin B Magic Red Assay

Human schwann cells were transduced with BacMAM cytosolic GFP (Thermo Fisher) for 36 h and loaded with Alexa Fluor 647 dextran (10 kDa) for 6 h, followed by a chase of 3 h. Cells were then stained with Cathepsin B Magic Red (Bio-rad) as per manufacturer's instructions before imaging. 25–30 cells were imaged per treatment, and experiments were repeated in triplicate. Images were analyzed in Imaris with the cell and peripheral lysosome constructed as mentioned. The number of peripheral lysosomes colocalizing with Cathepsin B were quantified and expressed as a percentage relative to controls.

BODIPY FL-ATP Staining

Human schwann cells on coverslips were transduced with BacMam lysosome RFP for 36 h, then treated and stained with BODIPY FL-ATP in media (5 μmol/L) for 30 min at 37°C, washed twice with PBS and imaged. The lysosome RFP-positive vesicles were analyzed by Imaris and classified as peripheral, juxtanuclear, or perinuclear lysosomes. Their percentages corresponding to control were then plotted in GraphPad Prism 6.0.

DRG Neuron-Schwann Cell Conditioned Media Assay

Rat Schwannoma cells (RT4-D6P2T) grown on poly-D-lysine coated coverslips were treated with gp120 in the presence/absence of inhibitors or controls for 30 min. Of 500 μL of the extracellular media, 200 μL was used for acid phosphatase or ATP assays to confirm lysosomal exocytosis. 100 μL of the conditioned media was added to 100 μL of Fluo-8/H2DCFDA stained primary rat DRG neurons (day 10 in culture), thus having a 1:1 ratio of conditioned media:DRG neuron media. Intracellular calcium and cytosolic ROS in DRG neurons were measured with a Zeiss LSM 800 confocal microscope.

Calcium Measurement

For Fluo-8 calcium imaging, DRG neurons were stained with Fluo-8 (2 μmol/L for 30 min at 37°C) in 1× assay buffer (HHBS with Pluronic F127 plus), followed by two washes with PBS and re-suspension in 100 μL of media prior to being taken for Schwann cell conditioned media assay. Imaging was done at Ex/Em - 490/525 nm with a 63X oil immersion lens. 25–30 cells were imaged per treatment, and the experiments were repeated in triplicate. Images were analyzed in Image J with the mean fluorescence intensity of cells (chosen as ROI) expressed as percentage. Control values were set at 100.

ROS Measurement

Cytosolic ROS was measured by staining DRG neurons with H_2DCFDA (5 μmol/L for 30 min at 37°C), followed by two washes and re-suspension in 100 μL of media before being taken for Schwann cell conditioned media assay. Imaging was done in the FITC channel. 25–30 cells were imaged per treatment, and the experiments were repeated in triplicate. Images were analyzed in Image J with the mean fluorescence intensity of cells (chosen as ROI) expressed as percentage. Control values were set at 100.

LAMP1-Positive Vesicle Positioning

Confocal microscopy acquired z-stack images were analyzed and processed in Imaris 9.2 (Bitplane, Zurich, Switzerland). LAMP1/RILP/BODIPY FL-ATP-positive vesicles were processed as spots, and the nucleus as surface using the Imaris for Cell Biologists module. The distance transformation in surface function was used to create inward facing concentric surfaces from the plasma membrane, and Imaris XT was used to calculate the number of spots. All image acquisition and analytical parameters (size, thresholding) were kept the same between experiments. Particle based colocalization was carried out for all experiments.

Statistical Analysis

All data were expressed as means ± SD. Statistical significance between two groups was analyzed with a Student's *t*-test, and statistical significance among multiple groups was analyzed with one-way ANOVA plus a Tukey *post hoc* test. $p < 0.05$ was considered to be statistically significant.

RESULTS

HIV-1 gp120 Induces Lysosomal Exocytosis

Characteristic hallmarks of lysosomal exocytosis are increased release of lysosomal hydrolases into extracellular media and the translocation of lysosomal membrane proteins to the plasma membrane (PM) (Zhang et al., 2007; Medina et al., 2011). Using these hallmarks, we determined the extent to which gp120 affects lysosomal exocytosis in primary hSCs. Release of lysosomal hydrolases into extracellular media was quantified by measuring activity of acid phosphatase in the media. Incubation of hSCs with recombinant HIV-1 gp120 for 24 h resulted in a concentration-dependent increase in release of lysosomal acid phosphatase into media (**Figure 1A**). Under these conditions, gp120 treatment did not induce significant cell death, as indicated by no changes in levels of released LDH (**Figure 1B**). A shorter treatment for 40 min with 8.3 nmol/L of HIV-1 gp120 also led to significant increase in acid phosphatase release into media (**Figure 1C**). This shorter treatment was therefore used for all subsequent experiments. The PM translocation of LAMP1 was assessed by surface biotinylation assay, and PM levels of LAMP1 were normalized to a control PM protein (α-cadherin). We demonstrated that gp120 (8.3 nmol/L) treatment for 40 min significantly increased PM protein levels of LAMP1 (**Figure 1D**). Furthermore, the PM translocation of LAMP1 was also assessed with surface staining of LAMP1, and levels of surface expression of LAMP1 was calculated as the ratio of LAMP1 immunofluorescent signal to total PM fluorescent signal as labeled with PKH26. gp120 (8.3 nmol/L) treatment for 40 min significantly increased surface expression of LAMP1 (**Figure 1E**). Together, these findings indicate that gp120 induces lysosomal exocytosis in hSCs.

HIV-1 gp120 Induces Redistribution of Lysosomes

Lysosome exocytosis requires two sequential steps. First, lysosomes are recruited to the close proximity of the cell surface (docking), and second, the pool of pre-docked lysosomes then fuses with the PM and releases lysosomal contents (Andrews, 2000; Martinez et al., 2000). The molecular trafficking machinery involved in these two steps is only partially known. To further determine mechanisms by which gp120 affects lysosomal exocytosis, we determined the effects of gp120 on the positioning of LAMP1-positve lysosomes. hSCs were treated with gp120 (8.3 nmol/L) for 40 min and stained with LAMP1 antibodies. Z-stacks were acquired every 0.4 μm in order to approximately position each lysosome in a single z plane. These images were then reconstructed in three dimensions with Imaris software; the cell boundary was either labeled by pan-cadherin antibodies or drawn from DIC images. As illustrated in **Figure 2A** concentric shells of 2 μm diameter were constructed, moving radially inward from the PM toward the nucleus, and labeled as Shell 1, 2, and 3. The lysosomes in Shell 1, 2, and 3 were labeled as peripheral, juxtanuclear, and perinuclear, respectively. As shown in **Figure 2B**, gp120 treatment increased the percentage of both peripheral and juxtanuclear lysosomes and decreased the percentage of perinuclear lysosomes. These findings indicate that gp120 causes a redistribution of LAMP1-positive lysosomes; lysosomes moving from the perinuclear to peripheral positions as a result of gp120 treatment. Given that these static images might not capture the dynamics of lysosomal exocytosis, we tracked the movement of LAMP1-positive lysosomes using live cell imaging. In hSCs transduced with LAMP1-GFP, gp120 promoted lysosomes trafficking to the PM, as indicated by increased number of LAMP1-positive lysosomes in the outermost Shell 1 (**Supplementary Figure S1A**). To rule out the possibility that the percentage changes of LAMP1-positive lysosomes in three shells is not a result of changes in lysosome biogenesis, total numbers of LAMP1-positive vesicles were quantified by immunostaining with LAMP1 antibodies. Treatment with gp120 (8.3 nmol/L) for 40 min did not change total number of LAMP1 positive vesicles (**Figure 2C**). Treatment with gp120 (8.3 nmol/L) for 40 min did change total protein levels of TFEB, a key transcription factor that regulates the biogenesis of lysosome and autophagy (**Figure 2D**). Furthermore, nuclear translocation of TFEB was determined with immunostaining, and gp120 (8.3 nmol/L) treatment for 40 did not induce significant change in nuclear translocation of TFEB (**Supplementary Figure S1B**). Together, these results indicate that gp120 induces lysosomal exocytosis in hSCs. Thus, our findings suggest that gp120 enhances the trafficking of lysosomes toward cell surfaces and promotes lysosomal exocytosis.

HIV-1 gp120-Induced Redistribution of Lysosomes Display Functional Heterogeneity

A recent study has shown that perinuclear lysosomes are more acidic and have higher cathepsin L activity than peripheral lysosomes (Johnson et al., 2016). This heterogeneity could be due to the stabilization of the v-ATPase subunit V1G1 by rab interacting lysosomal protein (RILP), a downstream effector of Rab7 that links Rab7 to dynein–dynactin and controls retrograde transport of late endosomes and lysosomes (Johansson et al., 2007). To further understand the underlying mechanism by which gp120 affects lysosome trafficking and lysosomal exocytosis, we determined the effects of gp120 on the colocalization of LAMP1 with RILP in hSCs. We found that gp120 (8.3 nmol/L) treatment for 40 min significantly lowered the association of RILP with peripheral lysosomes upon gp120 treatment but increased the association for juxtanuclear lysosomes (**Figure 3A**). These findings are consistent with our observations that gp120 induced the movement of lysosomes from the juxtanuclear to the peripheral position and enhanced lysosomal exocytosis. Following upon others' observations that

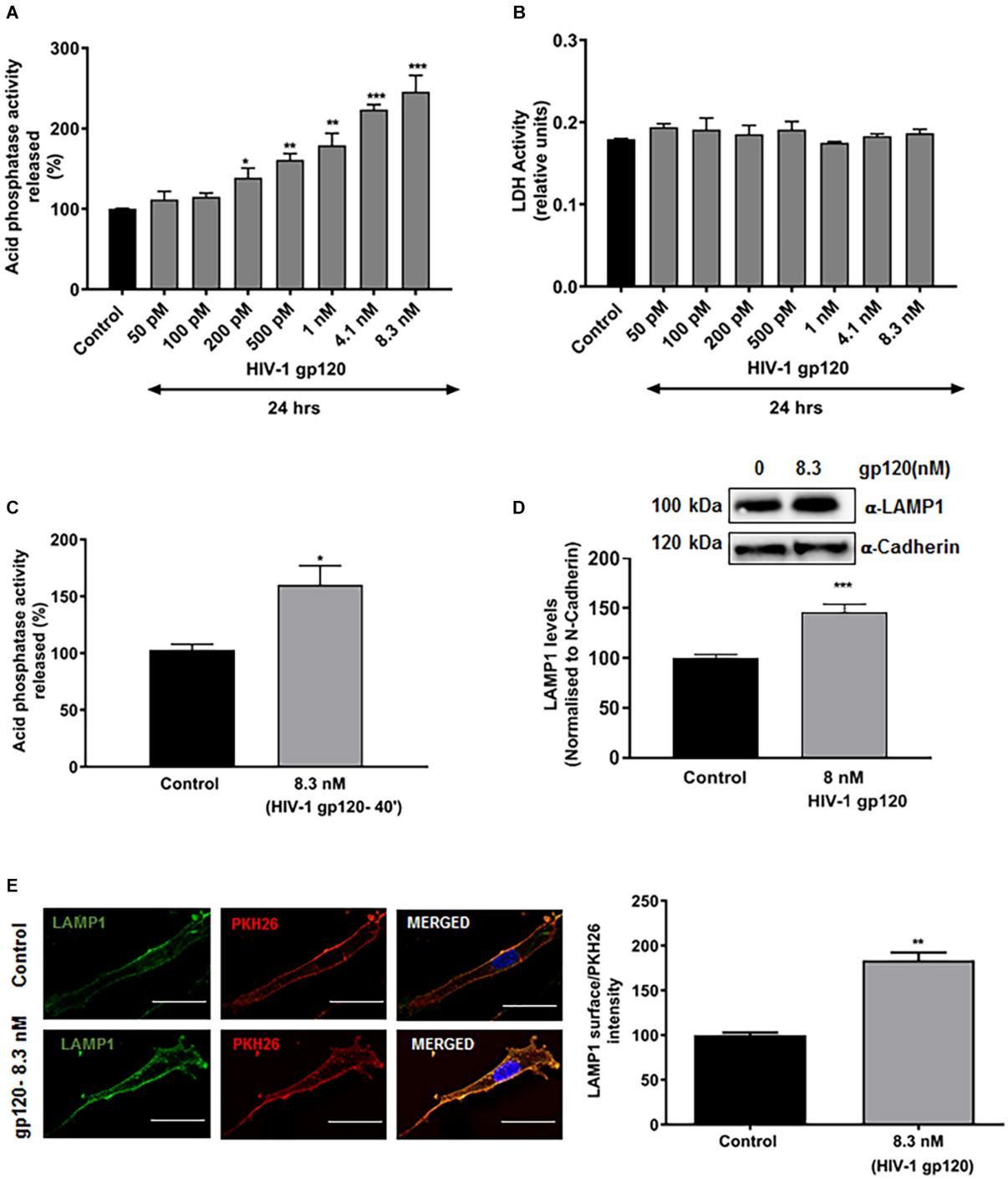

FIGURE 1 | HIV-1 gp120 induces lysosomal exocytosis in primary human Schwann cells (hSCs). **(A)** Compared to heat inactivated gp120 (control), gp120 caused a concentration-dependent increase in the activity of acid phosphatase in media of hSCs ($n = 5$, $^{*}p < 0.05$, $^{**}p < 0.01$, $^{***}p < 0.001$). **(B)** HIV-1 gp120 did not change release of LDH in hSCs. **(C)** gp120 treatment (8.3 nmol/L for 40 min) significantly increased the release of acid phosphatase in the media of hSCs ($n = 3$, $^{*}p < 0.05$). **(D)** In surface protein biotinylation assay, gp120 treatment (8.3 nmol/L for 40 min) increased PM levels of LAMP1 ($n = 3$, $^{***}p < 0.001$). **(E)** In surface protein labeling assay, gp120 treatment (8.3 nmol/L for 40 min) increased PM of LAMP1 ($n = 3$, $^{**}p < 0.01$; bar = 15 μm).

peripheral lysosomes are de-acidified compared to juxtanuclear and perinuclear lysosomes (Johnson et al., 2016), we assessed pH-dependent lysosome degradative capacity using a Magic Red Cathepsin B assay. This assay utilizes a fluorogenic substrate of the lysosomal hydrolase Cathepsin B, which is active under acidic pH, and loses activity upon de-acidification. The amount

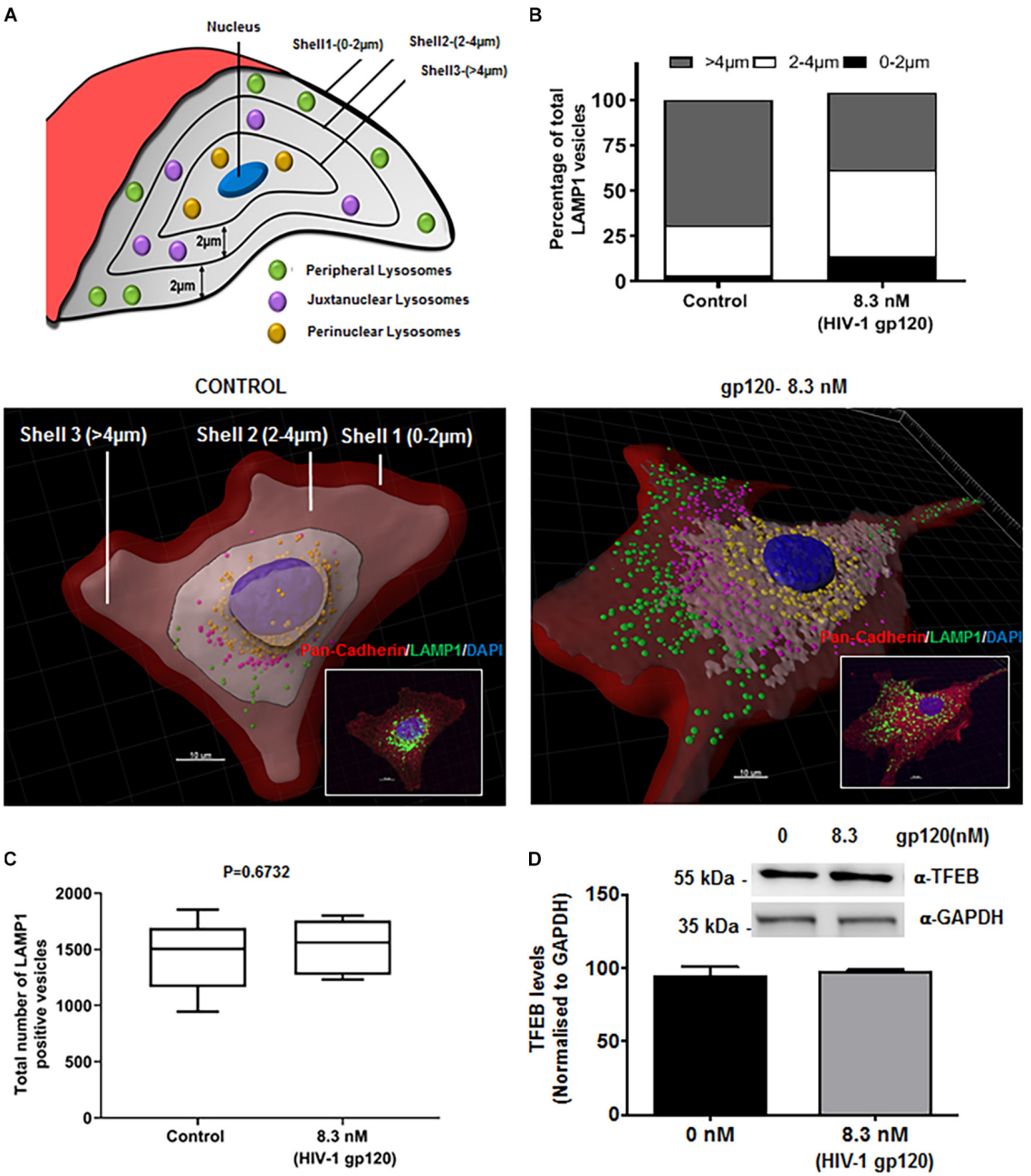

FIGURE 2 | HIV-1 gp120 causes lysosomal redistribution in hSCs. **(A)** Classification scheme of LAMP1 positive lysosomes in concentric shells labeled as peripheral (0–2 μm from PM), juxtanuclear (2–4 μm from PM), and perinuclear (>4 μm from PM) lysosomes. **(B)** As shown in representative LAMP1 staining (insert) and 3D reconstructed images, gp120 treatment (8.3 nmol/L for 40 min) increased the percentage of peripheral (green) and juxtanuclear (magenta) lysosomes and decreased the percentage of perinuclear (yellow) lysosomes. Plasma membranes were outlined with Pan-Cadherin (red) and the nucleus stained with DAPI (blue). **(C)** gp120 treatment (8.3 nmol/L for 40 min) did not change total numbers of LAMP1 positive lysosomes (n = 100) **(D)** gp120 treatment (8.3 nmol/L for 40 min) did not change TFEB protein levels in hSCs.

of fluorescence is therefore a direct output of active Cathepsin B, indicating the acidification status of the lysosome (Linke et al., 2002; Cheng et al., 2018). For this assay, hSCs were transfected with cytosolic GFP, and pulsed with Alexa Fluor 647 dextran (10 kDa) for 6 h followed by a chase of 3 h in order for the dextran to travel via the endocytic pathway to lysosomes. The hSCs were then treated with gp120 (8.3 nmol/L) for 40 min, stained with Magic Red Cathepsin B and imaged live by confocal microscopy. As expected, peripheral lysosomes had significantly lower levels of Magic Red fluorescence, indicating decreased activity of cathepsin B (**Figure 3B**). These findings indicate that the altered distribution of lysosomes upon gp120

treatment could be attributed to lysosome de-acidification. To further test the extent to which reduced v-ATPase activity and lysosome de-acidification promotes lysosome exocytosis, we treated cells with bafilomycin, a specific v-ATPase inhibitor, and determined the distribution of LAMP1-positive lysosomes. LAMP1 positive lysosomes were analyzed for their distance from the PM (cells outlined by Pan-Cadherin labeling) using the same methods as mentioned earlier in **Figures 2C,D**. Similar to that of gp120, treatment with bafilomycin increased the percentage of both peripheral and juxtanuclear lysosomes and decreased the percentage of perinuclear lysosomes (**Supplementary Figure S2**).

P2X4 Is Involved in gp120-Induced Lysosomal Exocytosis

Although lysosomes are recruited to being in close proximity to the cell surface in a Ca^{2+}-independent manner (Rodríguez et al., 1997; Andrews, 2000; Jaiswal et al., 2002), the fusion of pre-docked lysosomes with the PM requires Ca^{2+} elevation. Mounting evidence indicate that calcium released from lysosomes could mediate such a fusion event, and recently studies have shown that P2X4 cationic channels are localized to both plasma membranes and lysosomes and is regulated by its natural ligand ATP in a pH-dependent manner (Cao et al., 2015; Dong, 2015). Thus, gp120-induced lysosomal exocytosis could result from activation of P2X4 cationic channels. To determine the involvement of P2X4 channel in gp120-induced lysosomal exocytosis, we first characterized the subcellular localization of P2X4 in hSCs. We demonstrated that P2X4 channels colocalized with LAMP1-positive lysosomes in hSCs (**Figure 4A**). Using a surface biotinylation assay, we demonstrated that gp120 (8.3 nmol/L) treatment for 40 min increased PM levels of P2X4 (**Figure 4B**), indicating the involvement of P2X4 in gp120-induced lysosome exocytosis. To further confirm the role of P2X4 in gp120-induced lysosomal exocytosis, pre-incubation with Bx430, a selective allosteric antagonist of P2X4 (Ase et al., 2015), significantly blocked gp120-induced increases in release of lysosomal acid phosphatase (**Figure 4C**). We further determined the effect of a P2X4 agonist 2,3′-O-(4-benzoyl)benzoyl-ATP (BzATP) on lysosomal exocytosis (Emmett et al., 2008; Stokes et al., 2011). Similar to gp120, BzATP (5.0 μmol/L for 30 min) promoted lysosome exocytosis as indicated by increased activity of acid phosphatase released in media (**Supplementary Figure S3**). Thus, gp120 could induce lysosomal exocytosis by activating lysosomal P2X4 channels, and it is possible that gp120 affects the activity of P2X4 within the lumen of lysosomes because gp120 can be endocytosed (Berth et al., 2015; Wenzel et al., 2017). In support, we demonstrated that significant amounts of exogenous gp120-FITC trafficked to lysosomes in as early as 30 min with a Pearson's coefficient of 0.456 (**Supplementary Figure S4B**). It is known that the acidic pH of lysosome lumen has been shown to inhibit P2X4 channels (Huang et al., 2014). Therefore, upon gp120 treatment, lysosomes might move to the periphery, their luminal pH might increase (de-acidification), and as a result P2X4 receptors might be activated. To test this hypothesis, rat Schwannoma cells (RT4-D6P2T) were co-transfected with P2X4-tagged with pH sensitive fluorescent pHluorin123 and LAMP1-RFP. The pHluorin is a pH-sensitive GFP variant, the fluorescence of which remains quenched at acidic pH and increases as the pH increases to neutral (Xu et al., 2014). Cells co-transfected with P2X4-pHluorin123 and LAMP1-RFP were treated with gp120 (8.3 nmol/L) and imaged by time lapse microscopy for 20 min. As expected, gp120 increased P2X4-pHluorin123 fluorescence (**Figure 4D**), indicating gp120 de-acidifies P2X4 positive lysosomes. To confirm that RT4 rat Schwann cells behave the same as that of primary hSCs in response to gp120 treatment, we determined the effect of gp120 on lysosome exocytosis in RT4 rat Schwann cells. We found that the response of these rat Schwann cells to gp120 was similar to that of primary hScs; gp120 increased the release of lysosomal acid phosphatase in media of rat Schwann cells (**Supplementary Figure S4A**).

HIV-1 gp120 Modulates Lysosomal P2X4 via VNUT ATP Transporter

Lysosomal P2X4 activity has been shown to be dually regulated by luminal pH and ATP. One of the key lysosomal ATP transporters identified is VNUT (Vesicular Nucleotide Transporter or SLC17A9), responsible for ATP transport into lysosomes. VNUT has been shown to play a role in lysosomal exocytosis leading to extracellular release of ATP. To determine the involvement of VNUT in gp120-induced lysosome exocytosis, the lysosomal localization of VNUT in hSCs was first confirmed by immunocytochemistry, showing that 85% of LAMP1-positive lysosomes co-localized with VNUT, measured using mander's colocalization coefficient (MCC) in Imaris software (**Figure 5A**). Importantly, pretreatment with clodronate, a specific allosteric inhibitor of VNUT, blocked gp120-mediated acid phosphatase release (**Figure 5B**) as well as ATP release (**Figure 5C**) into the extracellular media (Kato et al., 2017). To further determine the involvement of lysosomal ATP in gp120-induced lysosomal exocytosis, we visualized directly lysosomal ATP and their redistribution upon gp120 treatment. Here, hSCs were transduced with LAMP1-RFP, labeled with BODIPY FL-ATP and imaged upon gp120 treatment. The majority of BODIPY FL-ATP staining was observed to be in the lysosomes. To determine the redistribution of lysosomal ATP, cell boundaries were drawn from DIC images and vesicles positive for both LAMP1 and BODIPY FL-ATP were classified based on their distance from the PM as mentioned earlier. As shown in **Figure 5D**, gp120 treatment resulted in a significant increase in the percentage of ATP positive lysosome in peripheral and juxtanuclear regions. Combined, these results suggest that lysosome de-acidification and ATP-mediated P2X4 activation could be a key process in gp120-induced lysosomal exocytosis.

HIV-1 gp120-Induced Schwann Cell Lysosomal Exocytosis Affects DRG Neuron Physiology

To further determine whether gp120-induced lysosomal exocytosis in Schwann cells could affect the function of DRG neurons and contribute to HIV neuropathy, conditioned media

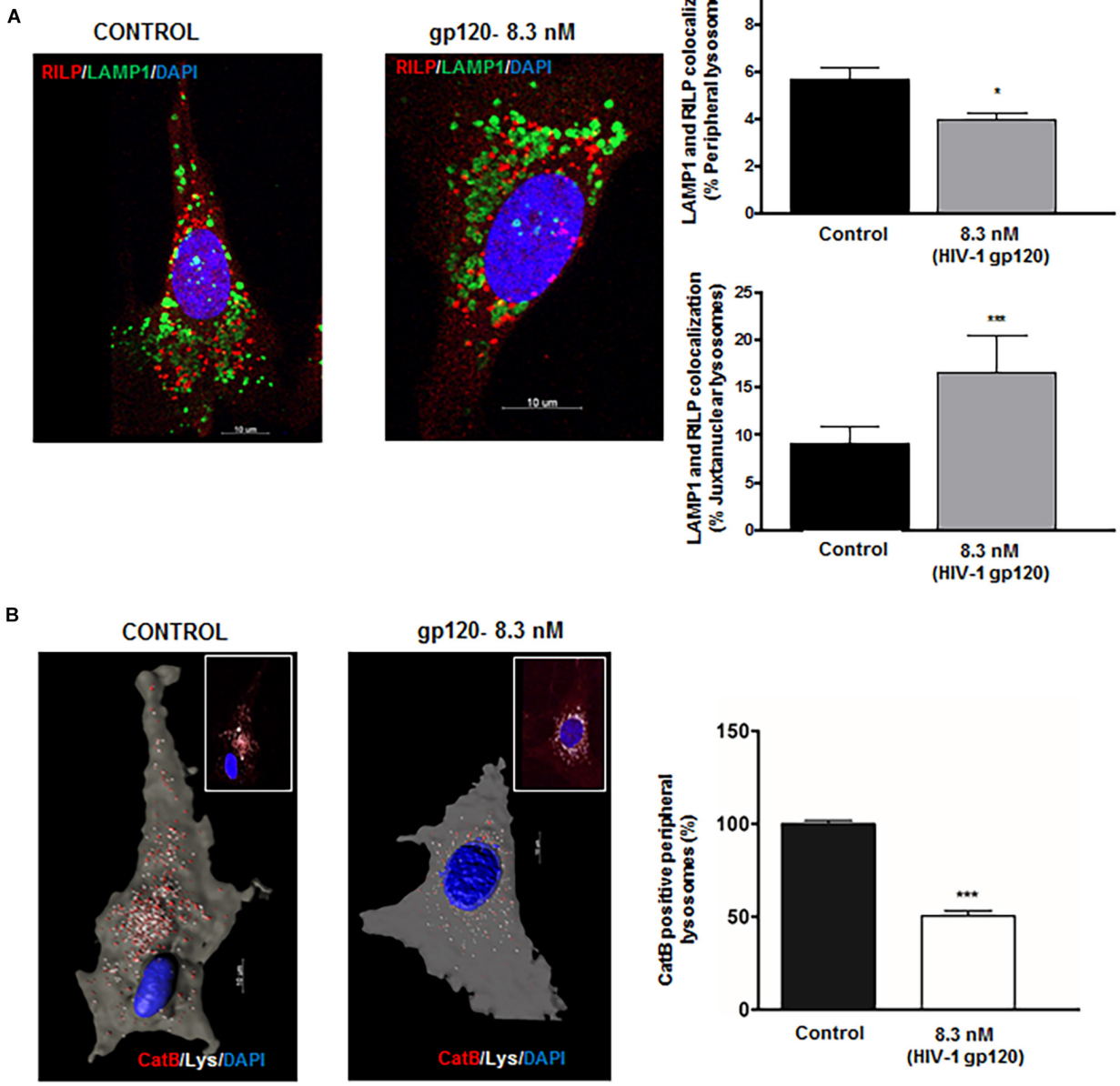

FIGURE 3 | HIV-1 gp120-induces redistribution of lysosomes displays functional heterogeneity. **(A)** gp120 treatment (8.3 nmol/L for 40 min) significantly decreased colocalization of LAMP1 (green) with RILP (red) in peripheral lysosomes, but increased colocalization of LAMP1 with RILP in juxtanuclear lysosomes ($n = 3$, $^{*}p < 0.05$, $^{***}p < 0.001$). **(B)** As shown in representative confocal (inset) and reconstructed Imaris images, gp120 treatment (8.3 nmol/L for 40 min) significantly reduced Cathepsin B activity (red) in peripheral (white) lysosomes ($n = 3$, $^{***}p < 0.001$).

of Schwann cells was used for treatment of DRG neurons. Here, RT4 rat Schwann cells were treated with HIV-1 gp120 for 45 min in the presence or absence of P2X4 blocker (Bx430) and VNUT inhibitor (clodronate), and the extracellular media was added to primary rat DRG neuronal cultures in a 1:1 ratio. Given that a rise in intracellular calcium and increasing the excitability of DRG neurons has been linked to heightened nociceptive sensation in neuropathic pain (Kostyuk et al., 2001; Chung and Chung, 2002; Yang et al., 2018), we measured intracellular calcium of DRG neurons with Fluo-8. We found that gp120-treated Schwann cell conditioned media elevated intracellular Ca^{2+} in DRG neurons, whereas conditioned media from P2X4 and VNUT inhibition (by Bx430 and clodronate, respectively) failed to induce a rise in intracellular calcium (**Figure 6A**). These findings indicate that gp120-induced lysosomal exocytosis of ATP in hSCs could be a key factor causing intracellular calcium to rise in DRG neurons. To further assess DRG neuronal function, cytosolic ROS was measured by staining with DCF-DA. As

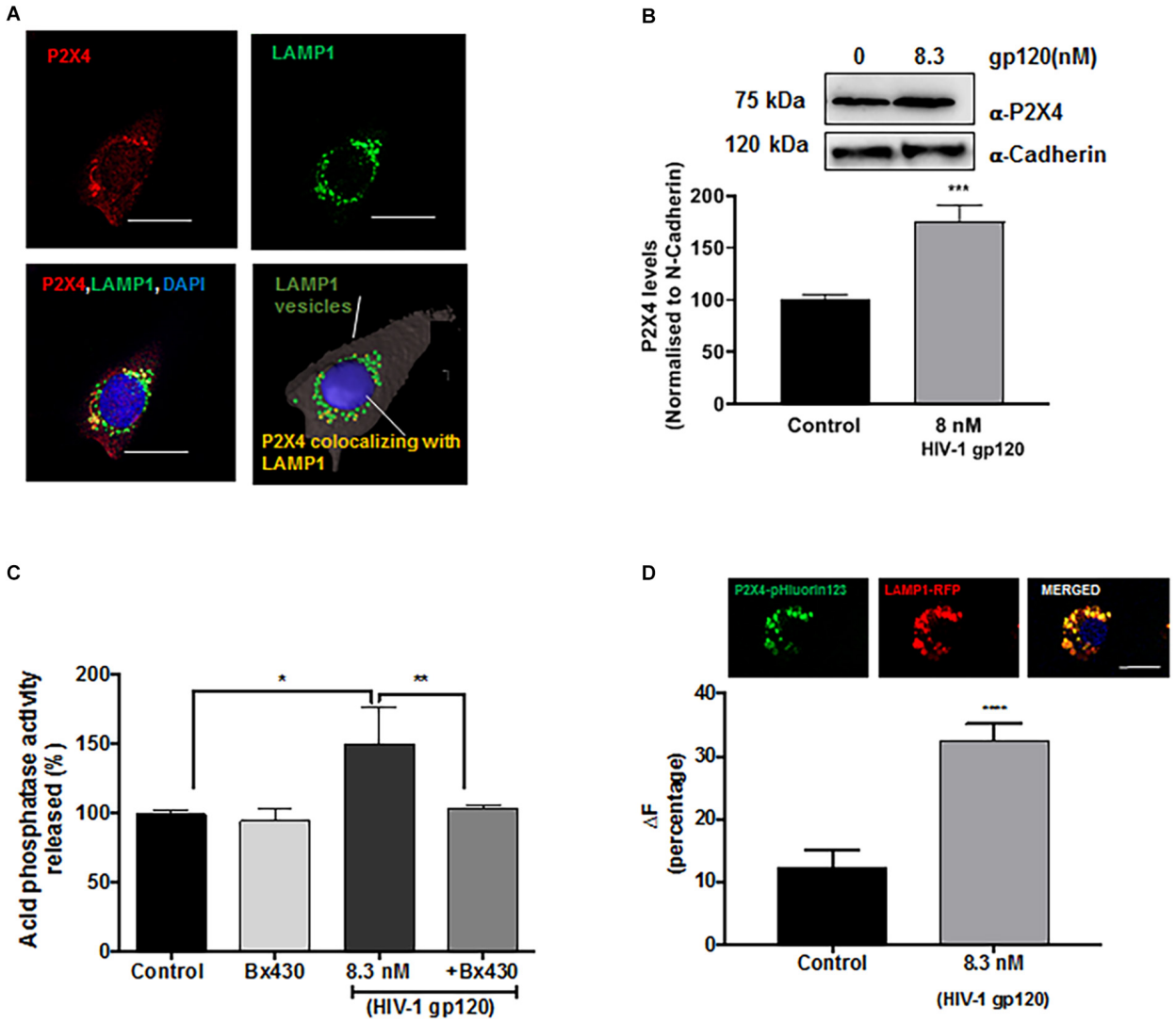

FIGURE 4 | Lysosomal P2X4 channel is involved in HIV-1 gp120 induced lysosomal exocytosis. **(A)** Representative confocal and reconstructed Imaris images show P2X4 (red) is colocalized with LAMP1 (green) positive lysosomes in hSCs (bar = 20 μm). **(B)** In surface biotinylation assay, gp120 treatment (8.3 nmol/L for 40 min) increased P2X4 translocation to the PM in hSCs ($n = 3$, $^{***}p < 0.001$). **(C)** An allosteric P2X4 regulator Bx430 (0.5 μmol/L) prevented gp120 (8.3 nmol/L for 40 min)-induced increases in the activity of acid phosphatase release in media of hSCs ($n = 3$, $^{*}p < 0.05$, $^{**}p < 0.01$). **(D)** As shown in RT4 rat Schwann cells co-transfection of P2X4-pHluorin123 (GFP) and LAMP1-RFP (bar = 10 μm), gp120 treatment (8.3 nmol/L for 40 min) increased fluorescence of P2X4-pHluorin123 ($n = 3$, $^{***}p < 0.001$).

shown in **Figure 6B**, incubation with gp120-treated Schwann cell conditioned media significantly increased DRG neuron ROS levels, whereas conditioned media from P2X4 and VNUT inhibition (by Bx430 and clodronate, respectively) failed to induce a rise in ROS levels. Because lysosomes have been shown to store ATP, which can be released upon exocytosis in other cell types (Zhang et al., 2007; Sivaramakrishnan et al., 2012; Beckel et al., 2018) and we found that gp120 increased the release of ATP into media (**Figure 5**), we determined effects of exogenous ATP on intracellular Ca^{2+} and ROS in DRG neurons. We found that ATP treatment increased both cytosolic Ca^{2+} and ROS in DRG neurons in a concentration-dependent manner (**Supplementary Figures S5A,B**).

DISCUSSION

HIV-associated distal symmetric polyneuropathy (DSP) is the most common neurological complication of HIV infection that results in chronic debilitating neuropathic pain. There is an urgent need for better understanding of its pathogenesis and for the development of effective therapeutic strategies. In the present study, we demonstrated that HIV-1 gp120 promoted the movement of lysosomes toward plasma membranes followed subsequently by lysosomal exocytosis and release of ATP; this process is achieved by gp120-induced activation of lysosome P2X4 via lysosome de-acidification and VNUT coupling. Such gp120-induced lysosomal exocytosis and release of ATP from

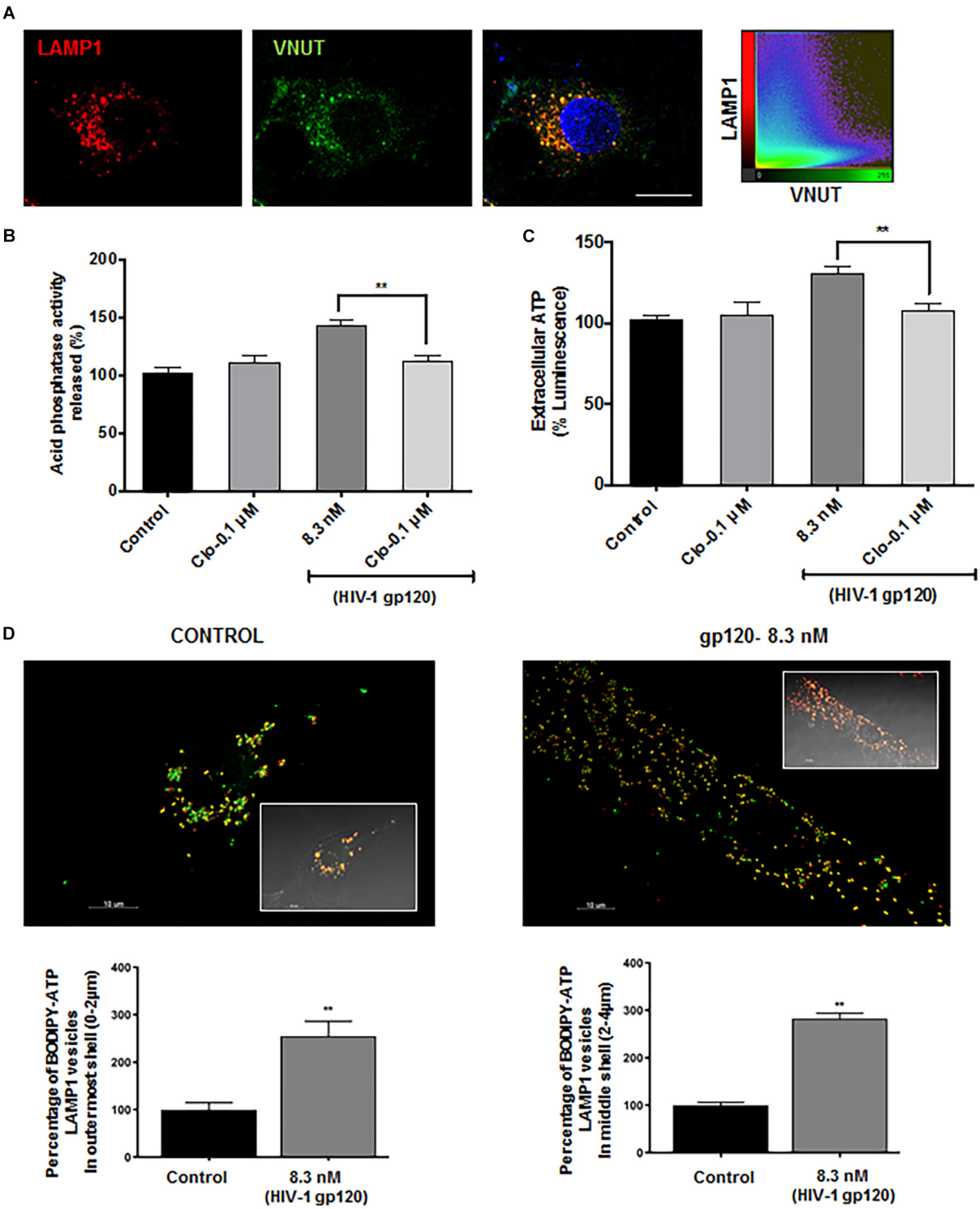

FIGURE 5 | Lysosomal ATP transporter-VNUT mediates HIV-1 gp120 induced lysosomal exocytosis. **(A)** Representative confocal images and scatterplot show the colocalization of VNUT (green) with LAMP1 (red) positive lysosomes in hSCs (bar = 15μm). **(B)** Inhibiting VNUT with clodronate (Clo, 0.1 μmol/L) prevented gp120 (8.3 nmol/L for 40 min)-induced increases in the activity of acid phosphatase release in media of hSCs ($n = 3$, $^{**}p < 0.01$). **(C)** gp120 treatment (8.3 nmol/L for 40 min) increased ATP levels in media of hSCs, and this effect was prevented by inhibiting VNUT with clodronate (Clo, 0.1 μmol/L) ($n = 3$, $^{**}p < 0.01$. **(D)** As shown in representative Imaris reconstructed and confocal images (inset), gp120 (8.3 nmol/L for 40 min) increased percentage of ATP (BODIPY FL-ATP, green) in peripheral and juxtanuclear lysosomes (LAMP1-RFP) ($n = 3$, $^{**}p < 0.01$).

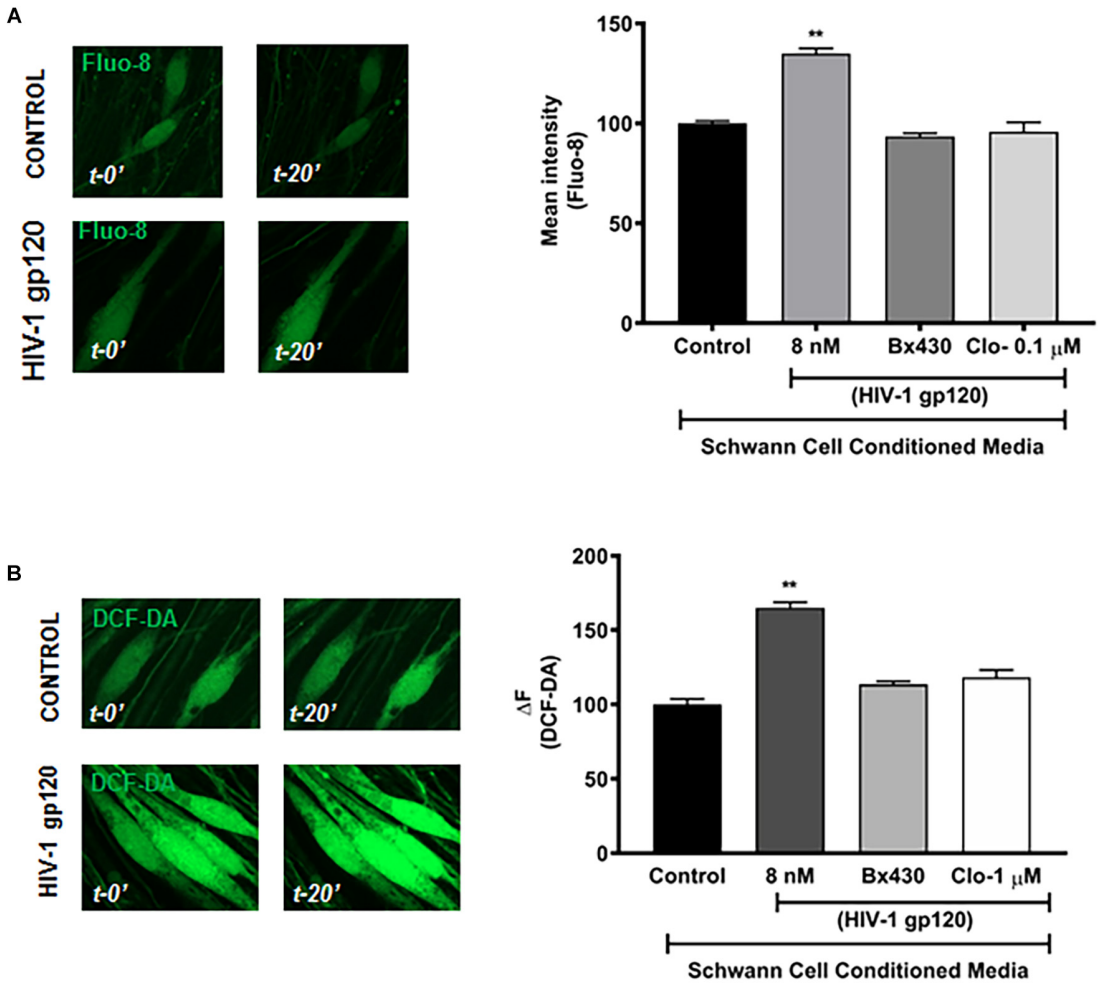

FIGURE 6 | HIV-1 gp120 conditioned RT4 Rat Schwann cell media increases cellular calcium and ROS in DRG neurons. **(A)** gp120 conditioned Schwann cell media, but not gp120 + Bx430 or gp120 + Clo conditioned media, increased intracellular calcium levels as measured by Fluo-8 in rat DRG neurons ($n = 3$, $^{**}p < 0.01$). **(B)** gp120 conditioned media, but not gp120 + Bx430 or gp120 + Clo conditioned media, increased cytosolic ROS levels as measured by DCF-DA in rat DRG neurons ($n = 3$, $^{**}p < 0.01$).

Schwann cells induced increases in cytosolic calcium and ROS in DRG neurons. Our results suggest that gp120-induced lysosomal exocytotic release of ATP might signal through P2X4 and VNUT in Schwann cells and thereby contribute to the pathogenesis of HIV-DSP.

The HIV-1 envelope glycoprotein gp120, which is non-covalently attached to the transmembrane gp41 protein, is expressed on the outer layer of the virus. As such, gp120 is readily shed from HIV-1 virions and infected cells (Gelderblom et al., 1987; Layne et al., 1992; Wyatt and Sodroski, 1998). Detectable levels of gp120 in plasma (0.5–15.6 ng/ml) and in spleen and lymph node (>0.3 ng/ml) is present in HIV-1 infected individuals (Oh et al., 1992; Santosuosso et al., 2009; Rychert et al., 2010). Even in HIV-infected individuals under ART with no detectable viral replication, gp120 can be detected in lymph nodes (Popovic et al., 2005). As the HIV-1 envelope protein, gp120 is critical for virus infection, because it is necessary for binding to specific cell surface receptors (CD4, CXCR4, and CCR5) on target cells and facilitating virus entry (Deng et al., 1996). Released free gp120 is a potent HIV virotoxin via either indirect mechanisms whereby gp120 promotes the release of pro inflammatory cytokines or other neurotoxic factors that elicit indirect neurotoxic effect (Kaul and Lipton, 1999; Bezzi et al., 2001), or direct mechanisms whereby gp120 elicits direct neurotoxic effect in the absence of glutamate receptor activation or pro-inflammatory cytokines (Bachis and Mocchetti, 2004; Bachis et al., 2006; Wenzel et al., 2017).

The role of gp120 in the pathogenesis of HIV-DSP has long been recognized. Higher levels of gp120 in the spinal dorsal horn of HIV neuropathic pain-positive individuals provides a clue that gp120 plays an important role in the development of HIV DSP (Yuan et al., 2014). Exposure of peripheral nerves to HIV-1 gp120 results in neuropathic pain (Herzberg and Sagen, 2001). HIV gp120 transgenic mice or rodents treated with gp120 develop neuropathic pain with pathological similarities with humans such as peripheral neuropathy, pain behavior, synaptic degeneration

and activation of glial cells (Nagano et al., 1996; Oh et al., 2001; Wallace et al., 2007; Hao, 2013; Burdo and Miller, 2014). Similar to gp120-induced neurotoxicity in CNS, gp120 could elicit direct neurotoxicity on DRG neurons (Apostolski et al., 1993, 1994) gp120 could activate macrophages, which in turn release neurotoxic inflammatory mediators that lead to indirect neurotoxicity, or gp120 acts on Schwann cells to release RANTES, which leads to DRG neurotoxicity via CCR5 activation (Keswani et al., 2003; Melli et al., 2006).

Additionally, there is evidence that organelle damage, such as mitochondrial dysfunction (Lehmann et al., 2011) and endoplasmic reticulum dysfunction (Hoke et al., 2009), contributes to the development of HIV DSP. However, virtually nothing is known about the involvement of lysosomes, which not only plays an important role in intercellular communication via lysosome exocytosis in CNS (Zhang et al., 2007; Li et al., 2008; Liu et al., 2011) but also play an important role in regulating Schwann cell function such as regulating myelination and the release of ATP, an important mediator of peripheral pain (Chen et al., 2012; Shin et al., 2014; Brosius Lutz et al., 2017). As such, we determined the extent to which and mechanisms by which gp120 affects lysosomal exocytosis in Schwann cells and contributes to HIV neuropathy.

Mechanism of gp120-Induced Lysosome Exocytosis in Schwann Cells

By measuring increased release of lysosomal hydrolases (acid phosphatase) into extracellular media and the translocation of lysosomal membrane proteins (LAMP1) to the PM, we demonstrated that gp120 promoted lysosome exocytosis in human Schwann cells. Because lysosomes docking (calcium independent) near the PM and subsequent fusion (calcium-dependent) with the PM are the two key steps to lysosome exocytosis (Andrews, 2000; Jaiswal et al., 2002; Tucker et al., 2004), we then determined the extent to which gp120 affected lysosome positioning, an important factor mediating cellular homeostasis including autophagy, apoptosis, exosome release and metabolic signaling (Korolchuk et al., 2011; Eitan et al., 2016; Jia et al., 2017). To estimate lysosomal positioning, we used published methods of classifying them as perinuclear, juxtanuclear, or peripheral lysosomes based on their distances from the PM in concentric rings (Fan and He, 2016; Johnson et al., 2016). Here, we used an increased ring diameter of 2 μm owing to the large size of hSCs, and we demonstrated that short-term treatment (40 min) with gp120 did not change total numbers of LAMP1-positive lysosomes but increased the numbers of peripheral and juxtanuclear lysosomes with concurrent decrease in the numbers of perinuclear lysosomes. Thus, gp120 increases the docking of lysosomes near the PM, which is consistent with enhanced lysosome exocytosis.

Lysosome trafficking in polarized cells occurs along microtubules and is mediated by plus-end directed kinesin (Hollenbeck and Swanson, 1990) and minus-end directed dynein motors (Harada et al., 1998) that are controlled by the action of GTPases such as Rab proteins (Progida and Bakke, 2016; Langemeyer et al., 2018). Rab7 is a specific marker for late endosomes-lysosomes (Feng et al., 1995; Meresse et al., 1995), and its downstream effector protein RILP induces recruitment of lysosomes to the dynein-dynactin complex preventing further cycling of Rab7 (Jordens et al., 2001). Here, we showed that gp120 decreased the association of peripheral lysosomes with RILP, thus further supporting the concept that gp120 promotes the trafficking of lysosomes progressing toward exocytosis (Johnson et al., 2016). We also demonstrated that gp120 increased the association of RILP with juxtanuclear lysosomes, which indicated that only the peripheral lysosomes undergo exocytosis. We further show that gp120 decreased cathepsin B activity in these peripheral lysosomes. Given that cathepsin B is more active in acidic environment, our findings are consistent with recent findings that lysosomes undergo progressive de-acidification as they move toward the PM (Johnson et al., 2016), and possibly these peripheral lysosomes have fulfilled their degradative functions and are destined for exocytosis.

Upon further investigating the underlying mechanisms whereby gp120 affects lysosomal trafficking to the cell periphery and lysosome exocytosis, we determined the involvement of P2X4, a fast and sensitive purinergic receptor that preferentially localizes to lysosomes (Xu et al., 2014) and its activity is dually regulated by intra-lysosome pH and intra-lysosome ATP (Huang et al., 2014; Cao et al., 2015). In the present study we did not focus on other purinergic receptors, such as P2X7 that have been implicated in modulating lysosomal pH (Takenouchi et al., 2009; Guha et al., 2013) because it has been shown that P2X7 receptors have ER and PM localization rather than lysosomes (Murrell-Lagnado and Robinson, 2013) owing probably to its longer C-terminal (Smart et al., 2003). We show that P2X4 is localized to LAMP1 vesicles in hSCs, an observation that is consistent findings in rat Schwann cells (Su et al., 2019). Importantly, blocking P2X4 with specific human P2X4 antagonist Bx430 attenuated gp120-induced lysosomal exocytosis. The activity of lysosomal P2X4 is normally inhibited under acidic luminal pH (Huang et al., 2014). As lysosomes undergo alkalization while moving toward the PM (Johnson et al., 2016), the de-acidification of lysosomes could activate P2X4. Using P2X4-pHluorin 123 construct, whose fluorescence increases with increasing pH, we demonstrated that gp120 treatment increased the fluorescence signal of lysosomes expressing P2X4-pHluorin 123, indicating gp120 increases lysosome pH (de-acidification).

However, increased lysosome pH itself is not sufficient to activate P2X4 as it is under the dual regulation of luminal pH and ATP. Consistent with others' findings (Shin et al., 2012), we demonstrated that lysosomes serve as ATP rich stores. Importantly, we demonstrated that gp120 treatment increased the percentage of ATP rich peripheral lysosomes. Thus, this population of ATP rich, de-acidified peripheral lysosomes is ideal for P2X4 activation, which probably reflects the calcium dependent second step of lysosomal exocytosis. We further showed that the ATP transporter VNUT was responsible for Schwann cell lysosomal ATP filling as inhibiting VNUT prevented gp120-induced lysosomal exocytosis and ATP release in the extracellular media. Thus, consistent with a report that functional coupling of VNUT and P2X4 underlies lysosome exocytosis (Zhong et al., 2016), our findings indicate such a

functional coupling of VNUT and P2X4 receptors play a role in gp120 induced lysosomal exocytosis. It is well known that lysosomal exocytosis is a calcium-dependent process; increases in intracellular calcium has been shown to promote the fusion of lysosomes within the vicinity of the PM and induce lysosomal exocytosis (Jaiswal et al., 2002). Calcium released via P2X4 receptors may also contribute to gp120-induced lysosomal exocytosis. Activation of PM P2X4 receptors allows the influx of Ca^{2+} leading to increased intracellular Ca^{2+}. Apart from calcium influx across PM, intracellular Ca^{2+} can be also increased via calcium released from lysosome lumen upon lysosomal P2X4 activation (Cao et al., 2015). Thus, calcium influx across PM and calcium release from lysosomes could both contribute to HIV-1 gp120-induced lysosomal exocytosis.

Together, our findings suggest that gp120 promotes the movement of lysosomes toward plasma membranes and subsequent lysosome exocytosis, and this process is achieved by gp120-induced activation of lysosome P2X4 via lysosome de-acidification and ATP enrichment. Currently, it is not clear how gp120 leads to lysosome de-acidification and ATP enrichment in Schwann cells. Given that gp120 has been shown to bind to CXCR4 receptors on Schwann cells (Keswani et al., 2003) and that gp120 can be endocytosed and localized to lysosomes within 30 min (**Supplementary Figure S4B**) (Costantini et al., 2015; Wenzel et al., 2017), gp120 could affect lysosome pH, lysosome ATP transport, and activity of lysosomal P2X4 either directly at the luminal side of lysosomes or indirectly via receptor-mediated signaling. Thus, further mechanistic studies are warranted.

The Functional Importance of gp120-Induced Lysosome Exocytosis in Schwann Cells

Schwann cells are the most abundant glial cells of the peripheral nervous system, ensheathing all axons of peripheral nerves as either myelinating or non-myelinating cells. In addition to its role as insulators of axons, Schwann cells are crucial for the proper function and maintenance of peripheral nerves by providing metabolic or trophic support (Beirowski et al., 2014; Feldman et al., 2017; Sasaki et al., 2018) and modulating responses to nerve injury (Jessen and Mirsky, 2016; Kim et al., 2018). On the other hand, the presence of axons is crucial to Schwann cells' ability to de-differentiate (Jang et al., 2017; Soto and Monje, 2017; Norrmén et al., 2018). Thus, disrupting Schwann cell function can compromise glial–axon communication that can lead to disturbed nerve homeostasis and ultimately lead to fiber loss, neurodegeneration, and pain.

In the central nervous system, lysosomal exocytosis represents a new pathway for gliotransmitter secretion from astrocytes (Zhang et al., 2007; Li et al., 2008; Liu et al., 2011). In Schwann cells, lysosome exocytosis has also been demonstrated and plays an important role in regulating myelination (Chen et al., 2012; Shin et al., 2012; Jung et al., 2014; Su et al., 2019). In particular, release of ATP via lysosome exocytosis has been demonstrated in Schwann cells (Shin et al., 2012). Numerous studies have shown the effect of extracellular ATP on Schwann cell physiology including its role on differentiation (Stevens and Fields, 2000), activation (Rodella et al., 2017), and its role in myelination (Ino et al., 2015) and in Wallerian degeneration (Shin et al., 2012, 2014). The over-expression of P2X4 in Schwann cells have recently been shown to promote remyelination via secretion of brain derived neurotrophic factor (Su et al., 2019), and another P2X receptor P2X7 has been shown to be involved in Charcot-Marie-Tooth disorder, a common inherited human neuropathy with demyelination (Nobbio et al., 2009). On the other hand, ATP is recognized as an important mediator of peripheral pain via activating the purinergic receptors and a rise in intracellular calcium in DRG neurons (Surprenant et al., 1996; Qi et al., 2011; Hattori and Gouaux, 2012; Masuda et al., 2016; Yamashita et al., 2016; Jurga et al., 2017; Ying et al., 2017; Yang et al., 2018).

In the present study, we explored the effect of gp120-induced lysosome exocytotic release of ATP from Schwann cells on DRG neuron function by treating primary culture rat DRG neurons with conditioned media from gp120-treated rat Schwannoma cells. We demonstrated that conditioned media from gp120-treated rat Schwannoma cells induced a rise in the levels of intracellular calcium and increase in cytosolic ROS in DRG neuron, both of which have been implicated in the development of peripheral neuropathy and/or HIV DSP (Salvemini et al., 2011; Materazzi et al., 2012; Iida et al., 2016). Importantly, conditioned media from gp120-treated rat Schwannoma cells in the presence of P2X4 or VNUT antagonists failed to induce rises in calcium and ROS in DRG neurons. Given that blocking either P2X4 or VNUT in Schwann cell attenuated gp120-induced lysosome exocytosis and the release of ATP into media, our findings suggest that ATP released via lysosome exocytosis from Schwann cells induces calcium rise in DRG neuron. However, our findings could not exclude the involvement of other factors released via lysosome exocytosis from Schwann cells. For instance, Schwann cell exosomes have been shown to interact with axons, and increased miRNA455-3p induction has been shown to be associated with HIV DSP (Lopez-Verrilli and Court, 2012; Lopez-Leal and Court, 2016; Jia et al., 2018; Zhou et al., 2018).

In summary, our findings suggest that HIV-1 gp120 promotes the movement of lysosomes toward plasma membrane followed subsequently by lysosomal exocytosis and the release of ATP; and this process is achieved by gp120-induced activation of lysosome P2X4 via lysosome de-acidification and VNUT coupling. Such gp120-induced lysosomal exocytosis from Schwann cells induces rises in cytosolic calcium and ROS in DRG neurons. Our results suggest that gp120-induced lysosomal exocytotic release of mediators including ATP from Schwann cells through P2X4 and VNUT signaling could be a possible mechanism for HIV-associated neuropathy. The mechanism identified here may have broader impact, because many viruses and bacteria enter host cells via endocytosis (Cossart and Helenius, 2014) and some viruses have been shown to release virions via lysosomal or autophagic exocytosis (Münz, 2017). It has been shown that virus-infected cells could release ATP that activates purinergic receptors on adjacent cells (Swartz et al., 2014; Manzoor et al., 2016) and affect viral infections including HIV, hepatitis virus, influenza, and dengue viruses (Taylor and Han, 2010; Corrêa et al., 2016; Leyva-Grado et al., 2017). Similar to viruses themselves, viral proteins such as HIV-1 Tat protein has been

shown to enter cells via endocytosis (Fields et al., 2015) and promote lysosome exocytosis (Fan and He, 2016). However, the potential role of virus or viral proteins in regulating purinergic receptors on lysosomes has not yet been studied. Thus, our findings provide a novel mechanism whereby viral proteins could affect lysosome purinergic receptors once entering the cell, and such a mechanism could occur in many other infectious diseases.

DATA AVAILABILITY

The raw data supporting the conclusions of this manuscript will be made available by the authors, without undue reservation, to any qualified researcher.

AUTHOR CONTRIBUTIONS

GD, JG, and XC designed the study. GD, NM, and ZA acquired the data. GD analyzed the data and drafted the manuscript. XC contributed to interpretation of the data, revising the work of intellectual content, and final approval of the version to be published. All authors approved the final version and agreed to be accountable for all aspects of the work in ensuring that questions related to the accuracy or integrity of any part of the work were appropriately investigated and resolved.

FUNDING

This study was funded by the National Institute of General Medical Sciences (P30GM100329 and U54GM115458), the National Institute of Mental Health (R01MH100972 and R01MH105329), and the National Institute of Neurological Diseases and Stroke (R01NS065957).

SUPPLEMENTARY MATERIAL

The Supplementary Material for this article can be found online at: https://www.frontiersin.org/articles/10.3389/fncel.2019.00329/full#supplementary-material

REFERENCES

Andrews, N. W. (2000). Regulated secretion of conventional lysosomes. *Trends Cell Biol.* 10, 316–321. doi: 10.1016/s0962-8924(00)01794-3

Apostolski, S., McAlarney, T., Hays, A. P., and Latov, N. (1994). Complement dependent cytotoxicity of sensory ganglion neurons mediated by the gp120 glycoprotein of HIV-1. *Immunol. Invest.* 23, 47–52. doi: 10.3109/08820139409063432

Apostolski, S., McAlarney, T., Quattrini, A., Levison, S. W., Rosoklija, G., Lugaressi, A., et al. (1993). The gp120 glycoprotein of human immunodeficiency virus type 1 binds to sensory ganglion neurons. *Ann. Neurol.* 34, 855–863. doi: 10.1002/ana.410340616

Ase, A. R., Honson, N. S., Zaghdane, H., Pfeifer, T. A., and Seguela, P. (2015). Identification and characterization of a selective allosteric antagonist of human P2X4 receptor channels. *Mol. Pharmacol.* 87, 606–616. doi: 10.1124/mol.114.096222

Aziz-Donnelly, A., and Harrison, T. B. (2017). Update of HIV-associated sensory neuropathies. *Curr. Treat. Options Neurol.* 19:36. doi: 10.1007/s11940-017-0472-3

Bacallao, K., and Monje, P. V. (2015). Requirement of cAMP signaling for schwann cell differentiation restricts the onset of myelination. *PLoS One* 10:e0116948. doi: 10.1371/journal.pone.0116948

Bachis, A., Aden, S. A., Nosheny, R. L., Andrews, P. M., and Mocchetti, I. (2006). Axonal transport of human immunodeficiency virus type 1 envelope protein glycoprotein 120 is found in association with neuronal apoptosis. *J. Neurosci.* 26, 6771–6780. doi: 10.1523/jneurosci.1054-06.2006

Bachis, A., and Mocchetti, I. (2004). The chemokine receptor CXCR4 and not the N-methyl-D-aspartate receptor mediates gp120 neurotoxicity in cerebellar granule cells. *J. Neurosci. Res.* 75, 75–82. doi: 10.1002/jnr.10826

Beckel, J. M., Gómez, N. M., Lu, W., Campagno, K. E., Nabet, B., Albalawi, F., et al. (2018). Stimulation of TLR3 triggers release of lysosomal ATP in astrocytes and epithelial cells that requires TRPML1 channels. *Sci. Rep.* 8:5726. doi: 10.1038/s41598-018-23877-3

Beirowski, B., Babetto, E., Golden, J. P., Chen, Y. Jr., Yang, K., Gross, R. W., et al. (2014). Metabolic regulator LKB1 is crucial for Schwann cell–mediated axon maintenance. *Nat. Neurosci.* 17, 1351–1361. doi: 10.1038/nn.3809

Berth, S., Caicedo, H. H., Sarma, T., Morfini, G., and Brady, S. T. (2015). Internalization and axonal transport of the HIV glycoprotein gp120. *ASN Neuro* 7:1759091414568186. doi: 10.1177/1759091414568186

Berth, S. H., Mesnard-Hoaglin, N., Wang, B., Kim, H., Song, Y., Sapar, M., et al. (2016). HIV glycoprotein Gp120 impairs fast axonal transport by activating Tak1 signaling pathways. *ASN Neuro* 8:1759091416679073.

Bezzi, P., Domercq, M., Brambilla, L., Galli, R., Schols, D., De Clercq, E., et al. (2001). CXCR4-activated astrocyte glutamate release via TNFalpha: amplification by microglia triggers neurotoxicity. *Nat. Neurosci.* 4, 702–710. doi: 10.1038/89490

Bilgrami, M., and O'Keefe, P. (2014). Neurologic diseases in HIV-infected patients. *Handb. Clin. Neurol.* 121, 1321–1344. doi: 10.1016/B978-0-7020-4088-7.00090-0

Brosius Lutz, A., Chung, W. S., Sloan, S. A., Carson, G. A., Zhou, L., Lovelett, E., et al. (2017). Schwann cells use TAM receptor-mediated phagocytosis in addition to autophagy to clear myelin in a mouse model of nerve injury. *Proc. Natl. Acad. Sci. U.S.A.* 114, E8072–E8080. doi: 10.1073/pnas.1710566114

Burdo, T. H., and Miller, A. D. (2014). Animal models of HIV peripheral neuropathy. *Future Virol.* 9, 465–474. doi: 10.2217/fvl.14.28

Cao, Q., Zhao, K., Zhong, X. Z., Zou, Y., Yu, H., Huang, P., et al. (2014). SLC17A9 functions as a lysosomal ATP transporter and regulates cell viability. *J. Biol. Chem.* 289, 23189–23199. doi: 10.1074/jbc.M114.567107

Cao, Q., Zhong, X. Z., Zou, Y., Murrell-Lagnado, R., Zhu, M. X., and Dong, X. P. (2015). Calcium release through P2X4 activates calmodulin to promote endolysosomal membrane fusion. *J. Cell Biol.* 209, 879–894. doi: 10.1083/jcb.201409071

Centner, C. M., Bateman, K. J., and Heckmann, J. M. (2013). Manifestations of HIV infection in the peripheral nervous system. *Lancet Neurol.* 12, 295–309. doi: 10.1016/S1474-4422(13)70002-4

Chen, G., Zhang, Z., Wei, Z., Cheng, Q., Li, X., Li, W., et al. (2012). Lysosomal exocytosis in schwann cells contributes to axon remyelination. *Glia* 60, 295–305. doi: 10.1002/glia.21263

Cheng, X. T., Xie, Y. X., Zhou, B., Huang, N., Farfel-Becker, T., and Sheng, Z. H. (2018). Characterization of LAMP1-labeled nondegradative lysosomal and endocytic compartments in neurons. *J. Cell Biol.* 217, 3127–3139. doi: 10.1083/jcb.201711083

Chung, J. M., and Chung, K. (2002). Importance of hyperexcitability of DRG neurons in neuropathic pain. *Pain Pract.* 2, 87–97. doi: 10.1046/j.1533-2500.2002.02011.x

Corrêa, G., de Lindenberg, C. A., Fernandes-Santos, C., Gandini, M., Petitinga Paiva, F., Coutinho-Silva, R., et al. (2016). The purinergic receptor P2X7 role in control of Dengue virus-2 infection and cytokine/chemokine production in infected human monocytes. *Immunobiology* 221, 794–802. doi: 10.1016/j.imbio.2016.02.003

Cossart, P., and Helenius, A. (2014). Endocytosis of viruses and bacteria. *Cold Spring Harb. Perspect. Biol.* 6:a016972. doi: 10.1101/cshperspect.a016972

Costantini, L. M., Irvin, S. C., Kennedy, S. C., Guo, F., Goldstein, H., Herold, B. C., et al. (2015). Engineering and exploitation of a fluorescent HIV-1 gp120 for live cell CD4 binding assays. *Virology* 476, 240–248. doi: 10.1016/j.virol.2014.12.019

Deng, H., Liu, R., Ellmeier, W., Choe, S., Unutmaz, D., Burkhart, M., et al. (1996). Identification of a major co-receptor for primary isolates of HIV-1. *Nature* 381, 661–666. doi: 10.1038/381661a0

Dong, X. (2015). P2X4 forms ATP-activated channels on lysosomal membranes regulated by luminal pH and SLC17A9 proteins. *Biophys. J.* 108:419a. doi: 10.1016/j.bpj.2014.11.2293

Eitan, E., Suire, C., Zhang, S., and Mattson, M. P. (2016). Impact of lysosome status on extracellular vesicle content and release. *Ageing Res. Rev.* 32, 65–74. doi: 10.1016/j.arr.2016.05.001

Ellis, R. J., Marquie-Beck, J., Delaney, P., Alexander, T., Clifford, D. B., McArthur, J. C., et al. (2008). Human immunodeficiency virus protease inhibitors and risk for peripheral neuropathy. *Ann. Neurol.* 64, 566–572. doi: 10.1002/ana.21484

Emmett, D. S., Feranchak, A., Kilic, G., Puljak, L., Miller, B., Dolovcak, S., et al. (2008). Characterization of ionotrophic purinergic receptors in hepatocytes. *Hepatology* 47, 698–705. doi: 10.1002/hep.22035

Fan, Y., and He, J. J. (2016). HIV-1 tat promotes lysosomal exocytosis in astrocytes and contributes to astrocyte-mediated tat neurotoxicity. *J. Biol. Chem.* 291, 22830–22840. doi: 10.1074/jbc.m116.731836

Feldman, E. L., Nave, K. A., Jensen, T. S., and Bennett, D. L. H. (2017). New horizons in diabetic neuropathy: mechanisms, bioenergetics, and pain. *Neuron* 93, 1296–1313. doi: 10.1016/j.neuron.2017.02.005

Feng, Y., Press, B., and Wandinger-Ness, A. (1995). Rab 7: an important regulator of late endocytic membrane traffic. *J. Cell Biol.* 131, 1435–1452. doi: 10.1083/jcb.131.6.1435

Fields, J., Dumaop, W., Elueteri, S., Campos, S., Serger, E., Trejo, M., et al. (2015). HIV-1 tat alters neuronal autophagy by modulating autophagosome fusion to the lysosome: implications for HIV-associated neurocognitive disorders. *J. Neurosci.* 35, 1921–1938. doi: 10.1523/JNEUROSCI.3207-14.2015

Fuller, G. N., Jacobs, J. M., and Guiloff, R. J. (1993). Nature and incidence of peripheral nerve syndromes in HIV infection. *J. Neurol. Neurosurg. Psychiatry* 56, 372–381. doi: 10.1136/jnnp.56.4.372

Gelderblom, H. R., Hausmann, E. H., Ozel, M., Pauli, G., and Koch, M. A. (1987). Fine structure of human immunodeficiency virus (HIV) and immunolocalization of structural proteins. *Virology* 156, 171–176. doi: 10.1016/0042-6822(87)90449-1

Gregg, E. W., Sorlie, P., Paulose-Ram, R., Gu, Q., Eberhardt, M. S., Wolz, M., et al. (2004). Prevalence of lower-extremity disease in the US adult population >=40 years of age with and without diabetes: 1999-2000 national health and nutrition examination survey. *Diabetes Care* 27, 1591–1597. doi: 10.2337/diacare.27.7.1591

Guha, S., Baltazar, G. C., Coffey, E. E., Tu, L. A., Lim, J. C., Beckel, J. M., et al. (2013). Lysosomal alkalinization, lipid oxidation, and reduced phagosome clearance triggered by activation of the P2X7 receptor. *FASEB J.* 27, 4500–4509. doi: 10.1096/fj.13-236166

Hall, C. D., Snyder, C. R., Messenheimer, J. A., Wilkins, J. W., Robertson, W. T., Whaley, R. A., et al. (1991). Peripheral neuropathy in a cohort of human immunodeficiency virus-infected patients. Incidence and relationship to other nervous system dysfunction. *Arch. Neurol.* 48, 1273–1274.

Hao, S. (2013). The molecular and pharmacological mechanisms of HIV-related neuropathic pain. *Curr. Neuropharmacol.* 11, 499–512. doi: 10.2174/1570159X11311050005

Harada, A., Takei, Y., Kanai, Y., Tanaka, Y., Nonaka, S., and Hirokawa, N. (1998). Golgi vesiculation and lysosome dispersion in cells lacking cytoplasmic dynein. *J. Cell Biol.* 141, 51–59. doi: 10.1083/jcb.141.1.51

Hattori, M., and Gouaux, E. (2012). Molecular mechanism of ATP binding and ion channel activation in P2X receptors. *Nature* 485, 207–212. doi: 10.1038/nature11010

Herzberg, U., and Sagen, J. (2001). Peripheral nerve exposure to HIV viral envelope protein gp120 induces neuropathic pain and spinal gliosis. *J. Neuroimmunol.* 116, 29–39. doi: 10.1016/s0165-5728(01)00288-0

Hoke, A., Morris, M., and Haughey, N. J. (2009). GPI-1046 protects dorsal root ganglia from gp120-induced axonal injury by modulating store-operated calcium entry. *J. Peripher. Nerv. Syst.* 14, 27–35. doi: 10.1111/j.1529-8027.2009.00203.x

Hollenbeck, P. J., and Swanson, J. A. (1990). Radial extension of macrophage tubular lysosomes supported by kinesin. *Nature* 346, 864–866. doi: 10.1038/346864a0

Huang, P., Zou, Y., Zhong, X. Z., Cao, Q., Zhao, K., Zhu, M. X., et al. (2014). P2X4 forms functional ATP-activated cation channels on lysosomal membranes regulated by luminal pH. *J. Biol. Chem.* 289, 17658–17667. doi: 10.1074/jbc.M114.552158

Iida, T., Yi, H., Liu, S., Huang, W., Kanda, H., Lubarsky, D. A., et al. (2016). Spinal CPEB-mtROS-CBP signaling pathway contributes to perineural HIV gp120 with ddC-related neuropathic pain in rats. *Exp. Neurol.* 281, 17–27. doi: 10.1016/j.expneurol.2016.04.012

Ino, D., Sagara, H., Suzuki, J., Kanemaru, K., Okubo, Y., and Iino, M. (2015). Neuronal regulation of schwann cell mitochondrial Ca(2+) signaling during myelination. *Cell Rep.* 12, 1951–1959. doi: 10.1016/j.celrep.2015.08.039

Jaiswal, J. K., Andrews, N. W., and Simon, S. M. (2002). Membrane proximal lysosomes are the major vesicles responsible for calcium-dependent exocytosis in nonsecretory cells. *J. Cell Biol.* 159, 625–635. doi: 10.1083/jcb.200208154

Jang, S. Y., Yoon, B. A., Shin, Y. K., Yun, S. H., Jo, Y. R., Choi, Y. Y., et al. (2017). Schwann cell dedifferentiation-associated demyelination leads to exocytotic myelin clearance in inflammatory segmental demyelination. *Glia* 65, 1848–1862. doi: 10.1002/glia.23200

Jessen, K. R., and Mirsky, R. (2016). The repair schwann cell and its function in regenerating nerves. *J. Physiol.* 594, 3521–3531. doi: 10.1113/JP270874

Jia, L., Chopp, M., Wang, L., Lu, X., Szalad, A., and Zhang, Z. G. (2018). Exosomes derived from high-glucose–stimulated Schwann cells promote development of diabetic peripheral neuropathy. *FASEB J.* 32, 6911–6922. doi: 10.1096/fj.201800597R

Jia, R., Guardia, C. M., Pu, J., Chen, Y., and Bonifacino, J. S. (2017). BORC coordinates encounter and fusion of lysosomes with autophagosomes. *Autophagy* 13, 1648–1663. doi: 10.1080/15548627.2017.1343768

Johansson, M., Rocha, N., Zwart, W., Jordens, I., Janssen, L., Kuijl, C., et al. (2007). Activation of endosomal dynein motors by stepwise assembly of Rab7–RILP–p150Glued, ORP1L, and the receptor βlll spectrin. *J. Cell Biol.* 176, 459–471. doi: 10.1083/jcb.200606077

Johnson, D. E., Ostrowski, P., Jaumouillé, V., and Grinstein, S. (2016). The position of lysosomes within the cell determines their luminal pH. *J. Cell Biol.* 212, 677–692. doi: 10.1083/jcb.201507112

Jordens, I., Fernandez-Borja, M., Marsman, M., Dusseljee, S., Janssen, L., Calafat, J., et al. (2001). The Rab7 effector protein RILP controls lysosomal transport by inducing the recruitment of dynein-dynactin motors. *Curr. Biol.* 11, 1680–1685. doi: 10.1016/s0960-9822(01)00531-0

Jung, J., Jo, H. W., Kwon, H., and Jeong, N. Y. (2014). ATP release through lysosomal exocytosis from peripheral nerves: the effect of lysosomal exocytosis on peripheral nerve degeneration and regeneration after nerve injury. *Biomed. Res. Int.* 2014:936891. doi: 10.1155/2014/936891

Jurga, A. M., Piotrowska, A., Makuch, W., Przewlocka, B., and Mika, J. (2017). Blockade of P2X4 receptors inhibits neuropathic pain-related behavior by preventing MMP-9 activation and, consequently, pronociceptive interleukin release in a rat model. *Front. Pharmacol.* 8:48. doi: 10.3389/fphar.2017.00048

Kaku, M., and Simpson, D. M. (2014). HIV neuropathy. *Curr. Opin. HIV AIDS* 9, 521–526. doi: 10.1097/COH.0000000000000103

Kato, Y., Hiasa, M., Ichikawa, R., Hasuzawa, N., Kadowaki, A., Iwatsuki, K., et al. (2017). Identification of a vesicular ATP release inhibitor for the treatment of neuropathic and inflammatory pain. *Proc. Natl. Acad. Sci. U.S.A.* [Epub ahead of print].

Kaul, M., and Lipton, S. A. (1999). Chemokines and activated macrophages in HIV gp120-induced neuronal apoptosis. *Proc. Natl. Acad. Sci. U.S.A.* 96, 8212–8216. doi: 10.1073/pnas.96.14.8212

Keswani, S. C., Polley, M., Pardo, C. A., Griffin, J. W., McArthur, J. C., and Hoke, A. (2003). Schwann cell chemokine receptors mediate HIV-1 gp120 toxicity to sensory neurons. *Ann. Neurol.* 54, 287–296. doi: 10.1002/ana.10645

Kim, S., Maynard, J. C., Strickland, A., Burlingame, A. L., and Milbrandt, J. (2018). Schwann cell O-GlcNAcylation promotes peripheral nerve remyelination via attenuation of the AP-1 transcription factor JUN. *Proc. Natl. Acad. Sci. U.S.A.* 115, 8019–8024. doi: 10.1073/pnas.1805538115

Korolchuk, V. I., Saiki, S., Lichtenberg, M., Siddiqi, F. H., Roberts, E. A., Imarisio, S., et al. (2011). Lysosomal positioning coordinates cellular nutrient responses. *Nat. Cell Biol.* 13, 453–460. doi: 10.1038/ncb2204

Kostyuk, E., Voitenko, N., Kruglikov, I., Shmigol, A., Shishkin, V., Efimov, A., et al. (2001). Diabetes-induced changes in calcium homeostasis and the effects of calcium channel blockers in rat and mice nociceptive neurons. *Diabetologia* 44, 1302–1309. doi: 10.1007/s001250100642

Langemeyer, L., Fröhlich, F., and Ungermann, C. (2018). Rab GTPase function in endosome and lysosome biogenesis. *Trends Cell Biol.* 28, 957–970. doi: 10.1016/j.tcb.2018.06.007

Layne, S. P., Merges, M. J., Dembo, M., Spouge, J. L., Conley, S. R., Moore, J. P., et al. (1992). Factors underlying spontaneous inactivation and susceptibility to neutralization of human immunodeficiency virus. *Virology* 189, 695–714. doi: 10.1016/0042-6822(92)90593-e

Lehmann, H. C., Chen, W., Borzan, J., Mankowski, J. L., and Hoke, A. (2011). Mitochondrial dysfunction in distal axons contributes to human immunodeficiency virus sensory neuropathy. *Ann. Neurol.* 69, 100–110. doi: 10.1002/ana.22150

Letendre, S. L., Ellis, R. J., Everall, I., Ances, B., Bharti, A., and McCutchan, J. A. (2009). Neurologic complications of HIV disease and their treatment. *Top. HIV Med.* 17, 46–56.

Leyva-Grado, V. H., Ermler, M. E., Schotsaert, M., Gonzalez, M. G., Lim, J. K., and García-Sastre, A. (2017). Contribution of the purinergic receptor P2X7 to development of lung immunopathology during influenza virus infection. *mBio* 8:e229-17. doi: 10.1128/mBio.00229-17

Li, D., Ropert, N., Koulakoff, A., Giaume, C., and Oheim, M. (2008). Lysosomes are the major vesicular compartment undergoing Ca2+-regulated exocytosis from cortical astrocytes. *J. Neurosci.* 28, 7648–7658. doi: 10.1523/JNEUROSCI.0744-08.2008

Linke, M., Herzog, V., and Brix, K. (2002). Trafficking of lysosomal cathepsin B—green fluorescent protein to the surface of thyroid epithelial cells involves the endosomal/lysosomal compartment. *J. Cell Sci.* 115, 4877–4889. doi: 10.1242/jcs.00184

Liu, T., Sun, L., Xiong, Y., Shang, S., Guo, N., Teng, S., et al. (2011). Calcium triggers exocytosis from two types of organelles in a single astrocyte. *J. Neurosci.* 31, 10593–10601. doi: 10.1523/JNEUROSCI.6401-10.2011

Lopez-Leal, R., and Court, F. A. (2016). Schwann cell exosomes mediate neuron-glia communication and enhance axonal regeneration. *Cell Mol. Neurobiol.* 36, 429–436. doi: 10.1007/s10571-015-0314-3

Lopez-Verrilli, M. A., and Court, F. A. (2012). Transfer of vesicles from schwann cells to axons: a novel mechanism of communication in the peripheral nervous system. *Front. Physiol.* 3:205. doi: 10.3389/fphys.2012.00205

Manzoor, S., Akhtar, U., Naseem, S., Khalid, M., Mazhar, M., Parvaiz, F., et al. (2016). Ionotropic purinergic receptors P2X4 and P2X7: proviral or antiviral? An insight into P2X receptor signaling and hepatitis C virus infection. *Viral Immunol.* 29, 401–408. doi: 10.1089/vim.2016.0008

Martinez, I., Chakrabarti, S., Hellevik, T., Morehead, J., Fowler, K., and Andrews, N. W. (2000). Synaptotagmin VII regulates Ca(2+) dependent exocytosis of lysosomes in fibroblasts. *J. Cell Biol.* 148, 1141–1150. doi: 10.1083/jcb.148.6.1141

Martyn, C. N., and Hughes, R. A. (1997). Epidemiology of peripheral neuropathy. *J. Neurol. Neurosurg. Psychiatry* 62, 310–318.

Masuda, T., Ozono, Y., Mikuriya, S., Kohro, Y., Tozaki-Saitoh, H., Iwatsuki, K., et al. (2016). Dorsal horn neurons release extracellular ATP in a VNUT-dependent manner that underlies neuropathic pain. *Nat. Commun.* 7:12529. doi: 10.1038/ncomms12529

Materazzi, S., Fusi, C., Benemei, S., Pedretti, P., Patacchini, R., Nilius, B., et al. (2012). TRPA1 and TRPV4 mediate paclitaxel-induced peripheral neuropathy in mice via a glutathione-sensitive mechanism. *Pflügers Arch.* 463, 561–569. doi: 10.1007/s00424-011-1071-x

Medina, D. L., Fraldi, A., Bouche, V., Annunziata, F., Mansueto, G., Spampanato, C., et al. (2011). Transcriptional activation of lysosomal exocytosis promotes cellular clearance. *Dev. Cell* 21, 421–430. doi: 10.1016/j.devcel.2011.07.016

Melli, G., Keswani, S. C., Fischer, A., Chen, W., and Hoke, A. (2006). Spatially distinct and functionally independent mechanisms of axonal degeneration in a model of HIV-associated sensory neuropathy. *Brain* 129(Pt 5), 1330–1338. doi: 10.1093/brain/awl058

Meresse, S., Gorvel, J. P., and Chavrier, P. (1995). The rab7 GTPase resides on a vesicular compartment connected to lysosomes. *J. Cell Sci.* 108, 3349–3358.

Monk, K. R., Feltri, M. L., and Taveggia, C. (2015). New insights on schwann cell development. *Glia* 63, 1376–1393. doi: 10.1002/glia.22852

Moriyama, Y., Hiasa, M., Sakamoto, S., Omote, H., and Nomura, M. (2017). Vesicular nucleotide transporter (VNUT): appearance of an actress on the stage of purinergic signaling. *Purinergic Signal* 13, 387–404. doi: 10.1007/s11302-017-9568-1

Moriyama, Y., and Nomura, M. (2017). Clodronate: a vesicular ATP release blocker. *Trends Pharmacol. Sci.* 39, 13–23. doi: 10.1016/j.tips.2017.10.007

Münz, C. (2017). The autophagic machinery in viral exocytosis. *Front. Microbiol.* 8:269. doi: 10.3389/fmicb.2017.00269

Murrell-Lagnado, R., and Robinson, L. (2013). The trafficking and targeting of P2X receptors. *Front. Cell. Neurosci.* 7:233. doi: 10.3389/fncel.2013.00233

Nagano, I., Shapshak, P., Yoshioka, M., Xin, K., Nakamura, S., and Bradley, W. G. (1996). Increased NADPH-diaphorase reactivity and cytokine expression in dorsal root ganglia in acquired immunodeficiency syndrome. *J. Neurol. Sci.* 136, 117–128. doi: 10.1016/0022-510x(95)00317-u

Nobbio, L., Sturla, L., Fiorese, F., Usai, C., Basile, G., Moreschi, I., et al. (2009). P2X7-mediated increased intracellular calcium causes functional derangement in schwann cells from rats with CMT1A neuropathy. *J. Biol. Chem.* 284, 23146–23158. doi: 10.1074/jbc.M109.027128

Norrmén, C., Figlia, G., Pfistner, P., Pereira, J. A., Bachofner, S., and Suter, U. (2018). mTORC1 Is transiently reactivated in injured nerves to Promote c-Jun elevation and schwann cell dedifferentiation. *J. Neurosci.* 38, 4811–4828. doi: 10.1523/JNEUROSCI.3619-17.2018

Oh, S. B., Tran, P. B., Gillard, S. E., Hurley, R. W., Hammond, D. L., and Miller, R. J. (2001). Chemokines and glycoprotein120 produce pain hypersensitivity by directly exciting primary nociceptive neurons. *J. Neurosci.* 21, 5027–5035. doi: 10.1523/jneurosci.21-14-05027.2001

Oh, S. K., Cruikshank, W. W., Raina, J., Blanchard, G. C., Adler, W. H., Walker, J., et al. (1992). Identification of HIV-1 envelope glycoprotein in the serum of AIDS and ARC patients. *J. Acquir. Immune Defic. Syndr.* 5, 251–256.

Orita, S., Henry, K., Mantuano, E., Yamauchi, K., De Corato, A., Ishikawa, T., et al. (2013). Schwann Cell LRP1 regulates remak bundle ultrastructure and axonal interactions to prevent neuropathic pain. *J. Neurosci.* 33, 5590–5602. doi: 10.1523/JNEUROSCI.3342-12.2013

Popovic, M., Tenner-Racz, K., Pelser, C., Stellbrink, H. J., van Lunzen, J., Lewis, G., et al. (2005). Persistence of HIV-1 structural proteins and glycoproteins in lymph nodes of patients under highly active antiretroviral therapy. *Proc. Natl. Acad. Sci. U.S.A.* 102, 14807–14812. doi: 10.1073/pnas.0506857102

Prior, D. E., Song, N., and Cohen, J. A. (2018). Neuromuscular diseases associated with human immunodeficiency virus infection. *J. Neurol. Sci.* 387, 27–36. doi: 10.1016/j.jns.2018.01.016

Progida, C., and Bakke, O. (2016). Bidirectional traffic between the golgi and the endosomes – machineries and regulation. *J. Cell Sci.* 129, 3971–3982.

Qi, J., Buzas, K., Fan, H., Cohen, J. I., Wang, K., Mont, E., et al. (2011). Painful pathways induced by TLR stimulation of dorsal root ganglion neurons. *J. Immunol.* 186, 6417–6426. doi: 10.4049/jimmunol.1001241

Rodella, U., Negro, S., Scorzeto, M., Bergamin, E., Jalink, K., Montecucco, C., et al. (2017). Schwann cells are activated by ATP released from neurons in an in vitro cellular model of miller fisher syndrome. *Dis. Model. Mech.* 10, 597–603. doi: 10.1242/dmm.027870

Rodríguez, A., Webster, P., Ortego, J., and Andrews, N. W. (1997). Lysosomes behave as Ca2+ regulated exocytic vesicles in fibroblasts and epithelial cells. *J. Cell Biol.* 137, 93–104. doi: 10.1083/jcb.137.1.93

Rychert, J., Strick, D., Bazner, S., Robinson, J., and Rosenberg, E. (2010). Detection of HIV gp120 in plasma during early HIV infection is associated with increased proinflammatory and immunoregulatory cytokines. *AIDS Res. Hum. Retroviruses* 26, 1139–1145. doi: 10.1089/aid.2009.0290

Salvemini, D., Little, J. W., Doyle, T., and Neumann, W. L. (2011). Roles of reactive oxygen and nitrogen species in pain. *Free Radic. Biol. Med.* 51, 951–966. doi: 10.1016/j.freeradbiomed.2011.01.026

Santosuosso, M., Righi, E., Lindstrom, V., Leblanc, P. R., and Poznansky, M. C. (2009). HIV-1 envelope protein gp120 is present at high concentrations in secondary lymphoid organs of individuals with chronic HIV-1 infection. *J. Infect. Dis.* 200, 1050–1053. doi: 10.1086/605695

Sasaki, Y., Hackett, A. R., Kim, S., Strickland, A., and Milbrandt, J. (2018). Dysregulation of NAD(+) metabolism induces a schwann cell dedifferentiation program. *J. Neurosci.* 38, 6546–6562. doi: 10.1523/JNEUROSCI.3304-17.2018

Schütz, S. G., and Robinson-Papp, J. (2013). HIV-related neuropathy: current perspectives. *HIVAIDS* 5, 243–251. doi: 10.2147/HIV.S36674

Shin, Y. H., Chung, H.-J., Park, C., Jung, J., Jeong, N. Y., and Neurobiology, M. (2014). Adenosine 5'-Triphosphate (ATP) inhibits schwann cell demyelination during wallerian degeneration. *Cell Mol. Neurobiol.* 34, 361–368. doi: 10.1007/s10571-013-0020-y

Shin, Y. H., Lee, S. J., and Jung, J. (2012). Secretion of ATP from schwann cells through lysosomal exocytosis during wallerian degeneration. *Biochem. Biophys. Res. Commun.* 429, 163–167. doi: 10.1016/j.bbrc.2012.10.121

Sivaramakrishnan, V., Bidula, S., Campwala, H., Katikaneni, D., and Fountain, S. J. (2012). Constitutive lysosome exocytosis releases ATP and engages P2Y receptors in human monocytes. *J. Cell Sci.* 125, 4567–4575. doi: 10.1242/jcs.107318

Smart, M. L., Gu, B., Panchal, R. G., Wiley, J., Cromer, B., Williams, D. A., et al. (2003). P2X7 receptor cell surface expression and cytolytic pore formation are regulated by a distal C-terminal region. *J. Biol. Chem.* 278, 8853–8860. doi: 10.1074/jbc.m211094200

Soto, J., and Monje, P. V. (2017). Axon contact-driven Schwann cell dedifferentiation. *Glia* 65, 864–882. doi: 10.1002/glia.23131

Stavros, K., and Simpson, D. M. (2014). Understanding the etiology and management of HIV-associated peripheral neuropathy. *Curr. HIVAIDS Rep.* 11, 195–201. doi: 10.1007/s11904-014-0211-2

Stevens, B., and Fields, R. D. (2000). Response of schwann cells to action potentials in development. *Science* 287, 2267–2271. doi: 10.1126/science.287.5461.2267

Stokes, L., Scurrah, K., Ellis, J. A., Cromer, B. A., Skarratt, K. K., Gu, B. J., et al. (2011). A loss-of-function polymorphism in the human P2X4 receptor is associated with increased pulse pressure. *Hypertension* 58, 1086–1092. doi: 10.1161/HYPERTENSIONAHA.111.176180

Su, W. F., Wu, F., Jin, Z. H., Gu, Y., Chen, Y. T., Fei, Y., et al. (2019). Overexpression of P2X4 receptor in Schwann cells promotes motor and sensory functional recovery and remyelination via BDNF secretion after nerve injury. *Glia* 67, 78–90. doi: 10.1002/glia.23527

Surprenant, A., Rassendren, F., Kawashima, E., North, R. A., and Buell, G. (1996). The cytolytic P2Z receptor for extracellular ATP identified as a P2X receptor (P2X7). *Science* 272, 735–738. doi: 10.1126/science.272.5262.735

Swartz, T. H., Esposito, A. M., Durham, N. D., Hartmann, B. M., and Chen, B. K. (2014). P2X-selective purinergic antagonists are strong inhibitors of HIV-1 fusion during both cell-to-cell and cell-free infection. *J. Virol.* 88, 11504–11515. doi: 10.1128/JVI.01158-14

Takenouchi, T., Nakai, M., Iwamaru, Y., Sugama, S., Tsukimoto, M., Fujita, M., et al. (2009). The activation of P2X7 receptor impairs lysosomal functions and stimulates the release of autophagolysosomes in microglial cells. *J. Immunol.* 182, 2051–2062. doi: 10.4049/jimmunol.0802577

Taylor, J. M., and Han, Z. (2010). Purinergic receptor functionality is necessary for infection of human hepatocytes by hepatitis delta virus and hepatitis B virus. *PLoS One* 5:e15784. doi: 10.1371/journal.pone.0015784

Tucker, W. C., Weber, T., and Chapman, E. R. (2004). Reconstitution of Ca2+-regulated membrane fusion by synaptotagmin and SNAREs. *Science* 304, 435–438. doi: 10.1126/science.1097196

Viader, A., Sasaki, Y., Kim, S., Strickland, A., Cayce Workman, S., Yang, K., et al. (2013). Aberrant schwann cell lipid metabolism linked to mitochondrial deficits leads to axon degeneration and neuropathy. *Neuron* 77, 886–898. doi: 10.1016/j.neuron.2013.01.012

Wallace, V. C., Blackbeard, J., Pheby, T., Segerdahl, A. R., Davies, M., Hasnie, F., et al. (2007). Pharmacological, behavioural and mechanistic analysis of HIV-1 gp120 induced painful neuropathy. *Pain* 133, 47–63. doi: 10.1016/j.pain.2007.02.015

Wenzel, E. D., Bachis, A., Avdoshina, V., Taraballi, F., Tasciotti, E., and Mocchetti, I. (2017). Endocytic trafficking of HIV gp120 is mediated by dynamin and plays a role in gp120 neurotoxicity. *J. Neuroimmune Pharmacol.* 12, 492–503. doi: 10.1007/s11481-017-9739-4

Wyatt, R., and Sodroski, J. (1998). The HIV-1 envelope glycoproteins: fusogens, antigens, and immunogens. *Science* 280, 1884–1888. doi: 10.1126/science.280.5371.1884

Xu, J., Chai, H., Ehinger, K., Egan, T. M., Srinivasan, R., Frick, M., et al. (2014). Imaging P2X4 receptor subcellular distribution, trafficking, and regulation using P2X4-pHluorin. *J. Gen. Physiol.* 144, 81–104. doi: 10.1085/jgp.201411169

Yamashita, T., Yamamoto, S., Zhang, J., Kometani, M., Tomiyama, D., Kohno, K., et al. (2016). Duloxetine inhibits microglial P2X4 receptor function and alleviates neuropathic pain after peripheral nerve injury. *PLoS One* 11:e0165189. doi: 10.1371/journal.pone.0165189

Yang, J., Xie, M. X., Hu, L., Wang, X. F., Mai, J. Z., Li, Y. Y., et al. (2018). Upregulation of N-type calcium channels in the soma of uninjured dorsal root ganglion neurons contributes to neuropathic pain by increasing neuronal excitability following peripheral nerve injury. *Brain Behav. Immun.* 71, 52–65. doi: 10.1016/j.bbi.2018.04.016

Yeh, T. M., Evans, S. R., Gulick, R. M., and Clifford, D. B. (2010). Vicriviroc and peripheral neuropathy: results from AIDS Clinical Trials Group 5211. *HIV Clin. Trials* 11, 51–58. doi: 10.1310/hct1101-51

Ying, M., Liu, H., Zhang, T., Jiang, C., Gong, Y., Wu, B., et al. (2017). Effect of artemisinin on neuropathic pain mediated by P2X4 receptor in dorsal root ganglia. *Neurochem. Int.* 108, 27–33. doi: 10.1016/j.neuint.2017.02.004

Yuan, S. B., Shi, Y., Chen, J., Zhou, X., Li, G., Gelman, B. B., et al. (2014). Gp120 in the pathogenesis of human immunodeficiency virus–associated pain. *Ann. Neurol.* 75, 837–850. doi: 10.1002/ana.24139

Zhang, Z., Chen, G., Zhou, W., Song, A., Xu, T., Luo, Q., et al. (2007). Regulated ATP release from astrocytes through lysosome exocytosis. *Nat. Cell Biol.* 9, 945–953. doi: 10.1038/ncb1620

Zhong, X. Z., Cao, Q., Sun, X., and Dong, X. P. (2016). Activation of lysosomal P2X4 by ATP transported into lysosomes via VNUT/SLC17A9 using V-ATPase generated voltage gradient as the driving force. *J. Physiol.* 594, 4253–4266. doi: 10.1113/JP271893

Zhou, M., Hu, M., He, S., Li, B., Liu, C., Min, J., et al. (2018). Effects of RSC96 schwann cell-derived exosomes on proliferation, senescence, and apoptosis of dorsal root ganglion cells *In Vitro*. *Med. Sci. Monit.* 24, 7841–7849. doi: 10.12659/MSM.909509

Conflict of Interest Statement: The authors declare that the research was conducted in the absence of any commercial or financial relationships that could be construed as a potential conflict of interest.

frontiers in Cellular Neuroscience

ORIGINAL RESEARCH
published: 23 July 2019
doi: 10.3389/fncel.2019.00331

Dopamine Receptor Blockade Attenuates Purinergic P2X4 Receptor-Mediated Prepulse Inhibition Deficits and Underlying Molecular Mechanisms

*Sheraz Khoja[1], Liana Asatryan[1], Michael W. Jakowec[2] and Daryl L. Davies[1]**

[1] Titus Family Department of Clinical Pharmacy, School of Pharmacy, University of Southern California, Los Angeles, CA, United States, [2] Department of Neurology, Keck School of Medicine, University of Southern California, Los Angeles, CA, United States

OPEN ACCESS

Edited by:
Chao Deng,
University of Wollongong, Australia

Reviewed by:
Rodrigo A. Cunha,
University of Coimbra, Portugal
Roberto Frau,
University of Cagliari, Italy

***Correspondence:**
Daryl L. Davies
ddavies@usc.edu

Specialty section:
This article was submitted to Cellular Neurophysiology, a section of the journal Frontiers in Cellular Neuroscience

Received: 02 March 2019
Accepted: 04 July 2019
Published: 23 July 2019

Citation:
Khoja S, Asatryan L, Jakowec MW and Davies DL (2019) Dopamine Receptor Blockade Attenuates Purinergic P2X4 Receptor-Mediated Prepulse Inhibition Deficits and Underlying Molecular Mechanisms. Front. Cell. Neurosci. 13:331. doi: 10.3389/fncel.2019.00331

Sensorimotor gating refers to the ability to filter incoming sensory information in a stimulus-laden environment and disruption of this physiological process has been documented in psychiatric disorders characterized by cognitive aberrations. The effectiveness of current pharmacotherapies for treatment of sensorimotor gating deficits in the patient population still remains controversial. These challenges emphasize the need to better understand the biological underpinnings of sensorimotor gating which could lead to discovery of novel drug targets for therapeutic intervention. Notably, we recently reported a role for purinergic P2X4 receptors (P2X4Rs) in regulation of sensorimotor gating using prepulse inhibition (PPI) of acoustic startle reflex. P2X4Rs are ion channels gated by adenosine-5′-triphosphate (ATP). Ivermectin (IVM) induced PPI deficits in C57BL/6J mice in a P2X4R-specific manner. Furthermore, mice deficient in P2X4Rs [P2X4R knockout (KO)] exhibited PPI deficits that were alleviated by dopamine (DA) receptor antagonists demonstrating an interaction between P2X4Rs and DA receptors in PPI regulation. On the basis of these findings, we hypothesized that increased DA neurotransmission underlies IVM-mediated PPI deficits. To test this hypothesis, we measured the effects of D1 and D2 receptor antagonists, SCH 23390 and raclopride respectively and D1 agonist, SKF 82958 on IVM-mediated PPI deficits. To gain mechanistic insights, we investigated the interaction between IVM and dopaminergic drugs on signaling molecules linked to PPI regulation in the ventral striatum. SCH 23390 significantly attenuated the PPI disruptive effects of IVM to a much greater degree than that of raclopride. SKF 82958 failed to potentiate IVM-mediated PPI disruption. At the molecular level, modulation of D1 receptors altered IVM's effects on dopamine and cyclic-AMP regulated phosphoprotein of 32 kDa (DARPP-32) phosphorylation. Additionally, IVM interacted with the DA receptors antagonists and SKF 82958 in phosphorylation of Ca^{2+}/calmodulin kinase IIα (CaMKIIα) and its downstream target, neuronal nitric oxide synthase (nNOS). Current findings suggest an involvement for D1 and D2 receptors in IVM-mediated PPI disruption via modulation of DARPP-32,

CaMKIIα and nNOS. Taken together, the findings suggest that stimulation of P2X4Rs can lead to DA hyperactivity and disruption of information processing, implicating P2X4Rs as a novel drug target for treatment of psychiatric disorders characterized by sensorimotor gating deficits.

Keywords: ivermectin, P2X4 receptors, dopamine receptors, prepulse inhibition, schizophrenia, DARPP-32

INTRODUCTION

Sensorimotor gating is an autonomic process of filtering irrelevant sensory information from salient ones in a stimulus-laden environment which is followed by execution of attention-dependent cognitive processes in order to respond to the salient stimuli (Braff and Geyer, 1990; Braff and Light, 2004; Powell et al., 2012). Prepulse inhibition (PPI) of acoustic startle reflex has been identified as an operational measure of sensorimotor gating since it is one of the forms of startle plasticity that resembles the mechanism of sensorimotor gating. PPI of acoustic startle reflex is defined as attenuation of behavioral response to a strong sensory stimulus (pulse) when preceded by a weaker stimulus (prepulse) by 30–500 ms (Graham, 1975; Hoffman and Ison, 1980; Ison and Hoffman, 1983). The observed reduction in response to the pulse stimulus occurs due to activation of inhibitory mechanisms in the central nervous system (CNS) which screens out incoming sensory stimuli until processing of the prepulse stimulus is completed. Hence, PPI serves as a mechanism to avoid interference between distinguishable stimuli (Kumari and Sharma, 2002). The inability to avoid this interference results in significant inundation or overflow of incoming sensory information leading to impairments in attention-dependent cognitive functions (McGhie and Chapman, 1961; Braff, 1993; Braff and Light, 2004). Deficits in PPI have been reported in a wide spectrum of neuropsychiatric disorders that are characterized by cognitive deficits including schizophrenia (Braff and Geyer, 1990; Geyer et al., 2001; Greenwood et al., 2007; Swerdlow et al., 2008; Swerdlow and Light, 2018), bipolar disorder (Perry et al., 2001), manic depressive disorder (Ludewig et al., 2002), Tourette syndrome (Swerdlow et al., 2001b) and autism spectrum disorders such as autism (Perry et al., 2007) and Fragile X syndrome (Frankland et al., 2004).

Previous investigations from our laboratory have reported a role for purinergic P2X4 receptors (P2X4Rs) in modulation of sensorimotor gating (Bortolato et al., 2013; Wyatt et al., 2013; Khoja et al., 2016). P2X4Rs belong to the 7-member P2X superfamily of cation permeable ligand gated ion channels (LGICs) gated by extracellular adenosine-5′-triphosphate (ATP) (North, 2002; North and Verkhratsky, 2006; Khakh and North, 2012). P2X4Rs are abundantly expressed on neurons and glial cells in the CNS (Abbracchio et al., 2009; Khakh and North, 2012). Ivermectin (IVM), a positive modulator of P2X4Rs, disrupted PPI regulation in male C57BL/6J mice and this effect was attenuated in mice deficient in the *p2rx4* gene [i.e., P2X4R knockout (KO) mice] (Bortolato et al., 2013) suggesting that IVM-mediated PPI deficits is P2X4R-dependent. Moreover, male P2X4R KO mice exhibited PPI deficits in comparison to their wildtype (WT) littermates (Wyatt et al., 2013). A possible mechanistic explanation for this behavioral outcome could be the reported increased expression of dopamine (DA) D1 and D2 receptors in the ventral striatum of P2X4R KO mice (Khoja et al., 2016). To further reinforce a role for DA neurotransmission in P2X4R-mediated PPI disruption, DA receptor antagonists significantly ameliorated PPI deficits in P2X4R KO mice (Khoja et al., 2016).

The propensity of IVM to reduce PPI function in C57BL/6J mice is reminiscent of non-selective DA receptor agonists including amphetamine, methamphetamine, cocaine, apomorphine, all of which have been shown to disrupt PPI function in rodents (Ralph et al., 1999; Ralph-Williams et al., 2002, 2003; Doherty et al., 2008). The ability of IVM to mimic pharmacological effects of DA receptor agonists is not surprising considering that we have previously shown that IVM can modulate DA-dependent behaviors and signaling pathways. For instance, IVM potentiated the effects of DA on motor behavior (Khoja et al., 2016). IVM significantly modulated phosphorylation of dopamine and cyclic AMP regulated phosphoprotein of 32 kDa (DARPP-32) (Khoja et al., 2016), which is a critical downstream target regulated by DA receptor agonists and antagonists (Svenningsson et al., 2000, 2003; Nairn et al., 2004; Borgkvist and Fisone, 2007; Bonito-Oliva et al., 2011). The findings from our laboratory and the numerous studies that have described a role for DA in PPI regulation forms the basis for our hypothesis that IVM is causing PPI disruption via activation of DA neurotransmission.

To investigate this hypothesis, we tested the effects of IVM (10 mg/kg, i.p.) on PPI function in the presence of DA receptor antagonists, SCH 23390 (for D1 receptors) and raclopride (for D2 receptors). We also tested the effects of IVM (5 mg/kg, i.p.) in combination with a selective D1 receptor agonist, SKF 82958. Furthermore, to gain mechanistic insights into interaction between IVM and DA receptor antagonists/D1 agonist in PPI regulation, we tested the effects of IVM on phosphorylation of signaling molecules linked to PPI regulation including DARPP-32, Ca^{2+}/calmodulin kinase IIα (CaMKIIα) and neuronal nitric oxide synthase (nNOS) in the ventral striatum in the presence of the dopaminergic drugs.

MATERIALS AND METHODS

Animals

Experimentally naïve 3–5 month old male C57BL/6J mice were used for the behavioral experiments and immunoblotting. Mice were either purchased from Jackson Laboratories (Bar Harbor,

ME, United States) or procured from our P2X4R KO breeding colony at University of Southern California (USC) that is maintained on a C57BL/6J background. P2X4R KO breeding colony has been described previously (Wyatt et al., 2013, 2014). It was ensured that there were no statistical significant differences in acoustic startle response or PPI% between C57BL/6J mice from Jackson Labs and our breeding colony during the baseline studies. 18–22 mice per treatment group were used for the PPI experiment involving IVM/DA receptor antagonists and 15–16 mice per treatment group were used for the PPI experiment involving IVM/D1 agonist. 3–12 mice per treatment group were used for the immunoblotting experiments. Mice were group housed in cages of 5 in a vivarium maintained at 22°C and 12 h/12 h light: dark cycle and allowed to acclimate to the behavioral testing room for a period of 1 week. All experiments were undertaken as per guidelines established by National Institute of Health (NIH) and approved by Institutional Animal Care and Use Committee (IACUC) at USC. Post completions of behavioral experiments, mice were sacrificed and brain tissues were collected for immunoblotting.

Materials

Ivermectin (Noromectin, 1% solution, Norbrook Inc, Lenexa, KS, United States) was diluted in 0.9% saline to achieve a concentration that would allow for an injection volume of 0.01 mL/g of body weight. Propylene glycol (Sigma–Aldrich, St. Louis, MO, United States) was used as vehicle control for IVM. SCH 23390, raclopride and SKF 82958 (Sigma-Aldrich, St. Louis, MO, United States) were diluted in 0.9% saline to achieve concentrations of 0.2 mg/mL, 0.6 mg/mL, and 0.02 mg/mL respectively that would allow an injection volume of 0.005 mL/g of body weight.

Acoustic Startle and PPI of Acoustic Startle Reflex

Apparatus

Acoustic Startle reflex and PPI session were tested as described previously (Wyatt et al., 2013; Khoja et al., 2016). The apparatus used for detection of acoustic startle and PPI (San Diego Instruments, San Diego, CA, United States) consisted of a standard cage placed in sound attenuated chambers with fan ventilation. Each cage consisted of a Plexiglass cylinder mounted on a piezoelectric accelerometric platform connected to an analog-digital converter. Background noises and acoustic bursts were conveyed by two separate speakers, each one oriented in a way that produced variation of 1 Db across startle cage. Both speakers and startle cages were connected to the main PC, which detected all the chamber variables. Before baseline or testing session, the machine was calibrated using digital sound level meter.

Startle and PPI Session

In the baseline session, mice were exposed to background noise of 70 Db and after an acclimation period of 5 min, were presented with 12 ms of 40 trials of 115 Db interposed with three trials of a 82 Db prestimulus preceding the 115 Db by 100 ms. Acoustic startle magnitude and PPI % were equivalent across all treatment groups. On the testing day, each mouse was exposed to an acclimation period of 5 min which comprised of background sound 70 Db, which continued for remainder of session. Each session consisted of three consecutive blocks of trials. During the first and third blocks, mice were exposed to five pulse alone trials of 115 Db. In the second block, mice were exposed to pseudorandom sequence of 50 trials, which consisted of 12 pulse alone trials, 30 trials of pulse preceded by 73, 76, or 82 Db (defined as PPI 3, PPI 6, and PPI 12 respectively; 10 for each level of prepulse loudness) and 8 no stimulus trials, wherein there was only background sound without any prepulse or pulse stimuli. Inter trial intervals were chosen between 10 and 15 s. PPI% was calculated as 100-[(mean startle amplitude for pre-pulse pulse trials/mean startle amplitude for pulse alone trials) × 100].

Ivermectin (or vehicle) (10 mg/kg, i.p. for DA receptor antagonist PPI experiment and 5 mg/kg, i.p. for D1 agonist PPI experiment) was injected 8 h prior to behavioral testing. This time-point is based on previous studies where we have shown correlation between pharmacological effects and maximal concentration (Cmax) as well as time to reach maximum concentration (Tmax) (Yardley et al., 2012; Bortolato et al., 2013). SCH 23390 (1 mg/kg, i.p.), raclopride (3 mg/kg, i.p.) or SKF 82958 (0.1 mg/kg, i.p.) was injected 10 min prior to behavioral testing.

Western Immunoblotting

Drug Treatments and Tissue Preparation

Ivermectin (or vehicle) was administered 8 h and 10 min prior to euthanasia. SCH 23390 (1 mg/kg, i.p.), raclopride (3 mg/kg, i.p.) or SKF 82958 (0.1 mg/kg) was injected 10 min prior to 8th h of IVM/vehicle administration and so, animals were euthanized 20 min post administration of dopaminergic drugs. The PPI testing duration is approximately 20 min and dopaminergic drugs were injected 10 min before the PPI session. Therefore, we chose to euthanize the mice 10 min post the 8th h of IVM/vehicle administration so that there is sufficient amount of time for the dopaminergic drugs to have an effect on IVM-mediated signaling pathways in the ventral striatum.

Ventral striatum was dissected out as per the landmarks described in the mouse brain atlas (Franklin and Paxinos, 2007). The brain tissues were homogenized in a buffer containing 50 mM tris-HCl pH (7.4), 150 mM NaCl, 0.5% sodium deoxycholate, 1% Triton-X-100, 0.1% SDS, 1% proteinase inhibitor cocktail (EMD Millipore, Temecula, CA, United States) and a cocktail of phosphatase inhibitors (1 mM sodium pyrophosphate, 10 mM sodium fluoride, 0.5 mM sodium orthovanadate, 10 mM β-glycerol phosphate, 1 μM microcysteine). In addition to these inhibitors, the homogenates were treated with 1% phosphatase inhibitors sets 1 and 2 (EMD Millipore, Temecula, CA, United States). Protein content was determined by BCA assay (Thermo Scientific, Rockville, IL, United States).

Immunoblotting Procedure

Ventral striatal tissues ran on 10% SDS-PAGE gels (50 μg/lane). Due to low volume of certain samples, protein concentrations of 40 μg/lane (for CaMKIIα) and 30 μg/lane (for nNOS) ran on some of the gels. The samples were then transferred

onto PVDF membranes using the Trans-turbo blot system (Bio-Rad, Hercules, CA, United States). Non-specific binding was blocked by incubating the membranes with 5% non-fat dry milk (Bio-Rad, Hercules, CA, United States) followed by incubation with primary antibodies overnight at 4°C. Incubation with loading control antibodies was performed at room temperature for 8 min. The phospho-specific antibodies used for immunoblotting were rabbit-anti-phospho-Thr34-DARPP-32 (1:350; EMD Millipore, Temecula, CA, United States), rabbit- anti-phospho-Thr286-CamKII (1:500; Cell Signaling Technology, Beverly, MA, United States), rabbit-anti-phospho-Ser897-nNOS (1:500; Abcam, Cambridge, United Kingdom). Rabbit polyclonal antibodies raised against DARPP-32 (1:1000; EMD Millipore, Temecula, CA, United States), CaMKIIα (1:1000; Cell Signaling Technology, Beverly, MA, United States) and nNOS (1:1000; Abcam, Cambridge, United Kingdom) which are not phosphorylation specific, were used to determine total amounts of protein. Mouse monoclonal antibodies raised against β-actin (1:20,000; Sigma-Aldrich, St. Louis, MO, United States), α-tubulin (1:20,000; EMD Millipore, Temecula, CA, United States) and α-vinculin (1:1000; Sigma-Aldrich, St. Louis, MO, United States) were used as loading control antibodies. Primary antibody incubation was followed by incubation with secondary antibodies including goat-anti-mouse and anti-rabbit antibody (Bio-Rad, Hercules, CA, United States) for 1 h at room temperature. After incubation with Clarity western plus substrate (Bio-Rad, Hercules, CA, United States), bands were visualized using chemiluminescence imaging on the ChemiDoc system (Bio-Rad, Hercules, CA, United States). Quantification of bands was performed using ImageJ software (NIH, Bethesda, MD, United States).

Statistical Analyses

To evaluate the effects of dopaminergic drugs on IVM-mediated PPI regulation, we performed repeated measures three way ANOVA using prepulse intensity as repeated variable and IVM treatment and SCH 23390/raclopride/SKF 82958 pre-treatments as independent variables, followed by Tukey's *post hoc* test for multiple comparisons. Non-repeated measures two way ANOVA followed by Tukey's *post hoc* test was used to analyze interactions between IVM and dopaminergic drugs in regulation of acoustic startle magnitude.

For the Western blotting analyses, the average densitometry values of vehicle treated samples was arbitrarily normalized to 1 and the samples from drug treatment groups were normalized by dividing each value by the average of vehicle treated samples. The degree of phosphorylation was calculated as ratio of normalized values of phosphorylated form to total form of protein and expressed as mean ± SEM. It was ensured that the densitometry values of treatment groups were normalized to their respective controls prior to combining the data from different membranes for statistical analyses. Non-repeated measures two way ANOVA with Tukey's *post hoc* test was used to investigate the interaction between IVM and the dopaminergic drugs in regulation of total levels and phosphorylation of various signaling molecules. Significance was set at $P < 0.05$. All data was analyzed using GraphPad Prism software (San Diego, CA, United States).

RESULTS

Pharmacological Blockade of D1 as Well as D2 Receptors Significantly Attenuated IVM-Mediated PPI Disruption in Mice

The impact of D1 and D2 receptor antagonism on IVM-mediated PPI regulation was assessed. There was a significant effect of prepulse intensity [$F(2,152) = 81.82$, $p < 0.001$] on the account of a gradual increase in PPI% as the prepulse stimulus intensity increases. In agreement with our previous findings (Bortolato et al., 2013), administration of IVM (10 mg/kg, i.p.) significantly disrupted PPI function [$F(1,76) = 8.983$, $p < 0.01$]. Treatment with D1 antagonist, SCH 23390, tended to affect PPI function as indicated by a non-significant trend toward effect of pre-treatment on PPI% [$F(1,76) = 3.306$, $p = 0.0741$]. In both cases, there was a significant treatment × prepulse intensity interaction [$F(2,152) = 4.040$, $p < 0.05$] as well as a pre-treatment × prepulse intensity interaction [$F(2,152) = 3.818$, $p < 0.05$] suggesting that the effects of IVM and SCH 23390 on PPI% were dependent upon the prepulse intensity. Most importantly, SCH 23390 significantly antagonized IVM-mediated PPI dysfunction as indicated by a significant treatment × pre-treatment interaction [$F(1,76) = 16.48$, $p < 0.001$]. Tukey's *post hoc* test revealed that IVM significantly reduced PPI% in comparison to its vehicle group at PPI 6 ($q = 6.447$, $p < 0.001$) and PPI 12 ($q = 6.735$, $p < 0.001$) (**Figure 1A**). IVM-mediated PPI disruption at both these prepulses was significantly reversed upon co-treatment with SCH 23390 ($q = 6.05$, $p < 0.01$ for PPI 6 and $q = 4.982$, $p < 0.05$ for PPI 12) (**Figure 1A**). Tukey's *post hoc* test also revealed that IVM significantly reduced PPI% in relation to SCH 23390-treated mice at PPI 6 ($q = 6.647$, $p < 0.001$) and co-treatment with IVM and SCH 23390 normalized IVM-induced PPI deficits (**Figure 1A**). In the context of acoustic startle reactivity, IVM significantly affected acoustic startle magnitude [$F(1,76) = 5.62$, $p < 0.05$] without any interaction with SCH 23390, indicating that IVM modulated startle response independent of D1 receptors (**Figure 1B**).

There was no significant effect of D2 antagonist, raclopride, on PPI function [$F(1,73) = 0.1442$, $p > 0.1$] indicating the inability of raclopride to independently modulate PPI. Similar to SCH 23390 treatment, raclopride significantly blocked IVM-mediated PPI disruption as indicated by a significant treatment × pre-treatment interaction [$F(1,73) = 11.51$, $p < 0.01$]. Co-treatment of IVM with raclopride significantly reversed the disruptive effects of IVM at PPI 6 ($q = 4.738$, $p < 0.05$) but, unlike SCH 23390, was unable to impede IVM-mediated PPI disruption at PPI 12 ($q = 2.197$, $p > 0.1$) (**Figure 1A**). Similar to SCH 23390-treated mice, administration of IVM significantly decreased PPI% in comparison to raclopride-treated mice at PPI 6 ($q = 5.163$, $p < 0.05$) and this effect was restored upon co-treatment with IVM and raclopride (**Figure 1A**). Noticeably, mice co-treated

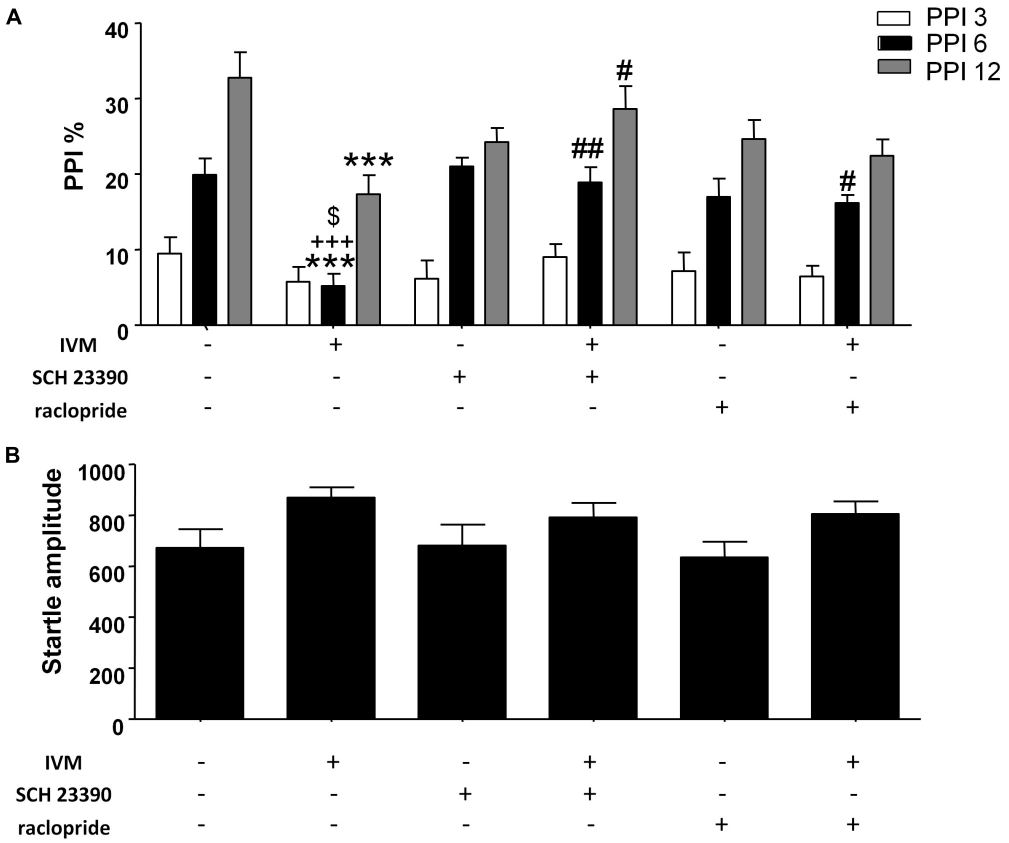

FIGURE 1 | Ivermectin (10 mg/kg) significantly disrupted PPI function in mice at PPI 6 and PPI 12. Co-treatment with SCH 23390 (1 mg/kg) significantly reversed IVM-mediated PPI disruption at both these prepulse intensities. Co-treatment with raclopride (3 mg/kg) reversed IVM-mediated PPI deficits at PPI 6, but not at PPI 12 **(A)**. Neither of the DA receptor antagonists significantly impacted IVM-mediated effects on startle magnitude **(B)**. IVM significantly affected startle magnitude. Values represent mean PPI % or startle amplitude ± SEM from 18 to 22 mice per treatment group. $^{***}P < 0.001$ versus control group. $^{\#}P < 0.05$, $^{\#\#}P < 0.01$ versus IVM-treated mice. $^{+++}P < 0.001$ versus SCH 23390-treated mice and $^{\$}P < 0.05$ versus raclopride-treated mice, Tukey's multiple comparison test.

with IVM and raclopride tended to have lower PPI % in comparison to mice treated with vehicle for IVM at PPI 12 ($q = 4.571$, $p = 0.0616$), suggesting the failure of raclopride to fully reverse the disruptive effects of IVM at PPI 12 (**Figure 1A**). Similarly, raclopride did not alter the significant effects of IVM on startle magnitude as revealed by a non-significant treatment × pre-treatment interaction (**Figure 1B**).

D1 Receptor Activation Did Not Potentiate the Effects of IVM on PPI Function

There was a non-significant trend toward effect of IVM treatment (5 mg/kg, i.p.) on PPI function [$F(1,57) = 3.626$, $p = 0.0619$] and treatment × prepulse intensity interaction tended toward statistical significance [$F(2,114) = 2.504$, $p = 0.0863$]. Treatment with D1 agonist, SKF 82958, did not have any significant effect on PPI function [$F(1,57) = 0.9509$, $p > 0.1$] (**Figure 2A**). Furthermore, there was no synergistic interaction between IVM and SKF 892958 on PPI% as indicated by a non-significant treatment × pre-treatment interaction [$F(1,57) = 1.304$, $p > 0.1$] (**Figure 2B**).

Pharmacological Modulation of Either D1 or D2 Receptors Significantly Altered IVM-Induced Changes in DARPP-32 Phosphorylation in the Ventral Striatum

We investigated the interaction between IVM and SCH 23390/raclopride on DARPP-32 phosphorylation in the ventral striatum on the basis of a critical role for DARPP-32 in PPI regulation (Svenningsson et al., 2003; Kuroiwa et al., 2012; Yabuki et al., 2013). There was no significant effect of IVM (10 mg/kg) or SCH 23390 treatment on DARPP-32 phosphorylation but there was a significant treatment × pre-treatment interaction suggesting that SCH 23390 altered the effects of IVM on DARPP-32 phosphorylation [$F(1,29) = 18.16$, $p < 0.001$]. Tukey's *post hoc* test confirmed that IVM significantly increased DARPP-32 phosphorylation in comparison to its vehicle ($q = 5.222$, $p < 0.01$) and this effect was significantly reversed upon co-treatment with SCH 23390 ($q = 5.658$, $p < 0.01$) (**Figures 3A,Bi**). Moreover, there was no significant treatment × pre-treatment interaction in regulation of total DARPP-32 levels indicating that SCH 23390 significantly modulated the effects of IVM on DARPP-32 phosphorylation without any impact on total protein levels.

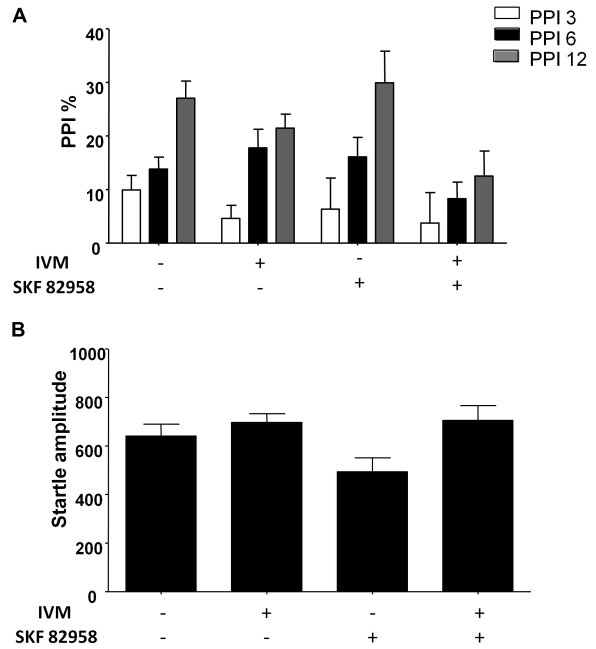

FIGURE 2 | D1 receptor stimulation by SKF 82958 (0.1 mg/kg) failed to potentiate IVM (5 mg/kg)-mediated PPI disruption. **(A)** There was no significant interaction between IVM and SKF 82958 in regulation of startle magnitude. **(B)** Values represent mean PPI % or startle amplitude ± SEM from 15 to 16 mice per treatment group.

On the other hand, raclopride did not exhibit any significant effect on DARPP-32 phosphorylation. Similar to SCH 23390, raclopride significantly antagonized IVM-induced increase in DARPP32 phosphorylation as indicated by a significant treatment × pre-treatment interaction [$F(1,23) = 5.419$, $p < 0.05$]. Tukey's *post hoc* test revealed a significant increase in DARPP-32 phosphorylation upon treatment with IVM alone ($q = 4.693$, $p < 0.05$) and co-administration with raclopride blocked the effects of IVM on DARPP-32 phosphorylation in relation to raclopride-treated mice ($q = 0.5589$, $p > 0.1$) (**Figures 3A,Bii**). However, co-administration with raclopride failed to reverse IVM-mediated increase in DARPP-32 phosphorylation (**Figures 3A,Bii**). Finally, similar to SCH 23390, raclopride does not modulate IVM's effects on total DARPP-32 levels as revealed by a non-significant treatment × pre-treatment interaction, indicating that the interaction between IVM and raclopride is specific to phosphorylation and not to total protein levels.

Considering that blockade of DA D1 receptors impedes IVM-mediated changes in DARPP-32 phosphorylation, we next evaluated whether DA D1 receptor activation can potentiate DARPP-32 phosphorylation in presence of IVM (5 mg/kg). There was a significant effect of SKF 82958 [$F(1,20) = 5.319$, $p < 0.05$] but not that of IVM treatment on DARPP-32 phosphorylation. In support of our hypothesis, SKF 82958 significantly up-regulated DARPP-32 phosphorylation in the presence of IVM as revealed by a significant treatment × pre-treatment interaction [$F(1,20) = 12.58$, $p < 0.01$]. Tukey's *post hoc* test confirmed that co-administration of IVM and SKF 82958 significantly up-regulated DARPP-32 phosphorylation in relation to IVM-treated mice ($q = 5.853$, $p < 0.01$), SKF 82958-treated mice ($q = 5.373$, $p < 0.01$) and tended to increase DARPP-32 phosphorylation in relation to mice treated with vehicle for IVM ($q = 3.664$, $p = 0.0759$) (**Figures 3A,Biii**). Finally, there were no significant effects of both IVM and SKF 82958 treatments on total DARPP-32 levels and the interaction between the two drugs was not significant.

Pharmacological Modulation of D1 and D2 Receptors Significantly Altered IVM-Mediated Changes in CaMKIIα Phosphorylation in the Ventral Striatum

CaMKIIα has been previously linked to regulation of information processing (Coultrap and Bayer, 2012) and pharmacological agents that are known to induce PPI deficits have been reported to cause alterations in CaMKIIα phosphorylation (Suemaru et al., 2000; Molteni et al., 2008; Cui et al., 2009). On the basis that P2X (Leon et al., 2006) and DA signaling (Anderson et al., 2008; Ng et al., 2010) have been associated with CaMKIIα regulation, we tested to determine if DA receptor modulation can regulate IVM-mediated effects on CaMKIIα phosphorylation. There was neither any significant effect of IVM (10 mg/kg) nor SCH 23390 treatment on CaMKIIα phosphorylation. However, SCH 23390 significantly blocked the effects of IVM on CaMKIIα phosphorylation as revealed by a significant treatment × pre-treatment interaction. [$F(1,31) = 6.343$, $p < 0.05$] with Tukey's *post hoc* test confirming that IVM significantly decreased CaMKIIα phosphorylation in relation to the vehicle group ($q = 3.852$, $p < 0.05$) (**Figures 4A,Bi**). Furthermore, SCH 23390 tended to decrease CaMKIIα phosphorylation in comparison to the control group ($q = 3.423$, $p = 0.0940$). Co-treatment of IVM and SCH 23390 blocked the effects of IVM on CaMKIIα phosphorylation in comparison to SCH 23390-treated mice ($q = 1.465$, $p > 0.1$) but failed to completely reverse IVM-induced decrease in CaMKIIα phosphorylation (**Figures 4A,Bi**). With respect to total protein levels, there was no significant effect of either IVM or SCH 23390 treatment on total CaMKIIα levels but the treatment × pre-treatment interaction tended toward statistical significance [$F(1,31) = 2.931$, $p = 0.0969$].

Raclopride did not exhibit any significant effect on CaMKIIα phosphorylation. However, there was a significant treatment × pre-treatment interaction [$F(1,28) = 10.39$, $p < 0.01$] suggesting that raclopride antagonized IVM-mediated effects on CaMKIIα phosphorylation. Tukey's *post hoc* test confirmed that IVM significantly decreased CaMKIIα phosphorylation ($q = 4.089$, $p < 0.05$) which was significantly reversed upon co-treatment with raclopride ($q = 5.116$, $p < 0.01$) (**Figures 4A,Bii**). In contrast to SCH 23390, there was a significant effect of raclopride on total CaMKIIα levels [$F(1,28) = 4.502$, $p < 0.05$] without any significant interaction with IVM suggesting that raclopride altered total protein levels independent of IVM treatment.

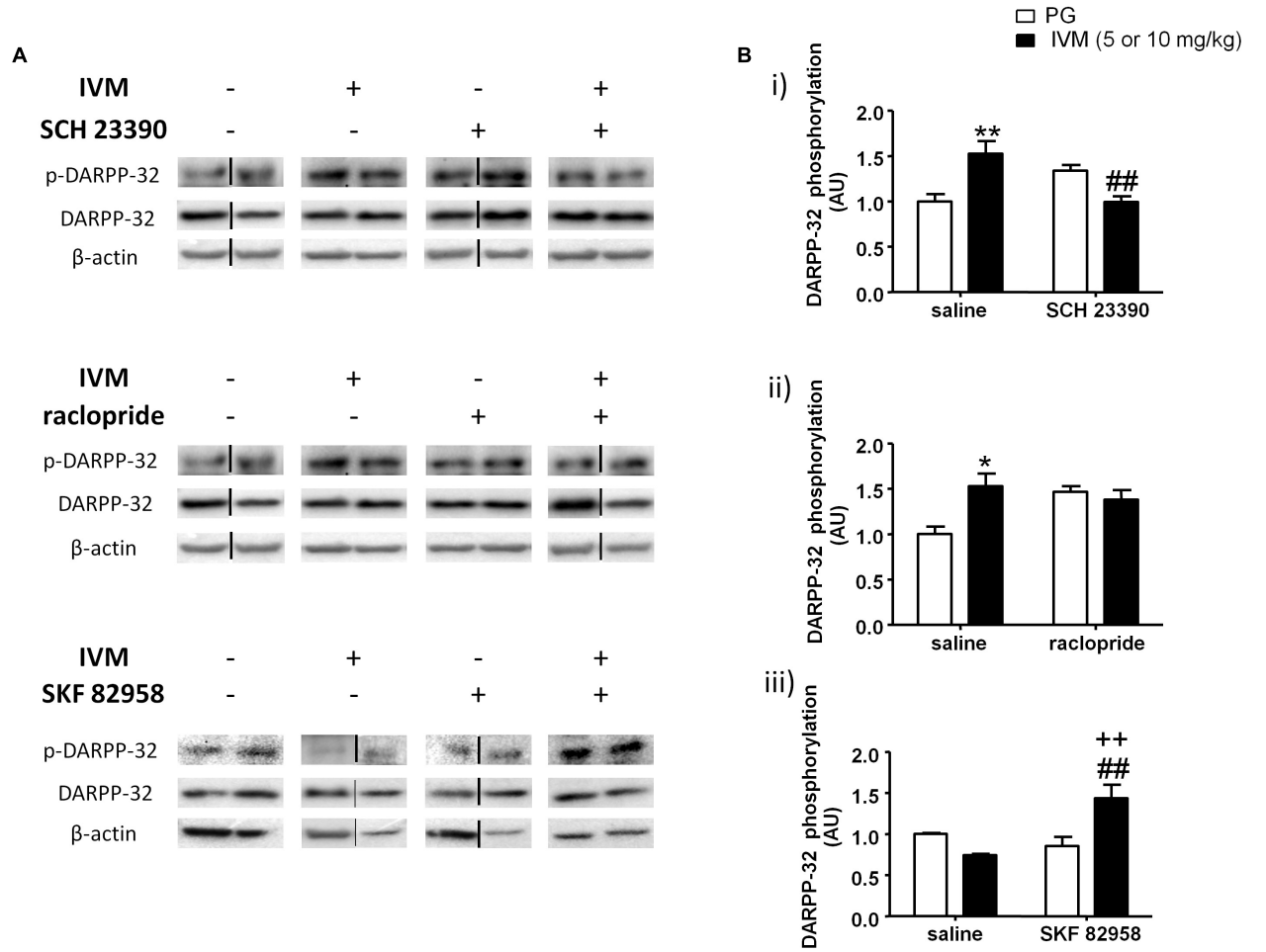

FIGURE 3 | Blockade of D1 receptors by SCH 23390 significantly reversed IVM (10 mg/kg)-mediated increase in DARPP-32 phosphorylation **(A,Bi)** in the ventral striatum. Blockade of D2 receptors by raclopride antagonized, but did not reverse, IVM (10 mg/kg)-mediated changes in DARPP-32 phosphorylation **(A,Bii)**. Stimulation of D1 receptors by SKF 82958 significantly interacted with IVM (5 mg/kg) in a synergistic manner **(A,Biii)**. The average of densitometry value of control group was arbitrarily normalized to 1. The treatment groups were normalized by dividing each value by the average of the control group. The data is presented as fold change of treatment group versus control group in that membrane. Values represent mean ± SEM from 4 to 10 mice per treatment group. Two representative bands from each treatment group from different gels are shown. IVM alone (or vehicle) images were used twice for the IVM/SCH 23390 and IVM/raclopride blots since both the DA receptor antagonist treatment groups (with or without IVM) ran on the same gel. Black solid lines between the bands indicate that the bands were cropped and spliced together either from different gels or non-consecutive lanes. Full scan of gel images can be found in the **Supplementary Figures S1–S3**. $^{*}P < 0.05$; $^{**}P < 0.01$ versus control group; $^{\#\#}P < 0.01$ versus IVM –treated mice (5 and 10 mg/kg); $^{++}P < 0.01$ versus SKF 82958-treated mice, Tukey's multiple comparison test.

DA D1 receptor activation by SKF 82958 induced independent changes in CaMKIIα phosphorylation [$F(1,14) = 5.053$, $p < 0.05$] that was significantly potentiated in the presence of IVM (5 mg/kg) as indicated by a significant treatment × pre-treatment interaction [$F(1,14) = 10.55$, $p < 0.01$]. Tukey's *post hoc* test detected that co-treatment of IVM and SKF 82958 significantly increased CaMKIIα phosphorylation in comparison to IVM-treated mice ($q = 5.936$, $p < 0.01$) (**Figures 4A,Biii**). Moreover, co-administration of IVM and SKF 82958 tended to enhance phosphorylation in relation to SKF 82958-treated mice ($q = 3.747$, $p = 0.0796$) (**Figures 4A,Biii**). Furthermore, there was a significant effect of both IVM [$F(1,14) = 9.404$, $p < 0.01$] and SKF 82958 [$F(1,14) = 9.723$, $p < 0.01$] treatments on total CaMKIIα levels without any significant interaction between the two treatments suggesting the inability of SKF 82958 to modulate IVM-induced changes in total CaMKIIα levels.

IVM Significantly Interacted With DA Receptor Antagonists/D1 Agonist in Regulation of nNOS Phosphorylation in the Ventral Striatum

P2X4Rs have been previously implicated in regulation of NOS activity and NO release in cardiac myocytes (Yang and Liang, 2012; Yang et al., 2015). Considering that NOS inhibitors have been reported to ameliorate PPI impairments induced by

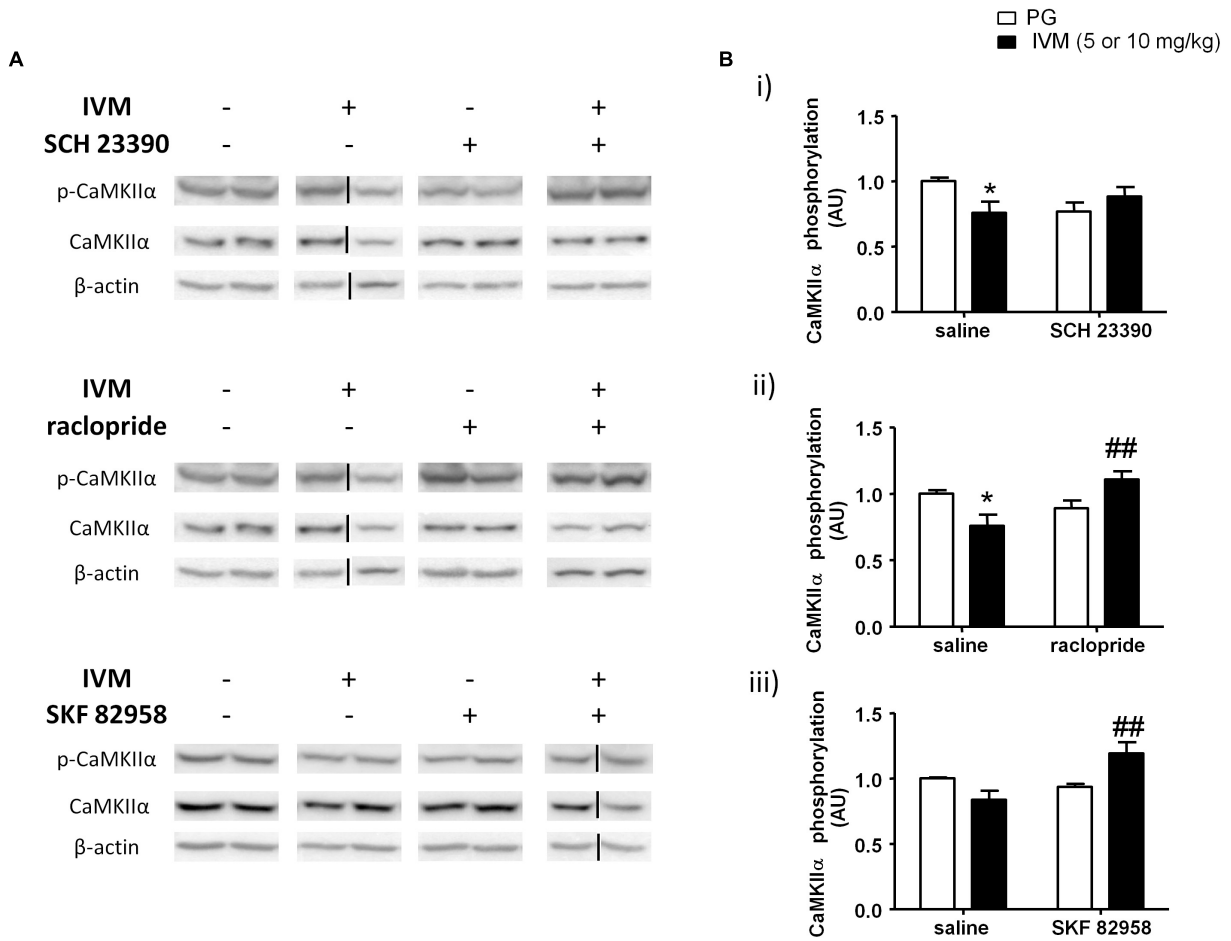

FIGURE 4 | IVM (10 mg/kg)-mediated decrease in CaMKIIα phosphorylation was significantly impeded by SCH 23390 **(A,Bi)** but reversed by raclopride **(A,Bii)** in the ventral striatum. IVM (5 mg/kg) synergistically interacted with SKF 82958 in regulation of CaMKIIα phosphorylation **(A,Biii)** in the ventral striatum. Details of normalization and analyses are presented in **Figure 3**. Values represent mean ± SEM from 3 to 11 mice per treatment group. Two representative bands from each treatment group are shown. IVM alone (or vehicle) images were used twice for the IVM/SCH 23390 and IVM/raclopride blots since both the DA receptor antagonist treatment groups (with or without IVM) ran on the same gel. Black solid lines indicated that bands were cropped and spliced from non-consecutive lanes or different gels. Full scan of gel images can be found in the **Supplementary Figures S4, S5**. $^{*}P < 0.05$ versus control group; $^{\#\#}P < 0.01$ versus IVM-treated mice (5 and 10 mg/kg), Tukey's multiple comparison test.

psychostimulants and the involvement of NO in PPI regulation (Wiley, 1998; Klamer et al., 2004; Fejgin et al., 2008; Issy et al., 2011, 2014), we hypothesized that nNOS could be one of potential substrates that underlies the antagonistic interaction between IVM and DA receptor antagonists in PPI regulation. There was a significant effect of SCH 23390 [$F(1,21) = 19.96$, $p < 0.001$], but not that of IVM (10 mg/kg), treatment on nNOS phosphorylation. In addition to regulating nNOS phosphorylation independently, SCH 23390 altered the effects of IVM as indicated by a significant treatment × pre-treatment interaction [$F(1,21) = 5.96$, $p < 0.05$]. Tukey's *post hoc* test detected a non-significant trend toward decrease in nNOS phosphorylation upon IVM treatment alone in comparison to the vehicle group ($q = 3.905$, $p = 0.0528$) which was significantly reversed upon co-administration with SCH 23390 ($q = 7.17$, $p < 0.001$) (**Figures 5A,Bi**). Furthermore, treatment with SCH 23390 alone significantly increased nNOS phosphorylation in comparison to IVM-treated mice ($q = 5.146$, $p < 0.01$) (**Figures 5A,Bi**). In regards to total protein levels, there was neither any significant effect of both the treatments nor was there any significant interaction suggesting that SCH 23390 altered effects of IVM on nNOS phosphorylation without any effect on total protein levels.

Similar to SCH 23390 treatment, administration of raclopride alone significantly affected nNOS phosphorylation [$F(1,20) = 4.839$, $p < 0.05$] and was able to significantly alter IVM-mediated effects on NOS phosphorylation as revealed by a significant treatment × pre-treatment interaction [$F(1,20) = 10.65$, $p < 0.01$]. Tukey's *post hoc* test confirmed that co-treatment of IVM and raclopride significantly increased nNOS phosphorylation in comparison to IVM-treated mice ($q = 5.741$, $p < 0.01$) (**Figures 5A,Bii**). There was a significant effect of IVM [$F(1,20) = 4.996$, $p < 0.05$], but not that of raclopride, treatment on total nNOS levels.

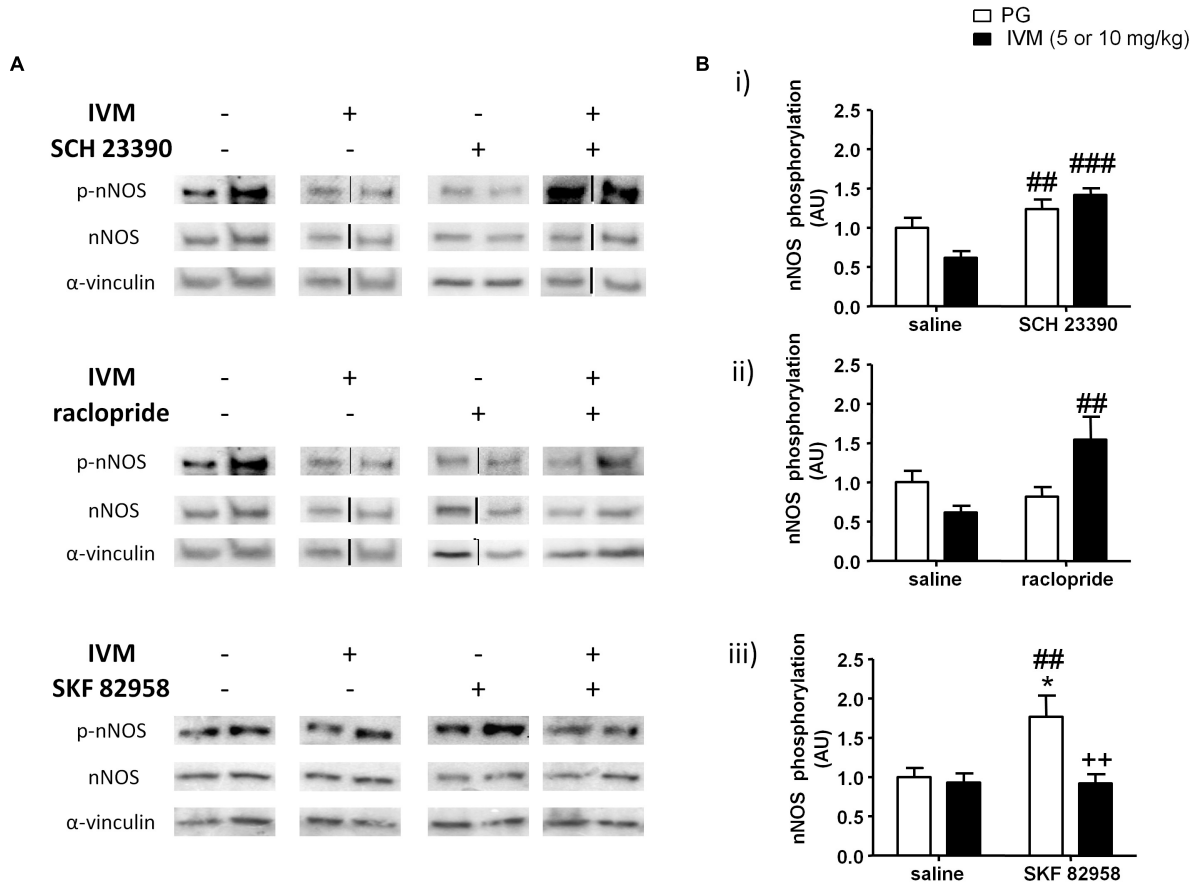

FIGURE 5 | SCH 23390 **(A,Bi)** and raclopride **(A,Bii)** significantly increased nNOS phosphorylation in presence of IVM (10 mg/kg) in the ventral striatum. IVM (5 mg/kg) significantly attenuated SKF 82958-induced increase in nNOS phosphorylation **(A,Biii)**. Details of normalization and analyses are presented in **Figure 3**. Values represent mean ± SEM from 4 to 12 mice per treatment group. Two representative bands from each treatment group are shown. IVM alone (or vehicle) images were used twice for the IVM/SCH 23390 and IVM/raclopride blots since both the DA receptor antagonist treatment groups (with or without IVM) ran on the same gel. Black solid lines between bands indicate that bands were cropped and spliced together from non-consecutive lanes or from different gels. Full scan of gel images can be found in the **Supplementary Figures S6, S7**. $^{*}P < 0.05$ versus control group; $^{\#\#}P < 0.01$, $^{\#\#\#}P < 0.001$ versus IVM-treated mice (5 and 10 mg/kg); $^{++}P < 0.01$ versus SKF 82958-treated mice, Tukey's multiple comparison test.

Additionally, the interaction between IVM and raclopride for total nNOS levels tended toward statistical significance [$F(1,20) = 3.347$, $p = 0.0823$].

In contrast to a high dose (10 mg/kg) of IVM; there was a significant effect of 5 mg/kg IVM on nNOS phosphorylation [$F(1,33) = 8.22$, $p < 0.01$]. Additionally, D1 receptor activation by SKF 82958 significantly increased nNOS phosphorylation alone [$F(1,33) = 5.524$, $p < 0.05$] and this effect was significantly attenuated by IVM as indicated by a significant treatment × pre-treatment interaction [$F(1,33) = 5.998$, $p < 0.05$]. Tukey's *post hoc* test detected a significant increase in nNOS phosphorylation upon SKF 82958 treatment alone in comparison to the control group ($q = 4.656$, $p < 0.05$) as well as IVM-treated mice ($q = 4.919$, $p < 0.01$) (**Figures 5A,Biii**). Most importantly, co-treatment with IVM and SKF 82958 significantly reduced nNOS phosphorylation in comparison to SKF 82958-treated mice ($q = 5.491$, $p < 0.01$) (**Figures 5A,Biii**). Finally, there was neither any significant effect of IVM or SKF 82958 treatment on total nNOS levels nor was there any significant interaction indicating that IVM was able to modulate SKF 82958-mediated changes in nNOS phosphorylation without any impact on total protein levels.

DISCUSSION

The current study investigated the mechanisms underlying IVM induced PPI disruption in C57BL/6J mice. PPI deficits induced upon P2X4R potentiation by IVM were significantly attenuated to a greater extent via antagonism of D1 than D2 receptors, implicating a more essential role for D1 than D2 receptors in IVM-mediated PPI dysfunction. Additionally, neither of the DA receptor antagonists modified the effects of IVM on startle magnitude suggesting that DA antagonists were able to restore IVM-induced information processing deficits without having any impact on auditory function. The findings from the DA receptor antagonist experiments are in agreement with previous investigations that have reported a more important role for D1

receptors than D2 receptors in PPI regulation in mice (Ralph-Williams et al., 2002, 2003; Ralph and Caine, 2005). For instance, non-selective DA receptor agonists such as apomorphine, cocaine or pergolide have been reported to disrupt PPI function in a D1 receptor-specific manner (Ralph-Williams et al., 2002, 2003; Doherty et al., 2008). Selective D1 agonists such as SKF 82958, SKF 81297 and dihydrexidine have also been shown to disrupt PPI functioning in C57BL/6J and 129S6 mice (Ralph-Williams et al., 2003; Ralph and Caine, 2005) at doses lower than those required to induce similar behavioral effects with rats (Wan et al., 1996; Swerdlow et al., 2000). Moreover, findings from our laboratory reported that D1 receptor antagonism rescued PPI dysfunction in P2X4R KO mice (Khoja et al., 2016). Taken together, the current body of evidence strongly suggests that D1 receptors have a prominent role in PPI regulation in mice.

In addition to the importance of D1 receptors in PPI regulation with mice; the role of D2 receptors cannot be disregarded based on our findings where raclopride significantly blocked IVM-mediated PPI dysfunction. Moreover, indirect DA receptor agonists including amphetamine and cocaine can disrupt PPI function via D2 receptor-dependent manner in mice (Ralph et al., 1999; Ralph-Williams et al., 2002; Doherty et al., 2008). In addition, multiple genetic knockout mouse models for dopamine transporter (DAT) (Ralph et al., 2001), disrupted in schizophrenia complex (DISC) (Lipina et al., 2010) and trace amine receptor-1 (TA1) (Wolinsky et al., 2007) exhibited PPI deficits that were linked to aberrant D2 receptor activity. In agreement with pharmacological and genetic findings, our laboratory has previously demonstrated that PPI deficits in P2X4R KO mice were also reversed by raclopride, in addition to SCH 23390, indicating that D2 receptors can be involved in PPI dysfunction in P2X4R KO mice (Khoja et al., 2016).

The findings from our IVM/P2X4R KO PPI investigations (and others) suggest a plausible D1–D2 receptor interaction in PPI regulation in mice. The argument for this hypothesis is reinforced by previous reports showing that antagonism of either D1 or D2 receptors can negate PPI deficits induced by D1 agonists in mice (Ralph and Caine, 2005). For example, administration of either D2 antagonist eticlopride or D1 antagonist SCH 39166 significantly restored SKF 82958-mediated PPI deficits in C57BL/6J mice (Ralph and Caine, 2005). A plausible explanation for this outcome is that activation of D1 receptors alone might not be sufficient enough to disrupt PPI function in rats but the ability of D2 receptors to induce PPI dysfunction is dependent upon the tonic activity of D1 receptors. Hence, based on our current findings, it appears that D1 receptors might be interacting with D2 receptors in the modulation of IVM-mediated PPI alterations and the tendency of raclopride to block IVM's behavioral effects might be dependent upon tonic activity of D1 receptors in C57BL/6J mice.

To gain insights into the molecular mechanisms by which IVM can induce PPI dysfunction, we investigated its interaction with dopaminergic drugs on DARPP-32 phosphorylation in the ventral striatum. Our findings suggest that positive modulation of P2X4Rs increased DARPP-32 phosphorylation in a D1 receptor dependent manner (**Figure 6A**). Although, raclopride was able to prevent IVM from further increasing DARPP-32 phosphorylation, it failed to reverse IVM-mediated increase in DARPP-32 phosphorylation, suggesting that the actions of IVM on DARPP-32 are D1-dependent. Enhanced phosphorylation of DARPP-32 at Thr 34 has been linked to PPI deficits mediated by various psychostimulants such as amphetamine, phencyclidine (PCP), lysergic acid diethylamide (LSD) and that these effects were significantly diminished in genetically modified mice wherein DARPP-32 phosphorylation at Thr34 is compromised (Svenningsson et al., 2003). D1 receptor activation on the striatonigral neurons (D1-expressing neurons) of the basal ganglia circuitry stimulates the cAMP/protein kinase-A (PKA) pathway which leads to increased phosphorylation of DARPP-32 at Thr34 (Svenningsson et al., 2004; Girault, 2012) (**Figure 6**) and possibly manifestation of PPI deficits in mice as demonstrated by selective D1 agonists (Ralph-Williams et al., 2003; Ralph and Caine, 2005). Taking these findings into perspective, the reversal of IVM-mediated changes in DARPP-32 phosphorylation by SCH 23390 may underlie the attenuation of IVM-mediated PPI deficits. Moreover, the failure of raclopride to reverse IVM-induced increase in DARPP-32 phosphorylation might explain the discrepancy between SCH 23390 and raclopride in restoration of IVM-induced PPI deficits. However, this inference cannot be supported by the current evidence that SKF 82958 failed to elicit PPI dysfunction in presence of IVM despite the synergistic interaction between SKF 82958 and IVM in augmentation of DARPP-32 phosphorylation in the ventral striatum. This discrepancy can be attributed to the notion that DARPP-32 alone cannot mediate PPI function considering that multiple other neural substrates may contribute to the alleviation of IVM-induced PPI disruption by SCH 23390. Furthermore, the high dose of SCH 23390 used in this study may involve pharmacological activity at other receptor targets such as agonism at 5-HT2C receptors (Briggs et al., 1991; Millan et al., 2001). Notably, 5-HT2C receptor agonists can rescue PPI deficits induced by psychomimetics (Marquis et al., 2007). Thus, the multi-pharmacological profile of SCH 23390 in amelioration of IVM-induced PPI deficits cannot be disregarded. Moreover, although the ventral striatum [which comprises of nucleus accumbens (NAc) core] is ascertained as an important site for PPI mediation; this behavior is regulated by the cortico-pallido-striatal-thalamic circuitry (Wan et al., 1995; Wan and Swerdlow, 1996; Swerdlow et al., 2008, 2011). Considering that DA receptor agonists induce PPI dysfunction and DA receptor antagonists reverse PPI deficits, it is presumably thought that increased DAergic function in the NAc (Swerdlow et al., 2001a), leads to inhibition of GABAergic neurons projecting toward the ventral pallidum (VP), which has a tonic control over the pedunculopontine nucleus (PPTg), which mediates PPI function (Fendt et al., 2001). Thus, disruption of underlying signaling cascades in any of these brain structures of this complex circuitry could possibly be linked to the antagonistic interaction between IVM and SCH 23390 which warrants further investigation. Detailed delineation of signaling pathways within the PPI circuitry maybe necessitated in elucidating the discrepancy between SCH 23390 and SKF 82958 in regulation of IVM-mediated behavioral effects.

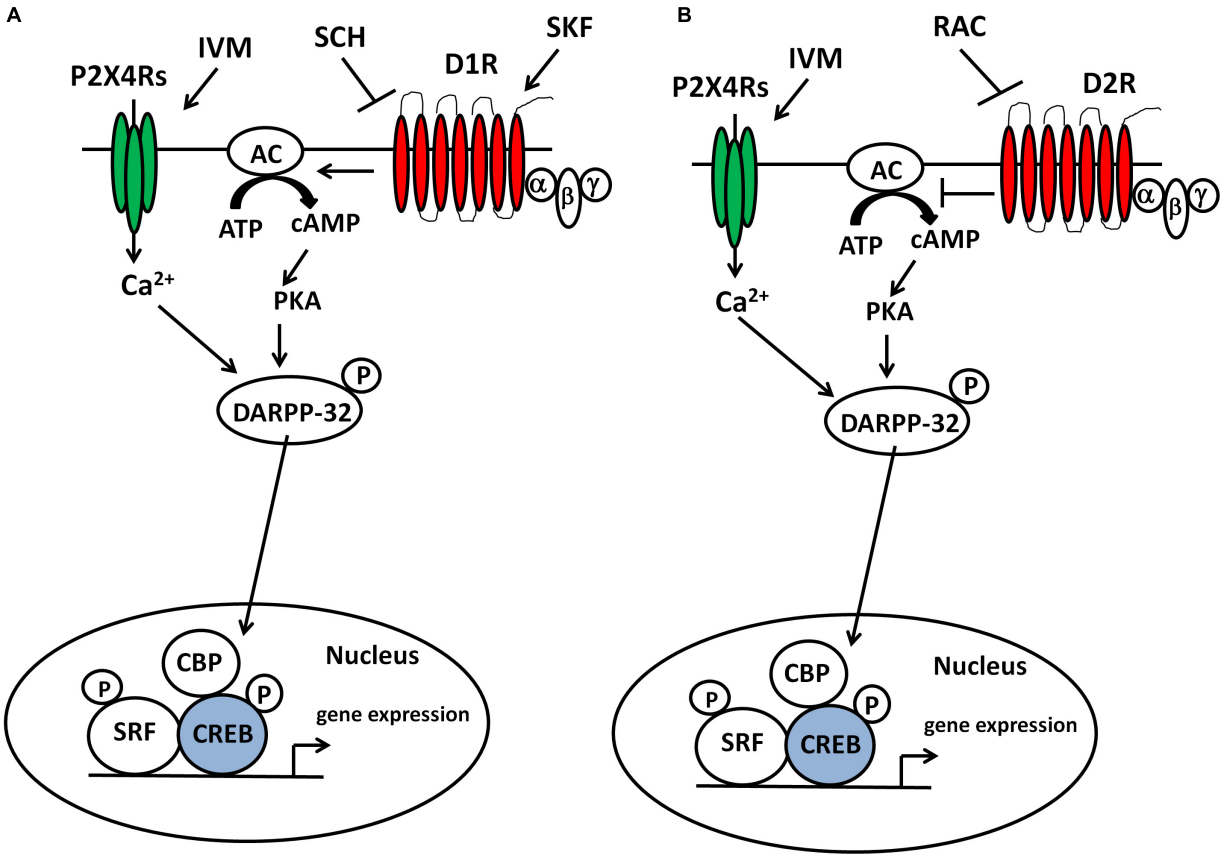

FIGURE 6 | IVM modulated DARPP-32 phosphorylation via P2X4R potentiation in a D1 receptor-dependent manner in the ventral striatum. Inter-dependence between P2X4Rs and D1 receptors in DARPP-32 phosphorylation may be relevant to regulation of transcription factors (e.g., CREB) and subsequent gene expression in the ventral striatum and DA-dependent behaviors such as sensorimotor gating **(A)**. The ability of raclopride to block IVM-mediated changes at behavioral and cellular level indicates a plausible interaction between P2X4Rs and D2 receptors in regulation of DA-dependent behaviors and signaling pathways **(B)**.

In addition to DARPP-32, we also evaluated the effects of IVM on other signaling molecules that may contribute to alterations in sensorimotor gating such as nNOS and its upstream regulator, CaMKIIα. CaMKIIα can phosphorylate nNOS at Ser897, leading to reduction in functional activity (Hayashi et al., 1999; Komeima et al., 2000). IVM decreased CaMKIIα phosphorylation in a D2-dependent manner since its effects were reversed by raclopride, but not by SCH 23390. Nevertheless, SCH 23390 was able to prevent IVM from further decreasing CaMKIIα phosphorylation suggesting that SCH 23390 might be reversing IVM-mediated effects on signaling pathways upstream of CaMKIIα phosphorylation. Interestingly, at a lower dose (5 mg/kg), IVM significantly potentiated the effects of SKF 82958 on CaMKIIα phosphorylation. A mechanistic explanation for this outcome is the synergistic interaction between IVM and SKF 82958 in DARPP-32 phosphorylation which could lead to up-regulation of CaMKIIα phosphorylation via inhibition of protein phosphotase-1 (PP-1) (Strack et al., 1997; Shioda and Fukunaga, 2017). Overall, these findings suggest that the dopaminergic control of IVM over CaMKIIα phosphorylation can be dose-dependent. While there is no direct evidence that links CaMKIIα to PPI regulation; results from our investigation mirror PPI disruptive agents such as indirect DA agonists (methamphetamine) (Suemaru et al., 2000) and *N*-Methyl-D-aspartate receptor (NMDAR) antagonists (PCP, ketamine) (Molteni et al., 2008; Cui et al., 2009) that have been reported to decrease CaMKIIα phosphorylation in mice and that this effect was fully restored upon D1 or D2 receptor antagonism. Additionally, CaMKIIα has been implicated in information processing (Coultrap and Bayer, 2012) and pathophysiology of psychiatric disorders characterized by cognitive abnormalities (Frankland et al., 2008; Yamasaki et al., 2008; Matsuo et al., 2009). If PPI deficiency can precede fragmentation of cognitive function (McGhie and Chapman, 1961); then alterations in CaMKIIα activity can be linked to PPI deficits in the clinical population.

On account of the significant reduction in CaMKIIα phosphorylation, IVM tended to reduce the phosphorylation of its downstream target, nNOS. Although raclopride, but not SCH 23390, was able to reverse IVM-mediated decrease in CaMKIIα phosphorylation; the pharmacological blockade of both D1 and D2 receptors significantly reversed IVM-mediated changes in nNOS phosphorylation. These results suggest that CaMKIIα could potentially be involved upstream in the effects of D2, but not D1, receptors on IVM-induced changes in

nNOS phosphorylation. Although D1 receptor activation can enhance nNOS activity via NMDARs-mediated Ca^{2+} currents which involves CaMKIIα (Cepeda et al., 1998; Lee et al., 2010), stimulation of D1 receptors can also lead to enhanced phosphorylation of nNOS at Ser897 via PKA activation (Missale et al., 1998; Neve et al., 2004) or protein kinase C (PKC) activation (Felder et al., 1989; Undie and Friedman, 1990) which could ultimately result in reduced nNOS activity (Bredt et al., 1992; Dinerman et al., 1994; Lee et al., 2010). In further support of the argument that CaMKIIα may not be involved in the interaction between P2X4Rs and D1 receptors in nNOS phosphorylation, IVM potentiated the effects of SKF 82958 in regulation of CaMKIIα phosphorylation but decreased SKF 82958-induced increase in nNOS phosphorylation.

The ability of IVM to increase nNOS activity (via reduced phosphorylation of nNOS at Ser897) can lead to increased DARPP-32 phosphorylation at Thr34 via the NO/cGMP/guanyl cyclase (GC)/protein kinase G (PKG) signaling cascade (Tsou et al., 1993; Nishi et al., 2005; Threlfell and West, 2013). Additionally, the ability of IVM to dampen SKF 82958-induced decrease in nNOS phosphorylation may provide a mechanistic explanation for the synergy between IVM and SKF 82958 in regulation of DARPP-32 phosphorylation. This could represent a potential mechanism underlying IVM-mediated increased DARPP-32 phosphorylation considering that P2X4Rs are LGICs localized on GABAergic interneurons (Amadio et al., 2007) that are enriched in nNOS (Bredt et al., 1990, 1991) and have been reported to play a role in modulation of NOS activity via the cGMP/GC/PKG pathway (Yang et al., 2015). Hence, it is more logical to assume that cGMP/PKG pathway is involved upstream of P2X4R-mediated effects on DARPP-32 phosphorylation rather than the canonical cAMP/PKA activity which is regulated by G-coupled protein receptors (GPCRs) (Pierce et al., 2002). Based on previous evidence that have supported an interaction between DA neurotransmission and nNOS activity (Sammut et al., 2006, 2007; Hoque et al., 2010; Hoque and West, 2012), the reversal of IVM-mediated decrease in nNOS phosphorylation by DA receptor antagonists may underlie their antagonistic interaction with IVM in regulation of DARPP-32 phosphorylation. However, future investigations testing the effects of IVM on NO and cGMP levels in presence of dopaminergic drugs would be warranted to confirm this hypothesis.

In contrast to CaMKIIα, there is a growing body of evidence that supports role of nNOS in PPI regulation in mice (Klamer et al., 2004; Salum et al., 2006; Fejgin et al., 2008; Issy et al., 2009, 2014). The ability of IVM to decrease nNOS phosphorylation at Ser897 and induce PPI deficits is in corroboration with current theory that increased NO signaling leads to PPI deficits. NOS inhibitors have been observed to attenuate PPI deficits mediated by DA receptor activation (amphetamine, methylphenidate) (Issy et al., 2009) or NMDARs antagonism (PCP) (Klamer et al., 2004; Fejgin et al., 2008) From a disease standpoint, multiple preclinical and clinical findings have linked increased NO signaling to pathophysiology of psychiatric disorders characterized by sensorimotor gating deficits including schizophrenia (Bernstein et al., 2001; Yao et al., 2004; Bernstein et al., 2005; Lauer et al., 2005; Nasyrova et al., 2015). Genetic deficiency of nNOS generates a mouse model that exhibits behavioral and neurochemical abnormalities that are reminiscent of psychiatric disorders (Tanda et al., 2009). Increased nNOS activity has been detected in several brain regions in schizophrenia (Karson et al., 1996; Bernstein et al., 2001; Baba et al., 2004). Furthermore, genetic polymorphisms in nNOS have been detected as risk factor for schizophrenia (Reif et al., 2006; Rovny et al., 2018). Overall, based on findings from previous reports and current investigation, the regulation of nNOS activity can contribute to dopaminergic control of IVM-mediated PPI deficits and P2X4Rs-mediated increase in nNOS activity can represent a novel mechanism underlying psychiatric disorders characterized by sensorimotor gating perturbations especially schizophrenia.

Deficits in PPI have been linked to a wide spectrum of "perceptual" disorders including schizophrenia (Braff et al., 1978, 1999; Braff, 1993; Kumari et al., 1999, 2000), bipolar disorder (Perry et al., 2001), obsessive–compulsive disorder (Swerdlow et al., 1993) and Tourette's syndrome (Swerdlow et al., 2001b) as well as to autism spectrum disorders such as autism (Perry et al., 2007) and Fragile X syndrome (Frankland et al., 2004). Mutant mouse models for susceptible genes that have been suggested to be involved in the pathophysiology of aforementioned diseases exhibit PPI dysfunction (Ralph et al., 2001; Duncan et al., 2004; Kinkead et al., 2005; Tanaka et al., 2006; Ohgake et al., 2009; Lipina et al., 2010; Willi et al., 2010; Vuillermot et al., 2011), making PPI a reliable endophenotype in the genetic studies of neuropsychiatric disorders (Braff et al., 2007; Powell et al., 2012). Moreover, several of the clinical typical and atypical anti-psychotics such as haloperidol, risperidone, clozapine, olanzapine, quetiapine have been demonstrated to ameliorate PPI deficits in genetic and pharmacological models of such diseases (Swerdlow and Geyer, 1993; Bast et al., 2001; Geyer et al., 2001; Kumari and Sharma, 2002; Levin et al., 2007). Thus, PPI has been elucidated as a useful behavioral assay in investigating molecular mechanisms of psychiatric diseases as well as screening of potential antipsychotic drugs. The ability of IVM to disrupt PPI function via P2X4R potentiation (Bortolato et al., 2013) as well as the reduced PPI function in the P2X4R KO mouse model (Wyatt et al., 2013) suggests a role for P2X4Rs in pathophysiology of psychiatric disorders characterized by sensorimotor gating perturbations. Additionally, our findings also suggest a role for DA neurotransmission in altering IVM-mediated effects on sensorimotor gating. Considering the link between dysregulated dopaminergic function and sensorimotor gating abnormalities in psychiatric diseases (Swerdlow et al., 1986; Braff and Geyer, 1990; Swerdlow and Geyer, 1993; Braff et al., 2001) has been well consolidated over past decades, our preclinical studies suggest a role for P2X4Rs in pathophysiology of psychiatric diseases. Moreover, we have also demonstrated that IVM can induce dysregulation in signaling molecules including DARRP-32, CaMKIIα and nNOS, all of which have been previously linked to psychiatric diseases characterized by sensorimotor gating abnormalities (Albert et al., 2002; Bernstein et al., 2005; Ishikawa et al., 2007; Frankland et al., 2008; Nasyrova et al., 2015; Wang et al., 2017). However, further investigations at the clinical level would be warranted to link *p2rx4* gene mutations

(leading to aberrations in functioning) with neuropsychiatric disorders in order to ascertain such a role for P2X4Rs in patients diagnosed with psychiatric illnesses. Until date, single nucleotide polymorphisms in human *p2rx4* gene have been only linked to hypertension and age-related macular degeneration (Caseley et al., 2014).

Although the findings from our current investigation provide novel mechanistic insights into role of P2X4Rs in regulation of sensorimotor gating, there are certain limitations of our study that needs to be acknowledged. First, we only identified the effects of IVM in regulation of signaling molecules in one brain region that is part of a complex neural circuitry that regulates PPI function (Swerdlow et al., 2001a, 2008). Hence, future investigations that will test the impact of dopaminergic drugs on IVM-mediated changes in DARPP-32, CaMKIIα and nNOS phosphorylation in other brain regions integral to PPI circuitry including medial prefrontal cortex (mPFC), ventral hippocampus and basolateral amygdala would be warranted. Elucidation of the interaction between P2X4Rs and DA receptors in these specified brain regions would provide a holistic overview of role of P2X4Rs in mechanisms of sensorimotor gating. Another major limitation of our study is the absence of translational applicability due to lack of specific P2X4R antagonists. Based on our results with IVM, antagonism of P2X4R function would alleviate sensorimotor gating deficits and represent a novel therapeutic strategy. An alternative approach is to use viral vectors that would specifically knockdown P2X4R expression in a brain region critical for PPI regulation such as the NAc, mPFC or ventral hippocampus. Lastly, we did not establish a link between DARPP-32, CaMKIIα or nNOS and the dopaminergic control of IVM-mediated PPI deficits. Hence, future experiments would include testing the impact of interaction between P2X4Rs and DA receptors on PPI regulation upon genetic ablation of these signaling molecules by viral vectors or in genetic knockout mouse models. Such investigations would be pivotal for establishing a role for DARPP-32, CaMKIIα and nNOS in IVM-mediated PPI deficits.

Overall, the current investigation provides novel insights into a potential interaction between P2X4Rs and DA receptors in modulation of PPI and that perturbation of this interaction could lead to manifestation of sensorimotor gating deficits and subsequent cognitive fragmentation. Most importantly, our findings support the development of P2X4R antagonists as potential anti-psychotics for treatment of diseases linked to DA-dependent sensorimotor gating dysfunction.

DATA AVAILABILITY

The datasets generated for this study are available on request to the corresponding author.

ETHICS STATEMENT

All experiments were undertaken as per guidelines established by the National Institutes of Health (NIH) and approved by the Institutional Animal Care and Use Committee (IACUC) at the University of Southern California, Los Angeles, CA, United States.

AUTHOR CONTRIBUTIONS

SK designed the research study, performed the experiments, analyzed the data, and wrote the manuscript. LA, MJ, and DD reviewed and edited the manuscript.

FUNDING

This work was supported by the National Institute on Alcohol Abuse and Alcoholism (NIAAA) Grant R01 AA022448 (to DD) and the USC School of Pharmacy, Los Angeles, CA, United States.

SUPPLEMENTARY MATERIAL

The Supplementary Material for this article can be found online at: https://www.frontiersin.org/articles/10.3389/fncel.2019.00331/full#supplementary-material

REFERENCES

Abbracchio, M. P., Burnstock, G., Verkhratsky, A., and Zimmermann, H. (2009). Purinergic signalling in the nervous system: an overview. *Trends Neurosci.* 32, 19–29. doi: 10.1016/j.tins.2008.10.001

Albert, K. A., Hemmings, H. C. Jr., Adamo, A. I., Potkin, S. G., Akbarian, S., Sandman, C. A., et al. (2002). Evidence for decreased DARPP-32 in the prefrontal cortex of patients with schizophrenia. *Arch. Gen. Psychiatry* 59, 705–712.

Amadio, S., Montilli, C., Picconi, B., Calabrei, P., and Volont, C. (2007). Mapping P2X and P2Y receptor proteins in striatum and substantia nigra: an immunohistological study. *Purinergic Signal.* 3, 389–398. doi: 10.1007/s11302-007-9069-8

Anderson, S. M., Famous, K. R., Sadri-Vakili, G., Kumaresan, V., Schmidt, H. D., Bass, C. E., et al. (2008). CaMKII: a biochemical bridge linking accumbens dopamine and glutamate systems in cocaine seeking. *Nat. Neurosci.* 11, 344–353. doi: 10.1038/nn2054

Baba, H., Suzuki, T., Arai, H., and Emson, P. C. (2004). Expression of nNOS and soluble guanylate cyclase in schizophrenic brain. *Neuroreport* 15, 677–680. doi: 10.1097/00001756-200403220-00020

Bast, T., Zhang, W. N., Heidbreder, C., and Feldon, J. (2001). Hyperactivity and disruption of prepulse inhibition induced by N-methyl-D-aspartate stimulation of the ventral hippocampus and the effects of pretreatment with haloperidol and clozapine. *Neuroscience* 103, 325–335. doi: 10.1016/s0306-4522(00)00589-3

Bernstein, H. G., Bogerts, B., and Keilhoff, G. (2005). The many faces of nitric oxide in schizophrenia. A review. *Schizophr. Res.* 78, 69–86. doi: 10.1016/j.schres.2005.05.019

Bernstein, H. G., Krell, D., Braunewell, K. H., Baumann, B., Gundelfinger, E. D., Diekmann, S., et al. (2001). Increased number of nitric oxide synthase immunoreactive Purkinje cells and dentate nucleus neurons in schizophrenia. *J. Neurocytol.* 30, 661–670.

Bonito-Oliva, A., Feyder, M., and Fisone, G. (2011). Deciphering the actions of antiparkinsonian and antipsychotic drugs on cAMP/DARPP-32 signaling. *Front. Neuroanat.* 5:38. doi: 10.3389/fnana.2011.00038

Borgkvist, A., and Fisone, G. (2007). Psychoactive drugs and regulation of the cAMP/PKA/DARPP-32 cascade in striatal medium spiny neurons. *Neurosci. Biobehav. Rev.* 31, 79–88. doi: 10.1016/j.neubiorev.2006.03.003

Bortolato, M., Yardley, M., Khoja, S., Godar, S. C., Asatryan, L., Finn, D. A., et al. (2013). Pharmacological insights into the role of P2X4 receptors in behavioral regulation: lessons from ivermectin. *Int. J. Neuropsychopharmacol.* 16, 1059–1070. doi: 10.1017/S1461145712000909

Braff, D., Stone, C., Callaway, E., Geyer, M., Glick, I., and Bali, L. (1978). Prestimulus effects on human startle reflex in normals and schizophrenics. *Psychophysiology* 15, 339–343. doi: 10.1111/j.1469-8986.1978.tb01390.x

Braff, D. L. (1993). Information processing and attention dysfunctions in schizophrenia. *Schizophr. Bull.* 19, 233–259. doi: 10.1093/schbul/19.2.233

Braff, D. L., Freedman, R., Schork, N. J., and Gottesman, I. I. (2007). Deconstructing schizophrenia: an overview of the use of endophenotypes in order to understand a complex disorder. *Schizophr. Bull.* 33, 21–32. doi: 10.1093/schbul/sbl049

Braff, D. L., and Geyer, M. A. (1990). Sensorimotor gating and schizophrenia. Human and animal model studies. *Arch. Gen. Psychiatry* 47, 181–188.

Braff, D. L., Geyer, M. A., and Swerdlow, N. R. (2001). Human studies of prepulse inhibition of startle: normal subjects, patient groups, and pharmacological studies. *Psychopharmacology* 156, 234–258. doi: 10.1007/s002130100810

Braff, D. L., and Light, G. A. (2004). Preattentional and attentional cognitive deficits as targets for treating schizophrenia. *Psychopharmacology* 174, 75–85. doi: 10.1007/s00213-004-1848-0

Braff, D. L., Swerdlow, N. R., and Geyer, M. A. (1999). Symptom correlates of prepulse inhibition deficits in male schizophrenic patients. *Am. J. Psychiatry* 156, 596–602. doi: 10.1176/ajp.156.4.596

Bredt, D. S., Ferris, C. D., and Snyder, S. H. (1992). Nitric oxide synthase regulatory sites. Phosphorylation by cyclic AMP-dependent protein kinase, protein kinase C, and calcium/calmodulin protein kinase; identification of flavin and calmodulin binding sites. *J. Biol. Chem.* 267, 10976–10981.

Bredt, D. S., Glatt, C. E., Hwang, P. M., Fotuhi, M., Dawson, T. M., and Snyder, S. H. (1991). Nitric oxide synthase protein and mRNA are discretely localized in neuronal populations of the mammalian CNS together with NADPH diaphorase. *Neuron* 7, 615–624. doi: 10.1016/0896-6273(91)90374-9

Bredt, D. S., Hwang, P. M., and Snyder, S. H. (1990). Localization of nitric oxide synthase indicating a neural role for nitric oxide. *Nature* 347, 768–770. doi: 10.1038/347768a0

Briggs, C. A., Pollock, N. J., Frail, D. E., Paxson, C. L., Rakowski, R. F., Kang, C. H., et al. (1991). Activation of the 5-HT1C receptor expressed in *Xenopus oocytes* by the benzazepines SCH 23390 and SKF 38393. *Br. J. Pharmacol.* 104, 1038–1044. doi: 10.1111/j.1476-5381.1991.tb12546.x

Caseley, E. A., Muench, S. P., Roger, S., Mao, H. J., Baldwin, S. A., and Jiang, L. H. (2014). Non-synonymous single nucleotide polymorphisms in the P2X receptor genes: association with diseases, impact on receptor functions and potential use as diagnosis biomarkers. *Int. J. Mol. Sci.* 15, 13344–13371. doi: 10.3390/ijms150813344

Cepeda, C., Colwell, C. S., Itri, J. N., Chandler, S. H., and Levine, M. S. (1998). Dopaminergic modulation of NMDA-induced whole cell currents in neostriatal neurons in slices: contribution of calcium conductances. *J. Neurophysiol.* 79, 82–94. doi: 10.1152/jn.1998.79.1.82

Coultrap, S. J., and Bayer, K. U. (2012). CaMKII regulation in information processing and storage. *Trends Neurosci.* 35, 607–618. doi: 10.1016/j.tins.2012.05.003

Cui, X., Li, J., Li, T., Ji, F., Bu, X., Zhang, N., et al. (2009). Propofol and ketamine-induced anesthetic depth-dependent decrease of CaMKII phosphorylation levels in rat hippocampus and cortex. *J. Neurosurg. Anesthesiol.* 21, 145–154. doi: 10.1097/ANA.0b013e31819ac2c0

Dinerman, J. L., Steiner, J. P., Dawson, T. M., Dawson, V., and Snyder, S. H. (1994). Cyclic nucleotide dependent phosphorylation of neuronal nitric oxide synthase inhibits catalytic activity. *Neuropharmacology* 33, 1245–1251. doi: 10.1016/0028-3908(94)90023-x

Doherty, J. M., Masten, V. L., Powell, S. B., Ralph, R. J., Klamer, D., Low, M. J., et al. (2008). Contributions of dopamine D1, D2, and D3 receptor subtypes to the disruptive effects of cocaine on prepulse inhibition in mice. *Neuropsychopharmacology* 33, 2648–2656. doi: 10.1038/sj.npp.1301657

Duncan, G. E., Moy, S. S., Perez, A., Eddy, D. M., Zinzow, W. M., Lieberman, J. A., et al. (2004). Deficits in sensorimotor gating and tests of social behavior in a genetic model of reduced NMDA receptor function. *Behav. Brain Res.* 153, 507–519. doi: 10.1016/j.bbr.2004.01.008

Fejgin, K., Palsson, E., Wass, C., Svensson, L., and Klamer, D. (2008). Nitric oxide signaling in the medial prefrontal cortex is involved in the biochemical and behavioral effects of phencyclidine. *Neuropsychopharmacology* 33, 1874–1883. doi: 10.1038/sj.npp.1301587

Felder, C. C., Jose, P. A., and Axelrod, J. (1989). The dopamine-1 agonist, SKF 82526, stimulates phospholipase-C activity independent of adenylate cyclase. *J. Pharmacol. Exp. Ther.* 248, 171–175.

Fendt, M., Li, L., and Yeomans, J. S. (2001). Brain stem circuits mediating prepulse inhibition of the startle reflex. *Psychopharmacology* 156, 216–224. doi: 10.1007/s002130100794

Frankland, P. W., Sakaguchi, M., and Arruda-Carvalho, M. (2008). Starting at the endophenotype: a role for alpha-CaMKII in schizophrenia? *Mol. Brain* 1:5. doi: 10.1186/1756-6606-1-5

Frankland, P. W., Wang, Y., Rosner, B., Shimizu, T., Balleine, B. W., Dykens, E. M., et al. (2004). Sensorimotor gating abnormalities in young males with fragile X syndrome and Fmr1-knockout mice. *Mol. Psychiatry* 9, 417–425. doi: 10.1038/sj.mp.4001432

Franklin, B. J., and Paxinos, G. (2007). *The Mouse Brain in Stereotaxic Coordinates*. Cambridge, MA: Academic Press.

Geyer, M. A., Krebs-Thomson, K., Braff, D. L., and Swerdlow, N. R. (2001). Pharmacological studies of prepulse inhibition models of sensorimotor gating deficits in schizophrenia: a decade in review. *Psychopharmacology* 156, 117–154. doi: 10.1007/s002130100811

Girault, J. A. (2012). Integrating neurotransmission in striatal medium spiny neurons. *Adv. Exp. Med. Biol.* 970, 407–429. doi: 10.1007/978-3-7091-0932-8_18

Graham, F. K. (1975). Presidential Address, 1974. The more or less startling effects of weak prestimulation. *Psychophysiology* 12, 238–248. doi: 10.1111/j.1469-8986.1975.tb01284.x

Greenwood, T. A., Braff, D. L., Light, G. A., Cadenhead, K. S., Calkins, M. E., Dobie, D. J., et al. (2007). Initial heritability analyses of endophenotypic measures for schizophrenia: the consortium on the genetics of schizophrenia. *Arch. Gen. Psychiatry* 64, 1242–1250. doi: 10.1001/archpsyc.64.11.1242

Hayashi, Y., Nishio, M., Naito, Y., Yokokura, H., Nimura, Y., Hidaka, H., et al. (1999). Regulation of neuronal nitric-oxide synthase by calmodulin kinases. *J. Biol. Chem.* 274, 20597–20602. doi: 10.1074/jbc.274.29.20597

Hoffman, H. S., and Ison, J. R. (1980). Reflex modification in the domain of startle: I. Some empirical findings and their implications for how the nervous system processes sensory input. *Psychol. Rev.* 87, 175–189. doi: 10.1037//0033-295x.87.2.175

Hoque, K. E., Indorkar, R. P., Sammut, S., and West, A. R. (2010). Impact of dopamine-glutamate interactions on striatal neuronal nitric oxide synthase activity. *Psychopharmacology* 207, 571–581. doi: 10.1007/s00213-009-1687-0

Hoque, K. E., and West, A. R. (2012). Dopaminergic modulation of nitric oxide synthase activity in subregions of the rat nucleus accumbens. *Synapse* 66, 220–231. doi: 10.1002/syn.21503

Ishikawa, M., Mizukami, K., Iwakiri, M., and Asada, T. (2007). Immunohistochemical and immunoblot analysis of Dopamine and cyclic AMP-regulated phosphoprotein, relative molecular mass 32,000 (DARPP-32) in the prefrontal cortex of subjects with schizophrenia and bipolar disorder. *Prog. Neuropsychopharmacol. Biol. Psychiatry* 31, 1177–1181. doi: 10.1016/j.pnpbp.2007.04.013

Ison, J. R., and Hoffman, H. S. (1983). Reflex modification in the domain of startle: II. The anomalous history of a robust and ubiquitous phenomenon. *Psychol. Bull.* 94, 3–17. doi: 10.1037/0033-2909.94.1.3

Issy, A. C., Lazzarini, M., Szawka, R. E., Carolino, R. O., Anselmo-Franci, J. A., and Del Bel, E. A. (2011). Nitric oxide synthase inhibitors improve prepulse inhibition responses of Wistar rats. *Behav. Brain Res.* 217, 416–423. doi: 10.1016/j.bbr.2010.11.016

Issy, A. C., Pedrazzi, J. F., Yoneyama, B. H., and Del-Bel, E. A. (2014). Critical role of nitric oxide in the modulation of prepulse inhibition in Swiss mice. *Psychopharmacology* 231, 663–672. doi: 10.1007/s00213-013-3277-4

Issy, A. C., Salum, C., and Del Bel, E. A. (2009). Nitric oxide modulation of methylphenidate-induced disruption of prepulse inhibition in Swiss mice. *Behav. Brain Res.* 205, 475–481. doi: 10.1016/j.bbr.2009.08.003

Karson, C. N., Griffin, W. S., Mrak, R. E., Husain, M., Dawson, T. M., Snyder, S. H., et al. (1996). Nitric oxide synthase (NOS) in schizophrenia: increases in cerebellar vermis. *Mol. Chem. Neuropathol.* 27, 275–284. doi: 10.1007/bf02815109

Khakh, B. S., and North, R. A. (2012). Neuromodulation by extracellular ATP and P2X receptors in the CNS. *Neuron* 76, 51–69. doi: 10.1016/j.neuron.2012.09.024

Khoja, S., Shah, V., Garcia, D., Asatryan, L., Jakowec, M. W., and Davies, D. L. (2016). Role of purinergic P2X4 receptors in regulating striatal dopamine homeostasis and dependent behaviors. *J. Neurochem.* 139, 134–148. doi: 10.1111/jnc.13734

Kinkead, B., Dobner, P. R., Egnatashvili, V., Murray, T., Deitemeyer, N., and Nemeroff, C. B. (2005). Neurotensin-deficient mice have deficits in prepulse inhibition: restoration by clozapine but not haloperidol, olanzapine, or quetiapine. *J. Pharmacol. Exp. Ther.* 315, 256–264. doi: 10.1124/jpet.105.087437

Klamer, D., Engel, J. A., and Svensson, L. (2004). The neuronal selective nitric oxide synthase inhibitor, Nomega-propyl-L-arginine, blocks the effects of phencyclidine on prepulse inhibition and locomotor activity in mice. *Eur. J. Pharmacol.* 503, 103–107. doi: 10.1016/j.ejphar.2004.09.042

Komeima, K., Hayashi, Y., Naito, Y., and Watanabe, Y. (2000). Inhibition of neuronal nitric-oxide synthase by calcium/ calmodulin-dependent protein kinase IIalpha through Ser847 phosphorylation in NG108-15 neuronal cells. *J. Biol. Chem.* 275, 28139–28143. doi: 10.1074/jbc.M003198200

Kumari, V., and Sharma, T. (2002). Effects of typical and atypical antipsychotics on prepulse inhibition in schizophrenia: a critical evaluation of current evidence and directions for future research. *Psychopharmacology* 162, 97–101. doi: 10.1007/s00213-002-1099-x

Kumari, V., Soni, W., Mathew, V. M., and Sharma, T. (2000). Prepulse inhibition of the startle response in men with schizophrenia: effects of age of onset of illness, symptoms, and medication. *Arch. Gen. Psychiatry* 57, 609–614. doi: 10.1001/archpsyc.57.6.609

Kumari, V., Soni, W., and Sharma, T. (1999). Normalization of information processing deficits in schizophrenia with clozapine. *Am. J. Psychiatry* 156, 1046–1051. doi: 10.1176/ajp.156.7.1046

Kuroiwa, M., Snyder, G. L., Shuto, T., Fukuda, A., Yanagawa, Y., Benavides, D. R., et al. (2012). Phosphodiesterase 4 inhibition enhances the dopamine D1 receptor/PKA/DARPP-32 signaling cascade in frontal cortex. *Psychopharmacology* 219, 1065–1079. doi: 10.1007/s00213-011-2436-8

Lauer, M., Johannes, S., Fritzen, S., Senitz, D., Riederer, P., and Reif, A. (2005). Morphological abnormalities in nitric-oxide-synthase-positive striatal interneurons of schizophrenic patients. *Neuropsychobiology* 52, 111–117. doi: 10.1159/000087555

Lee, D. K., Koh, W. C., Shim, Y. B., Shim, I., and Choe, E. S. (2010). Repeated cocaine administration increases nitric oxide efflux in the rat dorsal striatum. *Psychopharmacology* 208, 245–256. doi: 10.1007/s00213-009-1724-z

Leon, D., Hervas, C., and Miras-Portugal, M. T. (2006). P2Y1 and P2X7 receptors induce calcium/calmodulin-dependent protein kinase II phosphorylation in cerebellar granule neurons. *Eur. J. Neurosci.* 23, 2999–3013. doi: 10.1111/j.1460-9568.2006.04832.x

Levin, E. D., Caldwell, D. P., and Perraut, C. (2007). Clozapine treatment reverses dizocilpine-induced deficits of pre-pulse inhibition of tactile startle response. *Pharmacol. Biochem. Behav.* 86, 597–605. doi: 10.1016/j.pbb.2007.02.005

Lipina, T. V., Niwa, M., Jaaro-Peled, H., Fletcher, P. J., Seeman, P., Sawa, A., et al. (2010). Enhanced dopamine function in DISC1-L100P mutant mice: implications for schizophrenia. *Genes Brain Behav.* 9, 777–789. doi: 10.1111/j.1601-183X.2010.00615.x

Ludewig, S., Ludewig, K., Geyer, M. A., Hell, D., and Vollenweider, F. X. (2002). Prepulse inhibition deficits in patients with panic disorder. *Depress. Anxiety* 15, 55–60. doi: 10.1002/da.10026

Marquis, K. L., Sabb, A. L., Logue, S. F., Brennan, J. A., Piesla, M. J., Comery, T. A., et al. (2007). WAY-163909 [(7bR,10aR)-1,2,3,4,8,9,10,10a-octahydro-7bH-cyclopenta-[b][1,4]diazepino[6,7,1hi]indole]: a novel 5-hydroxytryptamine 2C receptor-selective agonist with preclinical antipsychotic-like activity. *J. Pharmacol. Exp. Ther.* 320, 486–496. doi: 10.1124/jpet.106.106989

Matsuo, N., Yamasaki, N., Ohira, K., Takao, K., Toyama, K., Eguchi, M., et al. (2009). Neural activity changes underlying the working memory deficit in alpha-CaMKII heterozygous knockout mice. *Front. Behav. Neurosci.* 3:20. doi: 10.3389/neuro.08.020.2009

McGhie, A., and Chapman, J. (1961). Disorders of attention and perception in early schizophrenia. *Br. J. Med. Psychol.* 34, 103–116. doi: 10.1111/j.2044-8341.1961.tb00936.x

Millan, M. J., Newman-Tancredi, A., Quentric, Y., and Cussac, D. (2001). The "selective" dopamine D1 receptor antagonist, SCH23390, is a potent and high efficacy agonist at cloned human serotonin2C receptors. *Psychopharmacology* 156, 58–62. doi: 10.1007/s002130100742

Missale, C., Nash, S. R., Robinson, S. W., Jaber, M., and Caron, M. G. (1998). Dopamine receptors: from structure to function. *Physiol. Rev.* 78, 189–225. doi: 10.1152/physrev.1998.78.1.189

Molteni, R., Pasini, M., Moraschi, S., Gennarelli, M., Drago, F., Racagni, G., et al. (2008). Reduced activation of intracellular signaling pathways in rat prefrontal cortex after chronic phencyclidine administration. *Pharmacol. Res.* 57, 296–302. doi: 10.1016/j.phrs.2008.02.007

Nairn, A. C., Svenningsson, P., Nishi, A., Fisone, G., Girault, J. A., and Greengard, P. (2004). The role of DARPP-32 in the actions of drugs of abuse. *Neuropharmacology* 47(Suppl. 1), 14–23. doi: 10.1016/j.neuropharm.2004.05.010

Nasyrova, R. F., Ivashchenko, D. V., Ivanov, M. V., and Neznanov, N. G. (2015). Role of nitric oxide and related molecules in schizophrenia pathogenesis: biochemical, genetic and clinical aspects. *Front. Physiol.* 6:139. doi: 10.3389/fphys.2015.00139

Neve, K. A., Seamans, J. K., and Trantham-Davidson, H. (2004). Dopamine receptor signaling. *J. Recept. Signal. Transduct. Res.* 24, 165–205.

Ng, J., Rashid, A. J., So, C. H., O'Dowd, B. F., and George, S. R. (2010). Activation of calcium/calmodulin-dependent protein kinase IIalpha in the striatum by the heteromeric D1-D2 dopamine receptor complex. *Neuroscience* 165, 535–541. doi: 10.1016/j.neuroscience.2009.10.017

Nishi, A., Watanabe, Y., Higashi, H., Tanaka, M., Nairn, A. C., and Greengard, P. (2005). Glutamate regulation of DARPP-32 phosphorylation in neostriatal neurons involves activation of multiple signaling cascades. *Proc. Natl. Acad. Sci. U.S.A.* 102, 1199–1204. doi: 10.1073/pnas.0409138102

North, R. A. (2002). Molecular physiology of P2X receptors. *Physiol. Rev.* 82, 1013–1067. doi: 10.1152/physrev.00015.2002

North, R. A., and Verkhratsky, A. (2006). Purinergic transmission in the central nervous system. *Pflugers Arch. Eur. J. Physiol.* 452, 479–485. doi: 10.1007/s00424-006-0060-y

Ohgake, S., Shimizu, E., Hashimoto, K., Okamura, N., Koike, K., Koizumi, H., et al. (2009). Dopaminergic hypofunctions and prepulse inhibition deficits in mice lacking midkine. *Prog. Neuropsychopharmacol. Biol. Psychiatry* 33, 541–546. doi: 10.1016/j.pnpbp.2009.02.005

Perry, W., Minassian, A., Feifel, D., and Braff, D. L. (2001). Sensorimotor gating deficits in bipolar disorder patients with acute psychotic mania. *Biol. Psychiatry* 50, 418–424. doi: 10.1016/s0006-3223(01)01184-2

Perry, W., Minassian, A., Lopez, B., Maron, L., and Lincoln, A. (2007). Sensorimotor gating deficits in adults with autism. *Biol. Psychiatry* 61, 482–486. doi: 10.1016/j.biopsych.2005.09.025

Pierce, K. L., Premont, R. T., and Lefkowitz, R. J. (2002). Seven-transmembrane receptors. *Nat. Rev. Mol. Cell Biol.* 3, 639–650. doi: 10.1038/nrm908

Powell, S. B., Weber, M., and Geyer, M. A. (2012). Genetic models of sensorimotor gating: relevance to neuropsychiatric disorders. *Curr. Top. Behav. Neurosci.* 12, 251–318. doi: 10.1007/7854_2011_195

Ralph, R. J., and Caine, S. B. (2005). Dopamine D1 and D2 agonist effects on prepulse inhibition and locomotion: comparison of Sprague-Dawley rats to Swiss-Webster, 129X1/SvJ, C57BL/6J, and DBA/2J mice. *J. Pharmacol. Exp. Ther.* 312, 733–741. doi: 10.1124/jpet.104.074468

Ralph, R. J., Paulus, M. P., Fumagalli, F., Caron, M. G., and Geyer, M. A. (2001). Prepulse inhibition deficits and perseverative motor patterns in dopamine transporter knock-out mice: differential effects of D1 and D2 receptor antagonists. *J. Neurosci.* 21, 305–313. doi: 10.1523/jneurosci.21-01-00305.2001

Ralph, R. J., Varty, G. B., Kelly, M. A., Wang, Y. M., Caron, M. G., Rubinstein, M., et al. (1999). The dopamine D2, but not D3 or D4, receptor subtype is essential for the disruption of prepulse inhibition produced by amphetamine in mice. *J. Neurosci.* 19, 4627–4633. doi: 10.1523/jneurosci.19-11-04627.1999

Ralph-Williams, R. J., Lehmann-Masten, V., and Geyer, M. A. (2003). Dopamine D1 rather than D2 receptor agonists disrupt prepulse inhibition of startle in mice. *Neuropsychopharmacology* 28, 108–118. doi: 10.1038/sj.npp.1300017

Ralph-Williams, R. J., Lehmann-Masten, V., Otero-Corchon, V., Low, M. J., and Geyer, M. A. (2002). Differential effects of direct and indirect dopamine agonists on prepulse inhibition: a study in D1 and D2 receptor knock-out mice. *J. Neurosci.* 22, 9604–9611. doi: 10.1523/jneurosci.22-21-09604.2002

Reif, A., Herterich, S., Strobel, A., Ehlis, A. C., Saur, D., Jacob, C. P., et al. (2006). A neuronal nitric oxide synthase (NOS-I) haplotype associated with schizophrenia modifies prefrontal cortex function. *Mol. Psychiatry* 11, 286–300. doi: 10.1038/sj.mp.4001779

Rovny, R., Marko, M., Katina, S., Murinova, J., Roharikova, V., Cimrova, B., et al. (2018). Association between genetic variability of neuronal nitric oxide synthase and sensorimotor gating in humans. *Nitric Oxide* 80, 32–36. doi: 10.1016/j.niox.2018.08.002

Salum, C., Guimaraes, F. S., Brandao, M. L., and Del Bel, E. A. (2006). Dopamine and nitric oxide interaction on the modulation of prepulse inhibition of the acoustic startle response in the Wistar rat. *Psychopharmacology* 185, 133–141. doi: 10.1007/s00213-005-0277-z

Sammut, S., Bray, K. E., and West, A. R. (2007). Dopamine D2 receptor-dependent modulation of striatal NO synthase activity. *Psychopharmacology* 191, 793–803. doi: 10.1007/s00213-006-0681-z

Sammut, S., Dec, A., Mitchell, D., Linardakis, J., Ortiguela, M., and West, A. R. (2006). Phasic dopaminergic transmission increases NO efflux in the rat dorsal striatum via a neuronal NOS and a dopamine D(1/5) receptor-dependent mechanism. *Neuropsychopharmacology* 31, 493–505. doi: 10.1038/sj.npp.1300826

Shioda, N., and Fukunaga, K. (2017). Physiological and pathological roles of CaMKII-PP1 signaling in the brain. *Int. J. Mol. Sci.* 19:E20. doi: 10.3390/ijms19010020

Strack, S., Barban, M. A., Wadzinski, B. E., and Colbran, R. J. (1997). Differential inactivation of postsynaptic density-associated and soluble Ca2+/calmodulin-dependent protein kinase II by protein phosphatases 1 and 2A. *J. Neurochem.* 68, 2119–2128. doi: 10.1046/j.1471-4159.1997.68052119.x

Suemaru, J., Akiyama, K., Tanabe, Y., and Kuroda, S. (2000). Methamphetamine decreases calcium-calmodulin dependent protein kinase II activity in discrete rat brain regions. *Synapse* 36, 155–166. doi: 10.1002/(SICI)1098-2396(20000601)36:3<155::AID-SYN1<3.0.CO;2-N

Svenningsson, P., Lindskog, M., Ledent, C., Parmentier, M., Greengard, P., Fredholm, B. B., et al. (2000). Regulation of the phosphorylation of the dopamine- and cAMP-regulated phosphoprotein of 32 kDa in vivo by dopamine D1, dopamine D2, and adenosine A2A receptors. *Proc. Natl. Acad. Sci. U.S.A.* 97, 1856–1860. doi: 10.1073/pnas.97.4.1856

Svenningsson, P., Nishi, A., Fisone, G., Girault, J. A., Nairn, A. C., and Greengard, P. (2004). DARPP-32: an integrator of neurotransmission. *Annu. Rev. Pharmacol. Toxicol.* 44, 269–296. doi: 10.1146/annurev.pharmtox.44.101802.121415

Svenningsson, P., Tzavara, E. T., Carruthers, R., Rachleff, I., Wattler, S., Nehls, M., et al. (2003). Diverse psychotomimetics act through a common signaling pathway. *Science* 302, 1412–1415. doi: 10.1126/science.1089681

Swerdlow, N. R., Benbow, C. H., Zisook, S., Geyer, M. A., and Braff, D. L. (1993). A preliminary assessment of sensorimotor gating in patients with obsessive compulsive disorder. *Biol. Psychiatry* 33, 298–301. doi: 10.1016/0006-3223(93)90300-3

Swerdlow, N. R., Braff, D. L., Geyer, M. A., and Koob, G. F. (1986). Central dopamine hyperactivity in rats mimics abnormal acoustic startle response in schizophrenics. *Biol. Psychiatry* 21, 23–33. doi: 10.1016/0006-3223(86)90005-3

Swerdlow, N. R., Breier, M. R., and Saint Marie, R. L. (2011). Probing the molecular basis for an inherited sensitivity to the startle-gating disruptive effects of apomorphine in rats. *Psychopharmacology* 216, 401–410. doi: 10.1007/s00213-011-2228-1

Swerdlow, N. R., and Geyer, M. A. (1993). Clozapine and haloperidol in an animal model of sensorimotor gating deficits in schizophrenia. *Pharmacol. Biochem. Behav.* 44, 741–744. doi: 10.1016/0091-3057(93)90193-w

Swerdlow, N. R., Geyer, M. A., and Braff, D. L. (2001a). Neural circuit regulation of prepulse inhibition of startle in the rat: current knowledge and future challenges. *Psychopharmacology* 156, 194–215. doi: 10.1007/s002130100799

Swerdlow, N. R., Karban, B., Ploum, Y., Sharp, R., Geyer, M. A., and Eastvold, A. (2001b). Tactile prepuff inhibition of startle in children with Tourette's syndrome: in search of an "fMRI-friendly" startle paradigm. *Biol. Psychiatry* 50, 578–585. doi: 10.1016/s0006-3223(01)01164-7

Swerdlow, N. R., and Light, G. A. (2018). Sensorimotor gating deficits in schizophrenia: advancing our understanding of the phenotype, its neural circuitry and genetic substrates. *Schizophr. Res.* 198, 1–5. doi: 10.1016/j.schres.2018.02.042

Swerdlow, N. R., Martinez, Z. A., Hanlon, F. M., Platten, A., Farid, M., Auerbach, P., et al. (2000). Toward understanding the biology of a complex phenotype: rat strain and substrain differences in the sensorimotor gating-disruptive effects of dopamine agonists. *J. Neurosci.* 20, 4325–4336. doi: 10.1523/jneurosci.20-11-04325.2000

Swerdlow, N. R., Weber, M., Qu, Y., Light, G. A., and Braff, D. L. (2008). Realistic expectations of prepulse inhibition in translational models for schizophrenia research. *Psychopharmacology* 199, 331–388. doi: 10.1007/s00213-008-1072-4

Tanaka, K., Shintani, N., Hashimoto, H., Kawagishi, N., Ago, Y., Matsuda, T., et al. (2006). Psychostimulant-induced attenuation of hyperactivity and prepulse inhibition deficits in Adcyap1-deficient mice. *J. Neurosci.* 26, 5091–5097. doi: 10.1523/JNEUROSCI.4376-05.2006

Tanda, K., Nishi, A., Matsuo, N., Nakanishi, K., Yamasaki, N., Sugimoto, T., et al. (2009). Abnormal social behavior, hyperactivity, impaired remote spatial memory, and increased D1-mediated dopaminergic signaling in neuronal nitric oxide synthase knockout mice. *Mol. Brain* 2:19. doi: 10.1186/1756-6606-2-19

Threlfell, S., and West, A. R. (2013). Review: modulation of striatal neuron activity by cyclic nucleotide signaling and phosphodiesterase inhibition. *Basal Ganglia* 3, 137–146. doi: 10.1016/j.baga.2013.08.001

Tsou, K., Snyder, G. L., and Greengard, P. (1993). Nitric oxide/cGMP pathway stimulates phosphorylation of DARPP-32, a dopamine- and cAMP-regulated phosphoprotein, in the substantia nigra. *Proc. Natl. Acad. Sci. U.S.A.* 90, 3462–3465. doi: 10.1073/pnas.90.8.3462

Undie, A. S., and Friedman, E. (1990). Stimulation of a dopamine D1 receptor enhances inositol phosphates formation in rat brain. *J. Pharmacol. Exp. Ther.* 253, 987–992.

Vuillermot, S., Feldon, J., and Meyer, U. (2011). Relationship between sensorimotor gating deficits and dopaminergic neuroanatomy in Nurr1-deficient mice. *Exp. Neurol.* 232, 22–32. doi: 10.1016/j.expneurol.2011.07.008

Wan, F. J., Geyer, M. A., and Swerdlow, N. R. (1995). Presynaptic dopamine-glutamate interactions in the nucleus accumbens regulate sensorimotor gating. *Psychopharmacology* 120, 433–441. doi: 10.1007/bf02245815

Wan, F. J., and Swerdlow, N. R. (1996). Sensorimotor gating in rats is regulated by different dopamine-glutamate interactions in the nucleus accumbens core and shell subregions. *Brain Res.* 722, 168–176. doi: 10.1016/0006-8993(96)00209-0

Wan, F. J., Taaid, N., and Swerdlow, N. R. (1996). Do D1/D2 interactions regulate prepulse inhibition in rats? *Neuropsychopharmacology* 14, 265–274. doi: 10.1016/0893-133X(95)00133-X

Wang, H., Farhan, M., Xu, J., Lazarovici, P., and Zheng, W. (2017). The involvement of DARPP-32 in the pathophysiology of schizophrenia. *Oncotarget* 8, 53791–53803. doi: 10.18632/oncotarget.17339

Wiley, J. L. (1998). Nitric oxide synthase inhibitors attenuate phencyclidine-induced disruption of prepulse inhibition. *Neuropsychopharmacology* 19, 86–94. doi: 10.1016/S0893-133X(98)00008-6

Willi, R., Weinmann, O., Winter, C., Klein, J., Sohr, R., Schnell, L., et al. (2010). Constitutive genetic deletion of the growth regulator Nogo-A induces schizophrenia-related endophenotypes. *J. Neurosci.* 30, 556–567. doi: 10.1523/JNEUROSCI.4393-09.2010

Wolinsky, T. D., Swanson, C. J., Smith, K. E., Zhong, H., Borowsky, B., Seeman, P., et al. (2007). The Trace Amine 1 receptor knockout mouse: an animal model with relevance to schizophrenia. *Genes Brain Behav.* 6, 628–639. doi: 10.1111/j.1601-183X.2006.00292.x

Wyatt, L. R., Finn, D. A., Khoja, S., Yardley, M. M., Asatryan, L., Alkana, R. L., et al. (2014). Contribution of P2X4 receptors to ethanol intake in male C57BL/6 mice. *Neurochem. Res.* 39, 1127–1139. doi: 10.1007/s11064-014-1271-9

Wyatt, L. R., Godar, S. C., Khoja, S., Jakowec, M. W., Alkana, R. L., Bortolato, M., et al. (2013). Sociocommunicative and sensorimotor impairments in male P2X4-deficient mice. *Neuropsychopharmacology* 38, 1993–2002. doi: 10.1038/npp.2013.98

Yabuki, Y., Nakagawasai, O., Moriguchi, S., Shioda, N., Onogi, H., Tan-No, K., et al. (2013). Decreased CaMKII and PKC activities in specific brain regions

are associated with cognitive impairment in neonatal ventral hippocampus-lesioned rats. *Neuroscience* 234, 103–115. doi: 10.1016/j.neuroscience.2012.12.048

Yamasaki, N., Maekawa, M., Kobayashi, K., Kajii, Y., Maeda, J., Soma, M., et al. (2008). Alpha-CaMKII deficiency causes immature dentate gyrus, a novel candidate endophenotype of psychiatric disorders. *Mol. Brain* 1:6. doi: 10.1186/1756-6606-1-6

Yang, R., Beqiri, D., Shen, J. B., Redden, J. M., Dodge-Kafka, K., Jacobson, K. A., et al. (2015). P2X4 receptor-eNOS signaling pathway in cardiac myocytes as a novel protective mechanism in heart failure. *Comput. Struct. Biotechnol. J.* 13, 1–7. doi: 10.1016/j.csbj.2014.11.002

Yang, R., and Liang, B. T. (2012). Cardiac P2X(4) receptors: targets in ischemia and heart failure? *Circ. Res.* 111, 397–401. doi: 10.1161/CIRCRESAHA.112.265959

Yao, J. K., Leonard, S., and Reddy, R. D. (2004). Increased nitric oxide radicals in postmortem brain from patients with schizophrenia. *Schizophr. Bull.* 30, 923–934. doi: 10.1093/oxfordjournals.schbul.a007142

Yardley, M. M., Wyatt, L., Khoja, S., Asatryan, L., Ramaker, M. J., Finn, D. A., et al. (2012). Ivermectin reduces alcohol intake and preference in mice. *Neuropharmacology* 63, 190–201. doi: 10.1016/j.neuropharm.2012.03.014

Conflict of Interest Statement: DD and LA are inventors on a patent for the use of ivermectin for treatment of alcohol use disorders.

The remaining authors declare that the research was conducted in the absence of any commercial or financial relationships that could be construed as a potential conflict of interest.

frontiers in Cellular Neuroscience

ORIGINAL RESEARCH
published: 26 July 2019
doi: 10.3389/fncel.2019.00340

Comparative Embryonic Spatio-Temporal Expression Profile Map of the *Xenopus* P2X Receptor Family

Camille Blanchard[1,2†], *Eric Boué-Grabot*[1,2] *and Karine Massé*[1,2*]

[1] Université de Bordeaux, Institut des Maladies Neurodégénératives, UMR 5293, Bordeaux, France, [2] CNRS, Institut des Maladies Neurodégénératives, UMR 5293, Bordeaux, France

P2X receptors are ATP-gated cations channels formed by the homo or hetero-trimeric association from the seven cloned subunits (P2X1-7). P2X receptors are widely distributed in different organs and cell types throughout the body including the nervous system and are involved in a large variety of physiological but also pathological processes in adult mammals. However, their expression and function during embryogenesis remain poorly understood. Here, we report the cloning and the comparative expression map establishment of the entire P2X subunit family in the clawed frog *Xenopus*. Orthologous sequences for 6 mammalian P2X subunits were identified in both *X. laevis* and *X. tropicalis*, but not for P2X3 subunit, suggesting a potential loss of this subunit in the *Pipidae* family. Three of these genes (*p2rx1, p2rx2,* and *p2rx5*) exist as homeologs in the pseudoallotetraploid *X. laevis,* making a total of 9 subunits in this species. Phylogenetic analyses demonstrate the high level of conservation of these receptors between amphibian and other vertebrate species. RT-PCR revealed that all subunits are expressed during the development although zygotic *p2rx6* and *p2rx7* transcripts are mainly detected at late organogenesis stages. Whole mount *in situ* hybridization shows that each subunit displays a specific spatio-temporal expression profile and that these subunits can therefore be grouped into two groups, based on their expression or not in the developing nervous system. Overlapping expression in the central and peripheral nervous system and in the sensory organs suggests potential heteromerization and/or redundant functions of P2X subunits in *Xenopus* embryos. The developmental expression of the p2rx subunit family during early phases of embryogenesis indicates that these subunits may have distinct roles during vertebrate development, especially embryonic neurogenesis.

Keywords: P2 receptors, purinergic signaling, embryogenesis, neurogenic placodes, sensory neurons, nervous system, *Xenopus laevis*

OPEN ACCESS

Edited by:
Christian Lohr,
Universität Hamburg, Germany

Reviewed by:
Ivan Manzini,
Justus Liebig University Giessen, Germany
Artur Llobet,
University of Barcelona, Spain

****Correspondence:***
Karine Massé
Karine.masse@u-bordeaux.fr

†Present address:
Camille Blanchard,
INSERM, U 1215, Neurocentre Magendie, Université de Bordeaux, Bordeaux, France

Specialty section:
This article was submitted to Cellular Neurophysiology, a section of the journal Frontiers in Cellular Neuroscience

Received: *20 March 2019*
Accepted: *10 July 2019*
Published: *26 July 2019*

Citation:
Blanchard C, Boué-Grabot E and Massé K (2019) Comparative Embryonic Spatio-Temporal Expression Profile Map of the Xenopus P2X Receptor Family. Front. Cell. Neurosci. 13:340. doi: 10.3389/fncel.2019.00340

INTRODUCTION

The nucleotide ATP, as the universal source of energy, is an essential intracellular molecule to the survival of cells and whole organisms. However, the discovery of the first P2 purinergic receptor at the beginning of the 1990s confirmed Geoffrey Burnstock's hypothesis that ATP acts also as an extracellular signaling molecule (Burnstock, 2014). In the last 25 years, numerous

studies demonstrated the fundamental importance of extracellular ATP in the physiology of all organs through the activation of ionotropic P2X and metabotropic P2Y receptors (Ralevic and Burnstock, 1998). Purinergic signaling pathway is not restricted to extracellular ATP actions. The metabolic breakdown of extracellular ATP by ectonucleotidases is a source of ADP and adenosine. Both ATP derivatives act as extracellular signaling molecule through the activation of P2Y and adenosine G-protein coupled receptors (Adora) respectively (Yegutkin, 2014). It is nowadays recognized that the purinergic signaling in various organs play important physiological roles but also in diseases, placing purinergic receptors and ectonucleotidases as theurapeutic targets (Burnstock, 2018). In particular, in the nervous system, ATP and adenosine are involved in neuromodulation, glial-neuron interaction, and sensory transmission but also in neuropathic pain, neurodegenerative diseases, and multiple sclerosis (Burnstock et al., 2011; Khakh and North, 2012; Burnstock, 2016, 2017; Boué-Grabot and Pankratov, 2017; Domercq et al., 2018). Although the purinergic signaling has received less attention in a developmental context, several recent studies have shown a role of extracellular ATP and its derivatives in progenitor cell proliferation, migration, differentiation and synaptogenesis (Del Puerto et al., 2013; Oliveira et al., 2016; Fumagalli et al., 2017; Rodrigues et al., 2018). Furthermore, the description of the ectonucleotidases and purinoreceptors embryonic expression profile *in vivo* provides indication of their implication during nervous system development (Massé and Dale, 2012).

Due to the high number of actors, their large and overlapping expression profile and the very broad range of the purinergic receptor sensitivities, deciphering *in vivo* the specific embryonic functions of each extracellular purine is quite challenging. We decided to tackle this by studying each member of purinergic receptors and ectonucleotidases family using the clawed frog *Xenopus* embryo due to its numerous advantages, e.g., large size, large number production, relative transparency, external development and rapid generation times. Moreover, as its developmental cycle is temperature dependent, it is possible to modulate the length of the early stages such a neurulation allowing to access easily to the embryos at all developmental stages. Although having a pseudo-allotetraploid genome, the recent development of *Xenopus* genetics has broadened the use of this model especially as animal model for human pathologies (Sater and Moody, 2017; Tandon et al., 2017). We have previously established the embryonic expression pattern of enpp and entpd ectonucleotidases and adenosine signaling pathway members in *Xenopus* embryos. The specific spatio-temporal expression profile of each member of ectonucleotidases and adenosine receptors, suggested that ATP, ADP and adenosine may have distinct and specific functions during vertebrate embryogenesis (Massé et al., 2006, 2010; Tocco et al., 2015). Indeed, we demonstrated that ADP, via the P2Y1 receptor, triggers eye development by regulating the expression of the eye field transcription factors, such as pax6 (Massé et al., 2007). *Xenopus* is therefore an ideal model to address the functional roles of the purinergic pathway during the early phases of vertebrate embryogenesis, phases that are difficult to study in other vertebrate models (Massé and Dale, 2012).

Here we characterized the *Xenopus* P2X receptor subunit family. P2X receptors are ATP-gated cation channels formed by homomeric or heteromeric association of three subunits, which are involved in numerous physiological and pathological processes (North, 2002; Khakh and North, 2006; North, 2016). Seven genes for P2X subunits have been cloned and shared a common topology with two membrane-spanning domains, a large extracellular domain containing the ATP binding sites and intracellular N and C termini (Kawate et al., 2009; Habermacher et al., 2016). We report the cloning of the entire family in *Xenopus* laevis and *tropicalis* and reveal the absence of the *p2rx3* gene in both of these species. Our phylogenetic data demonstrate a high degree of conservation of these *p2rx* sequences during vertebrate evolution. Analysis of the temporal and spatial expression of each amphibian subunit during *X. laevis* development showed that all identified subunits are expressed during development. Based on their expression or not in the nervous system, two groups of subunits can be proposed. Transcripts of all *p2rx* subunits, except *p2rx2.S* and *p2rx5.L*, are detected in the central and peripheral nervous system and their overlapping expression suggests potential hetero-oligomerization or redundant functions in the sensory system. A group of three subunits, *p2rx2.S, p2rx4.L, and p2rx5*, display specific expression in mesodermal derivatives suggesting these subunits may regulate renal and muscle development.

MATERIALS AND METHODS

Bioinformatics

Sequences were identified on the NCBI and Xenbase databases. BLAST (Basic Local Alignment Search Tool) searches were performed on the NBCI Nucleotide and on the Xenbase *Xenopus laevis* 9.1 genome databases (Altschul et al., 1990). This identification was based on *p2rx* subunits orthologs nucleotide alignments, using either predicted (from automated computational analysis) mRNA sequences from *Xenopus* genomic sequences or validated mRNA sequences from different species such as *Homo sapiens*, *Mus musculus*, *Rattus norvegicus*, *Danio rerio*, *Gallus gallus*, *Takifugu rubripes*, *Xenopus tropicalis,* and *Xenopus laevis*. Conceptual translation of cDNA and protein sequence analysis was performed on the ExPASy internet site using the program Translate Tool[1] (Artimo et al., 2012). Accession numbers of all sequences used in this study are given in **Supplementary Table S1**. Alignments were performed on the EMBL-EBI internet site using the program Pairwise sequence global alignment EMBOSS Needle and Multiple Sequence alignment Clustal Omega program (Needleman and Wunsch, 1970; Thompson et al., 1994). A phylogenetic tree was created on the Phylogeny.fr platform using muscle for multiple alignments, PhyML for tree building and TreeDyn for tree rendering (Dereeper et al., 2008).

[1] http://web.expasy.org/translate/

Embryos Culture

Xenopus laevis males and females were purchased from the CNRS *Xenopus* breeding Center (Rennes, France). Embryos were obtained by *in vitro* fertilization of eggs collected in 1X MMR (Marc's Modified Ringers) saline solution [100 mM NaCl, 2 mM KCl, 2 mM $CaCl_2$, 1 mM $MgSO_4$, 5 mM Hepes (pH 7.8), pH 7.4], from a hormonally [hCG (Agripharm), 750 units] stimulated *X. laevis* female by adding crushed testis isolated from a sacrificed male. Fertilized eggs were dejellied in 3% L-cysteine hydrochloride, pH 7.6 (Sigma-Aldrich), and washed several times with 0.1X MMR. Embryos were then cultured to the required stage in 0,1X MMR in presence of 50 mμ/mL of gentamycin sulfate (Sigma-Aldrich). The embryos were staged according to the Nieuwkoop and Faber table of *X. laevis* development (Nieuwkoop and Faber, 1994).

RT-PCR

RNA extraction from whole embryos and cDNA synthesis were performed as previously described (Massé et al., 2010). For each subunit, specific primers were designed, when possible, on two different exons with at least one primer positioned at exon junctions (**Supplementary Table S2**), in order to discriminate genomic from cDNA amplification. Furthermore, those chosen primers were selected to differentiate homeologs expression, with a restrictive annealing possibility on the other homeologous mRNA sequence. After optimization of the PCR conditions using a gradient PCR machine (Bio-Rad), PCR products were verified by sequencing (Beckman Coulter Genomics Company). To assess semi-quantitative PCR experiments, the quantity of input cDNA was determined by equalization of the samples with the constant gene *odc* (ornithine decarboxylase) (Bassez et al., 1990). Linearity of the signal was controlled by carrying out PCR reactions on doubling dilutions of cDNA. Negative controls (-RNA, -RT, and -cDNA) were also performed.

In situ Hybridization

Whole-mount *in situ* hybridizations were carried out as previously described (Massé et al., 2006, 2010; Blanchard and Massé, 2019). In order to detect the expression of each *p2rx* subunit, fragments of their cDNA, except for *p2rx4*, were subcloned into plasmid pBSKS, as described in **Supplementary Table S3**, in order to generate specific antisense and sense probes. Riboprobes were generated by *in vitro* transcription using a DIG RNA labeling kit following manufacturer's recommendations (Roche) after linearization of the corresponding plasmid (see **Supplementary Table S3** for details). Templates were designed in order to generate 250–600 bases riboprobes; when using larger riboprobes, a limited alkaline hydrolysis was performed. Riboprobe hybridization detection was carried out with an anti-DIG Alkaline Phosphatase antibody (Roche, Reference 11093274910) and the BM-Purple AP substrate (Roche Reference, 11442074001). After bleaching, embryos were photographed using the SMZ18 binocular (Nikon).

Embedding and Sectioning

After whole-mount *in situ* hybridization, embryos were gradually dehydrated in 100% gelatin/sucrose-PBS solution before an overnight incubation in 100% gelatin/sucrose solution. Identified embryos were embedded in Tissue-Tek OCT, frozen on dry ice and conserved at −80°C.The frozen blocks were sectioned on a cryostat at 10 μm thickness. Transverse sections were also performed with a razor blade on fixed embryos. Sections were photographed using the SMZ18 binocular (Nikon).

RESULTS

Cloning of the Different *p2rx* Subunit Genes

The *p2rx* subunit sequences were identified by bioinformatics analysis, this work having benefited from the recent *X. tropicalis* and *X. laevis* genome sequencing (Hellsten et al., 2010; Session et al., 2016). The accession numbers of the protein sequences of the amphibian subunits can be found in **Supplementary Table S1A**. Unexpectedly, no genomic sequences were identified for *p2rx3* subunit in both *X. laevis* and *X. tropicalis* genomes.

All *Xenopus tropicalis* sequences are available on the Xenbase website, although only as annotated and predicted by automated computational analysis from genomic sequences. Their identity as P2X subunits was confirmed by conducting two complementary analyses: (1) Blastx search of these predicted *X. tropicalis* sequences on the human protein database (NCBI) was first conducted. (2) *X. tropicalis* cDNA sequences were deduced from the genomic sequences and corrected by reference to the human sequences according to the Breathnach and Chambon rule (Breathnach and Chambon, 1981). The protein sequences were deduced from conceptual translation and aligned with their potential orthologs.

Regarding the *Xenopus laevis p2rx* subunits, the *p2rx4.L* and *p2rx7.L* sequences have been previously published (Juranka et al., 2001; Paukert et al., 2002). *P2rx1.L, p2rx2.L, p2rx5.L, and p2rx5.S* sequences were available on the Xenbase site, but only as annotated sequences. Sequences verification was performed as described above for the *X. tropicalis* sequences. *P2rx1 and p2rx6 X. tropicalis* protein sequences blast on the *Xenopus laevis* protein database (NCBI website) allowed us to identify the *p2rx1.L* sequence and two *X. laevis* hypothetical proteins, whose sequences were derived from genome annotation. The identity of these sequences as *p2rx1.S* and *p2rx6.L* subunits was confirmed as described above. A *p2rx2.S* genomic sequence was identified but no cDNA or protein sequences were available on the Xenbase or NCBI website. From this genomic sequence, we retrieved the cDNA sequence after checking the exon/intron boundary by comparison to the human *p2rx2* ones according to the Breathnach and Chambon rule (Breathnach and Chambon, 1981) and carried out several blasts on *Xenopus laevis* databases (NCBI website). Alignment of these different sequences allowed us to generate the consensus and complete sequence of *p2rx2.S* subunit cDNA. The protein sequence was then obtained by

conceptual translation and checked by blast on the protein databases (NCBI website).

Evolutionary Conservation of P2X Subunit Receptors

In order to characterize the evolution of P2X receptor subunits in vertebrates, we performed an alignment of all *Xenopus* protein sequences (**Supplementary Figure S1**). In *X. laevis*, *p2rx1*, *p2rx2*, *p2rx5* have two homeologs (L and S), whose protein sequences display high degree of identity (more than 90%, **Table 1A**). However, the percentage of identity between the different *X.laevis* p2rx subunit sequences is less than 50% with p2rx4.L sharing the highest identity percentage with p2rx5 homeologs. The identity percentage between p2rx7.L and its *X. laevis* paralogs sequences is less than 30%. This low percentage is certainly due to the presence of the long and most divergent C terminus domain of p2rx7.L in this analysis.

To address the evolutionary diversification of the P2X subunits in vertebrates, a phylogenetic analysis of P2X proteins was carried out (**Figure 1**). This resulting tree reveals a clear separation between the p2rx6 and p2rx5 proteins and the other p2rx family members, which could be subdivided into three groups, p2rx3 group, p2rx1 and p2rx2 group and p2rx4 and p2rx7 group. Each member is more related to its orthologs than to the other family members in the same species, suggesting that any function identified in *X. laevis* may well be conserved in other vertebrates (**Table 1B**). The percentage of identity between *Xenopus* and its orthologous proteins is between 44 and 76%, with p2rx7.L being the least conserved protein as it only shares 38–46% of identity with zebrafish and chick p2rx7 subunit respectively. P2rx4.L is the most conserved member during vertebrate evolution, with a percentage of identity higher to 49% with the other P2X4 vertebrate proteins.

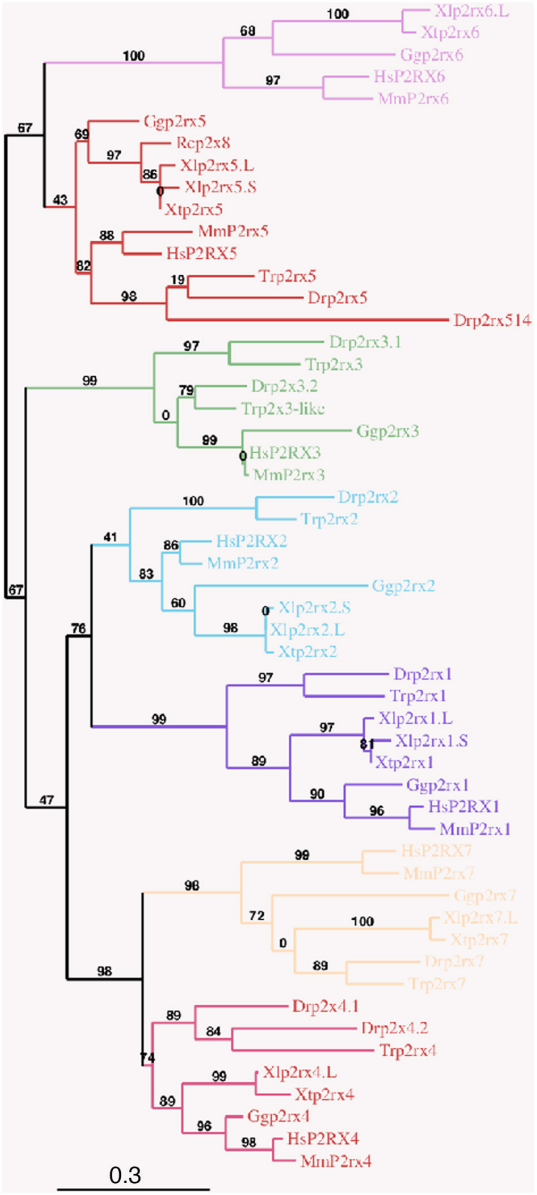

FIGURE 1 | Phylogenetic conservation of the vertebrate p2x receptor subunits. A phylogenetic tree of the p2rx subunits family based on African clawed frogs (*Xenopus laevis*, Xl and *Xenopus tropicalis*, Xt), human (*Homo sapiens*, Hs), mouse (*Mus musculus*, Mm), chicken (*Gallus gallus*, Gg), zebrafish (*Danio rerio*, Dr), Japanese puffer (*Takifugu rubripes,* Tr) and American bullfrog (*Rana catesbeiana*, Rc) was constructed on the plastform phylogeny.fr, using the Maximum Likelihood method. Bootstrap percentages (ranging from 0 to 100) are indicated at each node of the tree while branch lengths are representative of sequence substitution rates. P2rx1, 2, 3, 4, 5, 6, 7 subunit subfamilies are respectively colored in purple, blue, green, dark pink, red, light pink, and orange. The Genbank accession numbers of the different receptors are given in the **Supplementary Tables S1A,B** except for Rcp2rx8 (Accession Number: AAL24075.1).

Temporal Expression of the p2rx Gene Family During *X. laevis* Development

The temporal expression of the *p2rx* genes during embryonic development was assessed by RT-PCR (**Figure 2**). Adult brain cDNA was used as positive control. Each subunit displays a specific expression profile; however, the level of their expression increases during development to reach a maximum at stage 45, last embryonic stage tested during this experiment. The *p2rx1.L* subunit is expressed from late neurula stage whereas expression of its homeolog *p2rx1.S* is weakly detected from late segmentation to mid-neurulation and at a higher level during late organogenesis. The two *p2rx2* subunits display similar expression profile: both of these subunits are not expressed maternally and their zygotic expression can be detected from late segmentation stage, stage 9, although *p2rx2.L* seems more expressed during gastrulation. The *p2rx4.L* gene displays a specific expression profile, as being the only one subunit whose expression is detected at all stages tested, with a high level of maternal expression. This is in agreement with its previously published expression in oocytes (Juranka et al., 2001). The homeologs *p2rx5.L* and *p2rx5.S* are not maternally expressed. Zygotic expression of *p2rx5.L* is visible during neurulation whereas *p2rx5.S* expression is weakly detected at stage 33. Expression of these both homeologs is detected at a higher level from stage 41. The *p2rx6.L* subunit is the second *p2rx* gene being expressed maternally; however, its

TABLE 1A | Relatedness of the *X. laevis* p2x receptor subunits.

***X. laevis* protein**	**p2rx1.L**	**p2rx1.S**	**p2rx2.L**	**p2rx2.S**	**p2rx4.L**	**p2rx5.L**	**p2rx5.S**	**p2rx6.L**
p2rx1.S	91.7 (95.9)							
p2rx2.L	31.6 (50.9)	32.3 (53.6)						
p2rx2.S	31.8 (52.2)	32.8 (54.0)	94.1 (95.2)					
p2rx4.L	45.5 (64.2)	46.6 (63.7)	37.1 (55.9)	38 (56.9)				
p2rx5.L	43.6 (61.6)	42.8 (60.2)	37.4 (55.6)	39.1 (59.2)	46.9 (63.3)			
p2rx5.S	44.0 (61.7)	42.7 (59.9)	37.7 (56.0)	38.3 (58.1)	47.5 (63.2)	92.5 (96.1)		
p2rx6.L	34.5 (52.8)	35.4 (53.7)	34.0 (51.8)	33.7 (51.9)	42.4 (58.3)	44.5 (61.2)	45.9 (63.5)	
p2rx7.L	27.9 (40.0)	27.5 (39.5)	27.5 (39.5)	27.6 (40.9)	31.3 (45.0)	27.3 (40.8)	27.4 (40.5)	23.1 (35.9)

The percentages of amino acid identity and similarity (in bracket) between the different p2rx proteins were determined by pairwise alignment using the Needleman–Wunsch global alignment on the EMBL-EBI website.

TABLE 1B | Relatedness between the *X. laevis* p2x receptor subunits and their vertebrate orthologs.

		orthologs				
		X. tropicalis	***H. sapiens***	***M. musculus***	***G. gallus***	***D. rerio***
X. laevis proteins	p2rx1.L	94.4 (96.4)	59.6 (75.3)	59.3 (73.8)	60.8 (74.5)	51.6 (66.4)
	p2rx1.S	93.0 (97.1)	58.4 (76.4)	58.4 (75.7)	60.9 (76.3)	50.8 (67.1)
	p2rx2.L	96.8 (97.7)	48.1 (58.6)	50.5 (61.2)	48.4 (63.3)	44.3 (59)
	p2rx2.S	93.6 (95.0)	46.5 (56.9)	48.8 (58.9)	47.8 (62.7)	45.3 (60.6)
	p2rx4.L	91.0 (94.0)	66.2 (78.7)	66.6 (81.1)	68.9 (82.1)	56.2 (74.6)/ 49.8 (70.2)
	p2rx5.L	93.0 (97.1)	57.7 (72.3)	57.9 (71.9)	75.5 (85.5)	48.9 (61.4)
	p2rx5.S	93.2 (95.9)	57.5 (70.6)	57.5 (71.3)	76 (85.7)	50 (51.9)
	p2rx6.L	91.9 (95.6)	47.1 (60.5)	53.4 (67.3)	52.7 (67)	n.a
	p2rx7.L	81.6 (87.8)	45.7 (60.6)	45.1 (59.7)	46.6 (61.2)	38.4 (54.8)

The percentages of amino acid identity and similarity (in bracket) between the p2rx proteins were determined by pairwise alignment using the Needleman–Wunsch global alignment on the EMBL-EBI website. The Genbank accession numbers are given in the ***Supplementary Table S1****. No zebrafish p2rx6 subunit has been described (Kucenas et al., 2003). n.a, not applicable.*

zygotic expression is only detected at late organogenesis stages. The *p2rx7.L* gene displays another distinct expression profile with its expression only clearly visible at late organogenesis stages, from stage 41, suggesting no functional roles for this subunit at early embryogenesis stages.

Spatial Expression of the *p2rx* Gene Family During *X. laevis* Development

The spatial expression of these genes in the embryo was assessed by whole-mount *in situ* hybridization, performed from stage 5 to stage 41 with specific antisense riboprobes (**Figure 3**). Probes were designed in order to discriminate the expression of the homeologs except for *p2rx5* genes. Probes were designed in the 3′UTR region except for *p2rx5*, *p2rx6*, *p2rx7* for which genes probes are located in the coding region. For each subunit, controls were carried out with sense probes to discriminate specific and unspecific signals (see **Figure 4**). Sectioning of representative p2rx stained embryos was performed in order to further characterize their expression profile (**Figure 5**). As shown in **Figures 3**, **5**, p2rx subunits display specific and different, but also overlapping expression domains during *X. laevis* development. Expression profile of the different *p2rx* subunits is summarized in **Table 2**.

P2rx1 homeologs display distinct expression profile. The *p2rx1.L* subunit is not detected before stage 27 (**Figure 3**). At this stage and stage 33/34, its transcripts are localized in a very specific region of the hindbrain, in a two rows of laterally symmetrical neurons, in a ventral position along the dorso-ventral axis (**Figure 5**). At stage 33/34, *p2rx1.L* expression is also detected in the head region, in the branchial arches and in the cement gland, a mucus-secreting ectodermal structure. At later stages, staining is also found in the heart and in the vascular network between the heart and kidney (**Figure 3**). However, its expression in the notochord is unspecific as detected with the sense probe (**Figure 4**). Expression of the *p2rx1.S* homeolog is detected from cleavage stage (**Figure 3**). At stage 5, its expression is observed in some blastomeres at the animal pole. No specific signal was detected during gastrulation. During neurulation, its transcripts are detected in the developing nervous system and in the presumptive eye field. Its expression remains in the developing eye until stage 41. Transverse sections show expression in the retina layers (**Figure 5**). From stage 27/28, weak diffuse expression is observed in the head and dorsal region of the embryo. At later stages, strong *p2rx1.S* expression is observed into two specific domains of the neurogenic placodes and peripheral nervous system: in the fused ganglion of middle lateral line and glossopharyngeal nerves as well as in the

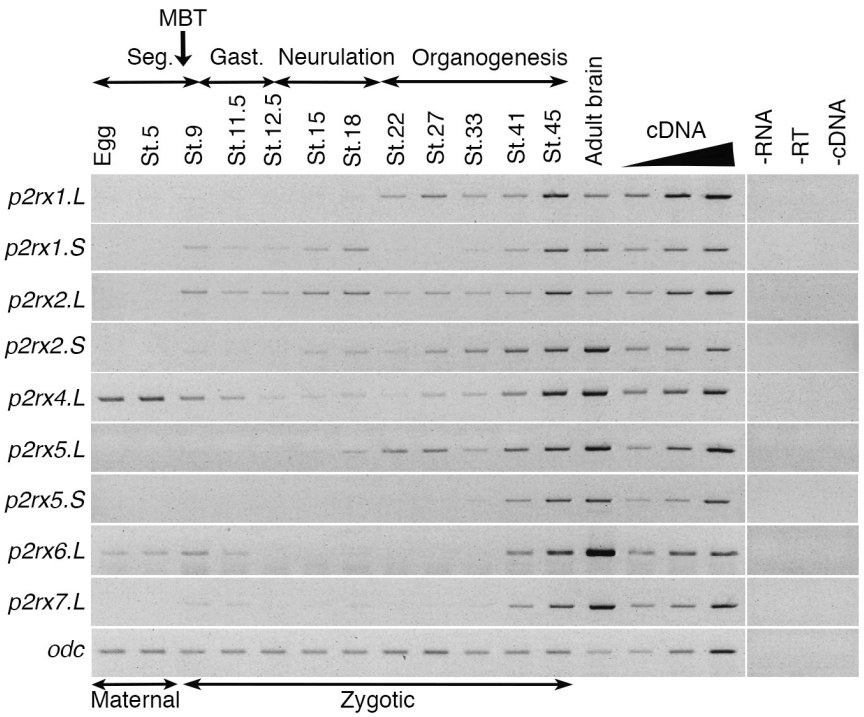

FIGURE 2 | Temporal expression profile of *p2rx* genes during embryogenesis. RT-PCR analysis showing the expression pattern of *p2rx* subunits in *X. laevis* unfertilized egg and embryos at different stages (St.). Adult brain cDNA was used as positive control and three negative controls (-RT, -RNA, -cDNA) were also performed. The linearity of the signal was controlled by carrying out PCR reactions on doubling dilutions of cDNA from stage 45 embryo, illustrated by the triangle. *Odc* (*ornithine decarboxylase*) was used as a loading control. The different phases of embryogenesis and the Mid-Blastula transition (MBT), the switch between maternal and zygotic expression, are indicated above the different embryonic stages. Seg, segmentation; Gast, Gastrulation.

trigeminal ganglion and ganglion of anterodorsal lateral line nerve (**Figure 5**).

The homeologs *p2rx2* also display different expression pattern. *P2rx2.L* transcripts are only detected in specific manner from early organogenesis stages, the staining during segmentation phase being observed with the sense probe (**Figure 3**). During organogenesis, *p2rx2.L* expression is mostly detected in developing mesoderm derivatives and nervous system. At early tailbud phase (st. 22/23), weak staining can be observed in the somites. At tailbud stages, staining is found in the ventral blood island from stage 27, in the duct of Cuvier from stage 33/34 and in the heart from stage 37 (**Figures 3**, **5**). At stage 41, expression can be observed in the gall bladder (**Figure 5**). Transcripts are also found in the head region, in the brain and the sensory organs such as eye and otic vesicule. At stage 41, staining in the eye is detected both in the retina, in the retinal ganglion and outer nuclear layers, and in the lens (**Figure 5**). From stage 37/38, *p2rx2.L* transcripts are detected in the trigeminal nerve (ophthalmic and maxillary branches) and strong expression is detected into specific regions of neurogenic placodes and peripheral nervous system : in the fused ganglion of middle lateral line and glossopharyngeal nerves and in ganglia of anteroventral lateral line and facial nerves (**Figures 3**, **5**). The *p2rx2.S* subunit displays a very tissue specific expression domain, with undetectable neural expression (**Figure 5**). No expression can be detected before stage 37 (**Figure 3**). From stage 37–41, its expression is only detected in the kidney region, in the pronephric glomus, as signal in the head and notochord is unspecific (**Figures 3–5**).

The *p2rx4.L* subunit also displays a very specific expression domain. As expected from the RT-PCR results, strong staining is observed in the animal pole in blastula and in the involuting mesoderm in gastrula embryos (**Figure 3**). However, no zygotic expression is detected before stage 33/34. At this stage, its transcripts are mostly found in the kidney. At stage 37/38, *p2rx4.L* is highly expressed in the proximal tubules (**Figure 5**). Expression is also observed in the pineal gland (epiphysis) (**Figure 3**).

The staining domain observed with the common *p2rx5* riboprobe, which does not discriminate the two homeologs, is also very specific, only in mesodermal and not neural tissues (**Figure 3**). From stage 22/23, *p2rx5* genes are only and highly expressed in the developing somites (**Figures 3–5**). This restricted muscle expression is unique to these members of the family.

The *p2rx6.L* and *p2rx7.L* genes are more weakly expressed in the embryo (**Figure 3**). At stage 33/34, weak *p2rx6.L* expression is observed in the somites. At stage 41, strong expression is detected in the head region and dorsal region of the embryo but this staining is unspecific as observed with the sense probe (**Figure 4**). However, the expression observed in the fused ganglion of middle lateral line and glossopharyngeal nerves is specific (**Figure 5**). The *p2rx7.L* subunit is only weakly but specifically detected at stage 41, in the head region, in the forebrain and midbrain and sensory organs (eye and otic vesicule) (see **Figures 4**, **5**).

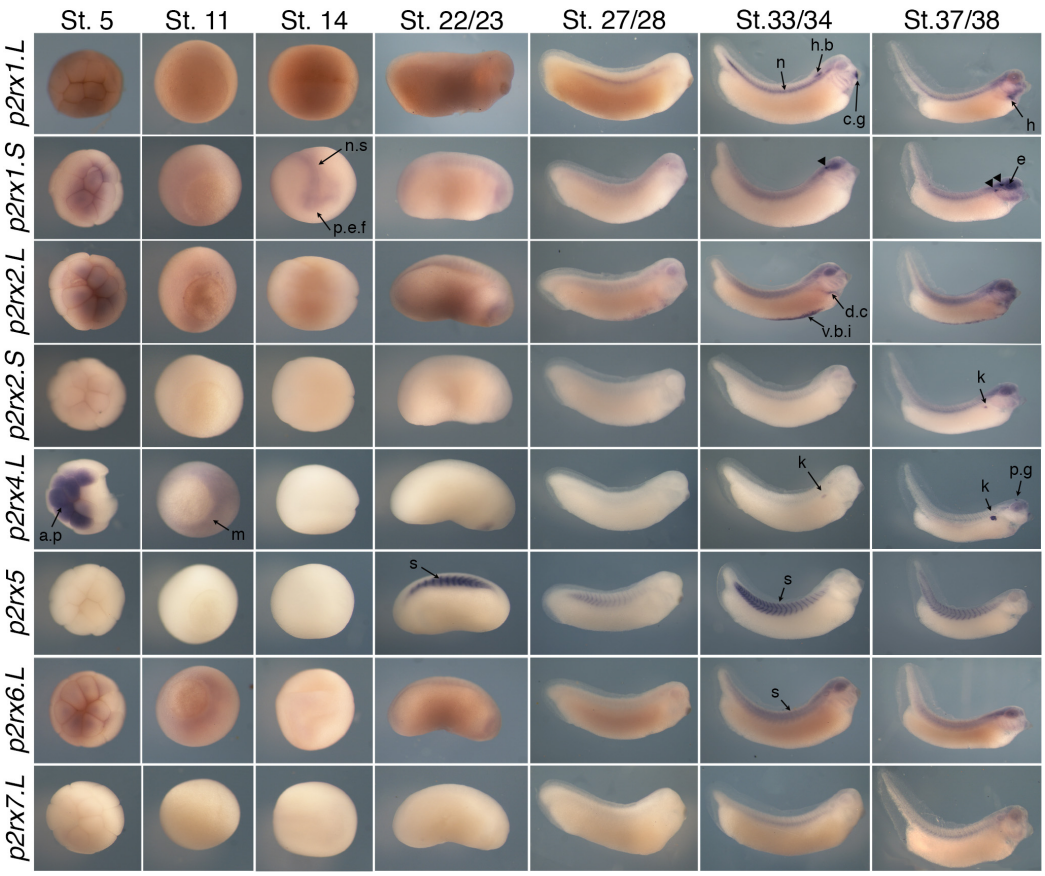

FIGURE 3 | Comparative spatial expression profile of *p2rx* genes during embryogenesis. Whole-mount *in situ* hybridization with specific DIG-labeled antisense RNA probes was performed on embryos from stages (St.) 5 to 37/38. Representative embryos were photographed at the magnification X20 for stages 5, 11, and 14 and X16 for later stages. Stage 5: animal pole view, stage 11: vegetal pole view, stage 14: dorsal view except for *p2rx1.S* (anterior view), later stages: lateral views, with dorsal is up and anterior is right. The arrowheads indicate the staining in the neurogenic placodes and peripheral nervous system detailed in **Figure 5**. a.p, animal pole; c.g, cement gland; d.c, duct of Cuvier; e, eye; h, heart; h.b, hindbrain; k, kidney; m, mesoderm; n, notochord; n.s, nervous system; p.e.f, presumptive eye field; p.g, pineal gland; s, somite; t.n, trigeminal nerve; v.b.i, ventral blood island.

DISCUSSION

We here report the cloning of the complete *p2rx* gene family in *Xenopus* in addition to p2rx4 and p2rx7 members previously identified (Juranka et al., 2001; Paukert et al., 2002). Moreover, we provide a complete expression map of all *p2rx* genes throughout *X. laevis* embryonic life. This is the first study to compare the expression of the entire p2rx family during the early phases of development, notably the earliest ones such as gastrulation and neurulation, corresponding to the specification and formation of the neural tube.

Evolutionary Conserved p2rx Subunit Genes Are Present in *Xenopus*, Except p2rx3

Our study reveals that all members of the *p2rx* family, except *p2rx3*, are present in *Xenopus laevis* and *tropicalis*. Phylogenetic analysis demonstrates the high degree of conservation during vertebrate evolution both at the protein and genomic level. The two transmembrane domains positions are conserved in all amphibian P2X subunits and the exons/introns boundaries are also conserved except for the boundary 11 (separating exons 11 and 12), which is only conserved between homeologs and orthologs. The full length of cDNAs, proteins and genomic sequences of all P2X subunits was used for our phylogenetic analysis. C-terminus tail sequences, encoded by exon 12 or exons 12 and 13 for p2rx7.L, were retained in our analysis although they correspond to the most variable domain in terms in length and sequences. The percentage of identity between the different *X. laevis* P2X subunits is similar to those shared by mammalian ones (North, 2002), the most conserved region being the transmembrane domains and the extracellular loop. Sixty four amino acids (AA) are conserved in all 15 *Xenopus* p2rx sequences, with 56/64 being located in the extracellular domain sequence. In the intracellular N-terminal domain, only a motif of 3 amino acids (Thr-X-Arg/Lys, with X being any amino acid) is conserved. This motif is a phosphorylation site by the Protein Kinase C modulating the desensitization rate of mammalian P2X receptors (Boué-Grabot et al., 2000b). In

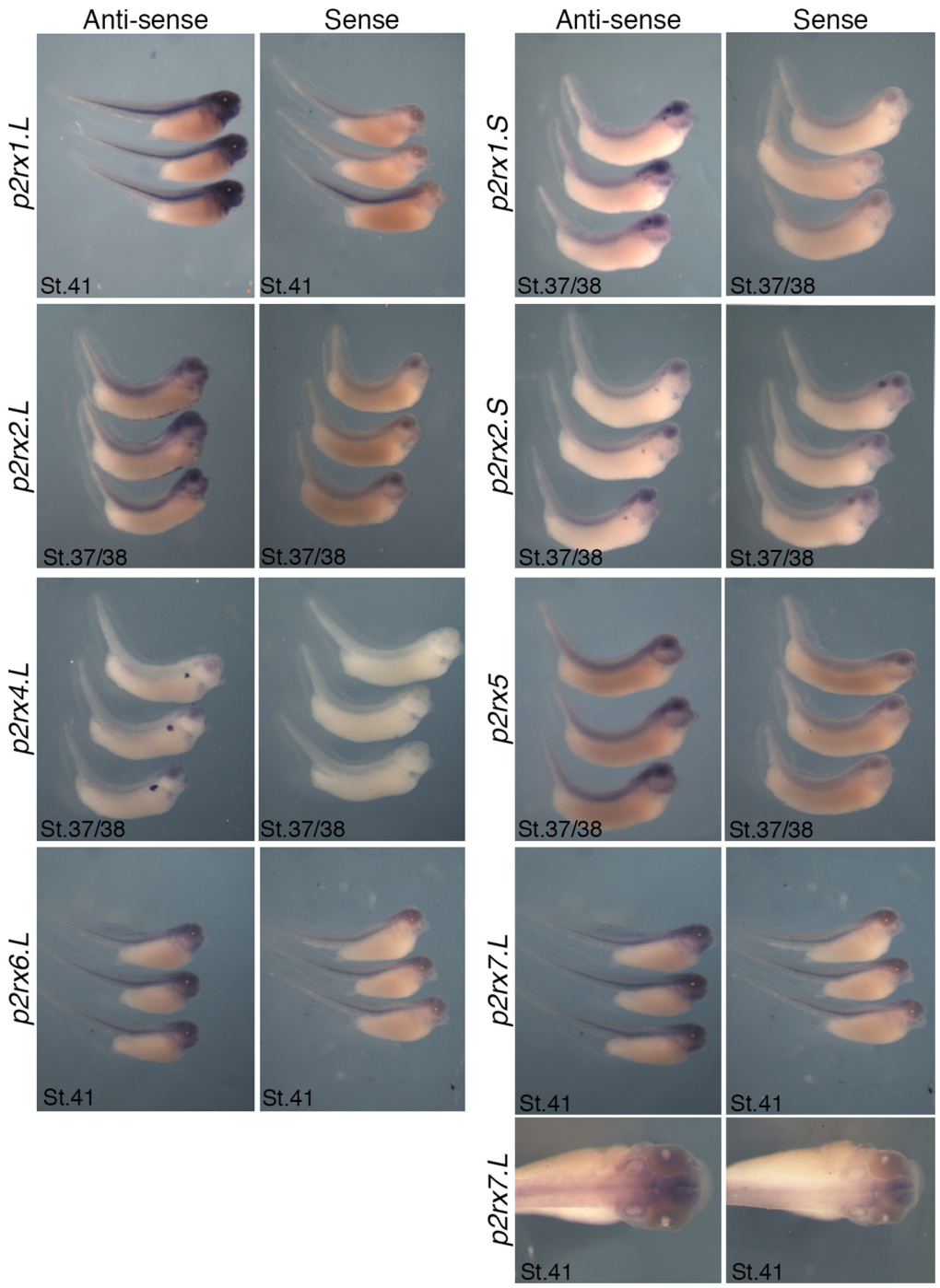

FIGURE 4 | Comparative staining obtained with the antisense and sense probes of p2rx genes. Lateral views of three representative embryos at stage 37/38 or stage 41stained with the antisense and sense probes for *p2rx1.L, p2rx1.S, p2rx2.L, p2rx2.S, p2rx4.L, p2rx6.L,* and *p2rx7.L*. subunits and *p2rx5* homeologs. Some unspecific staining, due to probe trapping, can be observed in the head region (brain ventricles, otic vesicle) and in the notochord. For *p2r7.L* subunit, a dorsal view of a representative embryo completes the lateral views. For lateral views, dorsal is up and anterior is right. For dorsal views, anterior is up.

the intracellular C-terminal domain, the consensus motif Tyr-XXX-Lys (with X being any amino acid) involved in surface targeting of mammalian P2X receptors is also conserved in all *Xenopus* P2X subunits (Chaumont et al., 2004). In the extracellular domain, the 10 cysteines (located at position 113, 124, 130, 147, 158, 164, 214, 224, 258, 267 in rat P2X2 and indicated with an asterisk on the **Supplementary Figure S1**) involved in tertiary structure of P2X subunit by disulphide bonds

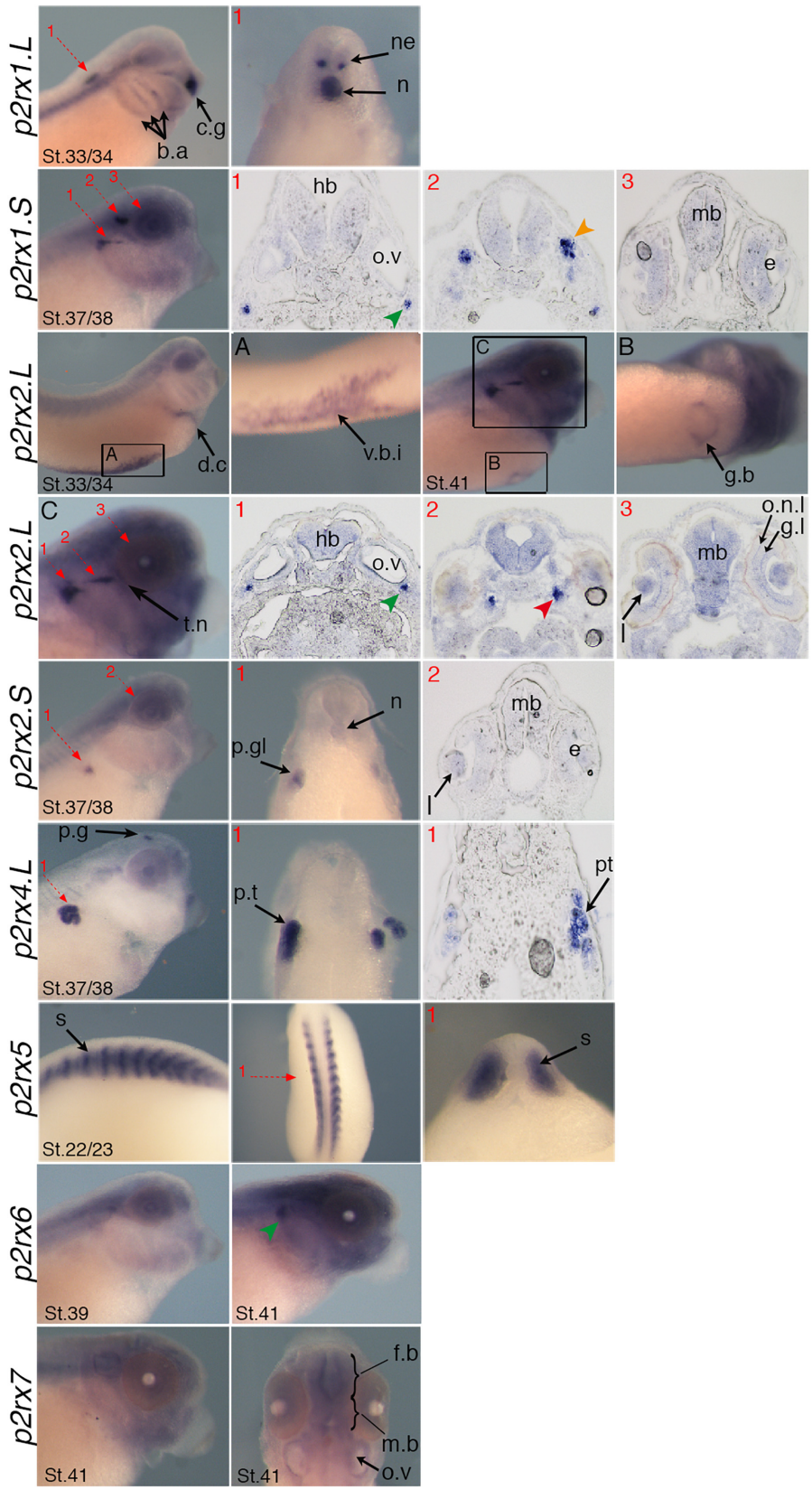

FIGURE 5 | Continued

FIGURE 5 | Specific expression domains of *p2rx* genes. Representative embryos from stages (St.) 22/23–41 displaying *p2rx* subunit expression detected by whole-mount *in situ* hybridization. To further characterize their expression profile, embryos stained for *p2rx* genes, except *p2r6.L* and *p2rx7.L*, were selected for scalpel sections and cryostat sections. Sections were performed on stage 22/23 for *p2rx5* stained embryos, on stage 33/34 for *p2rx1.L* stained embryos, on stage 37/38 for *p2rx1.S*, *p2rx2.S,* and *p2rx4.L* stained embryos and stage 41 for *p2rx2.L* stained embryos. The red numbered dotted arrows indicate the plan of the sections. For whole mount pictures, dorsal is up and anterior is right except for the *p2rx5 and p2rx7* subunits for which a dorsal view completes the lateral view. For section pictures, dorsal is up. The green arrowhead indicates the fused ganglion of middle lateral line and glossopharyngeal nerves, the orange one shows the trigeminal ganglion and ganglion of anterodorsal lateral line nerve and the red one the ganglia of anteroventral lateral line and facial nerves. c.g, cement gland; e, eye; fb, forebrain; g.b, gall bladder; g.l, ganglion layer; h, heart; hb, hindbrain; l, lens; mb, midbrain; n, notochord; o.n.l, outer nuclear layer; o.v, otic vesicle; p.g, pineal gland; p.gl, pronephric glomus; p.t, pronephric tubules; s, somite; t.n, trigeminal nerve; v.b.i, ventral blood island.

TABLE 2 | Summary of *p2rx* subunit expression domains in *Xenopus* late organogenesis stage embryos.

P2rx mRNA	1.L	1.S	2.L	2.S	4.L	5	6.L	7.L
Neural structures								
CNS Forebrain Midbrain Hindbrain Pineal gland Trigeminal nerve	+++	+++	++++++++		+++			++
Eye Retina		+	++					+
Otic Vesicle			+					+
Sensory ganglia ad.l.l. /t.g av.l.l./f.n m.l.l/g.n		++++++	++++++				+++	
Non neural structures								
Branchial arches	+							
Cement gland	++				+			
Gall bladder			++					
Eye Lens		+	++	+				
Kidney Glomus Tubules (P.T)				+++	++++			
Heart	+++		+					
Ventral blood island			+++					
Vascular system	++		++					
Somites			+			++++	+	

Expression levels are indicated on a semi quantitative scale. The number of crosses (+) indicates relative expression levels. ad.l.l./t.g, ganglia of anterodorsal lateral line and trigeminal nerves; av.l.l./f.n, ganglia of anteroventral lateral line and facial nerves; m.l.l/g.n, Fused ganglion of middle lateral line and glossopharyngeal nerves; CNS, Central Nervous System; System; P.T, Proximal Tubules.

formation are conserved in *Xenopus* (North, 2002). Furthermore, 7 of the 8 AA involved in ATP binding are also conserved [Lys70, Lys72, Phe188, Thr189, Asn296, Phe297, Arg298, Lys316 in zebrafish P2X4 (Habermacher et al., 2016); indicated with an black triangle on **Supplementary Figure S1**]. The Phe297 amino acid (indicated with an open triangle on **Supplementary Figure S1**) is conserved in all, except P2X2, *Xenopus* sequences. This is quite surprising as this phenylalanine is present in the mammalian P2X2 orthologous sequences.

Intriguingly, no genomic sequence for *p2rx3* was identified suggesting the loss of this subunit in *Pipidae*. Search on Ensembl and NCBI databases shows that this subunit is present in the different classes of vertebrates [mammalia, reptilia, aves, fish (cartilaginous, ray-finned fishes and coelacanths)] but not in agnatha. In vertebrates, P2X3 receptor is predominantly expressed in nociceptor sensory neurons of dorsal root and trigeminal ganglia and plays a key role in pain transduction (Vulchanova et al., 1997; Xiang et al., 1998; Boué-Grabot et al., 2000a; Norton et al., 2000; Kucenas et al., 2003; Appelbaum et al., 2007). In zebrafish or pufferfish, P2X3 is specifically expressed in trigeminal neurons and spinal cord Rohon-Beard cells and functional studies using transgenic animals showed its implication in sensory circuit formation during development (Kucenas et al., 2006, 2009; Palanca et al., 2013). In rodent P2X3 is similarly expressed in trigeminal and dorsal root ganglia sensory neurons and P2X3KO mice demonstrated its implication in nociception as well as sensory transduction (Cockayne et al., 2000; Souslova et al., 2000). Zebrafish p2rx3.2 is co-expressed with the ectonucleotidase entpdase3 in spinal cord Rohon-Beard cells (Appelbaum et al., 2007). We previously published entpdase3 expression in *Xenopus* Rohon-Beard cells (Massé et al., 2006), making amphibian *p2rx3* gene absence even more unexpected. Our *in situ* hybridization data show that *p2rx1.S*, *p2rx2.L,* and *p2rx6.L* are expressed in cranial neurogenic placodes, in the trigeminal ganglion and sensory lateral line system. Future work will have to address if one of these subunits could fulfill the functions of P2X3.

The Expression Patterns of *p2rx* Genes Are Temporally and Spatially Regulated

Xenopus laevis p2rx genes are all expressed during embryogenesis although their expression patterns differ during frog development. Only two subunits, *p2rx4.L* and *p2rx6.L*, are maternally expressed. *P2rx4* displays the highest level of expression in egg and early embryo stages (before the MBT), which is in agreement with its expression in oocytes (Juranka et al., 2001). Based on their zygotic expression, *p2rx* subunits

can be divided into two groups: those which are not expressed in the nervous system, *p2rx2.S and p2rx5*, and those which are expressed in the nervous system, although their expression can not be restricted to this tissue. For example, *p2rx4.L*, expressed in the pineal gland, is also highly expressed in the pronephros, *p2rx2.L* transcripts, found in sensory system, are also detected in the cardiovascular system or *p2rx1.L* expression detected at high level in an interneuron population in the hindbrain is also found in the cement gland. These distinct expression profiles suggest specific functions for these receptors during embryogenesis, during the formation of neural and non-neural tissues. However, as in mouse and zebrafish embryos, *p2rx7.L* does not seem to be involved during early embryogenesis as its expression is only detected weakly at late organogenesis stages (Kucenas et al., 2003; Appelbaum et al., 2007; MGI website). The absence of gross phenotype at birth of null P2X7 mice is in agreement with this result (Solle et al., 2001), although its activity has been reported, *in vitro*, as essential for mouse embryonic stem cells survival (Thompson et al., 2012).

Conserved Expression Domains in Mesodermic Derivatives

Several *p2rx subunits* display specific and almost restricted expression profile in two mesodermic derivatives, the kidney and somites. These expression patterns have been conserved during evolution. Our data demonstrate that *p2xr5* subunit is highly expressed in the somitic tissues. In rat and chick embryos, P2X5 is the earliest P2X receptors expressed in somites (Meyer et al., 1999; Ruppelt et al., 2001; Ryten et al., 2001). Somitic expression of this subunit has also been reported in zebrafish (Kucenas et al., 2003). *In vitro* studies demonstrated that P2X5 is involved in myogenesis and muscle progenitor cells (satellite cells) differentiation (Ryten et al., 2002; Araya et al., 2004; Martinello et al., 2011). Its possible implication during muscle regeneration makes this receptor a therapeutic target for musculoskeletal pathologies (Ryten et al., 2004; Burnstock et al., 2013). In rat, P2X2 and P2X6 are also expressed in developing skeletal muscles (Ryten et al., 2001). We observed *p2rx2.L and p2xr6.L* expression in *Xenopus* somites, although their transcripts are only detected at a low level compared to *p2rx5* somitic expression level. This suggests that P2X5 may be the major P2 receptor regulating somitogenesis. The easiness of *Xenopus* as an *in vivo* model for myogenesis makes this vertebrate embryo an ideal model to apprehend the functional roles of P2X5 during myogenesis (Sabillo et al., 2016).

P2rx4.L and p2rx2.S are both expressed at high level in the embryonic functional kidney, the pronephros, but in different regions: p2rx2.S is expressed in the glomus, the filtration unit, whereas *p2rx4* is expressed in the proximal tubules. No *p2rx* transcripts were detected in the distal pronephric region, e.g., the distal, and connecting tubules. In the rat metanephros, P2X2 is found in the glomerulus and collecting duct where it may be involved in ATP inhibitory effects on AVP-induced water permeability (Burnstock et al., 2014). In mammalian metanephros P2RX4 is one of the major P2X receptors and its expression is found along the entire nephron (glomerulus, proximal tubules, descending and ascending limb of Henle, distal tubules, and collecting duct) (reviewed in Bailey et al., 2000; Burnstock et al., 2014; Menzies et al., 2017). P2X4 and P2X4/6 receptors are involved in diverse physiological renal processes, depending on its nephron localization and but also in renal pathology, such as diabetic nephropathy (Chen et al., 2013; Menzies et al., 2017). Several evidence suggest that P2X4 may form complexes with P2X7 in the metanephros (Craigie et al., 2013) but we failed to detect any *p2rx6* or *p2xr7* expression in the developing amphibian pronephros, suggesting no renal hetero-oligomerization between P2X4 and these receptors in *Xenopus*. As in mammals, the *Xenopus* kidney is one of the major sites of expression of the purinergic receptors and ectonucleotidases. We previously published the renal expression of the ectonucleotidases entpdase 5 and enpp2, enpp4, enpp6 (Massé et al., 2010, 2006). Due to its simple structural organization, composed of a single enormous nephron, *Xenopus* pronephros may be an ideal model to address the functions of the P2X receptors and the purinergic signaling during kidney formation, renal physiology but also pathophysiology (Lienkamp, 2016; Krneta-Stankic et al., 2017).

Function During the Development of Central and Peripheral Nervous System

The developing nervous system is the major site of expression of the *p2rx* genes, with 7 out of the 9 genes displaying an expression in the central or peripheral nervous system. Surprisingly, only the expression of *p2rx1.S* was detected by *in situ* hybridization at stage neurula in developing nervous system, although *p2rx2.L, p2rx2.S* transcripts were amplified during neurulation by RT-PCR, a more sensitive technique, suggesting they may also be involved in neural tube formation. Little information is available regarding *p2rx* expression at neurula stages in other vertebrate models, although P2X3 seems to be the earliest subunit expressed during central nervous system formation (Massé and Dale, 2012; Burnstock and Dale, 2015). Developing central nervous system is a major site of expression of the *p2rx* genes, with 5 out of the 9 expressed in this tissue displaying diffuse and/or weak expresssion, for example *p2rx7.L,* or specific and strong expression. Such discrete domains are the pineal gland that expresses *p2rx4.L* or the subset of hindbrain neurons labeled with the *p2rx1.L* antisense probe. The ventral localization of these neurons suggests they might be a subset of interneurons or motor neurons (Thélie et al., 2015).

Several *p2xr* subunits are expressed in the cranial sensory peripheral nervous system at later organogenesis stages after the neurogenic placode differentiation (Schlosser and Northcutt, 2000). P2rx2.L is expressed in trigeminal ganglia. *p2rx1.S, p2rx2.S,* and *p2rx6.L are* expressed in *Xenopus* ganglia of the anterodorsal, anteroventral and middle lateral line nerves, which are mechanosensory organs, composed of mechanoreceptive neuromasts involved in the detection of water displacements and current and electric fields (Shelton, 1971; Winklbauer, 1989).

Although, p2xr3, the prototypic sensory P2X subtypes, is absent in *Xenopus laevis*, our data suggest that P2X receptors might have functional implication in sensory transmission rather than in neurogenic placode differentiation (Nakatsuka and Gu, 2006). *p2rx1.S, p2rx2.S,* and *p2rx6.L* mRNAs are colocalized into the ganglia of glossopharyngeal and middle lateral line nerves, suggesting co-expression of these subunits. Several biochemical evidences suggested the existence of P2X1/2 complexes, but still not confirmed *in vivo* (reviewed in Saul et al., 2013). However, existence of functional P2X2/6 channels and the co-expression of these two subunits in several rat neuronal populations have been demonstrated (Collo et al., 1996; King et al., 2000). Future work will need to address *in vivo* the potential oligo-heteromerization of these subunits during vertebrate neurogenesis.

Taken together, this work is a fundamental prerequisite to apprehend the developmental functions of P2X receptors during vertebrate embryogenesis. Specific gain or loss of function studies of the P2X subunits identified in this work should allow to decipher their functions during the early and late phases of the formation of the central and peripheral nervous system.

DATA AVAILABILITY

The datasets generated for this study can be found in Genbank, ID 2203640.

ETHICS STATEMENT

This study was carried out in strict accordance with the recommendations in the Guide for the Care and Use of Laboratory Animals of the European Community and approved by the ethical committee of Bordeaux.

AUTHOR CONTRIBUTIONS

CB performed the experiments, analyzed the data, and corrected the manuscript. EB-G made the figures and wrote the manuscript. KM supervised the work, analyzed the data, and wrote the manuscript.

FUNDING

This work was supported by funding from the University of Bordeaux and the CNRS.

SUPPLEMENTARY MATERIAL

The Supplementary Material for this article can be found online at: https://www.frontiersin.org/articles/10.3389/fncel.2019.00340/full#supplementary-material

REFERENCES

Altschul, S. F., Gish, W., Miller, W., Myers, E. W., and Lipman, D. J. (1990). Basic local alignment search tool. *J. Mol. Biol.* 215, 403–410. doi: 10.1016/S0022-2836(05)80360-2

Appelbaum, L., Skariah, G., Mourrain, P., and Mignot, E. (2007). Comparative expression of p2x receptors and ecto-nucleoside triphosphate diphosphohydrolase 3 in hypocretin and sensory neurons in zebrafish. *Brain Res.* 1174, 66–75. doi: 10.1016/j.brainres.2007.06.103

Araya, R., Riquelme, M. A., Brandan, E., and Sáez, J. C. (2004). The formation of skeletal muscle myotubes requires functional membrane receptors activated by extracellular ATP. *Brain Res. Brain Res. Rev.* 47, 174–188. doi: 10.1016/j.brainresrev.2004.06.003

Artimo, P., Jonnalagedda, M., Arnold, K., Baratin, D., Csardi, G., de Castro, E., et al. (2012). ExPASy: sIB bioinformatics resource portal. *Nucleic Acids Res.* 40, W597–W603. doi: 10.1093/nar/gks400

Bailey, M. A., Hillman, K. A., and Unwin, R. J. (2000). P2 receptors in the kidney. *J. Auton. Nerv. Syst.* 81, 264–270. doi: 10.1016/s0165-1838(00)00125-9

Bassez, T., Paris, J., Omilli, F., Dorel, C., and Osborne, H. B. (1990). Post-transcriptional regulation of ornithine decarboxylase in *Xenopus laevis* oocytes. *Development* 110, 955–962.

Blanchard, C., and Massé, K. (2019). "Developmental expression of ectonucleotidase and purinergic receptors detection by whole-mount *in situ* hybridization in embryos in the methods molecular biology," in *Purinergic Signaling*. Springer: Nature. doi: 10.1007/978-1-4939-9717-6_6

Boué-Grabot, E., Akimenko, M. A., and Séguéla, P. (2000a). Unique functional properties of a sensory neuronal P2X ATP-gated channel from zebrafish. *J. Neurochem.* 75, 1600–1607. doi: 10.1074/jbc.275.14.10190

Boué-Grabot, E., Archambault, V., and Séguéla, P. (2000b). A protein kinase C site highly conserved in P2X subunits controls the desensitization kinetics of P2X2 ATP-gated channels. *J. Biol. Chem.* 275, 10190–10195. doi: 10.1074/jbc.275.14.10190

Boué-Grabot, E., and Pankratov, Y. (2017). Modulation of central synapses by astrocyte-released atp and postsynaptic P2X receptors. *Neural Plast.* 2017:9454275. doi: 10.1155/2017/9454275

Breathnach, R., and Chambon, P. (1981). Organization and expression of eucaryotic split genes coding for proteins. *Annu. Rev. Biochem.* 50, 349–383. doi: 10.1146/annurev.bi.50.070181.002025

Burnstock, G. (2014). Purinergic signalling: from discovery to current developments. *Exp. Physiol.* 99, 16–34. doi: 10.1113/expphysiol.2013.071951

Burnstock, G. (2016). Purinergic mechanisms and pain. *Adv. Pharmacol.* 75, 91–137. doi: 10.1016/bs.apha.2015.09.001

Burnstock, G. (2017). Purinergic signalling and neurological diseases: an update. *CNS Neurol. Disord. Drug Targets* 16, 257–265. doi: 10.2174/1871527315666160922104848

Burnstock, G. (2018). The therapeutic potential of purinergic signalling. *Biochem. Pharmacol.* 151, 157–165. doi: 10.1016/j.bcp.2017.07.016

Burnstock, G., Arnett, T. R., and Orriss, I. R. (2013). Purinergic signalling in the musculoskeletal system. *Purinergic Signal.* 9, 541–572. doi: 10.1007/s11302-013-9381-4

Burnstock, G., and Dale, N. (2015). Purinergic signalling during development and ageing. *Purinergic Signal.* 11, 277–305. doi: 10.1007/s11302-015-9452-9

Burnstock, G., Evans, L. C., and Bailey, M. A. (2014). Purinergic signalling in the kidney in health and disease. *Purinergic Signal.* 10, 71–101. doi: 10.1007/s11302-013-9400-5

Burnstock, G., Krügel, U., Abbracchio, M. P., and Illes, P. (2011). Purinergic signalling: from normal behaviour to pathological brain function. *Prog. Neurobiol.* 95, 229–274. doi: 10.1016/j.pneurobio.2011.08.006

Chaumont, S., Jiang, L. H., Penna, A., North, R. A., and Rassendren, F. (2004). Identification of a trafficking motif involved in the stabilization and polarization of P2X receptors.: trafficking motif of P2X ATP-gated channels. *J. Biol. Chem.* 279, 29628–29638. doi: 10.1074/jbc.M403940200

Chen, K., Zhang, J., Zhang, W., Zhang, J., Yang, J., Li, K., et al. (2013). ATP-P2X4 signaling mediates NLRP3 inflammasome activation: a novel pathway

of diabetic nephropathy. *Int. J. Biochem. Cell Biol.* 45, 932–943. doi: 10.1016/j.biocel.2013.02.009

Cockayne, D. A., Hamilton, S. G., Zhu, Q. M., Dunn, P. M., Zhong, Y., Novakovic, S., et al. (2000). Urinary bladder hyporeflexia and reduced pain-related behaviour in P2X3-deficient mice. *Nature* 407, 1011–1015. doi: 10.1038/35039519

Collo, G., North, R. A., Kawashima, E., Merlo-Pich, E., Neidhart, S., Surprenant, A., et al. (1996). Cloning OF P2X5 and P2X6 receptors and the distribution and properties of an extended family of ATP-gated ion channels. *J. Neurosci.* 16, 2495–2507. doi: 10.1523/jneurosci.16-08-02495.1996

Craigie, E., Birch, R. E., Unwin, R. J., and Wildman, S. S. (2013). The relationship between P2X4 and P2X7: a physiologically important interaction? *Front. Physiol.* 4:216. doi: 10.3389/fphys.2013.00216

Del Puerto, A., Wandosell, F., and Garrido, J. J. (2013). Neuronal and glial purinergic receptors functions in neuron development and brain disease. *Front. Cell Neurosci.* 7:197. doi: 10.3389/fncel.2013.00197

Dereeper, A., Guignon, V., Blanc, G., Audic, S., Buffet, S., Chevenet, F., et al. (2008). Phylogeny.fr: robust phylogenetic analysis for the non-specialist. *Nucleic Acids Res.* 36, W465–W469. doi: 10.1093/nar/gkn180

Domercq, M., Zabala, A., and Matute, C. (2018). Purinergic receptors in multiple sclerosis pathogenesis. *Brain Res. Bull.* doi: 10.1016/j.brainresbull.2018.11.018 [Epub ahead of print].

Fumagalli, M., Lecca, D., Abbracchio, M. P., and Ceruti, S. (2017). Pathophysiological role of purines and pyrimidines in neurodevelopment: unveiling new pharmacological approaches to congenital brain diseases. *Front. Pharmacol.* 8:941. doi: 10.3389/fphar.2017.00941

Habermacher, C., Dunning, K., Chataigneau, T., and Grutter, T. (2016). Molecular structure and function of P2X receptors. *Neuropharmacology* 104, 18–30. doi: 10.1016/j.neuropharm.2015.07.032

Hellsten, U., Harland, R. M., Gilchrist, M. J., Hendrix, D., Jurka, J., Kapitonov, V., et al. (2010). The genome of the Western clawed frog *Xenopus tropicalis*. *Science* 328, 633–636. doi: 10.1126/science.1183670

Juranka, P. F., Haghighi, A. P., Gaertner, T., Cooper, E., and Morris, C. E. (2001). Molecular cloning and functional expression of *Xenopus laevis* oocyte ATP-activated P2X4 channels. *Biochim. Biophys. Acta* 1512, 111–124. doi: 10.1016/s0005-2736(01)00313-3

Kawate, T., Michel, J. C., Birdsong, W. T., and Gouaux, E. (2009). Crystal structure of the ATP-gated P2X(4) ion channel in the closed state. *Nature* 460, 592–598. doi: 10.1038/nature08198

Khakh, B. S., and North, R. A. (2006). P2X receptors as cell-surface ATP sensors in health and disease. *Nature* 442, 527–532. doi: 10.1038/nature04886

Khakh, B. S., and North, R. A. (2012). Neuromodulation by extracellular ATP and P2X receptors in the CNS. *Neuron* 76, 51–69. doi: 10.1016/j.neuron.2012.09.024

King, B. F., Townsend-Nicholson, A., Wildman, S. S., Thomas, T., Spyer, K. M., and Burnstock, G. (2000). Coexpression of rat P2X2 and P2X6 subunits in *Xenopus* oocytes. *J. Neurosci.* 20, 4871–4877.

Krneta-Stankic, V., DeLay, B. D., and Miller, R. K. (2017). *Xenopus*: leaping forward in kidney organogenesis. *Pediatr. Nephrol.* 32, 547–555. doi: 10.1007/s00467-016-3372-y

Kucenas, S., Cox, J. A., Soto, F., Lamora, A., and Voigt, M. M. (2009). Ectodermal P2X receptor function plays a pivotal role in craniofacial development of the zebrafish. *Purinergic Signal.* 5, 395–407. doi: 10.1007/s11302-009-9165-z

Kucenas, S., Li, Z., Cox, J. A., Egan, T. M., and Voigt, M. M. (2003). Molecular characterization of the zebrafish P2X receptor subunit gene family. *Neuroscience.* 121, 935–945. doi: 10.1016/s0306-4522(03)00566-9

Kucenas, S., Soto, F., Cox, J. A., and Voigt, M. M. (2006). Selective labeling of central and peripheral sensory neurons in the developing zebrafish using $P2X_3$ receptor subunit transgenes. *Neuroscience* 138, 641–652. doi: 10.1016/j.neuroscience.2005.11.058

Lienkamp, S. S. (2016). Using *Xenopus* to study genetic kidney diseases. *Semin. Cell Dev. Biol.* 51, 117–124. doi: 10.1016/j.semcdb.2016.02.002

Martinello, T., Baldoin, M. C., Morbiato, L., Paganin, M., Tarricone, E., Schiavo, G., et al. (2011). Extracellular ATP signaling during differentiation of C2C12 skeletal muscle cells: role in proliferation. *Mol. Cell. Biochem.* 351, 183–196. doi: 10.1007/s11010-011-0726-4

Massé, K., Bhamra, S., Allsop, G., Dale, N., and Jones, E. A. (2010). Ectophosphodiesterase/nucleotide phosphohydrolase (Enpp) nucleotidases: cloning, conservation and developmental restriction. *Int. J. Dev. Biol.* 54, 181–193. doi: 10.1387/ijdb.092879km

Massé, K., Bhamra, S., Eason, R., Dale, N., and Jones, E. A. (2007). Purine-mediated signalling triggers eye development. *Nature* 449, 1058–1062. doi: 10.1038/nature06189

Massé, K., and Dale, N. (2012). Purines as potential morphogens during embryonic development. *Purinergic Signal.* 8, 503–521. doi: 10.1007/s11302-012-9290-y

Massé, K., Eason, R., Bhamra, S., Dale, N., and Jones, E. A. (2006). Comparative genomic and expression analysis of the conserved NTPDase gene family in *Xenopus*. *Genomics* 87, 366–381. doi: 10.1016/j.ygeno.2005.11.003

Menzies, R. I., Tam, F. W., Unwin, R. J., and Bailey, M. A. (2017). Purinergic signaling in kidney disease. *Kidney Int.* 91, 315–323. doi: 10.1016/j.kint.2016.08.029

Meyer, M. P., Gröschel-Stewart, U., Robson, T., and Burnstock, G. (1999). Expression of two ATP-gated ion channels, $P2X_5$ and $P2X_6$, in developing chick skeletal muscle. *Dev. Dyn.* 216, 442–449. doi: 10.1002/(SICI)1097-0177(199912)216:4/5<442::AID-DVDY12>3.0.CO;2-Z

Nakatsuka, T., and Gu, J. G. (2006). P2X purinoceptors and sensory transmission. *Pflugers Arch.* 452, 598–607. doi: 10.1007/s00424-006-0057-6

Needleman, S. B., and Wunsch, C. D. (1970). A general method applicable to the search for similarities in the amino acid sequence of two proteins. *J. Mol. Biol.* 48, 443–453. doi: 10.1016/0022-2836(70)90057-4

Nieuwkoop, P. D., and Faber, J. (1994). *Normal Table of Xenopus Laevis (Daudin)*. New York, NY: Garland Publishing, Inc.

North, R. A. (2002). Molecular physiology of P2X receptors. *Physiol. Rev.* 82, 1013–1067. doi: 10.1152/physrev.00015.2002

North, R. A. (2016). P2X receptors. *Philos. Trans. R. Soc. Lond. B Biol. Sci.* 371:20150427. doi: 10.1098/rstb.2015.0427

Norton, W. H., Rohr, K. B., and Burnstock, G. (2000). Embryonic expression of a P2X(3) receptor encoding gene in zebrafish. *Mech. Dev.* 99, 149–152. doi: 10.1016/s0925-4773(00)00472-x

Oliveira, Á, Illes, P., and Ulrich, H. (2016). Purinergic receptors in embryonic and adult neurogenesis. *Neuropharmacology* 104, 272–281. doi: 10.1016/j.neuropharm.2015.10.008

Palanca, A. M., Lee, S. L., Yee, L. E., Joe-Wong, C., Trinh le, A., Hiroyasu, E., et al. (2013). New transgenic reporters identify somatosensory neuron subtypes in larval zebrafish. *Dev. Neurobiol* 73, 152–167. doi: 10.1002/dneu.22049

Paukert, M., Hidayat, S., and Gründer, S. (2002). The P2X(7) receptor from *Xenopus laevis*: formation of a large pore in *Xenopus* oocytes. *FEBS Lett.* 513, 253–258. doi: 10.1016/s0014-5793(02)02324-4

Ralevic, V., and Burnstock, G. (1998). Receptors for purines and pyrimidines. *Pharmacol. Rev.* 50, 413–492.

Rodrigues, R. J., Marques, J. M., and Cunha, R. A. (2018). Purinergic signalling and brain development. *Semin. Cell Dev. Biol.* doi: 10.1016/j.semcdb.2018.12.001 [Epub ahead of print].

Ruppelt, A., Ma, W., Borchardt, K., Silberberg, S. D., and Soto, F. (2001). Genomic structure, developmental distribution and functional properties of the chicken $P2X_5$ receptor. *J. Neurochem.* 77, 1256–1265. doi: 10.1046/j.1471-4159.2001.00348.x

Ryten, M., Dunn, P. M., Neary, J. T., and Burnstock, G. (2002). ATP regulates the differentiation of mammalian skeletal muscle by activation of a P2X5 receptor on satellite cells. *J. Cell Biol.* 158, 345–355. doi: 10.1083/jcb.200202025

Ryten, M., Hoebertz, A., and Burnstock, G. (2001). Sequential expression of three receptor subtypes for extracellular ATP in developing rat skeletal muscle. *Dev. Dyn.* 221, 331–341. doi: 10.1002/dvdy.1147

Ryten, M., Yang, S. Y., Dunn, P. M., Goldspink, G., and Burnstock, G. (2004). Purinoceptor expression in regenerating skeletal muscle in the mdx mouse model of muscular dystrophy and in satellite cell cultures. *FASEB J.* 18, 1404–1406. doi: 10.1096/fj.03-1175fje

Sabillo, A., Ramirez, J., and Domingo, C. R. (2016). Making muscle: morphogenetic movements and molecular mechanisms of myogenesis in *Xenopus laevis*. *Semin. Cell Dev. Biol* . 51, 80–91. doi: 10.1016/j.semcdb.2016.02.006

Sater, A. K., and Moody, S. A. (2017). Using *Xenopus* to understand human disease and developmental disorders. *Genesis* 55:e22997. doi: 10.1002/dvg.22997

Saul, A., Hausmann, R., Kless, A., and Nicke, A. (2013). Heteromeric assembly of P2X subunits. *Front. Cell. Neurosci.* 7:250. doi: 10.3389/fncel.2013.00250

Schlosser, G., and Northcutt, R. G. (2000). Development of neurogenic placodes in *Xenopus laevis*. *J. Comp. Neurol.* 418, 121–146. doi: 10.1002/(SICI)1096-9861(20000306)418:2<121::AID-CNE1>3.0.CO;2-M

Session, A. M., Uno, Y., Kwon, T., Chapman, J. A., Toyoda, A., Takahashi, S., et al. (2016). Genome evolution in the allotetraploid frog *Xenopus laevis*. *Nature* 538, 336–343. doi: 10.1038/nature19840

Shelton, P. M. (1971). The structure and function of the lateral line system in larval *Xenopus laevis*. *J. Exp. Zool.* 178, 211–231. doi: 10.1002/jez.1401780207

Solle, M., Labasi, J., Perregaux, D. G., Stam, E., Petrushova, N., Koller, B. H., et al. (2001). Altered cytokine production in mice lacking P2X(7) receptors. *J. Biol. Chem.* 276, 125–132. doi: 10.1074/jbc.M006781200

Souslova, V., Cesare, P., Ding, Y., Akopian, A. N., Stanfa, L., Suzuki, R., et al. (2000). Warm-coding deficits and aberrant inflammatory pain in mice lacking P2X3 receptors. *Nature* 407, 1015–1017. doi: 10.1038/35039526

Tandon, P., Conlon, F., Furlow, J. D., and Horb, M. E. (2017). Expanding the genetic toolkit in *Xenopus*: approaches and opportunities for human disease modeling. *Dev. Biol.* 426, 325–335. doi: 10.1016/j.ydbio.2016.04.009

Thélie, A., Desiderio, S., Hanotel, J., Quigley, I., Van Driessche, B., Rodari, A., et al. (2015). Prdm12 specifies V1 interneurons through cross-repressive interactions with Dbx1 and Nkx6 genes in *Xenopus*. *Development* 142, 3416–3428. doi: 10.1242/dev.121871

Thompson, B. A., Storm, M. P., Hewinson, J., Hogg, S., Welham, M. J., and MacKenzie, A. B. (2012). A novel role for P2X7 receptor signalling in the survival of mouse embryonic stem cells. *Cell. Signal.* 24, 770–778. doi: 10.1016/j.cellsig.2011.11.012

Thompson, J. D., Higgins, D. G., and Gibson, T. J. (1994). CLUSTAL W: improving the sensitivity of progressive multiple sequence alignment through sequences weighting, position-specific gap penalties and weight matrix choice. *Nucleic Acids Res.* 22, 4673–4680. doi: 10.1093/nar/22.22.4673

Tocco, A., Pinson, B., Thiébaud, P., Thézé, N., and Massé, K. (2015). Comparative genomic and expression analysis of the adenosine signaling pathway members in *Xenopus*. *Purinergic Signal.* 11, 59–77. doi: 10.1007/s11302-014-9431-6

Vulchanova, L., Riedl, M. S., Shuster, S. J., Buell, G., Surprenant, A., North, R. A., et al. (1997). Immunohistochemical study of the P2X2 and P2X3 receptor subunits in rat and monkey sensory neurons and their central terminals. *Neuropharmacology* 36, 1229–1242. doi: 10.1016/s0028-3908(97)00126-3

Winklbauer, R. (1989). Development of the lateral line system in *Xenopus*. *Prog. Neurobiol.* 32, 181–206. doi: 10.1016/0301-0082(89)90016-6

Xiang, Z., Bo, X., and Burnstock, G. (1998). Localization of ATP-gated P2X receptor immunoreactivity in rat sensory and sympathetic ganglia. *Neurosci. Lett.* 256, 105–108. doi: 10.1016/s0304-3940(98)00774-5

Yegutkin, G. G. (2014). Enzymes involved in metabolism of extracellular nucleotides and nucleosides: functional implications and measurement of activities. *Crit. Rev. Biochem. Mol. Biol.* 49, 473–497. doi: 10.3109/10409238.2014.953627

Conflict of Interest Statement: The authors declare that the research was conducted in the absence of any commercial or financial relationships that could be construed as a potential conflict of interest.

frontiers in Molecular Neuroscience

REVIEW
published: 07 August 2019
doi: 10.3389/fnmol.2019.00183

P2X7 Interactions and Signaling – Making Head or Tail of It

Robin Kopp†, Anna Krautloher*†, Antonio Ramírez-Fernández and Annette Nicke**

Walther Straub Institute of Pharmacology and Toxicology, Faculty of Medicine, LMU Munich, Munich, Germany

Extracellular adenine nucleotides play important roles in cell–cell communication and tissue homeostasis. High concentrations of extracellular ATP released by dying cells are sensed as a danger signal by the P2X7 receptor, a non-specific cation channel. Studies in P2X7 knockout mice and numerous disease models have demonstrated an important role of this receptor in inflammatory processes. P2X7 activation has been shown to induce a variety of cellular responses that are not usually associated with ion channel function, for example changes in the plasma membrane composition and morphology, ectodomain shedding, activation of lipases, kinases, and transcription factors, as well as cytokine release and apoptosis. In contrast to all other P2X family members, the P2X7 receptor contains a long intracellular C-terminus that constitutes 40% of the whole protein and is considered essential for most of these effects. So far, over 50 different proteins have been identified to physically interact with the P2X7 receptor. However, few of these interactions have been confirmed in independent studies and for the majority of these proteins, the interaction domains and the physiological consequences of the interactions are only poorly described. Also, while the structure of the P2X7 extracellular domain has recently been resolved, information about the organization and structure of its C-terminal tail remains elusive. After shortly describing the structure and assembly of the P2X7 receptor, this review gives an update of the identified or proposed interaction domains within the P2X7 C-terminus, describes signaling pathways in which this receptor has been involved, and provides an overlook of the identified interaction partners.

Keywords: C-terminus, protein-protein interaction (PPI), signaling/signaling pathways, P2X7 (purino) receptor, network

OPEN ACCESS

Edited by:
Eric Boué-Grabot, Université de Bordeaux, France

Reviewed by:
Hana Zemkova, Institute of Physiology (ASCR), Czechia
Toshi Kawate, Cornell University, United States

****Correspondence:***
Robin Kopp
Robin.Stocklauser@lrz.uni-muenchen.de
Anna Krautloher
a.krautloher@lrz.uni-muenchen.de
Annette Nicke
annette.nicke@lrz.uni-muenchen.de

† These authors have contributed equally to this work

Received: *31 May 2019*
Accepted: *11 July 2019*
Published: *07 August 2019*

Citation:
Kopp R, Krautloher A, Ramírez-Fernández A and Nicke A (2019) P2X7 Interactions and Signaling – Making Head or Tail of It. Front. Mol. Neurosci. 12:183. doi: 10.3389/fnmol.2019.00183

INTRODUCTION

The ATP-gated P2X receptors are trimeric ion channels with inter-subunit ATP-binding sites (Kaczmarek-Hájek et al., 2012). In contrast to most other ion channel families, six of the seven cloned subunits can form functional homomeric receptors but heteromeric receptors have also been identified, for example P2X2/3 and P2X1/5 receptors (Saul et al., 2013). A single P2X subunit has been structurally compared to a dolphin (**Figure 1A**) and contains two α-helical transmembrane domains (fluke) that are linked by a large extracellular domain [269–288 amino acids (aa) long] that is mostly formed by β-sheets (body) and several loop domains (head, dorsal fin, and flippers) (Kawate et al., 2009). The intracellular N- and C- termini are less conserved than the rest of the protein. The N-termini are 20–45 aa long, while the intracellular C-termini are more variable

in length with 29–87 aa for most subunits. P2X2, and in particular P2X7 contain considerably longer C-termini of 113/125 (human/mouse) and 240 aa, respectively. Human P2X5 and P2X6 have C-terminal sequences of 82 and 87 aa, respectively. Only in case of the ATP-bound open state of the human P2X3 receptor, a structure of these intracellular domains has been obtained so far (Mansoor et al., 2016). In this ATP-bound structure, the N- and C-termini form a network of three β-sheets (each formed by the C-terminus of one subunit and the N-termini of the two neighboring subunits) that is capping the cytoplasmic side of the pore. The termini appear to be disordered and flexible in the apo state.

The P2X7 receptor differs not only structurally but also functionally from all other P2X subtypes. In comparison, it has 10 to 100-fold reduced ATP sensitivity, suggesting that it functions as a "danger signal" detector for high ATP concentrations that are released at sites of tissue damage (Linden et al., 2019). A P2X7 splice variant (P2X7k) has been identified in rodents but not in humans, that can also be activated by extracellular nicotinamide adenine dinucleotide (NAD) via covalent enzymatic modification (ADP ribosylation) (Schwarz et al., 2012; Xu et al., 2012). The P2X7k variant also shows a higher ATP sensitivity.

Also, unlike other ion channels, P2X7 activation does not only open a non-selective cation channel, but in addition mediates a membrane permeability increase by forming a so-called "macropore" that can reach a diameter of 8.5 Å and allows the passage of large molecules such as the fluorescent dyes ethidium and YO-PRO1 (Di Virgilio et al., 2018b). P2X7 activation furthermore initiates a variety of signaling cascades that trigger caspase activation and cytokine release, plasma membrane reorganization, ectodomain shedding, and cell death to only name a few. Some of these effects are likely consequences of P2X7-dependent Ca^{2+} influx and/or K^{+} efflux, although a detailed description of the molecular interactions and signaling complexes involved is generally lacking. The C-terminus appears to be required for most of these effects and probably plays a role in positioning of the receptor in membrane microdomains (e.g., lipid rafts (Murrell-Lagnado, 2017) and/or signaling complexes (Kim et al., 2001)) that allow efficient signaling and/or direct interaction with signaling molecules.

It has to be mentioned, that considerable differences exist in the pharmacology of rat, mouse, and human P2X7 (Donnelly-Roberts et al., 2009). For example, at the rat isoform ATP and BzATP were 8 and 70 times more potent than at the mouse isoform and 10 and 25 times more potent than at the human isoform, respectively. While this could be attributed to single aa differences in the ligand-binding ectodomain of rat and mouse P2X7 (Young et al., 2007), a positive effect of the intracellular C-terminus on BzATP potency was shown in P2X7 chimeras, in which the human P2X7 C-terminus was replaced by the respective rat sequence (Rassendren et al., 1997). Likewise, sensitivity to divalent cations, dye-uptake efficiency and selectivity, and current kinetics largely differ between human and rodent isoforms and also between different cell types (Rassendren et al., 1997; Hibell et al., 2001; Janks et al., 2019) with the human and mouse isoforms being less efficient in dye uptake. However, despite these differences, the principal effects of P2X7 activation, such as dye uptake, interleukine-1β (IL-1β) release, phosphatidylserine-flip (PS)-flip, and blebbing appear to be present in all isoforms. Nevertheless, a systematic comparison is urgently needed.

P2X7 receptors are highly expressed in immune cells (in particular macrophages, T-cells, mast cells, and microglia), epithelial cells, oligodendrocytes of the CNS, and Schwann cells of the PNS (Di Virgilio et al., 2018a; Kaczmarek-Hájek et al., 2018). Their presence in neurons is more controversial (Illes et al., 2017; Miras-Portugal et al., 2017). Numerous studies describe P2X7 expression and function in astrocytes (Ballerini et al., 1996; Duan et al., 2003; Narcisse et al., 2005; Sperlagh et al., 2006; Norenberg et al., 2010; Oliveira et al., 2011; Sperlagh and Illes, 2014) while there is also contradictory evidence (Jabs et al., 2007). Thus, P2X7 detection in these cell types might depend on factors such as the species, tissue, model system, and activation state, or disease phase that is investigated. Furthermore, interpretation of findings depends on the sensitivity and/or specificity of the detection methods, as specificity of the most widely used antagonists (oxidized ATP and brilliant blue G) and the available P2X7 antibodies is questionable and proper control experiments (for example using P2X7 knockout animals) need to be performed (Sim et al., 2004; Anderson and Nedergaard, 2006).

The best-investigated and most widely accepted P2X7 functions are its roles in inflammation and immune signaling. Blockade or genetic ablation of the P2X7 receptor has early confirmed, that it is a major trigger of processing and release of pro-inflammatory IL-1β and resulted in amelioration of disease parameters in various experimental models ranging from inflammatory processes induced by infection, allograft rejection, and autoimmune diseases to numerous models of tissue or organ damage as well as various neurological diseases (Burnstock and Knight, 2018; Savio et al., 2018). In addition to its role in immune function and inflammation, which is often associated with the deleterious effects of its activation, P2X7 has also been shown to exert trophic roles, for example in microglia (Monif et al., 2009) or different cancer cells (Orioli et al., 2017). In humans, a truncated splice variant was identified that lacks the C-terminus and appears to serve mainly trophic functions (Adinolfi et al., 2010). In the following, we will provide an overview of the direct and indirect protein interactions and signaling pathways in which P2X7 has most commonly been involved.

INTERACTION OF THE P2X7 RECEPTOR WITH THE P2X4 RECEPTOR

Within the P2X receptor family, P2X4 shows the highest sequence similarity to P2X7 (47% amino acid identity of the human isoforms). The *P2rx4* gene is located just downstream of the *P2rx7* gene and they are thought to have originated from the same gene by gene duplication (Dubyak, 2007; Hou and Cao, 2016). Both subtypes show a widely overlapping expression pattern, in particular in immune cells and epithelial cells (Guo et al., 2007; Kaczmarek-Hájek et al., 2012), and have been linked to similar physiological and pathophysiological functions in inflammatory

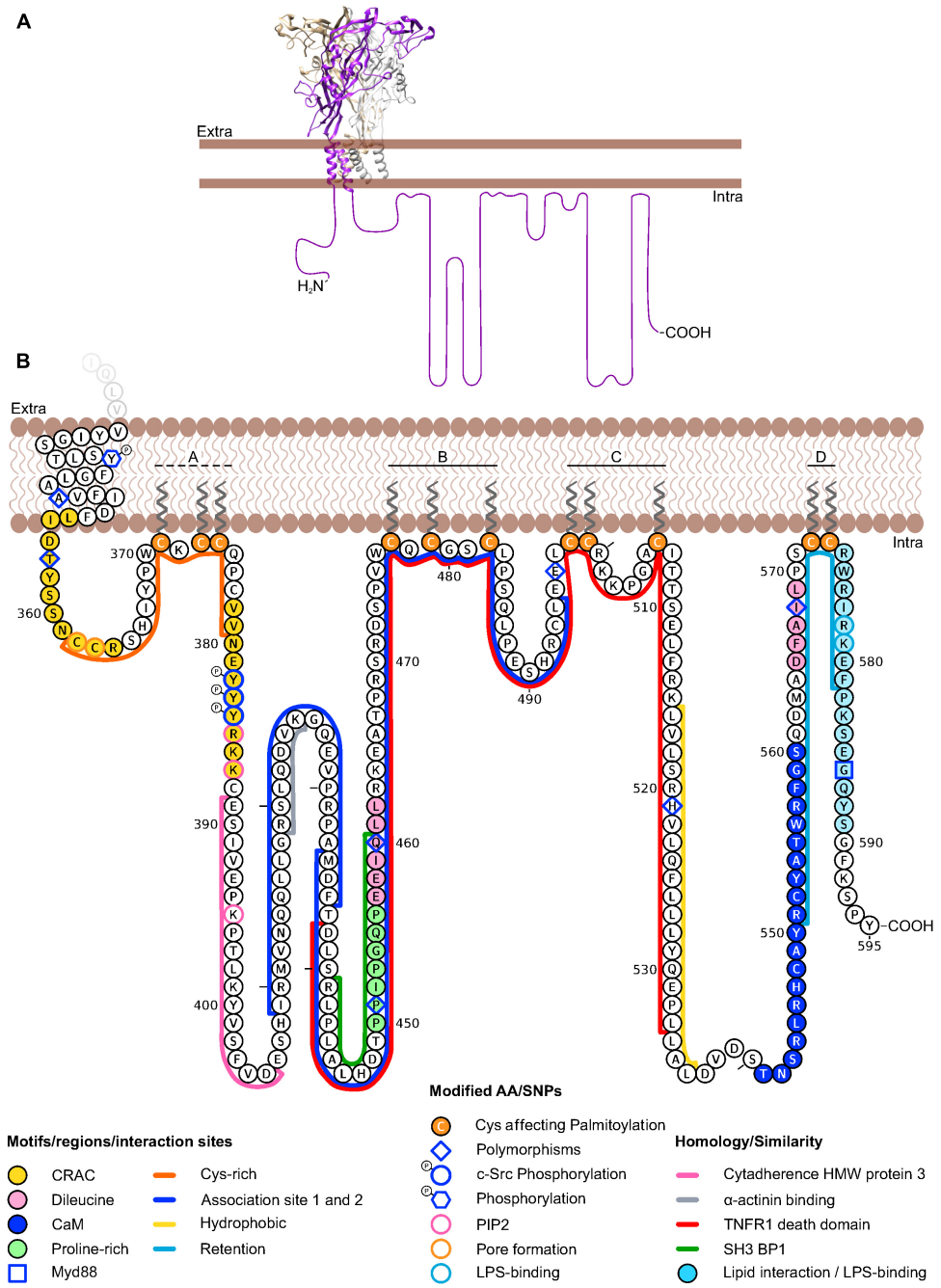

FIGURE 1 | Schematic representation of the human P2X7 receptor depicting details of its intracellular C-terminus. **(A)** Homology model (https://swissmodel.expasy.org/) based on the crystal structure of the panda P2X7 in the closed, apo state (PDB ID: 5U1L) is shown with the three P2X7 subunits represented in gray, brown, and purple. Note the dolphin-shaped structure of a single subunit with the transmembrane regions representing the fluke. The structure of the intracellular C-terminus has not been determined. The estimated length of one unfolded C-terminus is represented in scale to the crystallized domains. **(B)** Amino acid sequence of the human P2X7 intracellular C-terminus representing individual amino acid residues and domains discussed in the text. Note that some of the motifs/domains are putative and species variations are not considered. Groups of palmitoylated cysteines (A–D) according are shown. A dashed line indicates partial palmitoylation (Gonnord et al., 2008). The aa sequence was drawn with Protter and manually modified: http://wlab.ethz.ch/protter/ (Omasits et al., 2014).

processes, such as reactive oxygen species (ROS) production and the secretion of mature IL-1β and IL-18 through the activation of the NLRP3 inflammasome (Babelova et al., 2009; Kawano et al., 2012; Hung et al., 2013). For example, P2X4 was shown to affect the P2X7-mediated maturation and release of IL-1β, (Pérez-Flores et al., 2015) and a rapid initial P2X4-mediated Ca^{2+} influx was suggested to initiate this cascade (Sakaki et al., 2013). Both receptors have also been involved in phagosome

function (Qureshi et al., 2007; Kuehnel et al., 2009), autophagy, macrophage death (Kawano et al., 2012), as well as autocrine and paracrine activation of T cells via ATP-induced Ca^{2+} influx (Schenk et al., 2008; Yip et al., 2009; Woehrle et al., 2010; Manohar et al., 2012; Wang et al., 2014).

While heteromerisation of both subunits in trimeric complexes (Guo et al., 2007) was not confirmed (Torres et al., 1999; Nicke, 2008; Boumechache et al., 2009; Antonio et al., 2011), a number of studies provide evidence in favor of a direct physical association of both receptor types and/or a mutual functional interaction between both subtypes. Thus, both subunits could be co-immunoprecipitated from transfected cells, as well as various cell lines and primary cells (Guo et al., 2007; Boumechache et al., 2009; Weinhold et al., 2010; Hung et al., 2013; Pérez-Flores et al., 2015) and FRET studies on *Xenopus laevis* oocyte- and HEK293 cell-expressed subunits support a close association or heteromerisation (Pérez-Flores et al., 2015; Schneider et al., 2017). A close proximity within transfected HEK293 cells was also shown by *in situ* proximity ligation assays (Antonio et al., 2011). Functional evidence for an interaction was described in native and recombinant mammalian cells (Ma et al., 2006; Guo et al., 2007; Casas-Pruneda et al., 2009; Kawano et al., 2012; Pérez-Flores et al., 2015) but not in a more recent study (Schneider et al., 2017) in *Xenopus laevis* oocytes. Finally, a mutual interrelation between P2X4 and P2X7 mRNA and protein expression levels was described in kidney, E10 alveolar epithelial cells, and bone marrow derived dendritic cells (Weinhold et al., 2010; Craigie et al., 2013; Zech et al., 2016). To evaluate these results, it has to be considered, however, that the P2X4 subtype is mostly found intracellularly and co-localized with lysosomal markers (Bobanovic et al., 2002; Guo et al., 2007; Qureshi et al., 2007), whereas P2X7 is generally localized at the plasma membrane. Nonetheless, upon stimulation of the respective cells [e.g., via lipopolysacharide (LPS), CCL2/12 or ionomycin] an increased fraction of P2X4 receptors was found at the cell surface (Qureshi et al., 2007; Boumechache et al., 2009; Toulme et al., 2010; Toyomitsu et al., 2012).

STRUCTURE OF THE P2X7 C-TERMINUS AND ITS INVOLVEMENT IN P2X7 SIGNALING

The P2X7 C-terminus constitutes about 40% of the whole P2X7 protein (**Figure 1**) and amino acid sequence identity between rat, mouse, and human C-termini is 80%. Except for the domains described below, the so-called P2X7-tail shows no sequence homology to other proteins. It is supposed to be localized intracellularly, but contains a lipophilic stretch of 21 aa (residues 516–536 in human P2X7) that would be long enough to form another transmembrane domain or reentry loop. Deletion or truncation of the majority of this intracellular tail prevents P2X7-mediated effects such as dye uptake (Surprenant et al., 1996) and plasma membrane blebbing (Wilson et al., 2002), and alters channel kinetics (Becker et al., 2008), but does not impair cell surface expression or ion channel function (Smart et al., 2003; Becker et al., 2008). In the following, we will shortly explain the current understanding of P2X7 pore formation and then describe identified domains and motifs within the P2X7 tail, starting from the very terminus toward the second TM domain.

Pore Formation

A hallmark feature of P2X7 activation is the formation of a non-selective macropore. Both, naturally occurring splice variants of P2X7 and *in vitro* experiments with C-terminally truncated P2X7 receptors demonstrated that this property requires the C-terminus (Surprenant et al., 1996; Adinolfi et al., 2010). Basically two mechanisms of pore formation were discussed: According to the "pore dilation" hypothesis, pore formation is an intrinsic channel property and the consequence of a permeability increase from an initially cation selective channel to a non-selective pore. Alternatively, direct or indirect interaction with other pore forming proteins was suggested, with the large transmembrane channel Pannexin 1 (Panx1) representing the most prominent candidate (Pelegrin and Surprenant, 2006) (see below). Noteworthy, permeability to larger molecules like YO-PRO-1 or *N*-methyl-D-glucamine (NMDG) was also observed for P2X2 and P2X4 family members (Khakh et al., 1999; Virginio et al., 1999). However, at least for the P2X2 receptor this property appeared intrinsic to the receptor (Khakh and Egan, 2005; Chaumont and Khakh, 2008) and it was later shown that the time-dependent shift in the reversal potential of extracellular NMDG, that was generally interpreted as an increase in pore diameter, can also be the result of changes in intracellular ion concentration during whole-cell patch-clamp recordings (Li et al., 2015). While the mechanism of pore formation in P2X7 has been a long-standing debate (excellently reviewed in Di Virgilio et al., 2018b), more recent electrophysiological, photochemical, and biochemical experiments indicate that the pathway for larger molecules like NMDG or spermidine is also intrinsic to the P2X7 receptor and, similar to P2X2 (Li et al., 2015), the P2X7 channel is upon activation immediately permeable to both, small cations and large molecules (Riedel et al., 2007; Browne et al., 2013; Harkat et al., 2017; Karasawa et al., 2017; Pippel et al., 2017). Whether a P2X7-activated pathway for large anions that is observed in some cell types is also intrinsic to the P2X7 protein or mediated by a separate channel or pore, remains to be determined (Ugur and Ugur, 2019).

Trafficking and Lipid Interaction Domains (∼Residues 540–595)

In the search for domains in the P2X7 C-terminus that control P2X7 channel function, pore forming properties, and plasma membrane expression, truncated P2X7 versions were investigated (Smart et al., 2003) and it was found that 95% (i.e., the sequence up to residue 581) of the rat P2X7 C-terminus are required to mediate ethidium uptake in HEK293 cells. Truncations between aa 551–581 as well as some single point mutations (C572G, R574G, or F581G) in this region resulted in a loss of surface expression. Upon further truncation (residues 380–550), the ion channel but not the pore activity was regained. Thus it was suggested, that amino acid residues 551–581 contain a *retention motif* that is generally masked but becomes exposed

by truncations or single point mutations in this region and then inhibits surface expression. In support of a role of this region in receptor trafficking, the loss-of-function polymorphism I568N in this region of the human P2X7 was also found to inhibit cell surface expression (Wiley et al., 2003).

The supposed retention/retrieval region overlaps with a *lipid interaction or putative LPS-binding motif* (residues 574–589) that is homologous to the LPS binding domains of LPS-binding protein (LBP 44% identity) and bactericidal permeability-increasing protein (BPI 31% identity) and was shown to bind LPS *in vitro* (Denlinger et al., 2001). Both surface expression and LPS binding were abolished when the basic residues R578 and K579 were mutated in human P2X7 (Denlinger et al., 2003). LBP and BPI are pattern recognition proteins that, upon LPS-binding, can stimulate a defensive host response to gram-negative bacteria, although in different ways: LBP is a plasma protein, that increases the host cell's sensitivity to endotoxins by disaggregating, transporting, and binding LPS to other LPS-binding proteins, such as the pattern recognition receptor CD14. CD14 is a glycosylphosphatidylinositol (GPI)-anchored receptor that acts as a co-receptor for the toll-like receptor (TLR) 4 complex (Ranoa et al., 2013). Upon LPS binding, TLR4 induces via the adaptor protein myeloid differentiation primary-response protein 88 (MyD88) and the transcription factor NF-κB cytokine production. Interestingly, the very C-terminus of mouse P2X7, in particular G586 was described to directly interact with MyD88 (Liu et al., 2011) (see also Section "Proteins Involved in P2X7-Mediated Interleukin Secretion").

The soluble BPI has anti-endotoxin and direct bactericidal properties against gram-negative bacteria and can neutralize LPS, thereby inhibiting LPS-triggered cytokine production and an overshooting immune response (Weiss, 2003). Cytosolic LPS, experimentally delivered by cholera toxin B or by transfection of mouse bone marrow-derived macrophages, was shown to decrease the threshold for ATP-induced P2X7-associated pore opening, supposedly by allosteric modulation via the putative LPS binding motif in the P2X7 C-terminus (Yang et al., 2015). Internalization of LPS is facilitated by CD14. Accordingly, the presence of CD14 resulted in an increased co-localization of LPS and P2X7 in transfected HEK293 cells. A direct interaction between P2X7 and CD14 was also reported (Dagvadorj et al., 2015) (see also Section "Proteins Involved in P2X7-Mediated Interleukin Secretion").

Signaling requires the spatial organization (co-localization or sequestration) of its components in subcellular environments for example by protein scaffolds or membrane domains. The lipid interaction motif in P2X7 was not only suggested to serve as a binding domain for LPS, but also for phospholipids and thereby modulating the receptor's localization (Denlinger et al., 2001), for example in lipid rafts. An association between P2X7 and lipid rafts was found in T-cells, where P2X7 is ADP-ribosylated by ART2.2 (Bannas et al., 2005), in mouse lung alveolar epithelial cells (Barth et al., 2007), and in rat submandibular gland cells. In the latter, a lipid-raft pool and a non-raft fraction of P2X7 receptors were described that couple to different signaling pathways (Garcia-Marcos et al., 2006a). This would be in accordance with studies, showing that P2X7 modulates phospholipase A2, C, and D (el-Moatassim and Dubyak, 1992; Hung and Sun, 2002; Garcia-Marcos et al., 2006b; El Ouaaliti et al., 2012) (see also Section "P2X7 – Mediated Lipase Activation and Lipid Interactions"). Also functional regulation of P2X7 by phosphatidylinositol 4,5-bisphosphate (PIP2) was shown in patch-clamp experiments with *Xenopus laevis* oocytes. Although no direct binding of the P2X7 C-terminus and PIP2 could be observed, residues R385, K387 and K395 of the human P2X7 receptor were shown to be important for the interaction with PIP2 (Zhao et al., 2007).

Just upstream of the LPS binding motif, Gonnord et al. (2008) identified two *palmitoylated cysteine residues* (C572, C573) in mouse P2X7 that were essential for P2X7 surface trafficking. Likewise, two more proximal groups of cysteine residues (C477, C479, C482 and C498, C499, C506) were palmitoylated and required for surface expression. Mutation of the juxtamembrane cysteine residues C371, C373, and C374, however, showed only a 50% decrease in palmitoylation and reduced surface localization (Gonnord et al., 2008). Palmitoylation is a reversible posttranslational modification that increases membrane association and can also affect function, stability, and subcellular trafficking of proteins into membrane compartments, as for example the cholesterol- and sphingolipid-enriched lipid rafts.

Interestingly, the permeability of the P2X7 appears to depend not solely on the C-terminus, but also on the lipid composition of the cell membrane (Karasawa et al., 2017). In *in vitro* experiments with purified truncated panda P2X7 in artificial liposomes, phosphatidylglycerol and sphingomyelin facilitated YO-PRO-1 permeation, whereas cholesterol had an inhibitory effect. It was concluded that the palmitoylated cysteine residues in full-length receptors prevent the inhibitory effect of cholesterol by shielding the TM domains, while in C-terminally truncated P2X7, cholesterol can interact with the transmembrane helices and thereby limits its permeability. Thus, the pore forming properties of the P2X7 could be influenced by modulation of the membrane composition and may be cell-type specific (Di Virgilio et al., 2018b).

An unusual Ca^{2+}-dependent *calmodulin (CaM) binding motif* was functionally and biochemically identified in HEK293 cell-expressed rat P2X7 [residues I541-S560, Roger et al., 2008). In this sequence ([I-x(3)-L-x(10)-W]), key bulky amino acid residues form a 1-5-16 motif. CaM is a calcium sensor that modulates the function of a wide variety of enzymes and ion channels, but can also act as an adaptor, interacting with other target proteins (Villalobo et al., 2018). CaM binding to P2X7 was found to facilitate currents and blebbing. In human P2X7, both the CaM binding motif and current facilitation were not detected, but could be reconstituted by replacement of critical residues (T541I, C552S, and G559V) (Roger et al., 2010). P2X7 signaling via Ca^{2+}calmodulin-dependent kinase II (CaMKII) was also shown (Diaz-Hernandez et al., 2008; Gomez-Villafuertes et al., 2009).

The Death Domain (∼Residues 430–530)

Based on comparative sequence analysis, residues 438–533 of the human P2X7 were found to be similar (20% identity, 50% conservation) to the *death domain (DD)* of the human tumor

necrosis factor receptor 1 (TNFR1) (Denlinger et al., 2001). The DD is a subclass of protein motifs known as the death fold. It is a protein interaction domain that is contained in numerous proteins and enables them to oligomerize. Many DD-containing proteins are involved in apoptosis and inflammation.

Within the postulated P2X7 DD homology domain, a *proline-rich region* (residues 450–456) contains two overlapping PxxP motifs and may represent a canonical binding site for *cellular sarcoma tyrosine kinase (c-Src) homology 3 (SH3) domains* (Watters et al., 2001). An alignment (ClustalW) between the human SH3-domain binding protein 1 (Q9Y3L3) and residues 441–460 of the human P2X7 receptor shows a 40% sequence identity, in agreement with (Denlinger et al., 2001). SH3 domains are approximately 60 aa long modules that mediate protein interactions and are involved in various intracellular signaling pathways. They recognize *proline-rich regions* containing the PxxP motif (Kurochkina and Guha, 2013) and are present in phospholipases, tyrosine kinases and other signaling proteins (Kaneko et al., 2008). The interaction between the scaffolding protein MAGuK and the P2X7 receptor was suggested to be mediated via SH3 domains, but evidence is lacking (Kim et al., 2001).

There are also two sequences (457–462 and 565–569) with similarities to *a dileucine motif* ([D/E]xxxL[I/L]) (Wiley et al., 2011). This short signaling motif allows for interaction between cargo proteins and adaptor proteins for trafficking and controls endosomal sorting (Kozik et al., 2010).

C-terminal truncation of the human P2X7 at positions 408, 436, and 505 (Becker et al., 2008) lead to reduced ATP-induced inward currents and loss of its biphasic activation and deactivation kinetics when expressed in *Xenopus laevis* oocytes. In case of the 1–436 and 1–505 core receptors, the electrophysiological phenotype of the full-length receptor could be reconstituted by co-expression of a soluble tail construct (residues 434–595). Based on affinity purification, BN-PAGE, and cross-linking experiments a stable *association between the regions* 409–436 and 434–494 was identified, which provides the first information on molecular interactions within the P2X7 tail.

Between the sequence with homology to the death domain and the juxtamembrane region (see below) two regions with homology to *binding sites for cytoskeletal proteins* have been identified. Residues 389–405 of human P2X7 show 53% identity with the *cytadherence high molecular weight protein 3* from *Mycoplasma genitalium,* which binds actin filaments (Denlinger et al., 2001; Watters et al., 2001). Residues 419-425 in rat P2X7 (KSLQDVK) are homologous to the α*-actinin 2 binding sequence in the glutamate receptor NR1 subunit.* In support of a close interaction with the cytoskeleton, the cytoskeletal proteins α-actinin 4 and supervillin, which both interact directly with β-actin were identified in a search for possible interaction partners of rat P2X7 (Kim et al., 2001; Gu et al., 2009).

Juxtamembrane Region(s) (Residues 1–26 and 357–387)

Deletion of the juxtamembrane *cysteine-rich domain* (residues 362–379) was shown to affect the permeation and/or pore forming properties of rat and human P2X7 (Jiang et al., 2005; Robinson et al., 2014). Additionally, it was shown in a chimeric approach (Allsopp and Evans, 2015), that both the N- and the C-terminal juxtamembrane regions of the human P2X7 (including the cysteine-rich domain) are important for pore formation and regulation of channel kinetics. In the panda P2X7, serine-substitutions of C362 and C363 in this region resulted in complete inhibition of YO-PRO-1 uptake (Karasawa et al., 2017). Upstream (residues 354-364) and downstream (residues 378-387) of this cysteine-rich domain, there are at least two *cholesterol recognition amino acid consensus (CRAC) motifs* [(L/V)X1–5 YX1–5(K/R)] that are conserved in human and rodent P2X7. Further CRAC motifs have been identified in the N-terminus, the extracellular end of TM1, and the C-terminus of P2X7 (Robinson et al., 2014). Based on these findings, it was suggested that the juxtamembrane cysteine-rich domain framed by the CRAC motifs could alter the tilting angle of TM2 or act as a membrane anchor and thereby facilitate movements required for channel and/or pore opening (Allsopp and Evans, 2015; Karasawa et al., 2017). A similar anchor-like function that stabilizes the open state was ascribed to the cytoplasmic cap in the human P2X3, which is assumed to undergo profound reorganization upon channel activation (Mansoor et al., 2016).

Within the distal CRAC motif, three neighboring tyrosine residues (Y382-Y384) were identified that can be phosphorylated by the *c-Src tyrosine kinase* (Leduc-Pessah et al., 2017). In this study, it was found that Src kinase activation by morphine (via μ-opioid receptors) and subsequent P2X7 phosphorylation resulted in increased receptor expression and activity in rat spinal microglia. The resulting loss of morphine-induced analgesia linked P2X7 activity to the development of morphine tolerance.

Single Nucleotide Polymorphisms (SNPs) in the P2X7-Tail

The human P2X7 is highly polymorphic (Bartlett et al., 2014). The *T357S* polymorphism was found by ATP-induced influx measurements to cause a partial loss of function in human monocytes, lymphocytes, and macrophages, and was associated with impaired mycobacterial killing (Shemon et al., 2006; Miller et al., 2011). Interestingly, this SNP resulted in a complete loss of function when occurring in homozygote constellation or in combination with another loss-of-function SNP. A loss-of function phenotype was confirmed in *Xenopus laevis* oocytes and HEK293 cells overexpressing the mutant T357S P2X7 (Shemon et al., 2006).

Based on genetic studies, the *human Q460R* polymorphism has been associated with bipolar disorders and major depressive disorder (Barden et al., 2006; Lucae et al., 2006; McQuillin et al., 2009). ATP-induced ethidium uptake measurements in Q460R P2X7-transfected HEK293 cells revealed a slight reduction in pore formation (Fuller et al., 2009; Stokes et al., 2010). Interestingly, careful functional studies showed that this SNP is not *per se* compromised in its function, but shows impaired Ca^{2+} influx, channel currents, intracellular signaling, and also affected the sleep quality in a humanized Q460R P2X7 knock-in mouse model, if co-expressed with the respective non-polymorphic variant (Aprile-Garcia et al., 2016; Metzger et al., 2017).

The *E496A* SNP was found to prevent ATP-induced ethidium uptake, Ba^{2+} permeation, and induction of apoptosis in human B lymphocytes and was associated with cancer metastasis (Gu et al., 2001; Ghiringhelli et al., 2009). When expressed in *Xenopus laevis* oocytes or HEK293 cells and analyzed electrophysiologically, however, the E496A substitution had no effect on the ion channel functions of the receptor (Boldt et al., 2013).

The human loss-of-function SNP, *I568N*, was reported to prevent receptor trafficking and cell surface expression [see also Section "Trafficking and Lipid Interaction Domains (∼Residues 540–595)"] (Wiley et al., 2003), supposedly because of its localization within a sequence [DFAI(568)L] (Wiley et al., 2011) similar to a dileucine motif – [D/E]xxxL[I/L]– [(Kozik et al., 2010), compare Section "The Death Domain (∼Residues 430–530)"].

A gain of function in pore formation and IL- 1β secretion has been reported for the *human A348T* SNP (Stokes et al., 2010), whereas *H521Q* has been reported to represent a neutral SNP (Wiley et al., 2011).

The *murine P451L* loss-of-function SNP was identified by comparison of T-cells from different mouse strains (Adriouch et al., 2002). This SNP is found in the commonly used C57BL/6 strain, but not in BALB/c mice, rats, or humans. It impairs ATP-induced cation fluxes, pore formation, PS externalization, NAD-sensitivity as well as lysis and apoptosis of thymocytes (Schwarz et al., 2012; Rissiek et al., 2015), and has been associated with reduced pain sensitivity (Sorge et al., 2012). It lies within the SH3-binding domain [compare Section "The Death Domain (∼Residues 430–530)"].

P2X7 MEDIATED SIGNALING PATHWAYS

A multitude of downstream events have been identified upon P2X7 activation. In the following, we will focus on the proteins involved in the P2X7 activated signaling pathways rather than the physiological consequences or cell types in which these have been observed.

Release of IL-1β and Other Cytokines

The most investigated P2X7 function is probably its role in NLRP3 inflammasome assembly and subsequent maturation and release of IL-1β by macrophages and other immune cells. The pro-inflammatory IL-1β is a member of the interleukine-1 cytokine family, which comprises the IL-1 (IL-1α, IL-1β, IL-33, IL-1Ra), IL-18 (IL-18, IL-37), and IL-36 (IL-36Rα, IL-36α,β,γ, IL-38) subfamilies and includes pro- and anti-inflammatory cytokines (Dinarello, 2018). Due to its earlier identification and major role in host defense of the innate immune system and autoinflammatory diseases, IL-1β is so far best studied. Pro-IL-1β synthesis (and also that of NLRP3, see below) is induced by the transcription factor NF-κB, which in turn is activated upon binding of pathogen-associated molecular patterns (PAMPs), such as LPS, to the TLR4 (priming). Processing and release of mature IL-1β is then induced in a second step (activation) by inflammasome assembly and activation of caspase 1 by a diverse range of damage- or danger-associated molecular patterns (DAMPs), including ATP (Mariathasan et al., 2006).

Activation of caspase 1 by proteolytic conversion of pro-caspase 1 requires the NLRP3 inflammasome, a multiprotein complex that consists of the pattern recognition receptor NLRP3, the adaptor apoptosis-associated speck-like protein containing a caspase-recruitment domain (ASC), and the cysteine protease caspase 1 (Gross et al., 2011). In addition, never-in-mitosis A (NIMA)-related kinase 7 (NEK7) was recently identified as an essential component (He et al., 2016b; Shi et al., 2016).

K^+ efflux and depletion was early shown to constitute a critical step in ATP-induced IL-1β production (Perregaux and Gabel, 1998) and generation of the first P2X7 knockout mouse clearly demonstrated the involvement of the P2X7 in this process (Solle et al., 2001). More recently, K^+ depletion has been confirmed to represent an essential and sufficient requirement for inflammasome assembly induced by a diverse variety of DAMPs (Munoz-Planillo et al., 2013). However, while the P2X7 was generally assumed to represent the K^+ conduit, a recent study identified the two-pore domain K^+ channel TWIK2 as an ATP-responsive K^+ efflux channel (Di et al., 2018). According to this study, P2X7-induced cation influx generates the driving force for K^+ efflux. The molecular mechanisms of inflammasome assembly and caspase activation are little understood. Based on immunoprecipitation and co-localization studies in cell lines and primary mouse microglia, it has been suggested that the P2X7 is directly interacting with NLRP3 (Franceschini et al., 2015). Likewise, an interaction between P2X7 and the NLRP2 inflammasome was proposed in human astrocytes (Minkiewicz et al., 2013) (see also Section "Proteins Involved in P2X7-Mediated Interleukin Secretion").

In addition to K^+ depletion, cytosolic ROS production, either by NADPH oxidase or due to mitochondrial dysfunction, has been implicated in NLRP3 inflammasome activation and its exact role remains to be determined (He et al., 2016a). With the exception of the interleukine receptor antagonist (IL-1Ra), all IL-1 family members lack a signal peptide and are formed as precursor in the cytoplasm. Various mechanisms of non-classical IL-1β release mechanism including exocytosis via lysosomes, microvesicle shedding, exosome release, and release upon pyroptotic cell death have been proposed (for references and details see Dubyak, 2012; Giuliani et al., 2017). While PLC, PLA2 (Andrei et al., 2004), src kinase, p38, acid sphingomyelinase (Bianco et al., 2009), caspase 1 (Keller et al., 2008), and gasdermin (Evavold et al., 2018) have been involved, the exact mechanism(s) and P2X7 involvement remain(s) incompletely understood. In addition to IL-1β, numerous other cytokines, chemokines, and proteins have been shown to be released upon P2X7 activation (e.g., de Torre-Minguela et al., 2016).

ROS Formation/Mitochondrial Function

ROS are continuously generated by the mitochondrial electron transport chain or by activation of NADPH oxidases (NOXs). They represent important signaling molecules under physiological conditions. Under pathological conditions, increased ROS production contributes to immune signaling and killing of phagocytosed microorganisms, but also to deleterious effects such as protein, lipid, and DNA modification and damage. Seven NOX family members are known and the respective

NADPH oxidase complexes are subtype-specifically localized in internal and plasma membranes. They consist of the membrane integrated catalytic subunit with or without the p22phox protein and regulating cytosolic proteins including the Rho-GTPase Rac. NOX are activated by numerous receptors and NOX complex assembly and activity can be further regulated by Ca^{2+} signaling and subunit phosphorylation for example by protein kinase C isoforms, p38 and ERK1/2 MAP kinases, and phosphoinositide-3 kinase (PI3Ks) (Guerra et al., 2007; Spooner and Yilmaz, 2011; Haslund-Vinding et al., 2017; Belambri et al., 2018). P2X7-mediated NOX subunit phosphorylation and ROS production has been shown in microglia and macrophages (Parvathenani et al., 2003; Moore and MacKenzie, 2009; Lenertz et al., 2009) and few other cell types (Wang and Sluyter, 2013). The molecular mechanisms were suggested to involve kinase activation via Ca^{2+} influx (Guerra et al., 2007; Noguchi et al., 2008; Martel-Gallegos et al., 2013).

Interestingly, tonic stimulation by low levels of ATP was found to hyperpolarize the mitochondrial potential, increase mitochondrial Ca^{2+} content, and increase the cells' ATP content in transfected cells. This effect was dependent on the C-terminus and proposed to be due to a P2X7-mediated constant but low level Ca^{2+} transfer into the mitochondria that stimulates trophic effects whereas strong P2X7 stimulation causes mitochondrial Ca^{2+} overload and collapse and results in cell death (Adinolfi et al., 2005). P2X7-expressing cells also upregulated the glucose transporter and glycolytic enzymes, showed increased glycolysis, oxidative phosphorylation, and protein kinase B phosphorylation, and were able to proliferate even in the absence of serum and glucose (Amoroso et al., 2012) (see also Di Virgilio et al., 2017).

P2X7 – Mediated Lipase Activation and Lipid Interactions

Phospholipids, glycolipids, and cholesterol represent the major lipid components of animal plasma membranes. Cholesterol is an important constituent of lipid rafts and phospholipids can be broken down by phospholipases to produce different lipid second messengers or bioactive mediators of cellular signaling. Cholesterol as well as several phospholipases have been proposed to be involved in P2X7 signaling and function.

Phospholipase A2 (PLA2)

PLA2 phospholipases cleave phospholipids preferentially in the middle position of glycerol to release fatty acids and lysophospholipids.

Out of the six diverse groups of mammalian PLA2 enzyme families, the cytosolic PLA2α is the best-investigated enzyme. It belongs together with the β,γ,δ,ε, and ζ subtypes to the group IV family of cytosolic PLA2 (Leslie, 2015). cPLA2α preferentially catalyzes the hydrolysis of phospholipids to arachidonic acid and lysophospholipids, which are precursors for numerous bioactive lipids such as prostaglandins, leukotrienes, and epoxyeicosatrienoic acids (EETs). Ca^{2+}-independent PLA2 (iPLA2, group VI) are similar to cPLA2 but do not require Ca^{2+} for activation. Both types are also implicated in the regulation of intracellular membrane trafficking by the induction of changes in the membrane curvature that is required for membrane budding (Leslie, 2015).

cPLA2α is widely expressed in all tissues and regulated by its transcriptional level (e.g., induced by Ras and MAPK pathways and NF-κB, hypoxia-inducible factor, Sp1, and c-Jun), Ca^{2+}, and phosphorylation by MAPK. Ca^{2+} increase promotes its translocation to intracellular membranes, a requirement for arachidonic acid release. Phosphorylation by MAPKs can enhance its activity (Leslie, 2015). P2X7-mediated activation of cPLA2 and iPLA2 has been reported in immune and epithelial cells (Alzola et al., 1998; Chaib et al., 2000; Andrei et al., 2004; Kahlenberg and Dubyak, 2004; Garcia-Marcos et al., 2006b; Costa-Junior et al., 2011) and has been associated with various downstream effects such as PLD activation, kallikrein secretion, bioactive lipid generation, and pore formation as well as IL-1β processing, blebbing, and PS-flip (Garcia-Marcos et al., 2006b; Anrather et al., 2011; Costa-Junior et al., 2011; Norris et al., 2014; Wan et al., 2014; Alarcon-Vila et al., 2019; Janks et al., 2019). Janks et al. (2019) recently reported an involvement of undefined chloride channels downstream of PLA2 in some of these processes. The mechanism of PLA2 activation by P2X7 remains unclear but was suggested to involve MAP kinases, P-I4 kinase/PIP2 (Garcia-Marcos et al., 2006b; Wan et al., 2014) and/or n-SMase activation in lipid rafts (Garcia-Marcos et al., 2006a). In case of cPLA2, it might also be activated by Ca^{2+} influx through P2X7.

Phospholipase C (PLC)

In animals, PLC cleaves phosphatidylinositol-4,5-bisphosphate (PIP2) into the second messengers diacylglycerol and inositol-1,4,5,-triphosphate (Suh et al., 2008; Fukami et al., 2010). Besides PKC activation and mobilization of intracellular Ca^{2+} (via DAG and IP3, respectively) this process also influences the local concentration of PIP2 (an important membrane anchor and modulator of multiple processes and receptors) and the synthesis of the signaling molecule PIP3, which is generated by phosphatidylinositol 3-kinase (PI3K) from PIP2. Thirteen mammalian PLC isoforms that are organized in six groups are known and expressed in a tissue and/or cell-specific manner. In addition to the common catalytic and Ca^{2+}-binding domains all but the PLCζ isotype contain pleckstrin homology (PH) domains that can mediate interactions with phosphatidylinositol lipids, G protein βγ subunits, or other proteins. Furthermore, some isotypes have specific domains that contribute to their individual functions: thus the src homlogy (SH) domains in PLCγ allow its interaction with and activation by receptor and cytosolic tyrosine kinases. Ras-associating domains and Ras-GTPase exchange factor-like domains in PLCε mediate its interactions with members of the Ras family of small G proteins, and the long C-terminus of PLCβ contains determinants for Gq protein interactions, membrane binding, and nuclear localization (Suh et al., 2008; Fukami et al., 2010).

Several GPCRs, including some P2Y receptors, activate PLC. However, few reports exist on the activation of PLC by P2X7 (Carrasquero et al., 2010) and K^+ depletion has been suggested as a mechanism (Andrei et al., 2004; Clark et al., 2010). Also, modulation of PLC downstream effects by P2X7 has been

reported but appears to be indirect and not dependent on influx of extracellular Ca^{2+} (Garcia-Marcos et al., 2006b). In microglia, for example, it was found that P2X7-induced Ca^{2+} rise increases DAG lipase activity and thus favors production of the endocannabinoid 2-AG from DAG, which is generated by PLC (Witting et al., 2004). A negative modulation of P2X7 through the depletion of PIP2 (supposedly due to PLC) has also been reported (Zhao et al., 2007) and three residues in the C-terminus (R385, K387, K395) might be involved in this interaction. However, the mechanism could also be indirect as no direct PIP2-P2X7 interaction was identified (Bernier et al., 2013) [compare Section "Trafficking and Lipid Interaction Domains (∼Residues 540–595)"].

Phospholipase D (PLD)

PLDs represent a family of phosphodiesterases that catalyze the removal of head groups from glycerophospholipids (typically phosphatidylcholine), thereby generating the regulatory molecule phosphatidic acid (PA). More generally, this process represents a headgroup exchange by water and in the presence of primary alcohols generates phosphatidylalcohol. PA, due to its small negatively charged headgroup, can induce negative curvature of membranes if sufficient concentrations are reached. In addition, PAs can act as lipid anchors for numerous PA binding proteins and can modulate/activate various proteins, such as the NOX complex, kinases, PLC and G-protein regulatory proteins, to only name a few (Bruntz et al., 2014). PA can also be converted to DAG and lysophosphatidic acid.

In mammals, the two isoforms PLD1 and PLD2 occur almost ubiquitously, associate with membranes, and participate in processes that involve membrane remodeling such as vesicular transport and endocytosis but also many others. PLDs are activated by a variety of receptors (GPCRs, receptor tyrosine kinases, and integrins) and signaling molecules. Direct interaction and activation has been shown for PKC and the small Ras GTPases RhoA and ARF (Selvy et al., 2011; Bruntz et al., 2014). In a macrophage cell line, P2X7 activation was found to induce rapid PLD activation that was only partially dependent on Ca^{2+} and PKC (Humphreys and Dubyak, 1996) and subsequent studies in human and mouse macrophages showed that P2X7-dependent killing of intracellular pathogens requires PLD activation (Kusner and Adams, 2000; Fairbairn et al., 2001; Coutinho-Silva et al., 2003). In thymocytes, Ca^{2+}-dependent activation of PLD by P2X7 was shown (Le Stunff et al., 2004). What links P2X7 to PLD activation is not known in detail but influx of bivalent cations (Gargett et al., 1996), kinases (Hung and Sun, 2002; Perez-Andres et al., 2002; Pochet et al., 2003), and small G-protein interactions via the putative SH3 domain (Denlinger et al., 2001) have been involved.

Sphingomyelinase

Sphingomyelin is a phospholipid based on the unsaturated aminoalcohol sphingosine instead of glycerol. It is the most abundant sphingolipid with particularly high levels in the CNS and constitutes a major component of the plasma membrane. Due to its ability to bind cholesterol, it plays an important role in the formation of lipid rafts. Its content in the cell is regulated by *de novo* synthesis in the ER/Golgi (a multistep process involving sphingomyelin synthases) and its degradation by sphingomyelinases (SMases). SMases hydrolize sphingomyelin to phosphocholine and ceramide (sphingosine coupled via an amide bound to a fatty acid), a bioactive molecule that is involved in apoptosis, cell cycle, organization of membrane domains ("ceramide platforms"), inflammation, and various diseases (Gomez-Munoz et al., 2016). In addition, ceramide can be metabolized to further bioactive sphingolipids, such as the mitogenic sphingosine-1-phosphate.

Six types of SMases have been identified and were grouped according to the optimal pH value for their activation into acidic, alkaline and four neutral SMases. Of these, the lysosomal acidic a-SMase and Mg^{2+}-dependent neutral n-SMase2 are best characterized and considered the major candidates for ceramide production. n-SMase is located in Golgi and plasma membrane domains and regulated by transcription, anionic phospholipids, phosphorylation, and in response to several cytokines, including TNF-α and IL-1β (Shamseddine et al., 2015).

In thymocytes and macrophages, P2X7 has been involved in the *de novo* synthesis of ceramide and subsequent apoptosis (Lepine et al., 2006; Raymond and Le Stunff, 2006) and it was speculated that the P2X7 death domain might be involved in ceramide production in macrophages. Similarly, this domain was suggested to be involved in P2X7-induced activation of n-SMase in lipid rafts and subsequent PLA2 activation in submandibular gland cells. In a more recent study on astrocytes it was concluded that P2X7, via src kinase (maybe by interacting with the SH2 domain) and p38MAPK activation, induces translocation of a-SMase to the outer plasma membrane leaflet where it induces blebbing and shedding of IL-1β-containing micro particles (Bianco et al., 2009). It was also suggested that P2X7, via a-SMase activation can induce the rapid release of HIV-1-containing compartments from HIV-infected macrophages (Graziano et al., 2015).

P2X7 Effects on Membrane Organization and Morphology

Phosphatidylserine Exposure (PS-Flip) and Shedding

In healthy cells, PS is distributed to the inner leaflet of the plasma membrane. So-called flippases, most likely P4-ATPase ATP11C and its chaperone CDC50A, are required to keep this asymmetry (Segawa et al., 2014). Under certain conditions, for example during apoptosis, PS is translocated to the cell surface by scramblases (Segawa and Nagata, 2015). Anoctamin-6/TMEM16F (Ano6) and Xk-related protein 8 (Xkr8) were identified as scramblases (Suzuki et al., 2010, 2013) and proposed to account for Ca^{2+}-induced PS scrambling and a caspase/apoptosis-induced scrambling respectively (Suzuki et al., 2013). For the latter, simultaneous inactivation of ATP11C and activation of Xkr8 by caspases is required (Suzuki et al., 2013; Segawa et al., 2014).

Brief activation of P2X7 was shown to result in a reversible PS translocation, while prolonged activation results in irreversible exposure of PS and subsequent cell death (Mackenzie et al., 2005). A functional and physical interaction between P2X7

and the Ca^{2+} activated Cl^- channel Ano6 was identified and suggested to mediate the translocation of PS (Ousingsawat et al., 2015). However, the molecular mechanisms of this interaction are unclear and interaction between Ano6 and P2X7 was not confirmed in another study (Stolz et al., 2015).

Reversible PS flip is also part of a signal transduction pathway in response to pathological conditions and P2X7-mediated PS flip can lead to shedding of L-selectin (CD62L) (Elliott et al., 2005), a cell adhesion molecule that initiates leukocyte tethering, the first step of the adherens and migration cascade (Ivetic, 2018). Shedding of CD62L from human monocytes occurs precisely during transmigration and is important for the invasion and direction of migration (Rzeniewicz et al., 2015) and PS exposure increased the adhesion of cells to the endothelial cell layer (Manodori et al., 2000). Thus PS translocation appears to be relevant for leukocyte migration and P2X7-mediated PS flip might increase the membrane fluidity and plasticity of the cell and thereby facilitate the transmigration processes (Elliott et al., 2005; Qu and Dubyak, 2009).

In addition to CD62L (Jamieson et al., 1996; Gu et al., 1998; Labasi et al., 2002; Elliott et al., 2005; Sengstake et al., 2006; Scheuplein et al., 2009; Schwarz et al., 2012), shedding of low affinity immunoglobulin epsilon Fc receptor (CD23) (Gu et al., 1998; Chen et al., 1999; Sluyter and Wiley, 2002; Pupovac et al., 2015), complement receptor type 2 (CD21) (Sengstake et al., 2006), tumor necrosis factor receptor superfamily member 7 (CD27) (Moon et al., 2006), IL-6R (Garbers et al., 2011), CXCL16 (Pupovac et al., 2013), and vascular cell adhesion molecule 1 (VCAM-1) (Mishra et al., 2016) was reported upon P2X7 activation and was mainly linked to activation of membrane-associated metalloproteases, in particular the a disintegrin and metalloprotease domain-containing proteins (ADAM) 10 and ADAM17. Out of the 21 ADAM family members, these two have been studied the most. They are widely expressed by immune cells and their activity is controlled by multiple regulatory mechanisms (Grötzinger et al., 2017; Lambrecht et al., 2018). Interestingly, it was shown that PS exposure is required for ADAM17 activity (Sommer et al., 2016) and phosphorylation by ERK and p38 is important for its activation (Diaz-Rodriguez et al., 2002) and membrane trafficking (Soond, 2005), thus providing a direct link between metalloprotease activity and these described P2X7 signaling pathways.

Plasma Membrane Blebbing

Blebbing is the formation of spherical protrusions of the plasma membrane. It requires the detachment and/or local rupture of the actomyosin cortex from the membrane (bleb nucleation or initiation) as well as increased myosin activity and intracellular pressure (bleb expansion) and is reversed by subsequent reformation of an actin cortex at the blebbed membrane and myosin-driven retraction. While generally considered as a hallmark of apoptosis, blebbing is also involved in cell migration and cytokinesis (Charras, 2008; Paluch and Raz, 2013). The molecular details of these events are little understood but activation of the small G protein Rho by extra- or intracellular signals, its subsequent activation of the effector kinase Rho-associated kinase (ROCK), and phosphorylation of myosin light chain by ROCK appear to be central processes. In addition, proteins and lipids (such as PIP2) influencing the cortex-membrane interaction and alterations in the cell adhesion properties appear to play a role (Fackler and Grosse, 2008). P2X7 receptor activation causes reversible blebbing in native and recombinant systems (MacKenzie et al., 2001; Mackenzie et al., 2005). This effect is dependent on the P2X7 tail (Wilson et al., 2002) and in a Y2H screen an interaction with the epithelial membrane protein (EMP)-2 was identified and biochemically confirmed for the related proteins EMP-1, EMP-3, and peripheral myelin protein (PMP)-22, which are all widely expressed (references in Wilson et al., 2002). Overexpression of these proteins in HEK293 cells resulted in an increase of caspase-dependent apoptotic-like behavior and blebbing, although a specific interaction domain or mechanism was not identified. In subsequent studies, RhoA, ROCKI, and p38 MAP kinase (Morelli et al., 2003; Verhoef et al., 2003; Pfeiffer et al., 2004) have been shown to be involved in P2X7-induced blebbing and it was demonstrated that the signaling pathway that leads to blebbing is caspase independent and different from that promoting IL-1β release (Verhoef et al., 2003). However, dependence of blebbing on extracellular Ca^{2+}- was inconsistent in different studies and both Ca^{2+}-dependent and independent pathways leading to blebbing have therefore been proposed (Mackenzie et al., 2005). According to this model, the faster Ca^{2+}-dependent zeiotic form of membrane blebbing is a consequence of local Ca^{2+} overload that via induction of PS-flip leads to the disruption of plasma membrane actin interaction. In favor of this model, deregulation of Ca^{2+} entry as a consequence of CaM binding to the P2X7 C-terminus was found to facilitate blebbing (Roger et al., 2008). How Rho is activated remains unresolved. Based on findings in osteoblasts, it was proposed that P2X7 activation leads via PLD and PLA2 activation to LPA, and LPA, by activation of the LPA receptor (a GPCR), activates Rho (Panupinthu et al., 2007). Involvement of PLA2 activation in addition to an undefined Cl^- channel in blebbing is supported by a recent study on macrophages (Janks et al., 2019).

Additional effects of P2X7 on cellular membrane trafficking and organization have been reported. These include microvesiculation (MacKenzie et al., 2001; Bianco et al., 2005; Pizzirani et al., 2007), exosome release (Qu et al., 2009; Barberà-Cremades et al., 2017), phagosome maturation (Fairbairn et al., 2001), and formation of multinucleated giant cells (Lemaire et al., 2006). For review see Qu and Dubyak (2009).

Kinase Activation

Protein Kinase C (PKC)

PKCs are a family of serine/threonine kinases and represent central mediators of cytoplasmic signaling cascades that regulate a variety of cellular functions.

Three PKC subfamilies (classical, novel, and atypical) have been determined: The classical (PKCα, PKCβ, PKCγ) and the novel (PKCδ, PKCε, PKCθ, and PKCη) PKCs both require the second messenger DAG for activation. The cPKCs require Ca^{2+} as a cofactor while the nPKCs are Ca^{2+}-independent. The aPKCs

are independent of Ca^{2+} and DAG. Most PKCs are ubiquitously expressed. Their activation is associated with translocation of the enzyme from the cytosolic fraction to the plasma membrane or cell organelles. Besides mediating signal transduction from the plasma membrane, PKCs have been identified within the nucleus, where their role is less well studied (Lim et al., 2015).

P2X7-dependent translocation of Ca^{2+}-dependent PKCs has been described in osteoclasts (Armstrong et al., 2009) and Ca^{2+}-independent PKCs have also been involved in P2X7 signaling (Bradford and Soltoff, 2002; Gendron et al., 2003) although the molecular interactions and the source of DAG remained unclear in these studies. P2X7 modulation by PKC and its physical interaction with PKCγ was also suggested (Hung et al., 2005).

Mitogen Activated Protein Kinases (MAPK)

MAPKs are serine/threonine-specific protein kinases that are activated by phosphorylation as a result of a multi-level signaling cascade. Three types of MAPKs have been found to be phosphorylated upon P2X7 activation, the closely related extracellular signal regulated kinases ERK1 and ERK2, the c-Jun N-terminal kinases (JNKs), and the p38 MAPK (Hu et al., 1998; Armstrong et al., 2002). The ERK1/2 pathway is best investigated and starts with an extracellular ligand binding to its receptor, which then couples to and activates the small GTPase Ras, which via RAF kinases and mitogen-activated protein kinase kinases (MEK1/2) activates ERK1/2. ERK1/2 can regulate RNA translation and several transcription factors and plays an important role in cell division and proliferation. Activation of P38 and JNK MAPKs is more complex and includes numerous kinases that are mostly shared between both MAPKs. Activating stimuli include inflammatory signals and stress and these kinases are involved in apoptosis, proliferation, and inflammation.

Many studies have shown phosphorylation of these kinases following P2X7 activation (Humphreys et al., 2000; Panenka et al., 2001; Gendron et al., 2003). Activation of ERK1 was suggested to be mediated via Ca^{2+}, PI3K, c-Src (Gendron et al., 2003; Auger et al., 2005), and EGF receptor transactivation (Stefano et al., 2007). ERK activation was shown to depend mainly on the N-terminus of P2X7 since it was affected by N- but not C-terminal truncations (Amstrup and Novak, 2003).

Cellular Sarcoma Tyrosine Kinase (c-Src)

c-Src is a member of the Src kinase family and a protooncogene. It is via myristoylation associated with the plasma membrane and contains src homology (SH) domains 1–4. Its activation causes dephosphorylation of a tyrosine residue and opening of the SH2, SH3, and kinase domains and autophosphorylation. It can be activated by several membrane proteins and can activate various proteins, including focal adhesion proteins, adaptor proteins, and transcription factors and thereby directly or indirectly activates numerous signaling molecules including MAPKs.

Besides activating downstream signaling pathways, the P2X7 receptor itself could serve as a substrate for kinases or phosphatases. For example, Y343 in TM2 was assumed to be dephosphorylated upon receptor activation, since phenylalanine-substitution of Y343 in rat P2X7-expressing HEK293 cells prevented run-down of agonist-evoked currents as well as the effect of phosphatase inhibitors on currents and onset of membrane blebbing (Kim et al., 2001). Additionally, tyrosine residues Y382, Y383, and Y384 in rat P2X7 were found to be phosphorylated by c-Src (Leduc-Pessah et al., 2017).

Phosphoinositide 3-Kinase (PI3Ks)/Protein Kinase B (PKB Also Known as Akt)

PI3Ks are a family of kinases that, upon activation by receptors phosphorylate the hydroxyl group in position 3 of phosphatidylinositol, thereby generating various phosphoinositides that are able to recruit signaling proteins with phosphoinositide binding PH domains to membranes. Thus, the PH domains of the serine/threonine kinase protein kinase B and the phosphoinositide-dependent kinase (PDK1) bind to PtdIns(3,4,5)P3 (PIP3) and PtdIns(3,4)P2 (PIP2) and thereby localize to the plasma membrane where they interact.

PKB is a serine/threonine kinase that contains a PH domain, which binds with high affinity to phosphatidylinositol (3,4,5)-trisphosphate (PIP3) and is activated by the phosphoinositide-dependent kinase (PDK) 1 and the mammalian target of rapamycin complex 2 (mTOR2). This results in the activation of multiple substrates including mTOR. PKB is involved in antiapoptotic pathways, glucose metabolism, protein synthesis, and cell proliferation and tightly regulated. Numerous and complex effects of P2X7 on Akt have been reported. For example, in neuroblastoma cells and astrocytes, stimulation of P2X7 lead to Akt activation (Jacques-Silva et al., 2004; Amoroso et al., 2015). In another study on neuroblastoma cells, P2X7 inhibition was associated with neuritogenesis and increased Akt phosphorylation (Gomez-Villafuertes et al., 2009) and in pancreatic cancer cells, P2X7 activation was involved in activation of protein and lipid phosphatases that lead to nuclear Akt depletion and inhibited proliferation (Mistafa et al., 2010). Extra- and intracellular calcium, a c-Src-related tyrosine kinase, PI3K, and CaMKII have been involved in Akt activation by P2X7 (Jacques-Silva et al., 2004; Gomez-Villafuertes et al., 2009).

Neurotransmitter Release

A wealth of literature describes P2X7 localization and function in neuronal cells and its involvement in the release of various neurotransmitters and gliotransmitters. This effect is generally supposed to be a consequence of P2X7-mediated Ca^{2+} increase and beyond the scope of this review. Excellent overviews are given in Sperlagh and Illes (2014) and Miras-Portugal et al. (2017).

Role in Gene Transcription

P2X7 has been involved in the activation of several transcription factors, most of which play a role in inflammation.

Nuclear Factor κ-Light Chain Enhancer of Activated B Cells (NF-κB)

NF-κB is an ubiquitously expressed protein complex that acts as a rapid primary transcription factor (Zhang et al., 2017) and binds to so-called κB-motifs that are present in

numerous regulatory DNA regions. It is activated by stressful and pro-inflammatory stimuli such as cytokines, bacterial and viral antigens via a variety of cell surface receptors and initiates the transcription of genes involved in inflammation, proliferation, or survival. In unstimulated cells, NF-κB is bound in the cytoplasm to the inhibitor of κB (IκB). Phosphorylation of IκB by IκB kinase (IKK) leads to its degradation in the proteasome and enables NF-κB to translocate into the nucleus where it binds to target gene promoter sequences. In addition, activity of NF-κB is modulated by phosphorylation (Christian et al., 2016). Activation of P2X7 has been shown to lead to IκB degradation, NF-κB phosphorylation, nuclear translocation, and induced transcription in NF-κB reporter assays (Ferrari et al., 1997b; Aga et al., 2002; Korcok et al., 2004; Genetos et al., 2011; Kim et al., 2013). The signaling mechanisms have not been conclusively resolved but were suggested to involve ROS generation and caspase activation (Ferrari et al., 1997b), ERK1/2 and Akt, (Tafani et al., 2011), MAP kinases (Aga et al., 2004), and MyD88 (Liu et al., 2011). While it is generally accepted that P2X7-induced caspase 1 activation and subsequent IL-1β maturation requires TLR-induced NF-κB signaling (Kahlenberg et al., 2005), a role for P2X7-induced NF-κB signaling and IL-1β transcription (together with NLRP3 components) has also been shown in sterile inflammation upon mechanical trauma (Albalawi et al., 2017).

Nuclear Factor of Activated T Cells (NFAT)

The NFAT family consists of five (NFAT1-NFAT5) members and is related to the REL-NF-κB family of transcription factors (Serfling et al., 2012). NFAT1-NFAT4 are activated via CaM and the phosphatase calcineurin, by cell surface receptors that couple to Ca^{2+} mobilization. NFAT5 is activated by osmotic stress and not further discussed here. In its inactivated state, NFAT is phosphorylated and upon dephosphorylation by calcineurin, translocates to the nucleus. Here, it cooperates with other transcription factors (including the AP-1 and Rel family) to regulate immune function and inflammation as well as cell proliferation, cell differentiation and cancer growth. NFAT phosphorylation and inactivation is regulated by multiple kinases in the nucleus (e.g., GSK3) and/or cytoplasm (e.g., CK1). In addition, several other mechanisms, such as caspase 3 cleavage, can regulate NFAT (Müller and Rao, 2010).

In T cells, where NFAT function is best investigated, ATP release and autocrine or paracrine feedback signaling via P2X7 activation has been shown to lead to NFAT induction and release of IL-2 (Yip et al., 2009). In stimulated B cells, however, NFAT internalization in the nucleus was decreased by P2X7-induced membrane depolarisation (Pippel et al., 2015). In microglia cell lines, P2X7 signaling has been shown to activate NFAT proteins (Ferrari et al., 1999) and more recently, the inflammatory CC-motif chemokine ligand 3 (CCL3) was found to be released as a result of this signaling pathway (Kataoka et al., 2009).

Adinolfi et al. (2009) observed an induction in the expression of NFATc1 by heterologous expression of P2X7 in HEK293 cells that lead to promotion of growth and prevention of apoptosis. This effect was confirmed by P2X7 transfection in cancer cell lines and caused an increase in the tumor size and growth rate (Adinolfi et al., 2012). Likewise, transfection of P2X7 into osteosarcoma cells led to an increase in NFATc1 translocation to the nucleus and its activation has been associated with cell growth and proliferation (Giuliani et al., 2014).

Hypoxia Inducible Factor (HIF)

Hypoxia inducible factor is a heterodimeric (HIF-α and HIF-β) transcription factor that is upregulated under conditions of low oxygen availability and is implicated in tumor growth. P2X7-mediated upregulation of HIF-1α and ischemic tolerance was reported after ischemic insult in astrocytes (Hirayama et al., 2015; Hirayama and Koizumi, 2017) and P2X7 downmodulation reduced HIF-1α (Amoroso et al., 2015). HIF-1α has also been proposed to regulate the expression of P2X7 in the hypoxic microenvironment, which via Akt and Erk phosphorylation promotes nuclear translocation of NF-κB and tumor cell invasion (Tafani et al., 2011).

Other Transcription Factors

Other transcription factors that were reported to be induced upon P2X7 activation include activator protein 1 (AP-1) (Gavala et al., 2010), the early growth response transcription factors (Egr) (Stefano et al., 2007; Friedle et al., 2011), Runt related factor-2 (Runx2) (Yang et al., 2018), and cyclic AMP response element binding protein (CREB) (Ortega et al., 2011). For additional information please refer to Lenertz et al. (2011).

Cell Death

P2X7 is involved in different forms of cell death. While it is generally reported to cause apoptosis and/or necrosis, multiple alternative cytotoxic routes like pyroptosis and autophagy have also been described (Dubyak, 2012; Yang et al., 2015; Young et al., 2015). Whereas cell swelling and cytolysis could be explained by the plasma membrane permeabilizing properties of the P2X7 receptor (Surprenant et al., 1996) the exact mechanisms of different other forms of necrosis or apoptosis are not known in detail (for a recent review see Di Virgilio et al., 2017). Nevertheless, typical markers of apoptosis such as cytochrome c release, PS-flip, blebbing, cleavage of caspase-3, caspase-8, and caspase-9 have been observed in various systems (Ferrari et al., 1997a; Humphreys et al., 2000; Mackenzie et al., 2005).

DIRECT PROTEIN P2X7 INTERACTIONS OR INTERACTIONS WITHIN PROTEIN COMPLEXES

More than 50 proteins have been identified to physically interact with the P2X7 receptor (**Table 1**). Analysis of their STRING interaction network (**Figure 2**, Szklarczyk et al., 2019) shows that 22 of these proteins are involved in the innate immune response, in agreement with the proposed pro-inflammatory functions of P2X7. For the majority of the identified proteins, the interaction domains and the physiological consequences of this

TABLE 1 | Published P2X7 interaction partners (adapted from http://www.p2x7.co.uk).

Gene	Protein name	Uniprot ID (human)	Method	Cell system	References
ABL1	Tyrosine-protein kinase ABL1	P00519	Peptide array	*In vitro*	Wu et al., 2007
ACTB*	Actin, cytoplasmic 1 (β-actin)	P60709	IP-MS/WB	HEK293	Kim et al., 2001
			IP-MS	THP-1	Gu et al., 2009
ACTN4*	α-actinin 4	O43707	IP-MS/WB	HEK293	Kim et al., 2001
ANO6	Anoctamin-6	Q4KMQ2	IP-WB	HEK293	Ousingsawat et al., 2015
ARRB2	β-arrestin 2	P32121	IP-WB	CaSKI / HEK293	Feng et al., 2005
Bgn	Biglycan	P21810	IP-WB	Peritoneal macrophages	Babelova et al., 2009
CALM1*	Calmodulin	P0DP23	IP-WB	HEK293	Roger et al., 2008
					Roger et al., 2010
CASK	Peripheral plasma membrane protein CASK	O14936	Y2H	Liver cDNA library	Wang et al., 2011
Cav1/3	Caveolin-1	Q03135	PD/IP-WB	Alveolar epithelial E10 cells	Barth et al., 2008
			nPAGE/IP-WB	Alveolar epithelial E10 cells	Weinhold et al., 2010
			nPAGE-WB	HL-1	Pfleger et al., 2012
	Caveolin-3	P56539	nPAGE-WB	HL-1	Pfleger et al., 2012
CD14	Monocyte differentiation antigen CD14	P08571	IP-WB	HEK293	Dagvadorj et al., 2015
CD44	CD44 antigen	P16070	IP-WB	CHO-K1	Moura et al., 2015
CLTA/B/C/D	Clathrin		IP-WB	CaSKI / HEK293	Feng et al., 2005
CYFIP1	Cytoplasmic FMR1-interacting protein 1	Q7L576	IP-WB	Mouse prefrontal cortex	Li et al., 2017
DEFA1	Neutrophil defensin 1	P59665	PD-WB	HEK293	Chen et al., 2014
DNM1	Dynamin-1	Q05193	IP-WB	CaSKI / HEK293	Feng et al., 2005
EFNB3	Ephrin-B3	Q15768	Y2H	Liver cDNA library	Wang et al., 2011
EMP1/2/3	Epithelial membrane protein 1/2/3	P54849, P54851, P54852	Y2H, PD/IP-WB	HEK293	Wilson et al., 2002
Fyn	Tyrosine-protein kinase Fyn	P06241	IP-WB	OPCs, HEK293	Feng et al., 2015
GRB2	Growth factor receptor-bound protein 2	P62993	Peptide array	*In vitro*	Wu et al., 2007
GRK3	β-adrenergic receptor kinase 2	P35626	IP-WB	CaSKI / HEK293	Feng et al., 2005
HSP90AB1*	Heat shock protein HSP 90-β	P08238	IP-MS/WB	HEK293	Kim et al., 2001
			IP-WB	HEK293, peritoneal macrophages	Adinolfi et al., 2003
			IP-MS	HEK293	Gu et al., 2009
			IP-WB	PC12	Franco et al., 2013
HSPA1A*	Heat shock 70 kDa protein 1A/1B	P0DMV8	IP-MS/WB	HEK293	Kim et al., 2001
			IP-MS	HEK293	Gu et al., 2009
HSPA8*	Heat shock cognate 71 kDa protein	P11142	IP-MS/WB	HEK293	Kim et al., 2001
ITGB2	Integrin β-2	P05107	IP-MS/WB	HEK293	Kim et al., 2001
LAMA3	Laminin subunit α-3	Q16787	IP-MS/WB	HEK293	Kim et al., 2001
MPP3	MAGUK p55 subfamily member 3	Q13368	IP-MS/WB	HEK293	Kim et al., 2001
MYH9*	Myosin-9 (Myosin heavy chain, non-muscle IIa)	P35579	IP-MS/WB	THP-1	Gu et al., 2009
MyD88	Myeloid differentiation primary response protein MyD88	Q99836	IP-WB	HEK293	Liu et al., 2011
MYL12A/B*	Myosin regulatory light chain 12A, Myosin regulatory light chain 12B	P19105 O14950	IP-MS	THP-1	Gu et al., 2009
MYO5A	Unconventional myosin-Va	Q9Y4I1	IP-MS/WB	HEK293	Gu et al., 2009
NCK1	Cytoplasmic protein NCK1	P16333	Peptide array	*In vitro*	Wu et al., 2007
NLRP2/3	NACHT, LRR and PYD domains-containing protein 2	Q9NX02	IP-WB	Astrocytes	Minkiewicz et al., 2013
	NACHT, LRR and PYD domains-containing protein 3	Q9NX02	IP-WB	N13 microglia	Franceschini et al., 2015
NME2	Nucleoside diphosphate kinase B	P22392	IP-MS	HEK293	Gu et al., 2009
NOS1	Nitric oxide synthase, brain	P29475	IP-WB	Mouse brain	Pereira et al., 2013

(Continued)

TABLE 1 | Continued

Gene	Protein name	Uniprot ID (human)	Method	Cell system	References
P2RX4	P2X4 Receptor	Q99571	IP-WB	HEK293, BMDM	Guo et al., 2007
			IP-WB	BMDM	Boumechache et al., 2009
			nPAGE/IP-WB	Alveolar epithelial E10 cells	Weinhold et al., 2010
			PD/IP-WB	tsA 201	Antonio et al., 2011
			IP-WB	Primary gingival epithelial cells	Hung et al., 2013
			IP-WB	HEK293	Pérez-Flores et al., 2015
PANX1	Pannexin-1	Q96RD7	IP-WB	HEK293	Pelegrin and Surprenant, 2006
			IP-WB	J774.2	Iglesias et al., 2008
			IP-WB	Primary neurons	Silverman et al., 2009
			IP-WB	HEK293	Li et al., 2011
			IP-WB	N2a	Poornima et al., 2012
			IP-WB	HPDL	Kanjanamekanant et al., 2014
			PD-WB	N2a	Boyce and Swayne, 2017
PI4KA	Phosphatidylinositol 4-kinase α	P42356	IP-MS/WB	HEK293	Kim et al., 2001
PPIP5K1	Inositol hexakisphosphate and diphosphoinositol-pentakisphosphate kinase 1	Q6PFW1	IP-MS	THP-1	Gu et al., 2009
PMP22	Peripheral myelin protein 22	Q01453	Y2H, PD-WB	HEK293	Wilson et al., 2002
PRKCG	Protein kinase C γ type	P05129	IP-WB	Astrocyte cell line (RBA-2)	Hung et al., 2005
PTPN6	Tyrosine-protein phosphatase non-receptor type 6	P29350	IP-MS	THP-1	Gu et al., 2009
PTPRB	Receptor-type tyrosine-protein phosphatase β	P23467	IP-MS	HEK293	Kim et al., 2001
PYCARD	Apoptosis-associated speck-like protein containing a CARD (ASC)	Q9ULZ3	IP-WB	Primary neurons	Silverman et al., 2009
			IP-WB	Astrocytes	Minkiewicz et al., 2013
Snca	α-synuclein	P37840	IP-WB	Microglia cell line BV2	Jiang et al., 2015
SVIL	Supervillin	O95425	IP-MS/WB	HEK293	Kim et al., 2001
Tlr2/4	Toll-like receptor 2/4	O60603 O00206	IP-WB	Peritoneal macrophages	Babelova et al., 2009
TM9SF1	Transmembrane 9 superfamily member 1	O15321	Y2H	Liver cDNA library	Wang et al., 2011
TPR	Nucleoprotein TPR	P12270	IP-MS	HEK293	Gu et al., 2009
TRIM21*	E3 ubiquitin-protein ligase TRIM21 (52 kDa Ro protein)	P19474	IP-MS	THP-1; HEK293	Gu et al., 2009
TUBB*	Tubulin β chain	P07437	IP-MS	HEK293	Gu et al., 2009

Asterisks indicate proteins that are frequently found as contaminants in MS-based approaches (Mellacheruvu et al., 2013). PD, pull down; IP, immunoprecipitation; WB, western blot; MS, mass spectrometry; nPAGE, native PAGE; Y2H, yeast two-hybrid.

interactions have not been described. Only interaction partners that were studied in more detail and selected proteins will be briefly described in the following sections.

Proteins Involved in P2X7-Mediated Interleukin Secretion

Pathogen-associated molecular patterns like LPS activate innate immune responses via binding to TLR4. CD14 serves as a co-receptor of TLR4 to facilitate the cellular responses to LPS (Zanoni and Granucci, 2013). As described [see Section "Trafficking and Lipid Interaction Domains (∼residues 540–595)"], P2X7 harbors a potential LPS binding motif in its C-terminal domain (Denlinger et al., 2001) and CD14 was identified as a potential co-receptor of P2X7 that enables LPS internalization and binding to P2X7. Their physical interaction was shown in immunoprecipitation experiments with transfected HEK293 cells. LPS stimulation increased their co-localization and the amount of co-precipitated CD14 or P2X7 proteins (Dagvadorj et al., 2015).

MyD88 is another protein that is tightly associated with TLR function. TLR4 can signal through MyD88 to induce the synthesis of pro-inflammatory cytokines via the activation of NF-κB. In transfected HEK293 cells, it was shown that MyD88 physically interacts with P2X7, suggesting that MyD88 is responsible for P2X7-mediated NF-κB activation. The C-terminus of P2X7 and, in particular, the amino acid G586 was shown to be important for this interaction. Alanine substitution of G586 lead to a loss of P2X7 function, decreased caspase 1 cleavage activity, altered cellular localization, and impaired interaction between P2X7 and MyD88 in mouse, P2X7-expressing HEK293 cells and RAW264.7 cells (Liu et al., 2011).

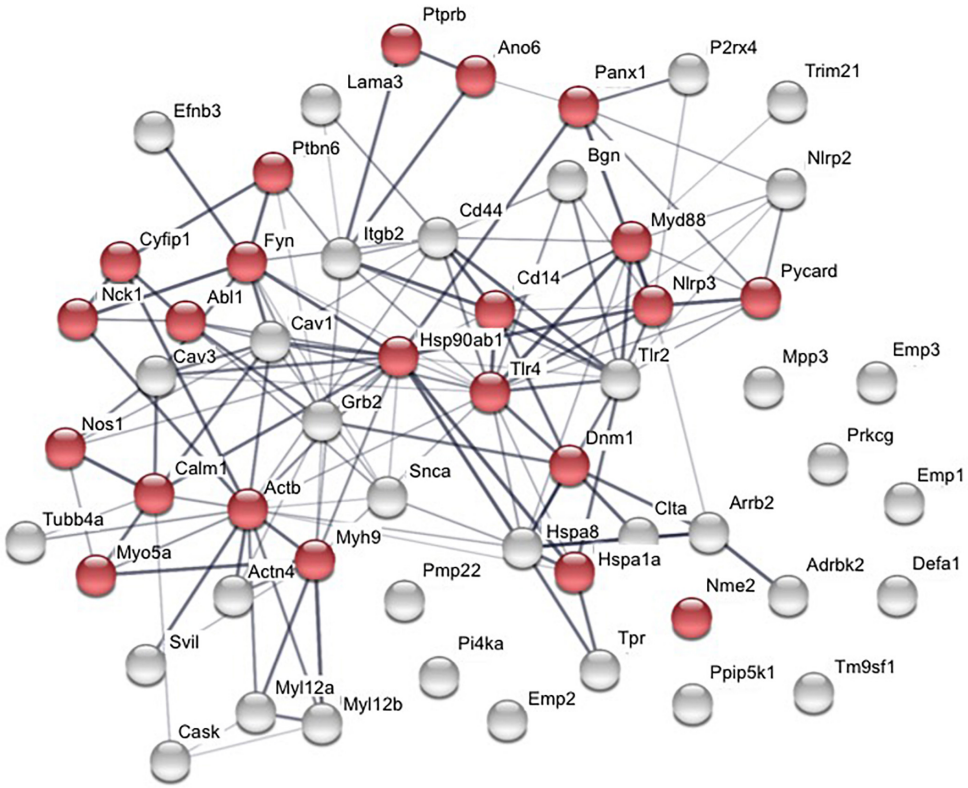

FIGURE 2 | Interaction network of published P2X7 interaction partners. Proteins were analyzed using STRING database (v11.0; Szklarczyk et al., 2019). Twenty-two proteins are involved in function of the innate immune system (shown in red). The thickness of the connecting lines indicates the strength of data support for physical and/or functional associations.

Inflammation is not only triggered by the binding of exogenous PAMPs to TLR4, but also mediated via endogenous structures. Soluble biglycan, a proteoglycan of the extracellular matrix, can activate TLR2 and 4 and stimulate inflammatory responses (Schaefer et al., 2005; Moreth et al., 2014). Co-precipitation experiments showed that biglycan can directly interact with P2X4 and P2X7 in peritoneal macrophages (Babelova et al., 2009). Interestingly, also TLR2 and 4 were co-precipitated with anti-P2X4 or anti-P2X7 antibodies in the presence of biglycan.

P2X7 was also found to directly interact with components of the inflammasome such as the adaptor protein ASC of the NLRP1 inflammasome in neurons (Silverman et al., 2009), ASC, and the NLR subunit of the NLRP2 inflammasome in astrocytes (Minkiewicz et al., 2013), and NLRP3 in N13 mouse microglial cells (Franceschini et al., 2015). For NLRP3 and P2X7 also a mutual relationship in mRNA and protein levels was detected and both proteins co-localize at discrete sites in the subplasmalemmal cytoplasm (Franceschini et al., 2015).

Pannexin-1

Pannexin-1 belongs to the pannexin family of channel-forming glycoproteins and has been reported to mediate the release of ATP (Chekeni et al., 2010). It can be activated by various stimuli (e.g., mechanical, caspase cleavage, cytoplasmic Ca^{2+}, membrane depolarization, extracellular ATP, and K^+; Penuela et al., 2013) and has been proposed to form the P2X7-associated macropore (Pelegrin and Surprenant, 2006). Indeed, several co-precipitation experiments revealed a physical interaction with the P2X7 receptor (Pelegrin and Surprenant, 2006; Iglesias et al., 2008; Silverman et al., 2009; Li et al., 2011; Poornima et al., 2012; Kanjanamekanant et al., 2014; Boyce and Swayne, 2017). However, negative pull-down experiments were also reported and more recent studies indicate that the macropore is an intrinsic property of P2X7 and opens immediately upon activation (Harkat et al., 2017; Karasawa et al., 2017; Pippel et al., 2017; Di Virgilio et al., 2018b). A functional interaction of P2X7 and pannexin in inflammasome activation was also described (Pelegrin and Surprenant, 2006; Locovei et al., 2007; Iglesias et al., 2008; Hung et al., 2013; Boyce et al., 2015; Boyce and Swayne, 2017) but is under discussion (Qu et al., 2011; Hanley et al., 2012; Alberto et al., 2013). As pannexin is considered to mediate the release of ATP, it might play a role upstream of P2X7 by controlling its activation (Chekeni et al., 2010; Isakson and Thompson, 2014).

Heat Shock Protein 90

Heat shock protein (HSP) 90 is a molecular chaperone and ATPase and one of the most abundant cytosolic proteins in eukaryotes. It is essential for protein folding and maturation and has been involved in many different pathologies, including

infections, cancer, and neurodegenerative diseases (Schopf et al., 2017). Two independent MS-based screening approaches in HEK293 cells identified HSP90 as potential interactor of P2X7 (Kim et al., 2001; Gu et al., 2009) and the cysteine-rich domain in the C-terminus was identified to be important for this interaction (Migita et al., 2016). Phosphorylation of HSP90 was shown to decrease P2X7 currents and membrane blebbing in HEK293 cells and rat peritoneal macrophages (Adinolfi et al., 2003). Nitration of the chaperone increased P2X7-dependent activation of the Fas pathway and subsequent apoptosis in PC12 cells (Franco et al., 2013). Fas (CD95) is a member of the tumor necrosis factor receptor (TNFR) superfamily and plays a central role in apoptosis. HSP90 was also found to be involved in P2X7 pore formation and P2X7-dependent autophagic death of dystrophic muscles (Young et al., 2015) as well as the activation of the P2X7/NLRP3 inflammasome pathway (Zuo et al., 2018). It was shown that HSP90 directly interacts with the LRR and NACHT domains of NLRP3 and is essential for inflammasome function and activity (Mayor et al., 2007).

Caveolin

Caveolins are the most abundant membrane proteins in caveolae and act as scaffolding and membrane curvature inducing proteins. Caveolae are invaginations of the plasma membrane and, similar to lipid rafts, enriched in cholesterol and glycosphingolipids (Patel and Insel, 2008). The caveolin family comprises three family members (caveolin-1, -2, -3). In E10 alveolar epithelial cells, P2X7 was found to be associated with caveolae and partially co-localized with caveolin-1 (Barth et al., 2007). A direct interaction of both proteins was shown via co-precipitation (Barth et al., 2008). This interaction was further verified via native PAGE, which indicated that both proteins are present in the same protein complex (Weinhold et al., 2010). Similar results were obtained in cardiomyocytes, where also caveolin-3 was detected (Pfleger et al., 2012). A mutual relation in expression and localization was shown (Barth et al., 2007; Weinhold et al., 2010).

Anoctamin Channels

Anoctamin channels (TMEM16 family) are calcium-activated Cl^- channels and are co-expressed with P2X7 in various cell types. Since a P2X7-mediated increase in anion conductance has been observed in several studies, a physical or functional interaction with anoctamin channels was investigated (Stolz et al., 2015). In *Xenopus laevis* and *Ambystoma mexicanum* oocytes [which lack endogenous anoctamin(s)], a functional interaction between heterologously expressed P2X7 and anoctamin-1 could be shown, but not for anoctamin-6 (Stolz et al., 2015). However, another study in the same year could show a P2X7-mediated activation of anoctamin-6 in *Xenopus laevis* oocytes, transfected HEK293 cells, and mouse macrophages and a physical interaction was also shown in co-immunoprecipitation experiments with transfected HEK293 cells (Ousingsawat et al., 2015).

Calmodulin

A novel CaM binding motif was identified in the C-terminus of rat P2X7 [compare Section "Trafficking and Lipid Interaction Domains (∼Residues 540–595)"]. The specific binding of CaM to this region was shown by co-immunoprecipitation and mutagenesis of the binding motif in HEK293 cells (Roger et al., 2008). Interestingly, this binding motif is absent in human and mouse P2X7 and indeed, an interaction of CaM with the human receptor could not be detected but reconstituted by mutagenesis (Roger et al., 2010). The binding of CaM facilitates and prolongs Ca^{2+} entry and was proposed to play a role in cytoskeletal rearrangements and membrane blebbing (Roger et al., 2008).

Myosin-9

The non-muscle myosin-9 was not only shown to co-precipitate with P2X7, but also to co-localize in the plasma membrane and membranes of intracellular organelles in a human monocytic cell line (THP-1 cells). A close association with P2X7 was confirmed by FRET experiments in HEK293 cells (Gu et al., 2009). It was proposed that P2X7 is anchored in the membrane by myosin-9 and activation of P2X7 via extracellular ATP leads to dissociation of the myosin-P2X7 complex and the formation of the large pore and membrane blebbing. It was further suggested that the integrity of this complex is required to regulate P2X7-mediated phagocytosis (Gu et al., 2010).

CONCLUSION

Blockade or genetic deletion of the P2X7 receptor has shown positive effects in numerous disease models and genetic association studies have linked SNPs of this receptor with various human diseases. While P2X7-induced cytokine secretion and/or cell death have been identified as important mechanisms that contribute to its pathophysiological role, the relevance and in particular, the molecular mechanism leading to the induction of many other identified P2X7-induced effects remain much less investigated. The extended P2X7 C-terminus has been involved in many P2X7-specific functions and is supposed to constitute a platform for intracellular interactions that initiate multiple signaling pathways. Although more than 50 interacting proteins have been identified (**Table 1**), their roles in receptor signaling, trafficking, regulation, or modification remain largely obscure and in most cases, the sites of interaction, the aa involved, and the molecular mechanisms are unknown. Many of the identified interactions are likely to depend on the type and/or state of the cell and might also be indirect or due to the association of proteins in larger domains or complexes (e.g., lipid rafts). However, the data need to be interpreted with caution as they include proteins that tend to interact with the solid-phase support or the used affinity tags and are frequently found as contaminants in affinity purification approaches followed by mass spectrometry (MS) (Mellacheruvu et al., 2013) (marked with asterisk in **Table 1**). It further has to be considered, that several proteins were identified in targeted rather than unbiased

screening approaches and most experiments were carried out in heterologous expression systems (in some of which P2X7 is not naturally occurring) and with overexpressed interaction partners, which might bear the risk of artificial aggregation.

In contrast to other receptor complexes, for which interaction partners have been defined (Schwenk et al., 2012, 2016; Hanack et al., 2015), few tight interactions that survived purification were identified for P2X7 and BN-PAGE analysis in mouse and rat tissues did not reveal bands that are reconcilable with complexes containing additional proteins besides the three P2X7 subunits (Nicke, 2008). Of the interaction partners identified in pull-down experiments, only few have been repeatedly identified or confirmed in independent studies. Thus, P2X7 interactions or complexes appear to be rather instable and the P2X7 tail might mainly have a structural role and/or serve as a scaffold for temporary and short-lived interactions in which Ca^{2+} signaling and interactions with membrane components are likely to play a major role. The specific molecular mechanisms involved are largely hypothetical and only few interaction sites have been determined by mutagenesis. Elucidation of these interactions and the downstream signaling pathways involved bears the potential to identify novel ways for therapeutic intervention.

AUTHOR CONTRIBUTIONS

AN conceived and supervised the project. All authors wrote, reviewed, and approved the manuscript. RK prepared the table. AK and RK designed the figures.

FUNDING

This work was supported by grants from the DFG (SFB 1328, A15) and the European Union's Horizon 2020 Research and Innovation Programme (Marie Skłowdowska-Curie Grant Agreement 766124) to AN.

ACKNOWLEDGMENTS

We would like to thank Isabel Müller for help with sequence comparisons.

REFERENCES

Adinolfi, E., Callegari, M. G., Cirillo, M., Pinton, P., Giorgio, C., Cavagna, D., et al. (2009). Expression of the P2X7 receptor increases the Ca2+ content of the endoplasmic reticulum, activates NFATc1, and protects from apoptosis. *J. Biol. Chem.* 284, 10120–10128. doi: 10.1074/jbc.M805805200

Adinolfi, E., Callegari, M. G., Ferrari, D., Bolognesi, C., Minelli, M., Wieckowski, M. R., et al. (2005). Basal activation of the P2X7 ATP receptor elevates mitochondrial calcium and potential, increases cellular ATP levels, and promotes serum-independent growth. *Mol. Biol. Cell* 16, 3260–3272. doi: 10.1091/mbc.e04-11-1025

Adinolfi, E., Cirillo, M., Woltersdorf, R., Falzoni, S., Chiozzi, P., Pellegatti, P., et al. (2010). Trophic activity of a naturally occurring truncated isoform of the P2X7 receptor. *FASEB J.* 24, 3393–3404. doi: 10.1096/fj.09-153601

Adinolfi, E., Kim, M., Young, M. T., Di Virgilio, F., and Surprenant, A. (2003). Tyrosine phosphorylation of HSP90 within the P2X7 receptor complex negatively regulates P2X7 receptors. *J. Biol. Chem.* 278, 37344–37351. doi: 10.1074/jbc.M301508200

Adinolfi, E., Raffaghello, L., Giuliani, A. L., Cavazzini, L., Capece, M., Chiozzi, P., et al. (2012). Expression of P2X7 receptor increases in vivo tumor growth. *Cancer Res.* 72, 2957–2969. doi: 10.1158/0008-5472.CAN-11-1947

Adriouch, S., Dox, C., Welge, V., Seman, M., Koch-Nolte, F., and Haag, F. (2002). Cutting edge: a natural P451L mutation in the cytoplasmic domain impairs the function of the mouse P2X7 receptor. *J. Immunol.* 169, 4108–4112. doi: 10.4049/jimmunol.169.8.4108

Aga, M., Johnson, C. J., Hart, A. P., Guadarrama, A. G., Suresh, M., Svaren, J., et al. (2002). Modulation of monocyte signaling and pore formation in response to agonists of the nucleotide receptor P2X(7). *J. Leukoc. Biol.* 72, 222–232.

Aga, M., Watters, J. J., Pfeiffer, Z. A., Wiepz, G. J., Sommer, J. A., and Bertics, P. J. (2004). Evidence for nucleotide receptor modulation of cross talk between MAP kinase and NF-κB signaling pathways in murine RAW 264.7 macrophages. *Am. J. Physiol. Cell Physiol.* 286, C923–C930. doi: 10.1152/ajpcell.00417.2003

Alarcon-Vila, C., Pizzuto, M., and Pelegrin, P. (2019). Purinergic receptors and the inflammatory response mediated by lipids. *Curr. Opin. Pharmacol.* 47, 90–96. doi: 10.1016/j.coph.2019.02.004

Albalawi, F., Lu, W., Beckel, J. M., Lim, J. C., McCaughey, S. A., and Mitchell, C. H. (2017). The P2X7 receptor primes IL-1β and the NLRP3 inflammasome in astrocytes exposed to mechanical strain. *Front. Cell. Neurosci.* 11:227. doi: 10.3389/fncel.2017.00227

Alberto, A. V. P., Faria, R. X., Couto, C. G. C., Ferreira, L. G. B., Souza, C. A. M., Teixeira, P. C. N., et al. (2013). Is pannexin the pore associated with the P2X7 receptor? *Naunyn Schmiedeberg's Arch. Pharmacol.* 386, 775–787. doi: 10.1007/s00210-013-0868-x

Allsopp, R. C., and Evans, R. J. (2015). Contribution of the juxtatransmembrane intracellular regions to the time course and permeation of ATP-gated P2X7 receptor ion channels. *J. Biol. Chem.* 290, 14556–14566. doi: 10.1074/jbc.M115.642033

Alzola, E., Perez-Etxebarria, A., Kabre, E., Fogarty, D. J., Metioui, M., Chaib, N., et al. (1998). Activation by P2X7 agonists of two phospholipases A2 (PLA2) in ductal cells of rat submandibular gland. Coupling of the calcium-independent PLA2 with kallikrein secretion. *J. Biol. Chem.* 273, 30208–30217. doi: 10.1074/jbc.273.46.30208

Amoroso, F., Capece, M., Rotondo, A., Cangelosi, D., Ferracin, M., Franceschini, A., et al. (2015). The P2X7 receptor is a key modulator of the PI3K/GSK3β/VEGF signaling network: evidence in experimental neuroblastoma. *Oncogene* 34, 5240–5251. doi: 10.1038/onc.2014.444

Amoroso, F., Falzoni, S., Adinolfi, E., Ferrari, D., and Di Virgilio, F. (2012). The P2X7 receptor is a key modulator of aerobic glycolysis. *Cell Death Dis.* 3:e370. doi: 10.1038/cddis.2012.105

Amstrup, J., and Novak, I. (2003). P2X7 receptor activates extracellular signal-regulated kinases ERK1 and ERK2 independently of Ca2+ influx. *Biochem. J.* 374(Pt 1), 51–61. doi: 10.1042/BJ20030585

Anderson, C. M., and Nedergaard, M. (2006). Emerging challenges of assigning P2X7 receptor function and immunoreactivity in neurons. *Trends Neurosci.* 29, 257–262. doi: 10.1016/j.tins.2006.03.003

Andrei, C., Margiocco, P., Poggi, A., Lotti, L. V., Torrisi, M. R., and Rubartelli, A. (2004). Phospholipases C and A2 control lysosome-mediated IL-1 β secretion: implications for inflammatory processes. *Proc. Natl. Acad. Sci. U.S.A.* 101, 9745–9750. doi: 10.1073/pnas.0308558101

Anrather, J., Gallo, E. F., Kawano, T., Orio, M., Abe, T., Gooden, C., et al. (2011). Purinergic signaling induces cyclooxygenase-1-dependent prostanoid synthesis in microglia: roles in the outcome of excitotoxic brain injury. *PLoS One* 6:e25916. doi: 10.1371/journal.pone.0025916

Antonio, L. S., Stewart, A. P., Xu, X. J., Varanda, W. A., Murrell-Lagnado, R. D., and Edwardson, J. M. (2011). P2X4 receptors interact with both P2X2 and P2X7 receptors in the form of homotrimers. *Br. J. Pharmacol.* 163, 1069–1077. doi: 10.1111/j.1476-5381.2011.01303.x

Aprile-Garcia, F., Metzger, M. W., Paez-Pereda, M., Stadler, H., Acuña, M., Liberman, A. C., et al. (2016). Co-Expression of wild-type P2X7R with Gln460Arg variant alters receptor function. *PLoS One* 11:e0151862. doi: 10.1371/journal.pone.0151862

Armstrong, J. N., Brust, T. B., Lewis, R. G., and MacVicar, B. A. (2002). Activation of presynaptic P2X7-like receptors depresses mossy fiber-CA3 synaptic transmission through p38 mitogen-activated protein kinase. *J. Neurosci.* 22, 5938–5945. doi: 10.1523/jneurosci.22-14-05938.2002

Armstrong, S., Pereverzev, A., Dixon, S. J., and Sims, S. M. (2009). Activation of P2X7 receptors causes isoform-specific translocation of protein kinase C in osteoclasts. *J. Cell Sci.* 122(Pt 1), 136–144. doi: 10.1242/jcs.031534

Auger, R., Motta, I., Benihoud, K., Ojcius, D. M., and Kanellopoulos, J. M. (2005). A role for mitogen-activated protein kinase(Erk1/2) activation and non-selective pore formation in P2X7 receptor-mediated thymocyte death. *J. Biol. Chem.* 280, 28142–28151. doi: 10.1074/jbc.M501290200

Babelova, A., Moreth, K., Tsalastra-Greul, W., Zeng-Brouwers, J., Eickelberg, O., Young, M. F., et al. (2009). Biglycan, a danger signal that activates the NLRP3 inflammasome via toll-like and P2X receptors. *J. Biol. Chem.* 284, 24035–24048. doi: 10.1074/jbc.M109.014266

Ballerini, P., Rathbone, M. P., Di Iorio, P., Renzetti, A., Giuliani, P., D'Alimonte, I., et al. (1996). Rat astroglial P2Z (P2X7) receptors regulate intracellular calcium and purine release. *Neuroreport* 7, 2533–2537.

Bannas, P., Adriouch, S., Kahl, S., Braasch, F., Haag, F., and Koch-Nolte, F. (2005). Activity and specificity of toxin-related mouse T cell ecto-ADP-ribosyltransferase ART2.2 depends on its association with lipid rafts. *Blood* 105, 3663–3670. doi: 10.1182/blood-2004-08-3325

Barberà-Cremades, M., Gómez, A. I., Baroja-Mazo, A., Martínez-Alarcón, L., Martínez, C. M., de Torre-Minguela, C., et al. (2017). P2X7 receptor induces tumor necrosis factor-α converting enzyme activation and release to boost TNF-α production. *Front. Immunol.* 8:862. doi: 10.3389/fimmu.2017.00862

Barden, N., Harvey, M., Gagné, B., Shink, E., Tremblay, M., Raymond, C., et al. (2006). Analysis of single nucleotide polymorphisms in genes in the chromosome 12Q24.31 region points to P2RX7 as a susceptibility gene to bipolar affective disorder. *Am. J. Med. Genet. Part B* 141, 374–382. doi: 10.1002/ajmg.b.30303

Barth, K., Weinhold, K., Guenther, A., Linge, A., Gereke, M., and Kasper, M. (2008). Characterization of the molecular interaction between caveolin-1 and the P2X receptors 4 and 7 in E10 mouse lung alveolar epithelial cells. *Int. J. Biochem. Cell Biol.* 40, 2230–2239. doi: 10.1016/j.biocel.2008.03.001

Barth, K., Weinhold, K., Guenther, A., Young, M. T., Schnittler, H., and Kasper, M. (2007). Caveolin-1 influences P2X7 receptor expression and localization in mouse lung alveolar epithelial cells. *FEBS J.* 274, 3021–3033. doi: 10.1111/j.1742-4658.2007.05830.x

Bartlett, R., Stokes, L., and Sluyter, R. (2014). The P2X7 receptor channel: recent developments and the use of P2X7 antagonists in models of disease. *Pharmacol. Rev.* 66, 638–675. doi: 10.1124/pr.113.008003

Becker, D., Woltersdorf, R., Boldt, W., Schmitz, S., Braam, U., Schmalzing, G., et al. (2008). The P2X7 carboxyl tail is a regulatory module of P2X7 receptor channel activity. *J. Biol. Chem.* 283, 25725–25734. doi: 10.1074/jbc.M803855200

Belambri, S. A., Rolas, L., Raad, H., Hurtado-Nedelec, M., Dang, P. M., and El-Benna, J. (2018). NADPH oxidase activation in neutrophils: role of the phosphorylation of its subunits. *Eur. J. Clin. Invest.* 48(Suppl. 2), e12951. doi: 10.1111/eci.12951

Bernier, L. P., Ase, A. R., and Seguela, P. (2013). Post-translational regulation of P2X receptor channels: modulation by phospholipids. *Front. Cell Neurosci.* 7:226. doi: 10.3389/fncel.2013.00226

Bianco, F., Perrotta, C., Novellino, L., Francolini, M., Riganti, L., Menna, E., et al. (2009). Acid sphingomyelinase activity triggers microparticle release from glial cells. *EMBO J.* 28, 1043–1054. doi:10.1038/emboj.2009.45

Bianco, F., Pravettoni, E., Colombo, A., Schenk, U., Möller, T., Matteoli, M., et al. (2005). Astrocyte-derived ATP induces vesicle shedding and IL-1 β release from microglia. *J. Immunol.* 174, 7268–7277. doi:10.4049/jimmunol.174.11.7268

Bobanovic, L. K., Royle, S. J., and Murrell-Lagnado, R. D. (2002). P2X receptor trafficking in neurons is subunit specific. *J. Neurosci.* 22, 4814–4824. doi: 10.1523/jneurosci.22-12-04814.2002

Boldt, W., Klapperstück, M., Büttner, C., Sadtler, S., Schmalzing, G., and Markwardt, F. (2013). Glu 496 Ala polymorphism of human P2X 7 receptor does not affect its electrophysiological phenotype. *Am. J. Physiol. Cell Physiol.* 284, C749–C756. doi: 10.1152/ajpcell.00042.2002

Boumechache, M., Masin, M., Edwardson, J. M., Górecki, D., and Murrell-Lagnado, R. (2009). Analysis of assembly and trafficking of native P2X4 and P2X7 receptor complexes in rodent immune cells. *J. Biol. Chem.* 284, 13446–13454. doi: 10.1074/jbc.M901255200

Boyce, A. K. J., Kim, M. S., Wicki-Stordeur, L. E., and Swayne, L. A. (2015). ATP stimulates pannexin 1 internalization to endosomal compartments. *Biochem. J.* 470, 319–330. doi: 10.1042/BJ20141551

Boyce, A. K. J., and Swayne, L. A. (2017). P2X7 receptor cross-talk regulates ATP-induced pannexin 1 internalization. *Biochem. J.* 474, 2133–2144. doi: 10.1042/BCJ20170257

Bradford, M. D., and Soltoff, S. P. (2002). P2X7 receptors activate protein kinase D and p42/p44 mitogen-activated protein kinase (MAPK) downstream of protein kinase C. *Biochem. J.* 366(Pt 3), 745–755. doi: 10.1042/BJ20020358

Browne, L. E., Compan, V., Bragg, L., and North, R. A. (2013). P2X7 receptor channels allow direct permeation of nanometer-sized dyes. *J. Neurosci.* 33, 3557–3566. doi: 10.1523/jneurosci.2235-12.2013

Bruntz, R. C., Lindsley, C. W., and Brown, H. A. (2014). Phospholipase D signaling pathways and phosphatidic acid as therapeutic targets in cancer. *Pharmacol. Rev.* 66, 1033–1079. doi: 10.1124/pr.114.009217

Burnstock, G., and Knight, G. E. (2018). The potential of P2X7 receptors as a therapeutic target, including inflammation and tumour progression. *Purinergic Signal.* 14, 1–18. doi: 10.1007/s11302-017-9593-0

Carrasquero, L. M., Delicado, E. G., Sanchez-Ruiloba, L., Iglesias, T., and Miras-Portugal, M. T. (2010). Mechanisms of protein kinase D activation in response to P2Y(2) and P2X7 receptors in primary astrocytes. *Glia* 58, 984–995. doi: 10.1002/glia.20980

Casas-Pruneda, G., Reyes, J. P., Pérez-Flores, G., Pérez-Cornejo, P., and Arreola, J. (2009). Functional interactions between P2X4 and P2X7 receptors from mouse salivary epithelia. *J. Physiol.* 587, 2887–2901. doi: 10.1113/jphysiol.2008.167395

Chaib, N., Kabre, E., Alzola, E., Pochet, S., and Dehaye, J. P. (2000). Bromoenol lactone enhances the permeabilization of rat submandibular acinar cells by P2X7 agonists. *Br. J. Pharmacol.* 129, 703–708. doi: 10.1038/sj.bjp.0703124

Charras, G. T. (2008). A short history of blebbing. *J. Microsc.* 231, 466–478. doi: 10.1111/j.1365-2818.2008.02059.x

Chaumont, S., and Khakh, B. S. (2008). Patch-clamp coordinated spectroscopy shows P2X2 receptor permeability dynamics require cytosolic domain rearrangements but not Panx-1 channels. *Proc. Natl. Acad. Sci. U.S.A.* 105, 12063–12068. doi: 10.1073/pnas.0803008105

Chekeni, F. B., Elliott, M. R., Sandilos, J. K., Walk, S. F., Kinchen, J. M., Lazarowski, E. R., et al. (2010). Pannexin 1 channels mediate 'find-me' signal release and membrane permeability during apoptosis. *Nature* 467, 863–867. doi: 10.1038/nature09413

Chen, J. R., Ben, J. G. U., Dao, L. P., Bradley, C. J., Mulligan, S. P., and Wiley, J. S. (1999). Transendothelial migration of lymphocytes in chronic lymphocytic leukaemia is impaired and involves down-regulation of both L-selectin and CD23. *Br. J. Haematol.* 105, 181–189. doi: 10.1111/j.1365-2141.1999.01278.x

Chen, Q., Jin, Y., Zhang, K., Li, H., Chen, W., Meng, G., et al. (2014). Alarmin HNP-1 promotes pyroptosis and IL-1β release through different roles of NLRP3 inflammasome via P2X7 in LPS-primed macrophages. *Innate Immun.* 20, 290–300. doi: 10.1177/1753425913490575

Christian, F., Smith, E., and Carmody, R. (2016). The Regulation of NF-κB subunits by phosphorylation. *Cells* 5, 12–12. doi: 10.3390/cells5010012

Clark, A. K., Wodarski, R., Guida, F., Sasso, O., and Malcangio, M. (2010). Cathepsin S release from primary cultured microglia is regulated by the P2X7 receptor. *Glia* 58, 1710–1726. doi: 10.1002/glia.21042

Costa-Junior, H. M., Marques-da-Silva, C., Vieira, F. S., Moncao-Ribeiro, L. C., and Coutinho-Silva, R. (2011). Lipid metabolism modulation by the P2X7 receptor in the immune system and during the course of infection: new insights into the old view. *Purinergic Signal.* 7, 381–392. doi: 10.1007/s11302-011-9255-6

Coutinho-Silva, R., Stahl, L., Raymond, M. N., Jungas, T., Verbeke, P., Burnstock, G., et al. (2003). Inhibition of chlamydial infectious activity due to P2X7R-dependent phospholipase D activation. *Immunity* 19, 403–412. doi: 10.1016/s1074-7613(03)00235-8

Craigie, E., Birch, R. E., Unwin, R. J., and Wildman, S. S. (2013). The relationship between P2X4 and P2X7: A physiologically important interaction? *Front. Physiol.* 4:216. doi: 10.3389/fphys.2013.00216

Dagvadorj, J., Shimada, K., Chen, S., Jones, H. D., Tumurkhuu, G., Zhang, W., et al. (2015). Lipopolysaccharide induces alveolar macrophage necrosis via CD14 and the P2X7 receptor leading to interleukin-1α release. *Immunity* 42, 640–653. doi: 10.1016/j.immuni.2015.03.007

de Torre-Minguela, C., Barbera-Cremades, M., Gomez, A. I., Martin-Sanchez, F., and Pelegrin, P. (2016). Macrophage activation and polarization modify P2X7 receptor secretome influencing the inflammatory process. *Sci. Rep.* 6:22586. doi: 10.1038/srep22586

Denlinger, L. C., Fisette, P. L., Sommer, J. A., Watters, J. J., Prabhu, U., Dubyak, G. R., et al. (2001). Cutting edge: the nucleotide receptor P2X7 contains multiple protein- and lipid-interaction motifs including a potential binding site for bacterial lipopolysaccharide. *J. Immunol.* 167, 1871–1876. doi: 10.4049/jimmunol.167.4.1871

Denlinger, L. C., Sommer, J. A., Parker, K., Gudipaty, L., Fisette, P. L., Watters, J. W., et al. (2003). Mutation of a dibasic amino acid motif within the C terminus of the P2X7 nucleotide receptor results in trafficking defects and impaired function. *J. Immunol.* 171, 1304–1311. doi: 10.4049/jimmunol.171.3.1304

Di, A., Xiong, S., Ye, Z., Malireddi, R. K. S., Kometani, S., Zhong, M., et al. (2018). The TWIK2 Potassium Efflux Channel in Macrophages Mediates NLRP3 Inflammasome-Induced Inflammation. *Immunity* 49, 56.e4–65.e4. doi: 10.1016/j.immuni.2018.04.032

Di Virgilio, F., Dal Ben, D., Sarti, A. C., Giuliani, A. L., and Falzoni, S. (2017). The P2X7 Receptor in Infection and Inflammation. *Immunity* 47, 15–31. doi: 10.1016/j.immuni.2017.06.020

Di Virgilio, F., Sarti, A. C., and Grassi, F. (2018a). Modulation of innate and adaptive immunity by P2X ion channels. *Curr. Opin. Immun.* 52, 51–59. doi: 10.1016/j.coi.2018.03.026

Di Virgilio, F., Schmalzing, G., and Markwardt, F. (2018b). The elusive P2X7 macropore. *Trends Cell Biol.* 28, 392–404. doi: 10.1016/j.tcb.2018.01.005

Diaz-Hernandez, M., del Puerto, A., Diaz-Hernandez, J. I., Diez-Zaera, M., Lucas, J. J., Garrido, J. J., et al. (2008). Inhibition of the ATP-gated P2X7 receptor promotes axonal growth and branching in cultured hippocampal neurons. *J. Cell Sci.* 121(Pt 22), 3717–3728. doi: 10.1242/jcs.034082

Diaz-Rodriguez, E., Montero, J. C., Esparis-Ogando, A., Yuste, L., and Pandiella, A. (2002). Extracellular signal-regulated kinase phosphorylates tumor necrosis factor α-converting enzyme at threonine 735: a potential role in regulated shedding. *Mol. Biol. Cell* 13, 2031–2044. doi: 10.1091/mbc.01-11-0561

Dinarello, C. A. (2018). Introduction to the interleukin-1 family of cytokines and receptors: drivers of innate inflammation and acquired immunity. *Immunol. Rev.* 281, 5–7. doi: 10.1111/imr.12624

Donnelly-Roberts, D. L., Namovic, M. T., Han, P., and Jarvis, M. F. (2009). Mammalian P2X7 receptor pharmacology: comparison of recombinant mouse, rat and human P2X7 receptors. *Br. J. Pharmacol.* 157, 1203–1214. doi: 10.1111/j.1476-5381.2009.00233.x

Duan, S., Anderson, C. M., Keung, E. C., Chen, Y., Chen, Y., and Swanson, R. A. (2003). P2X7 receptor-mediated release of excitatory amino acids from astrocytes. *J. Neurosci.* 23, 1320–1328. doi: 10.1523/jneurosci.23-04-01320.2003

Dubyak, G. R. (2007). Go it alone no more–P2X7 joins the society of heteromeric ATP-gated receptor channels. *Mol. Pharmacol.* 72, 1402–1405. doi: 10.1124/mol.107.042077

Dubyak, G. R. (2012). P2X7 receptor regulation of non-classical secretion from immune effector cells. *Cell Microbiol.* 14, 1697–1706. doi: 10.1111/cmi.12001

El Ouaaliti, M., Seil, M., and Dehaye, J. P. (2012). Activation of calcium-insensitive phospholipase A2 (iPLA 2) by P2X7 receptors in murine peritoneal macrophages. *Prostaglandins Other Lipid Mediat.* 99, 116–123. doi: 10.1016/j.prostaglandins.2012.09.005

Elliott, J. I., Surprenant, A., Marelli-Berg, F. M., Cooper, J. C., Cassady-Cain, R. L., Wooding, C., et al. (2005). Membrane phosphatidylserine distribution as a non-apoptotic signalling mechanism in lymphocytes. *Nature Cell Biol.* 7, 808–816. doi: 10.1038/ncb1279

el-Moatassim, C., and Dubyak, G. R. (1992). A novel pathway for the activation of phospholipase D by P2z purinergic receptors in BAC1.2F5 macrophages. *J. Biol. Chem.* 267, 23664–23673.

Evavold, C. L., Ruan, J., Tan, Y., Xia, S., Wu, H., and Kagan, J. C. (2018). The pore-forming protein gasdermin D regulates interleukin-1 secretion from living macrophages. *Immunity* 48 35.e6–44.e6. doi: 10.1016/j.immuni.2017.11.013

Fackler, O. T., and Grosse, R. (2008). Cell motility through plasma membrane blebbing. *J. Cell Biol.* 181, 879–884. doi: 10.1083/jcb.200802081

Fairbairn, I. P., Stober, C. B., Kumararatne, D. S., and Lammas, D. A. (2001). ATP-mediated killing of intracellular mycobacteria by macrophages is a P2X(7)-dependent process inducing bacterial death by phagosome-lysosome fusion. *J. Immunol.* 167, 3300–3307. doi: 10.4049/jimmunol.167.6.3300

Feng, J.-F., Gao, X.-F., Pu, Y.-y., Burnstock, G., Xiang, Z., and He, C. (2015). P2X7 receptors and Fyn kinase mediate ATP-induced oligodendrocyte progenitor cell migration. *Purinergic Signal.* 11, 361–369. doi: 10.1007/s11302-015-9458-3

Feng, Y.-H., Wang, L., Wang, Q., Li, X., Zeng, R., and Gorodeski, G. I. (2005). ATP stimulates GRK-3 phosphorylation and β-arrestin-2-dependent internalization of $P2X_7$ receptor. *Am. J. Physiol. Cell Physiol.* 288, C1342–C1356. doi: 10.1152/ajpcell.00315.2004

Ferrari, D., Chiozzi, P., Falzoni, S., Dal Susino, M., Collo, G., Buell, G., et al. (1997a). ATP-mediated cytotoxicity in microglial cells. *Neuropharmacology* 36, 1295–1301. doi: 10.1016/s0028-3908(97)00137-8

Ferrari, D., Wesselborg, S., Bauer, M. K., and Schulze-Osthoff, K. (1997b). Extracellular ATP activates transcription factor NF-kappaB through the P2Z purinoreceptor by selectively targeting NF-kappaB p65. *J. Cell Biol.* 139, 1635–1643. doi: 10.1083/jcb.139.7.1635

Ferrari, D., Stroh, C., and Schulze-Osthoff, K. (1999). P2X7/P2Z purinoreceptor-mediated activation of transcription factor NFAT in microglial cells. *J. Biol. Chem.* 274, 13205–13210. doi: 10.1074/jbc.274.19.13205

Franceschini, A., Capece, M., Chiozzi, P., Falzoni, S., Sanz, J. M., Sarti, A. C., et al. (2015). The P2X7 receptor directly interacts with the NLRP3 inflammasome scaffold protein. *FASEB J.* 29, 2450–2461. doi: 10.1096/fj.14-268714

Franco, M. C., Ye, Y., Refakis, C. A., Feldman, J. L., Stokes, A. L., Basso, M., et al. (2013). Nitration of Hsp90 induces cell death. *Proc. Natl. Acad. Sci.* 110, E1102–E1111. doi: 10.1073/pnas.1215177110

Friedle, S. A., Brautigam, V. M., Nikodemova, M., Wright, M. L., and Watters, J. J. (2011). The P2X7-Egr pathway regulates nucleotide-dependent inflammatory gene expression in microglia. *Glia* 59, 1–13. doi: 10.1002/glia.21071

Fukami, K., Inanobe, S., Kanemaru, K., and Nakamura, Y. (2010). Phospholipase C is a key enzyme regulating intracellular calcium and modulating the phosphoinositide balance. *Prog. Lipid Res.* 49, 429–437. doi: 10.1016/j.plipres.2010.06.001

Fuller, S. J., Stokes, L., Skarratt, K. K., Gu, B. J., and Wiley, J. S. (2009). Genetics of the P2X7 receptor and human disease. *Purinergic signal.* 5, 257–262. doi: 10.1007/s11302-009-9136-4

Garbers, C., Jänner, N., Chalaris, A., Moss, M. L., Floss, D. M., Meyer, D., et al. (2011). Species specificity of ADAM10 and ADAM17 proteins in interleukin-6 (IL-6) trans-signaling and novel role of ADAM10 in inducible IL-6 receptor shedding. *J. Biol. Chem.* 286, 14804–14811. doi: 10.1074/jbc.M111.229393

Garcia-Marcos, M., Pérez-Andrés, E., Tandel, S., Fontanils, U., Kumps, A., Kabré, E., et al. (2006a). Coupling of two pools of P2X7 receptors to distinct intracellular signaling pathways in rat submandibular gland. *J. Lipid Res.* 47, 705–714. doi: 10.1194/jlr.M500408-JLR200

Garcia-Marcos, M., Pochet, S., Marino, A., and Dehaye, J.-P. (2006b). P2X7 and phospholipid signalling: the search of the "missing link" in epithelial cells. *Cell. Signal.* 18, 2098–2104. doi: 10.1016/j.cellsig.2006.05.008

Gargett, C. E., Cornish, E. J., and Wiley, J. S. (1996). Phospholipase D activation by P2Z-purinoceptor agonists in human lymphocytes is dependent on bivalent cation influx. *Biochem. J.* 313(Pt 2), 529–535. doi: 10.1042/bj3130529

Gavala, M. L., Hill, L. M., Lenertz, L. Y., Karta, M. R., and Bertics, P. J. (2010). Activation of the transcription factor FosB/activating protein-1 (AP-1) is a prominent downstream signal of the extracellular nucleotide receptor P2RX7 in monocytic and osteoblastic cells. *J. Biol. Chem.* 285, 34288–34298. doi: 10.1074/jbc.M110.142091

Gendron, F. P., Neary, J. T., Theiss, P. M., Sun, G. Y., Gonzalez, F. A., and Weisman, G. A. (2003). Mechanisms of P2X7 receptor-mediated ERK1/2 phosphorylation

in human astrocytoma cells. *Am. J. Physiol. Cell Physiol.* 284, C571–C581. doi: 10.1152/ajpcell.00286.2002

Genetos, D. C., Karin, N. J., Geist, D. J., Donahue, H. J., and Duncan, R. L. (2011). Purinergic signaling is required for fluid shear stress-induced NF-κB translocation in osteoblasts. *Exp. Cell Res.* 317, 737–744. doi: 10.1016/j.yexcr.2011.01.007

Ghiringhelli, F., Apetoh, L., Tesniere, A., Aymeric, L., Ma, Y., Ortiz, C., et al. (2009). Activation of the NLRP3 inflammasome in dendritic cells induces IL-1B-dependent adaptive immunity against tumors. *Nat. Med.* 15, 1170–1178. doi: 10.1038/nm.2028

Giuliani, A. L., Colognesi, D., Ricco, T., Roncato, C., Capece, M., Amoroso, F., et al. (2014). Trophic activity of human P2X7 receptor isoforms A and B in osteosarcoma. *PLoS One* 9:e107224. doi: 10.1371/journal.pone.0107224

Giuliani, A. L., Sarti, A. C., Falzoni, S., and Di Virgilio, F. (2017). The P2X7 Receptor-Interleukin-1 liaison. *Front. Pharmacol.* 8:123. doi: 10.3389/fphar.2017.00123

Gomez-Munoz, A., Presa, N., Gomez-Larrauri, A., Rivera, I. G., Trueba, M., and Ordonez, M. (2016). Control of inflammatory responses by ceramide, sphingosine 1-phosphate and ceramide 1-phosphate. *Prog. Lipid Res.* 61, 51–62. doi: 10.1016/j.plipres.2015.09.002

Gomez-Villafuertes, R., del Puerto, A., Diaz-Hernandez, M., Bustillo, D., Diaz-Hernandez, J. I., Huerta, P. G., et al. (2009). Ca2+/calmodulin-dependent kinase II signalling cascade mediates P2X7 receptor-dependent inhibition of neuritogenesis in neuroblastoma cells. *FEBS J.* 276, 5307–5325. doi: 10.1111/j.1742-4658.2009.07228.x

Gonnord, P., Delarasse, C., Auger, R., Benihoud, K., Prigent, M., Cuif, M. H., et al. (2008). Palmitoylation of the P2X7 receptor, an ATP-gated channel, controls its expression and association with lipid rafts. *FASEB J.* 23, 795–805. doi: 10.1096/fj.08-114637

Graziano, F., Desdouits, M., Garzetti, L., Podini, P., Alfano, M., Rubartelli, A., et al. (2015). Extracellular ATP induces the rapid release of HIV-1 from virus containing compartments of human macrophages. *Proc. Natl. Acad. Sci. U.S.A.* 112, E3265–E3273. doi: 10.1073/pnas.1500656112

Gross, O., Thomas, C. J., Guarda, G., and Tschopp, J. (2011). The inflammasome: an integrated view. *Immunol. Rev.* 243, 136–151. doi: 10.1111/j.1600-065X.2011.01046.x

Grötzinger, J., Lorenzen, I., and Düsterhöft, S. (2017). Molecular insights into the multilayered regulation of ADAM17: the role of the extracellular region. *Biochim. Biophys. Acta Mol. Cell Res.* 1864, 2088–2095. doi: 10.1016/j.bbamcr.2017.05.024

Gu, B., Bendall, L. J., and Wiley, J. S. (1998). Adenosine triphosphate-induced shedding of CD23 and L-selectin (CD62L) from lymphocytes is mediated by the same receptor but different metalloproteases. *Blood* 92, 946–951.

Gu, B. J., Rathsam, C., Stokes, L., McGeachie, A. B., and Wiley, J. S. (2009). Extracellular ATP dissociates nonmuscle myosin from P2X(7) complex: this dissociation regulates P2X(7) pore formation. *Am. J. Physiol. Cell Physiol.* 297, C430–C439. doi: 10.1152/ajpcell.00079.2009

Gu, B. J., Saunders, B. M., Jursik, C., and Wiley, J. S. (2010). The P2X7-nonmuscle myosin membrane complex regulates phagocytosis of nonopsonized particles and bacteria by a pathway attenuated by extracellular ATP. *Blood* 115, 1621–1631. doi: 10.1182/blood-2009-11-251744

Gu, B. J., Zhang, W., Worthington, R. A., Sluyter, R., Dao-Ung, P., Petrou, S., et al. (2001). A Glu-496 to Ala polymorphism leads to loss of function of the human P2X7 receptor. *J. Biol. Chem.* 276, 11135–11142. doi: 10.1074/jbc.M010353200

Guerra, A. N., Gavala, M. L., Chung, H. S., and Bertics, P. J. (2007). Nucleotide receptor signalling and the generation of reactive oxygen species. *Purinergic Signal.* 3, 39–51. doi: 10.1007/s11302-006-9035-x

Guo, C., Masin, M., Qureshi, O. S., and Murrell-Lagnado, R. D. (2007). Evidence for functional P2X4/P2X7 heteromeric receptors. *Mol. Pharmacol.* 72, 1447–1456. doi: 10.1124/mol.107.035980

Hanack, C., Moroni, M., Lima, W. C., Wende, H., Kirchner, M., Adelfinger, L., et al. (2015). GABA blocks pathological but not acute TRPV1 pain signals. *Cell* 160, 759–770. doi: 10.1016/j.cell.2015.01.022

Hanley, P. J., Kronlage, M., Kirschning, C., Del Rey, A., Di Virgilio, F., Leipziger, J., et al. (2012). Transient P2X 7 receptor activation triggers macrophage death independent of toll-like receptors 2 and 4, caspase-1, and pannexin-1 proteins. *J. Biol. Chem.* 287, 10650–10663. doi: 10.1074/jbc.M111.332676

Harkat, M., Peverini, L., Cerdan, A. H., Dunning, K., Beudez, J., Martz, A., et al. (2017). On the permeation of large organic cations through the pore of ATP-gated P2X receptors. *Proc. Natl. Acad. Sci. U.S.A.* 114, E3786–E3795. doi: 10.1073/pnas.1701379114

Haslund-Vinding, J., McBean, G., Jaquet, V., and Vilhardt, F. (2017). NADPH oxidases in oxidant production by microglia: activating receptors, pharmacology and association with disease. *Br. J. Pharmacol.* 174, 1733–1749. doi: 10.1111/bph.13425

He, Y., Hara, H., and Nunez, G. (2016a). Mechanism and regulation of NLRP3 inflammasome activation. *Trends Biochem. Sci.* 41, 1012–1021. doi: 10.1016/j.tibs.2016.09.002

He, Y., Zeng, M. Y., Yang, D., Motro, B., and Nunez, G. (2016b). NEK7 is an essential mediator of NLRP3 activation downstream of potassium efflux. *Nature* 530, 354–357. doi: 10.1038/nature16959

Hibell, A. D., Thompson, K. M., Simon, J., Xing, M., Humphrey, P. P., and Michel, A. D. (2001). Species- and agonist-dependent differences in the deactivation-kinetics of P2X7 receptors. *Naunyn Schmiedebergs Arch. Pharmacol.* 363, 639–648. doi: 10.1007/s002100100412

Hirayama, Y., Ikeda-Matsuo, Y., Notomi, S., Enaida, H., Kinouchi, H., and Koizumi, S. (2015). Astrocyte-mediated ischemic tolerance. *J. Neurosci.* 35, 3794–3805. doi: 10.1523/JNEUROSCI.4218-14.2015

Hirayama, Y., and Koizumi, S. (2017). Hypoxia-independent mechanisms of HIF-1α expression in astrocytes after ischemic preconditioning. *Glia* 65, 523–530. doi: 10.1002/glia.23109

Hou, Z., and Cao, J. (2016). Comparative study of the P2X gene family in animals and plants. *Purinergic Signal.* 12, 269–281. doi: 10.1007/s11302-016-9501-z

Hu, Y., Fisette, P. L., Denlinger, L. C., Guadarrama, A. G., Sommer, J. A., Proctor, R. A., et al. (1998). Purinergic receptor modulation of lipopolysaccharide signaling and inducible nitric-oxide synthase expression in RAW 264.7 macrophages. *J. Biol. Chem.* 273, 27170–27175. doi: 10.1074/jbc.273.42.27170

Humphreys, B. D., and Dubyak, G. R. (1996). Induction of the P2z/P2X7 nucleotide receptor and associated phospholipase D activity by lipopolysaccharide and IFN-gamma in the human THP-1 monocytic cell line. *J. Immunol.* 157, 5627–5637.

Humphreys, B. D., Rice, J., Kertesy, S. B., and Dubyak, G. R. (2000). Stress-activated protein kinase/JNK activation and apoptotic induction by the macrophage P2X7 nucleotide receptor. *J. Biol. Chem.* 275, 26792–26798. doi: 10.1074/jbc.M002770200

Hung, A. C., Chu, Y. J., Lin, Y. H., Weng, J. Y., Chen, H. B., Au, Y. C., et al. (2005). Roles of protein kinase C in regulation of P2X7 receptor-mediated calcium signalling of cultured type-2 astrocyte cell line, RBA-2. *Cell. Signal.* 17, 1384–1396. doi: 10.1016/j.cellsig.2005.02.009

Hung, A. C., and Sun, S. H. (2002). The P2X(7) receptor-mediated phospholipase D activation is regulated by both PKC-dependent and PKC-independent pathways in a rat brain-derived Type-2 astrocyte cell line, RBA-2. *Cell. Signal.* 14, 83–92. doi: 10.1016/s0898-6568(01)00230-3

Hung, S. C., Choi, C. H., Said-Sadier, N., Johnson, L., Atanasova, K. R., Sellami, H., et al. (2013). P2X4 assembles with P2X7 and Pannexin-1 in gingival epithelial cells and modulates ATP-induced reactive oxygen species production and inflammasome activation. *PLoS One* 8:e70210. doi: 10.1371/journal.pone.0070210

Iglesias, R., Locovei, S., Roque, A., Alberto, A. P., Dahl, G., Spray, D. C., et al. (2008). P2X 7 receptor-Pannexin1 complex: pharmacology and signaling. *Am. J. Physiol. Cell Physiol.* 295, C752–C760. doi: 10.1152/ajpcell.00228.2008

Illes, P., Khan, T. M., and Rubini, P. (2017). Neuronal P2X7 receptors revisited: do they really exist? *J. Neurosci.* 37, 7049–7062. doi: 10.1523/jneurosci.3103-16.2017

Isakson, B. E., and Thompson, R. J. (2014). Pannexin-1 as a potentiator of ligand-gated receptor signaling. *Channels* 8, 118–123. doi: 10.4161/chan.27978

Ivetic, A. (2018). A head-to-tail view of L-selectin and its impact on neutrophil behaviour. *Cell Tissue Res.* 371, 437–453. doi: 10.1007/s00441-017-2774-x

Jabs, R., Matthias, K., Grote, A., Grauer, M., Seifert, G., and Steinhauser, C. (2007). Lack of P2X receptor mediated currents in astrocytes and GluR type glial cells of the hippocampal CA1 region. *Glia* 55, 1648–1655. doi: 10.1002/glia.20580

Jacques-Silva, M. C., Rodnight, R., Lenz, G., Liao, Z., Kong, Q., Tran, M., et al. (2004). P2X7 receptors stimulate AKT phosphorylation in astrocytes. *Br. J. Pharmacol.* 141, 1106–1117. doi: 10.1038/sj.bjp.0705685

Jamieson, G. P., Snook, M. B., Thurlow, P. J., and Wiley, J. S. (1996). Extracellular ATP causes loss of L-selectin from human lymphocytes via occupancy of P2Z purinoceptors. *J. Cell. Physiol.* 166, 637–642. doi: 10.1002/(sici)1097-4652(199603)166:3<637::aid-jcp19>3.3.co;2-1

Janks, L., Sprague, R. S., and Egan, T. M. (2019). ATP-gated P2X7 receptors require chloride channels to promote inflammation in human macrophages. *J. Immunol.* 202, 883–898. doi: 10.4049/jimmunol.1801101

Jiang, L.-H., Rassendren, F., Mackenzie, A., Zhang, Y.-H., Surprenant, A., and North, R. A. (2005). N-methyl-d-glucamine and propidium dyes utilize different permeation pathways at rat P2X7 receptors. *Am. J. Physiol. Cell Physiol.* 289, C1295–C1302. doi: 10.1152/ajpcell.00253.2005

Jiang, T., Hoekstra, J., Heng, X., Kang, W., Ding, J., Liu, J., et al. (2015). P2X7 receptor is critical in α-synuclein–mediated microglial NADPH oxidase activation. *Neurobiol. Aging* 36, 2304–2318. doi: 10.1016/j.neurobiolaging.2015.03.015

Kaczmarek-Hájek, K., Lörinczi, É, Hausmann, R., and Nicke, A. (2012). Molecular and functional properties of P2X receptors-recent progress and persisting challenges. *Purinergic Signal.* 8, 375–417. doi: 10.1007/s11302-012-9314-7

Kaczmarek-Hájek, K., Zhang, J., Kopp, R., Grosche, A., Rissiek, B., Saul, A., et al. (2018). Re-evaluation of neuronal P2X7 expression using novel mouse models and a P2X7-specific nanobody. *eLife* 7:e36217. doi: 10.7554/elife.36217

Kahlenberg, J. M., and Dubyak, G. R. (2004). Mechanisms of caspase-1 activation by P2X7 receptor-mediated K+ release. *Am. J. Physiol. Cell Physiol.* 286, C1100–C1108. doi: 10.1152/ajpcell.00494.2003

Kahlenberg, J. M., Lundberg, K. C., Kertesy, S. B., Qu, Y., and Dubyak, G. R. (2005). Potentiation of caspase-1 activation by the P2X7 receptor is dependent on TLR signals and requires NF-kappaB-driven protein synthesis. *J. Immunol.* 175, 7611–7622. doi: 10.4049/jimmunol.175.11.7611

Kaneko, T., Li, L., and Li, S. S. C. (2008). The SH3 domain–a family of versatile peptide- and protein-recognition module. *Front. Biosci.* 13, 4938–4952.

Kanjanamekanant, K., Luckprom, P., and Pavasant, P. (2014). P2X7 receptor-Pannexin1 interaction mediates stress-induced interleukin-1 β expression in human periodontal ligament cells. *J. Periodontal Res.* 49, 595–602. doi: 10.1111/jre.12139

Karasawa, A., Michalski, K., Mikhelzon, P., and Kawate, T. (2017). The P2X7 receptor forms a dye-permeable pore independent of its intracellular domain but dependent on membrane lipid composition. *eLife* 6, 1–22. doi: 10.7554/elife.31186

Kataoka, A., Tozaki-Saitoh, H., Koga, Y., Tsuda, M., and Inoue, K. (2009). Activation of P2X7 receptors induces CCL3 production in microglial cells through transcription factor NFAT. *J. Neurochem.* 108, 115–125. doi: 10.1111/j.1471-4159.2008.05744.x

Kawano, A., Tsukimoto, M., Noguchi, T., Hotta, N., Harada, H., Takenouchi, T., et al. (2012). Involvement of P2X4 receptor in P2X7 receptor-dependent cell death of mouse macrophages. *Biochem. Biophys. Res. Commun.* 419, 374–380. doi: 10.1016/j.bbrc.2012.01.156

Kawate, T., Michel, J. C., Birdsong, W. T., and Gouaux, E. (2009). Crystal structure of the ATP-gated P2X4 ion channel in the closed state. *Nature* 460, 592–598. doi: 10.1038/nature08198

Keller, M., Ruegg, A., Werner, S., and Beer, H. D. (2008). Active caspase-1 is a regulator of unconventional protein secretion. *Cell* 132, 818–831. doi: 10.1016/j.cell.2007.12.040

Khakh, B. S., Bao, X. R., Labarca, C., and Lester, H. A. (1999). Neuronal P2X transmitter-gated cation channels change their ion selectivity in seconds. *Nat. Neurosci.* 2, 322–330. doi: 10.1038/7233

Khakh, B. S., and Egan, T. M. (2005). Contribution of transmembrane regions to ATP-gated P2X2 channel permeability dynamics. *J. Biol. Chem.* 280, 6118–6129. doi: 10.1074/jbc.M411324200

Kim, J. E., Kim, D. S., Jin Ryu, H., Il Kim, W., Kim, M. J., Won Kim, D., et al. (2013). The effect of P2X7 receptor activation on nuclear factor-kappa B phosphorylation induced by status epilepticus in the rat hippocampus. *Hippocampus* 23, 500–514. doi: 10.1002/hipo.22109

Kim, M., Jiang, L. H., Wilson, H. L., North, R. A., and Surprenant, A. (2001). Proteomic and functional evidence for a P2X7 receptor signalling complex. *EMBO J.* 20, 6347–6358. doi: 10.1093/emboj/20.22.6347

Korcok, J., Raimundo, L. N., Ke, H. Z., Sims, S. M., and Dixon, S. J. (2004). Extracellular nucleotides act through P2X7 receptors to activate NF-κB in osteoclasts. *J. Bone Miner. Res.* 19, 642–651. doi: 10.1359/JBMR.040108

Kozik, P., Francis, R. W., Seaman, M. N. J., and Robinson, M. S. (2010). A screen for endocytic motifs. *Traffic* 11, 843–855. doi: 10.1111/j.1600-0854.2010.01056.x

Kuehnel, M. P., Rybin, V., Anand, P. K., Anes, E., and Griffiths, G. (2009). Lipids regulate P2X7-receptor-dependent actin assembly by phagosomes via ADP translocation and ATP synthesis in the phagosome lumen. *J. Cell Sci.* 122, 499–504. doi: 10.1242/jcs.034199

Kurochkina, N., and Guha, U. (2013). SH3 domains: modules of protein-protein interactions. *Biophys. Rev.* 5, 29–39. doi:10.1007/s12551-012-0081-z

Kusner, D. J., and Adams, J. (2000). ATP-induced killing of virulent Mycobacterium tuberculosis within human macrophages requires phospholipase D. *J. Immunol.* 164, 379–388. doi: 10.4049/jimmunol.164.1.379

Labasi, J. M., Petrushova, N., Donovan, C., McCurdy, S., Lira, P., Payette, M. M., et al. (2002). Absence of the P2X7 receptor alters leukocyte function and attenuates an inflammatory response. *J. Immunol.* 168, 6436–6445. doi: 10.4049/jimmunol.168.12.6436

Lambrecht, B. N., Vanderkerken, M., and Hammad, H. (2018). The emerging role of ADAM metalloproteinases in immunity. *Nat. Rev. Immunol.* 18, 745–758. doi: 10.1038/s41577-018-0068-5

Le Stunff, H., Auger, R., Kanellopoulos, J., and Raymond, M. N. (2004). The Pro-451 to Leu polymorphism within the C-terminal tail of P2X7 receptor impairs cell death but not phospholipase D activation in murine thymocytes. *J. Biol. Chem.* 279, 16918–16926. doi: 10.1074/jbc.M313064200

Leduc-Pessah, H., Weilinger, N. L., Fan, C. Y., Burma, N. E., Thompson, R. J., and Trang, T. (2017). Site-specific regulation of P2X7 receptor function in microglia gates morphine analgesic tolerance. *J. Neurosci.* 37, 10154–10172. doi: 10.1523/JNEUROSCI.0852-17.2017

Lemaire, I., Falzoni, S., Leduc, N., Zhang, B., Pellegatti, P., Adinolfi, E., et al. (2006). Involvement of the purinergic P2X7 receptor in the formation of multinucleated giant cells. *J. Immunol.* 177, 7257–7265. doi: 10.4049/jimmunol.177.10.7257

Lenertz, L. Y., Gavala, M. L., Hill, L. M., and Bertics, P. J. (2009). Cell signaling via the P2X(7) nucleotide receptor: linkage to ROS production, gene transcription, and receptor trafficking. *Purinergic Signal.* 5, 175–187. doi: 10.1007/s11302-009-9133-7

Lenertz, L. Y., Gavala, M. L., Zhu, Y., and Bertics, P. J. (2011). Transcriptional control mechanisms associated with the nucleotide receptor P2X7, a critical regulator of immunologic, osteogenic, and neurologic functions. *Immunol. Res.* 50, 22–38. doi: 10.1007/s12026-011-8203-4

Lepine, S., Le Stunff, H., Lakatos, B., Sulpice, J. C., and Giraud, F. (2006). ATP-induced apoptosis of thymocytes is mediated by activation of P2 X 7 receptor and involves de novo ceramide synthesis and mitochondria. *Biochim. Biophys. Acta* 1761, 73–82. doi: 10.1016/j.bbalip.2005.10.001

Leslie, C. C. (2015). Cytosolic phospholipase A(2): physiological function and role in disease. *J. Lipid Res.* 56, 1386–1402. doi: 10.1194/jlr.R057588

Li, J., Zhang, W., Yang, H., Howrigan, D. P., Wilkinson, B., Souaiaia, T., et al. (2017). Spatiotemporal profile of postsynaptic interactomes integrates components of complex brain disorders. *Nat. Neurosci.* 20, 1150–1161. doi: 10.1038/nn.4594

Li, M., Toombes, G. E. S., Silberberg, S. D., and Swartz, K. J. (2015). Physical basis of apparent pore dilation of ATP-activated P2X receptor channels. *Nat. Neurosci.* 18, 1577–1583. doi: 10.1038/nn.4120

Li, S., Tomić, M., and Stojilkovic, S. S. (2011). Characterization of novel Pannexin 1 isoforms from rat pituitary cells and their association with ATP-gated P2X channels. *Gen. Comp. Endocrinol.* 174, 202–210. doi: 10.1016/j.ygcen.2011.08.019

Lim, P. S., Sutton, C. R., and Rao, S. (2015). Protein kinase C in the immune system: from signalling to chromatin regulation. *Immunology* 146, 508–522. doi: 10.1111/imm.12510

Linden, J., Koch-Nolte, F., and Dahl, G. (2019). Purine release, metabolism, and signaling in the inflammatory response. *Ann. Rev. Immunol.* 37, 325–347. doi: 10.1146/annurev-immunol-051116-052406

Liu, Y., Xiao, Y., and Li, Z. (2011). P2X7 receptor positively regulates MyD88-dependent NF-κB activation. *Cytokine* 55, 229–236. doi: 10.1016/j.cyto.2011.05.003

Locovei, S., Scemes, E., Qiu, F., Spray, D. C., and Dahl, G. (2007). Pannexin1 is part of the pore forming unit of the P2X7 receptor death complex. *FEBS Lett.* 581, 483–488. doi: 10.1016/j.febslet.2006.12.056

Lucae, S., Salyakina, D., Barden, N., Harvey, M., Gagné, B., Labbé, M., et al. (2006). P2RX7, a gene coding for a purinergic ligand-gated ion channel, is associated with major depressive disorder. *Hum. Mol. Genet.* 15, 2438–2445. doi: 10.1093/hmg/ddl166

Ma, W., Korngreen, A., Weil, S., Cohen, E. B. T., Priel, A., Kuzin, L., et al. (2006). Pore properties and pharmacological features of the P2X receptor channel in airway ciliated cells. *J. Physiol.* 571, 503–517. doi: 10.1113/jphysiol.2005.103408

MacKenzie, A., Wilson, H. L., Kiss-Toth, E., Dower, S. K., North, R. A., and Surprenant, A. (2001). Rapid secretion of interleukin-1β by microvesicle shedding. *Immunity* 15, 825–835. doi: 10.1016/s1074-7613(01)00229-1

Mackenzie, A. B., Young, M. T., Adinolfi, E., and Surprenant, A. (2005). Pseudoapoptosis induced by brief activation of ATP-gated P2X7 receptors. *J. Biol. Chem.* 280, 33968–33976. doi: 10.1074/jbc.M502705200

Manodori, A. B., Barabino, G. A., Lubin, B. H., and Kuypers, F. A. (2000). Adherence of phosphatidylserine-exposing erythrocytes to endothelial matrix thrombospondin. *Blood* 95, 1293–1300.

Manohar, M., Hirsh, M. I., Chen, Y., Woehrle, T., Karande, A. A., and Junger, W. G. (2012). ATP release and autocrine signaling through P2X4 receptors regulate γδ T cell activation. *J. Leukoc. Biol.* 92, 787–794. doi: 10.1189/jlb.0312121

Mansoor, S. E., Lü, W., Oosterheert, W., Shekhar, M., Tajkhorshid, E., and Gouaux, E. (2016). X-ray structures define human P2X3 receptor gating cycle and antagonist action. *Nature* 538, 66–71. doi: 10.1038/nature19367

Mariathasan, S., Weiss, D. S., Newton, K., McBride, J., O'Rourke, K., Roose-Girma, M., et al. (2006). Cryopyrin activates the inflammasome in response to toxins and ATP. *Nature* 440, 228–232. doi: 10.1038/nature04515

Martel-Gallegos, G., Casas-Pruneda, G., Ortega-Ortega, F., Sanchez-Armass, S., Olivares-Reyes, J. A., Diebold, B., et al. (2013). Oxidative stress induced by P2X7 receptor stimulation in murine macrophages is mediated by c-Src/Pyk2 and ERK1/2. *Biochim. Biophys. Acta* 1830, 4650–4659. doi: 10.1016/j.bbagen.2013.05.023

Mayor, A., Martinon, F., De Smedt, T., Petrilli, V., and Tschopp, J. (2007). A crucial function of SGT1 and HSP90 in inflammasome activity links mammalian and plant innate immune responses. *Nat. Immunol.* 8, 497–503. doi: 10.1038/ni1459

McQuillin, A., Bass, N. J., Choudhury, K., Puri, V., Kosmin, M., Lawrence, J., et al. (2009). Case-control studies show that a non-conservative amino-acid change from a glutamine to arginine in the P2RX7 purinergic receptor protein is associated with both bipolar- and unipolar-affective disorders. *Mol. Psychiatry* 14, 614–620. doi: 10.1038/mp.2008.6

Mellacheruvu, D., Wright, Z., Couzens, A. L., Lambert, J. P., St-Denis, N. A., Li, T., et al. (2013). The CRAPome: a contaminant repository for affinity purification-mass spectrometry data. *Nat. Methods* 10, 730–736. doi: 10.1038/nmeth.2557

Metzger, M. W., Walser, S. M., Dedic, N., Aprile-Garcia, F., Jakubcakova, V., Adamczyk, M., et al. (2017). Heterozygosity for the mood disorder-associated variant Gln460Arg alters P2X7 receptor function and sleep quality. *J. Neurosci.* 37, 11688–11700. doi: 10.1523/JNEUROSCI.3487-16.2017

Migita, K., Ozaki, T., Shimoyama, S., Yamada, J., Nikaido, Y., Furukawa, T., et al. (2016). HSP90 regulation of P2X7 Receptor function requires an intact cytoplasmic C-terminus. *Mol. Pharmacol.* 90, 116–126. doi: 10.1124/mol.115.102988

Miller, C. M., Boulter, N. R., Fuller, S. J., Zakrzewski, A. M., Lees, M. P., Saunders, B. M., et al. (2011). The role of the P2X7 receptor in infectious diseases. *PLoS Pathog.* 7:e1002212. doi: 10.1371/journal.ppat.1002212

Minkiewicz, J., de Rivero Vaccari, J. P., and Keane, R. W. (2013). Human astrocytes express a novel NLRP2 inflammasome. *Glia* 61, 1113–1121. doi: 10.1002/glia.22499

Miras-Portugal, M. T., Sebastián-Serrano, Á, de Diego García, L., and Díaz-Hernández, M. (2017). Neuronal P2X7 receptor: involvement in neuronal physiology and pathology. *J. Neurosci.* 37, 7063–7072. doi: 10.1523/jneurosci.3104-16.2017

Mishra, A., Guo, Y., Zhang, L., More, S., Weng, T., Chintagari, N. R., et al. (2016). A Critical Role for P2X7 Receptor–Induced VCAM-1 shedding and neutrophil infiltration during acute lung injury. *J. Immunol.* 197, 2828–2837. doi: 10.4049/jimmunol.1501041

Mistafa, O., Ghalali, A., Kadekar, S., Hogberg, J., and Stenius, U. (2010). Purinergic receptor-mediated rapid depletion of nuclear phosphorylated Akt depends on pleckstrin homology domain leucine-rich repeat phosphatase, calcineurin, protein phosphatase 2A, and PTEN phosphatases. *J. Biol. Chem.* 285, 27900–27910. doi: 10.1074/jbc.M110.117093

Monif, M., Reid, C. A., Powell, K. L., Smart, M. L., and Williams, D. A. (2009). The P2X7 receptor drives microglial activation and proliferation: a trophic role for P2X7R pore. *J. Neurosci.* 29, 3781–3791. doi: 10.1523/jneurosci.5512-08.2009

Moon, H., Na, H. Y., Chong, K. H., and Kim, T. J. (2006). P2X 7 receptor-dependent ATP-induced shedding of CD27 in mouse lymphocytes. *Immunol. Lett.* 102, 98–105. doi: 10.1016/j.imlet.2005.08.004

Moore, S. F., and MacKenzie, A. B. (2009). NADPH oxidase NOX2 mediates rapid cellular oxidation following ATP stimulation of endotoxin-primed macrophages. *J. Immunol.* 183, 3302–3308. doi: 10.4049/jimmunol.0900394

Morelli, A., Chiozzi, P., Chiesa, A., Ferrari, D., Sanz, J. M., Falzoni, S., et al. (2003). Extracellular ATP causes ROCK I-dependent bleb formation in P2X7-transfected HEK293 cells. *Mol. Biol. Cell* 14, 2655–2664. doi: 10.1091/mbc.02-04-0061

Moreth, K., Frey, H., Hubo, M., Zeng-Brouwers, J., Nastase, M. V., Hsieh, L. T. H., et al. (2014). Biglycan-triggered TLR-2- and TLR-4-signaling exacerbates the pathophysiology of ischemic acute kidney injury. *Matrix Biol.* 35, 143–151. doi: 10.1016/j.matbio.2014.01.010

Moura, G., Lucena, S. V., Lima, M. A., Nascimento, F. D., Gesteira, T. F., Nader, H. B., et al. (2015). Post-translational allosteric activation of the P2X7 receptor through glycosaminoglycan chains of CD44 proteoglycans. *Cell Death Discov.* 1:15005. doi: 10.1038/cddiscovery.2015.5

Müller, M. R., and Rao, A. (2010). NFAT, immunity and cancer: a transcription factor comes of age. *Nat. Rev. Immunol.* 10, 645–656. doi: 10.1038/nri2818

Munoz-Planillo, R., Kuffa, P., Martinez-Colon, G., Smith, B. L., Rajendiran, T. M., and Nunez, G. (2013). K(+) efflux is the common trigger of NLRP3 inflammasome activation by bacterial toxins and particulate matter. *Immunity* 38, 1142–1153. doi: 10.1016/j.immuni.2013.05.016

Murrell-Lagnado, R. D. (2017). Regulation of P2X purinergic receptor signaling by cholesterol. *Curr. Top. Membr.* 80, 211–232. doi: 10.1016/bs.ctm.2017.05.004

Narcisse, L., Scemes, E., Zhao, Y., Lee, S. C., and Brosnan, C. F. (2005). The cytokine IL-1β transiently enhances P2X7 receptor expression and function in human astrocytes. *Glia* 49, 245–258. doi: 10.1002/glia.20110

Nicke, A. (2008). Homotrimeric complexes are the dominant assembly state of native P2X7 subunits. *Biochem. Biophys. Res. Commun.* 377, 803–808. doi: 10.1016/j.bbrc.2008.10.042

Noguchi, T., Ishii, K., Fukutomi, H., Naguro, I., Matsuzawa, A., Takeda, K., et al. (2008). Requirement of reactive oxygen species-dependent activation of ASK1-p38 MAPK pathway for extracellular ATP-induced apoptosis in macrophage. *J. Biol. Chem.* 283, 7657–7665. doi: 10.1074/jbc.M708402200

Norenberg, W., Schunk, J., Fischer, W., Sobottka, H., Riedel, T., Oliveira, J. F., et al. (2010). Electrophysiological classification of P2X7 receptors in rat cultured neocortical astroglia. *Br. J. Pharmacol.* 160, 1941–1952. doi: 10.1111/j.1476-5381.2010.00736.x

Norris, P. C., Gosselin, D., Reichart, D., Glass, C. K., and Dennis, E. A. (2014). Phospholipase A2 regulates eicosanoid class switching during inflammasome activation. *Proc. Natl. Acad. Sci. U.S.A.* 111, 12746–12751. doi: 10.1073/pnas.1404372111

Oliveira, J. F., Riedel, T., Leichsenring, A., Heine, C., Franke, H., Krugel, U., et al. (2011). Rodent cortical astroglia express in situ functional P2X7 receptors sensing pathologically high ATP concentrations. *Cereb. Cortex* 21, 806–820. doi: 10.1093/cercor/bhq154

Omasits, U., Ahrens, C. H., Müller, S., and Wollscheid, B. (2014). Protter: interactive protein feature visualization and integration with experimental proteomic data. *Bioinformatics* 30, 884–886. doi: 10.1093/bioinformatics/btt607

Orioli, E., De Marchi, E., Giuliani, A. L., and Adinolfi, E. (2017). P2X7 receptor orchestrates multiple signalling pathways triggering inflammation. autophagy and metabolic/trophic responses. *Curr. Med. Chem.* 24, 2261–2275. doi: 10.2174/0929867324666170303161659

Ortega, F., Pérez-Sen, R., Delicado, E. G., and Teresa Miras-Portugal, M. (2011). ERK1/2 activation is involved in the neuroprotective action of P2Y 13 and P2X7 receptors against glutamate excitotoxicity in cerebellar granule neurons. *Neuropharmacology* 61, 1210–1221. doi: 10.1016/j.neuropharm.2011.07.010

Ousingsawat, J., Wanitchakool, P., Kmit, A., Romao, A. M., Jantarajit, W., Schreiber, R., et al. (2015). Anoctamin 6 mediates effects essential for innate immunity downstream of P2X7 receptors in macrophages. *Nat. Commun.* 6, 6245–6245. doi: 10.1038/ncomms7245

Paluch, E. K., and Raz, E. (2013). The role and regulation of blebs in cell migration. *Curr. Opin. Cell Biol.* 25, 582–590. doi: 10.1016/j.ceb.2013.05.005

Panenka, W., Jijon, H., Herx, L. M., Armstrong, J. N., Feighan, D., Wei, T., et al. (2001). P2X7-like receptor activation in astrocytes increases chemokine monocyte chemoattractant protein-1 expression via mitogen-activated protein kinase. *J. Neurosci.* 21, 7135–7142. doi: 10.1523/jneurosci.21-18-07135.2001

Panupinthu, N., Zhao, L., Possmayer, F., Ke, H. Z., Sims, S. M., and Dixon, S. J. (2007). P2X7 nucleotide receptors mediate blebbing in osteoblasts through a pathway involving lysophosphatidic acid. *J. Biol. Chem.* 282, 3403–3412. doi: 10.1074/jbc.M605620200

Parvathenani, L. K., Tertyshnikova, S., Greco, C. R., Roberts, S. B., Robertson, B., and Posmantur, R. (2003). P2X7 mediates superoxide production in primary microglia and is up-regulated in a transgenic mouse model of Alzheimer's disease. *J. Biol. Chem.* 278, 13309–13317. doi: 10.1074/jbc.M209478200

Patel, H. H., and Insel, P. A. (2008). Lipid rafts and caveolae and their role in compartmentation of redox signaling. *Antioxid. Redox Signal.* 11, 1357–1372. doi: 10.1089/ars.2008.2365

Pelegrin, P., and Surprenant, A. (2006). Pannexin-1 mediates large pore formation and interleukin-1β release by the ATP-gated P2X7 receptor. *EMBO J.* 25, 5071–5082. doi: 10.1038/sj.emboj.7601378

Penuela, S., Gehi, R., and Laird, D. W. (2013). The biochemistry and function of pannexin channels. *Biochim. Biophys. Acta Biomembr.* 1828, 15–22. doi: 10.1016/j.bbamem.2012.01.017

Pereira, V. S., Casarotto, P. C., Hiroaki-Sato, V. A., Sartim, A. G., Guimaraes, F. S., and Joca, S. R. (2013). Antidepressant- and anticompulsive-like effects of purinergic receptor blockade: involvement of nitric oxide. *Eur. Neuropsychopharmacol.* 23, 1769–1778. doi: 10.1016/j.euroneuro.2013.01.008

Perez-Andres, E., Fernandez-Rodriguez, M., Gonzalez, M., Zubiaga, A., Vallejo, A., Garcia, I., et al. (2002). Activation of phospholipase D-2 by P2X(7) agonists in rat submandibular gland acini. *J. Lipid Res.* 43, 1244–1255.

Pérez-Flores, G., Lévesque, S. A., Pacheco, J., Vaca, L., Lacroix, S., Pérez-Cornejo, P., et al. (2015). The P2X7/P2X4 interaction shapes the purinergic response in murine macrophages. *Biochem. Biophys. Res. Commun.* 467, 484–490. doi: 10.1016/j.bbrc.2015.10.025

Perregaux, D. G., and Gabel, C. A. (1998). Human monocyte stimulus-coupled IL-1β posttranslational processing: modulation via monovalent cations. *Am. J. Physiol.* 275, C1538–C1547. doi: 10.1152/ajpcell.1998.275.6.C1538

Pfeiffer, Z. A., Aga, M., Prabhu, U., Watters, J. J., Hall, D. J., and Bertics, P. J. (2004). The nucleotide receptor P2X7 mediates actin reorganization and membrane blebbing in RAW 264.7 macrophages via p38 MAP kinase and Rho. *J. Leukoc. Biol.* 75, 1173–1182. doi: 10.1189/jlb.1203648

Pfleger, C., Ebeling, G., Blasche, R., Patton, M., Patel, H. H., Kasper, M., et al. (2012). Detection of caveolin-3/caveolin-1/P2X7R complexes in mice atrial cardiomyocytes in vivo and in vitro. *Histochem. Cell Biol.* 138, 231–241. doi: 10.1007/s00418-012-0961-0

Pippel, A., Beßler, B., Klapperstück, M., and Markwardt, F. (2015). Inhibition of antigen receptor-dependent Ca2+ signals and NF-AT activation by P2X7 receptors in human B lymphocytes. *Cell Calcium* 57, 275–289. doi: 10.1016/j.ceca.2015.01.010

Pippel, A., Stolz, M., Woltersdorf, R., Kless, A., Schmalzing, G., and Markwardt, F. (2017). Localization of the gate and selectivity filter of the full-length P2X7 receptor. *Proc. Natl. Acad. Sci.* 114, E2156–E2165. doi: 10.1073/pnas.1610414114

Pizzirani, C., Ferrari, D., Chiozzi, P., Adinolfi, E., Sandonà, D., Savaglio, E., et al. (2007). Stimulation of P2 receptors causes release of IL-1β-loaded microvesicles from human dendritic cells. *Blood* 109, 3856–3864. doi: 10.1182/blood-2005-06-031377

Pochet, S., Gomez-Munoz, A., Marino, A., and Dehaye, J. P. (2003). Regulation of phospholipase D by P2X7 receptors in submandibular ductal cells. *Cell. Signal.* 15, 927–935. doi: 10.1016/s0898-6568(03)00053-6

Poornima, V., Madhupriya, M., Kootar, S., Sujatha, G., Kumar, A., and Bera, A. K. (2012). P2X 7 receptor-pannexin 1 hemichannel association: effect of extracellular calcium on membrane permeabilization. *J. Mol. Neurosci.* 46, 585–594. doi: 10.1007/s12031-011-9646-8

Pupovac, A., Foster, C. M., and Sluyter, R. (2013). Human P2X7 receptor activation induces the rapid shedding of CXCL16. *Biochem. Biophys. Res. Commun.* 432, 626–631. doi: 10.1016/j.bbrc.2013.01.134

Pupovac, A., Geraghty, N. J., Watson, D., and Sluyter, R. (2015). Activation of the P2X7 receptor induces the rapid shedding of CD23 from human and murine B cells. *Immunol. Cell Biol.* 93, 77–85. doi: 10.1038/icb.2014.69

Qu, Y., and Dubyak, G. R. (2009). P2X7 receptors regulate multiple types of membrane trafficking responses and non-classical secretion pathways. *Purinergic Signal.* 5, 163–173. doi: 10.1007/s11302-009-9132-8

Qu, Y., Misaghi, S., Newton, K., Gilmour, L. L., Louie, S., Cupp, J. E., et al. (2011). Pannexin-1 Is required for ATP release during apoptosis but not for inflammasome activation. *J. Immunol.* 186, 6553–6561. doi: 10.4049/jimmunol.1100478

Qu, Y., Ramachandra, L., Mohr, S., Franchi, L., Harding, C. V., Nunez, G., et al. (2009). P2X7 receptor-stimulated secretion of MHC class II-containing exosomes requires the ASC/NLRP3 inflammasome but is independent of Caspase-1. *J. Immunol.* 182, 5052–5062. doi: 10.4049/jimmunol.0802968

Qureshi, O. S., Paramasivam, A., Yu, J. C. H., and Murrell-Lagnado, R. D. (2007). Regulation of P2X4 receptors by lysosomal targeting, glycan protection and exocytosis. *J. Cell Sci.* 120, 3838–3849. doi: 10.1242/jcs.010348

Ranoa, D. R. E., Kelley, S. L., and Tapping, R. I. (2013). Human lipopolysaccharide-binding protein (LBP) and CD14 independently deliver triacylated lipoproteins to Toll-like receptor 1 (TLR1) and TLR2 and enhance formation of the ternary signaling complex. *J. Biol. Chem.* 288, 9729–9741. doi: 10.1074/jbc.M113.453266

Rassendren, F., Buell, G. N., Virginio, C., Collo, G., North, R. A., and Surprenant, A. (1997). The permeabilizing ATP receptor, P2X7. Cloning and expression of a human cDNA. *J. Biol. Chem.* 272, 5482–5486. doi: 10.1074/jbc.272.9.5482

Raymond, M. N., and Le Stunff, H. (2006). Involvement of de novo ceramide biosynthesis in macrophage death induced by activation of ATP-sensitive P2X7 receptor. *FEBS Lett.* 580, 131–136. doi: 10.1016/j.febslet.2005.11.066

Riedel, T., Schmalzing, G., and Markwardt, F. (2007). Influence of extracellular monovalent cations on pore and gating properties of P2X7 receptor-operated single-channel currents. *Biophys. J.* 93, 846–858. doi: 10.1529/BIOPHYSJ.106.103614

Rissiek, B., Haag, F., Boyer, O., Koch-Nolte, F., and Adriouch, S. (2015). P2X7 on mouse T cells: one channel, many functions. *Front. Immunol.* 6:204. doi: 10.3389/fimmu.2015.00204

Robinson, L. E., Shridar, M., Smith, P., and Murrell-Lagnado, R. D. (2014). Plasma membrane cholesterol as a regulator of human and rodent P2X7 receptor activation and sensitization. *J. Biol. Chem.* 289, 31983–31994. doi: 10.1074/jbc.M114.574699

Roger, S., Gillet, L., Baroja-Mazo, A., Surprenant, A., and Pelegrin, P. (2010). C-terminal calmodulin-binding motif differentially controls human and rat P2X7 receptor current facilitation. *J. Biol. Chem.* 285, 17514–17524. doi: 10.1074/jbc.M109.053082

Roger, S., Pelegrin, P., and Surprenant, A. (2008). Facilitation of P2X7 receptor currents and membrane blebbing via constitutive and dynamic calmodulin binding. *J. Neurosci.* 28, 6393–6401. doi: 10.1523/jneurosci.0696-08.2008

Rzeniewicz, K., Newe, A., Rey Gallardo, A., Davies, J., Holt, M. R., Patel, A., et al. (2015). L-selectin shedding is activated specifically within transmigrating pseudopods of monocytes to regulate cell polarity in vitro. *Proc. Natl. Acad. Sci.* 112, E1461–E1470. doi: 10.1073/pnas.1417100112

Sakaki, H., Fujiwaki, T., Tsukimoto, M., Kawano, A., Harada, H., and Kojima, S. (2013). P2X4 receptor regulates P2X7 receptor-dependent IL-1β and IL-18 release in mouse bone marrow-derived dendritic cells. *Biochem. Biophys. Res. Commun.* 432, 406–411. doi: 10.1016/j.bbrc.2013.01.135

Saul, A., Hausmann, R., Kless, A., and Nicke, A. (2013). Heteromeric assembly of P2X subunits. *Front. Cell. Neurosci.* 7:250. doi: 10.3389/fncel.2013.00250

Savio, L. E. B., de Andrade Mello, P., da Silva, C. G., and Coutinho-Silva, R. (2018). The P2X7 receptor in inflammatory diseases: angel or demon? *Front. Pharmacol.* 9:52. doi: 10.3389/fphar.2018.00052

Schaefer, L., Babelova, A., Kiss, E., Hausser, H. J., Baliova, M., Krzyzankova, M., et al. (2005). The matrix component biglycan is proinflammatory and signals through Toll-like receptors 4 and 2 in macrophages. *J. Clin. Invest.* 115, 2223–2233. doi: 10.1172/JCI23755

Schenk, U., Westendorf, A. M., Radaelli, E., Casati, A., Ferro, M., Fumagalli, M., et al. (2008). Purinergic control of T cell activation by ATP released through pannexin-1 hemichannels. *Sci. Signal.* 1:ra6. doi: 10.1126/scisignal.1160583

Scheuplein, F., Schwarz, N., Adriouch, S., Krebs, C., Bannas, P., Rissiek, B., et al. (2009). NAD+ and ATP released from injured cells induce P2X7-dependent

shedding of CD62L and externalization of phosphatidylserine by murine T cells. *J. Immunol.* 182, 2898–2908. doi: 10.4049/jimmunol.0801711

Schneider, M., Prudic, K., Pippel, A., Klapperstück, M., Braam, U., Müller, C. E., et al. (2017). Interaction of purinergic P2X4 and P2X7 receptor subunits. *Front. Pharmacol.* 8:860. doi: 10.3389/fphar.2017.00860

Schopf, F. H., Biebl, M. M., and Buchner, J. (2017). The HSP90 chaperone machinery. *Nat. Rev. Mol. Cell Biol.* 18, 345–360. doi: 10.1038/nrm.2017.20

Schwarz, N., Drouot, L., Nicke, A., Fliegert, R., Boyer, O., Guse, A. H., et al. (2012). Alternative splicing of the N-terminal cytosolic and transmembrane domains of P2X7 controls gating of the ion channel by ADP-ribosylation. *PLoS One* 7:e41269. doi: 10.1371/journal.pone.0041269

Schwenk, J., Harmel, N., Brechet, A., Zolles, G., Berkefeld, H., Muller, C. S., et al. (2012). High-resolution proteomics unravel architecture and molecular diversity of native AMPA receptor complexes. *Neuron* 74, 621–633. doi: 10.1016/j.neuron.2012.03.034

Schwenk, J., Perez-Garci, E., Schneider, A., Kollewe, A., Gauthier-Kemper, A., Fritzius, T., et al. (2016). Modular composition and dynamics of native GABAB receptors identified by high-resolution proteomics. *Nat. Neurosci.* 19, 233–242. doi: 10.1038/nn.4198

Segawa, K., Kurata, S., Yanagihashi, Y., Brummelkamp, T. R., Matsuda, F., and Nagata, S. (2014). Caspase-mediated cleavage of phospholipid flippase for apoptotic phosphatidylserine exposure. *Science* 344, 1164–1168. doi: 10.1126/science.1252809

Segawa, K., and Nagata, S. (2015). An apoptotic 'Eat Me' signal: phosphatidylserine exposure. *Trends Cell Biol.* 25, 639–650. doi: 10.1016/j.tcb.2015.08.003

Selvy, P. E., Lavieri, R. R., Lindsley, C. W., and Brown, H. A. (2011). Phospholipase D: enzymology, functionality, and chemical modulation. *Chem. Rev.* 111, 6064–6119. doi: 10.1021/cr200296t

Sengstake, S., Boneberg, E. M., and Illges, H. (2006). CD21 and CD62L shedding are both inducible via P2X7Rs. *Int. Immunol.* 18, 1171–1178. doi: 10.1093/intimm/dxl051

Serfling, E., Avots, A., Klein-Hessling, S., Rudolf, R., Vaeth, M., and Berberich-Siebelt, F. (2012). NFATc1/A: the other face of NFAT factors in lymphocytes. *Cell Commun. Signal.* 10, 16–16. doi: 10.1186/1478-811X-10-16

Shamseddine, A. A., Airola, M. V., and Hannun, Y. A. (2015). Roles and regulation of neutral sphingomyelinase-2 in cellular and pathological processes. *Adv. Biol. Regul.* 57, 24–41. doi: 10.1016/j.jbior.2014.10.002

Shemon, A. N., Sluyter, R., Fernando, S. L., Clarke, A. L., Dao-Ung, L.-P., Skarratt, K. K., et al. (2006). A Thr357 to Ser polymorphism in homozygous and compound heterozygous subjects causes absent or reduced P2X7 function and impairs ATP-induced mycobacterial killing by macrophages. *J. Biol. Chem.* 281, 2079–2086. doi: 10.1074/jbc.M507816200

Shi, H., Wang, Y., Li, X., Zhan, X., Tang, M., Fina, M., et al. (2016). NLRP3 activation and mitosis are mutually exclusive events coordinated by NEK7, a new inflammasome component. *Nat. Immunol.* 17, 250–258. doi: 10.1038/ni.3333

Silverman, W. R., de Rivero Vaccari, J. P., Locovei, S., Qiu, F., Carlsson, S. K., Scemes, E., et al. (2009). The pannexin 1 channel activates the inflammasome in neurons and astrocytes. *J. Biol. Chem.* 284, 18143–18151. doi: 10.1074/jbc.M109.004804

Sim, J. A., Young, M. T., Sung, H. Y., North, R. A., and Surprenant, A. (2004). Reanalysis of P2X7 receptor expression in rodent brain. *J. Neurosci.* 24, 6307–6314. doi: 10.1523/JNEUROSCI.1469-04.2004

Sluyter, R., and Wiley, J. S. (2002). Extracellular adenosine 5'-triphosphate induces a loss of CD23 from human dendritic cells via activation of P2X 7 receptors. *Int. Immunol.* 14, 1415–1421. doi: 10.1093/intimm/dxf111

Smart, M. L., Gu, B., Panchal, R. G., Wiley, J., Cromer, B., Williams, D. A., et al. (2003). P2X7 receptor cell surface expression and cytolytic pore formation are regulated by a distal C-terminal region. *J. Biol. Chem.* 278, 8853–8860. doi: 10.1074/jbc.M211094200

Solle, M., Labasi, J., Perregaux, D. G., Stam, E., Petrushova, N., Koller, B. H., et al. (2001). Altered cytokine production in mice lacking P2X(7) receptors. *J. Biol. Chem.* 276, 125–132. doi: 10.1074/jbc.M006781200

Sommer, A., Kordowski, F., Büch, J., Maretzky, T., Evers, A., Andrä, J., et al. (2016). Phosphatidylserine exposure is required for ADAM17 sheddase function. *Nat. Commun.* 7, 11523–11523. doi: 10.1038/ncomms11523

Soond, S. M. (2005). ERK-mediated phosphorylation of Thr735 in TNF -converting enzyme and its potential role in TACE protein trafficking. *J. Cell Sci.* 118, 2371–2380. doi: 10.1242/jcs.02357

Sorge, R. E., Trang, T., Dorfman, R., Smith, S. B., Beggs, S., Ritchie, J., et al. (2012). Genetically determined P2X7 receptor pore formation regulates variability in chronic pain sensitivity. *Nat. Med.* 18, 595–599. doi: 10.1038/nm.2710

Sperlagh, B., and Illes, P. (2014). P2X7 receptor: an emerging target in central nervous system diseases. *Trends Pharmacol. Sci.* 35, 537–547. doi: 10.1016/j.tips.2014.08.002

Sperlagh, B., Vizi, E. S., Wirkner, K., and Illes, P. (2006). P2X7 receptors in the nervous system. *Prog. Neurobiol.* 78, 327–346. doi: 10.1016/j.pneurobio.2006.03.007

Spooner, R., and Yilmaz, O. (2011). The role of reactive-oxygen-species in microbial persistence and inflammation. *Int. J. Mol. Sci.* 12, 334–352. doi: 10.3390/ijms12010334

Stefano, L., Rössler, O. G., Griesemer, D., Hoth, M., and Thiel, G. (2007). P2X7 receptor stimulation upregulates Egr-1 biosynthesis involving a cytosolic Ca2+ rise, transactivation of the EGF receptor and phosphorylation of ERK and Elk-1. *J. Cell. Physiol.* 213, 36–44. doi: 10.1002/jcp.21085

Stokes, L., Fuller, S. J., Sluyter, R., Skarratt, K. K., Gu, B. J., and Wiley, J. S. (2010). Two haplotypes of the P2X 7 receptor containing the Ala-348 to Thr polymorphism exhibit a gain-of-function effect and enhanced interleukin-1β secretion. *FASEB J.* 24, 2916–2927. doi: 10.1096/fj.09-150862

Stolz, M., Klapperstück, M., Kendzierski, T., Detro-dassen, S., Panning, A., Schmalzing, G., et al. (2015). Homodimeric anoctamin-1, but not homodimeric anoctamin-6, is activated by calcium increases mediated by the P2Y1 and P2X7 receptors. *Pflugers Arch.* 467, 2121–2140. doi: 10.1007/s00424-015-1687-3

Suh, P. G., Park, J. I., Manzoli, L., Cocco, L., Peak, J. C., Katan, M., et al. (2008). Multiple roles of phosphoinositide-specific phospholipase C isozymes. *BMB Rep.* 41, 415–434. doi: 10.5483/bmbrep.2008.41.6.415

Surprenant, A., Rassendren, F., Kawashima, E., North, R. A., and Buell, G. (1996). The cytolytic P2Z receptor for extracellular ATP identified as a P2X receptor (P2X7). *Science* 272, 735–738. doi: 10.1126/SCIENCE.272.5262.735

Suzuki, J., Denning, D. P., Imanishi, E., Horvitz, H. R., and Nagata, S. (2013). Xk-related protein 8 and CED-8 promote phosphatidylserine exposure in apoptotic cells. *Science* 341, 403–406. doi: 10.1126/science.1236758

Suzuki, J., Umeda, M., Sims, P. J., and Nagata, S. (2010). Calcium-dependent phospholipid scrambling by TMEM16F. *Nature* 468, 834–840. doi: 10.1038/nature09583

Szklarczyk, D., Gable, A. L., Lyon, D., Junge, A., Wyder, S., Huerta-Cepas, J., et al. (2019). STRING v11: protein-protein association networks with increased coverage, supporting functional discovery in genome-wide experimental datasets. *Nucleic Acids Res.* 47, D607–D613. doi: 10.1093/nar/gky1131

Tafani, M., Schito, L., Pellegrini, L., Villanova, L., Marfe, G., Anwar, T., et al. (2011). Hypoxia-increased RAGE and P2X7R expression regulates tumor cell invasion through phosphorylation of Erk1/2 and Akt and nuclear translocation of NF-κB. *Carcinogenesis* 32, 1167–1175. doi: 10.1093/carcin/bgr101

Torres, G. E., Egan, T. M., and Voigt, M. M. (1999). Hetero-oligomeric assembly of P2X receptor subunits. Specificities exist with regard to possible partners. *J. Biol. Chem.* 274, 6653–6659. doi: 10.1074/jbc.274.10.6653

Toulme, E., Garcia, A., Samways, D., Egan, T. M., Carson, M. J., and Khakh, B. S. (2010). P2X4 receptors in activated C8-B4 cells of cerebellar microglial origin. *J. Gen. Physiol.* 135, 333–353. doi: 10.1085/jgp.200910336

Toyomitsu, E., Tsuda, M., Yamashita, T., Tozaki-Saitoh, H., Tanaka, Y., and Inoue, K. (2012). CCL2 promotes P2X4 receptor trafficking to the cell surface of microglia. *Purinergic Signal.* 8, 301–310. doi: 10.1007/s11302-011-9288-x

Ugur, M., and Ugur, O. (2019). A mechanism-based approach to P2X7 receptor action. *Mol. Pharmacol.* 95, 442–450. doi: 10.1124/mol.118.115022

Verhoef, P. A., Estacion, M., Schilling, W., and Dubyak, G. R. (2003). P2X7 receptor-dependent blebbing and the activation of Rho-effector kinases, caspases, and IL-1 β release. *J. Immunol.* 170, 5728–5738. doi: 10.4049/jimmunol.170.11.5728

Villalobo, A., Ishida, H., Vogel, H. J., and Berchtold, M. W. (2018). Calmodulin as a protein linker and a regulator of adaptor/scaffold proteins. *Biochim. Biophys. Acta Mol. Cell Res.* 1865, 507–521. doi: 10.1016/j.bbamcr.2017.12.004

Virginio, C., MacKenzie, A., Rassendren, F. A., North, R. A., and Surprenant, A. (1999). Pore dilation of neuronal P2X receptor channels. *Nat. Neurosci.* 2, 315–321. doi: 10.1038/7225

Wan, M., Soehnlein, O., Tang, X., van der Does, A. M., Smedler, E., Uhlen, P., et al. (2014). Cathelicidin LL-37 induces time-resolved release of LTB4 and TXA2 by human macrophages and triggers eicosanoid generation in vivo. *FASEB J.* 28, 3456–3467. doi: 10.1096/fj.14-251306

Wang, B., and Sluyter, R. (2013). P2X7 receptor activation induces reactive oxygen species formation in erythroid cells. *Purinergic Signal.* 9, 101–112. doi: 10.1007/s11302-012-9335-2

Wang, C. M., Ploia, C., Anselmi, F., Sarukhan, A., and Viola, A. (2014). Adenosine triphosphate acts as a paracrine signaling molecule to reduce the motility of T cells. *EMBO J.* 33, 1354–1364. doi: 10.15252/embj.201386666

Wang, J., Huo, K., Ma, L., Tang, L., Li, D., Huang, X., et al. (2011). Toward an understanding of the protein interaction network of the human liver. *Mol. Syst. Biol.* 7:536. doi: 10.1038/msb.2011.67

Watters, J. J., Sommer, J. A., Fisette, P. L., Pfeiffer, Z. A., Aga, M., Prabhu, U., et al. (2001). Macrophage signaling and mediator production. *Drug Dev. Res.* 104, 91–104. doi: 10.1002/ddr.1176

Weinhold, K., Krause-Buchholz, U., Rödel, G., Kasper, M., and Barth, K. (2010). Interaction and interrelation of P2X7 and P2X4 receptor complexes in mouse lung epithelial cells. *Cell. Mol. Life Sci.* 67, 2631–2642. doi: 10.1007/s00018-010-0355-1

Weiss, J. (2003). Bactericidal/permeability-increasing protein (BPI) and lipopolysaccharide-binding protein (LBP): structure, function and regulation in host defence against Gram-negative bacteria. *Biochem. Soc. Trans.* 31(Pt 4), 785–790.

Wiley, J. S., Dao-Ung, L.-P., Li, C., Shemon, A. N., Gu, B. J., Smart, M. L., et al. (2003). An Ile-568 to Asn polymorphism prevents normal trafficking and function of the human P2X7 receptor. *J. Biol. Chem.* 278, 17108–17113. doi: 10.1074/jbc.M212759200

Wiley, J. S., Sluyter, R., Gu, B. J., Stokes, L., and Fuller, S. J. (2011). The human P2X7 receptor and its role in innate immunity. *Tissue Antigens* 78, 321–332. doi: 10.1111/j.1399-0039.2011.01780.x

Wilson, H. L., Wilson, S. A., Surprenant, A., and Alan North, R. (2002). Epithelial membrane proteins induce membrane blebbing and interact with the P2X7 receptor C terminus. *J. Biol. Chem.* 277, 34017–34023. doi: 10.1074/jbc.M205120200

Witting, A., Walter, L., Wacker, J., Moller, T., and Stella, N. (2004). P2X7 receptors control 2-arachidonoylglycerol production by microglial cells. *Proc. Natl. Acad. Sci. U.S.A.* 101, 3214–3219. doi: 10.1073/pnas.0306707101

Woehrle, T., Yip, L., Elkhal, A., Sumi, Y., Chen, Y., Yao, Y., et al. (2010). Pannexin-1 hemichannel-mediated ATP release together with P2X1 and P2X4 receptors regulate T-cell activation at the immune synapse. *Blood* 116, 3475–3484. doi: 10.1182/blood-2010-04-277707

Wu, C., Ma, M. H., Brown, K. R., Geisler, M., Li, L., Tzeng, E., et al. (2007). Systematic identification of SH3 domain-mediated human protein-protein interactions by peptide array target screening. *Proteomics* 7, 1775–1785. doi: 10.1002/pmic.200601006

Xu, X. J., Boumechache, M., Robinson, L. E., Marschall, V., Gorecki, D. C., Masin, M., et al. (2012). Splice variants of the P2X7 receptor reveal differential agonist dependence and functional coupling with pannexin-1. *J. Cell Sci.* 125, 3776–3789. doi: 10.1242/jcs.099374

Yang, D., He, Y., Muñoz-Planillo, R., Liu, Q., and Núñez, G. (2015). Caspase-11 requires the Pannexin-1 channel and the purinergic P2X7 pore to mediate pyroptosis and endotoxic shock. *Immunity* 43, 923–932. doi: 10.1016/J.IMMUNI.2015.10.009

Yang, R., Yu, T., Kou, X., Gao, X., Chen, C., Liu, D., et al. (2018). Tet1 and Tet2 maintain mesenchymal stem cell homeostasis via demethylation of the P2rX7 promoter. *Nat. Commun.* 9:2143. doi: 10.1038/s41467-018-04464-6

Yip, L., Woehrle, T., Corriden, R., Hirsh, M., Chen, Y., Inoue, Y., et al. (2009). Autocrine regulation of T-cell activation by ATP release and P2X < *sub* > 7 < */sub* > receptors. *FASEB J.* 23, 1685–1693. doi: 10.1096/fj.08-126458

Young, C. N. J., Sinadinos, A., Lefebvre, A., Chan, P., Arkle, S., Vaudry, D., et al. (2015). A novel mechanism of autophagic cell death in dystrophic muscle regulated by P2RX7 receptor large-pore formation and HSP90. *Autophagy* 11, 113–130. doi: 10.4161/15548627.2014.994402

Young, M. T., Pelegrin, P., and Surprenant, A. (2007). Amino acid residues in the P2X7 receptor that mediate differential sensitivity to ATP and BzATP. *Mol. Pharmacol.* 71, 92–100. doi: 10.1124/mol.106.030163

Zanoni, I., and Granucci, F. (2013). Role of CD14 in host protection against infections and in metabolism regulation. *Front. Cell. Infect. Microb.* 3:32. doi: 10.3389/fcimb.2013.00032

Zech, A., Wiesler, B., Ayata, C. K., Schlaich, T., Dürk, T., Hoßfeld, M., et al. (2016). P2rx4 deficiency in mice alleviates allergen-induced airway inflammation. *Oncotarget* 7, 80288–80297. doi: 10.18632/oncotarget.13375

Zhang, Q., Lenardo, M. J., and Baltimore, D. (2017). 30 Years of NF-κB: a blossoming of relevance to human pathobiology. *Cell* 168, 37–57. doi: 10.1016/j.cell.2016.12.012

Zhao, Q., Yang, M., Ting, A. T., and Logothetis, D. E. (2007). PIP 2 regulates the ionic current of P2X receptors and P2X 7 receptor-mediated cell death. *Channels* 1, 46–55. doi: 10.4161/chan.3914

Zuo, Y., Wang, J., Liao, F., Yan, X., Li, J., Huang, L., et al. (2018). Inhibition of heat shock protein 90 by 17-AAG reduces inflammation via P2X7 receptor/NLRP3 inflammasome pathway and increases neurogenesis after subarachnoid hemorrhage in mice. *Front. Mol. Neurosci.* 11:401. doi: 10.3389/fnmol.2018.00401

Conflict of Interest Statement: The authors declare that the research was conducted in the absence of any commercial or financial relationships that could be construed as a potential conflict of interest.

frontiers in Cellular Neuroscience

BRIEF RESEARCH REPORT
published: 21 August 2019
doi: 10.3389/fncel.2019.00390

Stimulation of P2X7 Enhances Whole Body Energy Metabolism in Mice

Giacomo Giacovazzo[1†], Paola Fabbrizio[1†], Savina Apolloni[1], Roberto Coccurello[1,2] and Cinzia Volonté[1,3]*

[1] Preclinical Neuroscience, Fondazione Santa Lucia IRCCS, Rome, Italy, [2] Institute for Complex System (ISC), CNR, Rome, Italy, [3] Institute for Systems Analysis and Computer Science, CNR, Rome, Italy

The P2X7 receptor, a member of the ionotropic purinergic P2X family of extracellular ATP-gated receptors, exerts strong trophic effects when tonically activated in cells, in addition to cytotoxic effects after a sustained activation. Because of its widespread distribution, P2X7 regulates several cell- and tissue-specific physiological functions, and is involved in a number of disease conditions. A novel role has recently emerged for P2X7 in the regulation of glucose and energy metabolism. In previous work, we have demonstrated that genetic depletion, and to a lesser extent also pharmacological inhibition of P2X7, elicits a significant decrease of the whole body energy expenditure and an increase of the respiratory exchange ratio. In the present work, we have investigated the effects of P2X7 stimulation *in vivo* on the whole body energy metabolism. Adult mice were daily injected with the specific P2X7 agonist 2′(3′)-O-(4-Benzoylbenzoyl)adenosine 5′-triphosphate for 1 week and subjected to indirect calorimetric analysis for 48 h. We report that 2′(3′)-O-(4-Benzoylbenzoyl)adenosine 5′-triphosphate increases metabolic rate and O_2 consumption, concomitantly decreasing respiratory rate and upregulating NADPH oxidase 2 in *gastrocnemius* and *tibialis anterior* muscles. Our results indicate a major impact on energy homeostasis and muscle metabolism by activation of P2X7.

Keywords: P2X7 receptor, BzATP, energy expenditure, oxygen consumption, fatty acid oxidation

OPEN ACCESS

Edited by:
Eric Boué-Grabot,
Université de Bordeaux, France

Reviewed by:
Elena Adinolfi,
University of Ferrara, Italy
Hana Zemkova,
Institute of Physiology (ASCR), Czechia
Robson Coutinho-Silva,
Federal University of Rio de Janeiro, Brazil

***Correspondence:**
Cinzia Volonté
cinzia.volonte@cnr.it

[†]These authors have contributed equally to this work

Specialty section:
This article was submitted to Non-Neuronal Cells, a section of the journal Frontiers in Cellular Neuroscience

Received: *28 May 2019*
Accepted: *07 August 2019*
Published: *21 August 2019*

Citation:
Giacovazzo G, Fabbrizio P, Apolloni S, Coccurello R and Volonté C (2019) Stimulation of P2X7 Enhances Whole Body Energy Metabolism in Mice. Front. Cell. Neurosci. 13:390. doi: 10.3389/fncel.2019.00390

INTRODUCTION

The P2X7 receptor (Volonté et al., 2012; Di Virgilio et al., 2018), a member of the purinergic ionotropic P2X family of extracellular ATP-gated receptors, exerts a strong trophic effect when tonically activated in cells (Adinolfi, 2005), in addition to a well-recognized role in apoptotic cytotoxicity after a sustained activation (Di Virgilio et al., 2018). The receptor is present in cells of hematopoietic lineage including erythrocytes, monocytes, macrophages, dendritic cells, B and T lymphocytes, being also expressed by mast cells, fibroblasts, osteoblasts, osteoclasts and myocytes (Zhang et al., 2004). In the CNS, P2X7 receptors are described in astrocytes, microglia,

Abbreviations: BzATP, 2′(3′)-O-(4-benzoylbenzoyl)adenosine 5′-triphosphate; CD36, cluster of differentiation 36; CV, caloric value; EE, energy expenditure; h, hours; IC, indirect calorimetry; i.p., intraperitoneal; NOX2, NADPH oxidase 2; PBS, phosphate buffered saline; RER, respiratory exchange ratio; VCO_2, volume of CO_2 production; VO_2, volume oxygen consumption.

oligodendrocytes, Schwann cells, as well as in neurons from olfactory and lateral septal nuclei, cerebral cortex, striatum, and hippocampus (Volonté et al., 2012). Because of such a widespread distribution, P2X7 regulates several different tissue-specific and cell-specific physiological functions, being also involved in a number of disease conditions (Cotrina and Nedergaard, 2009; Fumagalli et al., 2017).

In the last few years, a new role has emerged for P2X7 in the regulation of glucose metabolism and energy homeostasis. Heterologous expression of P2X7 in HEK293 cells for instance upregulates glycolytic enzymes and the glucose transporter Glut1, thus promoting adaptation to unfavorable extracellular conditions (Amoroso et al., 2012). In intestinal epithelial cells, the activation of P2X7 modulates glucose transport through the downregulation of the glucose transporter Glut2 (Bilodeau et al., 2014). In pancreatic islet, an increase in glucose concentration stimulates P2X7 transcription, thus suggesting that glucose exerts also a feedback signaling inside the cells by stimulating the expression of regulatory P2X7. On the other hand, loss of P2X7 function in mice results in changes of adipocyte distribution and lipid accumulation. In particular, a significantly increased body weight, epididymal fat pad mass, lipid accumulation in adipocytes, and/or ectopic aggregation in the form of lipid droplets are observed in genetically depleted P2X7 male mice, although in the absence of any significant difference in food consumption (Beaucage et al., 2014). Moreover, in response to high-fat/high-sucrose diets, mice lacking P2X7 exhibit severe and rapid hyperglycemia, glucose intolerance and impaired beta cell function. P2X7 levels are elevated in pancreatic beta cells of obese patients, but downregulated in patients with type-2 diabetes mellitus (Glas et al., 2009). The suppression of the CD36, a membrane glycoprotein modulator of lipid homeostasis and immune responses, playing critical roles in the uptake of fatty acids and involved in neurodevelopment, metabolic disorders, aging, dementia and stroke (Zhang et al., 2018) attenuates P2X7 and adipogenic protein expressions and decreases adipocyte differentiation (Gao et al., 2017). However, in another study, the activation of the inflammasome pathway in the adipose tissue was found associated with hyperglycemia and hyperinsulinemia but not mediated by the P2X7 signaling axis (Sun et al., 2012).

In a previous work, we have demonstrated that genetic depletion and, to a lesser extent, also pharmacological inhibition of P2X7 elicits a pronounced decrease of the whole body EE and a significant increase of the RER, thus indicating a prevalent increase of carbohydrate oxidation. The relative sparing of fatty acids storage and concomitant defective energy homeostasis were also associated to body weight gain (Giacovazzo et al., 2018). Given the increasing importance of P2X7 in the regulation of cellular energy metabolism, either during physiological or tumor conditions (Amoroso et al., 2012; Savio et al., 2018), in the present work we have investigated by IC the effects of P2X7 activation in mice that underwent 7-days treatment with the best available selective and specific P2X7 agonist BzATP. We demonstrate a significant increase of metabolic rate and O_2 consumption, with a concomitant decrease of RER and increase in NOX2 expression in skeletal muscles, thus demonstrating a major impact on energy metabolism by activation of P2X7. Our results might contribute to shed further light on the role of P2X7 during metabolic diseases.

MATERIALS AND METHODS

Animals

C57BL/6J mice were originally obtained from Charles River Laboratories (Lecco, IT) and maintained in the indoor animal facility. Animals were housed in groups of 4–5 mice/cage in standard conditions with free access to food and water, at constant temperature (22° ± 1°C) and relative humidity (50%), with a regular 12 h light cycle (light 7AM–7PM). All animal procedures were performed according to European Guidelines for the use of animals in research (86/609/CEE) and requirements of Italian laws (D. L. 26/2014). The Animal Welfare Office, Department of Public Health and Veterinary, Nutrition and Food Safety, General Management of Animal Care and Veterinary Drugs of Italian Ministry of Health have approved the ethical procedure. All efforts were made to minimize animal suffering and the number of animals necessary for obtaining reliable results.

Pharmacological P2X7 Receptor Activation

Adult (15 weeks-old) C57BL/6J female mice were randomly grouped into vehicle- or treated-mice and daily i.p., administered, respectively, with vehicle PBS or the best available specific and selective P2X7 agonist BzATP (Sigma-Aldrich, Italy) used at 1 mg/Kg, (279.7 μM) for 7 days in standard feeding conditions. During the last 48 h (h) of treatment, mice were subjected to continuous IC recording.

Energy Metabolism

Energy expenditure, volume of oxygen consumption (VO_2) and RER were measured by an IC system (TSE Systems Manufacturer, model PhenoMaster/LabMaster®System for Automated Home Cage Metabolic Phenotyping) with a constant air flow of 0.35 L/min, as described (McLean and Tobin, 1988; Grobe, 2017). Mice were adapted for 24 h to the metabolic chamber prior to recording, and VO_2 and VCO_2 were measured every 20 min, for a total of 48 h (12 h dark-light phase comparison). Room temperature and humidity were kept constant (22° ± 1°C).

As index of substrate oxidation, we used the ratio between the volume of CO2 (VCO2) produced, and the volume of O2 (VO2) consumed (RER = VCO2/VO2). EE was then calculated according to the equation VO2 × (3.815 + (1.232 × RER)), as provided by the TSE manufacturer. In particular, EE is calculated in terms of CV that is the relationship between the heat and VO2, as reported in Graham (1917). The resulting equation for the CV is 3.815 + 1.232 * RER, and the heat is CV × $VO_{2subject}$, which is the rate of O2 consumed by each subject. Finally, the heat has been normalized using the estimated lean mass per mice, to express values as kcal/h/Kg.

The EE and RER for each of the sample points were evaluated across the 48 h of total recording. Locomotor activity was assessed during the indirect calorimetric assay by the number of infrared beams broken. Each cage of the calorimeter system is equipped with the InfraMot®device that uses "passive infrared sensors" to detect and record the motor activity of the mouse by the body-heat image and its spatial displacement across time. EE was also analyzed by considering animals' steady conditions or lack of motor activity (only values included between 0 and 3 activity counts were included) and indicated as resting EE (REE).

Time Course of Consecutive BzATP, A804598 and A804598 Plus BzATP Administrations in Mice

After adapting to the metabolic chambers for 24 h, adult (15 weeks-old) C57BL/6J female mice (n = 4) were i.p. injected with 1 mg/Kg BzATP and energy metabolism recorded for 24 h (day 1), then i.p. injected with 90 mg/Kg A804598 and energy metabolism recorded for additional 24 h (day 2), and finally (day 3) administered with A804598 followed (20 min after) by BzATP and energy metabolism recorded for the last 24 h. Results are expressed as VO_2 or EE (Kcal/hour/Kg).

Western Blotting

Total protein extracts from mice *gastrocnemius* and *tibialis anterior* muscles were obtained in homogenization buffer (15 mg of dry tissue/150 μl of 20 mM HEPES, pH 7.4, 100 mM NaCl, 1% Triton X-100, 10 mM EDTA) added with protease inhibitor cocktail (Sigma Aldrich). After sonication and centrifugation at 14000 × g (20 min at 4°C) supernatants were collected and assayed for protein content by Bradford detection kit (Bio-Rad Laboratories, Hercules, United States). Protein separation and analysis (15 μg/well) was performed by Mini-PROTEAN®TGX^{TM} Gels (BioRad, United States) and by transfer onto nitrocellulose membranes. After saturation with 5% non-fat dry milk (1 h at room temperature), membranes were probed with gp91phox antibody (1:1000, BD Transduction Laboratories, United States) in 5% non-fat dry milk overnight at 4°C, and incubated with HRP-conjugated secondary antibody (mouse 1:5000, Jackson Immunoresearch) for 1 h at room temperature. Detections were performed on X-ray film (Aurogene, United States), using ECL Advance detection kit (Amersham Biosciences, United States) and signal intensity visualized by Kodak Image Station and analyzed by ImageJ software (NIH, United States). Values were normalized with mouse anti-GAPDH (1:2500, Sigma-Aldrich, Italy).

Statistical Analysis

Data are expressed as means ± standard error of the means. Statistical analysis was performed by Student's t-test, or 1-way analysis of variance (ANOVA) followed by Tukey *post hoc* test. The accepted level of significance was set at $^*p < 0.05$.

RESULTS AND DISCUSSION

To investigate the role of P2X7 activation in the regulation of energy homeostasis, we have assessed the metabolic rate and the respiratory quotient of C57BL/6J mice treated once a day for 7 consecutive days with vehicle (PBS) or the best selective and specific available P2X7 agonist BzATP, by means of continuous IC analysis during the last 48 h of treatment in standard nutritional conditions (**Figure 1A**). To overcome sex-mixed results with low reproducibility, we have used only the female gender because of previously reported data (Giacovazzo et al., 2018). Our results indicate that BzATP at the concentration of 1 mg/Kg (i.e., within a range demonstrated to be effective in rodents (Gubert et al., 2016), shows quick absorption without accumulation in the peritoneal space. Moreover, BzATP is well tolerated presenting no signs of toxicity and apparent distress such as sunken flanks, neglected grooming, or piloerection, as evaluated by daily inspection of body appearance and behavioral parameters comprising locomotor activity. Mean body weight collected before BzATP treatment, and immediately before and after the IC analysis for 48 h, shows no differences with respect to untreated mice (**Figure 1B**). Moreover, the liver weight remains constant during the entire period of BzATP treatment (vehicle-treated mice 3,57 ± 0,02 gr/100 gr body weight, n = 2; BzATP-treated mice 3,89 ± 0,21 gr/100 gr of body weight, n = 4, not statistically significant difference).

Having established that BzATP at the used dosage demonstrates no evidence of toxic effects, and that BzATP-treated mice present no gross pathology on necropsy compared to saline-treated mice, we have then assessed the metabolic rate, expressed as continuous volume of oxygen consumption, demonstrating a marked increase of VO_2 intake across the 48 h period (**Figure 1C**). The *in vivo* IC analysis of EE demonstrates that the agonism at the P2X7 receptor produced a significant increase of metabolic rate (Kcal/h/kg) in terms of enhanced heat production and total EE (**Figure 2A**). Notably, the increase of EE is generated also in the lack of motor activity as detected during the overall resting period recorded across the entire light-dark cycle (**Figure 2B**). Moreover, the enhancement of EE is not attributable to significant changes of food intake (data not shown) and, consequently, to the contribution of food-induced thermogenesis. Next, we have collected data on the RER, in order to evaluate the differential level of nutrient substrate oxidation or, in other words, which energy source among carbohydrates, lipids or proteins is predominantly oxidized. Because the RER diminishes (**Figure 2C**) and more O_2 is consumed (**Figure 1C**), our results indicate an increase of fatty acid oxidation and a prevalent use of lipid storage as energy source after P2X7 receptor stimulation. Of note, these changes are detected with no evident alteration of motor behavior (**Figure 2D**).

Altogether, these results clearly show that during the entire circadian period and under standard nutritional conditions, both EE and REE are significantly increased by BzATP, while RER levels are decreased, thus demonstrating a major activation of energy metabolism induced by the stimulation of P2X7. These findings complement our recent evidence that both transgenic loss and pharmacological impairment of P2X7

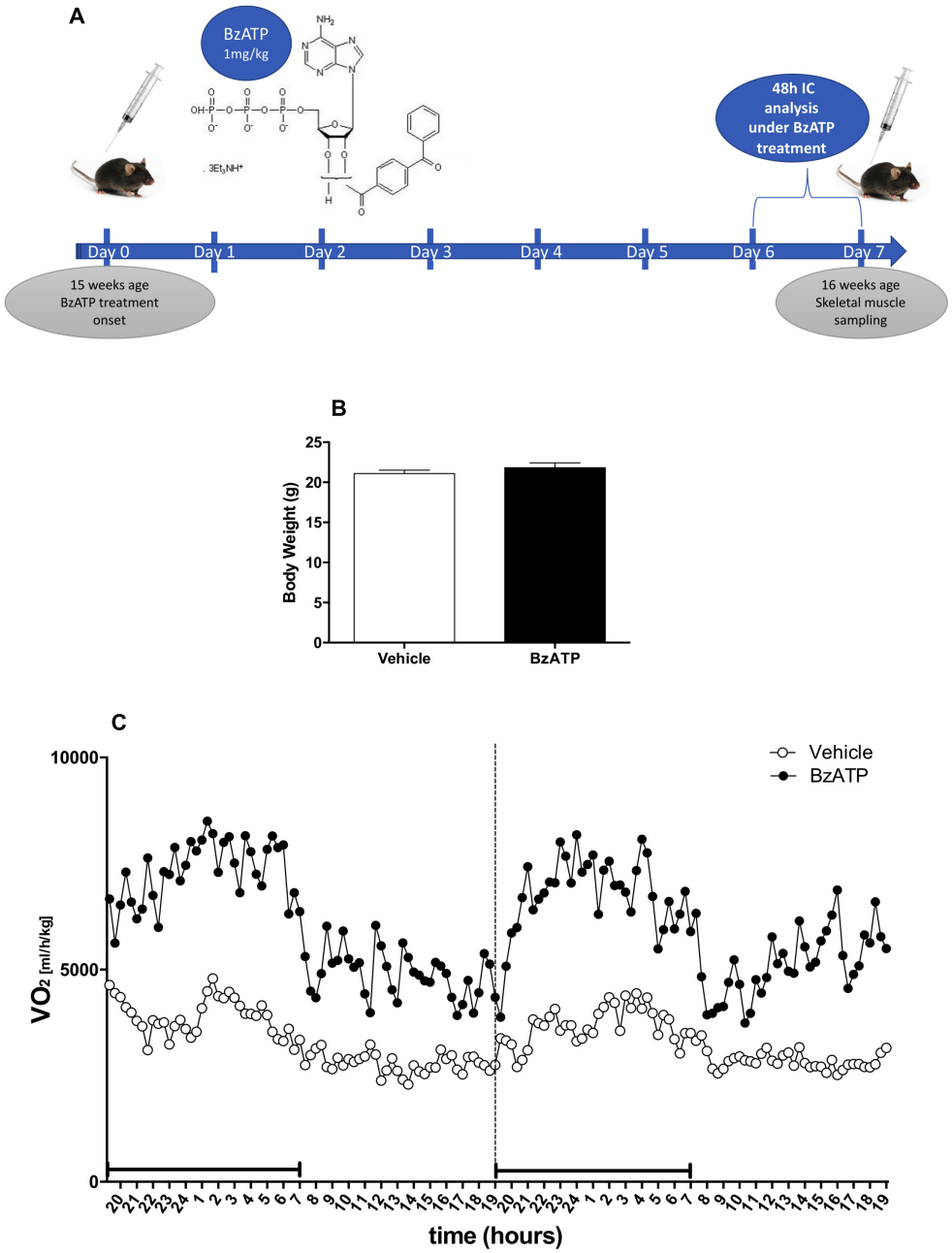

FIGURE 1 | Experimental plan and effects of 7-days BzATP administration on whole oxygen consumption. Adult (15 weeks-old) female C57BL/6J mice were daily i.p., administered with PBS or 1 mg/Kg BzATP for 7 days. At day 5, vehicle (n = 5) and BzATP-treated mice (n = 5), were introduced in the metabolic chambers to adapt for 24 h, and then subjected to IC recording for 48 h (days 6 and 7). **(A)** Schematic representation of experimental plan and execution. **(B)** Mean (± SEM) body weight (g) collected during the IC analysis for 48 h. **(C)** Mean (± SEM) of 48 h metabolic activity expressed as volume of oxygen consumption rate (VO_2) (ml/h/Kg), during the entire light/dark cycle. Black line below the recording time (X-axis) indicates the dark phase.

function conversely cause a robust decrease of metabolic rate and a lower ratio of fat to carbohydrate oxidation (Giacovazzo et al., 2018), thus generating lipid accumulation, increased fat mass distribution and, ultimately, the weight gain that is reported in P2X7-depleted mice (Beaucage et al., 2014). To further confirm the involvement of P2X7 in such events, we performed continuous IC recordings of C57BL/6J mice for 4 days, by registering basal activity for 24 h, followed by a single 1 mg/Kg BzATP i.p. administration and recording for 24 h, followed by a single i.p. administration of the specific P2X7 antagonist A804598 (90 mg/Kg, 24 h recording), and lastly BzATP (20 min pre-injection) followed by A804598 i.p. injection and final recording for 24 h. We demonstrate that the pre-administration of A804598 delays and attenuates the increase in

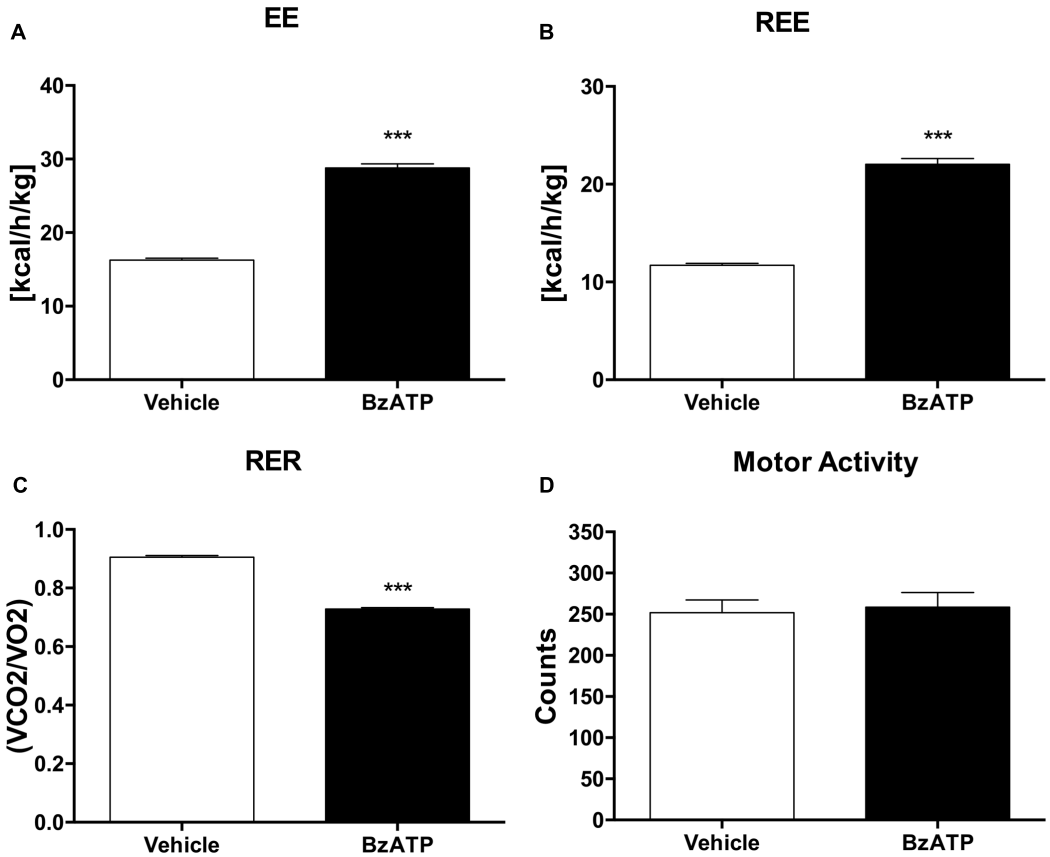

FIGURE 2 | BzATP increases energy expenditure and reduces respiratory exchange ratio. **(A)** Mean (±SEM) of 48 h EE expressed as Kcal emitted by whole body per hour, per Kg of body weight (Kcal/h/kg). **(B)** Mean of 48 h resting EE (REE) expressed as whole body EE in lack of motor activity (Kcal/h/Kg). **(C)** Mean (±SEM) of 48 h respiratory exchange ratio (RER), expressed as ratio of produced CO2 volume to used O2 volume (VCO_2/O_2). **(D)** Mean (± SEM) of 48 h locomotor activity (counts). (***P < 0,0001 vs. WT).

VO_2 consumption (**Figure 3A**) and EE (**Figure 3B**) induced by BzATP alone. These results further corroborate the previously observed implication of P2X7 in the decrease of whole body EE and increase of RER sustained by either pharmacological inhibition with the A804598 antagonist or genetic depletion of P2X7 (Giacovazzo et al., 2018).

As one of the largest tissue accounting for about 50% of body mass, the skeletal muscle is a major determinant of the whole-body metabolic rate (Zurlo et al., 1990), possessing a remarkable capacity to rapidly shift from carbohydrates to fatty acids utilization in response to increasing energy request and intensity of physical exercise (Kiens et al., 1993; Romijn et al., 1993; Van Loon et al., 2001). Indeed, the skeletal muscle readily responds to changing metabolic needs due not only to physiological, but also pathological stimuli, and the redox homeostasis appears to be a central modulator of muscle plasticity (Lambeth, 2004). Generation of reactive oxygen species (ROS) is for instance augmented in skeletal muscles as part of a physiological response to exercise, adaptation to increased workload and optimization of the contractile capacity (Forman et al., 2014). There is strong evidence that NOX2, a superoxide generating enzyme and major source of ROS under resting and contractile muscle conditions (Pearson et al., 2014), with its membrane-bound catalytic gp91phox and cytosolic regulatory p47phox subunits, can be accompanied by a change in mitochondrial content that is responsible for alterations in substrate utilization and whole body energy metabolism. Physical exercise is known to specifically increase NOX2 mRNA levels in the *gastrocnemius* (Loureiro et al., 2016). To investigate the potential involvement of NOX2 in regulating energy homeostasis by BzATP, we have next analyzed the expression profile of the glycoprotein gp91phox in the *gastrocnemius* (possessing both fast- and slow-twitch fibers) and *tibialis anterior* (with 95% fast-twitch fibers) muscles. Our results indicate that the content of gp91phox protein in both fiber types is remarkably increased in mice treated for 7 days with BzATP (**Figures 4A,B**). Because during muscle contraction there is a larger cytosolic ROS production with only a discrete mitochondrial signal (Sakellariou et al., 2012), the increased gp91phox expression may thus suggest that P2X7 activation plays a role in the contraction-induced intracellular signaling mediated by non-mitochondrial ROS sources such as NOX2. Notably, P2X7 activation by BzATP might also contribute to maintain a redox balance by inducing a physiological and transient ROS

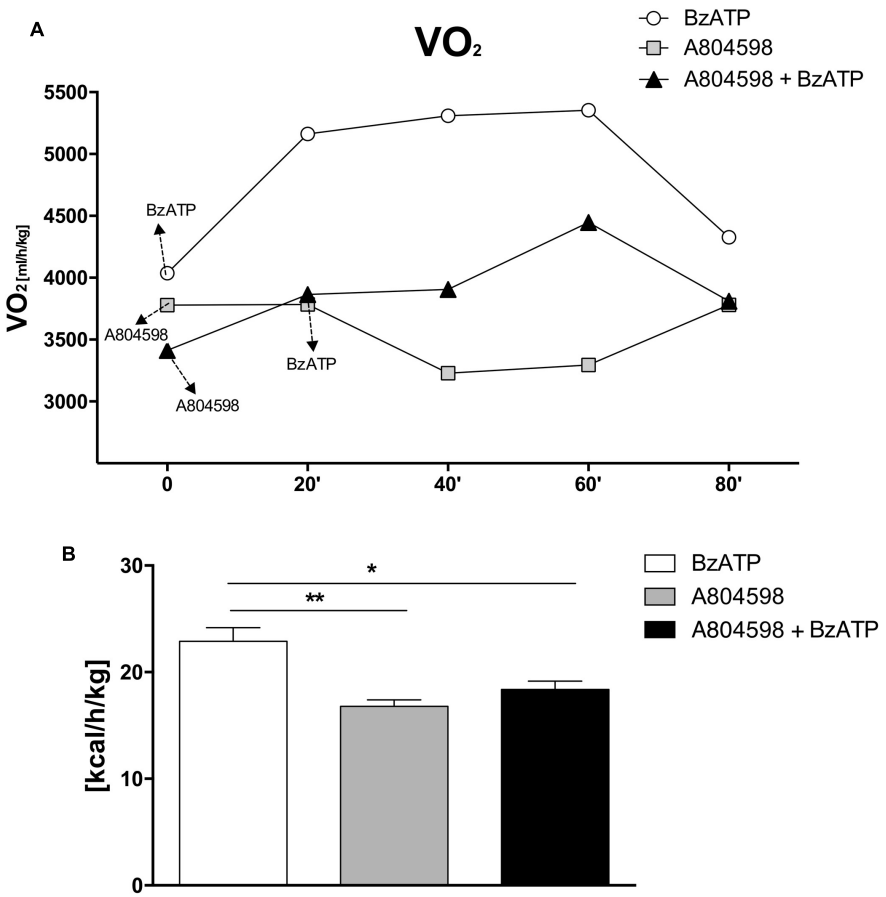

FIGURE 3 | A804598 administration prevents the BzATP-dependent increase of energy expenditure. Female C57BL/6J mice (n = 4) after adapting to the metabolic chambers for 24 h, were subjected to IC recording for 3 consecutive days according to the subsequent experimental design: day1, a single BzATP 1 mg/Kg i.p. injection and IC recording for 24 h,; day 2, a single A804598 90 mg/Kg i.p. injection and IC recording for 24 h; day 3, A804598 injection followed (after 20 min) by BzATP and IC recording for 24 h. **(A)** Mean (± SEM) 24 h metabolic activity is expressed as volume of oxygen consumption rate (VO_2) (ml/h/kg). **(B)** Mean (± SEM) EE energy expenditure is expressed as Kcal/h/Kg. (**P < 0,001 BzATP vs. A804598, *P < 0,005 BzATP vs. A804598 + BzATP).

generation (Ristow, 2014; Merry and Ristow, 2016). In this view, the BzATP-induced activation of P2X7 appears to mimic the effects produced by high-intensity training and, particularly, the increase of oxygen consumption (VO_2) (Trapp et al., 2008; Hazell et al., 2012) and the NOX2-dependent redox adaptation to endurance exercise that occur in both mixed (i.e., *gastrocnemius*) and fast-twitch glycolytic fiber types (i.e., *tibialis anterior*) (Henríquez-Olguín et al., 2019).

Overall, our results disclose and support a previously hypothesized function for P2X7 in shaping the whole-body energy metabolism (Giacovazzo et al., 2018). Here, we have shown that healthy mice challenged by BzATP display higher EE and higher oxidative capacity, with increased NOX2 expression in both mixed fast/slow-twitch and fast-twitch fibers. Because an increased oxidation of fatty acids reduces the carbohydrate utilization thus sparing the glycogen stores, and suppresses lactate production leading to increased endurance performance (San-Millán and Brooks, 2018), we suggest that a sustained activation of P2X7 might cause the remodeling of fatigue-resistance muscles and the reprogramming of the global muscle gene expression toward a slower, more oxidative transcription program.

Aging is associated with changing of muscle metabolism, adaptations in slow and fast fibers as well as a progressive decline of whole-body resting metabolic rate (Elia et al., 2000; Petersen et al., 2015). Altogether, muscle aging is associated to a drastic remodeling of muscle metabolism (e.g., decreased insulin sensitivity and mitochondrial capacity), structure (e.g., reduction of myofibers and muscle strength) and function (e.g., autophagy and contractile capacity) (Collino et al., 2013). Of note with aging, several glycolytic enzymes become overexpressed in the slow fibers, and a parallel upregulation and downregulation of glycogen metabolism is observed in slow and fast fibers of aged people, respectively (Rakus et al., 2015; Murgia et al., 2017). Since aging is also associated to muscle fiber type conversion, entailing a preferential loss of glycolytic fast-twitch fibers (Larsson, 1983), there is also the possibility that abnormal upregulation of glycogen metabolism in the slow fibers may, at least in part, accelerate the transition between fast- and slow-twitch fibers. In the light of our results, we might suggest that the potentiation

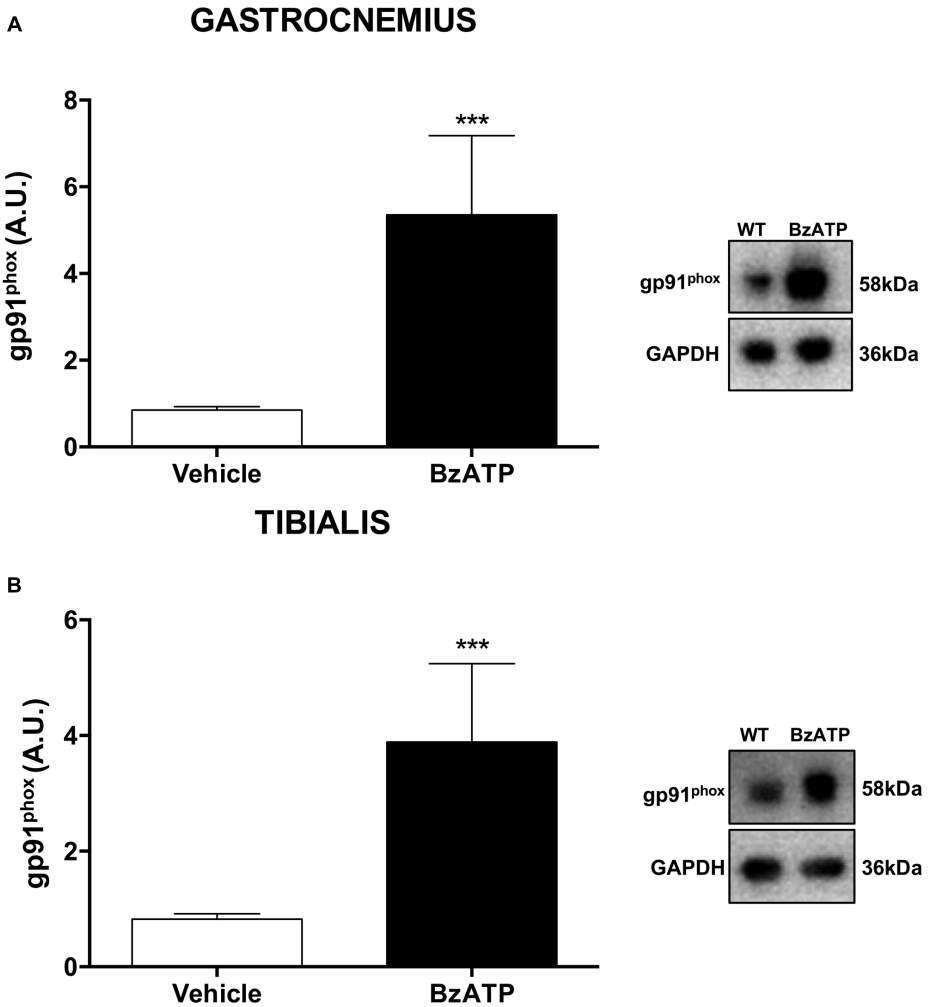

FIGURE 4 | BzATP enhances gp91phox expression in skeletal muscles of C57BL/6J mice. An equal amount of total *gastrocnemius* **(A)** and *tibialis anterior* **(B)** muscle lysates from vehicle and BzATP- treated mice (n = 3/group) were subjected to SDS-PAGE and Western Blotting with anti-gp91^{phox}. GAPDH was used for protein normalization. Data represent means ± SEM. Statistical significance was calculated by Student's t-test, as referred to vehicle, $^{*}p < 0.05$.

of P2X7 function in adult mice might contribute to restore a proper balance in either aged or pathologic carbohydrate-driven energy metabolism, by forcing the balance toward a prevalent oxidation of fatty acids and enhancement of metabolic rate. Further experiments on the role of P2X7 function will provide important insight about the fine-tuning of energy metabolism and redox homeostasis within the skeletal muscle cell.

DATA AVAILABILITY

The datasets generated for this study are available on request to the corresponding author.

ETHICS STATEMENT

The animal study was reviewed and approved by the Animal Welfare Office, Department of Public Health and Veterinary, Nutrition and Food Safety and General Management of Animal Care and Veterinary Drugs of the Italian Ministry of Health.

AUTHOR CONTRIBUTIONS

RC and CV contributed to the conception and design of the study. GG, PF, and SA contributed to the data acquisition and data analysis. All authors have approved the final version of the manuscript.

FUNDING

The Italian Ministry for Education, University and Research (MIUR) through Flagship Project NanoMAX B81J13000310005 to CV and RC, and the Italian Ministry of Health (Ricerca Corrente) have supported this work.

REFERENCES

Adinolfi, E. (2005). Basal activation of the P2X7 ATP receptor elevates mitochondrial calcium and potential, increases cellular ATP levels, and promotes serum-independent growth. *Mol. Biol. Cell.* 16, 3260–3272. doi: 10.1091/mbc.e04-11-1025

Amoroso, F., Falzoni, S., Adinolfi, E., Ferrari, D., and Di Virgilio, F. (2012). The P2X7 receptor is a key modulator of aerobic glycolysis. *Cell Death Dis.* 3:e370. doi: 10.1038/cddis.2012.105

Beaucage, K. L., Xiao, A., Pollmann, S. I., Grol, M. W., Beach, R. J., Holdsworth, D. W., et al. (2014). Loss of P2X7 nucleotide receptor function leads to abnormal fat distribution in mice. *Purinergic Signal.* 10, 291–304. doi: 10.1007/s11302-013-9388-x

Bilodeau, M. S., Arguin, G., and Gendron, F.-P. (2014). C/EBPβ regulates P2X7 receptor expression in response to glucose challenge in intestinal epithelial cells. *Biochem. Cell Biol.* 93, 38–46. doi: 10.1139/bcb-2014-98

Collino, S., Martin, F.-P., Karagounis, L. G., Horcajada, M. N., Moco, S., Franceschi, C., et al. (2013). Musculoskeletal system in the old age and the demand for healthy ageing biomarkers. *Mech. Ageing Dev.* 134, 541–547. doi: 10.1016/j.mad.2013.11.003

Cotrina, M. L., and Nedergaard, M. (2009). Physiological and pathological functions of P2X7 receptor in the spinal cord. *Purinergic Signal.* 5, 223–232. doi: 10.1007/s11302-009-9138-2

Di Virgilio, F., Schmalzing, G., and Markwardt, F. (2018). The elusive P2X7 macropore. *Trends Cell Biol.* 28, 392–404. doi: 10.1016/j.tcb.2018.01.005

Elia, M., Ritz, P., and Stubbs, R. J. (2000). Total energy expenditure in the elderly. *Eur. J. Clin. Nutr.* 54(Suppl. 3), S92–S103. doi: 10.1038/sj.ejcn.1601030

Forman, H. J., Ursini, F., and Maiorino, M. (2014). An overview of mechanisms of redox signaling. *J. Mol. Cell. Cardiol.* 73, 2–9. doi: 10.1016/j.yjmcc.2014.01.018

Fumagalli, M., Lecca, D., Abbracchio, M. P., and Ceruti, S. (2017). Pathophysiological role of purines and pyrimidines in neurodevelopment: unveiling new pharmacological approaches to congenital brain diseases. *Front. Pharmacol.* 8:941. doi: 10.3389/fphar.2017.00941

Gao, H., Li, D., Yang, P., Zhao, L., Wei, L., Chen, Y., et al. (2017). Suppression of CD36 attenuates adipogenesis with a reduction of P2X7 expression in 3T3-L1 cells. *Biochem. Biophys. Res. Commun.* 491, 204–208. doi: 10.1016/j.bbrc.2017.07.077

Giacovazzo, G., Apolloni, S., and Coccurello, R. (2018). Loss of P2X7 receptor function dampens whole body energy expenditure and fatty acid oxidation. *Purinergic Signal.* 14, 299–305. doi: 10.1007/s11302-018-9610-y

Glas, R., Sauter, N. S., Schulthess, F. T., Shu, L., Oberholzer, J., and Maedler, K. (2009). Purinergic P2X7 receptors regulate secretion of interleukin-1 receptor antagonist and beta cell function and survival. *Diabetologia* 52, 1579–1588. doi: 10.1007/s00125-009-1349-0

Graham, L. (1917). *The Elements of the Science of Nutrition*. Available at: https://books.google.it/books/about/The_elements_of_the_science_of_nutrition.html?id=joGZAoBs1jwC&redir_esc=y (accessed July 25, 2019).

Grobe, J. L. (2017). Comprehensive assessments of energy balance in mice. *Methods Mol. Biol.* 1614, 123–146. doi: 10.1007/978-1-4939-7030-8-10

Gubert, C., Fries, G. R., Pfaffenseller, B., Ferrari, P., Coutinho-Silva, R., Morrone, F. B., et al. (2016). Role of P2X7 receptor in an animal model of mania induced by D-amphetamine. *Mol. Neurobiol.* 53, 611–620. doi: 10.1007/s12035-014-9031-z

Hazell, T. J., Olver, T. D., Hamilton, C. D., and Lemon, P. W. R. (2012). Two minutes of sprint-interval exercise elicits 24-hr oxygen consumption similar to that of 30 min of continuous endurance exercise. *Int. J. Sport Nutr. Exerc. Metab.* 22, 276–283. doi: 10.1123/ijsnem.22.4.276

Henríquez-Olguín, C., Renani, L. B., Arab-Ceschia, L., Raun, S. H., Bhatia, A., Li, Z., et al. (2019). Adaptations to high-intensity interval training in skeletal muscle require NADPH oxidase 2. *Redox Biol.* 24:101188. doi: 10.1016/j.redox.2019.101188

Kiens, B., Essen-Gustavsson, B., Christensen, N. J., and Saltin, B. (1993). Skeletal muscle substrate utilization during submaximal exercise in man: effect of endurance training. *J. Physiol.* 469, 459–478. doi: 10.1113/jphysiol.1993.sp019823

Lambeth, J. D. (2004). NOX enzymes and the biology of reactive oxygen. *Nat. Rev. Immunol.* 4, 181–189. doi: 10.1038/nri1312

Larsson, L. (1983). Histochemical characteristics of human skeletal muscle during aging. *Acta Physiol. Scand.* 117, 469–471. doi: 10.1111/j.1748-1716.1983.tb00024.x

Loureiro, A. C. C., Rêgo-Monteiro, I. C., do Louzada, R. A., Ortenzi, V. H., Aguiar, A. P., de, et al. (2016). Differential expression of NADPH oxidases depends on skeletal muscle fiber type in rats. *Oxid. Med. Cell. Longev.* 2016:6738701. doi: 10.1155/2016/6738701

McLean, J. A., and Tobin, G. (1988). *Animal and Human Calorimetry*. Cambridge: Cambridge University Press, doi: 10.1017/CBO9780511663161

Merry, T. L., and Ristow, M. (2016). Mitohormesis in exercise training. *Free Radic. Biol. Med.* 98, 123–130. doi: 10.1016/j.freeradbiomed.2015.11.032

Murgia, M., Toniolo, L., Nagaraj, N., Ciciliot, S., Vindigni, V., Schiaffino, S., et al. (2017). Single muscle fiber proteomics reveals fiber-type-specific features of human muscle aging. *Cell Rep.* 19, 2396–2409. doi: 10.1016/j.celrep.2017.05.054

Pearson, T., Kabayo, T., Ng, R., Chamberlain, J., McArdle, A., and Jackson, M. J. (2014). Skeletal muscle contractions induce acute changes in cytosolic superoxide, but slower responses in mitochondrial superoxide and cellular hydrogen peroxide. *PLoS One.* 9:e96378. doi: 10.1371/journal.pone.0096378

Petersen, K. F., Morino, K., Alves, T. C., Kibbey, R. G., Dufour, S., Sono, S., et al. (2015). Effect of aging on muscle mitochondrial substrate utilization in humans. *Proc. Natl. Acad. Sci. U.S.A.* 112, 11330–11334. doi: 10.1073/pnas.1514844112

Rakus, D., Gizak, A., Deshmukh, A., and Wīniewski, J. R. (2015). Absolute quantitative profiling of the key metabolic pathways in slow and fast skeletal muscle. *J. Proteome Res.* 14, 1400–1411. doi: 10.1021/pr5010357

Ristow, M. (2014). Unraveling the truth about antioxidants: mitohormesis explains ROS-induced health benefits. *Nat. Med.* 20, 709–711. doi: 10.1038/nm.3624

Romijn, J. A., Coyle, E. F., Sidossis, L. S., Gastaldelli, A., Horowitz, J. F., Endert, E., et al. (1993). Regulation of endogenous fat and carbohydrate metabolism in relation to exercise intensity and duration. *Am. J. Physiol.* 265(3 Pt 1), E380–E391. doi: 10.1152/ajpendo.1993.265.3.E380

Sakellariou, G. K., Vasilaki, A., Palomero, J., Kayani, A., Zibrik, L., McArdle, A., et al. (2012). Studies of mitochondrial and nonmitochondrial sources implicate nicotinamide adenine dinucleotide phosphate oxidase(s) in the increased skeletal muscle superoxide generation that occurs during contractile activity. *Antioxid. Redox Signal.* 18, 603–621. doi: 10.1089/ars.2012.4623

San-Millán, I., and Brooks, G. A. (2018). Assessment of metabolic flexibility by means of measuring blood lactate, fat, and carbohydrate oxidation responses to exercise in professional endurance athletes and less-fit individuals. *Sport. Med.* 48, 467–479. doi: 10.1007/s40279-017-0751-x

Savio, L. E. B., Mello, P., de, A., da Silva, C. G., and Coutinho-Silva, R. (2018). The P2X7 receptor in inflammatory diseases: angel or demon? *Front. Pharmacol.* 9:52. doi: 10.3389/fphar.2018.00052

Sun, S., Xia, S., Ji, Y., Kersten, S., and Qi, L. (2012). The ATP-P2X 7 signaling axis is dispensable for obesity-associated inflammasome activation in adipose tissue. *Diabetes.* 61, 1471–1478. doi: 10.2337/db11-1389

Trapp, E. G., Chisholm, D. J., Freund, J., and Boutcher, S. H. (2008). The effects of high-intensity intermittent exercise training on fat loss and fasting insulin levels of young women. *Int. J. Obes.* 32, 684–691. doi: 10.1038/sj.ijo.0803781

Van Loon, L. J. C., Greenhaff, P. L., Constantin-Teodosiu, D., Saris, W. H. M., and Wagenmakers, A. J. M. (2001). The effects of increasing exercise intensity on muscle fuel utilisation in humans. *J. Physiol.* 536(Pt 1), 295–304. doi: 10.1111/j.1469-7793.2001.00295.x

Volonté, C., Apolloni, S., Skaper, S. D., and Burnstock, G. (2012). P2X7 receptors: channels, pores and more. *CNS Neurol. Disord. Drug Targets* 11, 705–721. doi: 10.2174/187152712803581137

Zhang, W., Chen, R., Yang, T., Xu, N., Chen, J., Gao, Y., et al. (2018). Fatty acid transporting proteins: roles in brain development, aging, and stroke. *Prostaglandins Leukot. Essent. Fat. Acids* 136, 35–45. doi: 10.1016/j.plefa.2017.04.004

Zhang, X. J., Zheng, G. G., Ma, X. T., Yang, Y. H., Li, G., Rao, Q., et al. (2004). Expression of P2X7 in human hematopoietic cell lines and leukemia patients. *Leuk. Res.* 28, 1313–1322. doi: 10.1016/j.leukres.2004.04.001

Zurlo, F., Larson, K., Bogardus, C., and Ravussin, E. (1990). Skeletal muscle metabolism is a major determinant of resting energy expenditure. *J. Clin. Invest.* 86, 1423–1427. doi: 10.1172/JCI114857

Conflict of Interest Statement: The authors declare that the research was conducted in the absence of any commercial or financial relationships that could be construed as a potential conflict of interest.

frontiers in Cellular Neuroscience

HYPOTHESIS AND THEORY
published: 21 August 2019
doi: 10.3389/fncel.2019.00365

The Purinome and the preBötzinger Complex – A Ménage of Unexplored Mechanisms That May Modulate/Shape the Hypoxic Ventilatory Response

*Robert J. Reklow[1], Tucaaue S. Alvares[1], Yong Zhang[1], Ana P. Miranda Tapia[1], Vivian Biancardi[1], Alexis K. Katzell[1], Sara M. Frangos[1], Megan A. Hansen[1], Alexander W. Toohey[1], Carol E. Cass[2], James D. Young[1], Silvia Pagliardini[1], Detlev Boison[3] and Gregory D. Funk[1]**

[1] Department of Physiology, Women and Children's Health Research Institute, Neuroscience and Mental Health Institute, Faculty of Medicine and Dentistry, University of Alberta, Edmonton, AB, Canada, [2] Professor Emerita, Department of Oncology, Faculty of Medicine and Dentistry, University of Alberta, Edmonton, AB, Canada, [3] Department of Neurosurgery, Robert Wood Johnson Medical School and New Jersey Medical School, Rutgers University, New Brunswick, NJ, United States

OPEN ACCESS

Edited by:
David Blum,
INSERM U1172 Centre de Recherche Jean Pierre Aubert, France

Reviewed by:
Swen Hülsmann,
University of Göttingen, Germany
Rodrigo A. Cunha,
University of Coimbra, Portugal

***Correspondence:**
Gregory D. Funk
gf@ualberta.ca

Specialty section:
This article was submitted to Cellular Neurophysiology, a section of the journal Frontiers in Cellular Neuroscience

Received: 18 January 2019
Accepted: 29 July 2019
Published: 21 August 2019

Citation:
Reklow RJ, Alvares TS, Zhang Y, Miranda Tapia AP, Biancardi V, Katzell AK, Frangos SM, Hansen MA, Toohey AW, Cass CE, Young JD, Pagliardini S, Boison D and Funk GD (2019) The Purinome and the preBötzinger Complex – A Ménage of Unexplored Mechanisms That May Modulate/Shape the Hypoxic Ventilatory Response. Front. Cell. Neurosci. 13:365. doi: 10.3389/fncel.2019.00365

Exploration of purinergic signaling in brainstem homeostatic control processes is challenging the traditional view that the biphasic hypoxic ventilatory response, which comprises a rapid initial increase in breathing followed by a slower secondary depression, reflects the interaction between peripheral chemoreceptor-mediated excitation and central inhibition. While controversial, accumulating evidence supports that in addition to peripheral excitation, interactions between central excitatory and inhibitory purinergic mechanisms shape this key homeostatic reflex. The objective of this review is to present our working model of how purinergic signaling modulates the glutamatergic inspiratory synapse in the preBötzinger Complex (key site of inspiratory rhythm generation) to shape the hypoxic ventilatory response. It is based on the perspective that has emerged from decades of analysis of glutamatergic synapses in the hippocampus, where the actions of extracellular ATP are determined by a complex signaling system, the purinome. The purinome involves not only the actions of ATP and adenosine at P2 and P1 receptors, respectively, but diverse families of enzymes and transporters that collectively determine the rate of ATP degradation, adenosine accumulation and adenosine clearance. We summarize current knowledge of the roles played by these different purinergic elements in the hypoxic ventilatory response, often drawing on examples from other brain regions, and look ahead to many unanswered questions and remaining challenges.

Keywords: hypoxia, P2 receptor, P1 receptor, ectonucleotidase, equilibrative nucleoside transporter, adenosine kinase

INTRODUCTION

The mammalian brain depends on a constant supply of oxygen (O_2) to meet its energy needs, and a host of adaptive responses have evolved to protect brain O_2 levels. Prominent among these is the biphasic hypoxic ventilatory response (Mortola, 1996) in which a fall in arterial O_2 detected at the carotid body chemoreceptors triggers, within the first minute of exposure, an adaptive (Phase 1) increase in breathing. If this increase does not immediately restore arterial O_2, the brain becomes hypoxic, triggering changes in brain chemistry and a maladaptive secondary hypoxic respiratory depression during which ventilation gradually decreases (4–5 min) to a lower steady-state (Phase 2) level. The secondary depression is especially pronounced in premature mammals, where ventilation falls below baseline and can become life-threatening (Mortola, 1996; Bissonnette, 2000; Moss, 2000).

Mechanistically, the biphasic hypoxic ventilatory response has been viewed for decades as the result of just two interacting processes; an initial peripheral, carotid body-mediated (Phase 1) excitation and a slower, centrally mediated hypoxic respiratory depression to a steady-state (Phase 2) level of breathing (Mortola, 1996; Moss, 2000). The mechanisms underlying this depression are not fully understood, but adenosine is strongly implicated (Mortola, 1996; Bissonnette, 2000; Moss, 2000). The key point is that according to this conventional view of the hypoxic ventilatory response, excitation of breathing during hypoxia derives solely from the peripheral nervous system; i.e., the only contribution of the central nervous system to the hypoxic ventilatory response is depression.

New evidence from key cardiorespiratory control sites is challenging this dogma. In relation to the cardiovascular system, C1 noradrenergic neurons involved in control of heart rate and blood pressure are powerfully excited by hypoxia and this excitation is important for homeostatic control (Guyenet, 2006). In the respiratory network, while the Phase 1 component of the hypoxic ventilatory response is mediated peripherally, our data from rodents strongly suggest that during hypoxia, astrocytes in the preBötzinger Complex (preBötC, critical site for generating breathing rhythm) detect hypoxia and release ATP, which, via $P2Y_1$ receptors, excites inspiratory neurons and increases ventilation, thereby attenuating the hypoxic respiratory depression (Gourine et al., 2005; Angelova et al., 2015; Rajani et al., 2017; Sheikhbahaei et al., 2018). Thus, unlike the majority of brain regions where hypoxia has depressant actions, the astroglial network of the preBötC appears to mount an excitatory response that partially counteracts the hypoxic respiratory depression, contributing to a vital homeostatic reflex.

The effects of extracellular ATP (ATPe), however, are not determined solely by its actions on P2 receptors. ATPe is rapidly broken down by ectonucleotidases (e.g., Cd39, CD73) into extracellular adenosine diphosphate (ADPe), adenosine monophosphate (AMPe) and ultimately adenosine (ADOe), a transmitter in its own right that signals via 4 types of P1 receptors, A1, A2A, A2B, and A3 (Haas and Selbach, 2000; Sebastiao and Ribeiro, 2009). Indeed a predominant effect of hypoxia (and ischemia) on brain chemistry is a widespread increase in the concentration of extracellular adenosine (ADOe) (reviewed by Dale and Frenguelli, 2009) that can derive from multiple sources including vesicular release of ATP as a transmitter/cotransmitter that is subsequently degraded, and export of intracellular ADO (ADOi) (reviewed by Latini and Pedata, 2001). In the brain ADOe acts primarily through low affinity A1 and A2A receptors to elicit a host of region-specific effects, largely by modulating glutamatergic transmission. A1 receptor-mediated inhibitory mechanisms, pre- and postsynaptic, are widespread and can be considered neuroprotective (Wei et al., 2011; Boison, 2013a, 2016). A2A receptors are primarily excitatory and engaged in adaptive processes, as heralded by their key role in synaptic plasticity in different brain areas (El Yacoubi et al., 2001, 2009; Pedata et al., 2001; Thauerer et al., 2012; Cunha, 2016; Canas et al., 2018; Lopes et al., 2019). Within the brainstem network that generates and controls breathing, ADOe is largely inhibitory, which in this network is maladaptive; i.e., for the body/brain to recover from hypoxia and restore O_2 homeostasis, ventilation and cardiac activity must increase. ADOe inhibits breathing most potently in premature and newborn mammals via A1 receptors in the preBötC (Herlenius et al., 1997; Herlenius and Lagercrantz, 1999; Huxtable et al., 2009; Zwicker et al., 2011) and A2A receptor-mediated excitation of brainstem GABAergic neurons (Koos et al., 2001, 2005; Wilson et al., 2004; Mayer et al., 2006). Indeed the inhibitory actions of ADOe on the central respiratory network are strongly implicated in the respiratory depression that is life-threatening in apnea of prematurity (AOP) (Martin and Abu-Shaweesh, 2005; Funk, 2013; Poalillo and Picone, 2013; Burnstock and Dale, 2015), and fatal in sudden infant death syndrome (SIDS) and sudden unexpected death in epilepsy (SUDEP) (Boison, 2013b; Richerson et al., 2016).

Thus, the actions of ATP in the preBötC are likely determined by the balance between the excitatory actions of ATP (and ADP) at P2 receptors and the inhibitory actions of its main metabolite, ADO, at P1 receptors (**Figure 1**). Indeed, this balance, which is controlled by a complex signaling system referred to as the *purinome* (Volonte and D'Ambrosi, 2009; **Figure 2**), is emerging as important in determining the degree of hypoxic respiratory depression (Funk, 2013; Angelova et al., 2015; Gourine and Funk, 2017; Rajani et al., 2017; Funk and Gourine, 2018a). The purinome includes: ATPe and P2 receptors (1,2 in **Figure 2**), ADOe and P1 receptors (4); ectonucleotidases that degrade ATP into ADO (3); equilibrative and concentrative nucleoside transporters (ENTs and CNTs, respectively) (King et al., 2006; Parkinson et al., 2011; Young et al., 2013) that move ADO across membranes down (ENTs) or against (CNTs) the ADO concentration gradient (5); and intracellular metabolic enzymes such as adenosine kinase (ADK) (Boison, 2013b) that keep ADOi levels low and control the direction of ADO transport by ENTs (7) (Boison, 2013b). Astrocytes also contribute through their ability to release and respond to ATP and ADO, degrade ATP and remove ADOe. This integrated view of the purinome has influenced epilepsy researchers in the development of novel strategies for manipulating endogenous levels of ADOe to combat seizures (Boison, 2012b; Richerson et al., 2016). Previous work exploring the contribution of purinergic signaling to the hypoxic ventilatory response has been neurocentric and

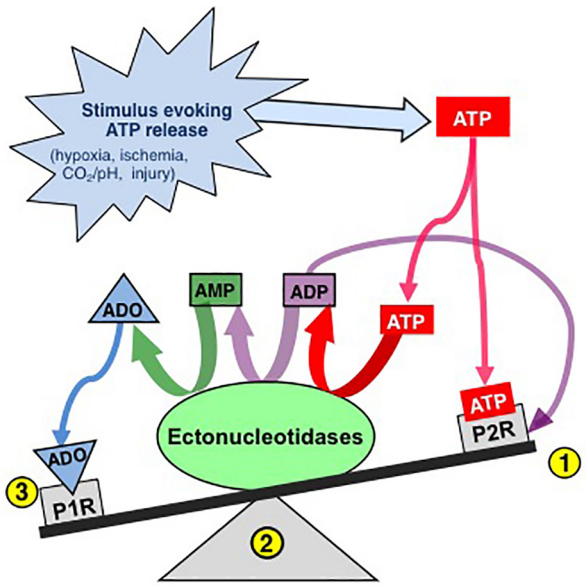

FIGURE 1 | The effects of ATP released into the extracellular space is determined by a balance between actions of ATP at P2 receptors and ADO, its main metabolite, at P1 receptors. Extracellular ATP has two main fates, binding to P2 receptors (1) or degradation by diverse ectonucleotidases (ECTOs) (2) with differential substrate affinities that degrade ATP and its by-products ultimately to adenosine (ADO). Extracellular ADO has three main fates, binding to P1 receptors, transport into the intracellular space or remaining where it is. The balance is dynamic and determined by a complex system referred to as the purinome (see **Figure 2**) (Modified with permission from Funk, 2013).

focused primarily on the actions of ADO at P1 receptors. Thus, contrary to the long-held view that the biphasic hypoxic ventilatory response is due to two competing processes, we propose at least three processes, a peripheral carotid body mediated excitation that underlies Phase 1, as well as central excitatory and inhibitory processes that interact to determine the time course and magnitude of the secondary depression; we also propose a key role for glia in this central excitation. Here, we first discuss the clinical significance of understanding the hypoxic ventilatory response. We then present our working hypothesis of the significance of purinergic signaling in the hypoxic ventilatory response from the broader perspective of the purinome, summarize what is known about the roles played by each component of the purinome in this response and highlight some of the important challenges/questions that remain. Our purpose is not to provide an exhaustive review of all purinergic mechanisms and their influence on information processing in the CNS, but to focus on those most relevant to understanding purinergic signaling in the preBötC and its contribution to the hypoxic ventilatory response. We draw from the insights about purinergic signaling that come from other systems, especially the Schaffer collateral-CA1 pyramidal neuron synapse in the hippocampus, and consider potential implications of identified mechanisms in the context of what is known in respiratory control. For those interested in the control of breathing, the goal is familiarity with the complexities of purinergic systems and potential implications for respiratory control in health and disease. For those with expertise in purinergic signaling, the goal is an appreciation of the unique opportunities for advancing understanding of purinergic signaling that might come with analysis of the central neuro-glial networks that control breathing [the contribution of purinergic signaling to hypoxia sensing in the carotid body is reviewed elsewhere (Lahiri et al., 2007; Conde et al., 2017; Leonard et al., 2018; Nurse et al., 2018)].

CLINICAL SIGNIFICANCE OF THE HYPOXIC VENTILATORY RESPONSE

Hypoxia and the secondary hypoxic respiratory depression are most severe and life threatening in infants who are born prematurely. This reflects that the brain circuits responsible for the generation and control of ventilation are immature and produce a breathing pattern that is interrupted by frequent apneas (periods where breathing stops; apnea of prematurity). Thus, a potentially fatal positive feedback loop can develop in which an apnea causes hypoxia, hypoxia evokes the hypoxic ventilatory response that features a strong secondary respiratory depression that can exacerbate the hypoxia. . .and so on. Apnea of prematurity affects ∼1% of all births in Canada; ∼3000 babies/yr (Statistics Canada., 2014). Risk decreases dramatically with gestational age; ∼15% of infants are affected at 32–33 weeks gestational age but nearly 100% at < 29 weeks (Poalillo and Picone, 2013). The mechanisms underlying the hypoxic respiratory depression and the greater depression in prematurity are not fully understood. The literature is confusing because the hypoxic respiratory depression varies greatly between species, changes developmentally, and likely involves multiple mechanisms. It also depends on whether the experimental apparatus used to deliver the hypoxic gas can deliver a rapid, step change in oxygen. The hypoxia-evoked, Phase 1 increase in ventilation peaks within the 1st min. If the transition from normoxia to hypoxia produced by the gas delivery system is too slow, the hypoxic stimulus will peak after secondary depressive mechanisms have been activated. The result is that the magnitude of both the Phase 1 increase in ventilation and the secondary depression will be underestimated. Nevertheless, it is clear that while the secondary depression is not entirely due to ADOe, ADOe plays a significant role (Martin and Abu-Shaweesh, 2005; Funk, 2013; Poalillo and Picone, 2013; Burnstock and Dale, 2015). Blockade of the respiratory depression by ADO receptor antagonists in a host of species suggests a causative role for ADOe (Martin and Abu-Shaweesh, 2005; Funk, 2013; Poalillo and Picone, 2013; Burnstock and Dale, 2015). Virtually all infants born prematurely who have apnea are treated with methylxanthines, purine based respiratory stimulants that antagonize the inhibitory actions of ADO (Schmidt et al., 2007, 2012). At higher doses that may be relevant clinically, methylxanthines may also inhibit phosphodiesterase activity (preventing cAMP breakdown) and voltage-gated calcium channels (Comer et al., 2001); i.e., the actions of caffeine may not all be mediated by P1 receptors.

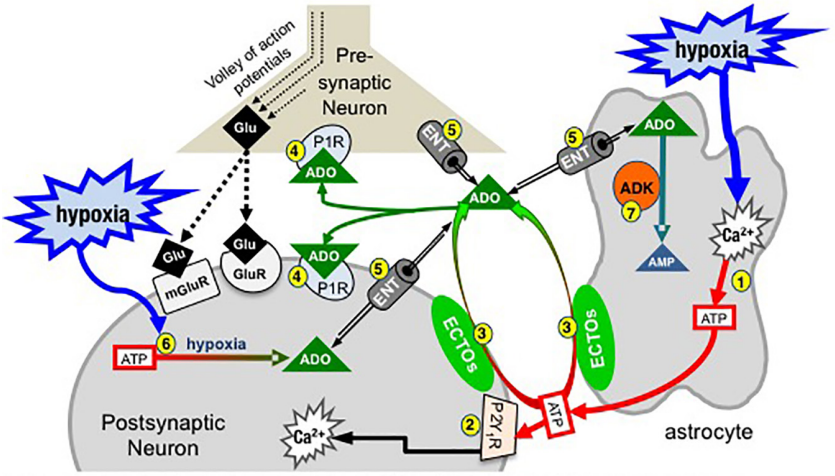

FIGURE 2 | Simplified schematic of the purinome at a glutamatergic, inspiratory, preBötC synapse: multiple factors determine the balance between ATP and ADO signaling. During inspiration, a volley of action potentials in the presynaptic neuron evokes glutamate release that depolarizes the postsynaptic inspiratory neuron via activation of glutamate receptors (ionotropic and metabotropic, mGluR). Hypoxia stimulates astrocytes, via a mitochondrial mechanism (not shown) that evokes increased intracellular Ca^{2+} and vesicular ATP release (1). (2) ATPe acts via neuronal P2 (primarily $P2Y_1$) receptors to excite inspiratory neurons and increase ventilation via a process involving increased intracellular Ca^{2+}. Extracellular ADO (ADOe) increases through breakdown of ATPe by ectonucleotidases (3) or ENT transport of accumulating ADOi (5). ADO acts pre- and postsynaptically via A1 receptors (or A2 receptors on GABAergic neurons, not shown) to inhibit ventilation (4). The direction of ADO transport via ENTs (5) is dependent on the [ADO] gradient. Hypoxia also causes accumulation of intracellular ADO (ADOi) from ATPi hydrolysis (6). ADK phosphorylates ADO into AMP (7), keeping ADOi low so that ENTs remove ADOe. The cytoplasmic form of ADK, at least in adult brain, is limited to astrocytes so that removal of ADOe becomes an astrocyte dependent process (Modified with permission from Funk, 2013).

Caffeine is the preferred methylxanthine for treatment of apnea of prematurity, due to its better safety profile, and efficacy (Shrestha and Jawa, 2017). However, there is still a need for alternate treatment strategies. First, ∼20% of apnea of prematurity patients do not respond to caffeine (Schmidt et al., 2007, 2012). On average such infants will spend an extra week on ventilator support and face greater rates of lung pathology, cognitive delay and cerebral palsy (Schmidt et al., 2007, 2012). Second, while generally a very safe drug, acute side effects include tachycardia, hypertension and tremors. In addition, high concentrations (which are more effective at reducing apneas) in preterm infants increase the incidence of cerebellar hemorrhage 2 years later, are associated with significant changes in motor performance (McPherson et al., 2015) and status epilepticus (Boison, 2011; Shrestha and Jawa, 2017). There is also the potential for long-term effects on sleep (Montandon et al., 2009). Hypoxia and hypoxic respiratory depression are also implicated in SUDEP, the sudden, unexplained death of persons with epilepsy (Boison, 2013b; Richerson et al., 2016; Vilella et al., 2018). SUDEP is a catastrophic event for which all persons with epilepsy are at risk; most deaths occur in middle age but it can happen at any age. The risk for SUDEP is not trivial. A cohort of children with epilepsy was observed for 40 years; SUDEP occurred in 9% of all patients and accounted for 38% of all deaths (Sillanpaa and Shinnar, 2010; Boison, 2012a). Respiratory arrest appears to be the major cause for SUDEP (Devinsky, 2011); a leading hypothesis, the ADO hypothesis of SUDEP, proposes that hypoxia and accumulation of ADOe during a seizure causes a fatal depression of the brainstem respiratory networks (Shen et al., 2010). No preventative strategies exist for SUDEP.

Intermittent hypoxia is also common in various forms of sleep disordered breathing in which a combination of a collapsible airway, high arousability, and high loop gain in chemosensory control systems give rise to cyclic apneas (Dempsey et al., 2012) and a dramatic increase in the risk of cardiovascular disease (Young et al., 1993; Young and Peppard, 2000; Leung and Bradley, 2001; Punjabi, 2008). While the hypoxic ventilatory response and hypoxic respiratory depression are not directly implicated in the cyclic apneas of obstructive sleep apnea, understanding all chemosensory systems, including the novel central hypoxia sensing mechanism under discussion here, is essential to resolve how central and peripheral chemosensory systems interact to cause high loop gain and cyclic apneas that are common in sleep disordered breathing (Dempsey et al., 2010, 2012; Dempsey and Smith, 2019).

Efforts to understand purinergic signaling in the hypoxic ventilatory response have largely focused on the inhibitory actions of ADO at P1 receptors, primarily because ADO is so strongly implicated in the profound hypoxic depression in apnea of prematurity (Martin and Abu-Shaweesh, 2005; Funk, 2013; Poalillo and Picone, 2013; Burnstock and Dale, 2015). Given the emerging picture that the balance between ATP and ADO signaling in the preBötC is important in determining the degree of respiratory depression during the hypoxic ventilatory response, this focus on ADO receptors needs to expand to other components of the purinome. Understanding how the various components of the purinome affect the balance between ATP and ADO signaling is key to manipulating purinergic signaling to modulate breathing. Indeed, the therapeutic potential of the purinome lies in the diversity of its ATP and ADO receptors,

transporters, and enzymes. This is fertile ground that has led to clinical drug trials for cardiac arrhythmias, pain, thrombosis, Parkinson's disease, psoriasis, dry eye, cystic fibrosis, glaucoma and cancer (Pacak et al., 2002; Koles et al., 2005; Burnstock, 2006; Jacobson et al., 2012; Boison, 2013b).

WORKING MODEL OF PURINERGIC SIGNALING IN THE PREBÖTC INSPIRATORY SYNAPSE DURING HYPOXIA

We first provide a brief summary of our working model of how the various components of the purinome in the preBötC might shape the hypoxic ventilatory response; note that not all of the indicated pathways have been demonstrated. This summary is followed by a detailed discussion of the data supporting involvement of purinergic signaling in each step of the proposed model that focuses on the types of preparations from which data were derived (culture, *in vitro*, or *in vivo* anesthetized/paralyzed/freely moving). When relevant data are not available from analysis of the respiratory network, we draw on insights made from analysis of glutamatergic synapses in other brain regions, in particular the hippocampus, where the modulation of glutamatergic signaling by purines (and all components of the purinome) is more completely understood.

At the core of the model (**Figure 2**) are three preBötC cells including an astrocyte, a presynaptic inspiratory glutamatergic neuron, and a postsynaptic, inspiratory glutamatergic neuron. During inspiration a volley of action potentials arrives at the presynaptic terminal, triggers the release of glutamate that acts at ionotropic (primarily AMPA) and metabotropic glutamate receptors and evokes an inspiratory burst. Modulation of rhythm by ATP and ADO during hypoxia is hypothesized to occur through modulation of excitability at multiple synapses like this one between key inspiratory, preBötC neurons that generate rhythm based on their excitatory connections with each other (Del Negro et al., 2018). During hypoxia, astrocytes in the preBötC respond with an increase in intracellular Ca^{2+} and vesicular release of ATP (1). ATPe has two main fates. It binds to P2, primarily $P2Y_1$, receptors on inspiratory neurons causing excitation and increased inspiratory frequency, at least in part by activating G_q proteins and increasing intracellular Ca^{2+} (Rajani et al., 2017) (2). ATPe, once released into the extracellular space, also immediately begins to undergo degradation by ectonucleotidases (3), producing extracellular ADPe (which is excitatory at $P2Y_1$ receptors), AMPe and finally ADOe, which binds to pre- and postsynaptic A1 receptors that inhibit inspiratory rhythm (4). This sets up the very dynamic interaction between the excitatory actions of ATPe (and ADPe) at P2 receptors (2) and inhibitory actions of ADOe at A1 receptors (4). The dynamics will be determined by all elements of the purinome that likely vary between brain regions, with development and also between the same brain region in different species (see discussion below comparing rat vs. mice (Zwicker et al., 2011). Excitation will be determined by the amount of ATP released, local P2 receptor expression patterns and levels, their downstream signaling cascades, as well as the expression level and local complement of ectonucleotidases that determine the rate of ATP removal. In addition, because different ectonucleotidases have different substrate affinities and reaction products with some preferentially producing ADP (which is excitatory via $P2Y_1$ receptors) while others preferentially produce ADO, the mixture of agonists that develops following ATP release depends on the local complement of ectonucleotidases. Inhibition will be determined by local P1 receptor expression patterns and levels, their downstream signaling cascades and the local concentration of ADOe. ADOe accumulates from ectonucleotidase-mediated degradation of adenine nucleotides but it can also come from ENT-mediated transport of ADOi (5) if the concentration of ADO accumulating inside cells from ATP hydrolysis (6) during hypoxia exceeds ADOe. Importantly, the availability of ADOe and hence the level of neuronal ADO receptor activation is largely under the control of ADK (7), expressed in astrocytes (at least in adults). Intracellular phosphorylation of ADO into AMP in astrocytes keeps ADOi levels sufficiently low to drive the influx of ADOe into astrocytes via ENT facilitated transport. Thereby, astrocytes assume a role as a metabolic sink for ADOe and for the termination of ADO receptor activation. The main points of **Figure 2** are first that the balance between P2 and P1 receptor signaling is very dynamic and determined by multiple factors, many of which remain to be examined for their impact on the hypoxic ventilatory response. Second, in contrast to the long-held view that the biphasic hypoxic ventilatory response results from just two interacting processes [an initial peripheral, carotid body-mediated (Phase 1) excitation and a slower, centrally mediated hypoxic respiratory depression (Mortola, 1996; Moss, 2000)], we propose that following the Phase 1 increase, central purinergic mechanisms, excitatory and inhibitory, interact in the preBötC and perhaps elsewhere to shape the remainder of the hypoxic ventilatory response.

While the initial increase indeed appears to be mediated by peripheral chemoreceptors, whether a central excitatory component helps shape the hypoxic ventilatory response during Phase 2 remains controversial and readers are referred to a recent Cross-Talk debate in the Journal of Physiology for a detailed discussion (Funk and Gourine, 2018a,b; Teppema, 2018a,b). Several points of consensus came from that Cross-Talk. First, there was general agreement that gradual recovery, or lack of recovery, of an excitatory component to the hypoxic ventilatory response following carotid body denervation is unlikely to be informative as the same data could be interpreted to support or refute either position. For example, while the frequently observed loss of an hypoxia-evoked increase in ventilation after carotid body denervation is compelling evidence that there is no central contribution to the hypoxia-induced increase in ventilation, there is an alternate interpretation. The lack of response could result from the loss of a tonic, non-chemosensory related carotid body input that is necessary for central hypoxia sensing mechanisms to be expressed. Indeed, unanesthetized dogs and goats with separately perfused, normoxic carotid bodies respond to central hypoxia with a slow onset increase in ventilation that is lost once the normoxic carotid bodies are denervated

(Daristotle et al., 1991; Curran et al., 2000). Conversely, gradual recovery of an excitatory ventilatory response to hypoxia in carotid body-denervated animals is often cited as strong evidence of a central contribution, but this recovered response could also be the result of plasticity. Indeed, carotid body denervation triggers considerable plasticity in peripheral and central neural networks involved in the control of breathing (Teppema and Dahan, 2010). Second, the need for reduced preparations to delineate cellular/ionic/molecular mechanisms of O_2 sensing was acknowledged, but so was the importance of acknowledging the limitations of data derived from such preparations. Finally, there was consensus that the real arbiter of the physiological relevance of central hypoxia sensing mechanisms is what happens in unanesthetized animals with intact carotid bodies when putative central oxygen sensing mechanisms are selectively (and reversibly) perturbed. Progress toward this goal, via the application of viral approaches to selectively (but not yet reversibly) manipulate central purinergic and glial signaling mechanisms *in vivo*, is summarized below.

COMPONENTS OF THE PURINOME AND THEIR ROLE(S) IN THE HYPOXIC VENTILATORY RESPONSE

Role for ATP and Astrocytes

Hypoxia-evoked ATP release of unknown origin was first detected using ATP sensors placed on the ventral medullary surface of anesthetized rats (Gourine et al., 2005; Angelova et al., 2015; Rajani et al., 2017). Hypoxia-induced increases in intracellular Ca^{2+} fluorescence of cortical astrocytes in anesthetized rats suggest that astrocytes are directly sensitive to hypoxia. Direct sensitivity was confirmed with the demonstration that cultured astrocytes respond to hypoxia with an increase in mitochondrial reactive oxygen species that activate PLC, causing an increase in intracellular Ca^{2+} and exocytotic release of ATP (not shown in **Figure 2**); ATP release was shown directly using TIRF (total internal reflection fluorescence) imaging to reveal hypoxia-induced disappearance of ATP-containing vesicles from the intracellular surface of astrocyte membranes (Angelova et al., 2015).

Astrocytic ATP release was also shown indirectly in awake, carotid body-intact animals using viral approaches to block astroglial vesicular release mechanisms (injection of adenoviral vectors that expressed either the light chain tetanus toxin or the dominant-negative SNARE protein in astrocytes) or increase ATP degradation (injection of lentiviral vector that increased ectonucleotidase expression on all cells) at the level of the preBötC; both treatments consistently reduced the hypoxic ventilatory response (Angelova et al., 2015; Sheikhbahaei et al., 2018). These treatments in anesthetized, carotid body intact or carotid body denervated rats similarly decreased the hypoxic ventilatory response (Angelova et al., 2015; Rajani et al., 2017).

These data make a strong case for an ATP-mediated, excitatory contribution to the hypoxic ventilatory response. A caveat remains regarding the case for an astrocytic contribution. The recent demonstrations that disruption of vesicular release mechanisms in astrocytes using the same viral tools attenuates the hypercapnic ventilatory response and exercise capacity as well as the hypoxic ventilatory response (Marina et al., 2017; Sheikhbahaei et al., 2018) have raised the concern that viral injection disrupts baseline astrocyte functions and impairs preBötC excitability. We consider this unlikely because control viruses were without effect on the hypoxic ventilatory response, the hypercapnic ventilatory response and exercise capacity. Thus, while it will be important to demonstrate that the viral tools used to disrupt astrocytic signaling *in vivo* do not globally impair preBötC responsiveness, we propose that the attenuation of respiratory responses to elevated ventilatory drive or metabolic demand following block of vesicular release mechanisms in preBötC astrocytes supports that astrocytes act as brain metabolic sensors (Marina et al., 2017).

P2 Receptors

ATP acts through seven subtypes of ionotropic P2X and eight subtypes of metabotropic P2Y receptors (Abbracchio et al., 2009; Burnstock, 2015; Burnstock and Dale, 2015). Our focus is on $P2Y_1$ receptors because they are exclusively responsible for the marked frequency increase evoked by ATP in the preBötC in medullary slices that generate inspiratory-related rhythm *in vitro*. However, $P2Y_1$ receptor effects are not always excitatory and vary between brain regions. For example, in hippocampus $P2Y_1$ receptor activation reduces glutamate release (Rodrigues et al., 2005), but also excites inhibitory interneurons (Kawamura et al., 2004). Lamina IX spinal cord neurons are also directly excited by $P2Y_1$ receptor activation (Aoyama et al., 2010). In the preBötC, MRS 2179 and MRS 2279 ($P2Y_1$ receptor antagonists) completely block the network response evoked by exogenous ATP *in vitro*, while PPADS and Suramin (general P2 antagonists with low affinity for $P2Y_1$ receptors) and TNP-ATP ($P2X_{1,3}$ antagonist) are without effect (Lorier et al., 2007; Huxtable et al., 2009, 2010). *In vivo*, bathing the ventral medullary surface of anesthetized rats with PPADS (10 μM) or unilaterally injecting the $P2Y_1$ antagonist MRS 2279 into the preBötC of paralyzed rats reduces the hypoxic ventilatory response, indicating that $P2Y_1$ receptors, and possibly other P2 receptors, contribute to the central, hypoxia-mediated increase in ventilation (Gourine et al., 2005; Angelova et al., 2015; Rajani et al., 2017). Potentiation of $P2Y_1$ receptor signaling may therefore be one approach through which respiratory activity could be enhanced to counteract respiratory depression.

These data add to a growing body of evidence that the preBötC is unique. Not only is it key for inspiratory rhythm generation (Feldman and Del Negro, 2006), generation of sighs (Li et al., 2016) and coordinating multiple orofacial behaviors (Kleinfeld et al., 2014a,b), it also mounts an excitatory response to hypoxia (Angelova et al., 2015; Gourine and Funk, 2017; Rajani et al., 2017). An important remaining task is to define 2nd messenger cascades, ionic mechanisms and neuronal phenotype(s) that underlie the ATP excitation of the preBötC that occurs during hypoxia. $P2Y_1$ receptors conventionally signal via the G_q cascade (Abbracchio et al., 2006), but the cascade activated in the preBötC has not been identified. Candidate ion channels, i.e.,

those that affect preBötC rhythm and are also modulated by $P2Y_1$ receptors, include TASK, KCNQ, L-, P-, Q-, and N-type voltage-gated Ca^{2+} channels, BK and SK, and I_{CAN} (Ca^{2+}-activated non-selective cation channels) (Rajani et al., 2016). A key question is whether the subgroup of preBötC neurons that respond to $P2Y_1$ receptor activation and mediate the increase in network frequency are excitatory (i.e., glutamatergic) or inhibitory (GABA- or glycinergic). The model in **Figure 2** depicts glutamatergic neurons as responsible but recent data indicate that preBötC frequency can be more dramatically increased via the activation of inhibitory preBötC neurons (Baertsch et al., 2018).

Ectonucleotidases

There are seven extracellular ectonucleotidase isoforms in the brain grouped into four families: E-NTPDase-1-3; E-NPP1 and 3; tissue non-specific alkaline phosphatase (TNAP); and ecto-5′-nucleotidase (Langer et al., 2008; Abbracchio et al., 2009). This diversity, combined with isoform diversity in substrate and end-product preferences and differential distribution in the brain underlies significant clinical potential and ongoing efforts to produce selective ectonucleotidase agonists/antagonists (al-Rashida and Iqbal, 2014). There is little doubt that ectonucleotidases help determine the balance between ATP and ADO signaling in the preBötC (Funk et al., 2008; Huxtable et al., 2009; Zwicker et al., 2011). However, that most ectonucleotidase inhibitors lack specificity and have off-target actions that interfere with respiratory network function means that most evidence is indirect. Evidence that ectonucleotidases affect preBötC network responses to ATP derives primarily from analysis of rhythmically active medullary slices *in vitro* and includes that: (i) hydrolysis-resistant ATP analogs, such as ATPγS (Lorier et al., 2007) and MRS 2365 (Huxtable et al., 2009) evoke greater frequency responses than ATP; (ii) frequency responses evoked by injection of ATP into the preBötC of rat and especially mouse slices are enhanced by the A1 receptor antagonist, DPCPX (Huxtable et al., 2009; Zwicker et al., 2011); (iii) diffusion of ATP through the preBötC is enhanced in tissue with reduced ectonucleotidase activity (Huxtable et al., 2009); (iv) ATP degradation, measured as the rate of phosphate produced by preBötC tissue punches incubated with ATP, is greatly slowed by the ectonucleotidase inhibitor POM1 (Huxtable et al., 2009); (v) ATP applied to the saline solution bathing rhythmically active slices has very poor access into the tissue; i.e., for an ATP sensor placed just above the slice surface to record the same ATP signal as when the same sensor is placed just 200 μm below the slice surface in the preBötC, the concentration of ATP in the bath must be raised 100-fold, suggesting limited diffusion but more likely significant ATP degradation (Funk et al., 2008).

Indirect evidence that differential ectonucleotidase expression is an important factor in shaping network response dynamics to ATP comes from comparing the responses evoked by injecting ATP into the preBötC of slices from rats and mice and correlating these data with real-time PCR data quantifying the relative expression patterns of ectonucleotidase transcripts in the preBötC of the two species. When applied to the preBötC of Wistar or Sprague-Dawley rats, a brief injection of ATP (10 s) evokes a two- to four-fold increase in frequency that peaks in the first 20–30 s and then falls, typically below baseline between 30 and 60 s postinjection before returning to baseline. In mice, however, the same ATP injection either has no effect or a much smaller effect on frequency (**Figure 3A**) (Zwicker et al., 2011). Importantly, the response of the mouse preBötC to ATP is the same as the rat if A1 ADO receptors are first blocked (**Figure 3C**). Rat and mouse responses to the selective $P2Y_1$ receptor agonist MRS 2365 are also very similar (**Figure 3B**). Thus, both networks share a common P2 receptor-mediated excitation (Zwicker et al., 2011). In mouse, however, it appears that ATP is degraded so quickly to ADO that the ATP excitation and ADO inhibition almost cancel each other out. That the complement of ectonucleotidases might be a factor in this differential ATP sensitivity is supported by the real-time PCR analysis of mRNA extracted from preBötC. The protein encoded by the dominant ectonucleotidase transcript in mice, TNAP (tissue non-specific alkaline phosphatase), which comprises 80% of total ectonucleotidase mRNA, converts ATPe directly to ADOe. In rats, however, the dominant isoform is ENTPDase 2 (its transcript comprises 55% of total ectonucleotidase mRNA, which has a much higher affinity for ATP than ADP so will preferentially produce ADP, an agonist at excitatory $P2Y_1$ receptors (**Figure 3D**). What remains is to determine protein expression (rather than mRNA) and enzyme activities in these different species as well as between different brain regions. The development of inhibitors that are selective for the different ectonucleotidase isoforms that are also devoid of off-target actions will open the door to answering key questions about the significance and therapeutic potential of manipulating ectonucleotidase activities.

Adenosine and Adenosine (P1) Receptors

ADO actions are mediated via four subtypes of G-protein coupled, P1 receptors. These are the A1 and A2A high-affinity subtypes and the A2B, and A3 low-affinity subtypes (Sebastiao and Ribeiro, 2009; Burnstock et al., 2011). While dogma holds that A1 and A3 receptors act through Gi/Go to inhibit, while A2A and A2B receptors act through Gs to stimulate, the classical adenylate cyclase – cAMP – protein kinase A signaling pathway (Fredholm et al., 2001; Thauerer et al., 2012), in the brain cAMP does not appear to be the main transducing system operated by A1 or A2A receptors (Cunha, 2016). P1 receptors may also signal through phospholipase C, Ca^{2+} and mitogen-activated protein kinases (MAPKs) (van Calker et al., 1979; Linden, 1991; Linden et al., 1991; Abbracchio et al., 1995; Fredholm et al., 2001; Schulte and Fredholm, 2003; Tomaselli et al., 2008). A2A receptors in the striatum can also couple to G_{olf} rather than Gs (Kull et al., 2000). All receptor subtypes are present in the CNS, but the high-affinity A1 and A2A subtypes are functionally the most important (Fredholm et al., 2001; Thauerer et al., 2012).

Measurements of ADOe concentrations made using multiple methods, all with limitations, underlie estimates of basal ADOe levels between 30 and 250 nM (Latini and Pedata, 2001). During hypoxia, local or global ischemia, or traumatic brain injury the concentration of ADOe is estimated to

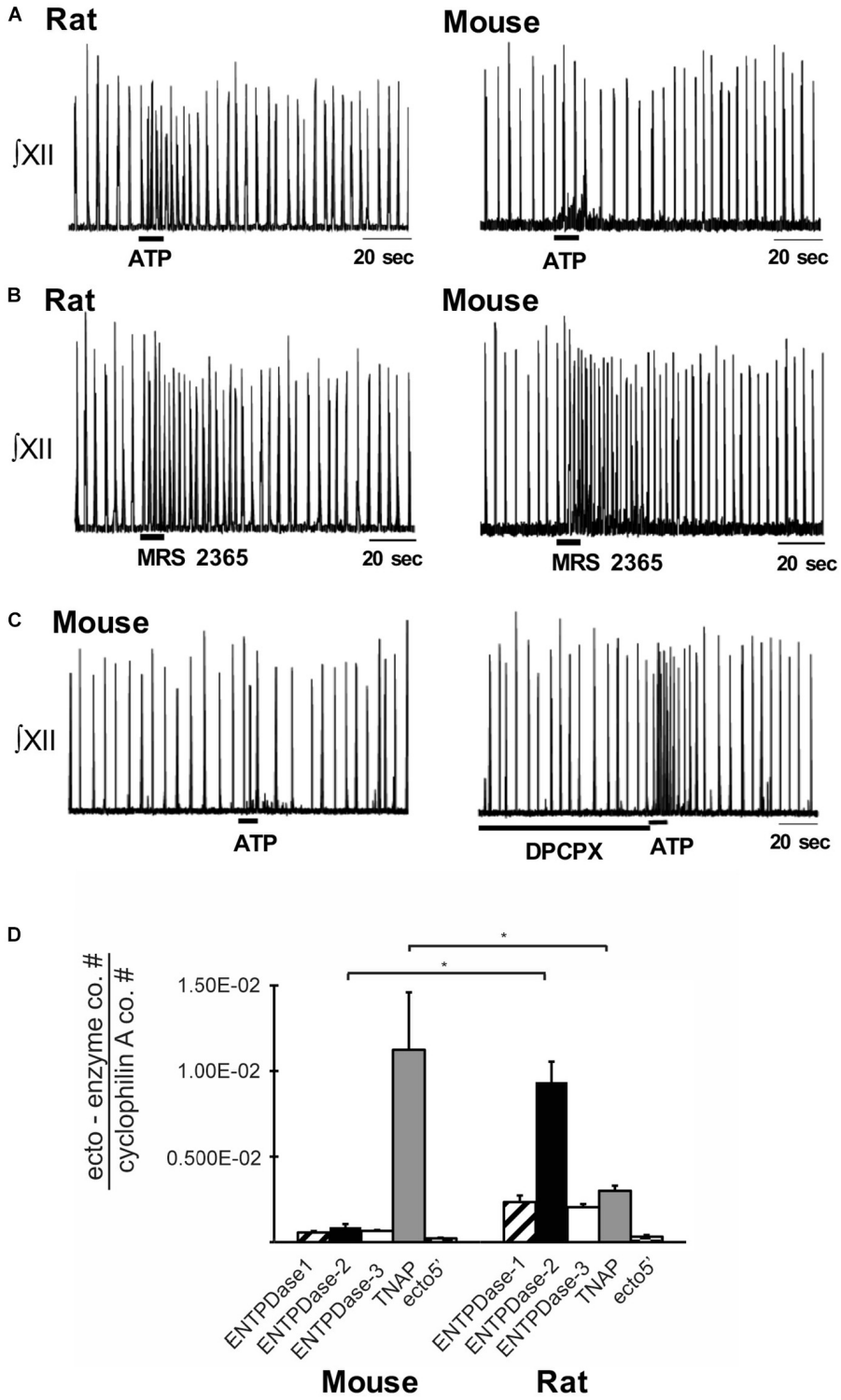

FIGURE 3 | Differential balance between the actions of ATP and ADO in rhythmically-active preBötC-containing slices from neonatal rat and mouse. Integrated XII nerve recordings (∫XII) from rhythmic slices of rat and mice showing baseline inspiratory-related rhythm *in vitro* and responses to local injection of ATP **(A)** or the $P2Y_1$ receptor agonist, MRS-2365, into the preBötC **(B)**. **(C)** Response of a mouse slice to ATP under control conditions and after preBötC injection of the A1 receptor antagonist DPCPX. **(D)** Real-time PCR analysis showing the percentage contribution of each ectonucleotidase isoform to the total ectonucleotidase mRNA extracted from mouse and rat preBötC punches. Error bars indicate SEM. *Significant difference between the compared columns. Reproduced with permission from Zwicker et al. (2011).

increase up to 100-fold into the μM range (3–30 μM) (Dunwiddie and Masino, 2001; Pedata et al., 2001; Wei et al., 2011). When considered in relation to the binding affinity of the different subtypes for ADO (calculated from *in vitro* binding studies; 3–30 nM for A1, 1–20 nM for A2A, 5 ± 20 μM for A2B and > 1 μM for A3 (Fredholm et al., 1994), ADOe concentration data suggest that basal levels of ADOe are sufficient to tonically activate A1 and A2A receptors. However, basal ADOe transmission appears to primarily to involve A1 receptors (Lopes et al., 2019). Lower affinity A2B and A3 receptors may be activated during hypoxia/ischemia/brain injury when ADOe concentrations increase pathologically (Latini and Pedata, 2001; Pedata et al., 2001).

A1 Receptors

A1 receptors are distributed throughout the body with the highest levels of expression in the brain, especially the cortex, hippocampus, cerebellum and dorsal horn of the spinal cord (Mahan et al., 1991; Dixon et al., 1996; Fredholm et al., 2000; Wei et al., 2011), A1 receptor expression is also high in brainstem regions essential for respiratory control (Reppert et al., 1991). As reviewed by Gomes et al. (2011), neuronal A1 receptors are located pre-, post- and extrasynaptically. A1 receptors are highly expressed in presynaptic terminals, especially at excitatory synapses (glutamatergic, cholinergic, serotonergic) (Gomes et al., 2011; Thauerer et al., 2012), where their activation generally inhibits neurotransmitter release (Yawo and Chuhma, 1993; Wu and Saggau, 1994; Gomes et al., 2011), reducing evoked PSPs and the frequency of mEPSPs. The main mechanisms underlying this inhibition include inhibition of voltage-gated Ca^{2+} channels and reduced sensitivity of the vesicular release apparatus to Ca^{2+} (Silinsky, 1984; Scanziani et al., 1992; Scholz and Miller, 1992; Ambrosio et al., 1997). Postsynaptic A1 receptors are primarily located in the postsynaptic density (Rebola et al., 2003) and their activation reduces the responses of hippocampal neurons to excitatory inputs via the inhibition of N-type Ca^{2+} channels, and NMDA receptor-mediated (but not AMPA receptor-mediated) synaptic inputs (de Mendonca et al., 1995).

At the level of the brainstem respiratory network, particularly the preBötC, A1 receptor actions appear dominant (Funk, 2013). A1 receptor antagonists increase basal frequency *in vitro* and *in vivo* and block the inhibitory actions of ADO on respiratory rhythm (Kawai et al., 1995; Schmidt et al., 1995; Kobayashi et al., 2001; Koos et al., 2001, 2005; Wang et al., 2005; Huxtable et al., 2009; Zwicker et al., 2011). In contrast, A2A and A2B receptor agonists have no effect on basal activity of rhythmic medullary slice (Mironov et al., 1999) or brainstem spinal cord preparations from mice (Brockhaus and Ballanyi, 2000), nor on the ADO-mediated inhibition of mouse slices (Mironov et al., 1999). As is well-documented in hippocampus and striatum, A1 receptor activation appears to modulate respiratory neuron and network excitability via pre- and postsynaptic mechanisms, but effects differ between subtypes of respiratory neuron, species and with development. Presynaptic A1 receptor-mediated inhibition of synaptic transmission has only been directly shown with mini PSC analysis in phrenic motoneurons in neonatal rats (Dong and Feldman, 1995). However, presynaptic A1 receptor mediated inhibition of inspiratory, excitatory and inhibitory inputs to rat XII motoneurons *in vitro* (Bellingham and Berger, 1994), mouse inspiratory neurons *in vitro* (Herlenius et al., 1997; Herlenius and Lagercrantz, 1999; Mironov et al., 1999) and cat stage 2 expiratory neurons *in vivo* (Schmidt et al., 1995) is inferred from A1 agonist-mediated reductions in respiratory (excitatory and inhibitory), evoked or spontaneous synaptic inputs (Brockhaus and Ballanyi, 2000). A1 receptor-mediated presynaptic inhibition may also be input- or neuron-specific because the inspiratory synaptic inputs to some inspiratory neurons in the brainstem spinal cord preparation are not unaffected by ADO while excitatory PSPs arriving during expiration are inhibited (Brockhaus and Ballanyi, 2000). Detailed analysis of the effects of ADO and A1 receptor agonists on the frequency and amplitude of miniPSCs in the different subtypes of respiratory neurons is essential to establish which synapses are under presynaptic A1 receptor control.

Postsynaptically, A1 receptor activation hyperpolarizes stage 2 expiratory neurons in adult cat *in vivo* via activation of postsynaptic conductance (likely a K^+ conductance) that decreases input resistance (Schmidt et al., 1995). Similarly, in the brainstem spinal cord preparation A1 receptor activation hyperpolarizes expiratory neurons and reduces input resistance (effects that persist in TTX), suggesting activation of a postsynaptic K^+ conductance (Herlenius and Lagercrantz, 1999). The membrane potential and input resistance of biphasic expiratory (Herlenius and Lagercrantz, 1999) and inspiratory neurons are unaffected by ADO in the absence (Brockhaus and Ballanyi, 2000) (or presence) of TTX (Herlenius and Lagercrantz, 1999). In inspiratory preBötC neurons of rhythmic mouse slices, A1 receptors inhibit intracellular cAMP production, which results in K_{ATP} activation and membrane hyperpolarization (Mironov et al., 1999). Similarly, A1 receptor-mediated hyperpolarization of inspiratory neurons in preBötC island preparations from mice is associated with significant reductions in neuronal input resistance (Vandam et al., 2008). Developmental and species differences must also be taken into account. For example, the A1 receptor-mediated inhibition of inspiratory rhythm in the rhythmic slice or brainstem spinal-cord preparation of rat is gone by postnatal day 2–3 (Herlenius et al., 1997, 2002; Huxtable et al., 2009), while in mouse it persists until at least 2 weeks of age (Funk and Reklow, unpublished observations).

Postsynaptic A1 receptors are also located at extrasynaptic sites (Tetzlaff et al., 1987). Their activation in hippocampal neurons enhances background K^+ currents and causes neuronal hyperpolarization (Greene and Haas, 1991). Basal ADOe tone in the CSF should be sufficient to activate these extrasynaptic receptors and contribute to a tonic, ADO-mediated inhibitory drive. The observation that global inhibition of ADO or A1Rs enhances respiratory rhythm in anesthetized adult cats (Schmidt et al., 1995), unanesthetized fetal sheep (Koos et al., 2001), lambs (Koos et al., 2005), rats *in vivo*, neonatal rats *in vitro* (Kawai et al., 1995; Wang et al., 2005), as well as fetal breathing movements in embryonic rats *in vivo* (Kobayashi et al., 2001) and fictive breathing *in vitro* (Huxtable et al., 2009), suggests that the respiratory network is also under tonic A1 receptor inhibitory control. However, whether this tone reflects activation of synaptic or extrasynaptic receptors is not known. Whether A1 receptors on astrocytes and microglia (van Calker and Biber,

2005; Haselkorn et al., 2010) influence respiratory network function also remains to be determined.

A2A Receptors

A2A receptors are expressed widely throughout the CNS, but more variably compared to A1 receptors. Expression levels are greatest in the olfactory tubercle and on medium spiny neurons of the striatum (Svenningsson et al., 1997a,b; Rosin et al., 1998). The majority of A2A receptors are located in synapses. In the striatum this includes significant pre-synaptic A2A receptor expression, but the majority of A2A receptors are postsynaptic (Rebola et al., 2005). While A2A expression levels in most other brain regions [including the cortex and hippocampus that show the highest levels of A1R expression (Dixon et al., 1996; Svenningsson et al., 1997a)] are substantially lower than in the striatum, levels are still sufficient to modulate neuronal excitability. For example, activation of presynaptic A2A receptors facilitates glutamatergic transmission in hippocampal CA1 neurons by blocking the inhibitory actions of presynaptic A1 receptors on glutamate release (Lopes et al., 1999, 2002). Postsynaptic A2A receptor mechanisms include potentiation of synaptic, but not extrasynaptic, NMDA receptor responses in hippocampal CA1 neurons (Mouro et al., 2018) and inhibition of the slow afterhyperpolarization in pyramidal neurons of the basolateral amygdala (Rau et al., 2015). As reviewed by Wei et al. (2011) and Cunha (2016), the blockade of A2A receptor-mediated effects appears to have little impact on synaptic transmission under baseline conditions but pharmacological or genetic block of A2A signaling attenuates synaptic plasticity/LTP at specific excitatory synapses. Neuronal and glial expression of A2A receptors can also change dramatically in response to specific conditions/stimuli such as epilepsy, further suggesting an important role in brain plasticity (Cunha, 2005).

Within the brainstem and preBötC, A1 receptor mechanisms appear to dominate but at higher levels of the CNS, possibly at the thalamus (Koos et al., 1998, 2000), A2A receptors also modulate breathing and contribute to the hypoxic respiratory depression. Injection of A2A receptor antagonists into the cisterna magna of sheep, pigs and rats reduces the hypoxic respiratory depression (Wilson et al., 2004; Koos et al., 2005; Mayer et al., 2006). Importantly, in pigs and rats the actions of the A2A antagonist on the hypoxic respiratory depression are reversed by the GABA receptor antagonist, bicuculline (Wilson et al., 2004; Mayer et al., 2006), suggesting that the A2A receptor-mediated inhibition is indirect via excitation of GABAergic neurons. The location of GABAergic neurons that receive the A2A receptor-mediated excitation is not known but it is likely rostral to the medulla and pons since A2 receptor antagonists have no effect on the actions of ADO in the rhythmic medullary slice (Mironov et al., 1999) or brainstem spinal cord preparation (Brockhaus and Ballanyi, 2000). Lack of an A2A receptor effect under these conditions does not mean A2A receptors have no role in modulation of respiratory networks. Just as A2A receptors appear important in plasticity in cortical circuits (Gomes et al., 2011; Cunha, 2016), activation of A2A receptors on phrenic motoneurons that drive the main inspiratory pump muscle of mammals can induce phrenic motor facilitation (Golder et al., 2008), a form of inducible plasticity in which inspiratory inputs to the phrenic motoneurons are potentiated. The critical role of the brainstem respiratory network in homeostasis has fueled the long-held view of the respiratory network as a hard-wired, immutable structure. This construct is gradually being replaced with the view that plasticity is likely key to the network's ability to adapt throughout life to diverse demands that are constantly changing on multiple time scales (e.g., during development, disease, aging, transitions to altitude, exercise, phonation, speech). A role for A2A receptors in plasticity at the motor output level of this network is clear (Golder et al., 2008; Johnson and Mitchell, 2013; Fuller and Mitchell, 2017a,b). Exploration of mechanisms that might underlie frequency plasticity within respiratory rhythm generating networks is in its infancy (Johnson et al., 2019).

The actions of low-affinity A2B and A3 receptors on respiratory networks are not known, but both have been implicated in modulating synaptic plasticity through actions on A1 receptor signaling. A2B receptors are located at glutamatergic terminals of the Schaffer collateral-CA1 pyramidal neuron synapse where they counteract the predominant A1 receptor-mediated inhibition of synaptic transmission (Goncalves et al., 2015). Similarly, an A3 receptor antagonist was reported to reduce the A1 receptor-mediated inhibition of excitatory inputs at these same synapses (Dunwiddie et al., 1997a; Lopes et al., 2003).

In summary, multiple lines of evidence indicate that ADOe plays an important role in modulating respiratory network activity and in shaping the hypoxic ventilatory response [see Ballanyi (2004) for review of other modulators that may contribute]. ADOe, whether applied exogenously or derived from the hydrolysis of extracellular ATP or from accumulated intracellular ADO that is transported to the extracellular compartment via equilibrative nucleoside transporters, depresses ventilation in virtually all mammals tested, at fetal (Bissonnette et al., 1990, 1991; Koos and Matsuda, 1990), newborn (Hedner et al., 1984, 1985; Lagercrantz et al., 1984; Runold et al., 1986, 1989; Herlenius et al., 1997), and adult stages (Eldridge et al., 1984; Wessberg et al., 1984; Yamamoto et al., 1994). In addition, despite significant species differences in the sensitivity of the secondary hypoxic respiratory depression to ADO antagonists (reviewed in Ballanyi, 2004), ADO receptor antagonists consistently attenuate the secondary hypoxic respiratory depression (Runold et al., 1989; Bissonnette et al., 1990, 1991; Koos and Matsuda, 1990; Yan et al., 1995; Koos and Maeda, 2001; Koos et al., 2005) and counteract respiratory depression in apnea of prematurity (Bhatt-Mehta and Schumacher, 2003). Despite this abundance of data (Koos et al., 2001, 2005; Wilson et al., 2004; Martin and Abu-Shaweesh, 2005; Funk, 2013; Burnstock and Dale, 2015), the relative contribution of ADOe and the four subtypes of ADO (P1) receptor to the respiratory depression and their site(s) of action are not clear. Variations in protocol, drugs, and developmental stage as well as species differences confound the animal literature (Funk, 2013; Heitzmann et al., 2016). A1 receptor signaling appears to dominate in the preBötC (Lorier et al., 2007, 2008; Huxtable et al., 2009; Zwicker et al., 2011; Angelova et al., 2015), where it may be the only P1 receptor mechanism operating,

at least in newborn rodents (rats and mice) (Mironov et al., 1999; Brockhaus and Ballanyi, 2000). Even within the confines of the preBötC, the action of A1 receptor activation varies developmentally and between species (Herlenius et al., 1997, 2002; Herlenius and Lagercrantz, 1999; Huxtable et al., 2009; Zwicker et al., 2011). There is significant need to understand in many species, throughout development, how the effects of ADO on preBötC activity change, as well as the magnitude of the increase in ventilation that can be achieved by inhibiting ADO receptors within the preBötC. Outside the preBötC, the neuroglial substrate responsible for the A2A receptor-mediated component of the hypoxic respiratory depression has yet to be defined and nothing is known in respiratory networks of the potential actions of A2B and A3 receptors.

Despite the efficacy of ADO receptor antagonists, especially caffeine, as respiratory stimulants that are highly effective in apnea of prematurity, ADO receptors may not be the best target for long-term manipulation of the balance between ATP and ADO signaling. First, as mentioned above, the observation that not all apnea of prematurity patients respond to ADO receptor antagonists highlights the need for alternate, non-ADO receptor focused methods of manipulating this balance. Second, P1 receptors are expressed throughout the body and brain, and potential for cardiovascular side-effects is high (Stella et al., 1993). Thus, even if more selective, higher affinity A1 receptor antagonists/agonists become available, it is unlikely that their oral or intravenous delivery would alter breathing without significant side-effects. A2A receptors are less widely expressed than A1 receptors but manipulation of their activity as a means to counteract hypoxic respiratory depression is not known. Blockade of presynaptic A2A receptor actions (which will inhibit glutamatergic transmission) is generally considered as neuroprotective but activation, rather than inhibition of post- and extrasynaptic A2A receptors may be beneficial (Gomes et al., 2011). In the context of Huntington's Disease, it remains unclear whether A2A agonism or antagonism is clinically favorable. In contrast, A2A receptor antagonists improve motor performance in animal models of Parkinson's Disease (Gomes et al., 2011), and are under examination for their potential clinical utility as a therapeutic strategy for Parkinson's Disease (Takahashi et al., 2018). In the context of SUDEP, caffeine increases survival time in animal models, hypothetically by reducing the inhibitory actions of ADOe on breathing (Shen et al., 2010). However, caffeine (Chroscinska-Krawczyk et al., 2011), or treatments that reduce ADOe, promote seizure (Fedele et al., 2005).

Sources of Extracellular Adenosine

A key piece of information lacking for the preBötC (and all parts of the respiratory network) that is critical for the rational development of alternate approaches to manipulate the purinome to enhance P2 and inhibit P1 signaling is the source, or sources, of ADOe. The source of endogenous ADOe during normal synaptic activity, during hypoxia or during any physiological/pathophysiological process is not known. Clearly the source of elevated endogenous ADOe (e.g., via export of ADOi or degradation of ATPe) will dictate the strategies that can be used to modify ADOe. ADOe can derive from multiple sources and release mechanisms that may differ depending on the nature and severity/duration of the stimulus (synaptic activity, hypoxia/ischemia, inflammation, excitotoxicity/traumatic brain injury), brain region and even cell type (Latini and Pedata, 2001). That the cellular source of ADOe can vary with stimulus was elegantly demonstrated when cultured neurons, astrocytes, and microglia (from rat) were deprived of oxygen-glucose (OGD, to model energy failure), exposed to H_2O_2 (to simulate oxidative stress), or given glutamate (to induce excitotoxicity) (Jackson et al., 2017). Cultured neurons were the primarily source of ADOe during OGD or glutamate exposure while microglia were the main source during oxidative stress. As reviewed by Latini and Pedata (2001) and in agreement with early studies in culture and using hippocampal slices (Meghji et al., 1989; Lloyd et al., 1993; Brundege and Dunwiddie, 1996), a majority of studies indicate that during ischemic or hypoxic conditions the main source of ADOe is formed intracellularly and exported. Importantly, while glia may be a dominant source of ADOe during hypoxia, elevated ADOe during hypoxia could come from endothelial cells, glial cells, and also neurons from anywhere along their cell membrane; i.e., not limited to synapses (Latini and Pedata, 2001). ADO release during hypoxia is only partially sensitive to TTX and Ca^{2+}-independent. This pattern of release differs markedly from normoxic conditions when depolarizing stimuli evoke an ADOe increase that is completely blocked by TTX, Ca^{2+}-sensitive and derived from presynaptic neuronal release of ATP that is subsequently degraded (i.e., ADOe production is sensitive to ecto-5-nucleotidase inhibitors) (Meghji et al., 1989; Lloyd et al., 1993; Brundege and Dunwiddie, 1996; Latini and Pedata, 2001; Parkinson et al., 2005; Wall and Dale, 2008; Zhang et al., 2012; Lietsche et al., 2016). The proposal that ADO can be released via exocytosis from synaptic vesicles (Wall and Dale, 2007, 2008; Klyuch et al., 2011, 2012; Corti et al., 2013) remains controversial, reflecting in part the speed with which ATP can be converted into ADOe and therefore the difficulty of excluding ATP as a source of ADOe (Cunha, 2016). It was shown early on that the actions of ATP at P2 receptors in different brain regions are followed by inhibitory actions that are caused by the rapid degradation of ATP via ectonucleotidases into ADO and activation of P1 receptors (Dunwiddie et al., 1997b; Cunha et al., 1998). The kinetics of this biphasic ATP-ADOe signaling action appear strongly influenced by the properties of ecto-5′-nucleotidase, the main extracellular enzyme that converts AMP into ADO. During periods of intense presynaptic activity and high ATP/ADP levels, it was proposed that ADO production from AMP is delayed until activity ceases and ATP/ADP levels decline, which removes the ATP/ADP inhibition of ecto-5′-nucleotidase (Dunwiddie et al., 1997b; Latini and Pedata, 2001). Such a biphasic response is clearly seen when ATP is applied exogenously into the preBötC of neonatal rats, but not in Swiss CD mice where the excitatory actions of ATP and inhibitory actions of ADOe more or less cancel each other out (Zwicker et al., 2011). This difference may reflect differential expression of ectoATPases in the two species. As mentioned above, the dominant ectonucleotidase transcript in mice is TNAP, which converts ATPe directly to ADOe. The dominant isoform in rat is ENTPDase 2, which preferentially

produces ADP from ATP (Zwicker et al., 2011). The kinetics of the ATP/ADO interaction that evolves in the preBötC in response to endogenously released ATP, and the involvement of specific ectoATPases in this relationship is not known. However, there is evidence that enzyme activity may be distributed to achieve spatially specific adenosine receptor activation. In hippocampus, production of ADOe by ecto-5′-nucleotidase has presynaptic inhibitory actions but also contributes to A2A receptor-mediated long-term potentiation of NMDA EPSCs (Rebola et al., 2008). In the striatum, ecto-5′-nucleotidase is localized to astrocytes but also prominently localized to A2A receptor-containing postsynaptic terminals where it mediates hypolocomotion and modulates working memory (Augusto et al., 2013).

Although the majority of studies (primarily in hippocampus) indicate that the main source of ADOe during ischemic or hypoxic conditions is formed intracellularly (Meghji et al., 1989; Lloyd et al., 1993; Brundege and Dunwiddie, 1996), this may not be case for regions involved in respiratory control. During hypoxia in fetal sheep, an important source of ADOe in the thalamic parafascicular locus, where A2A receptors contribute to the secondary hypoxic respiratory depression (Koos et al., 1998), appears to be extracellular; i.e., the hypoxia-induced increase in ADOe is unaffected by ENT inhibitors but reduced by inhibitors of ecto-5′- nucleotidase (Koos et al., 1997). Within the preBötC we also propose an extracellular source of ADOe during hypoxia; i.e., that hypoxia evokes ATP release from astrocytes via exocytosis, which is then degraded to ADOe. Whether ATPe released via exocytosis, and the subsequently produced ADOe, will diffuse to extrasynaptic receptors and have broad, generalized effects over the entire network, or have localized actions on specific preBötC neurons/synapses is not known. However, within the framework of the localized, bidirectional communication that is proposed to occur between pre- and postsynaptic terminals and astrocytes in the tripartite synapse (Araque et al., 1999; Covelo and Araque, 2018), and the observation that preBötC respiratory neurons differ markedly in their sensitivity to ATP/$P2Y_1$ and ADO receptor activation (Herlenius and Lagercrantz, 1999; Mironov et al., 1999; Thomas and Spyer, 2000; Lorier et al., 2007, 2008), neuroglial interactions in the preBötC are likely to be highly specialized, regionally and functionally; i.e., the effects of ATP/ADP/ADO released from astrocytes during hypoxia are likely to reflect activation of specific synapses and neurons.

Equilibrative Nucleoside Transporters

There are four ENT isoforms that move ADO passively, and bidirectionally across cell membranes. The direction of ADO transport is determined by the ADO concentration gradient. ENT1 and 2 carry out the majority of ADO transport across the outer cell membrane (Parkinson et al., 2011). ENT3 is intracellular and irrelevant in determining ADOe while ENT4 appears to function primarily in monoamine transport. Three isoforms of concentrative nucleoside transporters (CNTs) in the CNS are Na^+-coupled and indirectly consume ATP to move ADO against its concentration gradient, but there is no evidence that CNTs regulate ADOe under normal physiological conditions (Parkinson et al., 2011; Chu et al., 2013). Thus, our focus is on ENTs. They play a key role in maintaining ADOe under baseline conditions, as demonstrated by > 4-fold increases in ADOe in the striatum of freely behaving rats following transporter inhibition (Ballarin et al., 1991). Thus, they are increasingly recognized as potential targets in drug discovery, in part because ADOe is implicated in a range of significant health issues, including cardiovascular disease and sleep disorders (King et al., 2006).

Manipulation of ENTs to control ADOe requires that the source of the increased ADOe during hypoxia is known (Pearson et al., 2003; Pascual et al., 2005; Martin et al., 2007; Funk, 2013). As discussed above (*Sources of extracellular ADO*), if the main source of ADOe is from the ENT-mediated export of ADOi that accumulates during hypoxia, then ENT inhibition would be required to reduce ADOe in the preBötC. If, however, the main source of ADOe is from degradation of ATPe, then the objective would be to potentiate inward ENT-mediated transport and facilitate the clearance of ADOe. Multiple sources and mechanisms can contribute to an hypoxia-induced increase in ADOe. While ENT-mediated export may be a dominant source of ADOe during hypoxia/ischemia in some parts of the brain (Meghji et al., 1989; Lloyd et al., 1993; Brundege and Dunwiddie, 1996; Latini and Pedata, 2001), this may not be the case in the respiratory network. The role of ENTs in regulating ADOe during hypoxia has not been examined specifically in the preBötC. Under baseline conditions in the brainstem spinal cord of neonatal rats, the ENT inhibitor, dipyridamole, decreases inspiratory-related burst frequency, indicating that at least under these conditions ENT activity is important for clearing ADOe (Herlenius et al., 1997). In fetal sheep during hypoxia, however, a major source of ADOe implicated in the hypoxic respiratory depression (Koos et al., 1998) is from degradation of extracellular adenine nucleotides (Koos et al., 1997).

To gain insight into the potential source of ADOe during hypoxia in rodents, we have recently used whole-body plethysmography (Zwicker et al., 2014; Angelova et al., 2015) to compare the hypoxic ventilatory responses of adult, wild-type and three strains of transgenic mice from which ENT1, ENT2 or ENT1 and 2 were both knocked out from birth. All experiments were carried out in accordance with the guidelines of the Canadian Council on Animal Care and were approved by the University of Alberta Animal Ethics Committee (Protocols AUP256). Animals were placed in a whole-body, plexiglass plethysmograph that had inflow and outflow ports for continuous delivery of a steady flow of air (21% O_2, balance N_2 or 10% O_2/balance N_2). Pressure changes in the chamber were recorded with a pressure transducer (DP 103; Validyne, Northridge, CA), signal conditioner (CD-15; Validyne), analog-digital board (Digidata 1322), and Axoscope software (Molecular Devices, Sunnyvale, CA). Animals were allowed 30 min to become accustomed to the chamber. Baseline ventilatory parameters (frequency, relative tidal volume and relative minute ventilation) were then recorded for 10 min and gas composition was changed to 10% O_2/balance N_2 for 10 min and then returned to 21% O_2. Air flow and composition were controlled to produce a rapid transition from 21 to 10% O_2 (< 15 s). Note that measurements of frequency are quantitative while changes in tidal volume and minute ventilation (the product of frequency

and tidal volume) are semiquantitative (reported relative to baseline). The increase in ventilation from baseline to the peak observed during Phase 1 of the hypoxic ventilatory response was reported as 100%. Ventilation during Phase 2 (average between min 6–10 of hypoxic exposure) was calculated as a percentage of the peak increase recording during Phase 1 (**Figure 4A**). All strains showed a biphasic ventilatory response to hypoxia but the magnitude of the hypoxic respiratory depression was greatest in the ENT1/2 KO mice > ENT1 KO > ENT2 KO ≈ wild type mice (**Figure 4B**). The size of the blue bar indicates the magnitude of the depression; i.e., ventilation of the WT mice during Phase 2 was ∼70% of the peak seen during Phase 1 (i.e., during the hypoxic respiratory depression, ventilation fell ∼ 30% from the peak). In contrast, ventilation in the ENT1/2 KOs was 0% of peak, indicating that during Phase 2 ventilation fell all the way to baseline levels (100% depression). These data suggest that the main source of ADOe causing the hypoxic depression comes from breakdown of ATPe. If ADOe came via ENT-mediated outward transport of ADOi, one would expect the opposite – that ADOe would not increase in the ENT KOs and there would be no depression. The main limitation with these data is that ENTs are knocked out globally from birth in these animals, including from the carotid body. Thus, additional work with conditional and/or localized deletion/inhibition of ENT activity will be required to fully evaluate in respiratory networks the source of elevated ADOe during hypoxia, and the role of ENTs in the hypoxic ventilatory response. Such information is required to inform strategies on how to manipulate ENT function to reduce hypoxic respiratory depression.

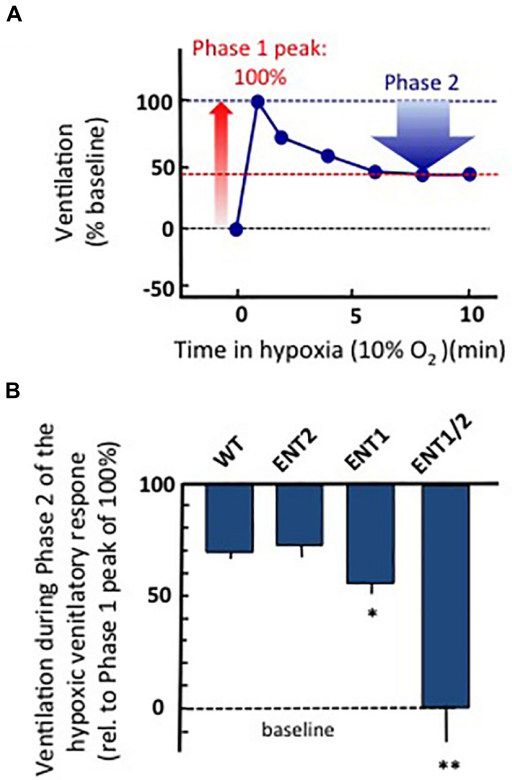

FIGURE 4 | Global knock out of ENTs increases the secondary hypoxic respiratory depression. **(A)** Cartoon showing the biphasic hypoxic ventilatory response, which comprises a Phase 1 increase followed by a secondary depression to a lower, steady-state level of ventilation in Phase 2. The Phase 1 increase was reported as 100%. Ventilation during Phase 2 was calculated as a percentage of the peak increase during Phase 1. In this mock example, ventilation during phase 2 was ∼45% of the phase 1 increase; i.e., ventilation fell by ∼55% from the peak during the hypoxic respiratory depression. **(B)** The level of ventilation (measured using whole-body plethysmography) during Phase 2 of the hypoxic ventilatory response is reported relative to the Phase 1 peak increase for unanesthetized wild type (WT), ENT2, ENT1, and ENT1/2 double knockout mice. *Represents sig. difference from WT, $p < 0.05$ or **$p < 0.01$. ANOVA was used in conjunction with Bonferroni *post hoc* multiple comparison test.

Adenosine Kinase

The impact of manipulating ENT activity on ADOe emphasizes the importance of ADOe metabolic clearance mechanisms in regulating ADOe under baseline, hypoxic and pathological conditions. ENT activity, however, is only part of the ADOe clearance equation. The direction of ADO transport by ENTs is determined by the ADO concentration gradient across the cellular membrane; ADOi must be maintained below ADOe for ENTs to effectively remove ADOe. As demonstrated in rat hippocampal slices (Lloyd and Fredholm, 1995), ADOi and ADOe are influenced by several intracellular enzymes. These include S-adenosyl homocysteine hydrolase, the low affinity, high capacity metabolic enzyme adenosine deaminase, that converts ADO into inosine, and the high affinity, low capacity enzyme ADK that phosphorylates ADOi to AMPi. Our discussion focuses on ADK because it has a higher affinity for ADO than adenosine deaminase, and in hippocampal and cortical networks it is the most important enzyme affecting intracellular levels of ADO and in controlling neuronal excitability and ADO signaling (Pak et al., 1994; Boison, 2013b). It is important to note that in the adult brain ADK is primarily expressed in astrocytes. Therefore ADOe and hence activation of ADO receptors on neurons is under the control of astrocyte-based metabolic clearance of ADOe. Dysregulation of ADK may be causative in some forms of epilepsy. The ADK hypothesis of epilepsy posits that acute insults to the brain lead to an initial and transient downregulation of ADK and an acute elevation of ADOe that is protective in the short term. However, the acute changes trigger maladaptive long term changes of the purinome including downregulation of astrocytic A1 receptors, upregulation of A2A receptors, and astrogliosis in conjunction with chronic overexpression of ADK, reduced ADOe and ultimately spontaneous focal seizure activity in astrogliotic regions (Boison, 2008). Pharmacological inhibition of ADK (Kowaluk and Jarvis, 2000), or ADO augmentation therapies developed to inhibit ADK and raise ADOe greatly reduce seizures in animal models of epilepsy (Boison, 2012b), whereas transgenic overexpression of ADK triggers seizures (Fedele et al., 2005). Whether ADK inhibition increases the risk of respiratory depression, and therefore SUDEP, is not known.

In fact, virtually nothing is known about the impact of ADK on either the baseline control of breathing or the hypoxic ventilatory response. Most exciting in terms of respiratory

control is that the ADK system changes dramatically during postnatal development (Boison, 2013b). ADK comes in long nuclear and short cytoplasmic isoforms, ADK-L and ADK-S, respectively. The nuclear isoform ADK-L has an epigenetic role as regulator of DNA methylation, whereas the cytoplasmic form ADK-S is responsible for regulating extracellular levels of adenosine and ADO receptor activation (Boison, 2013b; Williams-Karnesky et al., 2013). During fetal and early postnatal brain development there is a shift in the expression from ADK-L to more ADK-S and from neuronal expression toward astrocytic expression, suggesting a functional change from an epigenetic regulator of brain development toward a regulator of extracellular adenosine. Therefore, the major system responsible for clearing ADOe in the hippocampus is immature at birth. If the maturation of ADK follows a similar developmental profile in the brainstem respiratory network, it could contribute to the greater susceptibility of premature animals to hypoxic respiratory depression (Moss and Inman, 1989). Tools developed to study the role of ADK in epilepsy, including transgenic mouse lines (Tronche et al., 1999; Boison et al., 2002; Fedele et al., 2004) and adenoassociated viral vectors that knockdown ADK specifically in neurons or astrocytes (Theofilas et al., 2011), should be very instructive in advancing our understanding of the role played by ADK in respiratory control and the hypoxic ventilatory response.

In summary, we have reviewed evidence that purinergic signaling within the preBötC network modulates breathing rhythm and shapes the ventilatory response to hypoxia. Purinergic signaling in other brain regions may contribute to this reflex, but our discussion has focused on the preBötC because it is within this region that we have the strongest evidence that P2 and P1 receptor signaling and ectonucleotidase activity shape the hypoxic ventilatory response. Even for these components of the purinome many questions remain. These include: (i) the identity of signaling cascades and ion channels through which the different receptors modulate breathing rhythm; (ii) the significance of ectonucleotidase diversity for respiratory control; and (iii) the source of ADOe during hypoxia – degradation of ATPe or outward ENT-mediated transport of ADOi. Studies exploring the roles in the hypoxic ventilatory response of ADO transporters (the ENTs), and intracellular enzymes important in controlling ADOi and ADOe clearance (e.g., ADK) are only in their infancy. The developmental dynamics of purinergic signaling in the respiratory network also requires investigation, especially given the potential involvement of the purinome in the greater susceptibility of premature and newborn mammals to hypoxic respiratory depression. Additional key areas of future investigation not discussed above include how the effects of purinergic signaling on cerebral vasculature will affect network excitability, and how the mechanisms and dynamics of purinergic signaling differ between conditions like hypoxia, when ATP is released through physiologically relevant processes, and traumatic injury where ATP is released in high concentration from damaged/ruptured cells including red blood cells? A key translational challenge is to selectively manipulate the balance between ATP/ADO signaling to stimulate ventilation without simultaneously interfering with the beneficial actions of ADOe in other brain regions. To do so will require detailed understanding, not only of the purinome within the preBötC and other respiratory nuclei, but the rest of the brain as well.

ETHICS STATEMENT

All experiments were carried out in accordance with the guidelines of the Canadian Council on Animal Care and were approved by the University of Alberta Animal Ethics Committee (Protocols AUP256).

AUTHOR CONTRIBUTIONS

GF wrote the first draft of the manuscript. RR, TA, and GF contributed to the conception and design of the experiments described in **Figure 3**, while RR and TA completed these studies and performed the statistical analysis. RR, YZ, AM, VB, AK, SF, MH, and AT wrote the sections of the manuscript. JY and CC contributed the ENT knockout mice. DB consulted on ADK biochemistry and implications for respiratory control, and edited the manuscript. All authors contributed to the manuscript conception and revision, and read and approved the submitted version.

FUNDING

This work was supported by the Canadian Institutes of Health Research (CIHR, 53085 and 159551 to GF), Natural Sciences and Engineering Research Council (NSERC, 402532 to GF), Lung Association of Alberta and NWT, Women and Children's Health Research Institute (WCHRI), Canada Foundation for Innovation (CFI), and Alberta Science and Research Authority (ASRA). DB acknowledges funding through NIH grants R01 NS103740 and R01 NS065957. VB is supported by a WCHRI postdoctoral fellowship. RR and YZ received Ph.D. Scholarships from WCHRI. AK, AT, and MH received summer studentships from Alberta Innovates and WCHRI.

REFERENCES

Abbracchio, M. P., Brambilla, R., Ceruti, S., Kim, H. O., von Lubitz, D. K., Jacobson, K. A., et al. (1995). G protein-dependent activation of phospholipase C by adenosine A3 receptors in rat brain. *Mol. Pharmacol.* 48, 1038–1045.

Abbracchio, M. P., Burnstock, G., Boeynaems, J. M., Barnard, E. A., Boyer, J. L., Kennedy, C., et al. (2006). International union of pharmacology LVIII: update on the P2Y G protein-coupled nucleotide receptors: from molecular mechanisms and pathophysiology to therapy. *Pharmacol. Rev.* 58, 281–341. doi: 10.1124/pr.58.3.3

Abbracchio, M. P., Burnstock, G., Verkhratsky, A., and Zimmermann, H. (2009). Purinergic signalling in the nervous system: an overview. *Trends Neurosci.* 32, 19–29. doi: 10.1016/j.tins.2008.10.001

al-Rashida, M., and Iqbal, J. (2014). Therapeutic potentials of ecto-nucleoside triphosphate diphosphohydrolase, ecto-nucleotide

pyrophosphatase/phosphodiesterase, ecto-5'-nucleotidase, and alkaline phosphatase inhibitors. *Med. Res. Rev.* 34, 703–743. doi: 10.1002/med.21302

Ambrosio, A. F., Malva, J. O., Carvalho, A. P., and Carvalho, C. M. (1997). Inhibition of N-,P/Q- and other types of Ca2+ channels in rat hippocampal nerve terminals by the adenosine A1 receptor. *Eur. J. Pharmacol.* 340, 301–310. doi: 10.1016/s0014-2999(97)01451-9

Angelova, P. R., Kasymov, V., Christie, I., Sheikhbahaei, S., Turovsky, E., Marina, N., et al. (2015). Functional oxygen sensitivity of astrocytes. *J. Neurosci.* 35, 10460–10473. doi: 10.1523/JNEUROSCI.0045-15.2015

Aoyama, T., Koga, S., Nakatsuka, T., Fujita, T., Goto, M., and Kumamoto, E. (2010). Excitation of rat spinal ventral horn neurons by purinergic P2X and P2Y receptor activation. *Brain Res.* 1340, 10–17. doi: 10.1016/j.brainres.2010.04.053

Araque, A., Parpura, V., Sanzgiri, R. P., and Haydon, P. G. (1999). Tripartite synapses: glia, the unacknowledged partner. *Trends Neurosci.* 22, 208–215. doi: 10.1016/s0166-2236(98)01349-6

Augusto, E., Matos, M., Sevigny, J., El-Tayeb, A., Bynoe, M. S., Muller, C. E., et al. (2013). Ecto-5'-nucleotidase (CD73)-mediated formation of adenosine is critical for the striatal adenosine A2A receptor functions. *J. Neurosci.* 33, 11390–11399. doi: 10.1523/JNEUROSCI.5817-12.2013

Baertsch, N. A., Baertsch, H. C., and Ramirez, J. M. (2018). The interdependence of excitation and inhibition for the control of dynamic breathing rhythms. *Nat. Commun.* 9:843. doi: 10.1038/s41467-018-03223-x

Ballanyi, K. (2004). Neuromodulation of the perinatal respiratory network. *Curr. Neuropharmacol.* 2, 221–243. doi: 10.2174/1570159043476828

Ballarin, M., Fredholm, B. B., Ambrosio, S., and Mahy, N. (1991). Extracellular levels of adenosine and its metabolites in the striatum of awake rats: inhibition of uptake and metabolism. *Acta Physiol. Scand.* 142, 97–103. doi: 10.1111/j.1748-1716.1991.tb09133.x

Bellingham, M. C., and Berger, A. J. (1994). Adenosine suppresses excitatory glutamatergic inputs to rat hypoglossal motoneurons in vitro. *Neurosci. Lett.* 177, 143–146. doi: 10.1016/0304-3940(94)90065-5

Bhatt-Mehta, V., and Schumacher, R. E. (2003). Treatment of apnea of prematurity. *Paediatr. Drugs* 5, 195–210. doi: 10.2165/00148581-200305030-00006

Bissonnette, J. M. (2000). Mechanisms regulating hypoxic respiratory depression during fetal and postnatal life. *Am. J. Physiol. Regul. Integr. Comp. Physiol.* 278, R1391–R1400.

Bissonnette, J. M., Hohimer, A. R., and Knopp, S. J. (1991). The effect of centrally administered adenosine on fetal breathing movements. *Respir. Physiol.* 84, 273–285. doi: 10.1016/0034-5687(91)90123-z

Bissonnette, J. M., Hohimer, R., Chao, C. R., Knopp, S. J., and Notoroberto, N. F. (1990). Theophylline stimulates fetal breathing movements during hypoxia. *Paediatr. Res.* 28, 83–86. doi: 10.1203/00006450-199028020-00002

Boison, D. (2008). The adenosine kinase hypothesis of epileptogenesis. *Prog. Neurobiol.* 84, 249–262. doi: 10.1016/j.pneurobio.2007.12.002

Boison, D. (2011). Methylxanthines, seizures, and excitotoxicity. *Handb. Exp. Pharmacol.* 2011, 251–266. doi: 10.1007/978-3-642-13443-2-9

Boison, D. (2012a). A Breather for SUDEP. *Epilepsy. Curr.* 12, 111–112. doi: 10.5698/1535-7511-12.3.111

Boison, D. (2012b). "Adenosine augmentation therapy," in *Jasper's Basic Mechanisms of the Epilepsies*, 4th Edn, eds J. L. Noebels, M. Avoli, M. A. Rogawski, R. W. Olsen, and A. V. Delgado-Escueta (Oxford: OUP).

Boison, D. (2013a). Adenosine and seizure termination: endogenous mechanisms. *Epilepsy. Curr.* 13, 35–37. doi: 10.5698/1535-7511-13.1.35

Boison, D. (2013b). Adenosine kinase: exploitation for therapeutic gain. *Pharmacol. Rev.* 65, 906–943. doi: 10.1124/pr.112.006361

Boison, D. (2016). Adenosinergic signaling in epilepsy. *Neuropharmacology* 104, 131–139. doi: 10.1016/j.neuropharm.2015.08.046

Boison, D., Scheurer, L., Zumsteg, V., Rulicke, T., Litynski, P., Fowler, B., et al. (2002). Neonatal hepatic steatosis by disruption of the adenosine kinase gene. *Proc. Natl. Acad. Sci. U.S.A.* 99, 6985–6990. doi: 10.1073/pnas.092642899

Brockhaus, J., and Ballanyi, K. (2000). Anticonvulsant A(1) receptor-mediated adenosine action on neuronal networks in the brainstem-spinal cord of newborn rats. *Neuroscience* 96, 359–371. doi: 10.1016/s0306-4522(99)00544-8

Brundege, J. M., and Dunwiddie, T. V. (1996). Modulation of excitatory synaptic transmission by adenosine released from single hippocampal pyramidal neurons. *J. Neurosci.* 16, 5603–5612. doi: 10.1523/jneurosci.16-18-05603.1996

Burnstock, G. (2006). Purinergic P2 receptors as targets for novel analgesics. *Pharmacol. Ther.* 110, 433–454. doi: 10.1016/j.pharmthera.2005.08.013

Burnstock, G. (2015). Purinergic signalling and the autonomic nervous system in health and disease. *Auton. Neurosci.* 191:1. doi: 10.1016/j.autneu.2015.05.006

Burnstock, G., and Dale, N. (2015). Purinergic signalling during development and ageing. *Purinergic. Signal.* 11, 277–305. doi: 10.1007/s11302-015-9452-9459

Burnstock, G., Fredholm, B. B., and Verkhratsky, A. (2011). Adenosine and ATP receptors in the brain. *Curr. Top. Med. Chem.* 11, 973–1011. doi: 10.2174/156802611795347627

Canas, P. M., Porciuncula, L. O., Simoes, A. P., Augusto, E., Silva, H. B., Machado, N. J., et al. (2018). Neuronal adenosine A2A receptors are critical mediators of neurodegeneration triggered by convulsions. *eNeuro* 5:ENEURO.0385-18.2018. doi: 10.1523/ENEURO.0385-18.2018

Chroscinska-Krawczyk, M., Jargiello-Baszak, M., Walek, M., Tylus, B., and Czuczwar, S. J. (2011). Caffeine and the anticonvulsant potency of antiepileptic drugs: experimental and clinical data. *Pharmacol. Rep.* 63, 12–18. doi: 10.1016/s1734-1140(11)70394-2

Chu, S., Xiong, W., Zhang, D., Soylu, H., Sun, C., Albensi, B. C., et al. (2013). Regulation of adenosine levels during cerebral ischemia. *Acta Pharmacol. Sin.* 34, 60–66. doi: 10.1038/aps.2012.127

Comer, A. M., Perry, C. M., and Figgitt, D. P. (2001). Caffeine citrate: a review of its use in apnoea of prematurity. *Paediatr. Drugs* 3, 61–79. doi: 10.2165/00128072-200103010-00005

Conde, S. V., Monteiro, E. C., and Sacramento, J. F. (2017). Purines and carotid body: new roles in pathological conditions. *Front. Pharmacol.* 8:913. doi: 10.3389/fphar.2017.00913

Corti, F., Cellai, L., Melani, A., Donati, C., Bruni, P., and Pedata, F. (2013). Adenosine is present in rat brain synaptic vesicles. *Neuroreport* 24, 982–987. doi: 10.1097/WNR.0000000000000033

Covelo, A., and Araque, A. (2018). Neuronal activity determines distinct gliotransmitter release from a single astrocyte. *Elife* 7, e32237. doi: 10.7554/eLife.32237

Cunha, R. A. (2005). Neuroprotection by adenosine in the brain: from A(1) receptor activation to A (2A) receptor blockade. *Purinergic Signal.* 1, 111–134. doi: 10.1007/s11302-005-0649-641

Cunha, R. A. (2016). How does adenosine control neuronal dysfunction and neurodegeneration? *J. Neurochem.* 139, 1019–1055. doi: 10.1111/jnc.13724

Cunha, R. A., Sebasti, A. M., and Ribeiro, J. A. (1998). Inhibition by ATP of hippocampal synaptic transmission requires localized extracellular catabolism by ecto-nucleotidases into adenosine and channeling to adenosine A1 receptors. *J. Neurosci.* 18, 1987–1995. doi: 10.1523/jneurosci.18-06-01987.1998

Curran, A. K., Rodman, J. R., Eastwood, P. R., Henderson, K. S., Dempsey, J. A., and Smith, C. A. (2000). Ventilatory responses to specific CNS hypoxia in sleeping dogs. *J. Appl. Physiol.* 88, 1840–1852. doi: 10.1152/jappl.2000.88.5.1840

Dale, N., and Frenguelli, B. G. (2009). Release of adenosine and ATP during ischemia and epilepsy. *Curr. Neuropharmacol.* 7, 160–179. doi: 10.2174/157015909789152146

Daristotle, L., Engwall, M. J., Niu, W. Z., and Bisgard, G. E. (1991). Ventilatory effects and interactions with change in PaO2 in awake goats. *J. Appl. Physiol.* 71, 1254–1260. doi: 10.1152/jappl.1991.71.4.1254

de Mendonca, A., Sebastiao, A. M., and Ribeiro, J. A. (1995). Inhibition of NMDA receptor-mediated currents in isolated rat hippocampal neurones by adenosine A1 receptor activation. *Neuroreport* 6, 1097–1100. doi: 10.1097/00001756-199505300-00006

Del Negro, C. A., Funk, G. D., and Feldman, J. L. (2018). Breathing matters. *Nat. Rev. Neurosci.* 19, 351–367. doi: 10.1038/s41583-018-0003-6

Dempsey, J. A., and Smith, C. A. (2019). Update on chemoreception: influence on cardiorespiratory regulation and pathophysiology. *Clin. Chest. Med.* 40, 269–283. doi: 10.1016/j.ccm.2019.02.001

Dempsey, J. A., Smith, C. A., Blain, G. M., Xia, A., Gong, Y., and Teodorescu, M. (2012). "Role of central/peripheral chemoreceptors and their interdependence in the pathophysiology of sleep apnea," in *Arterial Chemoreception: from Molecules to Systems*, 758 Edn, eds C. A. Nurse, C. Gonzales, C. Peers, and N. R. Prabhakar (New York, NY: Springer), 343–350.

Dempsey, J. A., Veasey, S. C., Morgan, B. J., and O'Donnell, C. P. (2010). Pathophysiology of sleep apnea. *Physiol. Rev.* 90, 47–112. doi: 10.1152/physrev.00043.2008

Devinsky, O. (2011). Sudden, unexpected death in epilepsy. *N. Engl. J .Med.* 365, 1801–1811. doi: 10.1056/NEJMra1010481

Dixon, A. K., Gubitz, A. K., Sirinathsinghji, D. J., Richardson, P. J., and Freeman, T. C. (1996). Tissue distribution of adenosine receptor mRNAs in the rat. *Br. J. Pharmacol.* 118, 1461–1468. doi: 10.1111/j.1476-5381.1996.tb15561.x

Dong, X. W., and Feldman, J. L. (1995). Modulation of inspiratory drive to phrenic motoneurons by presynaptic adenosine A1 receptors. *J. Neurosci.* 15(5 Pt 1), 3458–3467. doi: 10.1523/jneurosci.15-05-03458.1995

Dunwiddie, T. V., Diao, L., Kim, H. O., Jiang, J. L., and Jacobson, K. A. (1997a). Activation of hippocampal adenosine A3 receptors produces a desensitization of A1 receptor-mediated responses in rat hippocampus. *J. Neurosci.* 17, 607–614. doi: 10.1523/jneurosci.17-02-00607.1997

Dunwiddie, T. V., Diao, L., and Proctor, W. R. (1997b). Adenine nucleotides undergo rapid, quantitative conversion to adenosine in the extracellular space in rat hippocampus. *J. Neurosci.* 17, 7673–7682. doi: 10.1523/jneurosci.17-20-07673.1997

Dunwiddie, T. V., and Masino, S. A. (2001). The role and regulation of adenosine in the central nervous system. *Annu. Rev. Neurosci.* 24, 31–55. doi: 10.1146/annurev.neuro.24.1.31

El Yacoubi, M., Ledent, C., Parmentier, M., Costentin, J., and Vaugeois, J. M. (2009). Adenosine A2A receptor deficient mice are partially resistant to limbic seizures. *Naunyn Schmiedebergs Arch. Pharmacol.* 380, 223–232. doi: 10.1007/s00210-009-0426-428

El Yacoubi, M., Ledent, C., Parmentier, M., Daoust, M., Costentin, J., and Vaugeois, J. (2001). Absence of the adenosine A(2A) receptor or its chronic blockade decrease ethanol withdrawal-induced seizures in mice. *Neuropharmacology* 40, 424–432. doi: 10.1016/s0028-3908(00)00173-8

Eldridge, F. L., Millhorn, D. E., and Kiley, J. P. (1984). Respiratory effects of a long-acting analog of adenosine. *Brain Res.* 310, 273–280. doi: 10.1016/0006-8993(84)91096-5

Fedele, D. E., Gouder, N., Guttinger, M., Gabernet, L., Scheurer, L., Rulicke, T., et al. (2005). Astrogliosis in epilepsy leads to overexpression of adenosine kinase, resulting in seizure aggravation. *Brain* 128(Pt 10), 2383–2395. doi: 10.1093/brain/awh555

Fedele, D. E., Koch, P., Scheurer, L., Simpson, E. M., Mohler, H., Brustle, O., et al. (2004). Engineering embryonic stem cell derived glia for adenosine delivery. *Neurosci. Lett.* 370, 160–165. doi: 10.1016/j.neulet.2004.08.031

Feldman, J. L., and Del Negro, C. A. (2006). Looking for inspiration: new perspectives on respiratory rhythm. *Nat. Rev. Neurosci.* 7, 232–242.

Fredholm, B. B., Abbracchio, M. P., Burnstock, G., Daly, J. W., Harden, T. K., Jacobson, K. A., et al. (1994). Nomenclature and classification of purinoceptors. *Pharmacol. Rev.* 46, 143–156.

Fredholm, B. B., Arslan, G., Halldner, L., Kull, B., Schulte, G., and Wasserman, W. (2000). Structure and function of adenosine receptors and their genes. *Naunyn Schmiedebergs Arch. Pharmacol.* 362, 364–374.

Fredholm, B. B., IJzerman, A. P., Jacobson, K. A., Klotz, K. N., and Linden, J. (2001). International union of pharmacology. XXV. Nomenclature and classification of adenosine receptors. *Pharmacol. Rev.* 53, 527–552.

Fuller, D. D., and Mitchell, G. S. (2017a). Respiratory neuroplasticity - overview, significance and future directions. *Exp. Neurol.* 287(Pt 2), 144–152. doi: 10.1016/j.expneurol.2016.05.022

Fuller, D. D., and Mitchell, G. S. (2017b). Special Issue: respiratory Neuroplasticity. *Exp. Neurol.* 287(Pt 2), 91–92. doi: 10.1016/j.expneurol.2016.11.004

Funk, G. D. (2013). Neuromodulation: purinergic signaling in respiratory control. *Compr. Physiol.* 3, 331–363. doi: 10.1002/cphy.c120004

Funk, G. D., and Gourine, A. V. (2018a). CrossTalk proposal: a central hypoxia sensor contributes to the excitatory hypoxic ventilatory response. *J. Physiol.* 596, 2935–2938. doi: 10.1113/JP275707

Funk, G. D., and Gourine, A. V. (2018b). Rebuttal from gregory D. Funk and Alexander V. Gourine. *J. Physiol.* 596, 2943–2944. doi: 10.1113/JP276282

Funk, G. D., Huxtable, A. G., and Lorier, A. R. (2008). ATP in central respiratory control: a three-part signaling system. *Respir. Physiol. Neurobiol.* 164, 131–142. doi: 10.1016/j.resp.2008.06.004

Golder, F. J., Ranganathan, L., Satriotomo, I., Hoffman, M., Lovett-Barr, M. R., Watters, J. J., et al. (2008). Spinal adenosine A2a receptor activation elicits long-lasting phrenic motor facilitation. *J. Neurosci.* 28, 2033–2042. doi: 10.1523/JNEUROSCI.3570-07.2008

Gomes, C. V., Kaster, M. P., Tome, A. R., Agostinho, P. M., and Cunha, R. A. (2011). Adenosine receptors and brain diseases: neuroprotection and neurodegeneration. *Biochim. Biophys. Acta* 1808, 1380–1399. doi: 10.1016/j.bbamem.2010.12.001

Goncalves, F. Q., Pires, J., Pliassova, A., Beleza, R., Lemos, C., Marques, J. M., et al. (2015). Adenosine A2b receptors control A1 receptor-mediated inhibition of synaptic transmission in the mouse hippocampus. *Eur. J. Neurosci.* 41, 878–888. doi: 10.1111/ejn.12851

Gourine, A. V., and Funk, G. D. (2017). On the existence of a central respiratory oxygen sensor. *J. Appl. Physiol.* 123, 1344-1349. doi: 10.1152/japplphysiol.00194.2017

Gourine, A. V., Llaudet, E., Dale, N., and Spyer, K. M. (2005). Release of ATP in the ventral medulla during hypoxia in rats: role in hypoxic ventilatory response. *J. Neurosci.* 25, 1211–1218. doi: 10.1523/jneurosci.3763-04.2005

Greene, R. W., and Haas, H. L. (1991). The electrophysiology of adenosine in the mammalian central nervous system. *Prog. Neurobiol.* 36, 329–341. doi: 10.1016/0301-0082(91)90005-l

Guyenet, P. G. (2006). The sympathetic control of blood pressure. *Nat. Rev. Neurosci.* 7, 335–346. doi: 10.1038/nrn1902

Haas, H. L., and Selbach, O. (2000). Functions of neuronal adenosine receptors. *Naunyn Schmiedebergs Arch. Pharmacol.* 362, 375–381. doi: 10.1007/s002100000314

Haselkorn, M. L., Shellington, D. K., Jackson, E. K., Vagni, V. A., Janesko-Feldman, K., Dubey, R. K., et al. (2010). Adenosine A1 receptor activation as a brake on the microglial response after experimental traumatic brain injury in mice. *J. Neurotrauma* 27, 901–910. doi: 10.1089/neu.2009.1075

Hedner, T., Hedner, J., Bergman, B., Mueller, R. A., and Jonason, J. (1985). Characterization of adenosine-induced respiratory depression in the preterm rabbit. *Biol. Neonate* 47, 323–332. doi: 10.1159/000242135

Hedner, T., Hedner, J., Jonason, J., and Wessberg, P. (1984). Effects of theophylline on adenosine-induced respiratory depression in the preterm rabbit. *Eur. J. Respir. Dis.* 65, 153–156.

Heitzmann, D., Buehler, P., Schweda, F., Georgieff, M., Warth, R., and Thomas, J. (2016). The in vivo respiratory phenotype of the adenosine A1 receptor knockout mouse. *Respir. Physiol. Neurobiol.* 222, 16–28. doi: 10.1016/j.resp.2015.11.005

Herlenius, E., Aden, U., Tang, L. Q., and Lagercrantz, H. (2002). Perinatal respiratory control and its modulation by adenosine in neonatal rat. *Ped Res.* 51, 4–12. doi: 10.1203/00006450-200201000-00004

Herlenius, E., and Lagercrantz, H. (1999). Adenosinergic modulation of respiratory neurones in the neonatal rat brainstem in vitro. *J. Physiol.* 518(Pt 1), 159–172. doi: 10.1111/j.1469-7793.1999.0159r.x

Herlenius, E., Lagercrantz, H., and Yamamoto, Y. (1997). Adenosine modulates inspiratory neurons and the respiratory pattern in the brainstem of neonatal rats. *Pediatr. Res.* 42, 46–53. doi: 10.1203/00006450-199707000-00008

Huxtable, A. G., Zwicker, J. D., Alvares, T. S., Ruangkittisakul, A., Fang, X., Hahn, L. B., et al. (2010). Glia contribute to the purinergic modulation of inspiratory rhythm-generating networks. *J. Neurosci.* 30, 3947–3958. doi: 10.1523/JNEUROSCI.6027-09.2010

Huxtable, A. G., Zwicker, J. D., Poon, B. Y., Pagliardini, S., Vrouwe, S. Q., Greer, J. J., et al. (2009). Tripartite purinergic modulation of central respiratory networks during perinatal development: the influence of ATP, ectonucleotidases, and ATP metabolites. *J. Neurosci.* 29, 14713–14725. doi: 10.1523/JNEUROSCI.2660-09.2009

Jackson, E. K., Kotermanski, S. E., Menshikova, E. V., Dubey, R. K., Jackson, T. C., and Kochanek, P. M. (2017). Adenosine production by brain cells. *J. Neurochem.* 141, 676–693. doi: 10.1111/jnc.14018

Jacobson, K. A., Balasubramanian, R., Deflorian, F., and Gao, Z. G. (2012). G protein-coupled adenosine (P1) and P2Y receptors: ligand design and receptor interactions. *Purinergic Signal.* 8, 419–436. doi: 10.1007/s11302-012-9294-9297

Johnson, R. A., and Mitchell, G. S. (2013). Common mechanisms of compensatory respiratory plasticity in spinal neurological disorders. *Respir. Physiol. Neurobiol.* 189, 419–428. doi: 10.1016/j.resp.2013.05.025

Johnson, S. M., Randhawa, K. S., Baker, T. L., and Watters, J. J. (2019). Respiratory frequency plasticity during development. *Respir. Physiol. Neurobiol.* 266, 54–65. doi: 10.1016/j.resp.2019.04.014

Kawai, A., Okada, Y., Muckenhoff, K., and Scheid, P. (1995). Theophylline and hypoxic ventilatory response in the rat isolated brainstem-spinal cord. *Respir. Physiol.* 100, 25–32. doi: 10.1016/0034-5687(94)00124-i

Kawamura, M., Gachet, C., Inoue, K., and Kato, F. (2004). Direct excitation of inhibitory interneurons by extracellular ATP mediated by P2Y1 receptors in the hippocampal slice. *J. Neurosci.* 24, 10835–10845. doi: 10.1523/jneurosci.3028-04.2004

King, A. E., Ackley, M. A., Cass, C. E., Young, J. D., and Baldwin, S. A. (2006). Nucleoside transporters: from scavengers to novel therapeutic targets. *Trends Pharmacol. Sci.* 27, 416–425. doi: 10.1016/j.tips.2006.06.004

Kleinfeld, D., Deschenes, M., Wang, F., and Moore, J. D. (2014a). More than a rhythm of life: breathing as a binder of orofacial sensation. *Nat. Neurosci.* 17, 647–651. doi: 10.1038/nn.3693

Kleinfeld, D., Moore, J. D., Wang, F., and Deschenes, M. (2014b). The brainstem oscillator for whisking and the case for breathing as the master clock for orofacial motor actions. *Cold Spring Harb Symp. Quant. Biol.* 79, 29–39. doi: 10.1101/sqb.2014.79.024794

Klyuch, B. P., Dale, N., and Wall, M. J. (2012). Receptor-mediated modulation of activity-dependent adenosine release in rat cerebellum. *Neuropharmacology* 62, 815–824. doi: 10.1016/j.neuropharm.2011.09.007

Klyuch, B. P., Richardson, M. J., Dale, N., and Wall, M. J. (2011). The dynamics of single spike-evoked adenosine release in the cerebellum. *J. Physiol.* 589(Pt 2), 283–295. doi: 10.1113/jphysiol.2010.198986

Kobayashi, K., Lemke, R. P., and Greer, J. J. (2001). Development of fetal breathing movements in the rat. *J. Appl. Physiol.* 91, 316–320.

Koles, L., Furst, S., and Illes, P. (2005). P2X and P2Y receptors as possible targets of therapeutic manipulations in CNS illnesses. *Drug News Perspect.* 18, 85–101.

Koos, B. J., Chau, A., Matsuura, M., Punla, O., and Kruger, L. (1998). Thalamic locus mediates hypoxic inhibition of breathing in fetal sheep. *J. Neurophysiol.* 79, 2383–2393. doi: 10.1152/jn.1998.79.5.2383

Koos, B. J., Chau, A., Matsuura, M., Punla, O., and Kruger, L. (2000). Thalamic lesions dissociate breathing inhibition by hypoxia and adenosine in fetal sheep. *Am. J. Physiol. Regul. Integr Comp. Physiol.* 278, R831–R837. doi: 10.1152/ajpregu.2000.278.4.R831

Koos, B. J., Kawasaki, Y., Kim, Y.-H., and Bohorquez, F. (2005). Adenosine A2A-receptor blockade abolishes the roll-off respiratory response to hypoxia in awake lambs. *Am. J. Physiol. Regul. Integr. Comp. Physiol.* 288, R1185–R1194.

Koos, B. J., Kruger, L., and Murray, T. F. (1997). Source of extracellular brain adenosine during hypoxia in fetal sheep. *Brain Res.* 778, 439–442. doi: 10.1016/s0006-8993(97)01207-9

Koos, B. J., and Maeda, T. (2001). Adenosine A(2A) receptors mediate cardiovascular responses to hypoxia in fetal sheep. *Am. J. Physiol. Heart Circ. Physiol.* 280, H83–H89. doi: 10.1152/ajpheart.2001.280.1.H83

Koos, B. J., Maeda, T., and Jan, C. (2001). Adenosine A(1) and A(2A) receptors modulate sleep state and breathing in fetal sheep. *J. Appl. Physiol.* 91, 343–350. doi: 10.1152/jappl.2001.91.1.343

Koos, B. J., and Matsuda, K. (1990). Fetal breathing, sleep state and cardiovascular responses to adenosine in sheep. *J. Appl. Physiol.* 68, 489–495. doi: 10.1152/jappl.1990.68.2.489

Kowaluk, E. A., and Jarvis, M. F. (2000). Therapeutic potential of adenosine kinase inhibitors. *Expert Opin. Investig. Drugs* 9, 551–564. doi: 10.1517/13543784.9.3.551

Kull, B., Svenningsson, P., and Fredholm, B. B. (2000). Adenosine A(2A) receptors are colocalized with and activate g(olf) in rat striatum. *Mol. Pharmacol.* 58, 771–777. doi: 10.1124/mol.58.4.771

Lagercrantz, H., Yamamoto, Y., Fredholm, B. B., Prabhakar, N. R., and Euler, C. (1984). Adenosine analogues depress ventilation in rabbit neonates. *Paediatr. Res.* 18, 387–390. doi: 10.1203/00006450-198404000-00018

Lahiri, S., Mitchell, C. H., Reigada, D., Ray, A., and Cherniack, N. S. (2007). Purines, the carotid body and respiration. *Respir. Physiol. Neurobiol.* 157, 123–129. doi: 10.1016/j.resp.2007.02.015

Langer, D., Hammer, K., Koszalka, P., Schrader, J., Robson, S., and Zimmermann, H. (2008). Distribution of ectonucleotidases in the rodent brain revisited. *Cell Tissue Res.* 334, 199–217. doi: 10.1007/s00441-008-0681-x

Latini, S., and Pedata, F. (2001). Adenosine in the central nervous system: release mechanisms and extracellular concentrations. *J. Neurochem.* 79, 463–484. doi: 10.1046/j.1471-4159.2001.00607.x

Leonard, E. M., Salman, S., and Nurse, C. A. (2018). Sensory processing and integration at the carotid body tripartite synapse: neurotransmitter functions and effects of chronic hypoxia. *Front. Physiol.* 9:225. doi: 10.3389/fphys.2018.00225

Leung, R. S., and Bradley, T. D. (2001). Sleep apnea and cardiovascular disease. *Am. J. Respir. Crit. Care Med.* 164, 2147–2165. doi: 10.1164/ajrccm.164.12.2107045

Li, P., Janczewski, W. A., Yackle, K., Kam, K., Pagliardini, S., Krasnow, M. A., et al. (2016). The peptidergic control circuit for sighing. *Nature* 530, 293–297. doi: 10.1038/nature16964

Lietsche, J., Imran, I., and Klein, J. (2016). Extracellular levels of ATP and acetylcholine during lithium-pilocarpine induced status epilepticus in rats. *Neurosci. Lett.* 611, 69–73. doi: 10.1016/j.neulet.2015.11.028

Linden, J. (1991). Structure and function of A1 adenosine receptors. *FASEB J.* 5, 2668–2676. doi: 10.1096/fasebj.5.12.1916091

Linden, J., Tucker, A. L., and Lynch, K. R. (1991). Molecular cloning of adenosine A1 and A2 receptors. *Trends Pharmacol. Sci.* 12, 326–328. doi: 10.1016/0165-6147(91)90589-k

Lloyd, H. G., and Fredholm, B. B. (1995). Involvement of adenosine deaminase and adenosine kinase in regulating extracellular adenosine concentration in rat hippocampal slices. *Neurochem. Int.* 26, 387–395. doi: 10.1016/0197-0186(94)00144-j

Lloyd, H. G., Lindstrom, K., and Fredholm, B. B. (1993). Intracellular formation and release of adenosine from rat hippocampal slices evoked by electrical stimulation or energy depletion. *Neurochem. Int.* 23, 173–185. doi: 10.1016/0197-0186(93)90095-m

Lopes, J. P., Pliassova, A., and Cunha, R. A. (2019). The physiological effects of caffeine on synaptic transmission and plasticity in the mouse hippocampus selectively depend on adenosine A1 and A2A receptors. *Biochem. Pharmacol.* 166, 313–321. doi: 10.1016/j.bcp.2019.06.008

Lopes, L. V., Cunha, R. A., Kull, B., Fredholm, B. B., and Ribeiro, J. A. (2002). Adenosine A(2A) receptor facilitation of hippocampal synaptic transmission is dependent on tonic A(1) receptor inhibition. *Neuroscience* 112, 319–329. doi: 10.1016/s0306-4522(02)00080-5

Lopes, L. V., Cunha, R. A., and Ribeiro, J. A. (1999). Cross talk between A(1) and A(2A) adenosine receptors in the hippocampus and cortex of young adult and old rats. *J. Neurophysiol.* 82, 3196–3203. doi: 10.1152/jn.1999.82.6.3196

Lopes, L. V., Rebola, N., Pinheiro, P. C., Richardson, P. J., Oliveira, C. R., and Cunha, R. A. (2003). Adenosine A3 receptors are located in neurons of the rat hippocampus. *Neuroreport* 14, 1645–1648. doi: 10.1097/01.wnr.0000088406.04452.44

Lorier, A. R., Huxtable, A. G., Robinson, D. M., Lipski, J., Housley, G. D., and Funk, G. D. (2007). P2Y1 receptor modulation of the pre-Botzinger complex inspiratory rhythm generating network in vitro. *J. Neurosci.* 27, 993–1005. doi: 10.1523/jneurosci.3948-06.2007

Lorier, A. R., Lipski, J., Housley, G. D., Greer, J. J., and Funk, G. D. (2008). ATP sensitivity of preBotzinger complex neurones in neonatal rat in vitro: mechanism underlying a P2 receptor-mediated increase in inspiratory frequency. *J. Physiol.* 586, 1429–1446. doi: 10.1113/jphysiol.2007.143024

Mahan, L. C., McVittie, L. D., Smyk-Randall, E. M., Nakata, H., Monsma, F. J. Jr., Gerfen, C. R., et al. (1991). Cloning and expression of an A1 adenosine receptor from rat brain. *Mol. Pharmacol.* 40, 1–7.

Marina, N., Turovsky, E., Christie, I. N., Hosford, P. S., Hadjihambi, A., Korsak, A., et al. (2017). Brain metabolic sensing and metabolic signaling at the level of an astrocyte. *Glia* 66, 1185–1199. doi: 10.1002/glia.23283

Martin, E. D., Fernandez, M., Perea, G., Pascual, O., Haydon, P. G., Araque, A., et al. (2007). Adenosine released by astrocytes contributes to hypoxia-induced modulation of synaptic transmission. *Glia* 55, 36–45. doi: 10.1002/glia.20431

Martin, R. J., and Abu-Shaweesh, J. M. (2005). Control of breathing and neonatal apnea. *Biol. Neonate* 87, 288–295. doi: 10.1159/000084876

Mayer, C. A., Haxhiu, M. A., Martin, R. J., and Wilson, C. G. (2006). Adenosine A2A receptors mediate GABAergic inhibition of respiration in immature rats. *J. Appl. Physiol.* 100, 91–97. doi: 10.1152/japplphysiol.00459.2005

McPherson, C., Neil, J. J., Tjoeng, T. H., Pineda, R., and Inder, T. E. (2015). A pilot randomized trial of high-dose caffeine therapy in preterm infants. *Pediatr. Res.* 78, 198–204. doi: 10.1038/pr.2015.72

Meghji, P., Tuttle, J. B., and Rubio, R. (1989). Adenosine formation and release by embryonic chick neurons and glia in cell culture. *J. Neurochem.* 53, 1852–1860. doi: 10.1111/j.1471-4159.1989.tb09252.x

Mironov, S. L., Langohr, K., and Richter, D. W. (1999). A1 adenosine receptors modulate respiratory activity of the neonatal mouse via the cAMP-mediated

signaling pathway. *J. Neurophysiol.* 81, 247–255. doi: 10.1152/jn.1999.81.1.247

Montandon, G., Horner, R. L., Kinkead, R., and Bairam, A. (2009). Caffeine in the neonatal period induces long-lasting changes in sleep and breathing in adult rats. *J. Physiol.* 587(Pt 22), 5493–5507. doi: 10.1113/jphysiol.2009.171918

Mortola, J. P. (1996). "Ventilatory responses to hypoxia in mammals," in *Tissue Oxygen Deprivation*, eds G. G. Haddad and G. Lister (New York, NY: Marcel Dekker), 433–477.

Moss, I. R., and Inman, J. G. (1989). Neurochemicals and respiratory control during development. *J. Appl. Physiol.* 67, 1–13. doi: 10.1152/jappl.1989.67.1.1

Moss, R. M. (2000). Respiratory responses to single and episodic hypoxia during development: mechanisms of adaptation. *Respir. Physiol.* 121, 185–197. doi: 10.1016/s0034-5687(00)00127-4

Mouro, F. M., Rombo, D. M., Dias, R. B., Ribeiro, J. A., and Sebastiao, A. M. (2018). Adenosine A2A receptors facilitate synaptic NMDA currents in CA1 pyramidal neurons. *Br. J. Pharmacol.* 175, 4386–4397. doi: 10.1111/bph.14497

Nurse, C. A., Leonard, E. M., and Salman, S. (2018). Role of glial-like type II cells as paracrine modulators of carotid body chemoreception. *Physiol. Genomics* 50, 255–262. doi: 10.1152/physiolgenomics.00142.2017

Pacak, K., Gendron, F. P., Benrezzak, O., Krugh, B. W., Kong, Q., Weisman, G. A., et al. (2002). Purine signaling and potential new therapeutic approach: possible outcomes of NTPDase inhibition. *Curr. Drug Targets* 3, 229–245.

Pak, M. A., Haas, H. L., Decking, U. K., and Schrader, J. (1994). Inhibition of adenosine kinase increases endogenous adenosine and depresses neuronal activity in hippocampal slices. *Neuropharmacology* 33, 1049–1053. doi: 10.1016/0028-3908(94)90142-2

Parkinson, F. E., Damaraju, V. L., Graham, K., Yao, S. Y., Baldwin, S. A., Cass, C. E., et al. (2011). Molecular biology of nucleoside transporters and their distributions and functions in the brain. *Curr. Top. Med. Chem.* 11, 948–972. doi: 10.2174/156802611795347582

Parkinson, F. E., Xiong, W., and Zamzow, C. R. (2005). Astrocytes and neurons: different roles in regulating adenosine levels. *Neurol. Res.* 27, 153–160. doi: 10.1179/016164105X21878

Pascual, O., Casper, K. B., Kubera, C., Zhang, J., Revilla-Sanchez, R., Sul, J. Y., et al. (2005). Astrocytic purinergic signaling coordinates synaptic networks. *Science* 310, 113–116. doi: 10.1126/science.1116916

Pearson, T., Currie, A. J., Etherington, L. A., Gadalla, A. E., Damian, K., Llaudet, E., et al. (2003). Plasticity of purine release during cerebral ischemia: clinical implications? *J. Cell Mol. Med.* 7, 362–375. doi: 10.1111/j.1582-4934.2003.tb00239.x

Pedata, F., Corsi, C., Melani, A., Bordoni, F., and Latini, S. (2001). Adenosine extracellular brain concentrations and role of A2A receptors in ischemia. *Ann. N. Y. Acad. Sci.* 939, 74–84. doi: 10.1111/j.1749-6632.2001.tb03614.x

Poalillo, P., and Picone, S. (2013). Apnea of prematurity. *J. Ped. Neon. Indiv. Med* .2, e020213.

Punjabi, N. M. (2008). The epidemiology of adult obstructive sleep apnea. *Proc. Am. Thorac. Soc.* 5, 136–143. doi: 10.1513/pats.200709-155MG

Rajani, R., Zhang, Y., Jalubula, V., Rancic, V., SheikhBahaei, S., Zwicker, J., et al. (2017). Release of ATP by preBötzinger complex astrocytes contributes to the hypoxic ventilatory response via a Ca2+-dependent P2Y1 receptor mechanism. *J. Physiol.* 596, 3245–3269. doi: 10.1113/jp274727

Rajani, V., Zhang, Y., Revill, A. L., and Funk, G. D. (2016). The role of P2Y1 receptor signaling in central respiratory control. *Respir. Physiol. Neurobiol.* 226, 3–10. doi: 10.1016/j.resp.2015.10.003

Rau, A. R., Ariwodola, O. J., and Weiner, J. L. (2015). Postsynaptic adenosine A2A receptors modulate intrinsic excitability of pyramidal cells in the rat basolateral amygdala. *Int. J. Neuropsychopharmacol.* 18:yv017. doi: 10.1093/ijnp/pyv017

Rebola, N., Canas, P. M., Oliveira, C. R., and Cunha, R. A. (2005). Different synaptic and subsynaptic localization of adenosine A2A receptors in the hippocampus and striatum of the rat. *Neuroscience* 132, 893–903. doi: 10.1016/j.neuroscience.2005.01.014

Rebola, N., Lujan, R., Cunha, R. A., and Mulle, C. (2008). Adenosine A2A receptors are essential for long-term potentiation of NMDA-EPSCs at hippocampal mossy fiber synapses. *Neuron* 57, 121–134. doi: 10.1016/j.neuron.2007.11.023

Rebola, N., Pinheiro, P. C., Oliveira, C. R., Malva, J. O., and Cunha, R. A. (2003). Subcellular localization of adenosine A(1) receptors in nerve terminals and synapses of the rat hippocampus. *Brain Res.* 987, 49–58. doi: 10.1016/s0006-8993(03)03247-5

Reppert, S. M., Weaver, D. R., Stehle, D. R., and Rivkees, S. A. (1991). Molecular cloning and characterization of a rat A1-adenosine receptor that is widely expressed in brain and spinal cord. *Mol. Endocrinol.* 5, 1037–1048. doi: 10.1210/mend-5-8-1037

Richerson, G. B., Boison, D., Faingold, C. L., and Ryvlin, P. (2016). From unwitnessed fatality to witnessed rescue: Pharmacologic intervention in sudden unexpected death in epilepsy. *Epilepsia* 57(Suppl. 1), 35–45. doi: 10.1111/epi.13236

Rodrigues, R. J., Almeida, T., Richardson, P. J., Oliveira, C. R., and Cunha, R. A. (2005). Dual presynaptic control by ATP of glutamate release via facilitatory P2X1, P2X2/3, and P2X3 and inhibitory P2Y1, P2Y2, and/or P2Y4 receptors in the rat hippocampus. *J. Neurosci.* 25, 6286–6295. doi: 10.1523/jneurosci.0628-05.2005

Rosin, D. L., Robeva, A., Woodard, R. L., Guyenet, P. G., and Linden, J. (1998). Immunohistochemical localization of adenosine A2A receptors in the rat central nervous system. *J. Comp. Neurol.* 401, 163–186. doi: 10.1002/(sici)1096-9861(19981116)401:2<163::aid-cne2>3.0.co;2-d

Runold, M., Lagercrantz, H., and Fredholm, B. B. (1986). Ventilatory effect of an adenosine analogue in unanaesthetized rabbits during development. *J. Appl. Physiol.* 61, 255–259. doi: 10.1152/jappl.1986.61.1.255

Runold, M., Lagercrantz, H., Prabhakar, N. R., and Fredholm, B. B. (1989). Role of adenosine in hypoxic ventilatory depression. *J. Appl. Physiol.* 67, 541–546. doi: 10.1152/jappl.1989.67.2.541

Scanziani, M., Capogna, M., Gahwiler, B. H., and Thompson, S. M. (1992). Presynaptic inhibition of miniature excitatory synaptic currents by baclofen and adenosine in the hippocampus. *Neuron* 9, 919–927. doi: 10.1016/0896-6273(92)90244-8

Schmidt, B., Anderson, P. J., Doyle, L. W., Dewey, D., Grunau, R. E., Asztalos, E. V., et al. (2012). Survival without disability to age 5 years after neonatal caffeine therapy for apnea of prematurity. *JAMA* 307, 275–282. doi: 10.1001/jama.2011.2024

Schmidt, B., Roberts, R. S., Davis, P., Doyle, L. W., Barrington, K. J., Ohlsson, A., et al. (2007). Long-term effects of caffeine therapy for apnea of prematurity. *N Engl. J. Med.* 357, 1893–1902. doi: 10.1056/NEJMoa073679

Schmidt, C., Bellingham, M. C., and Richter, D. W. (1995). Adenosinergic modulation of respiratory neurones and hypoxic responses in the anaesthetized cat. *J. Physiol.* 483(Pt 3), 769–781. doi: 10.1113/jphysiol.1995.sp020621

Scholz, K. P., and Miller, R. J. (1992). Inhibition of quantal transmitter release in the absence of calcium influx by a G protein-linked adenosine receptor at hippocampal synapses. *Neuron* 8, 1139–1150. doi: 10.1016/0896-6273(92)90134-y

Schulte, G., and Fredholm, B. B. (2003). Signalling from adenosine receptors to mitogen-activated protein kinases. *Cell Signal.* 15, 813–827. doi: 10.1016/s0898-6568(03)00058-5

Sebastiao, A. M., and Ribeiro, J. A. (2009). Adenosine receptors and the central nervous system. *Handb. Exp. Pharmacol.* 193, 471–534. doi: 10.1007/978-3-540-89615-9_16

Sheikhbahaei, S., Turovsky, E. A., Hosford, P. S., Hadjihambi, A., Theparambil, S. M., Liu, B., et al. (2018). Astrocytes modulate brainstem respiratory rhythm-generating circuits and determine exercise capacity. *Nat. Commun.* 9:370. doi: 10.1038/s41467-017-02723-2726

Shen, H. Y., Li, T., and Boison, D. (2010). A novel mouse model for sudden unexpected death in epilepsy (SUDEP): role of impaired adenosine clearance. *Epilepsia* 51, 465–468. doi: 10.1111/j.1528-1167.2009.02248.x

Shrestha, B., and Jawa, G. (2017). Caffeine citrate - is it a silver bullet in neonatology? *Pediatr. Neonatol.* 58, 391–397. doi: 10.1016/j.pedneo.2016.10.003

Silinsky, E. M. (1984). On the mechanism by which adenosine receptor activation inhibits the release of acetylcholine from motor nerve endings. *J. Physiol.* 346, 243–256. doi: 10.1113/jphysiol.1984.sp015019

Sillanpaa, M., and Shinnar, S. (2010). Long-term mortality in childhood-onset epilepsy. *N. Engl. J. Med.* 363, 2522–2529. doi: 10.1056/NEJMoa0911610

Statistics Canada. (2014). *Birth Database (CANSIM table 102–4512)*. Ottawa: Statistics Canada.

Stella, L., Berrino, L., Maione, S., de Novellis, V., and Rossi, F. (1993). Cardiovascular effects of adenosine and its analogs in anaesthetized rats. *Life Sci.* 53, 755–763. doi: 10.1016/0024-3205(93)90497-q

Svenningsson, P., Hall, H., Sedvall, G., and Fredholm, B. B. (1997a). Distribution of adenosine receptors in the postmortem human brain: an extended autoradiographic study. *Synapse* 27, 322–335. doi: 10.1002/(sici)1098-2396(199712)27:4<322::aid-syn6>3.0.co;2-e

Svenningsson, P., Le Moine, C., Kull, B., Sunahara, R., Bloch, B., and Fredholm, B. B. (1997b). Cellular expression of adenosine A2A receptor messenger RNA in the rat central nervous system with special reference to dopamine innervated areas. *Neuroscience* 80, 1171–1185. doi: 10.1016/s0306-4522(97)00180-2

Takahashi, M., Fujita, M., Asai, N., Saki, M., and Mori, A. (2018). Safety and effectiveness of istradefylline in patients with Parkinson's disease: interim analysis of a post-marketing surveillance study in Japan. *Expert Opin. Pharmacother.* 19, 1635–1642. doi: 10.1080/14656566.2018.1518433

Teppema, L. J. (2018a). CrossTalk opposing view: the hypoxic ventilatory response does not include a central, excitatory hypoxia sensing component. *J. Physiol.* 596, 2939–2941. doi: 10.1113/JP275708

Teppema, L. J. (2018b). Rebuttal from Luc J. Teppema. *J. Physiol.* 596, 2945. doi: 10.1113/JP276281

Teppema, L. J., and Dahan, A. (2010). The ventilatory response to hypoxia in mammals: mechanisms, measurement, and analysis. *Physiol. Rev.* 90, 675–754. doi: 10.1152/physrev.00012.2009

Tetzlaff, W., Schubert, P., and Kreutzberg, G. W. (1987). Synaptic and extrasynaptic localization of adenosine binding sites in the rat hippocampus. *Neuroscience* 21, 869–875. doi: 10.1016/0306-4522(87)90043-1

Thauerer, B., Zur Nedden, S., and Baier-Bitterlich, G. (2012). Purine nucleosides: endogenous neuroprotectants in hypoxic brain. *J. Neurochem.* 121, 329–342. doi: 10.1111/j.1471-4159.2012.07692.x

Theofilas, P., Brar, S., Stewart, K. A., Shen, H. Y., Sandau, U. S., Poulsen, D., et al. (2011). Adenosine kinase as a target for therapeutic antisense strategies in epilepsy. *Epilepsia* 52, 589–601. doi: 10.1111/j.1528-1167.2010.02947.x

Thomas, T., and Spyer, K. M. (2000). ATP as a mediator of mammalian central CO2 chemoreception. *J. Physiol.* 523(Pt 2), 441–447. doi: 10.1111/j.1469-7793.2000.00441.x

Tomaselli, B., Nedden, S. Z., Podhraski, V., and Baier-Bitterlich, G. (2008). p42/44 MAPK is an essential effector for purine nucleoside-mediated neuroprotection of hypoxic PC12 cells and primary cerebellar granule neurons. *Mol. Cell Neurosci.* 38, 559–568. doi: 10.1016/j.mcn.2008.05.004

Tronche, F., Kellendonk, C., Kretz, O., Gass, P., Anlag, K., Orban, P. C., et al. (1999). Disruption of the glucocorticoid receptor gene in the nervous system results in reduced anxiety. *Nat. Genet.* 23, 99–103. doi: 10.1038/12703

van Calker, D., and Biber, K. (2005). The role of glial adenosine receptors in neural resilience and the neurobiology of mood disorders. *Neurochem. Res.* 30, 1205–1217. doi: 10.1007/s11064-005-8792-8791

van Calker, D., Muller, M., and Hamprecht, B. (1979). Adenosine regulates via two different types of receptors, the accumulation of cyclic AMP in cultured brain cells. *J. Neurochem.* 33, 999–1005. doi: 10.1111/j.1471-4159.1979.tb05236.x

Vandam, R. J., Shields, E. J., and Kelty, J. D. (2008). Rhythm generation by the pre-Botzinger complex in medullary slice and island preparations: effects of adenosine A(1) receptor activation. *BMC Neurosci.* 9:95. doi: 10.1186/1471-2202-9-95

Vilella, L., Lacuey, N., Hampson, J. P., Rani, M. R. S., Sainju, R. K., Friedman, D., et al. (2018).). Postconvulsive central apnea as a biomarker for sudden unexpected death in epilepsy (SUDEP). *Neurology* 92, e171–e182. doi: 10.1212/WNL.0000000000006785

Volonte, C., and D'Ambrosi, N. (2009). Membrane compartments and purinergic signalling: the purinome, a complex interplay among ligands, degrading enzymes, receptors and transporters. *FEBS J.* 276, 318–329. doi: 10.1111/j.1742-4658.2008.06793.x

Wall, M., and Dale, N. (2008). Activity-dependent release of adenosine: a critical re-evaluation of mechanism. *Curr. Neuropharmacol.* 6, 329–337. doi: 10.2174/157015908787386087

Wall, M. J., and Dale, N. (2007). Auto-inhibition of rat parallel fibre-Purkinje cell synapses by activity-dependent adenosine release. *J. Physiol.* 581(Pt 2), 553–565. doi: 10.1113/jphysiol.2006.126417

Wang, J.-L., Wu, Z.-H., Pan, B.-X., and Li, J. (2005). Adenosine A1 receptors modulate the discharge activities of inspiratory and biphasic expiratory neurons in the meial regions o the nucleus retrofacialis of neonatal rat in vitro. *Neurosci. Lett.* 379, 27–31. doi: 10.1016/j.neulet.2004.12.042

Wei, C. J., Li, W., and Chen, J. F. (2011). Normal and abnormal functions of adenosine receptors in the central nervous system revealed by genetic knockout studies. *Biochim. Biophys. Acta* 1808, 1358–1379. doi: 10.1016/j.bbamem.2010.12.018

Wessberg, P., Hedner, J., Hedner, T., Persson, B., and Jonason, J. (1984). Adenosine mechanisms in the regulation of breathing in the rat. *Eur. J. Pharmacol.* 106, 59–67. doi: 10.1016/0014-2999(84)90678-2

Williams-Karnesky, R. L., Sandau, U. S., Lusardi, T. A., Lytle, N. K., Farrell, J. M., Pritchard, E. M., et al. (2013). Epigenetic changes induced by adenosine augmentation therapy prevent epileptogenesis. *J. Clin. Invest.* 123, 3552–3563. doi: 10.1172/JCI65636

Wilson, C. G., Martin, R. J., Jaber, M., Abu-Shaweesh, J., Jafri, A., Haxhiu, M. A., et al. (2004). Adenosine A2A receptors interact with GABAergic pathways to modulate respiration in neonatal piglets. *Respir. Physiol. Neurobiol.* 141, 201–211. doi: 10.1016/j.resp.2004.04.012

Wu, L. G., and Saggau, P. (1994). Adenosine inhibits evoked synaptic transmission primarily by reducing presynaptic calcium influx in area CA1 of hippocampus. *Neuron* 12, 1139–1148. doi: 10.1016/0896-6273(94)90321-2

Yamamoto, M., Nishimura, M., Kobayashi, S., Akiyama, Y., Miyamoto, K., and Kawakami, Y. (1994). Role of endogenous adenosine in hypoxic ventilatory response in humans: a study with dipyridamole. *J. Appl. Physiol.* 76, 196–203. doi: 10.1152/jappl.1994.76.1.196

Yan, S., Laferriere, A., Zhang, C., and Moss, I. R. (1995). Microdialyzed adenosine in nucleus tractus solitarii and ventilatory response to hypoxia in piglets. *J. Appl. Physiol.* 79, 405–410. doi: 10.1152/jappl.1995.79.2.405

Yawo, H., and Chuhma, N. (1993). Preferential inhibition of omega-conotoxin-sensitive presynaptic Ca2+ channels by adenosine autoreceptors. *Nature* 365, 256–258. doi: 10.1038/365256a0

Young, J. D., Yao, S. Y., Baldwin, J. M., Cass, C. E., and Baldwin, S. A. (2013). The human concentrative and equilibrative nucleoside transporter families. SLC28 and SLC29. *Mol. Aspects Med.* 34, 529–547. doi: 10.1016/j.mam.2012.05.007

Young, T., Palta, M., Dempsey, J., Skatrud, J., Weber, S., and Badr, S. (1993). The occurrence of sleep-disordered breathing among middle-aged adults. *N. Engl. J. Med.* 328, 1230–1235. doi: 10.1056/NEJM199304293281704

Young, T., and Peppard, P. (2000). Sleep-disordered breathing and cardiovascular disease: epidemiologic evidence for a relationship. *Sleep* 23(Suppl. 4), S122–S126.

Zhang, D., Xiong, W., Chu, S., Sun, C., Albensi, B. C., and Parkinson, F. E. (2012). Inhibition of hippocampal synaptic activity by ATP, hypoxia or oxygen-glucose deprivation does not require CD73. *PLoS One* 7:e39772. doi: 10.1371/journal.pone.0039772

Zwicker, J. D., Rajani, V., Hahn, L. B., and Funk, G. D. (2011). Purinergic modulation of preBotzinger complex inspiratory rhythm in rodents: the interaction between ATP and adenosine. *J. Physiol.* 589(Pt 18), 4583–4600. doi: 10.1113/jphysiol.2011.210930

Zwicker, J. D., Zhang, Y., Ren, J., Hutchinson, M. R., Rice, K. C., Watkins, L. R., et al. (2014). Glial TLR4 signaling does not contribute to opioid-induced depression of respiration. *J. Appl. Physiol.* 117, 857–868. doi: 10.1152/japplphysiol.00534.2014

Conflict of Interest Statement: DB is a co-founder of PrevEp LLC, and serves as scientific advisor for Hoffmann LaRoche.

The remaining authors declare that the research was conducted in the absence of any commercial or financial relationships that could be construed as a potential conflict of interest.

frontiers in Cellular Neuroscience

REVIEW
published: 04 September 2019
doi: 10.3389/fncel.2019.00401

Pleiotropic Roles of P2X7 in the Central Nervous System

Jean M. Kanellopoulos[1] *and Cécile Delarasse*[2]*

[1] CNRS, I2BC, Université Paris-Saclay, Orsay, France, [2] Inserm, Sorbonne Université, CNRS, Institut de la Vision, Paris, France

The purinergic receptor P2X7 is expressed in neural and immune cells known to be involved in neurological diseases. Its ligand, ATP, is a signaling molecule that can act as a neurotransmitter in physiological conditions or as a danger signal when released in high amount by damaged/dying cells or activated glial cells. Thus, ATP is a danger-associated molecular pattern. Binding of ATP by P2X7 leads to the activation of different biochemical pathways, depending on the physiological or pathological environment. The aim of this review is to discuss various functions of P2X7 in the immune and central nervous systems. We present evidence that P2X7 may have a detrimental or beneficial role in the nervous system, in the context of neurological pathologies: epilepsy, Alzheimer's disease, multiple sclerosis, amyotrophic lateral sclerosis, age-related macular degeneration and cerebral artery occlusion.

Keywords: purinergic receptor, P2X7, ATP, nervous system, neurodegenerative disease, neurologic disease, demyelinating disease, animal model

OPEN ACCESS

Edited by:
Eric Boué-Grabot,
Université de Bordeaux, France

Reviewed by:
Toshi Kawate,
Cornell University, United States
Francesco Di Virgilio,
University of Ferrara, Italy
James Saville Wiley,
University of Melbourne, Australia

****Correspondence:***
Cécile Delarasse
cecile.delarasse@upmc.fr

Specialty section:
This article was submitted to Cellular Neurophysiology, a section of the journal Frontiers in Cellular Neuroscience

Received: *24 May 2019*
Accepted: *19 August 2019*
Published: *04 September 2019*

Citation:
Kanellopoulos JM and Delarasse C (2019) Pleiotropic Roles of P2X7 in the Central Nervous System. Front. Cell. Neurosci. 13:401. doi: 10.3389/fncel.2019.00401

INTRODUCTION

The "purinergic hypothesis" was introduced in Burnstock (1972), based on his studies showing that response to ATP was similar to the response of non-adrenergic, non-cholinergic nerve stimulation of gut or bladder smooth muscles. Another important concept was introduced when ATP was shown to be released with various neurotransmitters in the peripheral and central nervous systems (CNS; Burnstock et al., 1972). Burnstock's hypothesis represents a major step in our understanding of purinergic signaling and Burnstock proposed pharmacological tools to discriminate between different receptor families for adenosine (P1 receptors) and for ATP/ADP (P2 receptors). P2-purinergic receptors are able to transduce signals triggered by the binding of extracellular adenosine 5′ triphosphate (eATP). However, eATP is rapidly degraded by several ecto-enzymes to adenosine 5′ diphosphate (ADP), adenosine 5′ monophosphate (AMP) and adenosine. ATP binds to plasma membrane receptors of the P2 family while adenosine stimulates other purinergic receptors called P1 receptors. The P2 family of receptors is divided in two subgroups, the ionotropic P2X receptors which bind ATP and metabotropic P2Y receptors able to bind ATP, ADP, UTP, and UDP.

The P2X7 receptor (P2X7) belongs to the P2X receptor family. The functions of P2X7 in inflammation and cell death have been studied extensively. The role of P2X7 in the immune system has been reviewed at length recently by Di Virgilio et al. (2017). In the CNS, the involvement of P2X7, in particular, in neuronal cell death is unclear, since the expression of P2X7 is still the subject of intense debate (Illes et al., 2017; Miras-Portugal et al., 2017). Interestingly, a recent in-depth study, using P2X7-transgenic reporter mice, cell-specific P2X7-deficient mice and P2X7-specific nanobodies (Kaczmarek-Hajek et al., 2018), showed that P2X7 is mainly expressed in glial cells. These important results are in agreement with a previous report that functional P2X7

are expressed on radial astrocytes of the cerebellar cortex called Bergmann cells (Habbas et al., 2011). However, using a humanized P2X7 conditional KO mouse line crossed to different tissue- or cell-specific Cre-recombinase transgenic mice, Metzger et al. (2017) have found that P2X7 mRNA is expressed in glutamatergic pyramidal neurons of the CA3 region of the hippocampus and in astrocytes, oligodendrocytes and microglia. Immune cells are involved in neurological diseases, such as multiple sclerosis in which an autoimmune response driven by T lymphocytes contributes to pathological processes. To a lesser extent, an inflammatory response also takes part in neurodegenerative diseases, as for example, in Alzheimer's disease (AD), amyotrophic lateral sclerosis (ALS) and age-related macular degeneration (AMD). In these pathologies, danger signals like amyloid-β peptides and ATP are released which activate the innate immune system leading to the development of a sterile inflammation (Chen and Nunez, 2010). Thus, P2X7 activities vary and are modulated by the pathological environment, the amount of extracellular ATP, the cell types involved, the level of P2X7 expression as well as the expression of co-receptors (TLR, pannexin 1) (Di Virgilio et al., 2017). The potential therapeutic effects of P2X7 inhibition by antagonists in different animal models of neurological diseases have been elegantly reviewed by Bartlett et al. (2014). In the present review, we will provide an overview of works highlighting the pleiotropic functions of P2X7 in the CNS in physiological and pathological conditions.

P2X7 CHARACTERISTICS

P2X7 Structure

Seven members of the P2X receptor family share the same predicted structure composed of a large extracellular loop of about 300 amino acids which binds ATP, two transmembrane domains, and two intracellular N- and C- termini. The P2X7 differs from other P2X receptors by its C terminus which is 200 amino acids longer. The first crystallographic structure of a P2X receptor was obtained by Kawate et al. (2009). It shows that the zebra fish P2X4 is organized as a trimer of P2X4 and a new fold named « dolphin like » was defined for each subunit. The same group published the structure of the ATP-bound to zebra fish P2X4 showing that two neighboring subunits were able to create a binding site for ATP and identified several residues involved in coordination of the phosphates of ATP as well as those interacting with adenine (Hattori and Gouaux, 2012). In addition, comparison of the free P2X4 with its ATP-bound form showed how the 6 transmembrane helices of the 3 subunits move from a closed to open state (Hattori and Gouaux, 2012). More recently, Karasawa and Kawate (2016) described the crystal structures of a truncated panda P2X7 in the presence of 5 different antagonists. They showed that the 5 drugs bind to the same pocket by hydrophobic interactions. This drug binding pocket is different from the ATP binding site (Karasawa and Kawate, 2016) and these antagonists behave as allosteric non-competitive inhibitors. Kasuya et al. (2017) have described the crystal structure of the chicken P2X7 in complex with the competitive inhibitor TNP-ATP. They found that the TNP-ATP molecule is positioned in the ATP binding pocket and identified the structural mechanism preventing channel activation.

P2X7 Channel/Pore

Brief activation of P2X7 by ATP in its tetra-anionic form, ATP^{4-}, opens cation-specific ion channels. Prolonged ligation of P2X7 results in the formation of non-selective membrane pores, permeable to molecules of molecular mass up to 900 Da. The molecular nature of this non-selective pore remains controversial. Two main hypotheses were proposed to explain pore formation, (1) P2X7 has the intrinsic ability to dilate and form the pore, (2) pore formation involves additional molecules such as plasma membrane hemichannels. The experimental evidence for or against the requirement of additional molecules to trigger the formation of the non-selective pore formation after P2X7 stimulation have been reviewed in detail by Di Virgilio et al. (2018). Several studies suggested that pannexin-1 (Pelegrin and Surprenant, 2006), connexin 43 (Beyer and Steinberg, 1991) and anoctamin 6 (Ousingsawat et al., 2015), a phospholipid scramblase, are involved in the formation of the non-selective pore. However, in mice deficient for pannexin-1 or connexin 43, the stimulation of P2X7 still triggers the formation of non-selective pores showing that these hemichannels of macrophages are dispensable (Qu et al., 2011; Alberto et al., 2013). Recently, purified panda P2X7 incorporated in proteoliposomes was able to form the non-selective pore after stimulation with ATP in the absence of other proteins. Thus, these findings strongly suggest that P2X7 possess an intrinsic ability to form a non-selective pore after ATP stimulation (Karasawa et al., 2017). In addition, a cysteine rich region containing C362 and C363 was demonstrated to be required for the formation of the non-selective pore. Mutations of these cysteine to serine eliminate YO-PRO-1 uptake. Palmitoylation of these cysteine plays a fundamental role in non-selective pore formation and it was proposed that these cysteine prevent the inhibitory effect of cholesterol (Karasawa et al., 2017). In addition, two elegant biochemical studies (Harkat et al., 2017; Pippel et al., 2017) strongly suggested that the non-selective pore formation is not due to a progressive dilation of the P2X7-channel letting large cations into cells. In contrast, ATP binding to P2X7 triggers the opening of a channel allowing the influx of small cations (Ca^{2+}, Na^{+}) and larger ones, such as YO-PRO1. Peverini et al. (2018) have recently analyzed and discussed current views on the permeability to large cations of P2X7 and other P2Xs following ATP stimulation in relation with the putative physiological roles of these non-selective pores.

However, several studies point out that other non-selective pores might be triggered by P2X7 stimulation. It was found that the non-selective pore formation was dependent of MAP-kinase activities (Donnelly-Roberts et al., 2004; Faria et al., 2005) and on second messengers such as Ca^{2+} (Faria et al., 2005). Faria et al. (2005) used a cell-attached configuration which allowed them to trigger or inhibit P2X7 located within the patch pipette or outside it on the plasma membrane. In peritoneal macrophages and 2BH4 cells, they found that a non-selective pore

formation occurred both within the patch pipette and outside of the plasma membrane, after ATP stimulation in or outside the pipette. Importantly, ATP application outside the membrane patch lead to pore formation inside the patch pipette even after P2X7 had been blocked with the pharmacological inhibitor o-ATP within the pipette. These data lead them to postulate that P2X7 stimulation generates a second messenger diffusing inside the cell and triggering the formation of a non-selective pore (Faria et al., 2005).

In addition, Schachter et al. (2008) have compared fluorescent dye uptakes after ATP stimulation in HEK293-P2X7 and macrophages. They found that while cationic dye uptake increased in both cell types after P2X7 stimulation, only macrophages were able to take up anionic dye and to form the p440 pS channels (Schachter et al., 2008). These results suggest that P2X7 stimulation triggers two different pores in macrophages, one for cationic and another one for anionic dyes.

Karasawa et al. (2017) have shown that P2X7 activity, especially pore formation, was highly dependent on the lipid composition of the liposomes in which the purified panda P2X7 was incorporated. Increase in cholesterol induced a decrease in P2X7 non-selective pore formation while phosphatidylglycerol and sphingomyelin enhanced it (Karasawa et al., 2017). Another study reports that P2X7-non-selective pore formation is increased by diminution of plasma membrane cholesterol concentration in human and mouse cells (Robinson et al., 2014). Interestingly, lipin-2 deficient macrophages produce lower levels of cholesterol than WT macrophages, this decrease boosts P2X7 activity leading to an increase in non-selective pore formation, K^+ efflux, NLRP3 activation and IL-1β/IL-18 release (Lorden et al., 2017). The physiopathological relevance of these observations is comforted by *in vivo* studies showing that LPS treatment of lipin-2ko mice induced highly significant increases in IL-1β and IL-18 serum levels compared to WT animals, an observation attributed in part to P2X7 hyperactivity (Lorden et al., 2017). Majeed syndrome patients have inactivating mutations of the *LPIN2* gene. The results obtained by Lorden et al. (2017) strongly suggest that auto-inflammatory disorders found in Majeed syndrome patients are due to an excessive production of mature IL-1β/IL-18 through P2X7 hyperactivity.

Several groups have reported that a pool of P2X7 is associated with detergent-resistant membranes (DRM) in different cell types (Garcia-Marcos et al., 2006; Barth et al., 2007; Delarasse et al., 2009; Gonnord et al., 2009) and that the two populations of P2X7 in the plasma membrane are associated with distinct receptor properties (Garcia-Marcos et al., 2006). Interestingly, the studies of Garcia-Marcos et al. (2006) indicate that the P2X7 involved in non-selective pore formation were those located outside the DRM, in membrane regions containing much less cholesterol.

Gonnord et al. (2009) have shown that P2X7 association with DRM requires the post-translational modification by palmitic acid of several P2X7 carboxy-terminal cysteins. Four regions of the carboxy terminus domain are involved in palmitoylation. Palmitoylation-defective P2X7 mutants showed a dramatic decrease of P2X7 cell surface expression due to their retention in the endoplasmic reticulum and proteolytic degradation in lysosomes and proteasomes. Thus, P2X7 palmitoylation plays a critical role in its association with the lipid microdomains of the plasma membrane and in the regulation of its half-life.

P2X7 Induced Cell Death or Proliferation

Prolonged ATP stimulation of P2X7 can lead to membrane blebbing and cell death by apoptosis or lysis/necrosis depending on the cell type. P2X7 is expressed by various hematopoietic cells such as thymocytes, lymphocytes, macrophages, dendritic cells. ATP treatment of mouse thymocytes induces two types of P2X7-dependent cell death: (1) a caspase-dependent apoptosis of a small subpopulation of thymocytes (mostly $CD4^+$); (2) a predominant Ca^{2+} independent lysis/necrosis of $CD4^+CD8^+$ thymocytes (Auger et al., 2005). Our analyses of the biochemical pathways triggered after ATP stimulation of thymocyte have shown that P2X7 ligation induces the sequential activation of a Src-kinase, a PI3-kinase (phosphoinositide 3-kinase), the ERK1/2 kinases (extracellular signal-regulated kinases) and finally the proteasome (**Figure 1**). Importantly, the pharmacologic inhibition of one of these enzymatic activities blocks the P2X7-induced thymocyte lysis. Surprisingly, we were unable to demonstrate these biochemical pathways of cellular death in T splenocytes (unpublished observations). The reason of this discrepancy may lie in the recent findings that P2X7-mediated cellular activities in heterogeneous sub-populations of T lymphocytes in the spleen are not directly related to the levels of P2X7 membrane expression but depend on the stage of activation/differentiation of these T cell subsets (Safya et al., 2018; Mellouk and Bobe, 2019).

In **Figure 1**, several examples of P2X7 induced cell death are shown. Various biochemical pathways are activated in different cell types undergoing necrosis/lysis, preventing the identification of a characteristic P2X7-induced cell death pathway. While necrotic/lysis induced by P2X7 stimulation remains ill defined, P2X7-dependent apoptosis and pyroptosis have been described more precisely at the molecular level. In particular, major breakthroughs have been made in our understanding of pyroptosis following P2X7-induced activation of NLRP3 inflammasome (cf. following paragraph).

While P2X7-dependent cell deaths have been described in many cellular models, the role of P2X7 in cell growth was discovered by Baricordi et al. (1999) who found that two different P2X7 negative lymphoid cell lines, transfected with a cDNA encoding P2X7, were able to grow in serum free medium. This increased proliferation was shown to be blocked by the antagonist o-ATP and was due to the release of ATP in the culture supernatants of these leukemic cell lines (Baricordi et al., 1999). More recently, basal stimulation of P2X7 was shown to increase the mitochondrial potential $\Delta\Psi$, the mitochondrial Ca^{2+} concentration and stimulate ATP synthesis (Adinolfi et al., 2005). The increase in cytosolic Ca^{2+} concentrations following basal stimulation of P2X7 was shown to increase the amount of nuclear NFATc1 (nuclear factor of activated T cell complex 1) leading to cell growth (Adinolfi et al., 2009). Surprisingly, the basal stimulation of P2X7 leading to cell growth was dependent on the carboxy-terminal tail of P2X7 and the non-selective pore activity (Adinolfi et al., 2005).

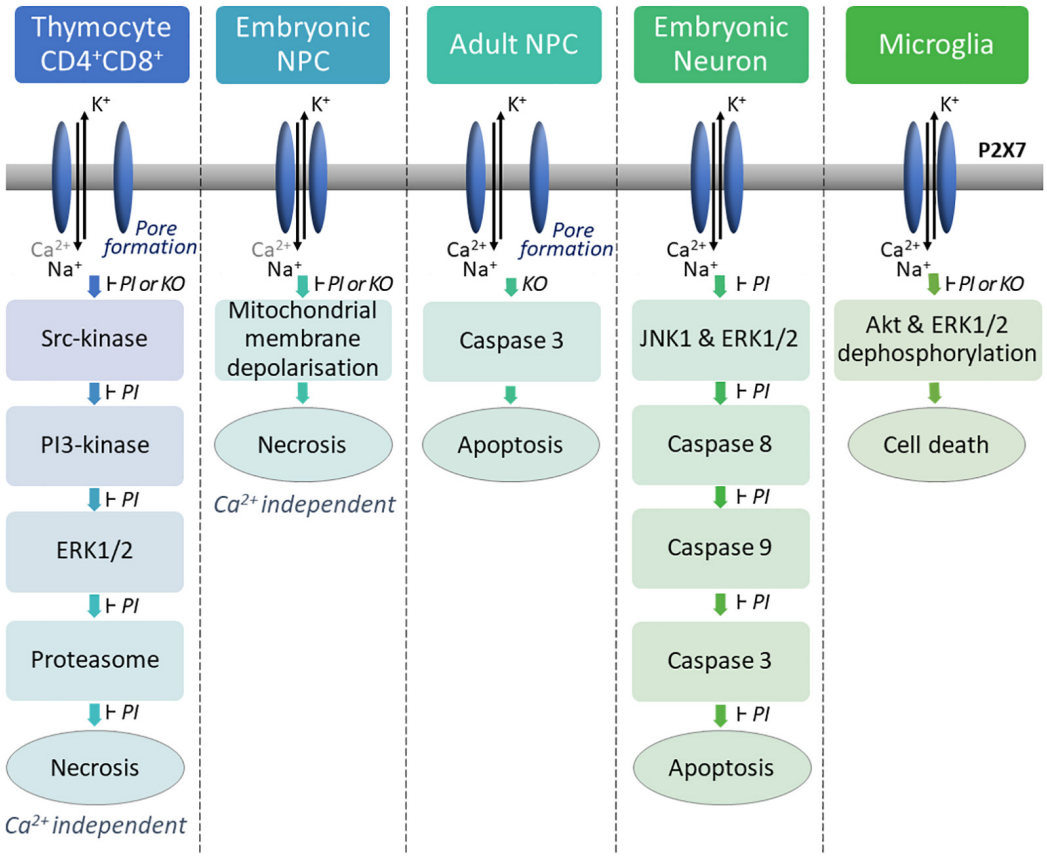

FIGURE 1 | P2X7 activation induces cell death via different molecular pathways depending on the cell type. In mouse thymocytes, P2X7 stimulation induces P2X7-dependent pore formation and a calcium-independent cell lysis via the successive activation of a SRC family tyrosine kinase, a phosphatidylinositol 3-kinase, the mitogen-activated protein (MAP) kinase (ERK/2) module, and the proteasome (Auger et al., 2005). In embryonic mouse NPCs, activation of P2X7 does not lead to pore formation but induces mitochondrial membrane depolarization leading to calcium-independent lysis of the cell (Delarasse et al., 2009). High concentration of ATP induces P2X7-dependent pore formation in mouse adult NPCs and activation of caspase 3 leading to cell death (Messemer et al., 2013). P2X7 stimulation induces apoptosis in embryonic rat cortical neurons *via* activation of the signaling pathways JNK1, ERK and caspases 8/9/3 (Kong et al., 2005). In newborn mouse microglia, P2X7 stimulation induces dephosphorylation of AKT, ERK1/2 and cell death (He et al., 2017). PI: Pharmacological inhibitors were used to specifically inhibit P2X7 or each down-stream enzyme of the pathway. Each of them were able to block P2X7-dependent cell death. KO: Cells from P2X7ko mice were used to analyze P2X7-dependent cell death pathway compared to cells from WT mice.

Further studies have shown that the T-cell receptor stimulation of T lymphocytes triggers the release of ATP which plays a crucial role in increasing cytosolic Ca^{2+} concentration, NFAT activation and IL-2 secretion (Yip et al., 2009). Additional evidence suggesting that P2X7 may trigger T cell growth or promote survival was provided by Adinolfi et al. (2010) They identified a shorter P2X7 natural splice variant [P2X7(B)] which lacks the carboxy-terminal tail and is expressed in T lymphocytes. P2X7(B) transfected in HEK293 cells was expressed as an homotrimer at the plasma membrane and had many properties of the longer isoform P2X(A) but was unable to form the non-selective pore. Interestingly, when P2X7(A) and P2X7(B) were co-transfected into HEK293 cells, they were able to form heterotrimers expressed at the plasma membrane and which have different properties. Their results suggest that if P2X7(A) is predominant in the heterotrimer, P2X7 will trigger the opening of the non-selective pore leading to cell death. In contrast, if the shorter isoform is in excess, P2X7 will stimulate growth (Adinolfi et al., 2010). However, the existence and functions of P2X7(A)/P2X7(B) heterotrimers in T lymphocytes is lacking at present.

Thus, P2X7 stimulation can lead to opposite effects: cell death or cell growth. The concentration of ATP used to trigger P2X7 bearing cells may explain these dramatically opposite outcomes. The studies of Stojilkovic's group (Khadra et al., 2013) have shown that naive P2X7 is activated and deactivated monophasically at low agonist concentrations, while at high concentrations P2X7 is activated with increased current amplitude and slow deactivation. They proposed a model explaining their data: at low agonist concentrations, only two ATP binding sites of the trimeric P2X7 are engaged and the channel opens to a low conductance state. Conversely, at higher agonist concentrations, all 3 binding sites are filled and the channel pore is dilated to a high conductance state.

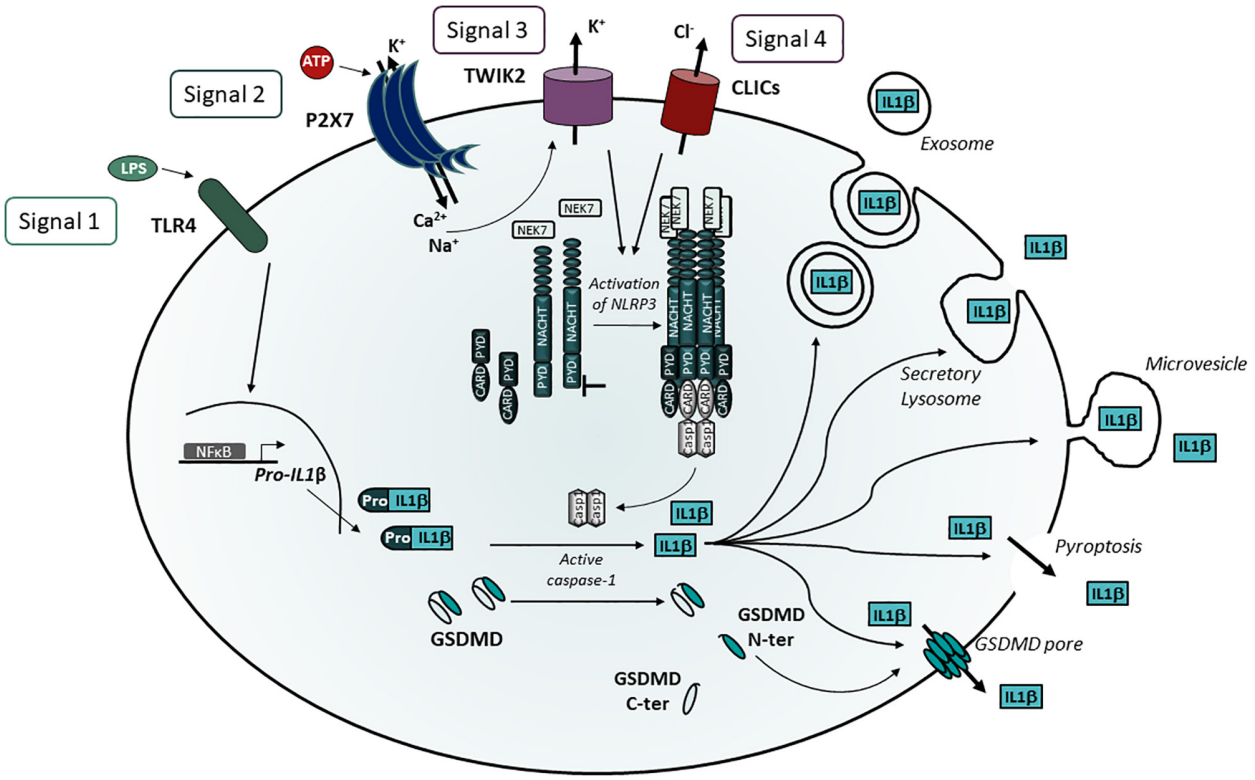

FIGURE 2 | P2X7 stimulation induces NLRP3 activation leading to IL-1β release. Maturation of IL-1β requires 4 signals: 1) TLR activation triggering pro-IL-1β transcription, 2) Ca^{2+} and Na^{+} influxes via P2X7 stimulation leading to activation of TWIK2, 3) K^{+} efflux via P2X7 and TWIK2 leading to NEK7 binding to leucine rich domain of NLRP3, 4) Potential translocation of CLICs to the plasma membrane and Cl^{-} efflux and activation of NLRP3. NLRP3 oligomerization recruits ASC and induces pro-caspase 1 cleavage leading to the cleavage of pro-IL-1β in mature IL-1β. Several pathways have been described for IL-1β release via exosomes, secretory lysosomes and microvesicles. However, the identification of GSDMD as a substrate of caspase 1 unraveled the role of the GSDMD-N domain in pore formation and pyroptotic cell death.

Activation of the NLRP3 Inflammasome

The role of P2X7 in the processing and release of IL-1β and IL-18 by microglia and macrophages is well established (Ferrari et al., 1997a,b; Di Virgilio, 2007). The maturation and release of these interleukins require four signals (**Figure 2**). The first signal via Toll-like receptors drives pro-IL-1β transcription and accumulation in the cytosol, while pro-IL-18 is constitutively expressed. The second signal via P2X7 triggers the influxes of Ca^{2+} and Na^{+} and the membrane efflux of K^{+} (Steinberg et al., 1987; Riedel et al., 2007) via P2X7 itself but also via TWIK2 (two-pore domain weak inwardly rectifying K^{+} channel 2), a K^{+} channel belonging to the K2P family (Di et al., 2018). The third signal corresponds to the K^{+} efflux via P2X7 and TWIK2 which is a potent activator of the NLRP3 inflammasome. However, TWIK2 does not control the activation of AIM2, NLRC4 and pyrin inflammasomes (Di et al., 2018). TWIK2 may act in synergy with P2X7 which was considered to be a K^{+} channel (Steinberg et al., 1987; Riedel et al., 2007) because in the absence of TWIK2, K^{+} efflux was strongly decreased but not abolished (Di et al., 2018). Surprisingly, in P2X7ko macrophages, ATP was still able to trigger K^{+} efflux through TWIK2 suggesting that an undefined ATP-sensitive receptor is able to stimulate TWIK2. Thus, more work is required to identify the signal generated by P2X7 to trigger TWIK2 and activate NLRP3. The mechanism by which a decrease in cytosolic K^{+} concentration leads to NLRP3 activation is not yet fully understood. However, studies have recently identified NEK7, a member of the NIMA (never in mitosis gene a)-related serine/threonine kinase family, as a component of the NLRP3 inflammasome activation (He et al., 2016; Schmid-Burgk et al., 2016; Shi et al., 2016). NEK7 was important for NLRP3 activation and formed molecular complexes with NLRP3 by the interaction of its catalytic region with the NLRP3 leucine rich repeat domain independently of its kinase activity (He et al., 2016; Shi et al., 2016). Importantly, He et al. (2016) established that the presence of high concentration of extracellular KCl (50 mM), known to block K^{+} effluxes, inhibited the interaction of NLRP3 with NEK7 in ATP-stimulated macrophages. These experiments suggest that NEK7 is a sensor of K^{+}. Recently, Sharif et al. (2019) described a cryo-electron microscopy structure of the human NLRP3 complexed to NEK7. Their interesting results show that the first half of the NEK7 C-lobe interacts with the leucin rich repeat of NLRP3 while the second part of the NEK7 C-lobe contacts the Nucleotide Binding Domain and the Helical Domain 2 of the NACHT region of NLRP3. The interaction between NLRP3 and NEK7 generates a complex which is inactive even after addition of ATP or ATP

analogs. Thus, these ligands do not trigger oligomerization of NLRP3-NEK7 complexes *in vitro* and the stimulus required for NLRP3-NEK7 inflammasome formation remains undefined yet. Interestingly, another protein, the thioredoxin interacting protein (TXNIP) able to interact with NLRP3 was identified by the yeast two-hybrid method using the leucine-rich repeats of NLRP3 as bait (Zhou et al., 2010). In the cytosol, TXNIP and thioredoxin, an antioxidant component, form a complex which dissociates in the presence of ROS. Subsequently, TXNIP interacts with NLRP3 and activates the NLRP3 inflammasome. Many structurally unrelated NLRP3 inflammasome activators among which silica, alum, monosodium urate crystals and ATP are able to activate NLRP3, most probably because they induce the production of ROS and the formation of TXNIP-NLRP3 complexes. To the best of our knowledge, it is not known yet whether the NEK7-NLRP3 or TXNIP-NLRP3 complexes co-exist in the same cells or whether they are triggered in different cell types.

The 4th signal results from the translocation of the Cl^- intracellular channels (CLICs) to the plasma membrane as described below (**Figure 2**).

Notably, inhibition of NLRP3 activation and IL-1β release by high extracellular concentrations of KCl is due to the blockade of both K^+ and Cl^- effluxes (Domingo-Fernandez et al., 2017; Tang et al., 2017; Green et al., 2018). Indeed, different pharmacological inhibitors of Cl^- channels prevent the secretion of IL-1β after stimulation of bone marrow derived macrophages (BMDM) by ATP (Domingo-Fernandez et al., 2017; Green et al., 2018). Importantly, it was established that the decrease in Cl^- effluxes induced a diminution of ASC specks formation in BMDM stimulated by LPS and ATP (Domingo-Fernandez et al., 2017; Tang et al., 2017; Green et al., 2018). The CLICs were shown to be involved in Cl^- effluxes and the knockdown by siRNA of CLIC1 and CLIC4 (Domingo-Fernandez et al., 2017) induced a strong diminution of pro-IL-1β and a total inhibition of mature IL-1β in the supernatant of LPS- and ATP- stimulated BMDM (Domingo-Fernandez et al., 2017). Since CLICS have redundant functions, another study used BMDM from CLIC1ko, CLIC4ko or CLIC5Ko mouse lines treated with siRNA against the other two Clic genes (Tang et al., 2017). Results of this strategy indicate that inhibition of CLIC1, CLIC4 and CLIC5 diminished ATP- and nigericin-induced caspase 1 maturation and IL-1β production and, in addition, established that CLICs activate NLRP3 by triggering Cl^- effluxes (Tang et al., 2017). Taken together these findings suggest that CLICs are acting downstream of K^+ effluxes, mitochondrial damage and ROS production which are also stimulating NLRP3 activation after ATP- or nigericin-treatment of BMDM (Tang et al., 2017). More recently, Green et al. (2018) found that ASC speck formation is dependent of Cl^- effluxes and is reversible but this pathway does not trigger the activation of caspase 1 and IL-1β secretion unless there is a simultaneous efflux of K^+ which stimulates the association of NEK7 to NLRP3. Thus, CLICs translocation to the plasma membrane and Cl^- efflux might be considered as a 4^{th} signal of NLRP3 activation.

NLRP3 is a large multimeric protein platform involved in the proteolytic cleavage of leaderless pro-IL-1β and pro-IL-18 to their active form by caspase 1. The activation of caspase 1 results from the binding of pro-caspase 1 by its caspase recruitment domain (CARD) to multimeric complexes composed of the Inflammasome NLRP3 and an adaptator called ASC (Apoptosis-associated speck like protein). ASC binds to the N-terminal pyrin domain (PYD) of NLRP3 by homotypic interaction via its PYD domain and recruits pro-caspase 1 by homotypic interactions of the CARD domains (**Figure 2**). The mature cytokines are then released from the cells. However, several pathways of secretion of mature cytokines have been described (Andrei et al., 1999; MacKenzie et al., 2001; Qu et al., 2007), and discussed (Lopez-Castejon and Brough, 2011). In LPS-activated human monocytes stimulated with exogenous ATP, Andrei et al. (1999) showed that mature IL-1β, active caspase 1 and cathepsin D co-localize in Lamp-1^+ endolysosomes which fuse with the plasma membrane and release these products in the extracellular medium. They also found that phosphatidylcholine-specific phospholipase C and calcium-dependent phospholipase A2 were required for lysosomal exocytosis (Andrei et al., 2004). Another pathway of mature IL-1β release was described in THP1, a human monocytic cell line. P2X7 activation induced the release of phosphatidyl serine positive microvesicles containing mature and immature IL-1β and active caspase 1 (MacKenzie et al., 2001). Using cultures of primary bone marrow-derived macrophages, a third pathway of IL-1β release was described, in which P2X7 activation leads to the production of multivesicular bodies containing exosomes loaded with IL-1β, caspase 1 and NLRP3 inflammasome components (Qu et al., 2007; Qu and Dubyak, 2009). Recently, two groups have shown that mouse caspases 1 and 11 or human caspases 4 and 5 are able to cleave the cytosolic protein gasdermin D (GSDMD; Kayagaki et al., 2015; Shi et al., 2015). After proteolytic cleavage, the NH_2-terminal fragment of GSDMD oligomerizes and forms pores in the cell plasma membrane (Ding et al., 2016; Liu et al., 2016; Sborgi et al., 2016). This leads to the release of inflammatory cytokines and pyroptotic cell death (Aglietti et al., 2016; Ding et al., 2016; Liu et al., 2016; Sborgi et al., 2016). In addition, several studies have suggested that the release of mature IL-1β is restricted to lytic macrophages (Liu et al., 2014; Cullen et al., 2015) and requires the lysis of macrophage plasma membrane. However, Evavold et al. (2018) and Heilig et al. (2018) have shown that blocking lysis of immortalized BMDM after NLRP3 inflammasome stimulation does not abolish the release of bioactive IL-1 which is then secreted through GSDMD pores. Interestingly, Ruhl et al. (2018) have recently disclosed that the endosomal sorting complexes required for transport (ESCRT) machinery is able to down-modulate GSDMD mediated pyroptosis and IL-1β secretion. These studies suggest that ESCRT-promoted ectosomes restore the injured plasma membranes by shedding GSDMD pores. This mechanism allows a GSDMD-mediated IL-1β release without cell lysis (reviewed in Evavold and Kagan, 2018). However, ATP (Evavold et al., 2018) and nigericin (Evavold et al., 2018; Heilig et al., 2018) triggered GSDMD-dependent pyroptosis preferentially while more potent NLRP3 activators (such as bacterial products or host-derived oxidized lipids) stimulated IL-1β release through GSDMD pores in absence of phagocyte lysis (Zanoni et al., 2017). In summary, following TLR activation of macrophages, P2X7 stimulation may trigger one of 4 different

identified biochemical pathways leading to IL-1β secretion i.e., (i) fusion of IL-1β containing endolysosomes with plasma membrane, (ii) release of microvesicles, (iii) release of exosomes filled with mature IL-1β, or (iv) IL-1β release through GSDMD cell lysis. However, additional work is needed to define in which cells and how P2X7 stimulation preferentially triggers one of these pathways. The study of NLRP3 positive cells lacking or expressing low levels of GSDMD in physiological conditions may uncover which IL-1β release pathway is triggered.

The finding that TWIK2 is involved in NLRP3 activation and processing of IL-1β, raises the question of studying TWIK2 impact in cell death. Indeed, TWIK2-deficient BMDMs show decreased ATP-induced cell death without affecting nigericin cell cytotoxicity. Thus, an interesting question is whether TWIK2 is implicated in the various P2X7-dependent cell deaths (**Figure 1**) or whether members of the K2P family other than TWIK2 have a role in cell death of different cell types.

P2X7 IN THE NERVOUS SYSTEM

Physiological Roles of P2X7 in the Nervous System

Neural progenitor cells (NPCs) express functional P2X7 as shown by patch-clamp recording on mouse primary NPCs culture (Delarasse et al., 2009; Messemer et al., 2013) and hippocampal brain slice from nestin-EGFP mice (Messemer et al., 2013). P2X7 was reported to induce cell death and also proliferation. In mouse embryonic NPCs, P2X7 activation with high concentrations of ATP or the agonist Bz-ATP induces necrosis along with impaired mitochondrial function, as evidenced by the loss of mitochondrial membrane potential (Delarasse et al., 2009). In these cells, P2X7-dependent cell death occurred in the absence of P2X7 pore formation (Delarasse et al., 2009). In contrast, in mouse adult NPCs, P2X7 stimulation with high amount of Bz-ATP induces pore formation, activation of the pro-apoptotic caspase 3 and cell death (Messemer et al., 2013; **Figure 1**). In embryonic rat cortical neurons, activation of P2X7 with the same range of Bz-ATP concentrations leads to apoptosis via activation of JNK1 (c-jun N-terminal kinase 1), ERK1/2 and caspase 8/9/3 pathway (Kong et al., 2005). Thus, P2X7-dependent signaling pathways appear to change with the developmental status of the cells. In addition, P2X7 stimulation with low amounts of Bz-ATP in rat embryonic NPCs induced neuronal differentiation rather than cell death and pore formation (Tsao et al., 2013). P2X7 properties of adult mouse NPCs depend on the presence of exogenous ATP and on its concentration (Leeson et al., 2018). When ATP concentration is low, NPCs are in resting state, whereas high concentration of ATP brings about inflammatory conditions (Leeson et al., 2018). Three different functions have been highlighted: (1) phagocytosis in the absence of ATP, (2) calcium influx and a decrease in proliferation in the presence of low amounts of ATP and (3) pore formation leading to cell death in response to high amount of ATP. Interestingly, in the absence of serum, P2X7 expressed by human NPCs and neuroblasts could participate in the clearance of apoptotic neuronal cells, as a scavenger receptor (Lovelace et al., 2015). Overall, these data indicate that in inflammatory conditions, high amount of ATP is released and P2X7 contributes to detrimental processes by inducing NPCs cell death (**Figures 3**, **4**). During embryonic development, P2X7 may be involved in the regulation of NPC population via phagocytosis of dead cells and proliferation of NPCs. The release of ATP from neighboring cells at a specific developmental stage and in a specific brain region may stop NPCs proliferation and induces NPC differentiation, thus P2X7 may also participate in neurogenesis (**Figures 3**, **4**).

Microglia is the resident immune cell of the CNS, and shares many functions with macrophages such as phagocytosis, pro-inflammatory cytokines release and production of reactive oxygen species (ROS) and nitric oxide (NO). P2X7 was shown to activate microglia and to induce their proliferation (Bianco et al., 2006; Monif et al., 2009). Down-regulation of P2X7 by siRNA oligonucleotide in rat primary microglia decreased cell proliferation (Bianco et al., 2006). On the other hand, overexpression of P2X7 on microglia in neuron-glia mixed cell cultures from rat hippocampus leads to an increased number of microglial cells (Monif et al., 2009). In both models, P2X7-dependent proliferation was observed, in the absence of added exogenous P2X7 agonist, indicating that ATP released by neighboring astrocytes and microglia was sufficient to induce proliferation under resting conditions (Bianco et al., 2006; Monif et al., 2009). Evidence that the trophic effect of P2X7 is mediated by the non-selective pore activity was obtained by using a point mutant of P2X7 (P2X7 G345Y) that can form an intact functional channel but is defective in non-selective pore formation. Transfection of rat microglia with this mutated P2X7 prevented cell growth (Monif et al., 2009). This confirms the involvement of the non-selective pore in cell proliferation, previously demonstrated in P2X7-transfected HEK293 cells (Adinolfi et al., 2005). *In vivo*, in the embryonic spinal cord of mouse at E13.5 stage, Rigato et al. (2012) also showed that P2X7 controls proliferation of microglia, but not their activation state by comparing WT and P2X7ko mice. In contrast, in microglia from the cortex of newborn mice, prolonged stimulation of P2X7 with high amount of Bz-ATP induced cell death that may be induced via dephosphorylation of Akt and ERK (He et al., 2017; **Figure 1**). Thus, in the presence of physiological amounts of ATP, P2X7 may control microglia proliferation in the CNS while sustained activation may induce cell death (**Figures 3**, **4**). Most studies have evaluated the death of cells on which P2X7 is activated by ATP. However, Skaper et al. (2006) have tested the impact of P2X7 stimulation of microglia on neighboring neurons. Co-cultures of rat cortical neurons with cortical microglia in the presence of ATP or Bz-ATP induced cortical neuron death. This effect was due to the release of superoxide and nitric oxide by P2X7 positive microglia stimulated with ATP and did not require direct contact between neuron and microglia. Thus, inhibition of P2X7 on microglia may protect neurons in some neurodegenerative diseases.

Age-related macular degeneration (AMD) is characterized by damage of the macula and central retina and the presence of extracellular deposits called drusen. Drusen are localized between the retinal pigment epithelium (RPE) and the Bruch's membrane (BM) accompanied with accumulation

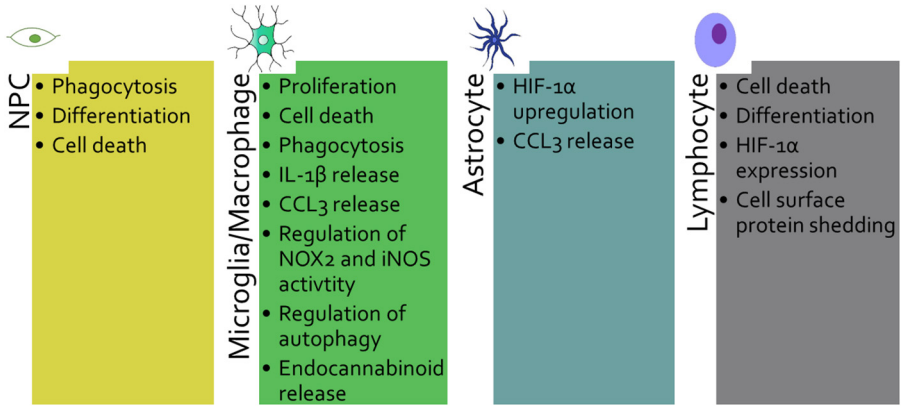

FIGURE 3 | P2X7 plays different roles depending on the cell type that expresses it: Neural progenitor cell (NPC), microglia/macrophage, astrocyte and lymphocyte. The various functions of P2X7 are listed for each cell type.

of macrophages (Guillonneau et al., 2017). In the absence of ATP, it was clearly established that P2X7 acts as a scavenger receptor conferring phagocytic properties to murine peritoneal macrophages, human monocytes, macrophages and microglia in the absence of serum (Gu et al., 2011; Gu and Wiley, 2018; Janks et al., 2018). Co-inheritance of P2X7 G150R and P2X4 Y315C polymorphisms was shown to impair phagocytosis of particles by monocytes harboring these variants and to be associated with late-stage AMD, suggesting an involvement of P2X7 in pathological processes (Gu et al., 2013). In addition, 18-month old P2X7-deficient mice display BM thickening, RPE cell loss and increased number of microglia/macrophages in the subretinal space compared to age-matched WT mice (Vessey et al., 2017). These findings suggest that default in P2X7-dependent phagocytic properties may be involved in accumulation of drusen deposits and the development of AMD (**Figures 3**, **4**).

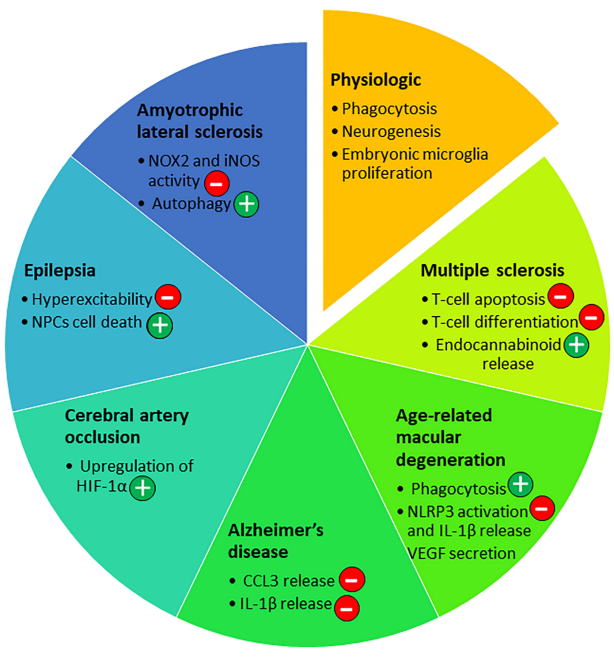

FIGURE 4 | P2X7 roles in the nervous system in physiological and pathological conditions. Depending on the disease of the nervous system and the progression of the pathology, P2X7 has been involved in different pathways [beneficial (+) or not (–)] that are listed in the diagram.

P2X7 Roles in Neurodegenerative Processes

Up-regulated expression of P2X7 has been observed in several neurodegenerative diseases: e.g., in astrocytes and microglia in AD (McLarnon et al., 2006; Martin et al., 2019), in microglia from spinal cord of MS and ALS (Yiangou et al., 2006), in astrocytes in MS (Narcisse et al., 2005; Amadio et al., 2017), in the optic nerve of MS patients (Matute et al., 2007) and in the neocortex and hippocampus of patients with epilepsy (Barros-Barbosa et al., 2016; Jimenez-Pacheco et al., 2016).

Epilepsy is a CNS disorder characterized by abnormal neuronal activity causing seizures. In mouse models, P2X7-deficient compared to WT animals show an increased susceptibility to pilocarpine-induced seizures. Pilocarpine activates muscarinic receptors leading to intracellular calcium release via IP3 production. In the absence of P2X7, desensitization of the muscarinic M1 receptor and pannexin 1 opening cannot be sustained, resulting in neuronal hyperexcitability involved in seizures (Kim and Kang, 2011). In addition, Rozmer et al. (2017) hypothesized that in the pilocarpine model, P2Y1 activation induced proliferation and migration of NPCs at ectopic site while P2X7 activation may counterbalance this pathologic effect by inducing the cell death of excess NPCs (**Figures 3**, **4**). In contrast, no difference between P2X7-deficient and WT mice was observed in the seizures induced either by kainic acid which activates glutamate receptors, and picrotoxin which inhibits GABAA receptors (Kim and Kang, 2011). Surprisingly, in the kainic acid-induced seizure model, inhibition by pharmacological inhibitors of P2X7 (A438079 & JNJ-47965567) reduced seizures and gliosis (Engel et al., 2012; Jimenez-Pacheco et al., 2016; Beamer et al., 2017).

This apparent discrepancy between results obtained with P2X7 selective pharmacological inhibitors and results found in the P2X7ko mice, may be explained by the level of P2X7 activation and the time at which P2X7 antagonists were administered. A constitutive deficit in P2X7 highlighted its physiological functions in the maintenance of the nervous system integrity. In the pilocarpine animal model of epilepsy, the study of P2X7-deficiency showed its potential roles in the control of the activity of neurons that express M1 receptors and in the regulation of neuronal networks by regulating NPCs population. Since pharmacological inhibitors were mostly applied during the acute phase of the kainic acid-induced disease, their effects suggest that at this later stage, high amounts of ATP are released and P2X7 present different properties i.e., release of IL-1β (Engel et al., 2012) and microglia proliferation in the hippocampus (Jimenez-Pacheco et al., 2016), which may contribute to pathological processes. Overall, these works illustrate that, depending on the model used and the pathological pathways involved, P2X7 may have a dual role i.e., P2X7 has protective role in physiological conditions while when the disease is advanced it worsens the pathological processes (Rassendren and Audinat, 2016).

In two independent studies, the degree of severity after middle cerebral artery occlusion (MCAO) was similar in WT and P2X7ko mice, indicating that P2X7 is not a major mediator of neuronal cell death in this model (Le Feuvre et al., 2003; Hirayama et al., 2015). Interestingly, a brief episode of sublethal ischemia protects neurons from cerebral ischemia, and this effect of ischemic tolerance is abolished in P2X7ko mice (Hirayama et al., 2015). These authors showed that P2X7 is up-regulated specifically in astrocytes but not in microglia during the tolerance episode and activation of P2X7 on astrocytes induces the transcription factor hypoxia inducible factor-1α (HIF-1α) upregulation and its target molecule erythropoietin, two neuroprotective factors. This study highlights a beneficial role of P2X7 up-regulation by astrocytes in ischemic tolerance and suggests that P2X7 may also have a protective effect in neurodegenerative diseases by inducing HIF-1α expression (**Figures 3**, **4**).

Amyotrophic lateral sclerosis (ALS) is a fatal neurodegenerative disease characterized by the progressive death of motor neurons in the brain and spinal cord (Taylor et al., 2016). In ALS mouse model (SOD1-G93A), the lack of P2X7 leads to an increased severity of the disease (diminished motor performance and amplified motoneuron loss) accompanied by an increased astrogliosis and microglial reaction with upregulation of the cytotoxic mediators NOX2 and iNOS (Apolloni et al., 2013a). These results are in contradiction with *in vitro* studies showing that P2X7 activation enhanced NOX2 activity in mouse primary microglia (Apolloni et al., 2013b). This discrepancy may be due in part to the origin of microglia, spinal cord *vs* brain cortex, and also to the environment of the cells. Indeed, depending on the level of activation, P2X7 can induce different polarization states of microglia. Brief activation of primary mouse microglia from SOD1-G93A mice was shown to promote autophagy while a sustained challenge increased inflammatory mediators' expression and inhibited autophagy (Fabbrizio et al., 2017). Thus, at the first stage of the disease, P2X7 may have a beneficial role by activating autophagy while persistent stimulation of P2X7 may inhibit autophagy and contribute to pathological inflammatory responses. These results indicate that P2X7 may have a dual role in ALS by controlling autophagy and NOX2 activation (**Figures 3**, **4**).

In vitro, short stimulation of P2X7 with ATP or Bz-ATP induces production of endocannabinoids by mouse microglia that may have beneficial effects (Witting et al., 2004). Indeed, the endocannabinoid, 2-arachidonoylglycerol, activates neuronal CB1 receptors which reduce glutamate release and inhibits excitotoxicity decreasing tissue destruction. Accordingly, the lack of P2X7 during experimental autoimmune encephalomyelitis (EAE), an animal model of multiple sclerosis (MS), results in the production of lower levels of endocannabinoids (Witting et al., 2006; **Figures 3**, **4**).

Alzheimer's disease is characterized by two main histological lesions: senile plaques composed of extracellular aggregates of amyloid β (Aβ) peptides and neurofibrillary tangles composed of intracellular aggregates of hyperphosphorylated tau protein. Using pharmacological inhibitors and neural cells from P2X7-deficient mice, we demonstrated that brief stimulation of P2X7 with ATP or Bz-ATP triggers the α-cleavage of the amyloid precursor protein (APP) (Delarasse et al., 2011; Darmellah et al., 2012). This beneficial pathway generates the neurotrophic and neuroprotective fragment sAPPα and simultaneously decreases the amount of toxic Aβ peptides. However, Leon-Otegui et al. (2011) showed, that sustained P2X7 stimulation with Bz-ATP on Neuro-2a cells activates the opposite pathway leading to Aβ peptides production. We thus explored the role of P2X7 *in vivo* in a mouse model of amyloid lesion, APPPS1 mice (Martin et al., 2019). We observed that lack of P2X7 in this model reduces the amyloid load in the brain independently of the sAPPα pathway. These studies highlight the conflicting roles attributed to P2X7 that may depend on the micro-environment in the brain. We can hypothesize that in physiological conditions, P2X7 may contribute to sAPPα release shown to trigger neurite outgrowth, synaptogenesis and proliferation of NPCs (Mattson, 1997; Caille et al., 2004). On the contrary, in the brain of AD mice, P2X7 no longer possess this property.

In the mouse amyloid model, J20, inhibition of P2X7 by the antagonist blue brilliant G was shown to reduce glycogen synthase kinase 3-beta activity, an important tau kinase (Diaz-Hernandez et al., 2012). This suggests a potential involvement of P2X7 in tau phosphorylation, however the effect of P2X7 on Tau pathology remains to be explored.

P2X7 Roles in Inflammatory Responses

Experimental evidence suggest that P2X7 contributes to AD inflammatory processes by activating NLRP3. Indeed, NLRP3 was shown to be an important mediator of neuroinflammatory responses in AD (Halle et al., 2008; Heneka et al., 2013) and intra-hippocampal injection of Aβ in mice increases the amount of IL-1β produced, only in the presence of an active P2X7 (Rampe et al., 2004; Sanz et al., 2009). However, we showed that P2X7-deficiency in transgenic AD mice did not significantly affect the release of IL-1β in the brain at advanced and very late stages

of the disease. Instead, P2X7 plays a critical role in Aβ peptide-mediated release of chemokines, particularly by increasing CCL3 levels. In effect, lower levels of CCL3 were detected in the brain of P2X7-deficient AD mice (Martin et al., 2019). In rat primary microglial cells, Kataoka et al. (2009) showed that ATP or Bz-ATP stimulation induced CCL3 release, which was partially blocked by pre-treatment with the antagonist BBG. In agreement with these results, we found no evidence of CCL3 release in the supernatants of microglia and astrocytes from P2X7-deficient mice after ATP, Bz-ATP or Aβ stimulation compared to WT cells (Martin et al., 2019). The discrepancy between acute (Sanz et al., 2009) vs. chronic AD models (Martin et al., 2019) may be explained by different activation status of microglia leading to the release of different inflammatory mediators after Aβ-stimulation of P2X7. For instance, in the absence of pre-stimulation with LPS, we observed CCL3 production in the supernatant of microglia that had been stimulated with ATP or Aβ peptides but we could not detect IL-1β release (Martin et al., 2019). Thus, we can hypothesize that, in the acute but not in the chronic AD model, the amount of ATP released, the P2X7 expression levels and the activation status of microglia favor P2X7-dependent IL-1β release (reviewed in Illes et al., 2019), but not in the chronic model. Interestingly, in mouse transgenic AD model, P2X7-dependent CCL3 release was associated with pathogenic $CD8^+$ T cell recruitment (**Figures 3**, **4**). This result supports the notion that P2X7 may be indirectly involved also in the recruitment of T lymphocytes in this disease, illustrating the complex involvement of P2X7 in inflammatory responses (Martin et al., 2019). Two different functions of P2X7, release of IL-1β and CCL3, have been highlighted in AD models and shown to contribute to the development of the disease. Thus, P2X7 antagonists are potentially pertinent pharmacological molecules to treat AD patients.

Likewise, depending on the AMD model studied, P2X7 appears to be involved in different ways. In physiological conditions, P2X7 was shown to contribute to the homeostasis of the retina as a scavenger receptor (Vessey et al., 2017). With age or light-challenge, CX3CR1-deficient mice develop subretinal macrophage accumulation associated with a significant loss of photoreceptors (Hu et al., 2015). In this model, P2X7 was up-regulated, leading to increased production of IL-1β. Treatment of CX3CR1-deficient mice with the P2X7 antagonist blue brilliant G (BBG) inhibited photoreceptor degeneration associated with subretinal inflammation (Hu et al., 2015). This study indicates that P2X7 up-regulation may have a pathogenic role in AMD via IL-1β release. Moreover, P2X7-deficiency did not affect photoreceptor loss after experimental retinal detachment, which could be explained by lower ATP and/or P2X7 levels in this model (Hu et al., 2015). There are two types of AMD, dry and wet, classified by the presence (wet) or absence (dry) of blood vessels that have disruptively invaded the retina from the choroid. In a model of dry AMD, P2X7 was shown to contribute to pathological processes via NLRP3 activation. In this model, P2X7-deficiency suppressed Alu RNA-induced RPE degeneration and caspase 1 activation (Kerur et al., 2013). In contrast, in a model of wet form of AMD, lack of P2X7 did not impact the volume of laser-induced choroidal neovascularization (CNV) but decreased the level of VEGF-A in the RPE and choroid (Mizutani et al., 2015). Interestingly, it was shown previously that stimulation of P2X7 with ATP or Bz-ATP triggers VEGF release from primary human monocyte (Hill et al., 2010) and also that VEGF secretion is reduced in P2X7-silenced B16 melanoma cells compared to WT B16 cells (Adinolfi et al., 2012). However, the cell origin of VEGF in the eye still has to be determined considering that P2X7 is exclusively expressed by microglia and endothelial cells in adult mouse retina (Kaczmarek-Hajek et al., 2018).

In summary, in AMD, P2X7 may act on different pathways such as phagocytosis, NLRP3 activation and/or VEGF-A production depending on the stage of the disease and the type of AMD (**Figures 3**, **4**). Intrinsic defect of P2X7 could lead to the development of AMD, while overactivation of P2X7 at late stage contributes to pathological processes via release of cytokines and production of VEGF.

P2X7 Role in Autoimmune Responses in the CNS

Multiple sclerosis is a demyelinating disease of the CNS characterized by an autoimmune response against myelin proteins. The role of P2X7 was assessed in experimental autoimmune encephalomyelitis (EAE), a mouse model of multiple sclerosis (MS). Brosnan's group used P2X7ko mice from Pfizer and observed that P2X7-deficient mice were more susceptible to EAE (Chen and Brosnan, 2006). This effect was due to a decreased number of apoptotic T lymphocytes in the brain and spinal cord of P2X7ko vs. WT mice, indicating that P2X7 is involved in autoreactive T cell death during EAE. Similarly, a recent study reported that retinoic acid up-regulates P2X7 in effector T cells of the intestine, thereby increasing their susceptibility to P2X7-dependent apoptosis. Intestinal T-cells are in contact with the gut microbiota and the authors have shown that this enhanced P2X7 expression is instrumental in the fine regulation of T-cell populations to avoid adverse inflammatory responses (Hashimoto-Hill et al., 2017). Taken together, these two studies emphasize the role of P2X7 in the control of deleterious T-cell responses by inducing T cell apoptosis (**Figures 3**, **4**).

In contrast, Sharp et al. (2008) observed that EAE incidence is reduced in P2X7-deficient mice when compared to WT animals. The discrepancy between these results and those of (Chen and Brosnan, 2006) come from the use of two different P2X7ko strains. Sharp et al. (2008) used the P2X7ko mice from Glaxo-Smith-Kline (GSK), that still express the P2X7(K) isoform, preferentially expressed in T-cells, but not the P2X7(A) isoform, present in macrophages and dendritic cells (Nicke et al., 2009; Taylor et al., 2009; **Box 1** and **Figure 5**). Thus, in the GSK P2X7ko mice, pathogenic T cells are eliminated in part by P2X7-dependent apoptosis in the CNS during EAE as observed in WT mice.

The persistence of $P2X7(K)^+$ T cells in the GSK P2X7ko animals does not explain why EAE incidence is reduced in the GSK P2X7ko mice compared to WT mice. We hypothesize that the lack of P2X7(A) isoform from macrophages, dendritic cells, microglia, mast cells and astrocytes could decrease the

BOX 1 | Additional background information on P2X7.

- The P2X7 sensitivity varies from 10 to 100-fold between species with agonist sensitivities of human P2X7 > rat P2X7 > mouse P2X7. P2X7 sensitivities to ATP and Bz-ATP vary between species (Donnelly-Roberts et al., 2009; Bartlett et al., 2014).
- Until the development of a new generation of P2X7 antagonists, a decade ago; the antagonists of P2X7 lacked specificity. For example blue brilliant G (BBG) also inhibits P2X1R and P2X4R (Young and Gorecki, 2018).
- In murine species, two main P2X7 isoforms were described. P2X7 isoform A (P2X7(A)) is the original full-length protein and P2X7 isoform K (P2X7(K)) results from the splicing of an alternative exon 1. Thus, P2X7(A) and (K) have different amino-acid residues in their NH2 and first transmembrane domains. In addition, P2X7(K) isoform which has an 8-fold higher ATP sensitivity than P2X7A, transduces signals more efficiently (Nicke et al., 2009; Bartlett et al., 2014; Rissiek et al., 2015). P2X7(A) and (K) are preferentially expressed by macrophages or T-lymphocytes, respectively (**Figure 5**).
- Two main P2X7 knock-out mice were studied. The Pfizer P2X7ko was generated by inserting a neomycin cassette into exon 13 (Solle et al., 2001) while the GlaxoSmithKline one was produced by inserting a lacZ transgene and a neomycin cassette into exon 1. It was found that the GSK P2X7ko strain of mice still expresses P2X7(K) isoform in T cells (Chessell et al., 2005), reviewed in Bartlett et al. (2014).
- In mouse, nicotinamide adenine dinucleotide (NAD) can also activate P2X7 via the transfer of an ADP-ribose group from NAD to P2X7. ADP-ribosylation of P2X7 is catalyzed by the ecto-ADP-ribosyltransferase ARTC2.2. T-cells are sensitive to NAD but not macrophages, this was attributed to their differential expression of P2X7 isoforms (Seman et al., 2003; Rissiek et al., 2015; **Figure 5**). In human, NAD is not an agonist of P2X7 because functional ART enzyme is not present on the cell surface of lymphocytes and macrophages.

contribution of these cells to inflammatory responses during EAE. In particular, mast cells which are considered to be important actors in EAE (Secor et al., 2000). probably lack P2X7(A) isoform in the GSK P2X7ko animals and thus will not open the brain blood barrier efficiently (Christy et al., 2013), will release lower levels of IL-1β and trigger less effectively T lymphocytes to produce GM-CSF (Russi et al., 2016). In addition, in the GSK P2X7ko mice the pathogenic macrophages have probably lost the P2X7(A) isoform and are unable to release IL-1β and other inflammatory molecules as WT macrophages do. Several reports have established that platelets contribute to pathological events during EAE (Langer et al., 2012; Starossom et al., 2015; Sonia et al., 2018). Platelets are found in the CNS before infiltration by encephalitogenic T lymphocytes (Sonia et al., 2018). They express P2Y1 and P2Y12 G-protein-coupled receptors and P2X1 only (Kahner et al., 2006; Hechler and Gachet, 2011; Mahaut-Smith et al., 2011). At early stages of EAE, platelets are able to degranulate and release several soluble factors in the CNS. Since platelets contains very large concentrations of ATP, they may activate P2X7(A) positive cells and increase inflammation in WT mice but not in GSK P2X7ko animals. P2X7 stimulation with ATP leads to CCL3 release by mouse primary microglia and astrocytes (Martin et al., 2019) and P2X7 activation with Bz-ATP induces CCL2 production by rat primary astrocytes (Panenka et al., 2001). These chemokines are involved in the recruitment of leucocytes, thus lack of P2X7 on glial cells may reduce infiltration of auto-reactive T-cells and macrophages in the brain. In addition, the disappearance of P2X7(A) isoform on oligodendrocytes could reduce their death and thus decrease demyelination (Domercq and Matute, 2019). Overall, this should lessen tissue lesions in the CNS and reduces EAE pathology in GSK P2X7ko mice.

The expression of P2X7 on HEK293 (stably transfected with P2X7) or increased expression of P2X7 in astrocyte in the brain of mice with sublethal ischemia, as well as long stimulation by Bz-ATP of primary mouse astrocyte triggers the expression of HIF-1α (Amoroso et al., 2012; Hirayama et al., 2015). HIF-1α is a metabolic sensor that decreases the number of $Foxp3^+$ regulatory T cells and stimulates Th17 cell development. Notably, HIF-1α ko mice are resistant to Th17-dependent EAE induction

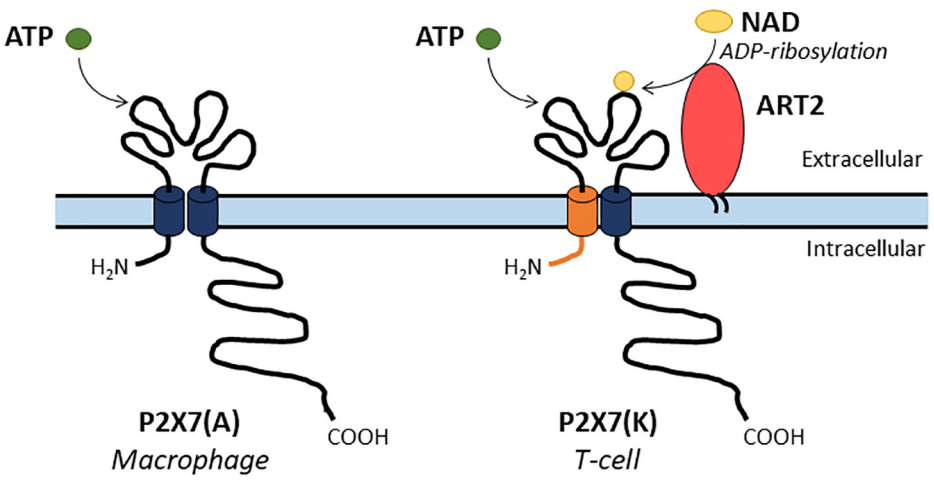

FIGURE 5 | Two main P2X7 isoforms have been described in mouse. A full-length P2X7(A) isoform is expressed by macrophages while the P2X7(K) isoform is expressed by T-cells and presents an alternate NH_2 and first transmembrane domains (depicted in orange). The P2X7(A) isoform is sensitive to ATP only while the P2X7(K) isoform is activated by both ATP or by covalent ADP-ribosylation by the enzyme ART2 in the presence of NAD.

(Dang et al., 2011). In addition, P2X7 activation also suppressed type 1 regulatory T-cell differentiation (Tr1) via an increased expression of HIF-1α in Tr1 lymphocytes (Mascanfroni et al., 2015). Thus, P2X7 might also be involved in EAE by controlling the balance between effector and regulatory T-cells via HIF-1α expression.

Genome-wide associated studies (GWAS) of patients with MS (International Multiple Sclerosis Genetics Consortium, 2007; Australia and New Zealand Multiple Sclerosis Genetics Consortium, 2009; International Multiple Sclerosis Genetics Consortium, 2011, 2013, 2018) identified multiple gene alleles associated with higher risk of MS but none of the highly polymorphic P2X7 genes. The frequency of P2X7 variants may vary depending on the variants studied (rare: mean allele frequency (MAF) <3% or common: MAF > 5%) and on the localization of the populations considered, i.e., a given P2X7 variant may be rare in certain groups and absent in others. When the frequency of the variants is rare, this low frequency may not be sufficient to determine whether certain variants are associated with particular pathologies through the GWAS method.

Gu et al. (2015) have genotyped 12 functional P2X7 variants in three case-control cohorts of MS patients and normal subjects. Interestingly, they identified a rare genetic variant of P2X7 R307Q that has lost P2X7 pore function and shows a protective effect against MS. In addition, they found that the R307Q variant is associated with another variant R270H with a partial loss of P2X7 pore function. In patients, the combination of these two variants may impair P2X7 function and reduces secretion of pro-inflammatory cytokines by activated macrophages in the CNS (Gu et al., 2015; Sadovnick et al., 2017). Sadovnick et al. (2017) sequenced the P2X7 and P2X4 of MS patients and healthy controls. They identified three rare variants (P2X7 T205M, P2X7 N361 S and P2X4 G135S) which co-segregate with MS in one family in which 6 individuals out of 13 were affected by the disease. The P2X7 T205M mutant has lost its plasma membrane expression and its phagocytic capacity. The two other mutations, P2X7 N361 S and P2X4 G135S, had minor impact on P2X4-P2X7 functions but additional studies are needed to determine whether these two rare variants are also risk factors in MS. These studies have shown that the mutations affect P2X7 functions in macrophages, however, it would be of great interest to evaluate whether these mutations affect T-lymphocytes which play a major role in MS.

To identify risk loci in late onset AD, several GWAS of AD patients were performed (Harold et al., 2009; Lambert et al., 2009; Jun et al., 2010; Hollingworth et al., 2011; Naj et al., 2011; Cruchaga et al., 2013; Lambert et al., 2013; Ramanan and Saykin, 2013; Marioni et al., 2018; Jansen et al., 2019; Kunkle et al., 2019). In these studies, about 29 loci were identified to be associated with higher risk of developing AD, but they did not include variants of *P2X7* gene. However, disease susceptibility may be due to the combined roles of different gene polymorphisms, which have minor individual effects but synergize when associated. Analyses of several linked variants could reveal the involvement of a particular biological pathway in the disease process (Marchini et al., 2005; Damotte et al., 2014). Thus, we performed gene pathway analyses based on published GWAS data (Lambert et al., 2009; Lambert et al., 2013). We analyzed polymorphisms in the *P2X7* gene as well as those found in genes involved in P2X7-dependent sAPPα release, NALP3/ASC inflammasome and caspase 1 activation, IL-1β production and IL-1β receptor genes (IL-1R1, IL-1R2, and IL-1RAcP). A global analysis of P2X7 pathways and a more detailed study of subnetworks did not identify any association with AD (unpublished observations). We believe that the strategy used by Gu et al. (2015) to identify P2X7 rare variants associated with MS should be applied to AD.

CONCLUSION

This review highlights the difficulties encountered in assigning a specific role to P2X7 in the nervous system (**Figures 3**, **4**). Whether beneficial or detrimental, the effects of P2X7 in neurological diseases vary, depending on the disease physiopathology and clinical stage. The impact of P2X7 in the CNS is determined by numerous factors such as (1) cell types expressing it, (2) levels of P2X7 at the cell surface, (3) isoforms of P2X7 expressed, (4) biochemical pathways triggered in different cell types, (5) the local concentrations of ATP and (6) the activities of ecto-nucleotidases. The complexity of P2X7 functions is underscored by the variety of responses triggered by P2X7 stimulation on the same cell type. Indeed, P2X7 stimulation of microglia leads to CCL3 secretion while IL-1β processing and release requires pre-stimulation by TLR ligands. In addition, several cytokines such as INFγ and TNFα trigger P2X7 expression in various cell types. Other factors that influence the lipid composition of plasma membrane could modify the localization of P2X7 in or out the lipid rafts on the cell surface. Consequently, this affects the formation of the non-selective pore and the stimulation of intracellular signaling pathways (Garcia-Marcos et al., 2006; Karasawa and Kawate, 2016). The level of ATP also influences P2X7 properties. Differentiation or cell death depend on ATP concentrations, as was shown for adult NPC (Leeson et al., 2018). In the absence of ATP and serum, it was clearly shown that P2X7 confers scavenger activity to monocytes and microglia (Gu et al., 2011; Gu and Wiley, 2018; Janks et al., 2018). However, at a later stage of the disease, when higher amounts of ATP are released, P2X7 has a pro-inflammatory role. In addition, several ecto-nucleotidases expressed at the cell surface may degrade ATP in ADP, AMP and adenosine and thus activate other purinergic receptors (Rodrigues et al., 2015). These receptors contribute to ATP release and can synergize or antagonize P2X7 functions. For example the expression of P2Y1 that induces the proliferation of NPCs may counterbalance P2X7-dependent cell death (Rozmer et al., 2017). P2X4 activation leads to BDNF production and release supporting remyelination after P2X7-mediated myelin damage (Domercq and Matute, 2019). In contrast, inhibition of P2X7 or of the adenosine receptor A2A is beneficial in mouse amyloid models of AD (Faivre et al., 2018; Martin et al., 2019). Data on *in vivo* physiological levels of ATP in the CNS and during neurodegenerative diseases would be a major information to determine the relevant functions of P2X7. Luciferase probes

were developed to measure ATP in animal models of colitis or tumor (Morciano et al., 2017), it would be very interesting to optimize this protocol for CNS related diseases.

The complex role of P2X7 in CNS diseases is reminiscent of the dual role of the Fas receptor and its ligand (FasL) in the pathogenesis and evolution of EAE (Sabelko-Downes et al., 1999). In their review, Sabelko-Downes et al. (1999) proposed a model in which encephalitogenic $FasL^+$ $CD4^+$ T lymphocytes enter the CNS and induce apoptosis of Fas^+ resident cells such as oligodendrocytes. Importantly, during the recovery phase of EAE, encephalitogenic T lymphocytes express Fas while the cytokine-stimulated CNS resident cells become $FasL^+$. Thus, they can eliminate the aggressive $CD4^+$ T cells by binding the Fas receptor. It is worth noticing that in EAE, P2X7 present on encephalitogenic T lymphocytes contributes to the elimination of T lymphocytes during the remission phase of the disease (Chen and Brosnan, 2006). In all these studies, the use of Fas/FasL or P2X7 deficient mice was of major interest in delineating the role of these receptors in EAE. However, the removal of P2X7 from a large number of cell types expressing it precludes refined analyses of its functions on well-characterized cell sub-populations. The availability of P2X7 conditional ko mice (Csoka et al., 2015) in which it is possible to restrain and/or induce the elimination of this receptor in CNS cell subpopulations would be of major interest to define its role in physiological or pathological situations.

P2X7 as a potential therapeutic target has been investigated in numerous diseases such as chronic inflammatory diseases, neurodegenerative pathologies associated with inflammation, cancer and mental disorders (reviewed in Di Virgilio et al., 2017; Savio et al., 2018; Young and Gorecki, 2018). Several pharmaceutical companies have produced pharmacological antagonists of P2X7 which have been tested in various diseases with mostly disappointing results (Di Virgilio et al., 2017; Savio et al., 2018; Young and Gorecki, 2018). However, recently, instead of using small molecules able to antagonize P2X7, Danquah et al. (2016) have immunized llamas with mouse or human P2X7 in native conformation and selected nanobodies able to inhibit or trigger P2X7 functions. They were able to identify one potent agonist of mouse P2X7, nanobody 14D5 and one potent antagonist, nanobody 13A7. They showed that 13A7 bivalent nanobodies were able to block P2X7 functions on primary mouse macrophages and T lymphocytes and significantly decreased inflammation in two mouse models: allergic contact dermatitis and experimental glomerulonephritis (Danquah et al., 2016). The potential use of these anti-P2X7 nanobodies with antagonist properties in human inflammation is strengthened by experiments showing that the anti-human P2X7 antagonist nanobody Dano1 inhibits IL-1β release from human monocytes at subnanomolar IC50. Interestingly, the inhibitory potency of Dano1 was 1000 times higher than two pharmacological inhibitors of P2X7 used in clinical trials (Danquah et al., 2016). These new nanobodies with powerful antagonist properties against the mouse and human P2X7 show promising therapeutic potential in various inflammatory and neurologic diseases (reviewed in Koch-Nolte et al., 2019).

AUTHOR CONTRIBUTIONS

JK and CD wrote the manuscript.

FUNDING

This work was supported by grant from the Agence Nationale de la Recherche (ANR-12-MALZ-0003-02-P2X7RAD). CD's laboratory is also supported by Inserm, CNRS and Sorbonne Université. JK is funded by CNRS and Université Paris-Saclay.

ACKNOWLEDGMENTS

We warmly thank Dr. Colette Kanellopoulos-Langevin and Dr. Iris Motta for critical review of our manuscript. We also thank Pr. Fritz Markwardt, Dr. Micaela Galante, and Xia Li for their expert feed-back on patch-clamp experiments.

REFERENCES

Adinolfi, E., Callegari, M. G., Cirillo, M., Pinton, P., Giorgi, C., Cavagna, D., et al. (2009). Expression of the P2X7 receptor increases the Ca2+ content of the endoplasmic reticulum, activates NFATc1, and protects from apoptosis. *J. Biol. Chem.* 284, 10120–10128. doi: 10.1074/jbc.M805805200

Adinolfi, E., Callegari, M. G., Ferrari, D., Bolognesi, C., Minelli, M., Wieckowski, M. R., et al. (2005). Basal activation of the P2X7 ATP receptor elevates mitochondrial calcium and potential, increases cellular ATP levels, and promotes serum-independent growth. *Mol. Biol. Cell* 16, 3260–3272. doi: 10.1091/mbc.e04-11-1025

Adinolfi, E., Cirillo, M., Woltersdorf, R., Falzoni, S., Chiozzi, P., Pellegatti, P., et al. (2010). Trophic activity of a naturally occurring truncated isoform of the P2X7 receptor. *FASEB J.* 24, 3393–3404. doi: 10.1096/fj.09-153601

Adinolfi, E., Raffaghello, L., Giuliani, A. L., Cavazzini, L., Capece, M., Chiozzi, P., et al. (2012). Expression of P2X7 receptor increases in vivo tumor growth. *Cancer Res.* 72, 2957–2969. doi: 10.1158/0008-5472.CAN-11-1947

Aglietti, R. A., Estevez, A., Gupta, A., Ramirez, M. G., Liu, P. S., Kayagaki, N., et al. (2016). GsdmD p30 elicited by caspase-11 during pyroptosis forms pores in membranes. *Proc. Natl. Acad. Sci. U.S.A.* 113, 7858–7863. doi: 10.1073/pnas.1607769113

Alberto, A. V., Faria, R. X., Couto, C. G., Ferreira, L. G., Souza, C. A., Teixeira, P. C., et al. (2013). Is pannexin the pore associated with the P2X7 receptor? *Naunyn Schmiedebergs Arch. Pharmacol.* 386, 775–787. doi: 10.1007/s00210-013-0868-x

Amadio, S., Parisi, C., Piras, E., Fabbrizio, P., Apolloni, S., Montilli, C., et al. (2017). Modulation of P2X7 receptor during inflammation in multiple sclerosis. *Front. Immunol.* 8:1529. doi: 10.3389/fimmu.2017.01529

Amoroso, F., Falzoni, S., Adinolfi, E., Ferrari, D., and Di Virgilio, F. (2012). The P2X7 receptor is a key modulator of aerobic glycolysis. *Cell Death Dis.* 3:e370. doi: 10.1038/cddis.2012.105

Andrei, C., Dazzi, C., Lotti, L., Torrisi, M. R., Chimini, G., and Rubartelli, A. (1999). The secretory route of the leaderless protein interleukin 1beta involves exocytosis of endolysosome-related vesicles. *Mol. Biol. Cell* 10, 1463–1475. doi: 10.1091/mbc.10.5.1463

Andrei, C., Margiocco, P., Poggi, A., Lotti, L. V., Torrisi, M. R., and Rubartelli, A. (2004). Phospholipases C and A2 control lysosome-mediated IL-1 beta secretion: implications for inflammatory processes. *Proc. Natl. Acad. Sci. U.S.A.* 101, 9745–9750. doi: 10.1073/pnas.0308558101

Apolloni, S., Amadio, S., Montilli, C., Volonte, C., and D'ambrosi, N. (2013a). Ablation of P2X7 receptor exacerbates gliosis and motoneuron death in the SOD1-G93A mouse model of amyotrophic lateral sclerosis. *Hum. Mol. Genet.* 22, 4102–4116. doi: 10.1093/hmg/ddt259

Apolloni, S., Parisi, C., Pesaresi, M. G., Rossi, S., Carri, M. T., Cozzolino, M., et al. (2013b). The NADPH oxidase pathway is dysregulated by the P2X7 receptor in the SOD1-G93A microglia model of amyotrophic lateral sclerosis. *J. Immunol.* 190, 5187–5195. doi: 10.4049/jimmunol.1203262

Auger, R., Motta, I., Benihoud, K., Ojcius, D. M., and Kanellopoulos, J. M. (2005). A role for mitogen-activated protein kinase(Erk1/2) activation and non-selective pore formation in P2X7 receptor-mediated thymocyte death. *J. Biol. Chem.* 280, 28142–28151. doi: 10.1074/jbc.m501290200

Australia and New Zealand Multiple Sclerosis Genetics Consortium, (2009). Genome-wide association study identifies new multiple sclerosis susceptibility loci on chromosomes 12 and 20. *Nat. Genet.* 41, 824–828. doi: 10.1038/ng.396

Baricordi, O. R., Melchiorri, L., Adinolfi, E., Falzoni, S., Chiozzi, P., Buell, G., et al. (1999). Increased proliferation rate of lymphoid cells transfected with the P2X(7) ATP receptor. *J. Biol. Chem.* 274, 33206–33208. doi: 10.1074/jbc.274.47.33206

Barros-Barbosa, A. R., Fonseca, A. L., Guerra-Gomes, S., Ferreirinha, F., Santos, A., Rangel, R., et al. (2016). Up-regulation of P2X7 receptor-mediated inhibition of GABA uptake by nerve terminals of the human epileptic neocortex. *Epilepsia* 57, 99–110. doi: 10.1111/epi.13263

Barth, K., Weinhold, K., Guenther, A., Young, M. T., Schnittler, H., and Kasper, M. (2007). Caveolin-1 influences P2X7 receptor expression and localization in mouse lung alveolar epithelial cells. *FEBS J.* 274, 3021–3033. doi: 10.1111/j.1742-4658.2007.05830.x

Bartlett, R., Stokes, L., and Sluyter, R. (2014). The P2X7 receptor channel: recent developments and the use of P2X7 antagonists in models of disease. *Pharmacol. Rev.* 66, 638–675. doi: 10.1124/pr.113.008003

Beamer, E., Fischer, W., and Engel, T. (2017). The ATP-Gated P2X7 receptor as a target for the treatment of drug-resistant epilepsy. *Front. Neurosci.* 11:21. doi: 10.3389/fnins.2017.00021

Beyer, E. C., and Steinberg, T. H. (1991). Evidence that the gap junction protein connexin-43 is the ATP-induced pore of mouse macrophages. *J. Biol. Chem.* 266, 7971–7974.

Bianco, F., Ceruti, S., Colombo, A., Fumagalli, M., Ferrari, D., Pizzirani, C., et al. (2006). A role for P2X7 in microglial proliferation. *J. Neurochem.* 99, 745–758.

Burnstock, G. (1972). Purinergic nerves. *Pharmacol. Rev.* 24, 509–581.

Burnstock, G., Satchell, D. G., and Smythe, A. (1972). A comparison of the excitatory and inhibitory effects of non-adrenergic, non-cholinergic nerve stimulation and exogenously applied ATP on a variety of smooth muscle preparations from different vertebrate species. *Br. J. Pharmacol.* 46, 234–242. doi: 10.1111/j.1476-5381.1972.tb06868.x

Caille, I., Allinquant, B., Dupont, E., Bouillot, C., Langer, A., Muller, U., et al. (2004). Soluble form of amyloid precursor protein regulates proliferation of progenitors in the adult subventricular zone. *Development* 131, 2173–2181. doi: 10.1242/dev.01103

Chen, G. Y., and Nunez, G. (2010). Sterile inflammation: sensing and reacting to damage. *Nat. Rev. Immunol.* 10, 826–837. doi: 10.1038/nri2873

Chen, L., and Brosnan, C. F. (2006). Exacerbation of experimental autoimmune encephalomyelitis in P2X7R-/- mice: evidence for loss of apoptotic activity in lymphocytes. *J. Immunol.* 176, 3115–3126. doi: 10.4049/jimmunol.176.5.3115

Chessell, I. P., Hatcher, J. P., Bountra, C., Michel, A. D., Hughes, J. P., Green, P., et al. (2005). Disruption of the P2X7 purinoceptor gene abolishes chronic inflammatory and neuropathic pain. *Pain* 114, 386–396. doi: 10.1016/j.pain.2005.01.002

Christy, A. L., Walker, M. E., Hessner, M. J., and Brown, M. A. (2013). Mast cell activation and neutrophil recruitment promotes early and robust inflammation in the meninges in EAE. *J. Autoimmun.* 42, 50–61. doi: 10.1016/j.jaut.2012.11.003

Cruchaga, C., Kauwe, J. S., Harari, O., Jin, S. C., Cai, Y., Karch, C. M., et al. (2013). GWAS of cerebrospinal fluid tau levels identifies risk variants for Alzheimer's disease. *Neuron* 78, 256–268. doi: 10.1016/j.neuron.2013.02.026

Csoka, B., Nemeth, Z. H., Toro, G., Idzko, M., Zech, A., Koscso, B., et al. (2015). Extracellular ATP protects against sepsis through macrophage P2X7 purinergic receptors by enhancing intracellular bacterial killing. *FASEB J.* 29, 3626–3637. doi: 10.1096/fj.15-272450

Cullen, S. P., Kearney, C. J., Clancy, D. M., and Martin, S. J. (2015). Diverse Activators of the NLRP3 inflammasome promote IL-1beta secretion by triggering necrosis. *Cell Rep.* 11, 1535–1548. doi: 10.1016/j.celrep.2015.05.003

Damotte, V., Guillot-Noel, L., Patsopoulos, N. A., Madireddy, L., El Behi, M., International Multiple Sclerosis Genetics Consortium, et al. (2014). A gene pathway analysis highlights the role of cellular adhesion molecules in multiple sclerosis susceptibility. *Genes Immun.* 15, 126–132. doi: 10.1038/gene.2013.70

Dang, E. V., Barbi, J., Yang, H. Y., Jinasena, D., Yu, H., Zheng, Y., et al. (2011). Control of T(H)17/T(reg) balance by hypoxia-inducible factor 1. *Cell* 146, 772–784. doi: 10.1016/j.cell.2011.07.033

Danquah, W., Meyer-Schwesinger, C., Rissiek, B., Pinto, C., Serracant-Prat, A., Amadi, M., et al. (2016). Nanobodies that block gating of the P2X7 ion channel ameliorate inflammation. *Sci. Transl. Med.* 8:366ra162. doi: 10.1126/scitranslmed.aaf8463

Darmellah, A., Rayah, A., Auger, R., Cuif, M. H., Prigent, M., Arpin, M., et al. (2012). Ezrin/radixin/moesin are required for the purinergic P2X7 receptor (P2X7R)-dependent processing of the amyloid precursor protein. *J. Biol. Chem.* 287, 34583–34595. doi: 10.1074/jbc.M112.400010

Delarasse, C., Auger, R., Gonnord, P., Fontaine, B., and Kanellopoulos, J. M. (2011). The purinergic receptor P2X7 triggers alpha-secretase-dependent processing of the amyloid precursor protein. *J. Biol. Chem.* 286, 2596–2606. doi: 10.1074/jbc.M110.200618

Delarasse, C., Gonnord, P., Galante, M., Auger, R., Daniel, H., Motta, I., et al. (2009). Neural progenitor cell death is induced by extracellular ATP via ligation of P2X7 receptor. *J. Neurochem.* 109, 846–857. doi: 10.1111/j.1471-4159.2009.06008.x

Di, A., Xiong, S., Ye, Z., Malireddi, R. K. S., Kometani, S., Zhong, M., et al. (2018). The TWIK2 potassium efflux channel in macrophages mediates NLRP3 inflammasome-induced inflammation. *Immunity* 49, 56–65.e4. doi: 10.1016/j.immuni.2018.04.032

Di Virgilio, F. (2007). Liaisons dangereuses: P2X(7) and the inflammasome. *Trends Pharmacol. Sci.* 28, 465–472. doi: 10.1016/j.tips.2007.07.002

Di Virgilio, F., Dal Ben, D., Sarti, A. C., Giuliani, A. L., and Falzoni, S. (2017). The P2X7 receptor in infection and inflammation. *Immunity* 47, 15–31. doi: 10.1016/j.immuni.2017.06.020

Di Virgilio, F., Schmalzing, G., and Markwardt, F. (2018). The elusive P2X7 macropore. *Trends Cell Biol.* 28, 392–404. doi: 10.1016/j.tcb.2018.01.005

Diaz-Hernandez, J. I., Gomez-Villafuertes, R., Leon-Otegui, M., Hontecillas-Prieto, L., Del Puerto, A., Trejo, J. L., et al. (2012). In vivo P2X7 inhibition reduces amyloid plaques in Alzheimer's disease through GSK3beta and secretases. *Neurobiol. Aging* 33, 1816–1828. doi: 10.1016/j.neurobiolaging.2011.09.040

Ding, J., Wang, K., Liu, W., She, Y., Sun, Q., Shi, J., et al. (2016). Pore-forming activity and structural autoinhibition of the gasdermin family. *Nature* 535, 111–116. doi: 10.1038/nature18590

Domercq, M., and Matute, C. (2019). Targeting P2X4 and P2X7 receptors in multiple sclerosis. *Curr. Opin. Pharmacol.* 47, 119–125. doi: 10.1016/j.coph.2019.03.010

Domingo-Fernandez, R., Coll, R. C., Kearney, J., Breit, S., and O'Neill, L. A. J. (2017). The intracellular chloride channel proteins CLIC1 and CLIC4 induce IL-1beta transcription and activate the NLRP3 inflammasome. *J. Biol. Chem.* 292, 12077–12087. doi: 10.1074/jbc.M117.797126

Donnelly-Roberts, D. L., Namovic, M. T., Faltynek, C. R., and Jarvis, M. F. (2004). Mitogen-activated protein kinase and caspase signaling pathways are required for P2X7 receptor (P2X7R)-induced pore formation in human THP-1 cells. *J. Pharmacol. Exp. Ther.* 308, 1053–1061. doi: 10.1124/jpet.103.059600

Donnelly-Roberts, D. L., Namovic, M. T., Han, P., and Jarvis, M. F. (2009). Mammalian P2X7 receptor pharmacology: comparison of recombinant mouse, rat and human P2X7 receptors. *Br. J. Pharmacol.* 157, 1203–1214. doi: 10.1111/j.1476-5381.2009.00233.x

Engel, T., Gomez-Villafuertes, R., Tanaka, K., Mesuret, G., Sanz-Rodriguez, A., Garcia-Huerta, P., et al. (2012). Seizure suppression and neuroprotection by targeting the purinergic P2X7 receptor during status epilepticus in mice. *FASEB J.* 26, 1616–1628. doi: 10.1096/fj.11-196089

Evavold, C. L., and Kagan, J. C. (2018). How inflammasomes inform adaptive immunity. *J. Mol. Biol.* 430, 217–237. doi: 10.1016/j.jmb.2017.09.019

Evavold, C. L., Ruan, J., Tan, Y., Xia, S., Wu, H., and Kagan, J. C. (2018). The Pore-forming protein gasdermin D regulates interleukin-1 secretion from living macrophages. *Immunity* 48, 35–44.e6. doi: 10.1016/j.immuni.2017.11.013

Fabbrizio, P., Amadio, S., Apolloni, S., and Volonte, C. (2017). P2X7 receptor activation modulates autophagy in SOD1-G93A mouse microglia. *Front. Cell. Neurosci.* 11:249. doi: 10.3389/fncel.2017.00249

Faivre, E., Coelho, J. E., Zornbach, K., Malik, E., Baqi, Y., Schneider, M., et al. (2018). Beneficial effect of a selective adenosine A2A receptor antagonist in the APPswe/PS1dE9 mouse model of Alzheimer's disease. *Front. Mol. Neurosci.* 11:235. doi: 10.3389/fnmol.2018.00235

Faria, R. X., Defarias, F. P., and Alves, L. A. (2005). Are second messengers crucial for opening the pore associated with P2X7 receptor? *Am. J. Physiol. Cell Physiol.* 288, C260–C271.

Ferrari, D., Chiozzi, P., Falzoni, S., Dal Susino, M., Melchiorri, L., Baricordi, O. R., et al. (1997a). Extracellular ATP triggers IL-1 beta release by activating the purinergic P2Z receptor of human macrophages. *J. Immunol.* 159, 1451–1458.

Ferrari, D., Chiozzi, P., Falzoni, S., Hanau, S., and Di Virgilio, F. (1997b). Purinergic modulation of interleukin-1 beta release from microglial cells stimulated with bacterial endotoxin. *J. Exp. Med.* 185, 579–582. doi: 10.1084/jem.185.3.579

Garcia-Marcos, M., Perez-Andres, E., Tandel, S., Fontanils, U., Kumps, A., Kabre, E., et al. (2006). Coupling of two pools of P2X7 receptors to distinct intracellular signaling pathways in rat submandibular gland. *J. Lipid Res.* 47, 705–714. doi: 10.1194/jlr.m500408-jlr200

Gonnord, P., Delarasse, C., Auger, R., Benihoud, K., Prigent, M., Cuif, M. H., et al. (2009). Palmitoylation of the P2X7 receptor, an ATP-gated channel, controls its expression and association with lipid rafts. *FASEB J.* 23, 795–805. doi: 10.1096/fj.08-114637

Green, J. P., Yu, S., Martin-Sanchez, F., Pelegrin, P., Lopez-Castejon, G., Lawrence, C. B., et al. (2018). Chloride regulates dynamic NLRP3-dependent ASC oligomerization and inflammasome priming. *Proc. Natl. Acad. Sci. U.S.A.* 115, E9371–E9380. doi: 10.1073/pnas.1812744115

Gu, B. J., Baird, P. N., Vessey, K. A., Skarratt, K. K., Fletcher, E. L., Fuller, S. J., et al. (2013). A rare functional haplotype of the P2RX4 and P2RX7 genes leads to loss of innate phagocytosis and confers increased risk of age-related macular degeneration. *FASEB J.* 27, 1479–1487. doi: 10.1096/fj.12-215368

Gu, B. J., Field, J., Dutertre, S., Ou, A., Kilpatrick, T. J., Lechner-Scott, J., et al. (2015). A rare P2X7 variant Arg307Gln with absent pore formation function protects against neuroinflammation in multiple sclerosis. *Hum. Mol. Genet.* 24, 5644–5654. doi: 10.1093/hmg/ddv278

Gu, B. J., Saunders, B. M., Petrou, S., and Wiley, J. S. (2011). P2X(7) Is a scavenger receptor for apoptotic cells in the absence of its ligand, extracellular ATP. *J. Immunol.* 187, 2365–2375. doi: 10.4049/jimmunol.1101178

Gu, B. J., and Wiley, J. S. (2018). P2X7 as a scavenger receptor for innate phagocytosis in the brain. *Br. J. Pharmacol.* 175, 4195–4208. doi: 10.1111/bph.14470

Guillonneau, X., Eandi, C. M., Paques, M., Sahel, J. A., Sapieha, P., and Sennlaub, F. (2017). On phagocytes and macular degeneration. *Prog. Retin. Eye Res.* 61, 98–128. doi: 10.1016/j.preteyeres.2017.06.002

Habbas, S., Ango, F., Daniel, H., and Galante, M. (2011). Purinergic signaling in the cerebellum: bergmann glial cells express functional ionotropic P2X7 receptors. *Glia* 59, 1800–1812. doi: 10.1002/glia.21224

Halle, A., Hornung, V., Petzold, G. C., Stewart, C. R., Monks, B. G., Reinheckel, T., et al. (2008). The NALP3 inflammasome is involved in the innate immune response to amyloid-beta. *Nat. Immunol.* 9, 857–865. doi: 10.1038/ni.1636

Harkat, M., Peverini, L., Cerdan, A. H., Dunning, K., Beudez, J., Martz, A., et al. (2017). On the permeation of large organic cations through the pore of ATP-gated P2X receptors. *Proc. Natl. Acad. Sci. U.S.A.* 114, E3786–E3795. doi: 10.1073/pnas.1701379114

Harold, D., Abraham, R., Hollingworth, P., Sims, R., Gerrish, A., Hamshere, M. L., et al. (2009). Genome-wide association study identifies variants at CLU and PICALM associated with Alzheimer's disease. *Nat. Genet.* 41, 1088–1093. doi: 10.1038/ng.440

Hashimoto-Hill, S., Friesen, L., Kim, M., and Kim, C. H. (2017). Contraction of intestinal effector T cells by retinoic acid-induced purinergic receptor P2X7. *Mucosal Immunol.* 10, 912–923. doi: 10.1038/mi.2016.109

Hattori, M., and Gouaux, E. (2012). Molecular mechanism of ATP binding and ion channel activation in P2X receptors. *Nature* 485, 207–212. doi: 10.1038/nature11010

He, Y., Taylor, N., Fourgeaud, L., and Bhattacharya, A. (2017). The role of microglial P2X7: modulation of cell death and cytokine release. *J. Neuroinflammation* 14:135. doi: 10.1186/s12974-017-0904-8

He, Y., Zeng, M. Y., Yang, D., Motro, B., and Nunez, G. (2016). NEK7 is an essential mediator of NLRP3 activation downstream of potassium efflux. *Nature* 530, 354–357. doi: 10.1038/nature16959

Hechler, B., and Gachet, C. (2011). P2 receptors and platelet function. *Purinergic Signal.* 7, 293–303. doi: 10.1007/s11302-011-9247-6

Heilig, R., Dick, M. S., Sborgi, L., Meunier, E., Hiller, S., and Broz, P. (2018). The Gasdermin-D pore acts as a conduit for IL-1beta secretion in mice. *Eur. J. Immunol.* 48, 584–592. doi: 10.1002/eji.201747404

Heneka, M. T., Kummer, M. P., Stutz, A., Delekate, A., Schwartz, S., Vieira-Saecker, A., et al. (2013). NLRP3 is activated in Alzheimer's disease and contributes to pathology in APP/PS1 mice. *Nature* 493, 674–678. doi: 10.1038/nature11729

Hill, L. M., Gavala, M. L., Lenertz, L. Y., and Bertics, P. J. (2010). Extracellular ATP may contribute to tissue repair by rapidly stimulating purinergic receptor X7-dependent vascular endothelial growth factor release from primary human monocytes. *J. Immunol.* 185, 3028–3034. doi: 10.4049/jimmunol.1001298

Hirayama, Y., Ikeda-Matsuo, Y., Notomi, S., Enaida, H., Kinouchi, H., and Koizumi, S. (2015). Astrocyte-mediated ischemic tolerance. *J. Neurosci.* 35, 3794–3805. doi: 10.1523/JNEUROSCI.4218-14.2015

Hollingworth, P., Harold, D., Sims, R., Gerrish, A., Lambert, J. C., Carrasquillo, M. M., et al. (2011). Common variants at ABCA7, MS4A6A/MS4A4E, EPHA1, CD33 and CD2AP are associated with Alzheimer's disease. *Nat. Genet.* 43, 429–435. doi: 10.1038/ng.803

Hu, S. J., Calippe, B., Lavalette, S., Roubeix, C., Montassar, F., Housset, M., et al. (2015). Upregulation of P2RX7 in Cx3cr1-deficient mononuclear phagocytes leads to increased interleukin-1beta secretion and photoreceptor neurodegeneration. *J. Neurosci.* 35, 6987–6996. doi: 10.1523/JNEUROSCI.3955-14.2015

Illes, P., Khan, T. M., and Rubini, P. (2017). Neuronal P2X7 receptors revisited: do they really exist? *J. Neurosci.* 37, 7049–7062. doi: 10.1523/JNEUROSCI.3103-16.2017

Illes, P., Rubini, P., Huang, L., and Tang, Y. (2019). The P2X7 receptor: a new therapeutic target in Alzheimer's disease. *Expert. Opin. Ther. Targets* 23, 165–176. doi: 10.1080/14728222.2019.1575811

International Multiple Sclerosis Genetics Consortium, (2007). Risk alleles for multiple sclerosis identified by a genomewide study. *N. Engl. J. Med.* 357, 851–862. doi: 10.1056/nejmoa073493

International Multiple Sclerosis Genetics Consortium, (2011). Genetic risk and a primary role for cell-mediated immune mechanisms in multiple sclerosis. *Nature* 476, 214–219. doi: 10.1038/nature10251

International Multiple Sclerosis Genetics Consortium, (2013). Analysis of immune-related loci identifies 48 new susceptibility variants for multiple sclerosis. *Nat. Genet.* 45, 1353–1360. doi: 10.1038/ng.2770

International Multiple Sclerosis Genetics Consortium, (2018). Low-frequency and rare-coding variation contributes to multiple sclerosis risk. *Cell* 175, 1679–1687.e7. doi: 10.1016/j.cell.2018.09.049

Janks, L., Sharma, C. V. R., and Egan, T. M. (2018). A central role for P2X7 receptors in human microglia. *J. Neuroinflammation* 15:325. doi: 10.1186/s12974-018-1353-8

Jansen, I. E., Savage, J. E., Watanabe, K., Bryois, J., Williams, D. M., Steinberg, S., et al. (2019). Genome-wide meta-analysis identifies new loci and functional pathways influencing Alzheimer's disease risk. *Nat. Genet.* 51, 404–413. doi: 10.1038/s41588-018-0311-9

Jimenez-Pacheco, A., Diaz-Hernandez, M., Arribas-Blazquez, M., Sanz-Rodriguez, A., Olivos-Ore, L. A., Artalejo, A. R., et al. (2016). Transient P2X7 receptor antagonism produces lasting reductions in spontaneous seizures and gliosis in experimental temporal lobe epilepsy. *J. Neurosci.* 36, 5920–5932. doi: 10.1523/JNEUROSCI.4009-15.2016

Jun, G., Naj, A. C., Beecham, G. W., Wang, L. S., Buros, J., Gallins, P. J., et al. (2010). Meta-analysis confirms CR1, CLU, and PICALM as alzheimer disease risk loci and reveals interactions with APOE genotypes. *Arch. Neurol.* 67, 1473–1484. doi: 10.1001/archneurol.2010.201

Kaczmarek-Hajek, K., Zhang, J., Kopp, R., Grosche, A., Rissiek, B., Saul, A., et al. (2018). Re-evaluation of neuronal P2X7 expression using novel mouse models and a P2X7-specific nanobody. *eLife* 7:e36217. doi: 10.7554/eLife.36217

Kahner, B. N., Shankar, H., Murugappan, S., Prasad, G. L., and Kunapuli, S. P. (2006). Nucleotide receptor signaling in platelets. *J. Thromb. Haemost.* 4, 2317–2326. doi: 10.1111/j.1538-7836.2006.02192.x

Karasawa, A., and Kawate, T. (2016). Structural basis for subtype-specific inhibition of the P2X7 receptor. *eLife* 5:e22153. doi: 10.7554/eLife.22153

Karasawa, A., Michalski, K., Mikhelzon, P., and Kawate, T. (2017). The P2X7 receptor forms a dye-permeable pore independent of its intracellular domain but dependent on membrane lipid composition. *eLife* 6:e31186. doi: 10.7554/eLife.31186

Kasuya, G., Yamaura, T., Ma, X. B., Nakamura, R., Takemoto, M., Nagumo, H., et al. (2017). Structural insights into the competitive inhibition of the ATP-gated P2X receptor channel. *Nat. Commun.* 8:876. doi: 10.1038/s41467-017-00887-9

Kataoka, A., Tozaki-Saitoh, H., Koga, Y., Tsuda, M., and Inoue, K. (2009). Activation of P2X7 receptors induces CCL3 production in microglial cells through transcription factor NFAT. *J. Neurochem.* 108, 115–125. doi: 10.1111/j.1471-4159.2008.05744.x

Kawate, T., Michel, J. C., Birdsong, W. T., and Gouaux, E. (2009). Crystal structure of the ATP-gated P2X(4) ion channel in the closed state. *Nature* 460, 592–598. doi: 10.1038/nature08198

Kayagaki, N., Stowe, I. B., Lee, B. L., O'rourke, K., Anderson, K., Warming, S., et al. (2015). Caspase-11 cleaves gasdermin D for non-canonical inflammasome signalling. *Nature* 526, 666–671. doi: 10.1038/nature15541

Kerur, N., Hirano, Y., Tarallo, V., Fowler, B. J., Bastos-Carvalho, A., Yasuma, T., et al. (2013). TLR-independent and P2X7-dependent signaling mediate Alu RNA-induced NLRP3 inflammasome activation in geographic atrophy. *Invest. Ophthalmol. Vis. Sci.* 54, 7395–7401. doi: 10.1167/iovs.13-12500

Khadra, A., Tomic, M., Yan, Z., Zemkova, H., Sherman, A., and Stojilkovic, S. S. (2013). Dual gating mechanism and function of P2X7 receptor channels. *Biophys. J.* 104, 2612–2621. doi: 10.1016/j.bpj.2013.05.006

Kim, J. E., and Kang, T. C. (2011). The P2X7 receptor-pannexin-1 complex decreases muscarinic acetylcholine receptor-mediated seizure susceptibility in mice. *J. Clin. Invest.* 121, 2037–2047. doi: 10.1172/JCI44818

Koch-Nolte, F., Eichhoff, A., Pinto-Espinoza, C., Schwarz, N., Schafer, T., Menzel, S., et al. (2019). Novel biologics targeting the P2X7 ion channel. *Curr. Opin. Pharmacol.* 47, 110–118. doi: 10.1016/j.coph.2019.03.001

Kong, Q., Wang, M., Liao, Z., Camden, J. M., Yu, S., Simonyi, A., et al. (2005). P2X(7) nucleotide receptors mediate caspase-8/9/3-dependent apoptosis in rat primary cortical neurons. *Purinergic Signal.* 1, 337–347. doi: 10.1007/s11302-005-7145-5

Kunkle, B. W., Grenier-Boley, B., Sims, R., Bis, J. C., Damotte, V., Naj, A. C., et al. (2019). Genetic meta-analysis of diagnosed Alzheimer's disease identifies new risk loci and implicates Abeta, tau, immunity and lipid processing. *Nat. Genet.* 51, 414–430. doi: 10.1038/s41588-019-0358-2

Lambert, J. C., Heath, S., Even, G., Campion, D., Sleegers, K., Hiltunen, M., et al. (2009). Genome-wide association study identifies variants at CLU and CR1 associated with Alzheimer's disease. *Nat. Genet.* 41, 1094–1099. doi: 10.1038/ng.439

Lambert, J. C., Ibrahim-Verbaas, C. A., Harold, D., Naj, A. C., Sims, R., Bellenguez, C., et al. (2013). Meta-analysis of 74,046 individuals identifies 11 new susceptibility loci for Alzheimer's disease. *Nat. Genet.* 45, 1452–1458. doi: 10.1038/ng.2802

Langer, H. F., Choi, E. Y., Zhou, H., Schleicher, R., Chung, K. J., Tang, Z., et al. (2012). Platelets contribute to the pathogenesis of experimental autoimmune encephalomyelitis. *Circ. Res.* 110, 1202–1210. doi: 10.1161/CIRCRESAHA.111.256370

Le Feuvre, R. A., Brough, D., Touzani, O., and Rothwell, N. J. (2003). Role of P2X7 receptors in ischemic and excitotoxic brain injury *in vivo*. *J. Cereb. Blood Flow Metab.* 23, 381–384. doi: 10.1097/00004647-200303000-00013

Leeson, H. C., Kasherman, M. A., Chan-Ling, T., Lovelace, M. D., Brownlie, J. C., Toppinen, K. M., et al. (2018). P2X7 receptors regulate phagocytosis and proliferation in adult hippocampal and SVZ neural progenitor cells: implications for inflammation in neurogenesis. *Stem Cells* 36, 1764–1777. doi: 10.1002/stem.2894

Leon-Otegui, M., Gomez-Villafuertes, R., Diaz-Hernandez, J. I., Diaz-Hernandez, M., Miras-Portugal, M. T., and Gualix, J. (2011). Opposite effects of P2X7 and P2Y2 nucleotide receptors on alpha-secretase-dependent APP processing in Neuro-2a cells. *FEBS Lett.* 585, 2255–2262. doi: 10.1016/j.febslet.2011.05.048

Liu, T., Yamaguchi, Y., Shirasaki, Y., Shikada, K., Yamagishi, M., Hoshino, K., et al. (2014). Single-cell imaging of caspase-1 dynamics reveals an all-or-none inflammasome signaling response. *Cell Rep.* 8, 974–982. doi: 10.1016/j.celrep.2014.07.012

Liu, X., Zhang, Z., Ruan, J., Pan, Y., Magupalli, V. G., Wu, H., et al. (2016). Inflammasome-activated gasdermin D causes pyroptosis by forming membrane pores. *Nature* 535, 153–158. doi: 10.1038/nature18629

Lopez-Castejon, G., and Brough, D. (2011). Understanding the mechanism of IL-1beta secretion. *Cytokine Growth Factor Rev.* 22, 189–195. doi: 10.1016/j.cytogfr.2011.10.001

Lorden, G., Sanjuan-Garcia, I., De Pablo, N., Meana, C., Alvarez-Miguel, I., Perez-Garcia, M. T., et al. (2017). Lipin-2 regulates NLRP3 inflammasome by affecting P2X7 receptor activation. *J. Exp. Med.* 214, 511–528. doi: 10.1084/jem.20161452

Lovelace, M. D., Gu, B. J., Eamegdool, S. S., Weible, M. W. II, Wiley, J. S., Allen, D. G., et al. (2015). P2X7 receptors mediate innate phagocytosis by human neural precursor cells and neuroblasts. *Stem Cells* 33, 526–541. doi: 10.1002/stem.1864

MacKenzie, A., Wilson, H. L., Kiss-Toth, E., Dower, S. K., North, R. A., and Surprenant, A. (2001). Rapid secretion of interleukin-1beta by microvesicle shedding. *Immunity* 15, 825–835. doi: 10.1016/s1074-7613(01)00229-1

Mahaut-Smith, M. P., Jones, S., and Evans, R. J. (2011). The P2X1 receptor and platelet function. *Purinergic Signal.* 7, 341–356. doi: 10.1007/s11302-011-9224-0

Marchini, J., Donnelly, P., and Cardon, L. R. (2005). Genome-wide strategies for detecting multiple loci that influence complex diseases. *Nat. Genet.* 37, 413–417. doi: 10.1038/ng1537

Marioni, R. E., Harris, S. E., Zhang, Q., Mcrae, A. F., Hagenaars, S. P., Hill, W. D., et al. (2018). GWAS on family history of Alzheimer's disease. *Transl. Psychiatry* 8:99.

Martin, E., Amar, M., Dalle, C., Youssef, I., Boucher, C., Le Duigou, C., et al. (2019). New role of P2X7 receptor in an Alzheimer's disease mouse model. *Mol. Psychiatry* 24, 108–125. doi: 10.1038/s41380-018-0108-3

Mascanfroni, I. D., Takenaka, M. C., Yeste, A., Patel, B., Wu, Y., Kenison, J. E., et al. (2015). Metabolic control of type 1 regulatory T cell differentiation by AHR and HIF1-alpha. *Nat. Med.* 21, 638–646. doi: 10.1038/nm.3868

Mattson, M. P. (1997). Cellular actions of beta-amyloid precursor protein and its soluble and fibrillogenic derivatives. *Physiol. Rev.* 77, 1081–1132. doi: 10.1152/physrev.1997.77.4.1081

Matute, C., Torre, I., Perez-Cerda, F., Perez-Samartin, A., Alberdi, E., Etxebarria, E., et al. (2007). P2X(7) receptor blockade prevents ATP excitotoxicity in oligodendrocytes and ameliorates experimental autoimmune encephalomyelitis. *J. Neurosci.* 27, 9525–9533. doi: 10.1523/jneurosci.0579-07.2007

McLarnon, J. G., Ryu, J. K., Walker, D. G., and Choi, H. B. (2006). Upregulated expression of purinergic P2X(7) receptor in Alzheimer disease and amyloid-beta peptide-treated microglia and in peptide-injected rat hippocampus. *J. Neuropathol. Exp. Neurol.* 65, 1090–1097. doi: 10.1097/01.jnen.0000240470.97295.d3

Mellouk, A., and Bobe, P. (2019). CD8(+), but not CD4(+) effector/memory T cells, express the CD44(high)CD45RB(high) phenotype with aging, which displays reduced expression levels of P2X7 receptor and ATP-induced cellular responses. *FASEB J.* 33, 3225–3236. doi: 10.1096/fj.201800867r

Messemer, N., Kunert, C., Grohmann, M., Sobottka, H., Nieber, K., Zimmermann, H., et al. (2013). P2X7 receptors at adult neural progenitor cells of the mouse subventricular zone. *Neuropharmacology* 73, 122–137. doi: 10.1016/j.neuropharm.2013.05.017

Metzger, M. W., Walser, S. M., Aprile-Garcia, F., Dedic, N., Chen, A., Holsboer, F., et al. (2017). Genetically dissecting P2rx7 expression within the central nervous system using conditional humanized mice. *Purinergic Signal.* 13, 153–170. doi: 10.1007/s11302-016-9546-z

Miras-Portugal, M. T., Sebastian-Serrano, A., De Diego Garcia, L., and Diaz-Hernandez, M. (2017). Neuronal P2X7 receptor: involvement in neuronal physiology and pathology. *J. Neurosci.* 37, 7063–7072. doi: 10.1523/JNEUROSCI.3104-16.2017

Mizutani, T., Fowler, B. J., Kim, Y., Yasuma, R., Krueger, L. A., Gelfand, B. D., et al. (2015). Nucleoside reverse transcriptase inhibitors suppress laser-induced choroidal neovascularization in mice. *Invest. Ophthalmol. Vis. Sci.* 56, 7122–7129. doi: 10.1167/iovs.15-17440

Monif, M., Reid, C. A., Powell, K. L., Smart, M. L., and Williams, D. A. (2009). The P2X7 receptor drives microglial activation and proliferation: a trophic role

for P2X7R pore. *J. Neurosci.* 29, 3781–3791. doi: 10.1523/JNEUROSCI.5512-08.2009

Morciano, G., Sarti, A. C., Marchi, S., Missiroli, S., Falzoni, S., Raffaghello, L., et al. (2017). Use of luciferase probes to measure ATP in living cells and animals. *Nat. Protoc.* 12, 1542–1562. doi: 10.1038/nprot.2017.052

Naj, A. C., Jun, G., Beecham, G. W., Wang, L. S., Vardarajan, B. N., Buros, J., et al. (2011). Common variants at MS4A4/MS4A6E, CD2AP, CD33 and EPHA1 are associated with late-onset Alzheimer's disease. *Nat. Genet.* 43, 436–441. doi: 10.1038/ng.801

Narcisse, L., Scemes, E., Zhao, Y., Lee, S. C., and Brosnan, C. F. (2005). The cytokine IL-1beta transiently enhances P2X7 receptor expression and function in human astrocytes. *Glia* 49, 245–258. doi: 10.1002/glia.20110

Nicke, A., Kuan, Y. H., Masin, M., Rettinger, J., Marquez-Klaka, B., Bender, O., et al. (2009). A functional P2X7 splice variant with an alternative transmembrane domain 1 escapes gene inactivation in P2X7 knock-out mice. *J. Biol. Chem.* 284, 25813–25822. doi: 10.1074/jbc.M109.033134

Ousingsawat, J., Wanitchakool, P., Kmit, A., Romao, A. M., Jantarajit, W., Schreiber, R., et al. (2015). Anoctamin 6 mediates effects essential for innate immunity downstream of P2X7 receptors in macrophages. *Nat. Commun.* 6:6245. doi: 10.1038/ncomms7245

Panenka, W., Jijon, H., Herx, L. M., Armstrong, J. N., Feighan, D., Wei, T., et al. (2001). P2X7-like receptor activation in astrocytes increases chemokine monocyte chemoattractant protein-1 expression via mitogen-activated protein kinase. *J. Neurosci.* 21, 7135–7142. doi: 10.1523/jneurosci.21-18-07135.2001

Pelegrin, P., and Surprenant, A. (2006). Pannexin-1 mediates large pore formation and interleukin-1beta release by the ATP-gated P2X7 receptor. *EMBO J.* 25, 5071–5082. doi: 10.1038/sj.emboj.7601378

Peverini, L., Beudez, J., Dunning, K., Chataigneau, T., and Grutter, T. (2018). New insights into permeation of large cations through ATP-Gated P2X receptors. *Front. Mol. Neurosci.* 11:265. doi: 10.3389/fnmol.2018.00265

Pippel, A., Stolz, M., Woltersdorf, R., Kless, A., Schmalzing, G., and Markwardt, F. (2017). Localization of the gate and selectivity filter of the full-length P2X7 receptor. *Proc. Natl. Acad. Sci. U.S.A.* 114, E2156–E2165. doi: 10.1073/pnas.1610414114

Qu, Y., and Dubyak, G. R. (2009). P2X7 receptors regulate multiple types of membrane trafficking responses and non-classical secretion pathways. *Purinergic Signal.* 5, 163–173. doi: 10.1007/s11302-009-9132-8

Qu, Y., Franchi, L., Nunez, G., and Dubyak, G. R. (2007). Nonclassical IL-1 beta secretion stimulated by P2X7 receptors is dependent on inflammasome activation and correlated with exosome release in murine macrophages. *J. Immunol.* 179, 1913–1925. doi: 10.4049/jimmunol.179.3.1913

Qu, Y., Misaghi, S., Newton, K., Gilmour, L. L., Louie, S., Cupp, J. E., et al. (2011). Pannexin-1 is required for ATP release during apoptosis but not for inflammasome activation. *J. Immunol.* 186, 6553–6561. doi: 10.4049/jimmunol.1100478

Ramanan, V. K., and Saykin, A. J. (2013). Pathways to neurodegeneration: mechanistic insights from GWAS in Alzheimer's disease, Parkinson's disease, and related disorders. *Am. J. Neurodegener. Dis.* 2, 145–175.

Rampe, D., Wang, L., and Ringheim, G. E. (2004). P2X7 receptor modulation of beta-amyloid- and LPS-induced cytokine secretion from human macrophages and microglia. *J. Neuroimmunol.* 147, 56–61. doi: 10.1016/j.jneuroim.2003.10.014

Rassendren, F., and Audinat, E. (2016). Purinergic signaling in epilepsy. *J. Neurosci. Res.* 94, 781–793. doi: 10.1002/jnr.23770

Riedel, T., Schmalzing, G., and Markwardt, F. (2007). Influence of extracellular monovalent cations on pore and gating properties of P2X7 receptor-operated single-channel currents. *Biophys. J.* 93, 846–858. doi: 10.1529/biophysj.106.103614

Rigato, C., Swinnen, N., Buckinx, R., Couillin, I., Mangin, J. M., Rigo, J. M., et al. (2012). Microglia proliferation is controlled by P2X7 receptors in a Pannexin-1-independent manner during early embryonic spinal cord invasion. *J. Neurosci.* 32, 11559–11573. doi: 10.1523/jneurosci.1042-12.2012

Rissiek, B., Haag, F., Boyer, O., Koch-Nolte, F., and Adriouch, S. (2015). P2X7 on mouse T cells: one channel, many functions. *Front. Immunol.* 6:204. doi: 10.3389/fimmu.2015.00204

Robinson, L. E., Shridar, M., Smith, P., and Murrell-Lagnado, R. D. (2014). Plasma membrane cholesterol as a regulator of human and rodent P2X7 receptor activation and sensitization. *J. Biol. Chem.* 289, 31983–31994. doi: 10.1074/jbc.M114.574699

Rodrigues, R. J., Tome, A. R., and Cunha, R. A. (2015). ATP as a multi-target danger signal in the brain. *Front. Neurosci.* 9:148. doi: 10.3389/fnins.2015.00148

Rozmer, K., Gao, P., Araujo, M. G. L., Khan, M. T., Liu, J., Rong, W., et al. (2017). Pilocarpine-induced status epilepticus increases the sensitivity of P2X7 and P2Y1 receptors to nucleotides at neural progenitor cells of the juvenile rodent hippocampus. *Cereb. Cortex* 27, 3568–3585. doi: 10.1093/cercor/bhw178

Ruhl, S., Shkarina, K., Demarco, B., Heilig, R., Santos, J. C., and Broz, P. (2018). ESCRT-dependent membrane repair negatively regulates pyroptosis downstream of GSDMD activation. *Science* 362, 956–960. doi: 10.1126/science.aar7607

Russi, A. E., Walker-Caulfield, M. E., Guo, Y., Lucchinetti, C. F., and Brown, M. A. (2016). Meningeal mast cell-T cell crosstalk regulates T cell encephalitogenicity. *J. Autoimmun.* 73, 100–110. doi: 10.1016/j.jaut.2016.06.015

Sabelko-Downes, K. A., Russell, J. H., and Cross, A. H. (1999). Role of Fas–FasL interactions in the pathogenesis and regulation of autoimmune demyelinating disease. *J. Neuroimmunol.* 100, 42–52. doi: 10.1016/s0165-5728(99)00191-5

Sadovnick, A. D., Gu, B. J., Traboulsee, A. L., Bernales, C. Q., Encarnacion, M., Yee, I. M., et al. (2017). Purinergic receptors P2RX4 and P2RX7 in familial multiple sclerosis. *Hum. Mutat.* 38, 736–744. doi: 10.1002/humu.23218

Safya, H., Mellouk, A., Legrand, J., Le Gall, S. M., Benbijja, M., Kanellopoulos-Langevin, C., et al. (2018). Variations in cellular responses of mouse T cells to adenosine-5'-triphosphate stimulation do not depend on P2X7 receptor expression levels but on their activation and differentiation stage. *Front. Immunol.* 9:360. doi: 10.3389/fimmu.2018.00360

Sanz, J. M., Chiozzi, P., Ferrari, D., Colaianna, M., Idzko, M., Falzoni, S., et al. (2009). Activation of microglia by amyloid {beta} requires P2X7 receptor expression. *J. Immunol.* 182, 4378–4385. doi: 10.4049/jimmunol.0803612

Savio, L. E. B., De Andrade Mello, P., Da Silva, C. G., and Coutinho-Silva, R. (2018). The P2X7 receptor in inflammatory diseases: angel or demon? *Front. Pharmacol.* 9:52. doi: 10.3389/fphar.2018.00052

Sborgi, L., Ruhl, S., Mulvihill, E., Pipercevic, J., Heilig, R., Stahlberg, H., et al. (2016). GSDMD membrane pore formation constitutes the mechanism of pyroptotic cell death. *EMBO J.* 35, 1766–1778. doi: 10.15252/embj.201694696

Schachter, J., Motta, A. P., De Souza Zamorano, A., Da Silva-Souza, H. A., Guimaraes, M. Z., and Persechini, P. M. (2008). ATP-induced P2X7-associated uptake of large molecules involves distinct mechanisms for cations and anions in macrophages. *J. Cell Sci.* 121, 3261–3270. doi: 10.1242/jcs.029991

Schmid-Burgk, J. L., Chauhan, D., Schmidt, T., Ebert, T. S., Reinhardt, J., Endl, E., et al. (2016). A Genome-wide CRISPR (Clustered Regularly Interspaced Short Palindromic Repeats) screen identifies NEK7 as an essential component of NLRP3 inflammasome activation. *J. Biol. Chem.* 291, 103–109. doi: 10.1074/jbc.C115.700492

Secor, V. H., Secor, W. E., Gutekunst, C. A., and Brown, M. A. (2000). Mast cells are essential for early onset and severe disease in a murine model of multiple sclerosis. *J. Exp. Med.* 191, 813–822. doi: 10.1084/jem.191.5.813

Seman, M., Adriouch, S., Scheuplein, F., Krebs, C., Freese, D., Glowacki, G., et al. (2003). NAD-induced T cell death: ADP-ribosylation of cell surface proteins by ART2 activates the cytolytic P2X7 purinoceptor. *Immunity* 19, 571–582.

Sharif, H., Wang, L., Wang, W. L., Magupalli, V. G., Andreeva, L., Qiao, Q., et al. (2019). Structural mechanism for NEK7-licensed activation of NLRP3 inflammasome. *Nature* 570, 338–343. doi: 10.1038/s41586-019-1295-z

Sharp, A. J., Polak, P. E., Simonini, V., Lin, S. X., Richardson, J. C., Bongarzone, E. R., et al. (2008). P2x7 deficiency suppresses development of experimental autoimmune encephalomyelitis. *J. Neuroinflammation* 5:33. doi: 10.1186/1742-2094-5-33

Shi, H., Wang, Y., Li, X., Zhan, X., Tang, M., Fina, M., et al. (2016). NLRP3 activation and mitosis are mutually exclusive events coordinated by NEK7, a new inflammasome component. *Nat. Immunol.* 17, 250–258. doi: 10.1038/ni.3333

Shi, J., Zhao, Y., Wang, K., Shi, X., Wang, Y., Huang, H., et al. (2015). Cleavage of GSDMD by inflammatory caspases determines pyroptotic cell death. *Nature* 526, 660–665. doi: 10.1038/nature15514

Skaper, S. D., Facci, L., Culbert, A. A., Evans, N. A., Chessell, I., Davis, J. B., et al. (2006). P2X(7) receptors on microglial cells mediate injury to cortical neurons *in vitro*. *Glia* 54, 234–242. doi: 10.1002/glia.20379

Solle, M., Labasi, J., Perregaux, D. G., Stam, E., Petrushova, N., Koller, B. H., et al. (2001). Altered cytokine production in mice lacking P2X(7) receptors. *J. Biol. Chem.* 276, 125–132.

Sonia, D., Souza, C., Li, Z., Luke Maxwell, D., Trusler, O., Murphy, M., et al. (2018). Platelets drive inflammation and target gray matter and the retina in autoimmune-mediated encephalomyelitis. *J. Neuropathol. Exp. Neurol.* 77, 567–576. doi: 10.1093/jnen/nly032

Starossom, S. C., Veremeyko, T., Yung, A. W., Dukhinova, M., Au, C., Lau, A. Y., et al. (2015). Platelets play differential role during the initiation and progression of autoimmune neuroinflammation. *Circ. Res.* 117, 779–792. doi: 10.1161/CIRCRESAHA.115.306847

Steinberg, T. H., Newman, A. S., Swanson, J. A., and Silverstein, S. C. (1987). ATP4- permeabilizes the plasma membrane of mouse macrophages to fluorescent dyes. *J. Biol. Chem.* 262, 8884–8888.

Tang, T., Lang, X., Xu, C., Wang, X., Gong, T., Yang, Y., et al. (2017). CLICs-dependent chloride efflux is an essential and proximal upstream event for NLRP3 inflammasome activation. *Nat. Commun.* 8:202. doi: 10.1038/s41467-017-00227-x

Taylor, J. P., Brown, R. H. Jr., and Cleveland, D. W. (2016). Decoding ALS: from genes to mechanism. *Nature* 539, 197–206. doi: 10.1038/nature20413

Taylor, S. R., Gonzalez-Begne, M., Sojka, D. K., Richardson, J. C., Sheardown, S. A., Harrison, S. M., et al. (2009). Lymphocytes from P2X7-deficient mice exhibit enhanced P2X7 responses. *J. Leukoc. Biol.* 85, 978–986. doi: 10.1189/jlb.0408251

Tsao, H. K., Chiu, P. H., and Sun, S. H. (2013). PKC-dependent ERK phosphorylation is essential for P2X7 receptor-mediated neuronal differentiation of neural progenitor cells. *Cell Death Dis.* 4:e751. doi: 10.1038/cddis.2013.274

Vessey, K. A., Gu, B. J., Jobling, A. I., Phipps, J. A., Greferath, U., Tran, M. X., et al. (2017). Loss of function of P2X7 receptor scavenger activity in aging mice: a novel model for investigating the early pathogenesis of age-related macular degeneration. *Am. J. Pathol.* 187, 1670–1685. doi: 10.1016/j.ajpath.2017.04.016

Witting, A., Chen, L., Cudaback, E., Straiker, A., Walter, L., Rickman, B., et al. (2006). Experimental autoimmune encephalomyelitis disrupts endocannabinoid-mediated neuroprotection. *Proc. Natl. Acad. Sci. U.S.A.* 103, 6362–6367. doi: 10.1073/pnas.0510418103

Witting, A., Walter, L., Wacker, J., Moller, T., and Stella, N. (2004). P2X7 receptors control 2-arachidonoylglycerol production by microglial cells. *Proc. Natl. Acad. Sci. U.S.A.* 101, 3214–3219. doi: 10.1073/pnas.0306707101

Yiangou, Y., Facer, P., Durrenberger, P., Chessell, I. P., Naylor, A., Bountra, C., et al. (2006). COX-2, CB2 and P2X7-immunoreactivities are increased in activated microglial cells/macrophages of multiple sclerosis and amyotrophic lateral sclerosis spinal cord. *BMC Neurol.* 6:12. doi: 10.1186/1471-2377-6-12

Yip, L., Woehrle, T., Corriden, R., Hirsh, M., Chen, Y., Inoue, Y., et al. (2009). Autocrine regulation of T-cell activation by ATP release and P2X7 receptors. *FASEB J.* 23, 1685–1693. doi: 10.1096/fj.08-126458

Young, C. N. J., and Gorecki, D. C. (2018). P2RX7 purinoceptor as a therapeutic target-the second coming? *Front. Chem.* 6:248. doi: 10.3389/fchem.2018.00248

Zanoni, I., Tan, Y., Di Gioia, M., Springstead, J. R., and Kagan, J. C. (2017). By capturing inflammatory lipids released from dying cells, the receptor CD14 induces inflammasome-dependent phagocyte hyperactivation. *Immunity* 47, 697–709.e3. doi: 10.1016/j.immuni.2017.09.010

Zhou, R., Tardivel, A., Thorens, B., Choi, I., and Tschopp, J. (2010). Thioredoxin-interacting protein links oxidative stress to inflammasome activation. *Nat. Immunol.* 11, 136–140. doi: 10.1038/ni.1831

Conflict of Interest Statement: The authors declare that the research was conducted in the absence of any commercial or financial relationships that could be construed as a potential conflict of interest.

frontiers in Cellular Neuroscience

ORIGINAL RESEARCH
published: 01 October 2019
doi: 10.3389/fncel.2019.00438

Caffeine Consumption During Pregnancy Accelerates the Development of Cognitive Deficits in Offspring in a Model of Tauopathy

*Stefania Zappettini[1], Emilie Faivre[2], Antoine Ghestem[1], Sébastien Carrier[2], Luc Buée[2], David Blum[2], Monique Esclapez[1] and Christophe Bernard[1]**

[1] Aix Marseille Univ, INSERM, INS, Institut de Neurosciences des Systèmes, Marseille, France, [2] Inserm, CHU Lille, LabEx DISTALZ, UMR-S 1172 - JPArc, Université de Lille, Lille, France

Psychoactive drugs used during pregnancy can affect the development of the brain of offspring, directly triggering neurological disorders or increasing the risk for their occurrence. Caffeine is the most widely consumed psychoactive drug, including during pregnancy. In Wild type mice, early life exposure to caffeine renders offspring more susceptible to seizures. Here, we tested the long-term consequences of early life exposure to caffeine in THY-Tau22 transgenic mice, a model of Alzheimer's disease-like Tau pathology. Caffeine exposed mutant offspring developed cognitive earlier than water treated mutants. Electrophysiological recordings of hippocampal CA1 pyramidal cells *in vitro* revealed that early life exposure to caffeine changed the way the glutamatergic and GABAergic drives were modified by the Tau pathology. We conclude that early-life exposure to caffeine affects the Tau phenotype and we suggest that caffeine exposure during pregnancy may constitute a risk-factor for early onset of Alzheimer's disease-like pathology.

Keywords: caffeine, development, Alzheimer, tauopathy, hippocampus, memory, learning, synaptic currents

OPEN ACCESS

Edited by:
Sonia Gasparini, LSU Health Sciences Center New Orleans, United States

Reviewed by:
Haruyuki Kamiya, Hokkaido University, Japan
Kelly Dougherty, Rhodes College, United States

***Correspondence:**
Christophe Bernard
christophe.bernard@univ-amu.fr

Specialty section:
This article was submitted to Cellular Neurophysiology, a section of the journal Frontiers in Cellular Neuroscience

Received: *18 July 2019*
Accepted: *13 September 2019*
Published: *01 October 2019*

Citation:
Zappettini S, Faivre E, Ghestem A, Carrier S, Buée L, Blum D, Esclapez M and Bernard C (2019) Caffeine Consumption During Pregnancy Accelerates the Development of Cognitive Deficits in Offspring in a Model of Tauopathy. Front. Cell. Neurosci. 13:438. doi: 10.3389/fncel.2019.00438

INTRODUCTION

Adult brain structure is primarily established in early life (Lenroot and Giedd, 2006). Disturbances in anatomical (number and connectivity of neurons) and functional (ability to engage alternative brain networks) development can interfere with crucial processes, including cell proliferation, neuronal migration (Crandall et al., 2004) and post-migration cortical connectivity (Guerrini and Dobyns, 2014). Disturbances can be genetic (e.g., a mutation) and environmental (e.g., maternal separation), resulting in increased risk to develop pathologies during early life such as cortical malformations, developmental delay, epilepsy, and/or autism (Barkovich et al., 2012; Guerrini and Dobyns, 2014), as well as during adulthood/aging, leading to dementia such as Alzheimer's Disease (AD)-related pathology (Borenstein et al., 2006; Whalley et al., 2006; Stern, 2012; Seifan et al., 2015).

Neuropathologically, AD is defined by the extracellular accumulation of amyloid beta (Aß) peptides into amyloid plaques, and the presence of intraneuronal fibrillar aggregates of hyper- and abnormally-phosphorylated tau proteins (Masters et al., 1985; Sergeant et al., 2008). Tau pathology is observed early in the brain stem and entorhinal cortex (Braak et al., 2011) and its progression from entorhinal cortex, to the hippocampus, and finally neocortex corresponds to the progression

of the symptoms in AD (Duyckaerts et al., 1997; Grober et al., 1999) supporting a pivotal role of Tau pathology in AD-related memory impairments. Various genetic and environmental risk factors are associated with dementia and/or AD (Reitz et al., 2011). Most of these environmental and lifestyle-related factors also impact AD lesions, and in particular Tau pathology. For instance, physical exercise (Belarbi et al., 2011), anesthetics (Le Freche et al., 2012; Whittington et al., 2013), or obesity/diabetes (Leboucher et al., 2013; Papon et al., 2013) modulate Tau pathology and associated memory disturbances.

Among the numerous existing environmental risk factors, those occurring during pregnancy and lactation can have important functional consequences. Exposure to psychoactive substances *in utero* can alter fetal brain development, leading to pathological states later in life for the offspring, including psychiatric disorders (Marroun et al., 2015; Skorput et al., 2015). Caffeine is the most frequently consumed psychoactive substance, including during pregnancy (Mandel, 2002; Greenwood et al., 2014). In mice, caffeine exposure during pregnancy and until weaning delays the migration and integration of GABA neurons, enhances seizure susceptibility, as well as alters brain rhythms and hippocampus-dependent memory function in the offspring (Silva et al., 2013; Fazeli et al., 2017). Although it is difficult to generalize rodent studies to humans, a study in mother–child pairs showed an association between caffeine exposure during pregnancy and impaired cognitive development (Galéra et al., 2015). Guidelines for pregnant women recommend to limit the amount of caffeine consumption to 200–300 mg/kg (American College of Obstetricians and Gynecologists, 2010). Whether early life exposure to caffeine may prime exposed offsprings to the development of neurodegenerative disorders later in life remains unknown. In the present study, we specifically aimed at determining whether Tau pathology related pathological traits would appear sooner in animals exposed to caffeine during brain development. To address this question, we evaluated the effects of early life caffeine exposure in offspring of the THY-Tau22 transgenic mouse model that progressively develops AD-like hippocampal Tau pathology, with ongoing deficits at 6–8 months of age and a full pathology and memory impairments occurring at 12 months of age (Van der Jeugd et al., 2013).

MATERIALS AND METHODS

Animals

Male mice were group housed to reduce stress (Manouze et al., 2019), in standard mouse cages under conventional laboratory conditions (12 h/12 h dark-light cycle, constant temperature, constant humidity, and food and water *ad libitum*). Animal care and experimental procedures were conducted in accordance with institutional guidelines and with the European Communities Council Directive 86/609/EEC and were approved by the Aix-Marseille University Chancellor's Animal Research Committee, Marseille (France). Since age is a highly important factor in studies related to Tauophaties as a major determinant of phenotype and disease progression, experiments were performed in 8 and 12 month-old mice.

Caffeine Treatment

This study is designed to mimic the situation in pregnant women consuming caffeine before and during their entire pregnancy until full-term birth, both in terms of time span of caffeine exposure and caffeine concentration. In the caffeine groups, female mice received caffeine via their drinking water. Caffeine treatment was started 2 weeks before mating — reflecting the situation in women who usually do not start consuming caffeine with the onset of pregnancy but did consume caffeine beforehand — and was continued up until postnatal day 15. This end point of the treatment period was chosen based on the assumption that, from a developmental point of view, term birth in humans (= end of gestational week 40) is approximately comparable to postnatal days 12/13 in rodents (Romijn et al., 1991; Clancy et al., 2001). Therefore, caffeine exposure during the entire pregnancy up until postnatal day 15 in mice would approximately reflect pregnancy until term birth in humans. Caffeine powder was dissolved in tap water at a concentration of 0.3 g/l and given as drinking water to the dam. This concentration was chosen based on previous findings that exposure to 0.3 g/l caffeine via drinking water results in a plasma caffeine concentration in rat dams that is similar to that found in the blood of humans drinking three to four cups of coffee per day (Adén et al., 2000) and in a plasma concentration of caffeine in rat pups at P7 similar to that found in the umbilical cord of human neonates whose mothers consume moderate amounts of coffee (up to three cups per day) (Björklund et al., 2008). In a previous study, we confirmed that this caffeine concentration in mice results in a serum concentration comparable to the one previously reported in rats (Silva et al., 2013). Also, we showed that this treatment regimen only affects maternal water intake on the first day of treatment, but not in the following time span (Silva et al., 2013), suggesting that 2 weeks of treatment prior to mating should be enough to reach stable caffeine concentrations in the dam at the onset of pregnancy.

From postnatal day 15 on, dams and offspring received pure drinking water. The water groups was never exposed to caffeine and received pure drinking water at all times.

Electrophysiology in Hippocampal Slices

The barrage of synaptic inputs received by neurons can characterize the functional state of neuronal networks. To quantify the excitatory and inhibitory inputs received by CA1 hippocampal pyramidal cells, we measured the frequency and amplitude of spontaneous and miniature excitatory and inhibitory post-synaptic currents in acute slices from wild type, wild type caffeine, Tau water, and Tau caffeine mice.

Number of animals per group: n = 8 cells, 8 slices, from 5 Wild type water mice vs. n = 8 cells, 8 slices, from 5 Wild type caffeine-exposed mice, vs. n = 9 cells, 9 slices, from 5 Tau water mice vs. n = 9 cells, 9 slices, from 5 Tau caffeine-exposed mice (8 months) and n = 8 cells, 8 slices, from 5 Wild type water mice vs. n = 8 cells, 8 slices, from 5 Wild type caffeine-exposed mice, vs. n = 7 cells, 7 slices, from 4 Tau water mice vs. n = 9 cells, 9 slices, from 5 Tau caffeine-exposed mice (12 months). Transverse cortical slices (350 μm)

were prepared with a vibroslicer Leica VT 1200S in a cold (lower than 4°C) cutting solution containing 140.0 mM potassium gluconate, 10.0 mM HEPES, 15.0 mM sodium gluconate, 0.2 mM EGTA, 4.0 mM NaCl, pH 7.2. After 20 min recovery in a preincubation solution (110 mM Choline chloride, 2.5 mM KCl, 1.25 mM NaH_2PO_4, 10 mM $MgCl_2$, 0.5 mM $CaCl_2$, 25 mM $NaHCO_3$, 10 mM D-glucose, 5 mM sodium pyruvate equilibrated with 5% CO_2 in 95% O_2 at room temperature), slices were perfused for at least 1 h with aCSF containing 126.0 mM NaCl, 25.0 mM $NaHCO_3$, 10.0 mM D-glucose, 3.5 mM KCl, 2.0 mM $CaCl_2$, 1.3 mM $MgCl_2.6H_2O$, and 1.2 mM NaH_2PO_4 equilibrated with 5% CO_2 in 95% O_2 at room temperature and transferred to a chamber containing the same aCSF, kept at a temperature between 33 and 35°C. Cells were recorded under visual control (Nikon FN1 microscope – Scientifica Patch Star manipulators) with an Multiclamp 700B amplifier and Digidata 1322 interface (Axon Instruments). Healthy-looking (based on infrared images) cells were selected. Although we do not know how cells containing neurofibrillary tangles would appear visually under the microscope, there is a possibility that the sampled cells may not be pathological, i.e., containing neurofibrillary tangles. PSCs were sampled at 10 kHz and low-pass filtered at 2 kHz. Currents were recorded using an internal pipette solution of 120.0 mM CsGluconate, 20.0 mM CsCl, 1.1 mM EGTA, 0.1 mM $CaCl_2.2H_2O$, 10.0 mM HEPES, 2.0 mM Mg-ATP, 0.4 mM Na-GTP, 2 mM $MgCl_2.6H_2O$, $CsOH.H_2O$ to adjust pH (pH 7.3, 280 mOsM). Inhibitory Post-Synaptic Currents (IPSCs) were recorded at a holding potential of +10 mV, the reversal potential for glutamatergic events; Excitatory PSCs (EPSCs) were recorded at −60 mV, the reversal potential for GABAergic events (Cossart et al., 2001). We also measured miniature excitatory post-synaptic currents (mEPSCs) and miniature inhibitory post-synaptic currents (mIPSCs) in acute slices from the four groups at 8 and 12 months, after the addition of TTX (1 μM). Average resistance series (RS) in neurons from 8 months wild type, wild type caffeine, Tau water and Tau caffeine mice were 35.3 ± 3.6, 34.91 ± 2.6, 23.58 ± 2.8, and 20.70 ± 3.1 MΩ, respectively (*$P < 0.05$ Wild type vs. Tau water and Tau caffeine, $P < 0.01$ Wild type caffeine vs. Tau caffeine*); in neurons from 12 months Wild type, Wild type caffeine, Tau water and Tau caffeine mice were 31.0 ± 2.9, 22.88 ± 3.0, 27.32 ± 3.6, and 24.34 ± 3.0 MΩ, respectively ($P > 0.05$). Although RS is in the range of that found in old control animals, we do not know why it is lower in Tau mice. A lower RS should improve the detection of small amplitude currents. Hence, the increase in frequency we find in Tau mice may be partly due to improved detection of synaptic events. We speculate that this would involve a minority of events, whilst the changes in frequency we describe are large. When the RS changed during the recording by more than 20%, the recording was terminated. Following break-in, the cells were allowed to dialyze and stabilize for 5 min. Cells were voltage clamped at −60 mV and recorded at that potential during 5 min. Then, the cells were voltage clamped at +10 mV, and after stabilization of the holding current, the cells were recorded during 10 min. The ACSF solution was then switched to one containing 1 μM of TTX. After 20 min of wash in recordings resumed first at +10 mV and then at −60 mV (5 min each). Recordings with a stable baseline were transferred into the Mini-Analysis software (Synaptosoft). The settings of the Mini-Analysis Program for the detection of synaptic events were set to conservative values: threshold amplitude (8 pA for s/mEPSCs, 10 pA for s/mIPSCs); area threshold (>10 pA.ms); rise time (<10 ms); and average baseline before onset (> 10 ms). These settings led to the detection of numerous false positives, including electrical artifacts, double detection of the same event, and multiple synaptic events occurring without a return to baseline. In the latter case, the events were kept for the inter-event interval distribution, but they were not used for amplitude analysis. All detected events were checked manually and false positives removed. All inter-interval and amplitude values in all conditions can be found in **Table 1**. All recorded cells were filled with biocytin for *post hoc* morphological identification, which was performed according to a previously described protocol (Esclapez et al., 1999). We did not notice obvious morphological differences between the different conditions. The two-sample Kolmogorov–Smirnov test was used for statistical analyses between groups. The level of significance was set at $P < 0.05$.

Barnes Maze

Barnes maze was used to compare cognitive deficits in learning and memory of 8- and 12-months Tau caffeine (n = 13 and 10), Tau water (n = 11 and 4) mice to the Wild type caffeine (n = 13 and 10) and Wild type (n = 11 and 8) groups. The maze was made from a circular, 13-mm thick, white PVC slab with a diameter of 1.2 m. Twenty holes with a diameter of 44.4 mm were made on the perimeter at a distance of 25.4 mm from the edge. This circular platform was then mounted on top of a rotating stool, 0.89 m above the ground and balanced. The escape cage was made by using a mouse cage and assembling a platform and ramp 25.4 mm below the surface of the maze. The maze was rotated clockwise after every three mice to avoid intra-maze odor or visual cues. All sessions were recorded using COP Security Monochrome CCD Camera (Model 15-CC20) and MyTV/x software (Eskape Labs).

The animals interacted with the Barnes maze in three phases: habituation (1 day), training (3 days), probes (2 days: 1 day after 1 week from the last trial day = Probe 1; 1 day after 2 weeks from the last trial day = Probe 2). Before starting each experiment, mice were acclimated to the testing room for 1 h. Then all mice (n = 2–4) from one cage were placed in individual holding cages where they remained until the end of their testing sessions. On the habituation day, the mice were placed in the center of the maze underneath a clear 3,500-ml glass beaker for 30 s while white noise was played through a sound system. Then, the mice were guided slowly by moving the glass beaker, over 10–15 s to the target hole that leads to the escape cage. The mice were then given 3 min to independently enter through the target hole into the escape cage. If they did not enter on their own during that time, they were nudged with the beaker to enter. The mice were allowed to stay in the escape cage for 1 min before being returned to the holding cage. Once all animals had completed the 1-session habituation, they were all returned to their home cage. In the training phase, mice were placed inside an opaque cardboard cylinder, 25.4 cm tall and 17.8 cm in diameter, in the

TABLE 1 | Characteristics (inter-event intervals and amplitudes) of spontaneous and miniature glutamatergic and GABAergic currents recorded *in vitro* in CA1 pyramidal cells in 8 and 12 month-old Wild type and Tau mice exposed or not to caffeine during early life.

	Wild type	Wild type caffeine	Tau water	Tau caffeine
Inter-event interval (ms)				
sEPSC 8 months	467.3 ± 48.25	428.1 ± 39.06	365.1 ± 23.81	383.8 ± 35.10
sEPSC 12 months	261.3 ± 20.04	285.8 ± 16.09	110.3 ± 9.22	232.5 ± 18.21
sIPSC 8 months	336.3 ± 26.59	217.4 ± 18.65	172.7 ± 8.65	456.7 ± 31.08
sIPSC 12 months	217.8 ± 12.13	154.1 ± 7.61	125.4 ± 10.43	107.4 ± 5.22
mEPSC 8 months	1676.0 ± 108.70	1243.0 ± 93.76	1106.0 ± 65.78	898.2 ± 77.12
mEPSC 12 months	1155.0 ± 89.12	1147.0 ± 87.90	447.8 ± 66.59	1001.0 ± 94.47
mIPSC 8 months	536.9 ± 37.85	902.0 ± 54.82	419.8 ± 24.81	869.0 ± 50.88
mIPSC 12 months	923.4 ± 62.00	449.0 ± 32.53	383.6 ± 31.76	373.8 ± 23.57
Amplitude (pA)				
sEPSC 8 months	15.14 ± 0.38	13.39 ± 0.30	16.25 ± 0.29	19.89 ± 0.84
sEPSC 12 months	19.64 ± 0.56	15.23 ± 0.37	19.25 ± 0.52	20.88 ± 0.72
sIPSC 8 months	24.58 ± 0.76	21.07 ± 0.42	25.95 ± 0.86	29.39 ± 0.95
sIPSC 12 months	20.77 ± 0.51	21.87 ± 0.44	23.43 ± 0.67	22.94 ± 0.57
mEPSC 8 months	11.59 ± 0.38	12.47 ± 0.28	16.98 ± 0.53	16.46 ± 0.76
mEPSC 12 months	17.05 ± 0.44	13.75 ± 0.30	17.17 ± 0.40	14.37 ± 0.26
mIPSC 8 months	19.67 ± 0.45	17.14 ± 0.35	20.26 ± 0.42	27.02 ± 0.71
mIPSC 12 months	17.25 ± 0.29	20.65 ± 0.67	19.22 ± 0.43	17.93 ± 0.36

center of the Barnes maze for 15 s. At the end of the holding period, a buzzer was turned on, the cylinder was removed, and the mice were allowed to explore the maze for 2 min. If a mouse found the target hole and entered the escape cage during that time, the end-point of the trial, it was allowed to stay in the escape cage for 1 min before being returned to the holding cage. If it did not find the target hole, the mouse was guided to the escape hole using the glass beaker. If a mouse still did not enter the escape cage after 1 min of nudging, it was picked up and manually put on the platform in the escape cage. This process typically took 5–7 min per mouse and was done with four mice at a time, providing a 20–30 min inter-trial interval. The total number of trials used was three trials on training days 1, 2, and 3. During the training phase, measures of primary latency were recorded. Primary latency was defined as the time to identify the target hole the first time, as mice did not always enter the hole upon first identifying it. On the probe day, 7 and 14 days after the last training day, the escape cage was removed. Each mouse was given 2 min to explore the maze. During the probe phase, measures of time spent per quadrant and holes searched (HS) per quadrant were recorded. HS was defined as nose pokes and head deflections over any hole. Primary HS was defined as the HS before identifying the target hole for the first time. For these analyses, the maze was divided into quadrants consisting of 5 holes with the target hole (goal) in the center of the target quadrant (goal zone). The other quadrants going clockwise from the goal zone were labeled: right, opposite, and left zone; all the data collected out of the goal zone are expressed as "other zone." Data are shown as means ± standard error of the mean (SEM). Two-way repeated measures ANOVA followed by Bonferroni *post hoc* analysis were used for probe day and training trials data, respectively. The level of significance was set at $P < 0.01$.

Biochemical and Molecular Evaluations

Animals were sacrificed at 6 months of age by cervical dislocation, brains harvested, left and right hippocampi dissected out using a coronal acrylic slicer (Delta Microscopies) at 4°C and stored at −80°C for biochemical and mRNA analyses. For Tau biochemistry, tissue was homogenized in 200 µl Tris buffer (pH 7.4) containing 10% sucrose and protease inhibitors (Complete; Roche Diagnostics), sonicated and kept at −80°C until use. Protein amounts were quantified using the BCA assay (Pierce), and samples diluted with lithium dodecyl sulfate buffer (2) supplemented with reducing agents (Invitrogen) and then separated on 4–12% NuPAGE Novex gels (Invitrogen). Proteins were transferred to nitrocellulose membranes, which were then saturated with 5% non-fat dried milk or 5% bovine serum albumin in TNT (Tris 15 mM pH 8, NaCl 140 mM, 0.05% Tween) and incubated at 4°C for 24 h with the primary antibodies. All primary antibodies used are described in **Table 2**. Appropriate HRP-conjugated secondary antibodies (anti-mouse PI-2000 et anti-rabbit PI-1000, Vector Laboratories) were incubated for 1 h at room temperature and signals were visualized using chemoluminescence kits (ECL, Amersham Bioscience) and a LAS4000 imaging system (Fujifilm). Results were normalized to actin or GAPDH and quantifications were performed using ImageJ software (Scion Software).

Neuroinflammatory markers were studied using quantitative PCR. Total RNA was extracted from hippocampi and purified using the RNeasyLipid Tissue Mini Kit (Qiagen). One microgram of total RNA was reverse-transcribed using the HighCapacity cDNA reverse transcription kit (Applied Biosystems). Quantitative real-time polymerase chain reaction (qPCR) analysis was performed on an Applied Biosystems™ StepOnePlus™ Real-Time PCR Systems using Power SYBRGreen PCR Master Mix (Applied Biosystems)

or TaqMan™ Gene Expression Master Mix (Applied Biosystems™). The thermal cycler conditions were as follows: 95°C for 10 min, then 40 cycles at 95°C for 15 s and 60°C for 25 s for SYBRGreen; and 95°C for 10 min, then 40 cycles at 95°C for 15 s and 60°C for 1 min for Taqman. Sequences of primers used in this study are given in **Table 3**. Cyclophilin A was used as a reference housekeeping gene for normalization. Amplifications were carried out in duplicate and the relative expression of target genes was determined by the $\Delta\Delta$Ct method.

RESULTS

Increased Synaptic Drive in Tau Water as Compared to Wild Type Control Mice at 8 Months

The excitatory and inhibitory synaptic drives received by CA1 pyramidal cells have not been characterized in Tau transgenic mice. We first characterized them in comparison with littermate wild type mice. We found that the frequency of sEPSCs and sIPSCs was increased by 34% (P = 0.0285) and 98% (P = 0.0135), respectively (**Figures 1A,E**), in Tau water (n = 9 cells, 9 slices, from 5 mice) as compared to wild type controls (n = 8 cells, 8 slices, from 5 mice). The distribution of sEPSC amplitudes was not different but sIPSCs showed a slight (5%) but significant (P = 0.0464) increase in amplitude in Tau mice as compared to wild type controls (**Figures 1B,F**). All inter-interval and amplitude values in all conditions are listed in **Table 1**. Since spontaneous currents are a mixture of action potential-dependent and independent (miniature) events, we measured miniature currents in the same cells in the presence of TTX (1 μM) to block action potentials. We found that the frequency of miniature EPSCs (mEPSCs) and IPSCs (mIPSCs) was increased by 68% (P = 0.0270) and 44% (P = 0.0263), respectively (**Figures 2A,E**), in Tau water (n = 9 cells, 9 slices, from 5 mice) as compared to wild type controls (n = 8 cells, 8 slices, from 5 mice). Although the amplitude of mIPSCs was not modified in Tau mice, the amplitude of mEPSCs was increased by 47% (P = 0.0253) as compared to Wild type controls (**Figures 2B,F**). The overall synaptic drive received by a neuron is a combination of action potential dependent and independent EPSCs and IPSCs. In order to assess their respective contributions, we calculated the frequency ratio for miniature/spontaneous and EPSC/IPSC events in each recorded cell. In Wild type controls the contribution of miniature events was around 20% and the contribution of EPSCs vs. IPSCs was also around 20%, ratios that were not statistically different in Tau water (**Figures 3A–D**). At 8 months, the data suggests that there is a general increase in the overall synaptic drive received by CA1 pyramidal cells in Tau mice, whilst both miniature/spontaneous and EPSC/IPSC ratios are not modified (**Figures 3E–H**).

Effects of Early Life Caffeine Exposure in Wild Type Mice Evaluated at 8 Months

We found that the frequency of sEPSCs and sIPSCs was increased by 17% (P = 0.0385) and 54% (P = 0.0144), respectively (**Figures 1A,E**), in Wild type caffeine (n = 8 cells, 8 slices, from 5 mice) as compared to wild type controls (n = 8 cells, 8 slices, from 5 mice). Caffeine exposure did not affect the amplitude of sEPSCs but decreased the amplitude of sIPSCs by 14% (P = 0.0262) (**Figures 1B,F**). The frequency of mEPSCs was increased by 42% (P = 0.0157) whilst the frequency of mIPSCs was decreased by

TABLE 2 | List of primary antibodies used for biochemical detection of Tau proteins on Western blot.

Name	Abbreviation	Epitope	Tissue	Type	Origin	Provider	WB
Anti-Phospho-Tau (AT270)	pT181	pT181	M	Mono	Mouse	Invitrogen #MN1050	1/1 000
Anti-Tau 1, clone PC1C6	Tau1	Non-phospho-S195, 198, 199, 202	M	Mono	Mouse	Millipore #MAB3420	1/10 000
Anti-Phospho-Tau (AT100)	pT212/S214	pT212/S214	M	Mono	Mouse	Invitrogen #MN1060	1/1 000
Anti-Phospho-Tau (Ser262)	pS262	pS262	M	Poly	Rabbit	Invitrogen #44-750G	1/1 000
Anti-Phospho-Tau (Ser396)	pS396	pS396	H/M	Poly	Rabbit	Invitrogen #44-752G	1/10 000
Anti-Phospho-Tau (Ser404)	pS404	pS404	M	Poly	Rabbit	Invitrogen #44-758G	1/10 000
Anti-total Tau (C-ter)	Cter	Cter last 15 aa of COOH terminus	M	Poly	Rabbit	Home-made	1/10 000
Anti-GAPDH	GAPDH	Mouse GAPDH FL1-335	H/M	Poly	Rabbit	Sigma-Aldrich #G9545	1/10 000

TABLE 3 | List of primers used for mRNA detection of neuroinflammatory markers by quantitative PCR.

Accession number	Forward primer	Reverse primer	Amplicon length
NM_011337.2	TGCCCTTGCTGTTCTTCTCT	GTGGAATCTTCCGGCTGTAG	112
NM_013652.2	GCCCTCTCTCTCCTCTTGCT	GAGGGTCAGAGCCCATTG	72
NM_013653.3	CTCACTGCAGCCGCCCTCTG	CCGAGCCATATGGTGAGGCAGG	51
NM_009853.1	GACCTACATCAGAGCCCGAGT	CGCCATGAATGTCCACTG	95
NM_001131020.1	CGCGAACAGGAAGAGCGCCA	GTGGCGGGCCATCTCCTCCT	104
NM_011905.3	GGGGCTTCACTTCTCTGCTT	AGCATCCTCTGCGATTTGACG	110
NM_013693.2	TGCCTATGTCTCAGCCTCTTC	GAGGCCATTTGGGAACTTCT	116
NM_008907.1	AGCATACAGGTCCTGGCATC	TTCACCTTCCCAAAGACCAC	126

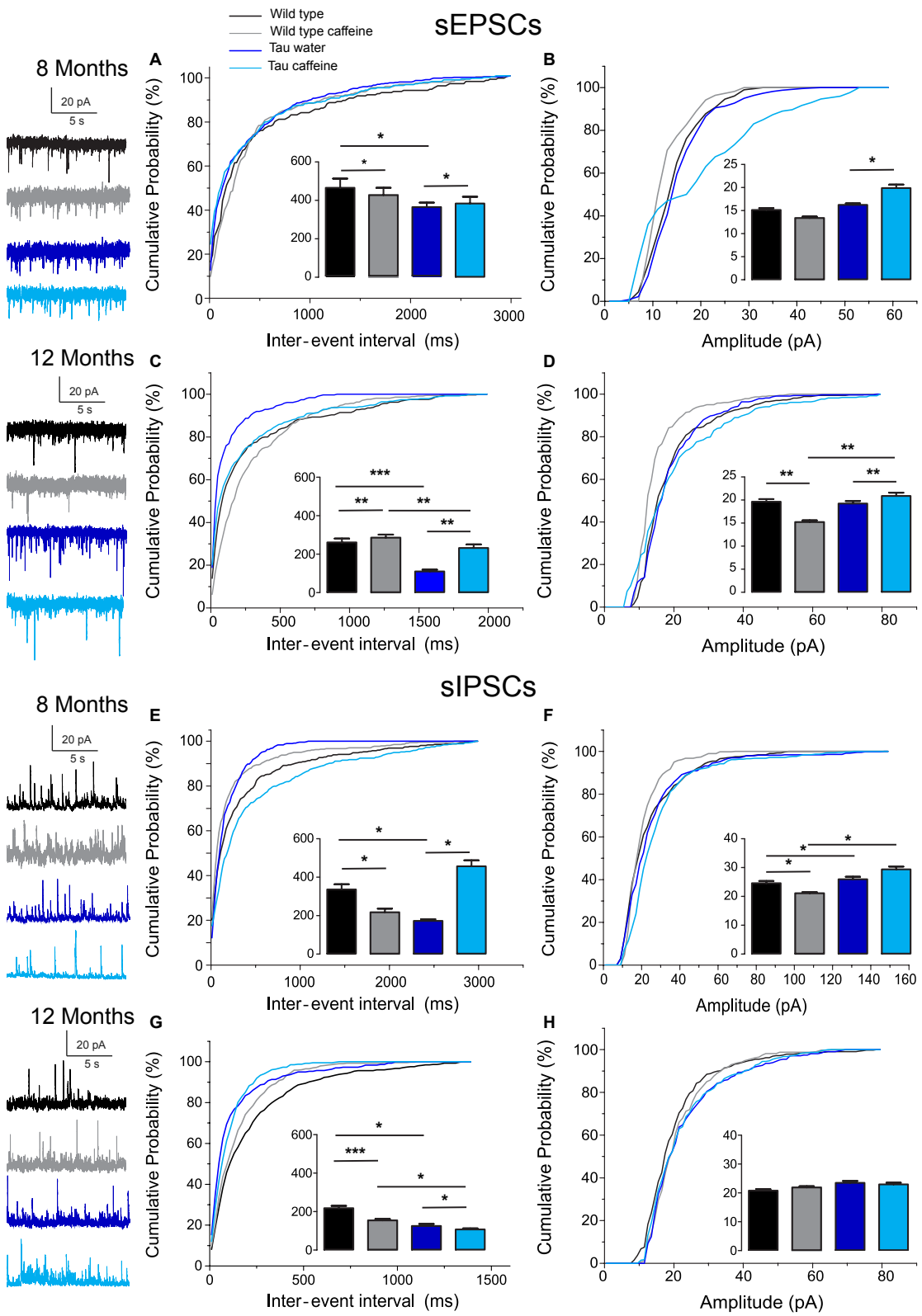

FIGURE 1 | Investigation of chronic caffeine exposure on spontaneous glutamatergic and GABAergic *in vitro* activities in 8 and 12 month-old Wild type and Tau mice. Representative traces of sEPSCs and sIPSCs recorded in CA1 hippocampal pyramidal cells of Wild type water (black), Wild type caffeine-treated (gray), Tau water (blue), and Tau caffeine-treated (light blue) mice are depicted on the left of the cumulative probability histograms [8 month-old sEPSCs: **(A,B)**; 12 month-old

(Continued)

FIGURE 1 | Continued
sEPSCs: **(C,D);** 8 month-old sIPSCs: **(E,F)**; 12 month-old sIPSCs: **(G,H)**]. Comparison between cumulative probability distributions was made using the Kolmogorov–Smirnov test (*$P < 0.05$; **$P < 0.01$; ***$P < 0.001$); bar graphs represent mean ± standard error. n = 8 cells, 8 slices, from 5, 8 month-old Wild type water mice vs. n = 8 cells, 8 slices, from 5, 8 month-old Wild type caffeine-treated mice; n = 8 cells, 8 slices, from 5, 8 month-old Wild type water mice vs. n = 9 cells, 9 slices, from 5, 8 month-old Tau water mice; n = 9 cells, 9 slices, from 5, 8 month-old Tau water mice vs. n = 9 cells, 9 slices, from 5, 8 month-old Tau caffeine-treated mice; n = 8 cells, 8 slices, from 5, 8 month-old Wild type caffeine-treated mice vs. n = 9 cells, 9 slices, from 5, 8 month-old Tau caffeine-treated mice; n = 8 cells, 8 slices, from 5, 12 month-old Wild type water mice vs. n = 8 cells, 8 slices, from 5, 12 month-old Wild type caffeine-treated mice; n = 8 cells, 8 slices, from 5, 12 month-old Wild type water mice vs. n = 7 cells, 7 slices, from 4, 12 month-old Tau water mice; n = 7 cells, 7 slices, from 4, 12 month-old Tau water mice vs. n = 9 cells, 9 slices, from 5, 12 month-old Tau caffeine-treated mice; n = 8 cells, 8 slices, from 5, 12 month-old Wild type caffeine-treated mice vs. n = 9 cells, 9 slices, from 5, 12 month-old Tau caffeine-treated mice.

41% (P = 0.0169) as compared to Wild type (**Figures 2A,E**). As for sEPSCs and sIPSCs, caffeine did not affect the amplitude of mEPSCs, but decreased mIPSC amplitude by 12.8% (P = 0.0216) as compared to Wild type (**Figures 2B,F**). Caffeine treatment did not affect the miniature/spontaneous and EPSC/IPSC ratios (**Figures 3A–D**). Thus, as reported in 3 months-old offspring of caffeine-exposed mice, there is an hyperactivity of GABAergic networks (Silva et al., 2013). However, we did not find hypoactivity of glutamatergic networks found in 3 months-old offspring (Silva et al., 2013), perhaps reflecting the time-dependent reorganization of hippocampal networks.

Effects of Early Life Caffeine Exposure in Tau Mice Evaluated at 8 Months

Tau mice exposed to caffeine during gestation and lactation (n = 9 cells, 9 slices, from 5 mice) showed a small decrease in sEPSC frequency by 10% (P = 0,0244) and a large decrease in sIPSC frequency by 62% (P = 0.0165) as compared to Tau water mice (**Figures 1A,E**). Therefore, although caffeine exposure resulted in increase of sIPSC frequency in wild type mice, it produced a decrease in Tau mice. Although caffeine exposure results in a decreased amplitude of sIPSCs in Wild type mice, the amplitude was not changed in Tau mice (**Figure 1F**). In contrast, the amplitude of sEPSCs was increased by 23% (P = 0.0408) in Tau caffeine mice as compared to Tau water mice (**Figure 1B**). As compared to the Tau water group, Tau mice exposed to caffeine during gestation and lactation showed a 38% (P = 0.0135) increase in mEPSC frequency and a decrease in mIPSCs frequency by 52% (P = 0.0256) (**Figures 2A,E**). In Tau caffeine, the amplitude of mEPSCs was not modified but the amplitude of mIPSCs was increased by 14% (P = 0.0285) as compared to Tau water mice (**Figures 2B,F**). Caffeine treatment did not affect the miniature/spontaneous and EPSC/IPSC ratios (**Figures 3A–D**).

Effects of Early Life Caffeine Exposure in Wild Type Mice Evaluated at 12 Months

Although early life exposure to caffeine resulted in a slight increase of sEPSC frequency at 8 months, it produced a decrease of sEPSC frequency by 19% (P = 0.0025) as compared to Wild type on water at 12 months (**Figure 1C**). The frequency of sIPSCs was increased by 59% ($P = 1.1151^{e-8}$) in Wild type caffeine mice, similarly to what we observed at 8 months. Caffeine treatment did not affect the amplitudes of sIPSCs but produced a decrease of sEPSC amplitude by 22% (P = 0.0026) (**Figures 1D,H**). Caffeine did not affect mEPSC frequency but increased mIPSC frequency by 106% ($P = 8.2161^{e-6}$) as compared to Wild type on water (**Figures 2C,G**), in contrast to that observed at 8 months. Caffeine exposure resulted in a decrease of mEPSC amplitude by 19% (P = 0.0391) but did not affect that of mIPSCs (**Figures 2D,H**). Therefore the most striking effect of early life exposure to caffeine in Wild type animals is the age-dependent large increase in GABAergic activity received by CA1 pyramidal cells.

Effects of Early Life Caffeine Exposure in Tau Mice Evaluated at 12 Months

In Tau caffeine mice (n = 9 cells, 9 slices, from 5 mice) we found a large decrease in sEPSC frequency by 53% (P = 0.0013) as compared to Tau on water mice (**Figure 1C**), in keeping with the effect of caffeine on sEPSC frequency described above in wild type mice exposed to caffeine. Although there was an increase in sEPSC at 8 and 12 months in Tau water mice, caffeine treatment prevented such increase. Although caffeine treatment results in a decreased sIPSC frequency at 8 months, we found an increase in sIPSC frequency by 17% (P = 0.0216) at 12 months as compared to Tau on water (**Figure 1G**). Caffeine exposure resulted in a slight increase of sEPSC amplitude by 9% (P = 0.0191) but did not change sIPSC amplitude as compared to Tau on water (**Figures 1C,G**). In Tau mice exposed to caffeine there was a large decrease in mEPSC frequency by 55% ($P = 4.99691^{e-50}$), while mIPSC frequency was not modified (**Figures 2D,H**). The amplitude of mEPSCs (but not that of mIPSCs) was decreased by 16% (P = 0.0391) as compared to Tau on water (**Figures 2D,H**). Thus, during aging, early exposure to caffeine exacerbates the increase in GABAergic drive received by CA1 pyramidal cells in Tau mice (**Figures 3E–H**).

Reorganization During Aging: Differences Between 8 Month- and 12 Month-Old Wild Type and Tau Mice on Water

Since our hypothesis is that early-life exposure to caffeine is accelerating the occurrence of phenotypic traits, we now compare the most striking modifications between 8 month- and 12 month-old animals. In both Wild type (n = 8 cells, 8 slices, from 5 mice) and Tau mice on water (n = 7 cells, 7 slices, from 4 mice) we found a large increase in sEPSC frequency by 87 and 231%, respectively, as well as in sIPSC frequency by 55 and 38%, respectively (**Figures 1A,C,E,G**). The amplitude of sEPSCs increased by 30 and 19%, respectively, in Wild type and Tau mice on water, while

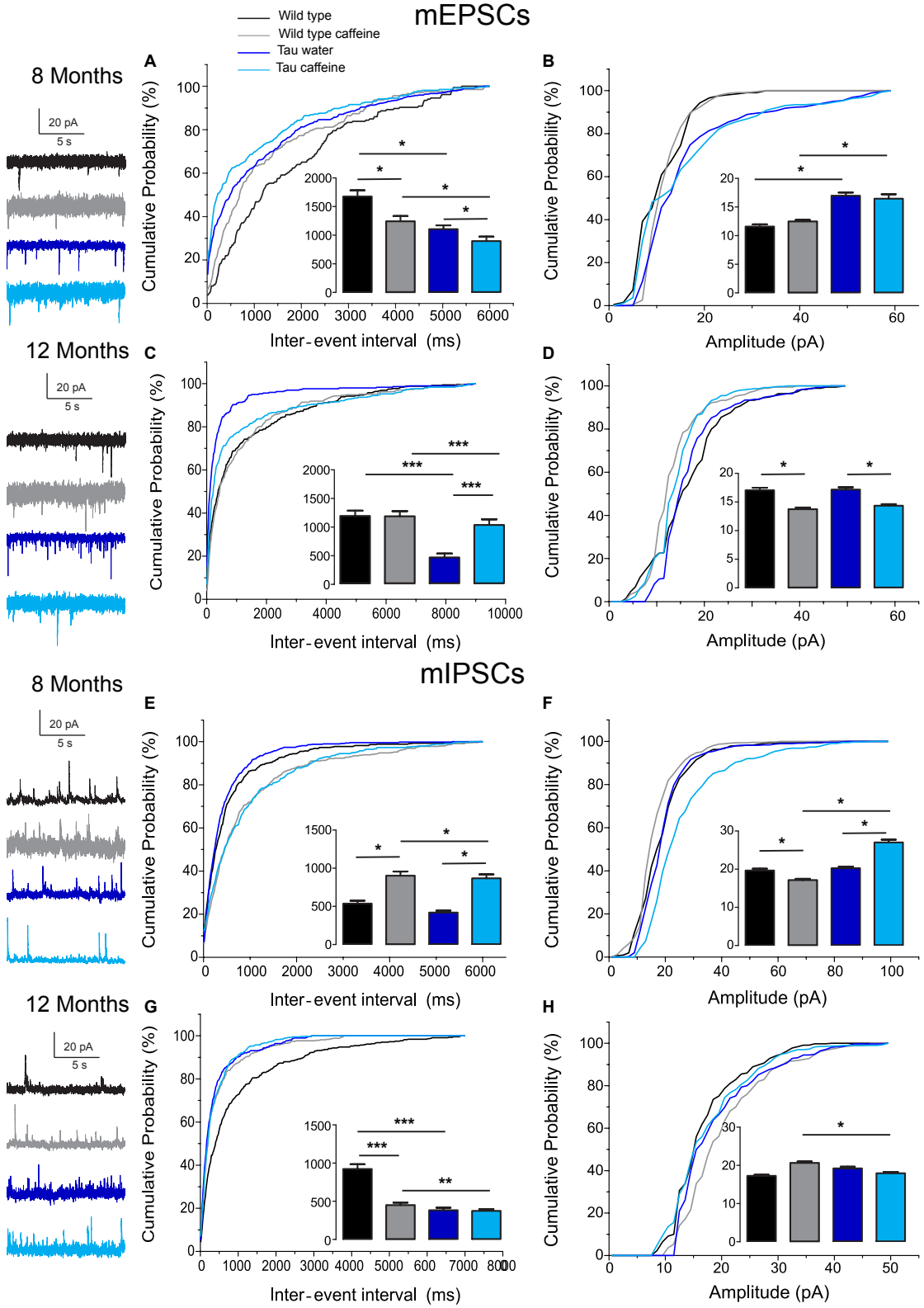

FIGURE 2 | Investigation of chronic caffeine exposure on miniature glutamatergic and GABAergic *in vitro* activities in 8 and 12 month-old Wild type and Tau mice. Representative traces of mEPSCs and mIPSCs recorded in CA1 hippocampal pyramidal cells of Wild type water (black), Wild type caffeine-treated (gray), Tau water (blue), and Tau caffeine-treated (light blue) mice are depicted on the left of the cumulative probability histograms [8 month-old mEPSCs: **(A,B)**; 12 month-old

(Continued)

FIGURE 2 | Continued
mEPSCs: **(C,D);** 8 month-old mIPSCs: **(E,F)**; 12 month-old mIPSCs: **(G,H)**]. Comparison between cumulative probability distributions was made using the Kolmogorov–Smirnov test (*$P < 0.05$; **$P < 0.01$; ***$P < 0.001$); bar graphs represent mean ± standard error. n = 8 cells, 8 slices, from 5, 8 month-old Wild type water mice vs. n = 8 cells, 8 slices, from 5, 8 month-old Wild type caffeine-treated mice; n = 8 cells, 8 slices, from 5, 8 month-old Wild type water mice vs. n = 9 cells, 9 slices, from 5, 8 month-old Tau water mice; n = 9 cells, 9 slices, from 5, 8 month-old Tau water mice vs. n = 9 cells, 9 slices, from 5, 8 month-old Tau caffeine-treated mice; n = 8 cells, 8 slices, from 5, 8 month-old Wild type caffeine-treated mice vs. n = 9 cells, 9 slices, from 5, 8 month-old Tau caffeine-treated mice; n = 8 cells, 8 slices, from 5, 12 month-old Wild type water mice vs. n = 8 cells, 8 slices, from 5, 12 month-old Wild type caffeine-treated mice; n = 8 cells, 8 slices, from 5, 12 month-old Wild type water mice vs. n = 7 cells, 7 slices, from 4, 12 month-old Tau water mice; n = 7 cells, 7 slices, from 4, 12 month-old Tau water mice vs. n = 9 cells, 9 slices, from 5, 12 month-old Tau caffeine-treated mice; n = 8 cells, 8 slices, from 5, 12 month-old Wild type caffeine-treated mice vs. n = 9 cells, 9 slices, from 5, 12 month-old Tau caffeine-treated mice.

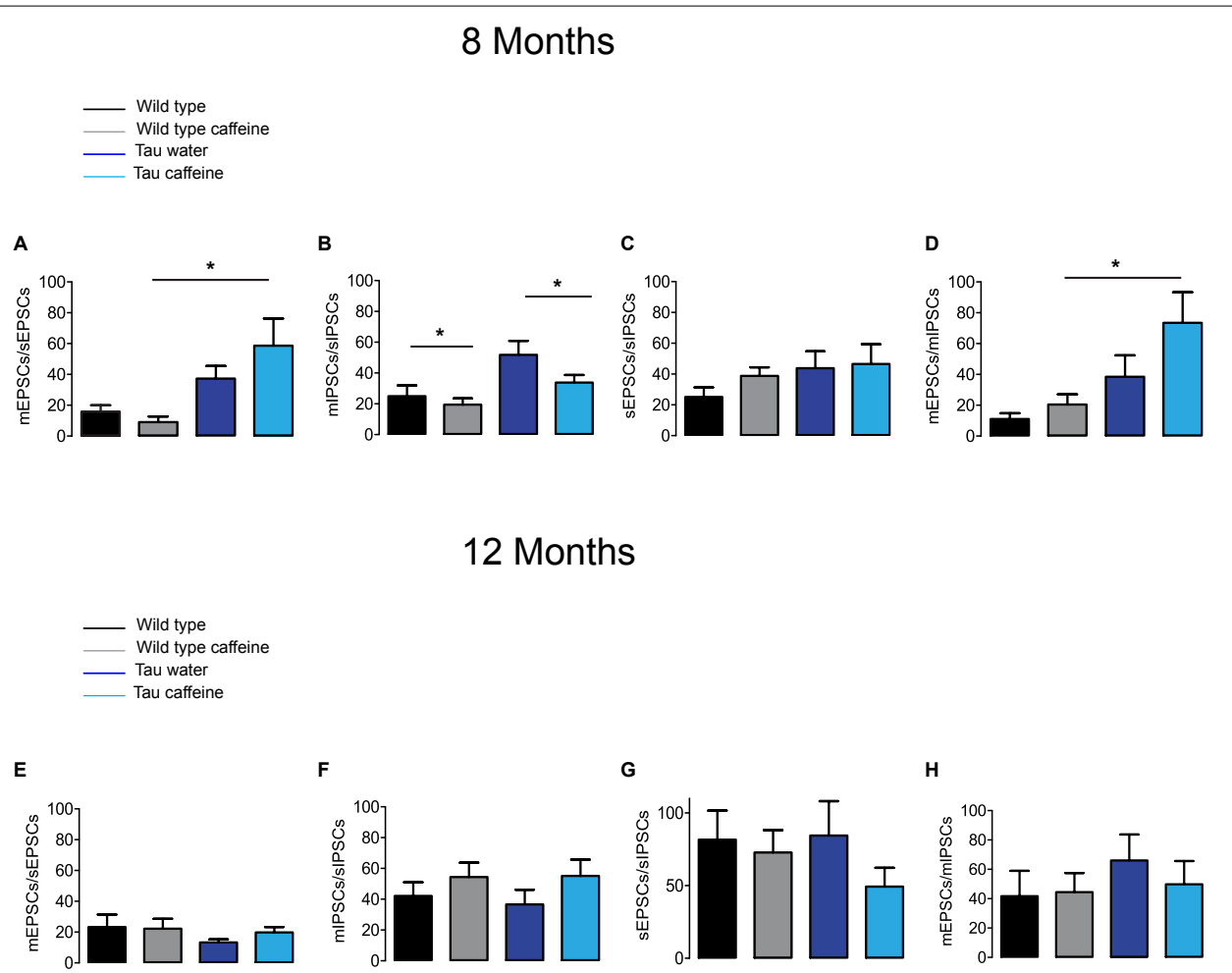

FIGURE 3 | Investigation of chronic caffeine exposure on miniature/spontaneous EPSC/IPSC ratios in 8 and 12 month-old mice. The ratios of the frequencies of mEPSCs to sEPSCs **(A,E)**, mIPSCs to sIPSCs **(B,F)**, sEPSCs to sIPSCs **(C,G)** and mEPSCs to mIPSCs **(D,H)** were analyzed for Wild type water (black), Wild type caffeine-treated (gray), Tau water (blue), and Tau caffeine-treated (light blue) 8 and 12 month-old mice. Bar graphs represent mean ± standard error; comparison between ratios was made using One way ANOVA Tukey–Kramer *post doc* test (*$P < 0.05$) n = 8 cells, 8 slices, from 5, 8 month-old Wild type water mice vs. n = 8 cells, 8 slices, from 5, 8 month-old Wild type caffeine-treated mice; n = 9 cells, 9 slices, from 5, 8 month-old Tau water mice vs. n = 9 cells, 9 slices, from 5, 8 month-old Tau caffeine-treated mice; n = 8 cells, 8 slices, from 5, 8 month-old Wild type caffeine-treated mice vs. n = 9 cells, 9 slices, from 5, 8 month-old Tau caffeine-treated mice; n = 8 cells, 8 slices, from 5, 12 month-old Wild type water mice vs. n = 8 cells, 8 slices, from 5, 12 month-old Wild type caffeine-treated mice; n = 9 cells, 9 slices, from 5, 12 month-old Tau water mice vs. n = 9 cells, 9 slices, from 5, 12 month-old Tau caffeine-treated mice; n = 8 cells, 8 slices, from 5, 12 month-old Wild type caffeine-treated mice vs. n = 9 cells, 9 slices, from 5, 12 month-old Tau caffeine-treated mice.

for sIPSCs we found a decrease by 20 and 26%, respectively (**Figures 1B,D,F,H**). The frequency of mEPSCs also increased at 8 months in both strains (81 and 72% respectively), but the frequency of mIPSCs decreased (42%) in Wild type whilst it increased (10%) in Tau mice (**Figures 2A,C,E,G**). The amplitude of mEPSCs increased by 47 and 1% in Wild type and Tau mice on water, respectively, while for mIPSCs it decreased by 13 and 5%, respectively (**Figures 2B,D,F,H**). During aging, at least for the two

time points considered in this study, there is a global increase of glutamatergic and GABAergic activity received in CA1 pyramidal cells. Interestingly, the fraction of action potential-dependent events is largely increased in 12 month-old wild type as compared to 8 months (since the contribution of mIPSCs is decreased).

Effects of Early-Life Exposure to Caffeine on Learning and Memory Performance

Hippocampal dependent memory was assessed using the Barnes maze test (Koopmans et al., 2003) in 8 month-old mice (n = 11 wild type water, 13 wild type caffeine-treated, 11 TAU water, 13 TAU caffeine-treated mice). Training was performed for 3 days (D1, D2, D3), with three trials (T1, T2, T3) per day. We found the typical learning curve in wild type mice on water as assessed by the latency to the target (**Figure 4G**). The learning curve was similar in Wild type caffeine mice, while a delay in learning was found in both Tau groups (treated or not with caffeine) with a significant difference at D1T2 and D2T1 between Wild Type and Tau mice (**Figure 4G**). No difference was found from D2T2. Thus, caffeine exposure by itself does not affect the learning curve, but the underlying Tau pathology does.

One week after the learning part, we performed a probe test (P1) and a second one, 1 week later (P2) to assess memory retention. The caffeine exposed Tau group showed a significant decrease in the number of holes searched in the GOAL area during P2 as compared to P1 (56%, P = 0.0383), which shows an impairment to remember the general location of the escape hole in Tau mice exposed to caffeine (**Figure 4A**). The latency to the escape hole was increased by 181% (P = 0.0003) in Tau caffeine mice at P2 (**Figure 4H**). The same trends were found in Wild type animals exposed to caffeine but it was not significant. Thus, caffeine exposed Tau mice show memory deficits. No difference was found in the number of holes searched in the GOAL ZONE and in the OTHER ZONE (**Figures 4B,C**), nor in the time in the quadrants in the GOAL, GOAL ZONE and OTHER ZONE (**Figures 4D–F**) for the 4 groups at P1 and P2.

We performed the same study in another series of 12 month-old animals (n = 8 wild type water, 10 wild type caffeine-treated, 4 TAU water, 10 TAU caffeine-treated mice). Surprisingly, in contrast to 8 month-old animals, the learning curves were similar in the four groups, although the TAU caffeine group showed a tendency for slower learning (**Figure 4O**). Both Tau water and Tau caffeine groups showed a decrease in the number of holes searched in the GOAL area at P2, by 45 and 36% respectively, but the decrease was not significant (**Figure 4I**). However, the latency at P2 showed an increase by 877.5% (P = 0.0122) and 249.9% (P = 0.0012) for Tau water and Tau caffeine, respectively (**Figure 4P**), confirming an impairment in memory retention for Tau mice exposed to an early caffeine consumption and the appearance of the same deficit in the Tau control group. This suggests that caffeine exposure in Tau mice enabled an earlier expression of memory deficits at 8 months. No difference was found in the number of holes searched in the GOAL ZONE and in the OTHER ZONE (**Figures 4J,K**), nor in the time in the quadrants in the GOAL, GOAL ZONE and OTHER ZONE (**Figures 4L–N**) for the 4 groups at P1 and P2.

Impact of Early Life Caffeine Consumption on Hippocampal Tau Phosphorylation and Related Neuroinflammatory Markers

THY-Tau22 mice exhibit progressive memory impairments in parallel with the development of hippocampal Tau hyperphosphorylation and neuroinflammation (Van der Jeugd et al., 2013; Laurent et al., 2017). At 6–8 months of age, Tau pathology and neuroinflammation are ongoing in the hippocampus of THY-Tau22 mice. The potentiation of memory deficits by early-life caffeine in Tau mice opened the possibility that Tau pathology itself or neuroinflammation might have been advanced, therefore we performed biochemical and qPCR experiments in an additional group of animals at the age of 6 months. Using sodium dodecyl sulfate-polyacrylamide gel electrophoresis, we evaluated Tau phosphorylation in both Tau experimental groups using antibodies raised against several Tau phosphoepitopes. None of the epitope studied was modified by early life exposure to caffeine (**Figure 5A**). As caffeine modulates neuroinflammation (Brothers et al., 2010; Laurent et al., 2014), we checked several neuroinflammatory markers previously described to be early or lately upregulated in the hippocampus of THY-Tau22 animals (Laurent et al., 2017). In general, in accordance with the absence of impact on Tau phosphorylation, early caffeine treatment did not modulate any of the neuroinflammatory markers studied. We could only evidence a slight reduction of the expression of the microglia CD68 markers in TAU mice treated with caffeine vs. Tau water animals (**Figure 5B**).

DISCUSSION

Psychoactive drugs ingested during pregnancy can have widespread deleterious effects in the fetus, in particular in the brain (Salisbury et al., 2009). Substances of abuse, such as alcohol, cannabis and cocaine, can directly alter the construction of the brain, in particular GABAergic circuits (Miller, 1986; Berghuis et al., 2007; Navi-Goffer and Mulder, 2009; Thompson et al., 2009). As the most widely consumed psychoactive drug, including during pregnancy, caffeine can also have body-wide effects (Temple et al., 2017). Previous works in control GIN (GFP-expressing Inhibitory Neurons) mice have shown that caffeine slows down the migration of GABA neurons resulting in a delayed insertion in the circuitry, both in the hippocampus and the cortex during the first postnatal week (Silva et al., 2013; Fazeli et al., 2017). Such alterations may have a direct impact on hippocampal network activity and performance during development (Salesse et al., 2011). Indeed, they are associated with enhanced sensitivity to epilepsy, hyperactivity *in vivo* and cognitive deficits later in life in offspring (Silva et al., 2013; Fazeli et al., 2017). Based on these studies, we hypothesized that the modifications produced by early life exposure to caffeine (acting as a first hit) would leave a long-term trace in the circuits, rendering them more vulnerable to a second hit, in line with the diathesis-disease theory (Bernard, 2016).

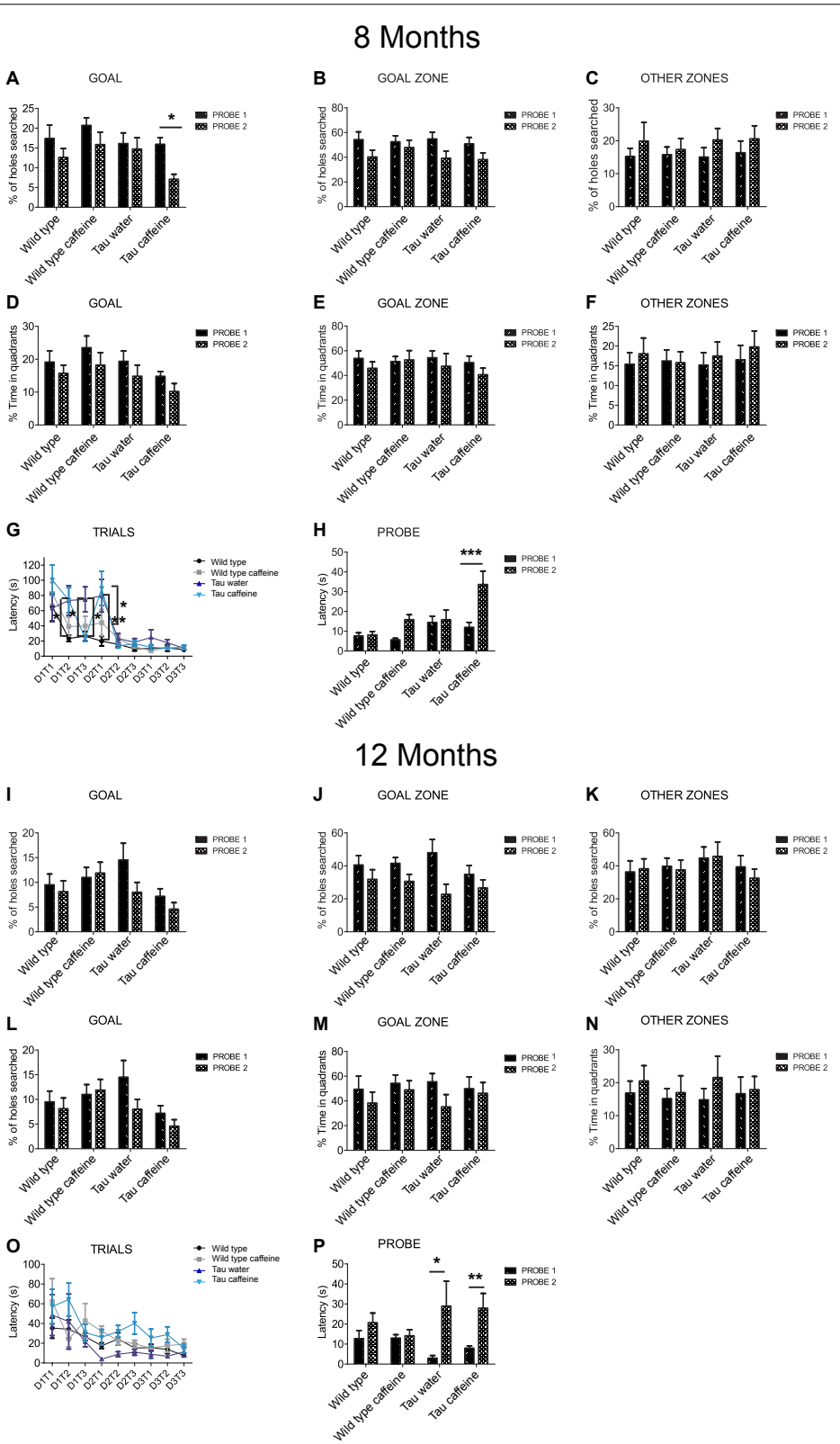

FIGURE 4 | Investigation of early-life exposure to caffeine on learning and memory performance. Barnes maze test was performed in 8 **(A–G)** and 12 **(I–O)** month-old mice. Training was performed for 3 days (D1, D2, D3), with three trials (T1, T2, T3) per day. For 8 and 12 month-old mice, the% of holes searched in

(Continued)

FIGURE 4 | Continued
GOAL **(A,I)**, GOAL ZONE **(B,J)** and OTHER ZONES **(C,K)**, the% time in quadrants **(D,L)**, GOAL ZONE **(E,M)** and OTHER ZONES **(F,N)** and the latency **(G,O)** were analyzed. To assess memory retention 1 week after the learning part, a probe test (P1) was performed and a second one, 1 week later (P2) on 8 and 12 month-old mice **(H,P)**. Two way ANOVA followed by Bonferroni *post hoc* test (*$P < 0.05$; **$P < 0.01$; ***$P < 0.001$). $n = 11$ Wild type water 8 month-old mice vs. 11 Tau water 8 month-old mice at D1T2; $n = 11$ Wild type water 8 month-old mice vs. 11 Tau water 8 month-old mice at D2T1; $n = 11$ Tau water 8 month-old mice vs. 11 Tau caffeine-treated 8 month-old mice at D1T3; $n = 11$ Tau water 8 month-old mice vs. 11 Tau caffeine-treated 8 month-old mice at D2T1; $n = 13$ Tau caffeine-treated 8 month-old mice at P1 vs. $n = 13$ Tau caffeine-treated 8 month-old mice at P2; $n = 4$ Tau water 12 month-old mice at P1 vs. $n = 4$ Tau water 12 month-old mice at P2; $n = 10$ Tau caffeine-treated 12 month-old mice at P1 vs. $n = 10$ Tau caffeine-treated 12 month-old mice at P2.

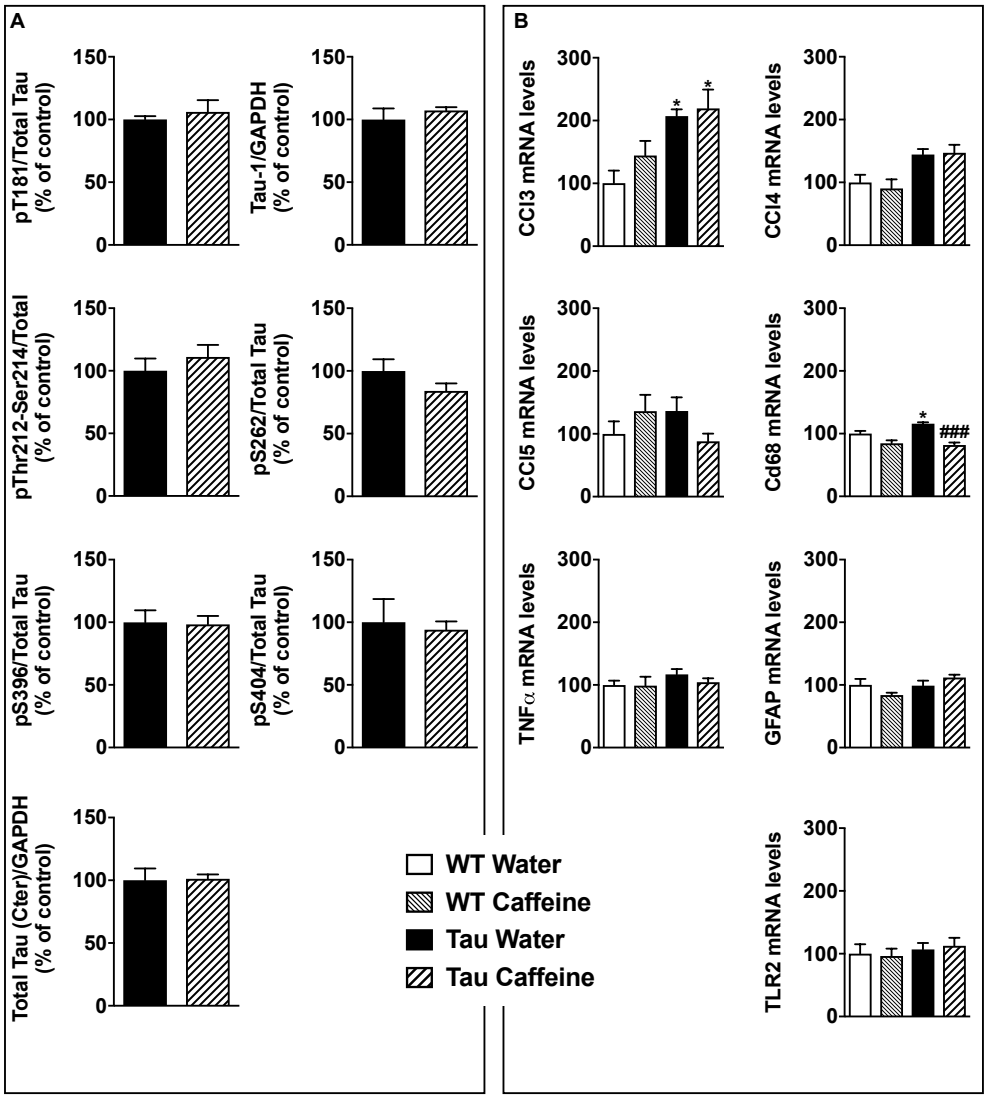

FIGURE 5 | Investigation of early-life exposure to caffeine on hippocampal Tau phosphorylation and associated neuroinflammatory markers. **(A)** Western blot analysis of tau phosphorylation in water or caffeine exposed THY-Tau22 offsprings using antibodies targeting physiological (pThr181, Tau-1, pSer262, pSer396, pSer404) and pathologic (pThr212/Ser214) Tau epitopes. Quantifications were performed over total tau levels (Cter). Total tau levels were quantified versus GAPDH, used as loading control ($n = 7$/group). **(B)** qPCR analysis of hippocampal neuroinflammatory markers associated with Tau pathology in the THY-Tau22 model ($n = 6$–10 per group).

This theory has been validated in the context of stress-induced vulnerability to epilepsy, depression and cognitive deficits, with the demonstration that social defeat (first hit) induces a state of vulnerability in some rats; a second hit being necessary to trigger a phenotype in the vulnerable population (Blugeot et al., 2011; Becker et al., 2015, 2019; Bouvier et al., 2016). If early-life exposure to caffeine constitutes a first hit and induces a state of vulnerability to a tauopathy, we reasoned that Tau mutant offspring exposed to caffeine would express phenotypic traits earlier than Tau mutants on water, in particular the cognitive

deficits and biochemical alterations known to occur in this mouse model. Since we wanted to bridge behavioral and molecular levels, we looked at the circuit level, focusing on the CA1 region, which is characterized by strong alterations in the GABAergic and glutamatergic circuits in caffeine exposed WT mice (Silva et al., 2013; Fazeli et al., 2017). Our ultimate goal was to be able to provide a coherent picture, linking all levels of analysis. However, the three levels of analysis do not provide a coherent picture.

The most salient feature of the results is the occurrence of deficits in spatial memory and learning already at 8 months in caffeine exposed Tau mice. These deficits occurred at 12 months in water exposed Tau mice and were still present at that age in caffeine Tau mice. In the present work, we used the Barnes maze, which is a terrestrial version of the Morris water maze and which is less stressful to mice than the Morris water maze (Harrison et al., 2009). We did not use other tests (such as anxiety and novel object recognition) to prevent interference when using different behavioral tests in succession. Interestingly, caffeine treatment did not alter spatial memory as assessed with the Barnes maze in Wild type mice, whilst caffeine-treated WT mice showed deficits in the object-location memory task (Silva et al., 2013). This suggests that specific types of memories are affected. The Barnes maze test is particularly useful in our case as WT mice exposed to caffeine do not display deficits, which would have added an independent variable, rendering the interpretation of the results more difficult. We can thus propose that early life exposure to caffeine accelerates the occurrence of the behavioral phenotype (with the caveat that we only looked at two time points). Humans have different genetic backgrounds and go through different life experiences, which will determine their sensitivity to the development of diseases, in particular neurological disorders (Bernard, 2016). The fact that caffeine exposure during early life produces an earlier occurrence of cognitive deficits in the Tau model used here may be relevant to a subset of human individuals. Said differently, exposure to caffeine during pregnancy may sensitize some but not all offsprings. Future studies will need to investigate other time points during aging, other cognitive tests and other models of AD. The experimental protocol is however highly time-consuming. We cannot rely on established aging colonies, since females need to be exposed to caffeine in the drinking water before mating until weaning. Then, it is necessary to wait until offspring reach the appropriate age.

Multiple mechanisms can be proposed to explain cognitive deficits in the Barnes maze (activation of the HPA axis, inflammation, metabolic defect, cell death, synaptopathy, channelopathy, epigenetic modifications, to name but a few). In THY-Tau22 mice, cognitive deficits have been associated with Tau pathological load and neuroinflammation (Van der Jeugd et al., 2013; Laurent et al., 2016, 2017, but see Burlot et al., 2015; Chatterjee et al., 2018). However, analysis of cardinal pTau and neuroinflammatory markers did not correlate with memory deficits in offspring exposed to caffeine. This result is in keeping with the proposal that cognitive decline may occur before the expression of molecular phenotypic traits in patients with AD (Jessen et al., 2014).

Since the hippocampus plays a key role is spatial memory, we were expecting circuit alterations in this region. To assess them, we measured glutamatergic and GABAergic synaptic currents received by hippocampal CA1 pyramidal cells. The results are very difficult to interpret because of the presence of three independent variables imposed by the experimental protocol. The first two independent variables are caffeine and Tau, both of which result in morpho-physiological alterations. The third independent variable is age, since we are considering two time points, 8 and 12 months. Yet, the *in vitro* approach provides interesting results in their complexity. Since our hypothesis was that caffeine exposure accelerates the occurrence of the phenotype, we start to discuss the age factor. In a given condition (WT mice or Tau mice), we were expecting to find whichever properties identified at 12 months in water treated animals at 8 months in caffeine exposed animals. In WT mice on water, we found an increase in both glutamatergic and GABAergic drives between 8 and 12 months. We can speculate that during normal aging, there is a gradual increase of the barrage of excitatory and inhibitory synaptic events received by CA1 pyramidal cells. More time points should be investigated to test this hypothesis. Several non-excluding mechanisms can explain such a rise, including an increase in the number of synapses, more active presynaptic cells, and a greater release probability from the presynaptic terminals. This result is consistent with that reported in the prefrontal cortex during aging (using later time points) for animals preserving their cognitive performances (Bories et al., 2013). Interestingly, in Tau mice on water, both glutamatergic and GABAergic drives were increased at 8 and 12 months as compared to their Wild type counterparts. In keeping with our results, most studies using Tau or Aß models report an increase in the excitatory drive as compared to Wild Type (Crimins et al., 2011; Dalby et al., 2014; Ovsepian et al., 2017), but see Rocher et al. (2008). Less data is available for the GABAergic drive. In the cortex of a different Tau model, there was no difference in sIPSC frequency at 9 months as compared to Wild Type (Crimins et al., 2011). The discrepancy with our results may stem from the type of mutant used and the brain region selected. Together, our results raise the intriguing possibility that the Tau mutation accelerates the aging process as assessed with the glutamatergic and GABAergic drives received by CA1 pyramidal cells.

Early life exposure to caffeine changed the apparent co-variance relationship between the two age and Tau independent variables. At 8 months, both GABAergic and glutamatergic drives were decreased in Tau caffeine mice as compared to Tau water mice. However, at 12 months, although the excitatory drive was decreased as compared to that measured in Tau water mice, the inhibitory drive was increased. Hence, contrary to our hypothesis, caffeine exposure does not accelerate the increase in synaptic barrage received by CA1 pyramidal cells that occurs in water exposed animal. We propose that the three variables tau-caffeine-age interact in non-linear fashion, thus constituting a complex system (the global behavior cannot be predicted from the observation of its independent components). This exemplifies the difficulty in interpreting the *in vitro* data. However, our data emphasize that caffeine exposure disrupts the effect of the pathogenic process characteristic of the Tau

phenotype in CA1 pyramidal cells. If there is a correlation between cognitive deficits and electrophysiological alterations at the circuit level, more parameters need to be measured (e.g., ion channels or metabolism). The possibility also exists that the CA1 region is not the most appropriate to establish such a correlation. *In vivo* recordings may also provide a different entry point into the underlying mechanisms, in particular measuring the properties of brain rhythms (theta, gamma) and sleep patterns.

CONCLUSION

We propose that early caffeine exposure produces physiological and cognitive alterations in a Tau pathological context, supporting our hypothesis that caffeine consumption during pregnancy may constitute a risk-factor for an earlier development of AD-related phenotypes. Future studies are needed using other mouse models, and, as importantly, to determine whether re-exposure to caffeine during adulthood is protective.

DATA AVAILABILITY STATEMENT

The datasets generated for this study are available on request to the corresponding author.

ETHICS STATEMENT

The animal study was reviewed and approved by Aix-Marseille University Animal Care and Use Committee.

AUTHOR CONTRIBUTIONS

SZ, EF, AG, and SC performed the experiments and analyzed the data. DB, ME, and CB designed the project. CB managed the project. All authors contributed to the writing of the manuscript.

FUNDING

This work was supported by a grant from Association France Alzheimer, Project No. AAP SM 2016/1567 and Aix-Marseille University. INSERM UMR-S1172 is supported by grants from Hauts-de-France (PARTEN-AIRR, COGNADORA), ANR (ADORATAU and ADOSTAsTRAU to DB; GRAND and TONIC to LB) and Programs d'Investissements d'Avenir LabEx (excellence laboratory) DISTALZ (Development of Innovative Strategies for a Transdisciplinary approach to ALZheimer's disease), Fondation pour la Recherche Médicale, France Alzheimer/Fondation de France, FHU VasCog research network (Lille, France), Fondation Vaincre Alzheimer, Fondation Plan Alzheimer, INSERM, CNRS, Université de Lille, Lille Métropole Communauté Urbaine, DN2M.

ACKNOWLEDGMENTS

We thank the Animal Facility (Lille, France) and Mélanie Besegher, Cyrille Degraeve, Caroline Declerck, Kim Letten, Yann Lepage, Benjamin Guerrin, Didier Montignies, Christian Meunier, Quentin Dekeyser, and Romain Dehaynin for animal care.

REFERENCES

Adén, U., Herlenius, E., Tang, L. Q., and Fredholm, B. B. (2000). Maternal caffeine intake has minor effects on adenosine receptor ontogeny in the rat brain. *Pediatr. Res.* 48, 177–183. doi: 10.1203/00006450-200008000-00010

American College of Obstetricians and Gynecologists, (2010). Moderate caffeine consumption during pregnancy. *Obstet. Gynecol.* 116(2 Pt 1), 467–468. doi: 10.1097/aog.0b013e3181eeb2a1

Barkovich, A. J., Guerrini, R., Kuzniecky, R. I., Jackson, G. D., and Dobyns, W. B. (2012). A developmental and genetic classification for malformations of cortical development: update 2012. *Brain* 135, 1348–1369. doi: 10.1093/brain/aws019

Becker, C., Bouvier, E., Ghestem, A., Siyoucef, S., Claverie, D., Camus, F., et al. (2015). Predicting and treating stress-induced vulnerability to epilepsy and depression. *Ann. Neurol.* 78, 128–136. doi: 10.1002/ana.24414

Becker, C., Mancic, A., Ghestem, A., Poillerat, V., Claverie, D., Bartolomei, F., et al. (2019). Antioxidant treatment after epileptogenesis onset prevents comorbidities in rats sensitized by a past stressful event. *Epilepsia* 60, 648–655. doi: 10.1111/epi.14692

Belarbi, K., Burnouf, S., Fernandez-Gomez, F. J., Laurent, C., Lestavel, S., Figeac, M., et al. (2011). Beneficial effects of exercise in a transgenic mouse model of Alzheimer's disease-like tau pathology. *Neurobiol. Dis* 42, 486–494. doi: 10.1016/j.nbd.2011.04.022

Berghuis, P., Rajnicek, A. M., Morozov, Y. M., Ross, R. A., Mulder, J., Urban, G. M., et al. (2007). Hardwiring the brain: endocannabinoids shape neuronal connectivity. *Science* 316, 1212–1216. doi: 10.1126/science.1137406

Bernard, C. (2016). The diathesis-epilepsy model: how past events impact the development of epilepsy and comorbidities. *Cold Spring Harb. Perspect. Med.* 6, a022418. doi: 10.1101/cshperspect.a022418

Björklund, O., Kahlstrom, J., Salmi, P., and Fredholm, B. B. (2008). Perinatal caffeine, acting on maternal adenosine A_1 receptors, causes long-lasting behavioral changes in mouse offspring. *PLoS One* 3:e3977. doi: 10.1371/journal.pone.0003977

Blugeot, A., Rivat, C., Bouvier, E., Molet, J., Mouchard, A., Zeau, B., et al. (2011). Vulnerability to depression: from brain neuroplasticity to identification of biomarkers. *J. Neurosci.* 31, 12889–12899. doi: 10.1523/JNEUROSCI.1309-11.2011

Borenstein, A. R., Copenhaver, C. I., and Mortimer, J. A. (2006). Early-life risk factors for Alzheimer disease. *Alzheimer Dis. Assoc. Disord.* 2006, 63–72. doi: 10.1097/01.wad.0000201854.62116.d7

Bories, C., Husson, Z., Guitton, M. J., and De Koninck, Y. (2013). Differential balance of prefrontal synaptic activity in successful versus unsuccessful cognitive aging. *J. Neurosci.* 33, 1344–1356. doi: 10.1523/JNEUROSCI.3258-12.2013

Bouvier, E., Brouillard, F., Molet, J., Claverie, D., Cabungcal, J. H., Cresto, N., et al. (2016). Nrf2-dependent persistent oxidative stress results in stress-induced vulnerability to depression. *Mol. Psychiatry.* 22:1795. doi: 10.1038/mp.2016.211

Braak, H., Thal, D. R., Ghebremedhin, E., and Del Tredici, K. (2011). Stages of the pathologic process in Alzheimer disease: age categories from 1 to 100 years. *J. Neuropathol. Exp. Neurol* 70, 960–969. doi: 10.1097/NEN.0b013e318232a379

Brothers, H. M., Marchalant, Y., and Wenk, G. L. (2010). Caffeine attenuates lipopolysaccharide-induced neuroinflammation. *Neurosci. Lett.* 480, 97–100. doi: 10.1016/j.neulet.2010.06.013

Burlot, M. A., Braudeau, J., Michaelsen-Preusse, K., Potier, B., Ayciriex, S., Varin, J., et al. (2015). Cholesterol 24-hydroxylase defect is implicated in memory impairments associated with Alzheimer-like Tau pathology. *Hum. Mol. Genet.* 24, 5965–5976. doi: 10.1093/hmg/ddv268

Chatterjee, S., Cassel, R., Schneider-Anthony, A., Merienne, K., Cosquer, B., Tzeplaeff, L., et al. (2018). Reinstating plasticity and memory in a tauopathy mouse model with an acetyltransferase activator. *EMBO Mol. Med.* 10:e8587. doi: 10.15252/emmm.201708587

Clancy, B., Darlington, R. B., and Finlay, B. L. (2001). Translating developmental time across mammalian species. *Neuroscience* 105, 7–17. doi: 10.1016/s0306-4522(01)00171-3

Cossart, R., Dinocourt, C., Hirsch, J. C., Merchan-Perez, A., De, F. J., Ben-Ari, Y., et al. (2001). Dendritic but not somatic GABAergic inhibition is decreased in experimental epilepsy. *Nat. Neurosci.* 4, 52–62. doi: 10.1038/82900

Crandall, J. E., Hackett, H. E., Tobet, S. A., Kosofsky, B. E., and Bhide, P. G. (2004). Cocaine exposure decreases GABA neuron migration from the ganglionic eminence to the cerebral cortex in embryonic mice. *Cereb. Cortex* 14, 665–675. doi: 10.1093/cercor/bhh027

Crimins, J. L., Rocher, A. B., Peters, A., Shultz, P., Lewis, J., and Luebke, J. I. (2011). Homeostatic responses by surviving cortical pyramidal cells in neurodegenerative tauopathy. *Acta Neuropathol.* 122, 551–564. doi: 10.1007/s00401-011-0877-0

Dalby, N. O., Volbracht, C., Helboe, L., Larsen, P. H., Jensen, H. S., Egebjerg, J., et al. (2014). Altered function of hippocampal CA1 pyramidal neurons in the rTg4510 mouse model of tauopathy. *J. Alzheimers. Dis.* 40, 429–442. doi: 10.3233/JAD-131358

Duyckaerts, C., Bennecib, M., Grignon, Y., Uchihara, T., He, Y., Piette, F., et al. (1997). Modeling the relation between neurofibrillary tangles and intellectual status. *Neurobiol. Aging* 18, 267–273. doi: 10.1016/s0197-4580(97)80306-5

Esclapez, M., Hirsch, J. C., Ben-Ari, Y., and Bernard, C. (1999). Newly formed excitatory pathways provide a substrate for hyperexcitability in experimental temporal lobe epilepsy. *J. Comp. Neurol* 408, 449–460. doi: 10.1002/(sici)1096-9861(19990614)408:4<449::aid-cne1>3.0.co;2-r

Fazeli, W., Zappettini, S., Marguet, S. L., Grendel, J., Esclapez, M., Bernard, C., et al. (2017). Early-life exposure to caffeine affects the construction and activity of cortical networks in mice. *Exp. Neurol.* 295, 88–103. doi: 10.1016/j.expneurol.2017.05.013

Galéra, C., Bernard, J. Y., van der Waerden, J., Bouvard, M.-P., Lioret, S., Forhan, A., et al. (2015). Prenatal caffeine exposure and child intelligence quotient at age 5.5 years: the Eden mother-child cohort. *Biol. Psychiatry* 80, 720–726. doi: 10.1016/j.biopsych.2015.08.034

Greenwood, D. C., Thatcher, N. J., Ye, J., Garrard, L., Keogh, G., King, L. G., et al. (2014). Caffeine intake during pregnancy and adverse birth outcomes: a systematic review and dose-response meta-analysis. *Eur. J. Epidemiol* 29, 725–734. doi: 10.1007/s10654-014-9944-x

Grober, E., Dickson, D., Sliwinski, M. J., Buschke, H., Katz, M., Crystal, H., et al. (1999). Memory and mental status correlates of modified Braak staging. *Neurobiol. Aging* 20, 573–579. doi: 10.1016/s0197-4580(99)00063-9

Guerrini, R., and Dobyns, W. B. (2014). Malformations of cortical development: clinical features and genetic causes. *Lancet Neurol.* 13, 710–726. doi: 10.1016/S1474-4422(14)70040-7

Harrison, F. E., Hosseini, A. H., and McDonald, M. P. (2009). Endogenous anxiety and stress responses in water maze and Barnes maze spatial memory tasks. *Behav. Brain Res.* 198, 247–251. doi: 10.1016/j.bbr.2008.10.015

Jessen, F., Amariglio, R. E., van Boxtel, M., Breteler, M., Ceccaldi, M., Chetelat, G., et al. (2014). A conceptual framework for research on subjective cognitive decline in preclinical Alzheimer's disease. *Alzheimers Dement* 10, 844–852. doi: 10.1016/j.jalz.2014.01.001

Koopmans, G., Blokland, A., van Nieuwenhuijzen, P., and Prickaerts, J. (2003). Assessment of spatial learning abilities of mice in a new circular maze. *Physiol. Behav.* 79, 683–693. doi: 10.1016/s0031-9384(03)00171-9

Laurent, C., Burnouf, S., Ferry, B., Batalha, V. L., Coelho, J. E., Baqi, Y., et al. (2016). A2A adenosine receptor deletion is protective in a mouse model of Tauopathy. *Mol. Psychiatry.* 21:97–107. doi: 10.1038/mp.2015.115

Laurent, C., Dorothee, G., Hunot, S., Martin, E., Delarasse, C., Buee, L., et al. (2017). [Tau and cognitive disorders: a role for T lymphocytes]. *Med. Sci.* 33, 817–819. doi: 10.1051/medsci/20173310002

Laurent, C., Eddarkaoui, S., Derisbourg, M., Leboucher, A., Demeyer, D., Carrier, S., et al. (2014). Beneficial effects of caffeine in a transgenic model of Alzheimer's disease-like tau pathology. *Neurobiol. Aging* 35, 2079–2090. doi: 10.1016/j.neurobiolaging.2014.03.027

Le Freche, H., Brouillette, J., Fernandez-Gomez, F. J., Patin, P., Caillierez, R., Zommer, N., et al. (2012). Tau phosphorylation and sevoflurane anesthesia: an association to postoperative cognitive impairment. *Anesthesiology* 116, 779–787. doi: 10.1097/ALN.0b013e31824be8c7

Leboucher, A., Laurent, C., Fernandez-Gomez, F. J., Burnouf, S., Troquier, L., Eddarkaoui, S., et al. (2013). Detrimental effects of diet-induced obesity onspathology are independent of insulin resistance instransgenic mice. *Diabetes Metab. Res. Rev.* 62, 1681–1688. doi: 10.2337/db12-0866

Lenroot, R. K., and Giedd, J. N. (2006). Brain development in children and adolescents: insights from anatomical magnetic resonance imaging. *Neurosci. Biobehav. Rev.* 30, 718–729. doi: 10.1016/j.neubiorev.2006.06.001

Mandel, H. G. (2002). Update on caffeine consumption, disposition and action. *Food Chem. Toxicol.* 40, 1231–1234. doi: 10.1016/s0278-6915(02)00093-5

Manouze, H., Ghestem, A., Poillerat, V., Bennis, M., Ba-M'hamed, S., Benoliel, J. J., et al. (2019). Effects of single cage housing on stress, cognitive, and seizure parameters in the rat and mouse pilocarpine models of epilepsy. *eNeuro* 6. doi: 10.1523/ENEURO.0179-18.2019

Marroun, H. E., Tiemeier, H., Franken, I. H. A., Jaddoe, V. W. V., Van Der Lugt, A., Verhulst, F. C., et al. (2015). Prenatal cannabis and tobacco exposure in relation to brain morphology: a prospective neuroimaging study in young children. *Biol. Psychiatry* 79, 1–9. doi: 10.1016/j.biopsych.2015.08.024

Masters, C. L., Simms, G., Weinman, N. A., Multhaup, G., McDonald, B. L., and Beyreuther, K. (1985). Amyloid plaque core protein in Alzheimer disease and down syndrome. *Proc. Natl. Acad. Sci. U.S.A* 82, 4245–4249. doi: 10.1073/pnas.82.12.4245

Miller, M. W. (1986). Effects of alcohol on the generation and migration of cerebral cortical neurons. *Science* 233, 1308–1311. doi: 10.1126/science.3749878

Navi-Goffer, S., and Mulder, J. (2009). The polarised life of the endocannabinoid system in CNS development. *Chembiochem* 10, 1591–1598. doi: 10.1002/cbic.200800827

Ovsepian, S. V., Blazquez-Llorca, L., Freitag, S. V., Rodrigues, E. F., and Herms, J. (2017). Ambient glutamate promotes paroxysmal hyperactivity in cortical pyramidal neurons at amyloid plaques via presynaptic mGluR1 receptors. *Cereb. Cortex* 27, 4733–4749. doi: 10.1093/cercor/bhw267

Papon, M. A., El Khoury, N. B., Marcouiller, F., Julien, C., Morin, F., Bretteville, A., et al. (2013). Deregulation of protein phosphatase 2A and hyperphosphorylation ofsprotein following onset of diabetes in NOD mice. *Diabetes Metab. Res. Rev.* 62, 609–617. doi: 10.2337/db12-0187

Reitz, C., Brayne, C., and Mayeux, R. (2011). Epidemiology of Alzheimer disease. *Nat. Rev. Neurol.* 7, 137–152. doi: 10.1038/nrneurol.2011.2

Rocher, A. B., Kinson, M. S., and Luebke, J. I. (2008). Significant structural but not physiological changes in cortical neurons of 12-month-old Tg2576 mice. *Neurobiol. Dis.* 32, 309–318. doi: 10.1016/j.nbd.2008.07.014

Romijn, H. J., Hofman, M. A., and Gramsbergen, A. (1991). At what age is the developing cerebral cortex of the rat comparable to that of the full-term newborn human baby? *Early Hum. Dev.* 26, 61–67. doi: 10.1016/0378-3782(91)90044-4

Salesse, C., Mueller, C. L., Chamberland, S., and Topolnik, L. (2011). Age-dependent remodelling of inhibitory synapses onto hippocampal CA1 oriens-lacunosum moleculare interneurons. *J. Physiol.* 589, 4885–4901. doi: 10.1113/jphysiol.2011.215244

Salisbury, A. L., Ponder, K. L., Padbury, J. F., and Lester, B. M. (2009). Fetal effects of psychoactive drugs. *Clin. Perinatol.* 36, 595–619. doi: 10.1016/j.clp.2009.06.002

Seifan, A., Schelke, M., Obeng-Aduasare, Y., and Isaacson, R. (2015). Early life epidemiology of Alzheimer's disease – a critical review. *Neuroepidemiology* 45, 237–254. doi: 10.1159/000439568

Sergeant, N., Bretteville, A., Hamdane, M., Caillet-Boudin, M. L., Grognet, P., Bombois, S., et al. (2008). Biochemistry of tau in Alzheimer's disease and related neurological disorders. *Expert Rev. Proteomics* 5, 207–224.

Silva, C. G., Metin, C., Fazeli, W., Machado, N. J., Darmopil, S., Launay, P.-S., et al. (2013). Adenosine receptor antagonists including caffeine alter fetal brain development in mice. *Sci. Transl. Med.* 5:197ra104. doi: 10.1126/scitranslmed.3006258

Skorput, A. G., Gupta, V. P., Yeh, P. W. L., and Yeh, H. H. (2015). Persistent interneuronopathy in the prefrontal cortex of young adult offspring exposed to ethanol in utero. *J. Neurosci.* 35, 10977–10988. doi: 10.1523/JNEUROSCI.1462-15.2015

Stern, Y. (2012). Cognitive reserve in ageing and Alzheimer's disease. *Lancet Neurol.* 11, 1006–1012. doi: 10.1016/S1474-4422(12)70191-6

Temple, J. L., Bernard, C., Lipshultz, S. E., Czachor, J. D., Westphal, J. A., and Mestre, M. A. (2017). The safety of ingested caffeine: a comprehensive review. *Front. Psychiatry* 8:80. doi: 10.3389/fpsyt.2017.00080

Thompson, B. L., Levitt, P., and Stanwood, G. D. (2009). Prenatal exposure to drugs: effects on brain development and implications for policy and education. *Nat. Rev. Neurosci.* 10, 303–312. doi: 10.1038/nrn2598

Van der Jeugd, A., Vermaercke, B., Derisbourg, M., Lo, A. C., Hamdane, M., Blum, D., et al. (2013). Progressive age-related cognitive decline in tau mice. *J. Alzheimers. Dis.* 37, 777–788. doi: 10.3233/JAD-130110

Whalley, L. J., Dick, F. D., and McNeill, G. (2006). A life-course approach to the aetiology of late-onset dementias. *Lancet Neurol.* 5, 87–96. doi: 10.1016/s1474-4422(05)70286-6

Whittington, R. A., Bretteville, A., Dickler, M. F., and Planel, E. (2013). Anesthesia and tau pathology. *Prog. Neuropsychopharmacol. Biol. Psychiatry* 47, 147–155. doi: 10.1016/j.pnpbp.2013.03.004

Conflict of Interest: The authors declare that the research was conducted in the absence of any commercial or financial relationships that could be construed as a potential conflict of interest.

frontiers in Cellular Neuroscience

ORIGINAL RESEARCH
published: 12 November 2019
doi: 10.3389/fncel.2019.00498

Generation and Characterization of Specific Monoclonal Antibodies and Nanobodies Directed Against the ATP-Gated Channel P2X4

Philine Bergmann[1†], Elvira Garcia de Paco[2,3†], Björn Rissiek[4], Stephan Menzel[1], Gudrun Dubberke[1], Jennifer Hua[2,3], François Rassendren[2,3‡], Lauriane Ulmann[2,3‡] and Friedrich Koch-Nolte[1‡]*

[1]Institute of Immunology, University Medical Center Hamburg-Eppendorf, Hamburg, Germany, [2]Institut de Génomique Fonctionnelle (IGF), University of Montpellier, CNRS, INSERM, Montpellier, France, [3]Laboratoire d'Excellence Canaux Ioniques d'Intérêt Thérapeutique (LabEx ICST), Montpellier, France, [4]Department of Neurology, University Medical Center Hamburg-Eppendorf, Hamburg, Germany

The P2X4 channel is involved in different physiological and pathological conditions and functions in the nervous system. Despite the existence of several mouse models for which the expression of the gene was manipulated, there is still little information on the expression of the protein at the cellular level. In particular, supposedly specific available antibodies have often proved to recognize unrelated proteins in P2X4-deficient mice. Here, we used an *in vivo* DNA vaccine approach to generate a series of monoclonal antibodies and nanobodies specific for human, mouse, and rat P2X4 channels. We further characterized these antibodies and show that they solely recognize the native form of the proteins both in biochemical and cytometric applications. Some of these antibodies prove to specifically recognize P2X4 channels by immunostaining in brain or sensory ganglia slices, as well as at the cellular and subcellular levels. Due to their clonality, these different antibodies should represent versatile tools for further characterizing the cellular functions of P2X4 in the nervous system as well as at the periphery.

Keywords: purinergic receptors, monoclonal antibody, nanobody, immunoprecipitation, cytometry

OPEN ACCESS

Edited by:
Eric Boué-Grabot, Université de Bordeaux, France

Reviewed by:
Philippe Séguéla, McGill University, Canada
Sheraz Khoja, University of Southern California, United States

****Correspondence:***
Lauriane Ulmann
lauriane.ulmann@igf.cnrs.fr

†These authors have contributed equally to this work

‡These authors share senior authorship

Received: *25 July 2019*
Accepted: *21 October 2019*
Published: *12 November 2019*

Citation:
Bergmann P, Garcia de Paco E, Rissiek B, Menzel S, Dubberke G, Hua J, Rassendren F, Ulmann L and Koch-Nolte F (2019) Generation and Characterization of Specific Monoclonal Antibodies and Nanobodies Directed Against the ATP-Gated Channel P2X4. Front. Cell. Neurosci. 13:498. doi: 10.3389/fncel.2019.00498

INTRODUCTION

ATP is an extracellular signaling molecule that acts through two main families of plasma membrane receptors: the P2Y receptors, which are G protein-coupled receptors, and P2X receptors (P2XR), which are ATP-gated cationic channels (Burnstock, 2006). There are seven P2X subunits (P2X1-7) that associate to form homotrimeric or heterotrimeric receptors. In contrast to other ligand-gated channels, whose expression is mostly confined to the nervous system, P2XRs are expressed in numerous tissues and cell types (Surprenant and North, 2009). While some P2XRs are preferentially expressed in the nervous system (P2X2, P2X3), others are only found in peripheral tissue (P2X1) or are widely expressed (P2X4, P2X5, P2X7). Among all of the P2XRs, P2X4 shows the most widespread expression. It is found in diverse tissues, such as the brain, kidney, heart, lung, and salivary glands; it is expressed by many different cell types, including immune, epithelial, endothelial, and neuronal cells (Suurväli et al., 2017). Compared to other

P2X receptors, P2X4 presents specific features. First, it is highly permeant to calcium; with a fractional calcium current close to 12–14%, P2X4 is as permeant to calcium as the NMDA receptors, and this is considered a major pathway for synaptic calcium influx (Egan and Khakh, 2004). Second, in resting cells, most P2X4 protein is localized in intracellular compartments along the endo-lysosomal pathway (Murrell-Lagnado and Frick, 2019). Signals that trigger the fusion of lysosomes with the plasma membrane bring a pool of intracellular P2X4 receptors to the cell surface. Third, P2X4 rapidly internalizes following its activation, possibly to protect the cell from calcium overload.

Despite recent advances, the pharmacology of P2X4 is still underdeveloped (Stokes et al., 2017). A few specific antagonists have been identified, showing species specificity and decent potencies. However, with a few exceptions, their efficacy *in vivo* is still poorly documented. Some insights into the physiological functions of P2X4 have been obtained through genetic ablation of its gene or down-regulation of its expression using RNA interference. These studies have implicated P2X4 in different pathologies (Tsuda et al., 2003; Sim et al., 2006; Yamamoto et al., 2006; Yang et al., 2014). A key feature of P2X4 is its expression in epithelial and endothelial cells, where luminal ATP triggers its activation. In endothelial blood vessel cells, shear stress due to high blood pressure evokes ATP release, which activates P2X4, which in turn triggers a calcium-dependent production of vasorelaxant nitric oxide (Yamamoto et al., 2006). Similarly, in lung epithelia, P2X4 activation is involved in mucus secretion (Winkelmann et al., 2019). Another key feature of P2X4 is its expression in different immune cells, such as myeloid cells and T lymphocytes. The functions of P2X4 are well documented in macrophages and microglia, where its activation triggers inflammatory and neuropathic pain, respectively (Ulmann et al., 2008, 2010). Of interest, while a strong P2X4 expression is observed in tissue-resident macrophages, it is not present in resting microglial cells. However, the expression of P2X4 is induced *de novo* in reactive microglia. In the CNS, the functions of P2X4 are still elusive. In BAC transgenic reporter mice, its expression was found to be sparse in the CNS, with a high level of expression in the hypothalamus, where it could control feeding behaviors (Xu et al., 2016). However, BAC transgenic reporter mice do not always accurately report on the actual expression of the gene of interest, as shown for the Genesat P2X7 eGFP-BAC reporter strain (Kaczmarek-Hajek et al., 2018).

Mapping P2X4 protein expression is still challenging. While there are two genetically modified mouse strains that allow *p2rx4* promotor activity to be followed: (1) a knock-in of the ß-galactosidase gene in the first exon; and (2) a BAC transgenic reporter mouse (Sim et al., 2006; Xu et al., 2016), these strains do not provide accurate information on the dynamics of receptor expression, as the half-lives of the receptor and the reporters likely differ. In addition, these reporter strains do not provide any information on the subcellular localization of the receptor. Cellular and biochemical characterization of proteins is facilitated by the use of antibodies. Regarding P2X4, several commercial and some homemade polyclonal antibodies are available. However, in our experience, the vast majority of these antibodies lack specificity, as they still show reactivity with proteins in P2X4-null mice. A considerable drawback of polyclonal antibodies is their inconsistency between different production lots, particularly when they originate from different immunized hosts (Roncador et al., 2016). This inconsistency presumably reflects the variability of the host immune response to a given immunogen. This is particularly problematic in the case of some commercial P2X4 antibodies for which validation of the specificity was performed on knockout mice samples for one given lot and then applied uniformly to other lots. An alternative to polyclonal antibodies are monoclonal antibodies, which because of their clonality, do not present variability issues and offer good reproducibility from lot to lot. However, because they recognize a single epitope, their signal intensity may be weaker and they may not work in all applications.

Here, we describe the generation and validation of a series of monoclonal rat antibodies and of recombinant llama nanobodies raised against either murine or human P2X4 in native conformation and demonstrate their utility for detecting P2X4 in living cells and fixed tissue and for immunoprecipitating P2X4 from undenatured cell extracts.

MATERIALS AND METHODS

Bone Marrow-Derived Macrophage (BMDM) Culture

Bone marrow-derived macrophage (BMDMs) were obtained from bone marrow cells by flushing the femurs and tibias of 6- to 12-week-old mice. The bone marrow was homogenized, and the resulting fresh bone marrow cells were cultured in Glutamax-DMEM medium (Invitrogen) containing 100 U/ml penicillin and 100 µg/ml streptomycin (Invitrogen), supplemented with 10% fetal calf serum (FCS; Biowest) and 30% L929 cell-conditioned medium (LCCM). Four days after seeding the cells, fresh medium was added, and cells were incubated for an additional 4 days. To obtain the BMDM, the supernatants were discarded, and the attached cells were washed with 10 ml of sterile PBS. The macrophages were detached by cell scraping, counted, seeded, and cultivated in tissue culture plates for 12 h before any further experimental procedure.

Mast Cell Degranulation Assay

Mast cells were obtained from the peritoneal cavity of C57BL/6 WT or P2X4$^{-/-}$ mice by lavage with 5 ml cold PBS + EDTA (2 mM, Gibco). Cells were resuspended in RPMI medium containing 10% FCS, and aliquots were incubated for 10 min at 37°C in the presence or absence of 2 mM ATP (Sigma). Mast cells were identified by flow cytometry as CD11b^{-}FcεR1^{+} using anti-CD11b (1/100, BioLegend, clone M1/70) and anti-FcεR1 (1/100, BioLegend, clone MAR-1) antibodies. ATP-induced degranulation of mast cells was evaluated by flow cytometry using antibodies against CD107a (1/100, BioLegend, clone 1D4B) and P2X4-specific monoclonal antibodies and nanobodies in order to detect the externalization of CD107a and P2X4 at the mast cell surface.

Culture of Cell Lines and Transfections

Human Embryonic Kidney 293 cells (HEK) were cultured in Glutamax-DMEM medium (Invitrogen) containing 1% 100 U/ml penicillin and 100 μg/ml streptomycin (Invitrogen) and supplemented with 10% FCS (Biowest). Transfections of plasmids expressing the appropriate protein of interest (eGFP, P2X receptors, as specified in the results or figure legends) were performed using 3 μl per 35-mm dish of Lipofectamine 2000 (Life Technologies) according to the manufacturer's recommendations.

Immunofluorescence

BMDM cells were plated on coverslips and fixed in 1% paraformaldehyde for 5 min at RT. Cells were then washed in PBS and blocked in PBS, 3% BSA for 1 h and incubated for 1 h at RT with the primary antibody [rat anti-P2X4 (Nodu 246), 1/1,000]. After three washes, cells were incubated for 30 min at RT with a specific Alexa 488 goat anti-rat secondary antibody (1/2,000).

Mice were euthanized by peritoneal injection of pentobarbital (300 mg/kg). Blood was removed with intracardiac perfusion of PBS. L4, L5, and L6 DRG (dorsal root ganglion) and brain were placed in 4% paraformaldehyde in 0.1 M phosphate buffer pH 7.4 for 2 h. Tissues were cut into 30 μm sections with a vibratome, rinsed with PBS, and blocked with 10% goat serum diluted in a 0.1% Triton X-100 solution for 1 h. Monoclonal rat anti-P2X4 (Nodu 246) antibody was added overnight at 4°C. After rinsing, slices were incubated for 2 h with an Alexa488-conjugated goat anti-rat IgG secondary antibody (1/1,000). Primary and secondary antibodies were diluted in PBS with 0.1% Triton X-100. After rinsing, sections were mounted with Fluorescent Mounting medium (Dako) and observed on an AxioImager Z1 apotome (Zeiss).

Western Blot

HEK cells were homogenized in lysis buffer (100 mM NaCl, 5 mM EDTA, 1% NP-40, 20 mM Hepes and complete protease inhibitor cocktail (Roche), pH 7.4). Lysates were clarified by centrifugation, and the protein concentration was determined using a protein assay kit (Bio-Rad). Proteins were separated on 12–4% NuPage precast gel (Life Technologies) and transferred onto a nitrocellulose membrane. The membrane was blocked with 5% non-fat dry milk/1% Tween20 in Tris-buffered saline (TBST) 1 h at RT. The membrane was then incubated o/n at 4°C with the appropriate antibody diluted in TBST: monoclonal rat anti-P2X4 (Nodu 246) or polyclonal rabbit anti-P2X4 antibody (1/500, Alomone Laboratory). After four washes in TBST, the membrane was probed with specific secondary antibodies conjugated to HRP (1/5,000) for 1 h at RT, revealed with SuperSignal West Pico Chemiluminescent Substrate (Pierce), and detected with a ChemiDoc^{TM} Imaging System (Bio-Rad).

Immunoprecipitation

Plasma membrane-enriched protein fractions were prepared from cultures of WT or P2X4 KO mouse BMDM. Cells were detached by cell scraping, counted, pelleted, and homogenized in a solubilization buffer [0.32 M sucrose, 10 mM Hepes, 2 mM EDTA, and complete protease inhibitor cocktail (Roche), pH 7.4] with 150 strokes of a Potter–Elvehjem homogenizer. Homogenates were centrifuged for 20 min at 1,264 rpm at 4°C to eliminate cell debris, and the supernatant was ultracentrifuged for 1 h at 70,000 rpm at 4°C. The resulting pellet was solubilized in Complexiolyte CL48 (Logopharm) supplemented with protease inhibitors (Roche) for 2 h at 4°C. Unsolubilized material (pellet; particles >336 S) was removed by centrifugation (30,000 rpm, 18 min, 4°C), transfected HEK cells were homogenized in lysis buffer [100 mM NaCl, 20 mM Hepes, 5 mM EDTA, 1% NP-40, and complete protease inhibitor cocktail (Roche), pH 7.4] 48 h after transfection. Lysates were clarified by centrifugation. The protein concentration of the lysates was determined using a protein assay kit (Bio-Rad). Freshly prepared solubilisates were incubated o/n at 4°C with Nodu 246 crosslinked to magnetic beads (Dynabeads, Invitrogen). The flow-through was discarded and the beads washed five times with wash buffer [CL48 diluted 1:4 in PBS and supplemented with complete protease inhibitor cocktail (Roche)], and sample buffer (Invitrogen) was added to separate the protein complexes from the beads. Proteins were resolved by SDS-PAGE, transferred to nitrocellulose membranes, and visualized using polyclonal rabbit anti-P2X4 (1/1,000, Alomone).

Flow Cytometry

The expression of cell surface molecules was assessed by detaching HEK or BMDM cells by cell scraping and then counting and centrifuging them. They were then incubated for 20 min on ice with rat anti-P2X4 (Nodu 246) diluted in wash buffer (PBS supplemented with 1% BSA). After washing, the cells were probed with a fluorochrome-conjugated goat anti-rat IgG secondary antibody (1/200) for 20 min on ice. For intracellular staining of P2X4, the same protocol as for surface staining was employed, except that 3% saponin was added to the wash buffer in order to permeabilize the cells (permeabilization buffer). Bivalent Nb-rabbit IgG heavy-chain antibodies were used at 1/100 dilution, and bound antibodies were detected with Alexa 647-conjugated goat anti-rabbit IgG (1/200). The expression of P2X4 was analyzed by flow cytometry (FACSCalibur II or FACS Canto, Becton Dickinson). In some experiments (peritoneal cells, BMDM), cells were unstimulated or incubated at 37°C either with ATP (2 mM) or ATP (2 mM) and ivermectin (IVM, 3 μM, Sigma-Aldrich) for 10 min prior to FACS analysis.

Targeting of the P2X4 Gene and Generation of Mutant Mice

Mice carrying a targeted null mutation of the P2X4 gene were described previously (Sim et al., 2006). Mice were housed under a standard 12 h light/dark cycle with food and water available *ad libitum*. Age varied between 6–12 weeks. APP/PS1; P2X4$^{-/-}$ were obtained by breeding P2X4$^{-/-}$ mice with the APPswe:PS1dE9 mice (Jackson Laboratory, stock# 034832). All procedures fully complied with French legislation (decree 87-848, October 19, 1987, and order, April 19, 1988), which implements the European directive (86/609/EEC) on research involving laboratory animals, and were performed according to the requirements of CNRS ethical standards.

Generation of P2X4-Specific Monoclonal Antibodies and Nanobodies

Rats and llamas were immunized with $P2X4^{Y378F}$-encoding mammalian expression vectors conjugated to gold particles by ballistic intradermal immunization, essentially as described previously (Möller et al., 2007; Eden et al., 2018). Spleen and lymph nodes were prepared from rats 4 days after the final boost; peripheral blood leukocytes were prepared from llamas 7 and 10 days after the final boost. Spleen and lymph node cells were fused to Sp2/0 myeloma cells, and hybridoma cells were selected in HAT medium in 96-well-plates. The VHH repertoire was PCR-amplified from cDNA of peripheral blood leukocytes and cloned into the pHEN2 phage display vector. The phage library was subjected to two rounds of panning on untransfected and $P2X4^{Y378F}$-transfected HEK cells. Sequencing of the VHH coding region identified families of enriched clones. The VHH coding region was cloned into the mammalian pCSE2.5 expression vector upstream of the hinge, CH2, and CH3 domains of rabbit IgG. Supernatants containing chimeric Nb-rabbit IgG heavy chain antibodies were collected 6 days after transfection, and supernatants from hybridoma cells 12–16 days after cell fusion. Cell supernatants were analyzed for the presence of P2X4-specific antibodies by immunofluorescence microscopy using CHO cells 24 h after co-transfection with expression vectors for P2X4 and GFP-NLS (nuclear localization signal) fusion protein. Bound antibodies were detected with PE-conjugated rat or rabbit IgG-specific secondary antibodies. P2X4-specific antibodies were purified by affinity chromatography on protein A-sepharose and conjugated *via* NH2-esters to Alexa fluorescent dyes. All procedures fully complied with German legislation, which implements the European directive (86/609/EEC) on research involving laboratory animals, and were performed according to the requirements of the University Medical Center Hamburg Eppendorf.

RESULTS

Generation of Rat Monoclonal Antibodies Against P2X4 Receptors

A combination of genetic and full-length protein immunization was used to maximize the chance of obtaining antibodies recognizing the native form of the receptor (Adriouch et al., 2005; Koch-Nolte et al., 2019). Gene gun immunization was used to immunize two rats according to the protocol shown in **Figure 1A**, either with a cDNA encoding mouse P2X4-Y378F (Rat RG23) or a mixture of mouse and human P2X4-Y378F cDNAs (Rat RG96), respectively. A final boost was performed using HEK cells transiently expressing either mouse P2X4 or both human and mouse P2X4. After terminal bleeding and fusion of splenocytes to Sp2/0 myeloma cells, individual hybridoma cells were selected by limit dilution, and the presence of antibodies recognizing P2X4 in the supernatant was tested by immunocytochemistry on CHO cells transiently transfected with either human or mouse P2X4-Y378F. **Figure 1B** shows examples of immune staining obtained using the supernatant of different hybridomas originating from rat RG96 (right panel) and pre-immune and immune sera from the same animal (left panel). The results show that two clones (Nodu 225 and Nodu 246) bind only mouse P2X4, while the other two (Nodu 19 and Nodu 344) only recognize human P2X4. The characteristics of the different hybridomas obtained are indicated in **Figure 1C**.

We next fully characterized the Nodu 246 monoclonal antibody, which specifically recognizes mouse P2X4, by immunostaining. We first evaluated its capacities to recognize native or denatured forms of the receptor *via* biochemical assay. We analyzed whether Nodu 246 could detect mouse P2X4 in a typical Western blotting experiment. Protein extracts from HEK cells transiently expressing either human P2X4 or Flag/HA-tagged mouse P2X4 were separated by SDS-PAGE and transferred to a nitrocellulose membrane. The blot was incubated sequentially with Nodu 246 and peroxidase-conjugated anti-rat IgG. Bound antibodies were visualized by enhanced chemiluminescence (**Figure 2A**). The results show that Nodu 246 is unable to detect denatured human or mouse P2X4, while a commercial polyclonal rabbit-antibody raised against a peptide conserved in mouse and human P2X4 reacts with protein bands at the expected molecular weight of ∼60 kD. These results indicate that Nodu 246 only recognizes mouse P2X4 in its native conformation. We next tested whether Nodu 246 could immunoprecipitate endogenous P2X4 from mouse BMDMs. Immunoprecipitation of P2X4 was performed on BMDM from either WT or P2X4-null mice. Immunoprecipitates were analyzed for the presence of mouse P2X4 by Western blotting using commercial P2X4 peptide-specific rabbit antibodies (**Figure 2B**). The results show that Nodu 246 efficiently immunoprecipitated P2X4 from WT BMDM but not from $P2X4^{-/-}$ cells. Similar experiments performed on HEK cells transiently expressing human P2X4 indicate that Nodu 246 is unable to immunoprecipitate the human receptor (not shown), confirming the results obtained by immunocytochemistry. Nodu 246 did not cross-react with human and mouse P2X7 receptors (data not shown); cross-reactivity to other subunits was not tested.

Nodu 246 was produced by cDNA immunization, a strategy aimed at producing antibodies that recognize native extracellular epitopes of membrane proteins (Möller et al., 2007; Eden et al., 2018). We thus analyzed the performance of Nodu 246 in flow cytometry experiments. We first used HEK cells transiently expressing mouse P2X4. As shown in **Figure 3A**, when tested on non-permeabilized HEK cells expressing P2X4, a specific fluorescence signal was present, although the number of events was relatively small and covered a large range of intensities. However, after permeabilization, the overall fluorescence signal increased, suggesting that even in transfected HEK cells, most P2X4 receptors are localized intracellularly. Similarly, in non-permeabilized mouse BMDM, Nodu 246 generated a weak fluorescent signal that was strongly enhanced upon permeabilization. No specific fluorescence signal was observed when the same experiments were performed on $P2X4^{-/-}$ BMDM (**Figures 3B,C**).

Next, we assessed the immunostaining performances of Nodu 246 on fixed primary cultured cells and tissue sections (**Figures 4A,B**). In a primary culture of permeabilized

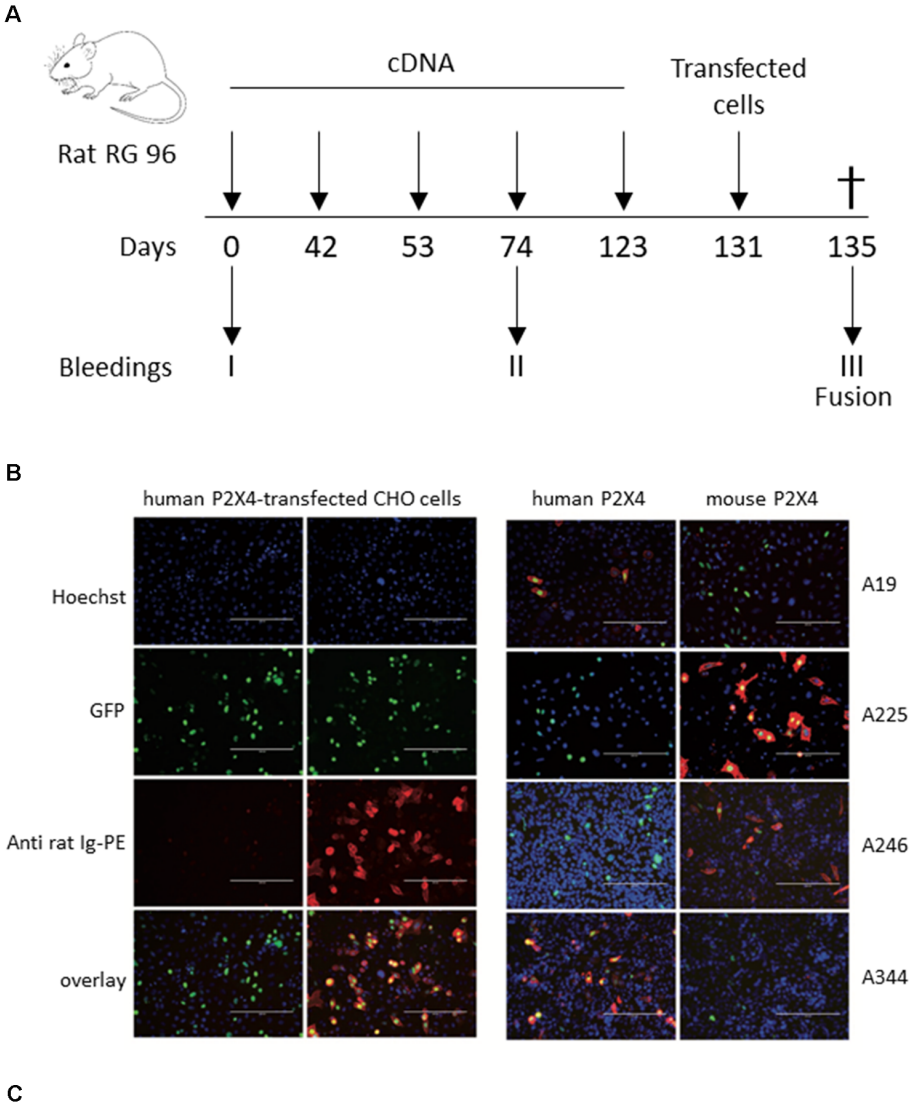

C

Rat	RG23	RG96	RG96	RG96	RG96	RG96	RG96
Clone	A194	A225	A246	A19	A128	A133	A344
Isotype	IgG2b, k	IgG2b, k	IgG2b, k	IgG2b, k	IgM, k	IgG2a, k	IgG2a, k
Species	h	m	m	h	h	h	h

FIGURE 1 | Identification of P2X4-specific monoclonal antibodies. **(A)** Schematic diagram of the rat immunization protocol. Rats were immunized five times by trans-dermic biolistic gene delivery (six shots per immunization) with expression vectors encoding either mouse WT P2X4 (rat RG23) or mouse and human P2X4-Y378F (rat RG96). Each rat received a final injection of CHO cells expressing either mouse P2X4 or a mixture of mouse and human P2X4-Y378F. Pre-immune sera were drawn at day 0 and immune sera at day 74, prior to the final boost at day 123. Terminal bleeding was performed on day 131, followed by cell fusion and hybridoma selection. **(B)** Pre-immune sera, immune sera (left panels, dilution 1/1,600) of rat RG96 and hybridoma supernatants derived from RG96 (right panels) were tested for reactivity with CHO-cells transiently co-transfected with expression constructs for nuclear GFP and either human P2X4 or mouse P2X4-Y378F, as indicated. Different hybridoma show specificity toward human or mouse P2X4 receptors. Scale bar: 200 μm. **(C)** Specific characteristics of the different identified hybridoma.

BMDM or microglia, the Nodu 246 signal was localized in intracellular compartments and co-localized with either CD68 or LC3b, suggesting an intracellular localization of P2X4 in the endo-lysosomal compartment (**Figures 4A,B**). No staining was observed in BMDM from P2X4$^{-/-}$ mice, supporting the specificity of the Nodu 246 antibody. Specificity was also

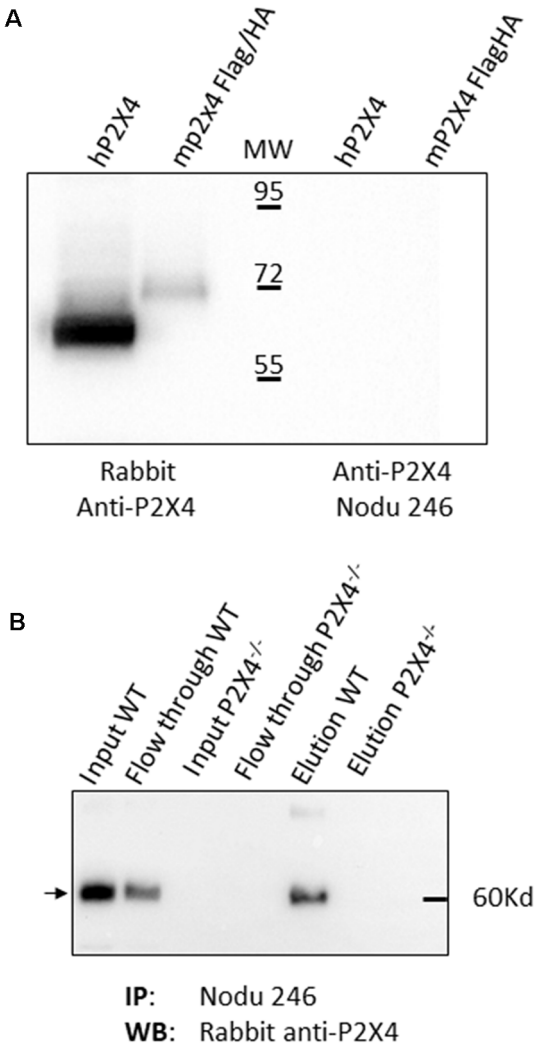

FIGURE 2 | Biochemical properties of Nodu 246 hybridoma. **(A)** Recognition of denatured human and mouse P2X4 receptors by mAb Nodu 246 was assessed by Western blotting. Protein extracts from a HEK cell line stably expressing the human P2X4 and HEK cells transiently transfected with an expression construct for Flag/HA-tagged mouse P2X4 were analyzed by Western blot after electrophoresis of cell lysates on an SDS-polyacrylamide gel. Blots were incubated either with a rabbit polyclonal anti-P2X4 peptide antibody (Alomone) or with rat monoclonal antibody Nodu 246. Bound antibodies were revealed with peroxidase-conjugated anti-rabbit IgG or anti-rat IgG. The monoclonal mAb Nodu 246 evidently does not recognize the denatured forms of human and mouse P2X4 (right panel), as opposed to the rabbit polyclonal anti-peptide antibody (left panel). **(B)** P2X4 in mouse WT and P2X4 KO bone marrow-derived macrophage (BMDM) was specifically immunoprecipitated with Nodu 246. Immunoprecipitated proteins were separated by electrophoresis on SDS-polyacrylamide gels and immunoblotted with a polyclonal rabbit anti-P2X4 peptide antibody (Alomone). The same protein extracts were loaded on both panels. Note the higher apparent molecular weight of the Flag/HA-tagged mouse P2X4 compared to human P2X4.

demonstrated in tissue sections of DRG (**Figure 4C**), showing, as previously reported, that P2X4 is expressed in a subset of sensory neurons (Lalisse et al., 2018). Specificity was also tested in the cortex of 12-month-old APP/PS1 mice (**Figure 4D**); non-specific staining was not observed in brain sections from P2X4$^{-/-}$ mice, while in the APP/PS1 mice, P2X4 was localized in specific intracellular compartments of reactive microglia clustered around amyloid deposits but not in microglia distant from the plaques. Dim immunostaining was also present in cortical neurons.

The specificity of Nodu 246 was not tested on recombinantly expressed P2X subunits. However, in P2X4-deficient mice, Nodu 246 did not stain macrophages, DRG, and brain sections, in which expression of all P2X subunits is well characterized, supporting the specificity of the Nodu 246.

Generation of Nanobodies Against P2X4 Receptors

Llama immunization was performed using a similar strategy as for rat, above. Two llamas were immunized four times at 2-week intervals using cDNA expression vectors encoding either mouse or human P2X4-Y378F, followed by a final boost with P2X4-transfected HEK cells. Blood was sampled 4 and 8 days following the last boost, and the VHH repertoire of vascular B cells was PCR-amplified and used for phage library construction. Positive clones were selected through two cycles of phage panning on HEK cells stably expressing recombinant human or mouse P2X4. Selected clones were produced as secreted periplasmic proteins carrying a C-terminal His6x-c-myc tag in *E. coli*. The specificity of the recombinant nanobodies was tested by immunofluorescent staining of CHO cells transiently co-transfected with expression vectors encoding human or mouse P2X4 and nuclear GFP. Bound nanobodies were detected using fluorochrome-conjugated monoclonal antibody directed against c-myc. **Figure 5A** shows representative results obtained for four different clones out of seven compared to an irrelevant nanobody. The seven VHH were subcloned into a eukaryotic expression vector so as to replace the C-terminal His6x-c-myc tag by the hinge, CH2, and CH3 domains of rabbit IgG, providing the basis for generating a bivalent nanobody-rabbit IgG heavy chain antibody (Rb-hcAb), which allows for increased avidity and easy production in eukaryotic cells. The species specificity of the different nanobodies produced as Rb-hcAb was assessed using flow cytometry of HEK cells transiently co-transfected with cDNA expression vectors encoding eGFP and either human, mouse, or rat P2X4 Y378F. **Figure 5B** shows an example of FACS sorting of HEK cells expressing either human, mouse, or rat P2X4, using GFP and a fluorochrome-conjugated secondary anti-rabbit-IgG antibody for detecting the Rb-hcAb constructed with nanobody 271 (Nb 271). **Figure 5C** shows the species specificity of the seven Nbs after gating on GFP-positive cells compared to cells incubated with the secondary antibody only. Two clones recognize human, mouse, and rat P2X4 (Nb 271 and Nb 284), two react only with human P2X4 (Nb 262, Nb 301), one reacts with both human and mouse P2X4 (Nb 258), one reacts with both human and rat P2X4 (Nb 318), and one reacts only with mouse P2X4 (Nb 325). Specificity was also tested on cells transfected with expression vectors for human and mouse P2X7 and P2X1. With the exception of Nb 301, which also recognizes both human and mouse P2X7, the other Nbs did not

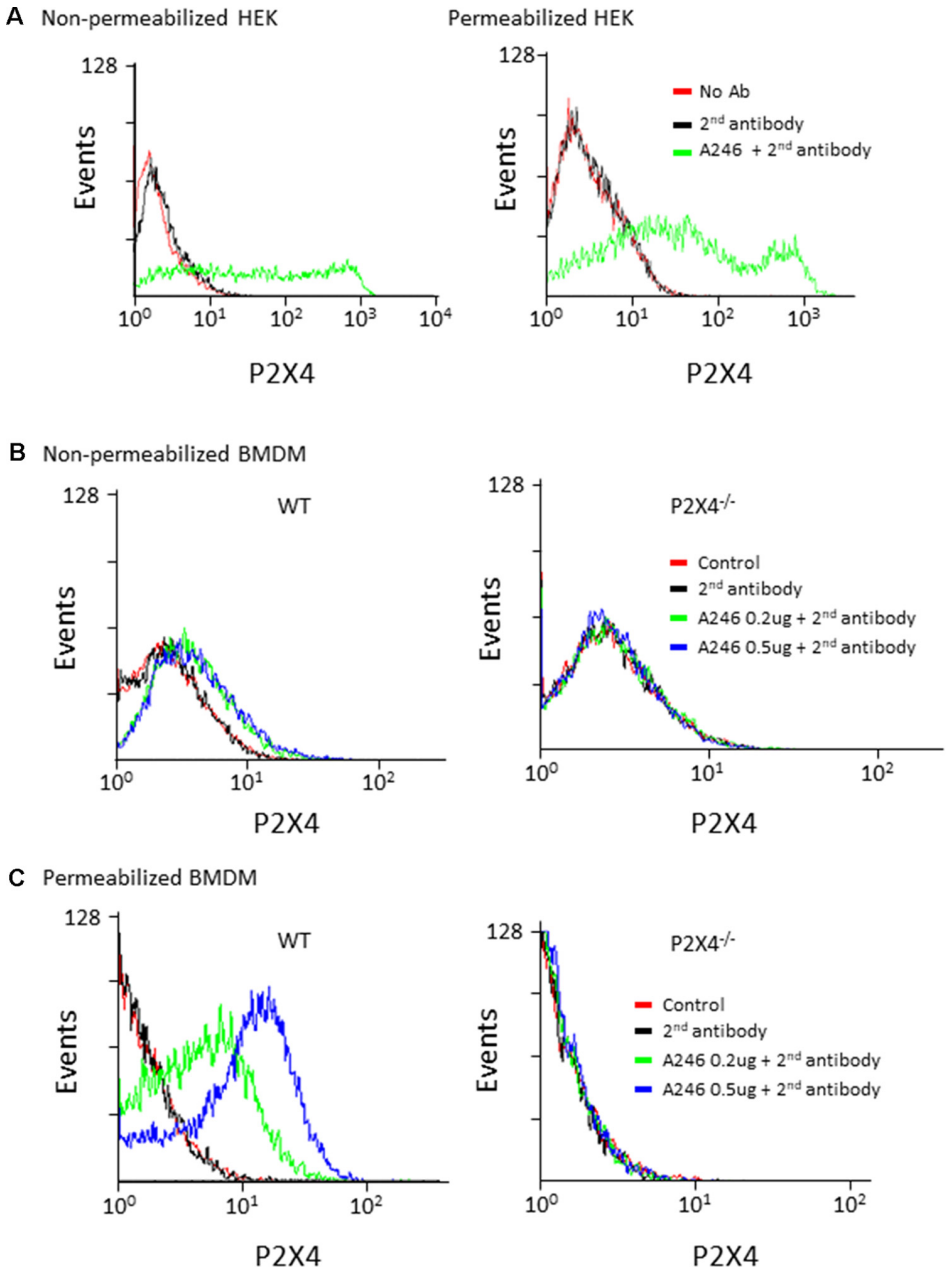

FIGURE 3 | Flow cytometry analysis of mouse P2X4 expression using Nodu 246. **(A)** Cell surface and intracellular expression of mouse P2X4 by P2X4-transfected and non-transfected HEK cells was assessed by flow cytometry after sequential incubation of cells with rat mAb Nodu 246 followed by a secondary PE-conjugated anti-rat-IgG antibody (2nd antibody), in non-permeabilized or permeabilized cells. Similar experiments were performed with BMDM obtained from WT and P2X4$^{-/-}$ mice. Cells were either non-permeabilized **(B)** or permeabilized **(C)**. Note that permeabilization greatly enhanced the detection of mouse P2X4 in BMDM, further supporting the intracellular localization of the native receptor.

show any cross-reactivity with P2X7 or P2X1 (data not shown). Specificity against other P2X subunits was not tested.

Treatment of mast cells with ATP reportedly evokes degranulation and lysosomal fusion with the plasma membrane (Wareham and Seward, 2016). We assessed whether the treatment of mouse mast cells with ATP induces exposure of P2X4 on the plasma membrane. Lysosomal fusion with the plasma membrane was visualized by flow cytometry using a fluorochrome-conjugated monoclonal antibody that recognizes the lysosomal protein Lamp1/CD107a (**Figure 6**). The results confirm that ATP stimulation strongly enhances the detection of Lamp1 in both WT and P2X4$^{-/-}$ mast cells, indicating a lysosomal fusion with the plasma membrane and exposure of Lamp1 at the cell surface. Detection by Nb 271 and 325 of endogenous P2X4 expressed by the peritoneal mast and BMDM cells was also analyzed by cytometry (**Figure 6**). A similar

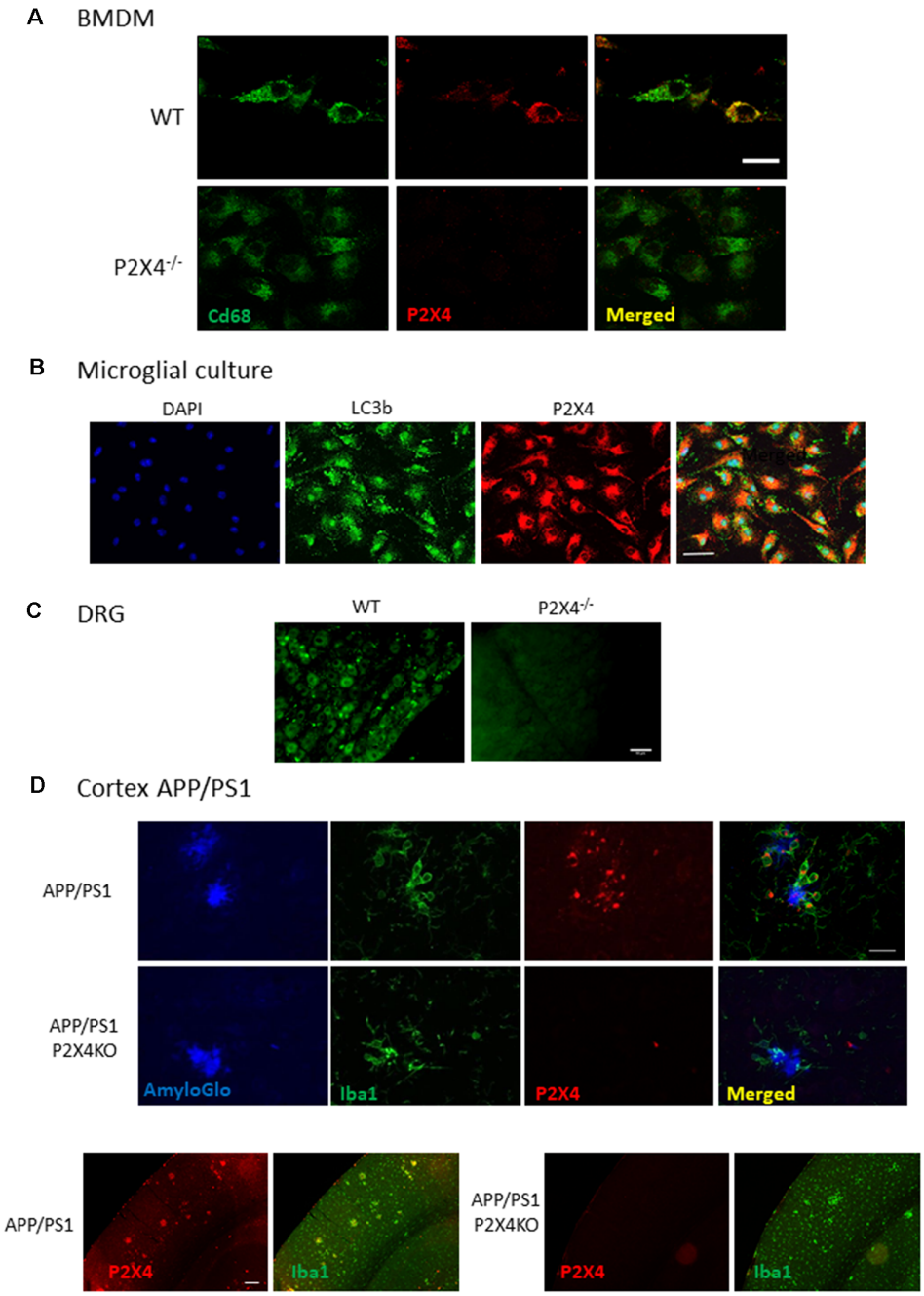

FIGURE 4 | Immunocyto- and -histochemistry with Nodu 246. **(A)** Co-immunostaining of WT and P2X4$^{-/-}$ BMDM with Nodu 246 and the lysosomal marker CD68. Scale bar: 5 μm. **(B)** Co-immunostaining of WT and P2X4$^{-/-}$ cultured mouse microglia using the rat-monoclonal antibody Nodu 246 and the lysosomal marker LC3b. Scale bar: 10 μm. **(C)** Immunostaining of dorsal root ganglion (DRG) of WT and P2X4$^{-/-}$ DRG. Scale bar: 50 μm. **(D)** Top panel, co-immunostaining of microglial cells (green, Iba1) and P2X4 (red, Nodu 246) and amyloid plaques (blue, AmyloGlo) in the cortex of brains from APP/PS1 and APP/PS1; P2X4$^{-/-}$ mice. P2X4 is localized in the intracellular compartments of activated microglia clustered around amyloid deposits. Scale bar 20 μm. Bottom panel, low magnification of the cortical region of APP/PS1 and APP/PS1; P2X4$^{-/-}$ mice stained with anti-Iba1 (green) and Nodu 246 (red). Note the dim P2X4 immunostaining in cortical neurons. Scale bar 50 μm.

experiment was performed with BMDM from WT and P2X4$^{-/-}$ using Nb271-rbhcAb. In this case, cells were either unstimulated or incubated, either with ATP (2 mM) or ATP and IVM (3 μM), for 10 min as above. As shown in **Figure 6B**, a specific signal was observed in WT but not in P2X4$^{-/-}$ BMDM. In contrast to peritoneal mast cells, a low level of P2X4 could clearly be detected on BMDM, even in the absence of ATP or IVM stimulation.

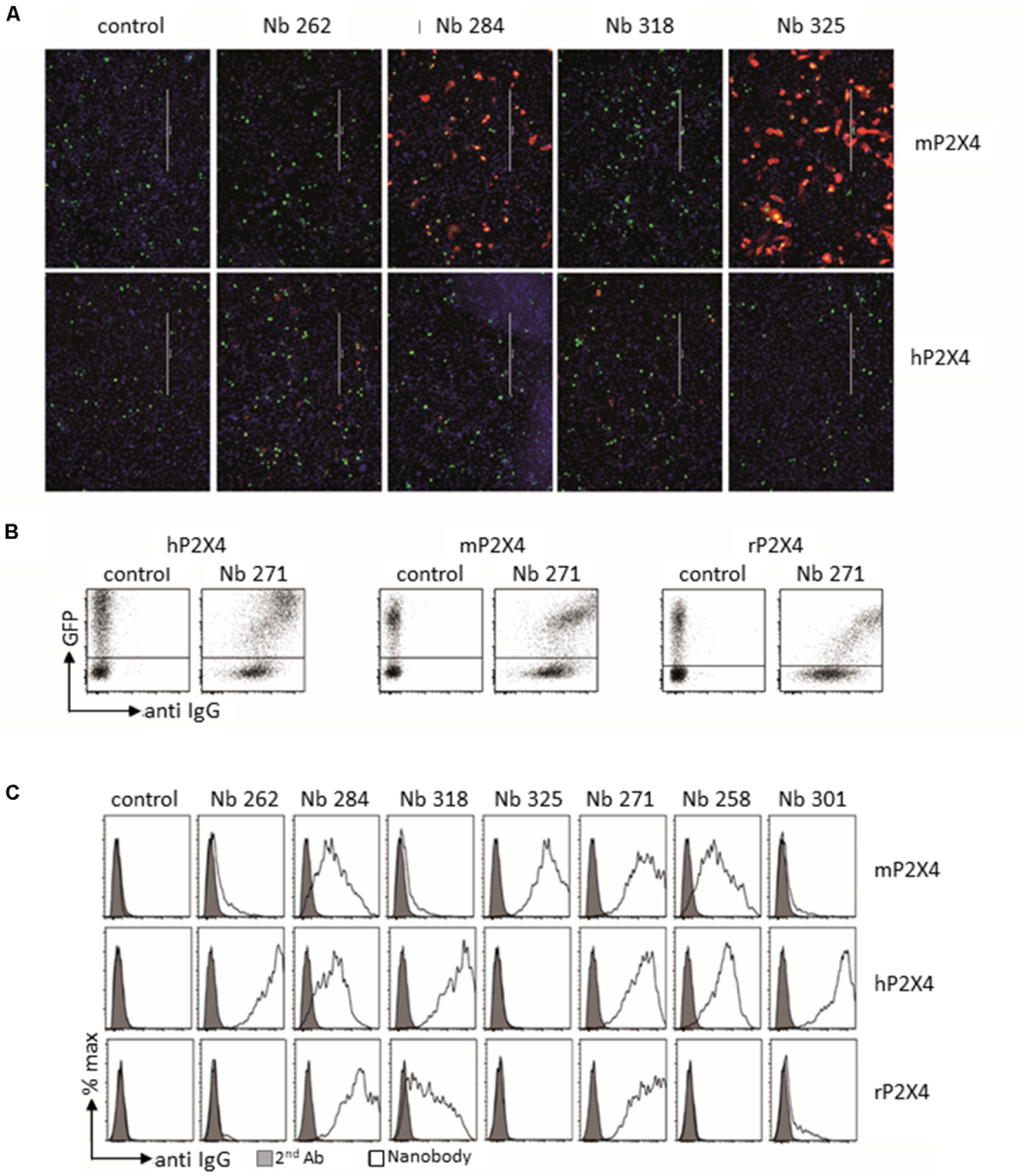

FIGURE 5 | Analysis of cloned nanobodies against mouse or human P2X4. **(A)** Immunofluorescence analysis of the reactivities of monovalent his6x-c-myc-tagged nanobodies with non-permeabilized CHO cells transiently co-transfected with GFP and either mouse (top panel) or human (bottom panel) P2X4 Y378F. Bound nanobodies were detected by sequential staining with a C-myc tag-specific mouse mAb followed by PE-conjugated rabbit anti-mouse IgG. Scale bar: 400 μm. **(B,C)** Flow cytometry analysis of the binding specificity of the different selected nanobodies. HEK cells were co-transfected with GFP and either human, mouse, or rat P2X4 Y378F. The FACS analyses in **(B,C)** were performed on transiently transfected HEK cells using bivalent Nb-rabbit IgG heavy chain antibodies. Bound antibodies were detected with Alexa 647-conjugated goat anti-rabbit IgG. **(B)** Example of results obtained with Nb 271, which binds all tested P2X4 receptors. **(C)** Binding specificity of the different selected nanobodies. Gray graphs correspond to control staining using only the secondary antibody. Nb isotype corresponds to a control with an unrelated isotype nanobody. The different staining protocols used to account for the stronger labeling intensity of human P2X4 transfected cells in **(B,C)** vs. **(A)**. The relative staining intensities of the nanobodies are the same in panels **(A,B)**, i.e., for mP2X4: 325 > 284 > 318 = 262 and for hP2X4: 262 > 318 > 284 > 325.

DISCUSSION

Antibodies are unique biological tools for characterizing protein expression, cellular distribution, and functions. There is a great diversity of antibody types, modes of immunization, species, and clonality, and assessing and validating their specificity is a major issue in the field (Baker, 2015; Roncador et al., 2016). This is particularly true for polyclonal antibodies, which are produced in limited amounts and require new validation for each new batch, assuming that batches correspond to different

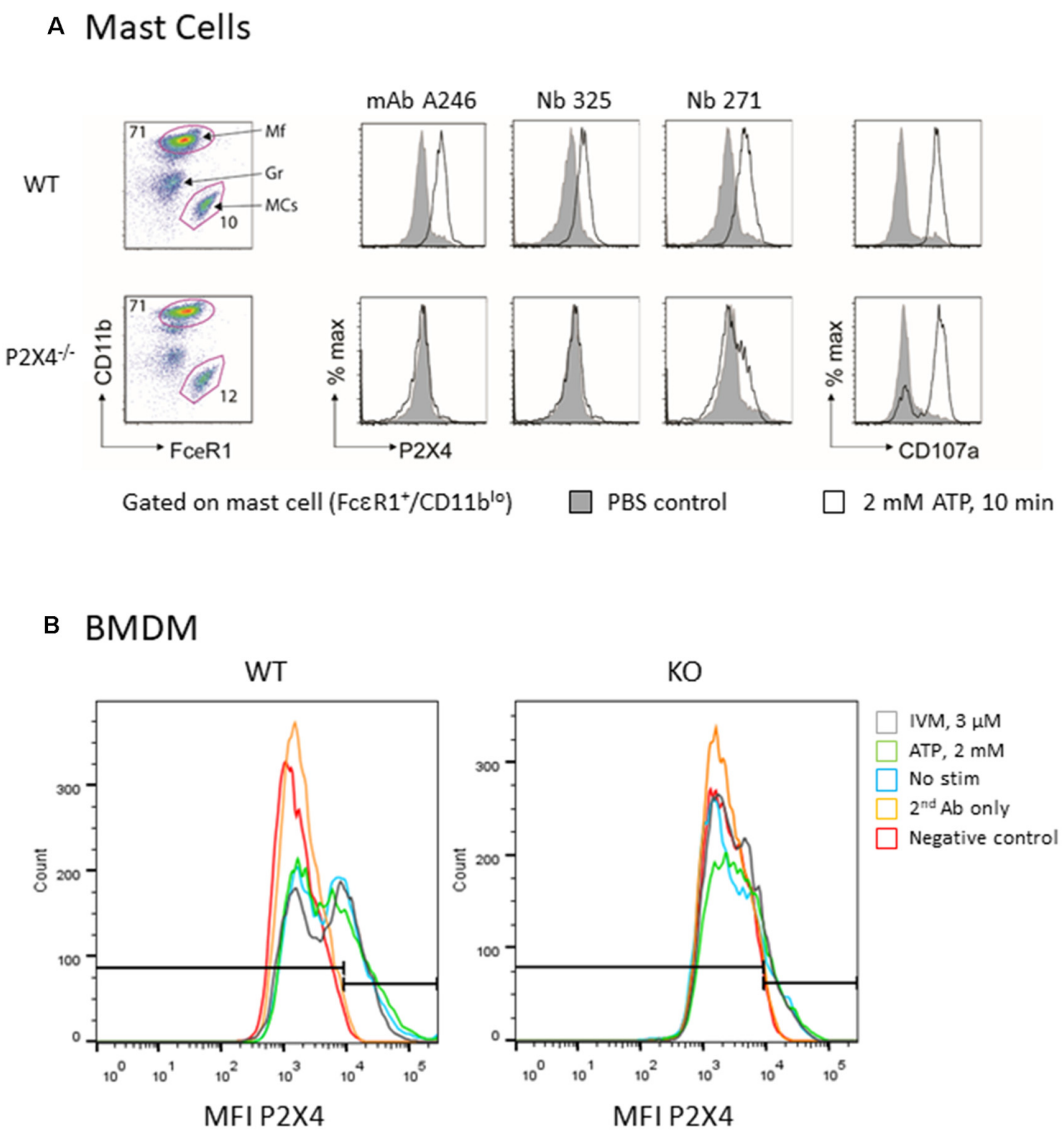

FIGURE 6 | Flow cytometry analysis of native mouse P2X4 expressed by peritoneal mast cells and BMDM. **(A)** Peritoneal cells from WT and P2X4$^{-/-}$ were stimulated (white) or not (gray) for 10 min with 2 mM ATP at 37°C. Cells were washed and incubated at 4°C with anti-CD11b-PerCO and anti-FcεR1-PE as well as with various antibodies directed against P2X4 and appropriate secondary antibodies (AF647 or AF488). CD107a (LAMP1-FITC) was used as a control experiment. Mast cells were identified as CD11b low, FcεR1+. mAb Nodu 246: rat monoclonal antibody; Nb 325, Nb 271: Nanobodies. **(B)** Similar flow cytometry experiments of WT and P2X4$^{-/-}$ BMDM using Nb 271 RbhcAb. Cells were stimulated as above with 2 mM ATP (ATP, green), 3 µM ivermectin (IVM, gray), or not stimulated (nanobody, blue). Negative controls were secondary antibody only (secondary antibody, orange) and unlabeled cells (Neg, red).

donors. Clonal antibodies such as monoclonal antibodies or nanobodies have the advantage of being unlimited, since they are either produced by immortalized hybridoma or cloned in eukaryotic expression vectors, respectively. This allows full characterization of their specificity and, once validated, the assurance of their reproducibility.

For different reasons, raising specific antibodies against transmembrane receptors is difficult. First, since these proteins contain one or more hydrophobic transmembrane domains embedded in the membrane leaflet, the purification of native membrane proteins for immunization is difficult. Second, producing recombinant membrane proteins in their native conformation is challenging. Thirdly, immunization with synthetic peptides derived from the amino acid sequence of a transmembrane protein does not ensure proper folding corresponding to that of the native protein. Resulting antibodies often do not recognize their target protein in native conformation. It is therefore important to improve the experimental design for generating membrane protein antibodies, leading to the generation of antibodies with increased specificity towards native protein. In this study, we used a specific strategy to generate monoclonal antibodies

and nanobodies recognizing native P2X4, a transmembrane ATP-gated channel. Animals were immunized through cDNA immunization, an approach that uses a repetitive injection of a eukaryotic expression plasmid encoding P2X4. This strategy allows *in vivo* transfection of cells of the immunized host, which will express the foreign protein in its native conformation and trigger the specific immune response (Möller et al., 2007; Eden et al., 2018). Because P2X4 receptors are normally intracellularly localized in lysosomes, we immunized with an expression vector encoding the Y378F P2X4 mutant, that is unable to internalize (Qureshi et al., 2007), instead of the WT receptor. Downstream characterization demonstrates that this strategy was highly efficient in generating antibodies recognizing the extracellular epitope of the native protein in both rats and llamas. All antibodies identified in this study only recognize P2X4 from mouse, rat, and/or human in their native conformation but not in their denatured form. This is likely due to the screening and selection strategies used for the identification of positives clones, which in both cases rely on binding of the antibody to the cell expressing the receptors. It is possible that a screening strategy based on denatured protein would have led to the identification of different clones with other specificities.

Antibodies targeting the extracellular region of receptors represent potential pharmacological tools for modulating their functions (Koch-Nolte et al., 2019). This is particularly true for nanobodies, which, owing to their small size and long CDR3 loops, can often access ligand-binding pockets and thus either activate or block receptors (De Genst et al., 2006; Stortelers et al., 2018). Concerning P2X receptors, blocking antibodies and nanobodies have been generated for mouse and human P2X7 (Danquah et al., 2016). These nanobodies show therapeutic potential, as they can reduce P2X7-evoked inflammation *in vivo*. A recent study reported the generation of a panel of antibodies that modulate human and mouse P2X4 receptors positively and negatively (Williams et al., 2019). These antibodies were raised against purified recombinant P2X4 proteins using either page display screening or immunization in rats and were further engineered to improve their biological activities. While these antibodies can reverse neuropathic pain when systemically administered in animal models, their biochemical and immunostaining properties were not reported.

Although the biological properties of all the antibodies identified in this study have not been deeply investigated, neither Nodu 246 nor Nb 284 show any blocking or activating properties (data not shown). Different factors can explain this lack of biological activity. First, the Y378F P2X4 mutant was used for immunization. Although this mutant shows no obvious altered sensitivity to ATP compared to wild type receptors, its constant presence at the plasma membrane may result in its inactivation by resting extracellular ATP concentrations. This inactivated conformation may bury the ATP-binding pocket region and its immunogenic potential. Alternatively, P2X4 receptors are heavily glycosylated compared to P2X7; this can act as a shield, preventing the antigenic regions of the binding pocket from being exposed during immunization. Further characterization of the binding epitopes of the antibodies would be required to achieve a better understanding of the lack of pharmacological effect of these antibodies and, potentially, to design new immunization strategies.

In addition to the production of highly specific monoclonal antibodies against P2X4 receptor, our results provide a methodological framework for generating antibodies against other membrane proteins that has widespread potential applications.

DATA AVAILABILITY STATEMENT

Genebank accession numbers for the different cDNAs used in this study are: Y07684.1 (human P2X4), AF089751.1 (mouse P2X4) and X87763.1 (rat P2X4).

ETHICS STATEMENT

The animal study was reviewed and approved by the animal welfare commission (Amt für Verbraucherschutz, Lebensmittelsicherheit und Veterinärwesen Hamburg, A8a/694).

AUTHOR CONTRIBUTIONS

FK-N and FR designed the study. PB, BR, SM, EG, GD, JH, and LU performed the experiments. LU, FK-N, and FR wrote the manuscript.

FUNDING

This work was funded by the Institut National de la Santé et de la Recherche Médicale (Inserm), the Centre National de la Recherche Scientifique (CNRS), the Agence Nationale de la Recherche (ANR-10-MIDI-0012), the Program Investissement d'Avenir (LabEx Ion Channel Science and Therapeutics), and la Fondation NRJ-Institut de France.

REFERENCES

Adriouch, S., Dubberke, G., Diessenbacher, P., Rassendren, F., Seman, M., Haag, F., et al. (2005). Probing the expression and function of the P2X7 purinoceptor with antibodies raised by genetic immunization. *Cell. Immunol.* 236, 72–77. doi: 10.1016/j.cellimm.2005.08.011

Baker, M. (2015). Antibody anarchy: a call to order. *Nature* 527, 545–551. doi: 10.1038/527545a

Burnstock, G. (2006). Purinergic signalling. *Br. J. Pharmacol.* 147, S172–S181. doi: 10.1038/sj.bjp.0706429

Danquah, W., Meyer-Schwesinger, C., Rissiek, B., Pinto, C., Serracant-Prat, A., Amadi, M., et al. (2016). Nanobodies that block gating of the P2X7 ion channel ameliorate inflammation. *Sci. Transl. Med.* 8:366ra162. doi: 10.1126/scitranslmed.aaf8463

De Genst, E., Silence, K., Decanniere, K., Conrath, K., Loris, R., Kinne, J., et al. (2006). Molecular basis for the preferential cleft recognition by dromedary heavy-chain antibodies. *Proc. Natl. Acad. Sci. U S A* 103, 4586–4591. doi: 10.1073/pnas.0505379103

Eden, T., Menzel, S., Wesolowski, J., Bergmann, P., Nissen, M., Dubberke, G., et al. (2018). A cDNA immunization strategy to generate nanobodies

against membrane proteins in native conformation. *Front. Immunol.* 8:1989. doi: 10.3389/fimmu.2017.01989

Egan, T. M., and Khakh, B. S. (2004). Contribution of calcium ions to P2X channel responses. *J. Neurosci.* 24, 3413–3420. doi: 10.1523/JNEUROSCI.5429-03.2004

Kaczmarek-Hajek, K., Zhang, J., Kopp, R., Grosche, A., Rissiek, B., Saul, A., et al. (2018). Re-evaluation of neuronal P2X7 expression using novel mouse models and a P2X7-specific nanobody. *Elife* 7:e36217. doi: 10.7554/eLife.36217

Koch-Nolte, F., Eichhoff, A., Pinto-Espinoza, C., Schwarz, N., Schäfer, T., Menzel, S., et al. (2019). Novel biologics targeting the P2X7 ion channel. *Curr. Opin. Pharmacol.* 47, 110–118. doi: 10.1016/j.coph.2019.03.001

Lalisse, S., Hua, J., Lenoir, M., Linck, N., Rassendren, F., and Ulmann, L. (2018). Sensory neuronal P2RX4 receptors controls BDNF signaling in inflammatory pain. *Sci. Rep.* 8:964. doi: 10.1038/s41598-018-19301-5

Möller, S., Jung, C., Adriouch, S., Dubberke, G., Seyfried, F., Seman, M., et al. (2007). Monitoring the expression of purinoceptors and nucleotide-metabolizing ecto-enzymes with antibodies directed against proteins in native conformation. *Purinergic Signal.* 3, 359–366. doi: 10.1007/s11302-007-9084-9

Murrell-Lagnado, R. D., and Frick, M. (2019). P2X4 and lysosome fusion. *Curr. Opin. Pharmacol.* 47, 126–132. doi: 10.1016/j.coph.2019.03.002

Qureshi, O. S., Paramasivam, A., Yu, J. C. H., and Murrell-Lagnado, R. D. (2007). Regulation of P2X4 receptors by lysosomal targeting, glycan protection and exocytosis. *J. Cell Sci.* 120, 3838–3849. doi: 10.1242/jcs.010348

Roncador, G., Engel, P., Maestre, L., Anderson, A. P., Cordell, J. L., Cragg, M. S., et al. (2016). The European antibody network's practical guide to finding and validating suitable antibodies for research. *MAbs* 8, 27–36. doi: 10.1080/19420862.2015.1100787

Sim, J. A., Chaumont, S., Jo, J., Ulmann, L., Young, M. T., Cho, K., et al. (2006). Altered hippocampal synaptic potentiation in P2X4 knock-out mice. *J. Neurosci.* 26, 9006–9009. doi: 10.1523/jneurosci.2370-06.2006

Stokes, L., Layhadi, J. A., Bibic, L., Dhuna, K., and Fountain, S. J. (2017). P2X4 receptor function in the nervous system and current breakthroughs in pharmacology. *Front. Pharmacol.* 8:291. doi: 10.3389/fphar.2017.00291

Stortelers, C., Pinto-Espinoza, C., Van Hoorick, D., and Koch-Nolte, F. (2018). Modulating ion channel function with antibodies and nanobodies. *Curr. Opin. Immunol.* 52, 18–26. doi: 10.1016/j.coi.2018.02.003

Surprenant, A., and North, R. A. (2009). Signaling at purinergic P2X receptors. *Annu. Rev. Physiol.* 71, 333–359. doi: 10.1146/annurev.physiol.70.113006.100630

Suurväli, J., Boudinot, P., Kanellopoulos, J., and Rüütel Boudinot, S. (2017). P2X4: a fast and sensitive purinergic receptor. *Biomed. J.* 40, 245–256. doi: 10.1016/j.bj.2017.06.010

Tsuda, M., Shigemoto-Mogami, Y., Koizumi, S., Mizokoshi, A., Kohsaka, S., Salter, M. W., et al. (2003). P2X4 receptors induced in spinal microglia gate tactile allodynia after nerve injury. *Nature* 424, 778–783. doi: 10.1038/nature01786

Ulmann, L., Hatcher, J. P., Hughes, J. P., Chaumont, S., Green, P. J., Conquet, F., et al. (2008). Up-regulation of P2X4 receptors in spinal microglia after peripheral nerve injury mediates BDNF release and neuropathic pain. *J. Neurosci.* 28, 11263–11268. doi: 10.1523/JNEUROSCI.2308-08.2008

Ulmann, L., Hirbec, H., and Rassendren, F. (2010). P2X4 receptors mediate PGE2 release by tissue-resident macrophages and initiate inflammatory pain. *EMBO J.* 29, 2290–2300. doi: 10.1038/emboj.2010.126

Wareham, K. J., and Seward, E. P. (2016). P2X7 receptors induce degranulation in human mast cells. *Purinergic Signal.* 12, 235–246. doi: 10.1007/s11302-016-9497-4

Williams, W. A., Linley, J. E., Jones, C. A., Shibata, Y., Snijder, A., Button, J., et al. (2019). Antibodies binding the head domain of P2X4 inhibit channel function and reverse neuropathic pain. *Pain* 160, 1989–2003. doi: 10.1097/j.pain.0000000000001587

Winkelmann, V. E., Thompson, K. E., Neuland, K., Jaramillo, A. M., Fois, G., Schmidt, H., et al. (2019). Inflammation-induced upregulation of P2X 4 expression augments mucin secretion in airway epithelia. *Am. J. Physiol. Lung Cell. Mol. Physiol.* 316, L58–L70. doi: 10.1152/ajplung.00157.2018

Xu, J., Bernstein, A. M., Wong, A., Lu, X.-H., Khoja, S., Yang, X. W., et al. (2016). P2X4 receptor reporter mice: sparse brain expression and feeding-related presynaptic facilitation in the arcuate nucleus. *J. Neurosci.* 36, 8902–8920. doi: 10.1523/JNEUROSCI.1496-16.2016

Yamamoto, K., Sokabe, T., Matsumoto, T., Yoshimura, K., Shibata, M., Ohura, N., et al. (2006). Impaired flow-dependent control of vascular tone and remodeling in P2X4-deficient mice. *Nat. Med.* 12, 133–137. doi: 10.1038/nm1338

Yang, T., Shen, J. B., Yang, R., Redden, J., Dodge-Kafka, K., Grady, J., et al. (2014). Novel protective role of endogenous cardiac myocyte P2X4 receptors in heart failure. *Circ. Heart Fail.* 7, 510–518. doi: 10.1161/CIRCHEARTFAILURE.113.001023

Conflict of Interest: The authors declare that the research was conducted in the absence of any commercial or financial relationships that could be construed as a potential conflict of interest.

Advantages of publishing in Frontiers

OPEN ACCESS
Articles are free to read for greatest visibility and readership

FAST PUBLICATION
Around 90 days from submission to decision

HIGH QUALITY PEER-REVIEW
Rigorous, collaborative, and constructive peer-review

TRANSPARENT PEER-REVIEW
Editors and reviewers acknowledged by name on published articles

Frontiers
Avenue du Tribunal-Fédéral 34
1005 Lausanne | Switzerland

Visit us: www.frontiersin.org
Contact us: info@frontiersin.org | +41 21 510 17 00

REPRODUCIBILITY OF RESEARCH
Support open data and methods to enhance research reproducibility

DIGITAL PUBLISHING
Articles designed for optimal readership across devices

FOLLOW US
@frontiersin

IMPACT METRICS
Advanced article metrics track visibility across digital media

EXTENSIVE PROMOTION
Marketing and promotion of impactful research

LOOP RESEARCH NETWORK
Our network increases your article's readership